IAEA-TECDOC-1691

Status of Fast Reactor Research and Technology Development

IAEA
International Atomic Energy Agency

STATUS OF FAST REACTOR RESEARCH AND TECHNOLOGY DEVELOPMENT

The following States are Members of the International Atomic Energy Agency:

AFGHANISTAN
ALBANIA
ALGERIA
ANGOLA
ARGENTINA
ARMENIA
AUSTRALIA
AUSTRIA
AZERBAIJAN
BAHRAIN
BANGLADESH
BELARUS
BELGIUM
BELIZE
BENIN
BOLIVIA
BOSNIA AND HERZEGOVINA
BOTSWANA
BRAZIL
BULGARIA
BURKINA FASO
BURUNDI
CAMBODIA
CAMEROON
CANADA
CENTRAL AFRICAN REPUBLIC
CHAD
CHILE
CHINA
COLOMBIA
CONGO
COSTA RICA
CÔTE D'IVOIRE
CROATIA
CUBA
CYPRUS
CZECH REPUBLIC
DEMOCRATIC REPUBLIC OF THE CONGO
DENMARK
DOMINICA
DOMINICAN REPUBLIC
ECUADOR
EGYPT
EL SALVADOR
ERITREA
ESTONIA
ETHIOPIA
FIJI
FINLAND
FRANCE
GABON
GEORGIA
GERMANY
GHANA
GREECE
GUATEMALA
HAITI
HOLY SEE
HONDURAS
HUNGARY
ICELAND
INDIA
INDONESIA
IRAN, ISLAMIC REPUBLIC OF
IRAQ
IRELAND
ISRAEL
ITALY
JAMAICA
JAPAN
JORDAN
KAZAKHSTAN
KENYA
KOREA, REPUBLIC OF
KUWAIT
KYRGYZSTAN
LAO PEOPLE'S DEMOCRATIC REPUBLIC
LATVIA
LEBANON
LESOTHO
LIBERIA
LIBYA
LIECHTENSTEIN
LITHUANIA
LUXEMBOURG
MADAGASCAR
MALAWI
MALAYSIA
MALI
MALTA
MARSHALL ISLANDS
MAURITANIA
MAURITIUS
MEXICO
MONACO
MONGOLIA
MONTENEGRO
MOROCCO
MOZAMBIQUE
MYANMAR
NAMIBIA
NEPAL
NETHERLANDS
NEW ZEALAND
NICARAGUA
NIGER
NIGERIA
NORWAY
OMAN
PAKISTAN
PALAU
PANAMA
PAPUA NEW GUINEA
PARAGUAY
PERU
PHILIPPINES
POLAND
PORTUGAL
QATAR
REPUBLIC OF MOLDOVA
ROMANIA
RUSSIAN FEDERATION
RWANDA
SAUDI ARABIA
SENEGAL
SERBIA
SEYCHELLES
SIERRA LEONE
SINGAPORE
SLOVAKIA
SLOVENIA
SOUTH AFRICA
SPAIN
SRI LANKA
SUDAN
SWEDEN
SWITZERLAND
SYRIAN ARAB REPUBLIC
TAJIKISTAN
THAILAND
THE FORMER YUGOSLAV REPUBLIC OF MACEDONIA
TOGO
TRINIDAD AND TOBAGO
TUNISIA
TURKEY
UGANDA
UKRAINE
UNITED ARAB EMIRATES
UNITED KINGDOM OF GREAT BRITAIN AND NORTHERN IRELAND
UNITED REPUBLIC OF TANZANIA
UNITED STATES OF AMERICA
URUGUAY
UZBEKISTAN
VENEZUELA
VIETNAM
YEMEN
ZAMBIA
ZIMBABWE

The Agency's Statute was approved on 23 October 1956 by the Conference on the Statute of the IAEA held at United Nations Headquarters, New York; it entered into force on 29 July 1957. The Headquarters of the Agency are situated in Vienna. Its principal objective is "to accelerate and enlarge the contribution of atomic energy to peace, health and prosperity throughout the world''.

IAEA-TECDOC-1691

STATUS OF FAST REACTOR RESEARCH AND TECHNOLOGY DEVELOPMENT

INTERNATIONAL ATOMIC ENERGY AGENCY
VIENNA, 2012

For further information on this publication, please contact:

Nuclear Power and Technology Development Section
International Atomic Energy Agency
Vienna International Centre
PO Box 100
1400 Vienna, Austria
Email: Official.Mail@iaea.org

Status of fast reactor research and technology development
– Vienna : International Atomic Energy Agency, 2012.
p. ; 30 cm. – (IAEA-TECDOC series, ISSN 1011-4289
; no. 1691)
ISBN 978-92-0-130610-4
Includes bibliographical references.

1. Liquid metal fast breeder reactors – Safety measures.
2. Nuclear power plants – Design and construction.
3. Nuclear reactors – Decommissioning. I. International
Atomic Energy Agency. II. Series.

IAEAL 12-00781

FOREWORD

In 1985, the International Atomic Energy Agency (IAEA) published a report titled “Status of Liquid Metal Cooled Fast Breeder Reactors” (Technical Reports Series No. 246). The report was a general review of the status of fast reactor development at that time, covering some aspects of design and operation and reviewing experience from the earliest days. It summarized the programmes and plans in all countries which were pursuing the development of fast reactors. In 1999, the IAEA published a follow-up report titled “Status of Liquid Metal Cooled Fast Reactor Technology” (IAEA-TECDOC-1083), necessitated by the substantial advances in fast reactor technology development and changes in the economic and regulatory environment which took place during the period of 1985–1998. Chief among these were the demonstration of reliable operation by several prototypes and experimental reactors, the reliable operation of fuel at a high burnup and the launch of new fast reactor programmes by some additional Member States.

In 2006, the Technical Working Group on Fast Reactors (TWG-FR) identified the need to update its past publications and recommended the preparation of a new status report on fast reactor technology. The present status report intends to provide comprehensive and detailed information on the technology of fast neutron reactors. The focus is on practical issues that are useful to engineers, scientists, managers, university students and professors, on the following topics: experience in construction, operation and decommissioning; various areas of research and development; engineering; safety; and national strategies and public acceptance of fast reactors.

The IAEA would like to express its appreciation to Mr. E. Fujita, who chaired this study. The IAEA is grateful to all those who helped in the preparation of this report, in particular, D. Caron. The report has been prepared with contributions from China, France, Germany, India, Italy, Japan, the Republic of Korea, the Russian Federation, the United Kingdom and the United States of America. The IAEA officers responsible for this publication were A. Stanculescu and S. Monti of the Division of Nuclear Power.

EDITORIAL NOTE

This publication has not been edited by the editorial staff of the IAEA. It does not address questions of responsibility, legal or otherwise, for acts or omissions on the part of any person.

The use of particular designations of countries or territories does not imply any judgement by the publisher, the IAEA, as to the legal status of such countries or territories, of their authorities and institutions or of the delimitation of their boundaries.

The mention of names of specific companies or products (whether or not indicated as registered) does not imply any intention to infringe proprietary rights, nor should it be construed as an endorsement or recommendation on the part of the IAEA.

CONTENTS

CHAPTER 1
BACKGROUND AND OVERVIEW

1.1. Background

Nuclear power currently provides about 14% of the world's electricity [1], primarily from thermal reactors cooled by water. In parallel with the development and construction of these thermal reactors, several Member States have undertaken research and development programmes on fast reactors cooled by liquid metal or gas, as well as their associated fuel cycles. Important among the research topics is the demonstration that key drivers which are important to the large-scale introduction of nuclear energy into the world's energy mix can be satisfied, including: economics, safety, natural resource utilization, reduction of waste, non-proliferation and public acceptance. Fast reactors with recycle have the potential to significantly enhance sustainability indices.

Twelve experimental fast reactors with thermal power ranging from 10–400 MW_{th} and six commercial size prototypes with electrical output ranging from 250–1200 MW_{el} have been constructed and operated. In total, nearly 350 reactor-years of operation have been acquired for fast reactors. Overall, the operational performance of these reactors has been remarkable, with noteworthy achievements such as thermal efficiencies of 43–45 %, which is the highest value in the nuclear power practice [2, 3]. Experience in the decommissioning of several of these reactors has been accumulated as well.

Great strides have been made in fast reactor technology, which encourage future development. The closed fuel cycle has been demonstrated, an effective breeding ratio was experimentally confirmed, fuel burnup in excess of 130 GW·d/t has been reached in several reactors with over 200 GW·d/t reached for some experimental pins and major steps towards commercial sodium-cooled fast reactor designs have been made [3]. The worldwide investment already made in the development and demonstration of the sodium-cooled fast reactors unique technology exceeds US$ 50 billion [4]. Research on fast reactors conducted during the period covered by this report has focused on advanced reactor designs that will meet sustainability goals simultaneously with those of improved economics and high levels of safety. This is accompanied by a renewed interest in alternative concepts for the coolant and fuel as a means by which to attain these goals.

It is now generally accepted that closed fuel cycle with fast reactors would be the main nuclear energy system that could provide sustainable nuclear energy contribution to the world community. In this report, the technology of fast reactors, in particular the technology of sodium-cooled fast reactors, is discussed. It must be acknowledged that, in order to reach the final goal of fast reactor development and deployment, the respective nuclear fuel cycle must also be developed. Fast reactors pose special problems to nuclear fuel cycle facilities; however, these problems are discussed in numerous other publications available and are not addressed in this report.

1.2. Fast neutron reactor potential

Fast neutron reactors offer great potential, examples of which include [5–9]:

(a) Increased uranium utilization

It is well known that fast reactors with closed fuel cycles have the potential to utilize uranium resources to the greatest extent possible. The key to this is the high fission

neutron yield per neutron absorbed in ^{239}Pu in a fast spectrum. It is necessary to close the fuel cycle for the repeated use of the same uranium. Considering practical fuel cycle losses (2–3%) and achievable burnups (100–200 GWd/t), it is possible to fission more than 80% of the natural uranium resources. Moreover, with the thermal efficiency of a fast reactor at ~ 0.4, compared to ~ 0.3 for a thermal reactor, the amount of energy that can be recovered per unit mass uranium is even greater.

(b) Fast nuclear power growth from the available resources through the breeding of fissile material

It is known that carbide, nitride and metal fuels have higher breeding potential compared to oxide fuels. While carbide fuel has difficulties in manufacturing and reprocessing, nitride fuel requires N-15 enrichment. Metal fuel has even higher breeding potential. These high breeding potentials of advanced fuels allow for fast growth of nuclear energy production in case this is desired.

(c) Reduction of radioactive waste

In thermal reactors, long-lived minor actinides which pose a radiological hazard (notably ^{237}Np, ^{241}Am, ^{242}Am, ^{243}Am and ^{244}Cm) are produced, as capture cross-sections are higher than fission cross-sections. In a fast neutron spectrum, minor actinides are not only produced at a lower rate due to lower capture to fission rations, but are also consumed through fission. Even with multiple recycle, the Pu isotopic composition can be maintained at a nearly constant value in a fast neutron reactor.

(d) Utilization of Th for ^{233}U production with low ^{232}U production

One of the identified problems associated with the thorium fuel cycle is the production of ^{232}U. In a thorium-fuelled thermal reactor, the ^{232}U production is typically in the range of 2000-4000 ppm; however, in a fast reactor with thorium loaded as a blanket material, this value reduces to the 500-1000 ppm range.

(e) Utilization of fission products and other radioactive isotopes

In the reprocessing cycle of a fast neutron reactor, important fission products which have commercial value are produced. Examples include: ^{137}Cs, produced in an abundance of about 31% of the Cs yield; ^{90}Sr, in an abundance of about 60% of the Sr yield; the platinoids Pd, Rh and Ru, the former is produced nearly free of radioactive contamination while the others are radioactive but decay to acceptable levels within a few years; and other examples such as ^{212}Pb, ^{212}Bi, ^{223}Ra and ^{227}Ac.

(f) Higher thermodynamic efficiency

1.3. Progress within the period 1999 – present

The period addressed during this report is from 1999 (the year in which the previous edition of the fast reactor status report was published) to the present. Operational performance of existing fast reactors during this interval was good and none experienced major complications. Two fast reactors in operation were definitively shut down after long and successful service lives, one was restarted subsequent to a long-term shutdown and one new fast reactor was commissioned. In the area of design achievements, several Member States have embarked on development programmes of advanced fast reactors. Research and development activities are focused on the anticipated deployment of advanced concept

sodium-cooled fast reactors, as well as demonstrators for the two alternative coolant concepts (heavy liquid metal and gas) in the near future.

1.3.1. Demonstration and prototype reactor operation

In France, the Phénix reactor was shut down after more than 35 years of service. In the course of operation, Phénix served as a technology demonstrator and an R&D support tool for later French and European sodium-cooled fast reactors. During the years of 1999–2002, Phénix underwent plant renovations and safety upgrades as part of its 720 EFPD lifetime extension to support the French programme on long-lived radioactive waste management. Overall, the last years of operation (2003–2009) were satisfactory and, more frequently, better than satisfactory. In 2007, Phénix broke several of its own records (grid connection time, operating cycle length and electrical production run without shutdown), earning it the 2007 Société française d'énergie nucléaire (SFEN) grand prize in recognition of its successful re-commissioning and its record operational performance. As a final contribution, a series of important end-of-life tests were conducted on Phénix at low and zero power; the results which will be deduced from these tests will serve as an experimental basis for core physics, thermal hydraulics and fuel issues; for investigations of the negative reactivity transients which occurred in 1989 and 1990; and for the programme to validate a wide range of sodium-cooled fast reactor computer codes.

In India, the Fast Breeder Test Reactor (FBTR) has been in operation since October 1985, producing over 330 GW·h of thermal and 10 GW·h of electrical energy. The core thermal power has been progressively increased from 10.6 MW (the initial rating for the carbide fuelled core) to 18.6 MW through the introduction of a carbide fuel consisting of more uranium and less plutonium, in an effort to attain the 40 MW design target (for the original MOX fuelled core). The burnup of the Mark I fuel assemblies which remained in the core has reached a peak value of 165 GWd/t without failure. The FBTR has been used as an irradiation tool to test fuel concepts for the Indian Pressurized Heavy Water Reactors (PHWRs) and the Prototype Fast Breeder Reactor (PFBR), as well as to conduct physics and engineering experiments to validate codes and systems. Several system upgrades and modifications have taken place and it is estimated that the residual life of this reactor is an additional 12 years at full power.

In Japan, the experimental fast reactor Joyo has been dedicated to the development of the sodium-cooled fast reactor. Various irradiation tests were successfully conducted together with the results from post irradiation examination. Joyo was granted the "Nuclear Historic Landmark Award" in 2006 by the American Nuclear Society, and reached its 30th anniversary on 24 April 2007. During the 15th periodical inspection of Joyo in 2007, it was found that there was obstacle in the in-vessel storage rack. This incident has necessitated the replacement of the upper core structure and the retrieval of the irradiation test device "MARICO-2" for Joyo re-start. Through these restoration works, Joyo has been used for the development of in-vessel inspection and repair techniques in SFRs.

The Japanese prototype fast breeder reactor Monju attained the first criticality in April 1994, but was shutdown on 8 December 1995 due to a sodium-leak incident which occurred in the secondary coolant system. After comprehensive reviews on the validity of fast breeder reactor development in Japan as well as the Monju safety, the plant modification work against sodium leakage was carried out in 2005–2007. Additional works aimed toward the Monju restart included verification of the entire plant soundness and improvement of the anti-seismic margin. Monju was restarted on 8 May 2010, over 14 years after its shutdown.

In the Russian Federation the BR-10 reactor was shut down in December 2002 after approximately 44 years of operation. As a result of its operation, substantial experience has been gained for fuels, materials, reactor systems and monitoring techniques, as well as a representative test facility for any technology that would later be realized in the subsequent Russian sodium-cooled fast reactors, namely BOR-60, BN-350 and BN-600. As to other applications, the BR-10 has been used as an isotope generator and to provide treatment to cancer patients. At present, the BR-10 reactor is being prepared for decommissioning and will serve as a basis for developing and testing sodium-cooled fast reactor decommissioning technologies.

The Russian BOR-60 reactor has been in operation since 1968, serving as both a test facility and supplying power to the grid. The number of unscheduled shutdowns during this period has been minimal, totalling only 1–2 events per year and due primarily to external initiating factors. Experimental tests performed at the BOR-60 facility during this period have focused on irradiation of fuels and materials, as well as testing of sodium, control and safety equipment. Subsequent to a thorough analysis, in December 2009, a second lifetime extension was approved for BOR-60, authorizing the reactor to operate through the end of 2014. The Russian BN-600 reactor has been operating as the third power unit of the Beloyarsk nuclear power plant since 1980, supplying over 112.5 billion kW·h of electricity to the grid. It now holds the distinction of being the largest operating fast reactor in the world and, moreover, the BN-600 ranks among the most reliable and stable nuclear power reactors in the Russian Federation. It has operated for the last nineteen years without steam generator leaks and for sixteen years without any sodium leaks in any of the sodium circuits. Work on lifetime extension began in 2006 and was successfully completed, permitting the BN-600 reactor to operate through the end of March 2020.

One sodium-cooled fast reactor, the China Experimental Fast Reactor (CEFR), the country's first fast reactor, has very recently been commissioned in July 2010. Presently, there are two sodium-cooled fast reactors under construction: the PFBR in India and the BN-800 in the Russian Federation, with anticipated commissioning dates of 2011 and 2014, respectively.

1.3.2. Design advances and technical achievements

In China, the conceptual design of the 600–900 MW_{el} China Demonstration Fast Reactor (CDFR) is ongoing. The next concept, currently under consideration, leading to the commercial utilization of fast reactor technology around 2030 is the 1000–1500 MW_{el} China Demonstration Fast Breeder Reactor (CDFBR). By 2050, China foresees to increase its nuclear capacity up to the level of 240–250 GW_{el}, to be provided mainly by fast breeder reactors.

In France, fast reactor technology development activities are determined by two French Parliament Acts, viz. the 13 July 2005 Act specifying the energy policy guidelines, and the 28 July 2006 Act outlining policies for sustainable management of radioactive waste, and requesting R&D on innovative nuclear reactors to ensure that, firstly, by 2012 an assessment of the industrial prospects of these reactor types can be made, and, secondly, a prototype reactor is commissioned by 31 December 2020 (with an industrial introduction of this technology in 2040–2050). To meet the stipulations of these laws, the Commissariat à l'Énergie Atomique (CEA) and its industrial partners (EdF and AREVA) are implementing an ambitious research and technology development programme aiming at the design and deployment of the 300–600 MW_{el} sodium cooled fast reactor prototype ASTRID. Within the framework of Euratom projects, CEA is also pursuing conceptual design studies for a 50-80 MW_{th} experimental prototype reactor called ALLEGRO.

In India, the next step foresees the construction and commercial operation by 2023 of 6 additional mixed uranium-plutonium oxide fuelled PFBR-type reactors (a twin unit at Kalpakkam and four 500 MW_{el} reactors at a new site to be determined). The design of these 6 fast breeder reactors will follow an approach of phased improvements of the first Kalpakkam PFBR design. Beyond 2020, the Indian national strategy is centred on high breeding gain ~ 1000 MW_{el} capacity reactors, and on the collocation of multi-unit energy parks with fuel cycle facilities based on pyro-chemical reprocessing technology.

In Japan, the R&D study of fast reactor cycle technology titled "Feasibility Study on Commercialized Fast Reactor Cycle Systems (F/S)" was carried out from JFY 1999 to JFY 2005. As a result of the F/S, the combination of sodium-cooled fast reactor with oxide fuel, advanced aqueous reprocessing and simplified pelletizing fuel fabrication was selected as the most promising concept of fast reactor cycle system. Following the publication of the F/S result and the establishment of the Japanese policy on FBR cycle technology development, the Japan Atomic Energy Agency (JAEA) launched the Fast Reactor Cycle Technology Development (FaCT) project in 2006, in cooperation with the Japanese electrical utilities. In the FaCT project, design and experimental study for the main concept will be implemented in order to present the conceptual designs of the commercial and demonstrative FBR cycle facilities by 2015, along with the development plan to realize them. R&D has progressed to the development stage, to establish the realization of innovative technologies that could meet development targets. The demonstration FBR will be launched around 2025. By around 2050, the commercial FBR cycle system will be deployed based on experiences with the demonstration FBR cycle system.

In the Republic of Korea, fast reactor development activities are performed within the framework of the Generation IV International Forum. Currently, R&D activities are focused on core design, heat transport systems, and mechanical structure systems. Specifically, R&D work covers a Passive Decay Heat Removal Circuit (PDRC) experiment, S-CO_2 Brayton cycle systems, a Na-CO_2 interaction test, and sodium technology. Design work on innovative sodium cooled fast reactor and fuel cycle concepts is pursued. The Republic of Korea is planning to develop and deploy a demonstration fast reactor by 2025–2028.

In the Russian Federation, the "Federal Target Programme (FTP) Nuclear power technologies of a new generation for the period of 2010–2015 and with outlook to 2020" development of closed fuel cycle technologies, and resolving the spent fuel issues. The spent fuel of existing and constructed light water reactors will be used to fuel the next generation fast reactors. The Russian fast reactor programme is based on extensive operational experience with experimental and industrial size sodium cooled fast reactors. Russia has also developed and gained experience with the technology of heavy liquid metal cooled (lead and lead-bismuth eutectic alloy) fast reactors. The fast reactor development programme includes life extension of both the experimental reactor BOR-60 and the industrial reactor BN-600, construction of the industrial sodium cooled fast reactor BN-800, and the design of the new experimental reactor MBIR (150 MW_{th}/.30 MW_{el})sodium cooled, uranium-plutonium oxide (alternatively uranium-plutonium nitride) fuelled], planned as replacement of BOR-60.

Within the framework of the programme, fast reactor technologies based on sodium, lead, and lead-bismuth eutectic alloy coolants (i.e. SFR, BREST-OD-300, and SVBR-100, respectively) will be developed simultaneously, along with the respective fuel cycles. The design of the advanced large-size sodium cooled commercial fast reactor BN-K is also ongoing.

In the United States of America, the current programmatic approach is centred on a long-term deployment of fuel cycle technologies, the initial analysis of a broad set of options, and on the use of modern science tools and approaches designed to solve challenges and develop better performing technologies. One major goal of the US programme is to develop an integrated waste management strategy. The focus of this work is on predictive capabilities for understanding repository performance. Another major research focus is in the area of used fuel separation technologies. Through the use of small-scale experiments, theory development, as well as modelling and simulation to develop fundamental understanding, innovative long-term options are being explored. The aimed at outcome of this work is waste reduction. Enhanced materials protection and control is another key goal in the US fast reactor programme. In this area the work focuses on the development of advanced techniques providing real-time nuclear materials management with continuous inventory (including for large through-put industrial facilities). The specific research and technology activities include the development of the "advanced recycle reactor" for closing the fuel cycle, and of the fast reactor needed for final transmutation/transuranics utilization systems. The near term focus is on sodium coolant technology. For future fast reactor technology deployment, the US programme focuses on two major research areas: capital cost reduction, and assurance of safety (including high system reliability).

1.4. Contents of this report

Chapter 2 details operating experience from the world's experimental, prototype and demonstration fast reactors with a thermal capacity of 8 MW_{th} or greater, which were constructed and, at a minimum, underwent pre-operational testing. These include Rapsodie, Phénix and Superphénix in France; KNK-II and SNR-300 in Germany; FBTR in India; Joyo and Monju in Japan; PFR in the United Kingdom; EBR-I, Enrico Fermi, EBR-II and FFTF in the United States; and BR-10, BOR-60, BN-350 and BN-600 in the Russian Federation (and, in the case of BN-350, the former Soviet Union). Descriptions of fast reactors of smaller capacity are not within the scope of this report.

Chapters 3 through 5 summarize the conceptual designs which adopt sodium, heavy liquid metal (i.e. lead or lead-bismuth) and gas coolant, respectively. Chapter 3 provides design descriptions and the current status of the three sodium-cooled fast reactors currently under construction or undergoing pre-operational testing, as well as conceptual design descriptions for other sodium-cooled fast reactors. Chapter 4 examines the motivations for and conceptual designs for fast reactors cooled by a heavy liquid metal. Similarly, Chapter 5 documents the conceptual design descriptions for gas-cooled fast reactors. Together, these chapters comprehensively document the sodium-cooled reference design as well as two alternatives, heavy liquid metal-cooled and gas-cooled, for which research is often conducted in parallel with that for the sodium-cooled designs.

Chapter 6 covers fast reactor core research and development. The aspects covered include: reactor physics, thermal hydraulics, fuel concepts, absorber elements, sodium coolant technologies, structural materials and instrumentation and control systems. Chapter 7 presents the status of fast reactor plant engineering technology development. Chapter 8 describes reactor core safety analysis as it pertains to fast reactors. In addition to describing the safety principles and presenting designed safety features, the chapter presents examples of design basis and beyond design basis safety analyses conducted for some representative fast reactors.

Finally, Chapter 9 provides a summary of reports of national strategies, international initiatives and an assessment of public acceptance as related to fast reactors. The chapter

concludes with some final remarks of the TWG-FR on the research and technology development of fast reactors.

REFERENCES TO CHAPTER 1

[1] INTERNATIONAL ATOMIC ENERGY AGENCY, Energy, Electricity and Nuclear Power Estimates for the Period up to 2030, Reference Data Series No. 1, IAEA, Vienna (2009).

[2] INTERNATIONAL ATOMIC ENERGY AGENCY, Fast Reactor Database, IAEA-TECDOC-1531, IAEA, Vienna (2006).

[3] INTERNATIONAL ATOMIC ENERGY AGENCY, Status of Liquid Metal Cooled Fast Reactor Technology, IAEA-TECDOC-1083, IAEA, Vienna (1999).

[4] MOUROGOV, V.M., et al., Liquid-metal-cooled-fast reactor (LMFR) development and IAEA activities, Energy, Vol. 23, No. 7/8, pp. 637-648 (1998).

[5] INTERNATIONAL ATOMIC ENERGY AGENCY, Status of Liquid Metal Fast Breeder Reactor Development in the USA, IAEA-TECDOC-791, IAEA, Vienna (1994).

[6] WALTERS, L.C., Thirty Years of Fuels and Materials Information from EBR-II, J. Nuc. Mat., Vol. 270, No. 39 (1999).

[7] HOFMAN, G.L., WALTERS, L.C., BAUER, T.H., Metallic Fast Reactor Fuels, Prog. Nuc. Ener., Vol. 31, No. 1 (1997).

[8] RAJ, B., MOHANAKRISHNAN, P., Reactor Physics and Safety Aspects of Fast Neutron Reactors with Associated Closed Fuel Cycles, Proc. PHYSOR'08, Interlaken, Switzerland, 14-19 September 2008, Paul Scherrer Institute (2008).

[9] ISHIKAWA, M., NAGATA, T., KONDO, S., Japanese Fast Reactor Program for Homogeneous Actinide Recycling, Proc. PHYSOR'08, Interlaken, Switzerland, 14-19 September 2008, Paul Scherrer Institute (2008).

CHAPTER 2
EXPERIENCE WITH SODIUM COOLED FAST REACTORS

2.1. Summary

Chapter 2 provides a résumé of many of the sodium-cooled fast reactors which have operated in the IAEA Member States. Historical context, design descriptions and experience in operation and (when appropriate) decommissioning are included for each. Table 2.1 shows fast reactors constructed and/or operated in IAEA Member States (MSs).

TABLE 2.1. FAST REACTORS CONSTRUCTED AND/OR OPERATED IN IAEA MSs

Plant (Location, IAEA Member State)	Reactor	Period of operation	Nominal full power (MW_t / MW_e)	References for further reading
CEFR (China)	China Experimental Fast Reactor	Under construction	65 / 20	Chapter 3 of the current report
Rapsodie (France)	-	January 1961 – April 1983	40 / -	Chapter 2.5 of the current report [24, 69, 71]
Phénix (France)	-	1973 - 2009	563 / 255	Chapter 2.8 of the current report
Superphénix 1 (France)	-	1985 - 1996	2990 / 1242	Chapter 2.14 of the current report
KNK-II (Germany)	Kompakte Natriumgekuhlte Kernreaktoranlage	1977 - 1991	58 / 20	Chapter 2.10 of the current report
SNR-300 (Germany)	Schneller Natriumgekühlte Reaktor	Not available[a]	762 / 327	Chapter 2.16 of the current report
FBTR (India)	Fast Breeder Test Reactor	1985 till present	40 / 13	Chapter 2.15 of the current report
PFBR (India)	Prototype Fast Breeder Reactor	Under construction	1250 / 500	Chapter 3 of the current report
PEC (Italy)	Prova Elementi di Combustibile	Never went critical	120 / 0	http://www-frdb.iaea.org/fulltext/13_fastReactorDesigns.pdf#PEC
Joyo (Japan)	-	April 1977 till present	50 to 140 / 15	Chapter 2.11 of the current report
Monju (Japan)	-	1st Criticality April 1994, Criticality after modifications May 2010	714 / 280	Chapter 2.17 of the current report
BR-10 (Russian Federation)	Bystrij Reactor (Fast Reactor)	1958 - 2002	8 / 0	Chapter 2.2 of the current report
BOR-60 (Russian Federation)	Bystrij Opytnyj Reactor (Fast Experimental Reactor)	April 1980 till present	55 / 12	Chapter 2.6 of the current report
BN-350 (Kazakhstan)	Bystrie neytrony (Fast neutrons)	July 1973 -June 1994	750 / 200 (+ water desalination)	Chapter 2.7 of the current report
BN-600 (Russian Federation)	Bystrie neytrony (Fast neutrons)	1981 till present	1470 / 600	Chapter 2.12 of the current report
BN-800 (Russian Federation)	Bystrie neytrony (Fast neutrons)	Under construction	2100 / 870	Chapter 2.6 of the current report
DFR (UK)	Dounreay Fast Reactor	Nov. 1959 - Oct.1962	60 / 15	http://www-frdb.iaea.org/fulltext/13_fastReactorDesigns.pdf#DFR
PFR (UK)	Prototype Fast Reactor	1974 - 1994	650 / 250	Chapter 2.9 of the current report
Clementine (USA)	First Fast Neutron, Experimental Reactor	1946 - 1952	0,025 (25 KW) / -	http://www.osti.gov/bridge/servlets/purl/6330462-UyJsvA/ http://www.osti.gov/bridge/servlets/purl/7011118-j16aqD/
EBR-I (USA)	Experimental Breeder Reactor I	1951 - 1963	1.2 / 0.2	Chapter 2.1 of the current report
LAMPRE 1 (USA)	Los Alamoa Molten Plutonium Reactor Experiment	1961 - 1963	1 / -	http://www.osti.gov/bridge/servlets/purl/6330462-UyJsvA/
EFFBR (Fermi 1) (USA)	Enrico Fermi Fast Breeder Reactor	1963 -1972	200 / 66	Chapter 2.3 of the current report
EBR-II (USA)	Experimental Breeder Reactor II	1964 - 1994	62.5 / 19	Chapter 2.4 of the current report
SEFOR (USA)	Southwest Experimental Fast Oxide Reactor	1969 - 1972	20 / 0	http://www.osti.gov/bridge/servlets/purl/6330462-UyJsvA/
FFTF (USA)	Fast Flux Test Facility	1980 - 1992	400 / 0	Chapter 2.13 of the current

[a] Construction of the SNR-300 was completed in 1985, but the reactor did not proceed to operation by decision of the German government.

2.2. Experimental Breeder Reactor-I operating experience

2.2.1. History

Enrico Fermi broached the idea of a fast reactor that bred plutonium in April 1944 [1]. Such a reactor, with no moderator and with fully enriched fuel in a compact core, would require a liquid metal coolant to adequately remove its heat. The idea was promoted enthusiastically by Walter Zinn, future director of Argonne National Laboratory, and the concept soon became the Experimental Breeder Reactor (EBR). Permission to construct this new type of reactor on a remote site in Idaho was granted in 1947 by the newly constituted Atomic Energy Agency (AEC).

Wet criticality took place in August 1951 and full power was achieved on December 20, it being the first time a reactor was used to generate electricity (Fig. 2.1). Proof of breeding was obtained in February 1952, when radiochemical analysis showed 1.00±0.04 ^{239}Pu atoms were produced in the blanket for each ^{235}U atom burned in the core [2].

FIG. 2.1. Light bulbs energized by electricity from EBR-I (December 20, 1951).

Fuel pins in the first core had fully-enriched U slugs NaK-bonded to steel cladding. A Mark II core of U-2%Zr was installed in 1954 and was found to exhibit a positive temperature coefficient of reactivity. During a test in October 1955 to further study this behavior, the core was inadvertently melted. The whole core was remotely removed using a temporary concrete cell placed on top of the reactor, complete with a lead-glass window and manipulators [3].

Later hot-cell examination revealed that the NaK bond had vaporized and driven molten fuel axially and radially from the core, an effective shutdown mechanism [4].

Because damage was limited to fuel that could be replaced, the core was re-designed to have pins contained in rigid hexagonal ducts of stainless steel to constrain fuel-pin bowing. The new Mark III core design had seven such ducted “assemblies”, containing pins of U-2% Zr metallurgically bonded to zircaloy-2. The Mark IV core had 60 smaller-diameter pins containing Pu-1.25% Al NaK-bonded to zircaloy. Both cores exhibited a negative power coefficient of reactivity, confirming the wisdom of using ducted assemblies. Analysis gave a

breeding ratio of ~ 1.27 for the Mark IV core versus a ratio near unity for the three ^{235}U cores, reflecting the higher number of fission neutrons for ^{239}Pu.

The reactor was shut down in 1963, when its successor, EBR-II, was close to completion on a site 20 miles away. EBR-I (as it had been known for some time) was declared a Registered Historic National Monument by President Johnson in August 1966. It was decommissioned in the early 1970s and made accessible to the public in 1976.

2.2.2. Design description

As its designers explained [5], the EBR was built to promote understanding of the principles of a fast breeder reactor. It was liquid-metal cooled and was of the simplest design because it was intended - and used - for purely experimental purposes; e.g., to understand fast neutron physics and to study reactivity effects and reactor control in an un-moderated system. Briefly, the reactor consisted of three parts:

- A core of small-diameter cylindrical fuel pins of near 90% ^{235}U enrichment;
- An inner blanket region with larger diameter pins, each containing natural U;
- An outer blanket region built from keystone-shaped bricks of natural U, each jacketed in 0.5 mm thick stainless and each weighing about 40 kg.

The core and inner blanket were cooled by a NaK alloy, which was liquid at room temperature. The NaK was contained by a double-walled tank that fitted closely around the inner blanket. The outer blanket was air-cooled, movable, and contained the reactor's 12 control rods. At the time experience with liquid metals was limited, and by restricting all moving parts to the air-cooled outer blanket any problems that might arise from having moving parts in NaK were avoided.

The Mark I core had 217 9.8-mm diameter pins, each containing two 108-mm long enriched U fuel slugs and giving the total ^{235}U mass of 52 kg required for criticality. The inner blanket region had 138 24.8 mm diameter pins, each containing 500-mm lengths of natural U in 5-mm thick stainless steel cladding. Figure 2.2 shows the grid plate used to position the core and inner blanket elements.

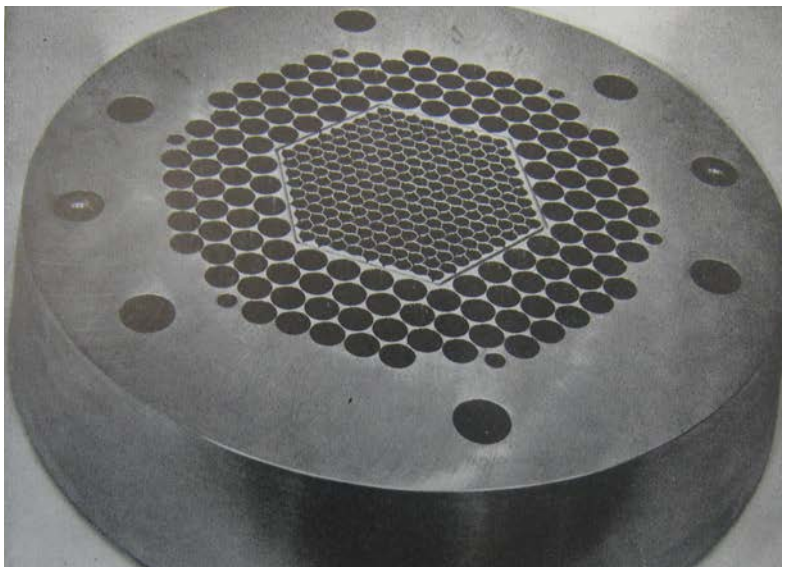

FIG. 2.2. 100-mm thick EBR grid plate used to position core and inner blanket elements.

Full reactor power was 1.2 MW, giving a peak flux of 1.1×10^{14} n/cm^2·s. The inlet and outlet temperatures of the primary NaK were 228°C and 316°C at a flow of 36 kg/s. A NaK-NaK heat exchanger, superheater, boiler, economizer and turbogenerator were used to produce approximately 200 kW of electricity. Details of these and other reactor systems are found in Refs [2-5], together with a review of the major insights into the physics of fast reactors which resulted from operating EBR as a research facility.

2.2.3. Core meltdown incident

As noted earlier, an experiment was being performed on November 29, 1955, to investigate the increased positive temperature coefficient associated with the Mark II core under certain operating conditions. On that day, intentional operation was underway at high core temperatures and with a short reactor period (60-s) when a sharp increase in reactor power occurred; fuel temperatures, as indicated by an in-fuel thermocouple, began to rise rapidly [4]. The safety rods were scrammed but it became obvious the reactor was not shutting down. The natural U outer blanket was next dropped from around the core, which immediately sent the reactor subcritical.

Brittan describes how analysis suggested that reactor power had peaked at around 14 MW_t and fuel temperatures had exceeded 1100°C in the center six rows of fuel pins in an egg-shaped region of the core disposed around the core center. Details of his analysis appear in [4]. Later examination of the Mark II core in the hot cells in Illinois (Figs 2.3 and 2.4) tended to confirm his scenario of events.

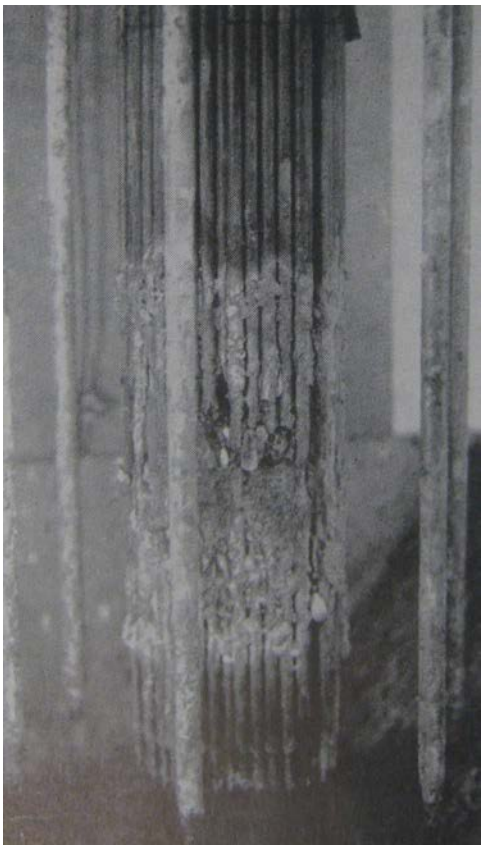

FIG. 2.3. View of EBR Mark II core after removal of outer row of pins.

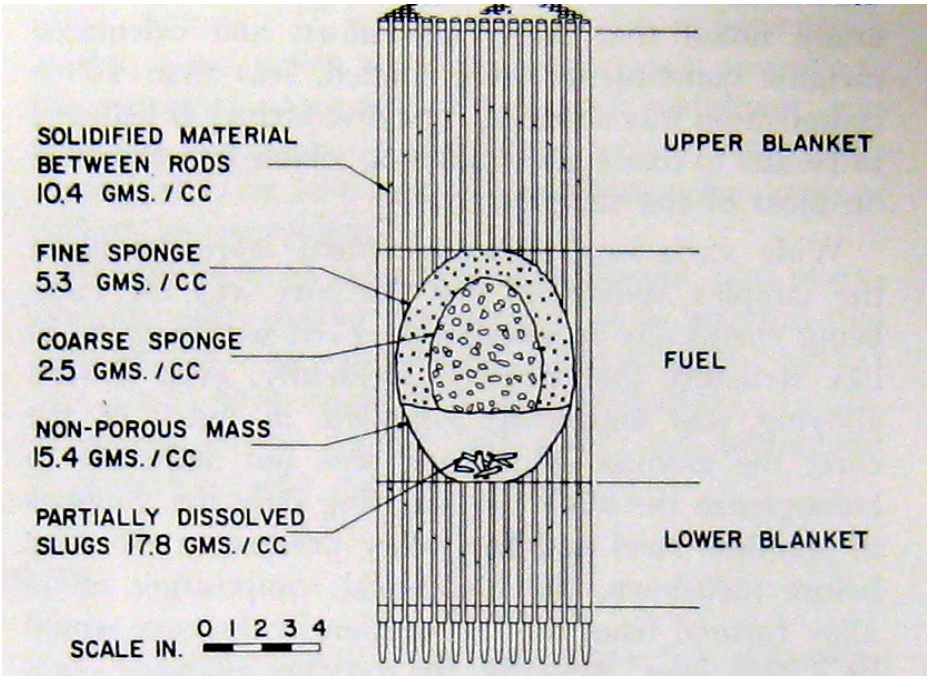

FIG. 2.4. Mapping of core damage from destructive examination.

2.3. BR-10 operating experience

2.3.1. Introduction

In January 1959, the first European experimental sodium cooled fast reactor BR-5 was put into operation at the IPPE in Obninsk. Two reconstructions of the reactor were implemented in 1971-1973 and in 1979-1983. The reactor was called BR-10 after the 1971-73 reconstruction.

At the BR-5/BR-10 reactor, all principal elements of sodium-cooled fast reactor technology were combined in one single facility, which was then successfully operated. Furthermore, nuclear fuel breeding was experimentally proven.

BR-5/BR-10 reactor successfully operated for almost 44 years before being shut down on December 6, 2002. Now BR-10 reactor is undergoing preparation for decommissioning.

2.3.2. Design description

The BR-5/BR-10 facility has a three-circuit loop-type layout of the primary system. The reactor was equipped with wide set of experimental tools - experimental channels and irradiation devices, neutron beams with neutron spectra that covered the range from thermal to fast neutrons. The reactor contained 5 dry instrumented experimental channels. A longitudinal section of the BR-10 reactor is presented in Fig. 2.5.

The main characteristics of the BR-5/BR-10 reactor are presented in Table 2.2 [6].

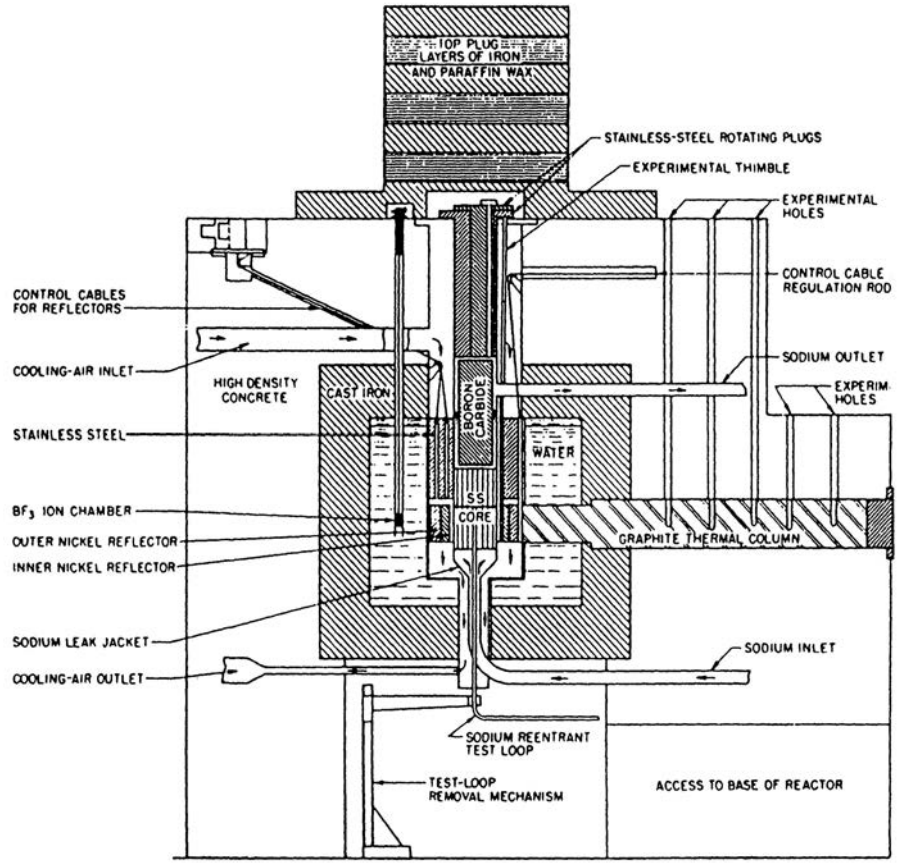

FIG. 2.5. A longitudinal section of the BR-10 reactor.

TABLE 2.2. BR-5/BR-10 MAIN CHARACTERISTICS

Parameter	Value	
	BR-5	BR-10
Overall plan		
Thermal power, MW	5	8
Number of heat removal loops	2	2
Primary circuit		
Coolant	Sodium	Sodium
Coolant temperature, °C		
Core inlet	430	350
Core outlet	500	470
Reactor core		
Maximum fast neutron flux density, $n \cdot cm^{-2} \cdot s^{-1}$	8.0×10^{14}	8.4×10^{14}
Fuel	PuO_2; UC	PuO_2; UN
Enrichment with fission material, %	90	90
Number of cells in the reactor	86-90	86-90
Secondary circuit		
Coolant	NaK	Sodium
Coolant temperature, °C		
AHX outlet	380	270
AHX inlet	450	370
Tertiary circuit		
Heat sink medium	Air	Air

2.3.3. Operating experience

As it was mentioned above, during BR-5/BR-10 operation two modifications of the reactor were carried out in 1971–1973 and in 1979-1983.

The modification project completed in 1973 had planned to increase the reactor power up to 10 MW. However, the reactor power was limited to 8 MW due to some problems in the reactor vessel air cooling system [7]. This reconstruction covered the following upgrading and modifications:

- Mechanical circulating pumps were replaced with electromagnetic pumps;
- The primary coolant was replaced;
- The secondary circuit sodium-potassium alloy was replaced with sodium;
- UC fuel was replaced with plutonium dioxide;
- An additional pair of air-sodium heat-exchangers was installed in the secondary circuit loops.

Before this reconstruction, high carbon content was observed in the sodium (40-170 ppm) due to its high content in the initial sodium, and ingress of lubricant from the lower bearings of the centrifugal pumps. Due to these measures, the carbon content in the sodium was decreased to 5-35 ppm. In the course of the second overhaul of the reactor, the following main procedures were performed:

- Replacement of reactor vessel with compensating cylinder because of high neutron fluence;
- Turning from plutonium dioxide to uranium mononitride UN;
- Installation of safety jackets on all main and auxiliary pipelines of the primary circuit from reactor vessel to shut-off valves;
- Replacement of lyre-shaped sections (adopting thermal expansion) of the main primary pipelines by bellows;
- Increase of reliability of normal and emergency power supply systems of the primary pumps and other measures increasing reactor safety.

As a result of the second reactor modification, unique experience has been gained in dismantling and replacement of such large size components as reactor vessels.

2.3.3.1. Core

In terms of the core state and fuel type used, the following 6 stages of BR-5/BR-10 reactor operation can be distinguished [6]:

1959–1964:	Plutonium dioxide fuel, reactor power of 5 MW;
1964–1971:	Uranium monocarbide fuel, reactor power of 5 MW;
1973–1979:	Plutonium dioxide fuel, reactor power of 8 MW;
1983–2002:	Uranium mononitride fuel, reactor power of 8 MW;
2003:	Core fuel unloaded, reactor shut down;
since 2004:	Dummy fuel assemblies in the core.

The capability of achieving significant burnup fractions was justified for various fuel compositions. The maximum burnup levels achieved for various fuel types are as follows: 14.1% h.a. - for plutonium dioxide, 6.1% h.a. - for uranium monocarbide, 9% h.a. - for uranium mononitride. For about 19 years, the core was operated with advanced nitride fuel.

Significant experience has been gained in reactor operation with failed fuel pins including fuel pins with artificial defects.

A system for on-line fuel pin cladding tightness monitoring was developed and adjusted in the BR-5/BR-10 reactor. Its operation was based on detection of delayed neutrons in the coolant. In addition there was periodical monitoring of gaseous fission product activity (xenon and krypton) in the cover gas of primary pump tanks. One of the significant results of the BR-10 operational experience is the substantiation of fuel pin design.

2.3.3.2. Sodium equipment and pipelines

The following values of operation time and lifetime of the main sodium equipment had been achieved during BR-5/BR-10 operation:

- Reactor vessel – 150 000 h;
- The primary circuit pipelines – 300 000 h;
- Intermediate heat exchangers – 300 000 h;
- Sodium electromagnetic pumps – 170 000 h;
- Air-sodium heat exchangers – 300 000 h.

The reactor vessel (Cr18Ni9Ti steel) replaced in 1980, had been exposed to an extremely high neutron fluence (8×10^{22} n/cm^2) that has not been reached by any other reactor vessel, nor by other non-replaceable in-vessel structures.

2.3.3.3. Coolant technology

Sodium technology, including special aspects related to radioactive sodium, has been mastered. Systems of coolant purification and control of coolant impurities have been developed and adjusted.

Technologies related to the removal of sodium residues after circuit draining, sodium washing-out (steam, steam-gaseous) of inner circuit surfaces and their decontamination had been developed. In the course of reactor operation, the primary circuit was subject to sodium washing-out by steam three times, in 1961, 1971 and 1980. Besides, both loops of the primary circuit underwent acid decontamination in 1961 and 1971.

2.3.3.4. Sodium leaks

The total number of sodium leaks that occurred in the BR-5/BR-10 reactor during its operation is 19. All the sodium leaks actually happened at the early stage of reactor operation, during the period when the sodium technology was being mastered and various equipment design solutions were being developed. There were no sodium leaks since 1986.

These leaks were caused by the following reasons [7]:

- Burn-through of the pipeline wall by electric heaters — 2 leaks
- Failures of level indicators in the pump vessels — 6 leaks
- Failures of sodium valves — 7 leaks
- Wrong sequence of procedures of heating pipeline with frozen sodium — 2 leaks
- Manufacture defect — 1 leak
- Crack in the pipeline wall — 1 leak

None of the leaks resulted in a radioactivity release exceeding allowable limits.

2.3.3.5.Additional areas of BR-10 application

Production of isotopes ^{32}P, ^{33}P, ^{35}S and ^{89}Sr by (n-p) reaction, ^{127}Xe, ^{131}I and ^{198}Au by (n-γ) reaction; ^{99}Mo by (n-f) reaction, etc. has been organized.

Treatment of cancer patients by using a fast neutron beam has been developed and about 500 patients have been treated.

A special device has been designed and constructed for the production of membranes having sterilization properties (pore diameter ranging from 0.5 μm to 5 μm, pores density 10^6 to 10^9 cm^{-2}). In this device, lavsan film was irradiated by the fission products in thermal neutron beam.

2.3.4. Experimental researches

A significant number of experimental studies were carried out at the BR-5/BR-10 during its operation:

- Tests of various fuel compositions (plutonium dioxide, uranium monocarbide and mononitride) and studies of burnup effect on the fuel characteristics;
- In-pile tests of various structural, moderating and absorbing materials and investigation of their behavior under neutron irradiation;
- Series of tests of core operation with failed fuel pins having artificial defects;
- Testing reactor passive shutdown system with hydraulically suspended absorbing rods;
- Studies of mass transfer and distribution of various impurities and nuclides (manganese, cesium, etc.) in the primary circuit;
- Development of the methods of monitoring the activity of fission and corrosion products in the coolant and on the primary pipeline walls;
- Study of corrosion impact of sodium on primary and secondary structural materials (stainless steel, X18H10T) that were being located in sodium from 49 000 hours to 210 000 hours at the temperature range of 300-450°C.

No significant corrosion of materials in the sodium circuits occurred during 40 years of operation, so it was possible to continue operation of the BR-10 reactor circuits (this study and laboratory tests of structural materials at 500°C had shown that the circuit components made of similar stainless steels can be used in sodium for 60 years without worsening of their properties due to corrosion in sodium, under the condition that the appropriate oxygen content in sodium is maintained).

2.3.5. Work on preparation for decommissioning

Now the BR-10 reactor is in the preparatory stage for its decommissioning. For the first time in Russia, technologies related to decommissioning sodium cooled fast reactors are under development; related experience is being accumulated.

Current status of the BR-10 reactor is as follows [8, 9]:

- All FSA have been unloaded from the core and replaced by the dummy subassemblies;
- All FSA of two core loadings with nitride fuel and part of FSA with UO_2 have been washed off sodium and placed in long-term storage;
- Sodium has been drained from the primary and secondary circuits to the storage tanks and frozen;

- The inner surfaces of the primary circuit have been cleaned from sodium and decontaminated;
- Both loops of the secondary circuit and inter-circuit heat exchanger of the central loop have been cleaned from sodium.

The plan of the BR-10 decommissioning has been developed. For its substantiation, experiments on the feasibility of various methods and technologies related to the treatment and conditioning of different reactor components have been conducted:

- Special facilities have been constructed for developing technology of conversion of sodium and NaK wastes into the safe condition by solid phase oxidation (SPO) method and appropriate studies are implemented;
- Technology of conversion of cold traps of the primary and secondary circuits and Caesium traps into the safe condition has been developed;
- Studies on alternative methods of cleaning pipelines and equipment from non-drained sodium residues by using nitrous oxide (N_2O) and conditioning radwaste of sodium-potassium coolant by water-vacuum method are carried out.

2.3.6. Conclusion

The test fast reactor BR-5/BR-10 was the first sodium cooled fast reactor in the USSR and Europe. It also has the longest period of operation among SFRs (almost 44 years).

The BR-10 reactor, together with the research work which has been carried out at this reactor was the pioneer in USSR and have made significant contributions to SFR technology worldwide. At the BR-5/BR-10, the first practical experience of sodium cooled fast reactor operation was gained, the possibility of fuel breeding in a SFR was confirmed, and sodium coolant technology was mastered. It provided a basis of SFR technology that was realized in BOR-60, BN-350 and BN-600 facilities subsequently.

Now the BR-10 reactor represents an experimental base for development of SFR decommissioning technologies.

2.4. Enrico Fermi Fast Breeder Reactor operating experience

2.4.1. History

The Enrico Fermi Fast Breeder Reactor (EFFBR) came about from the early conviction that nuclear power should be developed by industry as well as by the federal government. The AEC authorized industrial participation in 1951 and a consortium - Atomic Power Development Associates (APDA), led by the Dow Chemical and Detroit Edison Companies - chose a sodium-cooled successor to the EBR. A 200 MW_t loop-type design was developed rapidly and was approved by the AEC in 1955. Site preparation started in 1956, wet criticality was achieved in 1963, and operation at 100 MW_t began in July 1966. Figure 2.6 shows an aerial view of the EFFBR site.

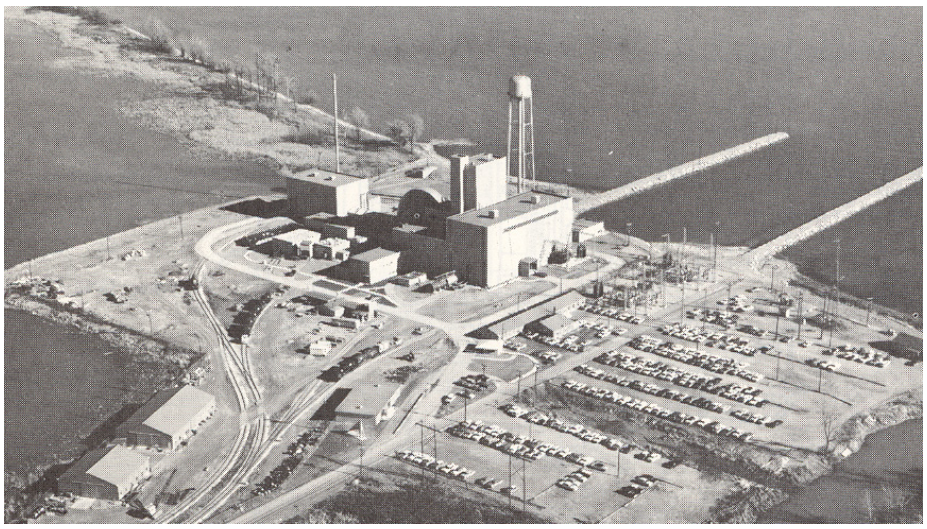

FIG. 2.6. Aerial view of the EFFBR site on Lake Erie 40 km NE of Toledo, Ohio.

The arc-cast U-10% Mo fuel was metallurgically bonded to Zr cladding by co-extrusion. Zirconium was used instead of steel out of fear of forming the U-Fe eutectic during an accident. A 12×12 array of 4-mm diameter pins was held in a 67.2-mm square steel duct, with corner pins replaced by steel rods. This inefficient square design was unique and was a hangover from when plates were being considered as the fuel form.

During final startup for 200 MW_t on October 5, 1966, a reactivity anomaly was detected at 34 MW_t and high outlet temperatures were measured over four assemblies. A fission-gas monitor showed large increases in activity so EFFBR was scrammed. A four-year recovery operation revealed that sodium flow to the assemblies had been partially blocked by one of six baffle plates around the nozzle of the inlet plenum. The plate had come adrift and lodged over the inlets to the four assemblies[1]; two of the assemblies were later found to exhibit fuel that had melted in-reactor.

After many reviews of the reactor safety systems and removal of the five other baffle plates, core reloading began in May 1970. Although oxide was considered as a new reload fuel, there were insufficient funds and the core was reloaded with the U-10% Mo fuel. Full power operation at 200 MW_t was reached uneventfully in October 1970. However the cost had been very high and two more short runs only were made at full power before EFFBR was shut down permanently in 1972 for purely financial reasons.

Decommissioning (mainly concerned with the disposal of fuel and sodium) began in January 1973 and was completed by November 1975 at a total cost of $6.9M. U-Mo fuel cut from the middle of core assemblies under water was packaged into casks and trucked to the Savannah River Project. Blanket assemblies and cut blanket sections were sent to the Idaho Chemical Processing Plant. Non-radioactive sodium was drained from the secondary system, loaded into 55-gallon drums and shipped to a West Virginia company for conversion into sodium methylate. Radioactive primary sodium was also loaded in 55-gallon drums and stored on-site

[1] The zirconium baffle plates were added to remove heat in the case of core melting and slumping in an accident — ironically, a feature added to improve safety in one area had caused problems in another.

for use by the Clinch River Project; it was eventually sent to Idaho for passivation along with the inventory of primary sodium from EBR-II.

Although EFFBR operating experience had been limited, much was learned about fast reactors, e.g., the compatibility of sodium with steels (excellent); the design, testing, maintenance and decommissioning of sodium systems and components; and inspection and removal techniques for in-core components. The total experience accumulated at the EFFBR was fully described by Alexanderson and others at APDA in 1979 [10].

2.4.2. Design description

The EFFBR was a three-loop sodium-cooled reactor with a rated power of 200 MW_t and generating ~ 60 MW_e. Cold-leg mechanical pumps were used to give nominal primary sodium inlet and outlet temperatures of 287 and 427°C for sodium flow rates of 1120 kg/s. The core contained 465 kg ^{235}U in the form of U-10%Mo fuel that contained 25.6% ^{235}U. A perspective view of the reactor is shown in Fig. 2.7.

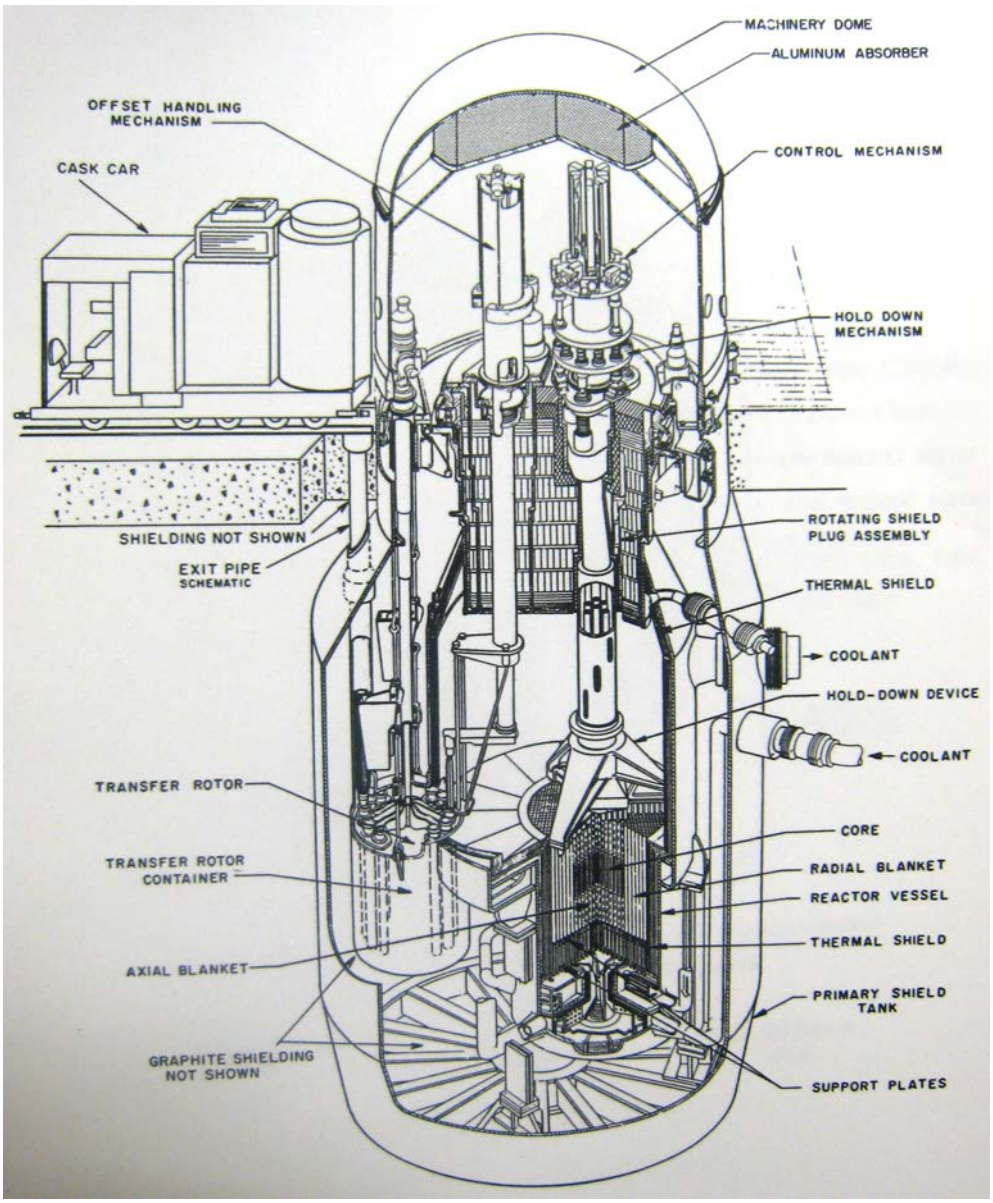

FIG. 2.7. Perspective view of the EFFBR.

Since the EFFBR was the first large fast reactor, the high decay heat of discharged fuel was an issue that had to be addressed during design. The method chosen was to place the discharged assemblies in finned pots where heat could be removed by radiation and convection, without recourse to forced cooling.

It was also recognized that large rotating plugs might be difficult to design for accuracy of positioning and sealing. Instead of having two rotating plugs (one within the other) as was later used at the smaller EBR-II, a single rotating plug and an offset fuel-handling mechanism were used to limit the overall size of the plug. Amorosi observed [11] that:

"Some 1000 fuel unloadings were accomplished with excellent performance. The rotating plug and offset handling mechanism, transfer rotor, and closure seal operated for over 10 years without replacement. Monitoring methods were developed to check out the position of the offset handling mechanism head and were used to assure its engagement with the proper [sub]assembly."

2.4.3. The fuel melting incident

As the former APDA engineer Page wrote [12], "the single event of greatest impact on the Fermi Project in terms of publicity, cost and schedule was the fuel melting incident that occurred 5 October 1966." The incident unfolded in the following way [13].

After successful completion of low-power test runs in 1965, the approach to 200 MW_t was to be carried out in discrete steps with appropriate measurements to ensure EFFBR behaved as expected. The approach included 53 hours at 100 MW_t in August 1966. During this run, thermocouple readings ~ 20°C higher than normal were noted over two core assemblies and a lower-than-expected value over another assembly. Because the elevated values were below the normal outlet temperature of the hottest assembly, these deviations were no cause for concern at the time.

On 5 October, it was planned to bring the reactor to 74 MW_t (a power already surpassed several times) in order to check two-loop operation and maybe to shed light on the cause of the anomalous thermocouple readings. Power was controlled manually up to 8 MW_t; after a brief hold the reactor was put onto automatic control for further increase. The meter recording the rate of change in power gave erratic signals and at 30 MW_t it was noted that the two operating control rods were withdrawn further than normal, which indicated some negative reactivity, one possibility being higher than expected heating.

Power was levelled at 34 MW_t at 15:05 when elevated temperatures were noted over two assemblies. These thermocouple readings were being studied at 15:09 when radiation monitors in the reactor building ventilation exhaust ducts alarmed, causing isolation of the containment. Power was reduced immediately, followed by manual scram at 15:20.

Later it was found that a fission product detector, which sampled the reactor cover gas, was being calibrated during the power rise on 5th October . The 3-minute cover-gas samples taken between 14:58 and 15:01 exhibited a 500-fold increase in activity for a power increase of only a few percent. As the EFFBR fuel burnup was low, this could only mean that melting of some U-Mo fuel had occurred in-reactor.

The search for melted fuel began by adding a device to the offset handling mechanism (OHM), which gauged the pulling force, required to lift an assembly. It was found that very

high OHM forces were required in the area of the two assemblies that had exhibited elevated exit temperatures. Finally, two assemblies - M-098 and M-127 - were found to be stuck together and could not be retrieved. By this time (March 1966), decay heat of the low burnup fuel was sufficiently low to allow primary sodium to be siphoned off to below the core support plate so that assemblies could be viewed directly.

A boroscope inspection revealed the two assemblies were stuck together over a limited area 250 mm below core midplane. A special wedge tool was devised to separate the two assemblies and allow discharge. Figure 2.8 shows the surface condition of the two assemblies when viewed in the hot cell. A later transverse section of assembly M-127 revealed local melting and destruction of the center sections of about 35 fuel pins.

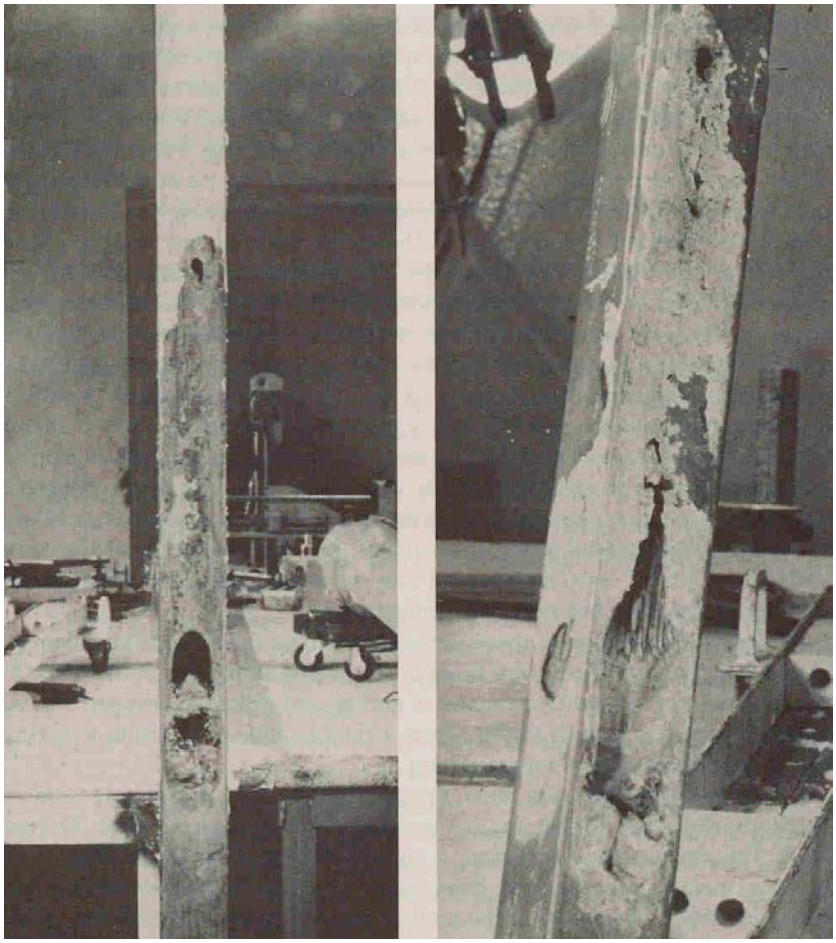

FIG. 2.8. External appearance of damaged EFFBR assemblies: M-098 (left) and M-127 (right).

The next objective was to find the cause of overheating. The melted condition of the assemblies suggested a foreign object might have led to local blockage of sodium flow. The hunt was then joined to find any such object. To aid in the search, the primary sodium was further drained in August 1967 down to the level of the lower plenum of the reactor, which presumably would be the point of entry. Indeed on the first sweep of the lower plenum, a boroscope revealed the object shown in the top photo in Fig. 2.9. It looked like a crumpled piece of folded metal and was quickly identified as one of six Zr baffle plates that had been added as a last-minute safety device around the nozzle in the high-pressure plenum region. Evaluation of the incident suggested that the cause for the baffle plate becoming detached

might have been the use of attachment screws that had an incorrect thermal expansion in-reactor so that the plate loosened at operating temperature.

Retrieval of the Zr baffle plate was time-consuming and arduous and was referred to as ‘deep reactor surgery’ in Alexanderson’s book, where it is well described. The bottom photo in Fig. 2.9 shows the offending baffle plate.

(a)

(b)

FIG. 2.9. View of Zr baffle plate in the reactor lower plenum (a); after retrieval and identification (b).

The EFFBR incident had an indelible effect on fast reactor safety in the USA and elsewhere. Overnight it created the fear of a ‘local fault’ in an LMR fuel assembly, which came to dominate thinking in the 1970s of how fast-reactor accidents might be initiated by real events. It certainly led to re-evaluation of the design of lower grid plates and sodium inlet orifices of assemblies to preclude the possibility of the starvation of sodium flow. It also led to an insistence on rigorous review of design changes, a vital component of quality assurance.

2.5. Experimental Breeder Reactor-II operating experience

2.5.1. History

The Experimental Breeder Reactor No. 2 (EBR-II) was designed and operated at the Idaho National Reactor Testing Site by Argonne National Laboratory for the US Department of Energy and its predecessor agencies. It was designed and constructed in the late 1950's to early 1960's, and began operation as a demonstration liquid-metal-cooled fast reactor power plant in 1964. EBR-II was used initially to demonstrate a closed fuel cycle for uranium alloy fuel, a task completed by 1969 [14]. Over the next 25 years it served as a versatile irradiation facility for LMR fuels and materials, and for safety experiments to study decay heat removal in sodium-cooled reactors [15, 16]. The operation of LMR fuels in the mild transient overpower (TOP) and run-beyond-cladding-breach (RBCB) modes were also extensively studied [17, 18].

Over 1984-94, EBR-II was a test bed for the Integral Fast Reactor (IFR) concept [19], using uranium-plutonium alloy fuel. Finally the reactor was used for initial tests of actinide burning. The reactor was shut down permanently in 1994 due to the termination of the DOE fast reactor development programme; it was defueled, drained of primary and secondary sodium, and put into a radiologically safe condition (SAFSTORE) by 2002.

EBR-II was a complete power plant generating 62.5 MW of thermal power with a steam-generating system and a turbine generator producing about 19 MW of electrical power. About 5 MW_e was used for site load and the balance was put on the grid for revenue generation. Operating experience of EBR-II over its 30-year lifetime provided valuable experience in the operation and maintenance of a pool-type sodium-cooled reactor. Milestones in the history of EBR-II are given in Table 2.3.

TABLE 2.3. MILESTONES IN EBR-II HISTORY

Milestone	Date
Start of construction	11-1956
'Wet' criticality	11-1963
First electricity to grid	08-1964
45 MW_t operation	03-1965
First experimental fuel test	05-1965
62.5 MW_t operation	09-1970
Steel reflector installed	06-1972
First decay heat removal test	03-1975
First RBCB test	02-1977
First IFR fuels test	12-1984
First actinide burning test	03-1992
Permanent shutdown	09-1994
Defueling complete	12-1996
Secondary Na disposed	04-1998
Primary Na disposed	05-1999
SAFSTORE achieved	03-2002

2.5.2. Design description

EBR-II was a conservatively designed, hybrid pool-type reactor with the reactor vessel and primary cooling system components submerged at the bottom of a primary vessel containing 329 m^3 of sodium. An argon cover gas was maintained over the surface of the sodium in the primary vessel to minimize the opportunity for air to contact the sodium. The primary cooling system consisted of two mechanical centrifugal pumps operated in parallel and pumping a total of 480 kg/s of sodium through the reactor at a pump discharge pressure of 0.39 MPa. The pumps took suction directly from the bulk sodium pool maintained at 371°C. The discharge from the pumps was piped into the bottom of the grid plenum assembly supporting the core. The flow from each pump was split into two flow streams to distribute coolant between the core driver fuel assemblies and the blanket/reflector section of the reactor. Figure 2.10 shows the layout of the primary vessel and primary components.

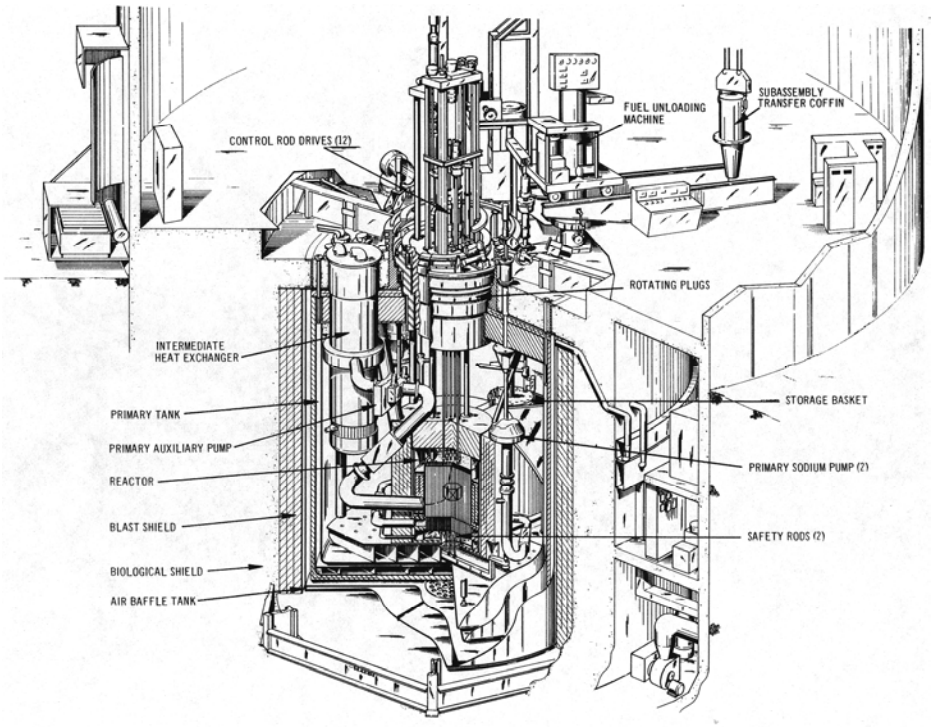

FIG. 2.10. Layout of the primary vessel and primary components of EBR-II.

The reactor vessel contained 637 hexagonal assemblies - 53 driver fuel assemblies, 60 inner and 510 outer blanket assemblies, plus 12 control rods and 2 safety rods. Eight high-worth control rods were later installed, allowing four control-rod positions to be used for four instrumented facilities, such as the breached-fuel test facility [20]. The top structure of the primary vessel consisted of two rotating plugs for fuel handling and supported twelve control rod drives in addition to the fuel handling components. To maintain a seal over the primary vessel cover gas, the rotating plugs employed a liquid Sn-Bi eutectic alloy in a circumferential trough at the periphery of each plug. A vertical blade attached to each rotating plug served as a “dip ring” submerged part way into each trough. This dip ring would travel in the alloy during plug rotation to maintain a liquid seal with cover gas on one side of the dip ring, and the reactor building air atmosphere on the other side.

Fuel assemblies were handled remotely under sodium. Irradiated assemblies were transferred to a storage rack along side the reactor vessel in the primary vessel sodium to allow for decay heat removal via convective cooling of the assembly prior to its removal from the primary vessel. In a similar manner, fresh fuel assemblies could be loaded into the storage rack in the primary vessel during reactor operation to stage them for loading into the reactor core when the reactor was shutdown for refueling. This fuel assembly staging system increased the operating efficiency of the reactor.

The sodium coolant exited the core at 473°C and flowed from the upper plenum of the reactor vessel to the intermediate heat exchanger (IHX). The IHX transferred heat from the nuclear-heated primary sodium to the secondary sodium in the intermediate loop. Primary sodium was then discharged from the IHX back into the sodium pool in the primary vessel. The IHX was a counter-flow shell and tube unit designed to be removable and replaceable, although this was never required. The primary sodium never left the primary vessel except for small sampling and purification streams that were pumped from the top of the primary vessel into shielded cells, then returned to the vessel. After initial sodium fill of the primary vessel in the early 1960's, the primary sodium was not drained from the vessel until after final shutdown of the reactor.

Figure 2.11 shows a schematic view of the EBR-II primary coolant system.

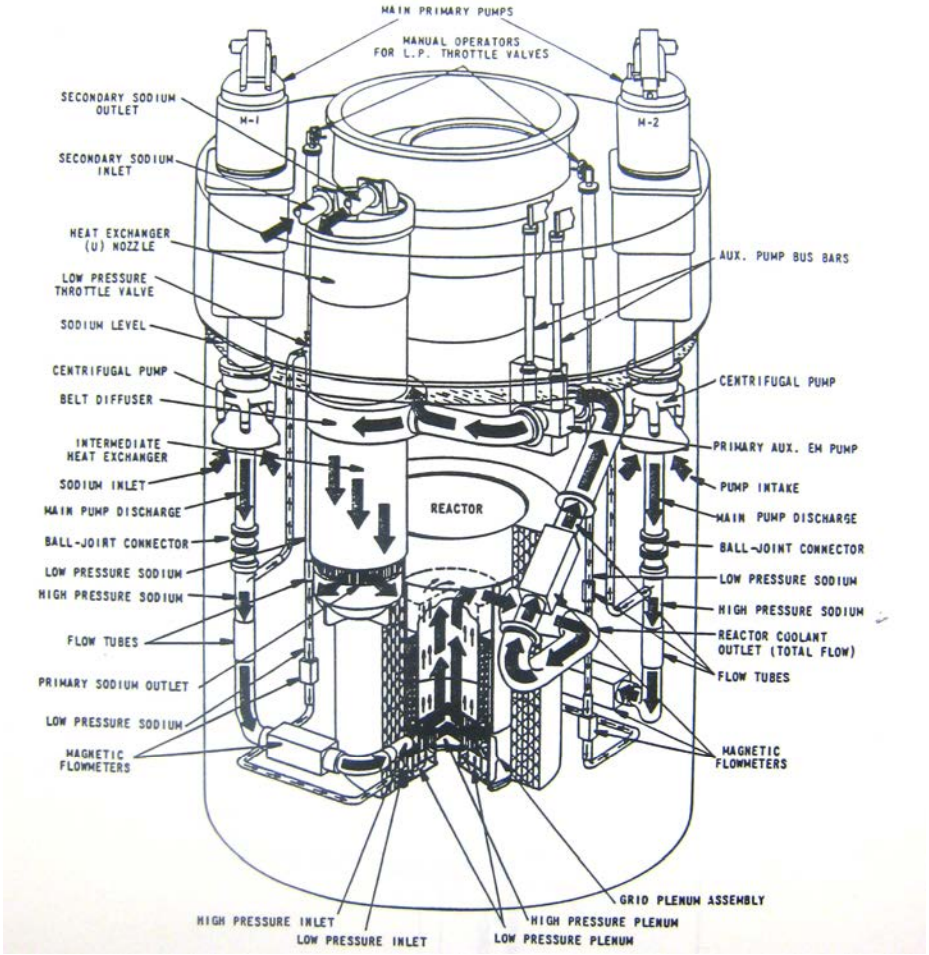

FIG. 2.11. EBR-II primary coolant system.

Secondary sodium was pumped from the IHX in the reactor building to the sodium boiler building where it passed through a series of superheaters and evaporators to create superheated steam. The secondary sodium pump was an electromagnetic pump located in the sodium boiler building. The secondary sodium system had its own sampling and purification system and had a storage tank sized to hold the entire volume of secondary sodium. Unlike the primary system, the secondary system could be drained of sodium for maintenance purposes.

The steam generating system consisted of two superheaters and initially eight evaporators (one evaporator was removed mid-life and converted to a superheater). Superheated steam from the steam generating system was piped from the sodium boiler building to the turbine generator in the power plant for electrical power production. The steam generator units were a conventional single pass, counter-flow shell and tube design, but with unique double-wall tubes that minimized the potential for sodium to come into contact with water or steam.

2.5.3. Operating experience

EBR-II operated quite reliably over its lifetime. The lifetime plant capacity factor was 57.6% including both the learning curve of the early operational years, and the last few years of operation when the plant operated at reduced capacity due to a shift in priorities of the US DOE. During its mid-life period from ~ 1976 to 1990, EBR-II consistently achieved annual capacity factors exceeding 70% with a high of 81% in 1987 [21]. This performance was notable, considering that EBR-II was a first-of-a-kind facility with test programmes that were often aggressive in nature.

A highlight of EBR-II operations was the successful completion of a series of tests that demonstrated the passive safety characteristics of this type of plant [16]. In April 1986 the final two tests in this series were performed to demonstrate safe response to severe accident scenarios. The scenarios studied were a loss-of-flow without scram and a loss-of-heat-sink without scram test. With no operator or engineering system intervention, in both tests (performed the same day) the plant responded in a benign manner ultimately reaching a steady state low power level with no adverse effects on the fuel or reactor structures. Furthermore, following plant restart to normal operating conditions, the driver fuel elements were taken to their qualified burnup level with no fuel failures. These tests demonstrated conclusively the passive response of this type of reactor system to significant upsets, and the robustness of the fuel and reactor systems.

The steam generators never experienced a sodium-to-water or sodium-to-steam leak, which differed from the typical experience with sodium-cooled power plants world-wide. The excellent performance of the EBR-II units was attributed to the robust duplex tube design of both the superheaters and evaporators. One superheater did experience a reduction in heat transfer efficiency, traced to relaxation of the pre-stress between the duplex tubes [22]. This unit was replaced with a modified evaporator and the steam generators experienced no other significant problems over the life of the plant.

Although the plant operated for thirty years it was in excellent condition at the time of final shutdown in 1994. Plant life extension and aging studies had indicated a probable lifetime of at least 50 years. Examination of the interior of the primary vessel following sodium drain showed the sodium-wetted surfaces to appear like new.

2.5.4. Maintenance experience

In addition to routine maintenance of both sodium and non-sodium systems, and of radiologically contaminated and clean systems, significant maintenance events associated with the reactor sodium systems included the following:

- Removal from the primary tank and refurbishment and re-installation of both primary sodium pumps (twice);
- Removal, replacement of the in-vessel transfer arm;
- Removal, replacement of control rod drive mechanisms (multiple times);
- Removal and repair of the core fuel handling gripper mechanism;
- Remote location and retrieval of a fuel assembly that was dropped onto the top of the core from the fuel transfer arm;
- Remote characterization and retrieval of a damaged fuel assembly in the fuel storage rack in the primary vessel [22];
- Retrieval of a damaged neutron source rod from the reactor vessel;
- Removal of a superheater from service due to long-term performance degradation, and replacement with an evaporator removed from service and modified to perform as a superheater [23];
- A sodium leak in a secondary sodium (non-radioactive) sampling line caused a fire in the sodium boiler building in the late 1960's. The leak was caused by a faulty welding procedure during maintenance activities. Damage was contained within the sodium boiler building, no injuries occurred, and there was no radiological release. The reactor was shutdown at the time of the incident. Several weeks were required for repair and recovery of the system. The maintenance procedures for working on sodium systems were changed to avoid similar problems following that incident.

A chronic maintenance problem at EBR-II was "sticking" of the rotating shield plugs during fuel handling. To install or remove a fuel assembly from the reactor, the two rotating plugs that provided top closure of the primary vessel were rotated to specific angular coordinates to place the fuel-handling gripper mechanism directly over any of the 637 assembly positions in the reactor. The rotating plugs used a liquid metallic alloy in a circumferential trough at the periphery of each plug to maintain a seal over the primary vessel cover gas. A blade on each plug served as a "dip ring" submerged part way into each trough. This dip ring would travel in the alloy during rotation to maintain a liquid seal, with cover gas on one side and reactor building air on the other. The alloy, a Sn-Bi eutectic, would become contaminated with oxide formation on the air side and with sodium aerosols from the reactor side, and form compounds which would inhibit rotation of the plugs.

The typical solution to this problem was to manually clean the surface of the seal alloy. The seal cleaning was very difficult due to very limited accessibility of the alloy in the troughs, but was usually effective in reducing sticking during rotation. However, the problem continued to worsen over the years until a system was developed for routine surveillance of the surface of the seal alloy using remote video technology to locate specific problem areas where contaminates accumulated, thus making seal cleaning more effective. For future designs, options to effectively eliminate this problem are available, e.g. inflatable seals.

In summary, the problem with the rotating plug seals was the only chronic maintenance or operational problem that had an ongoing negative impact on plant performance over much of the life of EBR-II. The experience with other plant systems and components was remarkably

good for a first-of-a-kind facility, and demonstrated that a pool-type sodium cooled fast reactor can be reliably operated and maintained over a significant operational lifetime.

The performance of EBR-II as a power producing fast reactor demonstration, test, and irradiation facility over its thirty years of operation was a good example of the potential of the technology. The experience base of EBR-II provides a valuable source of lessons learned that could be used to great advantage when developing the next generation of liquid-metal-cooled fast reactors.

2.6. Rapsodie operating experience

2.6.1. Introduction

The Rapsodie experimental reactor, the first French fast neutron reactor constructed and operated by the Commissariat à l'Énergie Atomique (CEA) at its Cadarache Centre, went critical on 28 January 1967 and was definitively shut down in April 1983. Rapsodie was designed, built and operated to obtain data on the physical behaviour of a fast neutron reactor under static and dynamic conditions, to offer information of direct use for the design of future liquid metal reactors, and to supply a fast neutron flux for irradiation tests of fuels and materials. During its 16 years of operation, more than 30 000 fuel pins of the driver core were irradiated, of which about 10 000 attained a burnup beyond 10%, 300 irradiation experiments were conducted and more than 1000 tests were performed.

The decision to stop operating the reactor was made after two successive defects were detected in the primary system containment. Before the final shutdown of the reactor, a series of end-of-life tests were conducted in April 1983. Pre-decommissioning operations were then conducted until 1986 and partial dismantling commenced in 1987, following the decision by the CEA to abandon, for budgetary reasons, a proposed Rapsodie appraisal programme. Presently, the remaining structures of the Rapsodie complex are being dismantled [69].

2.6.2. Design description

Rapsodie was a sodium-cooled, loop-type experimental fast neutron reactor, from which heat was removed by sodium-air heat exchangers; the reactor was not coupled to a turbine generator. The reactor vessel, its upper enclosures and the two primary loops, each equipped with a mechanical pump and an intermediate heat exchanger, were located within the reactor building (Fig. 2.12) and enclosed in Sercoter (a high density, rare earth oxide bearing) concrete cells to provide radiation shielding (Fig. 2.13). The secondary, non-radioactive sodium was piped to a conventional building containing the components of the two secondary loops comprising one sodium/air heat exchanger each. All the circuits and components were made of austenitic stainless steel, the main pipes and vessels having a double wall.

The reactor was initially operated at 24 MW_{th} and then, in 1970, at 40 MW_{th} after the modifications of the Fortissimo project were completed, the purpose of which was to enhance the experimental possibilities for the reactor.

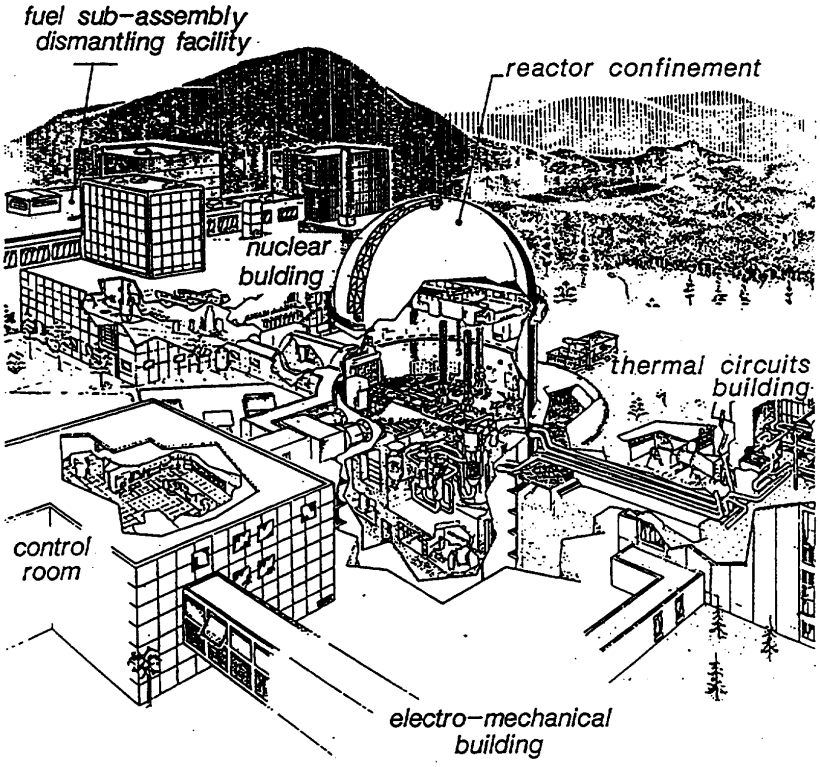

FIG. 2.12. Rapsodie facility.

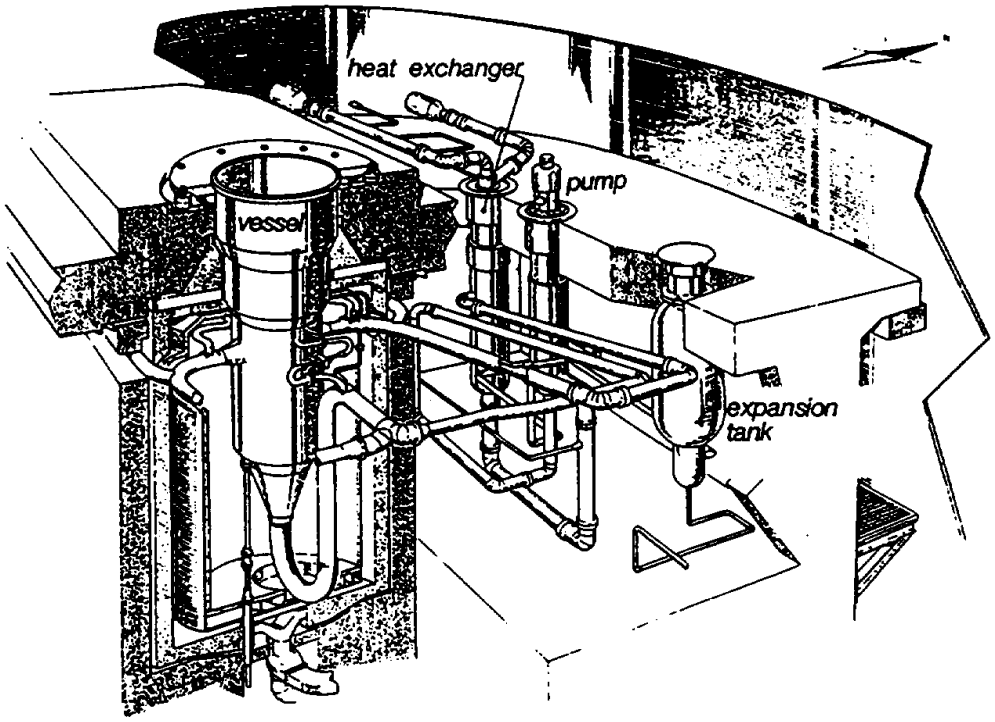

FIG. 2.13. Rapsodie reactor vessel depicted with one primary loop.

Key characteristics for these configurations are specified in Table 2.4.

TABLE 2.4. PRINCIPAL CHARACTERISTICS FOR THE RAPSODIE OPERATING MODES

Item	Value	
	Initial design	Fortissimo
Thermal power, MW	24	40
No. heat removal loops	2	2
Fuel type	PuO_2-UO_2	PuO_2-UO_2
Maximum neutron flux, 10^{15} n·cm^{-2}·s^{-1}	2	3.2
No. fissile assemblies and experimental rigs	64	58
Active core volume, excluding control rods, L	48.5	42.1
Primary coolant	Na	Na
Primary coolant temperature, °C		
Core inlet	405	400
Core outlet	495	510
Primary coolant flow rate, m^3·h^{-1}	890	970
Secondary coolant	Na	Na
Secondary coolant flow rate, m^3·h^{-1}	445	864

In 1980, subsequent to some incidents incurred and anomalies observed during the Fortissimo operation, the operating power of Rapsodie was reduced to 22.4 MW_{th}, which was high enough for irradiation needs but did not cause the defects to manifest. This was the maximum allowed power level until final shutdown of the reactor in 1983.

2.6.3. Operational experience

Over its lifetime, the operation of the Rapsodie reactor yielded 2.1×10^9 kW·h of thermal energy and was characterized by a load factor of ~ 50%.

2.6.3.1. Defects and operation interruptions

A distribution of the events which disrupted operation of the reactor is shown in Table 2.5.

TABLE 2.5. DEFECTS WHICH HAVE IMPACTED RAPSODIE OPERATION

	Defect	No. of occurrences	Time lost (EFPD)
Reactor components	Plugs	13	151
	Rods	50	74
	Fuel	61	261
Devices	Pumps	10	47
	Venting	15	13.5
Circuits	Sodium	10	592
	Gas	9	22.5
Monitoring	Software	101	21.5
	Electrotechnics	38	13
	Electronics	84	52
Systems	Handling	88	46
Total		479	1293.5

Of these, two defects of the primary system were influential in the decision to cease operation of Rapsodie. The first defect, which appeared in 1978, consisted of a sodium micro-leak:

radioactive sodium aerosols were found in the double wall of the reactor vessel. Investigations neither found any liquid sodium in the gap, nor located the defect. The safety authorities subsequently imposed a lower operating power (22.4 MW_{th} or ~ 60% of the nominal power) and, consequently, a lower primary coolant flow rate, which allowed the irradiation programme to continue but did not cause the leak to reappear. The second defect appeared in 1982 and consisted of a small leak from the nitrogen blanket surrounding the primary system. Indications of the unlikelihood to repair the latter within the given time frame and at a reasonable cost eventually led to the decision to shut down the reactor permanently.

2.6.3.2. Rapsodie end-of-life tests [24]

Before the final shutdown of the reactor, a sequence of end-of-life tests was conducted in April 1983. Two series of tests performed on the Rapsodie reactor, the purpose of which was to investigate the serviceability of the Rapsodie core and of the reactor as a whole under extreme conditions that were characterized by an exceedingly high temperature.

The first series of tests to be performed called for an experimental inquiry into the behaviour of fuel elements during fuel melting. Over the course of these tests, the fuel pin linear power observed on two test subassemblies reached 1000-1060 W/cm; i.e. two times greater than that normally used in commercial reactors.

The second series of experiments simulated the most serious accident, which consisted of the shutdown of the primary circuit and secondary circuit pumps, as well as the ternary circuit fans, and the non-operation of the safety rods. Here, reactor output reached 21.2 MW (more than 50% of the rated value), while the mean coolant temperatures at the reactor inlet and outlet came to 402 and 507°C, respectively. A comparison of calculation results and experimental data demonstrated that the fuel residing in the core shared a state of coalescence with the fuel element cladding and expanded with the cladding upon heating-up. It is in such instances precisely that good agreement is reached between the calculation results and the experimental data concerning the coolant temperature at the subassembly outlet.

2.6.4. Decommissioning and dismantling

2.6.4.1. Pre-decommissioning operations (1983 - 1985)

The pre-decommissioning operations include the preliminary actions prior to washing and rinsing the system, which might have otherwise caused corrosion damage. All the standard and experimental fuel assemblies were unloaded from the reactor vessel and stored either in the cooling pond or in a dry well. The fertile assemblies and the control rods were also unloaded and dismantled in a hot cell. Only the reflector assemblies, made of stainless steel or nickel, were left in place in the reactor vessel to be washed along with the vessel itself. At the same time, all the experimental devices were removed from the main vessel while certain components, pumps or IHXs were extracted from their respective vessels for decontamination. These operations were concluded with the blanking-off of all penetrations and vessels. The primary circuit was then drained of its sodium into the usual storage tank, while the storage tank containing the reserve of clean sodium was also emptied. Finally, the primary system was tightly sealed and kept under an inert atmosphere of argon and, later, nitrogen. In addition the secondary circuits were also drained of their sodium and later isolated from the IHXs [24, 70].

2.6.4.2. Decommissioning and partial dismantling (1986 - 1994)

The decommissioning operations involved in the partial dismantling programme were designed to eliminate the radioactivity as much as possible without exposing the operators excessively, to confine the residual radioactivity and, as a result, to minimize monitoring and surveillance measures pending complete dismantling. In the case of Rapsodie, the successive operations were:

- Removal and disposal of the steel and nickel reflector assemblies as waste.
- Washing and decontamination of the primary circuit. Washing was performed via in situ circulation of ethylcarbitol to neutralize the residual sodium, which remained after the primary circuit was drained. Decontamination consisted of cleansing with the alkali sodium hydroxide, rinsing with demineralized water, cleansing again with a sulfonitric acid mixture, rinsing again with demineralized water and finally applying a phosphate passivation solution.
- Dismantling of the primary circuit, of one secondary circuit and of the auxiliary systems of the reactor. Cutting was performed using plasma torches, except in high-risk areas where saws or chain-saws were used instead.
- Completion of the primary and secondary containment of the nuclear island. The first barrier was achieved by separating the reactor vessel from the primary and auxiliary circuits, closing the openings with welded plates and sealing an upper head cap onto the top of the vessel, within which a nitrogen atmosphere was maintained with a slight positive overpressure to prevent corrosion. The second barrier, which comprised the Sercoter concrete and steel liner (with steel housings to cover the holes on the reactor block), was linked to the building ventilation system via high efficiency filters (Figs 2.14 and 2.15).
- Dismantling of the auxiliary equipment used for handling, washing and storing nuclear materials or contaminated components.
- Destruction of the primary sodium and cleaning of the active area. The 37 tonnes of primary sodium were removed by direct transformation into aqueous sodium hydroxide using the NOAH process, for which the DESORA facility was designed and constructed onsite in 1992. Destruction operations lasted 2-3 months at the beginning of 1994, and the generated sodium hydroxide was sent to a COGEMA plant.

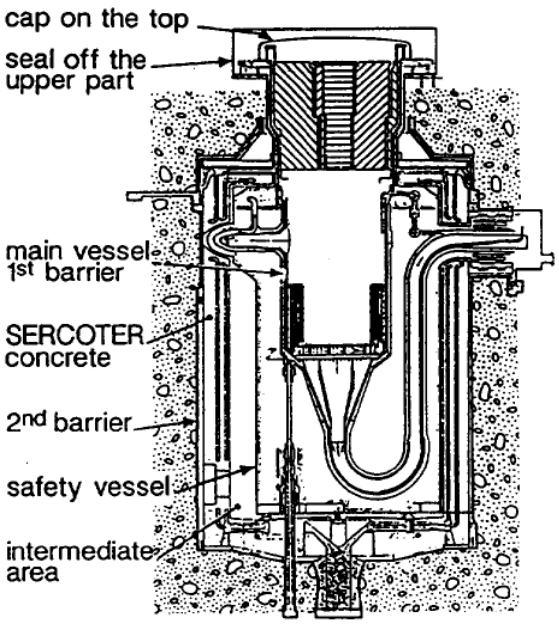

FIG. 2.14. Reactor block with the leak-tight barriers.

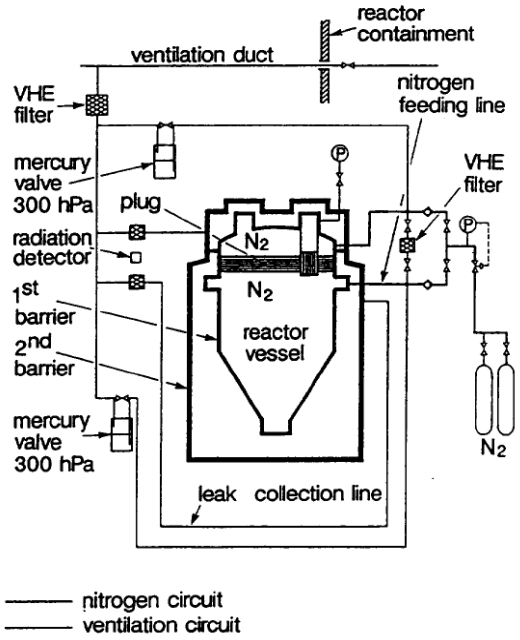

FIG. 2.15. Gas equipment of the two vessel's barriers.

Following the destruction of the primary sodium at the DESORA facility, it was decided to wash the sodium storage tank which had been used to store the sodium awaiting destruction using ethylcarbitol as was done 8 years earlier with the previous sodium storage tank. The amount of sodium left in the tank had been estimated, at that time, at ~ 100 kg. On 31 March 1994, several days after the beginning of this operation, a violent explosion occurred, causing casualties and heavy damage to the gallery. Investigation of the circumstances and possible causes of this accident have not yet been completed.

Low activity waste consisting of technological residues or thermal insulating materials was incinerated or compacted before being transferred to an ANDRA (the French national agency responsible for radioactive waste management) storage centre. Low activity metallic waste, which represented the largest volume, was eventually melted into ingots in a special furnace installed at the CEA's Marcoule Centre. Medium and high activity waste was stored at the Cadarache Centre. The liquid effluent produced by washing and decontaminating operations was transferred to the Liquid Waste Treatment Facility at Cadarache where it was neutralized, concentrated by evaporation and encapsulated in bitumen or cement. Upon completion of partial dismantling, several hundred tonnes of metallic material (steel and lead in particular) were returned to service, primarily in the form of biological radiation shielding.

2.6.4.3. Monitoring period and re-evaluation of the dismantling strategy

Up to the year 2003, the remaining part of the Rapsodie dismantling programme consisted of three steps:

(1) Cleaning operations and partial dismantling continued up to 2008;
(2) Surveillance during the period 2008-2020;
(3) Dismantling operations to be resumed in 2020.

However, in 2004, a new strategy was elaborated, discussed (in terms of cost evaluation, schedule, etc.) and adopted; it consists of two main steps:

- A cleansing period from 2004 to 2008 for the dismantling of auxiliary systems employed in the partial dismantling process. Furthermore, during this period, files were prepared and submitted by end-2007 to the safety authorities in order to obtain the necessary regulatory authorization required to proceed with the full dismantling of the reactor block and cleansing of buildings.
- A dismantling period from 2009 to 2017 for the dismantling of the reactor block and cleansing of the buildings. A regulatory authorization, granted in December 2009, was necessary to perform the dismantling phase.

The reference solution for dismantling of the reactor block involves the carbonation of the remaining primary sodium, specific treatment of two identified retention zones, cleaning of the carbonates using water and underwater dismantling of the internals using specific plasma-cutting and handling tools. After the water is drained, the primary and safety vessels, as well as the building, will be dismantled. The reactor internals, once extracted, will be cut up in a specially designed workshop. All reactor waste will be transported for storage at the waste disposal facilities of ANDRA.

2.6.5. Conclusion

Through the design, construction, operation and dismantling of Rapsodie, a wealth of knowledge and experience in the area of sodium-cooled fast reactors (including reactor physics, thermal hydraulics, fuel, materials and sodium technology) has been acquired and applied to future sodium-cooled fast reactor projects. Now, Rapsodie is in the final stages of dismantling, expected to be complete by the year 2020.

2.7. BOR-60 operating experience

2.7.1. Introduction

The experimental reactor BOR-60 is located at the Research Institute of Atomic Reactors (RIAR) in Dimitrovgrad. First criticality was reached in December 1968, and connection to the grid was in the beginning of 1969. Now the BOR-60 reactor is the only experimental fast reactor in Europe. The main target of the BOR-60 reactor consists in implementation of in-pile tests of various fuel compositions and structural materials; testing and substantiating various sodium equipment (steam generators, cold traps, etc.), sodium coolant technology, reactor control systems; justification of safety of sodium cooled fast reactors, etc.

2.7.2. Design description

The main technical parameters of the BOR-60 reactor are presented in Table 2.6 [25].

The reactor facility (RF) has a conventional three-circuit loop-type layout of the primary system. Sodium coolant in the primary and secondary circuits transfers heat from reactor through SG to the tertiary steam-water circuit and/or through "air-sodium" heat exchangers to outside air. RF BOR-60 consists of two loops of the primary and secondary circuits. A longitudinal section of the BOR-60 reactor is presented in Fig. 2.16 a general scheme of the BOR-60 reactor facility is shown in Fig. 2.17.

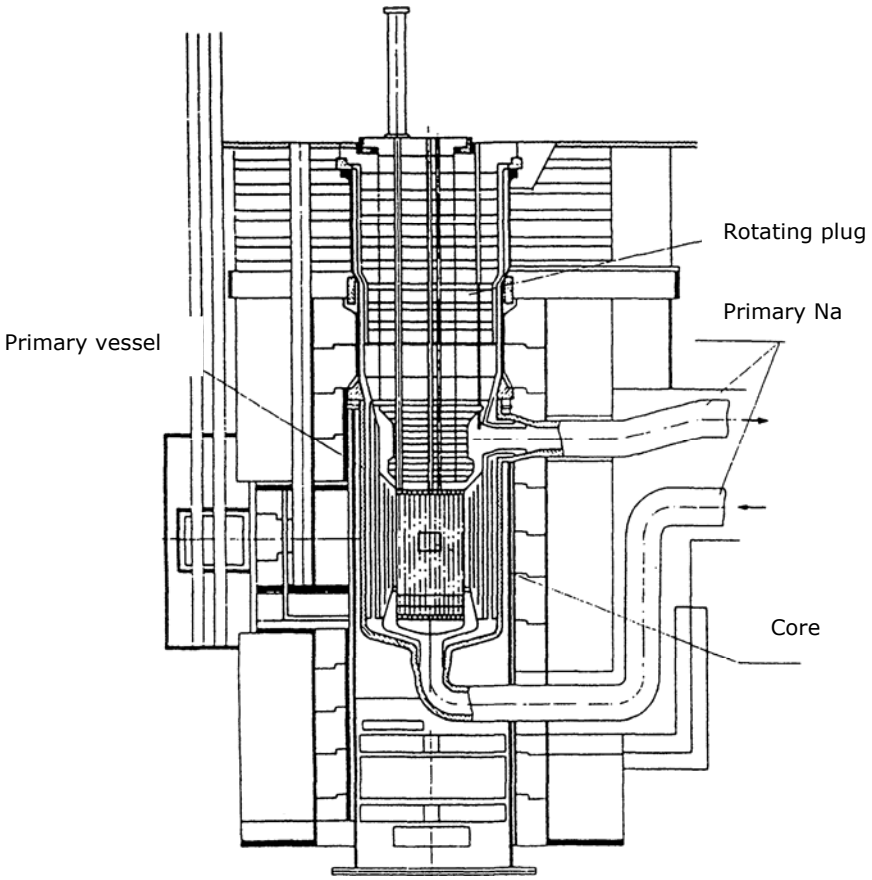

FIG. 2.16. BOR-60 reactor.

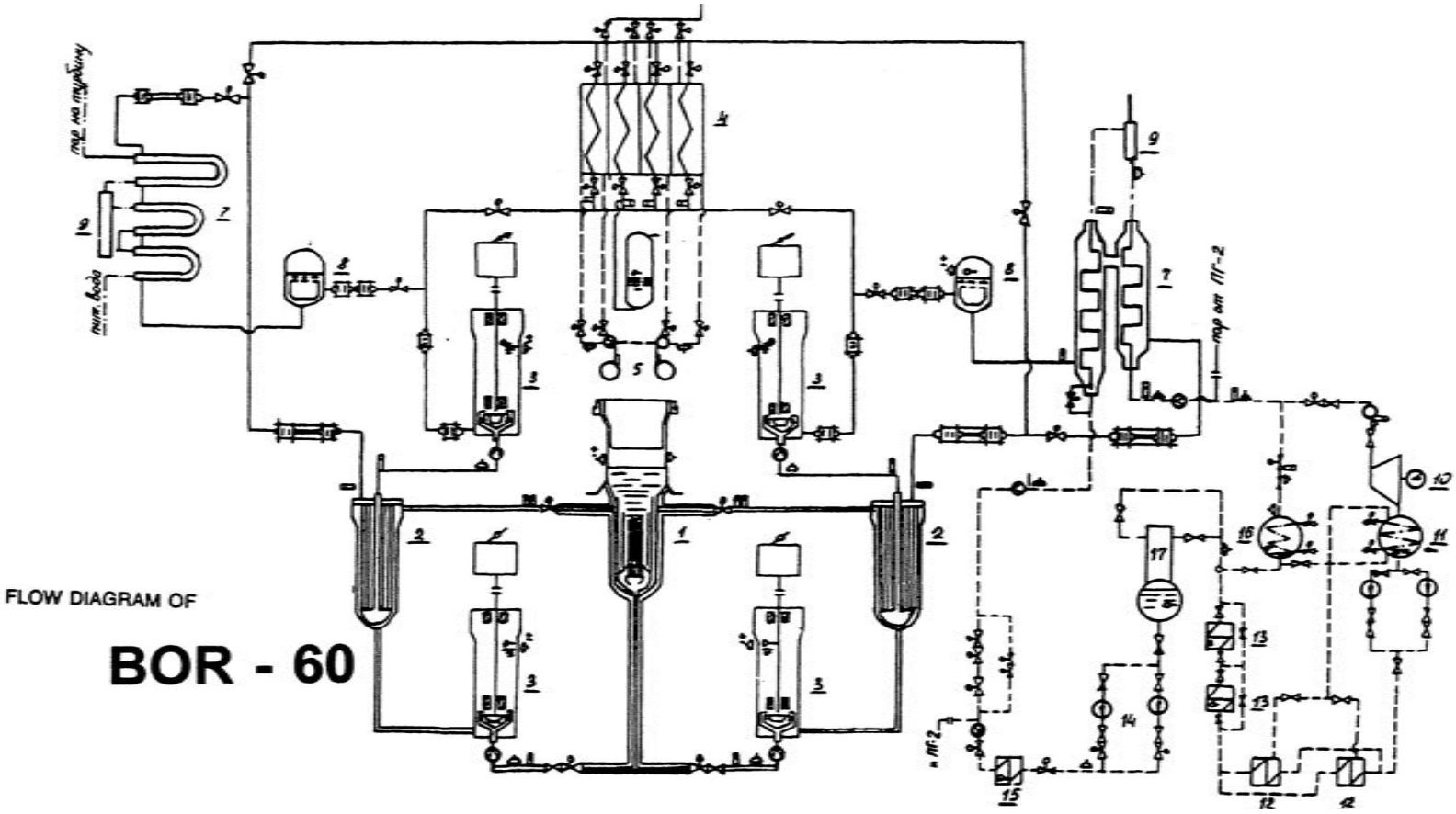

1-reactor, 2-IHX Na/Na, 3-pump, 4-HX Na/air, 5-ventilar, 6-exp. tank, 7-SG, 8-exp. tank SG, 9-separator, 10-turbine, 11-condenser, 12-heater, 13-low pressure heater, 14-pump, 15-high pressure heater, 16-condenser, 17-deaeator.

FIG. 2.17. General scheme of the BOR-60 reactor facility.

TABLE 2.6. BOR-60 MAIN TECHNICAL PARAMETERS

Parameter	Value
Overall plan:	
Thermal power, MW	Up to 60
Electrical power, MW	12
Heat supply capacity, Gcal/h	20
Operation reactor lifetime, year	20
Coefficient of utilization of calendar time	0.64-0.73
Primary circuit:	
Coolant	Sodium
Coolant temperature, °C	
Core inlet	Up to 360
Core outlet	Up to 530
Coolant flowrate through reactor, m^3/h	Up to 1200
Reactor core:	
Maximum neutron flux density, $n \cdot cm^{-2} \cdot s^{-1}$	3.7×10^{15}
Maximum core power density, kW/L	1100
Average neutron energy, MeV	0.45
Fuel	UO_2 or UO_2-PuO_2
Enrichment with ^{235}U, %	45-90
Maximum contents of Pu, %	Up to 40
Enrichment with ^{239}Pu, %	Up to 70
Fuel burnup rate, %/year	6
Neutron fluence per year, $n \cdot cm^{-2}$	5×10^{22}
Damage dose rate, dpa/year	Up to 25
Power rate non-uniformity factors:	
Axial	1.14
Radial	1.15
Volumetric	1.31
Number of cells in the reactor	256
Number of control rods:	
Automatic control rods	2
Shim rods	2
Safety rods	3
Absorber material	B_4C
Core coolant velocity, m/s	Up to 8
Core run duration, days	90
Run-to-run interval, days	45
Secondary circuit:	
Coolant	Sodium
Coolant flowrate in two secondary loops, m^3/h	Up to 1600
Thermal capacity of one steam generator, MW	30
Thermal capacity of air-sodium heat exchanger, MW	30
Tertiary circuit:	
Working fluid	Steam-water
Steam pressure, MPa	Up to 10
Main steam temperature, °C	Up to 500

2.7.3. Operating experience

As of 31.12.2006, the total time of the reactor power operation is 210 970 hours [9]. Electricity production by RF BOR-60 during this period is equal to 1.434 billion kW·h.

The distribution of unscheduled shutdowns of RF BOR-60 occurred for the period of its operation from 1970 till 2006 in accordance with initial events, is presented in Table 2.7 [8, 9, 25]. It is necessary to note that no events resulted in radiation consequences exceeding permissible limits.

TABLE 2.7. DISTRIBUTION OF UNSCHEDULED SHUTDOWNS OF BOR-60 REACTOR FACILITY CLASSIFIED BY INITIATING EVENT

Year	Control and safety system	Electrical equipment and energy supply	Mechanical equipment	Instrumentation	Personnel error	Total
1970	7	4	-	1	9	21
1971	4	5	5	-	6	20
1972	1	1	3	2	3	10
1973	4	3	6	4	4	21
1974	1	4	-	-	1	6
1975	-	1	6	-	2	9
1976	-	2	1	-	-	3
1977	1	6	1	1	2	11
1978	-	3	1	-	2	6
1979	1	2	1	-	3	7
1980	-	-	4	-	3	7
1981	1	3	3	-	3	10
1982	-	4	3	-	1	8
1983	-	1	1	-	1	3
1984	1	1	3	1	1	7
1985	2	-	1	-	2	5
1986	2	-	2	-	1	5
1987	2	-	1	1	1	5
1988	1	2	-	2	-	5
1989	-	1	-	-	-	1
1990	-	1	-	-	-	1
1991	-	1	1	1	1	4
1992	-	1	-	-	-	1
1993	-	4	-	1	-	5
1994	-	-	-	-	-	-
1995	-	-	-	-	-	-
1996	-	1	-	-	1	2
1997	-	-	-	-	-	-
1998	-	1	1	-	-	2
1999	1	-	-	-	-	1
2000	-	1	-	-	1	2
2001	-	1	-	-	-	1
2002	-	1	-	1	-	2
2003	-	-	-	-	-	-
2004	-	1	-	-	1	2
2005	-	1	-	1	-	2
2006	-	1	-	-	-	1
Total	29	58	44	16	49	196

Analysis of events presented in the table shows as follows:

- Number of shutdowns increased in those periods when new equipment was installed (1980–1982 - replacement of feed water pumps, 1985–1987 - substitution of the control and safety system equipment with a new one);
- Number of shutdowns caused by the personnel errors significantly decreased with operating experience, for instance, there were only 4 shutdowns due to personnel errors during last 20 years;
- Most reactor shutdowns were caused by the failures of external power supply system;
- The number of unscheduled shutdowns did not exceed 1–2 events per year for last 13 years and they were mainly caused by the failures of the power supply system.

These statistics testify to the high qualification of personnel, reliability and good quality of reactor equipment and well-thought-out technical decisions made in the RF BOR-60 design.

2.7.3.1. Core

In 1981, the reactor core was loaded with fuel elements having vibropacked pins with MOX-fuel based on reactor grade plutonium [26]. Introduction of a getter solved the problem concerning physical and chemical interaction of the fuel and cladding and assured high average fuel burnup (13-15% h.a.) [27]. Maximum burnup achieved in some pilot fuel elements was 32% h.a.

2.7.3.2. Isotopes production

Production of the following isotopes is implemented in BOR-60 reactor:

- Production of Sr^{89} from Y_2O_3 by the threshold reaction $Y^{89}(n,p)Sr^{89}$;
- Production of Gd^{153} radionuclide from europium oxide;
- Production of Ni^{63} isotope by the threshold reaction $Cu^{63}(n,p)Ni^{63}$.

Personnel of the BOR-60 reactor have gained a large amount of experience in the operation of equipment in contact with sodium [7, 26].

2.7.3.3. Reactor and in-vessel devices (IVD)

All IVD including control rod drives operate quite reliably. However, in the early stage of reactor operation, seizure of the large rotating plug occurred. No seizures of the small rotating plug have occurred. The study of this phenomenon showed that the seizure was caused by deposits of sodium aerosols on the cold surface of the reactor vessel above the liquid sodium level. In order to restore free rotation of the plug, some techniques were developed to eliminate the rotating plug seizure problem.

2.7.3.4. Main primary and secondary pumps

Only one pump (a primary pump) was replaced during the entire period of operation in 1973 because of high vibration. Studies revealed deformation of the pump shaft caused by incorrect application of heat treatment after the shaft components were welded together.

No failures have been detected in all other pumps. Maximum operation time of the pumps is ~ 180 thousand hours.

2.7.3.5. Primary and secondary valves

The total number of valves in the reactor facility is 77. The number of "open-close" cycles varies from 20 to 1100. The removable part of only one valve of 100 mm inner diameter has been replaced during reactor operation because of a loss of integrity of the bellows (without sodium release to the room).

2.7.3.6. Steam generator tests

RF BOR-60 represents an experimental base for testing various models of SG developed for sodium cooled FR.

The steam generator PGN-200M (a model of the BN-600 reactor steam generator) has been tested in RF BOR-60. It was in operation generating steam for 15 160 hours and it was decommissioned because of an inter-circuit leak. The leak was detected by detection of hydrogen in the argon cover gas of the pressure compensation tank. Studies have shown an ingress of ~ 3 kg of water into the secondary sodium and ~ 200 g of sodium into the water steam circuit. The leak occurred in the joint of one tube to the upper tube plate.

In 1979, tests were carried out in the micro-modular steam generator SG-1 to study the sodium-water interaction processes in case of small (up to 0.2 g/s) and large (up to 0.25 kg/s) water leaks. These tests allowed verification of various methods of leak detection, checking and confirmation of serviceability and reliability of SG safety systems, and also acquisition of experience on the elimination of leak consequences. A one-month period was required for the SG repair before it was put into operation.

Currently, two reverse type steam generators (OPG-1 and OPG-2) are in operation in BOR-60 reactor. This type of steam generator is designed in such a way that sodium runs in tubes and water-steam in the intertube space. The micromodular reverse type steam generator OPG-1 has been in operation from 1981 and its total testing time is equal to 138,608 hours (as of 31.12.2006), total testing time for the modular reverse type steam generator OPG-2 operated from 1991, is equal to 94 430 hours (as of 31.12.2006).

2.7.4. Experimental researches

Numerous tests of various types of fuel, structural materials of fuel subassembly wrappers and fuel pin claddings, absorber materials were carried out during the BOR-60 reactor operation [25, 26].

2.7.4.1. Fuel and fuel elements

- Sintered ceramic fuel (UO_2, $UPuO_2$, UC, UN, UPuC, UPuN, UPuCN);
- Vibropacked ceramic fuel ($UPuO_2$ UO_2);
- Metallic fuel (U, UPu, UZr, UPuZr);
- Cermet fuel (U-UO_2, U-PuO_2);
- Composite fuel ((UPuZr)C).

2.7.4.2. Absorber materials

- Control and safety rods (CrB_2, B_4C; Eu_2O_3, Eu_2O_3 + H_2Zr) ;
- Material samples (Ta, Hf, Dy, Sm, Gd, AlB_6, AlB_{12}, Eu_2O_3).

2.7.4.3. Structural materials

- Stainless steels;
- High nickel alloys;
- Refractory materials;
- Zirconium alloys;
- Graphite.

2.7.4.4. Electromechanical and other materials

- Electric insulation materials;
- Magnetic materials;
- Special ceramics;
- Biological shielding materials.

Also, accelerated tests of various structural materials are under way, in particular:

- Steels used for in-vessel devices (IVD) of LWR (VVER type);
- Zirconium alloys for VVER core;
- Vanadium based alloys in lithium environment for fusion reactors.

In-pile tests of experimental fuel pins related to the BREST-OD-300 lead cooled reactor have been carried out in the special independent loop AKST inserted in BOR-60 reactor.

2.7.4.5. Problems solved at the RF BOR-60

A number of significant problems of handling sodium, including radioactive sodium, have been solved at the RF BOR-60 [26, 28]:

- Maintenance of required level of impurities in sodium is provided by using cold traps; regeneration system of cold traps has been developed and put into operation;
- High-efficiency stationary system for purifying sodium from cesium radionuclides successfully operates;
- Cleaning equipment contacting with sodium and elimination of non-drainable sodium volumes from the equipment removed for repair or taken out from service has been developed on the base of new technologies.

It is noted that there were no leaks of sodium to the outside during the whole period of operation of the RF BOR-60.

At the RF BOR-60, a lot of experiments on safety substantiation of sodium cooled fast reactors were carried out. There were additional studies, e.g. neutron-physical and thermal hydraulic characteristics of the cores with various fuel types, complex investigations of local anomalies in BOR-60 operation and their diagnostics, implementation of series of experiments with sodium boiling into subassembly, etc. [28].

2.7.5. Work on extension of reactor lifetime

The initial design lifetime of the BOR-60 reactor facility was 20 years and was achieved in 1989. Life extension studies were conduction and permission was obtained for the operation of BOR-60 to 31 December 2009.

Further life extension work has been performed to allow continued operation to 2015. Among the requirements is the inspection of components to justify the continued operation [9].

In the framework of preparation for BOR-60 lifetime prolongation and substantiation of its safety, a significant amount of work has been performed in the following areas:

- Inspection of the condition of non-replaceable components, including the reactor vessel, and estimation of the possibility to extend their lifetime;
- Irradiation and investigation of samples of the BOR-60 reactor vessel material;
- Testing welds and material of pipelines and equipment of the circuits of RF BOR-60;
- Inspection of the condition of various components and systems of the RF and extension of their lifetime;
- Advanced analysis of RF BOR-60 safety, including updating of the list of initial events of beyond design basis accidents that should be analyzed for BOR-60 safety justification and their numerical estimation;
- Analysis of external impacts of rated magnitude as applied to the reactor building and RF components;
- Inspection of the condition of the building structures of RF BOR-60, etc.

In December 2009, Rostechnadzor has issued the license for an extended period of the BOR-60 operation up to 31 December 2014.

2.7.6. Conclusion

The experimental fast reactor BOR-60 successfully operated for more than 40 years.

In this period, a large number of irradiation tests of various fuel compositions, structural, absorbing materials etc. has been performed at the BOR-60 reactor; testing sodium equipment, various control and safety systems have been carried out and continue. RF BOR-60 represents the unique experimental facility that permitted testing and substantiating many technical and design decisions used in industrial NPP with fast reactors (BN-350, BN-600). The reactor facility personnel have gained the large experience on sodium coolant technology.

2.8. BN-350 operating experience

2.8.1. Design features

The BN-350 reactor plant is a constituent of Mangyshlak energy integrated works 10 km away from Aktau (former Shevchenko), Mangistauskaya Region of Kazakhstan on the shore of the Caspian Sea (Mangyshlak peninsula). It was designed and constructed as a two-purpose pilot-industrial power plant for electricity generation and heat production for seawater desalination. On 16 July 1993, twenty years had passed since the start of the reactor. Throughout that time BN-350 has been operated as a part of the industrial complex including the large capacity co-generation power plant and the distillate production works providing electricity and fresh water for Aktau and the adjoining industrial region, which is completely devoid of natural fresh water resources.

BN-350 has a loop arrangement of the primary circuit components, i.e. the primary sodium pumps, intermediate heat exchangers, and valves are disposed in separate compartments

(cells) and are connected with the reactor and interconnected by pipelines. The temperature expansions of the pipelines are accommodated by the bends.

The BN-350 reactor plant includes the following main components: fast sodium-cooled reactor, six primary loops, six intermediate (secondary) loops, steam generators, refuelling complex (integrated mechanical system), primary and secondary sodium purification system, and automated process control system, including the reactor control and protection system (CPS) and diagnostic systems for monitoring the operating state of the safety-related components and systems [24].

During power operation, core heat removal and transport to the working medium (steam water) are provided by a three-circuit flow scheme (Fig. 2.18).

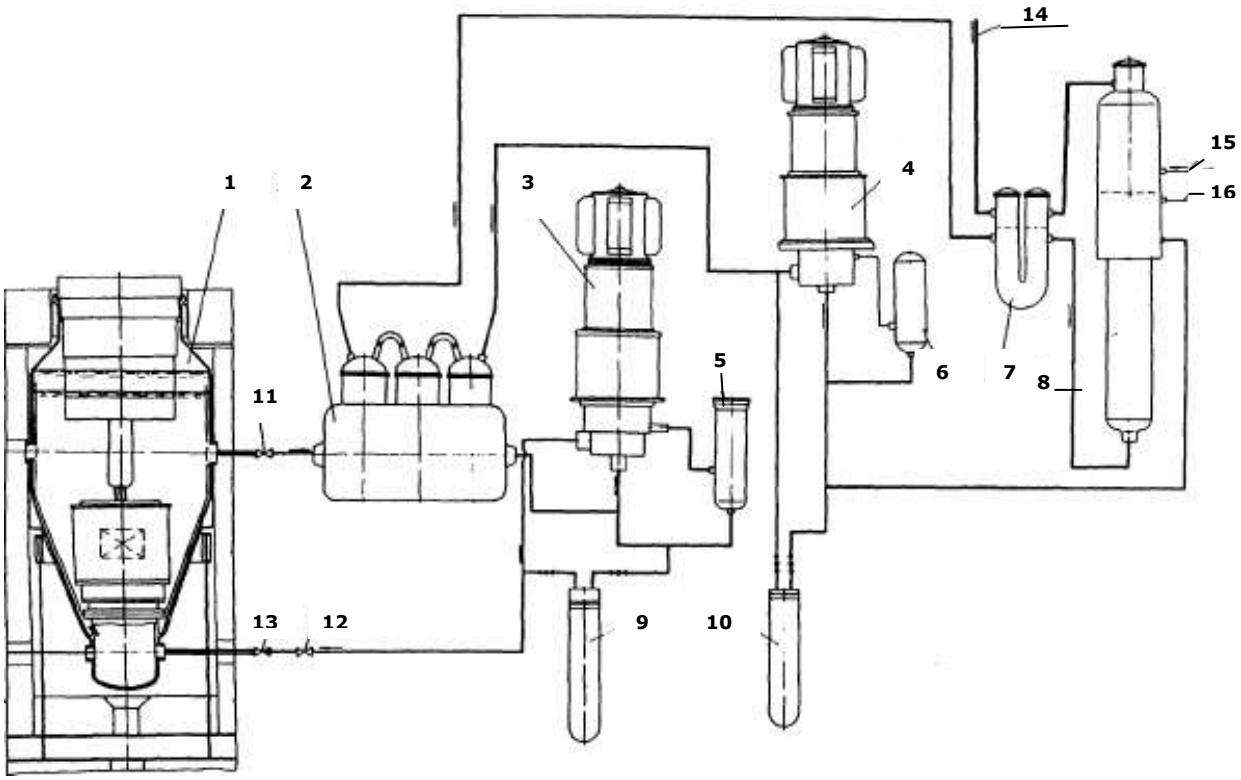

1-reactor, 2-intermediate heat exchanger, 3-primary coolant pump, 4-secondary coolant pump, 5,6-pump leakage drain tanks, 7-steam superheater, 8-evaporator, 9,10-filter-traps, 11-ND 600 gate valve, 12-ND 500 gate valve, 13-check valve, 14-main steam line, 15-feed water, 16-gas system line.

FIG. 2.18. BN-350 Principal flow diagram.

The primary circuit is composed of six IHX, six primary coolant pumps (PSP), and sodium pipelines with gate and non-return valves. The pressure chamber with the core diagrid and the upper mixing plenum above the core are the common sections of primary sodium flow path. Sodium flow is distributed from the diagrid into the core and the radial blanket fuel assemblies. A portion of the primary sodium (250 t/h) is removed from the pressure chamber through throttles and utilised for cooling the reactor vessel and its outlet nozzles.

There is a capability to isolate each primary loop from the reactor using two gate valves on the suction and pressure pipelines of the circuit. On the pressure pipeline of each loop downstream of the PSP a flap-type check valve is provided eliminating coolant backflow in the event of a PSP trip in one loop when the other PSP are operative. The secondary sodium

circuits comprise: IHX heat transfer tubes, pipelines, secondary sodium pumps and steam generators. Due to utilization of the reactor energy for fresh water production, the steam-water system has some specific features. Steam from the SG is supplied to turbines of two types: a condensing turbine (K-l00-45) and a back-pressure turbine (K-50-45). Exhaust steam flows from the back-pressure turbine and from intermediate bleeds of K-l00-45 turbine are supplied to the water desalination facilities.

At a heat output of 750 MW the reactor produces ~ 100 000 t per day of desalinated water and generates ~135 MW_e.

Basic data for the BN-350 reactor plant are given in Table 2.8 for an achieved power level of 750 MW.

TABLE 2.8. BN-350 BASIC OPERATING PARAMETERS

Parameter	Value
Reactor thermal output, MW	750
Primary sodium temperature, °C	
At reactor inlet	288
At reactor outlet	437
Sodium flow through reactor, t/h	14 100
Secondary coolant temperature, °C	
At SG inlet	420
At SG outlet	260
Sodium flow in secondary loop, t/h	3 400
Number of operating loops	5
Main steam parameters:	
Temperature, °C	405
Pressure, MPa	4.5
Steam flow, t/h	1070
Volume of primary sodium, m^3	500
Maximum electric output of power unit, MW	125-150
Distilled water output per day, t	100 000
Maximum neutron flux in core, n cm^{-2} s^{-1}	6×10^{15}
Design service life, year	20

The BN-350 reactor (Figs 2.19 and 2.20) includes: the reactor vessel which contains the core diagrid with neutron reflector and a set of core and blanket fuel assemblies; the reactor refuelling system; the above core structure with CPS drive mechanisms and in-core instrumentation guides.

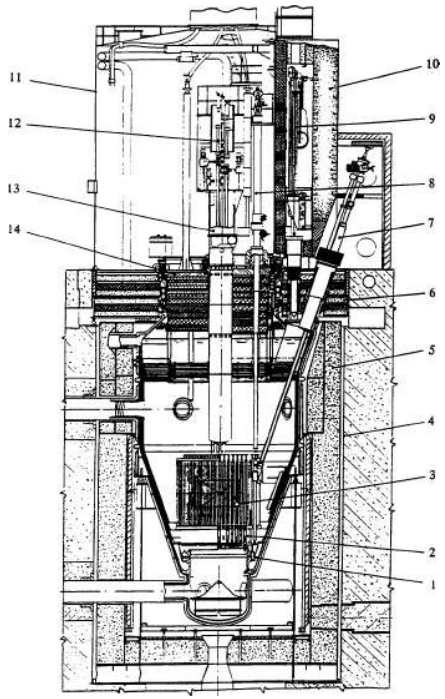

1-reactor vessel; 2-core diagrid; 3-reactor core; 4-reactor well liner; 5-lateral shield; 6-upper-stationary shield; 7-elevator, 8-refuelling mechanism; 9-FAs transfer mechanism; 10-fuel transfer cell; 11-protective dome; 12-control rod drive mechanism; 13-above core structure; 14-rotating plug.

FIG. 2.19. BN-350 Nuclear reactor.

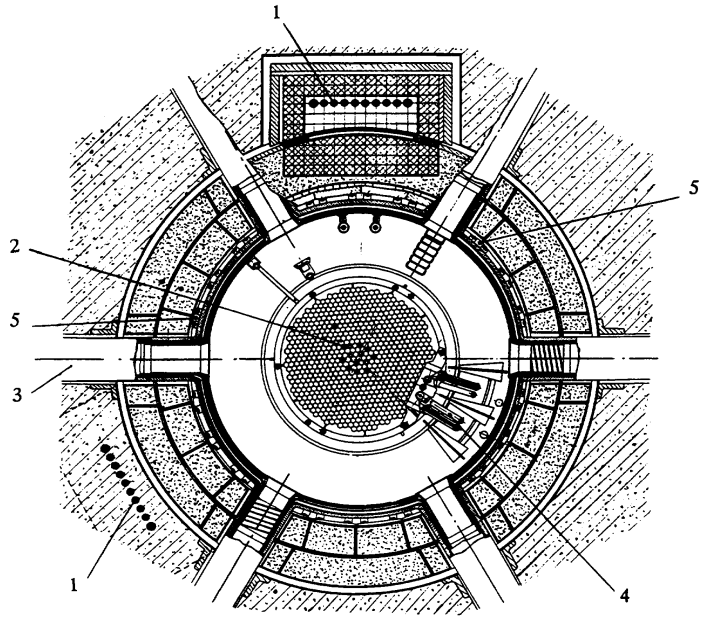

1-set of ionization chambers; 2-reactor core; 3-sodium outlet pipeline; 4-elevator; 5-channels for additional ionization chambers.

FIG. 2.20. BN-350 Reactor plan view (cross section).

The diameter of the cylindrical part of the reactor vessel is 6 000 mm, and the wall thickness is 30 mm. In the middle section of the vessel, there is a support belt by which the reactor is located on 16 roller bearings arranged on a support shell of 5 850 mm diameter transmitting the reactor weight load onto the foundations. The reactor vessel is enclosed in a guard vessel.

The reactor unit is set in a concrete well covered by the upper stationary shield, which is composed of steel shot and serpentine concrete layers. Between the reactor and the wall of the well is a radiation shield consisting of an iron ore concentrate-filled cage. Six cells enclosing the primary circuit thermo-mechanical equipment are adjoined to the reactor well.

2.8.2. Operating experience

2.8.2.1. General results of operation

More than twenty years of operation of the power unit associated with the BN-350 reactor have promoted the exploration of the new industrial region of Kazakhstan, which is rather rich in natural resources. The reactor's first criticality date was 29 November 1972, and power start-up was carried out on 16 July 1973. The extended start-up was explained by loss-of-integrity events in four evaporators (detected by the appearance of hydrogen in the gas plenum) when the SGs were filled with water. For that reason the power start-up was carried out with three loops available at a superheated steam pressure of 3.0 MPa (compared with the design value of 5.0 MPa), the reactor thermal power attained being approx. 200 MW. The reactor was designed for thermal output of 1 000 MW, but in the first stages of operation, its power level was limited by unsatisfactory operation of the steam generators. To ensure less demanding conditions for the operation of evaporators with field tubes, a maximum power of 130 MW was specified for each SG.

For the Czech-produced SGs "Nadjozhnost" the allowable power level was set somewhat higher - at 200 MWe. In addition, from an experiment carried out in 1976 on plant emergency cooling with loss-of-normal power, it was found that the available capacity of the steam-water system under these conditions allows normal development of the residual heat removal process at reactor power levels not higher than 750 MWth. Therefore, in further operation this power level was not exceeded, taking into account the power limitations imposed by the SGs as well.

During its operating life the reactor has operated at various power levels. The average load factor in respect to allowed power levels was 85%. Reduction in the load factor was caused basically by outages for refuelling and planned maintenance of the equipment. The reactor was shutdown for scheduled refuelling and maintenance two or three times a year (as a rule) with outage durations of 20–30 days. The main factor limiting the reactor power level was failure of the steam generators. At the same time, the reactor components and main circulating pumps have demonstrated stable, fault-free operation.

In the first years of plant operation, the reactor core posed certain problems due to the excessive heat rating of the fuel rods and considerable shape variation of the core structural items. Modernization of the core and switching to new structural materials allowed these problems to be solved.

The availability of stand-by components (six loops) and the ability to operate with different numbers of loops (from three to five), provided for stable operation of the reactor plant and production of electricity and fresh water. As a result, repair and replacement work on the steam generators (if necessary) was carried out without shutting down the reactor.

Simultaneously, with solving the paramount economic and social problems of provision of fresh water and electric energy for the prospective industrial regions of Kazakhstan, much experience was obtained from the construction and long-term operation of the power unit and BN-350 reactor, which was valuable for the further development of sodium cooled fast reactors. Among the results obtained, the following can be highlighted:

- Construction and long-term testing in the power reactor environment of such equipment as refuelling mechanisms and the main reactor components such as coolant pumps and CPS drive mechanisms, filter-traps, etc. which were then used without changes or with minor modifications in the next fast nuclear reactors - BN-600, BN-800, BN-600M.
- Construction and improvement of the main fast reactor core components: fuel assemblies (FAs), fuel rods, control rods and guide sleeves, which have the same dimensions as similar components of BN-600, BN-800 and BN-600M reactors.
- Development of sodium coolant technology and associated equipment for utilization in fast power reactors, providing safe operation of sodium systems, in particular fire safety.
- Investigation of safety-related physical and thermal-hydraulic characteristics of fast reactor cores.
- Investigation of hydrodynamics and heat transfer in sodium circuits under various operating conditions.
- Experience in construction and operation of heat-exchange equipment with systems for inter-circuit boundary integrity control.

BN-350 construction and operation experience became a reliable scientific and engineering basis for creation of the next fast nuclear power reactor, BN-600.

2.8.2.2.Radiological safety

Radiation doses to the BN-350 personnel have been associated mainly with repair and maintenance activities for sodium components in the primary circuit boxes. Radiation conditions in the rooms (except for the reactor well), depended substantially on the state of fuel rods in the core. In the initial period of the reactor plant operation when the first type core was used, numerous cladding failures caused a significant rise of fission fragment activity in the primary system.

In 1979 the gamma-radiation dose rate on the surface of the sodium equipment at reactor shutdown reached 8.90 μSv/s, 80% of which was attributed to cesium nuclides. Radiological conditions were improved significantly after completion (in 1979) of the core change over to the second type fuel design. It was promoted not only by reduction in the number of failed fuel rods, but also by clean-up of cesium from the primary coolant using a special trap with a graphite absorber. Since 1984 the gamma-radiation dose rate in the primary circuit rooms during outages did not exceed 1.5 μSv/s.

Due to the loop design of the reactor primary system, the reactor well is virtually inaccessible even at outages because of high radiation-induced activity of the reactor vessel structures. Transport of gaseous fission fragments into the upper part of the CRDM and to the oil system of the reactor coolant pumps turned out to be one of the reactor operating peculiarities, which degraded radiological conditions in the reactor servicing zones.

The major source of the reactor radiological impact to the environment was gaseous discharges from the equipment air-cooling system and from the reactor plant rooms through the vent stack. Resulting from the improvements in the fuel design and associated reduction in the number of failed fuel rods in the core to single events (which have become quite rare

lately) radioactivity of the plant discharges to the atmosphere determined by the radiation-induced activation of air in the reactor well cooling system. Daily release of gaseous nuclides was 0.55-0.74 TBq. Observations over many years of radioactivity of the flora and fauna, and radiological conditions in the local populated areas and in the sanitary restricted zone around the NPP, showed that those characteristics affected by natural and man-induced radiation sources correspond to background radiation levels.

2.8.2.3. Reactor core

The central part of the reactor contains a set of core and blanket FAs, guide sleeves for CPS rods and neutron reflectors installed in the diagrid. The diagrid is attached to the sodium pressure chamber. The internal plenum of the diagrid is divided into two chambers of high and low pressure. The sodium from the high pressure chamber is distributed for cooling the core FAs, control rods and FAs of the inner blanket. From the low pressure chamber the coolant goes for cooling FAs of the outer blanket. Core FAs arranged in the internal store around the outer blanket periphery are cooled by natural convection of coolant in the reactor vessel.

Coolant flow rate profiling in the core and in the radial blanket according to power distribution is provided by overlap of a certain portion of the orifices in the FA end fittings with throttling sleeves into which the FAs are inserted. To flatten the power distribution along the core radius for the initial reactor core FAs of two enrichment values (in uranium-235) were used: 17 and 26%. First-type core FAs had 169 fuel rods with cladding of 6.1 mm diameter and wall thickness of 0.35 mm. The fuel rod length was 1140 mm and the core height was 1060 mm, so the height of the gas plenum was very small - 50 mm which caused high stresses in the cladding from gaseous fission products. In the upper and lower parts of the core FA bundles of axial blanket rods were placed: 37 fuel rods of 12 mm diameter.

During the initial period of the reactor operation until 1979, when the first type core (fuel rod of 6.1 mm OD) was used, large number of fuel failures (loss-of-clad integrity events) occurred that caused a significant increase in fission fragment activity in the primary circuit and consequently resulted in deterioration of radiation conditions in the reactor plant rooms. Therefore the second type core design was developed with fuel rods of 6.9 mm OD. This advanced core provided for increased fuel burnup and more reliable operation of the fuel rods, mainly due to the following improvements:

- The gas plenum height in the fuel rod was increased at the expense of integration in one clad tube (6.9x0.4 mm) of core and axial blankets material (fissile and fertile) and reduction of the lower blanket height.
- The fuel assembly duct material Cr18Ni10Ti (austenitic steel) was replaced by stabilized austenitic steel Cr16Ni11Mo3 in a heat-treated state.
- The coolant pressure in the middle plane inside the duct was diminished by approx. 35% resulting in a decrease in duct deformation by radiation-induced creep.
- The power distribution over the core radius was flattened by the incorporation of a medium fuel enrichment (21%) zone between the existing core zones with "low" (17%) and "high" (26%) enrichment of fuel, resulting in a decrease of the fuel rod specific heat rating.

The above measures and reactor operation under derated power conditions resulted in a significant reduction in the number of defective fuel rods in the core. Further increase in fuel burnup is planned through utilization of the ferritic steel EP-450 for ducts and improved austenitic steel in cold-worked state for cladding. The basic parameters for different cores used in the reactor are given in Table 2.9.

TABLE 2.9. BN-350 REACTOR CORE DESIGN EVOLUTION

Parameter	Core type		
	1	2	3
Reactor heat output (max), MW	650		
Core dimensions, mm			
Active height	1060		
Equivalent diameter	1550		
Axial blankets height, mm			
Upper	600		
Lower	600		
Radial blanket thickness, mm	450		
Number of different fuel enrichment zones	2	2	3
Fuel enrichment (in ^{235}U), %			
LEZ*	17	17	17
MEZ	-	-	21
HEZ	26	26	26
Number of fuel assemblies			
LEZ	109	109	61
MEZ	-	-	48
HEZ	108	120	114
Cladding outer diameter and wall thickness, mm			
Core fuel rod	6.1×0.35	6.9×0.4	6.9×0.4
Lower axial blanket rod	12×0.4	6.9×0.4	6.9×0.4
Upper axial blanket rod	12×0.4	12×0.4	6.9×0.4
Radial blanket rod	14.1×0.4	14.1×0.4	14.1×0.4
Length of fuel rod, mm	1140	1800	2400
Length of gas plenum in fuel rod, mm			
Upper	50	50	380
Lower	-	250	310
Number of fuel rods in fuel assembly:			
Core fuel assembly	169	127	127
Blanket fuel assembly	37	37	37
Duct width across flats and thickness, mm	96×2	96×2	96×2
Structural material			
Cladding**	EI-847	ChS-68	
Duct	Cr18Ni10Ti	Cr16Ni11Mo3	
Fuel rod maximum linear rating, kW/m	28	40	43
Fuel rod cladding temperature (max), °C	550	570	600
Maximum fuel burnup, %h.a.	5.7	9.0	10.0
Maximum radiation dose, dpa	46	60	65
Core fuel life, ed	332^98	424-636	400-600
Refuelling interval, ed	83	106	100
UO_2 inventory in core, kg	7400	7800	7000
Average fuel burnup, MWd/kgU	38	54	58

*LEZ - "low" enrichment zone
*HEZ - "high" enrichment zone
*MEZ - "medium" enrichment zone**EI-847 – Cr16Ni15Mo3Nb
**ChS-68 – Cr16Ni15Mo2Mn2TiB

Simultaneously with the improvement of the core fuel operating performances, modifications have been introduced in the design of the control rods and guide sleeves by the use of radiation-resistant structural materials.

2.8.2.4. Control rod drive mechanisms (CRDM)

There are twelve CPS elements in the reactor: two power control rods, three emergency protection rods and seven reactivity compensating rods. For the entire period of operation the CRDM have functioned without any significant abnormalities.

In 1979 and 1980, there were difficulties in disconnecting the control rods from their drive lines before refuelling the reactor. Analysis revealed a potential for seizing the CRDM moving items in the guide tubes in the sodium-to gas transition zone by solidified sodium if coolant temperature were to diminish. To eliminate such events the sodium temperature in the refuelling mode was set at a higher level (230-240°C). After that minor modification there were no problems with movement of the control rods. The CRDM service life has been extended periodically with replacement (if necessary) of individual items on the basis of planned inspection results.

There are two sets of ionization chambers (10 chambers in each set) for neutron flux monitoring which are located in a concrete wall of the reactor well. Two additional ionization chamber suspensions were introduced (1976) in the immediate vicinity of the guard vessel wall, that significantly enhanced reactor subcriticality control during refuelling operations.

2.8.2.5. Refuelling equipment

The BN-350 refuelling system consists of two components:

- Complex of in-reactor refuelling mechanisms;
- Complex of out-of-reactor refuelling mechanisms.

The first complex is a constituent of the reactor and includes: two rotating plugs (large and small), refuelling mechanisms and loading-unloading elevators. This complex provides for loading and unloading of the main core items and their re-arrangement inside the reactor.

The rotating plugs are disposed eccentrically to each other. On the small rotating plug the refuelling mechanisms are mounted eccentrically. By rotating the plugs the refuelling mechanism is guided to any position in the core, radial blanket and in-vessel store, or to any control rod. The refuelling mechanism simultaneously with reshuffling of FAs rotates them for alignment with the hexagonal cells in the core.

The complex of out-of-reactor refuelling mechanisms includes:

- Fresh FAs drums;
- Fuel transfer cell transfer mechanism;
- Spent fuel drum;
- Washing cell fuel transfer mechanism;
- Loading-unloading elevator plug lifting mechanism.

Spent FAs and other items are transported into sockets in the washing cell and then transferred into the spent fuel water pool for decaying. The fuel transfer cell with its transfer

mechanism and the washing cell adjoin the reactor. New fuel assemblies are loaded into the reactor from the new fuel storage drum located beneath the refuelling cell. New fuel loading operations have not posed any difficulties during the reactor operating life.

According to the design, irradiated fuel assemblies were to be transported from the fuel transfer cell to the washing cell through the spent fuel storage drum located in a tank filled with Na-K alloy beneath the junction between the cells. Due to failure of the spent fuel storage drum (1976) a special lead-shielded flask was designed and manufactured for transporting spent fuel assemblies from the transfer cell to the washing cell.

It was noticed during operation that increased forces were required for rotation of the shield plugs. Probable causes were sodium vapor condensation in gaps or non-uniform heating of the hydraulic seals. Plug operation became normal after increasing the Pb-Bi eutectic working temperature to 200°C and temporary interruption of the plug air cooling system in the process of heating up the hydraulic seals. The refuelling mechanisms, elevators and fuel transfer mechanisms in the cells have been operated without significant disturbances. Minor disturbances were remedied through replacement and modernization of individual items. To improve the reliability of the mechanisms, a system to control installation and withdrawal forces was incorporated. During the entire period of reactor operation (till Oct. 1995) 56 planned refuelling cycles have been fulfilled. The time spent for one fuel assembly replacement was one hour. The total number of loading-unloading operating cycles of the elevators and fuel transfer mechanisms is ~ 3200.

2.8.2.6. Steam generators

The BN-350 steam generators consist of two super-heaters with U-shaped tubes and two evaporators with Field-type tubes inside which water flows under natural convection and partial evaporation conditions. The initial period of reactor plant operation was characterized by unreliable operation of the SGs. Numerous loss-of-integrity events occurred in the Field tubes of the evaporators. Metallographic examination of a great number of Field tubes showed the presence of microcracks in the tube-to-bottom weld joints. Mechanical deformation of the tube bottoms during cold stamping was acknowledged as the most probable cause of the microcracks. Growth of the microcracks could occur under the effect of internal stresses arising during welding the bottoms to the tubes and under cyclic thermal loads during evaporator operation. After repair of the Field-tube evaporators when outer tubes of 32×2 mm (OD × wall thickness) were replaced by 33×3 mm tubes with machined bottoms reactor plant operation was continued with five loops at thermal power of 650 MW. One of the repaired SGs failed later due to a large leak of water to sodium. It was dismounted and replaced with the micromodular SG "Nadjozhnost-1" of Czech fabrication (1980). Another SG of the same type "Nadjozhnost-2" was put into operation in 1982 instead of one of the Field-tube SGs which had been operated reliably since the reactor start up. In general, the plant operation demonstrated the reliability and high operating performances of the Field-tube SG design taking into account particularly their behavior in water-to-sodium leak events.

At the same time, the thermal-hydraulic disadvantage of the design was revealed by natural convection flow instability during emergency residual heat removal. The use of "Nadjozhnost"-type steam generator eliminates this disadvantage and in addition allows the removal of heat from the SG by air flowing outside the modules under forced or natural convection conditions. In January 1989, both these SGs failed due to stress-induced corrosion

on the steam-water side of the tubes promoted by non-uniform thermal-hydraulic conditions in the tube bundles. After repair the SGs were put again into operation in 1993.

2.8.2.7. Intermediate heat exchangers

Horizontal tube-and-shell IHX with three modules connected in series, made of U-shaped tubes are used in the BN-350. The IHX of each loop consists of two sections connected in parallel both for primary and secondary coolant flows. The IHX is located in a suction loop upstream of the primary coolant pump, while in the secondary circuit it is in a pressure loop downstream of the circulating pump. The IHX tube bundles can be removed if necessary and replaced with new ones. The most stressed units in the IHX are the fixing joints for the tube module covers and for the frame which stiffens the flat walls of the IHX body.

Measurements of temperatures and stresses in various items of the IHX were carried out during reactor plant operation. On this basis requirements were formulated to limit the rate of the IHX heating-up in steps of 10% specified power with delays of 5–10 h in each step. By 1995 the IHX have operated more than 160000 h at various power levels without any disturbances and failures.

2.8.2.8. Gate and check valves

Double-disk wedge gate valves with freezing seals of OD 500 mm and OD 600 mm (12 items) are used in the reactor plant. They are remotely operated and provide for disconnection of the primary circuit loops from the reactor. The total operating time of the primary circuit gate valves by January 1996 was approx. 180 000 h; the number of "closed-open" cycles for each OD 600 valve from the beginning of operation amounts to approx. 140. The operability and reliability of the valves has been proved during the reactor plant operation. Check valves are installed downstream of the reactor coolant pumps. The operation of these valves could not be checked on the pump test rigs. In the course of adjustment and commissioning on the reactor plant considerable displacements of primary pipelines were detected on the occasion of a trip of one of the pumps operating at maximum speed followed by check valve closure. The displacements were caused by a large backflow as the valve closed. A new design of check valve was developed which differs in that the mass of the gate member and the backflow on valve closure are smaller. The advanced valves are operating satisfactorily, which has made it possible to dispense with the reactor shutdown when a primary loop is switched off, thus realizing the design algorithm of loss of a single loop without scram.

2.8.3. Safety enhancement and equipment life extension

The reactor was developed on the basis of codes valid in the 1960s and therefore does not meet the up-to-date safety requirements fully. The possibility of further operation of BN-350 depends primarily on reactor safety enhancement.

In 1992, the design institutions together with the plant operator completed a review of the conformity of the reactor to the requirements of safety codes currently valid in this country. Resulting from the analysis, a list of deviations was compiled and the necessary measures for reactor plant upgrading were developed, part of which has been realized. The most important among those measures performed recently in the framework of reactor safety enhancement are as follows:

- From 1990, efforts have been under way to ensure safety under external dynamic loading, such as an earthquake. All necessary investigations have been completed to refine the parameters of the maximum design seismic impact. Calculations have been carried out to assess the building structures, pipelines, heat exchange equipment and the reactor main and guard vessels. Work has started on the reinforcement of individual equipment items and pipelines and provision of additional restraints. Analysis of the consequences of seismic impact on the reactor plant building structures, equipment and pipelines showed that the existing safety system such as the reliable power supply system, the feed water system and the reliable service water supply to components important to safety would be destroyed completely or partially under seismic impact of 6 units magnitude (MSK-64 scale) - the Maximum Design Earthquake accepted for the BN-350. Taking this fact into account a design was developed providing for the arrangement of safety equipment in the seismically robust part of the reactor building to ensure reactor residual heat removal under seismic impact conditions. A design was developed and is currently being realized providing for reactor seismic protection by triggering the shutdown system in response to signals from seismic sensors.
- Analysis of the influence on the reactor of explosion-hazardous industrial facilities situated in the vicinity of the site is complete and the corresponding measures for ensuring reactor safety have been developed.
- The control and protection system is being upgraded by renovation of its components and optimization of transient control algorithms.
- A core residual heat removal system for the event of coolant level lowering in the reactor below the outlet nozzles has been installed.
- An independent feedwater system for the SGs has been mounted and put into operation, as well as the air-cooling system for the micromodular SGs "Nadjozhnost-1 and -2". The electric valve drives are powered from a reliable power source.
- A diagnostic system for checking the state of the primary circuit pipeline metal is under development.

Lifetime extension implies analysis of the current state of main systems and components, determination of their residual lifetime, finding the items with expired lifetime and replacing them, and validation of the plant lifetime extension.

The preliminary findings resulting from this activity proved that components such as the reactor vessel, guard vessel, reactor support system, internal structures of the reactor, reactor coolant pump casings, and the bodies of the primary circuit check and gate valves still have a considerable lifetime reserve. The reactor operating record confirmed that its technical and economic performances during the entire period of service life, including recent years, are quite satisfactory. There are no symptoms of the reactor plant operating performance indicating deterioration. Based on the results of the ongoing work, a decision will be made on the possibility of continuing reactor operation.

2.8.4. Review of experimental programme

The BN-350 reactor plant has been used from the very beginning for tests and research activity aimed at enhancing safety and economic efficiency of reactor operation. The results of a considerable part of the experiments performed were used in the development of advanced fast nuclear reactor designs. Among the research work carried out, the following can be noted:

- Testing of structural materials for cladding and ducts of FAs with increased fuel burnup using the normal, experimental and special test fuel assemblies. The development and fabrication (1980) of a FA dimensional check system made it possible to obtain the required information on the deformation of core items associated with radiation-induced damage of structural materials.
- Testing of FAs with mixed uranium-plutonium oxide fuel and other types of nuclear fuel.
- Testing and post-irradiation investigation of absorber elements for control rods of enhanced efficiency and with extended service life.
- Testing of new control rods guide sleeves made of more radiation-resistant structural materials to improve reliability and to extend service life.
- Experiments with a special sodium boiling generator movable along the core height, involving recording of boiling initiation by acoustic and neutron sensors. The experiment confirmed the possibility of detecting sodium boiling and locating FAs in which the coolant is boiling.
- Investigation of reactivity effects and power distribution in the reactor core using indicators placed in capillary tubes integrated into the FAs and using a gamma-scanning technique.
- Experiments on the reactor plant emergency cooling using active and passive heat removal methods including natural convection of sodium in the circuits and cooling of the "Nadjozhnost" steam generators by air.
- Development and test of more effective systems for hydrogen monitoring and detection of leaks in both types of steam generators.
- Development and installation into the reactor of a small-size graphite absorber for removal of cesium nuclides from the reactor coolant and investigation of the efficiency of this technique.
- Investigation and perfection of reactor plant operation modes, modernization of the CPS and installation of additional sensors for control of reactor parameters.
- Experiments with large sodium fires and development of fire extinguishing techniques.
- Checking of new designs of advanced equipment and systems and substantiation of their utilization in other BN-type nuclear reactors.

2.9. Phénix operating experience

2.9.1. Design features

2.9.1.1. Reactor core

The reactor block is of an integrated design (pool) except for a few auxiliary circuits. The entire primary sodium system, containing 800 tonnes of radioactive sodium, is enclosed in the main reactor vessel, which is 11.8 m in diameter (Fig. 2.21).

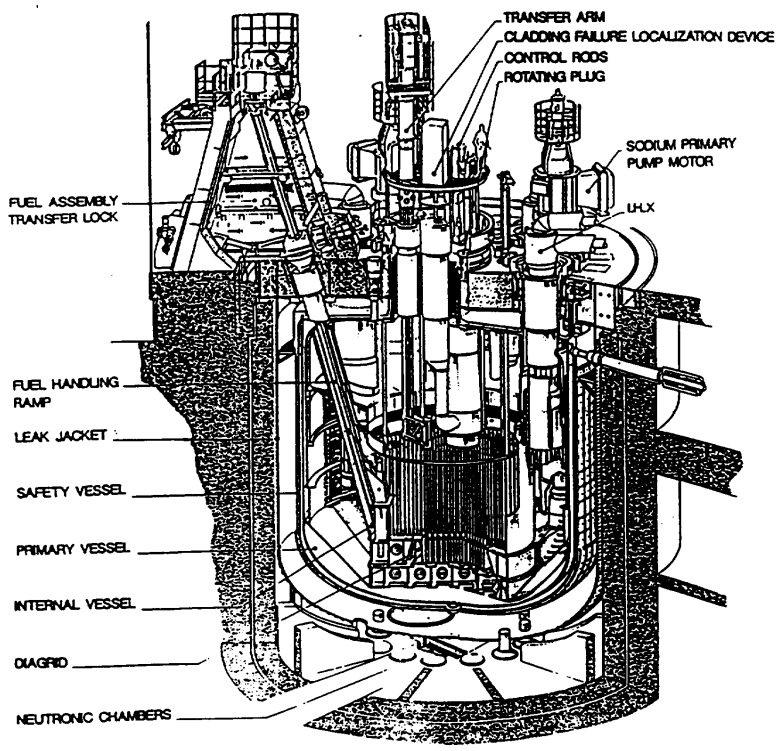

FIG. 2.21. Phénix cut-away view.

The fissile core, in which most of the reactor power is generated, is surrounded by a fertile blanket and neutron shielding to prevent activation of the secondary sodium flowing through the intermediate exchangers.

2.9.1.2. Vessel

The sodium in the main vessel is separated into two zones:

- Hot pool at the core outlet where the hot sodium flows into the intermediate heat exchangers (IHX);
- Cold pool taken from a peripheral annular space between the primary tank and the wall of the main reactor vessel, which contains the three main circuit circulating pumps and six heat exchangers, suspended from the upper slab (Since 1993, the reactor is operated with only two secondary loops. Thus only four IHX are operational, the two other spaces being plugged. The thermal power which was 563 MW is thus limited to 350 MW).

A number of other devices are located in the main vessel: the fuel transfer arm, the six control rods, the SAC (Complementary Shutdown System) implemented in 1996, neutron flux detectors, thermocouples, failed fuel detection and location devices, etc. An argon gas atmosphere is maintained above the sodium surface to prevent any contact with air.

The main vessel is closed at the top by a flat roof with penetrations for primary pumps and heat exchangers. It is associated with the cylindrical seating of a rotating plug in the slab penetrations forming the top of the reactor block. A safety vessel surrounds the main vessel. It has the double function of containing any sodium escaping by leakage, and preventing a drop in the sodium level of the main vessel which might affect core cooling. Finally, an outer containment vessel aims at containing any radioactive products that might escape from the

main vessel in the event of an accident. This containment is cooled by two interlaced water circuits which maintain the concrete of the reactor pit at a low temperature, and which are capable of acting as a standby cooling circuit for decay heat removal after shutdown, should all the secondary sodium circuits be out of service.

2.9.1.3. Heat transfer circuit

The three primary sodium pumps are variable speed units (150 to 970 rpm) delivering about 950 kg/s at 825 rpm (since 1993: about 670 kg/s at 540 rpm), which is their normal service speed. The circulating sodium enters the core at 400°C (since 1993: 380°C) and moves from there, at 560°C (since 1993: 530°C), to six (since 1993: four) IHX which are connected in pairs with three (since 1993: two) independent secondary loops.

Sodium must be kept very pure to prevent corrosion of the steel piping and plugging of circuit components. It is purified by cold traps operating on the principle of precipitation of any oxide in the sodium at low temperature. Secondary sodium, which is not radioactive, is circulated by a mechanical pump with a flow delivery of 700 kg/s. It enters the IHX at 350°C (since 1993: 320°C) and leaves at 550°C (since 1993: 520°C). Each secondary loop is connected to a steam generator consisting of 3 stages (evaporator, superheater, and reheater) with 12 modules in each stage.

2.9.2. Plant operation

The Phénix plant was built to demonstrate the facility's overall capacity of operating over time while meeting expected characteristics. Being a demonstration reactor of what was supposed to become a new reactor technology - the sodium-cooled fast neutron reactor - operation data were to be collected to serve teams working in parallel to the project and the construction of the next-to-come reactor, Superphénix and later the European Fast Reactor (EFR) project. Right from the beginning, the reactor was also used as an irradiation tool: a considerable amount of data was gained on fuel and sub-assembly structural materials, leading to a significant increase of fuel burnup. The closing of the fuel cycle was also achieved for the first time in 1980.

In the 1990s, the importance of Phénix as an irradiation tool increased further as part of the CEA R&D programmes on long-lived nuclear waste management and development of advanced fuel for reactors of the future.

2.9.2.1. The early years (1974-1980)

The first two years of operation were characterized by an overall smooth running of the plant and a plant availability of 75% was reached. During this period, knowledge of the facility was developed and operating parameters were revised to increase outputs significantly in comparison to the initial project parameters. From 1976 to 1978, leakage detected in the intermediate heat exchangers led to lengthy periods during which the plant was operated at two-thirds of its rated power, which confirmed the possibility of operating the Phénix plant using only two of the three secondary cooling circuits without any restrictions whatsoever. From April 1978 to March 1980, the plant once again experienced two years of continuous operation at full-power without any noteworthy incidents occurring. The availability factor (Fig. 2.22) was increased, rising above 80% during this period (84.8% in 1979).

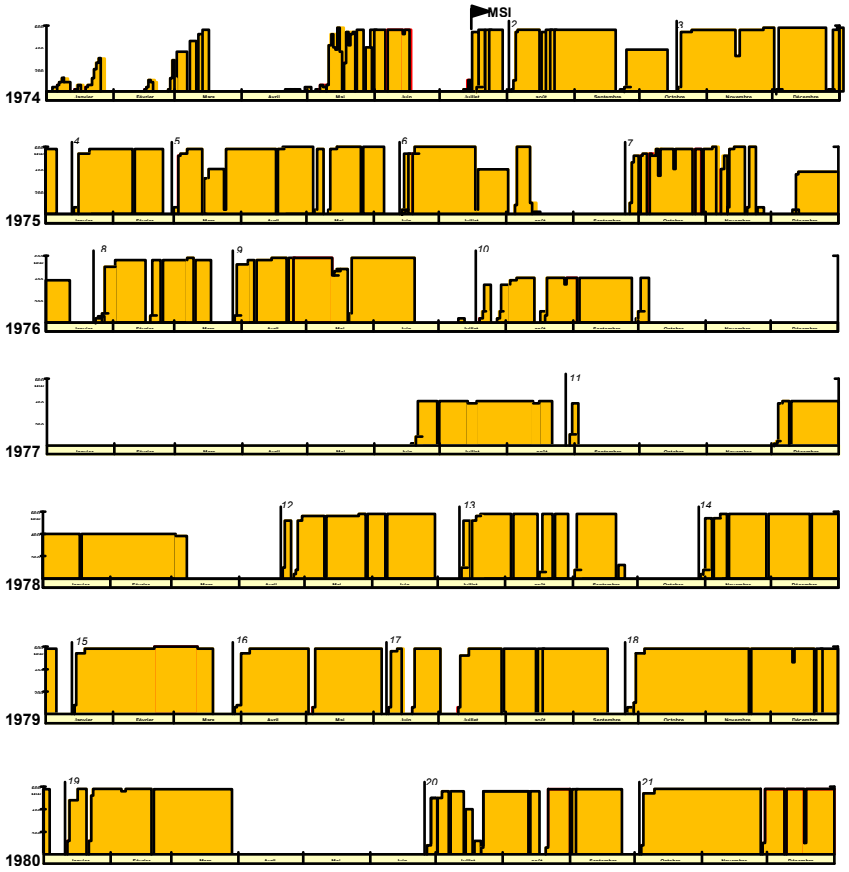

FIG. 2.22. Phénix availability factor during the early years (1974-1980).

2.9.2.2. Performance time (1980-1989)

After the success encountered during the early years, the challenge remained to operate the Phénix plant as stably and as continuously as possible. The operation teams thus focused to reduce the losses of availability of the plant, on preventive maintenance and constant improvements to the equipment and functions and on reducing reactivation time in the event of a shutdown.

In 1982 and 1983, four sodium-water reactions affected the reheater stages: the three steam generators were concerned. Once these incidents were solved, the plant was operated under good conditions: it continued to operate at full power until the second ten-yearly regulatory inspection and overhaul in spring 1989.

During this time, the plant improved on its own performances several times. 176 827 000 kWh were supplied to the electricity grid in January 1982. Between 25 August and 13 November 1983, the plant operated at full rated capacity for 81 days in a row. The plant topped the 10 billion kWh mark on 10 August 1982, and then went on to exceed 15 billion kWh supplied to the grid on 17 September 1986.

The total availability factor (Fig. 2.23) is slightly over 60% for the period between the industrial start-up (1974) and the second ten-yearly outage (1989).

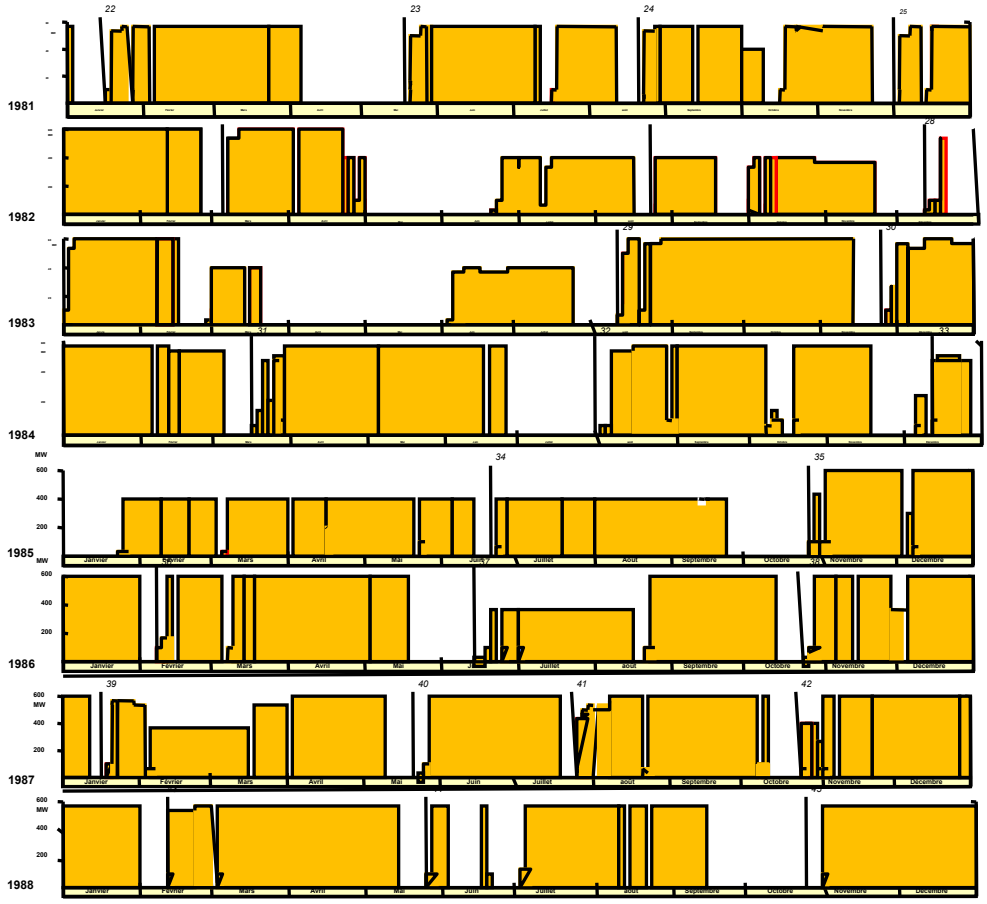

FIG. 2.23. Phénix availability factor during the performance time (1980-1989).

During this period, one-fourth of the time was at reduced power, in particular during the periods when the plant was operated with two out of three primary pumps or two out of three secondary circuits.

The plant's thermal efficiency reached 45.3% during the periods of stabilised operations: the best score held by any power plant of this generation, regardless of the plant's fuelling system (coal, petrol or nuclear).

2.9.2.3. Negative reactivity transients (1989–1993)

After the second ten-yearly regulatory inspection, the Phénix reactor experienced four extremely fast and high amplitude oscillations in the signal from the power range neutron chamber, which triggered automatic SCRAM when the negative reactivity threshold was reached. These four events, which took place in August and September 1989, then in September 1990, are labelled A.U.R.N. The first three occurred at a rating of 580 MW_{th}, and the last one at 500 MW_{th}, after operating periods between 4 and 15 days (Fig. 2.24).

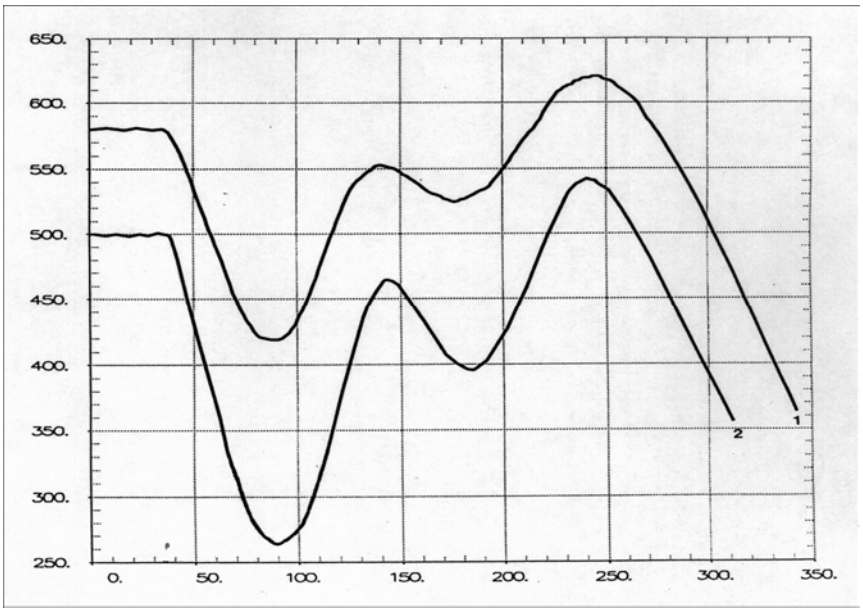

FIG. 2.24. The recordings from the power range neutron chambers, located beneath the main vessel, show a signal in the form of a double oscillation.

CEA then set up a very large investigation program, with the creation of a committee of experts, which presented at the end of 1991 the following two basic findings:

- The phenomenon which triggered the anomalies has not been clearly identified;
- However, there is a strong presumption that the variation in reactivity is due to a radial expansion of the sub-assemblies followed by a return to the centre (outward movement phenomenon).

The investigations have shown that the events were not the sign of internal reactor structure damage, in particular the core support structures, and that regardless of the mechanism initiating the incidents, there was no threat to reactor safety. With substantial reinforcement of the reactor surveillance, tests on instrumentation at very low power followed by a 10-day phase at power operation, the plant was authorized to resume operations.

Since 1991 monitoring of the reactor has increased in several fields: neutronic measurements, a SONAR device which follows the movement of the core sub-assemblies, acoustic detection in the core, measurement of the magnetic field in the vessel, structure displacement, specially designed fast measurement acquisition means, and special organization set up. There was no new negative reactivity transient event recorded. Further investigation into the cause of these transients is carried out in the framework of the Phénix end-of-life tests.

2.9.2.4. Safety upgrading and renovation phase (1993-2003)

From 1992, the role of Phénix as an irradiation facility emphasized the following: the reactor was necessary for irradiation experiments in support of the CEA R&D programmes on long-lived radioactive waste management in the context of line 1 of the 30 December 1991 law that French Parliament voted on this subject. An extension of the reactor lifetime by 720 EFPD (5 to 6 years) was then required and this necessity was again emphasized in 1997 with the announcement of the definitive shutdown of Superphénix reactor by the French Prime Minister.

In 1993, it was decided to pursue the operation of the plant with a maximum power of 350 MW_{th}. This new power (62% of the original nominal power) was sufficient for the irradiation experiments to be done. Consequently, only 2 out of the 3 secondary loops were necessary and the # 2 circuit was definitively stopped.

2.9.2.4.1. Seismic reinforcement

Following the seismic safety upgrade study, all the plant's buildings had to be reinforced especially the structural steelwork and the steel reinforcements in the reinforced concrete, but also disconnecting the buildings to prevent them from knocking together in the event of an earthquake. Special work was done inside and outside the reactor building. The most extensive reinforcement work was in the steam generator building.

All this work was done between January 1999 and August 2000.

2.9.2.4.2. Protection against sodium fires

Partitioning the steam generator building separated the area containing sodium pipes from the area containing pressurised steam or water pipes. The operation also separated the two secondary sodium circuits to be used in future (secondary circuit # 2 being abandoned).

The partitioning consisted of metal structures carrying insulating panels (about 1250). The first structural steelwork was put up in April 1999 and the work was completed at the end of January 2003. In addition, anti-whip devices were installed to prevent a failed pressurised steam or water pipe slapping violently against support structures; the work lasted from October 1999 to February 2001. All the steam generator casings were reinforced between March 1999 and April 2001, with a few final touches in late 2002.

2.9.2.4.3. Repair of the steam generators

From 1998, an inspection programme was run on the modules of the Phénix steam generators to assess their condition after 100 000 hours of power operation and make sure they were safe for the 720 effective full power days to come (about 30 000 hours). Examinations showed some cracks due to delay reheat cracking mechanism of the 321SS. The decision to repair the steam generators, and the method chosen, were validated in January 2001. The engineering work itself began in November 2001 and was completed in November 2002.

All in all, the repair of the steam generator modules required some 1500 welds, and about 8500 gammagraphy tests to check those welds

2.9.2.4.4. Inspections

As a requirement of the Safety Authorities, two major inspections (core support structures and core cover plug) had to be completed: any crack or disorder found might have led to definitive shut-down of the reactor.

These inspections were a first in the world and proved that inspecting the internal structures of a sodium reactor, although difficult, is perfectly possible.

The first major inspection, conducted between October and December 1999, was that of the welds on the conical shell supporting the core and connecting it to the main vessel. The method

chosen was inspection by ultrasound, a method developed especially for operation by CEA in 1998 and 1999. The inspection confirmed that there was no defect in the welds examined.

The core cover plug was examined by video inspection using optical devices on March and April 2001. The inspection concerned not only the outside of the core cover plug (external shell, bottom grid assembly, thermal shield bolting), but also inside, and some of the reactor block's internal structures: primary vessel, the penetrations of primary pumps and intermediate heat exchangers, etc. All the images obtained showed that the structures examined were in good condition.

Other verifications further demonstrated the good condition of the plant. In many cases the equipment used was purpose-designed. These operations revealed no abnormal defect after thirty years of operations.

2.9.2.4.5. Other work and innovations

The operating data acquisition platform, developed in 1991 to record parameters that might explain the negative reactivity trips, was replaced by a new system in 2001, as part of the renovation of the plant. Five hundred measuring channels are covered, at frequencies between 1 and 250 Hz. Acquisition of the most important measurements (80 channels) has redundancy. Reactor operation is only enabled if a minimum set of these measurements is operational.

Meanwhile, the computer handling fast processing of core temperatures (TRTC) and the computer handling centralised processing of information) from the plant to make it available to the operators in the control room (TCI have both been replaced by hardware of recent manufacture. The old and new equipments were tested in parallel throughout the 50th cycle before the old one was definitively stopped and removed from the control room.

2.9.2.5. Last operations period (2003-2009)

2.9.2.5.1. Preparatory work to resumption of operations

Early 2000, a specific organization was implemented to define and carry out exhaustive requalification tests of all equipment and circuits related to outage activities. Each component, affected by outage work, was tested phase by phase during specific test programmes.

During outage work, three quarters of the plant’s operational personnel were replaced. In terms of competencies, considerable effort was made to train staff, through on-the-job training, situational training and “apprentice coaching”, as well as conducting specific knowledge transmission classes and practical training using the Simfonix simulator. In parallel, more than a thousand different reactor control documents were updated.

2.9.2.5.2. Year 2003: restart of the reactor

Two sodium leaks occurred on March 2003 and May 2003. First, a valve bellow in the sodium purification circuit of the secondary circuit # 1 was no longer leaktight. Second, in May 2003, another sodium leak appeared in the electromagnetic pump of the steam generator # 3 hydrogen detection circuits.

Having issued the operational licence in January 2003 for the remaining six irradiation cycles, the Safety Authority then authorized to resume reactor power operations on 5 June 2003. The

reactor diverged on 15 June, the turbo-generator set was connected to the electric grid on July 4 and the plant reached its maximum authorised power of 350 MW_{th} on 6 July. The turbine clocked up its 100 000th hour connected to the electric grid on 1st September 2003.

The plant incurred its fifth sodium-water reaction on September 13, 2003. All the detection and automatic safety circuits functioned correctly. The faulty module was then removed and the pierced tube was assessed by CEA experts. All results were submitted to the Safety Authority for approval. In parallel, the module was replaced with a new module which was inspected and pressure-tested prior to installation. Permission to resume power was issued on 6 November 2003.

2.9.2.5.3. Years 2004 to 2007

Years 2004 to 2007 showed, on the whole, satisfactory operations despite some contingencies, which diminished the load factor and the production of electricity. During this period, an intensive programme of irradiations was carried out (see specific chapter).

In 2004, the electrical production was 626 GWh_e with an availability factor of 73%. The main contingency came from some disturbances on the SG evaporator module steam tube supports, seen by radiography. This contingency required obtaining further measurements and establishing a safety case to obtain the Safety Authority's authorization to start the next cycle with a programme of reinforced surveillance.

The year 2005 had excellent overall operation results: 262 days of equivalent rated power with more than 804 GWh_e produced and an availability factor of 85%. The main contingency which occurred was the insufficient load-bearing capacity of the complementary shut-down system. This led to replacing the system with its spare.

The reactor operation was excellent in early and late 2006 with an overall availability factor of 78% (192 days of operation). The main contingency came from the turbine (n°3 bearing, turning gear and the oil circuits) which led to a delay in restarting the plant after the outage of approximately 2 months. Furthermore, in October 2006, Phénix started to supply the Marcoule Centre with steam for its heating. These 6 680 tonnes of steam supplied in 2006 correspond to about 1 000 tonnes of CO_2 saved.

The year 2007 was the year of records:

- Phénix broke the European record of connection to the grid, for SFR: 151.2 days (153.34 critical days), beating its own record of 99 days which dated from 1990 and beating the Superphénix 122-day record which dated from 1996;
- The 54th cycle was Phénix's longest one without fuel reloading (96 EFPD);
- During this period, Phénix had its best electrical production in one go (without shutdown) with 510 GWh_e.

In August, the reactor was deliberately shutdown, following the discovery of a small sodium leak on a secondary loop pipe. This was three days prior to the beginning of the planned A8 outage. Finally Phénix ended with 184 days of operation, which represents a 69% load factor. The 23 000 tonnes of steam supplied to the Marcoule Centre for its heating account for savings of 3,600 tonnes of CO_2. The 2007 SFEN (French nuclear society) Grand Prize was awarded to the Phénix plant in recognition of its successful re-commissioning up to its record operational duration.

2.9.3. Feedback experience

During its 35 years of operation, Phénix encountered several events which are rich in terms of feedback for operating this type of reactors. In addition to those experiences identified earlier:

- Sodium leaks;
- Water-sodium reactions;
- Incidents on IHX;
- Clad failures;
- Sodium aerosols.

All these events, and others, led to losses of production. In Table 2.10 and Fig. 2.25, one will find the main reasons of these losses between 1974 and 1990. During this period, the average load factor was 59.6%.

TABLE 2.10. MAIN REASONS FOR THE EVENTS AT PHENIX IN 1974–1990

Item	Loss of power (MWh)	Loss of power distribution (%)	Loss of load factor (%)
Scheduled works	2268 287	15.1	6.14
Fuel handling (refueling)	1 675 540	11.2	4.54
Intermediate heat exchangers	4 142 673	27.6	11.21
Steam generator units	2 063 792	13.8	5.59
Turbo-generator and auxiliary circuits	1 077 502	7.2	2.91
Sodium leaks (not incl. IHX, SG)	390 230	2.6	1.06
Control rods	306 137	2.0	0.83
Fuel failure	145 725	1.0	0.39
Incidents during fuel handling	172 050	1.1	0.47
Sodium pumps drive	80 025	0.5	0.22
Computer systems	25 723	0.2	0.07
Control systems	247 964	1.65	0.67
Operator faults	49 145	0.3	0.13
Negative reactivity events	1 216 680	8.1	3.35
Miscellaneous (grid, tests)	1 129 891	7.5	3.1
TOTAL	14 991 361	100	40.58

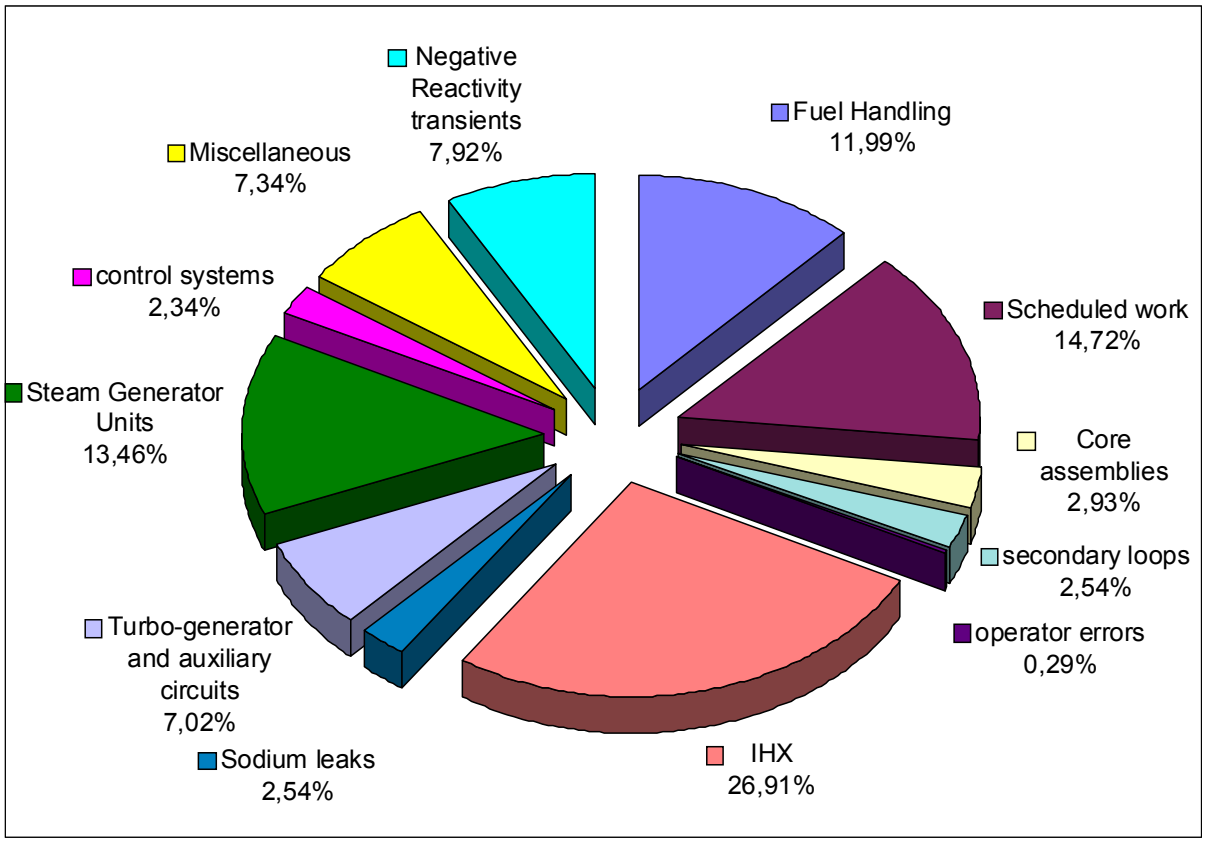

FIG. 2.25. Diagram of the main reasons for the events at Phénix in 1974-1990.

2.9.3.1. Sodium leaks

During its 35 years of operation, Phénix faced 31 sodium leaks with the following characteristics:

- The volumes of the leaks were from a few cm^3 to ~ 200 L;
- Very few primary sodium leaks (only small leaks on plugging-meters);
- Most of the leaks were located on welds of secondary loops and auxiliary circuits;
- The leaks were satisfactorily detected at an early stage;
- Usually no corrosion was found, except on one occasion when significant corrosion, due to a delayed detection, led to improvement of detection system;
- There were consequences on availability of the plant but never on its safety.

Table 2.11 gives an overview of sodium leaks from June 1973 to August 2007.

TABLE 2.11. SODIUM LEAKS FROM JUNE 1973 TO AUGUST 2007

Date	Plant conditions	Leak location	Detection method	Fluid and temperature	Leakage / corrosion	Cause
17 June 1973	Isothermal tests 400°C	Tee fitting on SG 3 auxiliary circuit	Fieldman	Na II 240°C	1 l – No corrosion	l = 20 mm crack on tee-to-pipe weld
18 Feb. 1974	Isothermal tests 400°C	Tee fitting on SG 2 auxiliary circuit	Fieldman then fire detection	Na II 240°C	Little quantity – No corrosion	Crack on weld
23 Feb., 1974	Filling up secondary circuit n°2	Plug on dilatation pot - SG 2 auxiliary circuit	Fieldman	Na II 180°C	Negligible quantity – No corrosion	Crack on plug-to-tube weld
20 Sept. 1974	Full power	SG 2 reheater inlet butterfly valve	Bead wires detection	Na II 550°C	20 L – Little corrosion	l = 200 mm crack on weld
14 March 1975	Full power	SG 2 reheater inlet butterfly valve installed in Oct. 1974	Bead wires detection	Na II 550°C	30 L	l = 60 mm crack on weld
16 July 1975	Full power	SG 2 inlet temporarily repaired butterfly valve	Bead wires detection	Na II 550°C	1 L	Crack on weld
11 July 1976	During power increase	Intermediate heat exchanger E (n°21) – Na II outlet header top plate	Fire detector	Na II ~ 550°C	10 L	Crack on top plate-to-internal shell weld
3 Oct. 1976	At 2/3 nominal power	Intermediate heat exchanger F (n°32) – Na II outlet header top plate	Spark plug detector	Na II 540°C	10 L	Crack on top plate-to-internal shell weld
31 Aug. 1977	At 2/3 nominal Power	Intermediate heat exchanger B (n°12) – Na II outlet header top plate	Spark plug detector	Na II 540°C	Slight leak	Crack on top plate-to-internal shell weld
April 22, 1982	Full Power	Secondary circuit n°1 “ACTINA” sampling circuit	Fieldman	Na II 550°C	Negligible leak	Leaking flange
16 Feb. 1983	Shutdown	SG 3 reheater rupture-disk mounting flange	Fieldman	Na II	Very slight leak	Leaking flange

Date	Plant conditions	Leak location	Detection method	Fluid and temperature	Leakage / corrosion	Cause
				250°C		
April 1983	Shutdown	Primary purification circuit: plugging meter #1	Fieldman	Na I 475°C	Negligible leak	Welding defect on temperature measurement thimble
1 Nov. 1983	Full Power	Primary purification circuit	Bead wires detection + aerosol detector	Na I ~ 475°C	Very slight leak	Welding defect
March 25, 1984	At 210 MWe	Intermediate heat exchanger C (n°31) – Na II outlet header internal shell	Spark plug detector	Na II 540°C	Very slight leak not evolving	Crack on weld on inner shell
6 Oct. 1984	Full power	SG 3 auxiliary sodium mixer – downstream elbow	Aerosols + fire detectors	Na II 430°C	Very slight leak – No corrosion	Crack on tee-to-mixer weld
16 Nov. 1984	Full power	Intermediate heat exchanger F (n°31) – Na II outlet header internal shell	Spark plug detector	Na II 550°C	2 l per day	Crack on weld on inner shell
5 May 1986	Full power	SG 3 reheater inlet tee	Bead wires detection	Na II 550°C	Several tens of litres + a few mm corrosion	Crack on weld
20 August 1986	Shutdown	Primary purification circuit : plugging meter #2	Bead wires detection	Na I	Very slight leak	Crack on weld
10 Oct. 1987	Full power	SG 3 hydrogen-detection circuit	Spectrophotometer + fire detector	Na II 475°C	A few litres	Crack on weld
14 Sept. 1988	Full power	Intermediate heat exchanger B (n°22) – Na II outlet header internal shell	Spark plug detector	Na II 550°C	Leak flow : 3 l/d - 0,7 l Na quantity	Crack on weld
12 Oct. 1988	Shutdown	SG 2 Na/H_2O reaction product discharge stack	Spark plug + fire detectors + spectrophotometer	Na II 180°C	~ 200 l	Leaking flange of discharge header

Date	Plant conditions	Leak location	Detection method	Fluid and temperature	Leakage / corrosion	Cause
May 1989	Shutdown	Na II purification circuit n°2 and 3 plugging meters	Fieldman	Na II	A few drops	Crack on weld
12 April 1991	Shutdown	Connection pipe between Na II auxiliary circuit n°2 and the mobile transfer station	Fieldman	Na II ~ 100°C	< 1 L	Leaking flange
June 1993	Shutdown	Secondary circuit n°3 Expansion tank(x 2)	Dye penetrant testing of the weld	Na II 350°C	A few litres – No corrosion	Crack on weld due to thermal stripping
13 Nov. 1998	Shutdown	Intermediate heat exchanger	Level drop in storage tank	Na II 250°C	~ 6 m^3	Intergranular crack on tubes
1 Dec. 2000	Shutdown	Intermediate heat exchanger H	Staff contamination by primary Na	Na I 180°C	~ 3 m^3	Intergranular crack on tubes
16 March 2003	Shutdown	Valve A1VR19	Spark plug detector	Na II 250°C	~ 20 L	Crack on valve bellow
4 May 2003	Shutdown	Electromagnetic pump of HD circuit #3	Spectrophotometer Na 101	Na II 180°C	~ 0.5 L	J3PG01 pump nozzle
18 August 2007	Full power	Secondary circuit n°3 Buffer tank downstream line	Bead wire detection on the weld	Na II 525°C	~ 1 L	
17 Feb. 2008	Full power	Electromagnetic pump of HD circuit #1	Spectrophotometer + fire detector	Na II 525°C	Negligible leak – No corrosion	Inlet of J1PG01 electromagnetic pump

2.9.3.2. Water-sodium reactions

During 35 years of operations, Phénix faced five sodium – water reactions:

(1) 29 April 1982 : SG2 re-heater module 12;
(2) 16 December 1982 : SG1 re-heater module 12;
(3) 15 February 1983 : SG3 re-heater module 12;
(4) 20 March 1983 : SG1 re-heater module 11;
(5) 13 September 2003 : SG1 re-heater module 12.

All of them were:

- On high ranked modules of re-heaters (four times module N°12 and once module N°11);
- Without the rupture of the disks;
- They led to numerous modifications and improvements on the circuits and the equipments.

The analysis of the first four incidents led to the following common observations:

- The reaction took place soon after a starting-up of the plant (< 5 days);
- The original failures are located at butt welds and on one of the 2 welds located at the hottest part of the tube.

The conclusions of the analysis were that the initial crack was due to a thermal fatigue phenomenon. The other effects were due to a wastage phenomenon:

- Piercing of the other linking tubes;
- Erosion on the shell.

As to the fifth reaction (September 2003), the origin of this incident was a manufacturing defect that evolved after cleaning of the module.

Many improvements and modifications were completed all along the entire life of Phénix to make the hydrogen detection systems faster and more reliable. These modifications were in various fields:

- Equipment: it's the field where the most numerous modifications were undertaken;
- Logic: to diminish the global response time and therefore to increase the sensitivity of the detection;
- Instructions for operators: for better behaviour towards such events.

Table 2.12 sums up the characteristics of all the five sodium-water reactions.

TABLE 2.12. CHARACTERISTICS OF SODIUM-WATER REACTIONS IN PHENIX

Na/H_2O Reaction N°	**1**	**2**	**3**	**4**	**5**
Number of leaking tubes	2	1	1	2	1
Wastage effect	Very important	Nil	Significant	Important	Significant
Scenario of the leaks	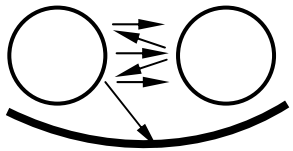	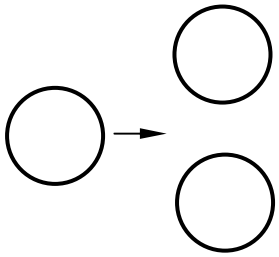	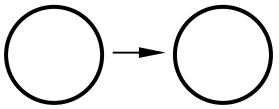	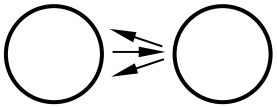	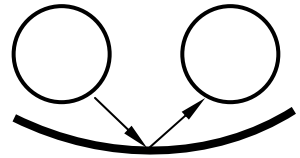
Section of holes on sodium side (mm^2)	13 + 60 + 90	7,4	7	6 + 35	24
Duration of the leak (min)	> 10	4	4	4	1,6
Estimation of the average leak flow rate (g/s)	20	12	5	12	20
Total quantity of water injected in sodium during the reaction (kg)	30 ± 8	3 ± 1	1,2 ± 0,3	4,1 ± 1,7	4 ± 1
Erosion on the Na shell	Yes on 1/4th of thickness i.e. 1,5 mm	No	No	No	Yes on 2/3rd of thickness i.e. 4,5 mm

2.9.3.3. Incidents of the intermediate heat exchangers

Concerning the intermediate heat exchangers (IHXs), Phénix faced eleven events of three types:

- Sodium leak in the inner space;
- Shutter command system jammed;
- Sodium leak in the tube bundle.

2.9.3.3.1. Sodium leak in the inner space

Sodium leaks from the Phénix IHXs took place at the secondary sodium outlet header: the thermal loading due to a difference of temperature between the inner and outer shells had been underestimated at the design stage.

All IHXs were repaired and design modifications were made:

- Addition of a mixer at the secondary sodium outlet from the tube bundle.
- Improvement of the flexibility of the IHX hot header between the top closure plate and the inner shell (Fig. 2.26).

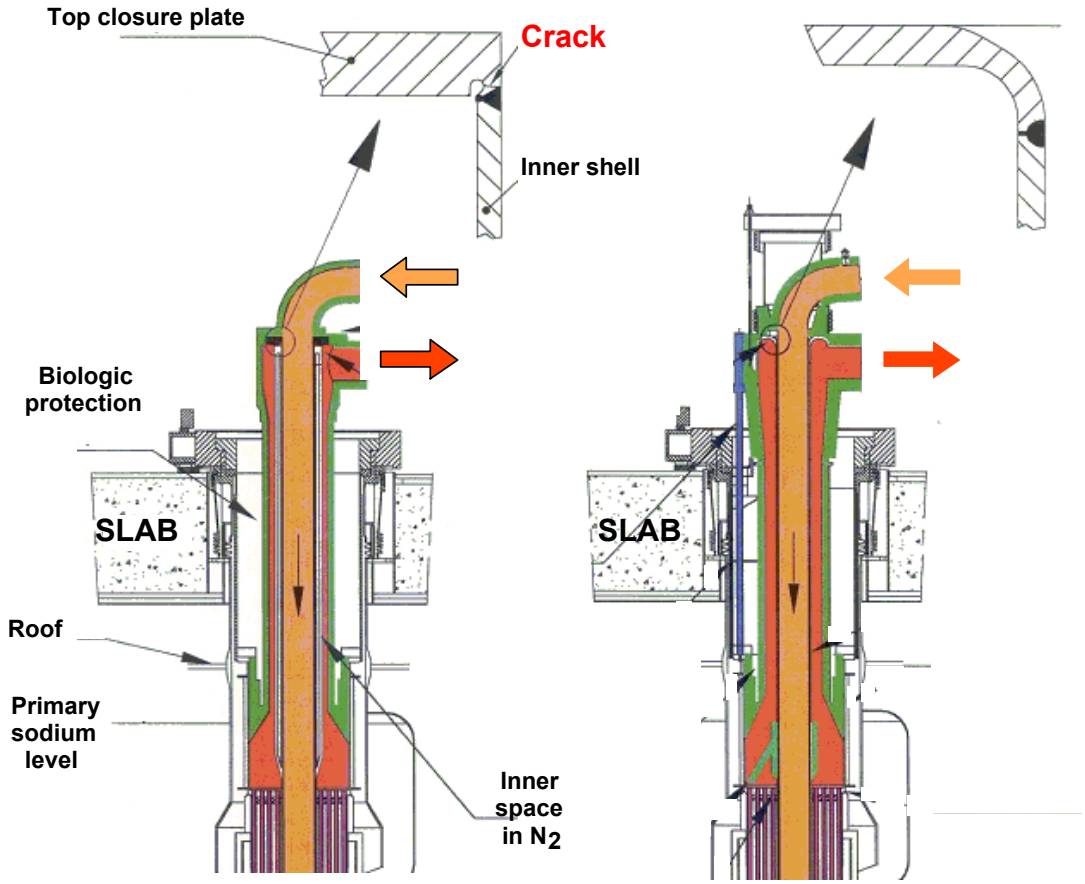

FIG. 2.26. Scheme of modification of connection between IHX top closure plate and inner shell.

2.9.3.3.2 Shutter command system jammed

Deposits of «mesos» were found in the lower part of the drive shaft, used to close the shutter, over a height of 500 to 1000 mm. These oxide mesos are produced by sodium aerosols in the presence of air and these mesos were the cause of the jamming. The modifications consisted in:

- Increasing the clearance between sleeve and drive shaft;
- Avoiding air ingress by efficiently sweeping the downcomers with gas;
- Carrying out operating tests on each drive shaft to «break» the solid mass of mesos as soon as it forms;
- Designing a new type of shutter command.

2.9.3.3.3 Sodium leak in the tube bundle

Two IHXs were found leaking:

- « I » IHX on 13 November 1998;
- « H » IHX on 1st December 2000.

The leaking tubes were found near the upper plate (Fig. 2.27).

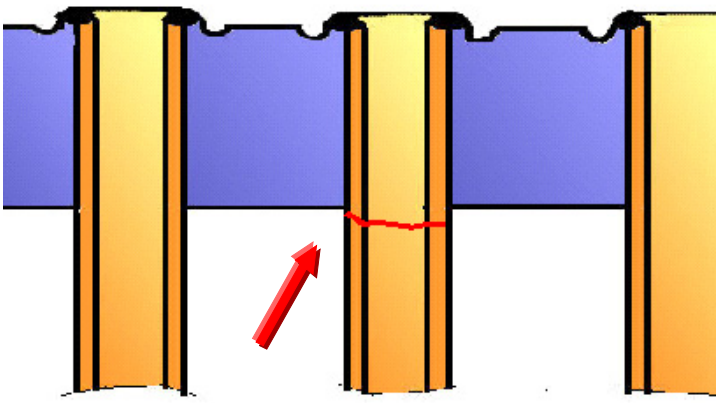

FIG. 2.27. Location of the sodium leaks in IHX tube bundle.

The result of metallurgical analysis was caustic stress corrosion due to the presence of polluted sodium hydroxide or sodium during the drained periods of the IHXs (air ingress during works on the secondary loop between 1995 and 1997).

2.9.3.4. Fuel behaviour

The fuel is uranium dioxide mixed with plutonium dioxide (UO_2-PuO_2). It is contained in about 110 hexagonal subassemblies, each containing 217 pins, which in turn consist of a stack of sintered oxide pellets, 5.5 mm in diameter, in stainless steel cladding. The pins are assembled in clusters in a stainless steel outer hexagonal shell, which also contains the upper and lower fertile blanket pins (depleted uranium oxide) and the upper neutron shielding.

The radial blanket is composed of depleted uranium dioxide pellets measuring 12.15 mm in diameter, in 90 assemblies of 61 pins each. The structural components of these subassemblies are identical with those of the fissile subassemblies, with sodium flow through the spike inserted into the diagrid.

Being a breeder reactor at the origin, Phénix closed the fuel cycle for the first time in 1980 and closed it 3 times altogether.

Due to improvements in the choice of specific steels, for wrapper and cladding, with low swelling properties, the average burnup increased from 50 000 MWd/t to 90 000 MWd/t (core 1) and 115 000 MWd/t (core 2) and even more than 150 000 MWd/t for some experimental subassemblies.

2.9.3.5. Clad failures

During the 35 years of operation, occurred:

- 15 fuel failures with delayed neutron signals (8 of them on experimental sub-assemblies);
- 11 gas leaks without neutron signal.

The detection and location systems have proved to be effective and reliable (location is based on sodium sampling from every fissile S/A outlet). They allowed an early detection and monitoring of the failures with, in most of the cases, a shut-down of the reactor before reaching the trip level. During these events, the contamination level of primary sodium was low (1200 Bq/g in ^{137}Cs). Table 2.13 shows the radioactive discharges from fuel failures.

TABLE 2.13. RADIOACTIVE DISCHARGES FROM FUEL FAILURES

Fuel failure	Date	Time		Maximal volumic activity of Ar gas blanket* (TBq/m^3)	Total released activity in Ar gas blanket* (TBq)	Total activity discharged to the atmosphere* (TBq)
		Gas leak	Fuel failure			
1	01.05.79	8 h	6 h	0.19	17.8	0.30
2	26.01.81	42 h	28 min	7.4×10^{-2}	17.4	0
3	09.07.81	39 min	8 min	0.19	**	1.9×10^{-2}
4	10.08.81	8 d	6 h 48 min	0.15	35.5	0.11
5	25.02.82	6 h 44 min	2 h 46 min	0.30	44.4	0.56
6	24.04.82	4.1 d	30 h	0.26	18.9	5.6×10^{-2}
7	07.10.82	52 d	1 h 31 min	3.7×10^{-2}	4.4	3.3×10^{-2}
8	21.05.85	8 h	51 h 30 min	3×10^{-2}	5.4	5.6×10^{-2}
9	29.10.85	< 4 min	6 min	1.1×10^{-2}	0.37	0
10	29.10.85	< 4 min	6 min	1.1×10^{-2}	0.37	0
11	05.03.86	7 min	36 h 12 min	0.3	24.4	0.63
12	03.08.87	380 d	123 d	0.15	**	0
13	21.08.87	602 d	18 d	0.15	**	0
14	02.03.88	64 h 30 min	48 h	5.6×10^{-2}	17.9	0.11
15	17.06.88	64 d	16 h	0.15	6.8	0

* This activity comes from leaks through penetrations of the slab
** Not evaluated

2.9.3.6. Fuel handling

Since 1974, Phénix has operated 178 spent fuel handling campaigns, representing:

- More than 10 000 movements;
- More than 15 000 hours of operation;
- Around 1 500 fuel assemblies dismantled (fissile or fertile).

These operations were performed without any major incident and their consequences, in terms of loss of power of the plant, were very small. No major component ever needed to be replaced. Some of the most significant difficulties are:

- Deformation under irradiation for fuel assemblies wrapper, initially made with austenitic steel, led to extraction / insertion difficulties. In such a case some of the surrounding assemblies had to be removed to the internal storage to complete the operation. This problem did not happen anymore with recent fuel assemblies with ferritic steel wrapper tube.
- Sodium aerosols accumulation led to significant maintenance operations (manual cleaning and removing of the sodium) on the lock valve on the fuel transfer ramp in 1980 and 1990, as well as on the transfer arm in 1993. The rotating plug operation was trouble free regarding aerosols deposits.
- Deterioration of a blowing seal led to a leak and pollution of the melting metallic seal of the rotating plug.
- Sodium/water reaction in the storage drum with a carrying assembly after washing in the hot cell.
- VISUS replacement after NaK leak on one of the wave-guides.

2.9.3.7. Sodium pumps

The primary and secondary pumps in Phénix are single input centrifugal pumps with radial suction and downwards-axial discharge. Some minor modifications were made during the early years such as modification of:

- The non return valve;
- The fixing of the shrinking ring on the hydrostatic bearing;
- Elimination of blind holes to prevent soda retention after cleaning.

After those modifications were completed, the performance of the pumps was good: the maximum number of operating hours for a primary pump is 220 000 hours. The number of unscheduled shutdowns caused by a primary pump is 21 and 24 by the secondary pump, essentially for electrical supply system reasons (failure of the thyristors from the motor speed variators). For the lifetime extension program, the pumps were completely refurbished: Parts of the pump were in good condition. Only manufacturing defects were found and those defects did not evolve during operation. Nevertheless, the non-return valve and moulded parts were replaced.

The upper bearing and tightness boxes represent a significant maintenance because of the checking of the quality of oil.

2.9.3.8. Sodium aerosols

Convection movements of the core cover gas, from hot areas, close to the level of sodium, towards colder zones carry sodium aerosols which can deposit on upper parts of the reactor.

This phenomenon led to jamming the IHX's shutter (see Section 2.7.3.3.2).

As to control rods, sodium aerosol deposits led to the partial blockage of some of them: this led to design modifications, improvements in the surveillance instrumentation, in the maintenance and in operation instructions. In particular, the latter includes periodic testing of the rods, even when the reactor is in operation.

However, no such phenomenon ever disturbed the rotating plug and all the systems and circuits used for fuel handling.

2.9.3.9. Radioactive impact

2.9.3.9.1. Staff radiation exposure

The radioactive level to which the personnel has been exposed is very low, for several reasons:

- The pool design of the reactor which confines the primary circuit.
- The near absence of fission products due to the small amount of clad failures, an early detection, identification and removal from the core.
- Good protection conditions, not only for fuel handling but also for big components like pumps or IHXs.

The main dose exposures result from specific inspections (storage drum, reactor vessel, etc.) or maintenance operations (fuel transfer devices, primary circuit, IHX, etc.): just in a few figures, there were 32 handling operation of IHXs and 22 of primary pumps; there were 17 decontaminations and repairs of IHXs, 7 of sodium pumps and 17 of CR mechanisms.

However, all these operations plus the normal operations of the plant only led to a total dose integrated by the personnel of 2.22 man-Sv (value cumulated from 1974 to the end of 2007), proving the radiological "cleanness" of this type of reactors. The diagram presented in Fig. 2.28 shows the dose evolution from 1974 to end of 2007.

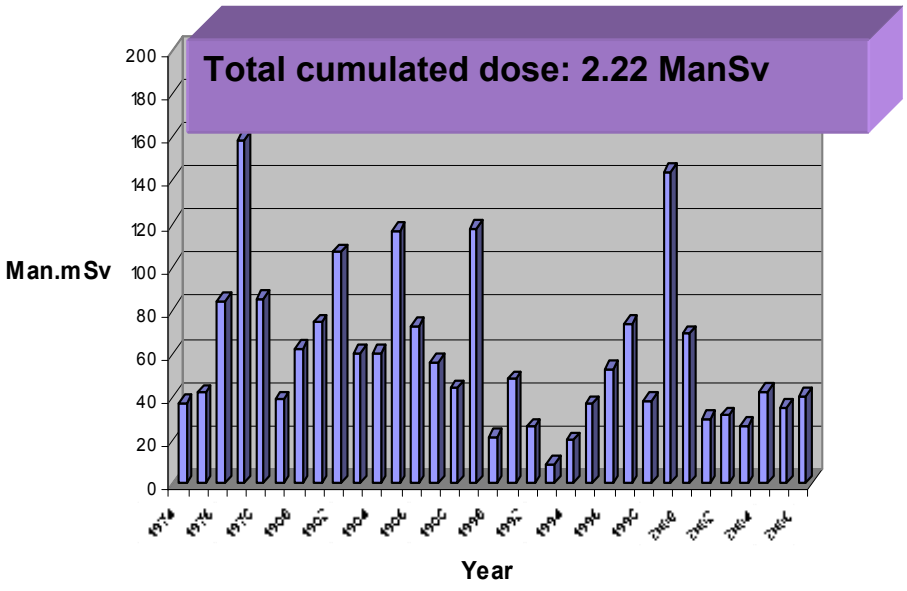

FIG. 2.28. Annual dose to the Phénix operators.

2.9.3.9.2 Liquid waste and gaseous discharge

Liquid wastes primarily come from subassembly, pump and IHX cleaning. They are not released directly from the plant but are transported to and treated by the facility which is on the Marcoule centre. Gaseous waste follows the activity from clad ruptures and is thus very low. Most of the time, this activity is at background level. Figures 2.29 and 2.30 show diagrams of these various activities.

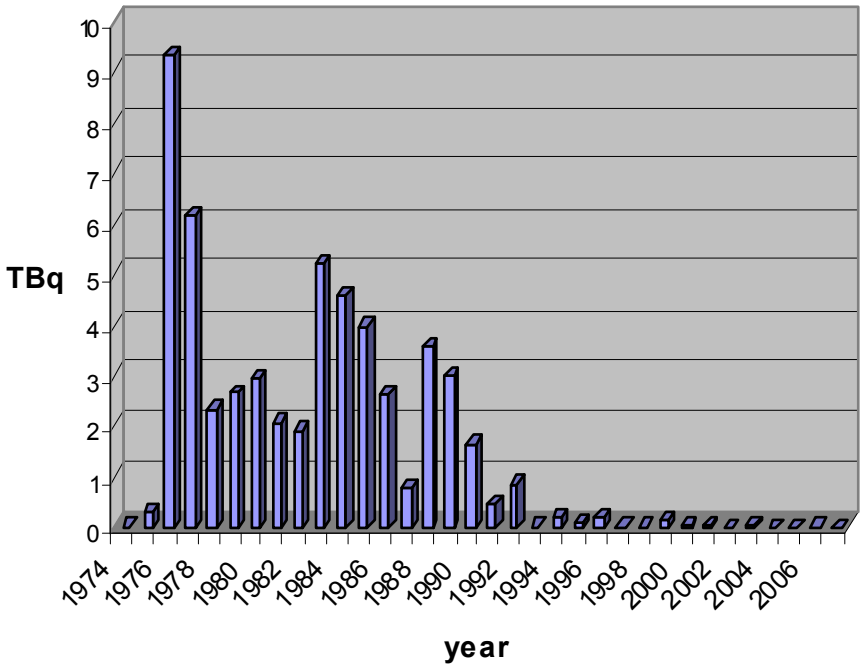

FIG. 2.29. Annual radioactive liquid effluent.

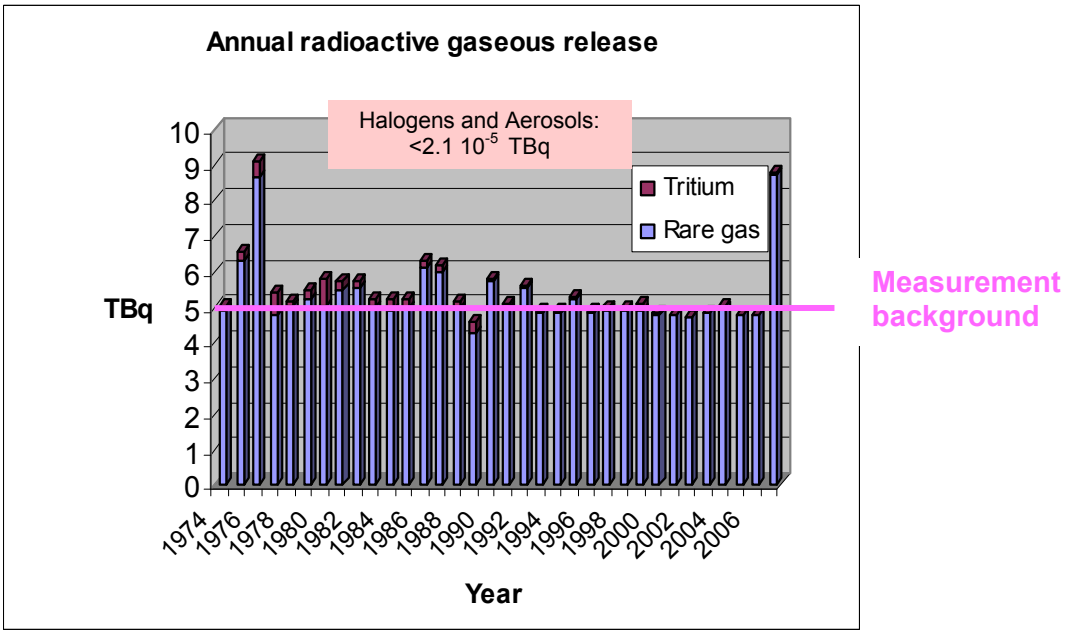

FIG. 2.30. Annual radioactive gaseous release.

2.9.4. The Phénix end-of-life-tests

2.9.4.1. Tests performed and test schedule

After 35 years of operation, a campaign of end of life tests was performed at Phénix before the final shutdown. The very first test was carried out in May 2008; however, most were performed after the end of the last electricity production cycle between May 2009 and January 2010. These tests aim to broaden the experimental base for validating neutron (ERANOS and DARWIN), thermal-hydraulic (TRIO_U and CATHARE) and fuel (GERMINAL) computer codes on the one hand, and on the other hand to provide a better understanding of the automatic shutdowns caused by a sudden drop in reactivity in 1989 and 1990. Ten different tests of four types were performed. The reactor conditions, test procedures and main measurements for each test are summarized in Table 2.14.

TABLE 2.14. THE PHÉNIX FINAL TESTS

Test	Initial reactor conditions	Test procedure	Main measurements
Thermal hydraulic tests			
Asymmetrical transient	Nominal*	Trip on one of the two secondary pumps producing a localized hot shock in the primary cold plenum.	Standard sodium temperatures and cold plenum thermometer pole.
Natural convection	120 MWth	Primary pumps trip then secondary pumps trip	Standard sodium temperatures and cold and hot plenum thermometer poles
Core physics tests			
Decay heat	Nominal	Scram	Standard sodium temperatures.
Control rod offsetting	Nominal	Radial power profile distortion by individual control rod movements	Standard sodium S/A outlet temperatures and control rod positions
Subassembly reactivity worth	Zero power	Criticality for different fuel, blanket and sodium S/As with different burnup in the core central position	Control rod positions Core reactivity
Control rod worth	Zero power	Control rod worth measurements by different static and dynamic methods	Control rod positions Core reactivity
Sodium void	Zero power	Criticality with a gas reservoir at different axial positions replacing a control rod	Control rod positions Core reactivity
Fuel test			
Partial fuel melting	300 MWth	Power increase from 300 MW to 370 MW in 3 minutes	Thermal power
Negative reactivity transient investigations tests			
Experimental carrier/blankets interactions	100 MWth	Temperature and sodium flow measurements on individual S/As for different power and primary flow levels	Thermal power Sodium flow in the DAC S/A Sodium outlet temperatures in DAC and blankets S/As Dose and maximum temperatures reached in the DAC S/A
Core flowering	Zero power	Reactivity effect of externally induced core flowering.	Control rod positions Core reactivity Mechanical device radial displacement

*Nominal: 350 MWth, 140 MWe

The year 2009 was mainly devoted to the tests along with finalizing the safety analysis documents, discussions with the IRSN (French Institute for Radioprotection and Nuclear Safety), technical support of the ASN (French Nuclear Safety Authority), finishing the fabrication of the experimental devices, operator training and performing the tests themselves, as per the schedule shown in Fig. 2.31.

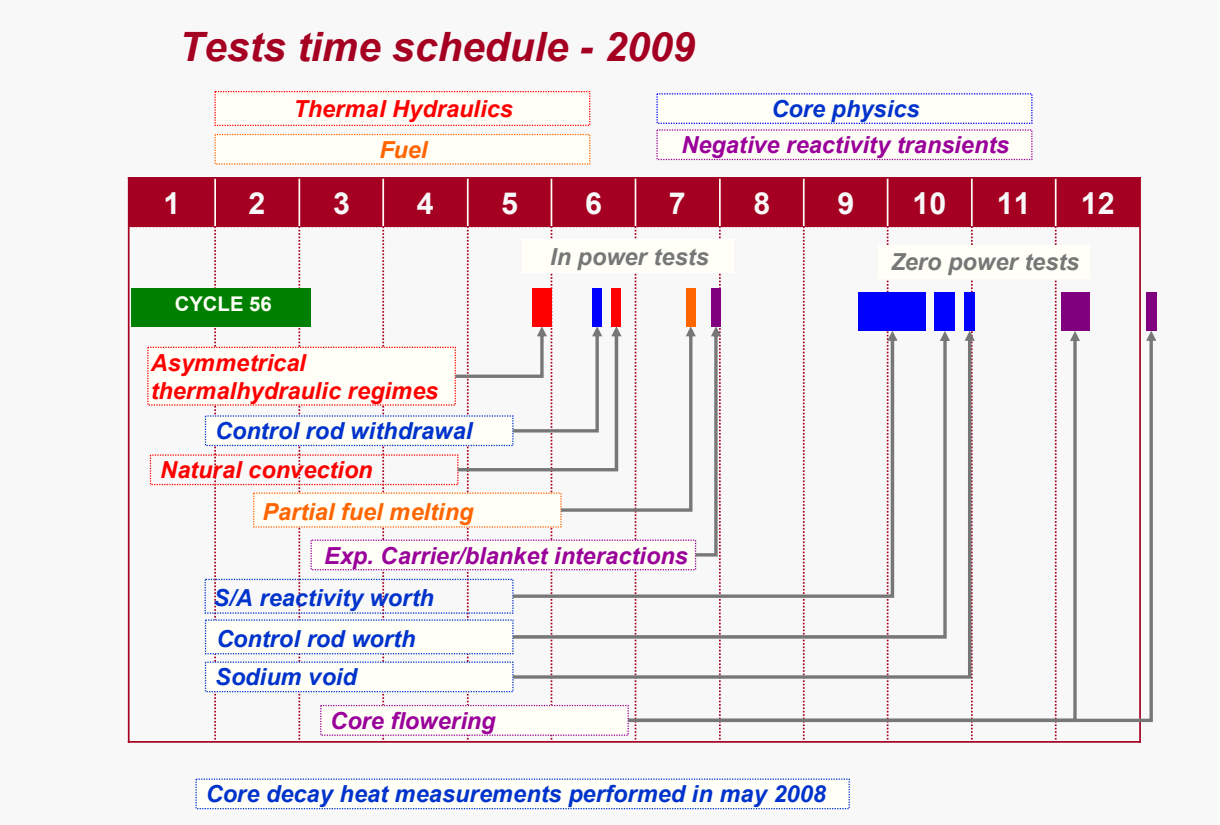

FIG. 2.31. Test schedule.

These tests were divided into two main phases: tests with power until the end of July, then tests with no power, which no longer require the use of the steam generators.

2.9.4.2. Special devices and training of personnel

Before conducting final tests on the reactor, considerable work was done to prepare the special devices required for these tests such as the COLTEMP temperature measuring pole qualification, the manufacture and acceptance of the cold plenum thermometer pole, the manufacture and tests on the mechanical device used for the core flowering tests and the installation of additional thermocouples on the secondary loops as well as temperature and air velocity measurements in the SG stacks. A thermal-hydraulic pole fitted with thermocouples and an Eddy current flowmeter (provided by IGCAR), enabling to monitor changes to individual flow rates of a sub-assembly was fabricated (Fig. 2.32).

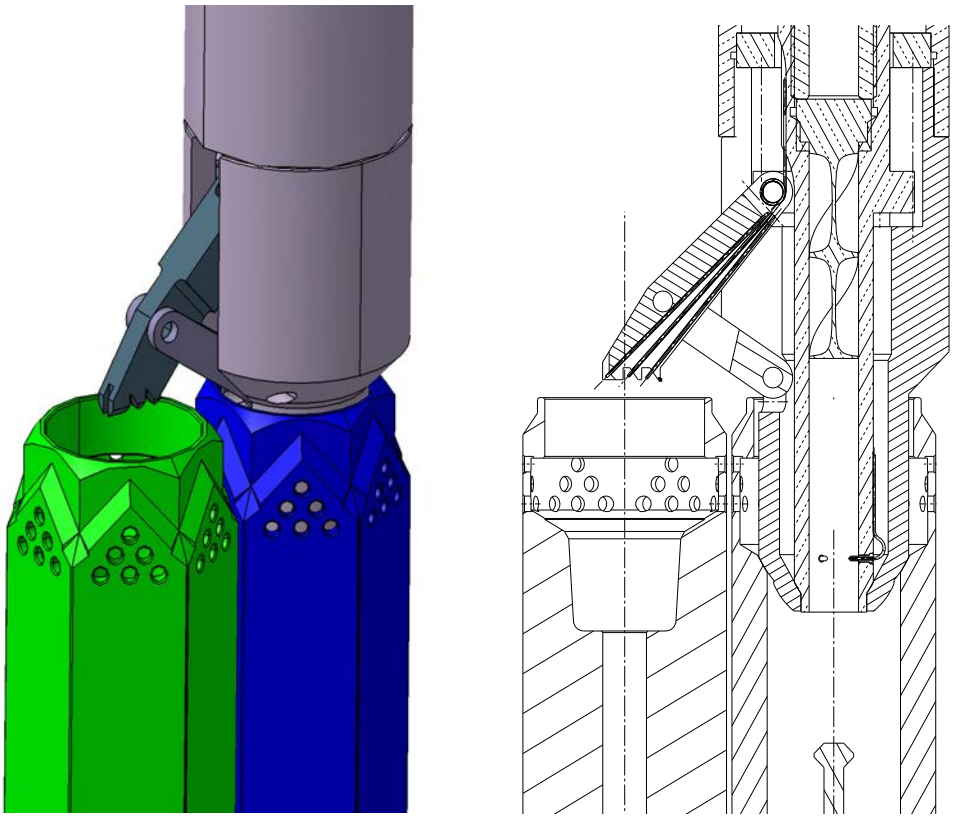

FIG. 2.32. Thermal-hydraulic measuring pole on the DAC.

Regarding the objects introduced into the core, an experimental sub-assembly with moderator (DAC) (Fig. 2.33) was modified to make it similar to those in the core in 1989 and 1990. A control rod was also modified so as to fit it with a helium-filled tank to measure the effect of partial drainage of sodium from the core.

FIG. 2.33. Experimental sub-assembly with moderator (DAC).

In agreement with the ASN, a training programme for the operating teams was set up. It consisted of presenting the operators with the test aims, their sequencing and related risks. To ensure successful testing, this programme also saw the operators take part in drawing up the operational documents, called Trial Instruction Programmes, as well as in running sessions on the SIMFONIX simulator, when this was possible.

2.9.4.3. Main results

2.9.4.3.1. Thermal hydraulic tests

Test # 1: Asymmetrical transient

Asymmetrical transient tests were obtained by tripping one of the two secondary pumps. The lack of cooling creates a cold shock in the cold plenum of the primary vessel at the outlet of the two intermediate heat exchangers (IHX) connected to the corresponding secondary circuit (Fig. 2.34).

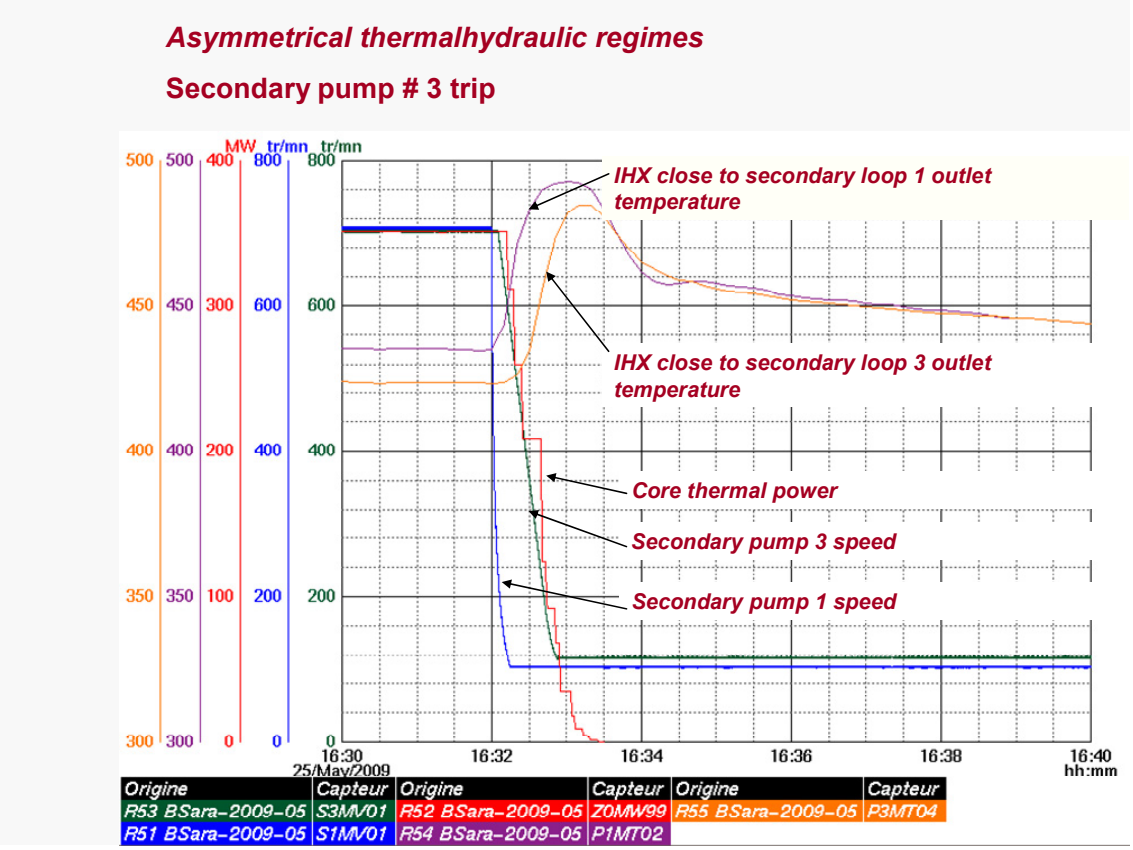

FIG. 2.34. Asymmetrical transient test – primary parameters.

The axial temperature distribution was recorded by the implemented new thermal pole (Fig. 2.35). The azimuthal distribution is also recorded by the standard reactor instrumentation giving a large data base for the qualification of thermal hydraulic codes.

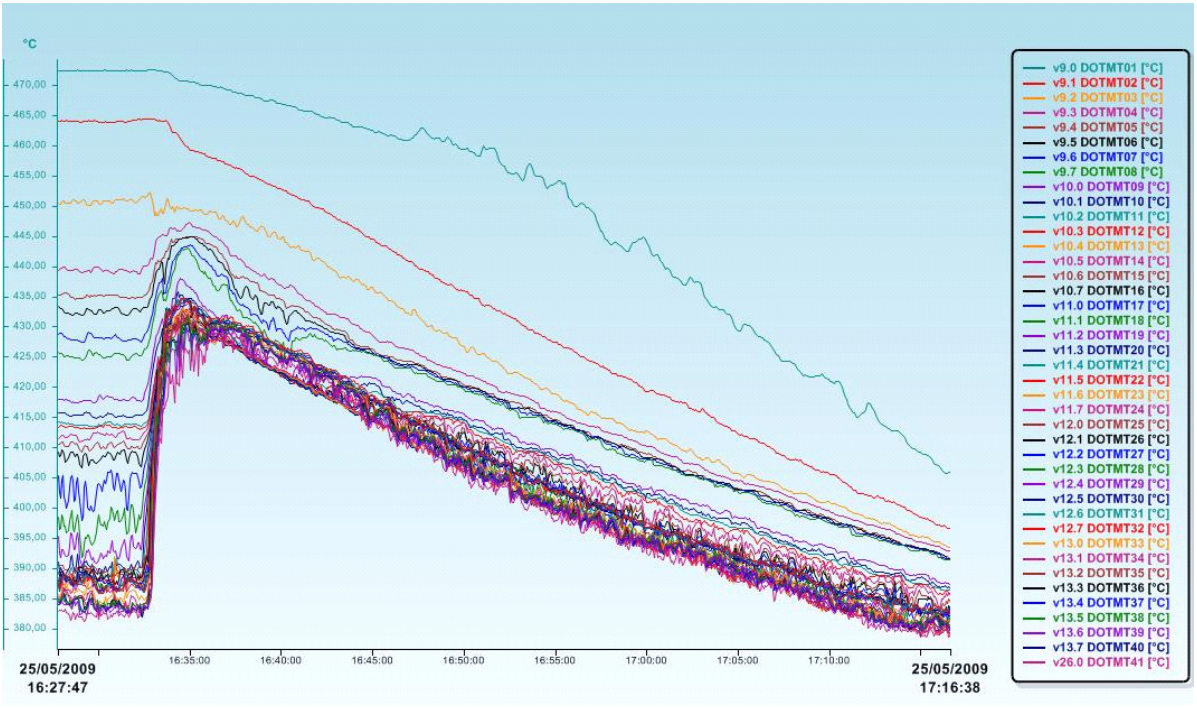

FIG. 2.35. Asymmetrical transient test – cold plenum thermal pole measurements.

Test # 2: Natural convection

For this test, all three primary pumps were tripped just after reactor scram. In a second phase of the test, the pump of one of the secondary circuits was also tripped (Figs 2.36 and 2.37).

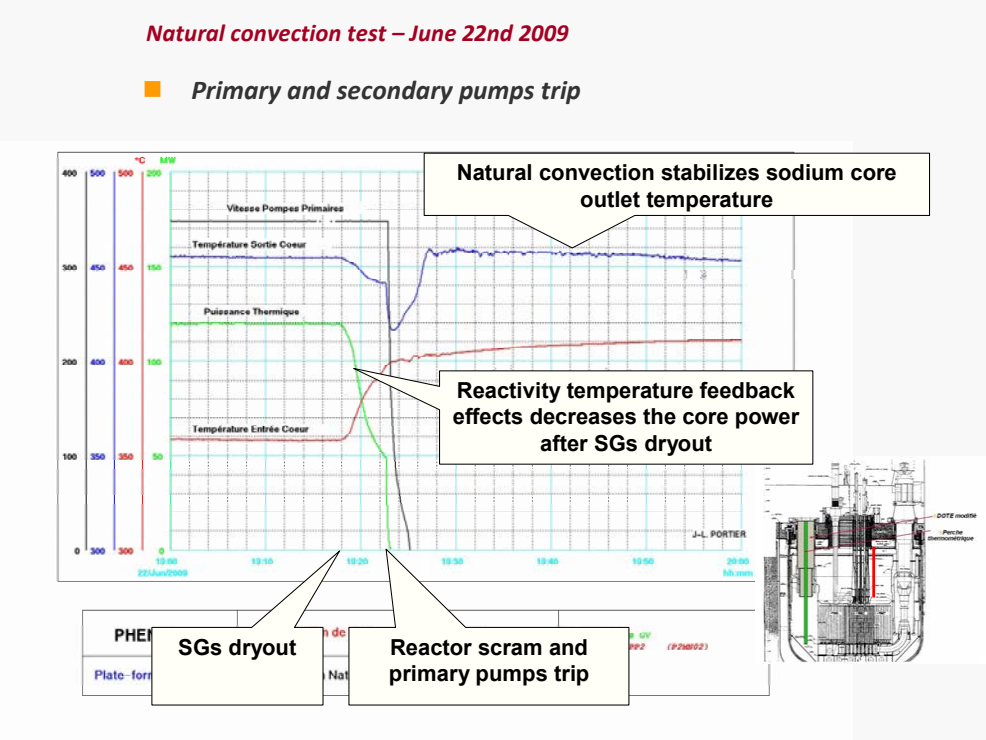

FIG. 2.36. Natural convection test – primary parameters.

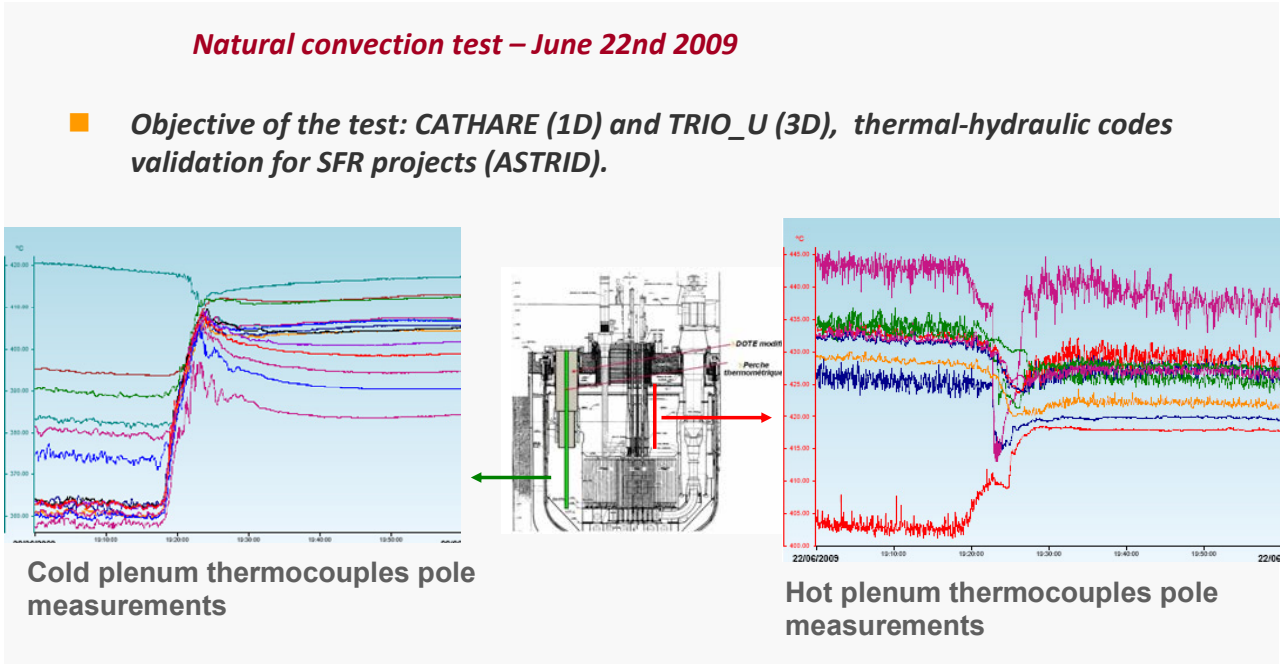

FIG. 2.37. Natural convection test – cold and hot plenum thermal poles measurements.

In the first phase, decay heat was removed first by thermal losses, and then by air natural convection through the steam generators casing. In the second phase, decay heat was removed by thermal losses. An international benchmark was launched by IAEA on this test.

2.9.4.3.2. Core physics tests

Test # 3: Decay heat

A calorimetric method based on the thermal balance of reactor circuits was used.

$$I\, d\Theta/dt = Dh + Sp - Tl$$

I: Thermal inertia of the whole system
Θ: Mean sodium temperature
Dh: Decay heat
Sp: Supplied power by other sources (pumps…)
Tl: Thermal losses

Using the sodium temperature measurements between 2 hours and 12 days after the reactor scram, the core decay heat was calculated with this equation.

Test # 4: Control rod offsetting

The aim of the "Operating with offset rods" test, carried out at the plant on 15–16 June 2009, was to study the influence of control rod position on the spatial distribution of power within the core. During the test the control rods were progressively offset in relation to each other while maintaining stable the total power. Four control rod configurations were studied:

(1) Six control rods in a curtain, within ±2 mm;
(2) Five rods in a curtain and one rod offset to –267 mm in relation to the curtain;
(3) Four rods in a curtain, one rod offset to –229 mm and another to +279 mm;
(4) Five rods in a curtain and one rod offset to +325 mm in relation to the curtain.

The deformations of fissile sub-assembly heat maps were measured. The deviations measured locally at the largest offsets were in the order of 10% (Fig. 2.38).

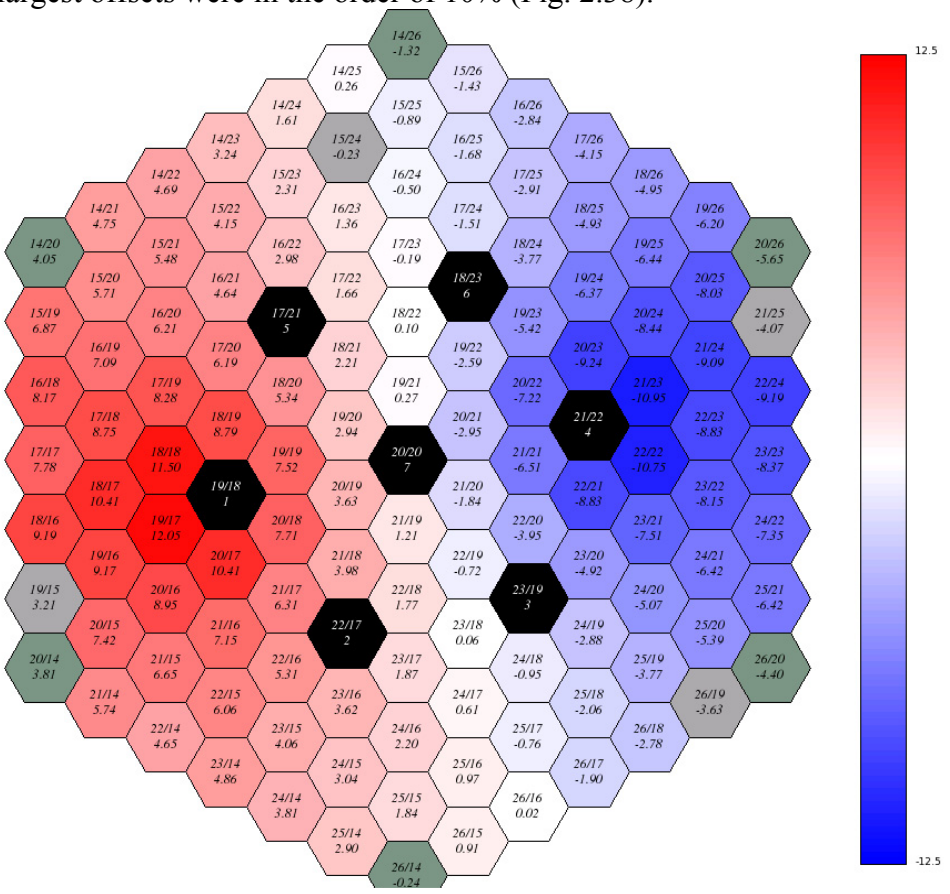

FIG. 2.38. Raw deviations measured during the maximum offset configuration (%).

The interpretation of the sub-assembly temperature measurements helped trace back to power and flux distribution deformations created by offsetting the control rods. In the final analysis, these results will provide the neutronic computer code qualification bases, required, in particular, in the design of future 4th Generation reactors. An international benchmark was launched by IAEA on this test.

Test # 5: Subassembly reactivity worth

The reactivity effect of fissile and fertile, fresh or spent sub-assemblies could be measured by substitution in the central position of the core (20-20). Six different configurations were studied:

(1) 1 standard fissile sub-assembly with high burnup;
(2) 1 fresh standard fissile sub-assembly;
(3) 1 experimental fissile sub-assembly (with low Pu content);
(4) 1 sub-assembly without fissile material (only sodium and steel);
(5) 1 fresh blanket sub-assembly;
(6) 1 blanket sub-assembly with high burnup.

The reactivity worth of these sub-assemblies was determined by measuring the critical height, with the worth of the control rods being reassessed at each configuration. The data acquired will provide the neutron computer code qualification bases.

Test # 6: Control rod worth

A control rod worth measurement test was performed from 17–22 October 2009, in core configurations representative of future Generation IV reactors. This test consisted of using different methods to measure the worth of control rod absorbers, by:

(i) Static methods when the reactor is subcritical;
(ii) Rod balancing when the reactor is critical;
(iii) Rod drop measurements (partial rod drop) (Fig. 2.39).

This test required:

- 31 approaches to criticality;
- 10 torque balancing measurements;
- 6 measurements per period;
- 24 rod drops from different heights (250 mm and 350 mm) (Fig. 2.39);
- 92 subcritical situations;
- 1 slow convergence (convergence time > 40 minutes).

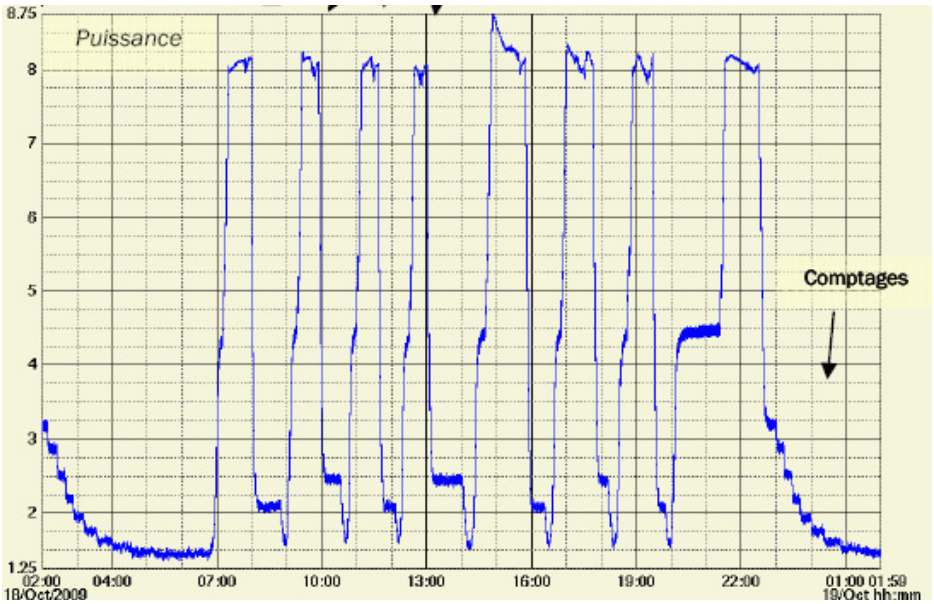

FIG. 2.39. Change in neutron flux during rod drops.

The data acquired during this absorber weighing campaign will be used to inter-compare the various experimental methods and provide the neutronic computer code qualification bases.

Test # 7: Sodium void

The assessment of the reactivity effect of introducing a gas bubble into the core of a sodium cooled fast neutron reactor is a key issue in the safety studies of future reactors using this technology. The final tests of the Phénix reactor represented a unique opportunity to experimentally check and to validate calculations made by the neutronic codes for such safety studies. The principle of the test was to simulate the displacement of a gas bubble in the core

by replacing the B_4C absorber contained in a control rod by a helium-filled tank Several measurement methods were applied to determine the reactivity effect of this helium tank the reactor being critical:

(i) Measurements by balancing the helium rod against the control rod;
(ii) Dynamic parameter measurements, monitoring the change in reactivity according to the continuous displacement of the helium "rod";
(iii) Measurements by helium "rod" drop.

The data acquired will provide static (ERANOS…) and dynamic (SIMMER…) neutronic computer code qualification and validation bases.

2.9.4.3.3. Fuel test

Test # 8: Partial fuel melting

Three rigs, specially designed to produce partial fusion of the fuel during a power ramp (Fig. 2.40), containing fuel pins at 0 at%, 4 at% and 8 at% burnup with and without central hole, were introduced into the core. The corresponding test took place in July 2009 and was fully controlled by the operating teams. Subsequent post irradiation examinations should give the full measure of the results. A fuel melted fraction of approx 10% in mass is locally expected at the maximum neutron flux axial level for some pins. These results will be used to complete the validation database of the fuel thermo-mechanical behavior code GERMINAL.

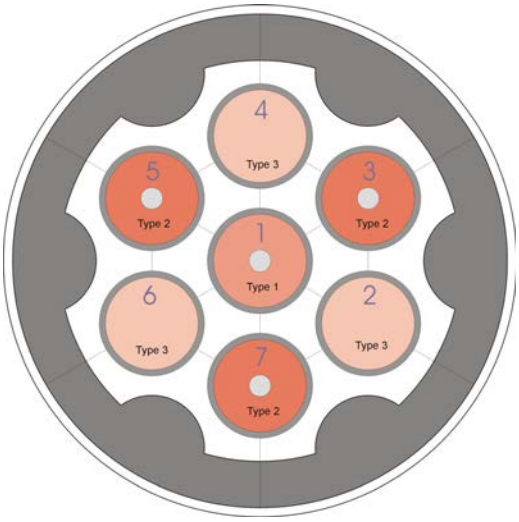

FIG. 2.40. Rig for partial fusion of the fuel.

Negative reactivity transients investigations tests

The most plausible scenario to explain the negative reactivity transients occurring in 1989 and 1990, consists of imagining that the core sub-assemblies sustained radial movements.

Test # 9: Experimental carrier/blankets interactions

One of the reasons for such movement would be the implosion of a sodium vapour bubble subsequent to its boiling in hot areas of the core at the level of experimental sub-assemblies (DAC) surrounded by blanket sub-assemblies. Such a configuration was reproduced

(Fig. 2.41) and flow rates as well as temperatures in the sub-assembly were recorded, at the end of the in power test period.

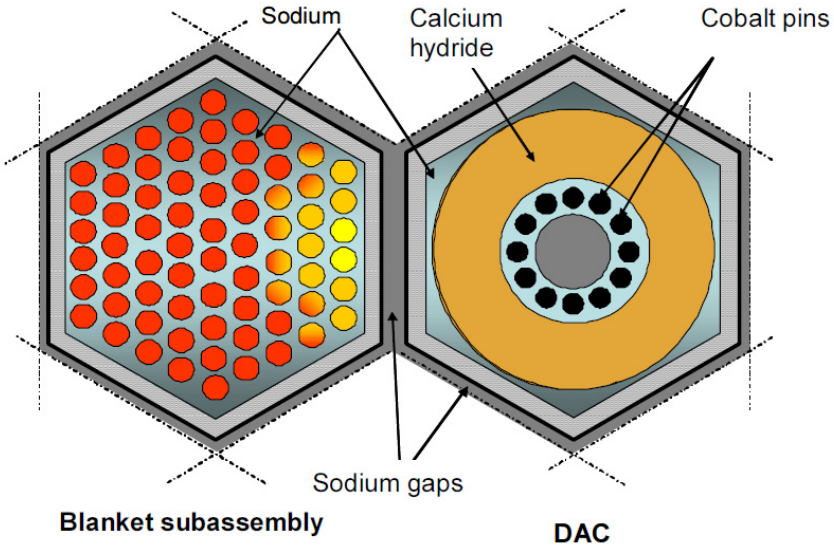

FIG. 2.41. "Blanket - DAC" configuration.

Special measurements of the sodium massflow inside the experimental DAC S/A were carried out with an Eddy current flowmeter developed by IGCAR at Kalppakam, India. During this test, thermal balances of both S/A were made at different sodium massflow regimes. With the help of detailed neutronic and thermal hydraulic models, the right effects of moderation on the blanket power and the thermal exchanges between S/A will be determined.

Test # 10: Core flowering

Furthermore, the reactivity effect of such radial movements was more closely identified by pushing apart the sub-assemblies, using a specific device (Fig. 2.42), at the end of the test period at zero power.

FIG. 2.42. Device to push apart sub-assemblies.

The mechanical device was placed at two different core positions: at the center and at the periphery. The effect of core flowering was measured at different temperatures in the range 180°C to 350°C. The mechanical behaviour of the core was close to what was expected. Very small changes on core radius give significant reactivity modifications, around -60 pcm/mm in case the device is operated at the central position. This effect is strongly reduced at the peripheral position of the device. The core compactness was not significantly affected by the temperature level.

2.9.4.4. Further steps of the programme

Now begins a new phase of in-depth interpretation of the test results by the DEN facilities at the origin of the request. Consequently the neutron physicists, thermal-hydraulics experts and fuel specialists will be able to capitalize on these results to complete the validation of the corresponding computer codes, ERANOS and DARWIN for neutronics, TRIO U and CATHARE for thermal-hydraulics and GERMINAL for fuel. The young engineers, specially recruited at CEA to prepare and conduct the tests along with the plant's teams, will join the fast reactor projects at CEA Cadarache center in their respective areas of specialization after having experienced a unique period in their professional career.

2.9.5. Conclusions

The 35 years of Phénix operations have brought a significant contribution to the development of fast reactors. It has fulfilled its original objective to demonstrate the viability of sodium-cooled fast reactors and has been throughout its lifetime an outstanding tool for fuel development and for conducting a wide range of irradiation experiments, in particular for minor actinide transmutation. Among many items, one can mention:

- Sustained operations were achieved at high load factor, given the prototype feature of the reactor, with gross thermal efficiency up to 45%.
- The reactor proved to be easy to operate with simple neutronic control and a large thermal inertia resulting from the integrated concept.
- Big primary components could be validated and their maintainability was demonstrated through a number of operations involving unloading of the component, cleaning and decontamination, repair or modification, requalification and reloading.
- Valuable experience was gained from sodium leaks and sodium-water reactions. It proved the efficiency of the protection against these events and it allowed further improvements of prevention, detection and mitigation.
- With a burnup doubled, the closing of the fuel cycle, the fuel was improved. Operation with failed fuel proved robustness of the fuel and benign consequences of failures.
- 35 years of operation provided a large amount of data on material behaviour and structural design.
- A unique experience of safety upgrading and lifetime extension programme that included some first-in-the-world inspections of reactor internal structures.
- Operations and maintenance of the plant only led to a total dose integrated by the personnel of 2.22 man-Sv (value at the end of 2007) proving the radiological "cleanness" of this type of reactor.

In the coming years, the valuable information collected during the end of life tests will serve as an experimental basis for core physics, thermal hydraulics and fuel issues; for investigations of the negative reactivity transients which occurred in 1989 and 1990; and for the programme to validate a wide range of sodium fast reactors computer codes.

2.10. PFR operating experience

2.10.1. Design features

The Prototype Fast Reactor (PFR) was built and operated at the United Kingdom Atomic Energy Authority's (UKAEA's) site at Dounreay in Scotland to validate and provide operational experience of a large pool-type fast reactor and as a test bed for the fuel, components, materials and instrumentation needed for an eventual commercial-sized station. It represented the climax of a programme which began in the early 1950s to ensure long-term security of the nuclear component of the UK's electricity supplies, should eventual shortages of new supplies of uranium limit the deployment of thermal reactor stations. As an initial experimental stage in this programme, a decision was made in 1954 to build the 60 MW_{th}, 15 MW_e Dounreay Fast Reactor (DFR), which subsequently operated from 1959 to 1977. The information and experience gained from DFR provided the necessary confidence that a commercial-sized fast reactor could be successfully built and operated. However, because a large increase in size between DFR and a commercial plant was necessary, the need for an intermediate plant incorporating the major steps in concept and scale was identified.

Thus, in 1966, approval was given for the building of PFR on land adjacent to DFR. PFR was designed to produce 250 MW_e from 600 MW_{th} core power and its design incorporated lessons learnt from the operation of DFR. DFR had used a 70-30 NaK alloy as coolant; PFR would use sodium which was less expensive and easier to handle. Coolant flow would be upwards through the core (in DFR the flow was downwards) to avoid gas entrainment. The fuel would be a ceramic - a mixed plutonium-uranium oxide in sealed stainless steel clad pins (in DFR the driver fuel was a vented enriched uranium method alloy) to achieve higher bum-up and to keep the coolant relatively clean. The sodium pumps would be mechanical centrifugal pumps (electromagnetic pumps were used in DFR) to obtain higher capacity in compact units. Finally, the steam generators (SGs) would be of an advanced highly-rated tube-in-shell design (whereas those in DFR were of a low-rated, double-walled matrix design). First criticality was achieved on 3 March 1974 and operation continued until 31 March 1994. Figure 2.43 shows the general arrangement of the reactor and the stern raising plant and Fig. 2.44 shows a cross-section of the primary circuit [24].

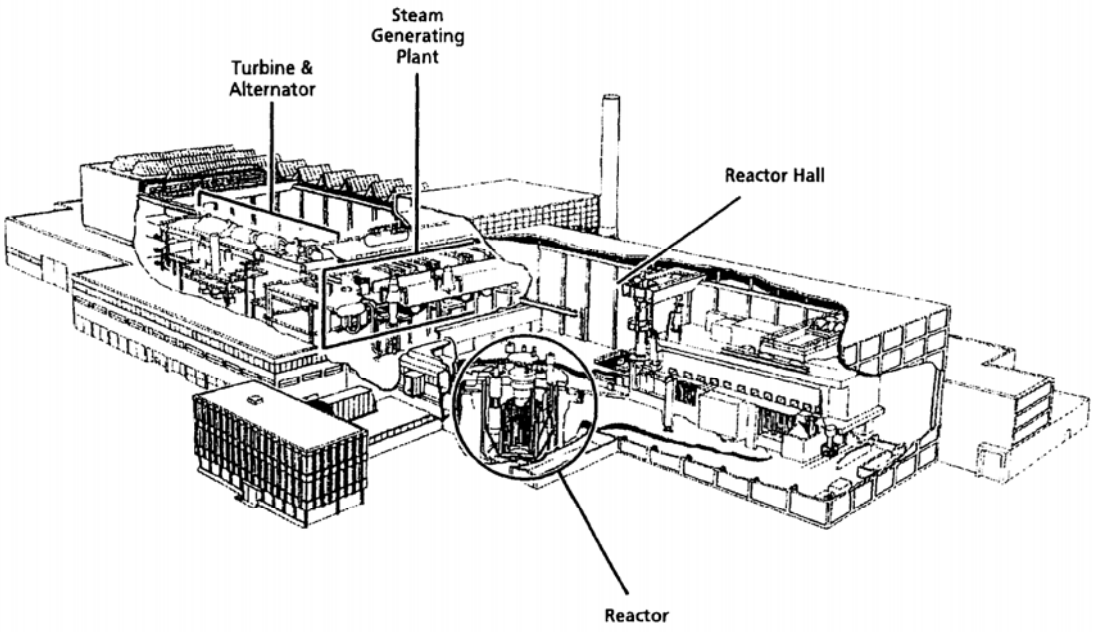

FIG. 2.43. PFR General arrangement of the reactor and steam generating plant.

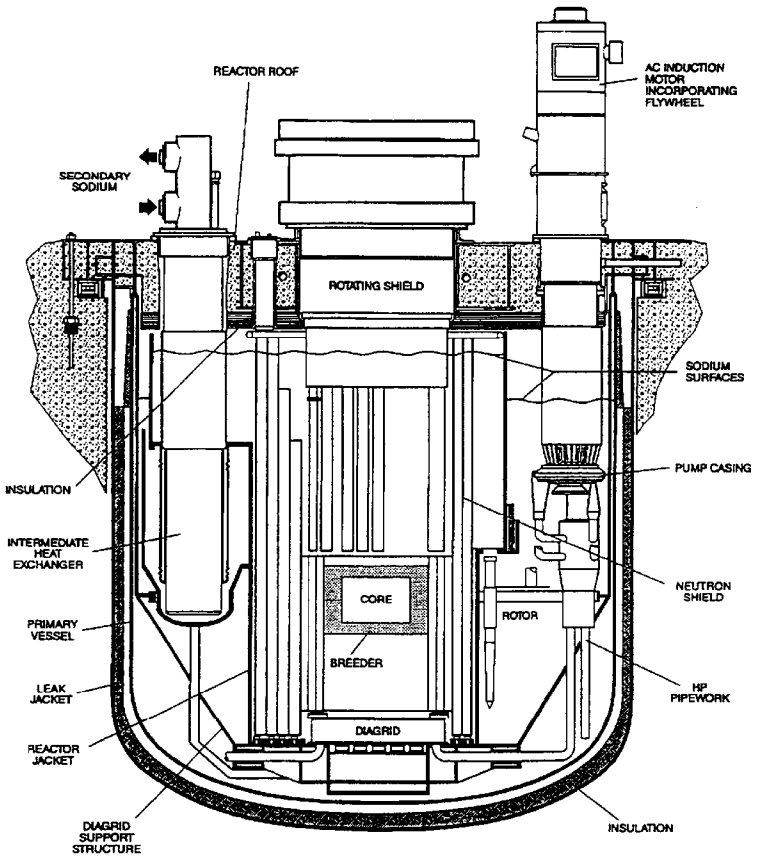

FIG. 2.44. PFR Cross-section of the primary circuit.

Heat from the 600 MW_{th}-rated core was transported to six IHXs within the primary vessel by sodium primary coolant pumped by three electrically-driven (1 MW) mechanical pumps. Sodium entered the core at a temperature of 400-430ºC; the core temperature differential was about 160°C. The 900 tonnes of primary sodium were contained in a primary vessel of 18/8/1 stainless steel, 12.2 m in diameter and 14.0 m deep, surrounded by a guard vessel made from medium carbon boiler grade steel.

Secondary sodium flowed through the shell side of each IHX and transported heat to the SG. There were three secondary circuits, each containing about 75 tonnes of sodium which was circulated by a mechanical pump similar to the primary sodium pumps and each coupling a pair of IHX to a set of SG consisting of an evaporator, a superheater and a reheater.

Each SG was of single-wall tube-in-shell design. The evaporators were of the forced-circulation type, with each of three circuits having a steam drum and a boiler circulating pump. Superheated steam from three circuits flowed to a common header to drive a 300 MW turbo-alternator. The main feed was via a 100% duty steam-driven pump with 10% electric- and 10% steam-driven pumps for start-up and post-trip use (later, a 50% capacity auxiliary electrically-driven pump was installed as a back-up). Appropriate water conditions were provided by a full-flow polishing plant, and the feed-heating by sets of low pressure direct contact and high pressure tube units. The underslung condenser was cooled by seawater.

The reactor core and its surrounding blanket was made up from an array of hexagonal subassemblies, 142 mm across flats. The assemblies were of a size appropriate to a full-scale commercial reactor, and provided a core 910 mm high and about 1550 mm in diameter.

Control was exercised through five boron carbide absorber rods, and a further five similar rods were available to shutdown the reactor. A radial breeder (blanket) surrounded the core and was itself bounded by stainless steel reflector assemblies to improve neutron economy. Outboard of the core and blanket was a graphite shield which essentially eliminated neutron activation of major removable components such as the primary pumps, valves and IHX, the secondary sodium, and the primary vessel itself. Special loops filled with eutectic NaK alloy as coolant were provided to reject decay heat from the primary coolant via air-cooled heat exchangers (AHX) to the atmosphere after reactor shutdown if SGs were not available for this purpose.

Fuel could be transferred from an adjacent preparation facility, the irradiated fuel cave (IFC), to a storage rotor within the primary vessel while the reactor was operating. This rotor reduced the time required for refuelling operations and, when irradiated fuel was discharged from the rotor to the IFC, reduced the number and complexity of the transfer flask movements because irradiated fuel removed from the core could be left to cool in the rotor before being moved to the IFC after the reactor had resumed operation. Transfers between the core and the storage rotor used a vertical lift pantograph charge machine working through a single rotating plug in the reactor roof; for such moves the reactor had to be shut down to allow the charge machine to be installed. Fuel discharged from the rotor after irradiation was first stored under sodium in the IFC until either it had been examined and returned to the reactor for further irradiation or was cool enough to be prepared for reprocessing (including steam cleaning to remove all traces of sodium) and then moved to a buffer store to await transfer to a reprocessing plant, also located on the Dounreay site.

2.10.2. Review of operating history

The operating history of PFR can be conveniently divided into two phases. For the first ten years, electrical output was limited, mainly because of a series of leaks in the tube-to-tubeplate welds of the steam generator units (SGU), and the highest load factor in any year was 12% (in 1978). After 1984, with the SG weld problems dealt with, plant performance improved. In the final year of operation the load factor was 56.5%. In this second decade of operation there was one major outage, in 1991/92. In contrast to experience with SG, unto 1991 the reactor and primary circuit were responsible for only a very small fraction of unplanned outage time; however, in mid-1991, a leakage of oil from a bearing of one of the primary pumps into the primary sodium led to suspension of reactor operation for 18 months.

2.10.2.1. The first decade, 1974-1984

The approach to criticality began in February 1974. The time from start of construction to filling of the primary circuit had been seven years compared with the four years planned, the delay being due principally to difficulties experienced in the welding of the reactor vessel roof. Nevertheless, the reactor was delivered at a cost of about £ 40 M.

Commissioning had proceeded without major problems though a water test of the sodium side of Circuit 3 had revealed a gas entrainment problem requiring modification of all shut-off circuits, and bearing problems on one of the primary pumps and two of the secondary pumps had needed attention.

Criticality was first achieved on 3 March 1974. Physics parameters for the core and for the reactivity effectiveness of, and interactions between, the control and shut-off rods agreed with prediction within the expected uncertainties. The hot dynamic test was completed in June,

when a small sodium leak was detected at a butt-joint of piping in a leak-jacketed section of one of the secondary loops. It was found to be due to a poor quality repair of a construction weld defect and was satisfactorily repaired in situ.

In October 1974, during early steam commissioning, a leak was detected in Superheater 3. This was found to have occurred in a tube-to-tube plate weld and was the first of 43 similar events - 2 in the superheaters, 1 in a reheater and 41 in the evaporators - which were to have a major influence on operations in the next seven years, with the highest incidence (11 leaks in the evaporators) in 1981. Thereafter, apart from a small leak in a tube-to-tubeplate weld of Superheater 3 in 1986, there were to be no more problems in this area, principally as a result of a major programme of sleeving carried out on the evaporator units. SG problems and their alleviation were thus to be the dominant influence on reactor operations in the first decade.

2.10.2.1.1. Steam generators

As has been observed, the first leak in a SG was experienced in a superheater, and though leaks in the ferritic steel evaporators were eventually to have most impact, experience with the superheater and reheater units, fabricated from stainless steel, will be reviewed first.

2.10.2.1.2. Superheaters and reheaters

The October 1974 leak in Superheater 3 was followed three months later by a similar leak in the tube-to-tubeplate weld of Superheater 2. In both cases, repair was effected by explosively plugging both ends of the faulty tube. Inspection of Superheater 3 revealed cracks in the tubeplate which were sufficiently accessible for removal by machining. After machining, the tubeplate thickness was adjudged to be sufficient for continued service. Inspection of Superheater 2 also revealed some tubeplate cracking, but in a region more difficult of access and machining was not possible. For this unit, a case for continued service was made, based upon plugging of tubes surrounding the failed one, passivation by sodium washing, a leak-before-break argument and the scheduling of periodic ultrasonic inspections of major shutdowns. No significant crack growth was observed in these inspections.

In 1976, a leak occurred in Reheater 3. Inspection showed that a significant amount of sodium had entered the tubes. Further examination showed that the tubeplate was irremediably damaged. The tube bundle was replaced by a flow restrictor in the sodium circuit to allow the associated evaporator and superheater to continue to be used. The reactor operated without failed reheater until 1984 when a replacement tube bundle was installed.

The original tube bundles of the superheaters and reheaters were fabricated, as has been observed earlier, in austenitic stainless steel, a design choice made to facilitate the achievement of the high temperature steam conditions being specified at the time by the UK electrical utilities. This steel is prone to chloride- and caustic-induced stress-corrosion cracking. This susceptibility was compounded in the superheaters and reheaters by an inability to stress relieve the tube-to-tubeplate welds after fabrication. Thus, when a leak occurred, secondary cracking was always a risk; moreover, crack propagation could be rapid.

This unfavourable experience, so early in the operating life of the steam generating plant, led to a decision to order a complete replacement set of superheater and reheater tube bundles of modified design to be fabricated in 9Cr1Mo ferritic steel. As in the original units, the new units were to have no under-sodium welds in the steam tubes, but, in addition, the need for difficult tube-to-tubeplate welds, and, indeed, for any welds separating the steam and sodium

environments, was eliminated by passing the steam tube through a sleeve projecting above the tubeplate, removing the joint to the steam header from the sodium environment. Each sleeve was brazed to the steam tube and welded to a seal plate. The new design also incorporated improvements to reduce flow-induced vibration of the tube bundles. These units were delivered to site in 1984, at which time it became possible to replace the missing reheated and thereby restore the full complement of SGU. The two remaining replacement reheaters and the three replacement superheaters were stored as strategic spares. One of the latter was used to replace Superheater 3 after the 1986 leak event and all of the others were deployed in 1987.

2.10.2.1.3. Evaporators

The operating conditions for the evaporators were less demanding than those of the superheaters and reheaters and these units were constructed from 2ViCr1Mo steel. The tubeplate and vessel material was unstabilised. However, a Nb-stabilised option was used for the tubes to reduce the risk of adverse effects due to decarburisation during service life.

A leak occurred after a tube-to-tubeplate weld failure in Evaporator 2 only a few days after the first superheater leak (in the same circuit), discussed in the previous section, had occurred. The unit was returned to service by plugging both ends of the defective tube. Further leaks occurred in the same evaporator and in Evaporator 3 early in 1976. Whilst the SGU leaks occurring in 1974 had tentatively been ascribed to weld defects undetected by the radiographic and visual inspections and the leak testing after fabrication, the occurrence of further leaks after nearly two years of service prompted closer examination and a technique was developed to remove a sample of the failed weld for examination before the tube was plugged. This was first applied to one of the early 1976 failures. Metallography indicated cracks on the water side. The welds were extremely hard. Up to that time such water-side cracking had not been observed in the laboratory, but subsequent experiments showed that hard, highly-stressed weld material could, in fact, develop cracks in good quality water. The phenomenon was described as "pure water stress corrosion cracking". The hard highly-stressed welds were a consequence of the style of the tube-to-tubeplate junction - a direct face weld joining a tube with 3 mm wall thickness to a 400 mm thick tubeplate.

There were further evaporator leaks in 1976–77, then none for a period of about eighteen months, followed by a further low level of incidence in 1979. Examination of weld samples in 1977 showed some partially penetrating sodium-side cracking. This prompted a programme to develop non-destructive methods of detecting partially-penetrating cracks.

Throughout this time, consideration had been given to methods of heat-treating or otherwise stress-relieving the welds. Bulk stress relief was considered but rejected because of difficulties in ensuring that there would be no distortion of the tubeplate. Local methods, including heat treatment of individual welds by glow discharge and elimination of tensile stresses in the surface layer by shot-peening, were therefore pursued. In the autumn of 1980, when it had become apparent that the rate of incidence of leaks was increasing, it was decided, after trials on a spare evaporator tube bundle, to shot-peen the bores of all of the 3000 tube-to-tubeplate welds in the operating units as a means of protecting them against pure water stress corrosion cracking. The possible benefit of shot-peening the sodium side of the welds was considered but adjudged to be not practicable. All of the evaporator units were shot-peened during the winter of 1980/81. Each unit was out of service for about two months. Most of the time was for preparation, inspection and reinstatement, the peening work itself taking only about a week.

Experience following this treatment was variable. One unit (evaporator 2) operated for a year after shot-peening before developing another leak. In the others the incidence continued to increase. Again defective welds were extracted for metallographic examination. These showed extensive sodium-side cracking. A survey using newly developed eddy current and ultrasonic methods, supported by selective radiography for validation and calibration, was initiated for the two units continuing to develop leaks. This found over 100 welds with sodium-side cracking in one unit, and about 20 in the other. This led to a major review of the tube-to-tubeplate weld problem.

With leaks having occurred in all three evaporators and a sodium-side origin of cracking in evidence, it was decided that the most practicable solution was to by-pass the suspect tube-to-tubeplate welds by using a sleeve. Each sleeve was a precisely machined cylindrical tube of a 9Cr1Mo steel inserted into the tubeplate and extending downwards into the top 75 mm of the tube. The upper end of the sleeve was explosively welded to the tubeplate and the lower end was braised into the inside of the tube.

Following extensive laboratory trials, four experimental sleeves were first fitted to operational evaporators towards the end of 1980. A further 11 evaporator weld leaks occurred in 1981 and a further 41 sleeves were fitted to by-pass defective and suspect welds. In parallel, work was in progress to examine whether the sleeving technique could be applied on a routine basis.

A trial installation of 200 sleeves was conducted on the spare evaporator tube bundle in the latter part of 1982. A decision was then made to sleeve all the 3000 tube-to-tubeplate junctions in the three evaporators. Work on two of the units was completed in 1983 and the third unit was sleeved by March 1984. It was installed in the summer and PFR operated for the first time with three fully-sleeved evaporators in August 1984. From then until end of PFR operation, there were no problems with the evaporators.

2.10.2.1.4. Temperature profiles in the reactor vessel

The vertical temperature profile up the wall of the primary vessel was required to be free from steep gradients to ensure that normal plant manoeuvering or trip action did not give rise to unacceptable thermal stresses as the sodium level in the vessel changed. The top of the vessel was at roof temperature, about 50°C, and the vessel wall at and below the sodium level was at the outer pool sodium temperature, about 400°C. The shape of the temperature profile in the section of the primary vessel (the "top strake") between these steady values was determined by the combined effect of the tapered external thermal insulation and the forced cooling by the roof cooling argon supply. During commissioning of the reactor, the temperature profile was found to have an unacceptably steep gradient in the region just above the sodium level, and this would result in unacceptable cyclic thermal stressing as the sodium level changed.

The roof cooling system was modified to deal with this; a more positive control of the cooling gas flow was achieved by installing independent diverter valves around the vessel circumference to reduce the cooling flow over the vessel. Structural analysis suggested possible creep ratchetting of the vessel in an inward radial direction and though, at the time when it was decided to introduce the remedial measures, no distortion of the vessel could be perceived, linear displacement transducers were fitted at five locations around the tank and at thirteen vertical positions to monitor the situation. In ten years of monitoring (1975-1985) no significant changes were detected in the surveys and monitoring was then discontinued.

2.10.2.1.5. Flow-mixing phenomena

PFR was fitted with extensive primary circuit instrumentation for use during the commissioning and operation of the plant. This instrumentation, supplemented by special rigs, proved to be invaluable, in association with laboratory facilities, in providing information on primary circuit performance, and, in particular, on flow-mixing phenomena. In the above-core plenum of PFR, temperature fluctuations arose in regions where the flows from core and breeder assemblies mixed. This subjected the above-core structure and its supports to thermal striping.

Extensive studies concluded that there were no constraints on operation which would restrict output at design power. In circumstances where SG leaks led to operation on less than three secondary circuits, a small flow of sodium at core outlet temperature past nominally-shut sleeve isolation valves in the IHX which were not in service provided a potential for mixing of sodium flows at core inlet and core outlet temperatures and hence to possible thermal striping damage to the IHX and their containment pods. These effects were extensively studied in laboratory rigs and resulted in the setting of limits on the core temperature rise when PFR was operating on less than three circuits.

2.10.2.1.6. Core distortions

PFR was designed before one of the two irradiation-induced phenomena affecting the dimensional stability of reactor core structural materials exposed to a high fast neutron flux had been discovered (void swelling) and before the other had been characterized (irradiation-induced creep). By the time operations began, however, the possible impact of both phenomena on the major core components (fuel assembly wrappers, pin cladding, and control rods and their guide tubes) had been evaluated. The guide tubes had been designed to be replaceable, but work was initiated to develop special tools to rotate the guide tubes during refuelling in order to extend their life.

In addition, development work to identify the swelling and creep-resistant alloys which would be necessary to tolerate these phenomena in a core designed to accommodate neither had proceeded sufficiently far to indicate that the austenitic steels chosen for the core components for PFR were far from optimum choices. It was decided, therefore, that major core components should be regularly monitored by measuring dimensional changes and curvatures as they were removed from the core and transferred to the fuel cave, and by using the charge machine at shutdowns to monitor length changes of fuel assemblies in situ. In addition, free movement of the control rods in their guide tubes was regularly monitored during operations. To guide the schedule of measurements, a predictive code, CRAMP, which modelled the core distortions due to void swelling, calculated the resultant stresses arising from swelling-induced interactions between components, and then estimated the creep-induced responses to these stresses, was developed.

The in-core life of some sub-assemblies, particularly those with solution treated austenitic stainless steel wrappers, was determined more by the irradiation-induced distortions than by the performance of the fuel itself. It was, however, possible in some cases to extend in-core life by rotating the assemblies so that bowing due to irradiation in a neutron flux gradient would be offset by further irradiation and the amount of bowing would not exceed that acceptable for extraction through the fuel discharge route. The risk of severe core component distortions thus needed continuous attention in the early years of operation but, in later years, the definition of management procedures based on earlier experience and the increasing use of

swelling-resistant alloys (ferritic steels or high-nickel alloys) in fabricating wrappers, guide tubes and other components effectively eliminated the problems.

2.10.2.1.7. Conventional plant

Although this paper is concerned primarily with experience of operation of the nuclear island, it is relevant to note that several improvements were made to the conventional plant during the first decade of operations, to increase availability and to reduce plant outages arising in this area. Early bearing failures on the turboalternator were remedied. The plant as originally designed had only a single steam-turbine driven feed pump, and a 50% capacity auxiliary electrically-driven pump was installed as back-up. Following trips initiated by the direct-contact feed heaters, improvements were made to their protection systems

Considerable work was undertaken to increase the capacity of the water treatment plants and the capacity for storing treated water. Ingresses of seaweed, restricting the seawater cooling flow to the main condenser and to other key plant ancillaries, caused reactor trips and significant loss of availability in the early years. Improvements to plant in the seawater pump house only partly alleviated the problem and in 1980 it was decided that a more radical solution should be sought. Modelling trials by a hydraulics consultancy led to a decision to construct a barrier with a low-tide by-pass channel on the foreshore at the seawater inlet. Construction was completed in 1987, and subsequent experience proved its effectiveness.

2.10.2.1.8. Station operations

Though the load factor of the station in the first ten years of operation never exceeded 12%, the first decade was also marked by many significant achievements. The primary circuit, the primary and secondary sodium pumps and the intermediate heat exchangers all proved to be very reliable in operation. Reactor availability figures of 80% and over were recorded in five of the years. The station was synchronised to the grid for the first time in January 1975 and in early February, with the reactor at 200 MW_{th}, 40 MW_e was exported from the site. In July 1976, operation at 500 MW_{th} generated 150 MW_e and full core power of 600 MW_{th} was reached on 25 February 1977; electrical generation was limited to 200 MW_e, however, because of the absence of Reheater 3 and operation of the steam plant outside its design conditions because of feed heating problems. Generation throughout the period up to 1983 was, however, intermittent, for reasons already discussed, and the maximum net generation in any one year was 9 678 MWd in 1978 at a load factor of 12.2%.

2.10.2.1.9. Fuel development

Major advances were made during the first decade of operation in the development of fuel, and PFR's Demountable Sub-Assembly (DMSA) facilities, in which independent clusters of up to 19 fuel pins could be irradiated to test both materials and design variants and to explore operational limits, provided a capability to mount a major fuel development programme. The initial target burnup for the PFR driver fuel was 7.5% (heavy atoms) and by the end of 1983 it was evident that this could be raised since, by that time, approaching 10 000 pins had exceeded the limit without failure and a significant number of pins had either exceeded or were approaching 10% burnup. It was, however, recognized that the variability in the swelling behaviour of the specified M316 austenitic stainless steel cladding (caused by minor variations in composition which could not be reliably controlled in the manufacturing process), the absolute magnitude of the swelling in the most susceptible batches, and doubts on the ability of the material to withstand fission gas plenum pressures at higher burnups

without exceeding creep design criteria, would never allow the achievement of the burnup targets then being contemplated for commercial stations (12.5 to 15%). However, the swelling resistance of the high nickel alloy, Nimonic PE16, had been recognized ever since the first experimental studies of void swelling at Dounreay in the mid-1960s and Nimonic PE16 was replacing the austenitic stainless steel as cladding in new batches of fuel.

Though there had been no fuel pin failures in the driver charge fuel, there had been a handful of failures in experimental fuels. These were not an operational problem. As has been noted, PFR's predecessor, the Dounreay Fast Reactor (DFR), was successfully operated for 18 years with metallic fuel in fully vented cladding. However, in designing PFR and switching to oxide fuel, it had been decided that the reference fuel would have hermetically sealed cans, though reservation of an option to include a partial loading (as much as one-third of the core) of vented fuel had led to the incorporation in the cover gas circuit of facilities to monitor and, if necessary, to deal with the presence of fission product gases. Equipment to locate fuel failures in the core was also provided.

Experience in the oxide fuel development programme in DFR had shown that the normal failure mode of a hermetically-sealed oxide fuel pin is the development of a thin crack in the cladding, releasing fission product gas into the coolant. Later - as much as 70 days or more later — the defect may develop to bring fuel into contact with sodium.

PFR was provided with delayed neutron signal instrumentation to detect this development and DFR experience indicated that this was the stage at which removal of the fuel became advisable; until this stage, the "gas leakers" were not an impediment to continued reactor operation. PFR experience with the failed experimental pins confirmed this strategy, and showed that the bulk delayed neutron detection system, located in the intermediate heat exchangers, provided adequate protection against a large rapidly developing failure.

2.10.2.1.10. PFR after ten years

With 10 years of operations completed in March 1984, it was appropriate to review the situation and to speculate on the future. The major impediment to sustained high power operation in the early years - the defective tube-to-tubeplate welds of the evaporators - was being dealt with by an engineering solution (the sleeving of every tube-to-tube plate junction to by-pass the suspect welds) and three fully sleeved units would be available for service later in the year.

After initial problems, which led to the removal of one of the reheaters, the superheaters and reheaters had been kept in service after plugging the tubes with defective welds and devising a technique for removing all traces of caustic from the undersides of the tube plates by washing with hot sodium. Replacement tube bundles for the superheaters and reheaters were due to be delivered to the site within the new few months and this would allow Reheater 3 to be brought back into service. Several parts of the conventional plant - valves, the dump system, the feed pump and the condenser coolant inlet channel - had all been modified to improve plant flexibility and the reliability of operations. All of the major components of the primary circuit — the pumps, IHX and the reactor control systems and instrumentation — had performed without problems. Most significantly, PFR was already showing excellent fuel performance with the prospect of even more significant advances as early choices of cladding and wrapper alloys, selected only for compatibility, fabricability and mechanical property qualities, were replaced by new materials more resistant to the endurance-limiting effects of void swelling and irradiation creep.

2.10.2.2. The second decade 1984–1994

2.10.2.2.1. Station operations

For most of 1984, only two secondary circuits, with sleeved evaporators, were available and this was the major factor reducing output. A sodium pump bearing seizure caused an extended shutdown as did a fire in a secondary circuit cell, resulting from a leak of some tens of kilograms of sodium after a small-bore pipe failure in the gas space hydrogen detection system of Superheater 1. A leak in one of the decay heat rejections loops (actually the fourth such leak, but the first to impede reactor operations) led to a decision to order new ones of modified design.

In 1985, PFR was able to operate, for the first time since the commissioning period, with a full set of SGUs. A reload-to-reload run of 135 days duration, generating 486 000 MW·h at a turbine load factor of 65%, was achieved during the year. This was a particularly bad year for seaweed ingress, with the new mid-tide barrier being not yet completed. It was estimated that 125 000 MW·h of generation was lost to this cause during the year. In 1986, a continuous turbine run from 23 August to 11 October generated 276 000 MW·h of electricity at a load factor of 92.5%. A fuel assembly still in serviceable condition at 15.9% h.a. burnup was discharged from the core for examination.

In 1987, a major tube failure in Superheater 2 led to PFR being off-line for 6.5 months while the aftermath was dealt with and the replacement tube bundles were deployed. There was also the first sodium leak from a reheater vessel. However, in spite of these problems, PFR returned a very creditable gross annual load factor of 41.8% during the year. In 1988, there were further problems with a reheated vessel leak, but the year saw a continuous high-power run of 41 days from 19 March to 29 April in which 230 100 MW·h of electricity were generated at a load factor of 94%.

PFR's best full calendar year of operation was 1989, with gross generation of 47 231 MW·d of electricity at an annual load factor of 51.8%. The station operated for 230 days. The major achievement of 1990 was the licensing of the station by the UK Nuclear Installations Inspectorate (NII). Prior to this the station had been licensed by its owner-operator's internal procedures, and independent licensing of the 16 year old plant was both a major achievement and a vindication of the standards previously used.

Operations in 1991 and 1992 were severely affected by a leakage of bearing oil from one of the primary pumps into the primary sodium coolant which took PFR out of service from 29 June 1991 until 30 December 1992. Operations then continued until 11 July 1993 - 119.5 effective full-power days in which 25 706 MW·d (gross) of electricity was generated at a load factor of 53%. A second run later in the year generated 14 955 MW·d (gross) of electricity at a load factor of 58%.

PFR was started up for the last time on 14 January 1994. An output of 240 MW_e was achieved on 16 January and operation continued at this level until the final shutdown on 31 March with load factor of 93%. So, in its final weeks of operation, PFR achieved its highest ever load factor for a single run. The continuous turbo alternator output of 18 160 MW·d exceeded the previous record of 13 570 MW·d set in March 1991. The total electricity generation in the last year of operation (April 1993 to March 1994) was 51 546 MW·d with a load factor of 56.5%.The previous best in any twelve-month period was 48 170 MW·d with a load factor of 52.8% achieved in 1989/90.

2.10.2.2.2. Fuel performance

One of the principal tasks of PFR was to demonstrate a reliable, safe and robust fuel capable of routinely achieving a high burn up target. Successful completion of this task is one of PFR's major achievements.

The major advances made in the second decade of PFR operations resulted from the introduction of Nimonic PE16 as the reference cladding alloy. The fuel assembly discharged at 15.9% burnup in 1986, mentioned earlier, gave the first indications of the benefit of this change. The pins showed maximum diametral increases of only 1%, with uniformly low diametral change profiles showing little pin-to-pin variability, compared with the 5-8% (maximum) diametral changes and highly peaked profiles showed by earlier examinations of pins clad in cold-worked M316 steel and irradiated to half the exposure. Destructive examination of the pins indicated that the fuel column was stable, that internal corrosion was low and that there was no evidence of any fuel/clad mechanical interaction resulting from containment of a high burnup swelling fuel in a non-distending cladding tube. This confirmed that higher burnups were probably feasible. Measurements of the PE16 wrapper showed trivial length increase, across-flats distension and bowing, and revealed no potentially life-limiting changes.

By 1990, irradiations of PE16 clad fuel pins in driver assemblies and in DMSAs had achieved more than 17% and 21% burnup respectively. Even with displacement doses of the order of 130 displacements per atom no life-limiting features could be identified in either the wrappers or the cladding.

Meanwhile materials irradiation experiments had shown ferritic/martensitic steels to be particularly resistant to void swelling, and while the high temperature mechanical strength of these materials seemed to preclude their use as pin cladding, application as wrapper materials seemed to be practicable. Accordingly, in the late 1980s driver fuel assemblies with wrappers of the ferritic/martensitic steel FV448 and pins clad in Nimonic PE16 were introduced into PFR. By the end of the reactor's working life, over 20 such assemblies had been loaded and seven of these had exceeded the 15% burnup (110 dpa) target; one had achieved the then world record, for a mixed-oxide driver charge assembly, of 19.8% burnup (155 dpa).

The fuel in all of these high bum-up assemblies was high intrinsic density annular pelleted mixed oxide, and this was the reference variant in the UK fast reactor fuel development program. It was, however, recognized that vibrocompacted fuel offers advantages with respect to fuel fabrication costs and this variant also featured in the programme. Almost 3000 pins containing vibrocompacted fuel were irradiated in PFR but failures in several pins due to fuel column instability at burnups in the range 1-10% confirmed the wisdom of concentrating on annular fuel and studies of vibrocompacted fuel ended in the mid-1980s.

In the drive for better commercial fast reactor station economics the possibility of annual refuelling became a design option. This led to consideration of lower mass-rated, larger diameter pins. PFR, with the capability to accept both DMSA and full assembly irradiations, was ideally suited to parallel testing of pin design variants of different diameters and a programme covering the range 5.84 to 8.5 mm was developed over the final few years of operation. Unfortunately the target burnups for the largest diameter pins (20%) could not be reached before the reactor operations ended, and the maximum attained was 10%.

Statistics illustrate the undoubted success of the fuels development programme in PFR. Approximately 98 000 pins were irradiated and, of these, over 40 000 exceeded the original 7.5% target burnup. The introduction of PE16 as cladding allowed over 2 400 pins to attain burnups in excess of 15% with about 320 of these having successfully exceeded 20% at the end of operations. The peak burnup achieved (in lead pins irradiated in DMSA) was 23.2% (135 dpa).

The overall failure rate of PFR fuel pins was remarkably low, considering the number of experimental variants examined in the programme. Of the 23 failure events which occurred in the 20 years of reactor operation, the majority could be linked either to experimental design features or to the less-stable vibrocompacted fuel form. In statistical terms, the failure rate for the vibrocompacted fuel pins irradiated in PFR was 7.4 in 1000 while for all annular variants the rate was 0.2 in 1000. It should be noted, in comparing these figures that the burnups experienced by vibrocompacted fuel pins were significantly lower than those achieved by annular fuel pins. The failure rate for pins clad in Nimonic PE16 was 0.21 in 1000. Four Nimonic PE16 clad driver fuel pins actually failed. Three of the failures were in pins which had exceeded 17.5% burnup. The fourth failure, which occurred at a burnup of 11.5%, arose from a suspected fabrication defect. In all four cases, the rate of development of the failures allowed adequate time for the reactor operators to observe the slow development of the failure, and in one case, irradiation was continued for 45 days after the leakage of fission product gas was detected. In no case was there any significant loss of fuel from the failed pin and there was no evidence of pin-to-pin failure propagation.

Breeder assembly operating conditions differ substantially from those experienced by the fuel assemblies. Breeder pins operate initially at a mass rating which is approximately one-tenth of that of fuel pins, but this rating increases as burnup proceeds. As the breeder assembly flow is set prior to irradiation to give acceptable pin cladding temperatures at end-of-life ratings, the pins are therefore overcooled at start-of-life and this, and the lower neutron fluxes experienced in the breeder zone, combine to increase the risk of mechanical interaction between the breeder pellets and the cladding. The target burnup for the PFR breeder was therefore set at a conservative 1%. More than 4 250 breeder pins exceeded this target in PFR, with apparently no failures. Examination of breeder pins clad in Nimonic PE16 and irradiated to burnups close to 3% showed no evidence of excessive plastic straining of the cladding. PFR experience therefore suggests that a burnup target of around 2% would be a reasonable initial aim in future reactors.

2.10.2.2.3. Specific aspects of operational experience

The performance of the SG which had so affected reactor operations in the first decade was to give little cause for concern in the second. The sleeved evaporators operated throughout the period without problems. There was, however, a failure in Superheater 2 on 27 February 1987 which led to a major leakage of steam into the secondary circuit sodium. Examination of this austenitic steel unit after the leak event revealed a fretting failure of a single tube which had been subjected to unexpected flow-induced vibration. In the sodium/water reaction event which followed, 39 neighbouring tubes also failed. This event rendered the unit unserviceable and it was decided to install one of the replacement tube bundles, stored on site as strategic spares since 1984, in its place. Consideration of the location of the fretting suggested that the possibility of a similar problem arising in the other original units could not be ruled out and it was decided to replace all of them. This led to a 6.5 months outage for the station. Observations of damage due to vibration in the units after removal indicated the wisdom of the decision.

The under-sodium leak in Superheater 2 was important for a number of reasons. It involved 40 tubes, yet the automatic protection system coped with the incident despite the severity being beyond that for which the system had been designed. In addition, analysis of data led to a complete reappraisal of the consequences of sodium/water reactions in SG. It also revealed the problems caused by not being able, in PFR, to clean up the intermediate heat exchangers independently of the contaminated secondary circuit - problems which took two months to circumvent. (Dump tanks of greater capacity would have eased the clean-up work). The main lesson for the future is that great care is needed in SG design to avoid tube vibration and that the earliest possible indication of a leak is essential if tube-to-tube failure progression is to be avoided.

The only other problem with the SG in the second decade was the observation of deteriorating welds in the stainless steel outer vessels of the superheaters and reheaters. Leaks in reheater vessels in 1987 and 1988 revealed cracks (in one case over 100 mm long) in the original interplate welds. Subsequent inspections of the other vessels revealed large but non-penetrating cracks, similarly located in two of the superheater vessels. All of the cracks were in welds which had been reworked during fabrication or where fabrication welds had overlapped. It was decided that the defects should be cut out after dumping the sodium and that the vessels should be repaired. However, one of the non-penetrating cracks in the Superheater 3 vessel was left in situ after assessment indicated low likelihood of rapid propagation. Strain gauges were fitted to the crack region as monitors. Two repair methods were used. In the earlier one, the excised region was filled with weld metal against a backing plate. One of these repairs was to be the cause of a further leak in 1990. In the later repair technique, a circular stub surrounding the defect area was welded on, the defect was then removed and the vessel was re-sealed by welding a cap on to the stub end. In subsequent years this method was evolved into a "stood off" patch, with the crack being left in situ with holes drilled at both ends to act as crack stoppers.

Investigation of the problem indicated that the cracks were initiated by delayed reheat cracking and grew by a high temperature brittle intergranular mechanism driven by the residual stress field.

The condition of the vessels became of increasing concern in the final years of operation and the need for regular examination significantly extended shutdown times. The basic problem was one of choice of material; a problem of availability of material during fabrication led to the use of a stabilised stainless steel and this resulted in a susceptibility to delayed reheat cracking.

2.10.2.2.4. Oil in sodium

The only primary circuit event ever to affect plant performance significantly occurred on 29 June 1991, when the reactor was manually tripped, following observations of overheating on the top bearing of a primary sodium pump. Remedial work was expected to take more than a week and, with a scheduled annual maintenance shutdown only two weeks away, it was decided to advance the shutdown and to begin preparatory work for the planned refuelling and maintenance.

It became clear that a significant quantity of oil (possibly up to 35 litres) had been lost from a primary pump upper bearing and had entered the primary sodium circuit. Replacement of the pump bearing and cleaning the primary sodium would be required before the reactor could return to power. To clean the primary sodium, it was necessary to rebuild the cold trap loop, which required procurement of a new basket, which was installed. The impurity burden in the primary circuit could be monitored through the plugging temperature of coolant within cold trap. When clean-up began this was 225°C but reduced steadily to below 170°C by the end of

the year, when the primary circuit was temperature cycled up to 420°C and then back to 310°C. This caused the plugging temperature to rise to 180°C, but a further phase of clean-up allowed to decrease the plugging temperature to 150°C.

The top bearing of the primary sodium pump concerned was replaced and the pump was successfully run-in at half speed, but when full speed tests were attempted, these had to be stopped as a result of high pressure in the oil drains tank - over five times the corresponding pressure on one of the other primary pumps. Further tests showed that the flow route from the bottom bearing and out through the pump case was restricted. Variations in pump speed cleared the blockage, which is believed to have been caused by oil degradation products.

Further suspicions of deposition of oil degradation products arose from observations that, just before the shutdown on 29 June, there had been indications of temperature increases in a number of core sub-assemblies, suggesting reduction of coolant flow through the inlet filters.

Attention therefore turned to the primary pump filters and it was decided to examine all of these, as well as some of the core sub-assembly filters, to check their condition. Removal of the pump filters was first implemented. Work to recover from the oil ingress problem, most particularly work to install new primary pump filters, occupied almost the whole of 1992. Deposits incorporating some carbon were found on all three filters removed. Some difficulty was experienced in fitting new filters because of the distortion of some thermocouple guide tubes and it was necessary to cut these away to complete the task.

Examination of a number of fuel assemblies also showed deposits on the inlet filters of those which had shown temperature increases prior to shutdown, but none on assemblies which had shown no increases. However, the deposits were sparse (about 0.5 g) and mainly of sodium. It was thought improbable that these were sufficient (even allowing for the possibility of some loss during handling) to cause the observed temperature rises and contamination of the cladding surfaces by adsorption of oil degradation products was postulated to be a contributory factor.

Work on the reactor was supported by laboratory studies to examine the effects of temperature, sodium and irradiation on both new and degraded oil. These included cooperative work with the Institute of Physics and Engineering at Obninsk to replicate in a rig the introduction of PFR pump bearing oil into flowing sodium upstream of a PFR subassembly filter. The totality of information acquired was submitted to the UK NII, the licensing authority, and consent to restart operations was given on 23 December. Criticality was achieved on 30 December 1992.

The outage of just over 18 months indicated the importance of designing to avoid any possibility of spillage of oil from pump bearings into the sodium coolant. There is, however, also a more general inference of the desirability of designing for easy removal of major circuit components to cope with unforeseen eventualities.

2.10.2.2.5. Decay heat removal loops

The normal route for the removal of decay heat in a fast reactor is via the secondary sodium circuits and the steam plant. Should this route not be available, decay heat in PFR could be rejected by one or more of three thermal syphon loops, each filled with eutectic NaK alloy. Each loop extracted heat through an immersed coil, intercepting some of the primary sodium as it flowed from the core towards an intermediate heat exchanger, and delivered the heat by

natural convection to the outside atmosphere through a NaK/air heat exchanger built into the wall of the secondary containment building.

In March 1975, a leak occurred as a result of failure in a welded pulled-tee connection between one of the forty parallel cooling tubes and the header in one of these AHX; the failure was attributed to a cold tear which developed during manufacture and a repair was effected by fitting a replacement tee. Similar leaks occurred in 1981 and 1982. Strain gauges and thermocouple were fitted to one of the loops and these revealed considerable temperature anomalies in a number of the tubes.

Measurements on the original heat exchangers and on a laboratory simulation suggested that the temperature differences between the tubes were caused by a reduction of NaK alloy flow, caused by gas locking in the bank of parallel cooling tubes, some of which were horizontal. In some cases, the flow reduction was compounded by deposition of impurities in places where the flow, and hence the temperature, was low. The temperature differences were sufficient to induce low frequency high strain fatigue as a consequence of normal plant manoeuvering. Vacuum filling of the heat exchangers and batch cold-trapping of the coolant improved but did not eliminate the problem.

Specimen pulled tees was subjected to cyclic strain and a stress versus cycles-to-failure curve was established. From this an allowable operating curve was derived, using measured plant data to define the strain history, and a damage account was maintained. Non-contacting displacement transducers were fitted to 240 positions on the heat exchangers to provide strain measurements to define fatigue development.

With these precautions, operation of the reactor was continued with visual examination of all the tube-to-header connections after specified fatigue damage increments. This, however, could only be an interim measure as it did not remove the underlying cause of the problem. In 1985, therefore, new heat exchangers for the decay heat removal loops were designed with this aim in mind. These new units incorporated heavier gauge headers, a modified geometry of the entry and exit connections of the tubes, a reduced-constraint tube support arrangement, and a slope (2 to the horizontal) in the tubes to reduce the possibility of gas locking. Two of the new AHX were installed in 1986 and a third in 1988. All three were heavily instrumented and performed as designed for the remainder of PFR's operating life.

2.10.3. Advanced technology developments

PFR was also used to test advanced technology developments of potential interest in future fast reactors. Thus, an under-sodium viewer was specially developed for PFR. Echoes of ultrasonic pulses were detected and stored in a computer for processing into a colour image, showing detail of the top of the core, which was submerged under 5 meters of sodium. The viewer could be mounted in three positions on the top rotating plug and rotation then allowed an annular scan from each position. The total viewing area covered about 60% of the top of the core. The computer-generated images were of excellent quality, and the orientation bars and code rings on individual assemblies could be clearly seen. Colour imaging allowed differentiation of the heights of the tops of the assemblies. Comparison of data from the viewer with data obtained by using the charge machine to measure the assembly heights showed excellent agreement; this comparison gave considerable confidence in the practice of using the charge machine to monitor wrapper growth. The viewer images also provided information on the lateral displacements of the tops of the assemblies due to bowing.

A single channel trip system was developed for CDFR to detect abnormal behaviour in a single fuel assembly and to shut down the reactor, if necessary. It was installed in PFR on a test basis to demonstrate its ability to detect circumstances needing shut-down action. The early problems with the SG highlighted a need to improve non-destructive methods of detecting small flaws in relatively inaccessible welds. A major programme of development work led to major refinements, particularly in ultrasonic techniques.

2.10.4. PFR safety and licensing

The design of the PFR was intended to minimize the frequency and severity of accidental releases of radioactivity. This was achieved by "defence in depth" incorporating:

- Sound engineering design coupled with a high standard of material specification, fabrication and pre-service inspection;
- The provision of instrumentation to detect divergences from normal operation and, if necessary, to initiate reactor shutdown using the fail safe shutdown system provided;
- The provision of multiple containment barriers between fuel and the environment, including a high pressure capability plant containment; (although the primary circuit is little above atmospheric pressure) and an overall building containment, both aimed at defence against very low probability accident situations;
- The provision of a reliable decay heat removal capability, and
- The use of redundancy, diversity, segregation and emergency power supplies to achieve a high degree of reliability for the operation of the engineered safeguards in (b) - (d) above.

The achievement of this policy was quantified in a probabilistic risk assessment (PRA) for the plant, judged against the frequency/severity criterion recommended for a prototype reactor at a remote location. PRA was used throughout PFR's history to improve the quality of the safety arguments. The 1974 risk assessment was revised in 1984, and again in 1990 as part of the preparations for licensing of the AEA by the NII.

2.10.4.1. Engineered safeguards

PFR was protected by an automatic protection system (APS) to detect abnormal conditions and to shut down the reactor automatically if necessary. The APS was designed to be fail safe, to be robust and to provide redundancy and diversity. There were two completely independent subsystems with separate power supplies operated from separate parameters, constructed from different hardware and feeding separate groups of control and shut-off rods. Of the total of ten rods, the insertion of any three would shut down the reactor.

There were multiple barriers between fuel and the environment. The fuel in each fuel pin was hermetically sealed within a strong stainless steel clad; the fuel pins were immersed in a sodium pool able to retain chemically a number of important fission products, should a fuel pin fail; the coolant was contained within the primary containment (the reactor vessel, the biological shield roof and, surrounding the reactor vessel, the leak jacket); over the biological shield roof was the secondary containment building which incorporated a post-incident clean-up plant. The latter ensured that any radioactive release to the environment, even following a major incident would be kept to a minimum. There must be a highly reliable means of removing decay heat from the primary circuit. To insure against non-availability of the secondary circuits and steam plant, PFR was provided with the three independent decay heat rejection loops.

2.10.4.2. Inherent safety properties

PFR possessed inherent safety features which would allow it to survive a range of very improbable incidents, even in the highly unlikely circumstances of failure of the engineering safeguards. The major inherent safety features were natural circulation (within the NaK filled decay heat rejection loops and of the primary sodium coolant) and the reactor's negative temperature and power coefficients. Loss of electrical supplies to the PFR would result in a trip of the reactor and the run down of the main coolant pumps. Because of flywheels the primary pump speed halving time was 10 s, and the pumps would stop after approximately 200 s, but for the clutching-in of the continuously running pony motors which maintained a pump speed of 10%. Should all three pony motors or their clutches fail to operate, reactor experiments demonstrated that natural circulation of the hot sodium in the core would transfer the core decay heat to the 900 t of primary coolant. The decay heat could then be transferred to the atmosphere via the naturally circulating decay heat rejection system without the sub-assembly outlet temperatures exceeding normal operating levels.

When the temperature of the PFR primary circuit changed there was a consequential change in the reactor power, which arose from a combination of structural and neutronic effects, the overall result of which was that an increase in temperature caused a decrease in power; that is, PFR had negative temperature and power coefficients. Negative power and temperature coefficients represented a potentially powerful safety feature in the highly unlikely case of a failure of the engineered safeguards, making the reactor remarkably robust against a loss of cooling event. It is also an inherent safety feature of pool type fast reactors that the personnel radiation dose is low, between one and two orders of magnitude lower than for light water reactors.

2.10.4.3. Licensing

For the early years of PFR operations, the station was licensed to operate by internal UKAEA procedures. In 1990, the UK government decided that, to ensure a publically demonstrable consistency of AEA's standards, all of its nuclear facilities became subject to licensing by the NII. After a thorough examination of the plant design, a review of the operating procedures and an assessment of experience from 16 years of reactor operations, PFR was given an NII license to continue operations in 1990. The successful licensing of a 16-year-old plant was a major achievement and confirmed the validity of the internal AEA practices previously in operation, and the soundness of the original design.

2.11. KNK II operating experience

2.11.1. Introduction

The Kompakte Natriumgekuhlte Kernreaktoranlage II (KNK II) is an experimental sodium-cooled fast power reactor of 20 MW_e electric output. It is located at the site of (at that time) Kernforschungszentrum Karlsruhe (Nuclear Research Center Karlsruhe), now Forschungszentrum Karlsruhe (Research Centre Karlsruhe). The KNK reactor originally was designed as a thermal reactor with an UO_2 core moderated by ZrH_2. This version, called KNK I, was successfully operated from 1971 until 1974. Between 1975 and 1977 the plant was modified into a fast reactor and provided with an unmoderated UO_2-PuO_2 core. This modified plant was called KNK II [29]. KNK II was put into operation in 1977. It was operated rather successfully till 1991. In 1991 the plant was finally shut down. Since then the decommissioning of the plant is going on and is close to completion.

2.11.2. Design description

The core of KNK II is a two-zone core, the inner fast zone was equipped with mixed oxide fuel elements, while the outer thermal zone contains UO_2 fuel only. To ensure the safe heat removal, the nuclear power system has been equipped with two parallel main heat transmission loops of the same capacity. Besides, an emergency cooling system has been provided for KNK II which is completely independent of the function of these loops and makes use of the possibility of direct nitrogen cooling of the reactor tank. In the main heat transfer system one activity-free secondary sodium circuit each has been provided for safety reasons between the active primary sodium loop and the water vapour loop. In all circuits the sodium is moved by forced convection through mechanical feed pumps. The steam generators heated by the secondary sodium are installed outside the safety containment. The main data of KNK II have been summarized in Table 2.15.

TABLE 2.15. MAIN PARAMETERS OF THE KNK II FAST REACTOR

General data	Value	Primary circuit system	Value
Thermal reactor power, MW	58	Number of circuits	2
Gross electric power, MW	21.35	Nominal pipe size, mm	200/400
Net electric power, MW	17.75	Mass flow per circuit, t/h	498
Gross efficiency, %	36.9	Reactor inlet temperature, °C	360
Net efficiency, %	30.7	Reactor outlet temperature, °C	525
Coolant	Sodium	Cover gas	argon
Reactor core		Intermediate heat exchangers	
Mean core diameter, mm	824	Design	Cross counter flow
Core height, mm	600	Material	10 CrMoNiNb9 10
Fuel elements in fast zone	7	Secondary circuit system	
Fuel elements in thermal (driver) zone	22	Number of circuits	2
Blanket elements (uranium)	5	Nominal pipe size, mm	200
Reflector elements (steel/ZrHx)	30	Flow per circuit, t/h	451
Reflector elements (steel)	19	Outlet temperature of IHX, °C	504
Rods of primary shutdown system	5	Inlet temperature of IHX, °C	322
Rods of secondary shutdown system	3	Maximum operating pressure, bar	13
Fuel inventory:		Steam generator	
Fast zone (UO_2-PuO_2), kg	164	Design	Counterflow (double tube coils) water/vapour inside sodium outside
Fast zone (Pu fiss), kg	36		
Thermal zone (UO_2), kg	525	Live steam flow, t/h	88
		Turbine	
Mean power density in fast zone/thermal zone, MW/t of HM	183/60	Design	Single casing condensation turbine
		Inlet temperature, °C	485
Average fast neutron flux in fast zone, n/cm^2	1.40E+15	Inlet pressure, atm	80
		Storage positions	
Total neutron flux in fast zone, n/cm^2	1.67E+15	Storage under sodium	56
		Dry storage	47

2.11.3. Operating experience

2.11.3.1. Steam Generators

The experience with KNK II steam generators was extremely good. Only one sodium – water reaction has occurred, this was right at the beginning of operation of KNK I. The reaction was easily detected via an alarm due to excessive argon pressure in the secondary system. Hydrogen detectors were not installed at that time. The failure was caused by a faulty weld. The plant was shut down manually, no serious consequences occurred.

After 13000 hours of operation, one steam generator module was replaced for thorough investigation of the material. The results of these investigations were favourable. Extremely low corrosion and corrosion and deposits were observed. The operation with the remaining therefore was continued. No further failures occurred.

2.11.3.2. Sodium pumps

One of the two primary sodium pumps was replaced in 1984 after more than 100 000 hours of operation in view of the vibrational behavior of that pump. Ever since start-up this pump had always shown a vibration level and behavior different to the other one. The replacement was undertaken as a preventive measure. No further problems occurred during the lifetime of the plant.

2.11.3.3. Sodium leaks

Very few sodium leaks occurred. They occurred exclusively in the secondary circuit. They developed as so called miniature leaks from material cracks, mostly in the neighborhood of inferior weldings. There were never leaks in the main piping system. This holds also for the main components, except the burst-disc at the steam generator pressure relief system.

2.11.3.4. Blockage of rotating top shield

Of some concern was the sudden blockage of the rotating top shield of the reactor vessel. It was developed during continuous operation of the reactor and was detected after shut down. The malfunction was caused by sodium aerosols leaving the surface of the tank sodium and condensing in the cold gaps of the top shield, thereby blocking the ball-bearings. There they could be detected visibly and scraped mechanically. After removal of the condensed aerosols a reasonable torque for the top shield could be achieved. It was even lowered later on when a method was applied which consisted in melting down the aerosols by heating up the shield. This was achieved by turning of the nitrogen cooling system during a limited period of time during the start up phase.

2.11.3.5. Gas entrainment into primary sodium

A phenomenon arose during the start-up of KNK II. It resulted in various dubious scrams at 60% power triggered by the signal “negative reactivity too high”. KNK II had a negative void coefficient, therefore sodium boiling, gas bubbles passing the core, but also fuel element or control rod movements could possibly be the origin of that phenomenon. An extensive research programme was launched. In total it lasted from 1978 to 1980.

It soon became evident, that sodium boiling could be excluded as the phenomenon occurred even at low power, furthermore there was no indication or signal for elevated temperatures. Radial core oscillations, fuel element levitation or control rod movement could also be excluded very soon. The only remaining reason was gas bubbles passing through the core.

This was confirmed by various experiments. It turned out, that small amounts of cover gas were entrained into the primary sodium. The gas was stored in dead volumes of the lower plenum below the core and was released infrequently, 8-10 times a day, in larger portions into the core, which caused the negative reactivity peaks.

Many possible solutions of the problem were considered, finally it was decided to use spin gas separators which were to be placed under the core. They would lead the gas into the reflector elements, which were much less sensitive with respect to reactivity.

This turned out to be the correct solution. The installation of the separators together with the second core of KNK II was a complete success. The gas bubble problem was solved.

The appropriate cooling of the fuel elements was never endangered by the gas bubbles.

2.11.3.6. Rod actuating equipment problem

A difficult problem in operation, though not a safety problem, was caused by blockages in the shutdown systems of KNK II. In total, four of those phenomena were discovered between 1986 and 1991.

The rod actuating equipment comprised components which were located between the absorber rod and the drive unit located above the reactor vessel. It incorporated a mechanical coupling, the scram magnets and the rotating spindle. It was located partly within the sodium of the reactor vessel, partly in the argon cover gas plenum and partly above the rotating plug. This extension over various compartments handling different media gave rise to the problem.

All but one event were caused by deposits causing sticking in the rod actuating equipment. The only exception was an event, in which apparently a metal chip caused the sticking.

When the quality of the cover gas is insufficient, the sodium in the rod actuating system is oxidized to sodium oxide whose dough like consistency impedes lifting movements of the equipment. These points to the solution of the problem: Cover gas has to be free form oxygen and moisture, especially during revision and handling outages. In addition, for requalification, a method of flushing the rod actuating equipment in hot sodium was developed.

2.11.3.7. Fuel pin failures

The KNK II was operated with two cores, which showed significant differences: The fuel rod diameter and consequently the in core residence time was increased, the fuel rod pitch was reduced, the (grid) spacer design was modified. Two new types of fuel fabrication methods were applied and the fuel density was increased. These modifications were to fulfill development needs of the second core SNR 300. There was not much experience with all modified parameters available.

The operating record of the fuel elements in the first core of KNK II was ample cause for satisfaction. The fuel elements not only had reached the target burnup of 60 000 MWd/t, but

even had exceeded it considerably. Only two fuel rods out of more than one thousand had developed leaks, these defects in turn had triggered off extensive R&D activities, they even provided valuable information, e. g. that exposed fuel goes not enter into a violent exothermal reaction with sodium. This proved the robustness of the first core of KNK II.

The situation was different with the second core of KNK II. As mentioned this core was to serve as a test bed for SNR 300.

The first two years of operation, 1983 and 1984, were without fuel element failures, however in the following years a total of seven fuel elements developed leaks at burnups between 27 000 and 47 000 MWd/t. They turned out to be a significant burden on the operation of KNK II. On the other hand, these defects proved to be a valuable early warning system for SNR 300. Had the SNR 300 plant ever been put into operation, it certainly would have had to be equipped with improved reload fuel.

2.11.4. The KNK Experimental programme

An experimental programme was run in KNK II which actually had been started back in 1971, still in KNK I, and had then become more and more extensive. These R&D activities were partly mixed with plant operation, for KNK II, by definition, was an experimental nuclear power plant in which electricity generation was not supposed to play the primary role. As a consequence, irradiation of the reactor cores, each of them a first-of-its-kind unit, could also have been assigned to the experimental programme, as could have been the detection and localization of fuel rod failures.

A number of experiments conducted in KNK II also were very important for the SNR 300. One example to be mentioned is the hydrogen detectors for the steam generators of the SNR 300, which had to be tested first in KNK II. Most important, however, was the test of the core outlet instrumentation for the SNR 300.

The whole experimental programme comprised 30 to 40 individual experiments in various areas. Only some examples can be described in the frame of this report.

2.11.4.1. Physics experiments

An important experiment in this area was the use of a boiling generator in the central position of KNK II. Its goal was to demonstrate, that sodium boiling, which could have arisen, for instance, in fuel element blockages, reliably could be detected by suitable instrumentation.

To generate the boiling signals, a dummy element with 18 electrically heated rods was used in the position of the central fuel element. Specially designed microphones were installed in various positions of the core to detect and transmit the boiling noise. The experiments were run with the nuclear part of the plant shut down, but with the full sodium flow in operation, in order to obtain representative cooling and temperature conditions. The outcome of these safety experiments was extremely satisfactory: boiling could be detected unequivocally by the sensors in all positions.

2.11.4.2. Irradiation experiments

Irradiation experiments occupied most of the capacity and time of the KNK II experimental programme. In most cases, cladding materials and structural materials, fuel rods, and absorber materials were irradiated.

The pressure tube test rig allowed eight tubular specimens to be irradiated in the central position at the same time. The specimens were subjected to internal pressures of up to 500 bar; their temperatures could be controlled with high precision up to 800°C. The pressure and the temperature could be set individually for each specimen. The eight specimens were arranged in the bottom part of an experimental plug, which accommodated also the measurement and control lines. For reactivity reasons, they had to be surrounded by a ring-shaped carrier element in the central position. The phenomena studied included creeping and the creep-rupture strength of the tubular specimens as a function of radiation, temperature, and stress. The German Fast Breeder Project was also interested in carbide fuel because of its capability of much higher power densities as compared to oxide fuel. Therefore in addition to the mixed oxide irradiated in many variants in the KNK II core, carbide fuel was irradiated in KNK II. In conclusion of the KfK activities in this field, therefore, a small carbide bundle was irradiated in KNK II. It consisted of 19 rods integrated in a carrier fuel element with 102 test zone rods. Irradiation was conducted between 1984 and 1988 and attained a burnup of 80 000 MWd/t.

2.11.4.3. Sodium chemistry and operation

The experimental programme on sodium chemistry, among other topics, looked into the development of methods of analyzing the coolant and the cover gas, the difficult area of sodium sampling, and tests of oxygen and carbon probes. In addition, corrosion and the development of protective coatings as a function of various operating conditions were studied in the steam generator. An extensive programme was conducted to analyze a large number of radionuclides in sodium, also as a function of the coolant temperature.On the basis of further studies it was possible, in the summer of 1988, to install in KNK II a so-called cesium trap and run it successfully for several campaigns. It removed from the primary coolant the long lived cesium nuclides, which contributed greatly to the exposure doses in plant compartments. Sorbents, such as RVC and Sigratex, turned out to be most effective in these traps.

The tritium content of the tertiary steam system was determined for many years. Tritium is produced in the nuclear fuel by ternary fission, also in the B_4C of the absorber rods and, because of its high diffusivity, migrates from the primary to the tertiary systems. The influence of the secondary cold trap on the concentration of tritium found in the steam generator region was of particular interest.These are just a few examples meant to give an impression of the variety of items in the experimental programme conducted in KNK II.

2.11.5. Decommissioning

2.11.5.1. Permits

The decommissioning permits (DPs) applied for under the Atomic Energy Act were based on the planned sequence of demolition steps. These procedures were planned and carried out outside in, i.e. progressing from conventional plant components to radioactively contaminated systems and, finally, the activated systems [30–34]. This approach is illustrated below in Fig. 2.45 and Table 2.16.

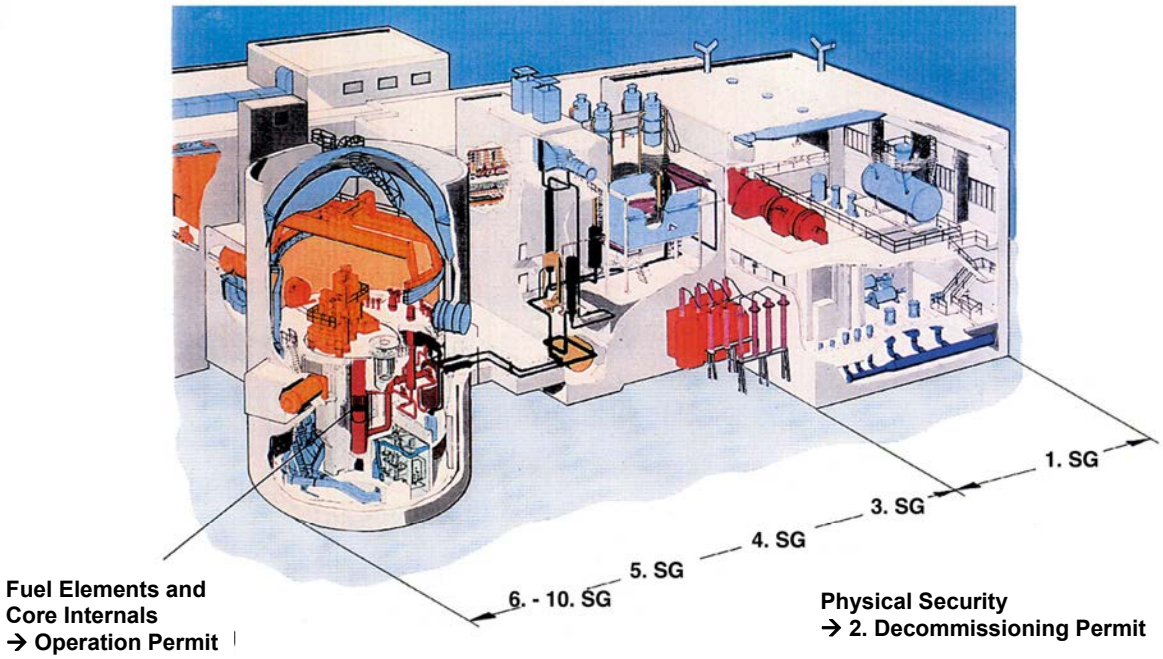

FIG. 2.45. Approach of demolition procedure of KNK II.

TABLE 2.16. SEQUENCE OF STAGES OF DEMOLITION PROCEDURE OF KNK II

Permit	Important steps
Operating permit	Unloading and disposal of all fuel elements and other movable core internals
1st DP (1993)	Decommissioning and removal of the water-steam circuit
2nd DP	Removal of the outer enclosure and reduction of physical protection
3rd DP	Disposal of secondary sodium (filling into 200 l drums and removal to Dounreay)
4th DP	Disposal of primary sodium Decommissioning, removal of fueling machine Removal of ex-vent air stack End of shift operation
5th DP	Removal and cleaning of secondary system with steam generators Decommissioning and removal of cooling tower
6th DP	Disassembly of turbine hall, steam generator building, and auxiliary facilities Demolition of argon system Removal and cleaning of withdrawable primary pump parts
7th DP	Infrastructure measures in preparation of disassembly of primary systems Removal of reactor control and protection systems
8th DP	Decommissioning and removal of primary sodium systems Removal of rotating shield of the reactor vessel
9th DP	Remote removal of reactor vessel Remote removal of primary shield Remote removal of the activated part of the biological shield Disposal of cold traps
10th DP (planned)	Removal of remaining systems Decontamination and clearance of buildings Release from the Atomic Energy Act Conventional demolition of buildings

Demolition up to and including the 8th DP more or less went as planned. However, possible amendments were applied for already at this stage in case it turned out during execution that a different approach would be preferable and easier to implement than the procedure originally planned, or if the primary systems allowed an approach to be used with lower collective doses.

Up until the end of the 8th DP there was division of labor between KBG (operator) and the KNK project management staff of the Research Center. The Research Center provided all facilities necessary for demolition while KBG organized demolition on the spot.

With the 9th DP, the Research Center also took over operations management for KNK and signed a contract for execution with the general contractor. This resulted in delays and cost increases. For this reason, the Research Center terminated this general contract in the spring of 2007.

In the course of demolition of the reactor vessel, it was discussed whether our plan to disassemble the reactor vessel in the dry mode under nitrogen, because of the residual sodium, was the best possible approach. Possibly, cleaning the reactor vessel from sodium prior to disassembly was preferable because of the possibility to employ thermal procedures [30–34].

2.11.5.2. Residual sodium

The primary and secondary sodium systems still contained sodium residues in the demolition phase. This residual sodium was a thin film on the insides or at lowest points of the system. Sometimes, for reasons not completely understood, sodium had not been drained completely, thus leaving residues in pipes or other components.

Sodium aerosol deposits in the cover gas compartments of the sodium systems turned out to be particularly critical. These sodium aerosol deposits could be highly reactive and, because of ^{137}Cs enrichment of the primary sodium, showed relatively high dose rates up to several 10 mSv/h.

The pipes and components had to be cleaned of sodium prior to delivery to HDB (Waste Treatment Department located at FZK) or conventional disposal. Various procedures were used in all of which the sodium reacted to caustic soda solution after addition of water or water vapor. Conversion with alcohol was not desired by our supervisory authority after the Rapsodie accident in 1994. No experience was available in Germany with the reaction of sodium and CO_2; hence this procedure was not considered.

2.11.5.2.1. Cleaning the secondary sodium system

The pipes and components were disassembled by mechanical techniques (sawing, milling, etc.) to such an extent that the reaction of water and sodium would not be able to build up pressure, and the sodium deposits on the insides were open to inspection.

Where pipes were filled with sodium completely or in part, that sodium was removed mechanically prior to final cleaning. These larger amounts of sodium were subsequently converted in the existing sodium wash plant.

A washing station outside the buildings was installed for component cleaning. This is where the parts were cleaned in three steps:

– The parts disassembled were placed in wire mesh crates and exposed to humid air for one or two weeks as required. Sodium reacted very slowly with normal airborne humidity but was likely to develop violent reactions when exposed to rain.
– When the sodium reaction was deemed to be complete, water was sprayed on the sodium through permanent nozzles.
– To be certain that the disassembled parts were free from sodium, the wire mesh crates were subsequently immersed in a water pool.

For safety reasons (groundwater protection), the washing station was a double-walled system with the double trough monitored for leakage. The caustic solution produced was drained into collection vessels and released to HDB as chemical liquid effluent. For sodium not radioactively contaminated, or for sodium only slightly contaminated with tritium, this method of sodium removal can be recommended.

2.11.5.2.2. Cleaning primary sodium systems

Cleaning in the sodium wash facility

The pipes and components were disassembled mechanically so as to fit into the washing vessels for cleaning. The washing vessel (Fig. 2.45a) was designed so that, at the most, the withdrawable part of a primary pump could be cleaned of sodium (diameter approx. 1 m, height approx. 6 m).

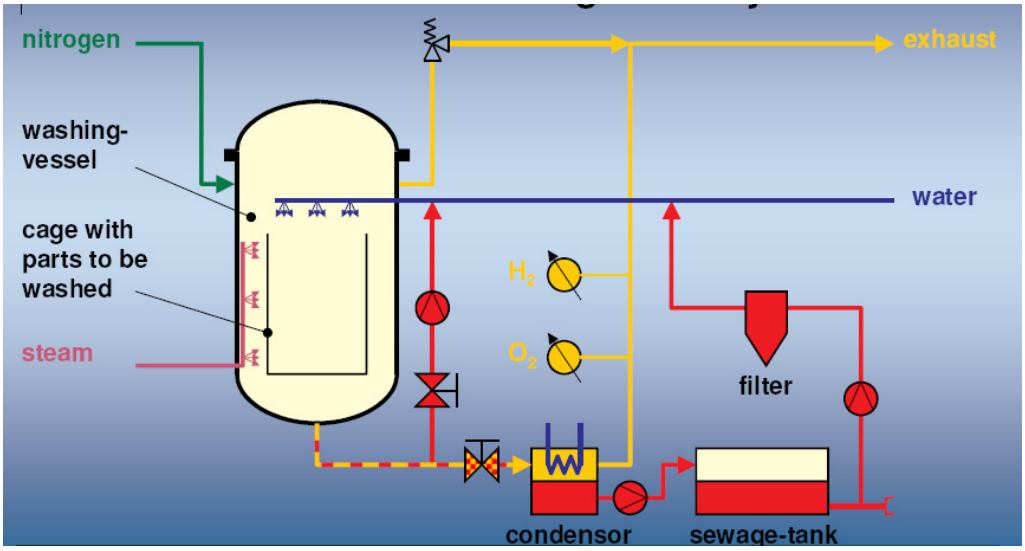

FIG. 2.45a. Scheme of the sodium wash facility.

The cleaning process was run as follows:

– Heating the filled vessel to approx. 200°C with hot nitrogen.
– Careful injection of superheated steam. The steam was metered so that the H_2-concentration in the off-gas did not become too high. When necessary, the nitrogen flow was increased.
– As soon as the main reactions had stopped, which could be seen from the evolution of hydrogen, the steam was added increasing amounts of demineralized water so that moist steam was sprayed.

– In order to be certain that all cracks had been cleaned, the part was sprayed with pure deionized water in another step, and then the entire vessel was filled.

After unloading, the vessel was dried for reloading. The caustic solution was filled into a collection vessel for radioactive liquid effluent. When that collection vessel was full, the liquid effluent was delivered to the HDB, where it will be evaporated in an evaporator. The condensate can then be passed on to the sewage treatment plant.

The sodium wash plant was left over from plant operation. For purposes of the 9th DP, where highly activated parts of the reactor vessel had to be cleaned, it was equipped with an additional shield.

Within the 6th DP, a sodium fire occurred when the last withdrawable component of a primary pump was to be placed into the washing vessel. That step had been carried out repeatedly during operation and was felt to be uncritical, also because of an existing special programme. When a plastic foil bag was opened a short distance above the washing vessel, some coagulated sodium aerosols fell out and immediately caught fire in the air. As the sodium was contaminated with ^{137}Cs, some compartments in the adjacent building were contaminated.

Cleaning large primary systems components

A procedure for large components was developed and qualified by the expert consultant which allowed the components to be cleaned in one piece.The example shown here is cleaning of the store for spent fuel elements. Figure 2.46 demonstrates schematic outline of fuel element store cleaning.

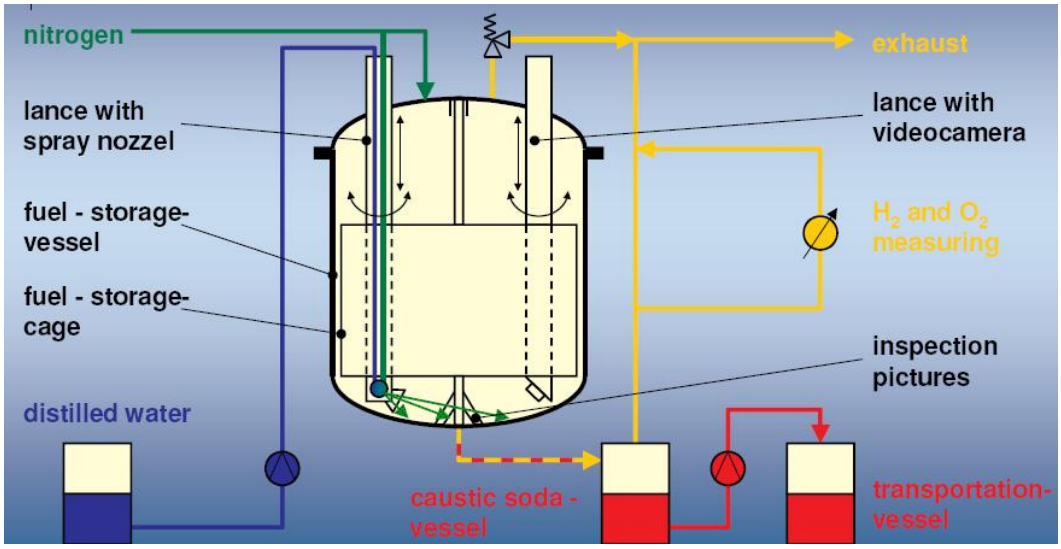

FIG. 2.46. Schematic outline of fuel element store cleaning.

First, the shielding plug was removed and the vessel was covered with a new plug. Two lances were introduced through the new plug. One lance carried a binary nozzle at its bottom end through which water and nitrogen were atomized.In order to keep hydrogen concentration low, the vessel at the same time was purged with nitrogen. The concentrations of nitrogen and oxygen were permanently monitored. The expert consultant had specified a limit of 2% for the hydrogen concentration. This limit was met easily by varying the water flow or the flow of purging nitrogen. There was another lance with a video camera and lighting system for

observation of the cleaning effect. Figure 2.47 shows the spray lance during the cleaning process. There were two possibilities to complete the cleaning process:

- For simple geometries, video inspection together with an expert consultant was planned;
- Where geometries were complicated, such as the rotating shields of the reactor vessel, the entire vessel was flooded with water.

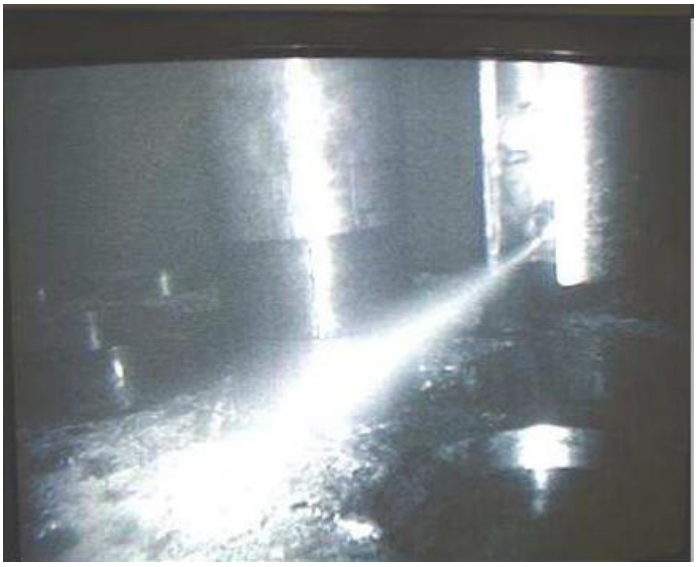

FIG. 2.47. Cleaning of the spent fuel storage vessel.

In this way, the following large components were cleaned:

(i) Sodium dump tank;
(ii) Fuel element store;
(iii) Large and small rotating shield of the reactor vessel;
(iv) Shielding plug of the fuel element store.

Conditioning with humid nitrogen of sodium surfaces and components containing sodium aerosol deposits

As sodium aerosols can be highly reactive when exposed to air, thus easily causing a sodium fire, a procedure was designed for chemical reactions on the surfaces of aerosol deposits. For this purpose, a so-called nitrogen humidification facility was developed. In that facility, the dry nitrogen was enriched with water to a relative humidity of 80 to 90%. For this humidification, an ultrasonic air humidifier was adapted to nitrogen conditions. Humid nitrogen was passed through the components or pipes, and the sodium on the surfaces was converted into sodium hydroxide. As sodium hydroxide no longer reacts with air, disassembly of these systems components became much safer.

2.11.5.2.3. Demolition of the primary and secondary sodium systems

In principle, the approach used on the primary and secondary sodium systems was similar. It basically ran like this:

- Removal of entire piping sections or components;
- Subsequent disassembly at work stations specially equipped for this purpose;
- Cleaning by the procedures mentioned in Section 2.10.5.2.

However, there were some special features to be borne in mind for the primary system:

- Pump casings were cleaned by milling away the inner surface with a special tool in the as-installed position of that component. In this way, most of the dose rate was removed as well.
- To dismantle the fuel element store, the pipe penetrations through the biological shield had to be cut in such a way that the vessel and the double tank were free to be lifted out of the cavity in the biological shield. A device working inside the pipes was developed and used for cutting the pipes.

2.11.5.3. Withdrawing the rotating shield of the reactor vessel

The rotating shield system of KNK (Fig. 2.48) consisted of a large rotating shield (blue) and an eccentric small rotating shield (red). Turning the rotating shields allowed any core position to be reached for fuelling. The so-called attachments to each of the rotating shields are shown in green colour.

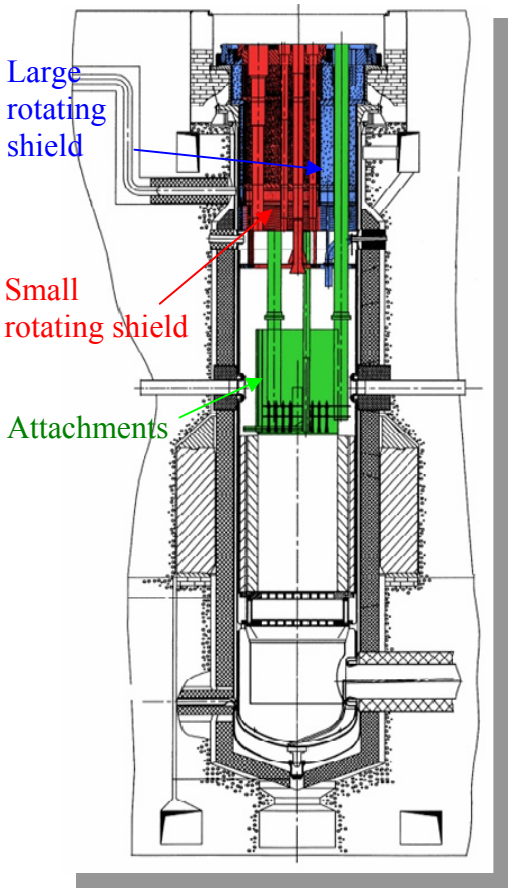

FIG. 2.48. Rotating shield system in the reactor vessel.

Special tools were manufactured and tested for removal. Initially, the two parts of the attachments were tensioned relative to each other in the area of the thermocouple distributor plates, and deposited on the reflector below by means of auxiliary tools. Next, a cutting system working inside the pipes was used to cut the lifting columns of the attachments in the area of the lower edge of the basalt box. This resulted in three components which could be removed separately. There were special shielding containers for withdrawing the parts in which the rotating shields and the attachments were cleaned as well.For each part there was a special container representing an optimum in terms of geometry, shielding effect, and load

carrying capacity of the crane. The rotating shields where cleaned by the technique described in Section 2.11.5.2.2, (b). As the geometry of the rotating shields was rather complicated making visual inspection almost impossible, the containers finally were completely filled with water for reliable removal of all sodium.

2.11.5.4. Disassembly of the reactor vessel

The reactor with its internals (Fig. 2.49) and the safety vessel together weighed approx. 43 t. Their total activity was approx. 1×10^{14} Bq. The maximum dose rate at the level of the center of the core was 27 Sv/h.

As there were still sodium residues in the reactor vessel, it was decided to conduct the disassembly step in the dry mode under nitrogen. A disassembly machine was built and tested which was then used to disassemble the vessel. The size of the parts was adapted to the size of a 200 L waste drum. In order to produce a minimum number of repository storage packages, disassembly plans were optimized. The sodium residues sticking to the parts of the reactor vessel were removed in the sodium washing facility prior to delivery of the waste drums to HDB. As mentioned above, the washing facility was equipped with an additional shield for this purpose. For milling, the disassembly machine was fixed and centered in the reactor vessel (Fig. 2.50). Movement in a total of six axes allowed all necessary cutting steps to be carried out.

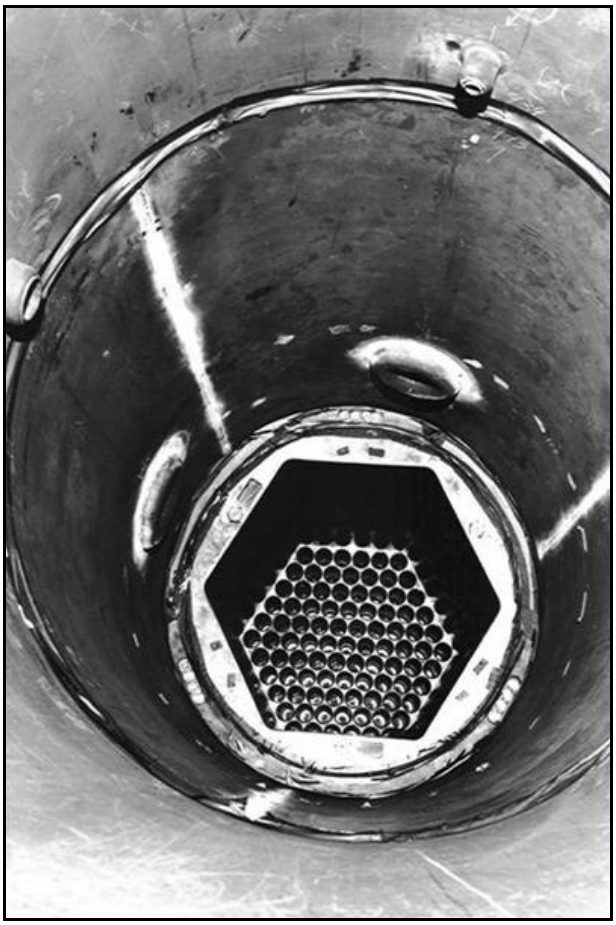

FIG. 2.49. Interior of the reactor vessel prior to disassembly.

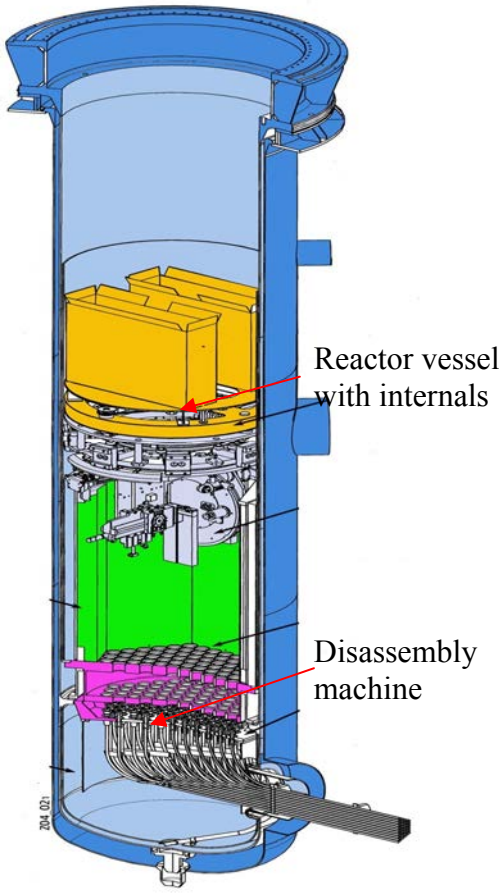

FIG. 2.50. Position of disassembly machine in the reactor vessel during its operation.

Figure 2.51 shows the disassembly machine, which allowed a variety of milling modules to be attached.

Figure 2.52 shows a reflector part being lifted out of the reactor vessel. For this purpose, a special lifting module was attached to the disassembly machine. As all parts still had to be washed, they were placed in washing baskets. A shielding bell was used to transport the washing baskets either into the washing facility or into a buffer store specially built.

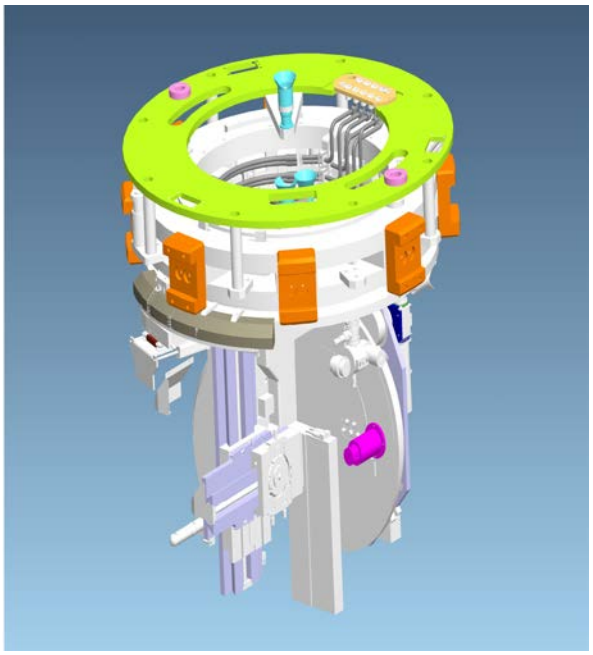

FIG. 2.51. Disassembly machine.

FIG. 2.52. Lifting reflector part from the reactor vessel.

After washing, the washing baskets were packaged in repository storage drums and transported to HDB in shipping casks (converted type-II casks) where they were conditioned for repository storage.

In the meantime, the entire reactor vessel has been disassembled.

2.11.5.5. Further procedure

After removal of the reactor vessel, the following parts still need to be removed remotely from within the biological shield (see Fig. 2.53):

- Thermal insulation (28 t of ceramic bricks and glass wool);
- Primary shield (90 t of grey cast iron);
- Activated part of the biological shield.

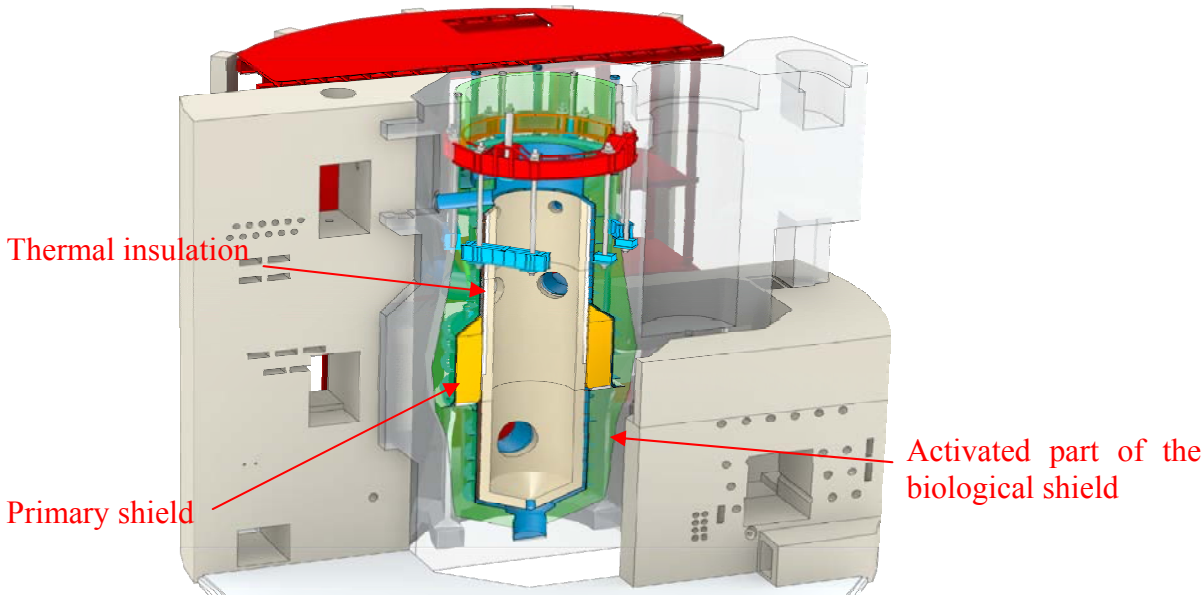

FIG. 2.53. Cut through the biological shield after removal of the reactor vessel.

The machines and facilities for this work are in various phases of procurement or testing.

A test rig is under construction in the former turbine hall of the MZFR to test the machines.

After remote removal of the systems still activated, disassembly of the remaining auxiliary systems and clearance measurement of the buildings can be started.

After clearance measurement pursuant to Section 29 of the Radiation Protection Ordinance, the buildings are to be released from the Atomic Energy Act and demolished by conventional techniques.

2.12. Joyo operating experience

2.12.1. Design features

The experimental fast reactor Joyo at Japan Atomic Energy Agency's Oarai Research and Development Center was constructed as the first step in sodium cooled fast reactor development in Japan. Its purposes are to provide the technical and engineering experience necessary for the construction of a prototype fast reactor and future fast reactors, and also for utilization as an irradiation facility for development of fuels and materials to be used for future fast reactors and fusion materials as well.

Joyo is a loop type sodium reactor with two sodium loops. The reactor vessel is a stainless steel (SUS304) with an inner diameter of 3.6 m, a wall thickness of 25 mm and a height of approximately 10 m. The vessel is double-walled and nitrogen gas fills the space between the walls. Argon gas covers the sodium and separates the sodium pool from the rotating plug. In-vessel storage rack for cooling radioactivity of spent fuel before taking out form the reactor vessel is installed around the reactor core (Fig. 2.54). A flow sheet of the cooling system is shown in Fig. 2.55.

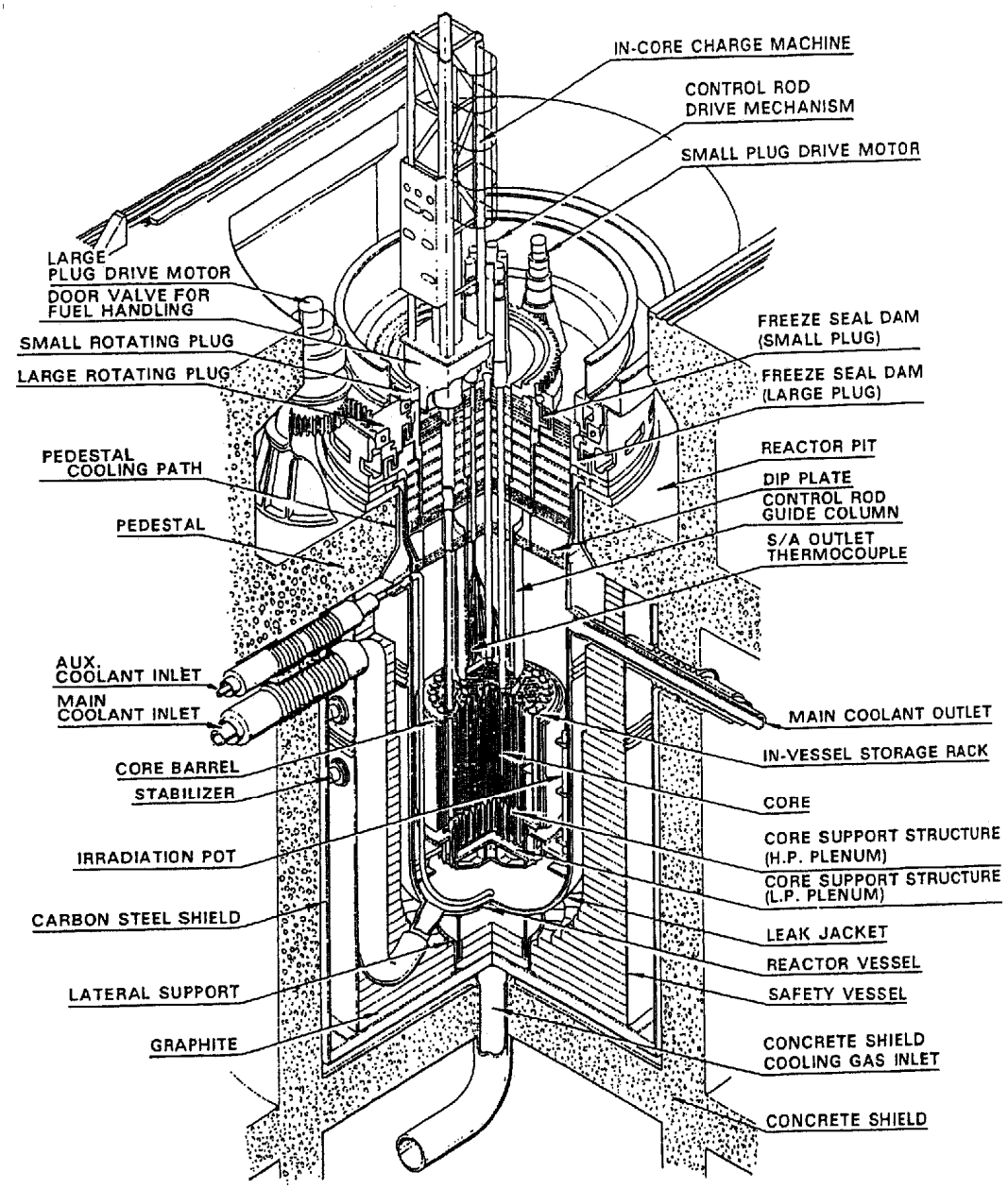

FIG. 2.54. Joyo cut-away view.

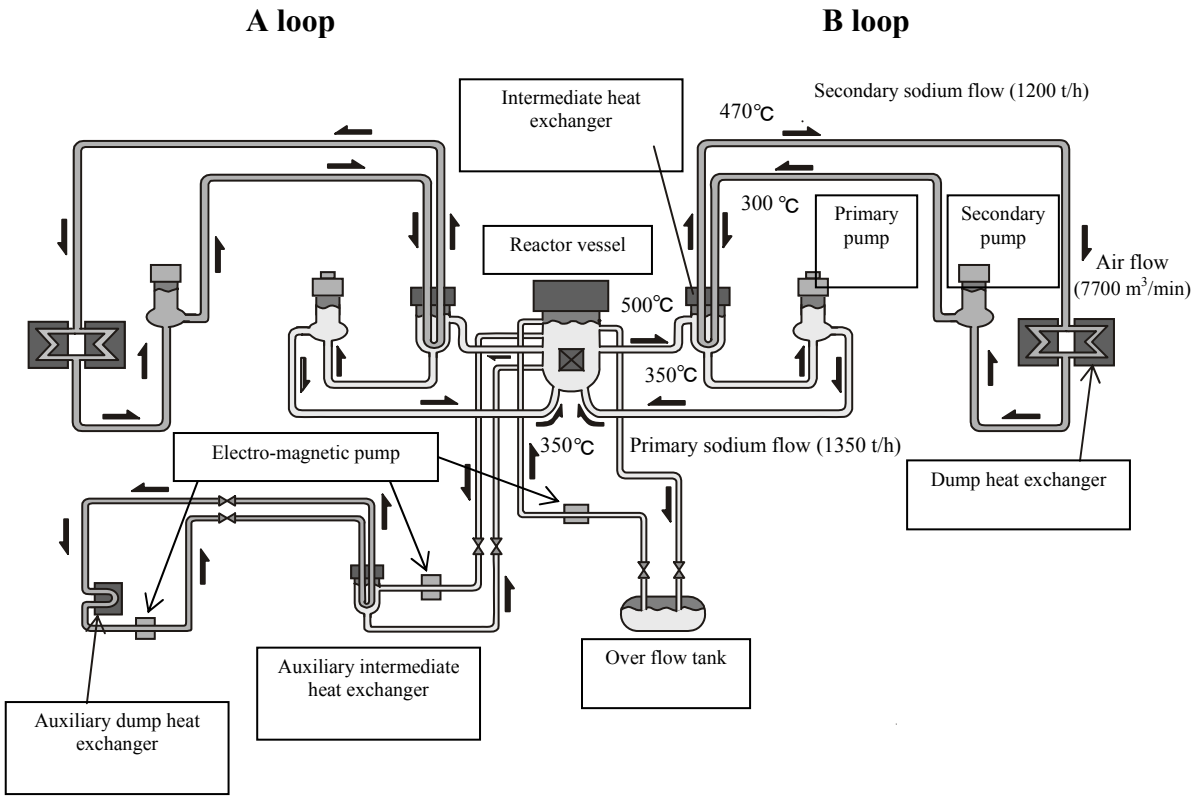

FIG. 2.55. Flow sheet of the cooling system of Joyo.

Joyo has two primary sodium loops, two secondary loops, and an auxiliary system. Approximately 200 tonnes of sodium is used for the cooling system in Joyo. The heat generated in the core is transported by the primary system sodium, which is circulated by a vertical-type, single-stage mechanical pump. The sodium enters the core at 350°C at a flow rate of 1 350 t/h/loop, and exits the reactor vessel at 500°C through 500 mm diameter piping. The maximum outlet temperature of the fuel assemblies is approximately 575°C. An intermediate heat exchanger (IHX) transfers the heat from the primary to the secondary sodium system, and the IHX separates radioactive sodium in the primary system from non-radioactive sodium in the secondary system. Secondary sodium loops transport the reactor heat from the IHX to the two air-cooled dump heat exchangers (DHX) with finned heat transfer tubes. The rated heat transfer rate of each DHX is 35 MW_{th}. All the generated heat is removed to the atmosphere by these DHX as Joyo has no steam generator. The auxiliary system, consisting of primary and secondary loops, is used for decay hear removal in case the mail cooling system is not available.

Mixed oxide (MOX) fuels with enriched uranium (U) and plutonium (Pu) are used to ensure the excess reactivity required for reactor operation. The ^{235}U enrichment of the MK-III core driver fuel is approximately 18%. The fissile Pu content (^{239}Pu + ^{241}Pu) / (U + Pu) is about 16 wt% in the inner core and about 21 wt% in the outer core.

Figure 2.56 shows an example of the MK-III core configuration.

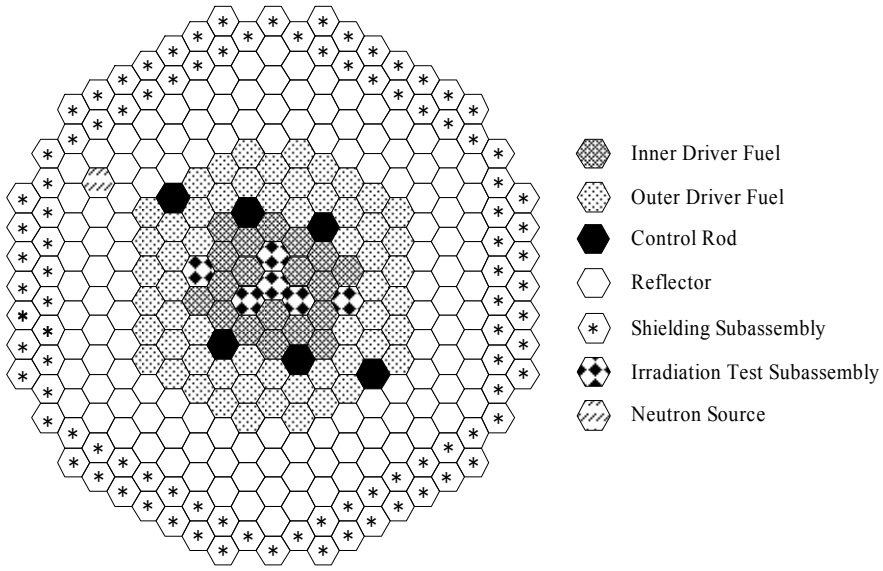

FIG. 2.56. Core configuration of MK-III equilibrium core.

The active core is cylindrical and about 80 cm in the equivalent diameter and 50 cm in height. It is a conventional two region core where the content of the fissile material of the inner and outer cores differ. There is a reflector region of stainless steel surrounding the core which is 25 to 30 cm thick. The shielding subassemblies with B_4C are loaded in the outer two rows of reactor grid to reduce the total neutron flux at the in-vessel spent fuel storage rack. All six of the control rods have the same poison-type design. The poison section contains B_4C enriched to 90% in ^{10}B, and there is a stainless steel follower section below it. The poison section is 650 mm long, which is also the axial distance the rod can move. In the MK-III core, two of six control rods were shifted from the third row to the fifth row to provide high-fast-neutron-flux loading positions for instrumented-type irradiation subassemblies.

2.12.2. Modification work for MK-III project

Joyo is expected to play a greater role in providing an irradiation field for irradiation tests to develop FBR and various other materials irradiation tests. An upgrading project named MK-III was initiated to satisfy those needs. The main objects of this project are the increase of neutron flux, the modification of the cooling system related to the power increase, the increase of irradiation periods, and the upgrading of irradiation technology.

2.12.2.1. Core design for high neutron flux

Extensive parametric calculations were performed to expand the irradiation field so that a large number of irradiation rigs could be irradiated simultaneously. The MK-III standard core design and basic core specifications were determined such that the fast neutron flux would be 1.3 times higher than in the MK-II core.

A. Design principle

The following principals were considered to achieve the desired performance of the MK-III core.

(1) Neutron flux. Improvement of irradiation performance requires that the high neutron flux region is significantly expanded. The goal of the higher fast neutron flux, which is about 1.3 times higher than in the MK-II core, is to shorten the irradiation period.

(2) Reactor power. Reactor power is 140 MW_t in order to achieve a balance between neutron flux and thermal output within the limitations of the modifications and scale of the cooling system.

(3) Loading of shielding subassembly. Shielding subassemblies containing B_4C have been loaded in the outside rows of the Joyo core matrix. Shielding subassemblies reduced the neutron flux level in the spent fuel storage rack area. Also, this allows the decay heat of the spent fuel in the fuel transfer pot to be removed by natural sodium convection within the rack.

B. Result of core design

The active core is cylindrical and about 80 cm in diameter and 50 cm in height. As a result, the fast neutron flux is up to 1.3 times higher than in the MK-II core, with 140 MW_t reactor power and a 420 W/cm (450 W/cm at the over-power condition) maximum linear heat rate in the fuel pins. Also, the irradiation test field space with a high neutron flux is about double that of the MK-II core. This was achieved by relocating two control rods and expanding the fuel region.

The comparison of the fast neutron flux between the MK-II core and the MK-III reference design core, along with their loading patterns, is shown in Fig. 2.57. The specifications of MK-I, MK-II and MK-III are shown in Table 2.17.

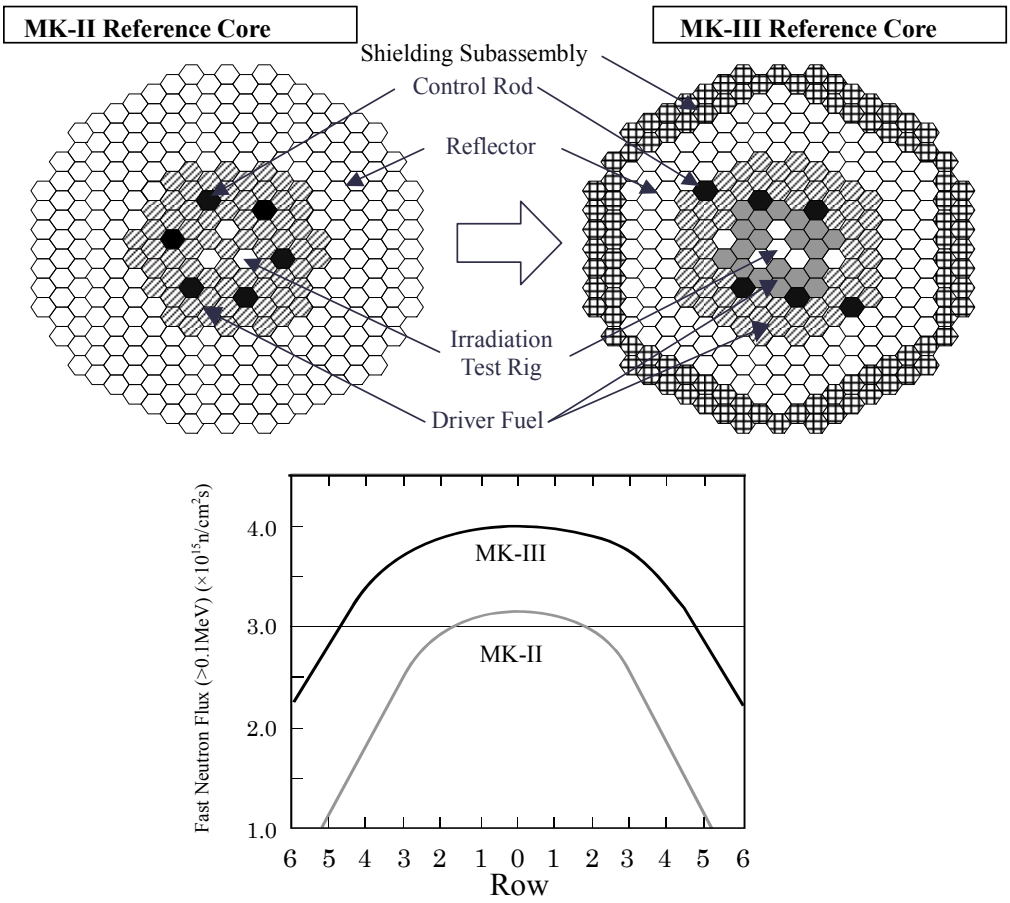

FIG. 2.57. Core modification and neutron flux distribution.

TABLE 2.17. BASIC SPECIFICATIONS OF JOYO

Item		MK-I	MK-II	MK-III
Reactor thermal output, MWt		50/75	100	140
Max. number of driver fuel S/A		82	67	85
Max. number of test fuel S/A		0	9	21
Core diameter, cm		80	73	80
Core height, cm		60	55	50
^{235}U enrichment, wt%		23	18	18
Pu content, wt%		18	30	30
Max. linear heat rate, W/cm		320	400	420
Max. neutron flux	Total, $\times 10^{15}$ n/cm^2.s	3.2	4.5	5.7
	Fast (> 0.1 MeW), $\times 10^{15}$ n/cm^2.s	2.2	3.2.	4.0
Max. burnup (pin average), GWd/t		42	75	90
	Flow rate, t/h	2,200	2,200	2,700
	Temp. (inlet), °C	370	370	350
	Temp. (outlet), °C	435/470	500	500
Blanket / reflector / shielding		Blanket/SUS	SUS/SUS	SUS/BC

With regard to the transformation to the MK-III core, the MK-III fuels were gradually loaded into the MK-II core without causing any delays in the fuels and materials irradiation test programmes.

2.12.2.2. Modification of cooling system

Modification of the cooling system in proportion to the increase in reactor power was required in the MK-III project. This involved evaluating the whole plant. We extensively examined the plant heat balance, instrument modifications of major equipment and their specifications. Thermal transient reduction countermeasures were also investigated for the instrumentation and control systems. In this examination, the following issues were considered:

- Integrity of the established facility;
- Impact to the unmodified facility and appropriate modification measures;
- Constraints in the design such as building structure;
- Adoption of the latest design standard and the latest design criteria;
- Best cost performance ratio;
- Potential problems related to the remaining reactor life.

(1) Design of cooling system

The heat balance of the cooling system was examined so that the scale of modification could be minimized. The basic configuration of the cooling system must accommodate the increase in ΔT of the coolant flow in order to raise the heat removal capacity in proportion to the reactor power increase. It was determined that the ΔT could be increased by simply lowering the cold leg temperature, since the maximum temperature of the primary and secondary systems remains at 500°C and 470°C, respectively. This is

desirable from the viewpoint of the material strength and structural integrity. With 40°C as the standard log-mean temperature difference (ΔT_m) of the IHX, the primary ΔT is 150°C. This assures the prevention of erosion in the coolant flow control mechanisms in the core and the temperature limit of the fuel cladding.

The coolant flow rate of the MK-III core is 122% of the MK-II core. In addition, it was confirmed that this flow rate was within the operation range of the existing primary circulation pump.

In the secondary system, the new ΔT is 170°C and the coolant flow rate was increased to 107% of that for the MK-II core. The drive motors of the main circulating pumps were modified due to the decrease in pressure of the secondary loop.

(2) Design of IHX

In considering factors such as reliability, operability, ease of construction, tie-in with the established facility, and effort, the same type of IHX must be employed. Since the enlargement of the IHX is difficult due to the constraints in the building, the thermal efficiency can be raised by suppressing bypass flow of sodium and by increasing ΔT_m. This made it possible for the primary heat removal capacity to be improved by 40%.

The 316FR type stainless steel, which was recently developed by JAEA, is employed as the structural material of the IHX and will be the lead material for the future FBR plant. This is an austenitic stainless steel that has improved high temperature creep properties that are applicable to the structural simplification of the plant for the commercialization of the FBR. The low carbon content and the optimization of the phosphorus and nitrogen content enhances its strength and is within the Japan Industrial Standard component range for type 316SS.

(3) Design of DHX

The heat removal capacity of the DHX was increased from 25 MW_t to 35 MW_t by changing the heat exchanger tubes in the main cooler from the conventional U type to Σ type, whereby the heat transfer area is about doubled. Other equipment such as air blowers, electric motors, vanes, and dampers also were replaced by high-performance ones. The materials and size of the heat exchanger tubes are the same as in the previous DHX because of their high reliability and performance during the past years.

2.12.2.3. Extension of irradiation period

The operating periods for irradiation are mainly limited by the loading and unloading requirements of irradiation rigs and driver fuel, and by the periodical plant inspections. These periods has been shortened due to modifications employed in the MK-III plant.

Since the heating rate of the spent fuel in the in-vessel storage rack is effectively reduced by the shielding subassemblies, the cooling pot with a coolant flow hole is no longer used. Also, the fuel handling process at the fuel storage racks in the reactor vessel has been simplified.

The fuel loading machine, cask car, fuel transfer machine, and fuel canning facility all were modified so that it is now possible to operate them automatically by remote control. In

addition, the general control system of the fuel handling facility was modified for automatic 24 hour operation. Therefore, the fuel exchange period can be shortened by up to one third.

During the periodical plant inspection periods, the control rod lower guide tube can be exchanged by the refueling machine, therefore shortening the change-out period from 20 days to 2 days. The change-out period of the irradiation devices were also examined. The periodical plant inspection period is 4 months, including the fuel exchange period. It was concluded that the reactor operating time for irradiation tests becomes 1.5 times longer in the MK-III plant.

2.12.2.4. Upgrading of irradiation technology

The development of irradiation technology has continued to expand the capability of FBR fuels and materials irradiations, and more than 10 types of irradiation devices have already demonstrated their practicality. The material irradiation rig with temperature control has been developed for creep strength testing with a temperature control accuracy of ±4°C under irradiation.

2.12.3. Operation experience

Figure 2.58 shows the operating history of Joyo.

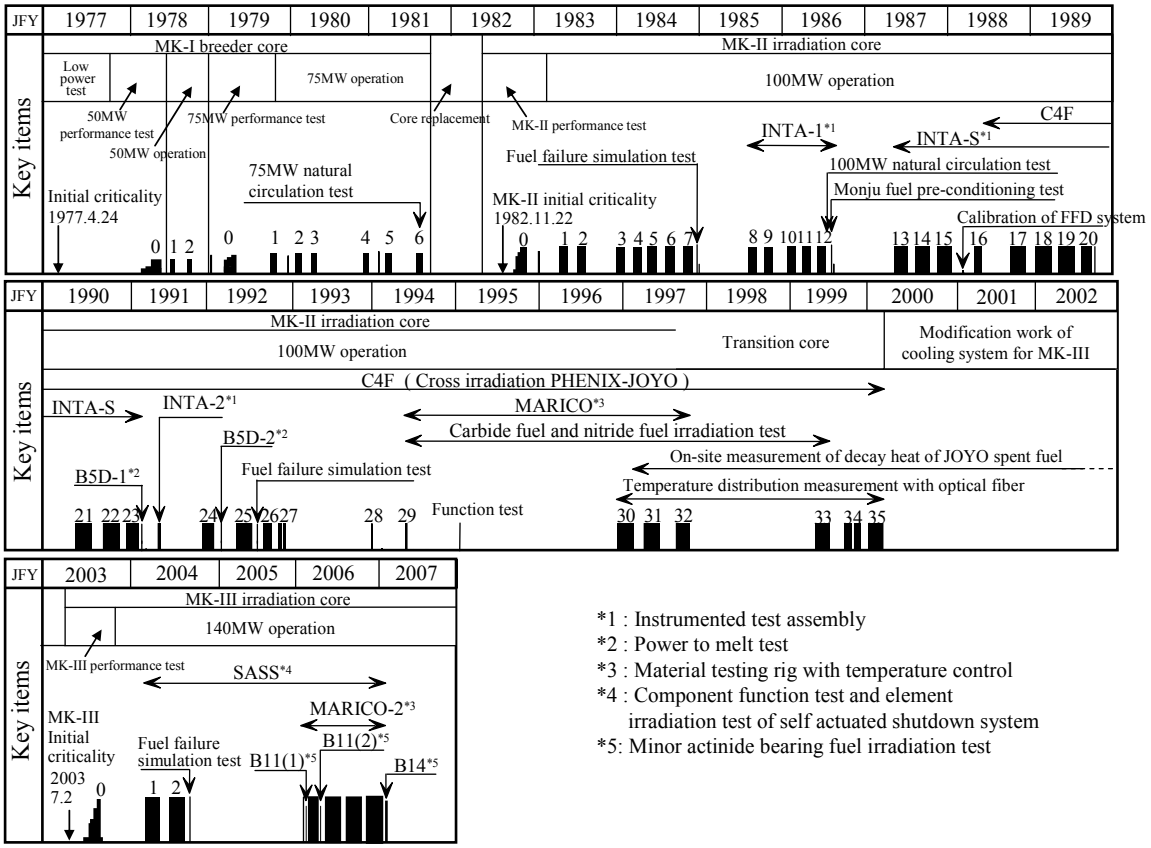

FIG. 2.58. Operation history of Joyo.

Joyo attained initial criticality as a breeder core (MK-I core) in April 1977. Joyo initially operated two 50 MW_t and six 75 MW_t duty cycles with the MK-I core. In this period there were about 260 reactor startups resulting from many kinds of tests such as those dealing with reactor physics, reactor dynamics, power ascension and transients. Through this programme, it was confirmed that the plant system satisfied the design objectives. In addition the breeding

ratio was verified by post-irradiation examination of the core and blanket fuel. The MK-I operation was completed at the end of 1981. From 1983 to 2000, Joyo operated with the MK-II core as an irradiation test bed to develop the fuels and materials for the prototype reactor Monju and future fast reactors. Several kinds of irradiation experiences have been accumulated in Joyo. One is monitoring of the driver fuels and control rods performance. Irradiation of test fuels and materials using irradiation test devices are other valuable irradiation test experience. Until the end of MK-II operation, 506 fuel assemblies were irradiated without any fuel pin failure, and a peak burnup value of 87 GWd/t and 144 GWd/t were attained for the MK-II driver fuel and irradiation test fuel respectively. From 2003, Joyo is operating with the MK-III core as a high performance irradiation test bed.

(1) Core management

A breeding ratio of 1.03 was confirmed during operation of the Joyo MK-I breeder core. On the other hand, the Joyo MK-II irradiation core was operated with a Pu conversion ratio of 0.3. This demonstrates that both breeding and consumption of Pu are feasible in the same LMFBR, with replacement of the core. Based on the irradiation results, the pellet peak burnup of driver fuel was increased step by step from 25 GWd/t to 85 GWd/t by improving the fuel design by optimizing the safety design margins and using new cladding materials that are anti-swelling and have higher strength at high temperatures. The linear heat rate of the driver fuels was also increased by rationalizing the safety margin of design with revision of maximum temperature of the fuels, based on the performance test evaluation. By the end of MK-III 6^{th} cycle operation, more than 70 000 fuel pins were irradiated without any fuel pin failure. This result indicates suitable management of the core and fuels, as well as high quality of fuel fabrication.

(2) Demonstration of Pu fuel recycle

Pu fuel recycle was demonstrated in 1984. Two MK-I driver subassemblies unloaded in 1981 were dismantled to remove the fuel pins, and ten fuel pins were transported to the Chemical Processing Facility (CPF) of Tokai works for the FBR fuel reprocessing tests in 1982. Approximately 56 g of Pu was extracted in the CPF and 25 g of Pu was used for processing MOX fuel pellets. The fuel pin which fabricated using these new fuel pellets was transported to the Irradiation Rig Assembling Facility (IRAF), adjacent to Joyo, where an irradiation test subassembly was assembled using this pin. This test assembly was irradiated in the MK-II core from the 5th duty cycle operation in 1984 to the 12^{th} duty cycle operation in 1986 up to a maximum burnup of 39 GWd/t, and integrity of these fuels was confirmed by PIE. Thus, small scale nuclear fuel cycle within an FBR was realized by Joyo and other MOX fuel facilities.

(3) Natural circulation test

The inherent safety of a fast reactor can be demonstrated by proving the natural circulation capability and establishing analytical techniques based on experiments. The natural circulation test from 100 MW_t was carried out at the end of the 12^{th} cycle of the MK-II core in 1986.

The test was initiated by tripping the primary and secondary sodium pumps manually without pony motor operation. This caused a reactor scram, and the blowers of the DHX were stopped immediately upon receipt of the reactor scram signal. The central driver fuel subassemblies underwent the most severe temperature transition during the tests. Figure 2.59 shows the outlet temperature of one of these subassemblies, together with primary coolant flow rate variations.

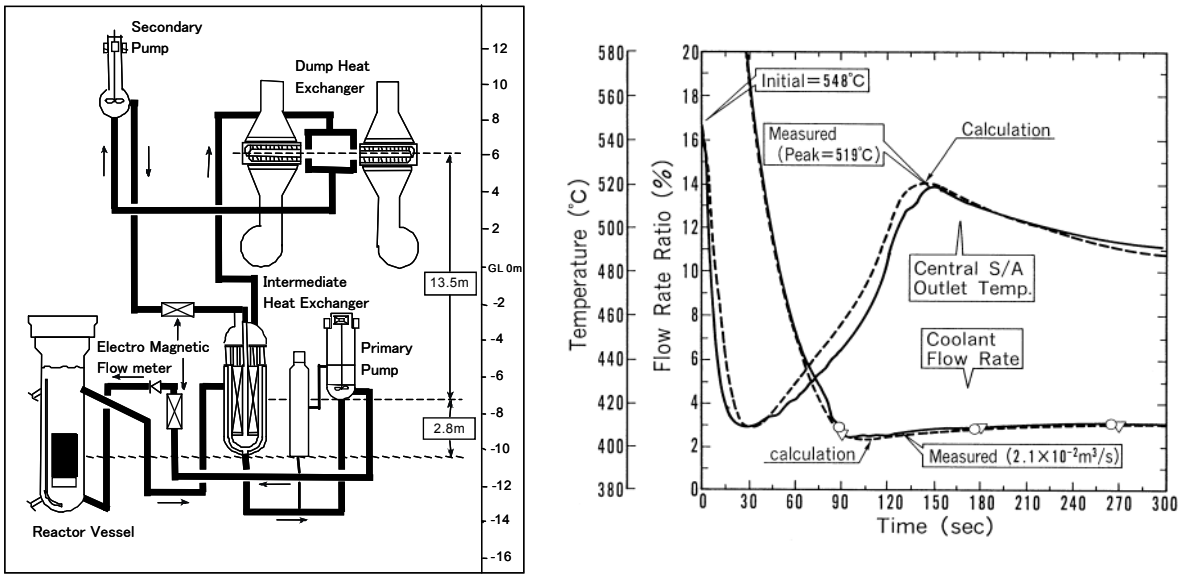

FIG. 2.59. Results of natural circulation test.

The peak temperature reached 519°C due to coolant flow rate reductions. This peak is significantly below the initial temperature of 548°C. Thus, it was shown that the temperature increase will not cause any safety-related problems, such as fuel cladding failure. The post analysis results from a plant wide dynamics code, MIMIR-N2, are in excellent agreement with the experimental data. The MIMIR-N2 analysis code includes all plant system models (core, primary cooling system and secondary cooling system) and was developed to analyze Joyo plant kinetics.

(4) Fuel failure simulation tests

When a fuel failure occurs in a nuclear reactor, it is essential to quickly detect the event and identify the failed fuel subassembly. As Joyo has not yet experienced any natural fuel pin failures, three fuel failure simulation tests had been conducted in the MK-II core. After the MK-III modification, performance of the fuel failure detection (FFD), the failed fuel detection and location (FFDL) systems, and the plant operation procedure in case of fuel failure needed to be demonstrated. The Joyo FFD system consists of both delayed neutron (DN) monitoring systems and a cover gas (CG) precipitating system. Two DN monitoring systems are located adjacent to the primary cooling loops to detect the delayed neutrons emitted from precursors released into the coolant sodium. The CG precipitating system detects the fission product ^{88}Rb, i.e., beta decay of ^{88}Kr released into the cover gas argon.

The fourth in-pile fuel failure simulation was conducted in the MK-III core. A test subassembly containing two fuel pins with an artificial slit on the fuel cladding tube was used for the irradiation test. The test fuel subassembly and the test results are shown in Fig. 2.60.

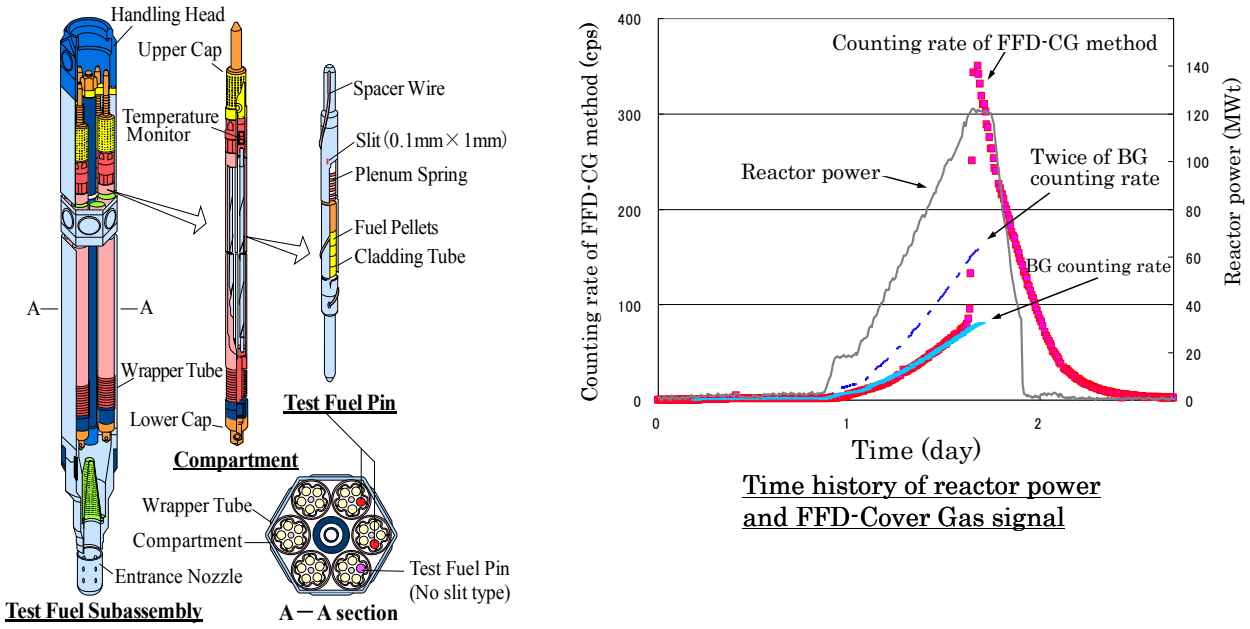

FIG. 2.60. Fuel failure simulation test.

When the reactor power reached 120 MW_t the fission gas released from test fuel pins was observed using several detectors of the FFD system. After the reactor shut-down, the subassembly which released fission gas was identified using the FFDL system. The test results will be also useful for preparing the future run-to-cladding- breach (RTCB) tests in Joyo.

(5) Reliability of sodium components

Operational experience in Joyo during about 30 years has shown excellent reliability of sodium-cooled, loop-type FBR. Particularly, sodium components, such as mechanical pumps, electromagnetic pumps, sodium service valves and sodium relating piping have been successfully operated. The structural materials of sodium components, such as stainless steel and ferrite alloy steel, have excellent compatibility with sodium. Sodium components are basically maintenance free, as they have no rubbing parts in the sodium. The primary cooling system of Joyo is equipped with two identical, motor-driven, centrifugal, free-surface mechanical pumps, as is the secondary cooling system. Cumulative operation time of the primary and secondary pumps amounts to 157 000 h and 169 000 h, respectively, including reactor shutdown periods (with 250ºC sodium temperature). Since the functional tests of MK-I, no trouble has been experienced with the inner assembly of any of these pumps.

(6) Irradiation test for MA-MOX fuel

An irradiation test for mixed oxide fuel containing minor actinides (MA-MOX) is performed in Joyo to investigate the irradiation behavior of this fuel. An irradiation subassembly consists of three types of fuel pins: test pins containing 3% and 5% americium (Am-MOX), fuel pins containing 2% americium and 2% neptunium (Np/Am-MOX) and reference MOX pins.

A MA-MOX fuel irradiation test series in Joyo named B11 is being conducted. A capsule type irradiation test subassembly, which enables the irradiation test of advanced fuel, such as those containing minor actinides, is used. Each test fuel pin is enclosed in a capsule to contain any

fuel and fission products in case of fuel failure. This irradiation test series includes initial structural change confirmation test (B11(1)), MA re-distribution confirmation test (B11(2)), and steady irradiation test (B11(3)). The fuel pin specifications containing MA are shown in Fig 2.61.

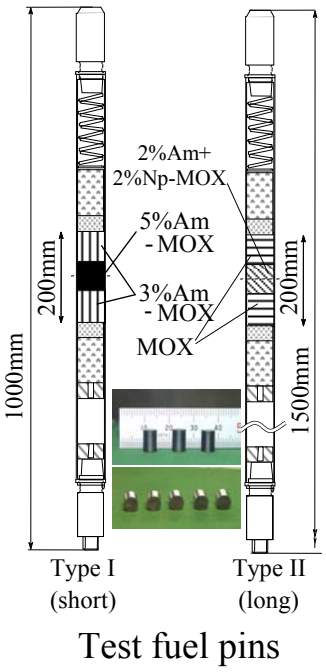

MA-MOX fuel pin specification

	Type I: Am-MOX	Type II: Np-Am-MOX
Diameter (mm)	6.5	5.4
O/M Ratio	1.95, 1.98	1.95, 1.98
Density (%TD)	93	93
Composition (%)	Pu 30, Am 3 or 5	Pu 30, Np 2+Am 2
LHR(W/cm)	427～431 *2	426～431 *2

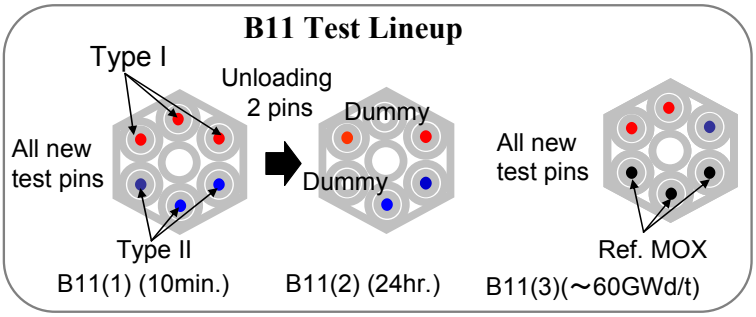

∗1: Referred to an article contributed FR'91 from CEA
∗2: Tentative evaluated values

FIG. 2.61. MA-MOX fuel pin specification.

As to fuels and materials irradiation, oxide dispersion strengthened ferritic steel (ODS), which is the most promising candidate for fuel cladding of future long life fuel, has been irradiated. Then, leading very high burnup irradiation tests will be started sequentially, and some rigs will open the door of planned fuel breach to investigate fuel life limit design. Targeted to realize economical fuel, short-process MOX fuel pellets, vipac MOX fuel or metal fuel will be tested in addition to conventional MOX fuel. The sodium bonded-type control rods with shroud tubes will be irradiated to demonstrate their long life. The B11(1) and B11(2) test were successfully conducted in 2006. In these tests, the maximum linear heat rate of the test fuel pin was set by the reactor power level, and the reactor power was raised continuously, held at 120 MW_t about 10 minutes in B11(1) and 24 hours in B11(2). The maximum linear heat rate was approximately 444 W/cm.

2.12.4. Planned schedule

The Joyo irradiation test programme is shown in Fig. 2.62.

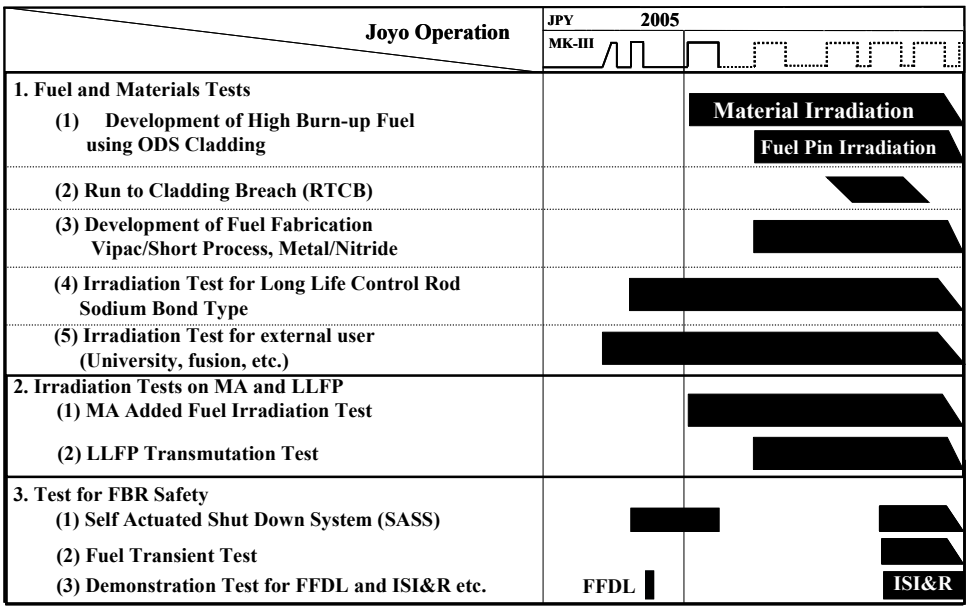

FIG. 2.62. Joyo irradiation test programme.

In the transmutation area, which is aimed at reducing the environmental burden of long-lived radionuclides, the irradiation test of moderator for incineration of ^{99}Tc and ^{129}I is planned. In the reactor engineering area, fuel slow transient safety testing, anticipated-transient testing without scram, and in-service inspection and repair demonstrations are being considered. The test results will be utilized in the fast reactor cycle technology development in Japan, which is similar to the Generation-IV study.

2.13. BN-600 operating experience

2.13.1. Introduction

The BN-600 reactor was constructed at the Beloyarsk NPP site and it is the 3rd power unit of the BNPP. It was connected to the grid on 8 April 1980. The design electrical power level of the reactor plant, 600 MW, was reached in December 1981.

Now the BN-600 reactor is the largest operating fast reactor in the world. For many years, the BN-600 reactor power unit is among the best NPP in the Russian Federation regarding reliable and stable operation.

2.13.2. Design description

The main technical parameters of the BN-600 power unit are presented in Table 2.18 [7, 35].

TABLE 2.18. THE MAIN CHARACTERISTICS OF THE BN-600 POWER UNIT

Item	Value
General parameters	
Thermal power, MWth	1470
Electric power, MWe	600
Number of circuits	3 (1 and 2 circuits - sodium, 3 circuit – steam-water)
Design lifetime, year	30
Primary circuit	
Arrangement	Pool-type
Reactor vessel support	At the bottom
Vessel cooling agent	Cold sodium
Number of heat removal loops	3
Inlet/outlet core sodium temperature, °C	377/550
Sodium flow rate, t/h	25000
Core and fuel	
Fuel	Uranium dioxide pellets
Max. fuel burnup, % h.a.	11.1
Diameter, mm	2058
Height, mm	1030
Intermediate heat exchanger	Shell-and-tube design, secondary sodium flowing on the tube side
Primary pump	
Design	Centrifugal, one stage
Rotating speed, rpm	250 - 970
Steam generator	
Design	Once-through, section & modular, 8 sections (3×8=24 modules)
Inlet/outlet sodium temperature, °C	518/328
Inlet/outlet water/steam temperature, °C	241/507
Live steam pressure, MPa	14
Secondary pump	
Design	Centrifugal, one stage
Rotating speed, rpm	250 - 750
Turbogenerator	Standard
Power, MW	210
Decay heat removal system:	
Primary and secondary circuits	Normal operation system
Third circuit	Steam generator - deaerator, emergency feedwater pumps
Refueling system	2 rotating plugs, vertical refueling mechanism
Fuel transfer system	Elevators with guide ramp
Spent fuel storage	In-vessel storage, sodium and water pools
Washing of subassemblies from sodium	Steam-gas-water

Heat transfer from the primary circuit to the secondary one is provided by two intermediate heat exchangers “sodium-sodium” in each loop. Heat from the secondary circuit to the steam-water medium of the tertiary circuit is transferred in sectional/modular steam generators (SG)

having 8 sections in each loop. Each SG section can be isolated from the secondary and tertiary circuit by cut-off valves.

The reactor facility can operate with two loops (when the third loop is shutdown) at a power level up to 70% of the rated value.

A general scheme of the NPP with the BN-600 reactor is shown in Fig. 2.63, the longitudinal section of the BN-600 reactor is presented in Fig. 2.64.

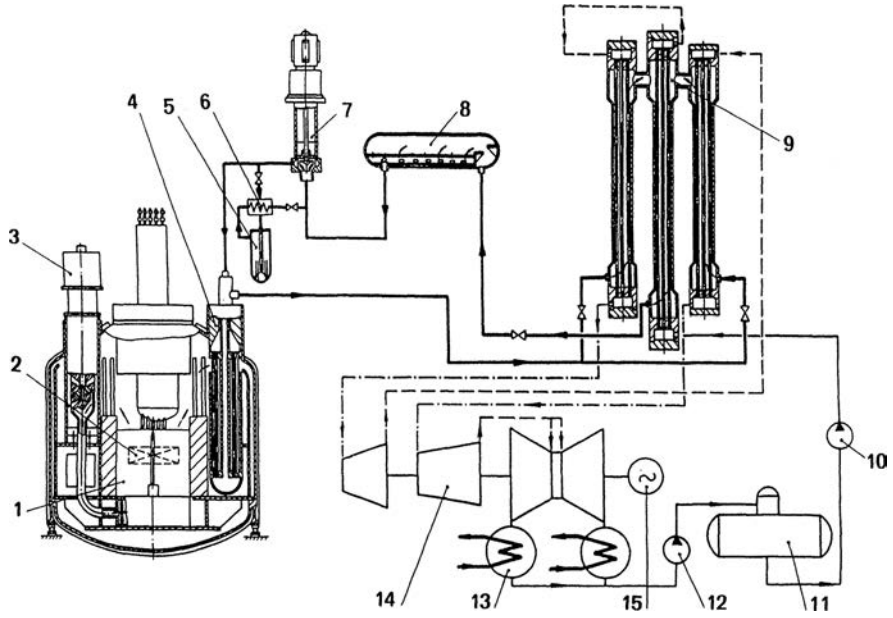

1-reactor, 2-reactor core, 3-reactor coolant pump, 4-intermediate heat exchanger, 5-filter-trap, 6-recuperator, 7-secondary coolant pump, 8-sodium expansion tank, 9-steam generator, 10-feedwater pump, 11-deaerator, 12-condensate pump, 13-condenser, 14-turbine plant, 15-turbogenerator.

FIG. 2.63. General scheme of the BN-600 power unit.

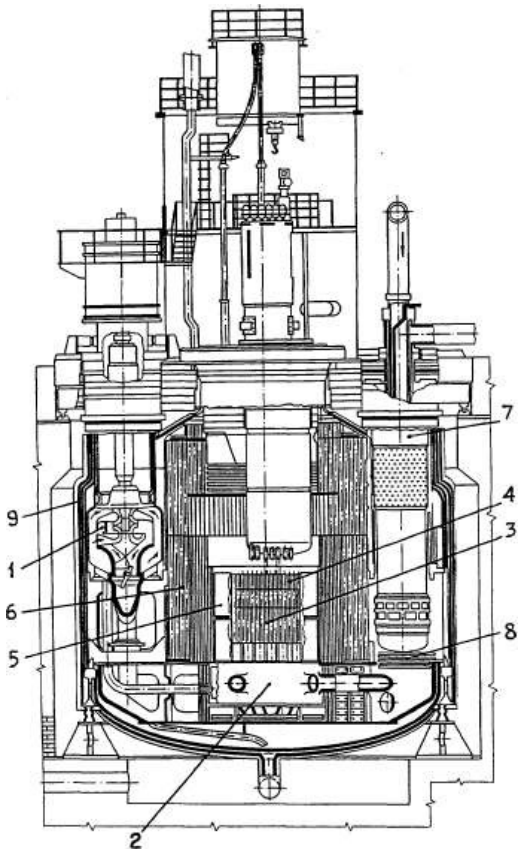

1 - pump, 2- high pressure header, 3 - core, 4 - blanket zone, 5 - spent assemblies storage, 6- in-vessel neutron shield, 7- heat exchanger, 8 - dumps, 9- reactor vessel

FIG. 2.64. BN-600 reactor.

The BN-600 reactor was successfully operated with the core 01M1 having a maximum design fuel burnup of 10% h.a. Complex research work was done to increase the design value of the burnup of fuel up to 11.1 % h.a. for a new BN-600 reactor core design 01M2 [36].

From spring 2004 till autumn 2005, a transition to the new core modification 01M2 with 4-fold reactor refueling was implemented. The new BN-600 reactor core has the same characteristics as the previous core configuration besides increased a design value of a fuel burnup and more prolonged refueling interval accordingly. Structural materials of fuel pin cladding and fuel subassembly duct remained the same. Main design characteristics of all the BN-600 reactor core modifications are shown in the Table 2.19.

TABLE 2.19. BN-600 REACTOR CORE DESIGNS EVOLUTION

Parameter	Reactor core type			
	1	M	M1	M2
Reactor thermal output (max.), MW	1470	1470	1470	1470
Reactor core diameter, mm	2058	2058	2058	2058
Active core height, mm	750	1000	1030	1030
Axial blankets height, mm				
Upper	400	300	300	300
Lower	400	380	350	350
Number of different fuel enrichment zones	2	3	3	3
Fuel enrichment in ^{235}U, %				
LEZ	21	17	17	17
MEZ	-	21	21	21
HEZ	33	26	26	26
Number of FA in core zones:				
LEZ	209	136	136	136
MEZ	-	94	94	94
HEZ	160	139	139	139
Core fuel cladding OD × wall thickness, mm	6.9×0.4	6.9×0.4	6.9×0.4	6.9×0.4
Fuel rod length, mm	2400	2400	2400	2400
Fuel rod gas plenum length, mm	808	653	653	653
Number of fuel rods in FA	127	127	127	127
Duct width across flats × wall thickness, mm	96×2	96×2	96×2	96×2
Core structural materials:				
Cladding*	EI-847	EI-847	ChS-68cw	ChS-68cw
Duct	Cr16Ni11Mo3	Cr16Ni11Mo3Ti	**	**
Fuel rod maximum linear heat rating, kW/m	54.0	47.2	≤48.0	≤48.0
Fuel rod cladding peak temperature, °C	~700	~700	~700	~700
Maximum fuel burnup, % h.a.	7.2	8.3	10	11.1
Maximum radiation dose to cladding, dpa	43.5	53.9	75.0	82.0
Fuel operating life, fpd	200/300	300/495	480	560/720
Core fuel cycle, fpd	100	165	160	120/160***
Fuel inventory in core, kg	8260	11630	12090	12090
Average fuel burnup, MW·d/kg U	42.5	44.5	60.0	70.0
Temp.-power reactivity effect, % Δk/k	-1.4	-1.3	-1.3	-

* EI-847 - Cr16Ni15Mo3Nb – austenitic steel, Chs-68cw - Cr16Ni15Mo2Mn2TiB – austenitic steel;
** Cr12MoBnVB – ferritic-martensitic steel;
*** 120 fpd – summer fuel cycle, 160 fpd – winter fuel cycle.

2.13.3. Operating experience

2.13.3.1. General information

As of 31 December 2009, the total time of reactor power operation had exceeded 206 000 hours, electricity production by the power unit during this period being over 112.5 billion kW·h.

The average load factor for the period of commercial operation of the BN-600 power unit since 1982 till 2009 inclusive, i.e. excluding initial stage of power mastering, is equal to 73.9%. As regards reliability indices, the BN-600 power unit is one of the best Russian NPP during a lot of years. Load factor behavior during commercial operation of the BN-600 power unit (upon reaching its design power level) is shown in Fig. 2.65 [37].

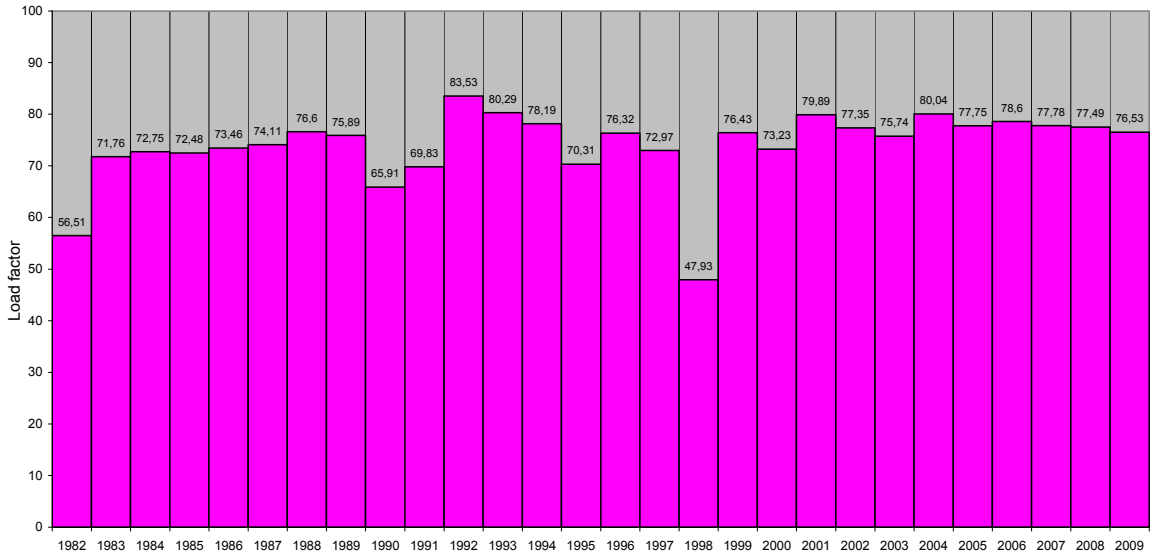

FIG. 2.65. Change of load factor during BN-600 power unit commercial operation.

Figure 2.66 shows the distribution of load factor losses on categories for the period of the BN 600 power unit operation since 1982 up to 2004 including [38].

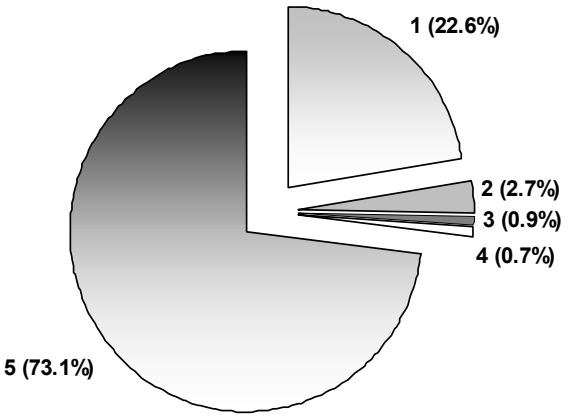

1 - scheduled inspections and core refuelings;

2 - failures of the equipment and personnel errors;

3 - other reasons (dispatching restrictions, decrease of efficiency of the 3rd circuit etc.);

4 - heat supplies;

5 - electric power production.

FIG. 2.66. Distribution of the reasons of load factor decrease of the BN-600 power unit.

During the considered period of power unit operation (1982-2004), 97 events related to unscheduled reactor shutdown or its power decrease have occurred. All these events refer to 0 and «out-of-scale» levels of INES, except for one event of the 1st level, thus confirming high safety level of the BN-600 power unit. In 60 cases, reactor power decreased down to 2/3 of rated value because of shutdown of one heat removal loop. It follows from Fig. 2.66 that only

2.7% loss of electricity production was caused by unscheduled reactor shutdowns and power decreases as a result of failures of technological components and personnel errors.

Distribution in time of events caused by failures of components and personnel errors is presented in Fig. 2.67.

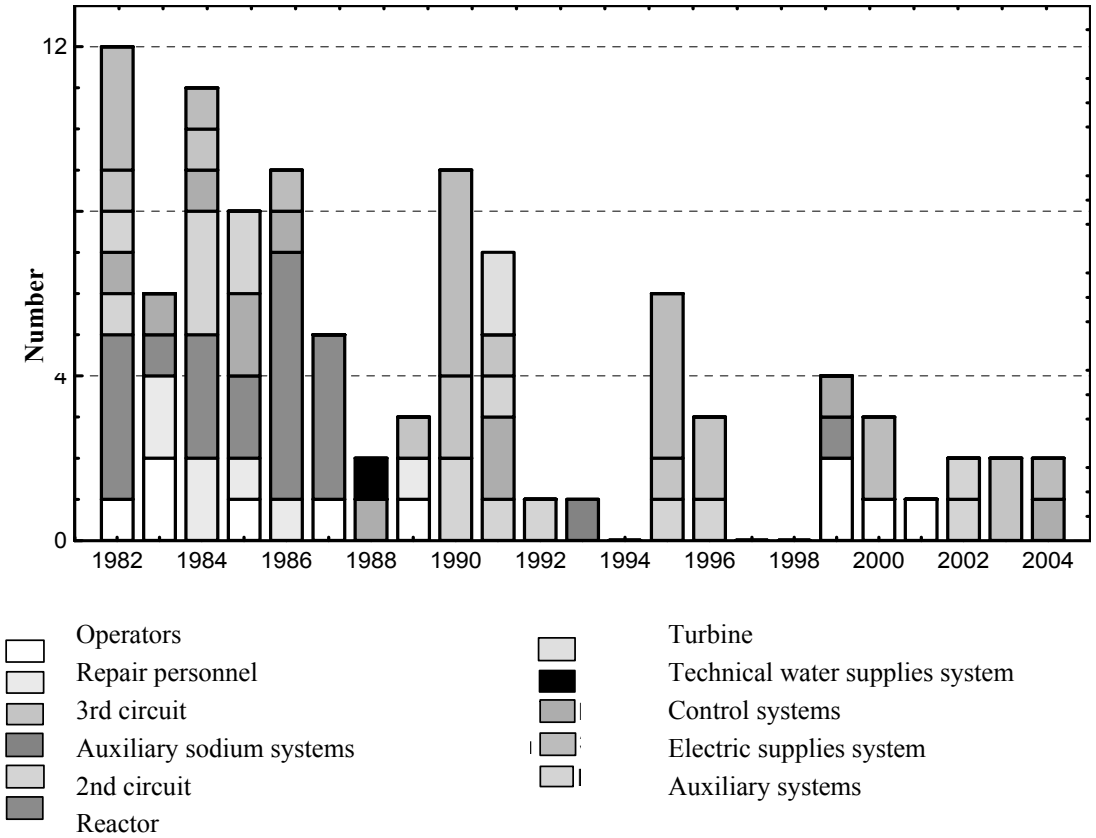

FIG. 2.67. Time distribution of events caused by failures of the equipment and the personnel errors.

Experience of the BN-600 reactor operation shows that in the recent period (upon mastering of SFR technology and adjustment of the main components) unscheduled losses of load factor which have been caused mainly by failures of the components of the third circuit were equal on an average to 1.1% per year. Scheduled value of load factor loss is caused by duration of power unit shutdown periods for carrying out scheduled preventive and repair work and reactor refueling. Now, the duration of annual reactor shutdown period for scheduled preventive repair (SPR) is mainly determined by the rated time of complete overhaul of the turbine generators (50 days) and time required for reactor refueling (twice a year). In the recent years of operation, average SPR duration has been about 71 days.

The BN-600 reactor, being more than 30 years in operation, has demonstrated high parameters of safety and operating reliability. During this period, the following achievements have been reached:

- Long-duration tests of large-size sodium components;
- Mastering sodium technology;
- Development and optimization of operating modes;
- Mastering technology of replacement and repair of sodium components including pumps and steam generators.

As of 2009, the following indices of the operating time and lifetime of the main components of the BN-600 reactor were achieved:

- Reactor vessel, primary circuit pipings – 205 000 h;
- Intermediate heat exchangers – 205 000 h;
- Sodium pumps – 105 000 h;
- Steam generators (evaporators) – 125 000 h.

The replacement of the following main equipment of the BN-600 power unit was implemented during its operation:

- 4 sets of the primary sodium main circulating pumps;
- 2 sets of the secondary sodium main circulating pumps;
- 1 set of mechanisms of the control and protection system (CPS);
- 3 sets of guide tubes of CPS rods;
- 1 set of evaporator modules of steam generators;
- 1 intermediate heat exchanger.

2.13.3.2. Steam generators

Sectional/modular steam generators (SG) used in the BN-600 reactor have demonstrated high performance for the whole period of power unit operation. During the whole period of SG operation, 12 leaks of steam and water into sodium have occurred; half of these leaks took place in the first year of operation because of manifestation of hidden manufacture defects. Intercircuit leaks took place mainly in the superheaters (6 events) and reheaters (5 events), while only one leak occurred in the evaporator (Table 2.20).

TABLE 2.20. LIST OF INTERCIRCUIT LEAKS IN BN-600 SG MODULES

Date	24.06. 1980	04.07. 1980	24.08. 1980	08.09. 1980	20.10. 1980	09.06. 1981	19.01. 1982	22.07. 1983	06.11. 1984	10.11. 1984	24.02. 1985	24.01. 1991
Leak place	RH	SH	RH	SH	SH	SH	SH	SH	E	RH	SH	RH
Leak size	L	L	S	S	S	S	L	S	S	S	S	S

RH – reheater, SH - superheater, E – evaporator, L – large leak, S – small leak

Note: Large leak is characterized with a change of main parameters of the secondary circuit (pressure of sodium and gas in sodium tank).

All listed SG leaks were suppressed by regular means, and thus they have not resulted in emergencies [39].

The last SG leak has taken place in January 1991. Thus, for over more than 19 years the SGs operate without any leaks, that testifies to successful SG design and to high quality of their manufacturing. A work programme aimed at the extension of design lifetime of evaporators of the steam generators (SG) was accomplished on the BN-600 power unit. This programme included special examination of condition of the evaporators, upgrading of water chemistry, decrease of the number of transients and accidents as compared to predicted values and carrying out chemical cleaning and water washing procedures on the regular basis for removal of low-density deposits. All these measures made it possible to justify extension of the lifetime of evaporators from 50 000 hours design value up to 105 000 hours and, hence, assure single replacement of the evaporators instead of three replacements planned for the

whole lifetime of the power unit. The scheduled replacement of SG evaporator modules has been carried out in the middle of 1990s.

2.13.3.3. Rotating plugs

Since 1995, seizure of the small rotating plug was observed during reactor refueling, and this seizure became stronger with time. In order to determine and eliminate the cause of this phenomenon, inspection of the small rotating plug with its lifting from the reactor was performed during scheduled preventive repair (SPR) combined with reactor refueling in 1998. It was confirmed that bearing unit was plugged with sodium and, besides, the small deformation of a lateral surface of the small rotating plug was revealed. The operations on replacement of the bearing unit and increase of a gap between the large and small rotating plugs by means of sweep and treatment of the lateral surface of the small plug were performed. Implementation of these works made it possible to restore design plug rotation force and now its operation is provided in accordance with regular mode without any deviations.

2.13.3.4. Sodium leaks

During BN-600 reactor operation, 27 sodium leaks have occurred.

Below is given the distribution of sodium leaks with respect to their causes (see also Section 6.5):

- Failures of SG sodium valves 5 leaks
- Defects of flange joints 5 leaks
- Wrong sequence of procedures of melting sodium in the pipeline 4 leaks
- Holes made by personnel 2 leaks
- Manufacture defects 3 leaks
- Sodium valve defects 2 leaks
- Cracks in the pipelines 6 leaks

Total number of leaks can be distributed with respect to the reactor facility components in the following way:

- Sodium reception system 5 leaks
- Cut-off valves of SG modules 5 leaks
- Auxiliary secondary systems 12 leaks
- auxiliary primary systems 5 leaks

All 27 sodium leaks that occurred during BN-600 reactor operation were detected in due time by control systems or operators.

Powders were used for confining and extinguishing non-radioactive sodium fires. It was only in one case of leak and fire of radioactive sodium from the primary circuit, that design algorithm of confinement of sodium fire consequences was implemented successfully: in this case radioactivity release (10.7 Ci) was well below permissible limit. There was no need in using drainage based fire fighting systems. Unique experience has been gained in the operation of sodium leaks confinement systems showing their effectiveness.

Since the time of issuing the previous edition of the status report on liquid metal-cooled fast reactors in 1999 [24], there were no sodium leaks from the sodium circuits of the BN-600 reactor. Last sodium leak outside took place in 1994. Thus, the BN-600 reactor operates for the last 16 years without any sodium leaks. It testifies to successful mastering sodium

technology by the power unit personnel and high parameters of reliability of the sodium equipment and communications. As a whole, it is possible to make the conclusion that the influence of specific features of the sodium coolant on economic indices and safety of the BN-600 power unit was minimal for all period of its operation.

2.13.4. Work on extension of unit lifetime

Design lifetime of power unit No 3 of Beloyarsk NPP with the BN-600 reactor is equal to 30 years and expires in 2010. A successful operation of the BN-600 power unit has allowed beginning works for substantiation of prolongation of its design lifetime from 30 up to 40–45 years.

Preliminary analytical studies were carried out on the substantiation of lifetime extension of non-replaceable components of the BN-600 reactor taking into account real data on modes of operation and obtained data on change of operating properties of structural materials. Results of studying behavior of operating characteristics of reactor plant structural materials after 200 000–300 000 hours of operation principally confirm an opportunity of such lifetime extension (LTE) for the BN-600 reactor plant.

During the 2002-2005 period, the first stage of the BN-600 preparation for its LTE was accomplished. At this stage the following activities were carried out:

- A complex of studies (including necessary research of structural material behaviour) aimed at a substantiation of an opportunity of lifetime extension of non-replaceable components of the BN-600 reactor plant was started;
- A comprehensive examination of the systems and components of the power unit has been completed. It allowed the determination of necessary additional research and a list of the equipment that should be replaced;
- The current safety level of the power unit has been estimated. An estimation has been made on the impact of identified deviations on the safety of the power unit. The measures for the elimination and the indemnification of safety deficiencies have been recommended;
- Works on management of the lifetime of recoverable components (evaluation of their status, maintenance service, repair).

In 2005, work on components replacement and their safety improvement required for LTE was also carried out. In particular:

- Manufacturing of steam generator modules was started (within the framework of preparation for LTE, replacement of all steam generators is planned);
- The outlet cascades of low pressure cylinder on No.5 turbine were replaced. A similar procedure is planned on the remaining two turbines;
- Work is going on to increase seismic stability of the power unit, as well as to modify measurement and automatic control system.

Since 2006 the stage of a direct preparation to LTE began. Now this activity has been successfully completed and the lifetime of the BN-600 reactor is extended up to 31 March 2020.

2.13.5. Conclusion

The successful operation of the power unit with BN-600 reactor during 30 years testifies to successful industrial development of technology of fast reactors with sodium coolant. Technology of replacement and repair of sodium equipment, including the main equipment (pumps, steam generators) also has been mastered.

The operational experience accumulated at the BN-600 reactor demonstrates that after mastering sodium technology by the personnel, the specific features of sodium coolant have no significant influence on safety and operational parameters of the power unit.

2.14. Fast flux test facility operating experience

2.14.1. History

The Fast Flux Test Facility (FFTF) was a 400 MW_t sodium-cooled loop-type fast reactor designed in the 1960s and built in the 1970s on the US-government owned Hanford Site in south-eastern Washington State. The FFTF was operated by Westinghouse Hanford on behalf of the US DOE as a facility to develop and test advanced fuels and materials. Early in the design phase the decision was made to not include the capability for producing electricity because the intent was to use the facility solely for research and not to complicate operations by the demand for power or because of possible steam generator problems. Figure 2.68 shows an aerial view of the FFTF in the 1990s.

FIG. 2.68. Aerial view of the FFTF site, clearly showing the containment dome of the reactor and its three sets of four air-dump heat exchangers.

AEC approval for the facility was given in 1965, and after a lengthy design and approval process, site preparation began in the summer of 1970 [40]. Reactor construction and sodium fill were completed by 1978. Prior to initial operation, the Nuclear Regulatory Commission and the Advisory Committee on Reactor Safeguards performed extensive reviews of the plant design and Final Safety Analysis Report, the same review process followed at commercial reactors [41]. Initial criticality took place on 9 February 1980, and full power operation was achieved on December 21, 1980. Following an additional year of extensive acceptance testing, FFTF was operated safely and successfully as an irradiation facility from 1982 to late 1992 [42].

Although several additional potential missions including medical and industrial isotope production were identified and demonstrated, in 1992 DOE ordered the shutdown of FFTF

because of a lack of economically viable missions and a decline in funding support in LMR development; similar reasons were to cause permanent shutdown of the EBR-II 21 months later. From 1994 through 1997, fuel was removed from the reactor and placed either in fuel storage vessels or in above-ground dry storage casks; 23 of its 100 operating systems were put into lay-up [43]. In early 1997, FFTF was ordered into standby condition while its possible role in tritium production was evaluated. The future for FFTF was debated over the next several years but in late 2001, decommissioning was resumed, including sodium drain and storage, fuel packaging for long term interim storage, and deactivation of the auxiliary plant systems. Decommissioning continues today [44].

2.14.2. Design description

The FFTF was a three-loop LMR operated at a peak power of 400 MW_t. and a peak flux of $\sim 7\times10^{15}$ n/cm^2·s. With a core inlet temperature of 360°C, three hot-leg centrifugal pumps supplied a primary sodium flow of 2 200 kg/s to give a core outlet temperature of 503°C. FFTF had neither steam generators nor blanket assemblies for breeding; instead it had air-dump heat exchangers and a reflector region of assemblies loaded with Inconel blocks. Figure 2.69 shows a perspective of the reactor.

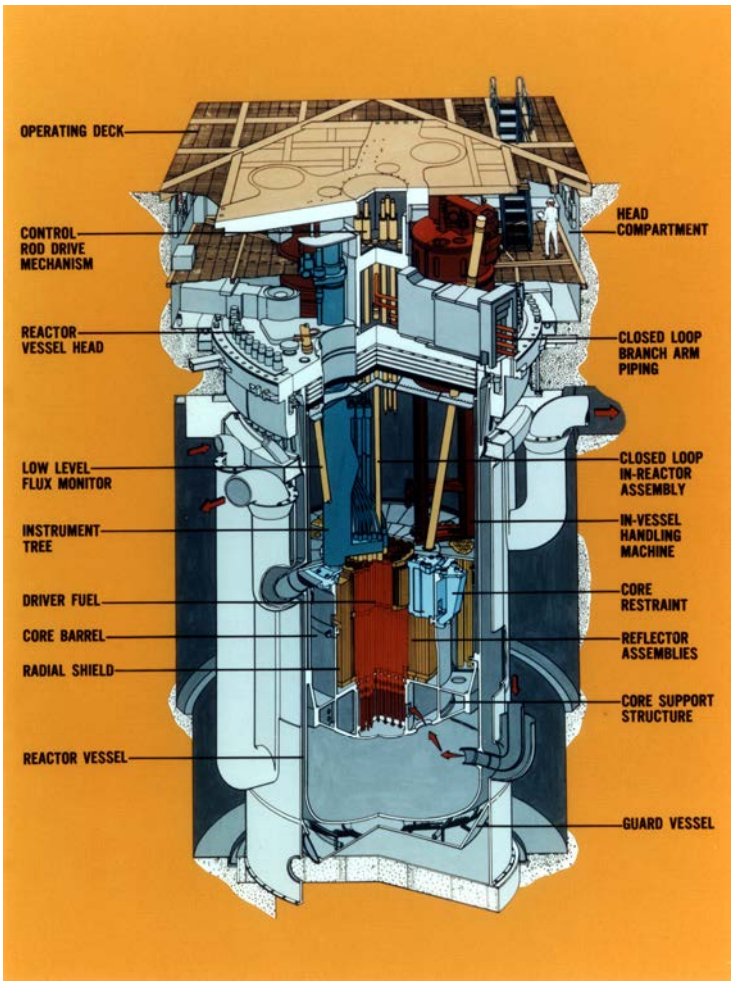

FIG. 2.69. Perspective view of the FFTF.

Design of the FFTF driver (core) assembly is shown in Fig. 2.70(a),(b).

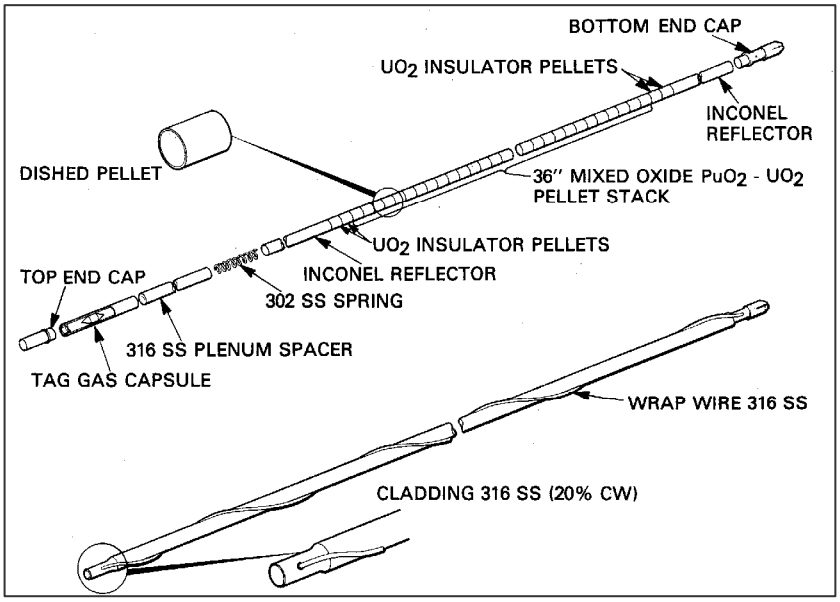

(a)

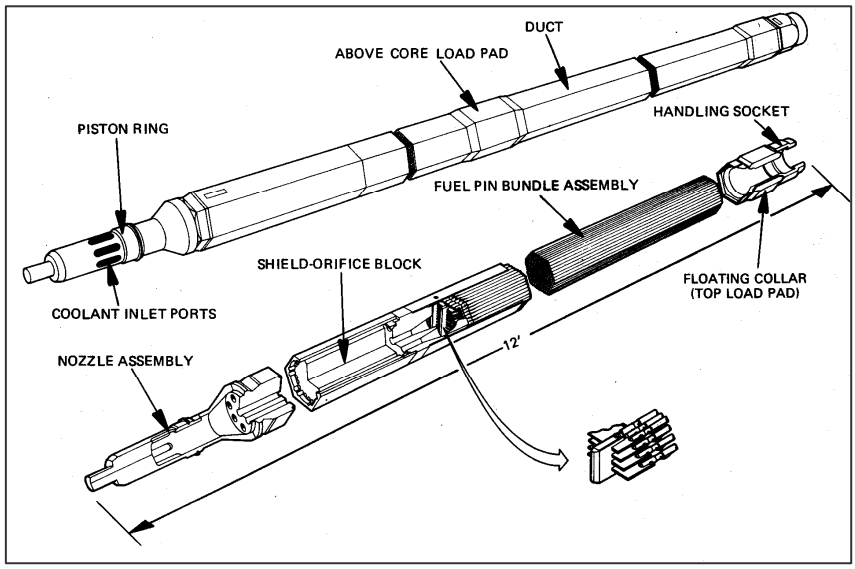

(b)

FIG. 2.70. FFTF Driver fuel:
S.S.-clad PuO_2-UO_2 fuel pin (a); Core assembly of 217 fuel pins (b).

A total of 217 5.8-mm diameter pins, each containing a 0.91-m column of PuO_2-UO_2 fuel pellets, were contained in 3.8-m long SS assembly in an hexagonal duct measuring 116 mm flat-to-flat and 3 mm in wall thickness. A typical FFTF core loading contained 74 such assemblies.

As befitted a modern irradiation facility, the FFTF had a great deal of instrumentation - sodium flow and exit temperature were measured for all core fuel, control and safety assemblies, and for selected reflector assemblies. Eight open test assembly core locations were fully instrumented. Two locations could accept a closed loop, although none was ever used.

2.14.3. Fuel handling experience

Spent fuel was discharged via the in-vessel handling machine (IVHM) loaded in one of three rotating plugs that each traverse one-third of the core. Three areas between the core barrel and the reactor vessel were used for In-Vessel Storage (IVS), where fuel could cool down in sodium-cooled Core Component Pots (CCPs) to the heat load allowed in the Closed-Loop Ex-Vessel Machine (CLEM). The CLEM transferred the spent fuel from IVS to the Interim Decay Storage (IDS) Vessel located in containment where it was allowed to cool further to the heat load allowed in the Bottom-Loading Transfer Cask (BLTC). The BLTC was used for transfer of the spent fuel out of containment. The BLTC was used both for removing spent fuel from the IDS Vessel and for bringing fresh fuel into CCPs in the IDS for preconditioning before loading in-core. The CLEM was used for both bringing fresh fuel in CCPs from IDS to the Reactor Vessel and moving spent fuel from the Reactor Vessel to IDS.

Despite its three separate machines, the total refueling system was used successfully for 14 major and 6 minor outages by the end of 1992, with the total transfer time steadily decreasing with time as experience was gained. Over all, there were >2 300 IVHM moves, >1 450 CLEM transfers, and >1 500 BLTC transfers. The only minor problems encountered were due to sodium vapor deposition in the machines (requiring regular filter changes) and maintenance of the computers that were used to control them [42]. As part of enhancing equipment operations and improving efficiency, the computer control systems for the IVHM, CLEM, BLTC and IDS were replaced in the Fuel Offload Project.

2.14.4. Operating experience

Like the EBR-II, the FFTF enjoyed remarkably trouble-free operation without significant problems with its fuel, components, or nuclear systems. For example, driver assemblies routinely reached peak burnups of 90-100 000 MWd/t and only one fuel failure was encountered out of 200 core assemblies (~ 40 000 fuel pins) taken to this goal exposure. From 1987 to final shutdown in 1992, a core demonstration test was performed of 6 blanket and 10 driver assemblies with cladding and ducts made from the low-swelling alloy HT-9; peak burnups reached an LMR record of 238 000 MWd/t without failure. Eleven cladding breaches in endurance tests of other experimental fuel pins were identified without difficulty using the gas-tag method that was originally developed at the EBR-II [45].

During 1986, a large number of plant tests were performed to more fully understand the passive safety characteristics of an oxide-fueled LMR [42]. Static and dynamic tests were carried out over a broad range of power, flow and temperature conditions, including demonstration of stable operation at low power under natural circulation cooling conditions. A passive safety enhancement device - the gas expansion module (GEM) - was developed and tested specifically to offset the excess reactivity in an oxide core during unprotected loss of flow.

Final tests in the series demonstrated the effectiveness of 9 GEM shutdown devices installed in the reactor: when the primary pumps were stopped at 50% power (200 MW_t) with the normal control-rod scram response disabled, the GEMs and inherent core reactivity feedback mechanisms acted to take the reactor sub-critical with only a transient 85°C rise in the sodium outlet temperature.

The primary and secondary pumps operated for over 200 000 hours without any major maintenance required. Pump coast-down times were periodically measured to detect mechanical problems and no adverse trends were observed. Similarly, the thermal performance of the intermediate heat exchangers were routinely monitored and remained

essentially unchanged from initial values. Electromagnetic pumps required little maintenance except for one that developed a pin-hole leak in 1984 due to flow tube deformation caused by sodium freeze/thaw cycles and cavitation/erosion at high sodium flow; it was promptly and easily replaced.

Other problems that occurred were also minor. For example, in Cycles 1-6 (1982-85) the primary system pressure drop increased from ~ 1040 kPa to ~ 1062 kPa over one year and then returned back to normal values over the next two years [46]. The phenomenon caused no real difficulty but needed explanation. Of several theories developed to explain the phenomenon, the only one that withstood the test of analysis and in-plant testing was an increase in surface roughness caused by deposition of small silicon-based crystals in the core inlet orifice blocks. The source was postulated to be Si leached from the core and hot-leg steel, possibly with some contribution from construction residues like SiC. The effect observed in FFTF was consistent with previous testing at Hanford to study hydraulic effects of Si leaching [47].

In early FFTF cycles, small random power fluctuations of about 2.5% peak-to-peak were noted. These fluctuations were characterized and shown to be attributable to control rod movement due to radial clearances in experimental rods with circular ducts. When the experimental rods were eventually removed, power fluctuations returned to the normal range of 0.1% to 0.5%.

One minor operating problem related to deformation of one of three fuel transfer ports in the reactor head; in November 1987 the shield plug in this port required a greater than normal force withdrawal force. Diagnostics showed the plug was stuck because the nozzle was tilted. In 1989 failure of an encapsulated depleted U shield in the nozzle vicinity, resulting in reaction of the U with air to cause swelling, was found to be the cause for the nozzle tilt. Some shielding was removed mechanically and the problem was solved.

This trouble-free operation of the FFTF - a tribute to its design - was manifest in a high plant factor (60-80%) through most of its operating lifetime. The years 1986, 1989 and 1991 were periods when plant safety testing and other special tests had significant impact on operations. The annual capacity factor of the FFTF is shown in Fig. 2.71.

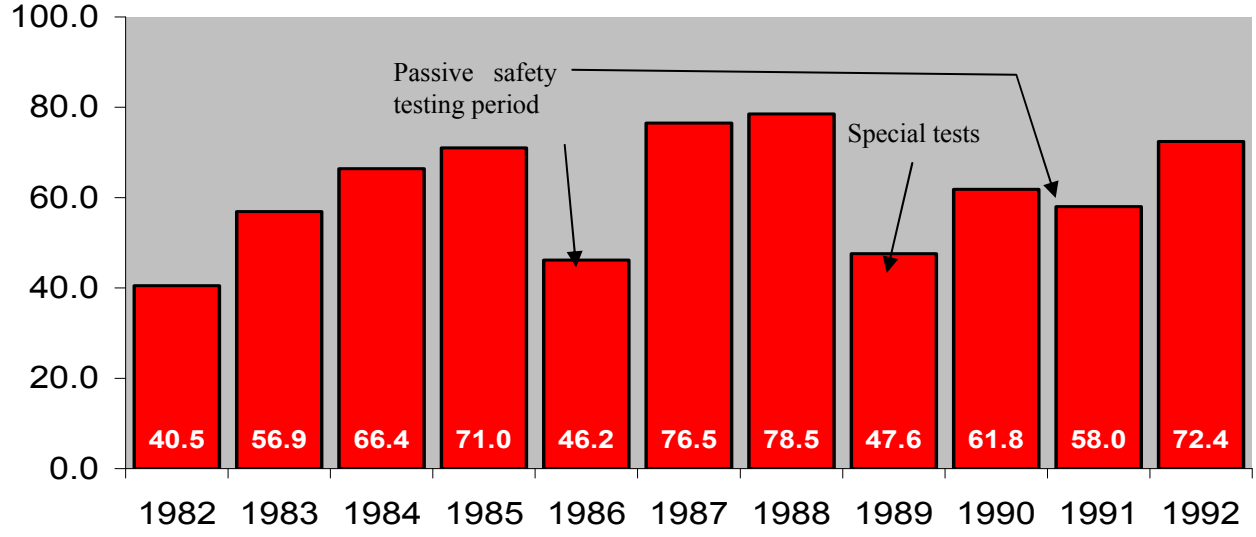

FIG. 2.71. Annual capacity factor of the FFTF.

2.15. Superphénix operating experience

2.15.1. Design features

Superphénix is the brand name of the nuclear steam supply system of the power plant located at the Creys-Malville site. Its design, derived from Phénix, is of the pool (or integrated) type. Primary sodium coolant is entirely enclosed in the main stainless steel vessel which contains the core, and in which are installed four primary pumps and eight intermediate heat exchangers, IHXs [24].

The reactor core is made up of 364 fissile subassemblies, in the form of uranium - 15% plutonium mixed oxide pellets stacked in 271 stainless steel cladding pins, with upper and lower depleted uranium oxide blankets. The fissile subassemblies are surrounded by 3 rows of fertile subassemblies of similar design containing only depleted uranium oxide, and by several rows of steel elements acting as neutron reflector and shielding.

The main vessel is closed above the free level of sodium and argon cover gas by a thick slab, made of a steel boxed structure filled with concrete, which carries all primary system structures and components, and provides neutron shielding to the operators who have to perform routine interventions on the reactor top. In its central section, the slab features two eccentric rotating plugs, which support fuel handling devices, and the core cover plug which supports the control rod drive mechanisms and the core instrumentation. The main vessel is surrounded by the safety vessel, also hanging from the slab, which is itself topped by a metallic dome. This dome can resist a pressure of 3 bar at a temperature of 180°C. The safety vessel and the dome make up the primary containment boundary, and the reactor building in reinforced concrete constitutes the secondary confinement boundary.

Thermal power extracted from the core by primary sodium is transferred by the 8 IHXs to 4 secondary loops which in turn supply the steam generators, housed in four buildings around the outside of the reactor building. The steam produced spins two turbine-generator sets of 620 MW_e each, at 3000 rpm.

Since the end of construction in 1984, the plant has seen three different stages of evolution:

- In 1984, with the building of the fuel storage pool building (APEC);
- In 1988, with the replacing of the sodium filled fuel storage drum by an argon-filled fuel transfer station (PTC);
- In 1993, with the modifications to improve means of prevention and handling of secondary sodium spray fires in the reactor building and the steam generator buildings.

2.15.1.1. The APEC and PTC

In the initial plant project, it was envisaged to ship the spent fuel subassemblies to a reprocessing plant after a period of one year in the sodium-filled storage drum. It was also planned to renew 50% of the core after a half-cycle of 320 EFPD. The storage drum could receive 409 subassemblies with a power of up to 28 kW individually. Removal of the subassemblies was carried out when the power had decayed to less than 7.5 kW.

In 1982, the necessity for large scale market introduction of fast reactors was less acute and therefore, there was less need for a dedicated reprocessing centre. This led the owner/operator, Centrale nucléaire européenne à neutrons rapides SA (NERSA), to decide on

the on-site construction of temporary storage capable of accommodating several spent cores. This is referred to as the APEC (Atelier Pour l'Evacuation du Combustible).

Then in 1988, a sodium leakage occurred, and the cost-benefit assessment of the storage drum repair resulted in NERSA's decision to eliminate it altogether and replace it with a gas-filled transfer chamber. This modification, which was made possible thanks to the existence of the APEC, in turn led to modification of the management mode of the core which is now based on frequency 1. The core is renewed entirely after a cycle of 2 to 3 years (640 EFPD). Replacing the subassemblies at a later stage requires 7 to 8 month delay, including an initial period of 2 months for decay of the first discharged subassemblies to a level of 7.5 kW. The APEC and the PTC make up two links of the handling line shown in Fig. 2.72.

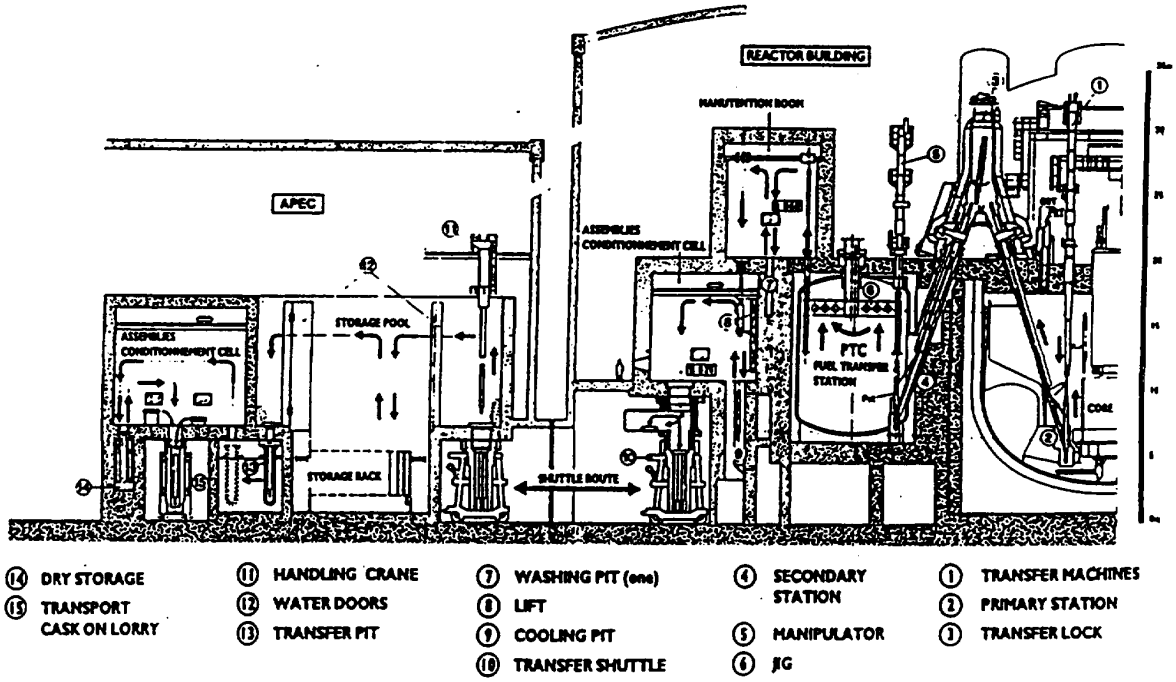

FIG. 2.72. Superphénix - evacuation line for fuel subassemblies.

Construction of the APEC covered the period 1984 to 1989, and that of the PTC lasted two years (1990/91).

The subassemblies are placed by the transfer machine in a sodium-filled container which is carried by the bucket in the A-frame. In the PTC, under argon, the container carrying the subassembly is placed on a pivot arm which transfers it to the handling line. The pivot arm has a third position to receive the new subassemblies to be loaded.

After washing, the subassemblies are placed in a transfer shuttle which can receive three subassemblies. The APEC offers storage for approximately 1 700 subassemblies shared between the pool with a capacity of about 1 400 subassemblies and a hall which can house about 300 subassemblies in casks under inert gas atmosphere. Unloading capacity of the handling line is about four to five subassemblies per day.

2.15.1.2. Sodium fire modifications

Initially the type of secondary sodium fire taken into account for safety resulted from a clean break of the largest piping (1 metre diameter), supposing that the sodium would spread in

pool form. In 1986, an important sodium spray fire (about 10 tonnes at 225°C) occurred in the solar plant at Almeria (Spain), destroying the major part of the installation. It was then decided to undertake the necessary work with the view, on the one hand, to improving prevention of such a fire risk, and on the other hand to guaranteeing safety in the hypothetical event of a spray fire resulting from the same clean pipe break.

As far as prevention is concerned, the improvements have involved mainly an extension of leak detection by beaded wire on the auxiliary piping, and placing of nearly 600 new detectors called "sandwich detectors" to cover the welds on the large piping (diameter exceeding 200 mm).

As far as consideration of consequences is concerned, the main modifications carried out in the four large rooms (1 000 m^3) housing secondary loops have been the installation of partitions creating 100 m^3 zones to limit build-up of pressure upon outbreak of fire; the piercing in the wall of the confinement building of 4 outlets equipped with flap valves set at 10 mbar to release the hot gases outside the reactor building; and the insulation of the concrete walls with stainless steel sheeting to contain the secondary sodium in the event of leak, to avoid reactions with sodium (Fig. 2.73).

In the four steam generator buildings, improvements involved mostly civil engineering provisions, including the creation of new outlets closed by panels attached with calibrated rupture bolts, to avoid excessive pressure build-up. In addition, the reliability of the sodium dump valves was improved in order to avoid aggravating the consequences of a fire should they fail.

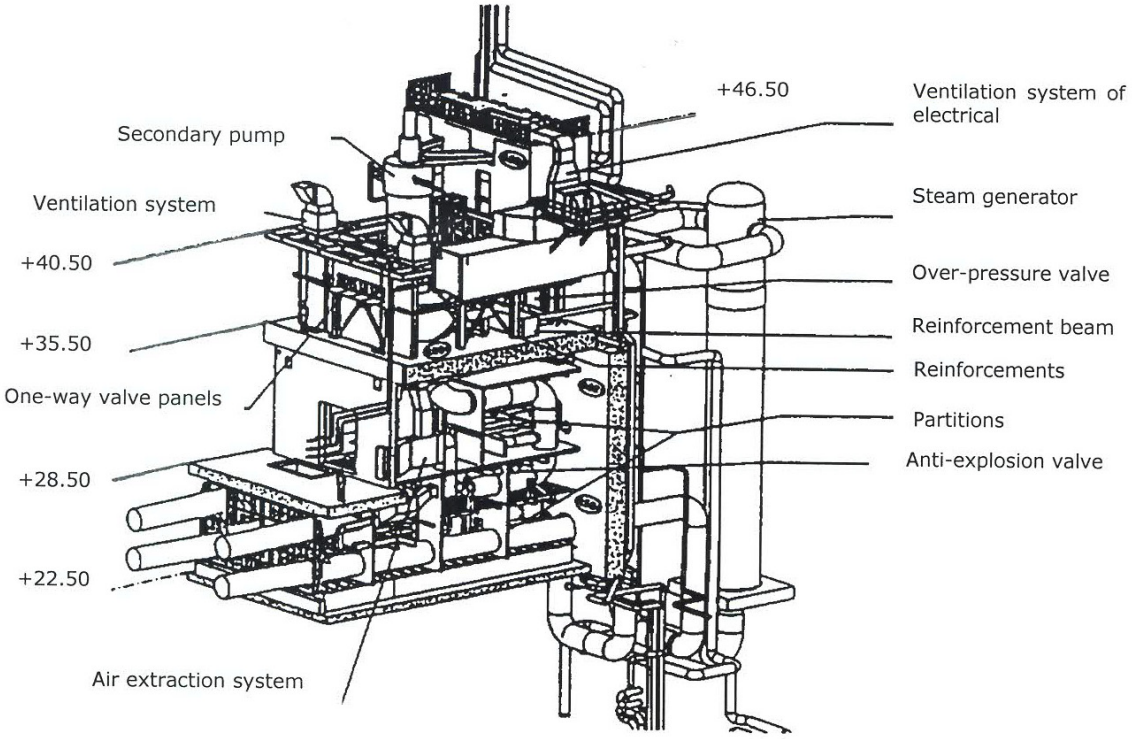

FIG. 2.73. Superphénix - disposition on secondary loop for sodium fire risk prevention.

2.15.2. Operating experience

(a) Sodium fill and isothermal testing

Successive filling of the storage drum, two secondary loops, the reactor block and lastly the two remaining secondary loops, took from June to December 1984. Filling the reactor block took 2 months, from 23 August to 31 October; after prior heating to about 150°C by circulation of hot nitrogen.

These filling operations were preceded by:

- Supply and on-site storage of 5650 tonnes of sodium, transported by 291 tankers, testing of the transfer piping under air;
- Leak-tightness checks of the intermediary containment (reactor main vessel and roof slab), the primary containment (safety vessel and the dome), and the storage drum under air, biological shielding checks by means of an 18 000 Ci source.

Isothermal tests started in January 1985 with an initial build-up in temperature limited to 395°C following the occurrence of sizeable oscillations of the shell which guides cold sodium flowing in an annular space along the inner side of the main vessel to act as a thermal shield facing the hot sodium plenum during increased primary pump speed. Following investigations carried out both on the reactor (visual examination by camera and displacement measurements through the "MIR" reactor inspection robot) and on mock-up under water, the origin of the problem could rapidly be attributed to a hydrodynamic coupling of the fluid and the structures, caused by vessel coolant sodium flow through the spillway (Fig. 2.74).

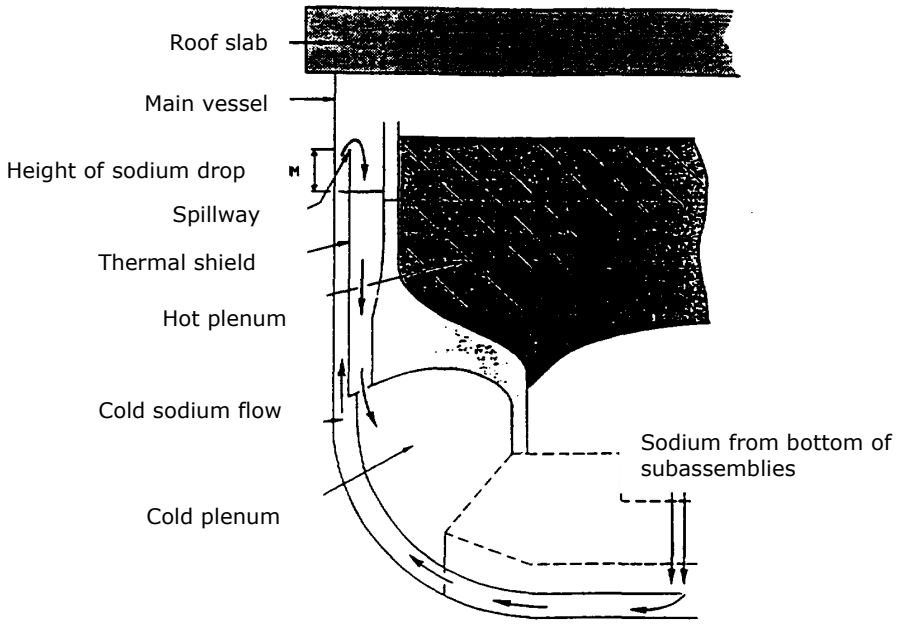

FIG. 2.74. Superphénix - thermal shield oscillations.

This problem was later resolved thanks to a slight modification in the foot of 19 subassemblies in order to get a 50% increase in the leakage rate towards the reactor bottom plenum, which feeds the main vessel wall cooling system, thereby reducing the height of the returning spillway. Efficiency of the modifications was successfully tested in the course of a second temperature build-up to 425°C in June 1985. The time period between the two

temperature build-ups was used to advantage for carrying out handling-line testing in sodium, and loading of the special device for introducing a neutronic chamber into the centre of the core. At the same time, testing of the turbines by auxiliary steam was carried out, as were tests on the feedwater plant and steam generators with sodium drained.

(b) Core loading and physics testing

The dummy, fissile material free, subassemblies used for isothermal tests were replaced by actual fuel subassemblies by applying an original method called checkerboard pattern which allowed criticality by loading the core in 4 batches. The first subassembly was loaded on 20th July and first criticality was achieved on 7th September 1985, with a core made up of 325 fissile subassemblies, as planned.

In October 1985, 33 fuel subassemblies were added to constitute the core for power build-up; it was with this core that zero power testing was carried out at no more than 30 MW_t:

- Control rod worth;
- Neutron flux distribution and fission rates;
- Calibration of neutron channels;
- Measurements of reactivity and feedback coefficients.

(c) Build-up of power

After obtaining the "first nuclear" steam on 31st December 1985, plant operation was managed through several stages. Start of power build-up was made on B turbine, as the A turbine was unavailable as a result of modifications in progress on the bypass circuit (experience feedback from PWR reactors). The following stages were planned:

(i) B turbine-generator testing - build up to 30% of nominal power;
(ii) Zero power physics testing;
(iii) Full power operation of B turbine-generator;
(iv) Fuel clad rupture detection systems testing;
(v) A turbine-generator testing and running both turbine-generator sets;
(vi) Stepwise build-up to nominal power;
(vii) Maintenance work;
(viii) Half-power operation due to unavailability of B turbine-generator.

After first connection to grid on 14th January 1986, build-up was soon interrupted due to, firstly detection of abnormal heating of one fuel subassembly that had to be replaced (a temporary plug in the foot had been overlooked), and secondly to several technical problems concerning the feedwater plant. Build-up was then interrupted in April and May to carry out necessary modification work and to complete the zero power physics testing programme.

B turbine reached full power (620 MW_e) on 30th June 1986, and this first build-up to 50% of nominal power was completed in July/August by calibration tests on the fuel clad rupture detection and localization systems.

When A turbine was available again, it was linked to the grid on 22nd August 1986, then nominal power build-up was achieved on both turbines on 12th September, full power being reached on 9th December 1986.

After various maintenance work, plant operation started again at the beginning of February 1987 but was again hampered successively by water hammer on the A auxiliary feedwater plant piping, putting it out of service for three months, then at the end of March by the detection of a sodium leak on the storage drum. This led to reactor shutdown at the end of May 1987, after a second calibration test on the clad rupture detection systems at 90% of nominal power.

2.15.2.1. First shutdown period

The two main activities of this shutdown period, which lasted from May 1987 until January 1989, were on the one hand, investigations on the storage drum which led to its replacement by the fuel transfer station (PTC), and on the other hand to the preparation of the reactor with a view to its resumption without the storage drum.

2.15.2.1.1. Investigations on the storage drum

Following detection, on 8th March, of the leak in its main drum by detectors situated at the bottom of the enclosing safety vessel, several actions were immediately envisaged.

- Pinpointing the leak where flow was assessed at approximately 20 L/hour;
- Installation of means of prevention in the event of a leak on the safety vessel;
- Installation of a draining circuit on the safety vessel to limit the quantity of sodium contained in it. The first draining occurred on 12th May and was repeated several times;
- Unloading the storage drum, which was carried out between April and July 1987.

Two hundred ninety non-radioactive dummy fuel subassemblies were stored on-site, 73 low radioactive steel subassemblies were stored in a cask in the APEC, and 49 various subassemblies were transferred into the reactor as a provision for operation without the storage drum. The location of the leak was determined at the beginning of September, and the storage drum was then definitively drained on 9th September. At the beginning of October, gamma radiography examination revealed that a crack had developed at the base of a weld on a support plate of the cooling circuit tubes (see Fig. 2.75).

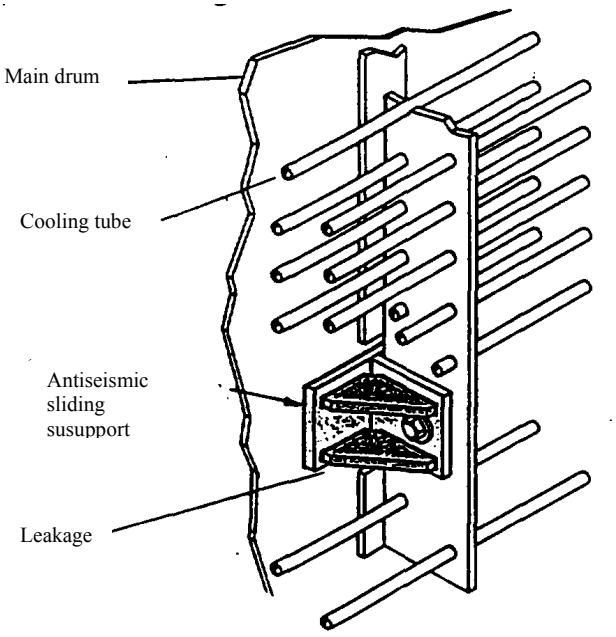

FIG. 2.75. Superphénix fuel storage drum leak location.

At the beginning of 1988, gamma radiographies showed that other indications of cracks existed in several zones of the main drum made of 15D3 ferritic steel and the first assessments of a sample, which were later on confirmed, showed that cracking by hydrogen, affecting these zones, was very severe.

The drum therefore appeared irreparable, and in March 1988 it was decided to replace the storage drum by a single fuel transfer station (PTC) while keeping the safety vessel made of the same ferritic steel. Finally, the decision to construct a new tank in stainless steel was taken in March 1989, after dismantling the internal structures and the storage drum.

2.15.2.1.2. Preparation of the reactor

As a preparation for resumption of power, a considerable programme of study and work was undertaken at the request of the Safety Authority; this mainly concerned:

- Re-examination of the design and fabrication of the reactor vessels, the secondary circuits, the decay heat removal circuits and inspection of the welds of the main vessel with the MIR inspection robot;
- Re-examination of accidental conditions and writing up of procedures to define necessary actions for handling a highly hypothetical situation resulting from a leak on the main vessel, subsequently followed by a leak on the safety vessel. Simultaneously a flask to unload fuel in the absence of the storage drum, while awaiting completion of the PTC, was studied and then manufactured.

At the same time, a campaign of work and modification aimed at improving the operation and availability of the installation was launched.

Examination of the main reactor vessel welds by the MIR robot travelling in the space between the vessels took place in the course of the summer 1988 and confirmed the sound quality of manufacture. On 29th November, examination of the overall status allowed concluding that the plant was fit for service, and on 12th January 1989 approval for resumption of power was granted by the Ministers in charge.

2.15.2.2. Resumption of operation

Resumption of operation was carried out through following steps:

- Neutronic and isothermal testing;
- Power build-up;
- Limited power operation due to high Rhône river temperature and low flow and a turbine-generator unavailable;
- Safety-related tests;
- Maintenance work and PTC civil work;
- Resumption of power.

After criticality, on 14th January 1989, and performance of neutronic and isothermal tests that were made necessary by the long shutdown of the installation, the plant was linked to the grid on 21st April, and reached full power on 16th June, i.e., in about 2 months.

The power build-up was disturbed by several incidents on equipment in the balance of plant, certain adjustments, and a spurious sodium leak alarm on a steam generator.

Power operation then continued but had to be reduced in compliance to the regulation on thermal releases because of a particularly low flow rate in the Rhône. After 17th August, operation continued with a single turbine, as the other had to be shut down following abnormal vibrations. There again, the main difficulties are attributable to the balance of plant: electric generator (hydrogen tightness), feedwater regulation valves and purge valves and fittings.

This period of operation ended on 7th September 1989 for a scheduled shutdown which was necessary for:

- Core rearrangement in order to recover a sufficient level of reactivity. Twelve diluent subassemblies were shifted to the outside of the core and replaced by 18 fuel subassemblies;
- Erection works linked to the PTC, which were not compatible with reactor operation.

This shutdown was preceded by two safety tests in September which allowed, on the one hand, to confirm the ability of Superphénix to evacuate decay heat by natural convection of the primary circuit and the secondary loops after reactor shutdown, and on the other hand, to demonstrate the absence of risk of a reactivity accident, caused by a passage of gas in the core following depressurization of one of the argon-filled sealing bells provided at intermediate heat exchanger penetrations through the internal vessel, which separates the hot from cold sodium plena.

The shutdown was used advantageously to carry out other preventive maintenance operations, and in particular replacing two tanks of the reactor argon circuit, constructed in the same ferritic steel as the storage drum, by two tanks in austenitic steel, repair on the turbine which had shown vibrations.

This shutdown was later considerably prolonged in order to carry out a test imposed by the Safety Authority, following the incident experienced at the Phénix plant, consisting of injections of radioactive tracing gas into the diagrid to demonstrate that the purge subassemblies were able to evacuate the gas and avoid the build-up of potentially dangerous gas pockets.

Plant operation resumed on 14 April 1990. Connection to the grid, which was delayed by a sodium leak of a few litres on an auxiliary secondary loop circuit, took place on 8 June 1990 and nominal power was reached 3 days later.

On 3 July, operation had to be interrupted following detection of an inadvertent air intake in the reactor argon circuit which caused oxidation of the primary sodium beyond allowable limits.

2.15.2.3. Second shutdown period

As soon as reactor shutdown took place, all actions needed to find the causes and consequences of the pollution incident were undertaken as follows:

- Investigations to identify the cause of the air inlet which, on 23 July, led to the incrimination of faulty compressor membranes on the primary argon activity measurement bypass;
- Sodium purification carried out in two campaigns, during which 3 sets of two purification cartridges were extracted from the reactor block. In January 1991, the sodium recovered a level at least equal to the purity prior to the incident;
- Repair of the installation and verification of the innocuous nature of the incident to components, involving, notably, endoscopic inspections, were completed in March 1991.

But this incident also led the Safety Authority to require, at the end of October 1990, a general re-examination of the organization of plant operation and further safety studies, in particular of the sodium fire risk in the secondary galleries, and feedback of experience from the Phénix incident.

Moreover on 27 May 1991 the Conseil d'Etat (Council of State) announced the partial cancellation of the Order of January 1989 approving plant operation without the storage drum; this prompted NERSA to accelerate work for completion of the PTC for commissioning as soon as possible. At the beginning of 1992, all equipment allowing evacuation of spent fuel from the reactor to APEC was available.

In other respects, this period was marked, on 13 December 1990, by the collapse of half the roof of the turbine hall due to an exceptionally heavy fall of snow, causing unavailability of one of the turbine-generator sets. Reconstruction work was undertaken rapidly on the turbine hall and repair of equipment was completed in October 1992.

In June 1992, the Safety Authority concluded that restarting Creys-Malville was possible subject to limitations and precautions, but on 29 June, the Prime Minister decided to defer the approval and requested a prior Public Enquiry and the immediate application of improvements to the prevention and handling of the sodium spray fire risk. Moreover, he requested the Minister of Research to write a report on the possible contribution of Creys-Malville to solving the nuclear fuel cycle back-end issue. NERSA then committed the necessary work which resulted in the submission, in July 1992, of a new licence application to the Ministry of Industry, backed up by a 900 page file in support to the Public Enquiry.

Further to the completion of sodium fire-related works and positive outcome of the Public Enquiry, a government decree was issued on 11th July 1994 sanctioning the new mission of the plant as an R&D tool for demonstrating the fast reactor capabilities for the management of the fuel cycle back-end, and the licence for resuming operation was granted on 3 August 1994.

2.15.2.4. Last operational period

The last operational period extended from August 1994 to December 1996, during which the most noticeable event was the occurrence, in January 1995, of a small leak at the argon feed tube of the gas sealing bell of one intermediate heat exchanger.

Precise location of the leak was performed by visual inspection using an endoscope inserted in the tube from above the reactor roof, and the repair was made by pressure expansion of an internal sleeve to plug the fault, without the need for removing the IHX. As a whole, this incident incurred 7 month downtime, including the inspections, the studies for defining the repair method and its validation through mock-up tests, and the revisiting of fabrication quality records for justifying the non generic character of the fault.

The 24 December 1996 was the last day of Superphénix operation, after which shutdown was planned for performing a regulatory inspection of steam generator tubes, and modification of the core configuration consistent with the new mission related to research on the fuel cycle back-end.

However, as these anticipated shutdown works were going on, the Council of State decided on 28 February 1997 the cancellation of the authorization decree issued in July 1994, and the definitive shutdown of the plant was confirmed by a Government order from 20 April 1998.

2.15.2.5. Operational performance summary

2.15.2.5.1. Availability

Since the first connection to the grid, the accumulated gross energy amounts to 8.3 billion kWh, and the energy extracted from the fuel represents 22.9 billion kWh, i.e. 319 EFPD.From the first connection to the grid until the last day of production, not accounting for unplanned outages specifically due to incidents, the reactor has been in normal operation, including planned outages, during about 53 months, broken down as follows:

- 8 months of start-up tests before connection to the grid;
- 34 months of power production, with connection to the grid;
- 11 months of planned outages for refuelling, in-service inspection and maintenance.

Excluding the power build-up phase in 1986, which was exceptionally long due to the performance of prototype plant tests, the average capacity factor 1987-1996 was 41.5%. However, it is worth noting that in the last operating period (August 1995 - December 1996), the gross electrical production amounts to 3.74 billion kWh, giving a capacity factor of about 57%.

2.15.2.5.2. Chronology of incidents

From the start of fuel loading in July 1985 until definitive shutdown in 1998, the plant has been affected by 101 abnormal events; all but one deemed 'safety significant'. The breakdown of incidents by origin of faults and time periods is shown in Table 2.21. It must be noted that this classification is not perfectly clear cut, since in most cases there is not a single cause of the incident; however it is aimed at giving a fair view on the overall picture.

TABLE 2.21. FREQUENCY OF INCIDENTS AT SUPERPHENIX (No of occurrences/year)

Period [*] (operation shaded)	1	2	3	4	5	6	7	8	9	10	11	12
Equipment	6	5.3	–	2.2	1.3	1.3	1.5	1.8	3	–	–	–
Design	8	3.8	1.2	1.1	2.5	–	0.8	0.9	–	–	–	–
Construction	4	0.8	–	–	2.5	1.3	–	–	–	–	–	–
Commissioning	2	3.8	2.4	–	–	–	–	–	–	–	–	–
Modification	4	–	–	–	–	–	–	0.9	–	–	–	–
Operation	8	2.3	3.6	2.2	1.3	1.3	5.3	3.4	3	2.7	3.2	1.7
Human factor	4	3	–	–	1.3	–	0.8	0.9	3	–	0.8	3.4

Note [*] The main periods of reactor operation are defined as follows:

(1) 19/07/1985 (start of fuel loading) to 14/01/1986 (1st connection to grid): plant commissioning, start-up tests;
(2) 1986 to 25/05/1987 (shutdown due to failure of fuel storage drum): build-up to nominal power;
(3) May 1987 to March 1988: modification of fuel transfer route;
(4) March 1988 to April 1989: waiting time for administrative procedures before restart;
(5) April 1989 to June 1990: operation including one scheduled outage;
(6) July 1990 to March 1991: shutdown due to the pollution of primary sodium by air intake in argon cover gas;
(7) March 1991 to July 1992: works for enhancing the mitigating provisions against sodium spray fire, and waiting time for administrative procedures;

(8) July 1992 to August 1994: public enquiry related to the restarting licence application;
(9) August 1994 to December 1994: operation;
(10) January 1995 to September 1995: shutdown due to the leakage of argon feed tube to the gas sealing bell of one IHX, and waiting time for administrative procedures;
(11) September 1995 to December 1996: operation;
(12) January 1997 to 20/04/1998 (decision on definitive shutdown): scheduled outage, followed by legal cancellation of the operation licence;

These periods can be gathered into three main categories as follows:

(a) From the beginning to mid-1987, during which 48 incidents occurred, *i.e.*, an average frequency of 24 per year; this high figure can be explained by the finding of a number of design and construction anomalies during commissioning and start-up.
(b) Three serious incidents (storage drum failure, primary sodium pollution, gas sealing bell leakage) caused long shutdown periods, which were further extended by lengthy administrative procedures. 36 incidents occurred during 7.75 years of cumulated shutdowns, *i.e.*, an average frequency of 4.6 per year.
(c) Reactor on-power: 16 incidents occurred during 3 years of cumulated operational periods (Nos 5, 9, and 11 in Table 21 above), *i.e.*, an average frequency of 5.3 per year.

Successive periods of production exhibit a steep reduction in the frequency of spurious shutdowns, which demonstrate that the 'teething troubles' that are common for all new plants, could be overcome eventually.It is also worth noting that the frequency of declared events averaged over the service life of Superphénix is about 8/year, which is the same as that observed on the whole fleet of French PWR plants after start of commercial operation. It is comparatively low after the initial period of commissioning and power build-up, either during shutdown or on-power operation.

2.15.2.5.3. Severity of incidents

The application of classification criteria defined by the INES severity scale for nuclear events leads to the following outcome:

- 2 incidents are classified level 2 (both because of plant unavailability duration criteria):
  - Fuel storage drum leak (March 1987);
  - Increase of primary sodium pollution beyond allowable range (July 1990).

- 6 incidents are classified level 1:
  - Emergency shutdown with loss of rundown inertia on 2 (out of 4) reactor coolant pumps (November 1985);
  - Overheating of one fuel subassembly (January 1986);
  - Fall of a temporary lifting crane during tests (October 1989);
  - Collapse of part of turbine hall roof due to accumulated snow (December 1990);
  - Inadvertent simultaneous opening of several containment barriers (May 1995);
  - Premature melting of the liquefiable metal seal of the large rotating plug, the reactor being still critical (May 1996).
- 72 incidents are unclassified by the scale.

2.15.2.5.4. Origin of incidents

The breakdown according to type of incident or cause of the fault is shown in Table 2.22.

TABLE 2.22. DISTRIBUTION OF INCIDENTS ACCORDING TO THEIR TYPES

Type of incident/cause of failure	Share, %
Operational procedures	33
Equipment failure	20
Design	15
Human error	15
Commissioning tests	8
Construction	6
Subsequent modifications	3

The following conclusions can be derived:

- Events originating from design, construction/modifications, and commissioning are dominant in the beginning of plant life, but only represent 32% of the total, which shows the effectiveness of corrective actions.
- Equipment failures and human errors together caused 35% of the events; this can be reduced by improving quality assurance for equipment procurement, preventative maintenance, training of personnel, preparation of interventions, etc. based on feedback from experience.
- Lastly, 33% of the events can be attributed to inadequate operating procedures or staff organization; they are not specific to fast reactor technology, which can, in turn, benefit from progress achieved in this respect on other nuclear power plants.

2.15.2.6. Feedback from experience

2.15.2.6.1. Core

Sub-critical approach, criticality and the different core rearrangements have shown very good agreement between measurements and predictive core physics calculations.

Operational features of the core stabilized by negative reactivity coefficients (Doppler, temperature, etc.) were confirmed. This neutronic stability, together with an important thermal inertia of the primary system, makes reactor control easy. Particularly at low power, uncoupling followed by recoupling of a turbine-generator set is performed without affecting the reactor.

However, larger than expected fluctuations were measured in sodium temperatures at subassembly outlets, particularly from fertile and fissile subassemblies on the core periphery, due to sodium recirculation in the hot plenum. This called for specific measurement campaigns and the adaptation of monitoring methods for these subassemblies.

2.15.2.6.2. Reactor unit

The behaviour of the reactor structures was on the whole in line with design predictions. The main problem was the appearance of oscillations in the thermal insulation baffle, triggered by pump running up during the isothermal tests. This prompted significant progress of theoretical knowledge in the area of fluid-structure hydrodynamic coupling.

The use on two occasions of the MIR robot and the excellent correlation between the measurements carried out during fabrication (1979) and those taken by the MIR demonstrate the feasibility of reactor vessel in-service inspection by ultrasonic techniques.

Numerous primary circuit components were handled with special flasks within the framework of tests or maintenance operations, thus confirming the maintainability of components in the sodium environment of the primary circuit.

Knowledge of the primary circuit behaviour for a large-sized pool-type fast reactor has been improved, on the one hand, thanks to natural convection tests, which showed that sodium circulation is established in the core within about 5 minutes, and on the other hand in relation to the hazards incurred by gas entraining through the core, thanks to tests carried out on the reactor and on several water mock-ups including one simulating the whole diagrid at 0.36 scale (SUPERPANORAMIX).

Lastly, the primary sodium pollution incident led to the installation of a chromatograph on the reactor argon circuit to monitor chemical purity of the primary argon. Besides, this incident gave the opportunity of gaining further knowledge on the chemistry of sodium (new tests on the Cadarache loop), on the performance of integrated cold traps, and on the workings of plugging indicators.

2.15.2.6.3. Large components

Experience feedback on large components remains significant in spite of the relatively short cumulated operating time. Primary and secondary pumps total more than 50 000 hours on main motor, and the continuous improvement of maintenance operations has allowed an increase in reliability and availability. As far as the steam generators are concerned, the sodium/water reaction detection systems have been improved on the basis of computing models validated through experience. The start-up tests have led to review the SG decompression-isolation sequences in order to comply with enhanced safety criteria.

2.15.2.6.4. Circuits

Numerous draining and filling operations (more than 30 for the secondary loops and more than 20 for the emergency decay heat removal circuits (RUR)) have allowed validation of the corresponding procedures.

Monitoring of sodium circuit piping displacements has only shown up abnormal behaviour on the RUR circuits where displacements, considering its considerable flexibility, differed from predictions and for which a specific follow-up has been implemented.

Sodium leak detection by beaded wires has shown problems of spurious earthing, and embrittlement of the nickel wire in the long run; this has required several interventions with, notably, a change from nickel to stainless steel. The beaded wire leak detection system has been further reinforced on secondary piping over 200 mm diameter by more robust sandwich-type detectors.

Apart from the storage drum leak of no external consequence, three sodium leaks which did not cause a fire, have occurred in ten years of operation:

- In 1985, a leak of a few cubic centimetres on the weld of a secondary loop thermocouple support due to vibration;
- In 1990, a leak of about 10 litres on a T-junction weld on a secondary loop auxiliary circuit due to thermal fatigue;
- In 1991, a small leak on a temperature measurement thimble on a secondary loop plugging indicator due to inadequate preheating procedure.

These incidents provided invaluable experience concerning monitoring techniques, interventions on sodium circuits and the dismantling of sodium systems. On the other hand, the storage drum incident has considerably increased knowledge on 15D3 ferritic steel. In addition practical consideration of sodium spray fires in the secondary loop rooms has led to progress in modelling the phenomena involved in the event of sodium leak. Spray fire tests with and without compartmenting have been carried out with flow rates up to 230 kg/s.

2.15.3. Decommissioning and dismantling

2.15.3.1. Licensing aspects

Following the definitive shutdown order on 20th April 1998, the Government issued, on 30th December 1998, a licence to undertake the first phase of decommissioning and dismantling (D&D) works, comprising:

(i) Core unloading and storage of fuel elements in the APEC;
(ii) Sodium draining;
(iii) Removal of non safety related equipment.

On 30th March 2006, two additional decrees have authorized, on the one hand, the complete dismantling of the reactor mechanical equipment and the demolition of buildings, on the other hand, the extension of APEC operating licence to enable accommodation of all fuel subassemblies (used and new) and other core elements taken out of Superphénix, and also of the concrete containers enclosing the waste produced by disposal of the sodium coolant.

2.15.3.2. On-site works

The following works were carried out:

- Removal of equipment of the conventional plant and power conversion systems that do not serve as necessary auxiliaries to the nuclear systems during their decommissioning;
- Installation of electrical trace heating and thermal insulation on the outer side of the safety vessel in order to prevent freezing of the primary sodium, as the residual power in the core was becoming too low to balance the natural thermal losses, and sodium heating by mechanical friction through running the primary pumps was not economical;
- Reconfiguration of some auxiliary systems (sodium transfer, gas and service water distribution), with the corresponding instrumentation and control systems, for meeting new functional requirements related to nuclear system decommissioning;
- Drilling of holes in some internal structures of the reactor, in order to enhance sodium flowing down to the vessel bottom and to minimize the volume of residues left after drainage.

2.15.3.2.1. Core unloading

The removal of core subassemblies was delayed because of a number of incidents affecting the fuel handling systems, notably the fuel evacuation route up to final washing, which had not been thoroughly utilized before and required maintenance and adjustment of operating procedures. The unloading of the first 2 rows of fertile subassemblies was carried out in the year 2000, and that of the fuel subassemblies in 2001. From February 2002 to February 2004, the absorber elements (control rods), experimental subassemblies, and the last row of fertile subassemblies, which required a special adaptation of the washing process, were unloaded.

The reflector and shielding steel elements around the core (1260 items) were unloaded in the period 2004-2008.

2.15.3.2.2. Equipment dismantling

In parallel to core unloading, miscellaneous small reactor devices including, e.g. control rod drives, and parts of reactor and core instrumentation and monitoring systems located above the reactor top closure, were removed, washed, cut into pieces and conditioned in waste containers. The same has started in 2009 and is still going-on for the main components: primary pumps and IHXs.

Main secondary and auxiliary sodium systems have been drained and the sodium has been sent to temporary storage tanks. Neutralization of the residual sodium film wetting the internal walls of piping and vessels has started in 2006, enabling the cutting and scrapping of equipment to be made. As of beginning 2010, the primary sodium still resides in the reactor, maintained in the liquid state by electrical heating as explained above.

2.15.3.2.3. Sodium disposal

A sodium processing facility, named TNA, has been erected in the former turbine hall, to perform the conversion of sodium into soda (sodium hydroxide). Thereafter, this will be incorporated in cylindrical containers made of concrete. The TNA plant has been commissioned at end 2009 and is due to operate for about 5 years to process 5 520 metric tonnes of sodium (3 300 t from the primary system; 1 550 t from the secondary and auxiliary systems; 670 t from the former in-sodium fuel storage tank, thereafter converted to in-gas PTC).

Existing sodium filling and draining systems have been modified, and new temporary piping have been erected as necessary to allow transferring sodium to and from temporary storage tanks and to the TNA facility.

2.15.3.2.4. Final dismantling stage

After sodium processing, from about 2014 on, the decontamination and dismantling of reactor structures and other systems involving radiological hazards (e.g. primary sodium and argon purification systems) will be undertaken. The fact is that some parts of the internal structures have been activated under neutron flux (e.g., stellite containing hard coatings of core elements holders), or contaminated by deposits of radioactive materials from the core, or of activated corrosion products entrained by the primary coolant flow. The removal of all potential sources of radiological exposure is due to be completed in around 2022, and the final dismantling stage will be the demolition of buildings, due to be completed in around 2025.

2.16. FBTR operating experience

2.16.1. Introduction

The Fast Breeder Test Reactor (FBTR) has been in operation since October 1985. FBTR is a 40 MWt, loop type, sodium cooled fast reactor, based on the French Rapsodie-Fortissimo design. One major design change in FBTR vis-à-vis Rapsodie-Fortissimo is the incorporation of a steam water circuit in place of the sodium-air heat exchanger in Rapsodie. Figure 2.76 shows the schematic flow sheet of the heat transport circuits.

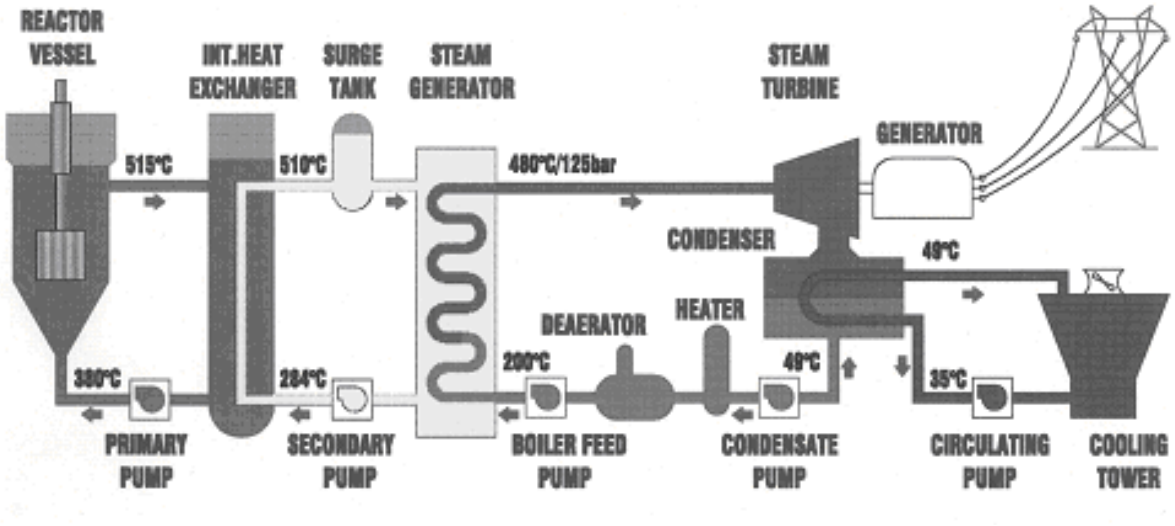

FIG. 2.76. Flow sheet of heat transport system.

Heat generated in the reactor is removed by two primary sodium loops, and transferred to the corresponding secondary sodium loops. Each secondary sodium loop is provided with two once-through steam generator modules. Steam from the four modules is fed to a common steam water circuit comprising a turbine-generator and a 100% dump condenser.

2.16.2. Design description

The reactor assembly is supported from the top. The reactor vessel houses the core and serves as a conduit for the primary sodium coolant flow through the core. Charging and discharging of subassemblies are done from the reactor top with the reactor in a shutdown state. The sodium inlet pipe joins the reactor vessel at the bottom and two sodium outlet pipes radially branch out of the vessel above the core. The reactor is closed at the top by the Large and Small Rotatable Plugs. The rotatable plugs are cooled by nitrogen. Liquid metal seals of tin-bismuth alloy, backed with inflatable seals, isolate the reactor cover gas from the reactor containment building atmosphere. The liquid metal seals are frozen during reactor operation and melted during rotation of the plugs. The space between the liquid metal seals and the inflatable seals, called the interseal space, is maintained in argon at a pressure higher than the reactor cover gas to prevent the leakage of active cover gas into the reactor building. The Small Rotatable Plug houses the Control Plug which carries six control rod drive mechanisms (CRDMs) and Core Cover Plate with thermocouples for monitoring the outlet temperatures of the fuel subassemblies (Fig. 2.77) [48].

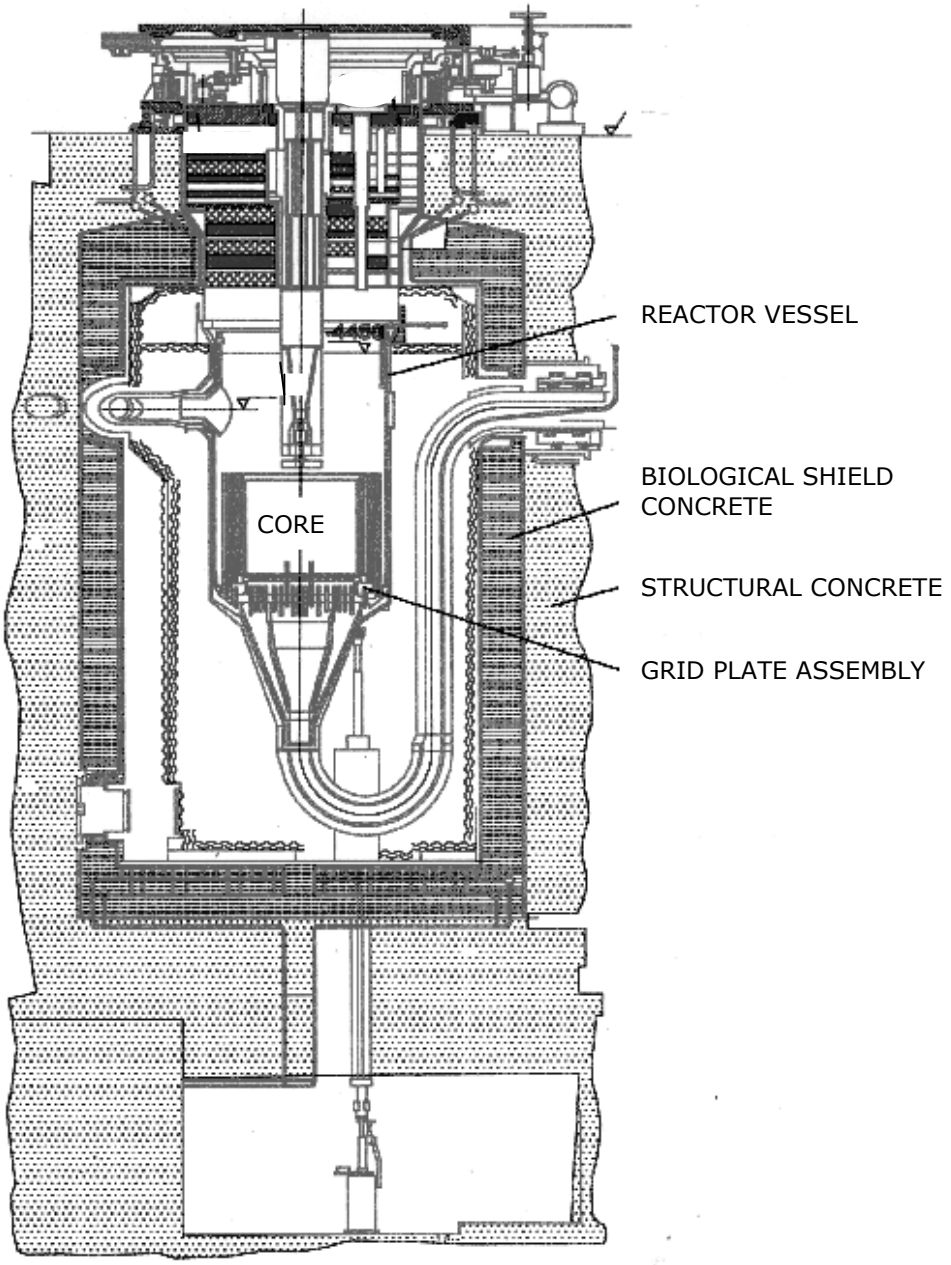

FIG. 2.77. Reactor assembly.

A steel vessel with thermal insulation surrounds the reactor vessel. Radial shielding is provided by borated concrete and structural concrete. The borated concrete is cooled by water pipes embedded close to its inner periphery. The entire reactor assembly is suspended from the top, with the load taken by structural concrete. The reactor is closed at the top by the Anti-Explosion Floor, which is bolted to tie-rods anchored on the structural concrete.

The core consists of 745 closely packed locations, with fuel at the centre, surrounded by nickel reflectors, thorium blankets and steel reflectors. The core is vertical and freestanding, with the subassemblies supported at the bottom by the grid plate and held down by collapsible hold-down springs. There are 23 storage locations in the outermost steel reflector row.

The sodium pumps are vertical, single stage centrifugal pumps with axial suction and radial discharge. Each pump has a fixed shell and a removable assembly comprising the impeller, diffuser and shaft. The shaft is supported by taper roller bearings at the top and guided by

hydrostatic bearings at the bottom. The pumps are driven by DC motors and powered by Ward Leonard drives with flywheels. Flow control is by controlling the speeds of the pumps.

The intermediate heat exchangers are vertical, counter-flow heat exchangers and transfer heat from the active primary sodium to the inactive secondary sodium. Primary sodium flows on the shell side and secondary sodium on the tube side. The shell is fixed and the tube bundles are removable. The steam generator modules are of once-through, counter-flow type, with sodium entering the shell side from top and water entering the tube side from bottom (Fig. 2.78).

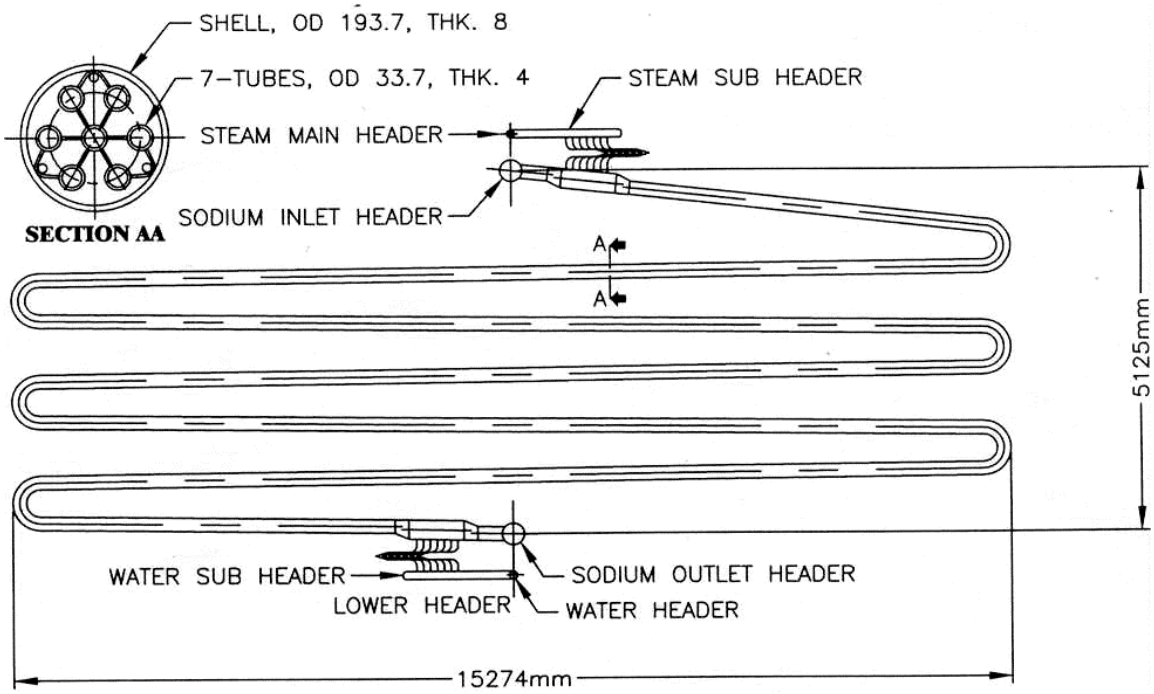

FIG. 2.78. Steam generator module.

The modules have a serpentine configuration, with evaporation and superheating occurring in a single pass. Due to the absence of blow-down, feed water chemistry is maintained within very stringent limits [49]. The steam generator modules are housed inside an insulated casing. By opening the trap doors of the casing, it is possible to remove decay heat from the reactor by natural convection.

2.16.3. Operating experience

2.16.3.1. Evolution of reactor core and power

Figure 2.79 schematically summarises the evolution of reactor core and power. As per the original design, the core of FBTR was rated for 40 MWt having 65 MOX fuel subassemblies of Rapsodie driver fuel composition (30% PuO_2 and 70% UO_2, with the latter enriched in ^{235}U to 85%).

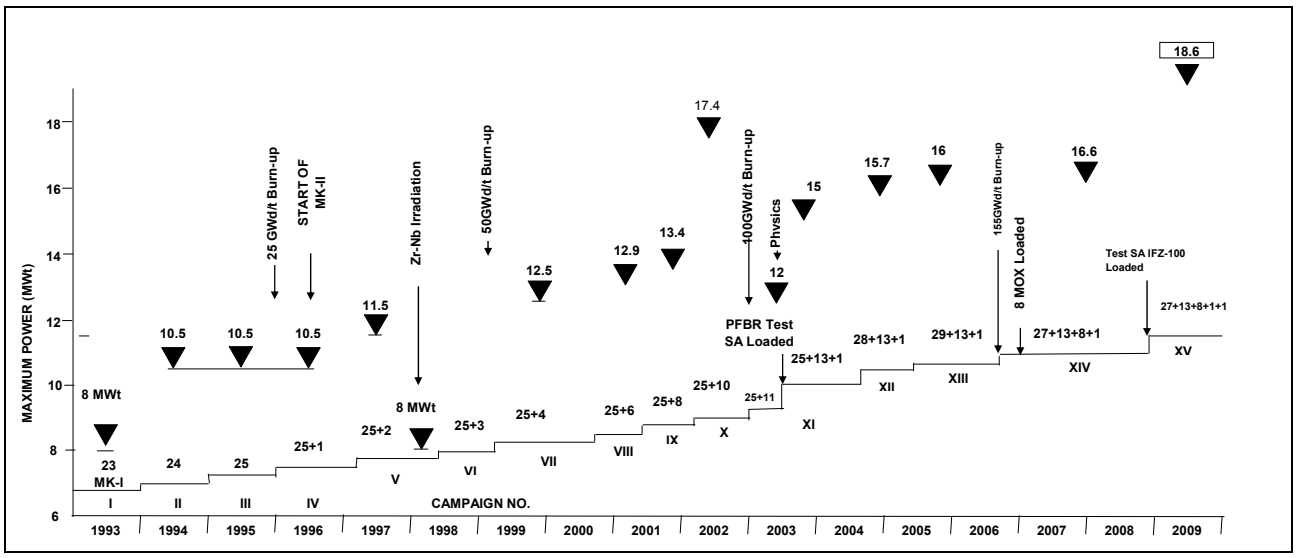

FIG. 2.79. Evolution of reactor core and power.

Due to the unavailability of highly enriched uranium, the option of using an alternate fuel rich in plutonium was studied. Compatibility of higher concentrations of oxides of Pu (>30%) with sodium and difficulties in fuel fabrication led to the choice of the carbide fuel for the first core of FBTR [50]. Being a unique fuel of its kind without any irradiation data, the core was redesigned as a small carbide core. Compared to the original design of 65 MOX fuel subassemblies rated for 40 MWt, the small carbide core was rated for 10.6 MWt and had 23 fuel subassemblies with 70% PuC and 30% UC composition (designated as Mark-I fuel). The core has since been progressively enlarged by adding fuel subassemblies to compensate for reactivity loss due to burnup.

With the intention to raise the reactor power to 40 MWt, it was decided in 1995 to go in for a full carbide core of 78 fuel subassemblies of 55% PuC + 45% UC composition (designated as Mark-II fuel). Fuel subassemblies of Mark-II composition were installed surrounding the Mark-I subassemblies in 1996. However, due to the progressive extension of the allowable burnup of Mark-I fuel from the initial target of 25 GWd/t to 155 GWd/t, the induction of Mark-II was suspended after loading 13 Mark-II fuel subassemblies.

A test fuel subassembly simulating the MOX fuel to be used in PFBR was loaded in the core in 2003. Also, in order to validate the fabrication practices for the MOX fuel being made for PFBR, eight MOX fuel subassemblies with high Pu content (44% PuO_2) were loaded in 2007.

The present core has 27 Mark-I (70% PuC+30% UC), 13 Mark-II (55% PuC + 45%UC) and eight high Pu MOX (44% PuO_2) fuel subassemblies, in addition to a test fuel subassembly simulating the PFBR fuel composition and a 54 pin (Mark-I) irradiation subassembly. The current core is rated for 18.6 MWt. The major characteristics of the reactor as per the original design and with the present core are given in Table 2.23.

TABLE 2.23. THE MAIN CHARACTERISTICS OF FBTR

Parameter	Initial design	Present core
Reactor type	Sodium cooled, loop type	
Reactor power, MWt / MWe	40 / 13.2	18.6 / 3
Fuel	MOX (30% PuO_2 + 70% UO_2 with 85% enrichment)	Mark I (70% PuC + 30% UC) Mark II (55% PuC + 45% UC)
No. of fuel subassemblies	65	27 Mark I + 13 Mark-II + 8 MOX+ 2 test fuel
Fuel pin diameter, mm	5.1	
No. of pins / subassembly	61	
Maximum linear heat rate of Mark-I driver fuel, W/cm	400	314
Maximum burnup, GWd/t	100	155
Peak neutron flux, $n/cm^2/s$	3.5×10^{15}	2.15×10^{15}
No. of control rods	6	
Control rod material	B_4C (90% enriched in B^{10})	
Reactor inlet sodium temperature, °C	380	381
Reactor outlet sodium temperature, °C	515	482
Primary sodium flow rate, m^3/h	1100	618
Feed water temperature, °C	190	
Steam temperature, °C	480	430
Feed water flow rate, t/h	70	33
Steam pressure, kg/cm^2	125	
Sodium inventory, t	150	
Steam generator	Once-through type, 7 tubes in shell, serpentine shaped	
Turbine-generator	16 stages, condensing type, 16.4 MWe, air cooled	
Bypass circuit	100% Dump condenser	

2.16.3.2. Construction and commissioning [51-55]

Construction started in 1972, and civil works were completed by 1977. Most of the components were installed in 1984. Commissioning was done in phases. Initially, the primary and secondary sodium systems were commissioned, without the steam generators in place. The reactor achieved first criticality on 18th October 1985. Low power physics experiments were conducted [56]. During an in-pile fuel transfer for measuring the worth of the 23rd fuel subassembly in May 1987, a major fuel handling incident took place. Reactor operation could be resumed only in May 1989. The various major milestones crossed so far are given in Table 2.24.

The reactor was operated up to a maximum power of 1 MWt till 1992 for intermediate power physics and engineering experiments. In the meantime, steam generator modules were connected to the secondary sodium circuits and the Steam Generator Leak Detection System was commissioned.

TABLE 2.24 MILESTONES CROSSED BY FBTR

Milestone	Date
First criticality	18 October 1985
Sodium valved in into SG	November 1989
Water valved in into SG	January 1993
Power of 10.5 MWt	December 1993
High power safety related experiments	1994–1995
MK-I reaches a burnup of 25 GWd/t	May 1996
Start of loading of MK-II fuel	October 1996
TG synchronised to grid	July 1997
Zr-Nb irradiation	1998–1999
MK-I reaches a burnup of 50 GWd/t	April 1999
Power of 17.4 MWt	March 2002
MK-I reaches a burnup of 100 GWd/t	September 2002
Start of PFBR test fuel irradiation	July 2003
MK-I reaches the target burnup of 155 GWd/t	July 2006

The steam water circuit was then commissioned, steam generators were put in water service and power was raised to 4 MWt in January 1993 and 8 MWt in April 1993. After completing high power physics and engineering experiments, power was raised to 10.2 MWt by the end of 1993. After completing the commissioning activities of the turbogenerator (TG) and auxiliaries, power was raised to 11.5 MWt and TG was synchronized to the grid in July 1997. The reactor has so far completed 15 irradiation runs, and reached the highest power level of 18.6 MWt. The major mission of FBTR from the 11th campaign onwards is the irradiation of test fuel simulating PFBR fuel composition.

2.16.3.3. Operation statistics

The operational statistics up to 31st March 2009 are summarized in Table 2.25. Figure 2.80 gives the histogram of reactor operation from 1993–2009.

TABLE 2.25. SUMMARY OF PERFORMANCE STATISTICS FROM 1985 (UP TO 31 MARCH 2009)

Parameter	Value
Maximum power, MWt	18.6
Maximum LHR, W/cm	400
Maximum bulk sodium temperature, °C	482
Operating time, h	41 835
Thermal energy produced, MWh	330 543
TG synchronisation time, h	8 148
Electrical energy generated, MWh	10 545
EFPD at LHR of 320 W/cm, d	968.3
Peak burnup of MK-I fuel, GWd/t	165
Longest operating campaign, d	72
Cumulative of four Na pump operation, h	62 8431
SG operation, h	24 655
No. of losses of reactivity / controlled shutdowns	270
No. of scrams	163
Cumulative dose to personnel, man-mSv	100
Cumulative stack release (Ar^{41}), GBq	19 000

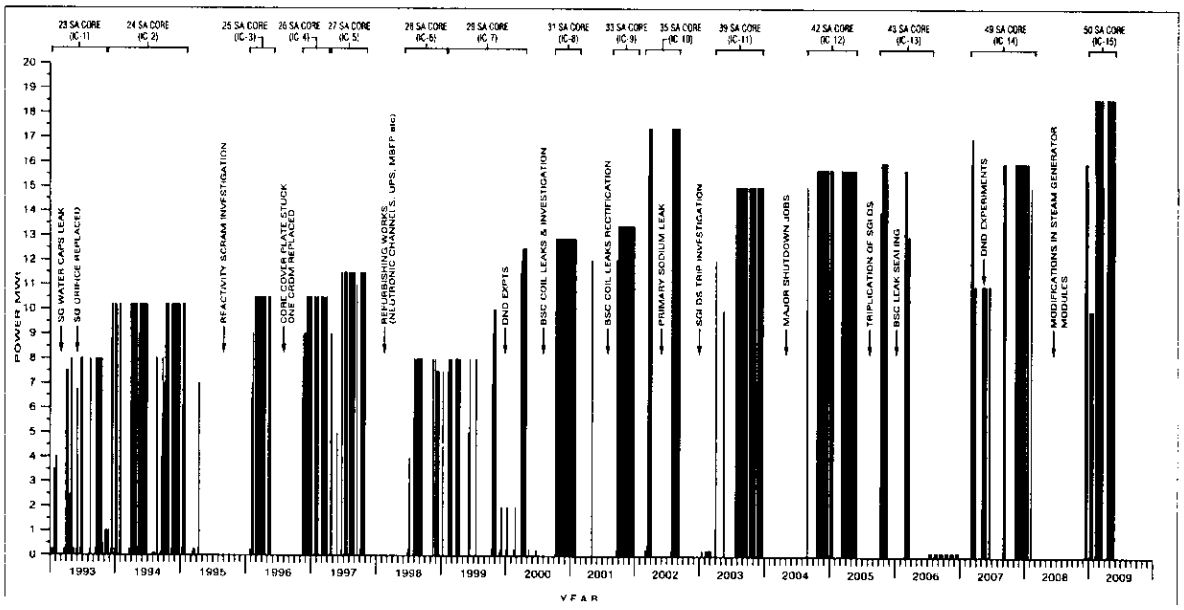

FIG. 2.80. Histogram of operation.

2.16.3.4. Fuel and material irradiation

In addition to being a self-driven irradiation facility for the Pu rich monocarbide fuel, the reactor has been utilised for studying the irradiation creep behaviour of Zr-Nb, which is being used in the Indian Pressurised Heavy Water Reactors [57]. The present mission of FBTR is to irradiate the MOX fuel (29% PuO_2) chosen for PFBR to the target burnup of 100 GWd/t at the design linear heat rating of 450 W/cm. The test fuel has so far seen a burnup of 92 GWd/t. In the coming years, FBTR will be deployed for irradiation of advanced fuels and structural materials contemplated for future fast reactors. In the 15th irradiation campaign, trial production of Sr^{89} from yttrium was demonstrated.

2.16.3.5. Physics and engineering experiments [58, 59]

In addition to routine measurements of control rod worths and reactivity coefficients of inlet temperature and power after every core configuration change, physics experiments carried out are: reactor kinetics experiments, void coefficient measurements, response of delayed neutron detection system to detect clad failure and flux mapping in sodium above core.

A series of safety related engineering tests was conducted in 1994-95, basically to validate the codes used in incident analysis. Normal plant incidents like off-site power failure and tripping of one pump in the primary, secondary or tertiary loops were studied and the sequence of events confirmed to be as per safety logic. Primary pump coast down characteristics, take over by the batteries and low speed running of the pumps were studied and found to be as per the design intent. As a precursor to the station black out test, natural convection tests in the secondary and primary loops were separately carried out.

A series of tests was conducted in 2007 for validating the delayed neutron detection (DND) system. A special subassembly with 19 perforated pins with U-Ni alloy was loaded at different core locations, and the contrast ratios were studied. The results were encouraging about the capability of the DND system to identify failed fuel, and localisation of the failed fuel from the contrast ratios.

2.16.3.6. Performance of the systems

Perhaps, the most gratifying performance is that of the unique carbide fuel. Being an untested fuel, it was initially rated for a linear power of 250 W/cm and burnup of 25 000 MWd/t [60]. Based on post-irradiation examination of the fuel at different stages (Fig. 2.81), it has been possible to raise its linear power to 400 W/cm and target burnup to 155 000 MWd/t. More than 1000 pins have so far reached the target burnup without any pin failure. PIE results indicate that at the high dpa levels, the wrapper dilation would limit the allowable burnup. One subassembly was irradiated up to 165 GWd/t to see the endurance limit of this unique fuel. It reached this burnup without failure.

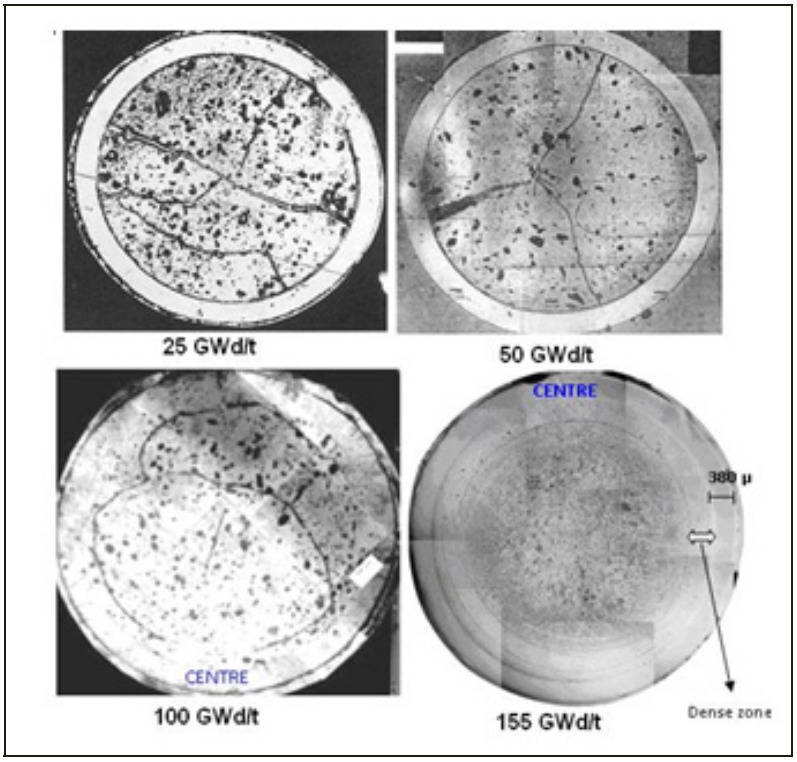

FIG. 2.81. Photomicrographs of fuel at 25, 50, 100 and 155 GWd/t burnup.

Performance of the safety critical and safety related systems has been excellent. Each sodium pump has operated for more than 150 000 h without any problem. Sodium purity is so well maintained that when viewed inside the reactor through the periscope, it shines as a mirror, so much so that many of the reactor internals could be inspected from their reflections in sodium.

Argon cover gas purity is so well maintained that even with the cold traps out of service for several months, the plugging temperature of sodium is found to be below 105°C.The steam generators, which are critical for the success of fast reactor programme, have operated for more than 24 500 h without any leak. The TG has been in service for more than 5000 hours at off-normal steam conditions (420°C as against the design value of 480°C, flow of 20 t/h as against the design value of 70 t/h). Inspection of the internals indicates no erosion of blades or diaphragms.

Figure 2.82 shows fuel pin bundles inside the hot cell.

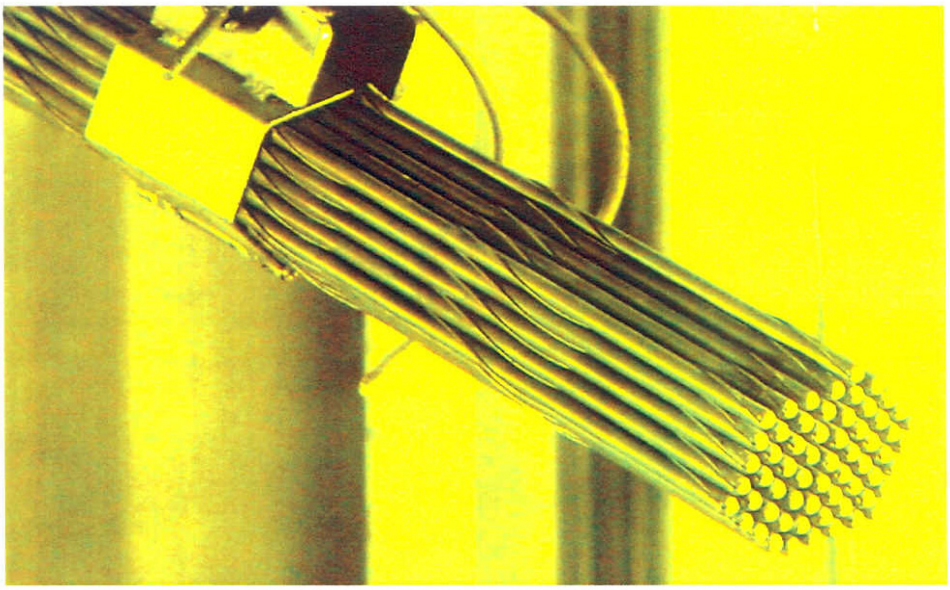

FIG. 2.82. Fuel pin bundles inside the hot cell.

The lower parts of control rod drive mechanisms have been replaced thrice due to leak from metallic bellows. Two control rods have also been replaced-one due to repeated dropping while raising, and the other since the CRDM gripper could not release the rod.

2.16.3.7. Technical challenges [61]

During commissioning, reactor vessel deflection was found high, beyond a sodium temperature of 270°C, due to circumferential variation of the reactor vessel temperatures in the cover gas region. It was due to convection loops formed by the cover gas in the annular gap between the large rotatable plug and the reactor vessel. This was solved by injecting helium in the gap, while admitting argon cover over the free sodium level below (Fig. 2.83). A dedicated helium injection circuit was added [62].

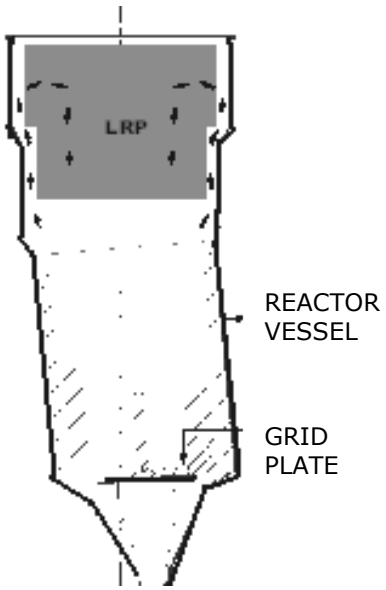

FIG. 2.83. Reactor vessel deflection.

During an in-pile fuel transfer for performing a low-power physics experiment in May 1987, a major fuel handling incident took place. The incident was due to the plug rotation logic during fuel handling remaining in bypassed state, resulting in the rotatable plugs being rotated with the foot of a fuel subassembly protruding into the core during the in-reactor transfer. The foot of the subassembly as well as the heads of 28 reflector subassemblies on the path of its rotation got bent. During the several manoeuvres to charge the subassembly, one reflector subassembly at the periphery got ejected by the bent foot of the fuel subassembly. In a complex mechanical interaction that took place during subsequent plug rotation, the sturdy guide tube which guides the gripper of the charging flask got bent by about 320 mm. The damaged fuel subassembly was retracted using extra force. The guide tube was cut below a set of equalisation holes using a specially designed remote cutting machine and removed in two pieces (Fig. 2.84).

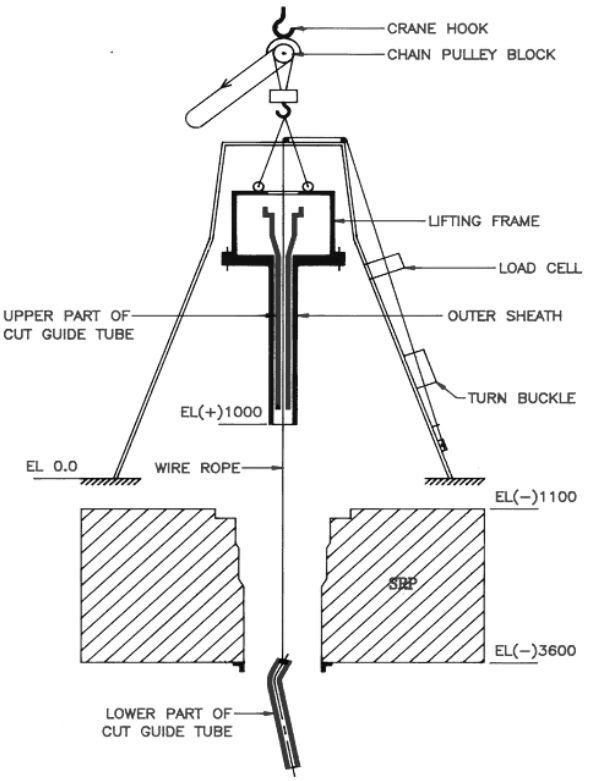

FIG. 2.84. Removal of bent guide tube from the reactor.

All care was taken to ensure that the cutting chips did not fall into the reactor. The damaged reflector subassemblies in the path of rotation were identified using periscope with sodium drained to uncover the subassembly heads, and removed using specially designed grippers. A limit switch was provided for the swivelling lock in the transfer flask and wired to the plug rotation logic to prevent plug rotation with the subassembly below the `transfer' position inside the core. Reactor operation could be resumed only in May 1989.

Subsequently, after valving in water into the steam generators, water started leaking through the cap of the orifice assembly at the bottom of a tube. All the caps were inspected and four defective caps were rectified. Subsequently, water leaks were observed across the gaskets in the orifice-meters in the water sub-headers of the steam generators. These were replaced by welded type orifices and power operation was resumed. Steam temperature variations among the tubes recently led to the finding that the spring loaded orifice assemblies at the bottom of most of the tubes had dropped due to fretting wear. They have been replaced by welded assemblies.

There were three reactivity incidents in 1994, 1995 [61] and again in 1998–99 [63]. Except that all these were positive reactivity incidents, the characteristics of all the three incidents were totally different in terms of magnitude, permanent gain and reproducibility. Though the exact causes could not be established even after extensive testing, they are suspected to be due to core deformations arising out of steep thermal gradients inherent in the small core. With the progressive expansion of the core, they are no longer seen.

The core cover plate housing the thermocouples for monitoring the subassembly outlet temperatures got stuck in fuel handling position in 1996, resulting in core temperature anomalies, especially of the MK-II fuel subassemblies in the core periphery. An eddy current flow meter has been developed for periodic monitoring of flows through the subassemblies during fuel handling, to supplement the core temperature supervision. The biological shield cooling coils inside the reactor cell developed water leaks in 2000 and were chemically sealed in 2001 [64]. The leaks are due to suspected crevice corrosion of fillet welds in the embedded pipes. The leak rates are monitored, and whenever leak rates exceed the prescribed limit, they are chemically sealed in-house. So far, leak sealing has been done six times.

There was an incident of about 75 kg of primary sodium leak in 2002 due to a defect in the body of a sodium valve [65]. The leak was contained within the inerted primary purification cabin and the system was normalised without any exposure or contamination.

2.16.3.8. Upgrades and modifications

Several modifications and improvements have been carried out subsequent to first criticality, based on operational experience feedback. The control power supplies of the secondary sodium instrumentation were segregated loop-wise in 1997–98, to avoid common mode failure. Several improvements were carried out in sodium pump speed control system to control the pump speed within ± 1 rpm in auto-mode operation. Wire type leak detectors have been installed on the steam generator shells to detect sodium leaks into the cabin. A dedicated argon bank to inert the steam generator cabin in the event of any sodium leak from the steam generator shell has been provided. During commissioning, one main boiler feed pump seized due to loss of thrust balance. This was traced to possible loss of net positive suction head. The pump was replaced by a maintenance friendly pump with lower allowable net positive suction head in 1997–98. The second pump has also been recently replaced.

The 220 V, 1-Φ, UPS system was replaced in 1998. All the battery banks were replaced in 1994–95, and again in 2005. The fire alarm system was replaced by a new, computer based analogue addressable system in 1998.

To obviate the need for a neutron source for start-up after long outages, two pre-start-up channels with boron coated chambers were inducted in service in 1992. The neutronic channels were completely replaced in 1998.

Due to obsolescence, both the computers of the Central Data Processing System were replaced — one in 1988 and the other in 1992. Both the sub-systems have again been replaced by embedded systems conforming to the latest safety standards. Over the years several new features have been added to the Central Data Processing System. These include additional personal computer based systems for monitoring reactor assembly temperatures, radiation and air activity levels, friction force measurement of control rod drive mechanisms and steam generator/turbine data logging. In addition, dedicated fast recording systems for reactivity incidents and an interrupt personal computer to scan all trip contacts every 20 ms and dump

the data on scram have been provided. An integrated message storage system to store all messages has also been added.

The feed water heaters of the steam-water circuit were of contact type, making them prone to level fluctuations during process parameter changes. These fluctuations resulted in cascade tripping of the condensate pumps, leading to reactor trip. In fact, most of the reactor trips have been originating from the steam water circuit. Hence these heaters were replaced by surface type heaters in 2004, and the reactor trips from steam-water system have since been negligible.

To avoid spurious reactor trips, the steam generator leak detection systems in both the secondary loops have been triplicated and wired to the reactor trip circuit in 2/3 voting logic. To detect water leaks at low sodium temperatures during power raising and hot shutdown, a thermal conductivity based hydrogen detection system has been installed in the cover gas of secondary sodium pumps. In order to avoid thermal striping stresses in the expansion tanks housing the secondary sodium pumps, the sodium overflow line was blanked and the cover gas pressure maintenance circuit was modified. The air-cooling system for the concrete surrounding the outlet pipe penetrations of the reactor assembly was modified recently in order to improve the cooling of the concrete.

The current core is likely to be the equilibrium core for some more time. With the limitation on the power realisable with this core, three out of the seven tubes were blanked in all the four steam generator modules in 2008. Several augmentations have been done in the auxiliary systems like service nitrogen, service water, demineralised water and ventilation systems.

2.16.3.9. Radiological safety

During the initial years of operation, higher radiation levels (45 mR/h max) were measured at some local spots in the reactor containment building (RCB) and shielding was augmented in these locations. The general radiation levels in all the accessible locations in the RCB during operation at 18.6 MWt power was 6-7 μGy/h. On top of the reactor, a streaming field of 10 μGy/h was seen at local spots. The total cumulative dose to personnel so far is 100 man-mSv and the total activity discharged through the stack is 19000 GBq of Ar^{41}. During the past 20 years, there has been no event of abnormal radioactivity release, personnel or area contamination. Due to the slight increase in cover gas leak rates in the recent years, a `cocoon' has been placed over the reactor to collect the active leaking gas and discharge it to the RCB exhaust.

2.16.4. Residual life assessment

As a part of the regulatory review, the residual life of the plant was assessed. The creep-fatigue damage seen by the components is found negligible. The reactor life is governed by the dpa levels seen by the grid plate. Flux levels at the grid plate location were measured using Np foils, and the residual life is estimated as about 12 EFPY.

2.16.5. Conclusion

The experience in construction, commissioning and operation of FBTR has been gratifying and the satisfactory performance of the fuel, sodium systems, steam generators and instrumentation during 25 years of operation has provided sufficient feedback to enable the launch of the PFBR project. In the years to come, it is planned to irradiate advanced structural materials and metallic fuels of varied designs in FBTR.

2.17. Construction and pre-operational testing of SNR-300

2.17.1. Introduction

SNR-300 was planned as an international project from the very beginning, i.e. about 1966. The final arrangement consisted of a three-country cooperation comprising Germany (70%), Belgium (15%), and the Netherlands (15%), involving the manufacturers, the utilities, and the R&D organizations.

The first nuclear license of SNR-300, which was necessary for the beginning of construction, was granted in December 1972. Construction of the Kalkar Nuclear Power Plant with SNR-300 reactor on the Rhine river banks began early in 1973. Start of power operation was originally scheduled for 1978/79, but really construction of the plant and pre-operational testing were completed by 1986 and early 1987 due to very complex the German licensing procedure based on a step-wise approach. Totally 16 licensing steps were made within period from 1972 till 1985.

The adverse political influence started in Germany as early as the late seventies, when the usefulness and the safety standards of nuclear power in general and SNR-300 in particular were questioned, was a reason of announcement of the German Federal Minister of Research and Development in March 1991 about unconditional abandonment of the project after a thorough evaluation of the overall situation. This has led finally to the fact that the development of fast reactor technology has been suspended in Germany.

2.17.2. Description

NPP SNR-300 was a prototype reactor project comparable to Phénix in France, to PFR in Great Britain, and Monju in Japan.SNR-300 is a loop-type reactor that has three parallel primary sodium heat transfer loops with the main heat transfer components external to the reactor vessel (Fig. 2.85).

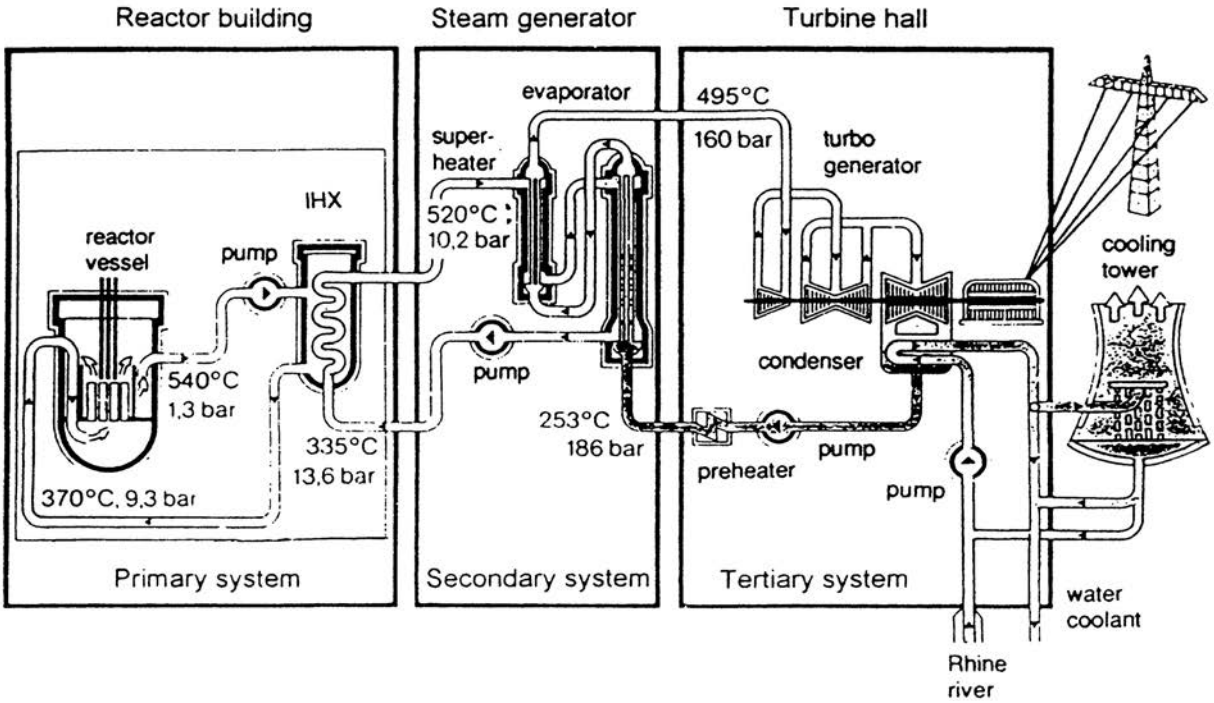

FIG. 2.85. Schematic flow scheme of the SNR-300.

The secondary heat transfer system, installed between primary system and water/steam system for safety reasons, is practically identical in both cases. It also consists of three parallel circuits. Live steam conditions and the achievable efficiency are very similar in all plants: 500°C, 165 bar, 40%. These are close to the conditions of coal-fired stations.

2.17.3. Construction and pre-operational testing

Construction of SNR-300 began in April 1973 and was essentially finished in mid 1985, when the leak and pressure tests of buildings and systems were successfully completed. Construction and pre-operational testing of a system were formally licensed together. However, construction and pre-operational testing were subject to a thorough supervision programme, which meant that individual erection and pre-operational testing events required a formal release. Some milestones of the construction period are listed in Table 2.26.

TABLE 2.26. IMPORTANT MILESTONES OF ERECTION WORK OF SNR-300

Time	Erection event
January 1981	Start of erection of components of mechanical and electrical auxiliary systems
Autumn 1981	Erection of reactor safety vessel
September 1982	Erection of reactor vessel
July 1983	Completion of radial breeder assembly fabrication
November 1983	Delivery of reactor cover plug, erection of primary pipe work
March 1984	Completion of erection of reactor vessel system (installation of cover plug)
September – November 1984	Delivery of helical tube steam generators
March 1985	Completion of fuel assembly fabrication

Pressure and leak tests were defined as the start of the pre-operational testing of the plant. Numerous pressure and leak tests were performed on:

- Primary system including the reactor vessel in December 1983;
- Secondary systems in February/March 1984 and January 1985;
- Containment system in October 1984.

The second striking step towards readiness for operation was the delivery of the sodium to the site, final filling of the respective systems (which had been preheated electrically or by the gas heating system), circulation of the sodium and operation of the purification plant. Approximately 1070 t of sodium were loaded into the dump tanks of the primary and secondary systems in four steps from July 1984 to February 1985.

Purification of the sodium in the dump tanks via the primary and secondary purification systems began in late September and December 1984, respectively. At the start of the measurements, the plugging temperatures were around 200°C, and it was possible to lower them to 130-120°C within a short time. Pre-heating, filling, and operation of the systems at higher temperatures were carried out in compliance with specific temperature and temperature difference criteria, which were stress analysis. The impurities in the sodium were well below the specified values. High temperature purification operation commenced in June 1985 instead of October as indicated in the revised schedule. The following targets were pursued during this testing phase:

- Increasing temperatures in approximately 30 K steps from around 200°C to 420°C and a subsequent temperature setback to 200°C; duration of this operation was about 30 days;
- Measurement of the quality of the sodium and the cover gas;

- Determination of the change of volume in the level holding tank (primary system) and in the secondary surge tanks caused by temperature changes in the main heat transfer loops during operation;
- Measurement of various hydraulic data;
- Measurements of heat losses from the systems (via the insulation for example), and plant room temperatures;
- Vibration measurements on the pipe work, and inspection of support and guidance structures;
- Temperature measurements at penetrations and temperature reduction sections of the pipe work.

In the primary system, the plugging temperature increased with the system temperature. A value of 200°C was measured for about 2 weeks, but it was then possible to lower it to 160°C and subsequently to 120°C. The hydrogen content in the cover gas of the primary system was reduced from 5 000 to approximately 600 vpm by way of continued purification of the sodium.

In the secondary system, a comparable plugging temperature variation resulted from similar changes in the system temperature. The final value here was also around 120°C. But in this case it was achieved within a few days. Although the plant room temperature and system heat loss measurements performed during the high temperature purification phase confirmed the design values in wide areas, it was necessary to rework the insulation in some regions (e.g. in the area around the main heat transfer systems), and to increase the flow-rates in subsections of the ventilation and nitrogen inertization systems using booster blowers to be installed at a later date. Hot flushing operation on the water/steam side was performed for the main heat transfer system at the beginning of April 1985, and for-the decay heat removal systems in May 1985. Good conductivity and iron values were obtained-in the cooling water relatively quickly.

Power testing of the decay heat removal systems commenced with the riling a steam generator group of one loop on the water side. To start with it was impossible to continue the test at 420°C due to the repair of the dump and leakage hold-up tanks, described later.

As a result of the temporarily insufficient dump tank capacity, the possible necessity of a dumping event was avoided by cautions operation of the main heat transfer systems at approximately 300°C with a main pump speed of about 30%. Especially in a loop-type reactor, the behaviour of the pipe work is of significant importance. Tests showed the following:

- After reference measurements with the hangers locked, the procedure included unlocking, increasing the pipework temperatures sodium filling and temperature variation. Calculated and measured displacements were in quite good agreement. Only a few spring or constant hanger forces had to be re-adjusted by less than 12%. Insulation weight tolerances were the reason for this deviation.
- Vertical movement of the pipework followed the temperature steps with a time lag due to friction in the insulation.
- The deviation in vertical displacement between calculation and measurement was within the specified tolerances.
- Low mass flow-rates in the circuits sometimes led to some stratification effects in the coolant.
- Low mass flow-rates in the circuits sometimes led to some stratification effects in the coolant.
- In very flexible parts of the pipework the sliding support bearings with a friction coefficient of ~ 0.1 had to be replaced by ball bearings with a friction coefficient of ~0.01 in order to reduce the number of earthquake shock absorbers and snubbers. A larger number of sliding support bearings than would otherwise have been necessary had to be installed.

- The auxiliary sodium service systems were checked, too, but to a lesser extent. The principal results were the same as for the main system.
- There were no significant vibrations of the primary and secondary pipework. During the start-up period before the core was in place, butterfly valves in the primary circuits served as throttle valves. This induced some vibration in the adjacent down-stream line, but it was judged not to be relevant for operating conditions with the core installed.

Table 2.27 summarizes the milestones of the pre-operational testing phase.

TABLE 2.27. MILESTONES IN THE PRE-OPERATIONAL TESTING PHASE OF SNR-300 UP TO JANUARY 1987

Milestones	Time/period
Approximately 900 partial and whole system pressure tests	June 1983 - April 1985
Single pressure and leak tests	
Primary system (closure of reactor plug)	12.83/(01.84)
Secondary systems 1/2/3	02.84/03.84/12.84
Containment system	28.09.84 - 01.10.84
Steel shell and containment building	05.04.85 - 06.04.85/
la area/lb area	08.02.85 - 09.02.85
Sodium delivery to the site	15.07.84- 13.05.85
Sodium filling into the dump tanks and start of purification operation in the primary/secondary systems	11.12.85/29.09.85
Sodium filling into the systems and start of circulation operation	
Primary system	28.04.85
Reactor tank and loop 1 (i.e. construction completed)	02.05.85/09.05.85
Loop 2 / Loop 3	24.11.84/07.02.85/
Secondary system loop 1 / loop 2 / loop 3	28.02.85
Emergency core cooling system	15./19.06.85
Na-cooled fuel store and cooling system	30.03.85-05.05.85
High temperature purification operation (primary and secondary systems)	28.06.85-15.09.85
NaK delivery and filling into floor cooling device (core catcher), circulation operation	10 09.85-21.11.85
Water/steam side	
Water flushing operation	April/May 1985
Steam generator filling and testing of a leg-specific decay heat removal system	interrupted on 13.08.85 until after dump tank repair
Inertization of Na-systems area Natural circulation tests	from 20.12.85 onwards 12.85 until 01.87

Further pre-operational testing was considerably impeded and delayed from the second half of 1985 until late 1986 by special unexpected events described later. Rectification of these events made it necessary to repeat various testing steps already carried out. Nevertheless, it was possible to inert the primary cell areas in December 1985. Thus in spring 1986, the plant was ready to accept the breeder and fuel assemblies which were available in the fabrication plants, despite the remedial work for the unexpected occurrences.

2.17.4. Unexpected occurrences and their remedy

In the present section, three occurrences which caused serious delays in the non-nuclear start-up schedule are described:

- Repair of the sodium dump and leakage hold-up tanks;
- Recovery of fragments of a broken vibration measurement lance;

- Increased hydrogen concentration in the reactor vessel and the sodium-cooled fuel store inert gas plenum.

2.17.4.1. Repair of sodium dump and leakage hold-up tanks

Ten sodium dump and leakage hold-up tanks made of ferritic material with the designation 15Mo3 were installed in the primary and secondary systems area. In August 1985 a small sodium leak in one of the dump tanks was discovered visually during a routine inspection walk. Due to the very small leak-rate no alarm was triggered by the smoke detectors. Thorough inspection showed that all ten tanks revealed transverse microcracks which penetrated the walls in the area of the weld seams. More detailed investigation showed that they had originated from the inside.

All parties concerned (manufacturer, safety experts, authorities) finally came to the conclusion that the cause was the adverse coincidence of the following parameters, which had led to the formation of cracks and their propagation through the wall about a year after filling with sodium:

- Microscopic cracks and geometric inhomogeneities as a result of the welding process;
- A rather high level of residual stresses after welding without subsequent heat treatment;
- Formation of iron hydroxide, especially FeO(OH), being the only corrosion product relevant for this question, during hydraulic pressure tests and the subsequent long storage times on the plant despite inert atmosphere;
- Formation of atomic hydrogen due to the reaction of the sodium with the iron hydroxide.

After the cause was identified, all welding seams, not only those directly affected, were removed on site under extremely difficult confined conditions and rewelded using improved welding parameters. This process took approximately 4.5 months, and was completed in accordance with a schedule drawn up for the operation. Ultrasonic tests shortly after repair and recharging with sodium and one year later showed no evidence of cracks. An examination of the complete plant for similar evidence showed that the cold trap vessels were also affected. However repair work on these was very much easier as disassembly and reassembly were relatively simple and repairs could be carried out in the workshop.

2.17.4.2. Salvage of debris from a broken vibration measurement lance

At the beginning of 1986, a vibration measurement lance, which had been installed for trial purpose in the central position of the core (which had not yet been loaded) had to be disassembled because the measuring signals indicated a fault. The lance had two inductive pick-ups, one for connection to the bottom of the gas bubble separator and one for connection to a special central grid plate insert.

When removal was attempted the lance jammed in the grid plate area. The reason was that the retention springs were not able to pull the coupling jaws of the inductive pick-up back into the original position. This was due to a sodium leakage in the pneumatic system with which the jaws were to be activated. During the attempt to free the lance by rotating it and increasing the tensile pull, it broke in the region of the upper inductive pick-up, roughly 2.5 m above the bottom. The 2.5 m long piece and some small parts remained in the reactor vessel and had to be salvaged. Fortunately, six dummy assemblies were positioned around the central position, which meant that the search for the parts could be limited to this small area.

Apart from a very small eyelet, which posed no risk to safety, it was possible to remove all the missing parts from the vessel using plastic bags to retain an inert atmosphere. For this purpose, the sodium level was lowered to the level of the grid plate, the argon was kept under a slight overpressure and the temperature was maintained at approximately 200°C.

The grab and lighting equipment were tested and optimized in an Interatom (now SIEMENS) test plant before being used in the reactor vessel. Use was made of valuable experience from the UK and France. The salvage process took approximately 2 months, and was completed to time according to the special work schedule drawn up for the purpose.

2.17.4.3. Penetration of moisture into the inert gas plenum of the reactor vessel

Handling tests carried out at the same time with the shutdown systems showed a certain sluggishness of the centering tube shifting device. The centering tube moves when resetting the reactor to handling operation. During this period the hydrogen content in the gas plenum of the reactor vessel behaved remarkably and seemed to increase continuously.

Detailed and systematic investigations finally clarified the cause for these unusually high hydrogen concentrations in the inert gas: a relatively high amount of moisture was penetrating from the venting apertures in the boxes attached to the rotating cover plug lid and the fixed cover ring containing basalt granulate shielding material. A number of very important constructional reasons had emphasized the need for venting into the plenum, e.g. to avoid being subject to pressure vessel regulations and to provide for thermal expansion. It must be admitted, however, that the rate at which the moisture was released from the basalt granulate and the total amount of water were definitely underestimated at the time of design and fabrication.

When disassembling three shutdown rod supports, thick deposits became obvious on the exterior, which, although they had impeded the movement of the centering tube, probably had no adverse effect on the shutdown function. Visual inspection of the inert gas plenum area showed that there were also thick deposits on other internals. The primary task was now to dry the basalt granulate in such a way that no more moisture could enter the plenum. For this purpose a system was installed by which fresh argon was forced through the basalt by applying pressure cycles and, after absorbing the moisture, was drained off in a controlled manner to the exterior. The basalt temperature was steadily increased during this operation by increasing the sodium temperature and partly heating the boxes.

The system was in operation with short interruptions from August 1986 until January 1987 when an adequate degree of dryness was obtained. Laboratory and simulation tests with basalt and basalt fills carried out in parallel permitted a quantitative evaluation of the drying process. The deposits were mostly concentrated in the area directly above the sodium level. It was therefore possible to dissolve them to a large extent by raising the level of sodium by about 500 mm and increasing the temperature to approximately 420°C. Above this area the deposits were mainly dissolved by hot sodium aerosols.

This occurrence had raised some fundamental questions, on the authority's side, not only with regard to elementary operational considerations but above all with a view to safety. Priority in the following discussions was given to the integrity of the heterogeneous weld seam in the upper area of the vessel and to the functioning of the shutdown systems.

Whereas the thick parts of the deposits on the internals adhered firmly and had to be removed mechanically from the disassembled parts, in the region of the heterogeneous weld seam of the tank, which was situated well above the sodium level in the vicinity of the cover, and accessible

from the inside through six small in-service inspection apertures on the circumference, only flake-like aerosols were found. They could easily be removed by suction, blowing or scraping. This was done through the apertures. Specimens of the deposits were also taken from six points and were thoroughly examined chemically and spectroscopically. The heterogeneous welding seam was also inspected through the apertures by cameras and endoscopes.

From the optical, metallurgical, chemical, and spectroscopic tests carried out with the deposits and the internal structures, there was no evidence at all of any actual damage at that time or to be expected later during operation. Careful attention was paid especially to indications of selective corrosion.

The deposits, which consisted of sodium, sodium oxides, and sodium hydroxides had apparently affected the surface of the structures to a certain degree by pitting: partly by general oxidation and partly by attacking the grain boundaries of the base material and the d-ferritic phase of the welds. A specific observation and materials testing programme was set up by agreement between the relevant experts and the authority in order to find out what long-term effect this attack could possibly have and how it could be kept under control.

The fast shutdown functions were not impeded to any measurable extent. This was proved by comparative measurements taken in April 1986 and February 1987. A basic inspection and functional testing programme for the shutdown systems and other internals was carried out in the framework of other functional tests on the reactor in order to corroborate the recent findings.

The permissible moisture and hydrogen levels during operation were investigated as a result, because the residual moisture from the basalt boxes and the fixed cover ring could not be completely removed either during the pre-operational testing phase (temperature too low) or during nuclear operation (asymptotic behaviour).

The conclusion of these investigations was that approximately 1000 vpm of H_2 in the inert gas plenum would not present any serious problem (actual value at that time: 350 vpm H_2). This corresponded to a moisture penetration-rate of about 400 g/day. The plugging temperature range from 120 to 150°C specified for continuous operation corresponded to much more than this ingress rate at an adequately available cold trap capacity. This meant that it could easily be controlled by cold trap operation. The same was true for the Na-cooled spent fuel storage vessel.

Although these significant unpredicted events caused strong setbacks to the pre-operational testing, the overall satisfactory completion must be emphasized. It must also be stressed that the remedies would not have been successful without the massive support of the R&D laboratories especially in the fields of chemistry and metallurgy. Positive results - in particular with respect to safety concerns - were obtained from, among others, the natural circulation tests via the main sodium heat transfer loops and via the emergency core cooling system, on which information is given below.

2.17.5. Achievements

Besides the valuable experience gathered during the pre-operational testing phase described above, the safety-related achievements should be emphasised, because they were finally able to demonstrate the tremendous potential of an LMFBR system with respect to passive decay heat removal by natural convection.

(a) Decay heat removal via the emergency core cooling system

For removal of decay heat, SNR-300 was equipped with 5 redundant systems, the 3 redundant legs of the primary, secondary, and tertiary heat transfer system, and the 2 redundant systems (i.e. 2 times 6 individual loops) of the emergency core cooling system. The emergency core cooling system was intended for use specifically on the very rare accidental occasions when the 3 parallel loops of the main heat transfer system were simultaneously inoperable, e.g. because of airplane crashes or large earthquakes [66]. Initial non-nuclear experiments, which were performed of course without nuclear heat, confirmed the respective design calculations for 2 operating modes: Emergency core cooling system (all active components operational) and Passive decay heat removal (no active components operational).

The primary, secondary and tertiary heat transfer system, and the emergency core cooling system were set to 400°C isothermal, the primary coolant loop dampers to minimum opening and the main pumps with the pony motors to 5% nominal speed. The flow-rate in the emergency core cooling system was raised by means of the electromagnetic pumps to 100%, but the air side dampers were closed and the blowers were switched off. For reasons of materials strength (to protect the components involved), another limit condition was that the sodium outlet temperature at the air cooler should not drop below 200°C. The experiment was started by opening the air outlet dampers after the blowers were switched on. The air inlet dampers were opened step by step. The cooling range was about 100 K and the core outlet temperature dropped by 40 K. With vessel temperatures of approximately 600°C and air dampers completely open, the overall design capacity of the emergency core cooling system was 12 MW, or 2 MW per individual loop. With these performance data and given a temperature of 400°C during the experiment, the cooling system removed 73% of the power, whereas a figure of only 67% was expected. When extrapolating to a vessel temperature of 600°C, the heat removal capacity was significantly beyond 100%.

SNR-300 had the potential for passive decay heat removal: even in the case of complete and unlimited failure of all active systems (station black-out) and without any supporting actions by the operating staff, none of the radioactivity barriers (cladding, primary system boundary, containment) would have been jeopardized [67]. This passive decay heat potential was based essentially on three principles:

(1) The high heat capacity of the sodium and the structural masses of the circuits, which were coupled thermodynamically to the core via natural circulation;
(2) The good natural circulation capability of the sodium circuits by provision of appropriate level differences between the heat exchanging components with respect to the heat source;
(3) Sufficiently high insulation heat losses from the sodium loops, which increased more than proportionally to the temperature increase.

The capacity of the concrete and steel of the reactor building to accumulate large quantities of heat and to discharge them to the environment slowly was of further importance. While principle 1 was determined by design, principles 2 and 3 had to be verified during pre-operational testing: Significant natural convection flow-rates caused by temperature differences of only some 10°C, consistent with the theoretical estimates, were observed in the primary and secondary circuits. The heat losses, mainly via the insulation of the heat transfer system, were measured using two different methods:

– The power input from the main pumps at various levels, the relevant equilibrium temperatures were measured;

– The systems were heated to 420°C, the heat sources were switched off, the temperature decay function was measured taking amount of calculated heat losses and heat capacities.

The previous analysis of passive decay heat removal had been based conservatively (for safety reasons) on theoretically-determined heat losses assuming ideal manufacturing and installation of the insulation and neglecting any penetrations, disturbances and other irregularities. It predicted a maximum temperature of 740°C. Later analyses utilizing the actual heat losses gave an upper temperature of 570°C after about 20 hours.

During pre-operational testing the natural convection capacity of the emergency core cooling system was also demonstrated. It was of particular interest in the R&D frame with regard to the follow-on project at that time, SNR2, for which passive decay heat removal via immersion coolers had been demanded by the customer.

The initial conditions of the experiments were the same as in the case of the emergency core cooling system tests described above. The EM-pumps were switched off. The dampers were opened partially to avoid sodium temperatures falling below 200°C in the cold legs. The heat removed by natural convection at the air side and at the Na-side amounted to 1.1 MW. This value was consistent with predictions of the given boundary conditions. The dampers of the air coolers, opened by simple manual operation, were introduced as an additional heat sink into the analysis of passive decay heat removal. A maximum temperature of 530°C was then reached after about 10 hours. The demonstrated temperatures lay very close to the normal operating temperatures (Fig. 2.86).

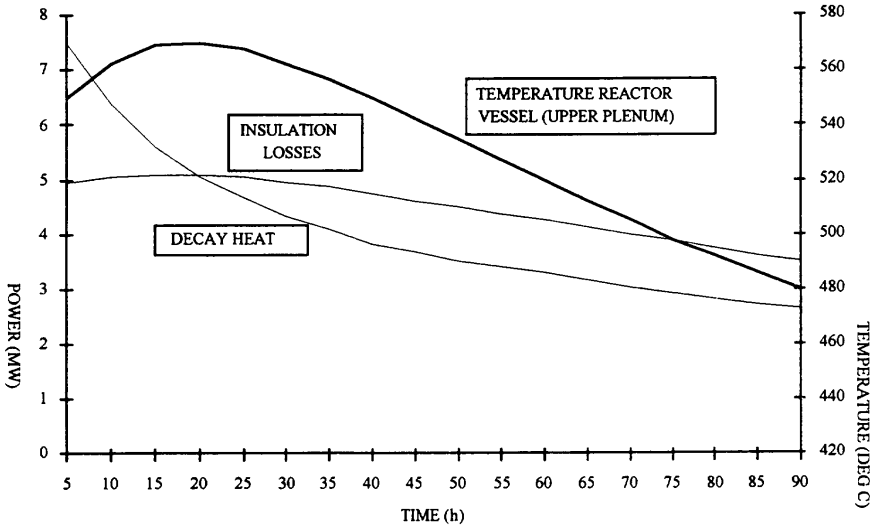

FIG. 2.86. Temperature variation in the reactor vessel upper plenum with natural circulation cooling.

(b) Natural circulation in the sodium loops of the main heat transfer system

The natural circulation potential of SNR-300 resulted from the system arrangement, and was determined analytically. As an important part of the pre-operational testing, natural circulation operations were first evaluated in the secondary loop. Primary and overall system tests were carried out and evaluated later. Natural circulation in the secondary system started under two different boundary conditions: switching off the secondary pump while operating the decay heat removal systems on the water side, and after draining the water side of the steam generator. In the first case, the flow-rate increased from 18 kg/s with a difference in temperature on the intermediate heat exchanger of 15 K, to 34 kg/s with a difference in

temperature of 34 K. During this process, the temperature increased continuously due to the heat supply from the primary pumps, and then decreased because of the heat transfer to the water/steam side. On reaching a temperature difference of 34 K as mentioned above, the water/steam side was switched off so that the evaporator outlet temperature increased again. A stable natural circulation flow-rate of slightly more than 1 kg/s/DT resulted. Calculations predicted approximately 0.5 kg/s/DT. Thus the design calculations were confirmed.

In the second case, the flow-rate increased to 30 kg/s with 60 K on the intermediate heat exchanger, and stabilized to 8 kg/s.

(c) Evaluation of the overall "passive" safety behaviour of the plant in case of decay heat removal

The tests on the safety potential of the plant described above, several of which exceeded the design and licensing basis, gave confidence in the plant safety, which until then had been only theoretically determined. This applied not only to the main heat transfer system in conjunction with the immersion coolers of the emergency core cooling system; it was also valid for other plant installations such as the sodium-cooled and gas-cooled fuel storage facilities, where significant amounts of decay heat would have been released. This was an important factor in the then current evaluations of accident management measures in the aftermath of the Chernobyl accident [67]. Under extremely unfavourable loading conditions component failure limits were reached after more than 40 hours for the sodium-cooled fuel store and after more than 100 hours for the gas-cooled store. Failure limits for the main heat transfer system components including the reactor vessel and the emergency core cooling system would not have been reached at all. The temperatures here would have decreased quite quickly. The main reason for this was the relatively large sodium volume in the reactor vessel and the adjoining primary and secondary systems which participated in the flow circulation to remove the heat, and the large system surfaces via which the heat dissipated into the surrounding rooms. The heat would have been stored in the steel and concrete masses of the building, and from there dissipated into the environment.

It is important to recall that in Germany, a total station black-out of at least 2 hours, during which absolutely no externally and internally produced energy is available apart from batteries, must be considered in the safety evaluation. Battery energy is only used to monitor important plant operating parameters during the station black-out period and to re-establish the grid connection when the grid becomes available again. Without being specifically designed for this purpose, the battery capacity of SNR-300 was sufficient for approximately 5 hours. From this, it was concluded that the available battery power would have a limited operating period to monitor plant parameters and re-establish the grid connection, but could not contribute to the decay heat removal function itself.

(d) Reassessment of safety design aspects in the light of important safety related events in other facilities

It is legally mandatory and usual practice in a licensing process in Germany to evaluate events in other facilities in the world which are obviously relevant to safety with respect to their possible implications for the facility which is the subject of the licensing process. This can possibly lead to a re-assessment of the safety design basis or even back-fitting measures. Three events in particular are worth reporting in this context: the sodium fire accident at the solar test power station at Almeria, Spain, in August 1986, the steam generator accident at the Prototype Fast Reactor (PFR), at Dounreay, Scotland in February 1987, and, quite naturally, the serious accident at Chernobyl in the then USSR, in April 1986.

At the solar test power station at Almeria, Spain, sodium was ejected from the main heat transfer system in the course of an obviously inexpert repair action, which resulted in tremendous damage to the whole facility. Sodium under unexpectedly high pressure in an apparently empty pipe was released and sprayed violently onto a valve flange over the leak. This resulted in the formation of very small droplets with large reacting surface. The reaction with the ambient air led to very high temperatures. The resulting damage was compatible with observations from recent experiments on mixed pool/spray fires. A generally-applicable analytical description was however not possible at the time. A similar accident would have been extremely improbable at SNR-300. In other operating facilities no leakage larger than a few kilograms per hour had ever occurred. Therefore, such an accident was not considered in the design basis either in operating plants or in plants in the design stage. The calculated course of accidents for design considerations is basically a maximum or limit estimate, firstly because, contrary to expectations, they start spontaneously from large pipe breaks (leak-before break behaviour not being accounted for), or secondly because an ideal spray cone which maximises the consequences can form only at a very few locations. An inexpert repair procedure such as at Almeria could be excluded for SNR-300, was shown by detailed comparison.

Contrary to the procedure adopted at Almeria, at SNR-300 the following steps had to be performed before commencing repair action.

- The system had to be depressurised, the sodium dumped, and the affected area doubly isolated;
- A sodium section had to be frozen in a controlled manner as an isolation measure;
- A written and verified repair procedure had to be prescribed.

The phenomenological application of the Almeria fire results the SNR-300 steam generator building was supported and confirmed by applying a physical spray cone model validated with respect to the findings of the Almeria fire and experiments. By this means the original design basis was proved to be still valid. Not only was the overriding goal of protection achieved by demonstrating the stability of the steam generator buildings, but also the mechanical and electrical installations necessary for mastering leakage were shown to remain fully functional.

In applying the spray cone model to the inertization area of the plant, the reaction of the sprayed sodium with oxygen was the decisive factor. Only a limited amount of oxygen is available, but the heat transfer area of the total sodium droplet surface to the ambient nitrogen atmosphere is much larger than that of the previously-assumed pool. This led - as calculations revealed — to higher gas temperatures compared with previous calculations, and as a consequence to higher room pressures. An evaluation of the dimensions of the concrete walls enclosing the rooms fortunately showed that the design requirements for these walls could be fulfilled for the higher pressures.

Re-examinations of the aerosol physics showed that the aerosol mass was higher than previous expectation. However, the containment of radioactivity was still guaranteed. With respect to environmental impact the change of data proved to be irrelevant.

The accident in a PFR superheater unit, a power plant of similar size to SNR-300 but of pool design, resulted in breach of 40 bundle tubes. A larger number were damaged to a certain extent, as post-accident evaluations revealed. The containment boundary of the intermediate heat exchanger, however, was not affected. Subsequent calculations showed that there was a sufficient safety margin, so that nuclear safety was not impaired. In the absence of detailed information about the accident, its origin and course had to be reconstructed and derived from

post-accident evaluations. Both could be put down to the choice of material, specific design features of the apparatus, and to incomplete monitoring of important operational parameters.

Because of these factors, immediate application to SNR-300 was not appropriate: the tubes consisted of ferritic steel which was practically insensitive to intercrystalline corrosion, and in addition the bundles were probably not sensitive to flow-induced vibrations so that the basic cause for the origin of the accident could be excluded. The monitoring instrumentation (H_2 in the coolant) was more reliable, since it was designed with redundancy and would have undergone regular maintenance. Limit estimates in connection with the recent licensing process for SNR-300 had also demonstrated that all the bundle tubes could fail simultaneously without endangering the containment boundary in the intermediate heat exchanger.

One essential finding from the course of the accident at PFR, however, was new, namely that under specific circumstances the bundle tubes could be damaged if they were heated up by a long-lasting and locally stable sodium/water reaction to the point of bursting. Until this accident at PFR, all experimental evidence had led to the assumption that the damage mechanism was local material erosion due to the impact of the reaction flame. The flame was assumed to originate at the location of the steam/water leak by reaction with sodium, and to impinge on the neighbouring tubes.

This new insight resulted in a specific analytical and experimental programme on behalf of SNR-300 at the R&D organizations. It finally led to the conclusion that also the loads produced by tube damage caused by overheating would not go beyond the design basis loads. This was basically due to the existence of bursting disks at both ends of the apparatus, a design feature not present at PFR. By this means the sodium would be expelled very quickly from the component so that the sodium/water reaction would close. Therefore, no adjustment or modification of the design measures to prevent and master a steam generator accident was necessary.

The very serious accident at Chernobyl brought up a series of important safety related technical questions, which obviously had and still have to be answered by all those building and operating nuclear facilities. More than that, the accident and its consequences are still having a considerable negative influence on public opinion and the political attitude towards nuclear energy in the whole world and especially so in Germany. Both factors played an important, if not decisive role, in the SNR-300 case. The Chernobyl case was taken by the licensing authority as an argument for a complete re-assessment of the overall safety design of SNR-300. This attitude in 1986 was the real starting point of the last act in the attempt to deal the deathblow to the project. Three phenomena were of prime concern: the positive void coefficient of reactivity during normal operation and in case of accidents, breach of radioactivity containment after core disruption accidents, and possible exothermal chemical reactions in the case of core disruption. Whereas the Reactor Safety Commission came to the conclusion that the points of concern were reliably protected by preventive and mitigative measures, the licensing authority demanded a complete re-assessment of the overall safety design. From a technical point of view, a comparison of the specific features which had most aggravated the course of the accident with the respective safety features of the SNR-300 led to the following conclusions [67]:

- Stable reactivity behaviour and good controllability characterize SNR-300, in contrast with unstable behaviour and complex spatial dependencies in the core of the RBMK-1000.
- Design deficiencies in the protection and emergency shutdown systems were — among other things — responsible for the accident at Chernobyl. All SNR-300 safety features, such as, for instance, redundancy, diversity, degree of automation, separation of

operational and safety tasks within the control system, security against uncontrolled access, efficiency and safety margins of the protection and fast acting shutdown systems, were far superior to those of RBMK-1000. For this reason reactivity excursion accidents could be classified hypothetical in SNR-300.

- Because of elementary physical properties the possible energy release in the case of a nuclear excursion were in principal much lower than in RBMK-1000.
- In addition to these far-reaching safety features, the primary circuit and the containment system including a so-called floor cooling device (core catcher) of SNR-300 were designed in such a way that even the consequences of a very unfavourable excursion accident could be mastered. At RBMK-1000 no mitigating features were installed.
- At RBMK-1000, exothermal chemical processes had escalated the accident consequences. In particular the protracted graphite fire had increased the radiological releases greatly.
- In SNR-300, the radioactivity enclosure (containment) was protected by inertization with nitrogen, steel cladding, and catch pans against large sodium leaks from pipe breaks or brought about by the consequences of a hypothetical power excursion accident, so that no exothermal reaction of any significance could have occurred. All in all, the re-assessment of various safety design features by the safety experts, and a review of events in other facilities, were about to converge to positive results when the decision to terminate the project was taken, since the licensing authority did not seem to follow the findings of the experts. The re-assessment had taken too long, and had led to further considerable delay and therefore to an increase of costs.

2.17.6. Epilogue

On 20 March 1991, the Federal Minister of Research and Technology announced after consultations with the industrial partners involved, that SNR-300 should not proceed to commence operation. He offered as a reason for this the politically-motivated delaying of the licensing process [68].

2.18. Construction and pre-operational testing of Monju

2.18.1. Overview of project

Monju, the prototype fast breeder reactor (FBR) which Japan Nuclear Energy Agency (JAEA; the successor of PNC and JNC) has built as part of the Japanese FBR development programme, has recently undergone plant modifications aiming mainly at reinforcing the safety measures against sodium leakage. Monju is a loop-type sodium-cooled fast breeder reactor with U-Pu mixed oxide fuel. It supplies 280 MW_e to the grid and is situated on the Tsuruga Peninsula facing the Sea of Japan, about 400 km west of Tokyo.

Work on the preliminary design of Monju started in 1968 before the final design of the experimental FBR Joyo, and the conceptual design started in 1969. Safety evaluations were conducted from 1980 to 1983, and the construction permit granted by the Prime Minister in May 1983. Construction started in 1985, and completed in April 1991. The pre-operational test started in May 1991 and initial criticality was achieved in April 1994. The sodium leak occurred in December 1995 at 40% rated power.

After the incident, Power Reactor and Nuclear Fuel Development Corporation (PNC) conducted the cause investigation, comprehensive safety review, and safety authority permitted plant modification in December 2002. The local governor of Fukui made pre-consent for plant modification work on February 2005. Japan Nuclear Cycle Development

Institute (JNC, the successor of PNC) started preparatory work for plant modification work in March 2005, after nine years of negotiations since the secondary sodium leakage. The main modification work was completed in May 2007 and the modified system function test in August 2007. The entire system function test is in progress since August 2007 which has achieved 43 tests in 114 tests by the end of January 2008. Monju resumed operation on 8 May 2010.

The FBR in Japan. The development of nuclear power in Japan is based on the premise that the FBR will become a major component of future nuclear capacity, alongside the LWR. In 1966, the Japan Atomic Energy Commission decided to go ahead with a national project to develop the FBR involving the government, universities and the private sector. The following steps were then taken:

- Basic research on plutonium fuel, sodium coolant, etc;
- R&D, including industrial development to bring components up to the point of practical application;
- The construction of an experimental reactor to confirm that the basic FBR technologies were ready for application;
- The construction of a prototype reactor to confirm the FBR's performance and to provide the basis for future commercialization.

In October 2005, the Atomic Energy Commission of Japan established a new "Framework for Nuclear Energy Policy", in which the future direction of research, development and utilization on nuclear fuel cycle in Japan was stated as follows:

- Nuclear energy, a basic energy source in Japan, contributes to supplying stable energy and controlling global warming;
- Development of the closed nuclear fuel cycle should be made steadily for the effective use of plutonium and uranium recovered by reprocessing spent fuel;
- Replacement of the current light water reactors (LWR) will start in around 2030; initially with an advanced type of LWR. The development of fast reactors (FR) aims at its commercial introduction around 2050.

PNC was established in October 1967 as the central development organization. On 1st October, 2005, the Japan Atomic Energy Agency (JAEA) was founded as the result of the integration of the Japan Atomic Energy Research Institute (JAERI) and JNC.

The role of Monju in the new "Framework for Nuclear Energy Policy":

- Monju is the centre of research and development for the commercialized fast breeder reactor cycle systems technology;
- In the initial stage of operation, Monju is expected to demonstrate its reliability as a FR power plant and to establish sodium handling technologies, through experiences in design, fabrication, construction, operation and maintenance of the plant. In the next stage, Monju should be used to verify the elemental technologies towards commercialized FR cycle systems, including the demonstration of burning minor actinides in FR to reduce the environmental burden caused by high-level radioactive wastes.

2.18.2. Research and development for Monju design

The R&D for Monju covered system design, core and fuel, heat transfer and fluid dynamics, structures and materials, instrumentation and safety. Research projects were started in the

early years, in concert with design studies, so that the results could be applied to Monju. The R&D aimed to:

- Introduce a "design by analysis" method instead of "design by test", and use partial- and reduced-scale models instead of full-scale models for verification tests as far as possible, based on Joyo experience;
- Develop steam generator technology and other systems not used in Joyo (such as a decay heat removal system) via a research programme going from basic research to performance with larger scale models;
- Prepare design codes and standards applicable to FBRs in general;
- Actively promote international co-operation in research and development (for instance, in the areas of fuel irradiation and core safety), and promote technical information exchange on systems and components with the USA and European countries;
- Summarize data and information on design and construction, and establish a method for carrying out effective R&D leading to commercial FBR.

2.18.3. Design and construction of Monju

2.18.3.1. Design features

Compared with the experimental reactor Joyo, the prototype reactor Monju has about seven times the thermal capacity (Joyo MK-II: 100 MW_t; Monju: 714 MW_t) and a provision for electricity generation. The principal design and performance data of Monju are shown in Table 2.28 [24].

TABLE 2.28. PRINCIPAL DESIGN AND PERFORMANCE DATA OF MONJU

Characteristic	Value
Reactor type	Sodium-cooled loop-type
Thermal power, MW	714
Electrical power, MW	~ 280
Fuel material	PuO_2-UO_2
Plutonium enrichment, inner/outer enrichment zone (% fissile plutonium)	
Initial core	15/20
Equilibrium core	16/21
Average burnup, MWd/t	80 000
Cladding material	Type 316 stainless steel
Power density, kW/L	283
Breeding ratio	1.2
Reactor inlet/outlet sodium temperature, °C	397/529
Secondary sodium temperature (IHX outlet/inlet), °C	505/325
Number of loops	3
Type of steam generator	Helical coil, once-through, separated in superheater and evaporator
Steam pressure (turbine inlet), MPa	12.7
Steam temperature (turbine inlet), °C	483
Refuelling system	Single rotating plug with fixed-arm fuel-handling machine
Refuelling interval (months)	6

Monju was designed in accordance with the same laws, regulations and standards which are applied to LWR in Japan, but with the addition of new standards peculiar to sodium-cooled FBR, for example those relating to high-temperature structural design.

2.18.3.2. Core and fuel

The hexagonal core consists of fuel assemblies, control rods and blanket assemblies, and a neutron shield which surrounds the blanket. There are two kinds of fuel assemblies with different plutonium enrichments, the higher enriched fuel assemblies are loaded in the outside region to level the radial power distribution. The initial burnup will be 80 000 MWd/t (average of unloaded fuel assemblies).

Refuelling is planned every six months approximately, and about one-fifth of the core and blanket fuel assemblies will be exchanged at each operating cycle.

2.18.3.3. Heat transport system

The stainless steel reactor vessel contains the core and core internals. The shield plug has a single rotating plug in which the upper core structure is installed (Fig. 2.87).

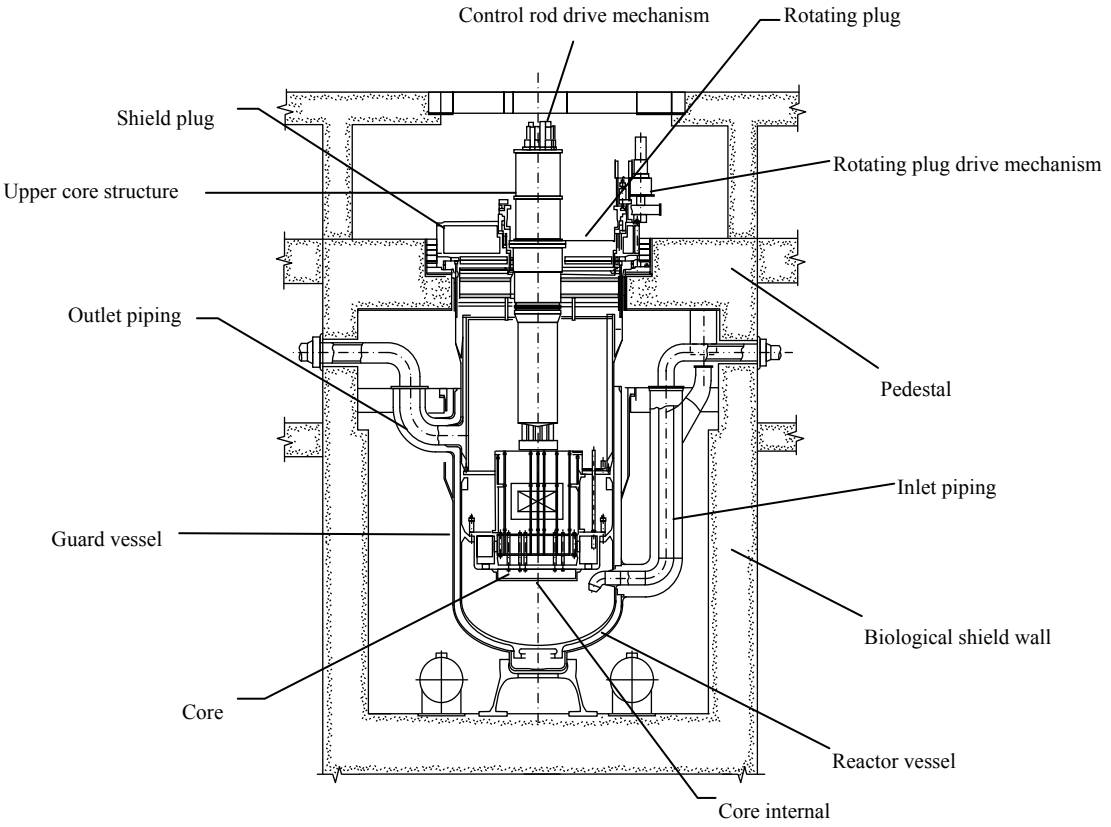

FIG. 2.87. Monju reactor system.

The upper core structure contains control rod drive mechanisms which position control rods consisting of three fine regulating rods, ten coarse regulating rods and six back-up safety rods.The heat generated in the reactor is removed by a loop-type sodium cooling system composed of three independent loops. It is transferred to a steam/water system through the primary and secondary sodium systems. The sodium inventory (total quantity of the primary, secondary and ex-vessel storage tank systems) is about 1 700 tonnes.Most of the piping which connects the primary system components is installed at high level, and guard vessels are provided for the reactor vessel, the primary main circulation pumps, the intermediate heat exchangers and the connecting piping. With this design, sufficient coolant for core cooling is guaranteed even if coolant leakage occurs. Moreover, compartments of systems with

radioactive sodium are kept in a nitrogen atmosphere and their floors and walls are lined with steel plates so that leaked sodium cannot ignite.

In addition to the main cooling system, there is an auxiliary cooling system to remove decay heat from the core when the reactor is shut down for refueling, or in an emergency. The auxiliary cooling system which is separated from the secondary sodium system has an air cooler in parallel with the steam generator. During shutdown, the primary and secondary sodium are circulated by the primary and secondary main circulation pumps driven by pony motors.

2.18.3.4. Spent fuel handling

Spent fuel is taken from the core and transferred to a tank in the lower part of an in-vessel transfer machine. This is done by a fuel handling machine of the pantograph fixed-arm type. After the fuel has been removed from the reactor vessel with an ex-vessel transfer machine, it is transferred through a containment equipment hatch. Later, it is stored in a fuel cooling pond after sodium cleaning.

2.18.3.5. Instrumentation and control

The normal start-up and shutdown of the reactor is achieved with regulating rods. A reactor shutdown system for emergency scram has been designed using the so-called "independent two" systems in which regulating rods and back-up safety rods are inserted. Monju's I&C is similar to that of a LWR, but with specific considerations for sodium cooled fast breeder reactor:

- The temperature difference between the reactor inlet and outlet is large;
- The main cooling systems have a large heat capacity and transport delay time;
- As a superheated steam turbine is used, the main steam temperature and pressure in the steam/water system have to be kept constant. For this reason, the main cooling system flow rate is controlled approximately proportional to the overall plant output power demand; at the same time, reactor power is controlled to follow the turbine/generator output power.

Reactivity changes during plant startup or shutdown, and changes related to fuel burnup, are controlled mainly with coarse regulating rods. Reactivity changes during power operation are mostly regulated with the fine regulating rods. The power is controlled manually below 40% of rated power, and automatically with set points from 40% to 100% of rated power. A delayed neutron method, a cover gas method and a tagging gas method are used to detect and locate fuel failure.

2.18.3.6. Structure, materials and a seismic design

PNC 316 steel (developed by PNC) is used as fuel cladding. SUS 304 steel is the main structural material, but 2.25 Cr-1 Mo steel and SUS 321 steel have been adopted for the heat transfer tube of evaporator and super-heater sections of the steam generator, respectively. The structural design was done in accordance with the High Temperature Structural Design Guide for Monju, based on PNC R&D results.

The seismic design was based primarily on the design considerations for LWR i.e. the foundation should be directly placed on a rock bed and the buildings should all be based on a rigid structure. Seismic considerations have led to any thin, long piping being supported by mechanical snubbers (primary system) or oil snubbers (secondary system). The containment vessel is reinforced and can sustain negative pressure inside.

2.18.3.7. Main components fabrication

The cylindrical reactor vessel is made of austenitic stainless steel about 7 m in diameter, 18 m high and 50 mm thick. To improve the structural reliability by reducing the number of welded parts, the vessel is composed of 12 pieces of ring forged metal and has only circumferential welds.

2.18.3.8. Fuel fabrication

In parallel with the construction of Monju, construction of the Plutonium Fuel Production Facility (PFPF, PNC's Tokai Works, 5 t MOX/y) started in July 1982. It was designed to develop fuel fabrication technologies as well as to fabricate fuels for Monju and Joyo. The construction was completed in October 1987. After test operation, production of Joyo fuel started in October 1988 as the first production campaign at PFPF. Production of the initial core fuel of Monju started in October 1989 and was completed in January 1994.

2.18.3.9. Construction

After Shiraki was chosen as the construction site in 1970, design, R&D and licensing for the construction of Monju went ahead. Preparation work started in 1983 and construction work proper began in October 1985. The installation of equipment was completed in April 1991 (Fig. 2.88).

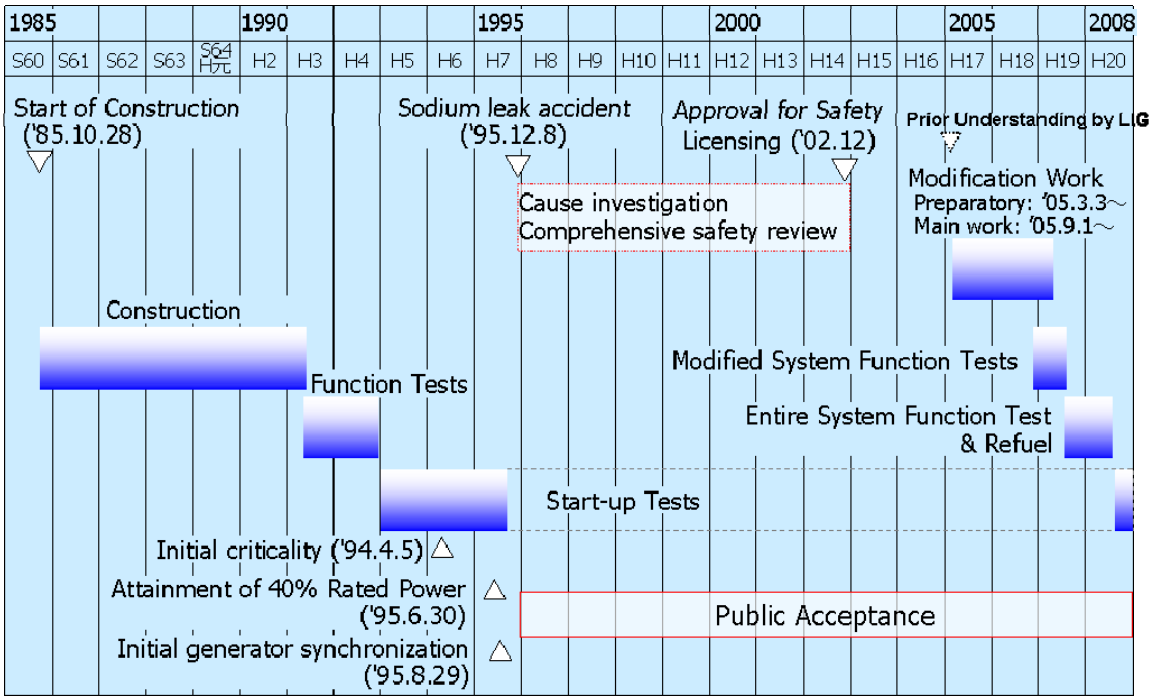

FIG. 2.88. Monju construction & tests schedule.

2.18.3.10. On-site work on buildings

The reactor cavity wall around the reactor vessel is made of serpentine concrete covered with steel plates. This steel cover is a structural member, being the support for the reactor vessel. It had to be installed with extreme precision, particularly with regard to remote refueling requirements. For this reason, each segment was fabricated in the factory and their dimensions are confirmed by temporary assembling before final assemble on site, maintaining tolerances of 1 mm or less.

2.18.3.11. Reactor construction

The reactor vessel and internals were constructed in this order: the guard vessel for the reactor vessel, the reactor vessel, the core internals, the shield plug, the upper core structure and then the control rod drive mechanism. In transportation, the guard vessel and the reactor vessel weighed about 500 t, therefore both were shipped to the site and transported from the wharf to the reactor vessel compartment by rollers taking more than five days. Installation work was conducted paying special attention to assure both installation accuracy and cleanliness of the components.

2.18.3.12. Organization

Many large Japanese companies, including those in the civil, electrical and component manufacturing areas, were involved in the construction of Monju, so it was truly a national project. There were about 20 main contractors and around 300 associated companies. The daily number of workers peaked at about 2700 in the busiest period of construction. Responsibilities for the construction of the main components and electrical facilities were shared as follows (these also apply for design and fabrication):

- Reactor structure - Mitsubishi Heavy Industries;
- Primary sodium system - Hitachi;
- Secondary sodium system - Toshiba;
- Fuel handling and storage facilities - Fuji;
- Civil works and buildings - five consortia composed of construction companies.

The FBR Engineering Company, established by the four companies named above, acted as a technical coordinator. On behalf of PNC, the Japan Atomic Power Company (JAPC) took responsibility for direct management of construction under the supervision of PNC. This allowed the project to benefit from the extensive experience of the Japanese electric power companies, which are shareholders of JAPC.

2.18.4. Pre-operational testing

Five main objectives of the pre-operational test are to:

(1) Confirm the functions and verify the safety and reliability required by the design of the systems and components in the plant;
(2) Verify the designs and evaluate the design margins based on pre-operational test data;
(3) Provide data from actual systems and components for the general FBR development effort;
(4) Ensure operators master operational techniques;
(5) Advance FBR technologies substantially.

Functional and performance testing of Monju components and systems were implemented in the following order: factory test, installation test, component function test, system function test and then system start-up test. System function test and system start-up test (classified as pre-operational test) started in May 1991 and December 1992, respectively. Because Monju is the first FBR to generate electricity in Japan, tests and inspections are conducted by the appropriate governmental organizations on the basis of the laws for nuclear power stations.

2.18.4.1. System function tests

System function tests were conducted to confirm the function and performance of the plant systems, following various tests and inspections during fabrication and construction. They were completed prior to fuel loading. The tests were composed of three phases:

- Testing the fuel handling system and control rod drive mechanism in air at room temperature prior to sodium charging;
- Tests in argon gas before charging sodium into the systems. Argon was used for preheating and heat-up;
- Testing the cooling systems, control systems, fuel handling systems, etc. after sodium charging.

There were about 300 system function tests, of which 240 are specific to the FBR.

2.18.4.2. System start-up test before sodium leak accident

System start-up test, aiming at confirmation and evaluation of the performance of the core, each system, and the entire plant, was started with fuel loading. It would be conducted along phases of criticality test, reactor physics test, nuclear heating test and power operation test. Safety and stable operating status of the plant and its design adequacy would be confirmed at full power.

Initial criticality was achieved with 168 fuel assemblies in April 1994. After the criticality test, reactor physics test were performed and the core reactivity worth, core reaction rate distribution, core flow rate distribution, etc., were measured.

The nuclear heating test was started on February 1995 and the reactor power was increased gradually. Monju was connected to the grid in August and the power-raising test was conducted. In the power-raising test, plant characteristics under power operation and transient conditions were confirmed up to 40% power.

2.18.4.3. Sodium leak accident in the secondary heat transport system

During the plant start-up for the plant trip test at 40% rated power, a sodium leak occurred in the Secondary Heat Transport System (SHTS), loop C, on 8 December 1995. The leak was occurred at the tip of the well tube of the temperature sensor installed near the outlet of intermediate heat exchanger in loop C. There were no adverse effects for personnel or the environment. The cause of the failure of the well tube was high-cycle fatigue due to flow-induced vibration. Monju has remained shutdown until today since this accident. During this period, periodical maintenance and improvements to enhance plant reliability has been conducted continuously.

Following the investigation into the cause of the accident, PNC (at the time) conducted a comprehensive safety review since December 1996 to review equipment, update descriptions given in manuals, reflect updated R&D knowledge and aspects of quality assurance activities. The result of this review and its innovation plan has been published in May 1997. Also, the safety authority (STA at the time) has conducted a comprehensive safety review itself and reported the result in March 1998. JAEA carried out its innovation plan methodically, and reported its response plan to the safety authority (METI) on 29 June 2001, responding to the requirements based on their comprehensive safety review. And JAEA was reporting the achievement of this response plan step by step, and finished the report at October 2007.

In June 2001, following the agreement of the local government of Fukui prefecture and Tsuruga city, JNC applied for the safety authority for the amendment of reactor installation permit regarding to the countermeasures against sodium leak etc., obtained permission in December 2002, and the clearance on the design and construction method and the construction plan were authorized in January 2004 by safety authority. Following the local government's agreement in February 2005, the preparatory work for the modification started in March and the main work started in September 2005. The main modification work has completed in May 2007, also the modified system function test has been conducted from December 2006 up to August 2007. The elements of modification work are summarized in Fig. 2.89 and the plant schedule is illustrated in Fig. 2.90.

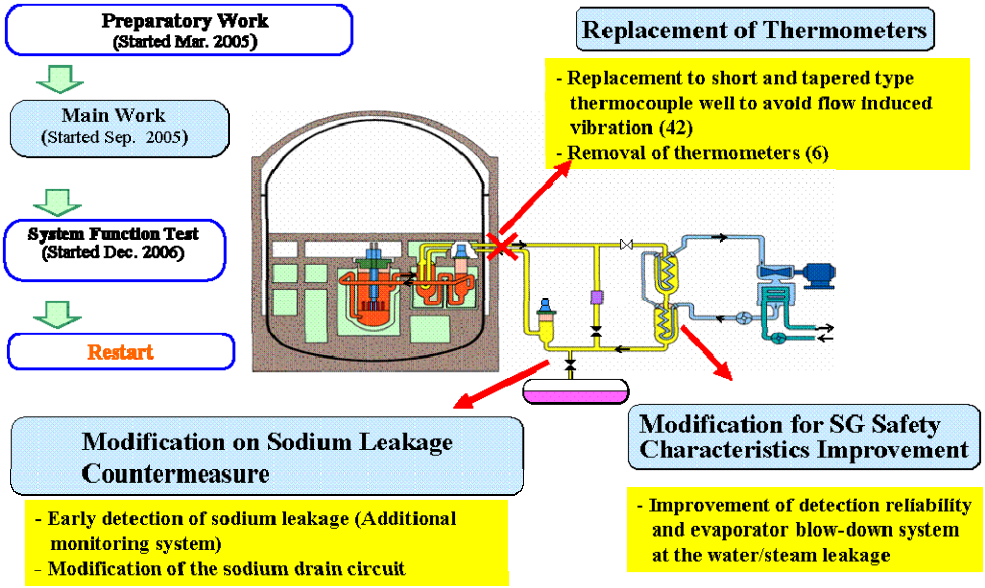

FIG. 2.89. Outline of Monju modification work.

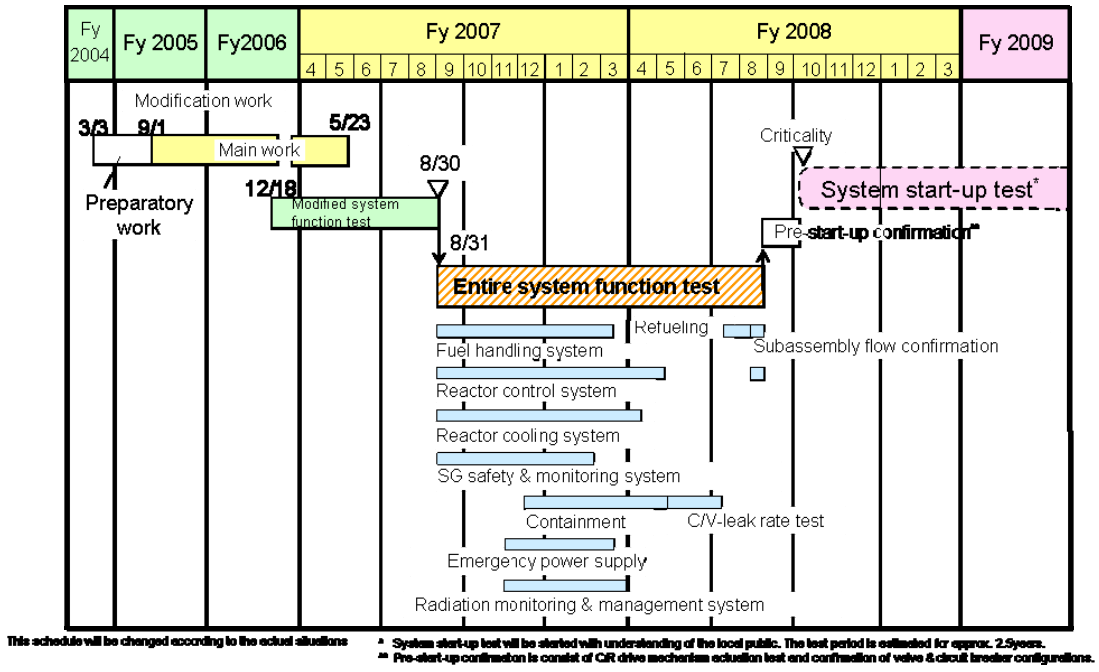

FIG. 2.90. Monju modification schedule.

Sequentially the entire system function test has started in August 2007, to confirm function and performance of systems not modified and entire plant. The test is scheduled up to May 2008, and restart, to resume the system start up test, is scheduled in October 2008 after refueling and pre-startup confirmation.

2.18.4.4. System start-up test after restart

The system start-up test (SST) has been suspended by sodium leak accident in 1995. Approximately 30% of the test items including most of the reactor physics test and plant performance test up to 40% rated power, were implemented before the accident.

After the entire system function test, SST which includes remaining test items and new test item, would be restarted. The SST programme will be divided into three stages shown in Fig. 2.91. The first and second stages will be conducted reflecting the past SST experiences and result of modification work.

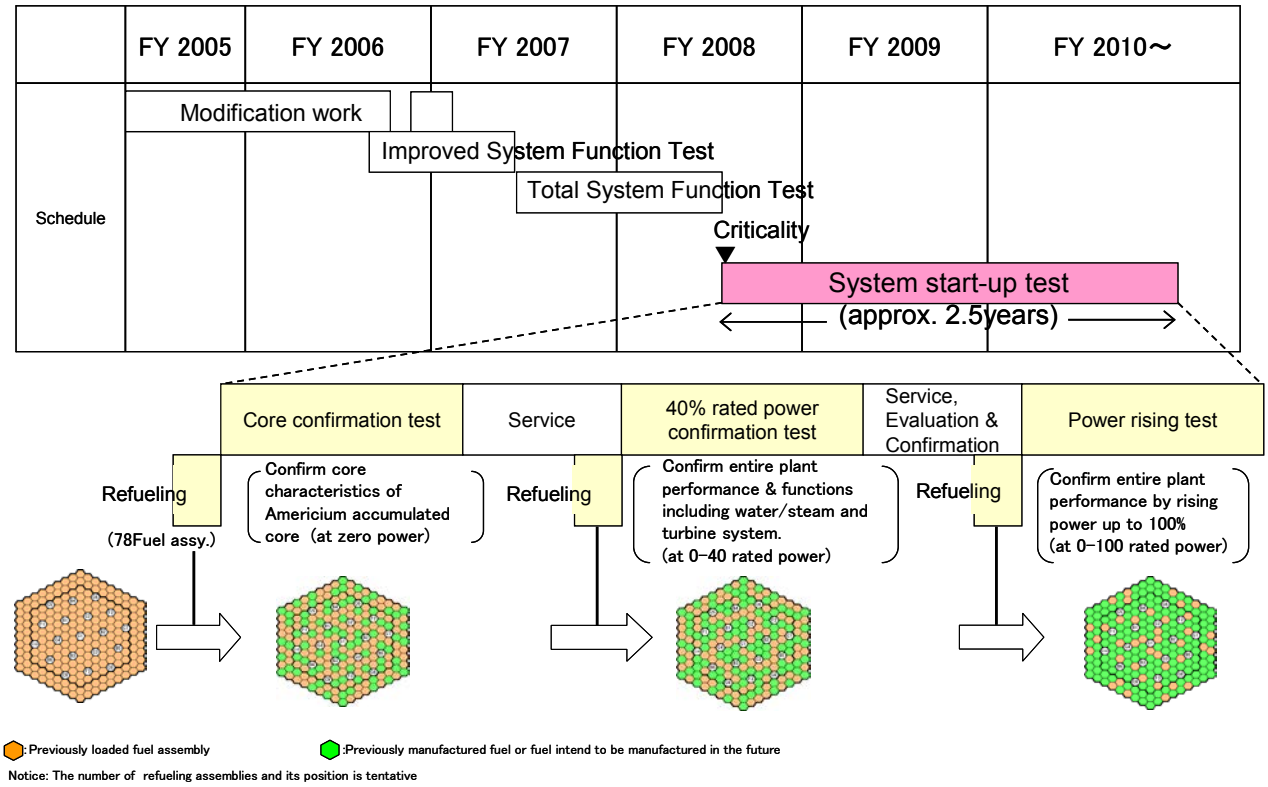

FIG. 2.91. Schedule of System Start-up Test (SST).

The reactor physics test will be conducted as the first stage in the condition of zero power critical core. The aim of this test is to confirm core characteristics after long-term shutdown. The core that includes relatively large amount of Am (ca. 2%) accumulated during the long-term reactor shutdown will be tested at zero power by measuring physical characteristics such as control rod reactivity worth, temperature coefficients. Before this first stage, about 80 fuel assemblies will be refuelled.

At the second stage, 40% rated power confirmation test will be conducted. The aim of the test is to confirm entire plant performance including water, steam and turbine-generator system up to 40% rated power. Before this stage, additional refuelling is planned.

At the final stage, power rising test will be conducted up to full power. The aim of this stage is to confirm entire plant performance. This stage includes plant control system performance test, automatic power raising test, plant thermo-dynamics transient test and plant scram test. Before this stage, additional refuelling is planned. Monju will provide a series of reactor physics data of the MOX-fuelled core having americium (Am) contents in the step-by step fuel exchange.

2.18.4.5. Monju operation plan after restart

Currently the R&D operation plan after restart is planned through two stages. In the first stage, Monju is expected to demonstrate its reliability as a FR power plant and establish sodium handling technologies. The operational data from Monju will be used to assess and validate the design of the core, plant systems and components. And operating and maintenance experience of Monju should be reflected the basic design of the demonstrated and commercialized FR plant.

In the second stage, Monju should be utilized to verify the elemental technologies towards commercialized FR cycle systems, including the demonstration of burning minor actinides in FR to reduce the environmental burden caused by high-level radioactive wastes.

At the same time, Monju is expected as a valuable R&D field for international cooperation. Figure 2.92 shows the Monju long-term R&D program. It includes demonstration test of long-life and high burnup advanced fuel, MA bearing fuel, etc.

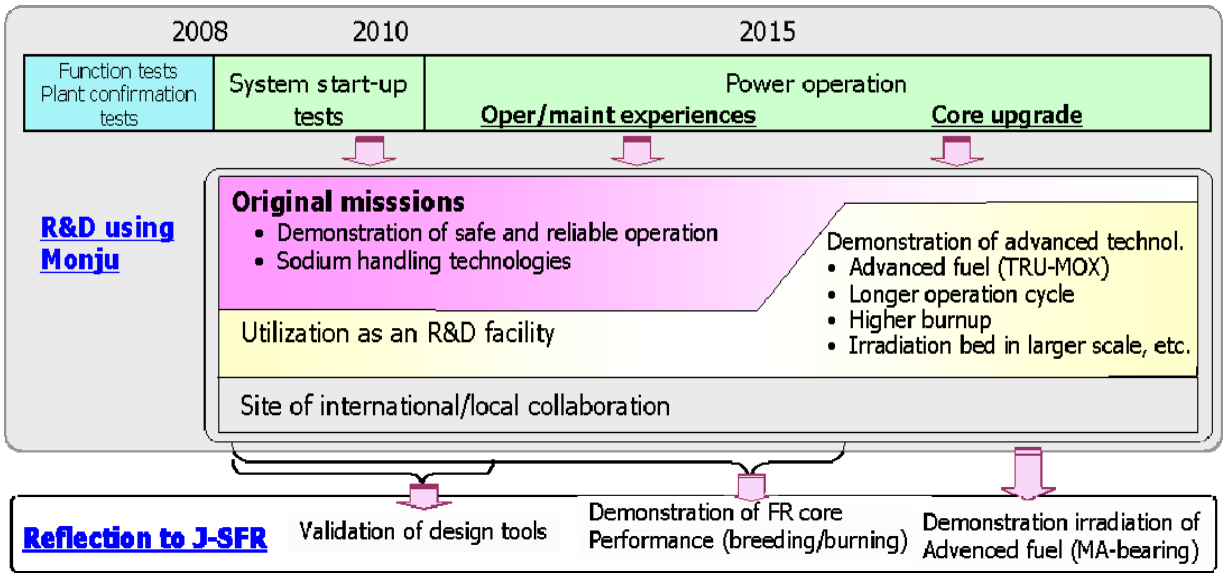

FIG. 2.92. R&D Programs using Monju.

REFERENCES TO CHAPTER 2

[1] "Notes on a Meeting of April 26, 1944" to be found in Collection of "Albert Wattenberg Papers, 1941-1996", Box 1 ECK-200, University of Illinois at Urbana Champaign, University Archives, Urbana, IL 61801. Publisher: American Institute of Physics (Center for History of Physics), College Park, MD, USA (2000).

[2] CROUTHAMEL, C.E., TURK, E., Determination of Nuclear Constants by Chemical Methods, Proc. Int. Conf. Peaceful Uses of Atomic Energy, Geneva, 1954, Vol. 7, published by United Nations New York (1955), paper P/721.

[3] KITTEL, J.H., NOVICK, M., BUCHANAN, R.F., DOE, W.B., Disassembly and Metallurgical Evaluation of the Melted-down EBR-I Core, Proc. Int. Conf. Peaceful Uses of Atomic Energy, Geneva, Switzerland, 1958, Vol. 7, published by United Nations New York (1959), paper P/2437.

[4] BRITTAN, R.O., Analysis of the EBR-I Core Meltdown, ibid, Vol. 7, No. 267, published by United Nations New York (1959), paper P/2156.

[5] LICHTENBERG, H., THALGOTT, F.W., KATO, W.Y., NOVICK, M., Operating Experience and Experimental Results obtained from a NaK-Cooled Fast Reactor, Proc. Int. Conf. Peaceful Uses of Atomic Energy, Geneva, Switzerland, 1954, Vol. 3, 243, published by United Nations New York (1955), paper P/813.

[6] NIKULIN, M.P., MAMAJEV, L.I., ASHURKO, YU.M., BAGDASAROV, YU.E., Experience Gained During BR-10 Reactor Operation, paper presented in the IAEA Technical Meeting on the Coordinated Research Project on Analyses of and Lessons Learned from the Operational Experience with Fast Reactor Equipment and Systems, Obninsk, Russian Federation, 14–16 February 2005.

[7] POPLAVSKY, V.M., ASHURKO, YU. M. et al, Review of fast reactor operational experience gained in Russia, in Operational and Decommissioning Experience with Fast Reactors, IAEA-TECDOC-1405, IAEA, Vienna, Austria (2004).

[8] POPLAVSKY, V.M., et al., Fast Reactors in Russia in 2005 and Further Trends of Their Development, paper presented in the IAEA Meeting of the Technical Working Group on Fast Reactors, Beijing, China, 15-19 May 2006.

[9] POPLAVSKY, V.M., et al., Review of Activities on Fast Reactors in Russia, paper presented in the IAEA Meeting of the Technical Working Group on Fast Reactors, Tsuruga-Kyoto, Japan, 14-18 May 2007.

[10] ALEXANDERSON, E. and WAGNER, H. (Editors), FERM-I, New Age for Nuclear Power, Item ID: 690004 / ISBN: 0-89448-017-0 (1979).

[11] AMOROSI, A.A., Concept and Design, ibid, pp. 131-162, ANS (1979).

[12] PAGE, E.M., The Fuel Melting Incident, ibid, pp. 225-254, ANS (1979).

[13] MCCARTHY, W.J., JENS, W.H., Enrico Fermi Fast Breeder Reactor: The reactor's fuel damage incident and its significance to future design, Nuclear News, ANS (November 1967).

[14] STEVENSON, C.E., The EBR-II Fuel Cycle Story, ANS, ISBN: 0-89448-031-6, (1987).

[15] SACKETT, J.I., Operating and Test Experience with EBR-II, the IFR Prototype, Progress in Nuclear Energy, Elsevier Science Ltd., Great Britain, Vol. 31, pp. 111-129 (1997).

[16] PLANCHON, H.P., The Experimental Breeder Reactor-II Inherent Shutdown and Heat Removal Tests-Results and Analysis, Nuclear Engineering Design, Vol. 91, p. 287 (1986).

[17] BOLTAX, A., NEIMARK, L.A., TSAI, H., KATSURAGAWA, M., SHIKAKURA, S., Reliability of Fast Reactor Mixed-Oxide Fuel during Operational Transients, Proc.

Conf. Fast Reactors and Related Fuel Cycles, Tokyo, 28 October-1 November 1991, Japan Atomic Energy Society (1991) Paper 6-6.
[18] STRAIN, R.V., BOTTCHER, J.H., GROSS, K.C., LAMBERT, J.D.B., UKAI, S., NOMURA, S., SHIKAKURA, S., KATSURAGAWA, M., Status of RBCB Testing of LMR Oxide Fuel in EBR-II, Paper 6-7, ibid.
[19] CHANG, Y.I., The Integral Fast Reactor, Nuc. Tech., Vol. 88, No. 129 (November 1989).
[20] OLP, R.H., et al., The Experimental Breeder Reactor (EBR-II) Breached Fuel Test Facility, paper presented in International Conference on Reliable Fuels for Liquid Metal Reactors, ANS (1982).
[21] KING, R.W., PORTER, D.L., Performance of Key Features of EBR-II and the Implications for Next Generation Systems, Proc. 10th Int. Conf. Nuclear Engineering, American Society of Mechanical Engineers, Arlington, VA, USA (2002).
[22] KING, R.W., FILEWICZ, E.C., Retrieval of Damaged Subassembly From Experimental Breeder Reactor-II Primary Tank, Nuclear Technology Journal, American Nuclear Society, Vol. 52, No. 1, pp. 32-42 (1981).
[23] LONGUA, K.J., PORTER, D.L., BUZZELL, J.A., Post-Service Examination of the EBR-II Superheater Duplex Tubes, paper presented in Annual Meeting of the American Nuclear Society, Los Angeles, USA (1982).
[24] INTERNATIONAL ATOMIC ENERGY AGENCY, Status of Liquid Metal Cooled Fast Reactor Technology, IAEA-TECDOC-1083, Vienna, Austria (1999).
[25] KOROLKOV, A.S., et al., Operating Experience with BOR-60: Basic Results and Prospects, paper presented in IAEA Technical Meeting on the Coordinated Research Project on Analyses of and Lessons Learned from the Operational Experience with Fast Reactor Equipment and Systems, Obninsk, Russian Federation, 14-16 February 2005.
[26] KOROLKOV, A.S., GADZHIEV, G.I., EFIMOV, V.N., MARASHEV, V.N., Operating Experience of the Reactor BOR-60, Atomnaya Energia, Vol. 91, issue 5, pp. 363-369 (November 2001).
[27] MAYORSHIN, A.A., TSYKANOV, V.A., GOLOVANOV, V.N., et al., Development and Tests of Fuel Elements of Fast Reactors with Vibroprocessed Oxide Fuel. Atomnaya Energia, Vol. 91, issue 5, pp. 378-385 (November 2001).
[28] GADZHIEV, G.I., EFIMOV, V.N., ZHEMKOV, I.YU., et al., Some Experimental Works Executed within 30 Years of Operation of the Reactor BOR-60, Atomnaya Energia, Vol. 91, issue 5, pp. 369-378 (November 2001).
[29] MARTH, W., The History of the Construction and Operation of the German KNK II Fast Breeder Power Plant, KFK 5456 (November 1994).
[30] BROCKMANN, K., PFEIFER, W., HILLEBRAND, I., Decommissioning of the Prototype Fast Breeder Reactor KNK in Germany, paper presented in Int. Conf. Safe Decommissioning for Nuclear Activities, Santiago, Chile, 10-14 November 2004.
[31] HILLEBRAND, I., BROCKMANN, K., MINGES, J., PFEIFER, W., BENKERT, J., WILLMANN, F., Rückbau KNK - Kalte Inbetriebsetzung und Durchführung der ersten Schnitte, Kontec (2005).
[32] BROCKMANN, K., HILLEBRAND, I., PFEIFER, W., Dismantling of the Reactor Vessel of the Compact Sodium Cooled Nuclear Reactor Facility (KNK), paper presented in ANS Topical on Decommissioning, Decontamination, & Reutilization, Denver, Colorado, USA, 7-11 August 2005.
[33] BROCKMANN, K., GRAFFUNDER, I., MINGES, J., PFEIFER, W., Progress and Difficulties in Dismantling KNK II Reactor, paper presented in IAEA Technical Meeting on The Decommissioning of Fast Reactors after Sodium Draining, CEA Cadarache, France, 26-30 September 2005.

[34] MINGES, J., BROCKMANN, K., THIESS, J., RUSS, J., WILLMANN, F., HALLER, H., Auslegung, Erfahrungen und Status des Rückbaus des Reaktortanks der KNK, Kontec (2007).
[35] SARAEV, O.M., OSHKANOV, N.N., et al., The experience of the BN-600 power unit operation. Atomnaya Energia, Vol. 80, issue 5, pp. 330-337 (May 1996).
[36] OSHKANOV, N., et al., The Main Results of Beloyarsk NPP Unit 3 Operation, paper presented in the IAEA Technical Meeting on the Coordinated Research Project on Analyses of and Lessons Learned from the Operational Experience with Fast Reactor Equipment and Systems, Obninsk, Russian Federation, 14-16 February 2005.
[37] ASHURKO, YU.M., Current Status of Activities in Fast Reactor and Accelerator Driven System Area, paper presented in IAEA Technical Meetings on Review of the Status of Accelerator Driven Systems and Fast Reactor R&D and Technology, Vienna, Austria, 4-8 December 2006.
[38] OSHKANOV, N.N., POTAPOV, O.A., GOVOROV, P.P., The evaluation of an operational performance of the power unit with the BN-600 fast reactor of Beloyarsk NPP for 25 years of operation. Nuclear Energetics, No. 1, pp. 3-9 (2005).
[39] INTERNATIONAL ATOMIC ENERGY AGENCY, Fast Reactor Operating Experience Gained in Russia: Analysis of Anomalies and Abnormal Operation Cases, IAEA-TECDOC-1180, Vienna, Austria, pp. 117-144 (2000).
[40] SHAW, M., The Role of the FFTF in the U.S. LMFBR program, Nuc. Eng. Int., Vol. 17, No. 195, pp. 613-15 (August 1972).
[41] NIELSEN, D.L., FFTF - A History of Safety and Operational Excellence, HNF-11406-FP (June 2002).
[42] SWAIM, D.J., WALDO, J.B., FARABEE, O.A., Ten Years Operating Experience at the Fast Flux Test Facility, Proc. Int. Conf. Fast Reactors and Related Fuel Cycles, Tokyo, Japan Atomic Energy Society (1991), Paper 2-3.
[43] Department of Energy Richland Operations Office, Fast Flux Test Facility. http://www.hanford.gov/page.cfm/FFT
[44] LESPERANCE, C.P., DOEBLER, S.V., BURKE, T.M., Closure of the Fast Flux Test Facility: Current Status and Future Plans, Proc. 11th Int. Conf. Environmental Remediation and Radioactive Waste Management (ICEM‘07), Brugge, Belgium, 2-6 September 2007, paper ICEM07-7279.
[45] LAMBERT, J.D.B., MIKAILI, R., GROSS, K.C., FRANK, S.M., CUTFORTH, D.C., ANGELO, P.L., Failed Fuel Identification Techniques for Liquid-Metal Cooled Reactors, Proc. Int. Conf. Fuel Management and Handling, British Nuclear Society, ISBN: 0 7277 2033 3 (March 1955).
[46] BURKE, T.M., YUNKER, W.H., CRAMER, E.R., Performance of the FFTF Heat Transport System During Cycles 1 and 2, Proc. 1st Nuclear Thermal Hydraulics Meeting, ANS (November 1983).
[47] YUNKER, W.H., Silicon Mass Transfer in Sodium Loops and the Resulting Thermal/Hydraulic Effects, 2nd Int. Conf., Liquid Metal Technology in Energy Production, CONF-800401, US-DOE (April 1980).
[48] SRINIVASAN, G., et al., The Fast Breeder Test Reactor - Design and Operating Experiences-, Nuclear Engineering & Design, 236 (2006).
[49] PANIGRAHI, B.S., et al., A decade’s experience in Chemistry Maintenance of Once-Through Steam Generators of FBTR, Progress in Nuclear Energy, Vol. 44, No. 4, pp. 315-320 (2004).
[50] GANGULY, C., et al., Development And Fabrication of 70% Pu- 30% UC Fuel for Fast Breeder Test Reactor in India, Nucl. Tech., Vol. 72 (January 1986).
[51] BHOJE, S.B., et al., Commissioning of Fast Breeder Test Reactor, Int. Conf. on Fast Breeders and Related Fuel Cycles, Kyoto, Japan (1991).

[52] KAPOOR, R.P., et al., Safety related Operating Experience with Fast Breeder Test Reactor, paper presented in Int. Topical Meeting on Sodium Cooled Fast Reactor Safety, Obninsk, Russian Federation, 3-7 October 1994.
[53] KAPOOR, R.P., et al., Operating Experience of Fast Breeder Test Reactor and its Utilization as an Experimental Facility, paper presented in 5th Asian Symposium on Research Reactors, Taejon, Korea, Republic of, 29-31 May 1996.
[54] RAMALINGAM, P.V., Operating Experience of FBTR, paper presented in 7th Int. Conf. on Nucl. Eng., Tokyo, Japan, 19-23 April 1999.
[55] KUMAR, S., et al., Fast Breeder Test Reactor- 15 Years Operating Experience, paper presented in IAEA Technical Meeting on Operational Experience and Decommissioning Experience with Fast Reactors, Cadarache, France, 11-15 March 2002.
[56] LEE, S.M., et al., Core Physics Parameters Measured in the Carbide Fuelled Fast Breeder Test Reactor, paper presented in Int. Conf. Physics of Reactors Operation, Design and Computation, Marseille, France, 23-27 April 1990.
[57] LEE, S.M., Status of fast reactor development in India: April 1998 – March 1999, paper presented in IAEA Technical Meeting on Status of National Programmes on Fast Reactors, Vienna, Austria, 18–19 May 1999.
[58] VAIDYANATHAN, G., et al., Dynamic Tests related to Under-Cooling events in FBTR, paper presented in Int. Topical Meeting on Sodium Cooled Fast Reactor safety, 3-7 October 1994, Obninsk, Russian Federation.
[59] SURESHKUMAR, K.V., et al., Physics and Engineering Experiments in Fast Breeder Test Reactor, paper presented in IAEA Technical Meeting on Operational Experience and Decommissioning Experience with Fast Reactors, 11-15 March 2002, Cadarache, France.
[60] INTERNATIONAL ATOMIC ENERGY AGENCY, RAJ, B., et al., Post Irradiation Examination of Mixed (Pu, U) C Fuels irradiated in Fast Breeder Reactor, IAEA-TECDOC-103, Vienna, Austria (1998).
[61] KAPOOR, R.P., et al., Unusual Occurrences in Fast Breeder Test Reactor, paper presented in IAEA Technical Committee Meeting on Unusual Occurrences during LMFBR Operation, 9-13 November 1998, Vienna, Austria.
[62] SRINIVASAN, G., et al., Thermo-Mechanical Behaviour of FBTR Reactor Vessel due to Natural Convection in Cover Gas Space, paper presented in 4th Int. Conf. on Liquid Metal Engineering and Technology, Avignon, France, 17-21 October 1988.
[63] LEE, S.M., Status fast reactor development in India: April 2000 – March 2001, paper presented in IAEA Technical Committee Meeting on Review of National Programmes on Fast Reactors and Accelerator Driven Systems (ADS), Almaty/Kurchatov City, Kazakhstan, 14–18 May 2001.
[64] LEE, S.M., Status fast reactor development in India: April 2001 – March 2002, paper presented in IAEA Technical Meeting to Review of National Programmes on Fast Reactors and Accelerator Driven Systems (ADS), Karlsruhe, Germany, 22–26 April 2002.
[65] CHETAL, S.C., Status of fast reactor development in India: April 2002 – March 2003, paper presented in IAEA Technical Meeting Review of National Programmes on Fast Reactors and Accelerator Driven Systems (ADS), Daejon, Korea, Republic of, 12-16 May 2003.
[66] MORGENSTERN, F.H., et al., The Decay Heat Removal Plan for SNR-300. A Licensed Concept, Proc. ANS/ENS International Meeting on Fast Reactor Safety and Related Physics (Conf. 761001), Chicago, USA, 5-8 October 1976.
[67] VOSSEBRECKER, H., et al., Evaluation of Special Safety Features of the SNR-300 in View of the Chernobyl Accident, INTERATOM-Report 35.02468.5, (March 1987).

[68] EITZ, A.W., VOGEL, J., RIETHMIILLER, R., Aktueller Stand des Projektes SNR 300 (Nukleare Inbetriebnahme nicht in Sicht), Energiewirtschaftliche Tagesfragen, 37. Jg. (1987) Heft 10.
[69] INTERNATIONAL ATOMIC ENERGY AGENCY, Status of Liquid Metal Cooled Fast Breeder Reactors, IAEA Technical Report Series No. 246, Vienna, Austria (1985).
[70] ASTEGIANO, J.C., et al., The status of fast reactors programme in France in 2006, paper presented in IAEA Meeting of the Technical Working Group on Fast Reactors, Tsuruga-Kyoto, Japan, 14-18 May 2007.
[71] INTERNATIONAL ATOMIC ENERGY AGENCY, Fast Reactor Database 2006 Update, IAEA-TECDOC-1531, Vienna, Austria (2007).

CHAPTER 3
SODIUM-COOLED FAST REACTOR DESIGNS

3.1. Introduction

Sodium-cooled fast reactors (SFRs) have the potential to play an important role in meeting growing energy needs worldwide in a safe, environmentally clean and affordable manner. A considerable amount of technological experience has already been acquired for the SFR system, thereby providing a sound basis for the further development and eventual deployment of new SFR designs. Furthermore Russia, China, and India are currently constructing the BN-800, CEFR and PFBR, respectively.

It is important to achieve a level of economic competitiveness that enables SFR deployment in accordance with market principles. Although SFR technology has been demonstrated in several countries, the electricity generation cost has been high compared to that of light water reactors. Thus a variety of innovative SFR design is being explored in each country.

The SFR system was identified in the Generation IV Technology Roadmap [1] as a promising technology to perform in particular the missions of sustainability, actinide management and electricity production if enhanced economics for the system could be realized. The main characteristics of the Gen-IV SFR that make it especially suitable for the missions identified in the Roadmap are:

- High potential to operate with a high conversion fast spectrum core with the resulting benefits of increasing the utilization of fuel resources;
- Capability of efficient and nearly complete consumption of trans-uranium as fuel, thus reducing the actinide loadings in the high level waste with benefits in disposal requirements and potentially non-proliferation;
- High level of safety obtained with the use of inherent and passive means that allow accommodation of transients and bounding events;
- Enhanced economics achieved with the use of high burnup fuels, reduction in power plant capital costs with the use of advanced materials and innovative design options, and lower operating costs achieved with improved operations and maintenance.

The SFR development approach is to rely on technologies already used for SFRs that have successfully been built and operated in France, Germany, India, Japan, the former Soviet Union, the United Kingdom and the United States. As a benefit of these previous investments in technology, the majority of the R&D needs that remain for the Gen-IV SFR in this plan are related to performance rather than viability of the system.

Japan, the Republic of Korea and the US are developing the reactor concept meeting Gen-IV objectives. Those are a large-size advanced loop-type reactor JSFR, an intermediate-size pool-type KALIMER-600, and a small-size modular type reactor (ABTR).

3.2. Sodium-cooled fast reactors under construction

3.2.1. BN-800

3.2.1.1. Introduction

Originally, it was planned to construct a small series of four power units with the BN-800 reactor located on two sites, namely: Beloyarsk NPP (BNPP) and South-Urals NPP (SUNPP). Now construction of one power unit with the BN-800 reactor is provided for the Beloyarsk NPP site (4th BNPP power unit) in accordance with the "Program of Development of Nuclear Power in the Russian Federation for 2000-2005 Period and up to 2010" authorized by the Russian Government.

In January 2010, the Federal Target Program (FTP) "Nuclear power technologies of a new generation for period of 2010-2015 and with outlook to 2020" has been approved by the Government of the Russian Federation. In accordance with this Program, a further development of sodium-cooled fast reactors is stipulated in Russia within the framework of creation of the new technological platform for nuclear power based on transition to closed nuclear fuel cycle (CNFC) with the 4th generation fast reactors. In this context, the BN-800 reactor would play the key role in the development of the main components and technologies of advanced CNFC of fast reactors and in this view the BN-800 reactor is considered now as a pilot reactor designed for demonstration of practical implementation of the concept of fast reactor in the CNFC.

3.2.1.2. Design description

BN-800 reactor design is a logical development of the BN-600 reactor design. An experience gained during BN-600 reactor operation allowed considerably improve technical decisions adapted to BN-800 reactor design and enhance its safety. It is necessary to mention the most important changes and modifications inserted into the BN-800 design comparing to the BN-600 design:

- One turbine for power unit;
- Steam reheating instead of sodium one;
- a special decay heat removal system dissipating heat outside through heat exchangers "sodium-air" (AHX) connected to the secondary circuit;
- Core catcher for collecting core debris in the case of its melting;
- A special sodium cavity over core to reduce sodium void reactivity effect;
- An additional passive shutdown system with hydraulically suspended rods.

The main technical parameters of the BN-800 power unit are presented in Table 3.1 [2].

TABLE 3.1. BN-800 MAIN DESIGN DATA

Parameter	Value
Overall plan:	
Reactor thermal power, MW	2100
Unit electrical power, MW	880
Unit net efficiency, %	40
Operating power variation range, % nominal	17-100
Equipment seismostability, MSK-64 units	7
Operation life, year	40
Breeding ratio	1.04
Primary system:	
Coolant temperature, °C	
Core inlet	354
Core outlet	547
Protective gas pressure, MPa	0.054
Gas plenum volume, m^3	110
Reactor vessel coolant mass, t	1000
Coolant flowrate, kg/s	8600
Pump delivery head, MPa	0.82
Number of circulating pumps	3
Reactor core:	
Equivalent core diameter, m	2.56
Active core height, m	0.88
Average core power density, MW/m^3	450
Number of core fuel assemblies	565
Fuel assembly duct width across flats, mm	96.0
Fuel assembly pitch, mm	100
Fuel	MOX sintered pellets
Initial core MOX-fuel inventory, kg	15880
Average Pu content in new fuel, %	20.5
Fertile material inventory (initial), kg	13810
Number of fuel rods per assembly	127
Fuel cladding outer diameter, mm	6.9
Fuel rod linear heat rating (max.), kW/m	48.5
Average fuel burnup, MW·d/kg	67
Maximum fuel burnup, % ha	9.9
Core lifetime, ed	465
Core refueling interval, ed	155
Reactor main vessel:	
Outer diameter, m	12.96
Overall height, m	14.0
Weight (empty), tons	216
Material	stainless steel Cr18Ni9
Secondary loop:	
Secondary coolant temperature, °C	
SG inlet	505
SG outlet	309
Secondary circuit sodium mass (three loops), t	980
Gas plenum volume (nominal power), m^3	20
Gas plenum pressure, MPa	0.245
Pump delivery head, MPa	0.42
Coolant flowrate, kg/s	2780
Number of SG sections	10
Number of DHR air cooler sections	2
Number of DHR electromagnetic pumps	2
Number of main circulating pumps	1
Tertiary circuit:	
Main steam pressure, MPa	13.7
Steam mass flowrate, kg/s	876
Feedwater temperature, °C	210
Main steam temperature, °C	490

A general scheme of the nuclear steam-supply system (NSSS) with the BN-800 reactor is shown in Fig. 3.1.

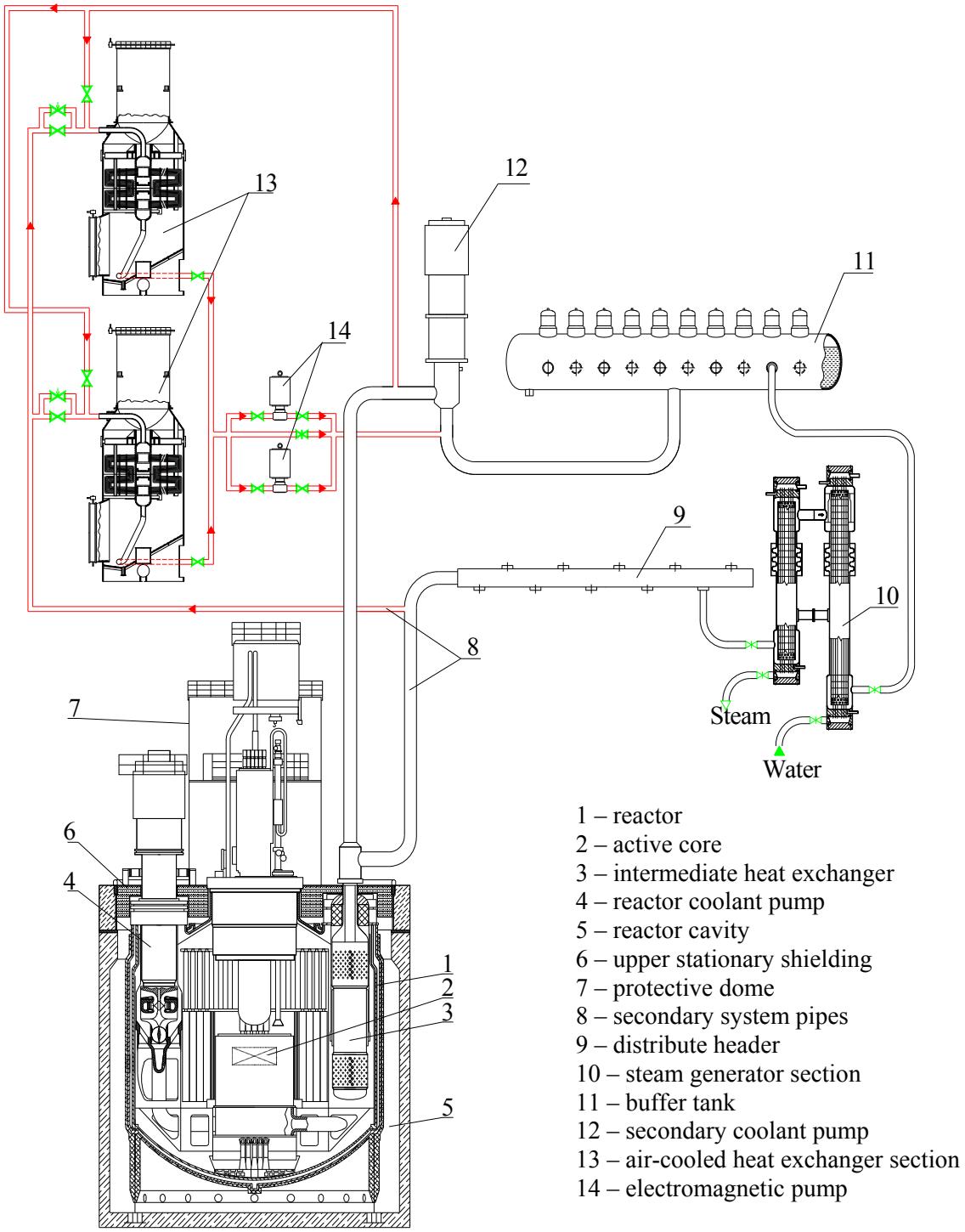

FIG. 3.1. General scheme of the NSSS with the BN-800 reactor.

The longitudinal section of the BN-800 reactor is presented in Fig. 3.2.

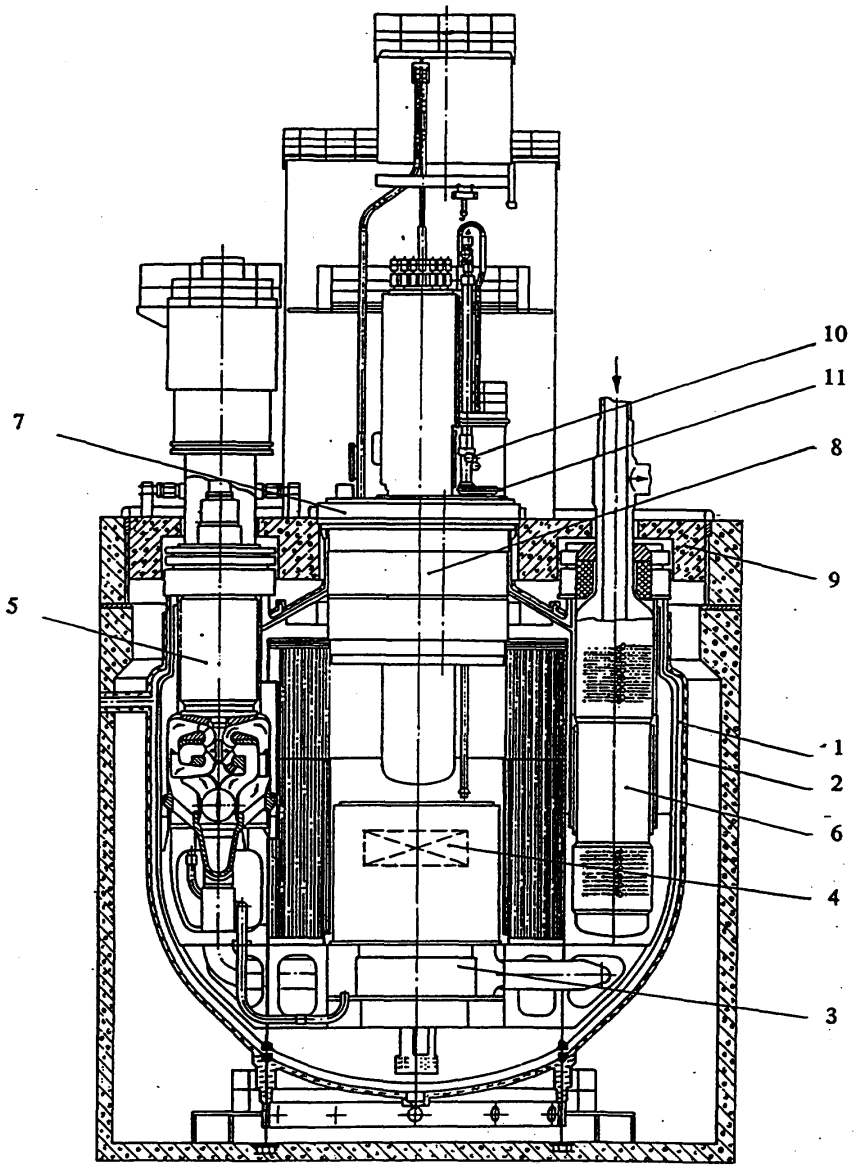

1-main reactor vessel, 2-guard vessel, 3-core diagrid, 4-reactor core, 5-reactor coolant pump, 6-intermediate heat exchanger, 7-large rotating plug, 8-above core structure, 9-upper stationary shield, 10-refuelling mechanism, 11-small rotating plug.

FIG. 3.2. Cross-section of the BN-800 primary circuit.

3.2.1.3. Current status

Construction completion and commissioning of the power unit No. 4 of the Beloyarsk NPP with the BN-800 reactor are planned for 2014.

Construction works are actively carried out on the power unit site. The facilities included into Start-up Back-up Complex (SBC) have been constructed and put into operation in 2004, including start-up and stand-by boiler-house, combined auxiliary building, on-site engineering and process communications etc. In 2007, construction of the foundation plates of the reactor compartment and the turbine hall of the main building has been completed and a reactor assembling building has been erected. In 2009, reactor silo has been built and assembling of reactor vessels began in it. Currently, the reactor compartment and the turbine hall of the main building are under construction and reactor vessels are assembled in the reactor silo.

Along with construction works on the site, manufacture of the power unit's components and their delivery to the site is carried out.

3.2.2. CEFR

3.2.2.1. Introduction

Following the basic nuclear energy development strategy with three steps: thermal reactor, fast reactor and fusion reactor, the development of nuclear power plants with PWRs has began and the engineering technology development of fast reactors has come to the date in the early 1990s in China. Based on two phases of fast reactor R&D, i.e. basic researches (1968–1987) and applied basic researches (1988-1993), targeting a ~ 60 MWt experimental fast reactor, in the framework of the National High-Tech Program, the China Experimental Fast Reactor (CEFR) project was launched in 1990 with the preparation of the pre-conceptual and conceptual designs.

The main purposes of the CEFR are to accumulate experience in fast reactor design, fabrication of components, construction, pre-operational testing and operation and maintenance. Additionally, the CEFR will serve as a fast neutron facility for irradiation testing of advanced fuels and materials, as a test bed which provides actual fast reactor conditions in order to develop advanced key components and as a completed real model or prototype to verify design and analysis computer codes and other design software.

The design philosophy adopted for the CEFR aims at similarity between it and the prospective commercialized fast reactors to be developed in the future. In particular, the main technical selections, temperature parameters and fuel parameters are selected such that they are similar to those of a commercial fast reactor. Additionally, the inherent safety properties of a sodium cooled fast reactor are utilized and passive safety measures are implemented in order to mitigate accidents to the greatest extent possible.

The CEFR is sodium cooled, 65 MWt experimental fast reactor with PuO_2-UO_2 fuel, but UO_2 as the first loading, and Cr-Ni austenitic stainless steel as fuel cladding and reactor block structure material. The pool-type reactor vessel is supported from the bottom and is equipped with two main pumps and two loops for primary and secondary circuits, respectively. The water-steam tertiary circuit is also two loops but the superheated steam is incorporated into one pipe which is connected to a turbine. The general timetable is as following:

Conceptual design	1990–1992.7
Technical co-design with Russia-FBR-Association	1994–1995
Preliminary design	1996–1997
Detailed design	1998–2003
Preliminary safety analysis report review	1998.5–2000.5
Architecture construction (first pot of concrete) started	2000.5
Reactor building construction completion	2002.8
Detailed design completed	2004.12
Reactor block installation started	2005.10
Pre-operational testing of systems started	2006.10
All installation work completed	2008.12
320 t nuclear grade sodium filled into primary, secondary and DHR systems	2009.6

3.2.2.2. Design description

3.2.2.2.1. CEFR core

The reactor core is composed of 81 fuel subassemblies, three compensation subassemblies and two regulation subassemblies; the latter two also serve as part of the first shutdown system (Fig. 3.3).

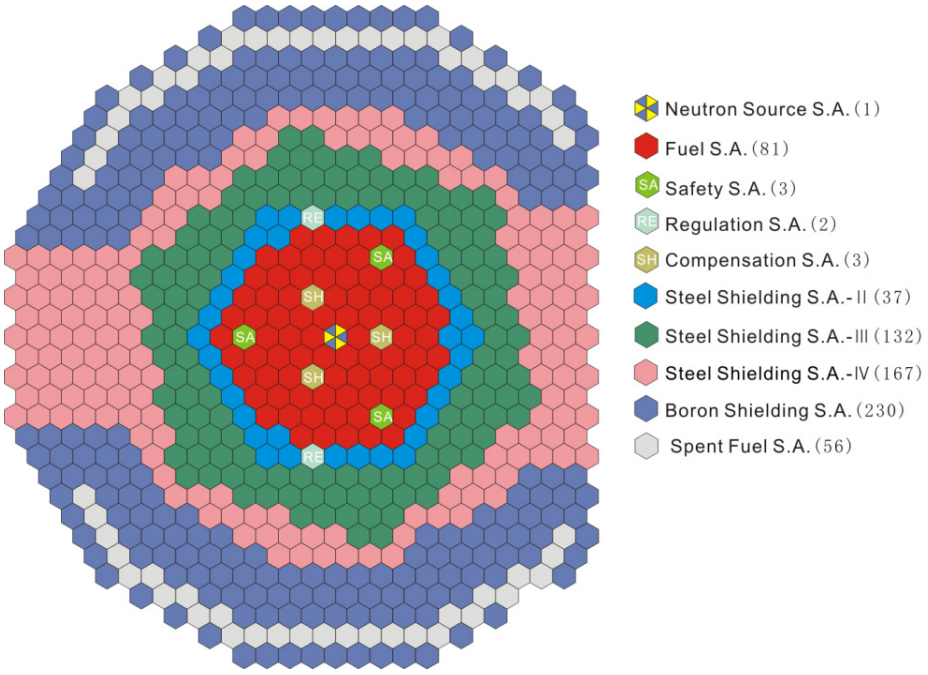

FIG. 3.3. CEFR Core.

Three safety subassemblies act as the secondary shutdown system. A total of 336 stainless steel reflector subassemblies and 230 shielding subassemblies, in addition to 56 positions for primary storage of spent fuel subassemblies, are included.

Each hexagonal fuel subassembly is composed of 61 fuel pins, each with a fuel pin cladding outer diameter of 6.0 mm and wrapped with a 0.95 mm thick wire. The fuel column has a height of 450 mm and the total length of the fuel subassembly is 2592 mm.

For the safety and compensation subassemblies 91% ^{10}B enriched B_4C is used, but natural boron B_4C (19.8% B-10) for the regulation subassemblies. Different mechanical designs have been adopted for the primary and secondary shutdown systems, with 2.5 s and 0.7 s as their drop down time, respectively.

The design limitation to the core which was fixed before the design is as following:

Thermal power, MW	65
Linear power (max.), W/cm	430
Operation cycle (min.), d	73
Inserting rate of reactivity (max.), β/s	0.07
Positive reactivity (each addition) (max.), β	0.4
Cladding temperature in normal operation (max.), °C	700

3.2.2.2.2. Reactor block

The CEFR block is composed of a main vessel and a guard vessel supported from bottom on the floor of reactor pit with the diameter 10 m and height 12 m (Fig. 3.4).

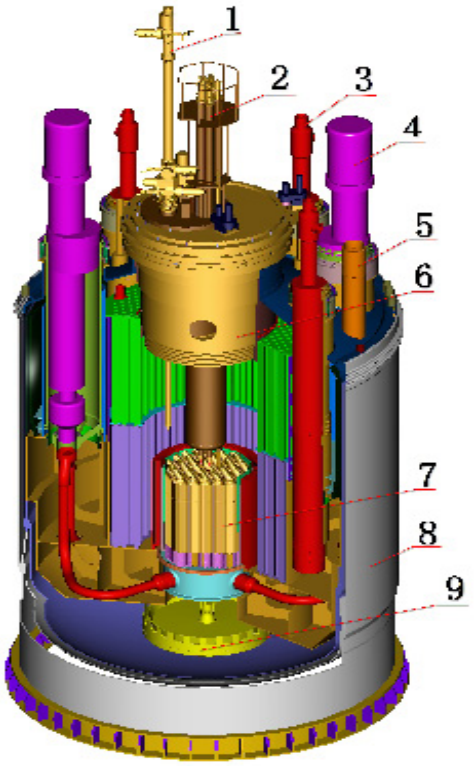

1. Fuel handling machine
2. Control subassemblies (8)
3. IHX (4)
4. Primary sodium pump (2)
5. Independent heat exchanger (2)
6. Double rotating plug
7. Core
8. Main vessel and guard vessel
9. Molten core catcher

FIG. 3.4. CEFR Reactor block.

The main vessel has an outside diameter of 8010 mm and diameter gap of 175 mm toward guard vessel. The narrow gap design permits the core to remain immersed in sodium in the event of an unexpected main vessel leak; however, at the consequence of increased difficulty to perform in-service inspection and repair of the main vessel. Using 2D Sn computer code the calculation shows that neutron fluence in the main vessel is about 1×10^{22} n/cm^2 during 30 years operation. The reactor core and its support structure are supported on lower internal structures. Two main pumps and four intermediate heat exchangers are supported on upper internal structures. These two structures are sat on the lower part of the main vessel. Two independent heat exchangers of the DHRS are hung from the shoulder of the main vessel. The double rotation plugs on which control rod driven mechanisms, fuel handling machine and some instrumentation structures are supported are located on the neck of the main vessel.

In the design, a molten core catcher is equipped even though there is no serious accident in which a significant part of core damage could happen based on the analysis of all the beyond design basis accidents for the CEFR [4].

3.2.2.2.3. Main heat transfer system

The primary circuit is composed of main pumps, four intermediate heat exchangers, reactor core support diagrid plenum, pipes and cold and hot sodium pools. In the cold pool, two primary

loops are separated from each other, but in hot pool they are connected. In normal operation the average sodium temperature in the cold pool is 360°C and in the hot pool it is 516°C.

As shown in Fig. 3.5 the secondary circuit has two loops, each one is equipped with one secondary pump, two intermediate exchangers (IHX), evaporator, super heater, expansion tank, and valves. The outlet sodium temperature of secondary circuit from IHX is 495°C. When it leaves the evaporator it will decrease to 310°C, and in outlet of super heater it is 463.3°C.

The tertiary water-steam circuit has one turbine generator, three low pressure heaters, one deoxygenate heater, one deionization system and feed water pumps. It provides 480°C/14 MPa superheated steam to the turbine.

Each evaporator is connected with one release-to-air valve and two safety release valves, but for superheater, one release-to-air valve and one safety release valve are equipped. And the by-pass system with de-temperature de-pressure valves equivalent to 67% full power are equipped for discharging the steam to the condenser when the turbine is not in operation.

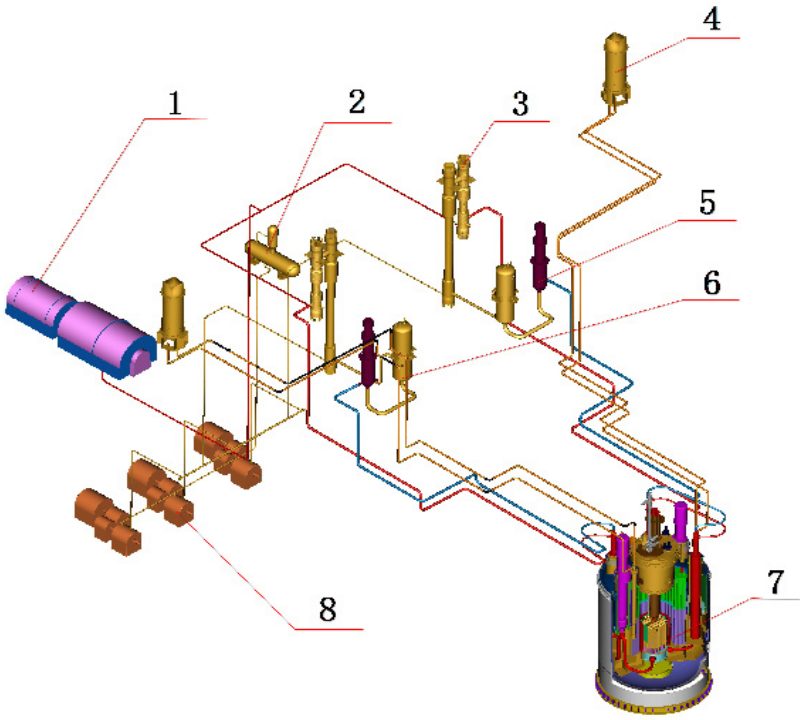

1. Turbine-generator
2. De-oxygen heater (1)
3. Steam generator (2)
4. Air cooler (2)
5. Secondary pump (2)
6. Buffer tank (2)
7. Reactor block
8. Feed water pump (2+1)

FIG. 3.5. CEFR Main heat transfer system.

3.1.2.2.4. Safety characteristics

The CEFR is located at the China Institute of Atomic Energy (CIAE), about 40 km away from Beijing City which has about 16 million inhabitants. According to the raising environment safety consideration, it is stipulated to have more strictly requests to radioactive materials release standards for normal operation, design basis accident (DBA) and beyond design basis accident (BDBA) than related national standards, as shown in Table 3.2.

TABLE 3.2. MAXIMUM LIMITS OF PUBLIC EFFECTIVE DOSE EQUIVALENT FROM THE CEFR [3]

States	GB6249-86	CEFR limits
Operational, mSv/a	0.25	0.05
DBA, mSv/accident	5	0.5
BDBA, mSv/accident	100	5

No any emergency intervention requirements for residents beyond 153 m from the reactor.

The safety characteristics of the CEFR derive from several technical features. The liquid sodium coolant and a pool configuration provide inherent protection and long times for corrective action for many abnormal events.

The use of liquid sodium coolant provides a low pressure system that is insensitive to postulated coolant boundary failures because coolant flashing cannot occur. All of the primary system sodium is contained within the reactor vessel, along with the core, the primary pumps, and the intermediate heat exchangers, except its purification system.

The CEFR is a small reactor, which has bigger heat inertia than many other pool reactors due to its relative primary sodium loading per MWt, is larger. The large heat capacity of the pool provides long time margins for corrective action in the event of loss-of -heat sink.

The CEFR core benefits from feedback effects providing the reactor with inherent safety characteristics. The core is designed with negative temperature coefficients, negative Doppler coefficients, and negative power coefficients.

These feedback properties are shown in Tables 3.3-3.6.

TABLE 3.3. TEMPERATURE REACTIVITY EFFECT $(PU,U)O_2/UO_2$ CORE, 250-360°C, %ΔK/K

	Cycle	
	Beginning	End
Sodium density	-0.169/-0.186	-0.170/-0.197
Axial expansion of reactor core	-0.037/-0.037	-0.038/-0.038
Axial expansion of lateral reflector	-0.019/-0.020	-0.020/-0.020
Radial expansion (diagrid plenum)	-0.204/-0.194	-0.205/-0.194
Doppler effect	-0.032/-0.020	-0.033/-0.020
Total	-0.461/-0.457	-0.466/-0.480

TABLE 3.4. POWER REACTIVITY EFFECT, HOT STANDBY-FULL POWER $(PU,U)O_2/UO_2$ CORE, %ΔK/K

	Cycle	
	Beginning	End
Sodium density	-0.107/-0.130	-0.112/-0.144
Sodium volume fraction exchange	-0.029/-0.026	-0.034/-0.029
Axial expansion of reactor core	-0.339/-0.312	-0.311/-0.257
Axial expansion of lateral reflector	-0.011/-0.010	-0.011/-0.010
Radial expansion (S.A. winding)	-0.020/-0.010	-0.020/-0.010
Doppler effect	-0.063/-0.027	-0.063/-0.030
Total	-0.569/-0.405	-0.556/-0.370

TABLE 3.5. DOPPLER CONSTANT OF CEFR CORE $(PU,U)O_2$ CORE, 10^{-3}ΔK/K

	kW (with Na)	Kd (without Na)
Fuel: 633-1593 K, Cladding: 633-1000 K	-0.878	-0.618
All materials 523-633 K	-1.574	-1.048
All materials 373-523 K	-1774	-1.142

TABLE 3.6. REACTIVITY EFFECT OF SODIUM LOST $(PU,U)O_2/UO_2$ CORE, %ΔK/K

Region lost sodium	Cycle	
	Beginning	End
Core (fuel section)	-2.366/-2.543	-2.404/-2.550
Core (fuel section + upper section of S.A)	-3.067/-2.856	-3.110/-2.948
Core (whole section of S.A)	-3.737/-3.644	-3.788/-3.774
Whole core (including central stainless steel rod and stainless steel reflector)	-5.190	-5.194

The reliable removal of accident decay heat after the shut-down of a nuclear reactor is an important safety criterion. For this reason, two independent passive decay heat removal systems (DHRS) are designed for the CEFR (as shown in Fig. 3.5). Each circuit consists of a Na-Na heat exchanger and a Na-air heat exchanger connected by an intermediate sodium loop. Each one is rated to a thermal power of 0.525 MWt under the working condition, the decay heat is removed by natural convection and circulation of primary and secondary coolant, and natural draft by air. To have the start-up of DHRS the air dampers of the air cooler stacks are opened by automatic signal of reactor protection system or opened mechanically by the operator staff in case of loss of any service power. Except for this procedure the CEFR DHRS is entirely passive. Table 3.7 gives the parameters of the DHRS of the CEFR.

TABLE 3.7. PARAMETERS OF ONE SET OF DHRS

Parameter	Working	Stand-by
Transfer power, MWt	0.525	0.052
Primary Na flow rate in DHX*, kg/s	5.8	1.66
Secondary Na flow rate in DHX, kg/s	2.93	1.37
Air flow rate in air cooler, kg/s	2.4	0.11
Primary Na temperature, °C		
Inlet at DHX	516	516
Outlet at DHX	444	490
Secondary Na temperature, °C		
Inlet at air cooler	514	515
Outlet at air cooler	373	485
Air temperature, °C		
Inlet at air cooler	50	50
Outlet at air cooler	264	496
Secondary Na pressure, MPa	0.6	0.402

* DHX: Decay Heat Exchanger in DHRS

The containment is designed to isolate the plant environment and staff from nuclear materials and fission product releases by a series of barriers. The cladding enveloping the fuel pellets represents the first barrier. The second barrier is composed of several containment vessels: (1) the main vessel doubled by the safety vessel for the primary circuit, (2) reactor vessel over-pressure protection system designed for reducing the pressure of Argon in the vessel by discharging the redundant Argon into special ventilation system passively. The most serious BDBA accident with the all power supply lost, all shut-down system failed and dampers of two air cooler closed until to 45 minutes have been calculated and analyzed. The result shows that the cladding temperature will reach the maximum value of 920°C in 40 s from accident happened and then the sodium temperature will crawl up to the maximum of 890°C in 50 s, less than boiling point 920°C at the situ pressure. And there is no fuel melting in the accident [4].

3.2.2.2.5. CEFR Main design parameters

The main design parameters of the CEFR are shown in Table 3.8.

TABLE 3.8. CEFR MAIN DESIGN PARAMETERS

Parameter	Value
Thermal power, MW	65
Electric power, net, MW	20
Reactor core,	
Height, cm	45.0
Diameter equivalent, cm	60.0
Fuel (first loading,	(Pu, U)O_2, [UO_2]
Pu, total, kg	150.3
^{239}Pu, kg	97.7
^{235}U- (enrichment), (first loading) kg (%)	42.6 (19.6%), [236.7 (64.4%)]
Linear power max, W/cm	430
Neutron flux, n/cm^2·s	3.7×10^{15}
Burnup, target max., MW·d/t	100 000
Burnup, first load max., MW·d/t	60 000
Inlet temp. of the core, °C	360
Outlet temp. of the core, °C	530
Diameter of main vessel (outside), m	8.010
Primary circuit	
Number of loops	2
Quantity of sodium, t	260
Flow rate, total, t/h	1328.4
Number of IHX per loop	2
Secondary circuit	
Number of loops	2
Quantity of sodium, t	48.2
Flow rate, t/h	986.4
Tertiary circuit	
Steam temperature, °C	480
Steam pressure, MPa	14
Flow rate, t/h	96.2
Plant life	30

3.2.2.3. Current status

About 500 pre-operation tests including with and without sodium, uni-system and multi-system, namely all pre-operation tests before physics start-up according to the CEFR commissioning programme have been completed. The outside view of CEFR is given in Fig. 3.6. It is envisaged that the first criticality and connection to the grid with 40% full power will be in the year 2010.

FIG. 3.6. CEFR reactor building.

3.2.3. PFBR

3.2.3.1. Introduction

A fast reactor programme, which includes the design, development and deployment of a national network of fast breeder reactors (FBRs), along with the associated reprocessing facilities and plutonium-based fuel fabrication facilities, represents the second stage of India's three-stage nuclear power programme. The fast reactor programme in India began in 1972 with the establishment of a research centre (then called Reactor Research Centre) dedicated to the development of fast reactor technology and the decision to construct the Fast Breeder Test Reactor (FBTR) at Kalpakkam (see Chapter 2). Based on the experiences gained internationally with FBRs, including FBTR, and the comprehensive research and technology development programme carried out in collaboration with a large number of academic and industrial organizations, a 500 MWe capacity Prototype Fast Breeder Reactor (PFBR) is being pursued.

3.2.3.2. Design description

PFBR is a 500 MWe, sodium cooled, pool type reactor with 2 primary and 2 secondary loops with 4 steam generators per loop. The reactor is located at Kalpakkam, close to the 2×220 MWe PHWR units of the Madras Atomic Power Station (MAPS). Kalpakkam is situated at 68 km south of Chennai on the coast of Bay of Bengal. The primary objective of the PFBR is to demonstrate techno-economic viability of fast breeder reactors on an industrial scale. The reactor power is chosen to enable adoption of a standard turbine as used in fossil power stations, to have a standardized design in reactor components resulting in further reduction of capital cost and construction time in future and compatibility with regional grids. The overall flow diagram comprising primary circuit housed in reactor assembly, secondary sodium circuit and balance of plant is shown in Fig. 3.7.

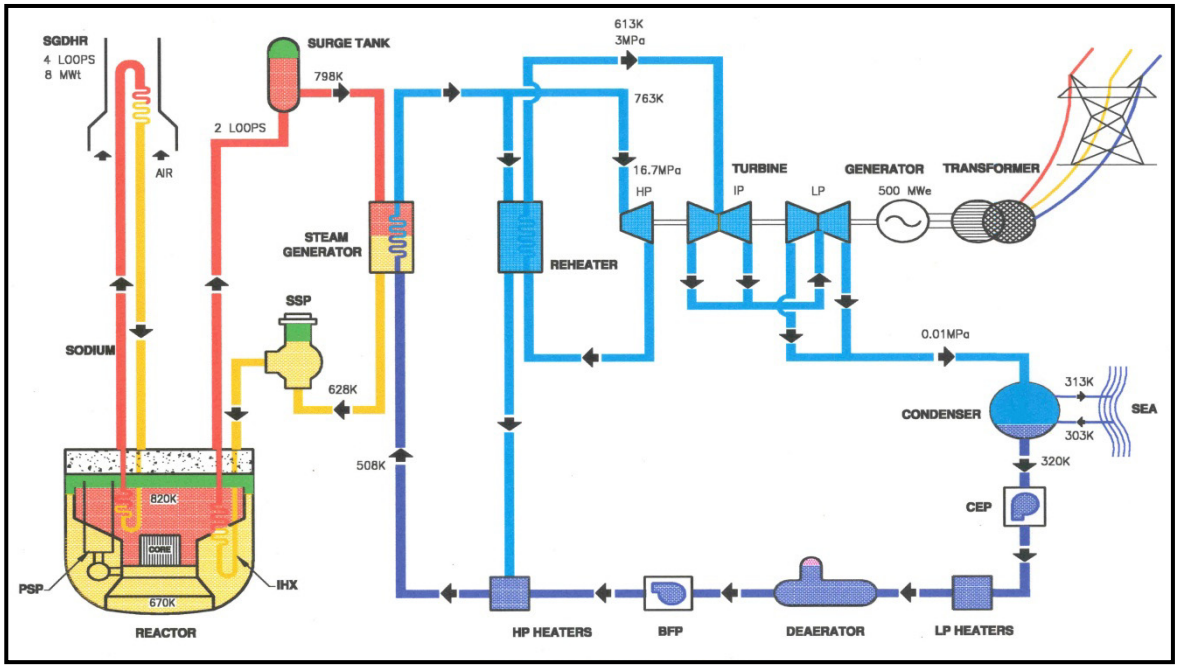

FIG. 3.7. PFBR Flow sheet.

In the reactor assembly (Fig. 3.8), the main vessel houses hot and cold sodium pools, separated by an inner vessel.

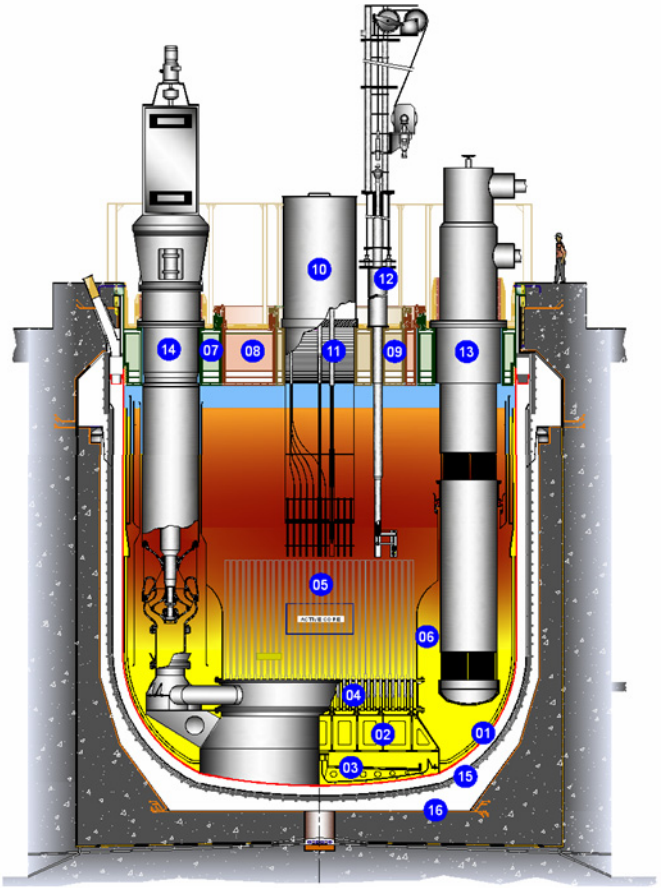

01	MAIN VESSEL
02	CORE SUPPORT STRUCTURE
03	CORE CATCHER
04	GRID PLATE
05	CORE
06	INNER VESSEL
07	ROOF SLAB
08	LARGE ROTATABLE PLUG
09	SMALL ROTATABLE PLUG
10	CONTROL PLUG
11	CSRDM / DSRDM
12	TRANSFER ARM
13	IHX
14	PRIMARY SODIUM PUMP
15	SAFETY VESSEL
16	REACTOR VAULT

FIG. 3.8. Schematic sketch of PFBR reactor assembly.

Both the pools have a free sodium surface blanketed by argon. The nuclear heat generated in the core is removed by circulating sodium from the cold pool which is at 670 K, to the hot pool which is at 820 K. The sodium from the hot pool transports the heat to four intermediate heat exchangers and joins back to the cold pool. While the circulation of sodium from the cold pool to the hot pool is maintained by two primary sodium pumps, the flow of sodium through the intermediate heat exchangers is driven by a level difference (1.5 m of sodium) between the hot and cold pool free surfaces. The heat from the intermediate heat exchangers is transferred to eight steam generators by sodium in the secondary circuit. Steam produced in steam generators is supplied to the turbo-generator.

The reactor core consists of about 1758 subassemblies including 181 fuel subassemblies (Fig. 3.9).

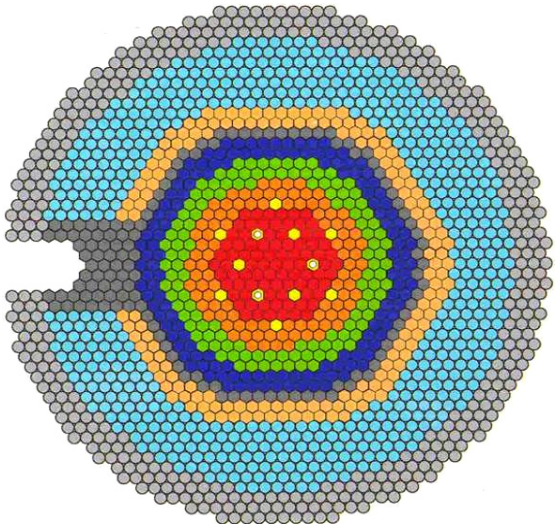

SYMBOL	TYPE OF SUBASSEMBLY	No.
	FUEL (INNER)	85
	FUEL (OUTER)	96
	CONTROL AND SAFETY ROD	9
	DIVERSE SAFETY ROD	3
	BLANKET	120
	STEEL REFLECTOR	138
	B_4C SHIELDING (INNER)	125
	STORAGE LOCATION	156
	STEEL SHIELDING	609
	B_4C SHIELDING (OUTER)	417
	TOTAL SUBASSEMBLIES	1758

FIG. 3.9. Core layout.

The core is supported by a grid plate, which also acts as a plenum for distributing the cold sodium. The grid plate rests on the core support structure, which, in turn is welded to the bottom portion of the main vessel at the triple point. The inner vessel is also supported at the periphery of grid plate. Thus, the main vessel supports the entire load of the core, the grid plate, the core support structure, the inner vessel and associated structures transmitting ~ 750 t at the triple point, apart from containing the primary sodium (~ 1150 t). The weight of the main vessel is 205 t, including the weight of thermal baffles, which protect the vessel from heat emanating from hot pool. The control plug, positioned just above the core, houses mainly 12 absorber rod drive mechanisms. The top shield covers the main vessel and supports the primary sodium pump, intermediate heat exchanger, control plug and fuel handling systems. The weight of the top shield, including that of the components supported by it and shielding, is ~ 1410 t. The reactor assembly weighing ~ 3520 t is supported at the top of the reactor vault.

For the core components, 20% cold worked D9 material is used to have better irradiation resistance. Austenitic stainless steel type 316 LN is the main structural material for the out-of-core components and modified 9Cr-1Mo (grade 91) is chosen for the steam generator. All reactor structures, systems and components are classified systematically based on their safety functions and the requirements under seismic events have also been identified. The PFBR is designed for a plant life of 40 y in compliance with design codes viz. RCC-MR (2002) and ASME-Section III (2003), respecting the safety criteria stipulated by Atomic Energy Regulatory Board. The important design data is given in Table 3.9.

TABLE 3.9. SUMMARY OF PFBR DESIGN DATA

Parameter	Value
Thermal power, MW_{th}	1250
Electric output, MW_{el}	500
Core height, mm	1000
Core diameter, mm	1900
Fuel	PuO_2--UO_2
Fuel pin outer diameter, mm	6.6
No. fuel pins per fuel assembly	217
Fuel clad material	20% CW D9
Diameter of main vessel, mm	12900
Primary circuit layout	Pool
Primary inlet / outlet temperature, °C	397 / 547
Steam temperature, °C	490
Steam pressure, MPa	16.6
Reactor containment	Rectangular
Plant life, y	40
No. shutdown systems	2
No. decay heat removal systems	2

The reactor assembly houses the cold and hot pool components, apart from the main vessel, the safety vessel and the top shield. The main cold pool components are the core catcher, the core support structure and the grid plate. The main hot pool components are the control plug and its internals, the inner vessel and the IHXs. The major design loadings for the cold and hot pool components are:

(I) Pressure loading for the primary pipe and grid plate
- Differential internal pressure
  - Nominal 0.643 MPa at 670 K
  - Maximum 0.78 MPa
- Differential sodium head across the thickness of inner vessel (at 820 K)
  - During normal operation 1.5 m of Na
  - During spill over 4.1 m of Na

(II) Temperature for cold pool components (sodium)
- During normal operation 670 K (397°C)
- During SGDHR 810 K (537°C) for 30 min (207 times)

(III) Maximum temperature for hot pool components (e.g. inner vessel, etc.)
- During normal operation 820 K (547°C)
- During SGDHR 895 K (622°C)

(IV) Core loads 4805.4 kN

(V) Radiation field (Max.)
- Neutron flux 9.7×10^{11} n/cm^{2}s(E > 0.1 MeV)
- Neutron fluence 6.9×10^{20} n/cm^2 (E > 0.1 MeV) (0.25 dpa)

(VI) Fluids in contact sodium / argon

The safety classification, seismic categorization, material of construction and design codes used for the main components are given in Table 3.10.

TABLE 3.10. DESIGN PARAMETERS FOR MAJOR COMPONENTS AND MATERIALS

Sl. No.	Component / system	Class			Seismic category	Material of construction
		Safety	Design	Manufacturing		
1	Main vessel	1	I	I	1	SS 316LN
2	Grid plate	1	I	I	1	- do -
3	Primary pipe	1	I	I	1	- do -
4	Core support structure	1	I	I	1	- do -
5	Inner vessel	2	I	I	1	- do -
6	Top shield	1	I	I	1	A48P2
7	Control plug	1 / 2 / 3	I / III	I / II / III	1 / 2	SS 316LN/ AISI 430/ A48 P2/ Fe 410WC
8	Safety vessel	2	I	I	1	SS 304 LN
9	Core catcher	1	I	I	1	SS 316LN

3.2.3.3. Current status

The nuclear island houses a total of seventeen buildings including safety related structures. Out of the seventeen buildings, eight buildings, namely the reactor containment building, the two steam generator buildings, the two electrical buildings, the control building, the radwaste building and the fuel building, are connected together as a single structure which is called the Nuclear Island Connected Building (NICB). The NICB is supported on a common raft foundation which covers an area of approximately 102 m×93 m and is 6 m thick. The construction of the NICB is completed, with the exception of the top roof of the reactor containment building, which remains open to facilitate the erection of the reactor assembly components (Fig. 3.10).

FIG. 3.10. Progress of NICB construction.

In this, the reactor vault construction has been successfully completed meeting the stringent dimensional tolerances required by the designers. The construction of the remainder of the nuclear island is nearing completion and other structures, which do not affect the project schedule, are at various stages of construction. The excavation works for the balance of plant have been completed and civil construction is in progress.

The nuclear steam supply system components have been manufactured successfully by the Indian industries, based on the experience gained through technology development. Manufacture of large size components like the safety vessel, main vessel, inner vessel and thermal baffles has been completed meeting the stringent tolerance requirements. The safety vessel, incorporated with delicate thermal insulation panels, is the first major nuclear equipment that has been erected successfully in June 2008 (Fig. 3.11). Subsequently, the safety vessel has been placed in it in December 2009.

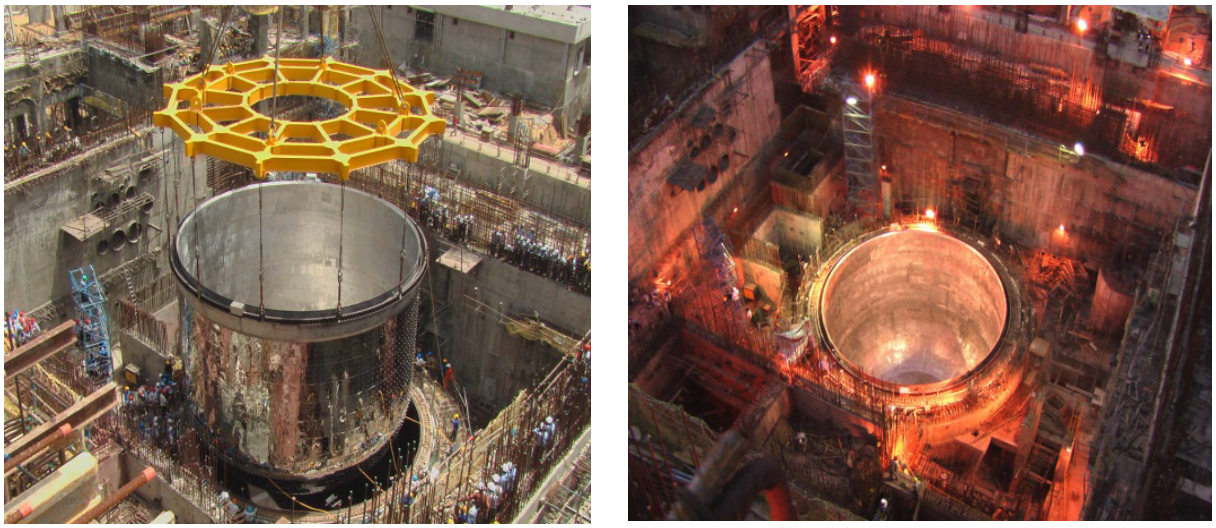

FIG. 3.11. Erection of safety vessel on the reactor vault.

As the manufacturing tolerances are very crucial for meeting the functional and structural integrity considerations, very stringent values have been specified. Better tolerances (form tolerances less than the half of the wall thickness) have been achieved consistently for all the large size components. This achievement is possible due to the extensive manufacturing development work completed as a pre-project activity as well as well co-ordinated efforts of task forces involving IGCAR and BHAVINI constituted for these purposes. Elegant methodology has been finalized for the subsequent erection of the main vessel along with the internals and top shield, respecting various erection tolerances and giving due consideration to time and economy.

The civil construction and equipment erection for the PFBR have been carried out in parallel, combining the use of sate-of-the-art erection equipments and construction methodologies and highly optimized construction sequences. It is planned to commission PFBR in 2011.

Figure 3.12 shows the manufacturing status of a few important components. About 1150 t of sodium has been transferred safely to storage tanks.

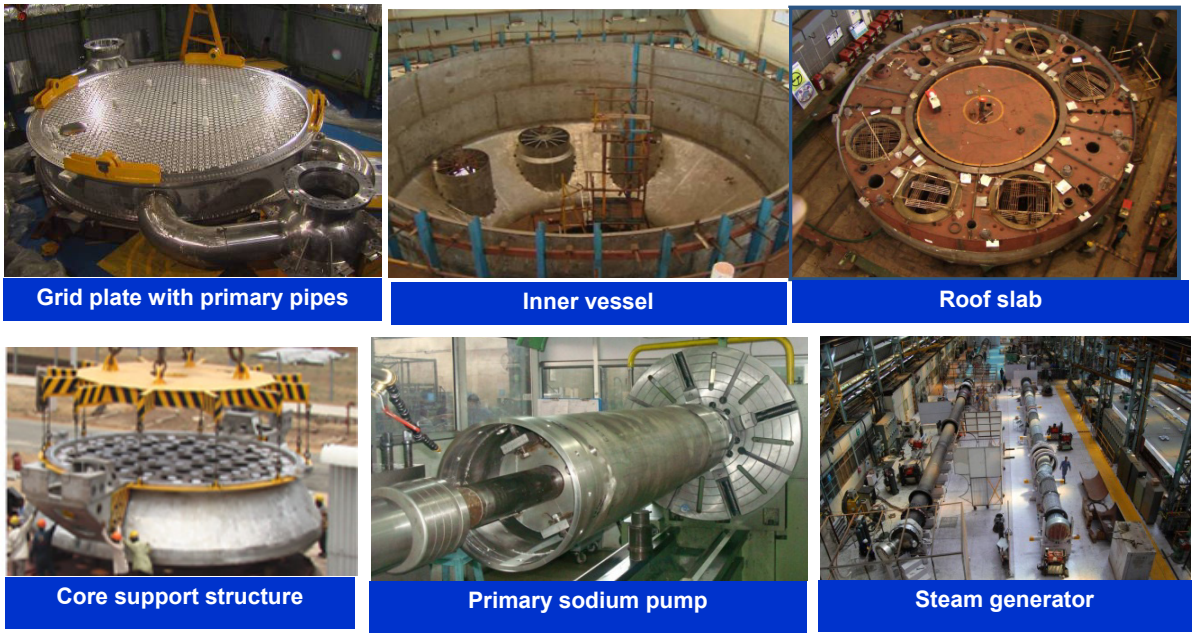

FIG. 3.12. Manufacturing status of a few important components.

3.3. Sodium-cooled fast reactor conceptual designs

3.3.1. ABTR

3.3.1.1. Introduction

The goals of the Global Nuclear Energy Partnership (GNEP) are to expand the use of nuclear energy to meet increasing global energy demand, to address nuclear waste management concerns and to promote non-proliferation. Implementation of the GNEP requires development and demonstration of three major technologies:

- Light water reactor (LWR) spent fuel separations technologies that will recover transuranics to be recycled for fuel but not separate plutonium from other transuranics, thereby providing proliferation-resistance;
- Advanced Burner Reactors (ABRs) based on a fast spectrum that transmute the recycled transuranics to produce energy while also reducing the long term radiotoxicity and decay heat loading in the repository;
- Fast reactor fuel recycling technologies to recover and refabricate the transuranics for repeated recycling in the fast reactor system.

The primary mission of the ABR Programme is to demonstrate the transmutation of transuranics recovered from the LWR spent fuel, and hence the benefits of the fuel cycle closure to nuclear waste management. The Advanced Burner Test Reactor (ABTR) is a fast reactor concept that could be the first step in demonstrating the transmutation technologies. It directly supports development of a prototype full-scale Advanced Burner Reactor, which would be followed by commercial deployment of ABRs. The primary objectives of the ABTR are:

- To demonstrate reactor-based transmutation of transuranics as part of an advanced fuel cycle;
- To qualify the transuranics-containing fuels and advanced structural materials needed for a full-scale ABR;
- To support the research, development and demonstration required for certification of an ABR standard design by the US Nuclear Regulatory Commission.

The ABTR should also address the following additional objectives:

- To incorporate and demonstrate innovative design concepts and features that may lead to significant improvements in cost, safety, efficiency, reliability, or other favorable characteristics that could promote public acceptance and future private sector investment in ABRs;
- To demonstrate improved technologies for safeguards and security;
- To support development of the US infrastructure for design, fabrication and construction, testing and deployment of systems, structures and components for the ABRs.

3.3.1.2. Design description

Based on these objectives, a pre-conceptual design of a 250 MWt ABTR was developed; the design is fully documented in the reference report and summarized here. In addition to meeting the primary and additional objectives listed above, the lessons learned from fast reactor programs in the USA and worldwide and the operating experience of more than a dozen fast reactors around the world, in particular the Experimental Breeder Reactor-II, have been incorporated into the design of the ABTR to the extent possible.

In order to demonstrate the transmutation of transuranics, the ABTR is required to provide a test environment prototypic of future commercial reactors, which implies that the reactor size should be large enough. On the other hand, a high power level means more complexity in engineering and higher project construction costs. Therefore, trade studies were conducted which concluded that ~ 250 MWt is a reasonable compromise balancing the prototypic irradiation environment and the project cost. The reactor core design parameters have been selected to be representative of commercial-scale reactors, which results in a moderate conversion ratio of ~ 0.6 and a plutonium or transuranics enrichment in the range where extensive irradiation databases exist. However, the core has flexibility to accommodate a wide range of conversion ratios by changing the assembly design parameters appropriately.

Based on the past trade studies and lessons learned from operating reactors, the pool-type arrangement was selected as the basis for the ABTR pre-conceptual design due to its potential for design simplicity, inherent passive safety, and economics. The key plant design parameters for the ABTR are summarized in Table 3.11.

TABLE 3.11. ABTR PLANT DESIGN PARAMETERS

Parameter	Value
Reactor power, MWt/ MWe	250/95
Coolant	Sodium
Coolant temperature, inlet/outlet , °C	355/510
Driver fuel	Reference: metal (~ 20% TRU, 80% U) Backup: oxide
Cladding and duct material	HT-9
Cycle length	4 months
Plant life	30 years with the expectation of life extension
Reactor vessel size, m	5.8 m diameter, 16 m height
Structural and piping material	Austenitic stainless steel
Primary pump	Reference: electromagnetic Backup: mechanical (centrifugal)
Power conversion cycle	Reference: supercritical CO_2 Brayton Backup: steam Rankine
Thermal efficiency	38%

The overall plant site arrangement is shown in Fig. 3.13.

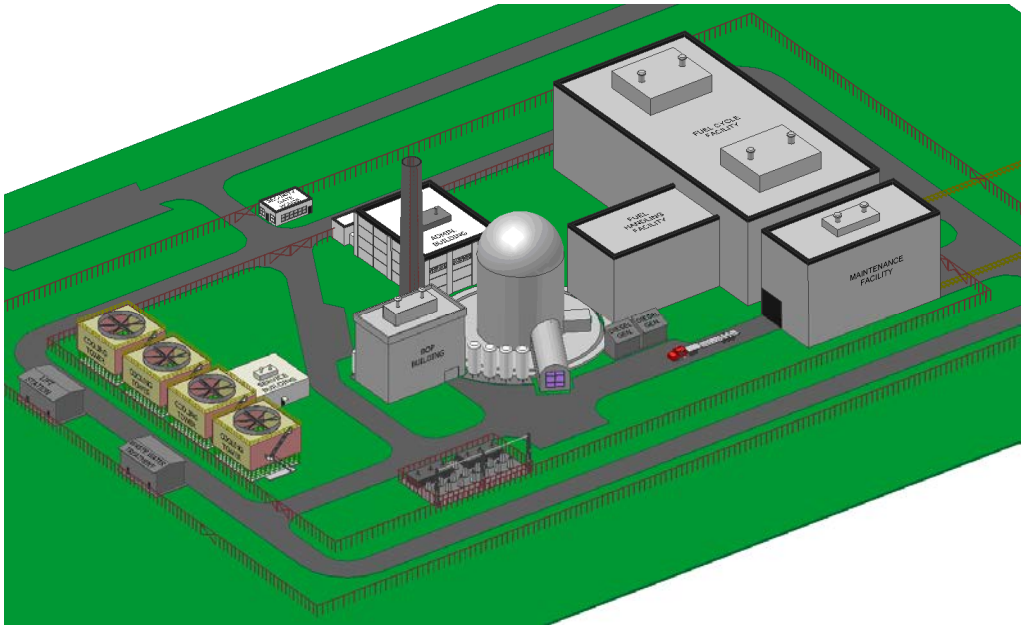

FIG. 3.13. Overall site view of the ABTR plant.

The major systems — the reactor vessel containing the reactor core and the primary heat transport system, the intermediate heat transport system with the sodium-to-CO_2 heat exchangers, and the Brayton cycle power conversion system — are shown in an elevation view in Fig. 3.14.

The reactor and the primary and secondary heat transport systems are located below grade. Note that all of the nuclear components of the plant are located on a nuclear island, which is seismically isolated from its foundations, which is also illustrated in Fig. 3.14.

The reactor core consists of 24 assemblies in an inner enrichment zone and 30 assemblies in an outer zone. Reactivity control and neutronic shutdown are provided by seven primary and three secondary control rod assemblies. A total of nine test locations are provided — six for fuel tests and three for material tests. This core design is the product of extensive trade studies involving power rating, conversion ratio, fuel type (metal, oxide), fissile material (weapons Pu, TRU from LWR spent fuel), control requirements and shutdown margin. The reference design uses weapons-grade plutonium-based ternary metal driver fuel as the initial core and envisions a gradual transition to transuranics-containing driver fuel as it is qualified and made available. It has a TRU conversion ratio of 0.65.

The primary system is configured in a pool-type arrangement (similar to that used successfully in EBR-II), with the reactor core, primary pumps, intermediate heat exchangers, and direct reactor auxiliary cooling system (DRACS) heat exchangers all immersed in a pool of sodium coolant within the reactor vessel. A schematic view of the primary system is shown in Fig. 3.15 and some specific dimensions are given in Fig. 3.16. The pool-type arrangement was selected because of its inherent simplicity and safety. All primary coolant piping is within the sodium pool, which greatly reduces the possibility of loss of coolant, and the sodium pool provides a large thermal inertia in the system. In addition, the reactor vessel is a simple structure having no penetrations. The hot sodium at core outlet temperature is separated from the cold sodium at core inlet temperature by a structure called the redan. The reactor vessel is exposed only to cold sodium, so it is not subjected to severe thermal transients. A guard vessel is provided as an additional passive safety feature.

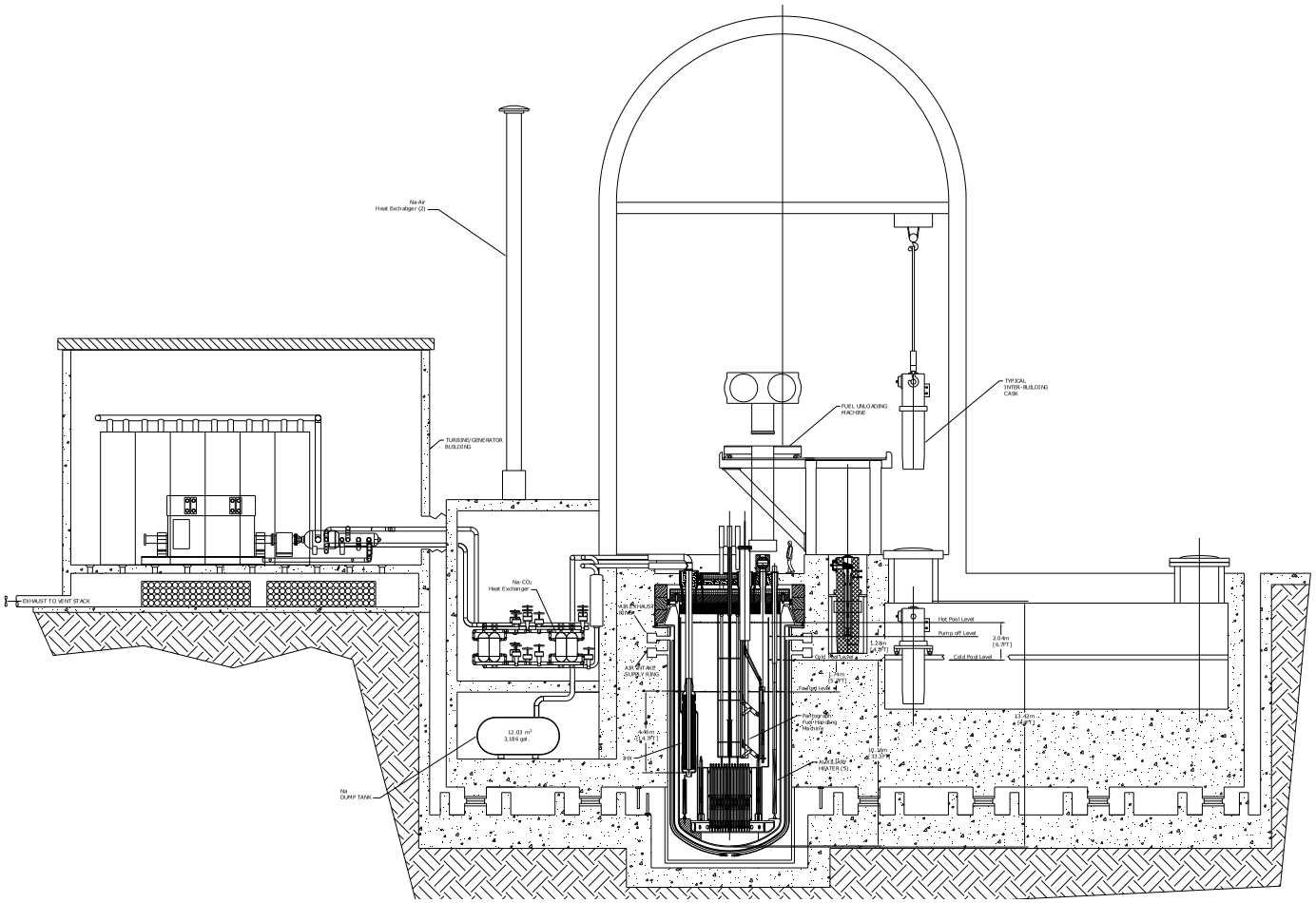

FIG. 3.14. Elevation view of primary system, intermediate system, and Brayton cycle power conversion system.

.

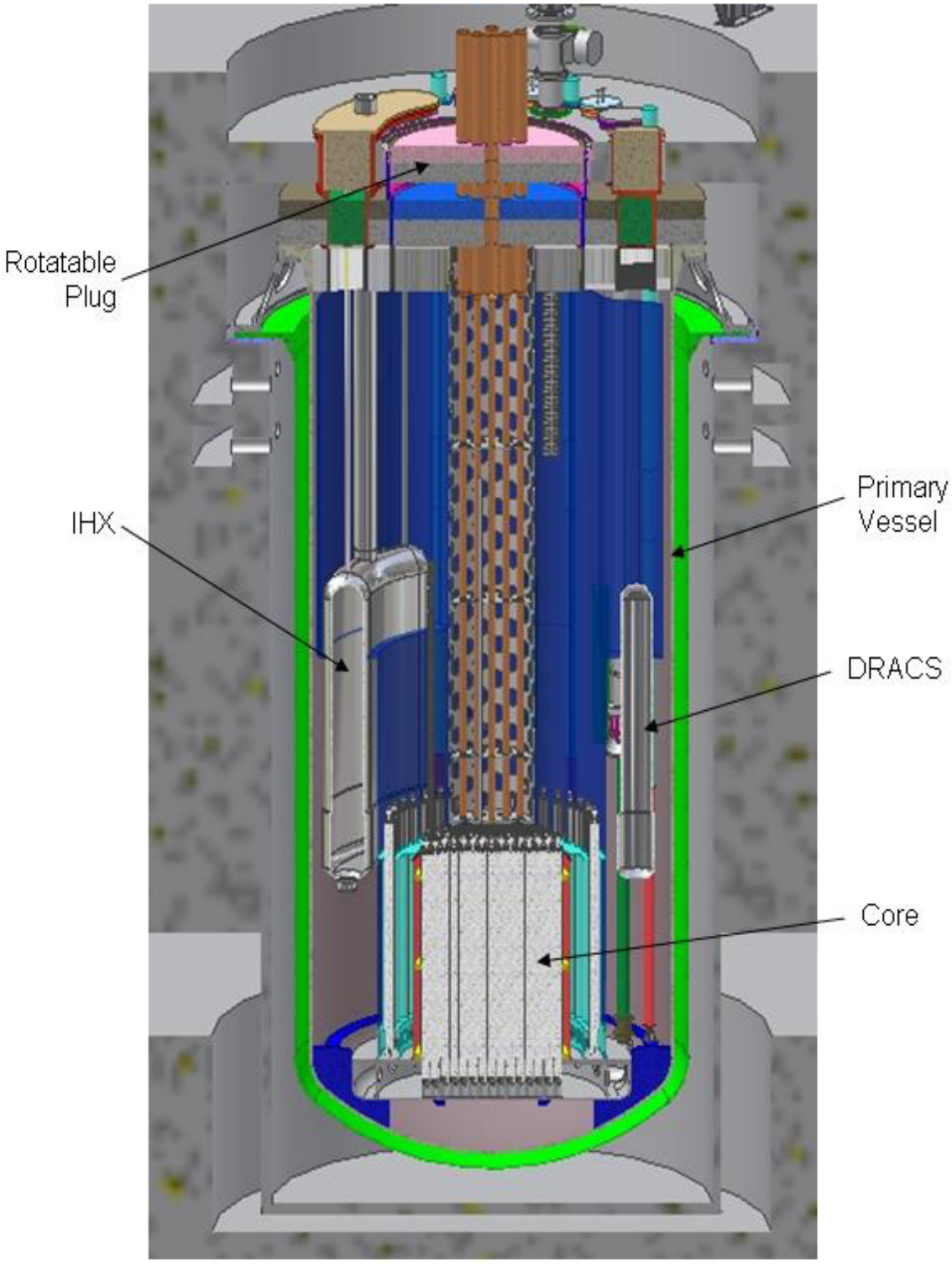

FIG. 3.15. Schematic view of primary system.

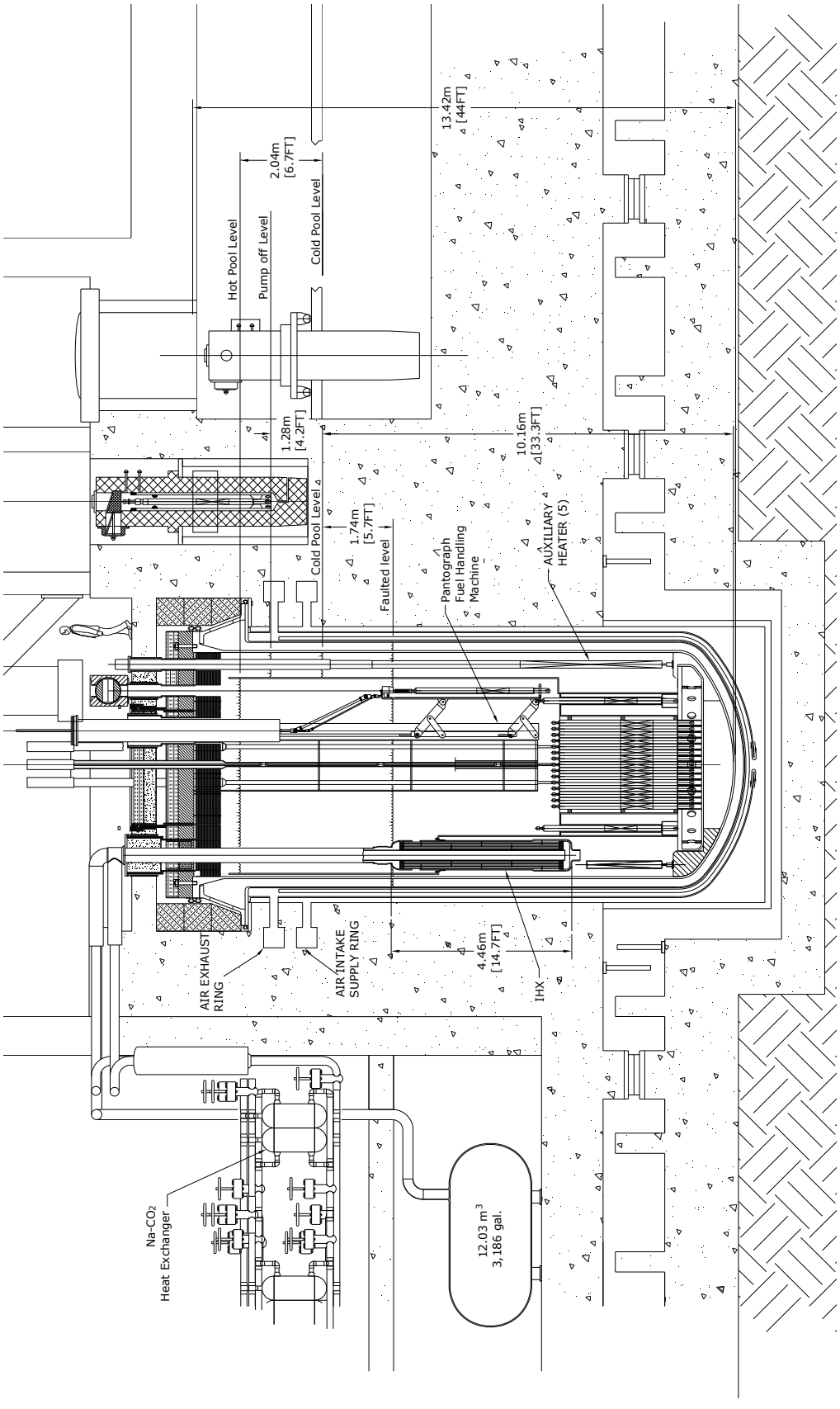

FIG. 3.16. Elevation view of primary system.

Within the reactor vessel, two primary electromagnetic pumps take suction from the lower regions of the cold pool and discharge the sodium into a header that distributes the sodium into main header with three feeder pipes, which distribute sodium evenly into the inlet plenum. The inlet plenum distributes the primary sodium to the inlet of the core assemblies, which are individually orificed for proper flow distribution. The sodium is heated as it flows through the core and exits the core assemblies into the outlet plenum. The hot sodium then rises into the redan and enters the inlet of the intermediate heat exchanger (IHX). After the primary sodium transfers its heat to the intermediate sodium, it exits the IHX into the lower regions of the cold pool. The IHX is contoured to the shape of the annular gap between the lower redan and the reactor vessel to minimize the overall diameter of the reactor vessel. The guard vessel that surrounds the reactor vessel will capture and contain any reactor vessel leakage and prevent the IHX inlet, DRACS heat exchangers, and core assemblies from being uncovered, maintaining a coolant natural circulation path for core cooling.

An innovative power conversion system using a Brayton cycle with supercritical CO_2 was selected for the reference design because of its simple layout with relatively few components, small turbo-machinery components and the potential for higher cycle efficiencies at higher sodium outlet temperatures. It also offers improved inherent safety because the potential for sodium-water chemical reaction is eliminated.

The intermediate sodium exits the IHX and flows to the Na-to-CO_2 heat exchanger located below grade on the nuclear island. This heat exchanger is part of the Brayton cycle power conversion system. The intermediate sodium heats the supercritical CO_2 which then flows into the turbine-generator performing work and generating electricity. The CO_2 then goes through a series of recuperator heat exchangers, coolers, and compressors before it re-enters the Na-to-CO_2 heat exchanger. The CO_2 rejects about 60% of its heat to a forced draft cooling tower which provides the ultimate heat sink. A schematic diagram of the reference power conversion system is shown in Fig. 3.17.

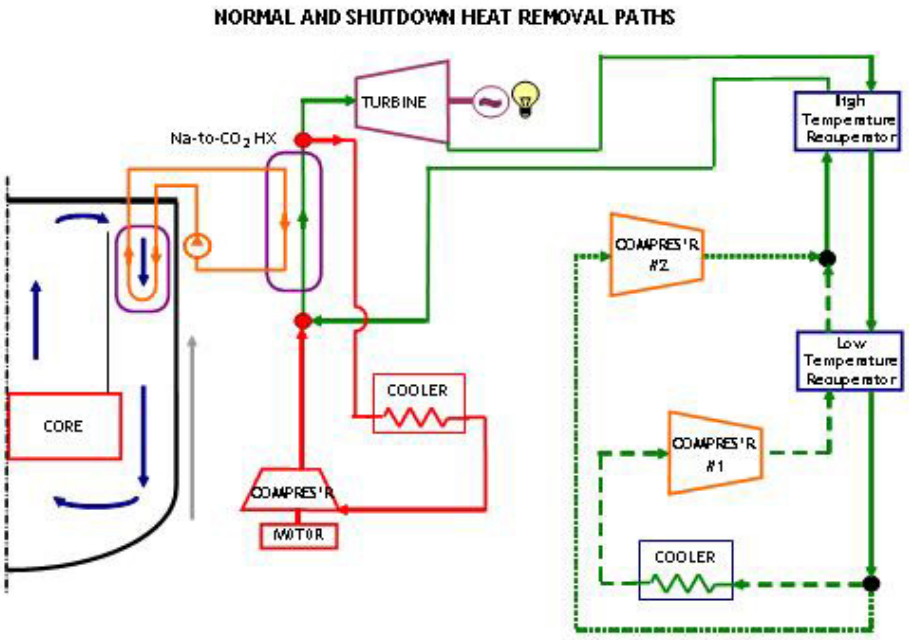

FIG. 3.17. Overall thermodynamic cycle.

Removal of decay heat from the reactor core is a fundamental safety function. In the reference ABTR design, normal decay heat removal is through the normal power conversion systems. However, a direct reactor auxiliary cooling system (DRACS) is provided, having both forced flow and natural convection capability. This system removes decay heat from the pool to the atmosphere using heat exchangers located in the cold part of the sodium pool and in the atmosphere above grade. If electrical power is available, forced flow can be used; in an emergency, natural convection flow can remove the decay heat.

The ABTR will have a short refuelling interval so efficient and reliable fuel handling is essential. The reference design provides in-vessel fuel storage cooled by natural convection. Movement of fuel into and out of the core is done using a simple and reliable pantograph-type fuel handling machine. This machine operates with a single rotatable plug in the vessel head, which simplifies the design of the head and allows a smaller reactor vessel diameter, both of which afford cost savings. Movement of fuel from the reactor vessel to the fuel handling building is done using a fuel unloading machine and inter-building transfer cask similar to the system used for many years at EBR-II.

The pre-conceptual design presented in the reference report reflects the results of extensive and detailed design analyses and trade-off studies. Areas that were the subject of special attention in the design analyses include the core design and in-vessel shielding analysis, the thermal-hydraulics of the vessel and the in-vessel structures and the various components in the heat transport systems. The performance of the reactor and heat transport systems during natural circulation transients and several design basis events was considered. These analyses are documented in Part III of the reference report.

3.3.2. PRISM

3.3.2.1. Introduction

The PRISM reactor is a modular sodium-cooled fast reactor whose development began as a joint project between General Electric (GE) and the US Department of Energy as part of the advanced liquid-metal reactor (ALMR) programme. Development has since continued at GE-Hitachi, and the design today incorporates Generation-IV objectives. The section provides a design overview and summary of the commercialization plan of PRISM.

3.3.2.2. Design description

3.3.2.2.1. Nuclear Steam Supply System (NSSS)

PRISM employs passive safety and uses a modular fabrication technique to expedite plant construction. Factory fabrication of the plant includes both the nuclear island and the Balance of Plant (BOP) facilities and components. One module (Power Block) includes two PRISM reactors; a full scale plant includes three Power Blocks. Design certification is accomplished by prototype testing of a single commercial scale Power Block. The principle design parameters for the largest PRISM are summarized in Table 3.12.

TABLE 3.12. PRISM PRINCIPLE DESIGN PARAMETERS (LARGEST ELECTRICAL OUTPUT)

Item	Value
Commercial plant	
Gross/net electrical output, MWe	2480/2280
Gross/net steam cycle efficiency, %	41/38
Number of power blocks	3
Number of reactor/plant	6
Plant availability, %	93
Power block	
Number of reactor modules	2
Gross/net electrical output, MWe	830/760
Number of steam generators	2
Steam generator type	Helical coil
Steam cycle	Superheated
Turbine speed, rpm	3600
Turbine throttle pressure / temperature, atm / °C	170 / 270
Feedwater temperature, °C	220
Reactor module	
Core thermal power, MWt	700 - 1000
Primary Na inlet/outlet temperature, °C	360/510
Secondary Na inlet/outlet temperature, °C	320/500

The commercial PRISM plant achieves large plant economics by utilizing six reactor modules and associated steam generating systems arranged in three identical Power Blocks. The plant net output can range from 1860 MWe to 2280 MWe (700 MWt to 1000 MWt). Plant electrical output depends on utility customer need. Examples in this description will use the larger (2280 MWe) size. Each Power Block features two identical reactor modules, each with its own steam generator, that jointly supply superheated steam to a single turbine-generator. Figure 3.18 provides a cut-a-way view of the NSSS and Fig. 3.19 is a cut away view of the PRISM reactor module.

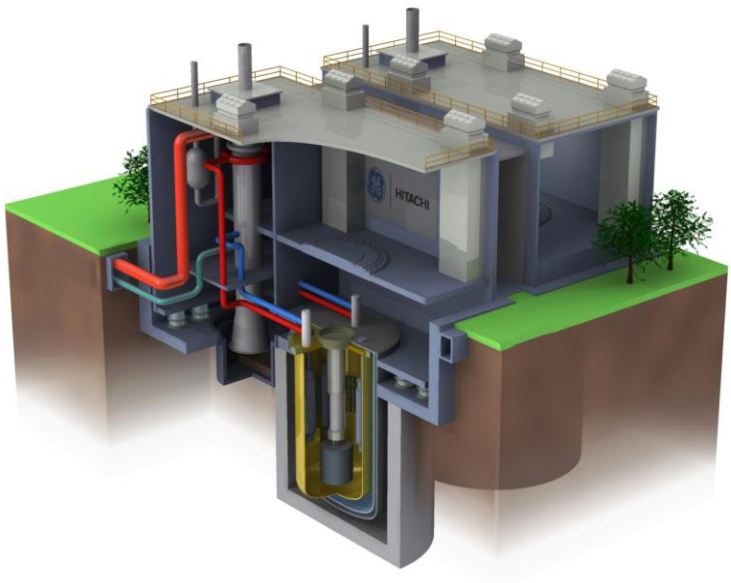

FIG. 3.18. 3D View of a PRISM Nuclear steam supply system.

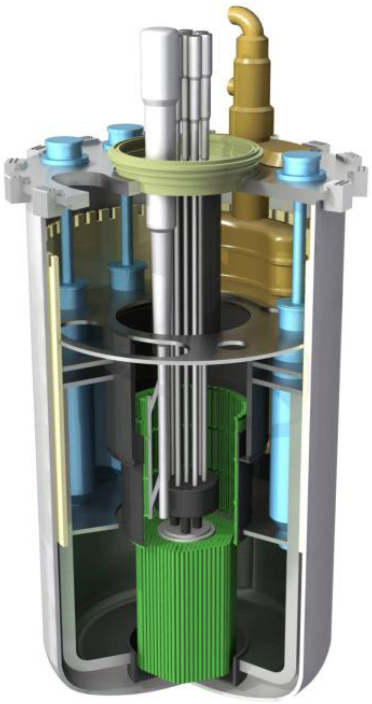

FIG. 3.19. 3D View of a PRISM Reactor module.

The PRISM power plant is physically divided into two areas: (1) Nuclear Island (NI) including the spent fuel service facility (Nuclear Fuel Recycling Center), and (2) BOP. This division of plant areas allow for a minimization of plant protection areas. The three Power Blocks consists of six reactors and six Steam Generators (SGs), which are housed in the reactor/SG complexes. The three turbine-generators are located in the balance of plant area. The Power Blocks are separated with a fence to allow for sequential construction of the individual Power Blocks.

The nuclear island consists of all of the facilities that require high security, contain radioactive materials, and those facilities that provide direct support to the facilities in the NI. The NI is inside a protected area enclosed by a double security fence and a vehicle barrier. All personnel, vehicle, and railroad access to the protected area are controlled from hardened security facilities.

A special gauge railroad system serves to transport the fuel transfer casks between the reactor facilities and the fuel service facility during refueling operations. The nuclear island warehouse, reactor maintenance facility, and radwaste facility are grouped together; the systems and access provisions are integrated for these structures. The control building includes the main control room.

The Nuclear Fuel Recycling Center (NFRC) is a design option that integrates spent fuel processing for both PRISM and LWRs, fuel assembly fabrication for PRISM, and waste storage operations into a single facility. It is located in a designated area of the NI within its own security and support facilities to permit independent ownership and/or operation. All PRISM fuel assemblies can be fabricated and recycled in the NFRC and are not shipped off-site. Core assemblies are transferred between the reactors and the facility inside fuel transfer casks via rail through the railroad gate.

The balance of plant includes the main turbine-generator facility which houses the three nominal 830 MWe turbine-generators and their supporting auxiliary systems, including the condensers, condensate polishers, feed heaters, and cycle pumps. This facility is located in the center of the plant near the steam generator facilities. The structure is surrounded with external condensate storage tanks, main stepup transformers and auxiliary transformers, chemical storage tanks, and the turbine lube oil storage tanks. Two separated railroad spurs and roadways provide maintenance access to the turbine generator buildings.

3.3.2.2.2. Reactor module

Each reactor module consists of the reactor vessel, reactor closure, containment vessel, internal structures, internal components, reactor module supports, and the reactor core. The reactor vessel can be fabricated in sizes 20–30 feet depending on costumer shipping constraints. The outermost structure of the reactor module is the containment vessel. A 20 cm gap between the reactor vessel and the containment vessel is filled with argon above the reactor cover gas pressure. The reactor cover gas is helium at a pressure of about one atmosphere at normal power conditions.

The reactor closure is a single plate with a rotatable plug and penetrations for the reactor equipment and primary sodium and cover gas service lines. Primary sodium purification is accomplished during reactor shutdown by a single cold trap system for a Power Block. There are no penetrations in the reactor vessel or the containment vessel. The reactor vessel is butt-welded to a lip on the underside of the closure. The containment vessel is bolted to the closure and sealed by welding. The reactor module is supported entirely from the closure by hold-down brackets.

PRISM uses metallic fuel for compatibility with coolant, inherent safety, and ease of fabricating metallic fuel in a hot cell. The reactor core is supported by a redundant beam structure attached at the bottom and the sides of the reactor vessel. A core barrel and support cylinder, extending from the core inlet plenum to above the core, contains storage racks attached to its inner surface for storage of spent fuel assemblies. A redundant structure designed to retain molten fuel is located immediately below the core inlet plenum. Two Intermediate Heat Exchangers (IHX) and four Electromagnetic (EM) primary pumps are suspended from the reactor closure. In addition, primary Control Rod Drives (CRD), ultimate shutdown rod drives, in-vessel instrumentation, and an In-Vessel Transfer Machine (IVTM) are suspended from the rotatable plug in the closure.

3.3.2.2.3. Reactivity control

Reactivity control for normal startup operation, load following, and shutdown is accomplished with control rods. Each control unit consists of a drive mechanism, a driveline, and a control assembly. A stepping motor, controlled by the Plant Control System (PCS), actuates a lead screw to insert and withdraw the absorber. The nine control rods have scram diversity and shutdown redundancy.

The primary shutdown system is backed-up by a secondary shutdown system (ultimate shutdown system). It utilizes magnetic latches, which can be actuated by either the Reactor Protection System (RPS), or automatically when the latch temperature exceeds the magnetic curie point temperature. Both shutdown systems are backed up by the inherent negative reactivity feedbacks of the reactor core. The inherent negative reactivity feedback response of the core to a temperature increase brings the core to a safe, stable, power state. PRISM has

this unique capability for accommodating the following severe, but extremely unlikely accidents:

- Inadvertent withdrawal of all control rods without automatic scram (RPS) or manual actuation (unprotected transient overpower);
- Loss of primary pump power and loss of all cooling by the IHTS without scram (unprotected loss of flow/loss of cooling);
- Loss of all cooling by the IHTS without scram (unprotected loss of cooling).

3.3.2.2.4. Primary heat transport system

Nuclear heat is removed from the reactor core by the Primary Heat Transport System (PHTS), which transfers the heat to the Intermediate Heat Transport System (IHTS) via the IHX, and then transfers the heat to the turbine-generator system via the Steam Generator System (SGS). One PHTS, one IHTS, and one SGS are associated with each reactor module. Within each reactor module, four electromagnetic pumps circulate the primary sodium through two intermediate heat exchangers, which transfer the heat to a single steam generator. The PHTS is contained within the reactor vessel. It is composed of the reactor core, the hot pool, the tube-side of the IHX, the cold pool, the EM pumps, the pump discharge piping, and the core inlet plenum.

3.3.2.2.5. Primary sodium pump

The reactor has four submersible EM pumps to provide primary sodium circulation within the reactor vessel. The pumps are inserted through penetrations in the reactor closure. The pump draws cold pool sodium from an inlet plenum beneath the pump. Within the pump, the sodium enters the tapered inlet section of the pump duct. The sodium discharges at the top of the pump and is passed radially outward into the pump outlet plenum from which it flows to the core inlet plenum.

3.3.2.2.6. Intermediate heat transport system

The IHTS consists of piping and components required to transport the reactor heat from the primary system, through the IHX, to the SGS. The IHTS is a closed loop system with an expansion plenum in the steam generator top head and an argon cover gas space to accommodate thermally induced system volume changes. Intermediate sodium is circulated by two EM pumps, each located in the cold leg of the loop in the steam generator facility, through the shell-side of the IHX and the shell-side of the steam generator. Guard pipes surrounding the IHTS pipes prevent secondary sodium leakage into the Head-Access-Area (HAA).

Hot leg sodium, is transported in separate stainless steel pipes from the two IHXs to the steam generator top head through vertical inlet nozzles. The cold leg piping returns the sodium to the IHX. The secondary sodium pumps are similar in design as ones employed in the primary system.

A sodium leak detection system provides early warning of any sodium-to-air leaks from the IHTS. In the event of a SG tube leak, the Sodium Water Reaction Pressure Relief System (SWRPRS) provides overpressure protection of the IHTS and IHXs. The SWRPRS consists of a safety grade rupture disk, a separator tank, a vent stack, and a hydrogen ignitor. To separate the reactants, the SWRPRS initiates the water-side isolation and blowdown of the SG system and purge of the SG tubes with nitrogen.

3.3.2.2.7. Steam generator system

The SGS is comprised of the steam generator, startup recirculation tank/pump, leak detection subsystem, and SG isolation valves. There is one SG system for each reactor module. Two SGs in a Power Block are connected together to feed one turbine-generator.

The steam generator is a vertically oriented, helical coil, sodium-to-water counter flow heat exchanger. The Helical Coil Steam Generator (HCSG) unit is designed to generate superheated steam. Sodium flows down the shell-side of the steam generator, while feedwater enters from the bottom. As the water flows upwards it is converted into super-heated steam.

3.3.2.2.8. Decay heat removal system

During normal operation, reactor shutdown heat is removed by the turbine condenser using the turbine bypass. An Auxiliary Cooling Systems (ACS) is provided as an alternative method for shutdown decay heat removal during maintenance or repair operations. The ACS uses natural or forced circulation of atmospheric air to remove heat as the air flows pass the shell side of the steam generator. The ACS consists of an insulated shroud around the steam generator shell with an air intake at the bottom through the annulus and an isolation damper located above the steam generator building. Natural circulation is initiated by opening the exhaust damper. The help of the safety grade Reactor Vessel Auxiliary Cooling System (RVACS), which has the capability to maintain reactor temperatures well below design limits, supplements the ACS. RVACS makes use of natural air convection to remove heat from the reactor module. For this reason, RVACS is always on and constantly removing heat from the reactor module. The RVACS layout is shown in Fig. 3.20.

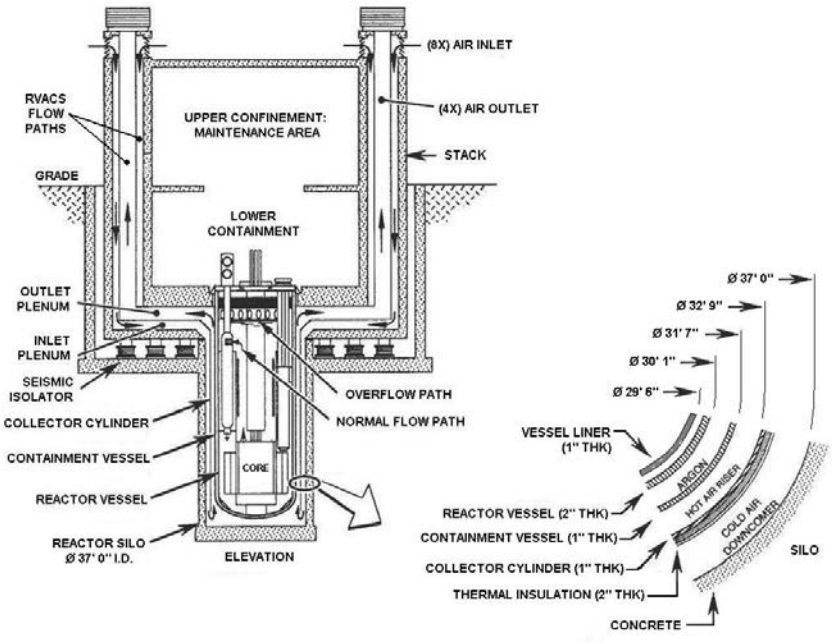

FIG. 3.20. RVACS.

In the highly unlikely event that the IHTS becomes unusable, PRISM will scram in response to a loss of its heat sink. The safety related RVACS will passively remove the residual heat. During the initial part of an RVACS-only transient, the temperatures of the reactor sodium and reactor vessel will rise, increasing the radiant heat transfer across the argon gap to the containment vessel.

The heat is then transferred from the containment vessel to the upwardly flowing atmospheric air around the vessel. The damage fraction to the reactor vessel and containment vessel from transient events that only use RVACS to remove residual heat is negligible.

The four RVACS stacks, extending above the reactor facility, are tornado hardened and incorporate eight separate air inlet openings and four separate air exhaust. The redundant air inlet and exhaust ducting, combined with substantial performance margins, make the RVACS extremely tolerant to accidental flow blockages and surface fouling.

3.3.2.2.9. Reactor refuelling system

Reactor refuelling occurs between 12 and 24 month intervals, depending on the fuel cycle. Fuel assemblies are allowed to decay in the reactor storage positions for one cycle before they are removed and transferred to the NFRC for processing. Within the reactor, core assemblies are moved between the core, storage racks, and a transfer station below the transfer port by the IVTM. An adapter is attached to the transfer port in the reactor closure during refuelling to provide the necessary system isolation. An Ex-Vessel Transfer Machine (EVTM) is positioned and a leak tight connection is made to the adapter.

The EVTM is used to exchange spent fuel and other core assemblies in the reactor with new assemblies from the transfer cask. The transfer cask is then returned to the NFRC where the spent fuel will be cleaned, inspected, and stored in an air-cooled storage rack.

3.3.2.2.10. Containment

The PRISM containment is one of three successive barriers (fuel cladding, primary coolant boundary and containment) to protect the public from accidental release of radioactivity from the reactor core. The containment consists of a lower containment vessel surrounding the reactor vessel and an upper containment structure over the reactor closure. To mitigate accidents that may release radionuclides through the reactor closure, the upper containment structure is designed to limit leakage to less than 1 volume % per day.

The lower portion of the containment consists of a stainless steel vessel. The containment vessel has no penetrations and is designed to remain leak tight. The 20 cm annulus between the reactor vessel and the containment vessel is sized to retain the primary sodium in the unlikely event of a reactor vessel leak. This design allows the reactor core, the stored spent fuel, and the inlets to the intermediate heat exchangers to remain covered with sodium. The annulus between the two vessels is filled with argon gas.

The upper portion of the containment has been designed to mitigate a postulated reactor closure breach associated with a Hypothetical Core Disruptive Accident (HCDA). It is defined by the HAA above the reactor deck. This containment volume is normally isolated from the primary sodium storage vault by means of a rupture disk. A secondary containment is provided by the permanent refuelling enclosure above the HAA.

3.3.2.2.11. Seismic isolation

Seismic isolation was adopted in the PRISM design to enhance seismic safety margins and to allow the application of a standard nuclear island design to sites with different soil and seismic characteristics. The reactor system, the intermediate heat transport system including the steam generator, all safety systems including the RVACS, the containment system, reactor

protection system, EM pump coast down system, and the sodium service facility are located on a common platform that is supported by seismic isolation bearings.

The seismic isolation bearings provide a horizontally flexible element between the basement and the nuclear island platform to absorb seismic shocks by allowing the superstructure to displace rather than remaining rigid. When compared to a non-isolated system, the isolation system reduces the horizontal seismic accelerations that are transmitted to the reactor module by a factor of three. Equally important, the facilities that are seismically isolated can be adapted to suit a large range of sites by adjusting the seismic isolator characteristics.

3.3.2.3. Conclusion

In the GE-Hitachi funded PRISM design effort, it was determined that the thermal rating of each NSSS could be set to best fit a utility customer's needs, and the operating conditions could be modified to optimize the efficiency of the steam cycle as shown in Table 3.12. Through the use of an outside financing firm the estimated N-th of a Kind (NOAK) capital cost of a PRISM plant has been determined to be competitive with other new Light Water Reactors (LWRs) and Advanced LWRs (ALWRs).

The follow-on GEH financed PRISM work is confirming earlier assessments that indicated that a modular SFR would be more than competitive with a large monolithic SFR plant concepts. Utilizing a pool type design SFR with metallic fuel, PRISM eliminates many of the required safety features needed in a loop-type SFR. The PRISM's NSSS is compatible with factory fabrication and design simplifications that are not feasible for larger monolithic plants.

Passive features that are utilized to simplify the design and reduce its capital and operating cost include passive reactor shutdown, passive shutdown heat removal, and passive reactor cavity cooling. The independence of each of the NSSS's in a modular design improves the capacity factor and reduces the need for the utility to maintain a large spinning reserve in the event that a reactor scram occurs. Inherent advantages of the modular approach include:

- No scale up from the module size is required to achieve a competitive bus bar cost;
- Factory fabrication rather than "stick" construction is used to improve quality, reduce cost, and shorten the construction schedule;
- Passive shutdown, passive shutdown decay heat removal, and passive post accident containment cooling systems are used to simplify design and operation, improve the safety, and reduce capital and operating costs;
- Class 1-E safety related emergency power requirements are reduced to a level that can be met with batteries avoiding the need for expensive high capacity diesels;
- The ability of each of the modular NSSS to operate independently of each other improves the plant capacity factor and reduces the need for the owner to maintain a large spinning reserve in the event that the plant scrams.

3.3.3. BN-1800

3.3.3.1. Introduction

"Strategy of Nuclear Power Development in Russia in the First Half of XXI Century", approved by the Russian Government in 2000, calls for using fast reactors assuring fuel breeding and, hence, more efficient consumption of uranium resources, as a basis of the future nuclear power of Russia.

Therefore, it was considered necessary to start designing an advanced large size fast reactor with sodium coolant and related components of closed nuclear fuel cycle. For this purpose, conceptual studies of the BN-1800 reactor intended for operation in the closed fuel cycle have been made.

While the BN-800 is interpreted as the pilot reactor designed for demonstration of feasibility of highly effective closed fuel cycle based on FR and optimization of conditions of FR operation in the closed fuel cycle, the BN-1800 reactor is designed as series FR to be used in closed fuel cycle thus providing the basis of the future nuclear power in the Russian Federation.

So, the main goal of the BN-1800 design development is to create commercial breeder reactor operating in closed fuel cycle for the large-scale multi-component nuclear power.

3.3.3.2. Design description

3.3.3.2.1. BN-1800 reactor design basis

Design approaches employed in the BN-1800 reactor are based on the use of sodium technology, structural materials and technologies previously proven in the process of design and operation of BN type reactors. These proposals were made taking into account experience gained in designing and operating of power fast reactors in our country (BN-350, BN-600, BN-800 and BN-1600), as well as foreign experience in creation of the large size commercial reactors with sodium coolant. First of all, the experience gained in the designing of the BN-1600 reactor was used, because BN-1800 reactor design is its logical evolution. Thus, it is possible to speak about continuity in the development of the SFR programme in the Russian Federation.

3.3.3.2.2. Stages of design development, current status of design

In 2001, a design proposal on NPP with the BN-1800 reactor featuring enhanced safety was developed by four organizations, namely: Institute for Physics and Power Engineering (IPPE), Experimental Design Bureau (OKBM), Scientific Research and Design Institute of St. Petersburg ATOMENERGOPROEKT (SPbAEP), and Experimental and Design Organization “GIDROPRESS” (OKB GP). The results of these studies have shown that the creation of SFR having both the enhanced safety and economic parameters comparable with thermal reactors and thermal power units on fossil fuel is a really feasible task.

On the basis of this design proposal, the additional researches on parameters and basic technical decisions proposed in the design of the BN-1800 reactor were carried out and the appropriate recommendations are made which will be a basis for development of a conceptual design.

Development of the conceptual design of the BN-1800 reactor now is conducted. Studies of various options of implementation of a fuel cycle of the BN-1800 reactor are also started.

3.3.3.2.3. BN-1800 reactor plant concept and its main features

The option of large-size sodium cooled fast reactor with pool-type configuration of the primary circuit and conventional three-circuit scheme of the NPP was taken as the initial preconditions for development of the concept of advanced commercial fast reactor. At a stage of development of the design proposal on the BN-1800 reactor, the task was put to estimate

potential capacities of such SFR option. With the purpose of achievement of high economic parameters of the power unit, the variant with transition to supercritical steam parameters in the third circuit has been considered in the design proposal [6].

Further the researches and optimization of parameters and technical decisions directed on the maximal increase of safety and competitiveness of commercial large-size sodium cooled fast reactor were carried out with the purpose of a choice of the most acceptable option for the subsequent development at the stage of the conceptual design. Optimization researches of reactor power have been executed (the variants with reactor power of 4200 MW_{th}, 3750 MW_{th} and 2500 MW_{th} have been examined). Various schematic variants of the tertiary circuit have been also analyzed (the variants with supercritical and moderate parameters of a thermal cycle have been examined).

The variant of NPP with thermal reactor power of 4200 MW_{th} and with moderate parameters of sodium and tertiary circuits has been accepted on the base of performed research as the basic one to the further studies (Fig. 3.21).

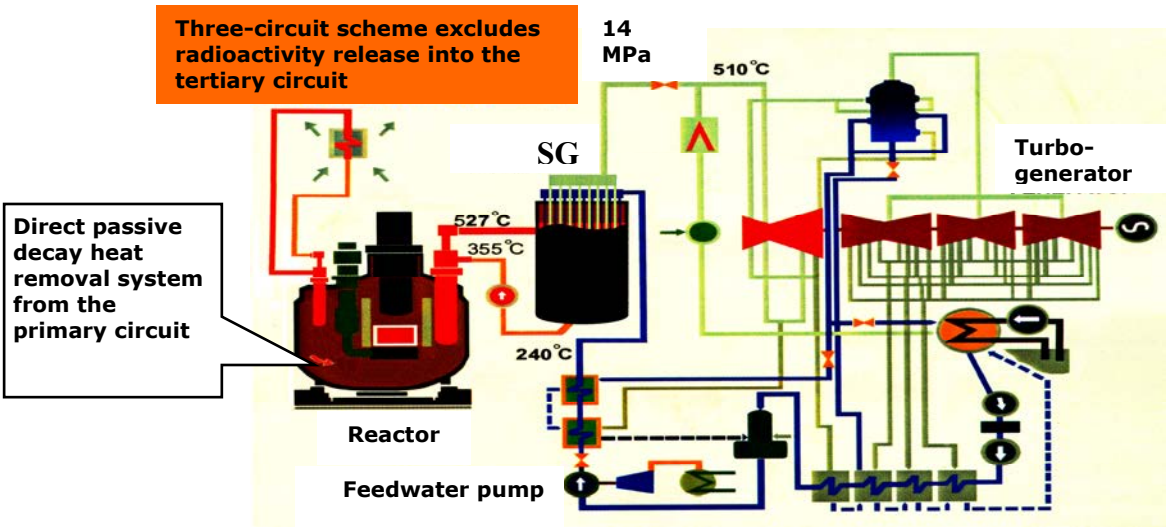

FIG. 3.21. The NPP variant with thermal reactor power of 4 200 MWth.

The basic characteristics of this variant are presented in the Table 3.13 [7].

TABLE 3.13. BN-1800 MAIN DESIGN DATA

Parameter	Value
Overall plan:	
Reactor thermal power, MW	4200
Unit electrical power, MW	1800
Operation life, year	60
Breeding ratio	1.2
Primary system:	
Coolant temperature, °C - core inlet - core outlet	 410 550
Protective gas pressure, MPa	0.055
Reactor vessel coolant mass, t	2350
Coolant flowrate, kg/s	23700
Pump delivery head, MPa	0.46
Number of circulating pumps	4
Reactor core:	
Equivalent core diameter, m	5.17
Active core height, m	0.85
Average core power density, MW/m^3	250
Number of core fuel assemblies	630
Fuel assembly duct width across flats, mm	184×3.5
Fuel	MOX (nitride fuel in future)
Number of fuel rods per assembly	271
Core fuel cladding OD × wall thickness, mm	9.5×0.6
Fuel rod linear heat rating (max.), kW/m	45
Average fuel burnup, % ha	11.1
Maximum fuel burnup, % ha	16.9
Core lifetime, ed	1650
Core refueling interval, ed	330
Reactor main vessel:	
Outer diameter, m	19.32
Overall height, m	19.4
Material	stainless steel Cr18Ni9
Secondary loop:	
Secondary coolant temperature, °C SG inlet SG outlet	 527 355
Secondary circuit sodium mass (four loops), t	870
Gas plenum pressure, MPa	0.254
Pump delivery head, MPa	0.4
Coolant flowrate, kg/s	4800
Tertiary circuit:	
Main steam pressure, MPa	14.0
Feedwater temperature, °C	240
Main steam temperature, °C	510
Steam reheating temperature, °C	250

A longitudinal section of the BN-1800 reactor is presented in Fig. 3.22.

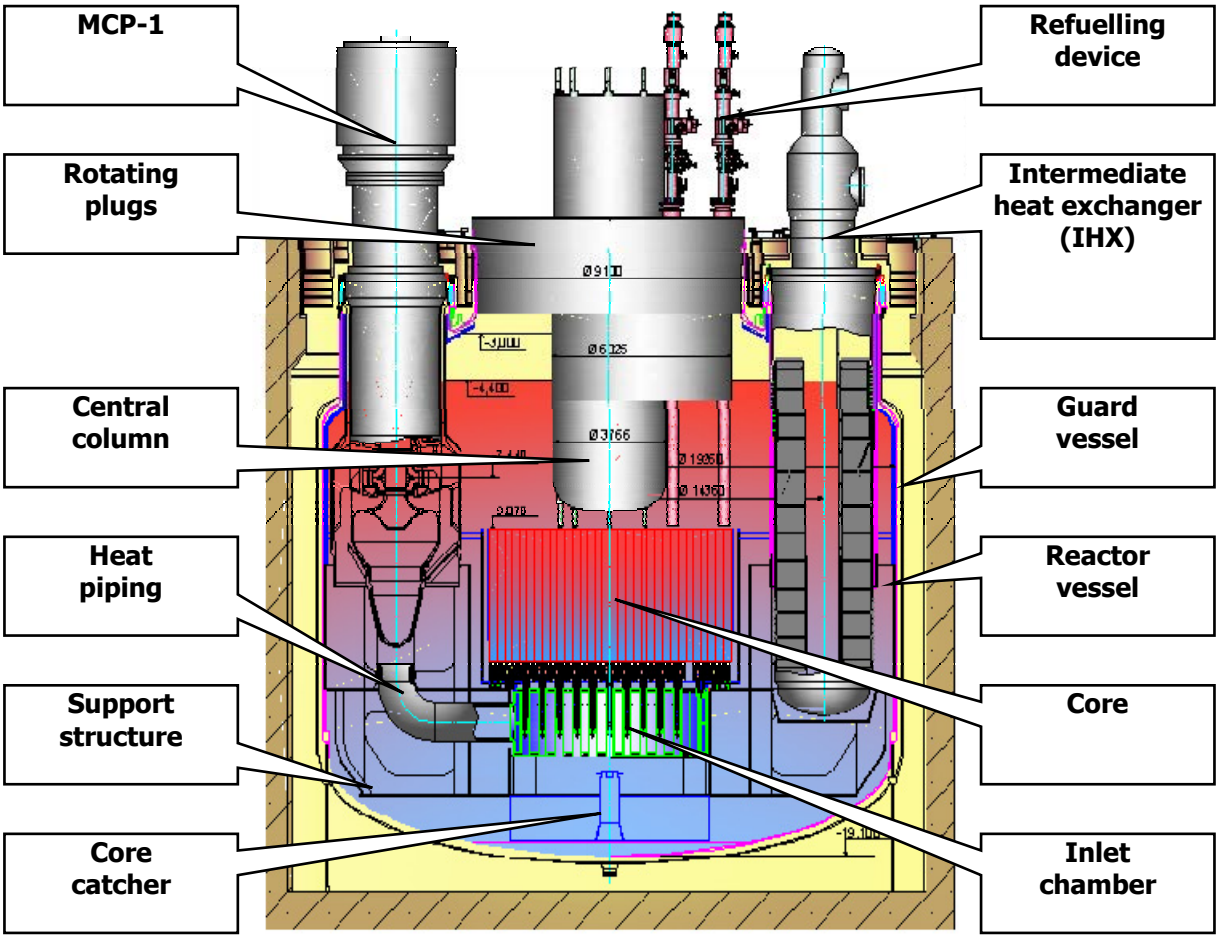

FIG. 3.22. Longitudinal section of the BN-1800 reactor.

The requirements corresponding to reactor plants of the fourth generation are taken into account at the development of the conceptual design of the BN-1800 reactor plant, in particular:

- Maximum use of inherent safety features;
- Providing high reliability of safety systems by the use of various passive safety devices;
- Elimination of the possibility of leaks and burning of radioactive sodium;
- Assurance of minimum impact on the environment.

The following conceptual technical and design decisions are accepted as a base:

- Pool type arrangement of the primary circuit is used with all sodium systems including cold traps located in the reactor vessel that makes it possible to eliminate in fact a danger of radioactive sodium release outside the reactor vessel and its fire;

- Number of loops in the primary circuit - 4 (each loop contains one IHX and one MCP-1);
- Number of loops in the secondary circuit - 4 (each loop contains one IHX, one MCP-2 and one SG);
- Once-through vessel-type SG of integrated type;
- Number of turbine units per power unit - 2;
- Steam reheating;
- Operation of the NPP at the stable (mainly, rated) power level is envisaged with load factor equal to at least 0.9;
- A closed nuclear fuel cycle excluding a stage of extraction of a pure plutonium is supposed;
- The exception of intermediate storage drums of fresh and spent FSA and organization of a capacious in-reactor vessel storage (IVS) of spent FSA (SFSA), providing exposure of SFSA over more than 1.5 years that allows carrying out a direct unloading of FSA from the IVS into washing cells and further into an exposure pool;
- The variant of decay heat removal system connected directly to the reactor vessel is considered as basic one;
- The variant with bottom support of the reactor vessel and loop-type variant of the hydraulic scheme of the basic circulation circuit of the primary sodium is considered as basic option.

3.3.3.3. Conclusion

Now in the Russian Federation, the development of the conceptual design of the BN-1800 fast reactor with sodium coolant is conducted, which is considered as series commercial power unit.

In accordance with the Strategy of Nuclear Power Development in the Russia Federation, it is supposed that the series FR will provide fuel breeding in closed fuel cycle and will be the basis of the nuclear power in Russia in the second half of the 21st century.

3.3.4. KALIMER

3.3.4.1. Introduction

The Korea Atomic Energy Research Institute (KAERI) has developed a sodium-cooled fast reactor KALIMER-600. The design objectives and the general design requirements of KALIMER-600 are given in Table 3.14. With a strong emphasis on proliferation resistance, the core design of KALIMER-600 is designed to not have a blanket. In addition, passive residual heat removal, shortened intermediate heat transfer system (IHTS) piping and seismic isolation are incorporated in the system design.

TABLE 3.14. KALIMER-600 DESIGN OBJECTIVES AND TOP-TIER DESIGN REQUIREMENTS

Design objectives	Sustainability Competitive economics	Enhanced safety Proliferation resistance
General design requirement	Reactor type	Pool-type sodium cooled fast reactor
	Plant size	600 MWe
	Plant design life	60 years
	Safety design philosophy	Emphasis on inherent safety mechanism
	Seismic design	Design basis earthquakes: 0.3 g seismic isolation
	Fuel type	Metal fuel
	Spent fuel	Spent fuel recycle by pyroprocessing
	Breeding ratio	1.0 no blanket assembly
Safety and investment protection	Accident resistance	Design simplification (large thermal capacity of the primary system)
		Diversified core shutdown mechanism (negative power reactivity effects)
	Core damage prevention	CDF $>10^6$ reactor year
		No fuel cladding liquid phase propagation during design basis events
		Highly reliable and diversified decay heat removal
Plant performance	Plant thermal efficiency	Net efficiency >39%
	Refuelling interval	≥ 18 months
	Spent fuel storage capacity in the reactor vessel	≥ 1 cycle discharge
	Load rejection capability	Should be able to accommodate 100% off-site load rejection without plant trip
	Operation, maintenance, and serviceability	Minimize the required numbers of operators (automatic inspection and diagnosis)
		Major equipment should be replaceable (human centered design)
	Construction cost	Design standardization

KALIMER-600 has a capacity of 600 MWe and a net plant efficiency of 39.4%. The core generates fission heat of 1523.4 MWt and is loaded with metal fuels of U-TRU-Zr. It is a pool type reactor and all the primary sodium is contained in a reactor vessel.

Table 3.15 summarizes the key design parameters of KALIMER-600.

TABLE 3.15. KALIMER-600 KEY DESIGN PARAMETERS

Item	Value
Overall	
Net plant power, MWe	600.0
Core power, MWt	1523.4
Gross plant Efficiency, %	41.9
Net plant Efficiency, %	39.4
Reactor	Pool Type
Number of IHTS Loops	2
Safety decay heat removal	PDRC
Seismic design	Seismic isolation bearing
Core	
Core configuration	Radially homogeneous
Core height, mm	940
Axial blanket thickness, mm	0
Maximum core diameter, mm	5209
Fuel form	U-TRU-10% Zr Alloy
Assembly pitch, mm	187.1
Moderator region height, mm	150
Fuel pin OD, mm	9.0
Fuel pin ID, mm (IC/MC/OC)	6.96/7.56/7.82
Cladding thickness, mm (IC/MC/OC)	1.02/0.72/0.59
Cladding material	Mod.HT9
PHTS	
Reactor core I/O temp., °C	390.0/545.0
Total PHTS flow rate, kg/s	7731.3
Primary pump	Centrifugal
Number of primary pumps	2
IHTS	
IHX I/O temp., °C	320.7/526.0
IHTS Total flow rate, kg/s	5800.7
IHTS Pump type	electromagnetic
Total number of IHXs	4
SGS	
Steam flow rate, kg/s	663.25
Steam temperature, °C	503.1
Steam pressure, MPa	16.5
Number of SGs	2

3.3.4.2. Design description

3.3.4.2.1. Reactor core design

The main design targets in order to meet the design requirements are as follows:

- Peak fast fluence $\leq 4.0 \times 10^{23}$ n/cm^2
- Breeding ratio without blanket ≈ 1.0
- Cycle length ≥ 18 months
- Average discharged burnup ≥ 80 MWd/kg
- Burnup reactivity swing < 1 \$

The KALIMER-600 core [8] was designed to have breakeven characteristics so as to produce exactly the amount of fissile material that it consumes, for proliferation resistance considerations. In order to further enhance the proliferation resistance, no blanket assembly was included in the design. However, the elimination of blanket caused the degradation of the sodium void reactivity worth and the Doppler coefficient. Therefore, the KALIMER-600 breakeven core has been optimized to reduce the sodium void reactivity worth.

The KALIMER-600 breakeven core uses a single enrichment fuel concept. The use of a single enrichment fuel leads to a spatially uniform distribution of conversion ratio and it makes the change of the power distribution from BOEC to EOEC small. As the result, the orifice design with use of a single enrichment fuels will become easier. On the other hand, special fuel assembly designs are required to control high power peaking factor under a single enrichment fuel core.

In the KALIMER-600 core, the cladding thickness is changed along the core regions for the purpose of a power profile flattening. The cladding thicknesses of the fuel rods in the inner, middle, and outer core regions are different, while the outer diameters of all the fuel rods are the same. Figure 3.23 shows the core configuration of the KALIMER-600 core.

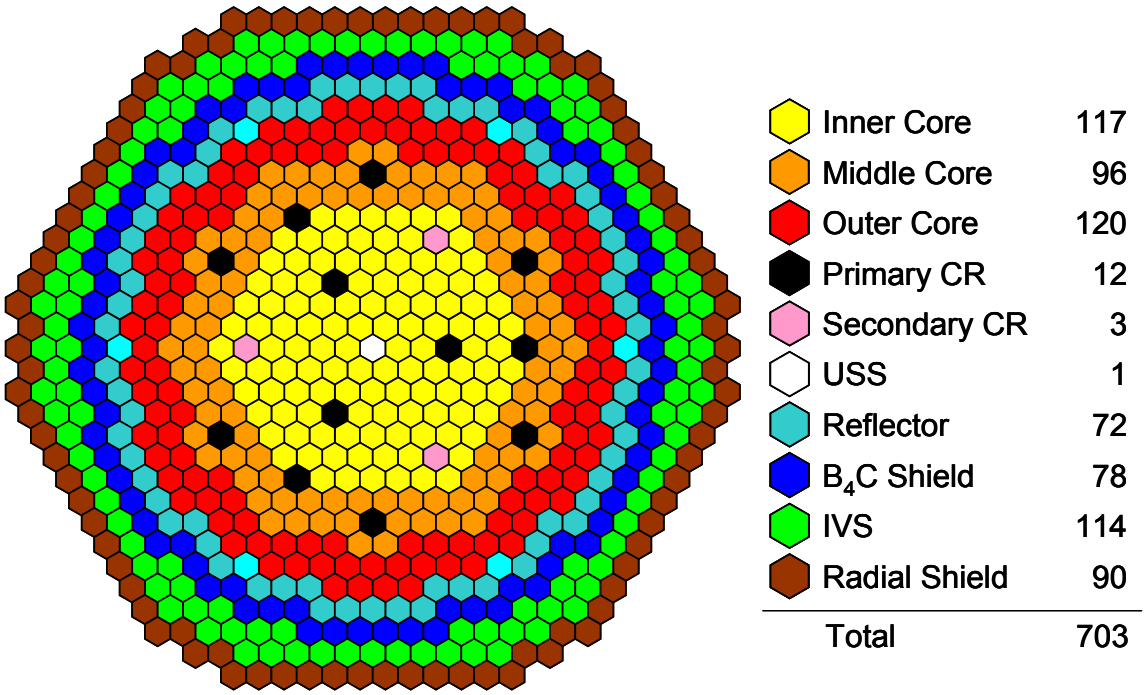

FIG. 3.23. KALIMER-600 Breakeven core layout.

The core is radially homogeneous and incorporates annular rings with fuels of a single enrichment. The active core consists of three fuel regions (i.e., inner, middle, and outer core regions) which have 117, 96, and 120 fuel assemblies, respectively. A 15 cm-thick (at hot state) graphite moderator region is placed just below the active fuel region. Each fuel assembly has 271 fuel pins with the pin pitch-to-diameter ratio (P/D) of 1.167. The fuel rods in the inner, middle, and outer core regions have 1.02 mm-, 0.72 mm-, and 0.59 mm-thick claddings, respectively, but their outer diameters are all the same (i.e., 9.0 mm). The fuel is U-TRU-10%Zr metal and the core structural material is modified HT9, chosen for its low irradiation swelling characteristics.

Table 3.16 shows the summary of nuclear performance of an equilibrium cycle.

TABLE 3.16. SUMMARY OF NUCLEAR PERFORMANCE OF EQUILIBRIUM CYCLE

Parameter	Value
Average conversion ratio	1.0
Cycle length (EFPM)	18
Burnup reactivity swing (pcm)	344
Number of batches, Inner/Middle/Outer cores	4/4/4
TRU wt% in fuel at BOEC	15.5
Average/peak fuel discharge burnup (MWd/kg)	80.4/125.4
Average power density (BOEC, W/cm^3)	148.5
Average linear power for fuel (W/cm)	168.3
Power peaking factors for fuel (BOEC/EOEC)	1.498/1.489
Peak discharge fast neutron fluence (10^{23} n/cm^2)	3.918
Sodium void worth (BOEC/EOEC, $)	7.4/7.6
Effective delayed neutron fraction, BOEC/EOEC	0.00351/0.00348

The cycle length is 18 EFPMs with the one-fourth of the fuel being replaced upon each refuelling. The burnup reactivity swing during a cycle is 344 pcm, less than 1 $. The average discharge burnup is 80.4 MWd/kg and peak discharge burnup is 125.4 MWd/kg. The cycle average breeding ratio is estimated to be 1.00. The sodium void worths for a voiding of the flowing sodium coolants both in the active core and the coolant channel of the upper gas plenum are 7.4 $ at BOEC and 7.6 $ at EOEC, respectively.

The reactivity control and shutdown system consists of fifteen control rods (twelve for primary control system and three for secondary control system) that are used for a power control, burnup compensation and a reactor shutdown. Each control rod unit consists of an array of tubes containing B_4C and provides two diverse scram methods; a gravity-driven rod drop and a powered-driven one.

3.3.4.2.2. Heat transport system design

The heat transport system of KALIMER-600 consists of Primary Heat Transport Systems (PHTS), Intermediate Heat Transport Systems (IHTS), Residual Heat Removal Systems (RHRS) and Steam Generating Systems (SGS). The PHTS removes the heat from the reactor core and transports the heat to the IHTS through the Intermediate Heat Exchangers (IHXs), and the IHTS transports the heat to the once through type Steam Generator (SG). The transported heat is used to convert water to superheated steam in the SG and the steam is provided to the turbine generator to produce electricity.

The PDRC system is designed to have a sufficient heat removal capacity enough to ensure that the system can be safely cooled down during an emergency shutdown condition, like a loss of a heat sink accident. The heat removal capacity of the proposed PDRC system is 16.5 MWt, which is equivalent to about 1% of the rated core thermal power with a 10% design margin. The PDRC component sizing was fulfilled based on the design capacity and the system conditions, conservatively defined with a primary sodium temperature of 545°C at the Decay Heat Exchanger (DHX) inlet and an air inlet temperature of 40°C.

The DHX is a shell-and-tube type counter-current flow heat exchanger. It is placed at a position higher than the cold pool free surface during a normal plant operation, and thus it is not directly in contact with the hot sodium. This feature makes the heat loss through the PDRC system during a normal plant operation fairly small. The sodium-air heat exchanger (AHX), placed above the reactor building, has the function of dumping the system heat load into the final heat sink, i.e., the atmosphere, and the counter-wound heat transfer tubes are helically arranged. Heat is transmitted from the primary sodium pool into the intermediate sodium loop via the DHX, and a direct heat exchange occurs between the sodium and the atmospheric air through the AHX sodium tube wall. When the normal heat transport path is not available, an adequate emergency core cooling method should be provided to accomplish a long-term cooling of the reactor core and a sodium coolant boundary without exceeding the temperature limit. Figure 3.24 shows a schematic drawing of the PDRC operation mode under a transient condition, e.g. a station blackout.

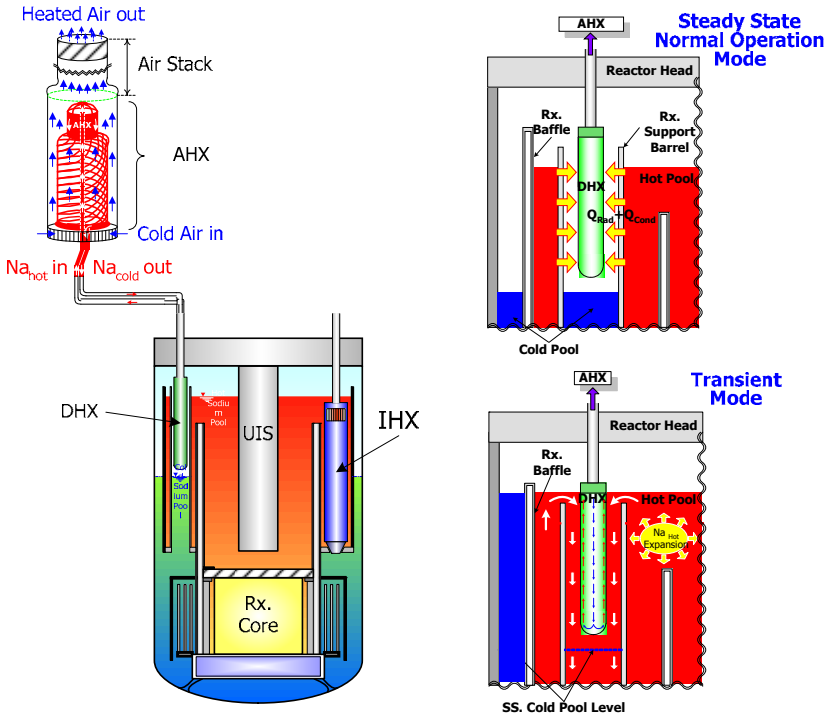

FIG. 3.24. Configuration and DHR Process of PDRC.

The net plant efficiency of KALIMER-600 is estimated to be 39.4%, which is higher than the Gen-IV standard requirements of 38%. In order to achieve such a high efficiency, the operating parameter of a 100% power operation is established as shown Fig. 3.25.

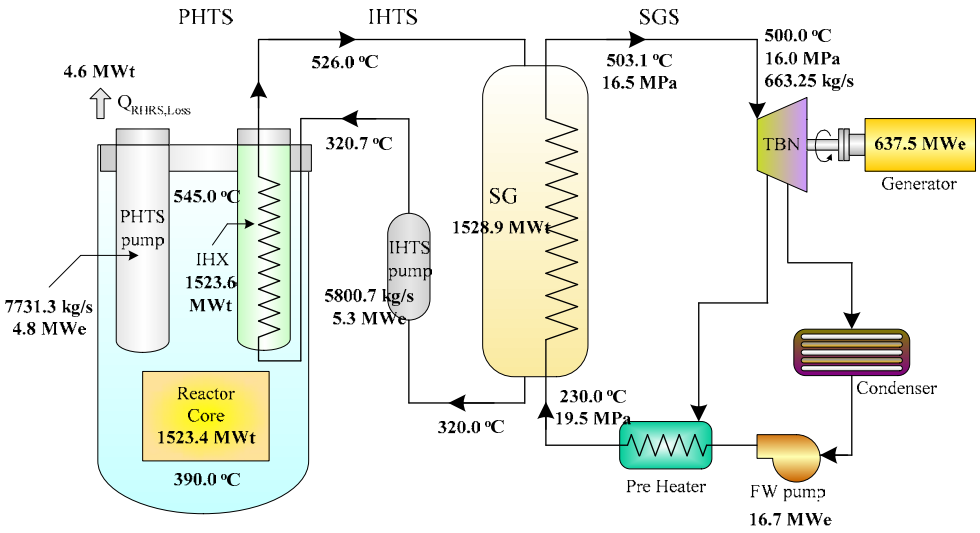

- **Net Plant Power = 600.0 MWe**
- **Gross Efficiency = 41.9 %**
- **Net Efficiency = 39.4 %**

FIG. 3.25. Plant operating parameters at 100% power.

3.3.4.2.3. Mechanical structure design

The main features of the mechanical structure design in KALIMER-600 are the seismically isolated reactor building, the reduced total pipe length of the IHTS, the simplified reactor support, and the compact reactor internal structures. The overall configuration of the KALIMER-600 reactor building and the internal configuration of the reactor vessel are shown in Fig. 3.26. A total of 164 seismic isolators (ϕ 1.2 m) are installed between the ground and lower basemat in the KALIMER-600 reactor building (W 49 m x D 36 m x H 54 m).

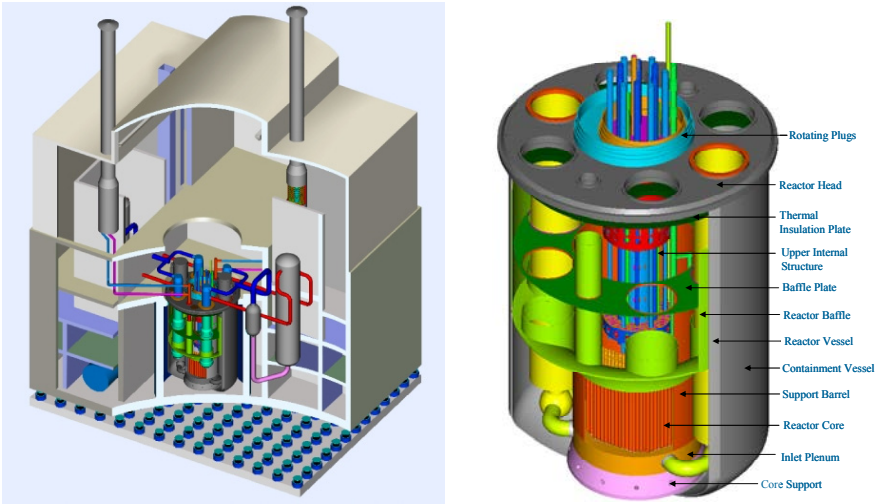

FIG. 3.26. KALIMER-600 reactor building and reactor vessel.

The reactor vessel, which is made of type 316 stainless steel, has overall dimensions of 18 m in height, 11.41 m in outer diameter, and 0.05 m in thickness. The total reactor weight is about 2 800 tons. The space inside the reactor vessel is thermally divided into two regions; that is the hot pool region and the cold pool region. The support barrel, the baffle plate and the

reactor baffle form the boundary of the two regions. The reactor vessel for KALIMER-600 is directly in contact with the cold sodium of 390°C. So, the reactor vessel can maintain its structural integrity for a 60 years design lifetime.

As for the reactor internals, a simple skirt type core support structure, integrated cylinder type support barrel, UIS and a core shield structure are conceptually designed and the design of the inlet pipe is simplified. The baffle annulus structure in the reactor internals can accommodate a large thermal difference between the hot pool and cold pool regions.

The reactor head in KALIMER-600 is the top closure of both the reactor vessel and the lower containment vessel. It provides a mechanical support for all the PHTS components including the IHXs, PHTS pumps, rotatable plug and the primary sodium. The reactor head is a single piece of welded steel plate that is 50 cm thick. It is designed to operate at temperatures lower than 150°C. This temperature is attained by the inclusion of 5 horizontal layers of stainless steel insulation and a shield plate below the reactor head. The top one of them is installed 45 cm below the bottom of the reactor head.

The KALIMER-600 containment design, shown in Fig. 3.27, provides defence-in-depth for a full spectrum of severe accidents including hypothetical core disruptive accidents (HCDAs).

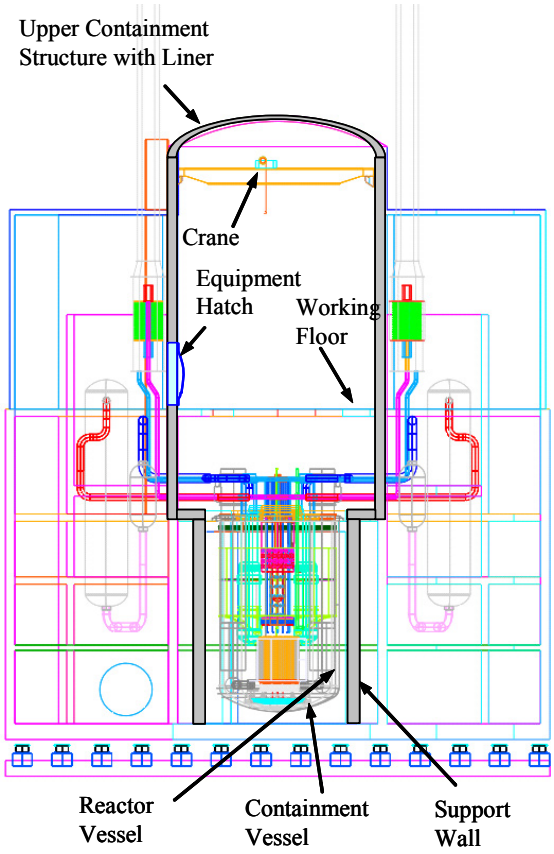

FIG. 3.27. Schematics of the containment dome.

It forms a low leakage, pressure-retaining boundary which completely surrounds the primary system boundary. The containment consists of the lower containment vessel designed to contain reactor vessel leaks and the upper containment structure which mitigates the

consequence of severe events such as an HCDA which are postulated to cause the introduction of radio-nuclides through the reactor head into the region above the reactor.

3.3.4.2.4. Safety analysis

The preliminary safety analyses have been performed to evaluate the plant response, the performance of the inherent safety features, and the margin to the plant safety limits. In the analyses, the system-wide transient and safety analysis code, SSC-K [9, 10] was used. The events analyzed were an unprotected transient over power (UTOP), an unprotected loss of flow (ULOF), and an unprotected loss of heat sink (ULOHS).

The UTOP is assumed to insert 39 cents, 2.6 cents per second for 15 seconds, by a withdrawal of all the control rods. The power reaches a peak of 1.55 times the rated power at 42 seconds, and stabilizes at 1.09 times the rated power after 8 minutes. The net reactivity starts out positive because of the reactivity from the control rods being removed, but turns downward once the negative reactivity feedback increases enough to counter the positive insertion. The equilibrium temperatures are re-established after the initial phase of the UTOP, where the core remains indefinitely hotter to offset the increased reactivity, which limits the maximum reactivity insertion during the event.

The ULOF event is initiated by a trip of all primary pumps followed by a coastdown. For a loss of flow accident, the power to flow ratio is the key parameter that determines the consequences of an accident. The reduction of a core flow due to the pump trips causes an initial peak in the fuel centreline temperature before the power begins to fall by the effects of a reactivity feedback. It is shown that the fuel damage due to the temperature increase during the initial phase of the transient is not a significant risk for this event.

The ULOHS accident is assumed to begin with a sudden loss of the normal heat sink by the IHTS and steam generators. The only heat removal is achieved by the PDRC. When the sodium heats up, a flow path of sodium from the core to the PDRC through the hot pool is formed and the PDRC heat removal rate is increased. The long-term cooling capability of the KALIMER-600 design was evaluated for different heat removal rates through the PDRC using the SSC-K linked with a simple long-term cooling model. It is shown that the limit of the PDRC capacity is about 15.4 MW. Therefore, the current PDRC design capacity of 16.5 MW has a margin of about 1.1 MW.

The analyses results for the unprotected events are summarized in Table 3.17 and Fig. 3.28, which imply the inherent safety characteristics of KALIMER-600.

TABLE 3.17. INHERENT SAFETY CHARACTERISTICS OF THE KALIMER-600

	Peak fuel centreline temp. (°C)	Peak clad temp. (°C)	Peak coolant temp. (°C)	Average core outlet temp. (°C)
DBE Limit	955	<700	1055	<5 hr: 650-700 >1 hr: 700-760
UTOP	798	697	637	630
ULOF	727	706	694	694
ULOHS	664	597	574	573

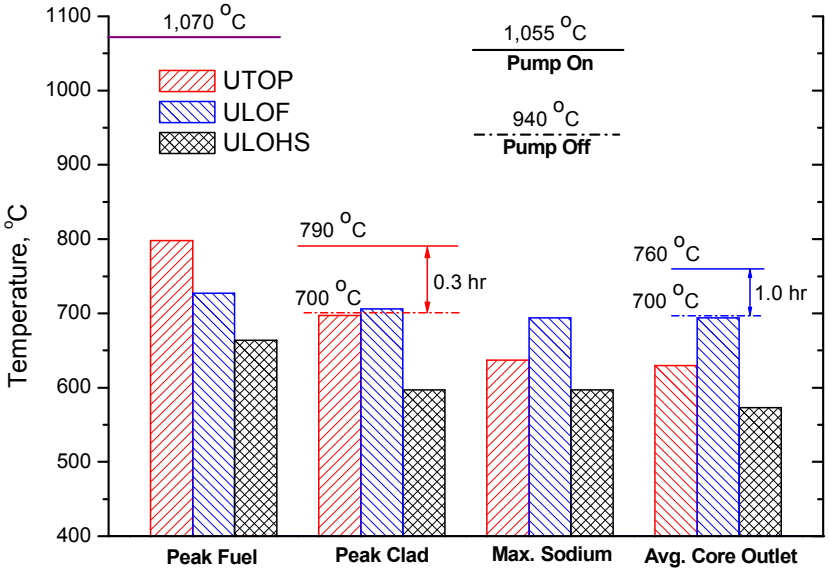

FIG. 3.28. Safety limits and margins for the ATWSs.

From these results it can be said that the KALIMER-600 design accommodates the various ATWS events without any threat to the plant's safety. The self- regulation of the power level without a scram is mainly due to the inherent and passive reactivity feedback mechanisms implemented in the design.

3.3.4.3. Current status

At the early stage of its development (Phase for basic LMR technologies: 1992–1997), the development efforts focused on basic R&D on core neutronics, thermal hydraulics and sodium technology, aiming at enhancing the basic liquid metal-cooled reactor (LMR) technology capabilities. The basic R&D efforts made at the early development stage have been extended to direct towards the development of the basic key technologies and the advanced fast reactor concept called KALIMER-600 (600 MWe) since 1997 under the revised nuclear R&D program. During Phases 1 and 2 (1997-2001), the conceptual design of KALIMER-150 (150 MWe) had been developed. During Phases 3 and 4 (2002–2006), the conceptual design of KALIMER-600 (600 MWe) have been developed.

In parallel with the KALIMER-600 system design, several items of R&D activities have been conducted. Current R&D items are a performance analysis of the PDRC system, experimental analysis of the sodium-water reaction phenomena, development of SIE ASME-NH code, waveguide sensor visualization, and development of safety analysis code.

A transient simulation method for the PDRC system has been developed and quantitative transient analyses results were provided by using the computer code POSPA [11]. By using the developed code, performance analysis of the PDRC system was carried out for a postulated design basis accident, i.e. a loss of a heat sink due to a station blackout.

Figure 3.29 shows the transient behaviour of the system temperature variations during the postulated condition.

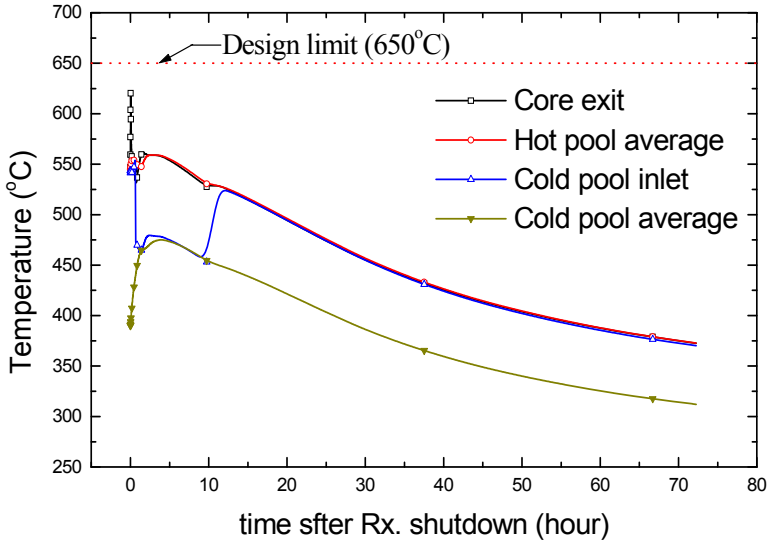

FIG. 3.29. Transient behaviour of the PDRC system.

As depicted in the figure, the core exit temperature reaches a peak of 621°C just after reactor shutdown and then it decreases. This is mainly due to the discrepancy between the core power decrease and the primary mass flow decrease, but the initial peak value satisfies the design limit of 650°C. This shows that, for the postulated design basis accident condition, the heat removal capacity of the provided PDRC system is sufficient. The self-wastage phenomena caused by small water/steam leaks were analyzed to evaluate the design criteria and design analysis procedures for the steam generators from the point of view of sodium-water reactions. A series of tests was carried out to investigate the enlargement rate of a nozzle hole itself with time for 2.25Cr-1Mo and Mod.9Cr-1Mo steel used for the heat transfer tube materials of an LMR steam generator. The initial size of the nozzle hole, which was used in the tests, was 0.2 mm in diameter and the initial leak rate was 0.38 g/sec H_2O. Enlargement rate of the nozzle hole itself was measured at 30 second intervals. As shown in Fig. 3.30, the phenomenon where the size of the nozzle hole became larger with an increasing duration of the steam injection appeared together from the two types of material.

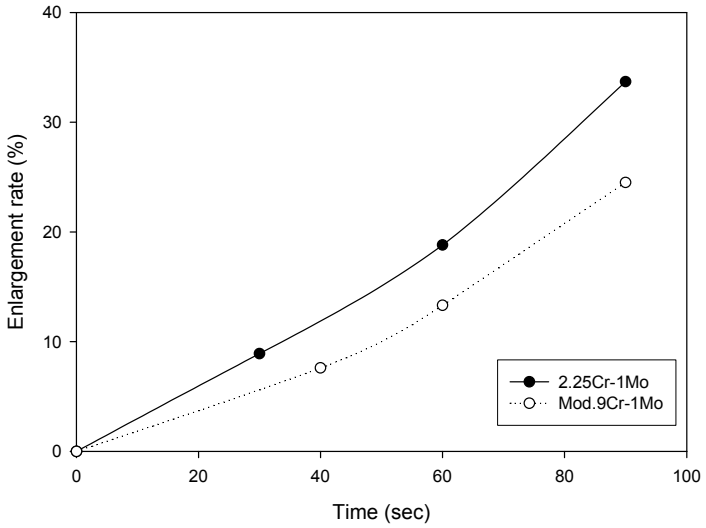

FIG. 3.30. Enlargement rate of the nozzle hole as a function of time.

Enlargement rate was slightly larger in the 2.25Cr-1Mo steel than in the Mod.9Cr-1Mo steel. Based on the cross-sectional area of a nozzle hole after a 90 second injection testing, it was estimated that the size of the nozzle hole became larger by about 1.34 times when compared with the initial value for the 2.25Cr-1Mo steel.

SIE ASME-NH code was developed to computerize the implementation of ASME Boiler and Pressure Vessels Code Section III Subsection NH rules including the time-dependent primary stress limits, the total accumulated creep ratcheting strain limits, and the creep-fatigue damage limits for both base metals and weldments. The computer code is an easy user interface program and can be an effective tool for the high temperature structural integrity evaluations of a SFR.

The waveguide sensor visualization technology was developed to inspect reactor internals by using some of the specific waveguides remaining in the hot sodium. The sensor can be applicable for the under-sodium visualization, ranging and dimensional gauging. To validate the visualization techniques for an underwater condition, a waveguide specimen was fabricated, which is a 250 mm long stainless steel plate, 15 mm wide and 1 mm thick. A C-scan visualization experiment for a similar shape of the reactor core was performed. The visualization image is clearly identified as shown in Fig. 3.31.

(a) Mock-up *(b) C-scan result*

FIG. 3.31 Visualization image of the reactor core mock-up using the waveguide sensor.

As the second verification, the test target is made of stainless steel with slits of different widths (2 mm, 1 mm, 0.8 mm and 0.5 mm) and loose parts (stepped plate, small nut and washer) on the surface. Figure 3.32 shows the visualization image of the test target. The loose part reflectors were identified clearly and the slit of a 2 mm width was observed successfully.

A detailed three-dimensional fuel subassembly thermal-hydraulic model has been developed and it was implemented in the system transient analysis code, SSC-K, which has been developed by KAERI for the evaluation of an abnormal transient or accident in a sodium-cooled fast reactor. The code is based on SSC-L, originally developed at BNL to analyze loop-type LMR transients [12].

The SSC-K code aims at handling a wide range of transients, including normal operational transients and anticipated unprotected events in a pool-type reactor. Therefore, both a model development and its verification have been continued because the dynamic response of the

primary coolant in a pool-type LMR, particularly the hot pool concept, can be quite different from that in the loop-type LMR.

Major modifications have been made for the hot pool model, core thermal-hydraulic model, reactivity model, and the passive decay heat removal system model. In particular, a one-dimensional hot pool model has been substituted with a more detailed two-dimensional hot pool (HP-2D) model [13] and a three-dimensional core thermal-hydraulic module has been added for an accurate prediction of the temperature and flow distribution in core subassemblies.

3.3.5. JSFR

3.3.5.1. Introduction [14, 15]

The Japan Atomic Energy Agency (JAEA) and electric utilities initiated the Feasibility Study (FS) in July, 1999 in collaboration with the Central Research Institute of Electric Power Industry (CRIEPI) and manufacturers, in order to effectively utilize the accumulated knowledge from the demonstration fast breeder reactor (DFBR) design, as well as the construction/operation experience from an experimental fast reactor, JOYO and a prototype fast breeder reactor, MONJU.

The objective of this study is "to present both an appropriate picture of commercialization of the FR cycle and the research and development (R&D) programs leading up to the commercialization in approximately 2015." Firstly, the five development targets have been established: safety, economic competitiveness, reduction of environmental burden, efficient utilization of nuclear fuel resources, and enhancement of nuclear non-proliferation.

3.3.5.2. Design description

3.3.5.2.1. Overview

An innovative concept of sodium-cooled FR named Japan Sodium-cooled Fast Reactor (JSFR) has been created through the FS and achieved the full satisfaction of development targets. This concept is recognized as a promising candidate for Generation IV system [17, 18]. JSFR is a sodium cooled, MOX (or metal) fuelled, advanced loop type fast reactor that evolves from Japanese fast reactor technologies and experience. There are two options of the reactor sizes, i.e. a large scaled reactor option generating 1 500 MWe and a medium scaled reactor option generating 750 MWe with the similar plant configuration.

The large-scale sodium-cooled reactor utilizes the advantage of "economy of scale" by setting the electricity output of 1500 MWe, proceeding to communization of facilities by designing as a twin plant [total electricity output of 3000 MWe], and reducing the amount of materials by design improvement. The schematic of the reactor and cooling system are shown in Figs 3.32 and 3.33.

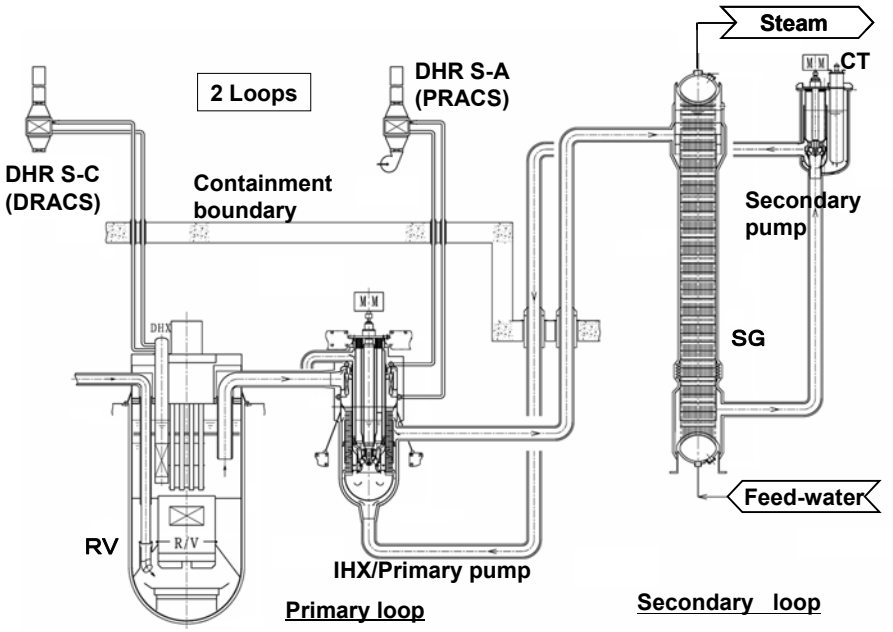

FIG. 3.32. Conceptual scheme of JSFR reactor and cooling system.

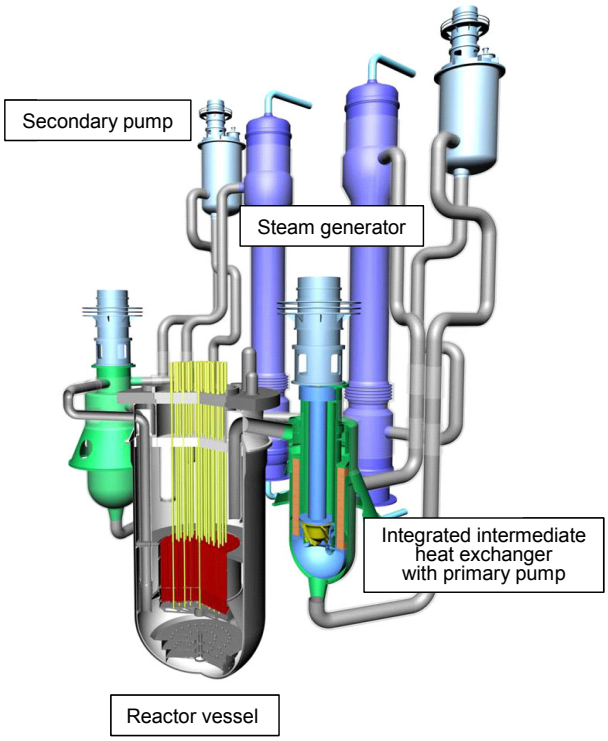

FIG. 3.33. Bird's-eye view of JFSR.

3.3.5.2.2. Reactor vessel and reactor internal structure [16, 19]

Figure 3.34 shows a conceptual scheme of the reactor vessel and reactor internal structure.

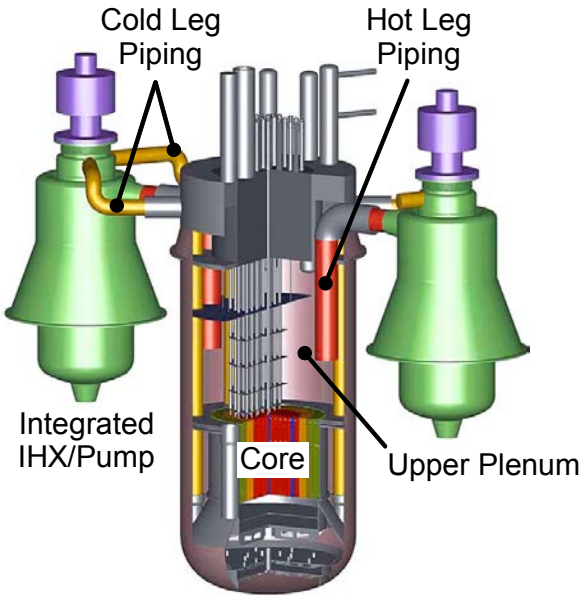

FIG. 3.34. Reactor vessel and primary piping system.

In order to reduce the amount of structural materials, the diameter and wall thickness of the reactor vessel are minimized and the reactor internal structures are simplified. The diameter, height, and wall thickness of the reactor vessel are 10.7 m, 21.2 m, and 30 mm, respectively.

A reactor vessel diameter of 10.7 m is realized by the compact design of the core and closure head structure. In this plant, a shell-less column–type upper internal structure (UIS) is adopted. The fuel handling machine (FHM) can enter into the center of this UIS, which has many control rod guide tubes. As this type of UIS makes it possible to conduct fuel handling with the UIS remaining just above the core, the diameter of a single rotating plug sets smaller, and this leads to the compact design of the closure head structure. The 30-mm wall thickness is realized by introducing the recriticality free technology that can mitigate mechanical energy release resulting from hypothetical core disruptive accident (CDA) and by introducing the seismic isolation technology that can mitigate seismic load.

In addition, a simple hot vessel design has been employed. Structural integrity against a thermal stress caused by an axial temperature profile around the liquid surface of the reactor vessel is ensured by establishment of an advanced elevated temperature structural design standard, which makes it possible to use an inelastic analysis, and by a direct assumption method of the thermal load. Further simplification of the structure is planned to reduce the amount of materials. Such simplification is attained by adopting a simple skirt-type core support structure, eliminating the vessel wall cooling system, eliminating the liquid-surface level control, etc. A dipped plate is employed to suppress a cover-gas entrainment in the coolant from the liquid surface of the reactor vessel because of an increased sodium velocity due to the compact design of the reactor vessel.

3.3.5.2.3. Reactor core and fuel [20]

The sodium cooled reactor core design studies in the FS, major consideration is concentrated on the following requirements.

(i) Core coolant void reactivity should be low enough to prevent the super-prompt criticality in the initiating phase of CDA. Measures of early discharge of molten fuel should be

considered in the core and fuel design to prevent the recriticality in the transition phase of CDA.

(ii) The target of core average discharge burnup is 150 GWd/t, and the total average discharge burnup (including blankets) ~60 GWd/t or more. The burnup target aims at the reduction of fuel cycle cost due to the economic competitiveness requirement. The high burnup also contribute to reduce the fuel mass capacity requirement of fuel cycle facilities.

(iii) Core should have flexible breeding capability in a viewpoint of uranium resource utilization. The target of maximum breeding ratio is from 1.1 to 1.2. The requirement of breeding capability is not only for the fuel breeding itself, but also for other requirements such as economic advantage, environmental burden reduction, etc. The core with high breeding capability possesses characteristic of high internal conversion ratio, which means the advantages for flexible core design management such as less blanket, enhanced capability for environmental burden reduction, longer reactor operation cycle duration.

(iv) From economics and proliferation resistance viewpoints, the core should have the capability of loading the low decontamination fuel associated with economical fuel recycle system. It should have also the capability of loading the fuel with a few percents of minor actinides (MA) from uranium resource utilization and environmental burden reduction viewpoints.

Figure 3.35 shows conceptual view of FAIDUS (Fuel Assembly with Inner Duct Structure) type subassembly.

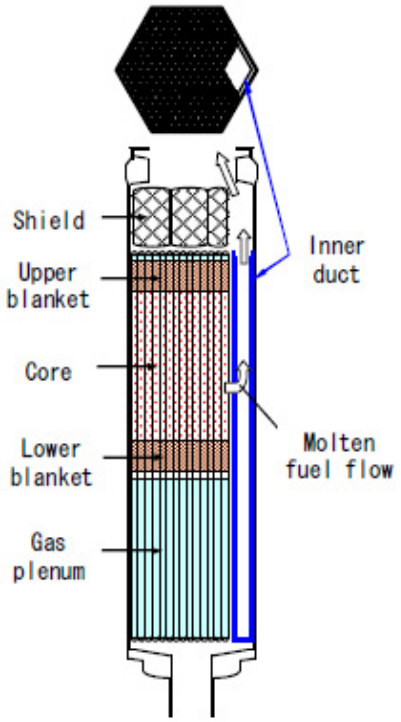

FIG. 3.35. FAIDUS type fuel subassembly.

In this subassembly, an inner duct is installed at the corner of the subassembly and a part of upper shielding element is removed. The molten fuel enters the inner duct channel and goes out directly into the outside without interfered by the upper shielding. The FAIDUS type is expected to have superior performance for molten fuel release at CDA to the precedent ABLE (Axial Blanket Elimination) type and have less issue for fabrication.

Figure 3.36 shows the configurations of the breeding core and beak even core.

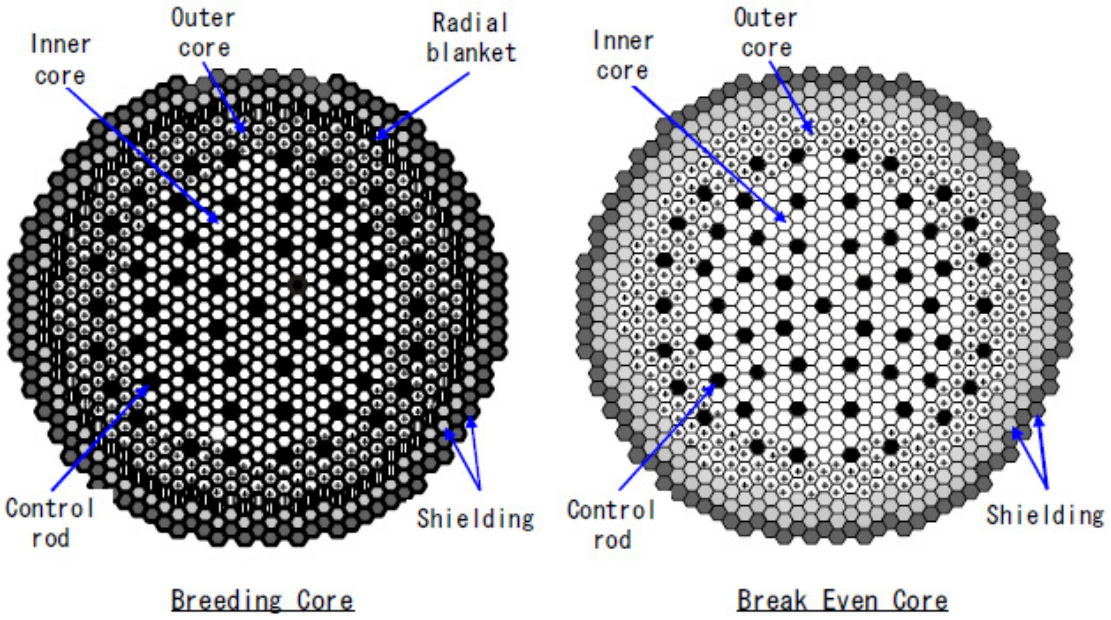

FIG. 3.36. Core configuration of oxide fuel core.

An advanced concept of large diameter fuel pin is applied into the oxide fuel core in order to obtain high internal conversion ratio. This leads to the break even breeding core, in which the breeding ratio is just above 1.0, without radial blanket. Total discharge average burnup (including blanket) achieves as high as about 100 GWd/t in refueling batch average including blanket. The achieved ave`raged burnup is extremely higher than conventional design with small diameter fuel pin. The cores have flexibility to be modified to breeding core with 1.1 of breeding ratio by adopting radial blanket. This advanced concept has economical advantage by consistently achieving high burnup and breeding with small amount of blanket. The major core performances of large scale core are as follows;

- The total average discharge burnup (including blanket) of breeding core is 90 GWd/t and break even core is 115 GWd/t. This means 50 ~ 90% higher value than the requirement of FS (60 GWd/t) could be attained.
- The operation cycle length is able to attain 26 months. This means 8 months longer than the requirement of FS.
- The breeding ratio of breeding core achieves over 1.1 and break even core is 1.03, so that this core has breeding flexibility corresponding to FR deployment scenario of FS.

3.3.5.2.4. Heat transport system

(a) Primary and intermediate heat transport systems [18, 19]

Concept of Cooling System. In order to select the most advantageous concept of the cooling system, the loop number, primary piping system, and applicability of the integration of components have been comprehensively examined from the viewpoint of the amount of materials, safety, maintainability, fabricability, etc. As a result of the examinations, the following were selected: two-loop cooling system, top-entry piping, integrated design of an IHX and a primary pump, and separated design of an SG and a secondary pump.

Shortened piping layout. The drastically shortened primary and secondary piping layout results in a compact plant configuration through a close arrangement of components, as well as a reduction of the amount of piping materials.

In particular, the primary hot-leg piping has been simplified. It is designed as a simple L-shaped piping and has a structure that absorbs a thermal expansion by only one elbow. Such a shortened piping layout with one elbow is realized with the aid of an adoption of Mod.9Cr-1Mo-steel which embodies high strength and low thermal expansion coefficient.

Reduction of loop number. The sodium-cooled system has some desirable characteristics: i.e., the high boiling point and the high heat conductivity of the sodium coolant that can raise the heat transfer capacity per unit volume of heat exchangers under low pressure condition. Owing to these desirable characteristics, it is possible to design heat exchangers that have a larger capacity by putting compact heat transfer structures in a vessel with a large diameter and a thin wall thickness.

The adoption of Mod.9Cr-1Mo-steel with high strength and high heat conductivity makes it possible to enlarge the heat transfer capacity further than that of the conventional design because a thinner heat transfer tube is available and it is easier to ensure the structural integrity against thermal stress by a large tube sheet. In this design, the capacity of the heat exchangers (i.e., the heat transfer capacity per one-cooling loop) has been enlarged as far as the fabricability and the structural integrity of the components are expected to be ensured, and then the number of loops has been reduced to two. According to the analytical estimation on this reduction effect, the two-loop system can reduce ~ 13% of the nuclear steam supply system (NSSS) weight and ~ 10% of the reactor building volume compared with the four-loop system.

Although the fuel integrity in a primary pump stick accident and the structural integrity of the large tube sheets of the heat exchangers against a thermal stress become critical issues with employing the two-loop cooling system, prospects for solution have been obtained through analytical examinations.

(b) IHX and reactor coolant pump

Type of pumps. Although there is an option of selecting electromagnetic pumps (EMPs) for the primary and secondary systems, conventional mechanical pumps have been selected for these systems in JSFR since long term R&D would be required to put a large EMP (more than three times as much as the EMP adopted in the Japanese DFBR design) to practical use.

Integration of IHX and reactor coolant pump. According to the comparison between the integrated and separated design of an IHX and a primary pump, the integrated design can reduce ~ 13% of the reactor and primary system weight and ~ 9% of the containment volume compared with the separated design. Thus, by integrating the IHX and the primary pump, the primary cooling system can be remarkably simplified.

In addition, in the case of the integrated design, improvements of maintainability are expected. That is, middle-leg piping between an IHX and a primary pump, on which it is difficult to do maintenance, can be eliminated, and in-place maintenance of the IHX tubes is easy by accessing to the IHX tubes through the center hole after withdrawal of the primary pump. For the above reasons, the integrated design has been selected. Figure 3.37 shows the conceptual scheme of the integrated components.

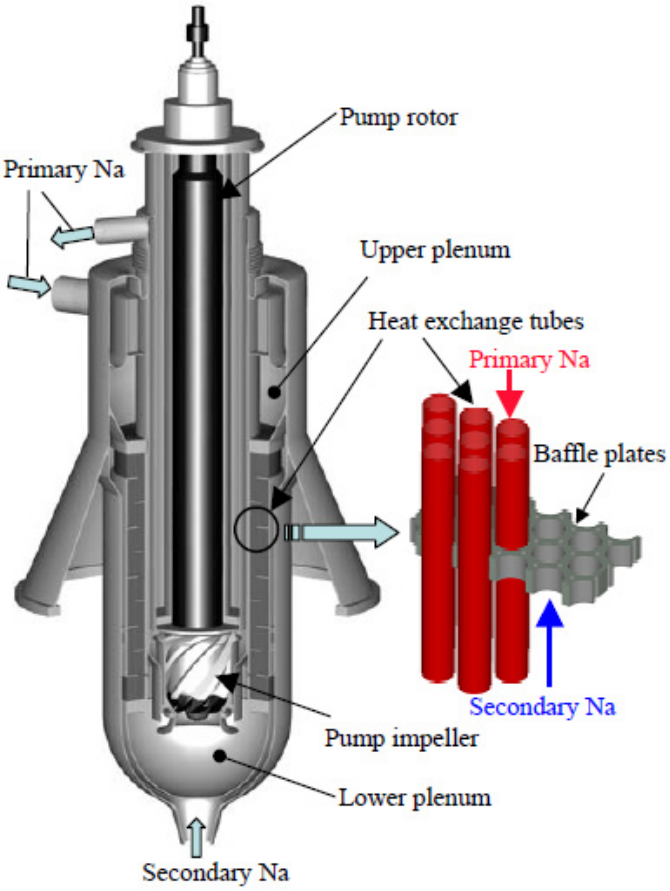

FIG. 3.37. Concept of the integrated IHX/pump component.

The integrated component is formed by installing the primary pump at the center of the IHX tube bundle. The IHX is designed as a no-liquid-surface type in order to allow high velocity of sodium coolant (~10 m/s) in the primary hot-leg piping without raising the cover-gas pressure in the reactor vessel. A straight heat transfer tube has been adopted.

The primary sodium flows within the tubes, and the secondary sodium flows zigzag outside of the tube. With the adoption of thinner heat transfer tubes made of Mod.9Cr-1Mo-steel, the heat transfer performance has been improved, and the tube bundle has become compact. The diameter and height of the integrated component are 4.3 and 14.2 m, respectively.

Although the integration of the IHX and the primary pump leads to a larger tube sheet diameter of the IHX, the adoption of Mod.9Cr-1Mo-steel with high strength and low thermal expansion ensures the structural integrity.

(c) Steam generator

JSFR adopts the integrated once-through-type SG with double-wall straight heat transfer tubes. Straight tube type SG has an advantage in construction cost due to fewer amounts of material and simpler fabrication (no bending of heat transfer tube) compared with helical type. The major specifications of SG are shown in Table 3.18.

TABLE 3.18. MAJOR SPECIFICATION OF SG

Item	Value
SG type	Double-wall straight tube type
Thermal capacity, MWt	1765
Tube diameter, mm	19.0
Tube pitch, mm	40.0
Effective tube length, m	29.0
Tube material	Mod.9Cr-1Mo steel
Sodium flow rate, kg/h	2.70×10^{6}
Steam/water flow rate, kg/h	2.884×10^{6}
Sodium temperature, °C	520 / 335
Main steam	497.2°C (19.2 MPa)

The detailed structure of the double-wall tube SG is shown in Fig. 3.38.

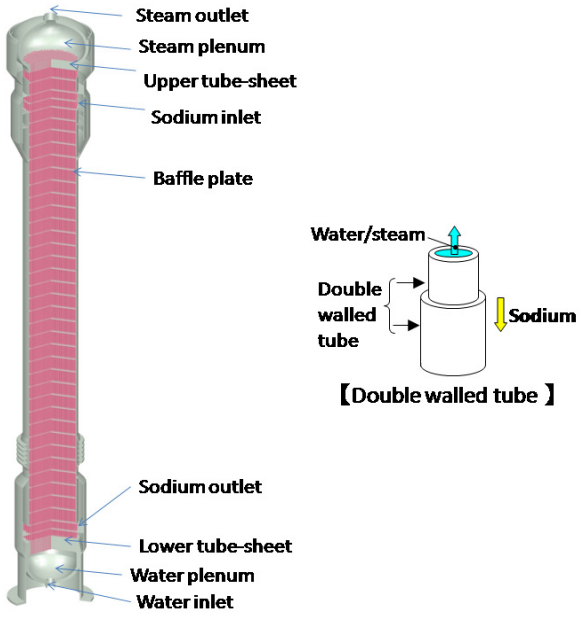

FIG. 3.38. Detail structure of double-wall SG.

Compact design of tube bundle is achieved by the improved performance in heat transfer that benefits from thinner heat transfer tubes made of Mod.9Cr-1Mo-steel. As a result, the effective length of heat transfer tube is about 29 m for the SG with capacity of 1765 MWt. As the thermal capacity of the SG is increased in order to pursue the economics of scale, the diameter of the SG shell becomes large. Then, it requires adoption of tube-plate with semi-spherical shape for the water-side pressure. A single plate type tube-plate is suitable in order to simplify both structure and plugging process of the tube-plate.

In the thermal hydraulic viewpoints, the provision of baffle-plates and a sodium flow down-up structure in a sodium inlet plenum of the SG can unify the radius sodium flow into the tube bundle, and the subsequently unified sodium flow contributes to flatten a horizontal temperature distribution in the bundle region. This is indispensable factor for preventing a tube buckling or

tube to tube-plate junction failure. The shell bellows can compensate the thermal expansion difference between the SG shell and tube bundle. Sodium fluids flow in the counter direction against the water fluids and in parallel with the heat transfer tubes to reduce the pressure loss and to evade tube-fretting. No water/steam hydraulics instability occurs by increasing waterside pressure without orifice. This orifice-less method serves to enhancement of the tube reliability in terms of preventing unpleasant phenomena like erosion or blockage at the orifice.

3.3.5.2.5. Safety system and features [22, 23]

(a) Reactor shutdown system (active and passive features)

The reactor shutdown system (RSS) consists of two independent active sub-systems (i.e. main and backup RSSs) with different design specifications; e.g., principle of detectors, driving mechanism of rods, etc. Each of them is designed to prevent fuel failure against DBEs. In addition the Curie-point magnet type self-actuated shutdown system (SASS), Fig. 3.39 [24] which is additionally introduced in the backup RSS as a passive shutdown feature ensures the prevention capability against the anticipated transients without scram (ATWS) combined with a robust structural core design. The ATWS is however addressed as DEC. SASS has been developed by both out- and in-pile experiments so far.

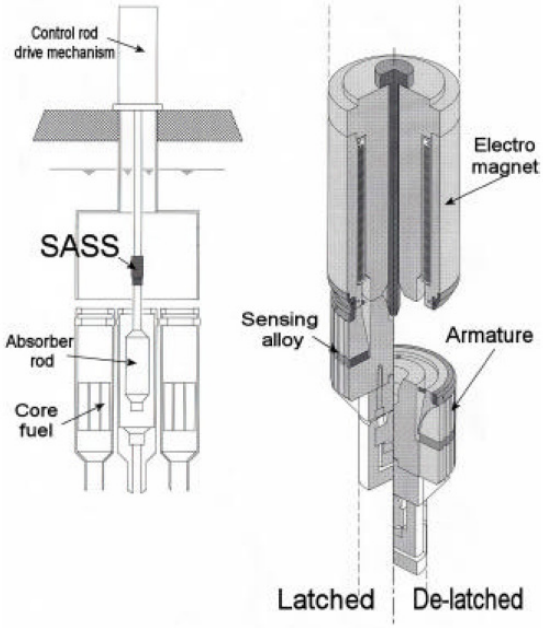

FIG. 3.39. Self actuated shutdown system (SASS).

(b) Decay heat removal system (passive features)

The combination of two PRACSs and one DRACS (see Fig. 3.40) has been selected from the viewpoint of safety and fluid stability of sodium-coolant at the condition of natural circulation. It was also confirmed that the decay heat removal capacity with the single failure condition such as one of the air cooler damper system mal-function is ensured.

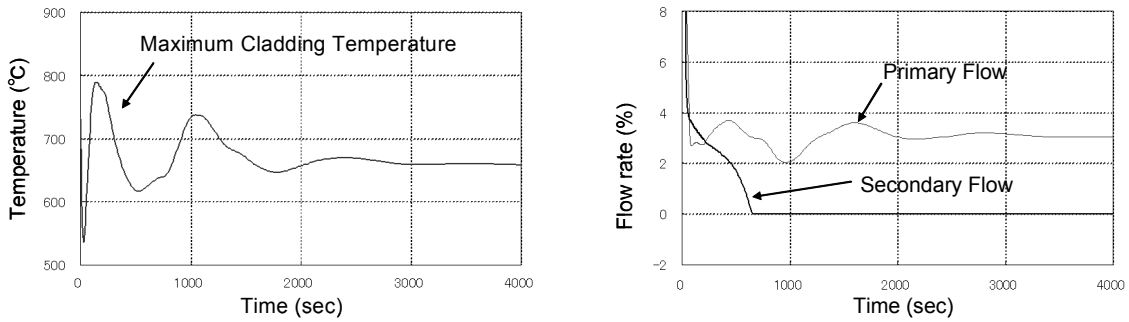

FIG. 3.40. Analytical result of the station blackout (2 PRACSs+DRACS).

3.3.5.2.6. Plant layouts [16, 18, 19]

Figure 3.41 shows the layout of the reactor building of JSFR. The reactor building is designed as a seismic isolated building, and the layout reflects the rationalization and compaction of the reactor and cooling system. In addition, communization of the balance-of-plant facilities has proceeded through the twin-plant design.

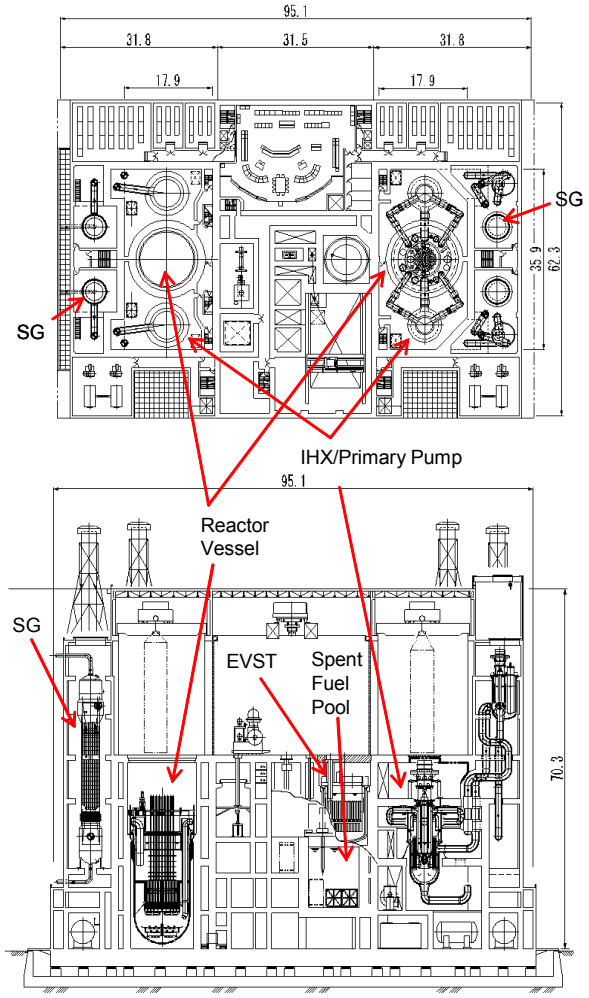

FIG. 3.41. Layout in the JSFR reactor building (twin plant).

The influence of sodium leakage coming from defects of materials is localized within the guard vessel or guard piping in this plant. Another cause of sodium leakage is overpressure to the wall. But, adoption of recriticality free measures eliminates such sodium leakage from the reactor vessel caused by a significant mechanical energy discharge in the CDA. Therefore, a simplified design of the reactor containment facility (reinforced concrete structure with an inner lining) is adopted from the point of view of radionuclide confinement, which is more important than pressure resistance.

3.3.5.2.7. Current status

JAEA launched a new Fast Reactor Cycle Technology Development (FaCT) Project in cooperation with the Japanese electric utilities in 2006. Design study and experimental study will be implemented in order to present the conceptual designs of commercial and demonstration FBR by JFY2015 with development plan to realize them. All the innovative technologies are planned to be developed in 10 years. The demonstration FBR will start to operate in around 2025.

3.3.6. EFR

3.3.6.1. Introduction

The European Fast Reactor (EFR) project was launched in 1988. It reached an important milestone in 1998 with the completion of the Concept Validation phase. The twin goals set by the customer utilities at the outset for the design have been demonstrated to be achievable: economic performance, with the power generation cost of a series-built EFR being competitive with its contemporary PWRs, and licensable in all participating countries, with a requirement for safety level which meets the ambitious targets for future nuclear plants. The European laboratories have provided extensive R&D support for validation of the design features necessary to meet these goals.

In Europe, the construction of fast reactors of increasing sizes under the national development programmes in France, Germany and the United Kingdom, had secured a solid foundation on which to base the development of the combined European expertise on fast reactor technology. The main milestones in these programmes were:

- Experimental reactors: DFR, Rapsodie, KNK II;
- Prototype power plants of 250 - 300 MWe: Phénix, PFR, SNR-300;
- Industrial sized power plant of 1200 MWe: Superphénix.

The continuing national study programmes had also resulted in well developed commercial fast reactor design proposals: CDFR, SNR-2, RNR-1500 (Superphénix-2).

Thereafter, the recognition of the potential benefits of pooling the experience and resources of the design and construction companies, the R&D organizations and the electrical utilities, led to the decision to pursue fast reactor development on the basis of a European collaborative venture (Fig. 3.42). Thus in 1988, the EFR collaboration was established and the participating organizations launched a programme of design and validation activities which was pursued for ten years.

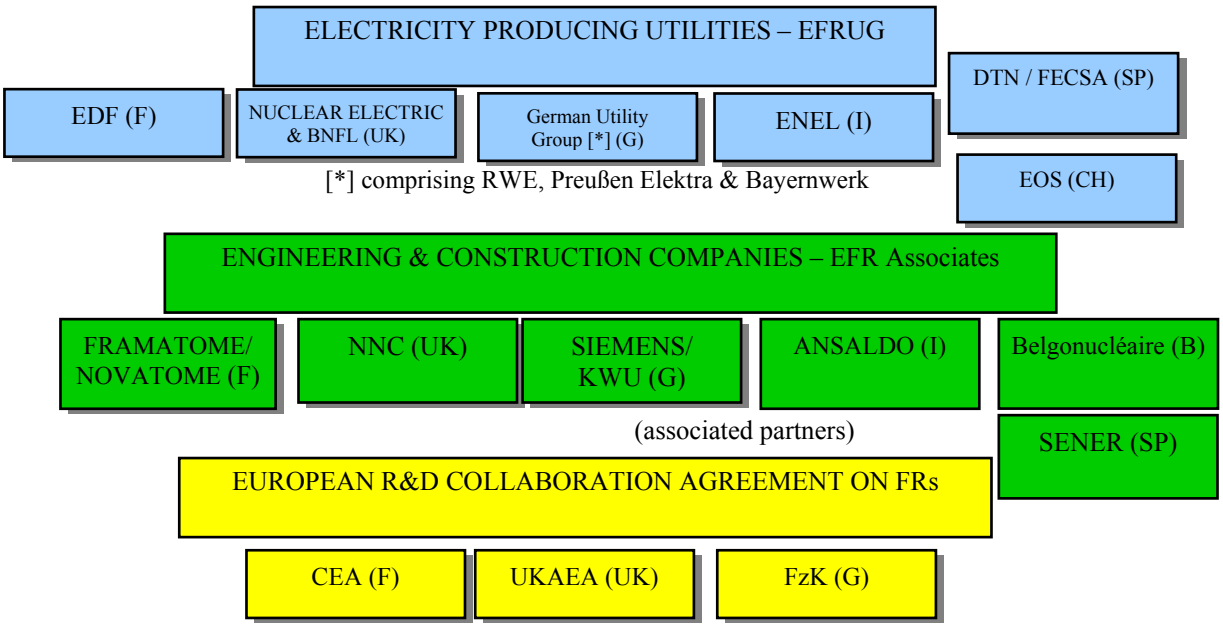

FIG. 3.42. EFR Programme participants.

During the first two year Conceptual Design phase (March 1988 - March 1990), the best features of the national commercial fast reactor projects were integrated into a compact EFR first consistent design along with alternative and fallback options.

This was followed by a three year Concept Validation phase (April 1990 – March 1993) in which the system engineering for EFR was completed and the R&D results were integrated into the design. Detailed studies concentrated on the analysis of crucial features of the Consistent Design, and on comprehensive assessments of the safety approach and the economic prospects.

The Concept Validation phase has achieved its intended objectives of a technically and economically well-established Nuclear Island design and a preliminary Non Site Specific Safety analysis Report (NSSSR), accompanied by initial probabilistic risk assessment studies.

In advance of any formal involvement of the national regulators, a review of the EFR safety approach and provisions was undertaken by a representative panel of assessors composed of eminent safety experts from various national organizations.

3.3.6.2. Design description

The objective was to produce a design which would both ensure high plant availability and meet the lifetime target of 40 years. This necessitated special attention to components and structures where failure would lead to prolonged outage for repair (of which the permanent reactor structures, the heat exchangers and the steam generators are particularly important), and the development of efficient in-service inspection and repair methods. The approach to meeting this objective was to use, as far as possible consistent with the other requirements, technology which was already verified or which could be expected to be fully endorsed by R&D. Consideration was also given to optimisation of parameters to ensure high component endurance coupled with continued study to develop well founded and validated design rules.

3.3.6.2.1. Layout of plant and buildings

The general site plan is, as an example, based on a river site with a cooling tower. The centre of the Nuclear Island (NI) is formed by the rectangular Reactor Building (RB) with three adjacent Steam Generator Buildings (SGBs). In addition the NI incorporates the Switchgear Buildings which house the essential and non-essential electrics and the main control room, and the Auxiliary Building housing the fuel and component handling equipment, decontamination facilities and stores for new and spent fuel.

The Reactor Building (RB)

The Reactor Building (RB) is designed to accommodate the reactor and its associated protection and cooling systems based on a six-circuit sodium cooling system for heat transfer to the steam generators (Fig. 3.43).

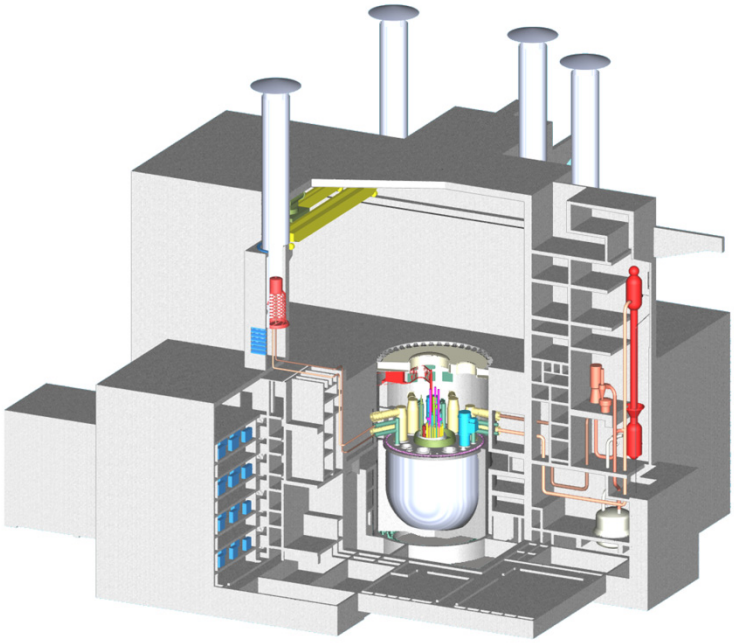

FIG. 3.43. EFR Nuclear island layout.

The three Steam Generator Buildings (SGBs) are arranged on the perimeter of the RB. The location of the SGBs is dictated by the component arrangement on the reactor roof. Each SGB is separated into two Steam Generator Compartments (SGCs). Each SGC comprises one secondary loop, one direct reactor cooling loop and parts of one feedwater/steam piping system, with their auxiliaries/ancillaries.

The switchgear buildings

The switchgear buildings are the buildings located in parts of the annulus around the RB, between the Steam Generator Buildings No 1 and 2 and Steam Generator Buildings Nos 3 and 1.

The turbine generator building

The turbine generator building contains all components of the water and steam plant including the turbine generator.

The reactor auxiliary building

The reactor auxiliary building is located adjacent to the reactor building between the steam generator buildings.

3.3.6.2.2. Reactor core

Two options are considered for the reactor core: a conventional homogeneous core and an axially heterogeneous core with an internal fertile slice just below core mid-plane. Both concepts have three radial core zones with different plutonium contents, and are fully compatible with each other. The inner zone contains 207 fuel subassemblies, while the intermediate and the outer zones are formed by 108 and 72 fuel subassemblies, respectively.

The core is surrounded by 78 breeder subassemblies in one row. The reactor core is 1 m high and, in the case of the axial heterogeneous concept, it comprises a 0.12 cm high internal breeder zone. Axial breeder blankets having a thickness of 0.15 m and 0.25 m are located above and below the reactor core, respectively. As a feature of the design flexibility with regard to the breeding characteristics, either the suppression of the axial and radial blanket, or the addition of axial blanket (up to a total of 0.8 m) and of one additional radial breeder row are possible. This feature is also important in connection with potential missions of fast reactors for plutonium management and transmutation of minor actinides (Fig. 3.44).

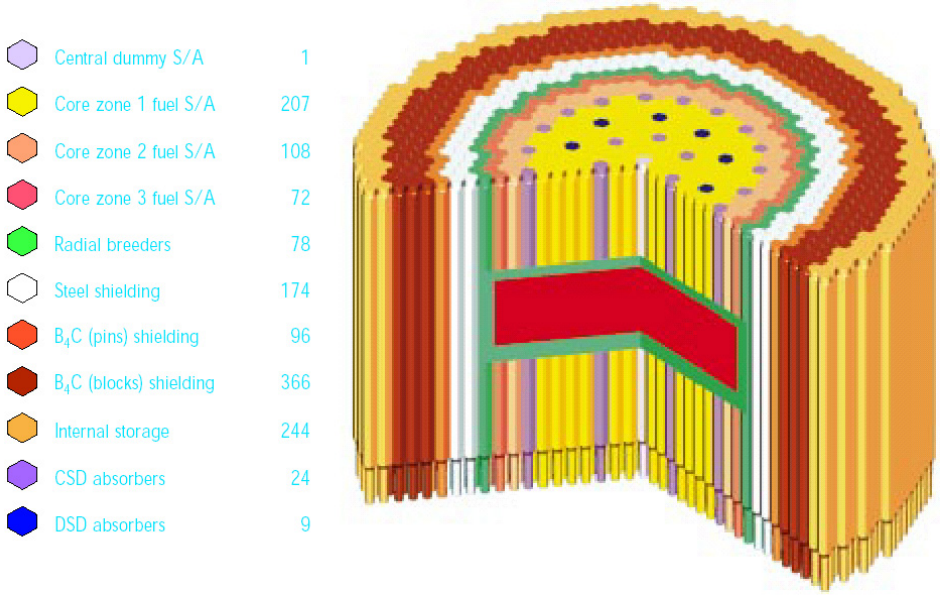

FIG. 3.44. EFR Core layout.

For core control, the EFR is equipped with two diverse fast acting shutdown systems. They are independent of each other from the sensors to the actuating trip systems. The latter are assigned to different electrical divisions where functional isolation of the different trip safety trains is provided. Each system on its own is capable of controlling all faults requiring rapid shutdown of the reactor.

3.3.6.2.3. Reactor unit

A compact reactor unit has been achieved with considerable simplification to the structures and components, and for surveillance (Fig. 3.45).

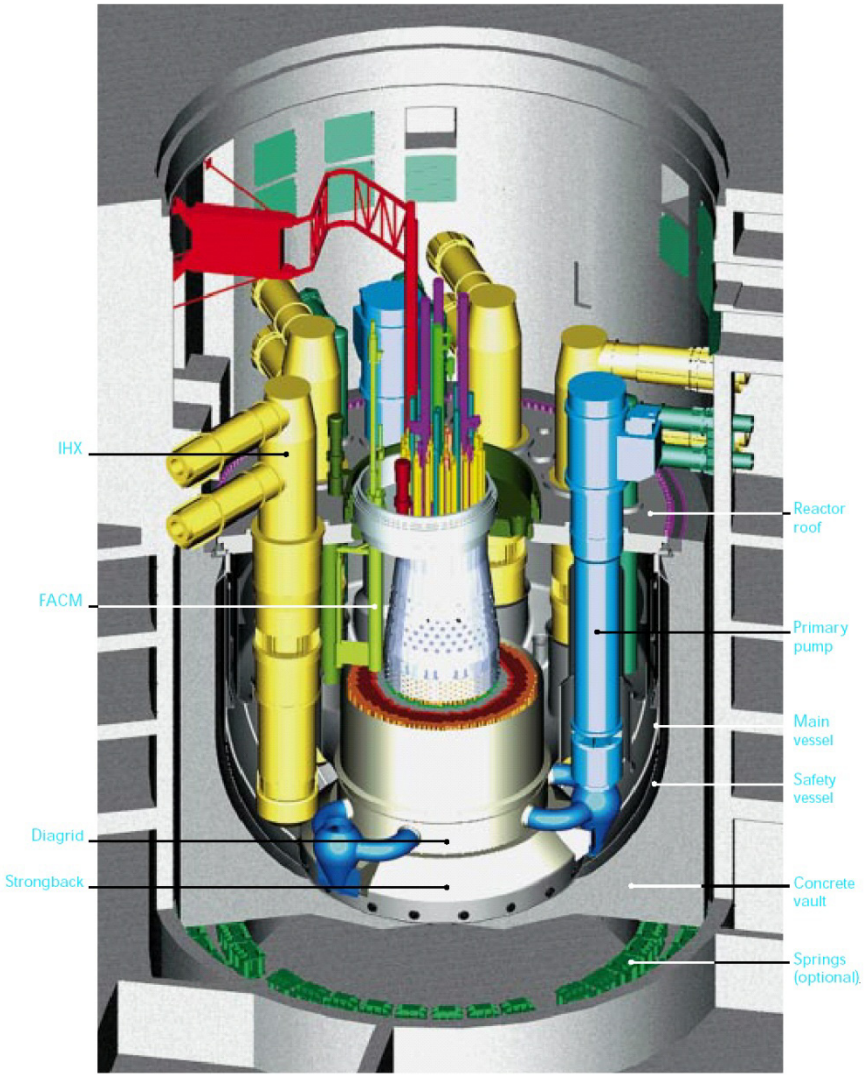

FIG. 3.45. EFR Reactor unit and primary system.

The large pool plant layout is an evolution from Superphénix taking full advantage of the national studies for CDFR, SNR-2 and Superphénix-2. The core, neutron shield and internal fuel store are supported by a diagrid which sits on a disc-shaped strongback to transfer the weight to the main vessel bottom. Sodium is circulated through the core by 3 primary pumps and the heat transferred to the secondary sodium by 6 intermediate heat exchangers (IHXs). Hot sodium leaving the core is separated from the cold sodium feeding the core by a single shell inner vessel. Decay heat can be rejected from the hot pool by the 6 dip coolers which form part of the direct reactor cooling (DRC) system.

A key to the compactness of the design is the reduction in the rotating plug diameter, made possible by providing intermediate 'set-down' locations for loading/unloading fuel subassemblies to/from the central area of the core. The smaller number of large components compared with Superphénix (6 IHXs instead of 8, and 3 pumps instead of 4), and simplification of the internal structures then lead to a main vessel diameter of only 17.2 m. A solid steel reactor roof (0.85 m thick) was adopted following design and manufacturing assessments which established the feasibility and advantage over the more conventional fabricated steel box structure with concrete filling used in large "pool" designs.

The *main* vessel is fabricated in austenitic steel and has been the subject of a number of improvements which simplify and enhance its structural integrity. The primary pumps have a top entry, single mixed flow impeller and a flywheel to extend the run-down time on loss of power supply. For the intermediate heat exchangers (IHXs) a simple straight tube design is used with the primary sodium on the shell side.

3.3.6.2.4. Intermediate heat transfer system

This system transfers the heat from the intermediate heat exchangers to the steam generator units during power operation and during operational decay heat removal via the water/steam plant after reactor shutdown. Additionally, it represents a barrier between the radioactive primary system and the non-radioactive water/steam system. The intermediate system comprises six independent secondary sodium loops, each consisting of one mechanical pump, one steam generator unit, one dump vessel and the piping connecting them to each other and to the intermediate heat exchanger located in the reactor vessel (Fig. 3.46).

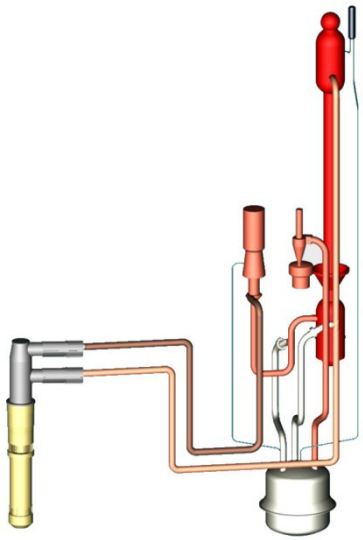

FIG. 3.46. EFR Intermediate heat transfer loop.

The steam generator units are once-through straight tube units with a tube bundle arranged in a circular pitch between two ferritic steel tube-plates. Sodium flow is outside the tubes.

3.3.6.2.5. Water/steam plant and turbine generator

Thanks to the high temperature of the steam at the outlet of the steam generator, it is possible to achieve a plant efficiency of over 40% and to design the water/steam plant in compliance with guidelines and quality requirements applied to conventional (fossil fired) power plants.

For this reason the conventional water/steam plant can be designed in accordance with standard utility/national practice, which leads to lower investment costs and minimises the special operator expertise required. It also allows the plant to be readily accommodated without real impact on the EFR NSSS.

The measures that have to be implemented in the water/steam system to provide protection against a steam generator accident are the only ones of safety related importance, in particular

with regard to protection of the intermediate heat exchanger as a part of the primary system boundary.

3.3.6.2.6. Direct reactor cooling systems (DRC)

The DRC systems provide highly reliable heat removal direct from the primary system in the event of the main heat transfer through the secondary system and the water/steam plant being unavailable. They comprise two direct reactor cooling systems (DRC 1 and DRC2) each consisting of three sodium-filled loops. All loops extract heat from the hot pool of the primary sodium by immersed Na/Na heat exchangers and reject the heat to the environment by Na/air heat exchangers (AHXs) arranged some 34 m above the Na/Na heat exchangers (Fig. 3.47).

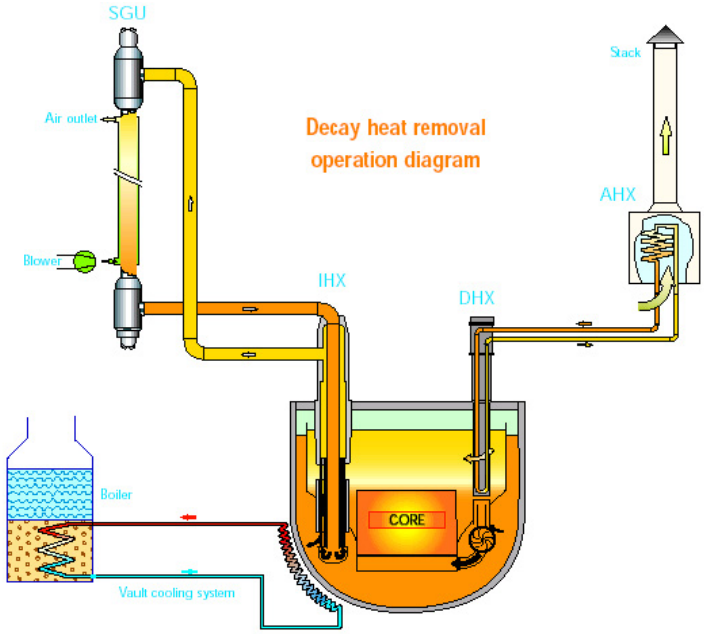

FIG. 3.47. EFR Decay heat transfer routes.

All six loops are rated for a thermal power of 15 MW in nominal conditions (primary sodium temperature at 530°C, ambient air at +35°C). DRC 1 relies exclusively on natural convection heat transfer, i.e., natural circulation on the sodium side and natural draught on the air side. DRC 2 is normally operated in forced flow, and each loop is equipped with a flow supporting electro-magnetic pump (EM pump) and with two fans in parallel on the air side. These active loops possess passive heat removal potential when the pump and fans are off, amounting to about 2/3 of that in the active flow mode.

The frequency target for the loss of DHR function is less than about 10^{-7} per year. Since the degree of redundancy of the DHR equipment in the water/steam system is determined only by operational and plant availability, and since the water/steam plant is not available after loss of station service power, the DHR reliability is essentially that of the DRC systems. The combination of three passive loops with three active loops also leads to an operational diversity between the two systems. The degree of diversity introduced into the DRC systems and the protection against the risk of large sodium fires on the reactor roof are appropriate to exclude common mode failures from design basis considerations.

3.3.6.2.7. Main auxiliary system

The primary sodium purification system consists of an in-vessel EM pump and an ex-vessel cold trap, heat exchangers and plugging meter, arranged in a shielded concrete cell with steel liner and inert gas. Each secondary sodium purification loop serves one main secondary loop and one direct reactor cooling loop. The purification system operates intermittently and does not serve the main loop and the DRC loop at the same time, so that the reliability of the DRC is not jeopardised.

3.3.6.2.8. Core subassembly handling systems

Refuelling takes place during scheduled reactor shutdowns, which occur at approximately annual intervals. Fuel subassemblies which are at the end of their life are removed from the core and placed in the in-vessel store. Fuel subassemblies which have been retained in the in-vessel store during the previous reactor operating period and, therefore, have a lower decay heat rating are transferred from the in-vessel store to the secondary fuel handling facilities. Other irradiated core components, such as breeder subassemblies and absorber rods, can be removed from the reactor vessel without using the internal store.

The in-vessel fuel handling system provides access to any core position by means of two eccentric rotating plugs in the reactor roof, a direct lift charge machine (DLCM) and a fixed arm charge machine (FACM). The DLCM is situated at the centre of the above core structure in the small rotating plug and covers the inner handling zone of the core.

The FACM, which covers the outer handling zone, is also located on the small rotating plug, but outside the above core structure. Take-over positions created in the core at the start of each fuel handling campaign provide the liaison between the two charge machines where the two handling zones overlap (Fig. 3.48).

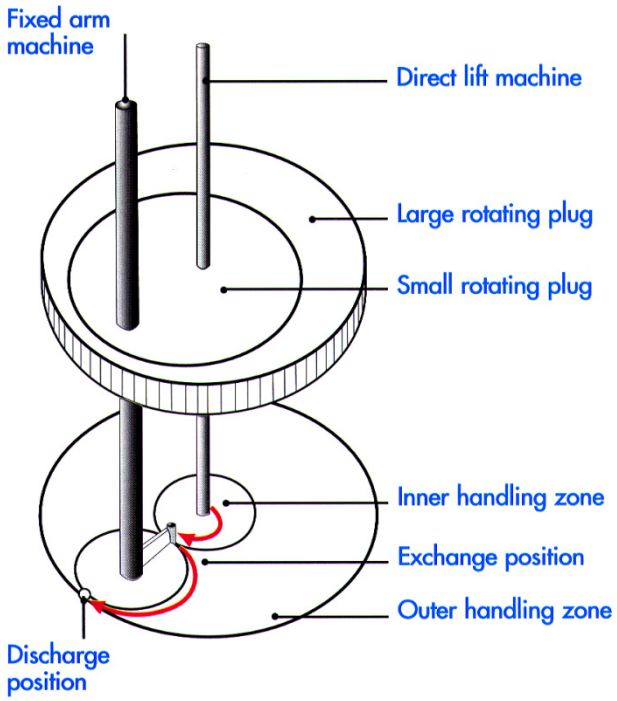

FIG. 3.48. EFR Primary fuel handling scheme.

Subassemblies are discharged from the reactor in a sodium filled bucket via the primary ramp of the A-frame system. The secondary ramp terminates in a transfer cell below the handling cell. New subassemblies are transferred from the new fuel store into the reactor vessel on a one-to-one basis in exchange for irradiated subassemblies.

3.3.6.3. R&D support of the design

During the EFR Concept Validation phase, the R&D organizations, which had already been working together for some time, embarked on a joint programme of activities focused on the key R&D requirements for EFR. This programme was split into 11 expert working groups (AGTs) which were responsible for the management of more than one hundred "work packages" comprising over 1 000 individual research tasks carried out in 13 research centres in 3 countries.

By the end of the concept validation phase most of the work had been completed by the R&D organizations with only a few exceptions related mainly to evolving design choices and long term work on material characterisation.

The following five years, were mainly dedicated to the consolidation of the results, with the benefit of the large R&D programmes in support of Superphénix and the activities related to new missions for fast reactor in the back end of the fuel cycle (such as the CAPRA/CADRA programme). Concept validation phase achievements is presented as follows:

3.3.6.3.1. The approach to competitive fast reactors

Demonstration of the economic potential was an important objective of EFR design studies, leading to thorough investigation of all components of the kWh cost, i.e. investment, fuel cycle and operation. Many lessons have been learnt from construction experience, the most recent being Superphénix in France, which has provided a wealth of information allowing the simplification and optimisation of future plant designs. There has also been considerable progress of knowledge in structural mechanics and design rules, which is reflected in the RCC-MR.

An economic assessment of EFR was performed as a joint activity between the utilities and the design and construction companies. This involved a number of qualified nuclear equipment manufacturers in Europe who provided quotations for the main components. Also, the major European fuel fabrication and reprocessing companies provided fuel service cost information enabling an assessment of the EFR fuel cycle costs to be carried out. As a result, the design work on EFR has achieved substantial reductions in material quantities for the NSSS compared to Superphénix, with corresponding construction cost savings (Fig. 3.49).

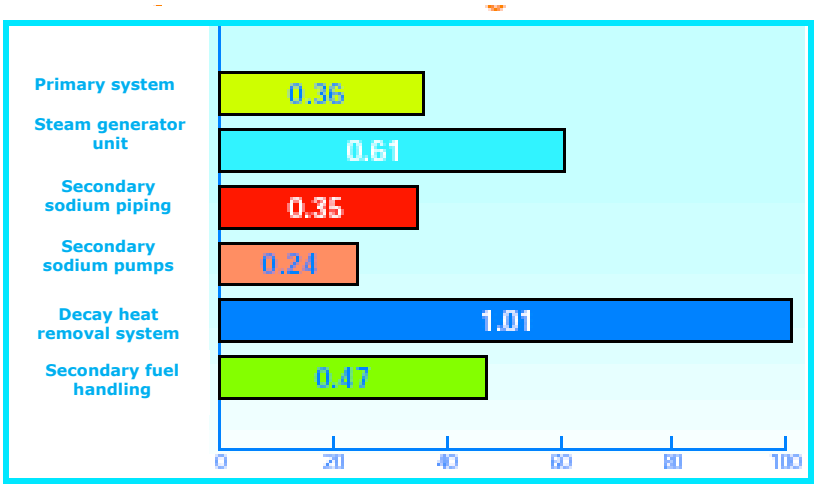

FIG. 3.49. EFR vs. SPX1 NSSS Comparison of steel weights (in relative terms t/kWe).

The comparison of generating costs between EFR and PWR carried out in France shows that, even compared to the very efficient PWR, the series EFR should be close to achieving competitiveness. Further progress in fast reactor technology and changes in the economic conditions (notably in the uranium market) would allow this to be achieved (Fig. 3.50).

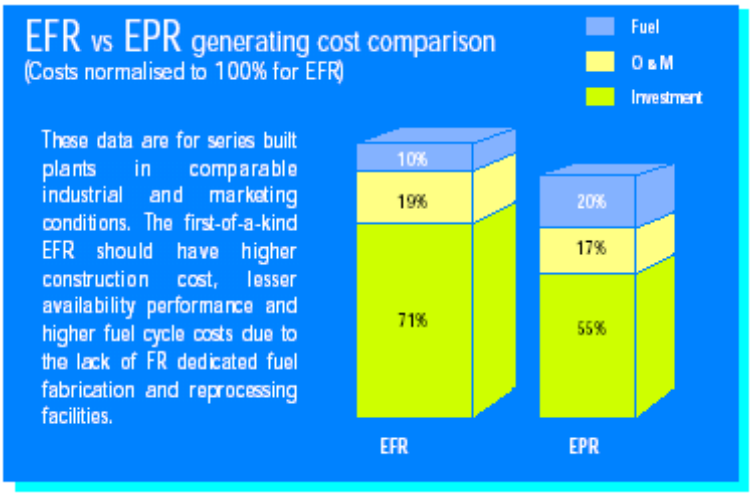

FIG. 3.50. EFR vs. EPR Generating cost comparison (French case).

3.3.6.3.2. The safety approach

A prime feature of the safety design of EFR is the extensive application of "defence in depth" principles. The successive protection levels include: careful design, high effort in quality assurance, extensive R&D to ensure a good design and performance, systems to protect and control failures or deviations from normal operation, protective systems and engineered safety provisions, physical barriers to confine any radioactive release, and ultimate risk minimization measures to enhance further the reliability of shutdown and decay heat removal, and the retention capability of the containment. Because the reactor is not pressurised and is located in a close-fitting pit, loss of coolant is precluded and core melt preventive measures are concentrated on enhanced shutdown and decay heat removal. Through these preventive measures the risk of core melt is extremely low (remote in the residual risk domain) and

beyond the objectives set by INSAG for future reactors. As such, there is no need for special containment provisions to meet the requirements on accident release limits. Nevertheless, according to the ALARP principle, strong primary and secondary containment are included, which further mitigate against postulated loadings.

The core design has been optimized for safety through: the fuel pin linear rating, chosen to prevent local fuel melting in the case of inadvertent absorber rod withdrawal, the core height chosen to minimise the positive reactivity effect of sodium voiding, and the Doppler coefficient to provide efficient reactivity feedback to rapid transients.

3.3.6.3.3. Reactor shutdown

Reactor shutdown is assured by two independent and diverse basic shutdown systems which guarantee very high reliability so as to relegate shutdown failure into the domain of residual risk. In the domain of residual risk, however, the "Third Shutdown Level" becomes effective. It consists of a bundle of additional engineered safety features which are incorporated in the design as a result of extensive risk-minimization studies. The system consists of active and passive subsystems and is supported by beneficial natural core behaviour.

The "Third Shutdown Level" is capable of maintaining core integrity in the case of a postulated failure of the two basic shutdown systems.

3.3.6.3.4. Decay heat removal

Decay heat removal (DHR) is normally achieved by means of the steam/water plant. This is backed up by two diverse DHR systems, both safety qualified. Also, complementary heat removal by air cooling of the steam generator outer shell surface is an effective risk-minimising measure.

3.3.6.3.5. The containment concept

The containment concept complies with the "defence-in-depth" principle, by providing a multiplicity of barriers between radioactive fission products and the operators and public at large. The high reliability of the first of these barriers, the fuel cladding, has been confirmed by the operating experience of prototype FRs.

The challenge for EFR is that it must satisfy the same level of safety as future LWRs and be capable of being licensed in each of the participating countries. An important achievement has been to demonstrate the potential licensability by means of an independent review of the essential elements of the safety case by a group of prominent safety experts from France, Germany, and the UK. This review allowed in-depth discussions on the general approach, the main safety functions and the proposed risk minimization measures. The outcome was as follows: on core melt; adequately low levels of risk are achievable, on sodium fire hazards and in-service inspection; significant progress has been made with EFR compared to previous fast reactor designs, and on decay heat removal; the improvements incorporated in the design are judged satisfactory.

The review concluded, notably, that the approach adopted for EFR results in level of safety comparable with that of future PWRs. It also provided useful advice on areas where work would substantiate the EFR safety case further, e.g. some additional studies were recommended concerning: the containment; additional demonstration of the validity of the

chosen "plant states" as part of the ALARP principle implementation, and common cause failures; due to the concentration of safety equipment on the reactor roof: it is necessary to show that measures have been taken to make the risk acceptably low. In conclusion, the final view expressed by the independent experts was that "they were favourably impressed by the progress that has been made with the current EFR design, and they consider that it provides a sound basis from which to proceed to licensing application in each of the participating countries".

3.3.6.4. Conclusion

The EFR design provides a sound basis for the commercial exploitation of fast reactor. The final outcome of the EFR programme is a fully integrated and consistent advanced commercial fast reactor design, approaching the objectives set by the utilities related to safety and economic competitiveness compared with future European LWR plants. It is a design which takes full benefit of the operating experience gained from fast reactors in Europe and around the world, and which includes innovative and advanced features bringing benefits in safety, reliability and economics, which have been validated by extensive R&D.

EFR is, and will remain, a reference commercial fast reactor design against which new innovations, either specific fast reactor features or alternative concepts, can be compared and judged.

REFERENCES TO CHAPTER 3

[1] GIF-002-00, A Technology Roadmap for Generation IV Nuclear Energy Systems (December 2002).

[2] ASHURKO, Yu.M., Current Status of Activities in Fast Reactor and Accelerator Driven System Area, paper presented in IAEA Technical Meeting Review of the Status of Accelerator Driven Systems and Fast Reactor R&D and Technology, Vienna, Austria, 4-8 December 2006.

[3] MI, XU, The Status of Fast Reactor Technology Development in China, paper presented in IAEA Technical Meeting Review of National Programmes on Fast Reactors and Accelerator Driven Systems (ADS), Karlsruhe, Germany, 22–26 April 2002.

[4] Primary Safety Analysis Report of CEFR, Vol. 16, Fast Reactor Department, CIAE (2001) (in Chinese).

[5] CHANG, Y.I., et al., Advanced Burner Test Reactor Preconceptual Design Report, ANL-ABR-1, Argonne National Laboratory (September 2006).

[6] POPLAVSKY, V.M., et al., BN-1800: a next generation fast breeder, Nuclear Engineering International, Vol. 49, No. 599, pp. 20–24 (June 2004).

[7] ASHURKO, YU.M., Current Status of Activities in Fast Reactor and Accelerator Driven System Area, paper presented in IAEA Technical Meeting Review of the Status of Accelerator Driven Systems and Fast Reactor R&D and Technology, Vienna, Austria, 4-8 December 2006.

[8] HONG, S.G., et al., A New Design Concept of the Kalimer-600 Core, Proc. ICAPP '07, Nice, France, 13–18 May 2007.

[9] KWON, Y.M., LEE, Y.B., CHANG, W.P., HAHN, D., SSC-K Code User's Manual (Rev.0), KAERI/TR-1619/2000, Korea Atomic Energy Research and Institute (2000).

[10] CHANG, W.P., et al., Model Development for Analysis of the Korea Advanced Liquid Metal Reactor, Nuclear Engineering and Design, Vol. 217, pp. 63–80 (2002).

[11] EOH, J.H. et al., Transient Performance Analysis of the Passive DHR System in KALIMER-600, paper presented in '06 Spring Meeting, Kang-chon Resort, Korea, Republic of, 2006.
[12] AGRAWAL, A.K. et at., An Advanced Thermohydraulic Simulation Code for Transients in LMFBRs (SSC-L Code), BNL-NUREG-50773, Brookhaven National Laboratory (1973).
[13] LEE, Y.B., et al., Development of a Two-Dimensional Model for the Thermohydraulic Analysis of the Hot Pool in Liquid Metal Reactors, Annals of Nuclear Energy, Vol. 29, pp. 21–40 (2001).
[14] JAPAN ATOMIC ENERGY AGENCY and THE JAPAN ATOMIC POWER COMPANY, Phase II Final Report of Feasibility Study on Commercialized Fast Reactor Cycle Systems -Executive Summary (March 2006).
[15] SAGAYAMA, Y., Feasibility Study on Commercialized Fast Reactor Cycle Systems (1) Current Status of the Phase-II Study, Proc. GLOBAL 2005, Tsukuba, Japan, 9–13 October 2005 (Editor: Hajimu Yamana) Atomic Energy Society of Japan, ISBN: 4-89047-133-2, paper No. 380.
[16] HISHIDA, M., et al., Progress on the planned design concept of sodium-cooled fast reactor, Proc. GLOBAL 2005, Tsukuba, Japan, 9-13 October 2005 (Editor: Hajimu Yamana) Atomic Energy Society of Japan, ISBN: 4-89047-133-2, paper No. 068.
[17] KOTAKE, S., et al., Feasibility study on commercialized fast reactor cycle systems: current status of the FR system design, Proc. GLOBAL 2005, Tsukuba, Japan, 9-13 October 2005 (Editor: Hajimu Yamana) Atomic Energy Society of Japan, ISBN: 4-89047-133-2, paper No. 435.
[18] ICHIMIYA, M., et al., A promising sodium-cooled fast reactor concept and its R&D plan, Proc. GLOBAL 2003, Louisiana, USA, 16-20 November 2003, ANS, ISBN: 0-89448-677-2 (2003) paper 0434.
[19] SHIMAKAWA, Y., et al., An innovative concept of a sodium-cooled reactor to pursue high economic competitiveness, Nuclear Technology, Vol. 140, pp. 1-16 (October 2002).
[20] MIZUNO, T., et al., Advanced Oxide Fuel Core Design Study for SFR in "Feasibility Study in Japan", Proc. GLOBAL 2005, Tsukuba, Japan, 9-13 October 2005 (Editor: Hajimu Yamana) Atomic Energy Society of Japan, ISBN: 4-89047-133-2, paper No. 434.
[21] JAPAN ATOMIC ENERGY AGENCY, Feasibility Study on Commercialized Fast Reactor Cycle Systems Technical Study Report of Phase II-(1) Fast Reactor Plant Systems, JAEA-Research 2006-042, p. 1807 (2006) (in Japanese).
[22] KUBO, S., et al., Status of conceptual safety design study of Japanese sodium-cooled fast reactor, Proc. GLOBAL 2005, Tsukuba, Japan, 9-13 October 2005 Proc. GLOBAL 2005, Tsukuba, Japan, 9-13 October 2005 (Editor: Hajimu Yamana) Atomic Energy Society of Japan, ISBN: 4-89047-133-2, paper No. 221.
[23] NIWA, H., et al., LMFBR Design and its Evolution: (3) Safety System Design of LMFBR, GENES4/ANP2003, No. 1154, Kyoto, Japan, 15-19 September 2003.
[24] MORIHATA, M., AONO, H., ARIYOSHI, M., IKARIMOTO, I., Development of Self Actuated Shutdown System for FBR in Japan, paper presented in Int. Conf. Nuclear Engineering, Nice, France, 26-30 May 1997.
[25] SAGAYAMA, Y., Launch of fast reactor cycle technology development project in Japan, Proc. GLOBAL 2007, Boise, Idaho, USA, 9–13 September 2007, ISBN: 0-89448-055-3.

CHAPTER 4
HEAVY LIQUID METAL-COOLED FAST REACTOR DESIGNS

4.1. Introduction

The term Lead-Cooled Fast Reactor (LFR) usually applies to a fast reactor utilizing either of two Heavy Liquid Metal Coolant (HLMC) materials. The first is Pb itself which has a melting temperature of 327.45°C and an atmospheric boiling temperature of 1743°C. The second is lead-bismuth eutectic (LBE) which is composed of 45.0 at% Pb and 55.0 at% Bi with a melting temperature of 124.5°C and an atmospheric boiling temperature of 1670°C. The Pb and LBE densities at 480°C are 10 470 and 10 100 kg/m^3, respectively.

Heavy Liquid Metal Coolants have several key inherent properties which, if taken advantage of by the designer together with specific design options, can potentially reduce the cost and improve the safety of a LFR relative to Sodium-Cooled Fast Reactors (SFRs) of the same electrical power level. Some experts believe that LFRs can even be economically competitive with Light Water Reactors (LWRs). These are the main drivers of interest in LFR development together with the traditional sustainability benefits of fast reactors.

As above mentioned, Pb has a high boiling temperature of about 1740°C which is well above the temperatures at which the steel cladding and structures lose their strength and melt. The Pb is therefore a low pressure coolant and does not flash should a leak develop in the primary coolant system boundary, while enabling the traditional advantages of a low pressure compact liquid metal system. The high boiling temperature of heavy liquid metal coolant also provides a pathway to operation at higher temperatures not limited by coolant boiling such that the greater efficiency benefits of advanced energy conversion systems such as the supercritical carbon dioxide Brayton cycle can be exploited more effectively.

Lead coolant does not interact vigorously with water/steam or air and is calculated not to react chemically with CO_2 working fluid above about 250°C, which is well below the Pb melting temperature of 327°C. Thus, with CO_2 there is no formation of combustible gas or exothermic energy release. Compatibility of Pb with the working fluid whether water/steam or CO_2 makes it possible to eliminate the need for an intermediate cooling circuit, reducing the plant capital cost and enhancing plant reliability.

Lead has a low absorption of neutrons. This permits the fuel pin lattice to be opened up by increasing the coolant volume fraction without a significant reactivity penalty. Increasing the coolant volume fraction increases the hydraulic diameter for coolant flow through the core reducing the core frictional pressure drop. As a result, natural circulation is more effective and can transport a greater fraction of the core power. Adoption of an open lattice core configuration with wide openings for crossflow between the fuel pins also eliminates flow blockage accident initiators in which the coolant flow entering at the bottom of the core is postulated to be locally blocked.

The high heavy liquid metal coolant density (ρ_{Pb} = 10 400 kg/m^3) limits the system size by the need to accommodate seismic events, e.g. by using two-dimensional seismic isolators. On the other hand, the high density limits void growth and downward penetration following postulated in-vessel HX tube rupture such that significant void is not transported to the core [1] but instead rises benignly to the lead free surface to be removed from the vessel by a

passive pressure relief system. This further contributes to the feasibility of eliminating the intermediate coolant circuit.

Experiments carried out at the Forschungszentrum Karlsruhe have shown that iodine, cesium, and cesium-iodide (i.e. fission products having low melting and boiling points) are absorbed and immobilized by lead-bismuth eutectic at temperatures of 400 and 600°C. Caesium forms inter-metallic compounds in LBE while iodine forms PbI_2 which has a melting temperature of 850°C. Thus, the heavy liquid metal coolant is a trap for these low melting point and low boiling point radionuclides. However, formation of PbI_2 did not consume all of the iodine in the experiments; some iodine escaped absorption and was released from the LBE free surface in the experiments.

The heavy liquid metal coolant has a higher density than that of oxide fuel. Thus, in an oxide-fueled LFR if a severe accident leads the system temperatures above that at which the cladding and other in-vessel structures melt, the pieces of solid oxide fuel and molten cladding and structure will float to the top of the Pb where they may spread over the available surface area. The streaming of neutrons from the surface can be expected to prevent criticality.

Although heavy liquid metal coolant dissolves Fe, Cr, and Ni from unprotected steels at rates which increase with temperature, active maintenance of the dissolved oxygen potential in the coolant within a proper concentration window and limiting velocities to values of ~ 1 m/s or less has been well established as a means for forming protective oxide layers (Fe_3O_4 at temperatures below ~ 570°C) significantly retarding the dissolution rate and avoiding the formation of solid PbO particulate [2]. The systems for monitoring the dissolved oxygen potential and maintaining the oxygen level in the desired regime must be designed to have a high reliability such that the probability of failure of the systems in modes that could threaten the long-term integrity of the cladding or other structures, or result in the formation of solid debris that might locally block flow channels, is sufficiently low.

It has recently been demonstrated that T91 ferritic/martensitic (F/M) steel cladding is protected from Pb corrosive attack at velocities at least as high as 3 m/s and temperatures as high as 550°C by “aluminizing” using the treatment currently applied in the GESA IV apparatus at the Forschungszentrum Karlsruhe [3]. Aluminizing might offer protection at higher temperatures and velocities as well. Oxygen control is not required to protect steel from corrosion below about 425°C.

Pump impellers shall be subjected to significantly higher velocities in a LFR. One promising material worthy of investigation for pump impellers is Ti_3SiC_2 manufactured by 3-ONE-2, LLC [4, 5]. It can be pressed, slip cast, and injection molded. It is machinable or can be thermally sprayed onto metals to form coatings. It is described as stiff, thermal shock resistant, damage tolerant, tough, and fatigue resistant. Its corrosion resistance has been tested at Argonne National Laboratory by exposure to Pb with low oxygen potential at 800 and 650°C for 1000-hours in a quartz Harp loop [6]. No evidence of Ti_3SiC_2 attack by Pb was observed. An extensive investigation shall be carried out at the Forschungszentrum Karlsruhe and an entire impeller manufactured from Ti_3SiC_2 will be tested in the CHEOPE III lead loop at the ENEA Center in Brasimone, Italy.

Lead coolant has a high melting temperature of 327°C while lead-bismuth eutectic (LBE) melts at 125°C. Some LFRs utilize lead-bismuth eutectic (LBE) mainly because of its lower melting temperature. For heavy liquid metal coolant, a means of heating the reactor system must be provided to melt the coolant and maintain it in a molten state prior to startup. Freezing

and thawing of the coolant that could result in damaging stresses in fuel pins and structures must be avoided. For a fresh core, the non-nuclear heating system must have a high reliability to avoid freezing until a significant decay heat source builds up in the fuel. The use of a pool-type configuration with its low surface-to-volume reduces the risk of freezing. The Russians have developed a procedure for deliberately freezing and thawing a LBE-cooled reactor system mainly involving slow heat removal or addition at varying elevation along the reactor vessel. The low shrinkage of LBE during solidification and the rather high plasticity and low strength in the solid state facilitate elimination of damage as the alloy solidifies and is cooled down to ambient temperature. The stresses developing when LBE surrounds a structure and freezes are controlled during the freezing-thawing procedure by assuring a very low freezing rate (i.e., a low rate of temperature decrease) and melting the solidified coolant downwards from the free surface. Lead coolant has a greater shrinkage than LBE upon solidification. The safety evaluation of operational transients and postulated accidents must include events involving overcooling of the heavy liquid metal coolant and assessment of the potential for local freezing of the coolant (e.g., on the outside of heat exchanger tubes) and its effects.

Neutron capture in Bi-209 presents in LBE leads to a decay chain resulting in the isotope ^{210}Po, which is an alpha emitter having a half life of 138 days. If the coolant interacts with moisture, polonium hydride can form. Polonium hydride is volatile and represents an airborne hazard. The generation of ^{210}Po with LBE is the main reason for using Pb coolant for which the amount of ^{210}Po is reduced by two to three orders of magnitude relative to LBE. However, ^{210}Po is not completely eliminated due to Bi impurities as well as creation of ^{209}Bi from transmutation reactions. Operations such as refueling or repair as well as responses to events involving coolant leakages must therefore protect workers from the effects of ^{210}Po and minimize its release to the environment. For example, when welding was carried out on a pipeline of the Russian 27/VT LBE-cooled land prototype reactor containing LBE residue on the inside surface of the pipeline, the radioactivity of air in the reactor hall increased for a short time by a factor of four over the permissible limit due to ^{210}Po. The Russians have developed measures including radiation control zones at work sites, drawing air out of areas with spills or high alpha activity combined with the use of fine fiber aerosol filters, protective clothing and respirators, use of caissons with pressurized air, removal of spilled or frozen LBE, applying easy-to-remove polymer films to polonium-contaminated surfaces, and prohibiting cutting, welding, etc. in areas of high polonium contamination.

Lead is a toxic substance and health hazard which adversely affects numerous body systems and causes forms of health impairment and disease that arise after periods of exposure as short as days or as long as several years. Regulations and procedures for protecting industrial and construction workers from the health hazards of lead are well established and routinely implemented. Regulations for working with lead have not impeded the charging, startup, operation, or modification of any LBE or lead experiment loops or facilities.

4.2. Development of lead and lead-bismuth cooled fast reactors

Major contributions in the development of lead technology have been carried out by Russian scientists and industries actively pursuing lead-cooled reactor technology for more than 50 years. In the early 1950s in Russia, research and design on the use of lead-bismuth alloy as the coolant for nuclear reactors was initiated by Academician A. I. Leipunsky at the Institute of Physics and Power Engineering (IPPE) in Obninsk. The principal objective of these efforts was the design and construction of nuclear reactors for submarine propulsion.

The 70 MWt 27/VT land prototype started power operation at IPPE in 1959. In 1963, the first nuclear submarine with a heavy liquid metal cooled reactor was put into operation. It was designated by the former Soviet Union (USSR) as “Project 645, Submarine K-27” and by the North Atlantic Treaty Organisation (NATO) as “November class K-27 variant” and utilized two 73 MWt reactors. Since 1971, two series of nuclear powered submarines termed by the former USSR as “Projects 705 and 705K” and by NATO as “Alfa class” have been put into operation. They utilized a single 155 MWt reactor and were distinguished by their steam – supply systems, one type of which was designed by the Experimental Design Bureau of Machine Building (OKBM) and the other was designed by the Experimental Design Bureau “Gidropress” (OKB Gidropress). In total, there have been constructed seven nuclear submarines of the Project 705/705K type and the one of the “Project 645” type. In addition, the KM-1 land based prototype mainly supporting Project 705K was put into operation at the A. P. Aleksandrov Scientific Technical Research Institute (NITI) in Sosnovy Bor in 1978.

During the land-based testing of prototype reactors and submarine operations, a number of technical difficulties were encountered and lessons were learned. Among these were the formation of solid masses in the coolant which penetrated into the core and caused local coolant blockage; local coolant freezing; and the formation of ^{210}Po. Consequently, in addressing these issues, a large experience base has been acquired in the areas of lead coolant technology, corrosion performance and mass transfer in lead-bismuth circuits.

Based on this extensive experience and subsequent worldwide research and development efforts, several designs have been developed of new nuclear reactors for electric energy production.

The Generation IV (GEN IV) Technology Roadmap [7], prepared by GIF member countries, identified the six most promising advanced reactor systems and related fuel cycles, and the R&D necessary to develop these concepts for potential deployment. Among the promising reactor technologies being considered by the GIF, the LFR has been identified as a technology with great potential to meet the needs for both remote sites and central power stations.

In the GEN IV technology evaluations, the LFR system was top-ranked in sustainability because it uses a closed fuel cycle, and top-ranked in proliferation resistance and physical protection because it employs a long-life core. It was rated ‘good’ in safety and economics. Safety was considered to be enhanced by the choice of a relatively inert coolant. The LFR was primarily envisioned for missions in electricity and hydrogen production and actinide management. Given its R&D needs for fuel, materials, and corrosion control, the LFR system was estimated to be deployable by 2025. The LFR system features a fast-neutron spectrum and a closed fuel cycle for efficient conversion of fertile uranium. The LFR can also be used as a burner of all actinides from spent fuel and as a burner / breeder with thorium matrices.

The GIF LFR Provisional System Steering Committee has prepared a draft of the System Research Plan (SRP) for the Lead-Cooled Fast Reactor [8] with molten lead as the reference coolant and lead-bismuth as a backup option.

Figure 4.1 illustrates the basic approach being recommended in the LFR SRP. It portrays the dual track viability research program with convergence to a single, combined demonstration facility (demo, also called Technology Pilot Plan - TPP) leading to eventual deployment of both types of systems.

This approach consists of the design of a small transportable system of 10–100 MWe size that features a very long refueling interval, and of a larger system, rated at about 600 MWe,

intended for central station power generation. Following the successful operation of the demo (a technology pilot plant) around the year 2018, a prototype development effort is expected for the central station LFR, leading to industrial deployment at the horizon of 2025-2030.

In line with the GIF-SRP for the LFR, the following sections provide a brief overview of the different LFR concepts under development worldwide.

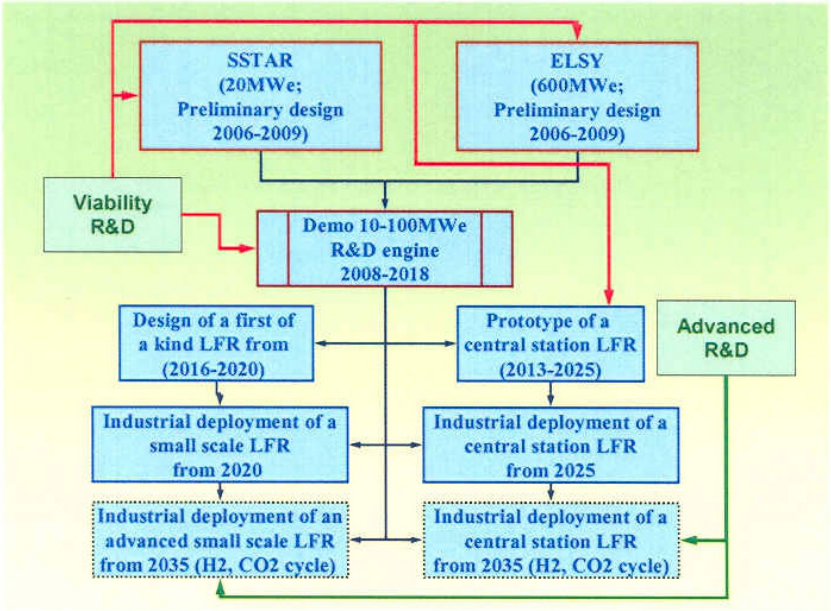

FIG. 4.1. LFR GIF-SRP Conceptual framework.

4.3. ELSY

4.3.1. Introduction

A major step in favor of the LFR occurred when EURATOM decided to fund the European Lead-cooled SYstem (ELSY) — a Specific Targeted Research Project of the 6th European Framework Program (FP6) — proposed to investigate the economical feasibility of a lead-cooled, critical reactor of 600 MWe power for nuclear waste transmutation [9–12].

Since September 2006, a consortium of twenty organizations (from industry, research centres and universities) including seventeen from Europe, two from Republic of Korea and one from United States has been pursuing the development of ELSY.

The ELSY project, scheduled to last three years, aims at demonstrating the possibility to design a competitive and safe lead-cooled fast power reactor using simple engineered features. This prospect is appealing also to private investors who have offered to participate in the initiative. This would create the conditions for advancing the ELSY activity even beyond the current sponsorship under Euratom's FP6.
The use of compact, in-vessel steam generators and a simple primary circuit (Fig. 4.2) with all internals possibly being removable are among the reactor features needed for competitive electric energy generation and long-term protection of investment.

Table 4.1 provides the preliminary parameters of ELSY.

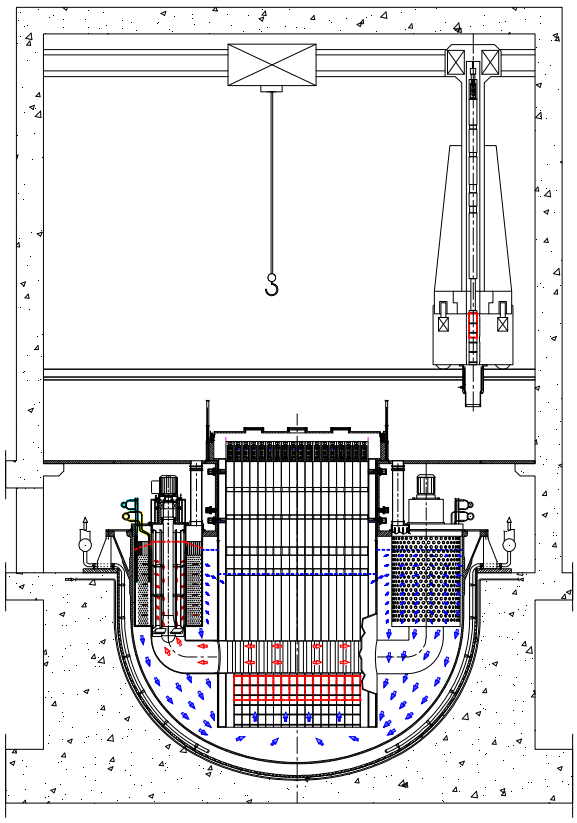

FIG. 4.2. ELSY Primary system arrangement.

TABLE 4.1. MAIN PARAMETERS OF THE ELSY PLANT

Parameter	Value
Power, MWe	600
Thermal efficiency	40%
Primary coolant	Pure lead
Primary system	Pool type, compact
Primary coolant circulation	Forced, at power, natural circulation + Pony motors for DHR
Primary pressure loss, bar	~ 1.5
Core inlet temperature, °C	~ 400
Core outlet temperature, °C	~ 480
Fuel	MOX with consideration also of nitrides and dispersed minor actinides
Fuel cladding material	T91 (aluminized)
Fuel cladding temperature, °C	(max)~ 550
Main vessel, m	Austenitic stainless steel, hung, short-height ~ 9; diameter ~ 12,5
Safety vessel	Anchored to the reactor pit
Steam generators	N° 8, integrated in the main vessel
Secondary cycle	Water-superheated steam at 180 bar, 450°C
Primary pumps	N° 8 mechanical, in the integrated in the steam generators
Internals	Removable
Inner vessel	Cylindrical
Hot collector	Small-volume, above the core
Cold collector	Annular, outside the inner vessel, free level higher than free level of hot collector
DHR coolers	N° 4, DRC loops + a Reactor vessel air cooling system
Seismic design	2D isolators supporting the reactor building

4.3.2. Description of the ELSY concept

The ELSY power plant is tentatively sized at 600 MWe (about 1500 MWth) because only plants of the order of several hundreds MWe are expected to be economically affordable on the existing, well-interconnected European grids.

In the ELSY design, sustainability represents one of the leading criterion. It requires the efficient utilization of the natural U resources and of the accumulated Plutonium (Pu), as well as the minimization of Minor Actinides (MAs) and Long-Lived Fission Products (LLFPs) building up. The fast neutron spectrum allows obtaining a self-breeder core with a U-Pu fuel and, at the same time, allows reducing significantly the MAs production with respect to thermal reactors.

More precisely, ELSY is conceived as an "adiabatic reactor", meaning that it has a unitary Conversion Factor and burns its own Minor Actinides. Nevertheless room will be provided for burning a larger amount, to cope the Minor Actinides legacy.

A challenging design goal is the respect of the relatively low max temperature assumed for the cladding (≅ 550°C). In fact, since the average Pb outlet core temperature (T_{out}) is 480°C (see Table 4.1), the clad temperature specification implies a rather flat T_{out} distribution. A further difficulty is introduced by the open square solution, because it does not permit to exploit different FA orificing, to locally regulate the Pb flow rate.

The 1530 MWth core (Fig. 4.3a,b) has been analysed with the ERANOS 2.0 code by a 3D geometry model. The spatial calculations have been carried out with the VNM-VARIANT TGV (Variational Nodal Method) code, which is a transport code based on the variational-coarse mesh nodal method that can adopt a 3D XYZ geometry.

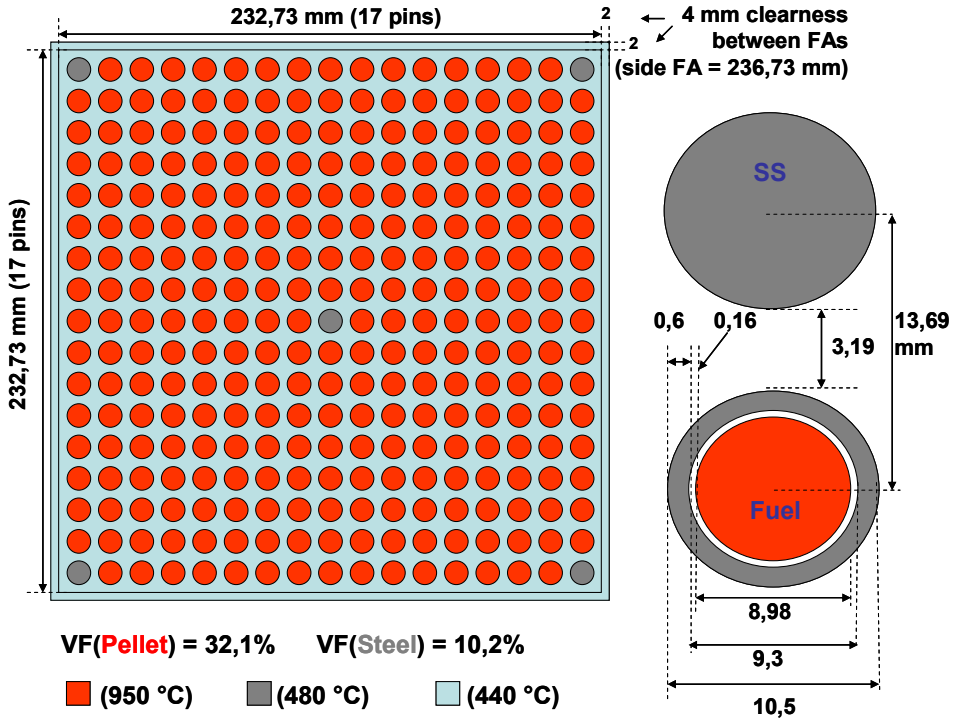

(a)

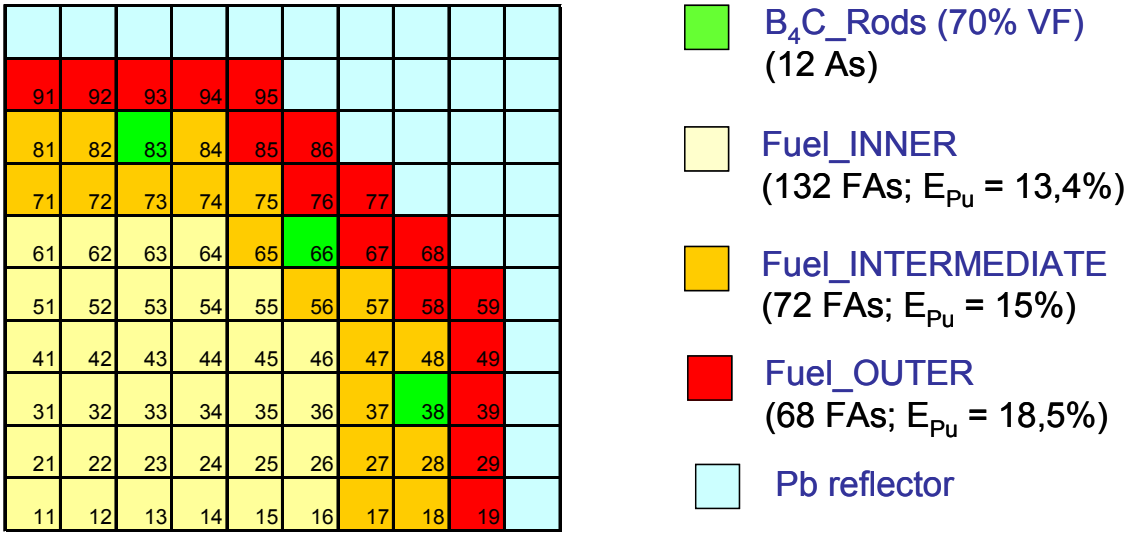

(b)

FIG. 4.3a,b. The ELSY 1530 MW(th) core design.

Figures 4.4 and 4.5 show the calculated average and max PD values for each FA (AvePD and MaxPD), respectively. It results evident that the 150 $W \cdot cm^{-3}$ postulated limit on PD is respected in each zone and a good "radial" flattening has been obtained with the adopted FA distribution (132 inner, 72 intermediate, 68 outer).

106,3	100,1	92,8	90,4	85,8				
109,0	101,0		93,2	109,7	97,0			
119,6	113,8	106,8	105,8	102,9	111,7	97,7		
112,9	110,1	106,2	102,7	106,1		111,7	97,0	
115,6	113,8	110,7	106,9	101,8	106,1	102,9	109,7	85,8
118,6	117,1	114,5	111,0	106,9	102,7	105,8	93,2	90,4
121,2	120,0	117,7	114,5	110,7	106,2	106,8		92,8
123,2	122,1	120,0	117,1	113,8	110,1	113,8	101,0	100,1
124,2	123,2	121,2	118,6	115,6	112,9	119,6	109,0	106,3

FIG. 4.4. ELSY core: FA AvePD results obtained by the 3D model (at BOL).

138,5	130,6	121,0	119,7	118,5				
133,2	125,9		118,2	138,6	127,2			
139,2	135,1	130,2	127,5	123,5	139,0	129,0		
128,7	126,8	123,0	119,7	127,7		139,0	127,2	
131,2	129,5	126,6	123,1	119,5	127,7	123,5	138,6	118,5
134,1	132,7	130,1	126,8	123,1	119,7	127,5	118,2	119,7
136,5	135,3	133,0	130,1	126,6	123,0	130,2		121,0
138,2	137,0	135,3	132,7	129,5	126,8	135,1	125,9	130,6
138,9	138,2	136,5	134,1	131,2	128,7	139,2	133,2	138,5

FIG. 4.5. ELSY core: FA MaxPD results obtained by the 3D model (at BOL).

Table 2 resumes the main power parameters of the core. The average power per FA is 5.6 MW (5.9, 5.5 and 5.1 in the inner, intermediate and outer zones, respectively). The axial form factors in each fuel zone (ff_ax_INN, INT, OUT), defined as the ratio between the Max PD and the average PD of the same hottest FA (MaxAve_PD), vary from 1.12 (in the inner zone) up to 1.24 (in the outer one). Also the "radial" form factor values in each fuel zone (ff_rad_INN, INT, OUT), here defined as the ratio between the MaxAve_PD and the average PD on the entire zone, increases from the centre (1.09) toward the boundary (1.13).

As reference for the control rods system, an anti-reactivity of 15 $ (some 5000 pcm) has been set. To this purpose, the analysis carried out has been devoted to reduce the number of control rods, by searching the positions in the core that assure the required anti-reactivity. These "optimal" positions have been identified between the intermediate and the outer fuel zones, making possible to control the reactor by 12 B_4C elements (70% B_4C VF).

Furthermore, a system of absorbers (with 15% B_4C VF) positioned above the active zone has been considered. It could be able to compensate the low cycle swing, without perturbing the radial power distribution. In this case the 12 conventional control rods (70% B_4C VF) would be utilised only for safety and refuelling purposes.

The Reactor Vessel (RV) has a fixed cover that is basically a large annular steel plate with a central main steel Upstand to accommodate the extended Cylindrical Inner Vessel (CIV). The fixed reactor cover plate incorporates penetrations which host the reactor components. The remaining inner part of the reactor cover is not conventional, because it consists of essentially the packed heads of the fuel/dummy assemblies that extend over the reactor cover plate. The cold collector is located in the annular space between the RV and the CIV. The fuel assemblies are withdrawn from and plug into the core using a simple handling machine that operates in the cover gas at ambient temperature, under full visibility.

The fuel elements, whose weight is supported by lead, are fixed at their upper end in the cold gas space, well above the lead surface. This avoids the classical problem of a core support grid immersed into the coolant which would require a tricky ISI in lead environment.The core consists of an array of open fuel assemblies (FAs) of square pitch surrounded by reflector-assemblies, a configuration that presents reduced risk of coolant flow blockage. An alternative solution with closed hexagonal FAs is retained as a fall-back option.

Each FA contains, at its bottom end, a fuel pin bundle with structural grids similar to the grids of a PWR. The FA foot is free from mechanical supports (no core grid of classical design) except for the radial interlocking contact with adjacent FAs and Dummy Assemblies (DAs). FAs and DAs create a self-standing structure.

The outer DAs ring is installed, with a gap of a few mm, inside the CIV which acts as a core barrel, representing a back up supplementary core radial constraint. The gap and the free horizontal displacements of the FAs will facilitate refueling in case of FA deformation; in fact no clearance is provided among the FAs during reactor operation, in order to avoid the possibility of reactivity insertion through core compactness. The upper part of the FA is peculiar to this novel ELSY design, because it extends well above the fixed reactor cover, and the FA heads are directly accessible for handling from the above reactor cell. This innovative approach is favoured by lead properties, i.e.:

(i) Low vapour pressure;
(ii) Buoyancy effect resulting from its high density.

The anticipated advantages are:

- The elimination of the core support grid with the associated stringent requirement of ISI which would be difficult to perform in lead. The elimination of the core support grid represents a plus in investment protection, taking into account the near impossible replacement of such a component in large size reactors.
- The elimination of the need to lock the FAs to the core support grid. Because of the buoyancy resulting from the high density of lead, a conventional approach might require the locking of the FAs to the core support grid.
- The elimination of in-vessel fuel transfer equipment. This type of machine has never been designed or tested in lead. In addition, reactor compactness would require the use of a pantograph machine which would require a tricky and uncertain development.

Considering the high temperature and lead environment, any approach that foresees the use of in-vessel refuelling equipment would represent a tremendous R&D effort and substantial associated technical risk, especially because of the need to develop reliable bearings operating in lead, an unknown technology at present. For these reasons the adopted design approach represents a real breakthrough.

The Steam Generator is composed of a stack of spiral-wound tubes arranged in the bottom-closed, annular space formed by vertical outer and inner shrouds (see Fig. 4.6). The inlet and outlet ends of each tube are connected to the feed water and steam headers, respectively, both arranged above the reactor cover plate.

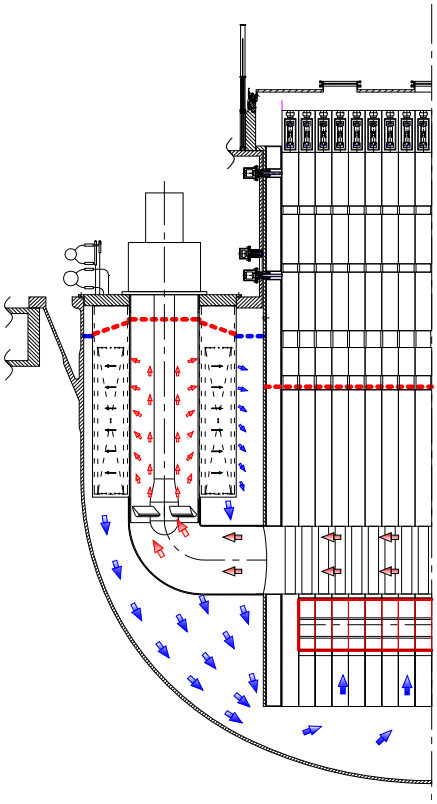

FIG. 4.6. The innovative steam generator-primary pump arrangement of ELSY.

An axial-flow Primary Pump, located inside the inner shell, provides the head required to force the coolant to flow radially from the inner to the outer perforated shrouds through the SG spirals tubes (see Fig. 4.6). Therefore the hot primary coolant enters the pump-steam

generator assembly from the bottom and flows radially through the SG spiral tubes arranged at different vertical levels. This ensures that the coolant will flow over steam generator bundles even in the event of reduction in the primary coolant level in case of leakage from the reactor vessel. As a by-product, the SG unit can be positioned at a higher level in the downcomer and the RV shortened, accordingly. All reactor internal structures are removable and in particular the SG Unit, because it's upper part is bolted to the reactor cover plate and can be withdrawn by radial and vertical displacements, which disengage the unit from the reactor cover plate.

Corrosion of structural materials in lead is one of the main issues of LFR, deemed so critical that several international organizations consider LFR only for long term deployment. However, material corrosion is very dependent from temperature and lead speed. In order to overcome this issue, three main design provisions have been adopted in ELSY:

- Max primary coolant temperature of 480°C;
- Max primary coolant speed of 2 m/s;
- Elimination of mechanism operating inside the primary coolant to drastically reduce the type of materials to be developed.

Limitation of the temperature and primary coolant speed allows the use of industrial materials such as AISI 316, AISI 321, T91, even if an effort for development of an alluminization process of fuel cladding material remains necessary. A material under test (Maxthall) seems to be suitable for the pump impeller which is the only remaining component moving at high speed in lead. All types of bearing have been eliminated by design: bearings supporting the pump shaft and mechanism of the control rods are in gas atmosphere, refueling machine in lead is no more necessary. Safety is based both on the inherent safety characteristic of lead as well as on the specific engineered solution identified in ELSY to meet the safety objectives.

Molten lead has the advantage of allowing operation of the primary system at low (atmospheric) pressure. Low doses to the staff can also be anticipated, owing to lead low vapor pressure, high capability of trapping fission products and high gamma radiation shielding. In the case of accidental air ingress, in particular during refueling, any produced lead oxide can be reduced to metal by injection of hydrogen gas and the reactor operation safely resumed. Despite the high density of lead, pressure drops can be kept pretty low (about one bar inside the core and a total pressure drop of the primary system of about 1.5 bar) because low neutron energy losses in lead allows larger fuel rods pitches. Moreover, lead allows a reliable natural circulation of the primary coolant which results in a suitable grace time for operation and simplification of control and protection systems.

In case of leakage from the reactor vessel, the free level of the coolant can be designed such as to guarantee the coolant circulation through, and the safe heat removal from, the core. Any leaked lead would solidify without significant chemical reaction affecting the operation or performance of surrounding equipments or structures.

Fuel dispersion dominates over fuel compaction, thus reducing considerably the likelihood of the occurrence of severe re-criticality events in the case of core disruption. In fact the lead density, which is slightly higher than the fuel one, and convective streams make rather difficult to achieve scenarios leading to fuel aggregation with subsequent formation of a secondary critical mass, in the event of postulated fuel failure. The use of MOX fuel containing MA increases Proliferation Resistance because of the difficulties in partitioning pure Pu from this nuclear material.

The use of a coolant chemically inert with air and water and operating at atmospheric pressure greatly enhances Physical Protection. There is reduced need for robust protection against the risk of catastrophic events, initiated by acts of sabotage, because there is a little risk of fire propagation. There are no credible scenarios of significant containment pressurization. The innovative reactor layout such as primary pumps installed in the hot collector, besides the economic advantages, improves several safety-related aspects, such as:

- Moderate volume of hot collector and large volume of cold collector;
- DHR coolers immersed in the cold collector. This favors the natural circulation and eliminates the interference between hot coolant streaming from the core and cold coolant from the outlet of the DHR coolers.
- Free-level of the cold collector, in normal operation, higher than the free-level of the hot collector. This, in case of primary pump shutdown, favors a mild transition from forced to natural circulation of the coolant and hence ensures adequate heat removal from the core during a transient.

Installation of SGs inside the vessel is the real challenge of a LFR design. In operation there is the need for SGs of:

- A sensitive and reliable leak detection system;
- A highly reliable steam generator depressurization and isolation system.

High reliability requires redundancy of the leak detection system achieved by means of:

(i) Acoustic system,
(ii) Steam detection in the reactor cover gas, and
(iii) Pressure increase detection of the reactor cover gas.

Fast depressurization from 180 bar in few seconds will be achieved operating both water side as well as steam side because of the use of ferrules at inlet of the SG tubes. Careful attention has been also given to the issue of mitigating the consequences of the SG tube rupture (SGTR) accident to reduce the risk of pressurization of the primary boundary. To this end, three provisions have been conceived: The first provision is the elimination of the risk of failure of the water and steam collectors inside the primary boundary by installing them outside the reactor vessel. This provision aims to eliminate by design a potential initiator of a severe accident of low probability but potentially catastrophic consequences (see Fig. 4.7).

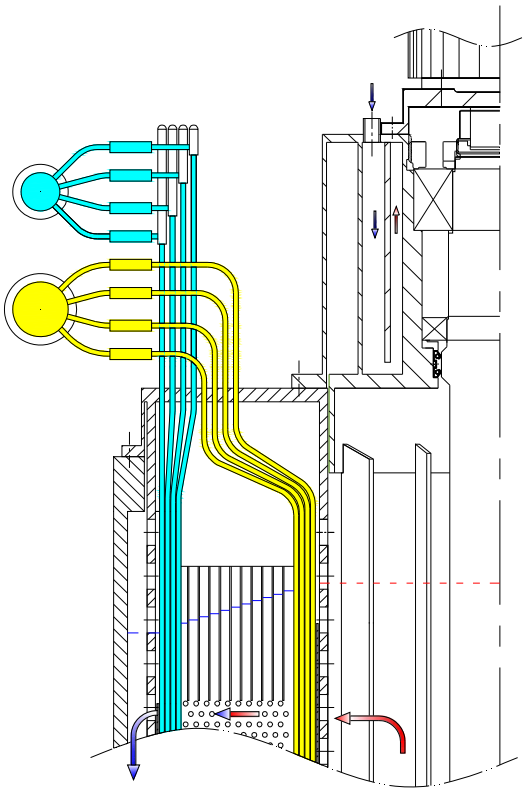

FIG. 4.7. Steam generator collectors arrangement.

The second provision (to be confirmed in term of feasibility) is the installation on each tube of a check valve close to the steam header and of an excess flow valve close to the feed water header. With these valves any leaking tube is promptly isolated.

The third provision aims at ensuring that the flow of any feedwater-steam-primary coolant mixture be re-directed upwards and the risk of potentially disruptive pressure surges within the reactor vessel prevented by design. To this purpose in the event of a SGTR the normal radial flow is deviated upwards by design features that are fully passive and are actuated by pressurization in the SG bundle.

Pressure relieving ducts, each with two rupture discs, installed on top of each SG unit, hydraulically connect the reactor cover gas plenum with the Above-Reactor Enclosure in case of inner pressure surge, particularly brought about by the SGTR accident. The evaluation of the pressure evolution as well the pressure waves propagation inside the primary system in case of SGTR is part of the ELSY program.

The fact that molten lead does not react violently with air or water gives the designer some freedom in the choice of the liquid for the DHR coolers, the use of air and water remaining the preferred approach.

A simple system for decay heat removal is the Reactor Vessel Air Cooling System (RVACS) which consists basically of an annular tube bundle of U-tubes arranged in the reactor pit with atmospheric air flowing pipe-side in natural or forced circulation (see Fig. 4.8). RVACS is a reliable system, but its use without other systems can only be considered for small-size reactors since the vessel outer surface is relatively large in comparison with the reactor power.

A Reactor Pit Cooling System (RPCS) is additionally included for use during in-service inspection of the reactor vessel.

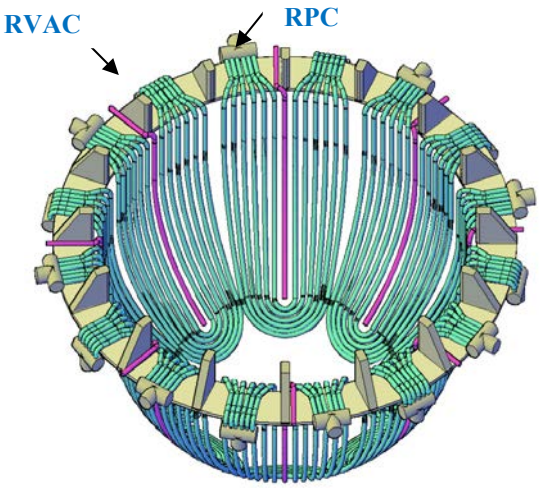

FIG. 4.8. Schematic layout of RVACS and RPCS pipe bundle of ELSY.

In the case of ELSY, the RVACS performance is sufficient only in the long term (about one month after shut down) and a Direct Reactor Cooling (DRC) system is needed, equipped with coolers immersed in the primary system. Stringent safety and reliability requirements of the DRC system will be achieved by redundancy and diversification. The DRC system is made of four loops; two loops operating with water (the W-DHR loops) and the remaining loops with water and/or air (the WA-DHR loops) (Fig. 4.9).

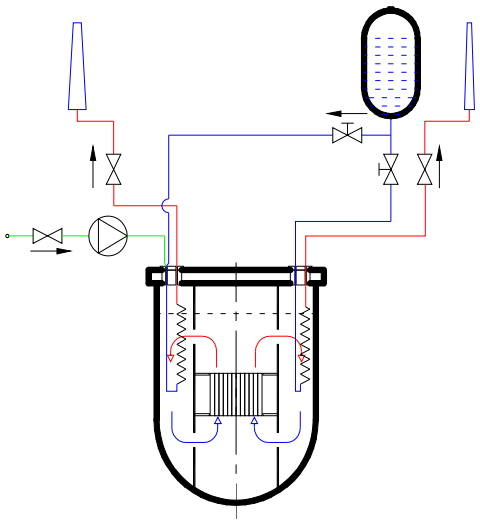

FIG. 4.9. DRC W-DHR (right-side) and WA-DHR loops, process scheme showing stored cooling water interconnection.

Each W-DHR loop is made of a cooling water Storage Tank, a water-lead Dip Cooler, interconnecting piping, and steam vent piping to discharge steam to the atmosphere. The two W-DHR loops with the contribution of the RVACS are sufficient to remove the decay heat in order to respect the temperature limit of 650°C specified for the 4th Category, service level D, over a week's time from reactor shut down. Each WA-DHR loop is made of an inlet air duct,

an air-lead Dip Cooler and an outlet air duct. The inlet air duct is equipped with an electric fan supplied by batteries. Isolation valves are installed in the inlet air and outlet ducts.

A connection of the WA-DHR Dip Cooler to the cooling water storage tank of a W-DHR loop is also provided to for improved cooling with a mixture of air and water. The two WA-DHR loops with the contribution of the RVACS and the use of the water of the W-DHR loops in the short term from the reactor shut down, are sufficient to remove the decay heat in order to respect the temperature limit of 650°C established for the 4th Category, service level D. In the long term operation with air natural circulation is sufficient to respect the temperature limit. The Dip Cooler tube bundle is made of bayonet tubes (see Fig. 4.10).

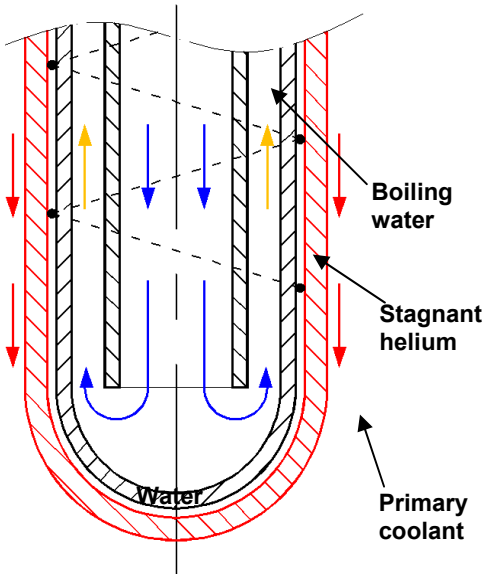

FIG. 4.10. Bayonet tubes of the DHR dip coolers.

The bayonet consists of three concentric tubes, the outer two of which have the bottom end sealed. Water evaporation or air heating takes place in the annulus between inner tube and the intermediate tube. The annulus between the outer tube and intermediate tube is filled with He gas at a pressure higher than the lead pressure at the bottom end of the bundle. All annuli are interconnected to form a common He gas plenum, the pressure of which is continuously monitored. A leak from either walls of any of the outer tubes, is promptly detected because of depressurization of the common gas plenum.

The bayonets of the ELSY DRC Dip Coolers are different with respect to classical bayonets, which consist each of only a pair of concentric tubes. The two outer tubes do not constitute a double walled tube, but are mechanically and, thermally decoupled. This configuration allows to localize the most part of the thermal gradient between lead and boiling water across the gas layer, avoiding both risk of lead freezing and excessive thermal stresses across the tube walls during DHR steady state operation and transients.

4.3.3. Current status and summary

As briefly summarized in the following, the main features identified to get ELSY in compliance with the GEN IV goals are either based on the properties of lead as a coolant or specific design innovations to be engineered in the project.

4.3.3.1. Sustainability

Since lead is a coolant with low neutron absorption and scattering, it is possible to maintain a fast neutron flux even with a large amount of coolant in the core. This allows an efficient use of neutrons, a breeding ratio of about 1 without fertile assemblies, long core life and a high fuel burn-up. A breeding ratio significantly larger than one, requiring expensive fertile fuel subassemblies in the core, is not necessary because deployment of additional FR units can be afforded with a first core load based on enriched uranium. This strategy is of particular interest for new nuclear countries whose fast reactor nuclear deployment should not be conditioned by an anticipated LWR program.

The fast neutron flux significantly reduces net MA generation, Pu recycling in a closed cycle being the condition recognized by GEN IV for waste minimization. The potential capability of the LFR system to safely burn considerable amounts of recycled minor actinides within the fuel will add to the attractiveness of the LFR.

4.3.3.2. Economics

A simple plant will be the basis for reduced capital and operating cost. A pool-type, low-pressure primary system offers great potential for plant simplification. The use of in-vessel Steam Generator Units (SGU's), and hence the eliminating the intermediate circuit, is expected to provide competitive generation of electricity in the LFR. The configuration of the reactor internals will be as simple as possible. The very low vapor pressure of molten lead should allow relaxation of the otherwise stringent requirements of gas-tightness of the reactor roof and possibly allow the adoption of simple fuel handling systems. Reduction in the risk to capital results from the potential of removable/replaceable in-vessel components.

4.3.3.3. Safety and reliability

Molten lead has the advantage of allowing operation of the primary system at atmospheric pressure. A low dose to the operators can also be predicted, owing to its low vapor pressure, high capability of trapping fission products and high shielding of gamma radiation. In the case of accidental air ingress, in particular during refueling, any produced lead oxide can be reduced to lead by injection of hydrogen and the reactor operation is safely resumed.

The moderate ΔT between the core inlet-outlet temperatures reduces the thermal stress during transients, and the relatively low core outlet temperature minimizes creep in steels.

It is possible to design fuel assemblies with fuel pins spaced as in the case of fuel assembly of the water reactor. This results in a moderate pressure loss through the core of about one bar, in spite of the high density of lead, with associated improved heat removal by natural circulation and the possibility of an innovative reactor layout such as the installation of the primary pumps in the hot collector to improve several aspects affecting safety. In case of leakage of the reactor vessel, the lower free level of the coolant will be sufficient to ensure the coolant circulation through the core and the safe decay heat removal. Any leaked lead would solidify without significant chemical reactions affecting the operation or performance of surrounding equipment.

With high-density lead as a coolant, fuel dispersion dominates over fuel compaction, making the occurrence of complex sequences leading to re-criticality less likely. In fact lead, with its higher density than oxide fuel and its natural convection flow, makes it difficult to lead to fuel

aggregation with subsequent formation of a secondary critical mass in the event of postulated fuel failure.

4.3.3.4. Proliferation resistance and physical protection

The use of MOX fuel containing MA increases proliferation resistance. The use of a coolant chemically compatible with air and water and operating at ambient pressure enhances Physical Protection. There is reduced need for robust protection against the risk of catastrophic events, initiated by acts of sabotage because there is a little risk of fire propagation and because of the passive safety functions. There are no credible scenarios of significant containment pressurization.

4.4. PBWFR, SLPLFR and CANDLE: current status of R&D

The R&D activities on LFR performed by the Japan Atomic Energy Agency (JAEA), the Central Research Institute of the Electric Power Industry (CRIEPI) and the Tokyo Institute of Technology in Japan are summarized as follows.

4.4.1. LFR research in JAEA

LFR design study and the related fundamental corrosion experiments were carried out within the framework of "Feasibility Study on Commercialized Fast Reactor Cycle Systems" from 1999 to 2005.

LBE as a fast reactor coolant is comprised of the eutectic mixtures: 45% Pb and 55% Bi. The boiling point of LBE is high at 1 670°C, and it is possible to realize low-pressure cooling systems. The high boiling point has also an advantage from the viewpoint of coolant boiling in the core damage accident.

An LBE-cooled reactor has a potential to simplify system design by deleting intermediate cooling systems, because chemical reactivity of LBE in contact with water and air is small. Furthermore, LBE has excellent nuclear properties.

On the other hand, a significant property of LBE is its high solubility for chemical elements that are components of steel used as cladding or structural material. Experimental studies to solve the corrosion problem have been carried out in Japan since 2001. The maximum cladding temperature must be restricted to control corrosion. At the early stage of this study, the maximum cladding temperature was set to 650°C, and then it was changed to 570°C based on the outcomes of some experimental studies [13]. As a result, the core inlet and outlet coolant temperatures are 285°C and 445°C, respectively.

The specific gravity of LBE is twelve times greater than that of sodium. This property affects structural integrity, a particular concern for high seismicity in Japan. According to the feasibility study, it is estimated the LFR plant size in Japan would be limited to less than a medium-scale size of around 750 MWe, even with adoption of 3D seismic isolation [14, 15].

It was found that the LFR has potential as a future fast reactor system; however, this concept needs several fundamental research efforts to establish technical feasibility. In 2006, a combination of the sodium-cooled fast reactor (SFR) with MOX fuel core, the advanced aqueous reprocessing process and the simplified pelletizing fuel fabrication was selected as currently the most promising conceptual system of the FR cycle technologies that has

potential to satisfy the performance criteria through R&D efforts in Japan. A new project, Fast Reactor Cycle Technology Development Project (FaCT Project) was launched in JFY2006 focusing on development of the selected concept. Therefore, in Japan the LFR is no longer considered a candidate fast reactor option and no budget for research activities including LFR design study has been allocated in the FaCT project.

4.4.2. LFR research in CRIEPI

The LBE-cooled fast reactor is one of the candidates of the next generation nuclear reactor. CRIEPI (Central Research Institute of Electric Power Industry) started the LBE studies from the proposal of an innovative steam generator for the sodium cooled fast breeder reactor with direct contact heat transfer between the LBE in the intermediate loop and water.

To clarify the heat transfer performance of LBE in the intermediate loop and the two phase flow characteristics of LBE, water and steam, the "CRIEPI Pb-Bi Test Loop on Thermal Hydraulics" was constructed in 1997. The heat transfer performance around the tube and the gas lift performance of the LBE tested in the loop have been clarified [16].

Another important issue in the use of LBE is material compatibility. To clarify the corrosion characteristics of LBE, the "CRIEPI Static Corrosion Test Facility" was constructed in 2001. The objective of this facility was to understand the corrosion behavior of stagnant LBE at 650°C on high chromium martensite stainless steel, which is a promising candidate of structural material for LFRs. A series of corrosion tests were performed jointly by CRIEPI and JAEA.

4.4.3. LFR research in Tokyo Institute of Technology

Tokyo Tech proposed a small long-life fast reactor cooled by LBE, and presented a preliminary design in 1991. Since then, the importance of the Tokyo Tech's study has become gradually widely recognized and as a result, programs were supported to promote LFRs in the following areas:

- Po behavior, treatment, cross-section measurements (FY 1998–2000);
- Corrosion (materials test, oxygen control) (FY 1999–2001);
- CANDLE burnup (FY2001-2003);
- Steam lift-pump reactor designs and basic research (FY2002-2004).

4.4.3.1. PBWFR and SLPLFR

In the reactor called Pb-Bi Cooled Direct Contact Boiling Water Fast Reactor (PBWFR) [17–19], direct contact boiling provides significantly high heat transfer. The PBWFR electric power is 150 MW. The design limit of the cladding temperature is 650°C. The LBE core outlet temperature is 460°C. The LBE temperature rise across the core is 150°C. The conditions of the secondary coolant steam are the same as those of conventional BWRs. The PBWFR plant is equipped with a Reactor Vessel Air Cooling System (RVACS) and a Primary Reactor Auxiliary Cooling System (PRACS), and an auxiliary water supply tank to cope with a loss of feedwater. Hydrogen is dissolved in feedwater at a concentration of 100-500 ppb to keep oxygen concentration in LBE around 10^{-5}wt%.

The second reactor concept, called the Steam Lift Pump Type LFR (SLPLFR) [20], has SGs in the reactor vessel, and subcooled water is injected into LBE above the core at a low flow rate. The resulting steam condenses in a dedicated heat exchanger, which also serves as the

re-heater of the feedwater. In comparison with PBWFR, SLPLFR is expected to have higher thermal efficiency with higher LBE temperature, lower pressure in the primary loop, and no Po or LBE droplet contamination in the turbines.

4.4.3.2. CANDLE

For the CANDLE reactor [21, 22], the neutron flux shape and the nuclide and power density distributions remain constant but move in an axial direction. The solid fuel is fixed at each position and no movable reactivity control mechanisms are required. The change of excess reactivity during burn-up is theoretically zero for ideal equilibrium conditions. The core characteristics, such as power feedback coefficients and power peaking factors, do not change over the operational life. Since the k-infinity of replacement fuel is less than unity, the transport and storage of such fuels is easy and safe.

Application of this burn-up strategy to LFRs with metallic or nitride fuels enables the following excellent characteristics; fissile material is required only for the nuclear ignition region of the initial core, and only natural or depleted uranium is required for the remaining region of the initial core and for succeeding cores. The average burn-up of the spent fuel is about 40%; that is equivalent to 40% utilization of the natural uranium without reprocessing or enrichment. Ongoing basic research in support of this concept includes the following items:

- Corrosion testing of structural and cladding materials;
- Testing of Pb-Bi-water direct contact boiling;
- Testing of oxygen control with steam injection into Pb-Bi;
- Testing of Pb-Bi droplet removal in steam flow;
- Assessment of Polonium behavior in the coolant system.

Concerning the budget and schedule of the current program, Tokyo Tech is preparing an application for follow-on projects in the LFR program. The LFR program is strongly supported by the Center of Excellence – Innovative Nuclear Energy Systems (COE-INES).

4.5. PEACER

4.5.1. Introduction

A group of researchers at Seoul National University (SNU) began a feasibility study on accelerator-driven nuclear waste transmutation concept proposed by LANL, U.S.A. Then the Nuclear Materials Laboratory at SNU (SNUMAT, hereafter) had begun experimental investigations on Pb-Bi eutectic alloy (LBE) as an alternative coolant to sodium for use in spent nuclear fuel waste transmutation systems. Positive experimental verification of its physico-chemical properties had pushed SNUMAT to initiate the development of the first dedicated transmutation fast reactor design cooled by LBE, designated as Proliferation-resistant Environment-friendly Accident-tolerant Continuable and Economical Reactors (PEACER) [23–25].

The first design had a pancake-shaped fast reactor core with metallic fuels containing transuranic (TRU) elements extracted from LWR spent fuels by on-site pyrochemical partitioning processes under through multi-national controls. The upper core region of PEACER has thermalized neutrons for stabilization of long-living fission products including technetium and iodine. Coolant exit temperature was judiciously chosen to be 400°C in order to ensure 60 year design life of structural materials including steam generator and 3 year life of fuel cladding material, even with the high corrosivity of LBE.

The Nuclear Transmutation Energy Research Center of Korea (NUTRECK) was established at SNU in 2002 as a dedicated R&D institution to further explore the transmutation technology utilizing heavy liquid metal coolant and pyrochemical partitioning process along the line of multinational nuclear approaches. A design optimization by using 3D CAD led the development of PEACER-300 with a 300 MWe capacity.

4.5.2. Description of the PEACER concept

A set of design criteria for PEACER was established when the first conceptual design effort was begun for LBE-cooled transmutation reactor with the financial support of Ministry of Science and Technology of the Republic of Korea. Taking into account anticipated energy shortage in developing countries and international concern over growing proliferation risk as well as long term safety of spent fuel repositories, design criteria for the transmutation systems have been established, as shown in Fig. 4.11.

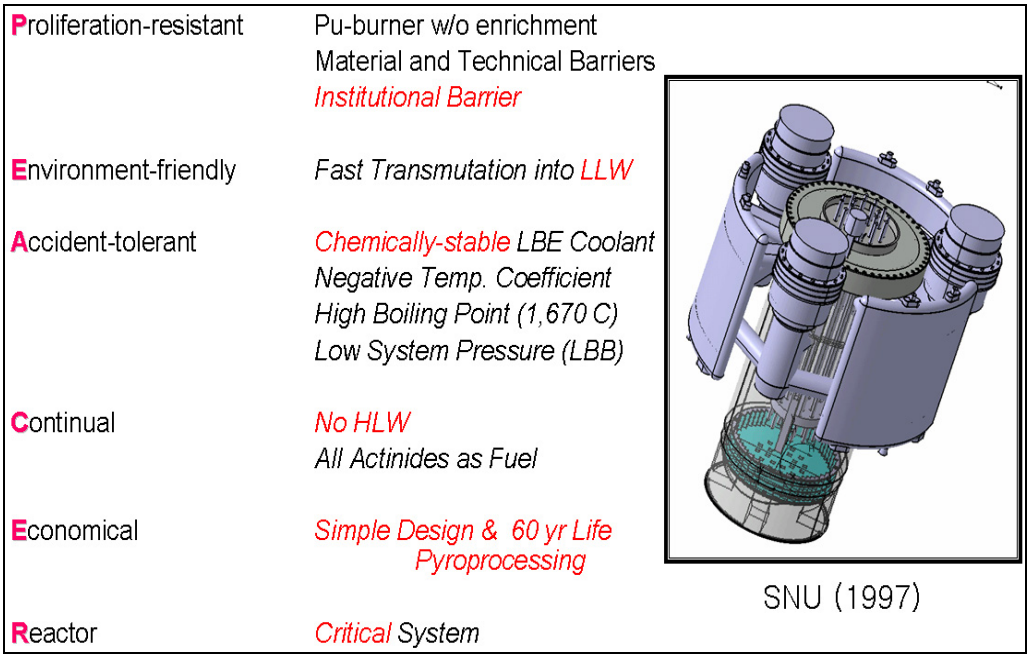

FIG. 4.11. Korean design criteria of nuclear transmutation energy systems and PEACER design attributes to address each criterion.

It is interesting to note that GEN-IV design goals that came a few years later, are clearly consistent with the PEACER criteria The chance for diverting any intermediate materials from the transmutation system by clandestine groups must be sufficiently ruled out. As a materials barrier, the transmutation reactor should burn fissile isotopes to leave spent fuel from a transmutation system with adequate concentrations of even mass-number isotopes such that intense heat and spontaneous neutrons are generated. As the engineering barrier all intermediate process materials containing spent nuclear fuel materials should have intense radiation such that access to process materials by any clandestine operation would be impossible. Institutional barrier must be superimposed in order to prevent any state-wide attempt to divert nuclear materials.

Transmutation technology is designed to reduce toxicity and longevity of radioactive materials. Final waste form discharged from a transmutation system should be acceptable for available sites for ultimate disposal. Not all countries have geological conditions to accept

high-level wastes that require environmental controls for up to one million years. Nuclear power including fusion energy is the ultimate energy source for sustainable world. However even nuclear fusion is expected to generate high-level waste. Therefore desirable transmutation system should be capable of adequately burning long-living wastes, discharging only low-intermediate level wastes since disposal of the latter can be disposed of in sustainable manners in most countries.

Lessons learned from the past nuclear accidents including TMI-2 and Chernobyl had highlighted the fact that human error is one of the most important causes that will persist in the future systems. Therefore passive safety characteristics must be embedded in the design of transmutation system, paying particular attention to large quantity of intensely radioactive materials within the partitioning system. Passivity of accident mitigation system design should be high enough to tolerate worst conceivable human error under control without leading to large early release events. Physical attacks on nuclear energy system are recognized as conceivable threat. Adequate protection against airborne attack as well as natural disasters such as earthquake should be assured. The same level of passive safety is required for all associated systems including spent fuel partitioning facility.

Uranium supply is expected to last only about hundred years while growing number of countries explore nuclear power generation. Transmutation systems should be able to produce electricity and heat using spent nuclear fuel wastes from operating thermal reactors and of their own, by having capability of burning even mass-number isotopes including uranium-238 and thorium-232. The capability will expand fuel resources to supply the world until nuclear fusion will become economically viable. It was recognized that even nuclear fusion reactors, even when completely developed, will produce high level wastes and transmutation technology like PEACER will be required to operate in symbiotic cycles in order to make fusion energy environmentally acceptable. In addition, nuclear transmutation system should generate energy without producing greenhouse gases.

Overall cost of energy from nuclear transmutation system should be competitive with other commercial means, including fossil energy. Cost figures include all expenses from spent fuel handling and processing to final waste disposal as well as construction, operation and decommission of the facility. It is mandated that PEACER design must have economical competitiveness against advanced light water reactors. The concentration of odd mass-number isotope in discharged fuels from PEACER core is designed to decrease below that of even mass-number isotopes by minimizing TRU build up through maximization of neutron leakage so that materials barrier nature can be introduced in discharged fuels.

The PEACER core design also yields a high support ratio (the ratio of amount of transuranic element burnt in the transmutation core over the amount produced from light water reactor core for the same electricity generation), exceeding two (2.0). The high support ratio goal could be achieved by using high diameter-to-height ratio for the reactor core. Peripheral thermal trap areas are introduced to produce epi-thermal neutrons for the stabilization of long living fission products, as shown in Fig. 4.12.

Rated Power	850 MWt (300 MWe), 35% efficiency
Feed Fuel Material	LWR and HWR SNF
Feed Fuel Composition	U-TRU-Zr (57.2/31.9/10.9) Metallic Fuel with Pb-bonding Smeared Density : 67% 3 Enrichment and 3 Batch Tc, I in Thermal Traps
Fuel Cycle Strategy	Annual Reload & In-house Pyroprocess
Support Ratio	2.06 for TRU (CR=0.6) 2.64 for Tc, I
Fuel Assembly	PWR Style 17 X 17 Array
Pitch-to-Diameter Ratio	1.44
Core Shape	Pancake Design with High Leakage 50 cm H X 382 cm D
Scram Systems	Dual B_4C Absorber Assemblies
Coolant	Pb-Bi Eutectic with O_2 Control Operating Temp.: 300 ~ 400 ºC

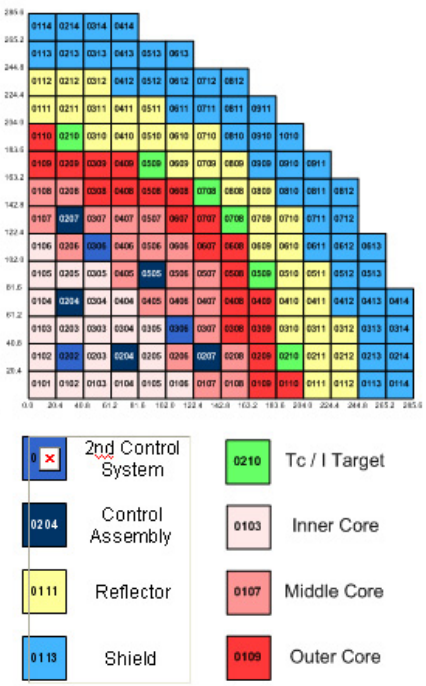

FIG. 4.12. PEACER-300 core design characteristics.

As a result, long-lived fission products including Tc and I can be stabilized in its epithermal neutron spectra at a support ratio of about 2.64. Metallic fuel form is chosen for PEACER core for higher negative temperature coefficient and better compatibility with pyrochemical process. The metallic fuel rod consisted of about 60% U, 30% TRU and the remainder as zirconium is bonded to HT-9 cladding with pure Pb, to have overall smeared density of about 67%. Reaction layer depth of metallic uranium-zirconium fuel bonded with liquid lead has been measured to be about 46 micrometer after 1 000 hour exposure at 650°C. PEACER fuel is expected not to exceed the temperature even during accidental conditions.

To address concern of the use of LBE as to flow accelerated corrosion and vibration of reactor core structure including fuel cladding, relatively low flow speed is used with low power density. Fuel assemblies have square lattice with high pitch-to-diameter ratio without channel boxes so that cross flow can attenuate thermal peaking. Thermal peaking is further reduced by having three enrichment zones, as shown in Fig. 4.12.

The first conceptual design, PEACER-550, had been verified by a systematic review process that confirmed overall soundness in design. However some design deficiencies were identified particularly in thermal-hydraulics and safety analyses. These deficiencies have been resolved by installing an improved design method interfaced with 3D CAD. The final design for PEACER-300 is shown in Fig. 4.13 and the final design characteristics are given in Table 4.2.

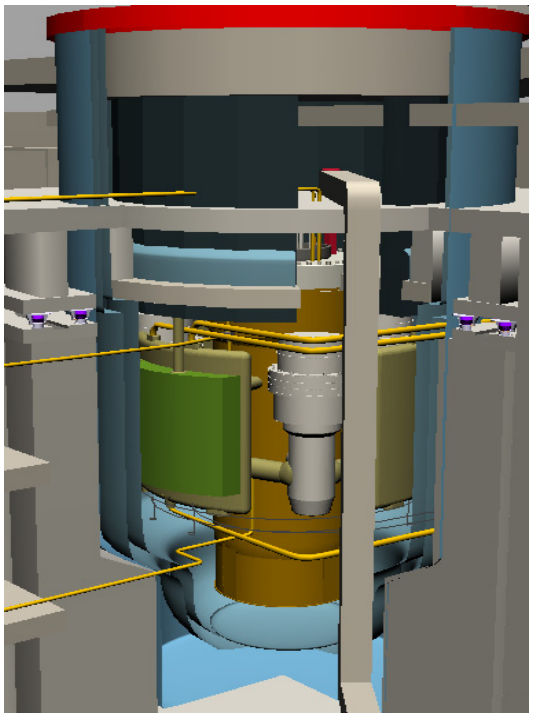

FIG. 4.13. 3D CAD Drawing of PEACER-300 MWe.

TABLE 4.2. PRINCIPAL SYSTEM DESIGN PARAMETERS OF PEACER-300

Parameter	Value
Power (MWe/MWt/efficiency)	300/850/35.3
Core outlet/inlet coolant temperature (°C)	400 / 300
Primary coolant	Pb-Bi (45-55 Wt. %) eutectic alloy
Primary system cover gas pressure (atm)	1.0
Primary coolant flow rate (kg/sec)	58 000
Average power density, MWt/ m^3	205
Average discharge burnup (GWd/t)	76.6
Fuel composition	U-TRU-Zr (57-32-11 Wt. %) 3 TRU Enrichment Zoning Smeared Density : 67%
Fuel assembly	PWR yype open lattice (square array without wrapper)
Cladding material	HT-9
Fuel/coolant volume fraction	0.159/0.677
Fuel assembly lifetime (year)	3
Fuel pin diameter, cm	0.832
Fuel rod pitch to diameter ratio	1.44
Active core dimensions: height / diameter, m	0.50/3.82
Energy converter / balance of plant	Superheated steam cycle
Fuel cycle strategy	Full actinide recycle using pyrochemical partitioning facility
In core management	3 Batch annual reload
Passive safety	Negative temperature coefficient and Pb-Bi natural circulation
Emergency decay heat removal	Guard vessel cooling by natural circulation of air; always in effect and enhanced by LBE flooding during emergency
Design seismic acceleration (g) (horizontal, vertical)	3D Seismic Isolators (0.3, 0.2)
Electric capacity factor	90%

Proliferation-resistance, Environment-friendliness, Accident-tolerance, Continuity, and Economy have been assessed for PEACER-300. The assessment has assured that PEACER has unique advantages over similar other fast reactor designs. Each of three primary loops for PEACER-300 is equipped with a once-through steam generator and a centrifugal pump. Reactor inlet and outlet temperatures (300-400°C) are judiciously chosen with considerations on materials endurance, transient operability and thermal efficiency. By taking advantage of chemical stability of LBE, the balance of plant with standard superheated Rankine cycle is directly coupled to the primary coolant system through steam generators.

Accident-tolerance requirement mandated the development of a Reactor Auxiliary Vessel Air Cooling System (RVACS). It is expected that RVACS will provide passive cooling capability for decay heat for PEACER-300. An innovative passive water cooling system for the reactor vessel outer wall has been introduced to allow for the system up-scaling from 300 MWe to large scale systems with passive safety. As LBE has high density, earthquake can exert severe load on structural components. Therefore seismic isolators are extensively employed for entire plant including pyrochemical partitioning facility. Three dimensional seismic isolators are applied for all the reactor systems, including the containment.

Pyrochemical partitioning process originally developed at ANL and ORNL, U.S.A. has been employed so that spent fuels with intense radiation can be handled with increased proliferation resistance and the significantly greater margin against criticality accident compared with the conventional wet processing. Analyses of final waste disposal site performance have shown that the final vitrified waste from pyrochemical partitioning processes of PEACER can be qualified as the low-level waste, provided that TRU recovery factor, defined as the ratio of TRU input to the processor to that to final waste forms, exceed 20 000. Liquid metal cathode technology invented at ANL, U.S.A. co-separation of transuranic elements leading to dirty fuel standards. However solid cathode extraction method has been employed in PEACER in order to avoid Am loss during Cd distillation process. Finally selective oxidation and reduction processes are added to reach a very high TRU recovery factor (over 20 000) so that final waste can meet US Class C low level waste standard [26].

Although the pyrochemical process has inherently high proliferation resistance, a provision for institutional barriers is desired. For this reason, PEACER is required multi-national consortium is to be established for its peaceful institution.

Key technologies for successful PEACER deployment include transmutation reactor core neutron spectrum zoning (fast and epi-thermal), highly decontaminating pyrochemical processes, excellent natural circulation under accidental conditions, advanced Pb-Bi coolant technology for system life/toxicity management and overhung structural design with 3D seismic isolations. In order to effectively coordinate design parameters with sophisticated technological interactions, a new powerful design methodology, designated as Solver-Interfaced Virtual Reality (SIVR) [27] has been invented at NUTRECK.

The new Solver-Interfaced Virtual Reality tool tailored for PEACER development, PEACER-SIVR, has been evolved from CATIA and free Virtual Reality Modeling Language (VRML) such that 3-D CAD data can be directly used for the input preparation of nuclear solver codes and for 3-D visualization of outputs, facilitating easier design changes. Results of PEACER 3D design effort are illustrated in Fig. 4.14.

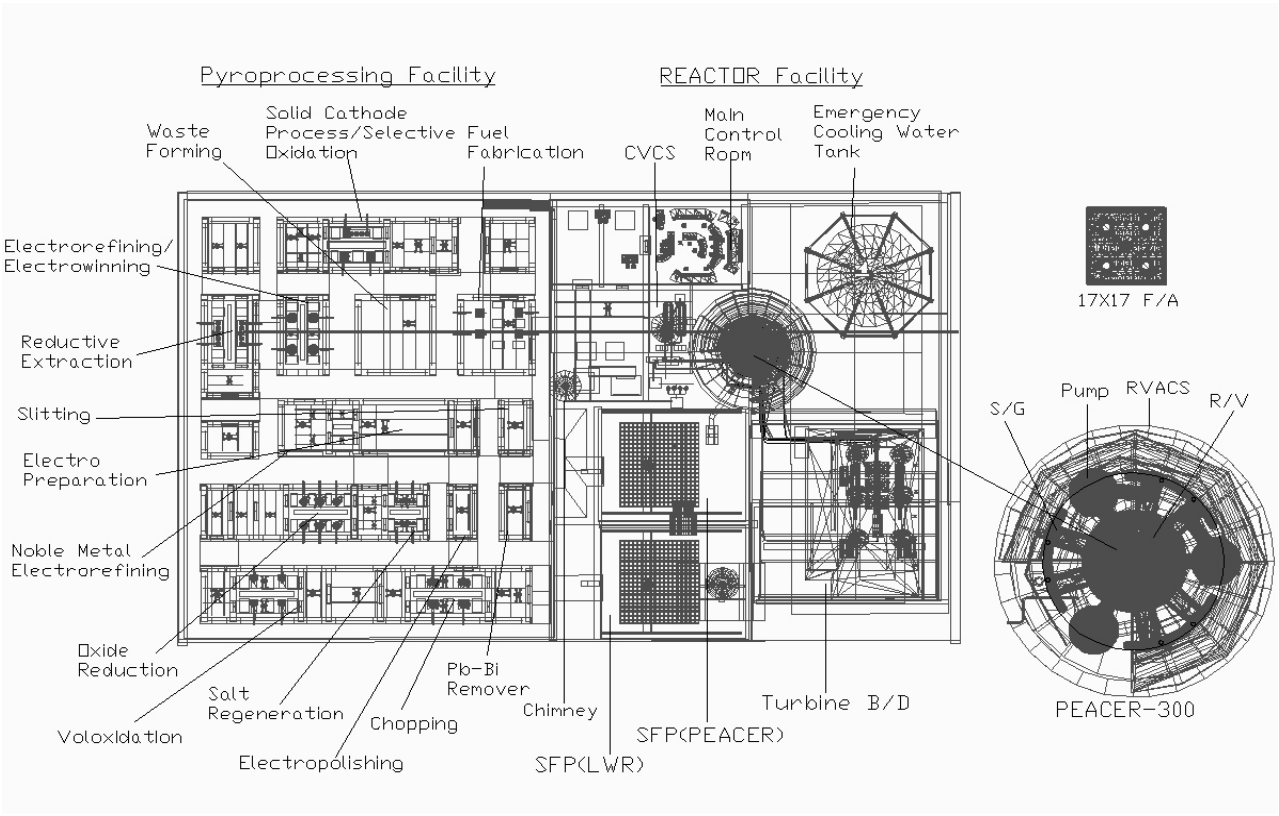

FIG. 4.14. Planar drawing of PEACER-300 MWe.

HELIOS (Heavy Eutectic liquid metal Loop for the Integral test of Operability and Safety of PEACER (Fig. 4.15) has been developed by scaling of PEACER-300 design [28].

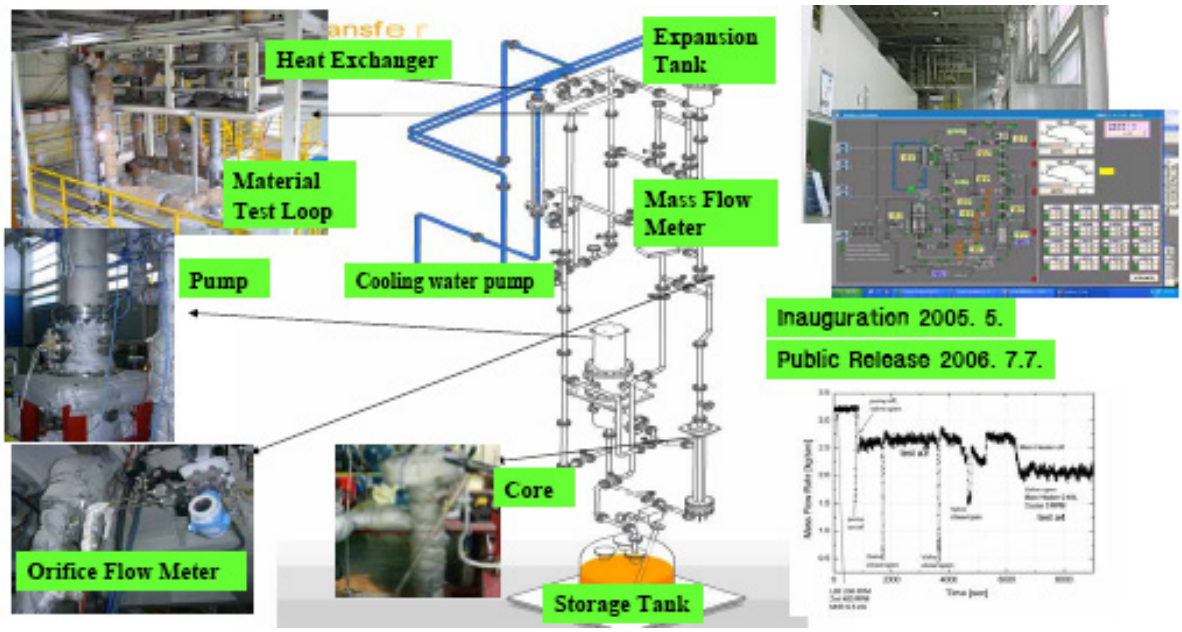

FIG. 4.15. Thermal-hydraulically scaled integral test loop, HELIOS.

The world's tallest Pb-Bi loop has been constructed with the full utilization of 3D CAD in 2005. The operability, natural circulation capability, and materials corrosion resistance have been successfully tested. As results, the reliability, chemical stability, safety, and economy of

PEACER-300 have been demonstrated through scale-up prediction procedures to warrant continued R&D towards a demonstration reactor design development, deployment validation engineering tests.

4.5.3. Current status and summary

The operability, natural circulation capability, and materials corrosion resistance have been successfully tested using the world's tallest Pb-Bi loop, HELIOS, as shown in Fig. 4.15. As result, the coolant management reliability, chemical stability, passive safety, and materials durability of PEACER-300 design have been demonstrated to warrant continued R&D towards a demonstration reactor design development, deployment validation engineering tests. Thermal-hydraulic data produced at HELIOS is being utilized for code benchmark studies.

Since LBE cooled or lead cooled system has not been built for commercial system, confidence in western world can be reinforced by a demonstration even in a small scale. A small reactor named as PATER (Proliferation-resistant, Accident-tolerant Transmutation Experimental Reactor) is being developed at NUTRECK for demonstrating most design goals of PEACER in combination with a small mock-up of PATER that will be constructed using a electrically heated core for multi-purposes. PATER will be used for demonstrating fuel integrity and the adequacy of ^{210}Po-removal process.

4.6. SVBR-75/100

4.6.1. Introduction

In 1950, lead-bismuth (LBE) coolant in fast reactor was first examined by A.I. Leypunsky in his paper [29], while assessing the possibility of constructing a breeder reactor. However, the low heat-transfer properties of LBE, relative to those of sodium, do not permit a high power density in the core, as is required for a short doubling time of plutonium, even at breeding ratio (BR) considerably higher than one. For that reason, when fast breeder reactors were further developed in Russia, sodium was selected as coolant.

Nowadays, the presence of sufficient explored and accumulated stocks of uranium have allowed to postpone to the future the need of a short Pu doubling time in FR and to guarantee a high rate of development of nuclear power without consumption of natural uranium. For this reason it has become possible to reconsider the use of lead-bismuth as coolant in FRs.

In Russia, the design studies of LBE-cooled FRs are carried out within the framework of the development of a modular small power lead-bismuth cooled SVBR-75/100, i.e. a lead-bismuth fast reactor of equivalent electric power from 75 to 100 MW_e, depending on the steam parameters [30, 31].

The development of SVBR-75/100 is based on the experience gathered in Russia with design and operation of several LBE facilities, which now allows:

- Use of mastered LBE technology;
- Use of almost all basic components, units and equipment devices of the reactor installation, which have been verified by operational experience in LBE;
- Capability to master primary and secondary circuits;
- Use of existing fuel infrastructure.

4.6.2. Description of the SVBR-75/100 concept

The flow diagram of the SVBR-75/100 is presented in Fig. 4.16.

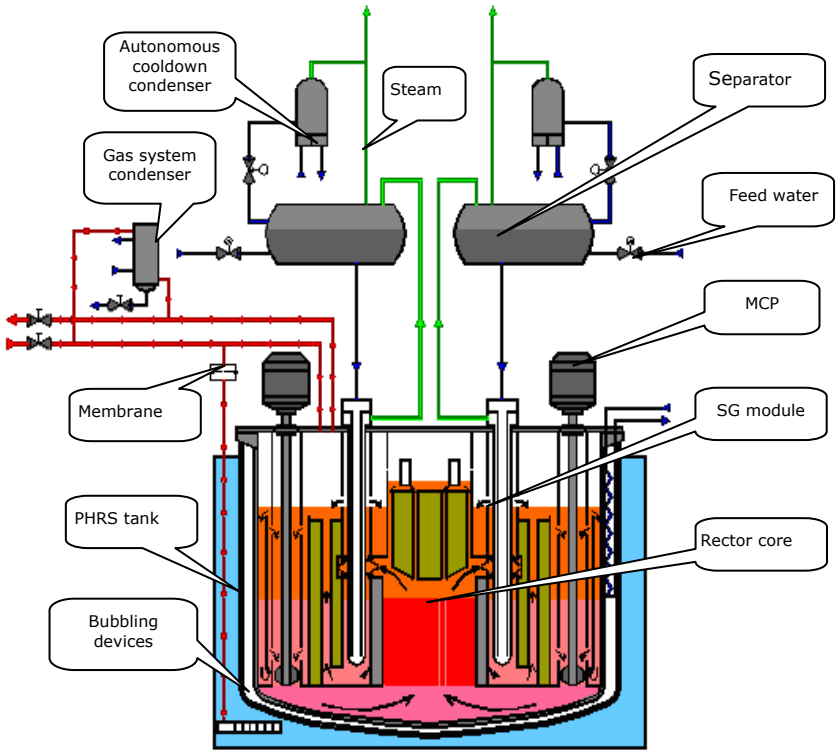

FIG. 4.16. The flow diagram of SVBR-75/100.

The figure shows the main components and sub-systems of the primary circuit which includes: a core, steam-generator (SG) modules, main circulation pumps (MCP), in-vessel radiation shielding; the primary system is installed in the vault of the reactor monoblock (RMB).

The secondary system includes: SG modules, feedwater and steam pipelines, separators and autonomous cooling condensers. The protection gas system includes: gas system condensers, a membrane-protection device, a bubble device and pipelines.

The heating system is designed for heating the RMB prior to filling it with coolant and keeping the hot state and includes a set of pipelines installed between the RMB basic and safeguard vessels, along which the heating steam is conveyed.

The coolant technology system includes mass-exchangers, gas mixture ejectors, sensors of oxygen activity in LBE; its function is to maintain the LBE quality, inhibiting structural materials corrosion.

The safety systems are represented by: an emergency protection (EP) system of the reactor, a system to localize leaks in the SG, an autonomous cooling system (ACS), and a passive heat removal system (PHRS). All these systems, except the emergency shutdown system of the reactor (i.e. EP), guarantee normal operation as well as reactor safety functions. The reactor components include a fuel handling system – composed of an adapter box with a gate valve, refueling pressure suits for extracting the shielding plug (the upper shield of the reactor) and

the core basket, a refueling container - for unloading the spent fuel subassemblies (FSA) into the capsules filled in with lead and installing a new core basket with fresh fuel.

The basic parameters of SVBR-75/100 are presented in Table 4.3. The basic equipment of SVBR-75/100 is installed in the tight box-containment, 11.5 m high (Fig. 4.17).

TABLE 4.3. BASIC PARAMETERS OF SVBR-75/100

Parameter	Value
Thermal power (nominal), MW	280*
Electric power, MW	101.5*
Steam-production, t/h	580*
Steam parameters: pressure, MPa	9.5*
temperature, °C	307*
Feeding water temperature, °C	241*
LBC temperature, °C: at the core outlet	482*
at the core inlet	320*
Core dimensions: D×H (diameter × height), m	1.645 × 0.9
Average power density of the core, kW/l	140*
Average linear load of the fuel element, kW/m	~ 24.3*
Fuel cladding dimensions (outer diameter × thickness), mm	12 × 0.4
Cladding material	steel EP-823 (ferrite-martensite class)
Thickness of side reflector (stainless steel), mm	250
Fuel (UO_2): U-235 loading, kg	~ 1470*
U-235 enrichment, %	16.1*
Number of control rods (boron carbide)	37
The core lifetime, thousands of full power hours	~ 53
The time interval between refuelings, year	~ 8
The number of SG	2
The number of SG modules	2 × 6
The number of MCP	2
Power of the MCP electric driver, kW	450
Head of the MCP, MPa	~0.55
Lead-bismuth eutectics (LBE) volume in the primary circuit, m^3	18
Dimensions of the reactor vessel: D×H (diameter × height), m	4.53×6.92

* Note: The presented characteristics are those of SVBR-75/100 being a component of the modular NPP with two units of 1600 MW each [32]. If SVBR-75/100 is used as a component of other NPP, these characteristics may be changed.

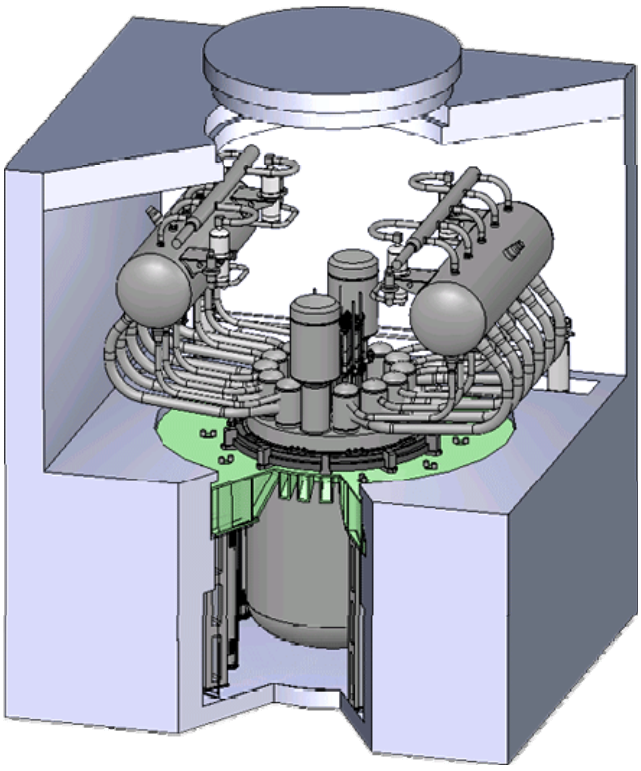

FIG. 4.17. SVBR-75/100 equipment arrangement.

In the lower part of each box there is a concrete well to host the PHRS tank. The reactor monoblock is installed inside the PHRS tank and is fastened on the head ring of the tank roof. Installed in the PHRS tank there are also 12 dipped vertical heat-exchangers which transfer heat from the PHRS tank to the cooling water of an intermediate circuit. Over the PHRS tank in the upper part of the box there is the reactor equipment, including two steam separators and two cooling condensers. The high elevation of the separators has been selected in order to guarantee the coolant natural circulation in the secondary circuit in all reactor operation modes. The gas system condensers are installed in the upper part of the box in the separate concrete compartment.

All the equipments of the primary circuit are installed inside the vessel of the RMB. The removable unit composed of the core, the control rods and a shielding plug is installed in the centre of the reactor block and it is surrounded by an in-vessel radiation shielding (boron carbide) with SG and MCP modules placed inside it (see Fig. 4.18).

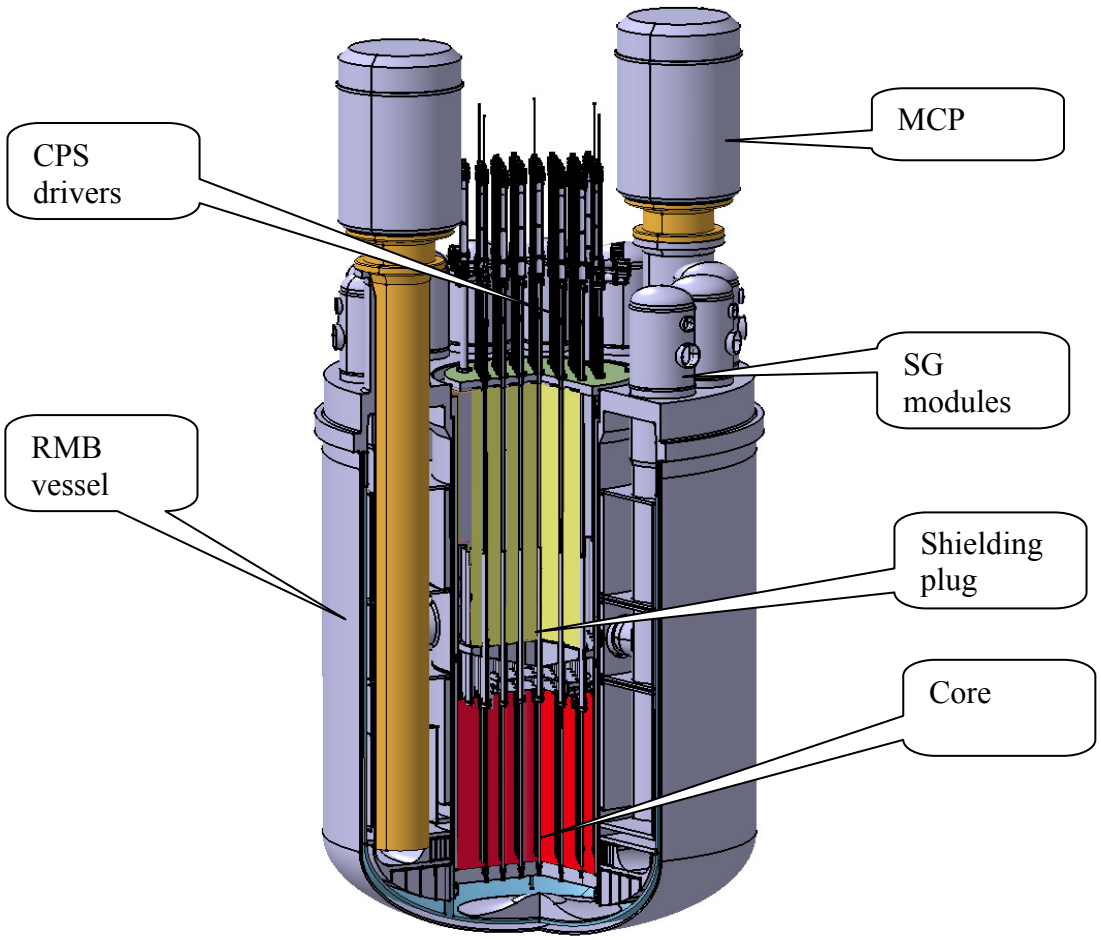

FIG. 4.18. Equipment arrangement in the RMB vessel of SVBR-75/100.

The two circuits for primary coolant circulation (the main and the auxiliary one), are wholly realized by components of the in-vessel devices, without using pipelines and valves.

Within the main circulation circuit (MCC), the coolant flows according to the following scheme. Being heated in the core (cross section of the core is shown in Fig. 4.19), coolant flows to the inlet of the medium part of the inter-tube chamber of 12 SG modules connected in parallel each other.

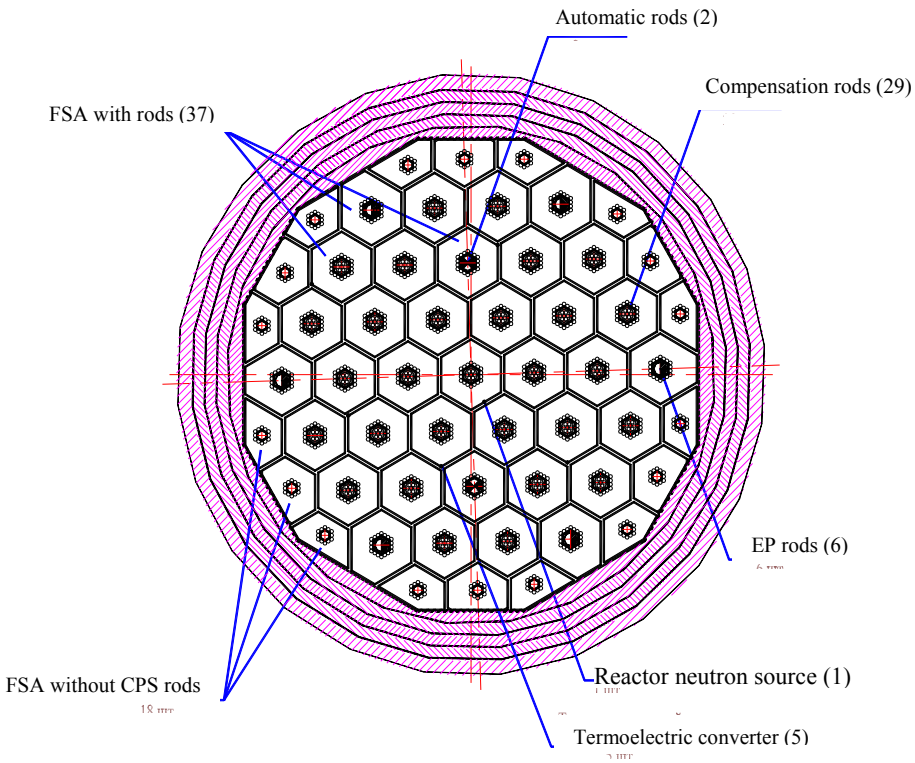

FIG. 4.19. Cross section of the SVBR-75/100 core.

Then coolant is divided into two flows. One flow moves upwards in the inter-tube chamber and enters into the peripheral buffer chamber with a free level of the “cold” coolant. Another flow moves downwards and enters into the outlet chamber out of which it goes to the channels into in-vessel radiation shielding. Coolant flow moves upwards through in-vessel radiation shielding and cools it, and then it enters into the peripheral buffer chamber as well. Out of the peripheral buffer chamber, the main coolant flow goes over the downcomer circular channel along the RMB vessel via the inlet chamber to the MCP suction. Another part of coolant goes to the MCP suction over the circular channel formed with a vessel and MCP shaft. Out of the MCP the coolant flows over the two channels installed in the block of the lower zone of in-vessel radiation shielding into the distributing chamber, from which it goes to the reactor inlet chamber, thus closing the MCC circuit.

The circulation scheme adopted for the MCC - with free levels of coolant in the upper part of the RMB and channels of SG modules coupled with a low flow rate of coolant on the downcomer sections of the circuit - provides reliable separation of the water from the coolant in the event of accidental failure of tightness in the SG tubes.

Several computations and analyses have revealed that - if a conservative approach is adopted - the safety operating limit is not achieved in the case of the following postulated accidental events:

- Unauthorized withdraw of the most effective absorbing rod;
- A blockage of coolant flow cross section at the core inlet up to 50%;
- Shut down of all main circulation pumps;
- Interruption of steam to the turbine and of feedwater supply;
- Guillotine rupture of several SG tubes;
- Leak in the reactor vessel;

- LBE freezing in the SG;
- Black-out of the NPP.

SVBR-75/100 safety does not depend on the state of the systems and equipments of the turbine-generator installation. The reactor inherent safety properties provided by reactor feedbacks, the natural properties of LBE and the reactor structure allow to guarantee safety functions (except for the emergency protection function) and normal operation. Passive actuation of the following systems is provided:

- At increasing LBE temperature over a dangerous value, emergency protection of the reactor operates passively due to fusible locks in the nodes of coupling the absorbing rods with the driver's rods, even in case of mechanical damage of servo-drivers;
- Decay heat removal when there is no heat removal via the SG is provided passively by heat transfer via the monoblock vessel to water of the PHRS tank and then by boiling water in the tank with steam release to the atmosphere (the "grace" period is about five days);
- In the event of several SG tubes rupture or shut-off of the gas system condenser, at increasing steam pressure in the gas system over 1 MPa, localization of SG leak is provided passively due to damage of the breaking membrane and discharging steam into the bubbler, i.e. the PHRS tank.

As several simulations have revealed, safety potential of SVBR-75/100 is characterized by the following: even in case of simultaneous postulated initial events as damage of shielding shell, reinforced-concrete overlapping over the reactor and tightness failure of the primary circuit gas system with direct contact between LBE surface in the reactor monoblock and atmospheric air, total black-out of the NPP, no reactor runaway, no explosion, no fire occurs, and radioactivity release to the environment does not reach values requiring population evacuation beyond the NPP fence. The probability of an severe core damage is considerably lower than the value specified in the regulatory guides.

The "standard" reactor modules of ~100 MWe can be used in different applications, e.g.:

- Modular NPP of small, medium or large power;
- Regional NHEPP of 200-600 MW_e which are located not far from the cities;
- Refurbish of NPP units whose reactors have expired their lifetime;
- Nuclear desalination systems.

In particular, technical and economical assessments have shown that a number of SVBR-75/100 modules can replace the 2nd, 3rd, and 4th unit of the Novovoronezh NPP (NVNPP) at half the capital cost of replacing the same power capacity [33]. With the purpose of using SVBR-75/100 modules in large-scale nuclear power plants, SSC RF IPPE, FSUE EDO "Gidropress" and FSUE "Atomenergoproekt" have developed a conceptual design of a NPP which consists of two power units of 1600 MW_e each [32]. A nuclear steam-supply system (NSSS) consisting of 16 SVBR-75/100 reactor modules and a turbine of 1600 MW_e in each power unit is arranged in the main building (see Fig. 4.20).

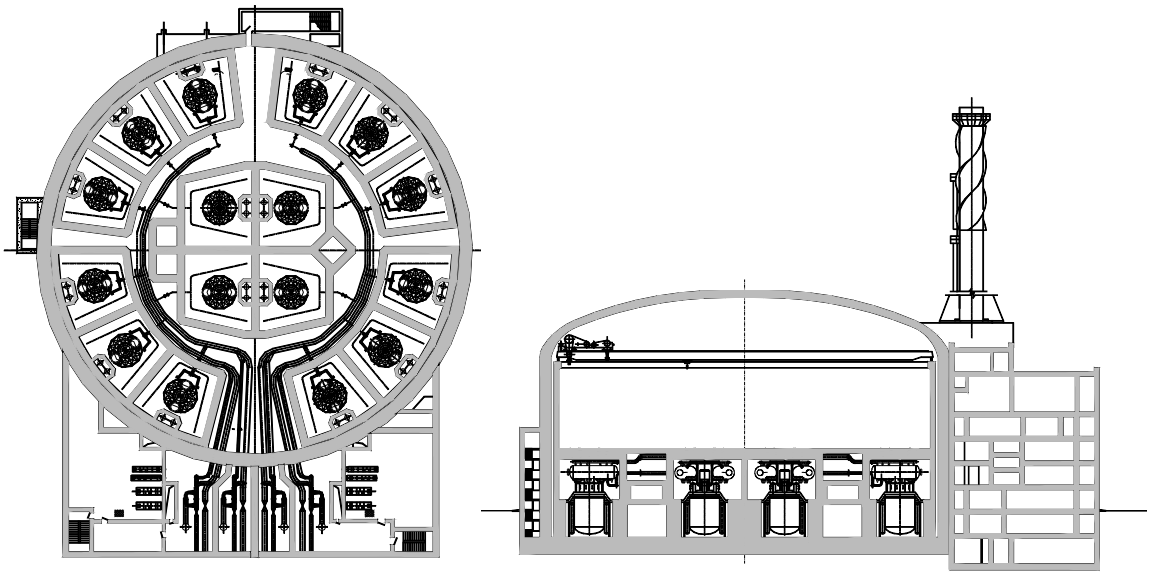

FIG. 4.20. A plan and a longitudinal section of the main building of the NSSS of SVBR-75/100.

The main parameters of the NPP with two NSSS SVBR-1600 are summarized in Table 4.4.

TABLE 4.4. BASIC PARAMETERS OF A NPP COMPOSED OF SVBR-75/100 MODULES

Parameter	Value
Rated power of the power unit, MW_e	1625
Number of units at the plant	2
Electric power necessary for plant own needs, %	4.5
Net efficiency of the plant, %	34.6

A modular design of the NSSS power unit allows ingload factor (LF) not less than 90% under long reactor operation. When a reactor module is shut down for refuelling, power of the unit reduces slightly. Modular NPPs also allow fabrication of the single modules in a factory, easy water or ground transportation of the modules to the NPP site and, definitely, reduced construction times.

4.6.3. Current status and summary

The conceptual design of the SVBR-75/100 reactor applied to NPP with two power units of 1600 MW_e each has been developed. The conservative approach adopted for designing the reactor allows to considerably reducing the overall R&D effort. The SVBR-75/100 is particularly suitable for modular NPPS and for replacing units of NPPs whose reactors have expired their lifetime. In particular, SVBR-75/100 modules could replace the shutdown 2nd unit of the NVNPP.

4.7. BREST-OD-300

4.7.1. Introduction

The lead-cooled fast reactor is one of the alternative fast reactors under development in Russia. The future of this concept will substantially depend on the success of development of the lead coolant technology. The reference Russian design of a medium-size lead cooled fast reactor is BREST-OD-300 [34].

In contrast with sodium a previous experience in using pure lead as a coolant in fast reactors is absent. Actually, operative experience in Russia exists as far as the use of lead-bismuth eutectic alloy in power reactors for submarine propulsion. At a certain extent, this experience can be used in the development of lead cooled fast reactors.

Nevertheless, reactor technology with use of lead as a coolant is innovative and, therefore, it requires implementation of appropriate R&D for its validation, including, in particular, activities in the field of coolant technology, safety, environmental impact, etc.

The mixed U-Pu nitride fuel - which is supposed to be used in the BREST-OD-300 design - also requires implementation of the appropriate research, as well as experimental test and qualification, as there is no significant experience with this type of fuel worldwide.

A conceptual design study of the BREST-OD-300 reactor was developed in 1995. Furthermore, a feasibility study of the BREST-OD-300 NPP with an On-Site Nuclear Fuel Cycle (OSNFC) for the Beloyarsk NPP Site was issued in 2002 [35]. It includes design reports on reactor facility (RF), NPP and OSNFC equipments.

In the same period, engineering developments were implemented at a conceptual level; they confirmed the feasibility of BREST reactors with different power (600, 1200 MW) based on the same principles laid down in the development of the BREST-OD-300 design. The present goal is to implement all necessary R&D in order to finalize the basic design of the BREST-OD-300.

4.7.2. Description of the BREST-OD-300 concept

BREST-OD-300 reactor facility is a two-circuit steam generating power unit including a reactor with steam generators (SG), pumps, fuel assembly (FA) loading system, a control and protection system (CPS), a concrete vault with a heat shield, a steam-turbine unit, a system for heat removal during cool-down, a reactor heat-up system, a reactor overpressure protection system, a gas purification system and other auxiliary systems [34, 35].

The adopted fuel is mixed mononitride (UN-PuN) which exhibits high density (14.3 g/cm^3) and high conductivity (20 W/m·K) and is compatible with lead and the fuel cladding of chromium ferritic-martensitic steel. In order to reduce the fuel temperature and thus make the release of fission products from the fuel relatively low, the gap between the fuel and the cladding is filled with lead which ensures a suitable thermal fuel-coolant contact. To provide a significant coolant flow area, increase the level of power removed by natural lead circulation, reduce the coolant preheating temperature and, primarily, exclude the cooling losses in the damaged FA in case of local flow rate blockage, all core FAs do not have shrouds. The FA design allows radial coolant overflow in the core which prevents overheating of the damaged FA.

The reflector assemblies have leak-proof cans. The first row of these assemblies is used as control element channels and the assemblies in rows 2 to 4 can contain long-lived iodine and technetium for transmutation and also contain ^{90}Sr and ^{137}Cs as a stable heat source for prevention of hypothetical coolant freezing. Instead of traditional flattening of the radial power density distribution by means of different fuel enrichments, this is achieved by means of a core composed of three zones with fuel elements having different diameters, but the same plutonium content. Such a method guarantees a suitable flattening of the lead temperatures at the core outlet, as well as the respect of the maximum fuel cladding temperatures. To reduce the neutron leakage, to better leveling the neutron flux, ensure the operation conditions without cycle reactivity change and attain the complete fuel breeding in the core (CBR ~ 1), traditional uranium shields have been replaced with an effective lead reflector whose albedo characteristics are better than those of uranium dioxide.

Heat is removed from the reactor core through forced lead coolant (LC) circulation by pumps. The LC is pumped to the height of ~ 2 m relative to the lead level in the suction chamber and supplied to the free level of the annular pressure chamber. The lead further goes down to the core support grid, flows upward through the core where it is heated up to the temperature of 540°C, and is supplied to the common "hot" coolant drain chamber. Then it goes up and flows over the SG inlet cavities and inter-tube space via the distribution header nozzles. As it goes down in the inter-tube space, the LC transfers heat to the secondary coolant flowing inside the SG tubes. Cooled-down to ~ 420°C, the LC goes up in the annulus and flows out the pump suction chamber, wherefrom it is pumped again to the pressure chamber (Fig. 4.21).

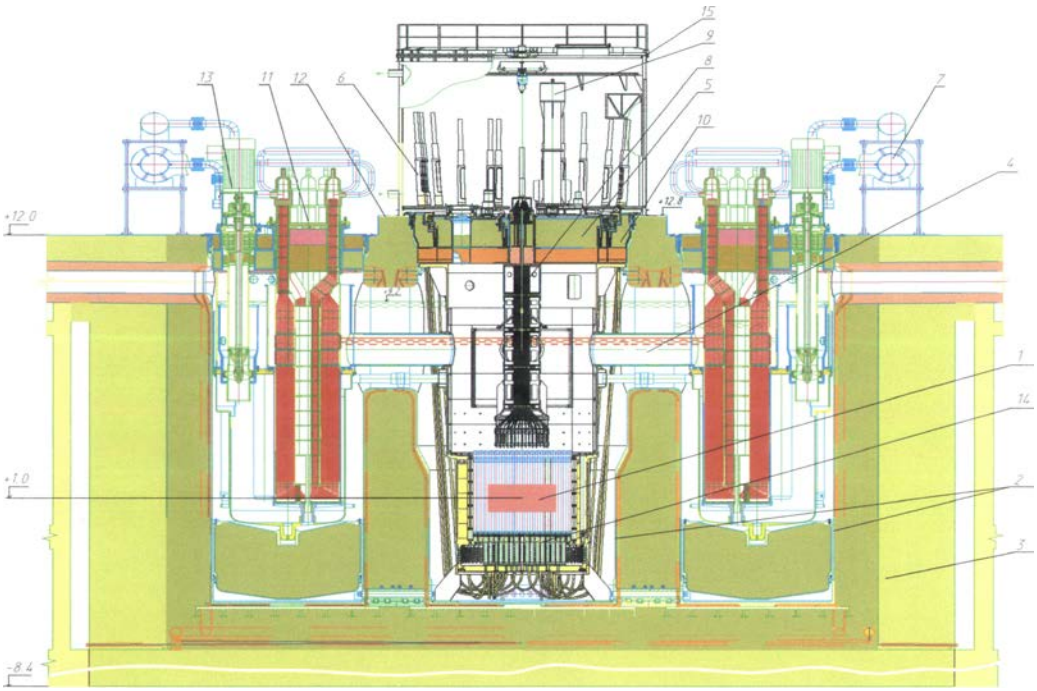

1-reactor core; 2-reactor vessel; 3-concrete; 4-piping collector; 5-large rotating plug; 6-control rod drive mechanism; 7-decay heat removal system; 8- upper core structure; 9-fuel handling machine; 10-small rotating plug; 11-steam generator; 12-upper stationary shield slab; 13-main pump; 14-core support structure; 15-protective dome

FIG. 4.21. The BREST-OD-300 reactor.

Main technical characteristics of the BREST-OD-300 are presented in Table 4.5.

TABLE 4.5. MAIN CHARACTERISTICS OF BREST-OD-300 REACTOR

Parameter	Value
Overall plan:	
Reactor thermal power, MW	700
Unit electrical power, MW	300
Breeding ratio	1.05
Load factor	0.82
Primary system:	
Coolant temperature, °C Core inlet Core outlet	 420 540
Reactor vessel coolant mass, t	~8600
Coolant flowrate, kg/s	41600
Max coolant velocity in the core, m/s	1.67
Pump delivery head, MPa	0.225
Number of the primary loops	4
Number of circulating pumps	4
Reactor core:	
Equivalent core diameter, m	2.296
Active core height, m	1.1
Number of zones with different fuel rod sizes	3
Average power density in the fuel, MW/m^3	510
Number of core fuel assemblies	145
Fuel assembly duct width across flats, mm	166.5
Fuel assembly pitch (at nominal temperature), mm	169
Fuel	PuN-UN-MA
Total Pu inventory in the core (all isotopes), kg	2260
Number of fuel rods per assembly	156/160*
Core fuel cladding outer diameter, mm	9.4/9.8/10.5
Core fuel cladding wall thickness, mm	0.5
Fuel rod linear heat rating (max.), kW/m	41.9/39.5/32.6
Average fuel burnup, MW·d/kg	61.45
Maximum fuel burnup, MW·d/kg	91.7
Core lifetime, ed	1500
Core refueling interval, ed	300
Reactor main vessel:	
Outer diameter, m	6.88
Overall height, m	14.14
Material	Cr16Ni10
Secondary circuit:	
Number of turbo-generators	1
Main steam pressure, MPa	27.0
Feedwater temperature, °C	355
Main steam temperature, °C	525

* - 156 – inner zone, 160 – medium and outer zones

The difference in the “cold” and “hot” coolant levels resulting from the pump operation excludes the abnormal lead flow rate through the SG in case of trip of one or more pumps and provides the flow inertia during fast pump trip by the coolant leveling in the pressure and suction chambers.

BREST-OD-300 uses a mixed integral/loop configuration of the primary circuit, as the SG and MCP are installed outside the reactor central vessel. As compared to the integral traditional fast reactor designs, the BREST concept has reduced dimensions and volume of the primary circuit. The reactor and the steam generators are located in the thermally shielded concrete vault, without using a metal vessel. The concrete temperature is kept below the allowable limit by means of natural air circulation.

The absence of high pressure in the primary lead circuit and a relatively high lead freezing temperature contribute to crack self-healing, which excludes loss-of-core-cooling accidents and outflow of radioactive lead from the reactor vessel.

The safety analysis has shown that all considered initial events involving a fast introduction of reactivity up to its full margin (spontaneous movement of all CPS control rods, steam throw to the core at a SG tube rupture, etc.), interruption of the forced coolant circulation (trip or arrest of all pumps), loss of secondary heat sink or lead supercooling at the core inlet and so on, do not lead to accidents with fuel damage and inadmissible radioactive or toxic releases, even in the case of a failure of the reactor active safety systems.

Accidents are avoided thanks to the intrinsic safety features of BREST, including reactivity fuel temperature coefficient, coolant and core design components, and also coolant pressure and temperature at the core inlet and outlet. For this reason BREST can be considered an intrinsically safe reactor. However, the search for the weaknesses in the design of the reactor and its safety systems in terms of safety continues, and it is not excluded that the list of predominantly passive engineered features for overcoming accidents caused by previously ignored initial events will be expanded.

An accident with a SG tube rupture is one of the most adverse events for BREST-OD-300. To reduce the consequences of a potential accident with a steam generator (SG) tube rupture, a mixed integral/loop configuration of the primary circuit is adopted, with SGs and MCP installed outside the reactor central vessel. Together with the selected lead circulation pattern and steam dump from the reactor gas volume to the localization system, such configuration excludes the ingress of the hazardous steam into the core and reactor overpressure.

The use of chemically inert, high-boiling molten lead in the primary circuit allows adoption of a two-circuit unit configuration, with a supercritical steam system as secondary circuit.

The secondary circuit is a non-radioactive circuit consisting of steam generators, main steam lines, a feedwater system and one turbine unit with supercritical steam parameters. A standard K-300-240-3 turbine unit with three-cylinder (HPC+MPC+LPC) steam condensation turbine with intermediate steam superheating and a rotation speed of 3000 rev/min is used. The nominal steam flowrate to the turbine is about 1000 t/h. An oxygen neutral water at supercritical pressure is used in the secondary loop. Such provision does not require removal of oxygen and make the deaerator in the secondary circuit unnecessary. The intermediate steam superheating system contains two steam-to-steam heat exchangers (SSHX). The SSHX heating fluid is steam extracted from the main steam lines upstream of the turbine at a flowrate of 600 t/h. Downstream of the SSHX, all cooled fluid flowrate is supplied via

throttling control valves as the heating fluid to the feedwater mixing preheater (FWMP) where it additionally heats the water downstream of the high pressure preheater to the temperature of 355°C at the pressure of 170 kg/cm^2.

The feedwater preheating at such a temperature is necessary to prevent the lead coolant freezing (T_{melt}=327°C) in the primary circuit in emergency conditions. It is for the same purpose that cutoff valves (two for each SG) are installed on the pipelines for feedwater supply to the steam generators. They are closed automatically both by the "passive drive" and the "active drive" in response to respective emergency signals.

Feedwater pumps (FWP-2) (two working pumps and one standby pump) supply feedwater from the FWMP to each steam generator via control units with the main and starting control valves. The FWP-2 speed is controlled in the range from 70 to 100% of the nominal value. Each FWP-2 is equipped with a recirculation line. The common header serves as a starting recirculation line to the FWMP (the capacity of 350 t/h) with a control valve for warming up the entire system prior to the water supply to the SG. The peculiarity of the secondary circuit is that it is not charged with safety functions for emergency heat removal from the reactor.

The main building's structures have been designed based on the "Regulations for Aseismic Design of Nuclear Power Plants". The magnitude of 6 is assumed in the design as the design-basis earthquake and the magnitude of 7 on the MSK-64 scale is assumed as the ultimate design-basis earthquake. The buildings are separated from each other with an aseismic temperature-deformation joint.

The reactor building and the other structures are mounted on a single monolithic reinforced concrete foundation plate. In order to reduce the seismic inertia forces, the building has been designed to be symmetrical with the footprint of 65×74 m and separated with intercoupled vertical bearing diaphragms (Fig. 4.22).

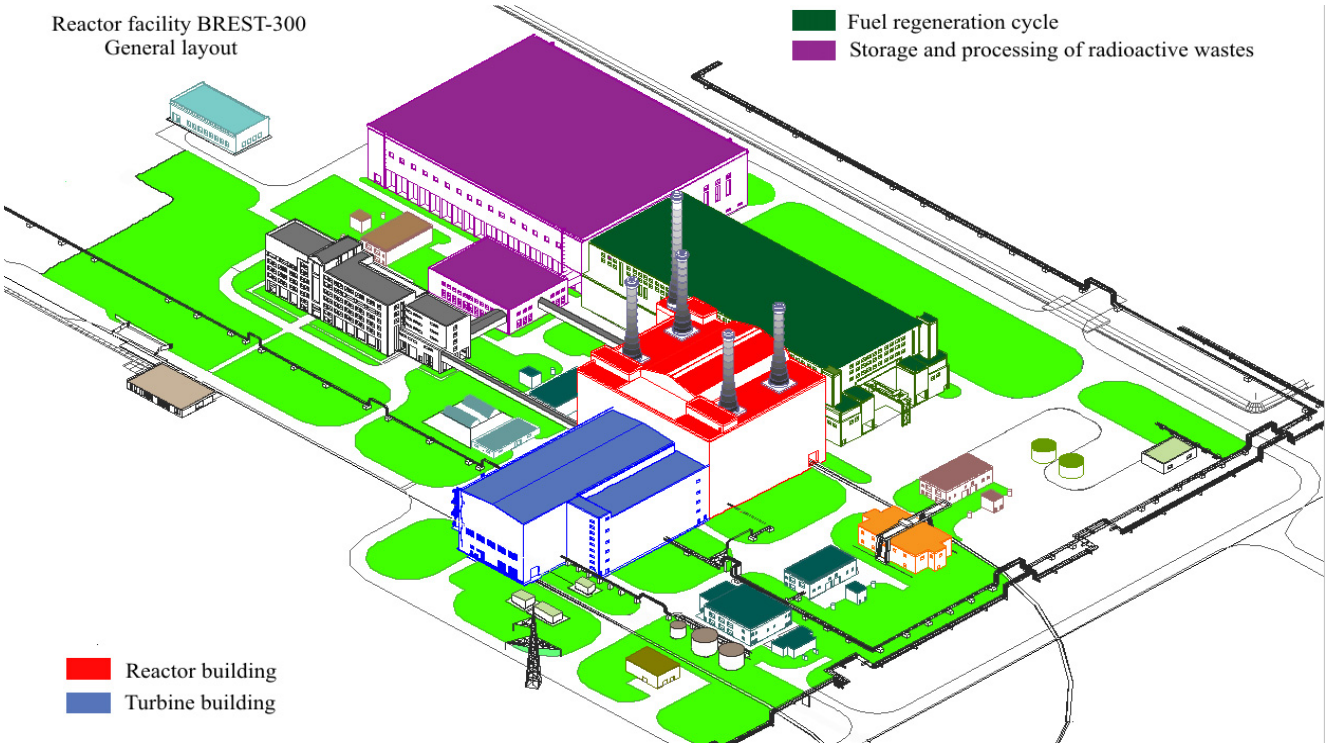

FIG. 4.22. Overall view of the BREST-OD-300 NPP.

Around the nuclear island there are auxiliary buildings that serve as an additional protective barrier and ensure the reliable behavior of the monolithically interconnected structures.

4.7.3. Current status and summary

The BREST-OD-300 power unit is designed as a pilot and demonstration unit intended for studying the reactor facility operation in different modes and optimizing all processes and systems that support the reactor operation. Furthermore, BREST-OD-300 is also considered the prototype of a fleet of medium-size power reactors. Indeed, after the operational tests, the unit will be commissioned for electricity supply to the grid.

4.8. SSTAR and STAR-LM

4.8.1. Introduction

It is widely recognized that the developing world is the next area for major energy demand growth, including a demand for new and advanced nuclear energy systems. With limited existing industrial and grid infrastructures, there will be an important need for future nuclear energy systems that can provide small or moderate increments of electric power (10 700 MWe) on small or immature grids in developing nations. More recently, the Global Nuclear Energy Partnership (GNEP) has identified, as one of its key objectives, the development and demonstration of concepts for small and medium sized reactors (SMRs) that can be globally deployed while assuring a high level of proliferation resistance. Lead-cooled systems offer several key advantages in meeting these goals.

The small Lead-Cooled Fast Reactor (LFR) concept known as the Small Secure Transportable Autonomous Reactor (SSTAR) has been under ongoing development as a small reactor for international deployment under the US Department of Energy Generation IV Nuclear Energy Systems Initiative, anticipating the GNEP objectives [36-40]. It is a concept expressly developed to provide energy security to developing nations, while incorporating features to achieve nonproliferation goals.

SSTAR incorporates concepts that are reflected in the Global Nuclear Energy Partnership (GNEP). In particular, the user-supplier paradigm has been part of LFR work in the U.S. since its inception; the focus has been on Secure Transportable Autonomous Reactor (STAR) fast reactor converters (Conversion Ratio ~ 1) suitable for deployment in developing nations. STARs offer an alternative approach to actinide management by "storing" actinides in long core lifetime (e.g. 15- to 30-year) fissile self-sufficient operating power reactors. Thus, instead of burning minor actinides (MAs) in Advanced Burner Reactors, the MAs are incorporated into a comparable number of STARs which return the fissile resources at the end of the core lifetime.

4.8.2. Description of the SSTAR concept

SSTAR has been developed as a modular fast reactor concept at the low end of the power spectrum, 19.8 MWe (45 MWt), but can be scaled up to 175 MWe (400 MWt) if desired (named STAR-LM) with optional potable water production using a portion of the reject heat. As a SMR, SSTAR has the potential to serve the following markets:

(i) Clients looking for energy security at small capital outlay;
(ii) Cities in developing nations;
(iii) Deregulated independent power producers in developed nations.

The SSTAR pre-conceptual design integrates three major features in a pool vessel configuration: primary coolant natural circulation heat transport; lead (Pb) coolant; and transuranic nitride fuel.

The high Pb boiling temperature (1740°C) exceeding the temperatures at which traditional cladding and structural materials lose their strength and melt offers a pathway to reactor operation at higher temperatures not limited by coolant boiling at which the benefits of more efficient power conversion using the supercritical carbon dioxide (S-CO_2) Brayton cycle can be realized provided that suitable cladding and structural materials are developed for service in Pb at the system temperatures. Lead has a low neutron absorption (e.g., relative to sodium) permitting the core to be opened up by increasing the coolant volume fraction without significant reactivity penalty decreasing the core frictional pressure drop making natural circulation more effective. Shippable LFRs with significant power (181 MWe/400 MWt; i.e., STAR-LM) can be designed with natural circulation at power levels exceeding 100% nominal. Natural circulation eliminates main coolant pumps and loss-of-flow accident initiators. The high Pb density (ρ_{Pb} = 10400 kg/m^3) limits void growth and downward penetration following postulated in-vessel heat exchanger (HX) tube rupture eliminating significant void transport to the core [1] such that HXs can be located inside of the reactor vessel eliminating the need for an intermediate coolant circuit between the primary coolant and working fluid. Lead is calculated not to react chemically with the CO_2 working fluid above ~ 250°C which is less than the 327°C Pb freezing temperature. Lead does not react vigorously with air. Lead is also expected not to react vigorously with water or steam making it possible to eliminate the intermediate circuit when a Rankine steam cycle is utilized as the power converter.

Experiments carried out at the Forschungszentrum Karlsruhe have shown that iodine, cesium, and cesium-iodide (i.e., fission products with low melting and boiling points) are absorbed and immobilized by lead-bismuth eutectic (LBE) at temperatures of 400 and 600°C. Cesium forms inter-metallic compounds in LBE while iodine forms PbI_2.

Transuranic nitride fuel offers a number of potential benefits provided that it can be demonstrated to perform suitably well in steady state and transient irradiation tests and can be reliably manufactured to meet the performance requirements. The high transuranic nitride fuel decomposition temperature (estimated > 1350°C) would enable the fuel to maintain its integrity at temperatures above those at which cladding and structural materials lose their strength and melt further supporting the pathway to operation at higher temperatures. The high transuranic nitride atom density enables the fuel volume fraction to be further reduced further contributing to increasing the coolant volume fraction facilitating natural circulation. Transuranic nitride has the potential for low volumetric swelling and fission gas release per unit burnup allowing the gap size between fuel pellets and cladding to be reduced and reducing thermal creep of the cladding resulting from internal pressurization by released fission gas. Nitride is compatible with Pb coolant and bond as well as ferritic/martensitic (F/M) steel cladding. The fast neutron spectrum core with Pb and transuranic nitride has strong reactivity feedbacks enabling autonomous load following, inherent power shutdown to match the heat removal from the reactor, and enabling core designs having low burnup reactivity swing over long time.

Use of Pb coolant also introduces a number of potential negatives that need to be considered. The high coolant density requires greater vessel thicknesses and costs to support the coolant weight and accommodate seismic loadings. The effective reactor power level may be limited

by the need to accommodate seismic loads. Reliance upon natural circulation may result in a taller reactor vessel and internal components adding to cost. There is a need to supply non-nuclear heating to assure that the coolant doesn't freeze. There is a need to deal with the effects of accidental freezing of coolant and thawing of frozen coolant. Although heavy liquid metal coolant dissolves Fe, Cr, and Ni from unprotected steels at rates which increase with temperature, active maintenance of the dissolved oxygen potential in the coolant within a proper concentration window has been well established as a means for forming protective oxide layers (Fe_3O_4 at temperatures below ~ 570°C) at velocities below ~ 1 m/s significantly retarding the dissolution rate and avoiding the formation of solid PbO particulate [2]. It has recently been demonstrated that T91 ferritic/martensitic (F/M) steel cladding is protected from Pb corrosive attack at velocities at least as high as 3 m/s by "aluminizing" using the treatment currently applied in the GESA IV apparatus at the Forschungszentrum Karlsruhe [3].

Figure 4.23 illustrates SSTAR which is a pool-type reactor; the Pb coolant is contained inside of a reactor vessel surrounded by a guard vessel.

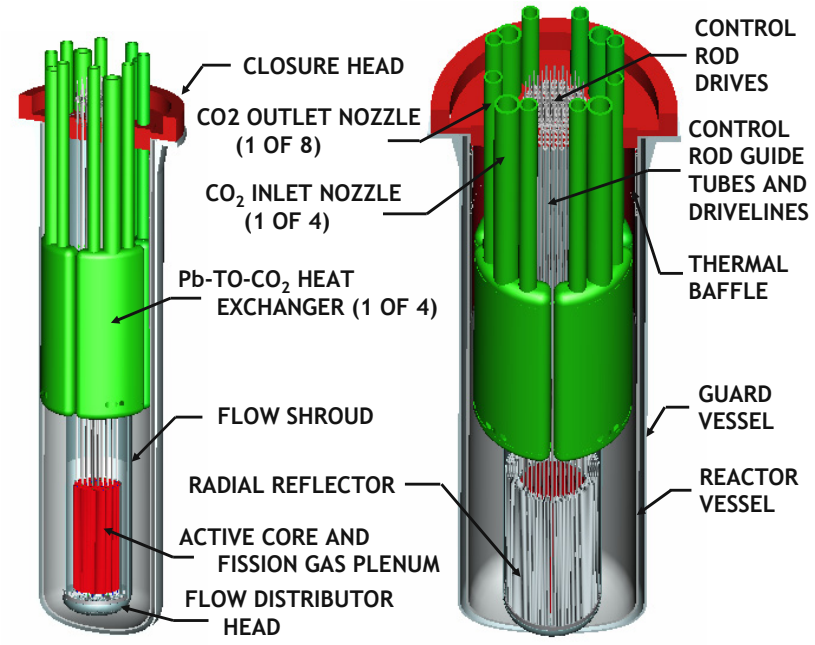

FIG. 4.23. Small Secure Transportable Autonomous Reactor (SSTAR).

Lead is chosen as the coolant rather than lead-bismuth eutectic to reduce the amount of alpha-emitting ^{210}Po isotope formed in the coolant by two to three orders of magnitude relative to LBE, and to eliminate dependency upon bismuth which might be a limited resource. The Pb coolant flows through a perforated flow distributor head located beneath the core; this structure provides an essentially uniform pressure boundary condition at the inlet to the core. The Pb flows upward through the core and a chimney above the core formed by a cylindrical shroud. The vessel has a height-to-diameter ratio large enough to facilitate natural circulation heat removal at all power levels up to and exceeding 100% nominal, and to accommodate the Pb free surface elevation such that the nominal flowpath is maintained by the faulted free surface height in the event of a reactor vessel leak. The coolant flows through openings near the top of the shroud and enters four modular Pb-to-CO_2 HXs located in the annulus between the reactor vessel and the cylindrical shroud. Inside each HX (Fig. 4.24), the Pb flows downwards over the exterior of tubes through which the CO_2 flows upwards.

The CO_2 enters each HX through a top entry nozzle which delivers the CO_2 to a lower plenum region in which the CO_2 enters each of the vertical tubes. The CO_2 is collected in an upper plenum and exits the HX through two smaller diameter top entry nozzles. The Pb exits the HXs and flows downward through the annular downcomer to enter the flow openings in the flow distributor head beneath the core.

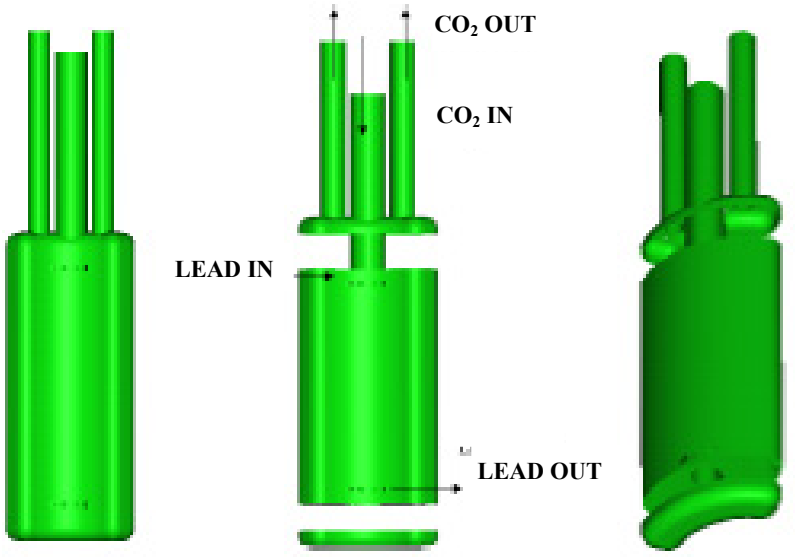

FIG. 4.24. SSTAR Pb-to-CO_2 heat exchanger.

SSTAR does not incorporate an intermediate heat transport circuit. This is a simplification possible with Pb coolant which is calculated not to react with the CO_2 working fluid below ~ 250°C. A safety grade passive pressure relief system is provided on the reactor system to vent CO_2 from the reactor in the event of a heat exchanger tube rupture. A deliberate escape channel located between the HXs and the reactor vessel/thermal baffle enables CO_2 to rise benignly to the Pb free surface. A thermal baffle is provided in the vicinity of the Pb free surface. The annular space between the baffle and reactor vessel is filled with argon cover gas to thermally insulate the reactor vessel and mitigate thermal stresses that would otherwise result from exposure to the Pb during startup and shutdown transients when the Pb temperature varies between the cold shutdown temperature of 420°C and the nominal core outlet temperature of 567°C.

The SSTAR core shown in Fig. 4.25 is an open lattice of large diameter (2.5 cm OD) fuel pins on a triangular pitch (p/d = 1.185) that does not consist of removable fuel assemblies.

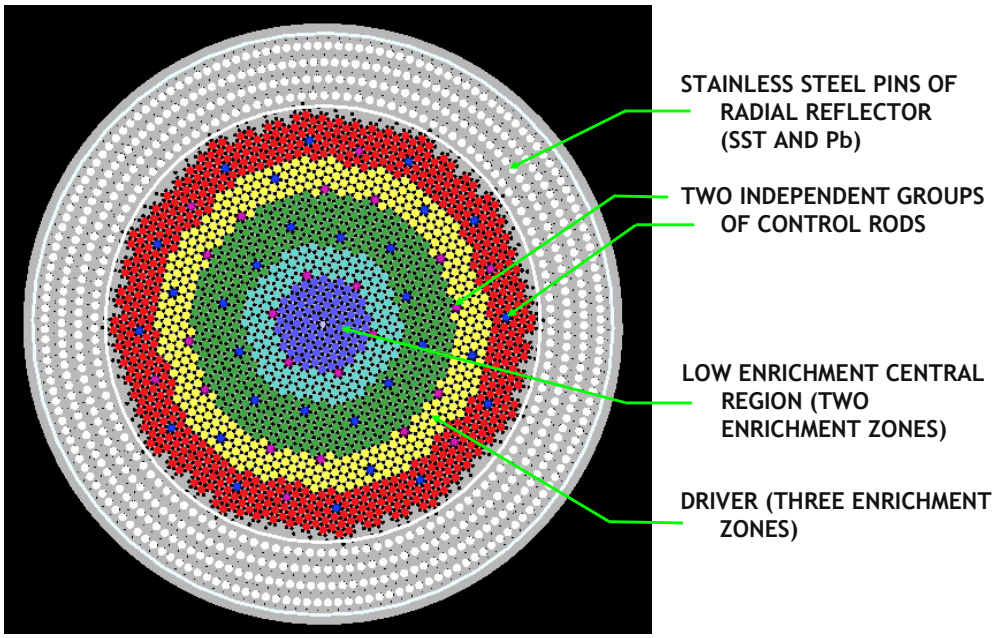

FIG. 4.25. SSTAR 30-Year Core with all Fuel pins are shown – primary control rod locations are shown in magenta and secondary control rod locations in blue colour.

The fuel pins are permanently attached to an underlying support plate. This configuration restricts access to fuel and eliminates fuel assembly blockage accident initiators. The compact active core which is 1.22 m in diameter by 0.976 m in height is removed as a single cassette during refueling and replaced by a fresh core. The active core diameter is selected to minimize the burnup reactivity swing over the 30-year core lifetime. The power level of 45 MWt is conservatively chosen to limit the peak fluence on the cladding to 4×10^{23} neutrons/cm^2 which is the maximum exposure for which HT9 cladding has been irradiated. This fluence is also assumed as a reference criterion for other cladding materials for which long-term irradiation data is unavailable. The core incorporates two low enrichment zones in the core central region which helps to reduce the burnup reactivity swing. Three driver enrichment zones reduce the peak-to-average power. Primary and secondary sets of control rods are uniformly dispersed throughout the active core. The radial reflector consists of an annular "box" containing 50 volume % stainless steel rods and 50 volume % Pb with a small flowrate of Pb to remove the small power deposition in the reflector. Stainless steel is necessary to shield the reactor vessel from neutrons reducing the fluence at the reactor vessel.

The reference cladding material incorporates Si-enhanced steel to retard the oxidation rate of the cladding resulting from exposure to dissolved oxygen in the coolant. A promising approach for the cladding may be weldment of a surface layer of Si-enhanced steel upon F/M steel to form a layered billet which is co-extruded [41]. The Si-enhanced layer provides improved corrosion resistance but has poor irradiation stability. The substrate provides structural strength and irradiation stability. The fuel pellets are bonded to the cladding by molten Pb to reduce the temperature difference between the pellet outer surface and cladding inner surface.

The fuel pins are held by two levels of grid spacers similar to the approach followed in Light Water Reactor (LWR) fuel assemblies. The grid spacer configuration is shown in Figs 4.26 and 4.27.

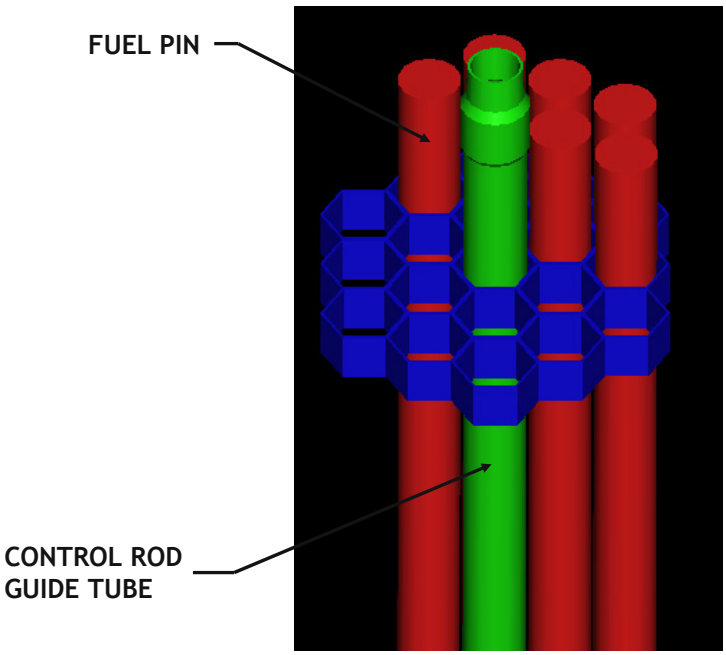

FIG. 4.26. Illustration of SSTAR fuel pins held by grid spacers welded to control rod guide tubes.

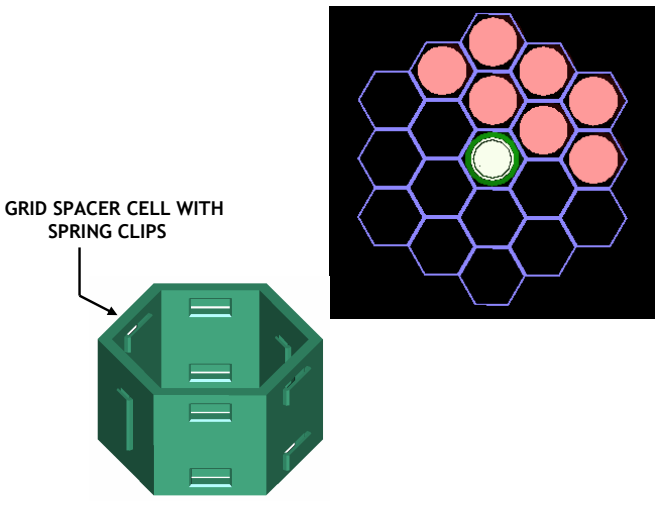

FIG. 4.27. Illustration of SSTAR core grid spacer cell.

A grid spacer is welded to a control rod guide tube; the grid spacer holds the surrounding fuel pins by means of spring clips allowing for thermal expansion of the fuel pins relative to the control rod guide tube.

Two sets of control rods are provided for independence and redundancy of scram. The control rods incorporate boron carbide absorber with enhancement of the isotope, ^{10}B. Small adjustments of the control rods are carried out to compensate for small changes in the burnup reactivity swing. Each control rod moves inside of a control rod guide tube occupying a position in the triangular lattice (Fig. 4.28).

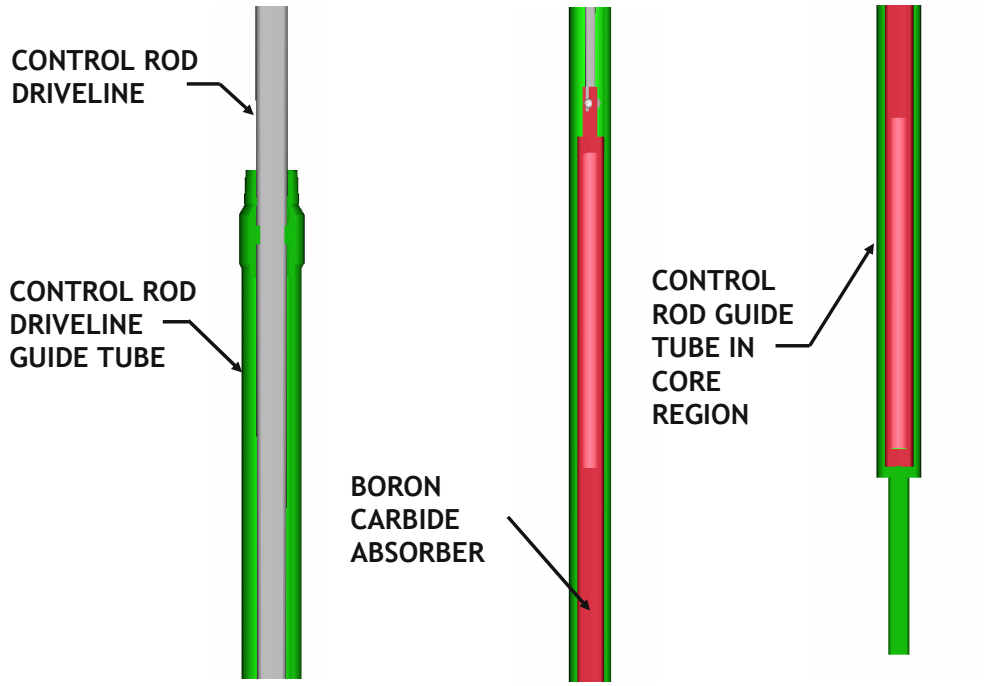

FIG. 4.28. SSTAR control rod, control rod driveline, and control rod driveline guide tube.

Control rod drivelines are shrouded by guide tubes above the core (distinct from the control rod guide tubes inside the core) and are connected to control rod drives located above the upper closure head.

Normally, refueling equipment is not present on the site. Refueling equipment including a crawler crane is brought onsite only following the 30-year core lifetime. The control rods are inserted into the core, “locked” to prevent their withdrawal, and detached from the control rod drivelines. The upper closure head for the guard and reactor vessels is removed together with the control rod drives and drivelines, the spent core is removed from the vessel, the core is placed inside of a shipping cask and transported to a fuel cycle support center located in a fuel cycle state. A fresh core is installed in the reactor vessel, the closure head is re-installed, drivelines are attached to control rods, and the refueling equipment is removed from the site. Additional proliferation resistance features of SSTAR are discussed in Ref. [42].

SSTAR incorporates two independent and redundant safety grade active shutdown systems. The low burnup reactivity swing of the 30-year lifetime core decreases the excess reactivity requirements reducing the amount of reactivity insertion that would accompany the unintended withdrawal of one or more control rods.

SSTAR currently incorporates a single safety grade emergency heat removal system which is the Reactor Vessel Auxiliary Cooling System (RVACS) for decay heat removal should the normal heat removal path involving the Pb-to-CO_2 HXs be unavailable. The RVACS involves heat removal from the outside of the guard vessel due to natural circulation of air which is always in effect. Because the RVACS represents only a single safety grade system, it would be required to have a high reliability with respect to seismic events or sabotage. To provide for greater reliability of emergency decay heat removal beyond that corresponding to a single RVACS system, it is planned to incorporate multiple safety grade Direct Reactor Auxiliary Cooling System (DRACS) HXs inside of the reactor vessel to provide for independent and redundant means of emergency heat removal.

Conversion of the core thermal energy to electricity is accomplished using a supercritical carbon dioxide (S-CO_2) Brayton cycle energy converter providing higher plant efficiencies and lower balance of plant costs than the traditional Rankine steam cycle operating at the same reactor core outlet temperature. The interest in higher plant efficiencies has heretofore driven interest in operation of SSTAR at higher Pb temperatures to take advantage of the increase in plant efficiency with temperature of the S-CO_2 Brayton cycle. The increase in cycle efficiency with turbine outlet temperature calculated for SSTAR is shown in Fig. 4.29.

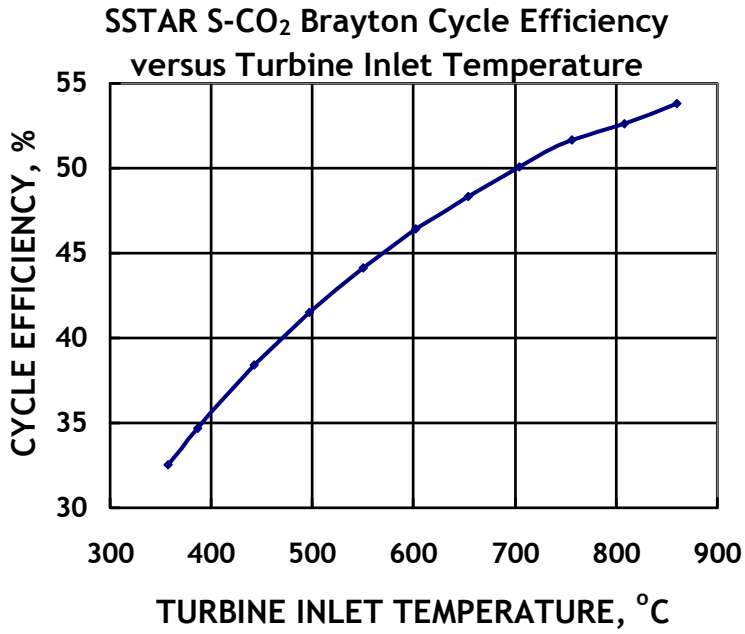

FIG. 4.29. Efficiency of S-CO_2 Brayton cycle versus turbine inlet temperature.

Table 4.6 provides SSTAR conditions and dimensions.

TABLE 4.6. CONDITIONS AND DIMENSIONS FOR SMALL SECURE TRANSPORTABLE AUTONOMOUS REACTOR (SSTAR)

Item	Value
Power, MWe (MWt)	19.8 (45)
Coolant	Pb
Fuel	Transuranic nitride (TRUN) enriched to Nearly 100 % N^{15}
Enrichment, %	1.7/3.5/17.2/19.0/20.7 TRU/HM, 5 radial zones
Core lifetime, years	30
Core inlet/outlet temperatures, °C	420 / 567
Coolant flow rate, kg/s	2107
Power density, W/cm^3	39.4
Average (peak) discharge burnup, MWd/kg HM	81 (131)
Burnup reactivity swing, $	< 1
Peak fuel temperature, °C	841
Cladding	Co-extruded Si-enhanced steel layer for corrosion resistance and ferritic/martensitic steel substrate for structural strength and irradiation resistance bonded to fuel pellets by Pb
Peak cladding temperature, °C	650
Fuel/coolant volume Fractions	0.45 / 0.35
Fuel pin diameter, cm	2.50
Fuel pin triangular Pitch-to-diameter ratio	1.185
Active core dimensions Height/diameter, m	0.976 / 1.22
Core hydraulic diameter, cm	1.371
Pb-to-CO_2 HXs Type	Shell-and-tube
Number of Pb-to-CO_2 HXs	4
HX tube length, m	4.0
HX tube inner/outer diameters, cm	1.0 / 1.4
Number of tubes (all HXs)	10 688
HX tube pitch-to-diameter ratio	1.222
HX Pb hydraulic diameter, cm	0.904
HX-core thermal centers separation height, m	6.80
Reactor vessel dimensions height/diameter, m	12.0 / 3.23
Reactor vessel thickness, cm	5.08
Average Pb coolant velocity through core, m/s	0.47
Pb coolant velocity through grid spacers, m/s	0.85
Gap between reactor vessel and guard vessel, cm	12.7
Gap filling material	Air
Guard vessel thickness, cm	5.08
Air channel thickness, cm	15
Air ambient temperature, °C	36
Working fluid	Supercritical CO_2
CO_2 turbine inlet temperature, °C	552
Minimum CO_2 temperature in cycle, °C	31.25
Max/min CO_2 pressures in cycle, MPa	20 / 7.4
CO_2 flow rate, kg/s	245
Net generator output, MWe	19.8
Supercritical CO_2 Brayton cycle efficiency, %	44.2
Net plant efficiency, %	44.0

A peak cladding inner surface temperature of 650°C has been adopted as a goal for SSTAR. This is comparable to the peak cladding temperature of ~ 630°C of the Russian BREST-OD-300 design which reflects the optimism of the Russians to operate at such temperatures with EP-823 Si-enhanced F/M steel cladding. Reactor and S-CO_2 Brayton cycle conditions calculated for a 650°C peak cladding temperature are shown in Fig. 4.30.

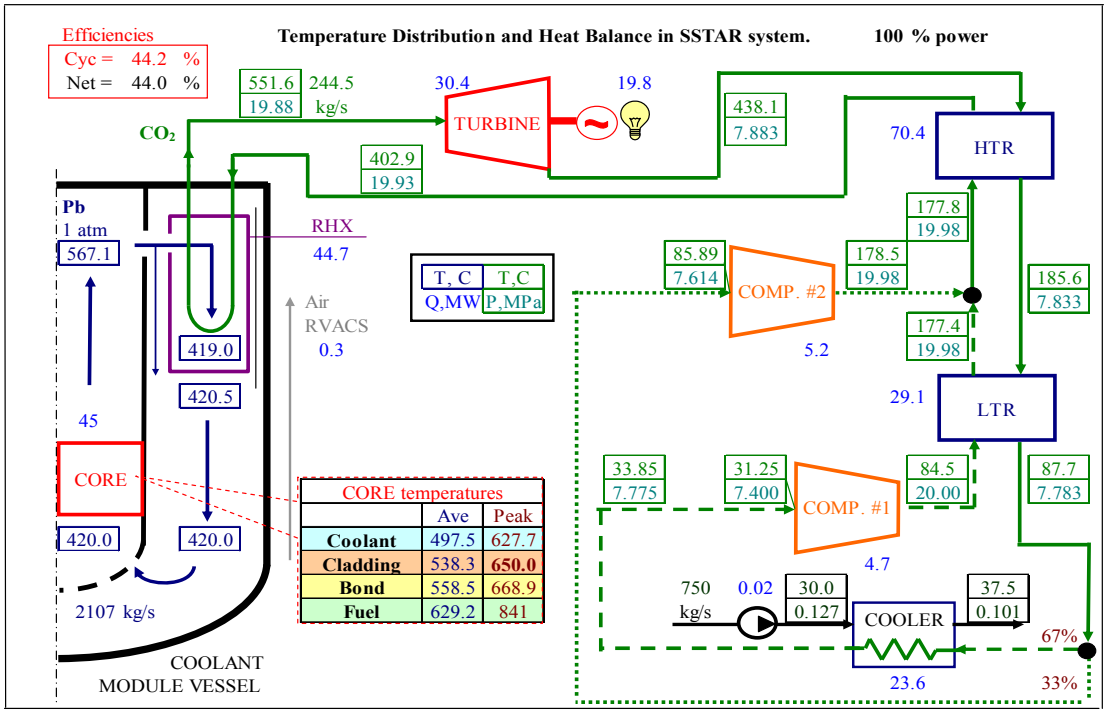

FIG. 4.30. Conditions calculated for SSTAR with S-CO_2 Brayton cycle energy converter.

The coupled reactor-S-CO_2 Brayton cycle plant system thermal hydraulic pre-conceptual design has been optimized to maximize the cycle efficiency. For a 650°C peak cladding temperature, a reactor core outlet temperature of 567°C is achieved resulting in a Brayton cycle efficiency of 44.2% and a net plant efficiency of 44.0%. Remarkably small sizes are calculated for the centrifugal (i.e., radial flow) compressors and the axial flow turbine. The small turbomachinery sizes reflect the high density of supercritical CO_2 (e.g., relative to gaseous helium) such that the flow area for energy transport with supercritical CO_2 is much less than that required for a gas such as He in a gas Brayton cycle or steam in a Rankine cycle steam turbine.

An autonomous load following capability is needed for deployment on small or immature electric grids. A control strategy has been developed for the S-CO_2 Brayton cycle energy converter whereby the cycle is automatically controlled such that the heat removal from the Pb-to-CO_2 HXs is adjusted such that the generator power matches the load demand from the electric grid. The control strategy enables autonomous load following by the reactor whereby the core power automatically adjusts itself due to the strong reactivity feedbacks of the fast spectrum core with Pb coolant and transuranic nitride fuel such that the core power matches the heat removal from the Pb-to-CO_2 HXs. In particular, it is not necessary for the reactor core power to be changed through the motion of control rods except for startup and shutdown operations.

The automatic control strategy enables load following by the reactor and controllability of the S-CO_2 Brayton cycle near the critical point. The automatic control strategy includes:

- Turbine bypass control for fast changes in heat removal at all load levels;
- Additional inventory control between 90 and 35% nominal load (limited by the inventory control tank volume) tending to maintain cycle temperatures;
- Cooler bypass control to maintain the CO_2 temperature at the inlet to the first stage of the main compressor (i.e., the lowest temperature in the cycle) close to the critical temperature (30.98°C) and preventing it from decreasing below the critical temperature resulting in the onset of two-phase flow;
- Cooler cooling water flow rate control preventing full opening or closing of the cooler bypass valve;
- In addition, compressor surge prevention systems precluding surge which could cause compressor damage in specific postulated accidents.

Autonomous load following enabled by the S-CO_2 Brayton cycle automatic control strategy simplifies operator requirements and enhances plant reliability.

4.8.3. Scale-up of SSTAR concept: STAR-LM

SSTAR can be scaled-up to a 175 MWe (400 MWt) natural circulation LFR called the Secure Transportable Autonomous Reactor with Liquid Metal (STAR-LM). The 400 MWt power rating represents the ability of single-phase natural circulation heat transport of the Pb primary coolant to transfer core power to in-vessel heat exchangers inside of a reactor vessel with an assumed transportability height limitation for rail transport of about 18.9 meters. It operates with core outlet and inlet temperatures of 578 and 420°C, respectively. STAR-LM units are deployable as a sequence of clustered modules installed over time at a single site to serve the needs of a growing consumer base. For example, six modules provide 1086 MWe of capacity.

For the manufacture of H_2 when a full-fledged hydrogen economy arrives, STAR-H2 (Hydrogen) is a 400 MWt STAR-LM version intended for hydrogen generation using a Ca-Br thermochemical ("water cracking") cycle. Deployment would follow SSTAR and STAR-LM when cladding and structural material for operation in Pb up to 800°C are developed. STAR-H2 could provide all primary energy and potable water for a city of ~ 75 400. STAR-H2 operates with core outlet and inlet temperatures of 793 and 664°C, respectively. The balance of plant involves a cascade of H_2 production (and O_2 production) via the Ca-Br cycle, in-house electricity production using the S-CO_2 Brayton cycle, and water desalination. A possible approach for materials for STAR-H2 involves the use of high temperature materials resistant to attack by Pb and having sufficient structural strength and irradiation stability. One promising material worthy of investigation is Ti_3SiC_2 manufactured by 3-ONE-2, LLC [4, 5]. It can be pressed, slip cast, and injection molded. It is machinable or can be thermally sprayed onto metals to form coatings. It is described as stiff, thermal shock resistant, damage tolerant, tough, and fatigue resistant. Its corrosion resistance has been tested at Argonne National Laboratory by exposure to Pb with low oxygen potential at 800 and 650°C for 1000 hours in a quartz Harp loop [6]. No evidence of Ti_3SiC_2 attack by Pb was observed. Conditions and dimensions for STAR-LM are provided in Table 4.7.

TABLE 4.7. CONDITIONS AND DIMENSIONS FOR SECURE TRANSPORTABLE AUTONOMOUS REACTOR WITH LIQUID METAL (STAR-LM)

Item	Value
Power, MWe (MWt)	175.4 (400)
Coolant	Pb
Fuel	Transuranic Nitride (TRUN) Enriched to Nearly 100 % N^{15}
Enrichment, %	13.3/18.2/21.3 TRU/HM, 3 Radial Zones
Core lifetime, years	15
Core inlet/outlet temperatures, °C	438 / 578
Coolant flow rate, kg/s	19708
Power density, W/cm3	42
Average (peak) discharge burnup, MWd/kg HM	83 (136)
Burnup reactivity swing, %Δk ($)	0.61 (1.97)
Peak fuel temperature, °C	744
Cladding	Co-extruded Si-enhanced steel layer for corrosion resistance and ferritic/martensitic steel substrate for structural strength and irradiation resistance bonded to fuel pellets by Pb
Peak cladding temperature, °C	650
Fuel/coolant volume fractions	0.21 / 0.66
Fuel pin diameter, cm	1.30
Fuel pin triangular pitch-to-diameter ratio	1.536
Active core dimensions height/diameter, m	2.0 / 2.459
Core hydraulic diameter, cm	2.082
Pb-to-CO_2 HXs type	Shell-and-tube
Number of Pb-to-CO_2 HXs	4
HX tube length, m	6.0
HX tube inner/outer diameters, cm	0.5 / 0.9
Number of tubes (all HXs)	63288
HX tube pitch-to-diameter ratio	1.632
HX Pb hydraulic diameter, cm	1.742
HX-core thermal centers separation height, m	9.623
Reactor vessel dimensions height/diameter, m	16.9 / 5.5
Reactor vessel thickness, cm	5.08
Average Pb coolant velocity through core, m/s	0.65
Pb coolant velocity through grid spacers, m/s	1.16
Gap between reactor vessel and guard vessel, cm	12.7
Gap filling material	Pb-Bi eutectic
Guard vessel thickness, cm	5.08
Air channel thickness, cm	15
Air ambient temperature, °C	36
Working fluid	Supercritical CO_2
CO_2 turbine inlet temperature, °C	559
Minimum CO_2 temperature in cycle, °C	31.25
Max/Min CO_2 pressures in cycle, MPa	20 / 7.4
CO_2 flow rate, kg/s	2260
Net generator output, MWe	175.4
Supercritical CO_2 Brayton cycle efficiency, %	44.3
Net plant efficiency, %	43.9

Conditions for the STAR-LM S-CO_2 Brayton cycle power converter are shown in Fig. 4.31.

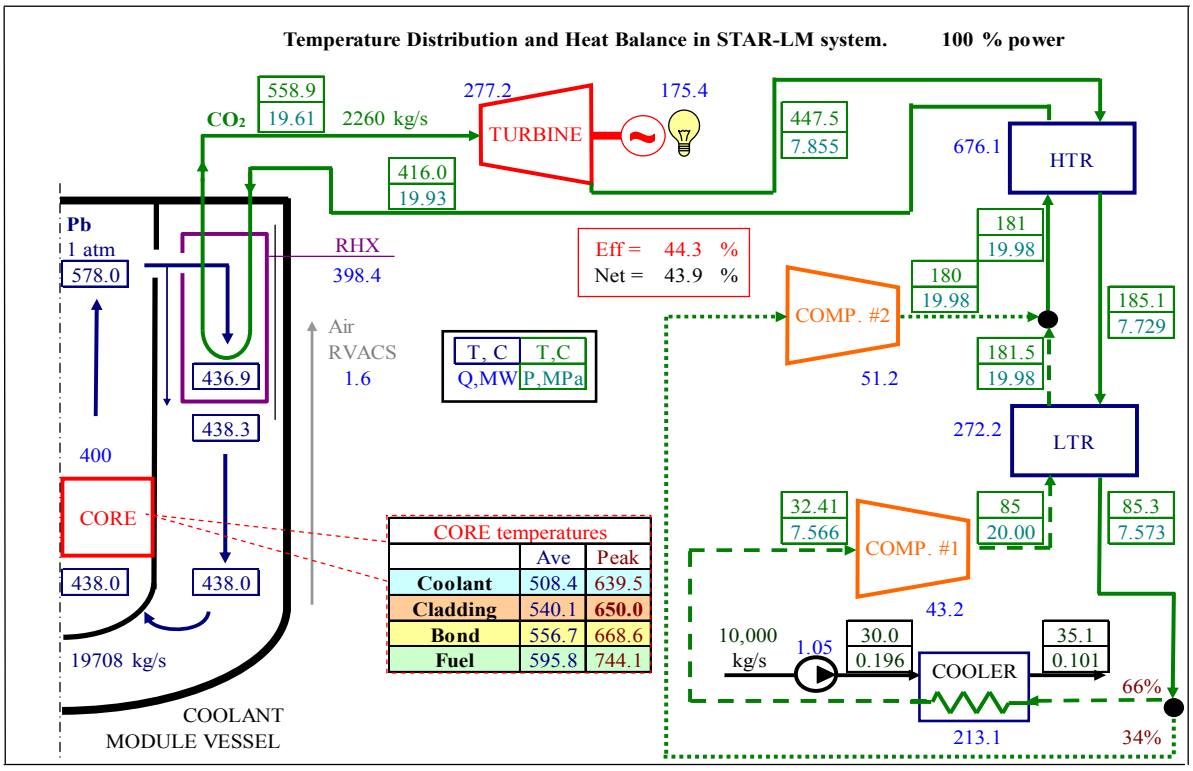

FIG. 4.31. Conditions calculated for STAR-LM with S-CO_2 Brayton cycle energy converter.

4.8.4. Current status and summary

The SSTAR LFR has been shown through preconceptual design analyses to be a viable concept for a small fast reactor converter for international deployment providing proliferation resistance, fissile self-sufficiency, autonomous load following, simplicity of operation and reliability, transportability, as well as a high level of passive safety. Interest in achieving higher plant efficiencies has heretofore driven interest in operation of SSTAR at higher Pb temperatures to take advantage of the increase in plant efficiency with temperature provided by the S-CO_2 Brayton cycle power converter. A peak cladding temperature of 650°C has been used as a goal; at this temperature, a reactor core outlet temperature of 567°C is achieved resulting in a net plant efficiency of 44.0%. It was always recognized that this would require the development of cladding and structural materials for long-term service in Pb coolant up to 650°C peak temperature with corrosion protection provided by active maintenance and control of the dissolved oxygen potential in the coolant together with limitation of the Pb coolant velocities giving rise to the formation of protective oxide layers on the steel cladding and structures. SSTAR development is being supported by ongoing testing in the DELTA loop at Los Alamos National Laboratory of alloy specimens with special treatments or coatings which might enhance corrosion resistance at the temperatures at which SSTAR operates.

The next step on the path towards realization of the LFR is the development and deployment of a technology pilot plant (i.e., a LFR demonstration reactor) which implements innovative engineering features enabling lead to show its economic potential and industrial attractiveness. The technology pilot plant would operate at lower temperatures enabling the use of existing materials such as T91 F/M steel and Type 316 austenitic stainless steel that have been shown to have corrosion resistance to lead-bismuth eutectic with active oxygen control at temperatures below ~ 550°C in experiments carried out in the DELTA loop and elsewhere.

REFERENCES TO CHAPTER 4

[1] FARMER, M.T., SIENICKI, J.J., Analysis of Transient Coolant Void Formation During a Guillotine-Type Tube Rupture Event in the STAR-LM System Employing a Supercritical CO_2 Brayton Cycle, Proc. 12th Int. Conf. on Nuclear Engineering (ICONE12), Arlington, Virginia, USA, 25-29 April 2004, Paper ICONE12-49227.

[2] LI, N., Lead-Alloy Coolant Technology and Materials –Technology Readiness Level Evaluation, paper presented in 2nd COE-INES Int. Symposium on Innovative Nuclear Energy Systems (INES-2), Yokohama, Japan, 26-30 November 2006.

[3] WEISENBURGER, A., HEINZEL, A., MUELLER, G., MUSCHER, H., RUSANOV, A., T91 Cladding Tubes with and without Modified FeCrAl Coatings Exposed in LBE at Different Flow, Stress and Temperature Conditions, paper presented in IV International Workshop on Materials for HLM Cooled Reactors and Related Technologies, Rome, Italy, 21-23 May 2007.

[4] BARSOUM, M.W., EL-RAGHY, T., The MAX Phases: Unique Carbide and Nitride Materials, American Scientist, Vol. 89, p. 334 (July-August 2001).

[5] See www.3one2.com (3-ONE-2 LLC, 4 Covington Place, Voorhees, NJ 08043, USA).

[6] BARNES, L.A., DIETZ RAGO, N.L., LEIBOWITZ, L., Corrosion of Ternary Carbides by Molten Lead, in Press (Journal of Nuclear Materials).

[7] GIF-002-00 (Graphics Interchange Format-002-00), Gen IV Technology Roadmap (December 2002).

[8] Private communication (System Research Plan for the Lead-cooled Fast Reactor, LFR, Draft document of the LFR Provisional Steering Committee, May 2006).

[9] CINOTTI, L., AÏT ABDERRAHIM, H., BENAMATI, G., FAZIO, C., KNEBEL, J., LOCATELLI, G., MONTI, S., SMITH, C.F., SUH, K., Lead-Cooled Fast Reactor, paper presented in EU Research and Training in Reactor Systems (FISA 2006), Luxembourg, 13-16 March 2006.

[10] CINOTTI, L., SMITH, C.F., SIENICKI, J.J., AÏT ABDERRAHIM, H., BENAMATI, G., LOCATELLI, G., MONTI, S., WIDER, H., STRUWE, D., ORDEN, A., HWANG, I.S., The Potential of the LFR and the ELSY Project, Proc. ICAPP '07, Nice, France, 13-18 May 2007, ISBN: 9781604238716, Curan Associates, Inc. (February 2008).

[11] CINOTTI, L., AÏT ABDERRAHIM, H., BENAMATI, G., CORSINI, G., LE CARPENTIER, D., LOCATELLI, G., MONTI, S., ORDEN, A., STRUWE, D., TUCEK, K., The ELSY Project, Proc. PHYSOR 2008, Interlaken, Switzerland, 14-19 September 2008, Paul Scherrer Institute (2008).

[12] ALEMBERTI, A., CARLSSON, J., MALAMBU, E., ORDEN, A., CINOTTI, L., STRUWE, D., AGOSTINI, P., MONTI, S., European Lead Fast Reactor ELSY, paper presented in 7th European Commission Conference on Euratom Research and Training in Reactor Systems (FISA 2009), Prague, Czech Republic, 22-24 June 2009.

[13] FURUKAWA, T., et al., Corrosion Behavior of FBR Candidate Materials in Stagnant Pb–Bi at Elevated Temperature, Journal of Nuclear Science and Technology, Vol. 41, No. 3, pp. 265-270 (March 2004).

[14] HAYAFUNE, H., et al., Conceptual Design Study of Pb-Bi Cooled Fast reactor Plant System in the Feasibility Study in Japan, Proc. GLOBAL 2005, Tsukuba, Japan, 9-13 October 2005 (Editor: Hajimu Yamana), Atomic Energy Society of Japan, ISBN: 4-89047-133-2, paper no. 457.

[15] KOTAKE, S., et al., Feasibility Study on Commercialized Fast Reactor Cycle Systems/Current Status of the FR System Design, Proc. GLOBAL 2005, Tsukuba, Japan, 9-13 October 2005 (Editor: Hajimu Yamana), Atomic Energy Society of Japan, ISBN: 4-89047-133-2, paper no. 435

[16] KINOSHITA, I., NISHI, Y., FURUYA, M., Study on Applicability of Direct Contact Heat Transfer Steam Generations for LMFBRs, 8th Int. Conf. on Nuclear Engineering (ICONE-8), ICONE-8769, Baltimore, MD, USA, 2-6 April 2000.
[17] TAKAHASHI, M., IGUCHI, T., OTSUBO, A., KONDO, M., HATA, K., HARA, K., UCHIDA, S., OSADA, H., KASAHARA, Y., MATSUZAWA, K., SAWA, N., YAMADA, Y., KUROME, K., Design and Experimental Study for Development of Pb-Bi Cooled Direct Contact Boiling Water Small Fast Reactor (PBWFR), Proc. ICAPP '04, Pittsburgh, PA, USA, 13-17 June 2004, ANS, ISBN: 0-89448-680-2.
[18] UCHIDA, S., TAKAHASHI, M., KOYAMA, K., YAMADA, Y., Conceptual and Safety Design of Pb-Bi Cooled Direct Contact Boiling Water Fast Reactor (PBWFR), Proc. ICAPP'05, Seoul, Korea, Republic of, 15-19 May 2005, ISBN: 9781604236934, Curran Associates, Inc. (April 2007) paper 5172.
[19] TAKAHASHI, M., TORII, H., Conceptual Study of Lead-Bismuth-Cooled Fast Reactor (PBWFR) and Its Applicability to Chemical Industrial Complex, paper presented in Tokyo Tech-MIT Symposium, Kamakura, Japan, 23-25 July 2007.
[20] TAKAHASHI, M., SOFUE, H., IGUCHI, T., MATSUMOTO, M., PRAMONO, Y., HUANG, F., MATSUZAWA, T., UCHIDA, S., NOVITRIAN, H.N., Experimental Simulation of Steam Lift Pump and Steam Generation for Pb-Bi Cooled Direct Contact Boiling Water Fast Reactor, Proc. ICAPP'05, Seoul, Korea, Republic of, 15-19 May 2005, ISBN: 9781604236934, Curran Associates, Inc. (April 2007) paper 5164.
[21] TAKAKI, N., MATSUI, K., TASHIMO, M., SEKIMOTO, H., Potential role of CANDLE reactor on sustainable development and non-proliferation, paper presented in 2nd COE-INES International Symposium on Innovative Nuclear Energy Systems (INES-2), Yokohama, Japan, 26-30 November 2006.
[22] YAN, M.YU., SEKIMOTO, H., Small Long Life CANDLE Fast Reactor Research, paper presented in 15th Int. Conf. Nuclear Engineering (ICONE-15), Nagoya, Japan, 22-26 April 2007.
[23] HWANG, I.S., JEONG, S.H., PARK, B.G., et al., The concept of a Proliferation - resistant, Environment - friendly, Accident - tolerant, Continual and Economical Reactor (PEACER), Progress in Nuclear Energy, 37(1-4), 217 (2000).
[24] HWANG, I.S., A Sustainable Regional Waste Transmutation System: PEACER, Plenary Invited Paper, ICAPP'06, Reno, NV, U.S.A., 4-6 June 2006.
[25] LIM, J.Y., KIM, M.H., KIM, C.H., HWANG, I.S., Proliferation Resistance and Transmutation Capability of PEACER Core, Proc. GLOBAL 2003, New Orleans, LA, USA, ANS, ISBN: 0-89448-677-2 (2003).
[26] PARK, B.G., HWANG, I.S., PEACER Pyrochemical Processing for Low-Level Waste Production in PEACER, paper presented in ICAPP '02, Hollywood, FL, USA, 9-13 June 2002.
[27] LEE, H.W., et. al, Solver-Interfaced Virtual Reality Approach for Life-cycle Management of Nuclear Energy Systems, Proc. ICAPP '05, Seoul, Korea, Republic of, 15-19 May 2005, ISBN: 9781604236934, Curran Associates, Inc. (April 2007).
[28] JEONG, S.H., BAHN, C.B., CHANG, S.H., OH, Y.J., NAM, W.C., RYU, K.H., NAM, H.O., LIM, J., LEE, N.Y., HWANG, I.S., Operation Experience of LBE Loop: HELIOS, Proc. ICAPP '06, Reno, NV, USA, 4-6 June 2006, paper no. 6284.
[29] LEYPUNSKY, A.I., Fast Neutron Systems, Book: A.I. Leypunsky, Selected Papers, Reminiscence, Naukova Dumka, Kiev, Ukraine, p. 62 (1990).
[30] INTERNATIONAL ATOMIC ENERGY AGENCY, Multipurpose Lead-Bismuth Cooled Small Power Modular Fast Reactor SVBR-75/100, Proc. Int. Conf. Innovative Technologies for Nuclear Fuel Cycles and Nuclear Power, 23–26 June 2003, Vienna, Austria (2003), paper CN-108-36.

[31] STEPANOV, V.S., KLIMOV, N.N., BOLVANCHIKOV, S.N., KULIKOV, M.L., Reactor Module SVBR-75/100: Improved Safety, Transportability, Opportunities of Multipurpose Usage, paper presented in 2nd Int. Conf. Heavy-Liquid Metal Coolant in Nuclear Technologies (HLMC-2003) Obninsk, Russian Federation, 2003.
[32] ZRODNIKOV, A.V., DRAGUNOV, YU.G., TOSHINSKY, G.I., STEPANOV, V.S., et al., NPPs Based on Reactor Modules SVBR-75/100, Atomnaya Energiya, 91, Issue 6 (2001).
[33] IGNATENKO, YE.I., ZRODNIKOV, A.V., STEPANOV, V.S., KRUSHENITSKY, V.N., VIKIN, V.A., et al., Renovation of the First Generation NPP Units Withdrawn from Operating after Expiring their Lifetime by Mounting Reactor Installations SVBR-75 with Lead-Bismuth Liquid Metal Coolant in the Steam-Generators' Boxes, paper presented in 8th Annual Conference of Russia Nuclear Society, Ekaterinburg, Russian Federation, 1997.
[34] ADAMOV, E.O., ORLOV, V.V., Naturally Safe Lead-cooled Fast Reactor for Large-scale Nuclear Power, Moscow, Russian Federation (2001).
[35] GABARAEV, B.A., FILIN, A.I., Development of a BREST-OD-300 NPP with an On-Site Fuel Cycle for the Beloyarsk NPP, Implementation of the Initiative by Russian Federation President V.V. Putin, 11th International Conference on Nuclear Engineering, Tokyo, Japan, 20-23April 2003, paper ICONE11-36410.
[36] SIENICKI, J.J., MOISSEYTSEV, A.V., SSTAR Lead-Cooled, Small Modular Fast Reactor for Deployment at Remote Sites – System Thermal Hydraulic Development, Proc. ICAPP '05, Seoul, Korea, Republic of, 15-19 May 2005, ISBN: 9781604236934, Curran Associates, Inc. (April 2007) paper 5426.
[37] YANG, W.S., SMITH, M.A., KIM, S.J., MOISSEYTSEV, A.V., SIENICKI, J.J., WADE, D.C., Lead-Cooled, Long-Life Fast Reactor Concepts for Remote Deployment, Proc. ICAPP '05, Seoul, Korea, Republic of, 15-19 May 2005, ISBN: 9781604236934, Curran Associates Inc. (April 2007) paper 5102.
[38] SIENICKI, J., WADE, D., MOISSEYTSEV, A., YANG, W.S., KIM, S.J., SMITH, M., ALIBERTI, G., DOCTOR, R., MATONIS, D., STAR Performer, Nuclear Engineering International, p. 24 (July 2005).
[39] SIENICKI, J.J., MOISSEYTSEV, A., WADE, D.C., NIKIFOROVA, A., Status of Development of the Small Secure Transportable Autonomous Reactor (SSTAR) for Worldwide Sustainable Nuclear Energy Supply, Proc. ICAPP '07, Nice, France, 13-18 May 2007, ISBN: 9781604238716, Curran Associates, Inc. (February 2008) paper 7218.
[40] SIENICKI, J.J., WADE, D.C., MOISSEYTSEV, A., Role of Small Lead-Cooled Fast Reactors for International Deployment in Worldwide Sustainable Nuclear Energy Supply, Proc. ICAPP '07, Nice, France, 13-18 May 2007, ISBN: 9781604238716, Curan Associates, Inc. (February 2008) paper 7228.
[41] LIM, J.Y., BALLINGER, R.G., Alloy Development for Lead-Cooled Reactor Service, paper presented in MIT-Tokyo Technical Symposium on Innovative Nuclear Energy Systems, Massachusetts Institute of Technology, Cambridge, Massachusetts, USA, 2-4 November 2005.
[42] SIENICKI, J.J., WADE, D.C., Nonproliferation Features of the Small Secure Transportable Autonomous Reactor (SSTAR) for Worldwide Sustainable Nuclear Energy Supply, Transactions of the American Nuclear Society, Vol. 93, p. 340 (2005).

CHAPTER 5
GAS-COOLED FAST REACTOR DESIGNS (FRANCE, JAPAN, EUROPEAN UNION, RUSSIAN FEDERATION AND USA)

5.1. Introduction

Gas-cooled fast reactors have several potential advantages over liquid metal-cooled fast reactors. For example, the coolant is inert (avoiding metal-water reactions and corrosion), it is transparent (potentially yielding an advantage in inspection) and advanced thermodynamic cycles promise higher thermal efficiencies. However, certain disadvantages in terms of safety must be addressed. The low thermal inertia and poor heat transfer properties are important considerations in depressurization events. The current consensus reached on the approach to the depressurized decay heat accidents is a combination of both active and passive means (e.g. a guard containment surrounding the primary system can be utilized to provide back-up pressure). This back-up pressure plus whatever natural convection is available at this pressure level will be utilized to reduce significantly the blower power of the active decay heat removal system. This makes it possible to use passive power supplies, such as batteries without the need for startup. The target is to remove the need for electric power in these situations.

In this chapter, contributions will be presented on the gas-cooled fast reactor programmes in France, Switzerland, the European Union and Japan, within the framework of the Generation IV International Forum (the GIF), and within the national programmes of the Russian Federation and the United States.Gas-cooled fast reactors developed in the framework of GIF.

5.1.1. Background

The GEN-IV Gas-cooled Fast Reactor (GFR) system features a fast-spectrum helium-cooled reactor and a closed fuel cycle. Through the combination of a fast neutron spectrum and full recycle of actinides, GFRs minimize the production of long-lived radioactive waste and also make it possible to utilize available fissile and fertile materials (included depleted uranium) two orders of magnitude more efficiently than thermal spectrum systems. Similar to thermal-spectrum helium cooled systems, the high outlet temperature of He coolant offers the possibility to deliver electricity, hydrogen or process heat with high conversion efficiency. The GFR therefore has the potential to fulfil two possible missions. In accordance with these missions, two main plant layouts were being considered.

The high-temperature, helium-cooled, direct Brayton cycle reactor system (850°C core outlet temperature) is a longer-term option to be considered for high temperature co-generation capability and system compactness. This presents challenges for high temperature fuels/materials R&D and He turbo-machinery development. The indirect cycle with helium as primary coolant and supercritical CO_2, as well as consideration of other gases, as secondary working fluid is an option to be considered for near-term sustainability of the nuclear fuel cycle and/or feasibility studies of potential design options. The challenge here is to establish a significant level of efficiency improvement over previous fast reactor designs through engineering design R&D.

In the USA around the early 1960s, groups formed to explore the advantages of gas-cooling for fast reactor applications. A legacy already existed at this early point for the use of gas-cooling of nuclear reactor cores through the early utilization for gas-cooled thermal reactor plants, both in the USA and in Europe. There was a precedent technology base to build

upon and expand. In the USA, the effort lead by (Gulf) General Atomics centred on helium gas. In Europe, the UK started from the CO_2 cooled Magnox reactors, but eventually the European effort also coalesced around helium in the work of the European Community and KFK and KWU in Germany. Helium gas is:

- Single phase and capable of being used at both high temperatures and low temperatures without decomposing. There are no sudden changes in properties with two phase transformation.
- Chemically inert: it neither burns in air nor reacts with water to produce hydrogen. As a result of its inertness, it does not provide much of a corrosive medium for heat exchangers, pipes or seals constructed from either metals or ceramics. It does not react with the major fuel systems, oxides, carbides or nitrides of the actinides.
- Not activated by and is essentially transparent to neutrons so there is less coupling between the thermal fluid behaviour of the coolant and the neutronic behavior of the core. It is also optically transparent.

It was realized by this early generation of GCFR (Gas-Cooled Fast Reactor) designers and safety analysts that these properties of helium could lead to a fast reactor (FR) plant without the need for intermediate loops, hydrogen or extraordinary fire mitigation systems, washing stations or double walled steam generators. Monitoring and inspections could be performed through optical means. Moreover, given good fuel performance quality with low failure rates, component maintenance has the potential to be much simpler. It was also realized early that there was the potential for advanced generations of direct Brayton cycle gas turbine plants replacing the legacy Rankin cycle steam generator plants. This would require the development of an advanced generation of high-temperature compatible materials, in particular a whole new choice of fuel systems and elements. To leverage off the major investment in LMR technology, the GCFR designers chose to design plants in the temperature range of the Liquid Metal Fast Breeder Reactors (LMFBRs) so that major R&D items such as LMR fuel technology could also be used in the GCFR plants [1, 2]. In addition, High temperature Gas-Cooled Reactor (HTGR) technology was also leveraged to provide the components such as the Pre-stressed Concrete Reactor Vessel (PCRV), steam generators, gas circulators and clean-up systems. It was envisioned that this early generation GCFR based on essentially “off the shelf” items would be the first step in the ultimate sequence to an advanced generation of fast reactors. These would not only have the neutronic functional versatility unique to fast systems, such as breeding, sustainability or even transmutation, but also have the high temperature functional capability unique to gas reactors such as high efficiency, direct Brayton cycle machines and process heat applications in addition to electricity generation applications.

5.1.2. GEN-IV programme

However, even with these potential advantages and with this long-term vision, it was widely accepted that helium gas coolant did not have the attractive heat transfer and heat transport properties of sodium previously mentioned. It is the classical balance between operation and maintenance and the safety of postulated accidents. Given the early momentum in sodium LMFBR development and the investment already made in that technology, it was not possible to alter the course of the early decisions which had already been made in favour of sodium technology.

The GCFR effort both in the U.S. and in Europe was discontinued in the late 1970s to the early 1980s and the national FR efforts concentrated on CRBR in the U.S, Superphénix in France and Monju in Japan. Unfortunately, these decisions did not proceed completely

according to plan. International policy, non-proliferation concerns, environmental opposition to nuclear power and operating experience resulted in the cancellation of CRBR before completion of construction, decommissioning of Superphénix well before its design life time and the forced cold shutdown of Monju for the last ten years. The resulting a hiatus in FR development has been world-wide and has persisted for more than ten years. Given this hiatus, not only in FR development but also nuclear reactor development in general, USDOE took the lead and undertook the task of forging an international initiative to form a collaborative effort at the international level between the reactor R&D organizations of a number of nations to jointly develop the next generation of nuclear power plants, the "Generation IV" (or Gen IV) plants to be deployed in the mid 21st century. This global partnership is the Generation IV International forum (GIF) and of the six reactor types selected for further development, three of these are FRs. In particular, it was decided that given the hiatus in sodium LMR development, it would be the opportune moment to revisit the GCFR, now termed the GFR. Revisiting this technology would determine whether or not the promising advantages of the gas coolant for operation and maintenance identified thirty years previously actually had the potential to be in the basis of a design that could fulfil the Gen IV goals with regard to economics, safety, non-proliferation and sustainability Towards this objective, France, the USA and Japan participated in the GIF with the intent to jointly re-explore the GFR option. They were joined in this endeavor by Euratom, the UK and Switzerland. Before the formal signing of the GIF multilateral agreement on the GFR, the System Arrangement, still had not yet been signed, the parties cooperated under the framework of bilateral agreements. All sides collaborated such that the various bilateral work scopes complied with the multilateral GIF framework. In the USA, these bilateral agreements on the development of the GFR took the form of I-NERI projects with CEA of France.

Furthermore, in the specific case of the GFR the international parties had jointly formulated an International Collaboration Plan (ICP) comprised of the bilateral work scopes with the intent that this ICP will become Annex 1 of the Design and Safety Project Arrangement for the GFR [3] following formal signing of the system arrangement.

This chapter summarizes the design and safety analysis work on the GFR performed over the last few years by these international partners under this ICP and latterly under the auspices of the GFR Conceptual Design and Safety Project within the GIF. In accordance with the GIF GFR System R&D Plan [4], this work covered the Exploratory Phase where several design options and concepts were investigated to provide the basis for down selection. The End of the Exploratory Phase occurred at the end of FY2005. Down selection of the different GFR design and safety options was completed in FY2006 and, as outlined in the GIF System R&D plan, the GFR Preliminary Viability Report was completed at the end of FY2007. This report made laid the foundations for the work to be performed during the GFR Conceptual Design and Viability phases in the period 2008–2012. Unfortunately, both the US and the UK declined to sign the GFR System Arrangement and at the time of writing, whilst valuable activities continue in the US, the Gen IV GFR system studies were continued only by France, Switzerland, Japan and the European Union.

The next subsection details the design criteria and objectives which were set for these Exploratory Phase studies based on the Gen-IV goals. The bulk of the chapter then outlines key features of the concept, core, primary and safety system, and plant layout which have resulted from the design and safety analyses of the French, the USA and the integrated European efforts. Each section concludes with a summary of the status of the related R&D programme.

5.1.3. Design criteria and objectives

The key feasibility issues for the GFR as required by the work scope outlined in the ICP are:

- High temperature refractory and confining fuels;
- Structural materials for high temperatures and doses;
- Safety case with low thermal inertia and poor heat transfer properties of coolant particularly at low pressures:
- Decay heat removal strategies;
- Core melt exclusion strategies.

With these feasibility issues in the background, the general objectives of the parties to the ICP were to design a gas-cooled fast reactor system with:

- A high level of safety:
  (i) Successful decay heat removal under wide range of pressurized and depressurized conditions;
  (ii) Survive loss of active reactivity shutdown capability without core damage;
- A full recycling of actinides;
- Highly proliferation resistant;
- Attractive in terms of economics:
  (i) High thermal efficiency;
  (ii) Direct gas cycle as reference with indirect cycles as an alternative;
  (iii) Hydrogen as a commercial product;
- A power range from 300 MW(e) (modular) to 1200 MW(e) (economy of scale);
- Helium as the reference coolant with consideration of other gases, such as S-CO_2, for the secondary side of the indirect cycle options.

In the initial stages of the effort, design goals and criteria were specifically formulated for these GFR design objectives and documented to meet the GEN-IV criteria/metrics on sustainability, non-proliferation, economics and safety [5, 14]. To aid in the design effort, the high-level GEN-IV goals have been translated into specific GFR design and safety criteria [6]. These are as follows:

(a) Sustainability goals and criteria

Sustainability was judged to be the key goal for the GFR system. This means extensive use of uranium and calls for the recycling of actinides in a closed cycle. Furthermore, waste minimization requires recycling both Pu and the minor actinides in an integral homogeneous recycling of all actinides present in used fuel. There is also consensus in the project to minimize feedstock usage with a self-sustaining cycle, which only requires depleted or reprocessed U feed. This calls for a self-generating core with a breeding gain near zero. In order not to penalize the GFR long-term deployment, and based on considerations of both the anticipated available Pu stockpiles (mainly in water reactor irradiated fuels) and the period of time for GFR fleet development, it is recommended that the initial Pu inventory in the GFR core may not be much higher than 15 tonnes per GW(e).

(b) Non-proliferation goals and criteria

To avoid separated material in the fuel cycle, the programme considered minimizing the use of fertile blankets (none) and percent fissile (< 20%). The objective of high burnup together with actinides recycling results in spent fuel characteristics (isotopic composition) unattractive for handling. High burnups are the final objective (10-15 at% or more).

Minimization of fuel transport would help non-proliferation concerns and could be realizable, if very compact facilities can be designed, with on-site fuel treatment.

(c) Economic goals and criteria

High outlet temperature (850°C) for high thermal efficiency and hydrogen production, and direct cycle for compactness are reference objectives. Other options, provided the targeted efficiency is preserved and attractive system arrangement can be found, are not excluded (for example indirect cycle with a reduced He outlet temperature on the primary side and super-critical CO_2 as working fluid on the secondary side). Unit power will be considered in the range from 300 MW(e) (modularity) up to larger 1500 MW(e) size (economy of scale). Generation IV objectives for construction time and costs are considered.

(d) Safety goals and criteria

The design goal of no off-site radioactivity release requires the efficiency, simplicity, robustness, reliability, and economics of all systems and physical barriers. At core level, the use of refractory fuels with a very high capacity to confine fission products at high temperature (1600°C, or above) and robust structural materials is an objective.Finally, the specification range for the power density affects economics (minimization of fuel inventory, Am production, fuel cycle cost, compactness of the primary vessel), sustainability (in-core Pu inventory per GW(e)) and safety (in particular, decay heat removal in case of depressurization events). Economics and sustainability call for rather high values and safety for lower ones. The tentative range between 50 and 100 MW/m^3 seems to be a good compromise between HTR values of about 7 MW/m^3 and classical LMFBR values of more than 200 MW/m^3.With these specific design and safety criteria in mind and although the GFR System and Project Arrangements had not been signed, the GIF GFR international partners (France, Japan, US, UK, Switzerland and the European Union) started to work together on the Gas-Cooled Fast Reactor (GFR) design and safety, using existing cooperation frameworks. As mentioned previously on the road to the preliminary viability assessment, the SRP organizes the design work in an initial two year period of exploratory studies followed by two additional years for pre-conceptual design studies on a limited number of GFR options. As there were a number of options to be evaluated during the exploratory phase, the GFR GIF international partners agreed to share between them the work on several combinations of options and to cooperate together at the end of the exploratory phase on a first down selection of options [7]. These seven combinations of options were defined as follows:

(1) 600 MW(th) case: high volumetric power, challenging dispersed fuel (high ratio fuel/matrix) and high temperature direct cycle;
(2) 600 MW(th) step to case 1: high volumetric power, challenging dispersed fuel (high ratio fuel/matrix), He at lower temperature as primary coolant and SC CO_2 as secondary coolant;
(3) 2 400 MW(th) cercer case: high volumetric power, more accessible dispersed fuel (50/50) and high temperature direct cycle;
(4) 2 400 MW(th) pin case: high volumetric power, SiC cladded fuel and high temperature direct cycle;
(5) 2 400 MW(th), or more, particle fuel case: moderate volumetric power, particle fuel and high temperature direct cycle;
(6) 2 400 MW(th), or more, pin case: moderate volumetric power, SiC cladded oxide fuel and high temperature direct cycle;
(7) Generic 2 400 MW(th) indirect cycle (He, S-CO_2).

With the exception of option 6, all the other options utilize high density fuel with either carbide or nitride as the actinide compound.The US work focused on option 4 which is therefore the focus of the US summary given in this section. However, even though the consensus has settled on helium as this international collaboration's choice for the primary coolant, there has also been separate work on Supercritical Carbon Dioxide (S-CO_2) GFR primary cooled systems; the work has been performed primarily in the United States of America and Japan.

5.1.4. Indirect cycle 2400 MW(th) GFR design (France)

5.1.4.1. System definition

A "reference" design (fuel, core, primary system, safety systems, energy conversion, plant layout, etc) was decided early in the project (2005, end of exploratory studies) with the objectives to pre-design the various components and to perform a safety analysis of the GFR concept as a whole. The data and results presented hereafter are part of the GEN-IV report: "GFR preliminary viability report".

5.1.4.1.1. Fuel and core design

An innovative refractory fuel element is shown in Fig. 5.1 and consists of:

- The fissile compound is UPuC (high thermal conductivity, high density);
- The clad is made with a SiC-SiC composite ceramic completed with an inner metallic liner (leaktighness of the "first barrier").

Innovative to many aspects, the fuel element is a key issue in the GFR feasibility. It is supported by a significant R&D effort. The core design is shown in Fig. 5.2.

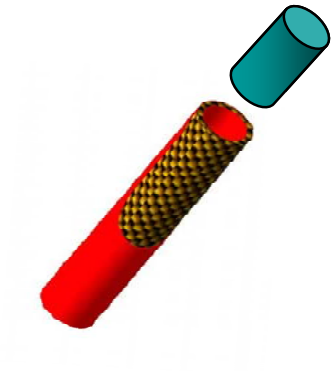

FIG. 5.1. GFR pin-type fuel element.

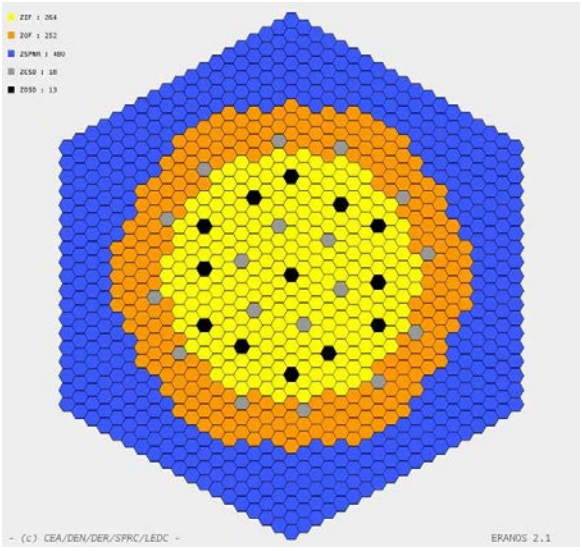

FIG. 5.2. GFR core design.

The core design targets a high enough core power density (minimization of the Pu inventory), plutonium and minor actinides recycling capabilities [8]:

- 2 400 MW(th), 100 MW/m^3 (trade-off neutronics performance vs safety issue);
- T°inlet/outlet RPV: 400/850°C (trade-off energy conversion η vs materials and safety issues);

– pressurized coolant: 7 MPa ; primary designed with limited ΔP to ease the gas circulation: $\Delta P_{core} \leq 0.15$ MPa; core designed with favourable reactivity effects.

5.1.4.1.2. Plant design

The primary circuit is illustrated in Fig. 5.3.

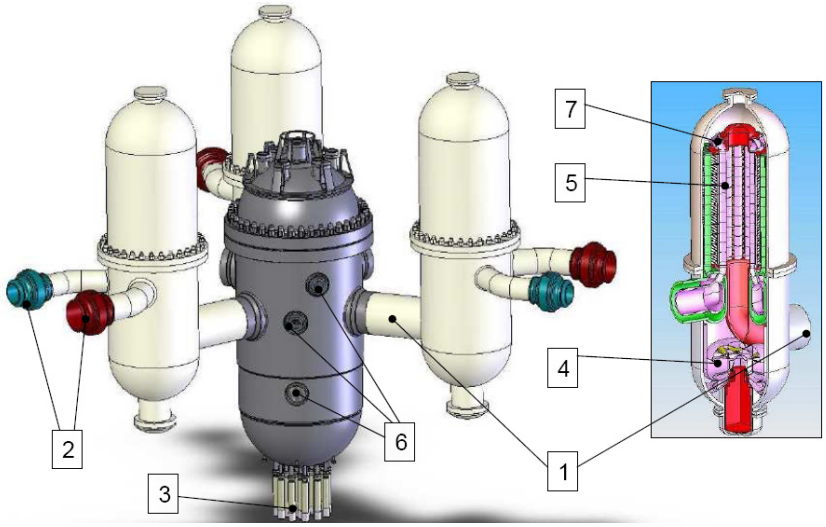

1 – primary cross-duct; 2 – secondary pipes with isolating valves; 3 – control rod drive mechanisms;
4 – primary blower and associated motor; 5 – compact heat exchanger modules;
6 – pipe connections for DHR systems; 7 – primary isolation valve

FIG. 5.3. GFR reactor pressure vessel and IHX vessels.

Concerning the energy conversion, the reference option is the indirect combined cycle, with He-N_2 mixture for intermediate gas cycle. Electrical energy is generated partly by the secondary circuit gas turbines (auxiliary alternators: 3×130 MW(e)), and partly by steam turbine (main alternator: 1×730 MW(e)) mounted in the tertiary circuit. The cycle efficiency is close to those of the direct cycle (45%), with lower inlet core temperature (400°C, no extensive thermal shielding required).

5.1.4.1.3 DHR means

The Decay Heat Removal (DHR) safety function is based on the control of both gas circulation and gas inventory [9]:

– The primary circuit, the core in particular, is designed to ease the gas circulation and enhance the natural convection capabilities ;
– The core cooling is ensured either using the normal loops or dedicated DHR loops;
– a close containment concept – functionally, a gas-tight envelope enclosing the primary circuit – is considered in order to limit the loss of pressure in case of depressurization (a “backup” pressure results from the equilibrium between the close containment and primary volumes) ;
– One of the dedicated DHR loop is design to cope with the failure of the close containment.

The primary circuit and close containment are depicted in Fig. 5.4.

FIG. 5.4. Views of the primary circuit integrated in the close containment.

The strategy to actuate the various systems is the following (risk minimization, PSA analysis):

- For the most frequent situation (i.e. integrity of the primary circuit) and Anticipated Transient Without Scram (ATWS), the use of normal loops (main blowers operated with pony motors supplied by diesel), using for the heat sink either the steam generator (with by-pass of the turbine) or dedicated air coolers (back-up system, operated in case of loss of the electrical grid);
- For other situations, the use of dedicated DHR systems designed to face up to the nominal primary pressure as well as to the large range of possible backup pressure after depressurization (Fig. 5.5). This system is composed of (design at end 2008):

  (i) Reactor High Pressure (RHP) cooling system: 3×100% with blowers as normal systems (0.4-7 MPa) and 2×100% with natural convection as backup systym;
  (ii) Reactor Low Pressure (RLP) cooling system: 1×100% with blower designed for very low pressure (0.4-0.2 MPa).

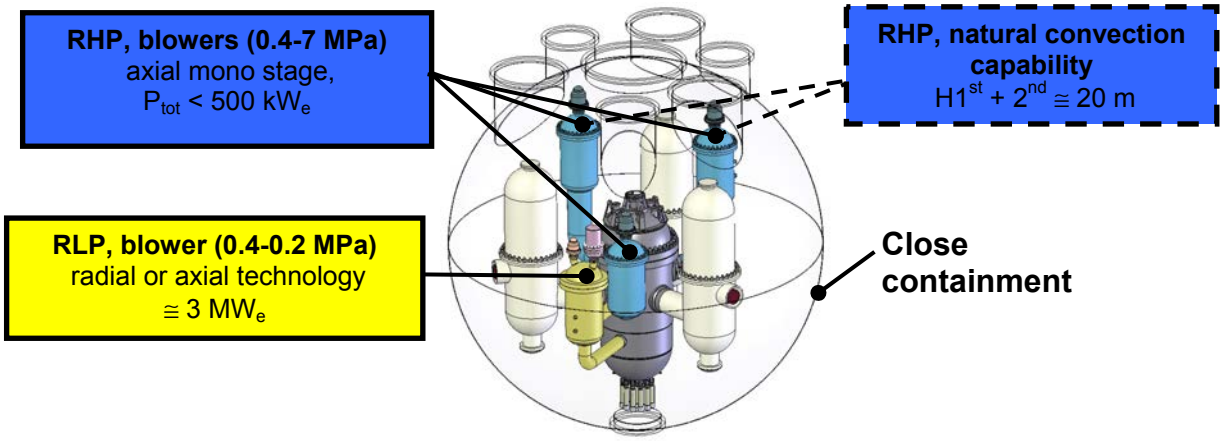

FIG. 5.5. View of primary system, dedicated DHR loops inside the close containment.

5.1.4.2. Current status of R&D (safety aspects)

5.1.4.2.1. Safety approach

Beyond a fundamental set of safety objectives defined by the IAEA, as a fourth generation reactor, the GFR must include specific qualitative objectives aimed to increase public confidence. Among others, the need of minimal emergency protection action of the population around the site is one of these objectives. The governing principle of the safety approach is grounded on the defence in depth principle (DiD), the existence of physical barriers, the safety functions aimed at protecting these barriers and the ALARA principle regarding the radiation protection of the facility's staff. The physical barriers enabling the fission products to be confined are, successively, the metallic liner of the fuel assembly, the primary circuit boundary and finally the containment.

The adequacy of the provisions retained in the design can be judged using a variety of deterministic and probabilistic methods. In general terms, the plant is deterministically designed against the identified list of the operating conditions using well-established design criteria to ensure suitable safety margins (Fig. 5.6).

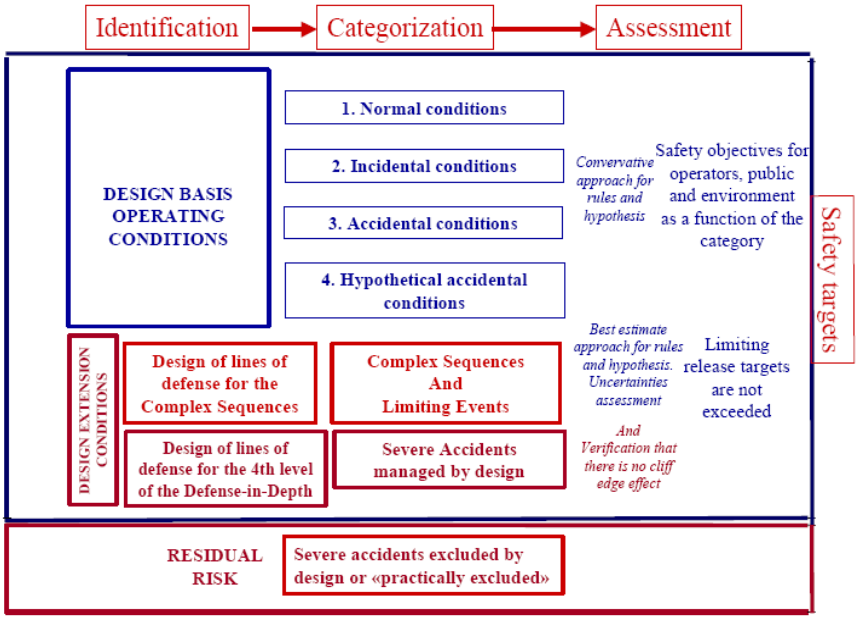

FIG. 5.6. Sketch of the methodology for the safety analysis.

A probabilistic assessment is also currently performed to verify that there are no vulnerable areas in the design with the potential for high-risk sequences. In this way, probabilistic safety assessment can identify any requirement for additional design features for preventing or mitigating accidents.

5.1.4.2.2. Study of the Reference

The preliminary acceptance criteria retained for the assessment of the Design Basis Accidents (DBA) are:

- Category 3 situations :
  (i) Clad temperature < 1450°C;
  (ii) Upper plenum temperature < 1250°C;
- Category 4 situations, the more limiting criterion being considered among:
  (i) Fuel temperature < 2000°C;
  (ii) Clad temperature < 1600°C;
  (iii) Upper plenum temperature < 1250°C;
  (iv) No degradation of the fluid channel able to prevent the core cooling.
- Categories 3 and 4 : a controlled state must be reached at the end of the sequence.

The reference situations analyzed result from the combination of the initial state of the reactor (full power), of an initiating event (IE) and of the single aggravating failure inducing the most adverse effect on the consequence of the transient. The single aggravating failures considered were:

- Failure of a Diesel train (when relevant considering the IE);
- Failure of a blower when actuated;
- Failure of the opening of a DHR loop;
- Failure of the closing of a main loop (required to operate normally the DHR loops).

The following Category 3 reference situations have been studied:

- Loss Of Off-site Power (LOOP) longer than 2 hours;
- Small break in the primary circuit;
- Small break in the IHX;
- Small break in the secondary circuit.

The following Category 4 reference situations have been studied:

- Large break in the IHX;
- Large break in the primary circuit (Fig. 5.7).

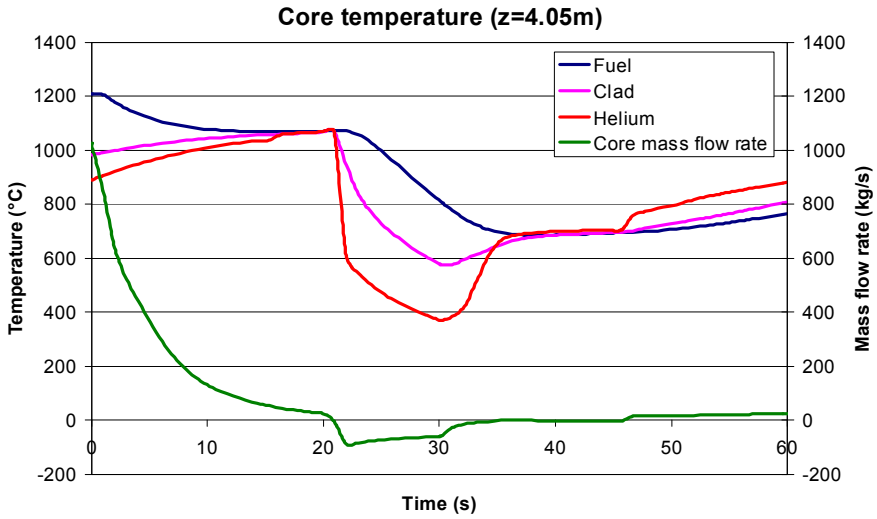

FIG. 5.7. LB-LOCA, calculated core mass flow rate and temperatures.

All the plant transients (about 30 cases) have been simulated using the CATHARE 2 computer code.

Additional Design Basis Situations:

- LOOP combined with multiple failures;
- Small primary break combined with multiple failures;
- Control of the small primary breaks IEs with the DHR system operating with a natural convection flow.

Finally, for most likely events, significant margin is available between the overheating calculated in the transient and the acceptance criteria. Moreover, the dimensioning, the redundancy and the diversification of the DHR system enable a postulated partial core bypass due to an erroneous configuration of coolant pathway to be faced, with a large temperature margin up to the criteria for most situations. In the case of a very fast depressurization the criteria are also met, but with a more limited margin [10].

5.1.4.2.3. Study of the DEC situations

As in the previous analysis, the pressurized situations can be distinguished from the depressurization situations (blackout versus primary breaks). The category 4 acceptance criteria should be fulfilled for the Design Extension Conditions (DEC) except for the possible severe accidents situations. The exhaustiveness within the DEC is not aimed since most of the transients presented here have been retained to assess the robustness of the DHR system design.

Consideration of the design extension situations was undertaken taking into account multiple failures of redundant facilities in the DHR systems, together with cross failures of independent components. As a first approach, only the safety systems were considered (shutdown plus DHR systems). Despite this very conservative approach (all systems except those affected by the accidents should be considered in DEC, including the main primary loops), the transient analysis showed, in pressurized and intermediate pressure (IHX rupture) situations, that the DHR system is able to control complex sequences resulting from multiple failures combined with an erroneous primary flow path configuration, including in natural circulation operation [11].

The lessons learnt from the study of very unlikely situations resulting from a fast depressurization combined with an erroneous primary flow path configuration and with multiple failures, will lead to the design of support systems enabling the valves to be operated adequately for a correct flow path configuration in the DHR system. Moreover, considering the limited thermal inertia of the GFR core and of its coolant on the one hand, and the specific power of the core and the absence of high negative feed-back reactivity, on the other, the prevention of severe accidents relies mainly on the refractory properties of the core materials and on the reliability of the shutdown system.

5.1.4.2.4. PSA supporting the GFR design

PSA enables weak points in the design of the reactor to be identified, due to its broad framework and its exhaustive purpose. As a result, a homogenous safety design should result from a valuable use of PSA results avoiding a family of sequences contributing too greatly to the overall risk number. Since this kind of study is performed using an iterative process with the design, it has been called a Probabilistic Engineering Assessment (PEA). Finally, the PEA

could help to locate the IEs and the resulting sequences in the risk domain for IEs which are questionable and/or difficult to categorize. Moreover, regarding severe accidents, it provides a preliminary assessment of the safety improvement resulting from the planned mitigation measures as well to prioritize the R&D efforts.

The IEs and their occurrence frequencies, considered in this fist version of the PEA are consistent with those investigated in the deterministic approach presented before. The failure of the various systems have been modelled with fault trees connected to event trees modelling the accidental sequences, thus permitting the whole quantification of the Core Damage Frequency (CDF) as usual in a level 1 PSA. When support calculations of the sequences were not performed, the final state leading to core damage was considered to be the loss of a main safety function.

The various sources of uncertainties were taken into account as follows:

- The reliability of natural convection thanks to a specific methodology based on uncertainties propagation in thermal-hydraulic calculations;
- The technological uncertainties on very innovative components thanks to a risk factor taking into the possible inability to design or to manufacture the component;
- The physical uncertainties due to the risk for a component to not fulfil its mission.

Starting from an initial configuration or architecture of support systems, successive modifications were performed in the probabilistic model (Fig. 5.8) according to the preponderant minimal cut-sets (MCs) screening (i.e. “vertical” screening of results).

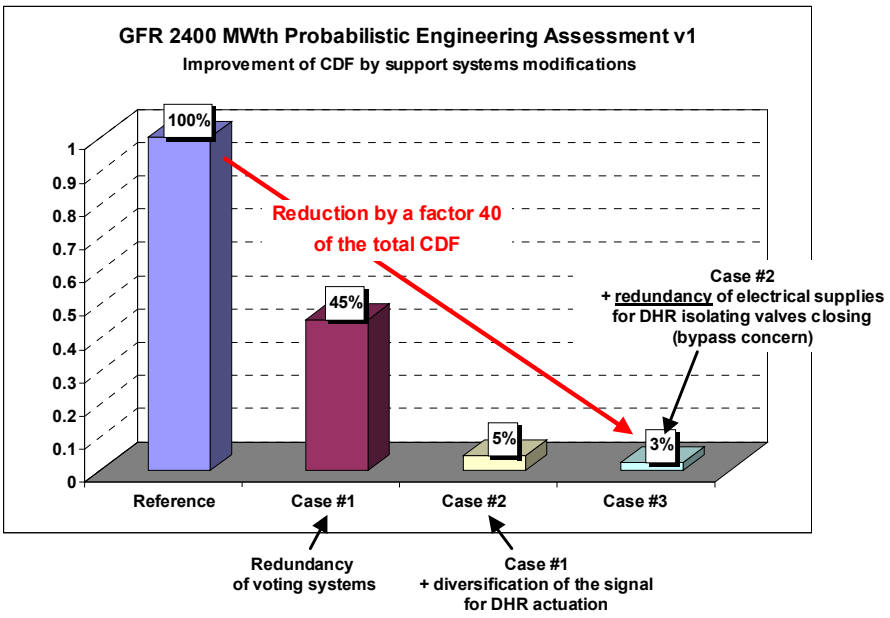

FIG. 5.8. Risk reduction process implemented thanks to PEA.

The DHR system presented earlier already takes into account the outputs of the PSA analysis.

5.1.4.2.5. Consideration of severe accidents

An R&D programme is being devised in order to adequately identify the severe plant situations that will be managed by design from that to practically eliminate. Several families of severe accident scenarios leading to severe plant conditions have been preliminarily identified. An approach was proposed to distinguish those families depending on the integrity of the safety barriers, the magnitude and the dynamics of the phenomena induced by the accidents and the possible associated threshold effects. A preliminary set of situations was identified by means of this approach; they are featured depending on:

- The dynamics, the linearity and the scale of the phenomena;
- The tightness of the barriers, the state of the close containment and of the systems available;
- The core geometry and its coolability;
- The reactivity control (neutronic and chemical), the criticality control and the related power extraction capability;
- The factors governing the course of the accident and the possibility of controlling them in order to control the accident;
- The knowledge of the phenomena coming into play during the accident;
- The overall ability to control the accident or the possibility of demonstrating its practical elimination.

Moreover, the ability of the GFR to withstand severe plant conditions relies mainly on the behaviour of the core materials at a high temperature, including a chemically aggressive atmosphere due to nitrogen ingress, possible water ingress and more improbably due to air ingress. As a result, experimental tests are under way in order to assess the capability of the highly refractory GFR core materials to sustain the accidents associated with severe plant conditions. For this objective, one checks by experimental tests the behaviour of UPuC and SiC-SiCf at 2000°C under several atmospheres. Oxidation is expected on composites since dissociation may occur for mixed carbide. As far as the air ingress situation is concerned, experimental studies, carried out between 1000°C and 1700°C, showed two oxidation features: a passive oxidation with the formation of a protective SiO_2 layer at low temperature and high oxygen partial pressure, and an active oxidation with the formation of an unstable SiO layer at high temperature and low oxygen partial pressure.

The passive oxidation regime would not lead to a loss of clad mechanical properties. On the contrary, the active regime must be demonstrated to be reached only for a limited duration and a limited core region. Thermal-hydraulic calculations are foreseen in order to assess the flow rate and the oxygen partial pressure crossing the core in a plausible air ingress accident.

The next step of this study will be to assess the heat and the kinetics of the oxidation reactions with air and with steam, and to assess the nitriting consequences. If there is a risk of obtaining a flammable atmosphere in the containment due to the oxidation products (CO in case of air oxidation and H_2 in case of steam oxidation), the concentration of the flammable mixture will be kept under the limit enabling a dangerous loading of the containment (for example with nitrogen dilution, recombiners or igniters) to be prevented.

5.1.4.2.6. Final remarks

Research studies conducted on the GFR led to a first consistent design of the reactor and its fuel. The design basis of the GFR is still evolving; however, major design directions have

been decided. The foregoing discussion described the preliminary safety analysis. The architecture that is used correctly covers the potential defects fitted to this system, thanks to the following elements:

- A fuel element that uses refractory materials and withstands high temperatures;
- A gas voiding reactivity effect in the core naturally not significant;
- robustness and progressiveness in the DHR means.

In particular, the preliminary safety analysis, as deep as it has been carried out up to now, pointed out that the current design allows the decay heat to be removed in any accidental situations (pressurized or not, even in case of large leak, including an additional single failure or multiple failures), thanks to different systems of moderate power supply and to a close containment. In addition, the natural convection capabilities could be retained in most of the situations, including small break LOCAs, leading to a real advantage in terms of DHR strategy robustness and progressiveness. All pressurized accidental situations can be managed in a passive way, including the situation of the total loss of electrical powers.

The prior objective targeted for 2012 is the demonstration of viability for the fuel, and, more broadly, for the reactor, for this type of technology.

5.1.5. Direct cycle 2400 MW(th) pin core design (United States of America)

Figure 5.9 shows the GEN-IV concept for the direct cycle GFR.

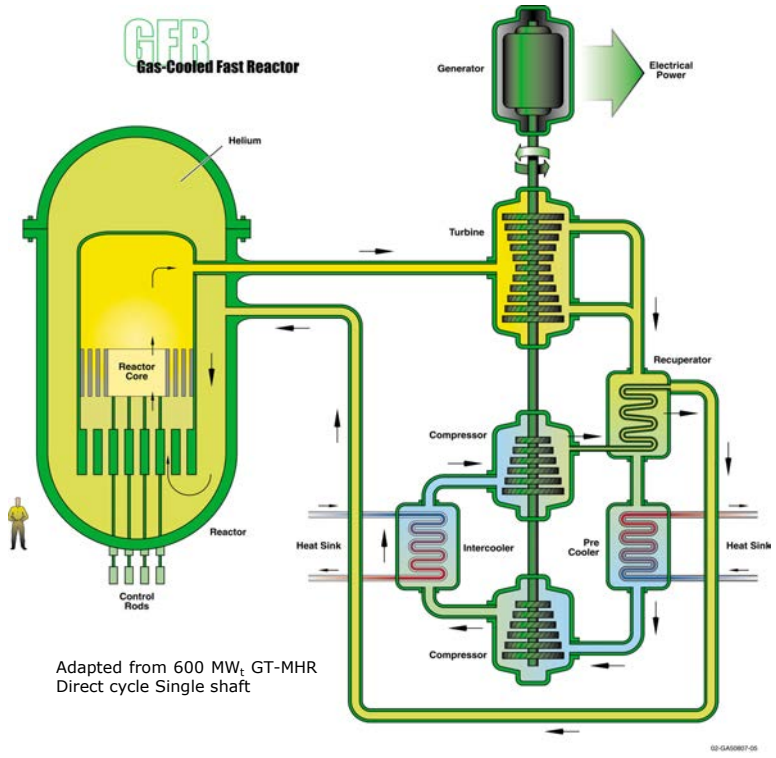

FIG. 5.9. Conceptual GFR system.

As a direct adaptation from the US GEN-IV VHTR/NGNP Program, the 600 MW_t Power Conversion Unit (PCU) is utilized in this US GFR. It was planned to rely on the R&D work of the VHTR/NGNP to develop the PCU. Four 600 MW_t modules of this PCU would be utilized in the US direct cycle GFR. The full power operating conditions are shown in Table 5.1.

TABLE 5.1. FULL POWER OPERATING CONDITIONS

Item	Value
Reactor	
Core power, MW_t	2400
Core inlet/outlet temperatures, °C	490/850
Core upper plenum inlet pressures, MPa	7.07
Helium mass flow rate, kg/s	1280
Turbomachinery	
Turbine mass flow rate, kg/s	320
Turbine inlet/outlet temperatures, °C	850/510
Turbine inlet/outlet pressures, MPa	7.02/2.65
Compressor inlet/outlet temperatures, °C	33/112
Compressor inlet/outlet pressures, MPa	2.60/7.24
Compressor overall pressure ratio	2.82
Recuperator	
Mass flow rate, kg/s	322
Hot side inlet/outlet temperatures, °C	510/131
Cold side inlet/outlet temperatures, °C	112/490
Precooler	
Mass flow rate, kg/s	322
Inlet/outlet temperatures, °C	131/33
Intercooler	
Mass flow rate, kg/s	322
Inlet/outlet temperatures, °C	112/33

As discussed later, some adjustments will have to be made in the core inlet and outlet pressures to account for the differences in the core design pressure drop between the GFR concept and the VHTR. This is due to the difference in the approach to passive decay heat removal. The 850°C core outlet temperature should lead to plant conversion efficiencies >45% and allow the thermo-chemical production of hydrogen.

5.1.5.1. Primary and safety system

In agreement with the GIF partners the effort was focused on metal for the primary system vessel. Since the work of thirty years ago focused on the PCRV, it was decided to make an assessment of the use of a metal primary vessel similar to the current approach for the VHTR. The results would then be compared with those for the PCRV and a selection made after the pre-conceptual design phase in accordance with the SRP. The current US design was therefore based on the primary system of the Peach Bottom HTGR built by General Atomics in the late 1960s in the USA Peach Bottom I was a high temperature gas cooled thermal reactor which has all the features that are being incorporated into the high temperature GFR. This includes the bottom entry control rods, hot plenum shroud, top refuelling, metal vessel, and concentric piping. The design was successfully built and operated and many of the GFR designs presented in the status report by the various national groups look very similar to the Peach Bottom design. Continuation of the US design effort on the primary system would be focused on the Peach Bottom design as the starting point. The overall plant dimensions are

driven by the reactor vessel (RV) and PCU requirements. In turn, the RV radial dimensions are based upon the core diameter and the reflector and shielding thicknesses needed. The RV height is based on the Shutdown Cooling System (SCS) height and ducting, the core height, the PCU cross vessel location and refuelling reach concerns. The dedicated DHR heat exchangers and electric blowers are incorporated into the four SCS pods which are connected to the vessel through the concentric duct arms shown in Fig. 5.2. The electric motors are top mounted external to the pod. Based on the results from the R&D studies on decay heat removal (DHR) under both depressurized and pressurized conditions, it was decided to enclose the primary system together with the balance-of-plant in a guard containment capable of maintaining back pressures in the 7-8 bar range. These guard containment design pressures are attainable with current LWR technology. This residual back pressure then allows the capability of natural convection in the primary systems to remove core decay heat completely passively within about twenty four hours of the occurrence of a depressurization accident initiator without the need for electric power. However for the first twenty four hours, low power DHR circulators would be needed in this hybrid active-passive safety scheme. The low power requirements for this situation can be easily met by the use of station batteries with a volume of a few cubic meters. Compressed gas could also be an alternative. Future R&D would also examine the possibility of utilizing the residual decay heat to drive turbo-compressor sets to maintain the low level of core flow required to maintain the temperature limit.

5.1.5.2. Plant configuration

The Guard Containment (GC) design studies for the US 2400 MW_t GFR focused on the layout for the concrete option [12] which is shown in Fig. 10. For the concrete in the GC to retain its strength, the normal operating temperature must be held below 93°C, and no hotspot can exceed 315°C. To avoid this problem during LOCA conditions, the GC inner cavity design was revised and enlarged to include not only the RV but the PCU vessels and the SCS units as well. An open internal containment option was designed using metallic support structures for the reactor vessel, the PCU vessels and the SCS units. The PCU vessels have the same overall dimensions as that designed for the 600 MW_t GT-MHR, and they are supported at cross vessel elevations in five places with four snubbers for lateral seismic restraint at the bottom. The vertical supports at the cross vessel elevation allow for axial movement due to thermal expansion along the cross vessel axis and also permit y-axis movement due to differential thermal expansion effects. The RV is supported in a framing structure of tube steel columns and horizontal beams to allow for cross vessel and piping penetrations while restraining horizontal movement. Snubbers are used for lateral seismic restraint. The SCS units are supported on steel braced framing, and the SCS duct from the RV takes the additional moment due to any growth of RV in the downward direction. An elevation view of this layout is shown in Fig. 5.10.

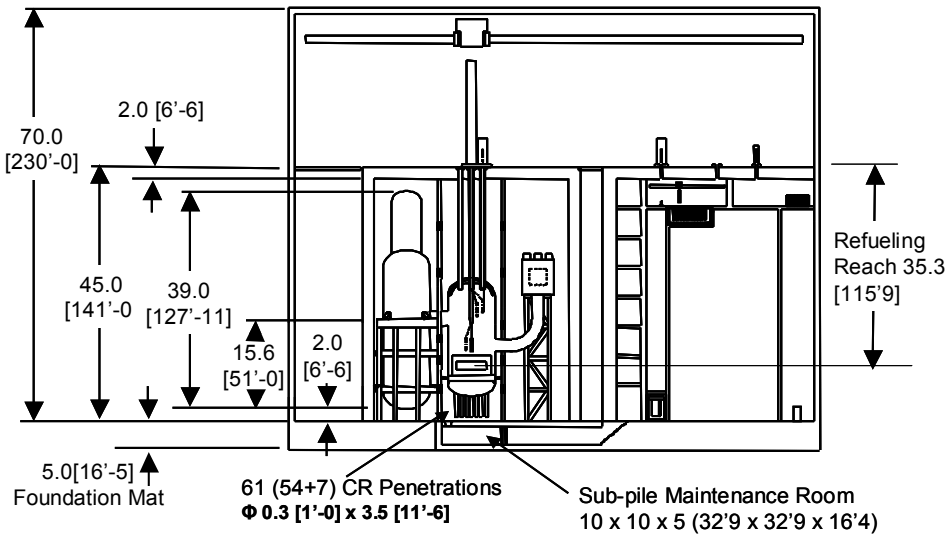

FIG. 5.10. 2400 MW_t GFR reactor building elevation view.

As shown in Fig. 5.10, a flat roof structure was adopted for the enlarged GC rather than a dome-like structure. This provides a lay down area for equipment if needed during core refueling, and it simplifies fuel cask transfer to the storage area. The RV support framing provides internal support to the long span flat roof top slab thus reducing the thickness to about 2 m. On the bottom, the GC is attached to a foundation mat, 5 m thick, as indicated in the figure. The GFR design is similar to the Peach Bottom I design in that it has an up-flow core to aid in cooling under loss of pressure or forced flow conditions. As in the Peach Bottom reactor, the control rods are inserted from the bottom and withdrawn below the lower head to minimize their operating temperatures. Access to the control rods for maintenance and repair is through a "sub-pile Maintenance Room" as shown in Fig. 5.10. The height of the GC is dictated by the dimensions of the PCU vessels, and this height in turn sets the reach required of the refueling system, which is 35.3 m as indicated in the figure. Since the refueling arm and the fuel elements have to be withdrawn into a transfer cask and refueling machine, this in turn sets the height requirement for the reactor building (70.0 m). The reach of 35.3 m for refueling is feasible and the penetrations in the top head will be designed with adequate stiffness to allow for smooth refueling without any significant alignment problems for the given reach. A plan view of the GC layout including the plant building and refueling areas is shown in Fig. 5.11.

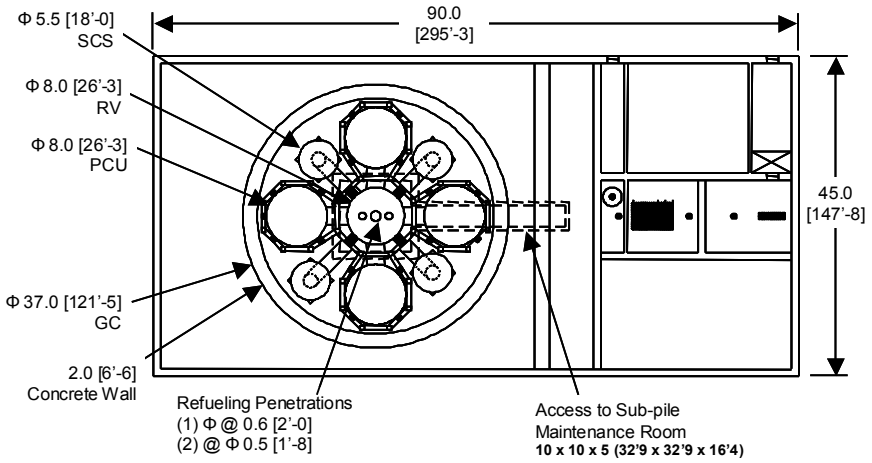

FIG. 5.11. 2400 MW_t GFR guard containment layout – plan view.

This view shows the overall reactor building width and length (45 m by 90 m), and the diameters of the GC, the 4 PCU vessels, the RV, and the 4 SCS units. The GC has an outside diameter of 37 m, and a wall thickness of 2 m. The containment structures for the various units inside the GC are also shown along with the access to the Sub-pile Maintenance Room. Three refueling penetrations are shown on the RV in the layout. The central one is for the refueling arm itself, and the other two are for removal of the individual fuel elements into the fuel transfer cask located on the roof of the GC. The steel support framing structures are sized to support a combination of the dead, live, and seismic loads imposed by the PCU and RV vessels and the SCS units.

5.1.5.3. Core design

The pin core alternative serves as a backup to the CEA plate core design presented in [6, 13, 14] s such, it has the classical subassembly configuration of the past GCFR designs which is in turn based on the LMR assembly designs. A pin bundle composed of a number of axially oriented pins, tied together at the top and bottom of the pin by fuel support grids, is located within a hexagonal can with walls. The bundle has in addition spacer plates located at regular intervals to maintain rigidity of the pin bundle. This is to mitigate thermal bowing and flow-induced vibration effects. Each pin is composed of a tube of cladding material within which are positioned a column of separate fuel pellets in a stack. End caps are used to seal the tube. The GCFR pellets were dished and had a central internal hole to minimize the effects of swelling and pellet clad interaction. This will be the starting point for the current GFR pin design. The fission gas released from the fuel pellet during the irradiation history is collected in designated regions of the pin which serve as either top or bottom fission gas plenums. This feature will be retained in the GFR design, at least initially. The main difference between the current GFR pin and the past GCFR pin is in the selection of the high temperature cladding material. Currently it is expected that the smooth cladding tube will be fabricated of SiCf/SiC composite material. SiC composite tubing fabrication experiments at Kyoto University [16] showed trends for thicker tubing and shorter fabrication lengths. The judgment to date has been that monolithic SiC tubes (α or β phase) would not have the required strength both for fission gas retention or fuel handling needs. The conclusion being that higher strength SiC/SiC composites should be the pathway forward. Factoring in the results from Kyoto University it was decided to increase the pin design cladding thickness by a factor of 2 and to decrease the tubing length by a 1/2. This led to a split segment pin (two segments) with thick clad. The concept has a 0.5 m upper axial reflector length but the fission gas plenum has been split in two. There is a top 0.5 m upper axial plenum length, and a bottom 0.5 m lower axial plenum length. The 1.34 m active core length remains the same but is symmetrically split between the two segments. The 0.5 m lower axial reflector length in the bottom segment is a duplicate of the top segment geometry. An increase to 1 mm fuel clad thickness leads to a 9.57 mm fuel pin outside diameter. There are no axial blankets and there is out-off-pin above and below core shielding similar to EBR-II.

In addition to thermal margin design calculations, evaluations were also made of thermal bowing and axial flow-induced vibration. This was factored into the subassembly design. Figure 5.12 shows the fuel subassembly plane view for both the fuel (only) subassembly and the fuel with control rod subassembly. The 2 400 MW_t core layout which will utilize this bundle pin concept is presented in Fig. 5.13.

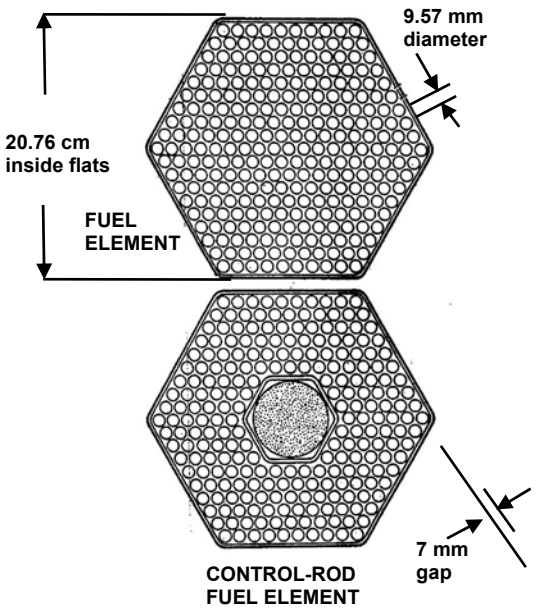

FIG. 5.12. Subassembly design.

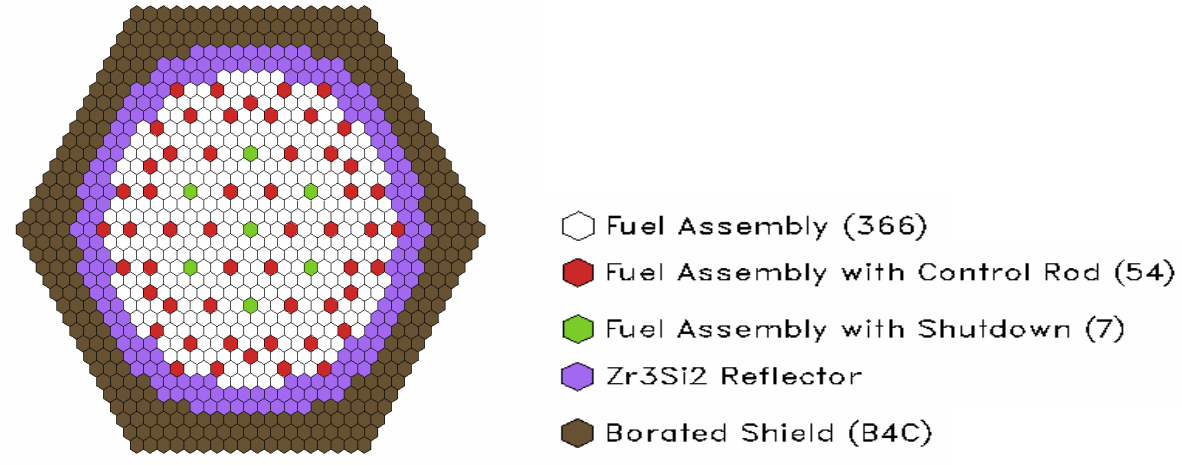

FIG. 5.13. 2400 MW_t Backup pin core reference layout.

This was the pin core option back-up to the 2 400 MW_t CEA plate core design. There are no external blankets, either internal or radial. Details regarding this core layout are available in [14] where the core design work was performed and documented. It is a 2 400 MW_t core with equilibrium TRU recycle and a conversion ration of ~ 1.0. It has a 3 cycle residence time and 10% average discharge burnup with 786 EFPD cycle length. The H/D ratio is 0.28 and the active core diameter (equivalent) is 4.77 m. This translates to a hex-to-hex active core diameter of 5.1 m.

Table 5.2 shows core design parameters. Note that the core power density has been de-rated from the GCFR of thirty years ago. This is in accordance with the decay heat removal strategy for accident situations.

TABLE 5.2. 2400 MW_T CORE DESIGN SUMMARY

	BOEC	EOEC
Item	Value	
Delayed neutron fraction $\times 10^3$	3.46	3.40
Prompt neutron lifetime, μs	2.67	2.15
Doppler temperature coefficient, ¢/K	-0.30	-0.28
Radial expansion coefficient, $/cm	-0.42	-0.41
Axial expansion coefficient, $/cm	-0.15	-0.13
Depressurization reactivity, $	1.09	1.15
Power, MW_t	2400	
Power density, W/cm^3	100.0	
Height / diameter ratio	0.282	
Cycle length, EFPD	786	
Cycles in core	3	
Charge enrichment (TRU/HM), %	15-20	
Enrichment zones	5	
BOEC heavy metal loading, t	56.6	
EOEC heavy metal loading, t	54.6	
BOEC TRU loading, t	10.3	
EOEC TRU loading, t	10.4	
Average discharge burnup, %	9.9	

5.1.5.4. Current status of related R&D

5.1.5.4.1. Depressurized decay heat removal accidents [17]

With the advent of the GEN-IV initiative to develop an entirely new generation of nuclear reactor plants, there is now the opportunity to revisit the design of the gas-cooled fast reactor (GFR) and enhance the safety case. The GFR safety approach for the passive removal of decay heat in a protected depressurization accident with total loss of electric power needs to be different from that taken for the HTRs [18]. The HTR conduction cool-down mode [19, 20] to the vessel wall boundary for economically attractive cores is not feasible in the case of the GFR because the high power densities require decay heat fluxes well beyond those achievable by heat conduction and radiation heat transfer modes. A set of alternative novel design options has been evaluated for potential passive safety mechanisms unique to the GFR. Focusing on the core design, in particular fuel forms, and the implications of alternatives for the passive removal of decay heat it is evident that the pebble fuel has a unique possibility which the other major fuel forms, pin and block/plate would have difficulty to emulate. In addition to heat transfer, there is the possibility of mass transfer. Table 5.3 summarizes the potential passive decay heat removal mechanisms [23-26].

TABLE 5.3. PASSIVE DECAY HEAT REMOVAL SYSTEMS

Mass transfer
— Fuel dump system
Heat transfer
— Radiation/Conduction cool-down to
- Vessel boundary
- Core internal heat sinks (cooled or un-cooled)
- Primary system heat sinks (cooled or un-cooled)
— Natural convection heat transport to
- Vessel boundary
- Core internal heat sinks (cooled or un-cooled)
- Primary system heat sinks (cooled or un-cooled)
— Special devices
- Heat pipe
- Cold finger
Inertia
— Increasing fuel form thermal inertia
— Increasing flow coast-down times

The NERI and I-NERI GFR projects supported by DOE have explored the possibility of achieving an enhanced safety case for the GFR by utilizing these mechanisms. The main focus of those efforts, have been on the effect of core fuel form configuration on the feasibility of these passive decay heat removal mechanism for the GFR. The major alternatives for fuel forms are:

— Clad pins with fuel pellets;
— Block or plates with dispersion or coated particle fuel kernels;
— Pebbles with coated particle fuel kernels.

The DOE supported I-NERI project [21] and NERI project [22] have produced results for a small modular pebble bed GFR (300 MW_t), and a larger modular reactor (600 MW_t) with either a pin-type or block-type GFR core design. Based on the sum total of these lessons learned, a number of conclusions can be drawn for each of the potential mechanisms identified in Table 5.3.

What has been selected for further development is the natural convection option with a plate/pin type de-rated core and a hybrid passive/active approach. The guard containment will still be utilized but it will be sized for an LWR containment range backup pressure with an initial pressure of 1 bar. The assessment has shown that a significantly higher back pressure is required for total natural convection driven removal of significant decay heat levels at GFR target power densities.

The lower back-up pressure, plus whatever natural convection is available at this pressure, will be utilized to significantly reduce the blower power of the active DHR system sized to remove 2-3% decay power. The objective is to be able to have such low power requirements so that power supplies such as batteries without the need for startup, can be utilized. This lower back-up pressure should be sufficient to support natural convection removal of 0.5% decay heat which occurs at ~ 24 hours. So there should be no more need for active systems/power supply after the initial period of one day. Furthermore, since there will be a decay of the after-heat from 2-3% to 0.5% in this time period, credit should be taken in probability space for loss of active systems during the 24 hours. The safety approach will then

be a probabilistic one. Work was performed in the US-France I-NERI GFR project [27] to further evaluate this hybrid passive/active approach to heat removal for depressurized decay heat accidents.

5.1.5.4.2. Fuel development

GFR fuel is a high fissile density fuel and cannot contain graphite because it will cause excessive moderation and has poor mechanical properties under fast irradiation. Therefore there is no large thermal mass as in thermal reactors. This translates to temperatures possibly reaching as high as 1600°C quickly and maintaining this temperature for several hours. A novel fuel must be developed that will withstand high temperatures but not compromise neutronic performance. Most materials are eliminated based on melting temperature. Of the remaining materials, many have unfavorable neutron absorption cross sections, such as the refractory metals. This leaves only a handful of materials refractory carbides and nitrides. Refractory ceramics have been considered for the gas cooled fast reactor (GFR) because of their high temperature stability at approximately 1 000°C under normal operation and up to 1 600°C during a loss of coolant accident. Refractory ceramics of ZrC, ZrN, TiC, TiN and SiC are candidates for both structural and fuel matrix materials due to their neutronic performance, thermal properties, chemical behavior, crystal structure, and physical properties. The transition metal carbides and nitrides (ZrC, ZrN, TiC and TiN) have a NaCl type FCC structure. The 6H-SiC is a common form of SiC that has a hexagonal structure. Silicon carbide (SiC) has been chosen as the reference matrix materials for the fuel because it has shown favorable irradiation properties and has the largest property data base. The fuel concept is a SiC matrix uranium/plutonium carbide ((U,Pu)C) dispersion fuel. The US fuel R&D work focused on two different fuel configurations:

(1) 15 cm hexagonal blocks composed of stacked horizontal plates with coolant holes; and
(2) A refractory clad pin type fuel.

This summary discusses efforts to develop fabrication methods for the block/plate type fuel and a SiC clad pin type fuel and initial irradiation studies.

Block/plate type fuel fabrication development

It was initially proposed that the block type fuel be fabricated through a reaction forming process. In this type of reaction bonding the carbon source is not graphite or carbon powder but rather a carbonaceous pre-form made by pyrolyzing a polymeric precursor. A pore forming agent is added to the precursor solution creating the porous network. Porosity is formed by the polymerization occurring around the dispersed inert pore forming agent. After the polymer is formed it is pyrolyzed leaving only an amorphous carbon pre-form. This pre-form is then infiltrated with silicon forming a network of SiC with isolated grains of residual free silicon. This process is particularly attractive for its near net shape fabrication capabilities. After the pre-form is pyrolyzed it can easily be machined into complex shapes, which can then be infiltrated while maintaining good dimensional stability [28]. The main disadvantage for this process in regard to fuel fabrication is the large amount of shrinkage which occurs during pyrolyzation. In order to reduce the shrinkage filler material is added which then has an effect on the perform microstructure and the infiltration properties.

In summary the hybrid process of reaction bonding/forming being developed for block type fuel fabrication is a viable process as is shown by the dense samples of SiC obtained to date. However, there are a very large number of variables that must be optimized for the process to

consistently produce samples suitable for irradiation. These variables include filler power composition and size distribution, amount of pore former used in the polymer, pressing pressure used for pellet production, fuel particle loading among others. SiC fabrication processes share the common trait of being very sensitive to a number of variables, this process included. As more variables are optimized and held constant fuel loadings will be increased to the maximum amount, however, this maximum may also change for any given set of parameters. Also over coating the fuel particles will be examined as a solution to proper fuel packing in the samples.

Pin type fuel fabrication

Work on advanced gas cooled reactor fuel in the United Kingdom was conducted in the late 1960s. Uranium carbide (UC) was produced by mixing uranium oxide and carbon powders in the proper ratios with a small amount of binder. These powders were then agglomerated into spheres and reacted and sintered. Following sintering, the spheres were coated with pyrocarbon in a fluidized bed coater. These spheres were then incorporated into a graphite/α-SiC powder mix and pressed into a cylindrical pellet. A second annular pellet was also pressed without a fuel phase and the fuelled pellet inserted into the annulus. This assembly was then extruded to form rods. These rods were placed in contact with molten silicon. As the silicon infiltrated the porous rods β-SiC precipitated out on the α-SiC grains forming a dense reaction bonded SiC clad/SiC matrix dispersion fuel. This fuel was irradiated to 5% fissions per initial metal atom and showed good irradiation properties; both gaseous and metal fuel fission product retention was very good [29]. Although this fuel was destined for a thermal gas cooled reactor, the same process is a viable fabrication route for SiC clad GFR fuel.

As with the hybrid process described above, although optimization difficulties have been encountered by the work to-date this process should still be considered a viable fabrication route. Again, the largest hurdle to successful fuel fabrication is the number of variable that must be kept constant and optimized. This process can be done through a series of parametric comparisons and careful study of results.

Irradiation study of candidate ceramics [30]

The US program has investigated the micro-structural changes in GFR candidate ceramics due to proton irradiation and heavy ion irradiation. 6H-SiC was identified to be the best among 5 ceramics on microstructure stability under Kr ion irradiation at 800°C. The radiation induced increase in lattice spacing in TiC and TiN is approximately ~ 4 times smaller than in ZrC and ZrN. It appears that among the 5 ceramics, the one with lighter molecular weight performs better on the microstructure stability under heavy ion irradiation at 800°C. Si and Ti atoms are smaller and lighter than Zr atom, leading to a difference in the strength of the covalent bonds between SiC, TiC (or TiN) and ZrC (or ZrN) that may affect the recovery of radiation induced defects. The better micro-structural performance of TiC over ZrC under Kr ion irradiation is consistent with the work on neutron irradiated TiC and ZrC at a low temperature and dose. While 6H-SiC was identified as the best ceramics based on the micro-structural stability under Kr irradiation among the 5 ceramics in the previous work, the same conclusion can not be made in the proton irradiation study, possible due to the relatively low dose. In this work, ZrN shows less micro-structural change to proton irradiation as compared to ZrC and SiC. There are 5 ceramics (ZrC, ZrN, TiC, TiN and 6H-SiC) irradiated with 2.6 MeV protons at a temperature

of 800°C to a single dose for each ceramic in the range of 1.5 to 3.0 dpa depending on the material.

Post-irradiation examination reveals the micro-structural changes due to proton irradiation. The change of lattice constant evaluated using HOLZ patterns is not observed for the irradiated samples up to 1.5 dpa for 6H-SiC and up to 3.0 dpa for ZrC and ZrN. In contrast to Kr ion irradiation at 800°C to 10 dpa, the proton-irradiated ceramics at 3.0 dpa show less irradiation damage to the lattice structure evidenced by the visibility of the HOLZ line pattern and Kikuchi pattern. The proton irradiated ZrC exhibits faulted loops which are not observed in the Kr ion irradiated sample. The irradiated ZrN shows the least micro-structural change form proton irradiation. The microstructure of 6H-SiC irradiated to 3.0 dpa consists of black dot type of defects at high density.

A follow-on neutron irradiation at 800°C using the Advanced Test Reactor (ATR) at the Idaho National Laboratory have been carried out but at a much lower dose level (~ 1 dpa at 800°C). This is test GFR-F1. However, a high dose neutron irradiation at high temperature will be needed to verify the results from this screening work.

The FUTURIX-MI irradiation program between the CEA and the DOE, in which French and US candidate materials were irradiated in Phénix from 2007 to 2009, will provide this critical neutron irradiation data to the GFR materials program.

5.1.5.4.3. Structural material development [31]

Currently, insufficient physical property data exist to qualify candidate material for gas-cooled fast reactor (GFR) designs. The target for this US effort is to develop advanced tailored microstructures that will improve radiation resistance, creep resistance, and oxidation resistance, helping to establish metallic materials capable of supporting GFR designs.

The first goal is to improve high temperature creep strength and resistance to environmental attack by optimizing grain boundary structural orientations (a technique known as grain boundary engineering – GBE). Thermal mechanical treatment is performed on candidate metal alloys to maximize the fraction of low-energy grain boundaries. Following treatment, the changes to microstructure are characterized and response to mechanical loading, radiation, and environmental attack are examined. The focus is on Alloy 800H, an austenitic alloy designed for high temperature boiler components, alloy 617, a Ni-base alloy being considered for high-temperature reactor piping, and T-91, a low carbon (9Cr-MoVNb) ferritic-martensitic alloy designed for lower temperature boiler components and being considered for higher temperature pressure vessels.

The second goal is to characterize radiation resistance of candidate GFR metallic materials with focus on Alloy 800H. Candidate metallic materials for the GFR have not typically been used for high dose core components so an understanding of the radiation resistance is unknown. Therefore, radiation response of these alloys will be characterized by examining the changes in microstructure in samples irradiated with high-energy ions and when available, neutrons from a test reactor. Several important results have been achieved, specifically:

- Grain boundary distributions have been altered to increase the fraction of low-energy boundaries in a ferritic-martensitic steel, T91, in an Fe-base austenitic alloy, 800H, and in a Ni-base alloy, 617;
- The grain boundary optimization in T91 has been shown to improve the creep resistance;

- The grain boundary optimization in 800H has been shown to reduce unwanted oxide spallation in alloy 800H;
- The optimized grain boundary distributions have proven to be stable in all three alloys to certain limiting temperatures. The 617 stability studies indicate the stability is very dependent on the grain boundary character distributions, pointing to the possibility that the improved grain boundary distributions may be stable to higher temperatures than currently achievable.

To a limited extent, the radiation stability of alloy 800H has been examined using heavy ion irradiation. The studies show typical radiation hardening. These studies were to be complemented by future data from samples irradiated in ATR, HFIR, and Phénix. The HFIR samples include material that has undergone the GBE treatment.

5.1.6. ALLEGRO experimental reactor (Europe)

5.1.6.1. Objectives and context

On the Gas Fast Reactor (GFR) development roadmap, the Experimental and Technology Demonstration Reactor (ALLEGRO) is the first necessary step towards an electricity generating prototype. It is a low power (~ 75 MW_t) helium-cooled fast reactor including the following main objectives:

- Qualification of GFR fuel and sub-assembly concept;
- Demonstration of core operation and control with the appropriate instrumentation;
- Establishment of a first GFR safety reference framework;
- Acquisition of first of a kind GFR operating feedback experience.

In the GFR fuel development plan, ALLEGRO is located in between the irradiation of samples in material testing reactors and the full demonstration at a GFR electricity generating prototype scale. Launched in 2005 for 4 years, the Gas Cooled Fast Reactor Specifically Targeted Project (GCFR STREP) of the EURATOM 6^{th} framework program includes pre-conceptual ETDR (previous ALLEGRO name) design and safety studies.

The CEA is mainly in charge of core physics, reactor system design and global plant layout. Nexia Solutions is in charge of sub-assembly design, whereas AMEC is in charge of the absorbers and control and instrumentation and NRG of reflector and shielding studies. The GoFastR program, which started in 2010 and will last for three years, includes new partners for ALLEGRO, particularly from central Europe, namely Czech Republic (RC-Rez) and Hungary (AEKI and University of Budapest).

5.1.6.2. Core design

The core design includes a two-step approach:

- First core (start-up core) using conventional MOX fuel and steel cladding with some experimental GFR fuel sub-assemblies,
- Second core (refractory core) using only GFR reference fuel (carbide fuel with ceramic cladding).

The start-up core is composed of 81 MOX fuel S/As with 6 control/shutdown rods (CSD) and 4 diverse shutdown (DSD) rods. After one year of operation, the core will be loaded with

experimental GFR S/As. The objective is to irradiate these S/As for about 2000 equivalent full power days with acceptable representative GFR conditions. Table 5.4 compares the irradiation performances and parameters on the experimental GFR S/A and the GFR 2 400 MW_t reference (here on the so called 12/06F plate core). These performances can be considered as quite acceptable as about 2000 efpd would be needed to reach the relevant GFR burnup.

TABLE 5.4. COMPARISON OF IRRADIATION CHARACTERISTICS OF A CARBIDE S/A IN GFR AND IN THE ALLEGRO MOX CORE

For one GFR S/A, for one irradiation year (365 efpd)	GFR 2400 12/06F core	ALLEGRO 75 MW MOX core (Frequency 1)
GFR S/A Pu enrichment, %	17.3	30.5 (× 1.8)
Maximum fast flux (E>0.1 MeV), $n \cdot cm^{-2} \cdot s^{-1}$	12.4×10^{14}	8.4×10^{14} (-32%)
Maximum burnup, at%	2	1.8 (-10%)
Maximum dose, dpa SiC	22	15 (-32%)
Dose/burnup ratio, dpa SiC/at%	11.0	8.3 (-25%)

Other important characteristics are the safety neutronic coefficients of the MOX core which are gathered in Table 5.5. It can be noticed that the void effect remains quite low whereas the Doppler Effect always tends to stabilize the power in case of fuel temperature increase

TABLE 5.5. SAFETY NEUTRONIC COEFFICIENTS OF THE MOX CORE

Safety coefficient	Value
β_{eff}, pcm	360
Doppler (between 180 and 880°C), $	-1.1
Void, $	+0.3

5.1.6.3. System design

The preliminary system design is based on intermediate loops with two primary helium loops able to remove 75 MW without energy conversion. It includes two intermediate heat exchangers compatible with the helium inlet/outlet temperatures of both the start-up and demonstration cores (respectively 260/530°C — compatible with the MOX fuel option — and 400/850°C). The secondary loops include pressurized water, which avoids the issue of high temperature materials which would have been raised with a gas-gas heat exchanger option. The final heat sink is the atmosphere. An additional circuit reservation has been made to possibly test high temperature processes or components using part of the reactor power (10 MW).

A global view of the ALLEGRO primary circuit is shown in Fig. 5.14, while Fig. 5.15 illustrates the primary circuit in the reactor building. The thin metallic guard containment encloses the primary system ensuring a backup pressure of 3 bar in case of LOCA. Heavy concrete structures are disposed around the reactor vessel to protect the personnel during maintenance.

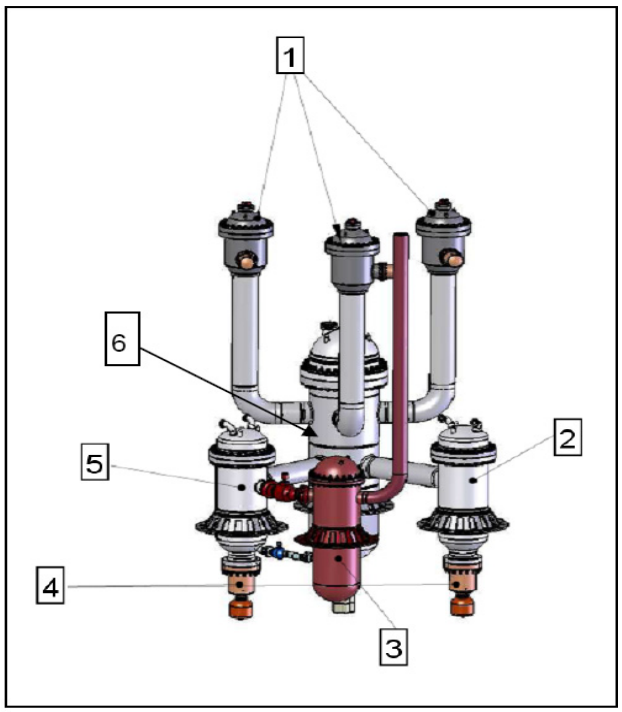

Legend :

1-3x100% DHR Systems forced or natural convection mode

2- IHX 40 MWatt U Tube Helium water

3- Optional IHX He/He 10 MWatt

4-2 main blowers with pony motor assist

5- Same than 2

6- Reactor pressure vessel

FIG. 5.14. Overview of the ALLEGRO primary system.

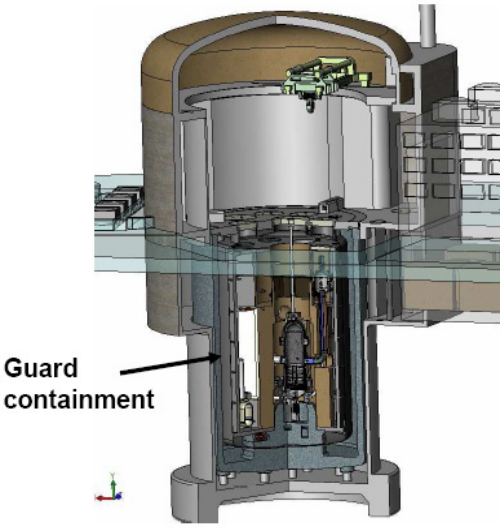

FIG. 5.15. ALLEGRO reactor building.

5.1.6.4. R&D work plan

In parallel to the pre-conceptual design process, the ALLEGRO R&D plan has been launched to qualify the appropriate calculation tools (ERANOS, CATHARE,…) and the specific helium technology necessary in addition to the VHTR mainstream development. This includes in particular:

- A core physics test program in MASURCA;
- Air and helium tests on reduced size sub-assemblies (ESTHAIR);
- System transient analysis codes benchmarking and qualification;
- High temperature resistant thermal barriers (1250°C for one hour);
- DHR blowers with quite large specifications (from 3 to 70 bar with constant mass flow rate);
- Specific instrumentation for core thermal monitoring and fuel handling;
- Specific GFR environment purification systems.

The R&D plan is now broadened at the European level through the 7th Framework Program ADRIANA project which aims at identifying the needs and research infrastructures for SFR, GFR and LFR systems.

5.2. BGR-1000

5.2.1. Background

Lately, conceptual studies of gas-cooled fast reactors are renewed in Russia, the basis for which originates from long-term Russian experience in the development of helium-cooled fast reactor (BGR) concepts. Based on these considerations, recommendations have now been made on the development of the new BGR concepts. Power units with BGRs are assumed to be used for electricity production and (in the future) for energy and technology purposes. The development of the conceptual design of two-circuit nuclear power plant with BGR-1000 reactor for production of steam with super-high parameters is under way, and the status is presented subsequently. Additional information beyond the information presented in this section regarding the Russian BGR programme can be found in references [32-35].

5.2.2. BGR-1000 reactor design basis

The conceptual studies conducted in the framework of designing a reactor facility (RF) with the BGR-1000 reactor are based on synthesis of developed reactor technological decisions for high-temperature and light water reactors (VVER-type). In particular, within the framework of this design it is assumed to use the results of studies on substantiation of application of coated microfuel particles in light water reactors like VVER. The similar approach allows hope for an appreciable reduction of volume of R&D works and maximum use of design and technological decisions used in light water reactors.

5.2.3. Stages of design development and the current status of the design

At present, formation of the concept of the RF with the BGR-1000 reactor is carried out. At the current stage of concept development, the following studies have been performed:

- The general concept of the facility has been formulated, including the qualitative analysis of possible design decisions for the core and equipment of the primary circuit, choice of fuel types and configuration of fuel elements;
- Preliminary evaluation of neutron-physics and thermal hydraulic characteristics of the core has been performed;
- Some preliminary assessments of safety potential of proposed conceptual decisions are executed.

5.2.4. BGR-1000 reactor plant concept and its main features

The following initial preconditions are taken for development of the BGR-1000 gas-cooled fast reactor concept:

- Option of two-circuit and two-loop facility with helium in the primary circuit with moderate temperature at the reactor outlet and with steam-water in the secondary circuit with supercritical parameters is chosen;
- The reactor is located in a metallic vessel;
- The basic equipment has a block-type or block/loop-type arrangement into a leak tight containment made of pre-stressed reinforced concrete;
- The fuel microparticles with dense mixed monocarbide (or mononitride) fuel and multilayered ceramic coating are chosen as fuel elements (option with mixed dioxide fuel is considered as an alternate);

- The core consists of fuel assemblies (FA) filled with fuel microparticles in a fixed bed, with the cross-axial coolant flow;
- Control rods are placed into guide tubes inside FA;
- S team generators have vertical direct-flow arrangement with steam generation in tubes (working substance moves upwards);
- Refueling is performed with removing the reactor vessel head and filling core with water;
- Residual heat during refueling is removed by the active system of normal flooding and residual heat removal (NFRHRS);
- In the events with fast loss of coolant, the core is cooled with water provided by ECCS sub-systems (similar to those used in the new generation VVER reactors), in particular, by passive water supply from high- and low-pressure water tanks, and by active water supply from containment sumps;
- In accidents with total loss of power, residual heat is removed into the air using the passive heat removal system, similar to those developed for the new generation VVER.

A schematic of coolant flow through a FA of the core is shown in Fig. 5.16.

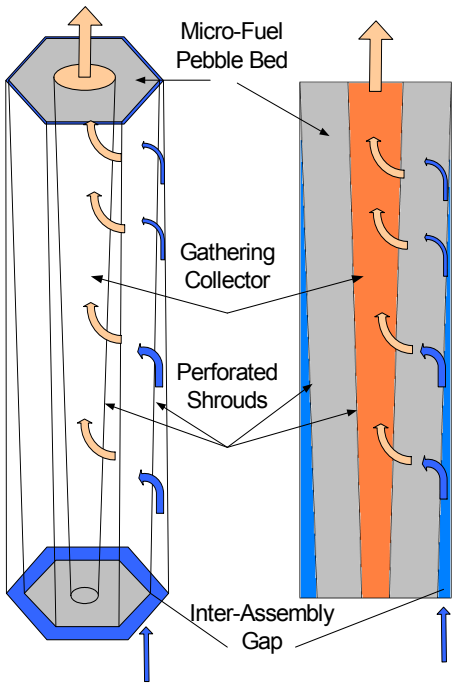

FIG. 5.16. Schematic of coolant flow through FA of the BGR-1000 reactor.

A longitudinal section of the BGR-1000 reactor is presented in Fig. 5.17.

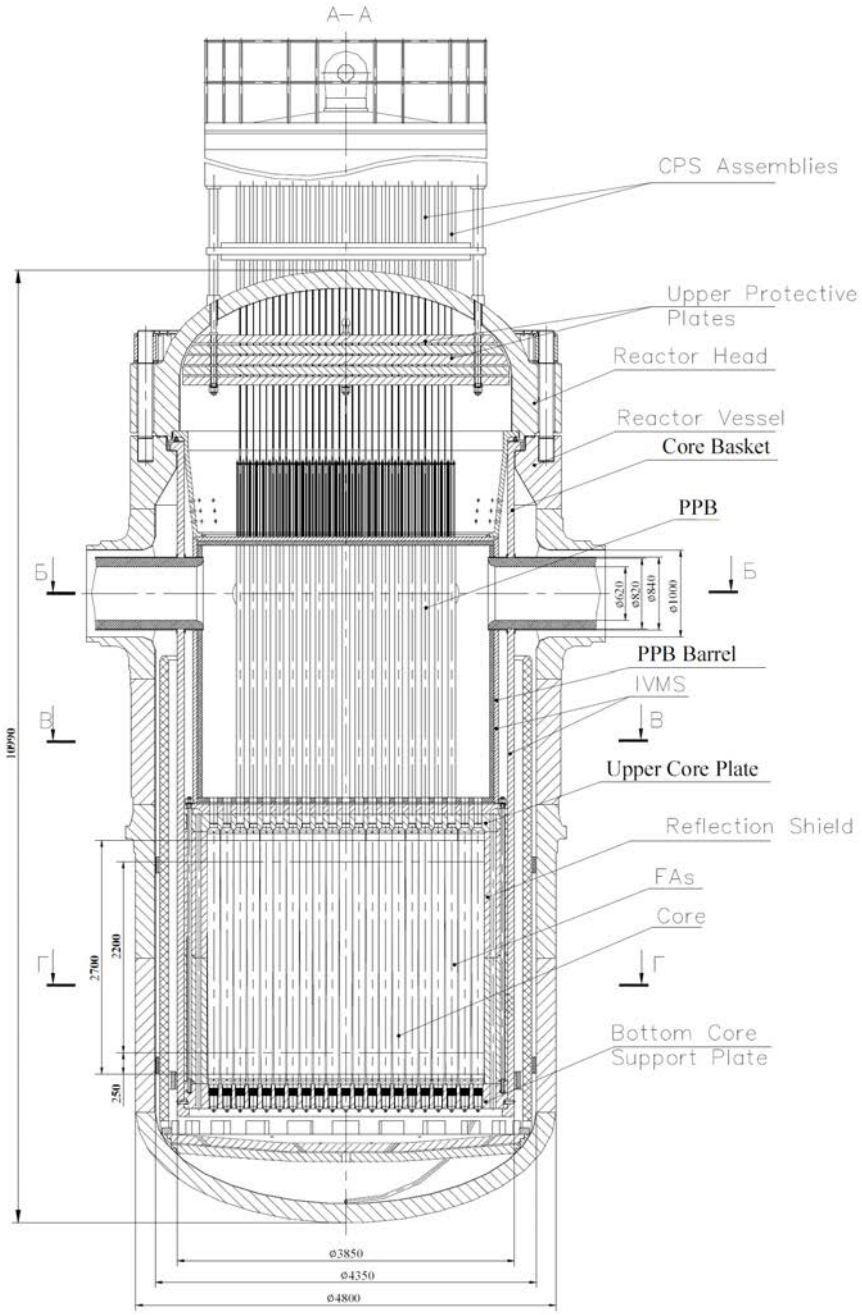

FIG. 5.17. BGR-1000 reactor vertical cross-section.

Under normal operating conditions, thermal energy is removed from reactor by forced circulation of helium that is provided by four main circulation blowers and transferred inside main pipes of large diameter to three steam generators and one superheater.

The basic technical parameters of the BGR-1000 reactor facility are presented in Table 5.6.

TABLE 5.6. BGR-1000 BASIC TECHNICAL PARAMETERS

Parameter	Value
Overall plan:	
Reactor thermal power, MW	2000
Unit electrical power, MW	1000
Design lifetime, year	60
Average capacity factor per lifetime	0.87
Breeding ratio	1.05
Primary circuit:	
Coolant	Helium
Primary circuit pressure, MPa	16
Coolant temperature, °C	
Core inlet	350
Core outlet	750
Coolant flowrate, kg/s	900
Pressure drop, MPa	below 0.5
Number of main circulation gas blowers	4
Power of main circulation gas blowers, MW	4×10=40
Reactor core:	
Core volume, m^3	12.82
Core effective radius, m	1.36
Core height, m	2.2
Number of FA in the core (zone 1 / zone 2 / zone 3)	295 (121/114/60)
Number of FA in the radial blanket (2 rows)	138
Bottom axial blanket thickness, m	0.25
Top axial blanket thickness, m	0.25
Fuel assembly duct width across flats, mm	150.0
FA positioning pitch, mm	151.0
Fuel	(U, Pu)C
Effective fuel density, g/cm^3	12.0
Pu contents in the core (zone 1 / zone 2 / zone 3), mass.%	10.5/16.5/20.0
Total heavy metal load of the core, kg	35951
Fissile plutonium load, kg	3640
Share of fissile Pu isotopes in the load, %	10.1
Total reactor thermal power, MW	2000
Core thermal power, MW	1890
Axial blankets thermal power, MW	39
Radial blanket thermal power, MW	71
Average fuel burnup, % ha	9.7
Maximum fuel burnup, % ha	13.6
Core fuel lifetime, ed	1800
Radial blanket fuel lifetime, ed	600
Refueling interval, ed	600
Secondary circuit:	
Working substance	Water-steam
Total capacity, MW	1908
Superheated steam pressure after SG, MPa	30
Superheated steam temperature after SG, °C	650
Feedwater temperature, °C	300
Steam pressure at intermediate reheater inlet, MPa	3.5
Steam temperature at intermediate reheater, °C	
Inlet	310
Outlet	650

Based on the results of the preliminary analysis of different options, the following key provisions concerning the BGR-1000 core were adopted for further detailed development:

- Three-zone power profiling by varying plutonium contents in the fuel and providing equal fuel shares in all parts of the core;
- Maintenance of a volumetric fraction of the fuel practically constant along FA height;
- Presence of the top and bottom axial blankets;
- Presence of the radial blanket consisting of two rows of FA and surrounded by reflection shield;
- Spherical fuel microparticles with outer diameter of 2 mm and three-layer coating (inner layer is made of porous pyrocarbon, PyC; medium layer is made of dense PyC; outer layer is made of silicon carbide, SiC).

5.2.5. Conclusion

Presently in Russia, research of gas-cooled fast reactors is conducted at the conceptual level. These studies are carried out within the framework of development of the helium-cooled fast reactor BGR-1000 concept. It is supposed that these reactors can be used for electricity production and technological application in the future.

REFERENCES TO CHAPTER 5

[1] ARGONNE NATIONAL LABORATORY, PROJECT STAFF, EBR-II System Design Descriptions: Volume II Primary System, Chapter 2, Reactor, Argonne National Laboratory report (June 1971).

[2] VECA, A.R., SYNDER, H.J., RAU, P., PEEHS, M., Fuel Element Design for the 330 MWe Gas-Cooled Fast Breeder Reactor, Nuclear Engineering and Design, 40, pp. 81-99 (1977).

[3] GIF GFR PROVISIONAL DESIGN AND SAFETY PROJECT MANAGEMENT BOARD, Annex 1: GFR System Integration Design and Safety Project Plan, GFR D&S PPMB Draft Annex to the Project Arrangement (August 2005).

[4] GIF GFR PROVISIONAL SYSTEM STEERING COMMITTEE, GFR System Research Plan for the Gas-Cooled Fast Reactor R&D Program Plan, GIF Draft Report (April 2006).

[5] U.S. DOE NUCLEAR RESEARCH ADVISORY COMMITTEE AND THE GENIV INTERNATIONAL FORUM, A Technology Roadmap for Generation-IV Nuclear Energy Systems, GIF-002-00 (December 2002).

[6] ROUAULT, J., WEI, T.Y.C., I-NERI France-U.S. GFR Project: Synthesis of Main Design Trends, Proc. ICAPP '05, Seoul, Korea, Republic of, 15-19 May 2005, ISBN: 9781604236934, Curran Associates, Inc. (April 2007) paper 5188.

[7] ROUAULT, J., WEI, T., MIZUNO, T., CODDINGTON, P., MITCHELL, C., GFR Design and Safety Provisional Project Management Board Views on GFR Options to be Studied in the Pre-conceptual Design Phase, Draft GFR D&S PPMB Report (May 2006).

[8] RICHARD, P., et al.,Status of the pre-design studies of the GFR core, Proc. PHYSOR 2008, Interlaken, Switzerland, 14-19 September 2008, Publisher: Paul Scherrer Institute, JRC Publication No: JRC46854 (2008).

[9] MALO, JY., et al., Gas-cooled Fast Reactor 2400 MWth, end of preliminary viability phase, Proc. ICAPP '08, Anaheim, USA, 8-12 June 2008, ANS, ISBN: 0-89448-061-8 (2008), paper 8175.

[10] BERTRAND, F., et al., Preliminary safety analysis of the 2400 MWth Gas-cooled Fast Reactor, Proc. ICAPP '08, Anaheim, USA, 8-12 June 2008, ANS, ISBN: 0-89448-061-8 (2008) paper 8184.
[11] POETTE, C., et al., ALLEGRO, The European Union's Experimental Gas-Cooled Fast Reactor Project, Proc. ICCAP'08, Anaheim, USA, 8-12 June 2008, ANS, ISBN: 0-89448-061-8 (2008) paper 8175.
[12] VENKATASH, M., BAXTER, A., General Atomics, personal communication (September 2006).
[13] FELDMAN, E.E., HOFFMAN, E.A., KULAK, R.F., THERIOS, I.U., WEI, T.Y.C., Large GFR Core Subassembly Design, ANL-GENIV-50, Argonne National Laboratory report (August 2005).
[14] FARMER, M.T., HOFFMAN, E.A., PFEIFFER, P.A., THERIOS, I.U., WEI, T.Y.C., "Pin Core Subassembly Design," ANL-GENIV-070, Argonne National Laboratory Report (April 2006).
[15] GARNIER, J.C., et al, GFR SYSTEM – Progress of CEA pre-conceptual design studies, Proc. ICAPP '05, Seoul, Korea, Republic of, 15-19 May 2005, ISBN: 9781604236934, Curran Associates, Inc. (April 2007) paper 5305.
[16] MIZUNO, T., JAEA, private communication (March 2005).
[17] WEI, T.Y.C., HEJZLAR, P., FELDMAN, E.E., WILLIAMS, W.C., A Semi-Passive Approach to GFR Depressurized Decay Heat Removal Accidents, Proc. ICAPP '05, Seoul, Korea, Republic of, 15-19 May 2005, ISBN: 9781604236934, Curran Associates, Inc. (April 2007).
[18] MELESE, G., Thermal and Flow Design of Helium-Cooled Reactors, Chapter 10, ANS, Lagrange Park (1986).
[19] LABAR, M.P., SHENOY, A.S., SIMON, W.A., CAMPBELL, E.M., Status of GT-MHR for Electricity Production, paper presented in World Nuclear Association Symposium, London, UK, 3-5 September 2003.
[20] GITTUS, J.H., ESKOM Pebble Bed Modular Reactor, Nuclear Energy, Vol. 38, No. 4, pp. 215-221 (1999).
[21] ROUAULT, J., WEI, T.Y.C., Development of GEN-IV Advanced Gas-Cooled Reactor with Hardened/Fast Neutron Spectrum, Transactions of the American Nuclear Society, Vol. 88, p. 191 (June 2003).
[22] FELDMAN, E.E., WEI, T.Y.C., et al., Cold Finger Concept for Passive Decay Heat Removal in Gas-Cooled Reactors, Transactions of the American Nuclear Society, Vol. 88, p. 681, (June 2003).
[23] HEJZLAR, P., DRISCOLL, M.J., TODREAS, N.E., The Long Life Gas Turbine Fast Reactor Matrix Core Concept, paper presented in International Congress on Advanced Nuclear Power Plants, Hollywood, Florida,USA, 9-13 June 2002.
[24] LUDEWIG, H., Brookhaven National Laboratory, private communication (2003).
[25] WILLIAMS, W.C., HEJZLAR, P., SAHA, P., Analysis of a Convection Loop for GFR Post-LOCA Decay Heat Removal, Paper ICONE12-49360, Proc. ICONE12, 12th International Conference on Nuclear Engineering, Arlington, Virginia USA, 25-29 April 2004.
[26] HEJZLAR, P., WILLIAMS, W.C., DRISCOLL, M.J., Hot Channel Flow Starvation of Helium Cooled GFRs in Laminar Natural Convection, Transactions of the American Nuclear Society, Vol. 91, p. 202 (November 2004).
[27] GARNIER, J.C., CHAUVIN, N., ANZIEU, P., FRANCOIS, G., WEI, T.Y.C., TAIWO, T., MEYER, M., HEJZLAR, P., LUDEWIG, H., BAXTER, A., Feasibility Study of an Advanced GFR, Design Trends and Safety Options, Status of France and U.S. Studies,

Proc. GLOBAL 2003, New Orleans, USA, 16-20 November 2003, ANS, ISBN: 0-89448-677-2 (2003).
[28] CHIANG, Y., MESSNER, R.P., TERWLIILIGER, C.D., Reaction-formed Silicon Carbide, Materials Science and Engineering, A 144, pp. 63-74 (1991).
[29] SHENNAN, J.V., Dispersed Ceramic Fuels for the Advanced Gas-Cooled Reactors, Chemical Engineering Progress Symposium, Nuclear Engineering, Part XVIII, No. 80, Vol. 63, pp. 96-110.
[30] GAN, J., ALLEN, T., Generation IV GFR Materials Program FY-2006 Summary Report, Idaho National Laboratory Report (October 2006).
[31] ALLEN, T., WAS, G., GAN, J., personal communication (July 2006).
[32] PONOMAREV-STEPNOY, N., et al., Development of Fast Helium Reactor in Russia, Atomnaya Energia, Vol. 94, issue 4, pp. 262-270 (2003).
[33] ALEKSEEV, P.N., et al., Development of Conceptual Proposal for a Nuclear Facility with the Gas Cooled Fast Reactor BGR-1000 Using Coated Microfuel and Technologies of Light Water Reactors, Proc. PHYSOR-2006, Vancouver, BC, Canada, 14-16 September 2006, paper C106.
[34] ALEKSEEV, P.N., et al., Nuclear Facility with the Gas Cooled Fast Reactor BGR-1000 Using Coated Particles and Technologies of Light Water Reactors, Proc. ICAPP '07, Nice, France, 13-18 May 2007, ISBN: 9781604238716, Curran Associate, Inc. (February 2008) paper 7292.
[35] Strategy of Nuclear Power Development in Russia in the First Half of XXI Century. Moscow, Atominform (2001).

CHAPTER 6
STATUS OF FAST REACTOR CORE RESEARCH AND DEVELOPMENT

6.1. Introduction

Notwithstanding their history, fast reactors to this day remain the topic of intensive research and development (R&D) efforts, due in large part to the nature of fission induced by fast neutrons and the associated innovative technologies that are proposed or adopted for such systems. As a result, new, often more stringent, engineering design criteria are imposed on the development of fast neutron reactors, demanding extensive R&D effort in order to identify and eventually qualify candidate concepts, data and calculation methodologies. The R&D of fast reactor technologies continues in many specific fields, among them the measurement and evaluation of nuclear data, reactor physics and thermal hydraulics calculations, fuel concepts and performance, materials performance, coolants and coolant technologies, and the design of instrumentation and control systems. Each of these research foci is addressed within this chapter.

6.2. Reactor physics

6.2.1. Nuclear data

6.2.1.1. Nuclear data library

The measured nuclear data are sent to one of the four Nuclear Data Centers where all measured data are compiled and stored in an internationally agreed-upon exchange format, EXFOR. The Nuclear Data Centers are:

(1) Nuclear Energy Agency (NEA) Data Bank in Paris, which serves OECD countries other than those which have their own centers;
(2) National Nuclear Data Center (NNDC) at Brookhaven National Laboratory, USA;
(3) Russian Nuclear Data Center at Obninsk, Russia; and
(4) International Atomic Energy Agency (IAEA) Nuclear Data Section (NDS) which serves countries not covered by the other three centers and provides a coordinating role.

An evaluation of the available measured nuclear data is necessary to produce a recommended file of cross-section data for a nuclide, or an evaluation of fission product yields or the radioactive decay data for a nuclide. This is because there are often several sets of measurements or gaps in the measured data which must be filled using theory. Inconsistent data must be examined and a best estimate made, taking into account any theoretical constraints. There are several evaluation projects which coordinate the efforts of the scientists working in the field and make plans to meet the data requirements. All cross-section evaluation projects now use the ENDF/B format to store their data [1]. The IAEA Nuclear Data Section periodically issues an Index of Nuclear Data Libraries in the IAEA-NDS-7 series [IAEA Nuclear Data Service at http://www-nds.iaea.org], and this should be consulted for information about the current status.

In the United States, evaluated nuclear reaction data are made available to users in applied and basic nuclear science through ENDF/B files. The Cross Section Evaluation Working Group (CSEWG), which was founded in 1966, is the organization that oversees the development of this database. Major releases of the ENDF/B files are summarized in Table 6.1.

TABLE 6.1. MAJOR RELEASES OF ENDF/B LIBRARIES

ENDF/B	I	II	III	IV	V	VI	VI.8	VII.0
Year	1968	1970	1972	1974	1978	1990	2001	2006

After an initial two-year release cycle, recent major releases have occurred at widely-spaced intervals, and interim releases, containing certain cross section advances, have occurred more frequently. The most recent version of the ENDF/B file is ENDF/B-VII, which was released in December 2006 [2, 3]. The major advances of the ENDF/B-VII file over the previous ENDF/B files are:

(1) New cross sections for U, Pu, Th, Np and Am actinide isotopes, with improved performance in integral validation criticality and neutron transmission benchmark tests;
(2) More precise standard cross sections for neutron reactions on H, ^{6}Li, ^{10}B, Au and for ^{235}U and ^{238}U fission;
(3) Improved thermal neutron scattering;
(4) Development of an extensive set of neutron cross sections on fission products;
(5) Large suite of photonuclear reactions;
(6) Extension of many neutron- and proton-induced evaluations up to 150 MeV;
(7) Many new light nucleus neutron and proton reactions;
(8) Post fission beta-delayed photon decay spectra;
(9) New radioactive decay data;
(10) New methods for uncertainties and covariance data;
(11) New actinide fission energy deposition.

Through extensive validation using radiation transport codes to simulate measured critical assemblies, major improvements in the ENDF/B-VII files are:

(i) Long-standing under-prediction of low enriched uranium thermal assemblies is removed;
(ii) ^{238}U and ^{208}Pb reflector biases in fast systems are largely removed;
(iii) Good agreement with ENDF/B-VI.8 for simulations of thermal high-enriched uranium assemblies is preserved;
(iv) Under-prediction of fast criticality of ^{233}U, ^{235}U and ^{239}Pu assemblies is removed; and
(v) Intermediate spectrum critical assemblies are predicted more accurately.

The Joint Evaluated File Project, JEF, was started in the early 1980s as a cooperative effort between member countries of the OECD NEA Data Bank. The first evaluated nuclear data library, JEF-1, was released in 1985 [4]. The preliminary version of JEF-2 was produced early in 1990, and the improved version, JEF-2.2, was produced in 1993 [5]. The JEF libraries follow the ENDF-6 format, and this has made it possible to easily include evaluations from other libraries. Through an extensive programme of benchmark testing, JEF-2.2 has been validated both for thermal and fast reactor applications, as well as for many other special applications, such as criticality, decay heat and radiation shielding, including a special emphasis on the major structural materials. A large number of laboratories throughout Western Europe have been engaged in this data processing and validation phase [6]. The development of the JEF-2 library has been closely linked to the European Fusion File Project, EFF, and the associated European Activation File, EAF. The JEF and EFF are currently being combined within the framework of the Joint European Fission and Fusion File project to produce the JEFF-3 library. The latest version of the JEFF library, JEFF-3.1, was released in May 2005 [7]. The neutron general purpose library contains incident neutron data

for 381 materials from H to ^{255}Fm. The activation library (based on the European Activation File, EAF-2003) contains 774 different targets from H to ^{275}Fm. The radioactive decay data library contains data for 3852 isotopes, of which 226 are stable. The thermal scattering law library covers nine materials, and the fission yield library covers 19 isotopes of neutron-induced fission yield from ^{232}Th to ^{245}Cm, and three isotopes with spontaneous fission yields (^{242}Cm, ^{244}Cm and ^{252}Cf).

The Nuclear Data Center of the Japan Atomic Energy Agency (JAEA/NDC) plays a leading role in the production of nuclear data libraries in Japan. The JAEA/NDC coordinates nuclear data activities in cooperation with the Japanese Nuclear Data Committee (JNDC), which was founded in 1963. They started data evaluation for the Japanese Evaluated Nuclear Data Library (JENDL) in 1970. The driving force to start JENDL was Japan's fast reactor projects. The first version JENDL-1 was released in 1977 for fast-reactor applications [8]. The second version JENDL-2, which was intended for applications to thermal and fast reactors, was made available in 1982 [9]. A series of the third versions JENDL-3.1 [10], JENDL-3.2 [11], and JENDL-3.3 [12], which can be used even in fusion and is regarded as general purpose, has been published since 1989. The current version JENDL-3.3, which was released in 2002, contains data for 337 nuclides. In addition to these general purpose files, the JAEA/NDC released special purpose files. The latest one is the JENDL Actinoid File 2008 (JENDL/AC-2008) [13], which contains data for 79 nuclides from Ac to Fm. In the evaluation for JENDL/AC-2008, small corrections (less than 1%) were made to the ^{233}U, ^{235}U, ^{238}U, ^{239}Pu, ^{240}Pu, ^{241}Pu and ^{237}Np data in order to improve the reproducibility of the integral data measured in small fast reactors. A new general-purpose library JENDL-4 [14] was released in 2010. In JENDL-4, much emphasis is placed on the improvements of MA and FP data.

BROND is the Russian evaluated nuclear data library. The current version is BROND-2.2. The Chinese evaluated nuclear data file is CENDL. The current version is CENDL-3.0 [15] and is maintained by the Chinese Nuclear Data Center of the China Institute of Atomic Energy.

KEDAK [16] is the German evaluated nuclear data. The KEDAK development was discontinued long ago. New evaluated data employed in reactor analyses come mainly from the European (JEF 2.2, JEFF 3.0, JEFF 3.1), Japanese (JENDL 3.2, JENDL 3.3), and US (ENDF/B 6.8 and ENDF/B 7.0) data libraries. The preliminary results available from the literature and obtained at FZK with the most recent data such as JEFF 3.0/3.1, JENDL 3.3 and ENDF/B 7.0 show a significant reduction of deviations for results related to experiments in critical facilities performed in the past. This leads to a strong reduction of uncertainties for principal parameters of conventional fast reactor designs (as compared to the state of the art at times when the fast reactor programmes were intensively developed worldwide, i.e. ca. 15 years ago and earlier). However, for new Liquid Metal Fast Reactor (LMFR) designs (with fuel containing a significant amount of minor actinides) the uncertainties still seem to be rather high (compared to "design" needs), almost no relevant integral measurements being available.

FENDL is the Fusion Reactor Technology Evaluated Nuclear Data Library Project coordinated by the IAEA Nuclear Data Centre specifically for the ITER Fusion Project. Files are selected from the available libraries following validation studies. Data are available for 71 materials relevant for fusion at 300 K. The latest version, FENDL-2.1, was released in December 2004. IRDF is the International Reactor Dosimetry File Project coordinated by the IAEA Nuclear Data Section.

Assessment of nuclear data uncertainty is important for assuring that nuclear systems will be safe, reliable, and cost effective, since nuclear data uncertainties impact key nuclear system

characteristics such as criticality, reactivity feedback coefficients, kinetics parameters, reactivity loss during irradiation, peak power value, conversion ratio, decay heat, radiotoxicity, etc. The nuclear data should be accompanied by estimates of uncertainties that correspond to the methods or techniques used in determining the nuclear data, including covariance data. However, the covariance data are frequently missing from evaluated nuclear data files because evaluators are not accustomed to providing uncertainty estimates. The available covariance date in the evaluated data files are summarized in [17]. The OECD/NEA Data Bank has extracted the relevant covariance data from the current evaluated data files and processed them into the same multigroup structure used for sensitivity calculations. The derived covariance is called "NEA-K Covariance Matrix," and the data selected in NEA-K are provided in Table 6.2. Recently, some trials were made to generate covariance data for the ENDF/B-VII library [18] and nuclear data uncertainty calculations were performed using the covariance data [19].

TABLE 6.2. NEA-K COVARIANCE DATA

Nuclide	Reaction	Origin of data
^{235}U	ν, fission, inelastic, elastic, (n,γ), (n,2n)	JENDL-3.3
^{238}U	ν, inelastic, elastic, (n,2n)	JENDL-3.3
	(n,γ), fission	IRDF-2002 [a)]
^{237}Np	Fission	IRDF-2002
^{239}Pu	ν, inelastic, elastic, (n,γ), (n,2n)	JENDL-3.3
	Fission	IRDF-2002
^{240}Pu	fission, inelastic, elastic, (n,γ), (n,2n)	JENDL-3.3
^{241}Pu	ν, fission, inelastic, elastic, (n,γ), (n,2n)	JENDL-3.3
^{241}Am	Fission	IRDF-2002
C	elastic, (n,γ)	ENDF/B-V
H	elastic, (n,γ)	ENDF/B-V
O	Inelastic, elastic	ENDF/B-V
^{52}Cr	inelastic, elastic, (n,γ), (n,2n)	ENDF/B-VI
^{56}Fe	inelastic, elastic, (n,γ), (n,2n)	ENDF/B-VI
^{23}Na	inelastic, elastic, (n,γ), (n,2n)	ENDF/B-VI
^{206}Pb	inelastic, elastic, (n,γ), (n,2n)	ENDF/B-VI
^{207}Pb	inelastic, elastic, (n,γ), (n,2n)	ENDF/B-VI
^{208}Pb	inelastic, elastic, (n,γ), (n,2n)	ENDF/B-VI
Si	inelastic, elastic, (n,p), (n,α)	ENDF/B-VI
^{90}Zr	inelastic, (n,γ), (n,2n)	JENDL-3.3
^{10}B	(n,α)	IRDF-2002
^{58}Ni	inelastic, elastic, (n,γ), (n,2n)	JEF-3

[a)] International Radiation Dosimetry File

In Japan, to meet the increasing needs for nuclear data uncertainty information, JENDL-3.3 [12] contains the covariance data for 20 important nuclides. These covariances were mainly obtained from measurements or nuclear model calculations which the evaluated mean data were based on. In addition, the simultaneous evaluation [20] yielded the covariance matrices for the fission cross sections of ^{233}U, ^{235}U, ^{238}U and ^{239}Pu, ^{240}Pu, ^{241}Pu in the energy region above several tens of keV. The matrices represent not only the correlation of individual fission cross sections

between different incident energies but also that of a fission cross section with another fission cross section, e.g., ^{235}U(n,f) vs. ^{239}Pu(n,f). The covariances of resolved resonance parameters were obtained [21] for several nuclides. After the release of JENDL-3.3, additional work was done to estimate the covariances which were not contained in JENDL-3.3 [22-24].

6.2.1.2. Group constants

Reactor codes cannot use evaluated nuclear data libraries directly because the volume of data is usually large and the data have a complicated structure. Therefore special code systems are used to process the evaluated nuclear data into more compact and simple forms.

Most reactor neutronics codes use group cross-section data sets, the exception being some Monte Carlo codes which use continuous energy nuclear data. The group cross section sets (or group constants libraries) contain energy-group-averaged cross sections, resonance self-shielding parameters, transfer matrices and other auxiliary data. For routine reactor calculations, few-group and broad-group cross sections are usually used. The number of groups depends upon the complexity of the code, the parameters being calculated (accurate perturbation theory calculations of effects such as sodium voiding need at least 30 groups) and the available computation resources. In addition to the broad-group data sets used for routine calculations, there are the fine-group (about 2000 groups) libraries which permit an accurate treatment of resonance shielding in heterogeneous geometries. Resonance shielding is generally treated using the Bondarenko self-shielding factor (f-factor) method [25] and the subgroup method [26], these being parameterizations of the resonance structure from which effective cross sections can be calculated for particular compositions and temperatures. An alternative approach developed at ANL is based on detailed spectrum calculations for specific compositions and temperatures [27] by representing all the resonance structures explicitly. At present, this approach is most widely used in the USA for fast reactor modelling.

The most widely used computer code to process evaluated nuclear data into group cross section libraries is the NJOY code [28, 29]. The code was developed from the ancestor MINX [30] to interpret the multigroup cross sections from ENDF/B files. The latest version is NJOY99. It is a cleaned-up version of NJOY97 with more progress towards Fortran-90 style block constructs. Recently added features include capabilities for high-energy libraries (up to 150 MeV), options for detailed treatment of charged particles, probability tables for unresolved range self-shielding treatment, and the capability to handle photonuclear reactions. In addition, a code may be needed to convert the data produced by NJOY into the form required by a particular code scheme. For the treatment of resonance shielding, auxiliary codes can be required to produce the appropriate parameters (e.g. the CALENDF code [31] for subgroup parameter calculations).

There are other processing codes, such as GRUKON [32], AMPX [33] and ETOE-2 [34]. The AMPX code is a processing code used in the SCALE code system. It processes ENDF/B-formatted evaluated files to generate temperature-dependent point-wise cross sections, including resonance self-shielding factors for resolved and unresolved resonances. It produces the probability tables for unresolved resonances, processes S(α,β) data for thermal moderators, and processes cross-section uncertainty data for use in sensitivity/uncertainty analyses [35]. The ETOE-2 code processes the ENDF/B data and prepares the binary cross section and Legendre polynomial data files for the MC^2-2 multigroup cross section generation code [36]. The MC^2-2 data library generated consists of eight files containing:

(1) Administrative file;
(2) Function table file;

(3) Unresolved resonance data;
(4) Resolved resonance data;
(5) Smooth tabulated non-resonant data;
(6) Inelastic and (n,2n) distributions;
(7) Fission spectra data;
(8) Legendre data.

The current fine-group energy structure chosen to form the MC^2-2 libraries is 2082 groups with constant lethargy (1/120) from 15 MeV to 0.4 eV, but the ETOE-2 code allows any number of ultra-fine group lethargy intervals. The ETOE-2 code was recently updated to process the ENDF/B-VI and –VII data. The R-Matrix (Reich-Moore) parameters for resolved resonances are converted to multi-pole parameters [37] that preserve the general features required by the traditional resonance integral concept and the Doppler-broadening algorithm in the MC^2-2 code without comprising rigor.

Deterministic neutron calculations are usually made in two stages, with the first stage being the production of group cross sections for specific regions of the reactor, such as the core and blanket regions of subassemblies. In this first stage, resonance shielding effects are treated and flux fine structure effects allowed for. This involves a "cell calculation" for each region, followed by flux averaging of the cross sections. Calculations over the whole reactor are then made in the second state using these equivalent homogeneous cross sections.

The space-averaging of group cross sections for a fast reactor fuel subassembly may sometimes be done simply by treating the assembly on a radial plane as a homogeneous mixture of fuel, coolant and steel materials, not taking into account heterogeneity effects. This is because, for fast reactors, in many cases these effects are of minor importance compared with their significance for thermal reactors. This is essentially due to the fact that the dimensions of the substructures (e.g. the pin diameter of about 6 mm or 8 mm) are small compared with the mean free path of fast neutrons. However, the heterogeneity cannot be completely neglected, and cell codes are then used to treat the effects more accurately. Special care has to be taken in the determination of anisotropic diffusion constants, especially for “voided” conditions, i.e. for cases when coolant is removed or has been lost from regions of the core. Under these conditions, neutron streaming along preferential flight paths in low-density channels becomes possible. The accurate treatment of the heterogeneity of subassemblies is of most importance for calculations of reactivity effects such as control rod worth and sodium void and Doppler reactivity effects. Heterogeneity effects are also important in calculations for critical assembly geometries, particularly for those assembled from plates. Some examples of cross section preparation systems are given in the following paragraphs.

The best-known tool in the USA for fast reactor group constant generation is the MC^2-2/SDX system [27, 36]. Using the libraries generated by ETOE-2, the MC^2-2 code solves the ultra-fine group neutron slowing-down equations for specific compositions and temperatures with explicit representation of resonances. It accommodates high-order anisotropic scattering representations and provides numerous capabilities such as isotope mixing, delayed neutron data processing, free-format input, and flexibility in output data selection. The extended transport P1, extended transport B1, consistent P1, and consistent B1 fundamental mode ultra-fine-group equations are solved. Resolved and unresolved resonances are treated explicitly by the generalized J^* integral formulation based on the narrow resonance approximation including overlapping and Doppler broadening effects [38]. A fundamental mode

homogeneous unit cell calculation is performed by solving the multi-group slowing-down equation above the resolved resonance energy and the continuous slowing down equation below this range [39]. Equivalence theory is used to treat heterogeneity effect. Alternative hyper-fine group integral transport calculation (RABANL) is available as an option. RABANL performs a homogeneous or heterogeneous (pin or slab) unit cell calculation over the resonance region (resolved and unresolved). Neutron cross sections are generated by RABANL for the homogeneous unit cell and for each heterogeneous region in the pin or slab unit cell calculation.

MC^2-2 calculations provide composition and temperature-dependent cross sections in a user specified energy group structure. Broad-group cross sections for whole-core calculations can be obtained directly from these MC^2-2 calculations. However, space-dependent broad group cross sections are typically determined in multiple steps. In the first, composition and temperature-dependent cross sections are generated in an intermediate (~ 230) group structure from MC^2-2 calculations. Using these intermediate group cross sections, whole-core diffusion or transport calculations are then performed with relatively simple core models. Earlier calculations used the SDX code, which performs one-dimensional diffusion theory calculation using the intermediate-group library and cell-averaged resonance cross sections. Detailed heterogeneity effects are treated through spatial self-shielding factors and cell-averaged intermediate-group cross sections, which are obtained from integral transport calculations for unit cells. More recent calculations for generating broad-group cross sections utilize intermediate-group transport solution for whole-core problem in two-dimensional R-Z geometry obtained with TWODANT [40]. It is noted that SDX provides a gamma-processing capability by interfacing with AMPX or NJOY generated files. This capability permits a consistent calculation of gamma-production data accounting for the resonance and spatial self-shielding of the capture and fission cross sections.

The Russian codes used in practice, such as TRIGEX [41], JAR [42], GEFEST and SYNTES [43], have an opportunity of calculations with 26 and smaller number of groups. The code complexes have the uniform built-in constant maintenance based on use of system CONSYST/ABBN and constants libraries ABBN-93 [44]. In contrast with previous version ABBN-78 [45], the constants in ABBN-93 are based on library of files of the evaluated nuclear data FOND-2.2 [46], which were transformed into the group form by GRUCON and NJOY codes. The libraries ABBN-93 include group constants of materials for 28 and 299 neutron energy groups - from 0 up to 20 MeV, and for 15 photon groups - from 0 up to 11 MeV. Effect of thermalization in the ABBN-93 system is taken into account by thermalization P0 and P1 matrices of scattering depending on material temperature within region of neutron energy below 4.65 eV. The 299-group micro- and macro-constants for calculated materials, prepared by CONSYST code [47], are reduced into 26 groups with weight of the flux and current neutron spectra calculated with B2-approximation, and are transformed by PRECON code [Baran48] into the format ARAMACO [49] used by the codes. These constants can be reduced into smaller number of groups if it is necessary for calculations. For this purpose, spatial-dependent 26 grouped fluxes calculated by codes are used as the weight functions. In standard calculations, the grouped micro- and macro-constants are prepared for homogeneous fuel subassembly contents. However, FFCP code can be called by option and applied for estimation of the heterogeneous effects [50] using a method of the first flight collision probability together with a method of subgroups for more correct description of resonance structure of cross-sections [51]. Change of fuel isotope contents under burnup modelling is calculated by CARE code [52]. All constants are recalculated newly at each step of burnup. A Monte-Carlo MMKKENO code [53] is used for

more exact evaluation of critical parameters and reactivity effects, and also for analysis of experiments carried out at fast critical assemblies and operating reactors. Constants for the MMKKENO code are prepared by CONSYST code with 299 groups and with P5-approximation for scattering anisotropy and taking into account thermalization effects.

So-called "benchmark" experiments executed at physical critical assemblies of zero power and operating reactors and well evaluated are used for validation of nuclear constants and calculation methods. Some corrections are frequently inserted into calculation and experimental results to provide equality between their conditions and conditions of benchmark model. Comparison of calculation and experimental data allows making a conclusion about accuracy of calculation prediction of neutronics characteristics of designed reactor facilities and necessity of increase of this accuracy by implementation of new experiments or by correction of constants. Here are used adjustment procedures based on the Generalized Least Square Method or Maximum Likelihood Method. Covariance matrix of constant's uncertainties obtained as a result of adjustment procedure enables to evaluate a component of calculation uncertainty caused by nuclear data being prevailing today. There are created the international banks of evaluated benchmark experiments for the purpose of validation, such as ICSBEP [54], IRPhEP [55] and SINBAD [56].

In the Russian Federation, for these purposes the system of codes and archives INDECS [57] is developed which includes libraries of the evaluated benchmark experiments and related calculation results LEMEX, of sensitivity factors LSENS, of covariance matrices of constants LUND, and also includes CORE code for statistical analysis of data. Comparison between required accuracy of calculation of the basic neutronics characteristics of sodium cooled fast reactor of BN-800 type and achieved accuracy evaluated by the use of the INDECs system and constants system ABBN [58] is presented in Table 6.3.

TABLE 6.3. REQUIRED AND ACHIEVED ACCURACY OF CALCULATION RESULTS FOR A SODIUM COOLED FAST REACTOR OF THE BN-800 TYPE

Parameter	Required accuracy	Achieved accuracy
k_{eff}	0.5%	0.7%
Doppler-effect	10%	10%
Rate of reactivity decrease per 1% burnup	0.07%Δk/k	0.10%Δk/k
Control rods efficiency	5%	5%
Sodium void reactivity effect	0.3%Δk/k	0.3%Δk/k
Local energy release	2%	2%
Breeding gain	0.03	0.03

In the past, France and the UK had their own fast reactor group cross section data libraries and corresponding processing codes [59, 60], and these are still in use for some project studies. As part of the European Fast Reactor Project, these national systems have been replaced by the ECCO cell code and its library [26]. The ECCO library has been derived from JEF-2.2 using NJOY and CALENDF [61], which includes 1968-group library for 37 main resonant nuclides, 33-group library for fast-spectrum applications, 175-group library for shielding calculations, and 172-group library for thermal-spectrum applications. The ECCO cell/lattice code uses the subgroup method to treat resonance self-shielding effect. ECCO prepares self-shielding cross sections and matrices by combining a slowing-down treatment in many groups (1968) with subgroup method within each fine group. In the reference calculation scheme, ECCO treats the heterogeneous geometry in fine groups for the 37 most

important nuclides while broad group libraries (33 or 172 groups) are used for the less important nuclides. The subgroup method takes into account the resonance structure of heavy nuclides by means of probability tables and by assuming that the neutron source in uniform in lethargy within a given fine group. The effective cross sections and matrices produced by ECCO code are subsequently used in full-core ERANOS calculations. Many types of geometries are available in ECCO code, such as 2D rectangular lattice of cylindrical and/or square pins within a square tube, 3D slab and 2D hexagonal lattice [62].

The Japanese fast reactor group cross section sets are usually in 70 group form [63]. Now data sets based on the JENDL-3.2 and JENDL-3.3 libraries are in use. Cell calculations [64] are usually a standard option in the preparation of effective cross sections. Recently homogenisation techniques for control rods based on "reaction rate preservation" have been implemented in the cross section preparation scheme [65]. The effective 70 group cross sections are usually collapsed to 6-18 groups using 2D RZ spectra for use in 3-dimensional calculations, except the evaluation of sodium void reactivity which needs the fine energy treatment.

Recently in Japan, an ultra-fine energy calculation system has become available [66]. A cel calculation code SLAROM-UF has been developed for fast reactor analyses to produce effective cross sections with high accuracy in practical computing time, taking full advantage of fine and ultra-fine group calculation schemes. The fine group calculation covers the whole energy range in a maximum of 900-group structure. The structure is finer above 52.5 keV with a minimum lethargy width of 0.008. The ultra-fine group calculation solves the slowing down equation below 52.5 keV to treat resonance structures directly and precisely including resonance interference effects. Effective cross sections obtained in the two calculations are combined to produce effective cross sections over the entire energy range. Calculation accuracy and improvements from conventional 70-group cell calculation results were investigated through comparisons with reference values obtained with continuous energy Monte Carlo calculations. It was confirmed that SLAROM-UF reduces the difference in k-infinity from 0.15% to 0.01% for a JOYO MK-I fuel subassembly lattice cell calculation, and from 0.21% to less than a statistical uncertainty of the reference calculation of 0.03% for a ZPPR-10A core criticality calculation.

The German fast reactor libraries were developed and maintained at FZK since long time, the significant past achievements consist of the KFKINR [67] 26-group ABBN type cross-section set (that included f-factors for taking into account resonance self-shielding effects). It should be noted that currently multi-group data sets, which are employed by deterministic (in contrast to Monte-Carlo) codes are usually obtained in a semi-automatic manner by processing “point-wise” data that can be retrieved from the evaluated nuclear data files. The procedure was less straightforward in the past.

Continuing earlier work on more temporarily used predecessors, the KFKINR library was obtained by collecting different sources of data (including those coming KEDAK and from measurements performed at FZK) and then intensively tested for a large series of experimental fast reactor models, in particular for those, which were representative for the SNR-300 fast reactor core. The experimental results were then used for adjusting the KFKINR nuclear data for important nuclides, such as ^{238}U. Thus, an important part of data in KFKINR does not correspond to a particular evaluated data library.

Experimental activities on “differential” cross-section measurements at FZK were mainly redirected towards cross-section measurements relevant for astrophysics. It should be

mentioned that the corresponding energy region (few keV to few hundreds keV domain) is also important for fast reactor analyses. However, many nuclides relevant for astrophysics (for which measurements have been performed) are less important for fission reactor studies. In support of the cross-section measurements, the code FITACS [68] has been established and maintained at FZK; this code is still used worldwide.

The KFKINR library is essentially frozen. However, the KFKINR 26-group data were used as a basis for establishing an 11-group library (including f-factors) for safety studies [69]. The reduction of the number of energy groups (from 26 to 11) was highly desirable due to application of this library in spatial kinetics models such as the SIMMER code [70] in which neutron flux calculations are performed many times during the transient. Later on, the 11-group library was modified and extended [71] for SIMMER safety analyses in nuclear waste burners [72]. In particular, data for minor actinides were taken from recent evaluated nuclear data libraries mentioned before. Data for some important isotopes, as e.g. for ^{238}U, remained unchanged and are still related to the 26-group KFKINR dataset. Currently, the 11-group dataset is mainly applied for SIMMER and related analyses (that are usually performed in order to validate the SIMMER neutronics model with respect to a particular application).

In addition to KFKINR, a 69-group (below 20 MeV) cross-section set - developed at FZK in early 1990s (following the WIMS approach and using evaluated nuclear data files), primarily for water-cooled reactors [73] - is also used for analyses of systems with fast neutron spectra. Currently, the updated 69-group dataset and datasets derived on its basis are employed at FZK, in particular for ADS studies (for that purpose, additional data on cross-sections can be taken into account in the energy region above 20 MeV) performed with the KAPROS code system [74] that is coupled [75] with the SAS4A code [76].

Since the second half of 1990s, the ERANOS nuclear code and data system [77] development of which was initiated in the framework of the European Fast Reactor project and is conducted by CEA, France in cooperation with European partners, has been employed at FZK. This system includes the ECCO cell code [78] and related datasets (33-group, 172-group, 1968-group datasets being available, the latter one for a restricted number of "important" nuclides only) based on the evaluated nuclear data files. The most recent version of ERANOS is expected to be available at FZK before end of 2007 and will include libraries based on JEFF 3.1. The datasets, which are currently used at FZK are based on JEF 2.2. A particular feature of the ECCO code and data libraries is the capability of using the probability table (or subgroup) approach for taking into account resonance self-shielding effects. This approach offers more options (compared to the direct application of f-factors) for accurate cross-section processing, in particular for heterogeneous reactor cell models (it should be mentioned that average cross-sections and f-factors can be potentially employed to compute the subgroup parameters, that could be a relatively complicated task, and vice versa, that is a straightforward option). The maintenance and developments of ERANOS datasets is performed by CEA, unlike other datasets employed at FZK, which are modified and extended at FZK in accordance with actual needs when new data evaluations become available. The validation of the ERANOS data and code system for LMFR applications based on a large experimental data base accumulated by CEA has been performed over the years from the MASURCA zero-power critical assembly, as well as from other facilities or reactors. This data base includes in particular physics measurements performed in the Phénix and Superphénix plants [62]. The analysis of recent experiments (CIRANO [79, 80], COSMO

[81], MUSE programmes in MASURCA) has made it possible to extend the ERANOS domain of validity to plutonium-burning cores.

Thus, until recently three main data options were available at FZK. The 11-group dataset was employed for SIMMER and related studies. The 69-group set (and datasets derived on its basis) were employed with KAPROS. The ECCO (33/172/1968-group) datasets were employed with ERANOS. The choice of a particular option to be used for a particular research topic was strongly dependent on the problem to be solved and on researcher's background. The abovementioned codes employ data stored in different formats. Recently, efforts were paid to facilitate data exchange in the CCCC format [82] that is employed by SIMMER.

Since the beginning of this century, using of Monte-Carlo (MC) codes, in particular [83], and related point-wise data libraries become increasingly popular worldwide for reactor core analyses as it offers a straightforward way to take into account resonance self-shielding, heterogeneity, and complex geometry effects while paying a higher computation cost and introducing statistical uncertainties in the obtained results. Any further discussion of the advantages and disadvantages of MC codes as compared to deterministic ones will be omitted here. Several MCNP data libraries are used at FZK, while the MCNP results are often compared or complemented when it is possible by corresponding "deterministic" ones: to better understand physical phenomena and to increase the reliability of obtained results. An important condition for these comparisons is: using the same basic evaluated nuclear data.

Recently, a new multigroup code and data system, C^4P [84], has been developed at FZK. The main incentive was to improve the nuclear data basis for SIMMER and related studies. The C^4P library (in the extended - to properly take into account thermal neutron scattering – CCCC format) includes 560 "neutron" groups below 20 MeV (higher energy data and gamma cross-sections are not considered here). The number of energy groups in the library was chosen so that for all simplified (with respect to geometry) models of advanced reactors (including LM-, gas-, water-cooled and molten salt systems) the deterministic calculations (with this library) and MCNP calculations (with point-wise cross-sections, based on the same evaluated data) would provide essentially the same results with respect to criticality and major reactivity effects (assuming that deviations in criticality below 200 pcm are acceptable). For fast reactor analyses, either a 30-group or a 100-group library condensed (including f-factors) from the 560-group "master" library is often employed.

Most of the described multigroup data libraries and related data processing codes include options for generating data for isotope mixtures, e.g. for Fe-nat from Fe isotopes, which are based either on the probability table or f-factor approach. An option, recently developed for C^4P, performs "merging" of isotope-wise data in a different way. This option employs an original concept of "extended" probability tables [85]. These tables can often be derived from f-factors and averaged cross-sections in a more easy and accurate manner than conventional probability tables or subgroups. Unlike the conventional approach, the "extended" subgroup parameters are determined independently for the total cross-section and for all pairs (total, partial cross-section) so that several (for the total and for each partial cross-section) sets of subgroup fractions (or weights) and several sets of total subgroup cross-sections are effectively used in a particular energy group. Application of these extended sets of parameters is, however, limited to the task of "merging" isotope-wise data; unlike the conventional subgroups they cannot be directly employed in neutron transport models.

It should be mentioned that some of the described data libraries include alternative evaluations based on the abovementioned evaluated nuclear data files. The availability of alternative evaluations is often used to investigate the effect of different data on the computed reactor parameters. If the calculations are performed for systems, which are assumed to be waste burners and contain a significant amount of minor actinides, the results may depend strongly (e.g. by more than 1000 pcm for criticality) upon the choice of nuclear data. The results are usually less sensitive (to this choice) if more conventional fuel compositions are considered. The effect of other (i.e. non-actinide data) also becomes smaller recently, after JEFF 3.1 and ENDF.B 7.0 libraries have been released, partly due to the fact that similar evaluated data for some nuclides (e.g. for some lead isotopes) are accepted in these libraries. Thus, the data uncertainties may in reality be larger than the observed deviations due to using of different nuclear data libraries.For certain problems, such as computations of the "effective" delayed neutron fraction or burnup modelling, auxiliary parameters, such as delayed neutron data or branching ratios are necessary. For certain codes, these data can be provided as part of the input, so that e.g. ERANOS inputs created in the past can be used for the corresponding computations. For certain codes, e.g. applied for burnup studies and mentioned in the following, special libraries in proprietary format are kept and modified from time to time.

A more recent approach, as e.g. is currently the case for computing delayed neutron parameters for SIMMER-related studies, is to use "directly" the point-wise data (nu-bar, delayed neutron spectra, etc.) in ENDF format and performing the group averaging "online"; that is possible to do in a fast manner (due to the fact that self-shielding effects can be neglected) and facilitates computations with different multigroup cross-section libraries. A similar approach has been recently used for accessing data relevant for burnup modelling from the auxiliary data files of JEFF 3.1, such as fission products, decay data and activation cross-section. An additional advantage (compared to abovementioned alternative options) of this approach is that location-dependent reaction branching ratios may be employed in cases, in which the neutron flux spectra vary appreciably in space.

In India, a 25 group library which was a forerunner of CARNAVAL-IV cross-section library of Cadarache was used [86] for the design of the Fast Breeder Test Reactor (FBTR). Using indigenous and IAEA processing codes, a new 25 group library was derived from JENDL-2. In the original adjusted 25 group library, ^{241}Pu and Ni cross-sections were deficient and had not been subjected to any adjustment. Thus a revised library called CV2M was also derived for Prototype Fast Breeder Reactor (PFBR) design [87] by replacing the above two isotope cross-sections with those derived from JENDL. For better prediction of burnup reactivity fall, new lumped fission product multigroup cross-sections were also prepared and added to this cross-section set, for different burnup levels of PFBR core [88]. This modified library was compared with the unadjusted 25 group library fully derived from JENDL-2 mentioned earlier. By analyzing the ZPPR-13 experimental results it was concluded that CV2M predictions are better than the newer unadjusted library [89]. Presently for PFBR design and analysis a 26 group cross-section library derived from BNAB-93 [90] is also being used.

With respect to basic R&D studies in nuclear data, two important aspects were studied for the first time:

(1) Effect of energy dependence of the dilution (background) cross-section on the group-average cross-section [91];
(2) Effect of temperature dependence of the unshielded group cross-section [92].

The former study found that the historical Bondarenko assumption works reasonably well. The latter study found that the present procedure in practice of forcing an upper limit of unity to the self-shielding factor, could at times lead to wrong effective group cross-sections. In group cross-sections, self-shielding factor can be allowed to go above unity. To compute complex resonance integrals numerical approximations were suggested which are very accurate. In one case, Pade approximations were used for $J(\theta,\beta)$ and its temperature derivative [93], and in a subsequent work new rational approximations were developed for Reich-Moore collision matrices found in ENDF/B [94, 95].

In the Republic of Korea, all the nuclear design and evaluation are performed with the K-CORE System [96] of KAERI for the neutronics analysis of fast reactors. The evaluation procedure for the nuclear design and analysis consists of three parts: neutronics cross section generation, flux solution and burnup calculation, and reactivity calculation. The evaluation procedure for the nuclear design and analysis is schematically shown in Fig. 6.1.

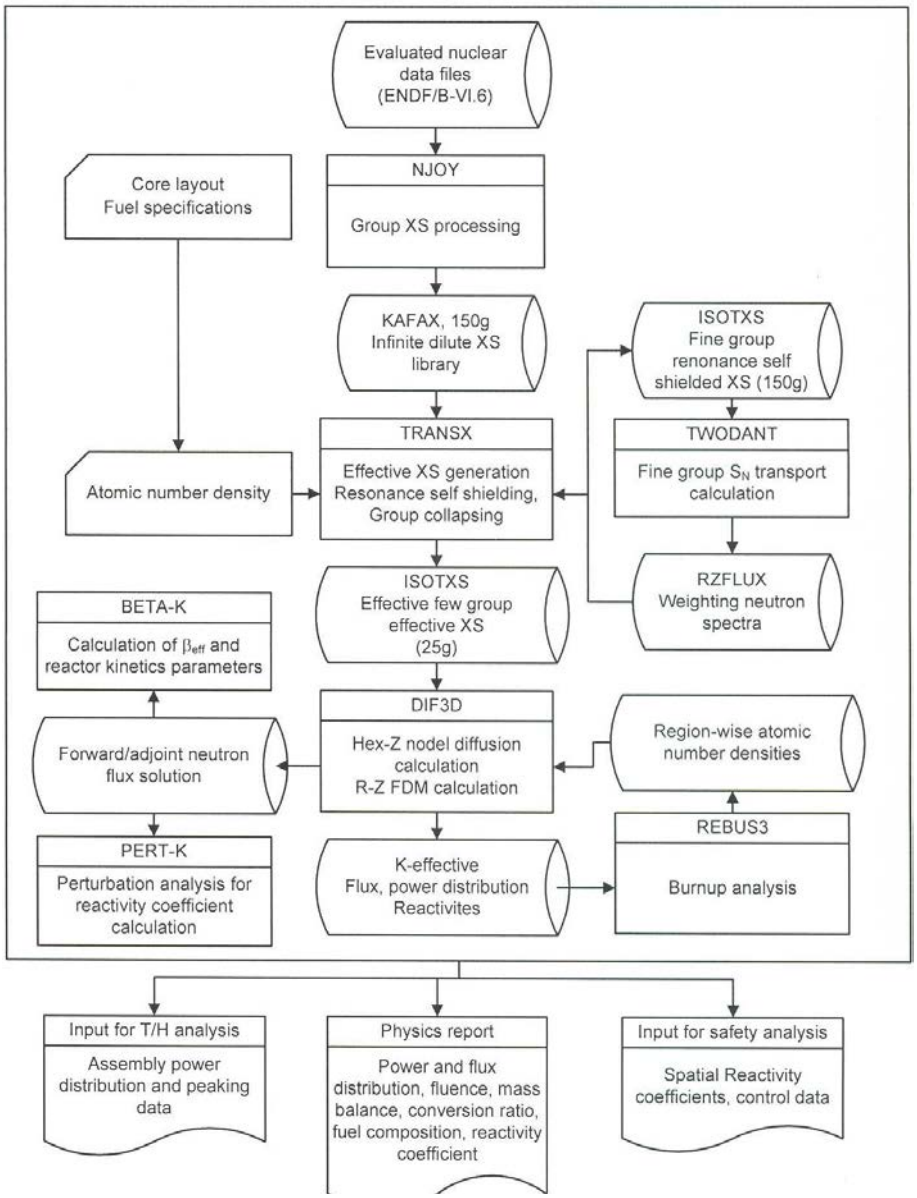

FIG. 6.1. K-CORE System.

The nuclear evaluation process is initiated by the generation of regionwise microscopic cross sections, based upon the self-shielding f-factor approach. 150-group neutron cross section library version KAFAX (KAERI Fast XS)/E66 [97] is prepared for general applications, based on ENDF/B-VI evaluated nuclear data files using the NJOY data processing. KAFAX contains infinite dilute cross sections for various.

Composition-dependent, region-wise microscopic cross sections are generated by utilizing the effective cross section generation module consisting of TRANSX [98] and TWODANT [40] codes and the pre-processed KAFAX library. For this process, nuclide densities and other composition and geometry information for each region are separately provided, based on the core layout and core component design determined previously.

The effective cross section generation module provides multi-group cross section libraries in a format that can be directly applicable to discrete ordinates (S_N) approximation and diffusion calculations in the flux solution module. The data processing in this module includes resonance and spatial self-shielding corrections, reactor and cell flux solutions, and cross section group collapsing. Resonance self-shielding calculations for each region are based upon the Bondarenko f-factor approach using narrow resonance (NR) approximation. Cell homogenization over each region is performed to obtain the cross section data for a homogenized mixture. Neutron spectra for collapsing the cross section data to fewer group libraries is obtained from S_N approximation flux solution calculations for a two-dimensional reactor model as desired. The pre-processed 150-group library is generated using a fixed library neutron spectrum typical of a fast reactor.

The 25 group cross section library is used for basic neutronic computations. The reference region-wise temperatures used in the data processing calculations are taken from the core thermal-hydraulic analysis for the steady-state full-power operating condition. Cell calculations are carried out with elevated temperatures to generate fuel cross sections for calculating the Doppler Effect. A set of cross sections is also generated for the sodium void reactivity calculation by removing all flowing sodium from fuel assemblies.

6.2.2. Neutronics calculation methods

6.2.2.1. Diffusion, transport, Monte Carlo methods

6.2.2.1.1. Diffusion method

Due to the improved efficiency of transport theory methods and advances in computer hardware, the use of transport theory methods for reactor core calculations is now increasing. However, diffusion theory still remains the main tool for fast reactor designs primarily because (1) the application of the diffusion approximation is satisfactory for most purposes in the active core region, and (2) the diffusion equation is relatively simple, and its properties and the appropriate methods to solve it have long been well known. Applicability of the diffusion approximation requires that the condition of a nearly isotropic distribution of angular neutron fluxes is sufficiently well satisfied. This means that the application of the diffusion approximation becomes questionable in the immediate neighborhood of local neutron sources, external boundaries and internal interfaces between material regions with different nuclear properties. Depending on the neutron energy and geometrical arrangement of materials inside a reactor, the allowed range of application may also be restricted within strongly absorbing media (control rods) and within components surrounding the reactor (blankets, reflectors, etc), where one could expect that the neutrons would exhibit a

pronounced preference for the outward flight direction, which is not in accordance with the diffusion theory assumption of nearly uniform angular distributions of neutrons.

The methods and codes applied to solve the multi-dimensional diffusion equation are well established. Most of the current whole-core diffusion theory codes are based on the advanced nodal methods developed mainly in early 1980s, although finite difference methods are still in use. The finite difference methods calculate a single value of the average flux in each mesh interval, or on each surface of the mesh interval for a regular geometry grid in XYZ, RZ, triangular-Z, or hexagonal-Z geometry with each mesh interval having constant cross sections. The most frequently cited three-dimensional diffusion codes based on finite-difference methods for fast reactor calculations are DIF3D [99], TRIGEX [100], DEGEN [101], CITATION [102], 3DB [103], and D3D [104].

The nodal codes solve the three-dimensional diffusion equation in Cartesian and/or hexagonal geometries using the homogenized assembly cross sections. Among dozens of different nodal methods, those based on the transverse integration procedure are most widely used in production analysis. In these methods, the transverse leakages are typically approximated with quadratic polynomials, and the resulting set of one-dimensional equations is generally solved with the nodal expansion method or the analytic nodal methods. However, the final algebraic equations are formulated in various forms and solved with different solution and acceleration schemes including Krylov subspace, domain decomposition, coarse-mesh rebalancing, and non-linear iterative methods. The most frequently cited nodal codes for fast reactor applications are DIF3D [105] and HEXNOD [106].

Applications of the advanced nodal method were significantly extended in the last decade. Due to the high efficiency of nodal method and advances in computer hardware, the whole-core analysis can now be performed in a fraction of a minute. This has led to the direct use of advanced nodal codes for whole-core depletion calculation [107]. Various three-dimensional, spatial kinetics capabilities were also developed based on the advanced nodal methods. These high fidelity kinetics methods are important for core transients involving significant variations of the flux shape.

6.2.2.1.2. Transport method

In some applications diffusion theory may be too approximate, especially if a pronounced angular dependence of the neutron flux exists in a reactor region. Whole-core multi-dimensional deterministic transport theory calculations were very slow and almost impractical in the 1970's. But progress in computers and calculation methods has led to the increasing use of transport theory calculations for fast reactor applications. Efficient methods for multi-dimensional neutron transport calculations have been developed and applied in computer codes during the last 20 years, including the traditional spherical harmonics method [108], the discrete ordinate method [109–116], the method of characteristics [117], the transverse-integration nodal transport method [65, 106, 118, 119], the variational nodal transport method [120–122], and the collision probability method [123].

In the last decade, the discrete ordinate methods were significantly improved for three-dimensional whole-core transport theory calculation. The production codes include ATTILA [112], PARTISN [114], PENTRAN [115], THREEDANT [111], and TORT [116]. These codes solve the multi-group transport equation on two- and three-dimensional orthogonal or unstructured meshes. Various spatial discretization schemes are employed including the diamond and weighted diamond difference, linear and exponential

discontinuous, discontinuous finite element, nodal, and characteristic methods. The source iteration approach is used to solve the discretized equations with various acceleration schemes such as the diffusion synthesis acceleration, coarse mesh rebalancing, partial current rebalancing, and multi-grid methods. Parallel computation capabilities are available in PARTISN, PENTRAN, and TORT. The time-dependent transport equation can also be solved using the PARTISN code, where the Crank-Nicholson method is used for time differencing.

In 1980s, nodal transport methods based on the transverse integration procedure were intensively developed, because these methods provide the larger part of the transport correction to diffusion theory at a very low additional cost to the nodal diffusion method. The transverse integration approach involves transversely integrating the neutron balance equation to reduce it to a set of one-dimensional equations containing a transverse leakage term as an extra source term. Nodal balance equations are then derived from the set of coupled one-dimensional neutron balance equations, each of which is obtained via transverse integration along a different orthogonal direction. This method was originally developed for rectangular nodes. When applied to a hexagonal node, however, the transverse leakage becomes very complicated and contains non-physical singular terms of step function and delta-function types, which destroys the nice features appearing in the nodal equations for rectangular nodes. In the HEXNOD code [106], the approach is simply to ignore these singular terms. To compensate for ignoring these terms, the transversely averaged flux is artificially modified to retain the neutron balance equation in a hexagonal node. The advantage of this technique is that the nodal equations remain essentially identical to those for rectangular nodes (except, of course, for having three instead of two sets of nodal equations on a radial plane). This method works reasonably well for fast reactor core calculations like control rod worth calculations [106]. Another approach to handling the singular terms in the transverse leakage is to split each singular term into two parts, each of which is not singular by itself. This approach is implemented in the HEXTR code

The variational nodal transport method based on the second-order formulation of transport equation was more recently developed and implemented in the VARIANT code [122] for fast reactor applications, which solves multi-group transport problems in two- and three-dimensional Cartesian and hexagonal geometries. This method guarantees nodal balance and permits refinement using hierarchical complete polynomial trial functions in space and spherical harmonics or simplified spherical harmonics in angle. The even angular parity flux equations are solved within the nodes, and the continuity between nodes is provided by even- and odd-parity flux moments. The final algebraic equations are cast into a response matrix form and solved with red-black partial current iterations. Recent developments include a spatial kinetics capability, a sub-element method to treat the within-node heterogeneities, and a first-order spherical harmonics method to treat voided nodes. The VARIANT code was also incorporated in the European system of codes ERANOS [124].

The last direction in transport theory methods development to be mentioned here is the collision probability method. This method is usually used for cell problems, but has also been applied to reactor and shielding calculations [123]. The collision probability method starts from the integral transport equation and requires calculating the probabilities, P_{ii} and P_{ij}, respectively, that a neutron born or traveling in region i of a cell will have its next collision either in the same region i or in some other region j. The numerical integrations are facilitated by using some reciprocity and addition relationships. For simple geometries (one-dimensional plane, cylindrical, and spherical geometries, in particular) the calculation of the probabilities P_{ii} and P_{ij} is straightforward (involving exponential integrals, Bickley functions and

associated functions). It is more complicated to calculate P_{ij} for a sophisticated system, such as an array of pins (or more complex geometries). Some simplifying modelling assumptions must be made regarding the starting distribution of neutrons. There are two alternatives: (1) use a flat source distribution within a fairly small volume element, which leads to simple expressions for the collision probabilities but may demand a fine subdivision; (2) use a fairly coarse subdivision into a few, fairly large volume elements, which requires improved approximations for a source distribution (i.e. linear or quadratic shapes). The optimum choice must be found between these two possibilities. An interesting approach was suggested in [125] involving calculating collision probabilities in complex geometry systems using Monte Carlo codes. This approach removes the geometric limitations of the method.

6.2.2.1.3. Monte Carlo method

Several codes are available for carrying out a direct Monte Carlo simulation of a reactor problem using detailed geometrical models and continuous energy (or very fine group) representation of nuclear data. These can be used to provide reference values and investigate the effects of approximations in deterministic methods. Some widely used Monte Carlo codes are MCNP [126], MORSE [127], KENO [128], MVP [129], TRIPOLI [130] and VIM [131], among others.

Monte Carlo codes are relatively rarely used in fast reactor design, partly because they are usually time consuming. This also must be a reflection of the success of the standard deterministic methods, which involve a hierarchy of approximations, usually beginning from a simple cell or fundamental mode treatment of fine energy, followed by calculations in a more complex geometry in a coarser energy mesh, and finally a whole reactor three-dimensional calculation with few energy groups and a coarser spatial mesh.

The best of these deterministic methods, correctly applied, give a perfectly adequate treatment of most reactor problems. However there are some important benefits from a more direct model of the physical problem. The current deterministic methods involve so many specialized approximations, the focus of many man-years of specialists' effort during their development, that their range of validity is sometimes well understood only by their originators. It is difficult to conceive of a way in which the next generation of users of these codes, or even a group maintaining them, could become fully conversant with them. Under these circumstances, there is always a danger that a code will be incorrectly applied to some new problem which appears to be not too dissimilar to established problems but is actually outside the range of validity of the method, producing misleading results.

If difficulties of this kind are to be avoided, potential users will have to be trained to an exceptionally high level in the modelling techniques used in the old methods, and the overhead in doing this will be high. The Monte Carlo method could be the remedy. Due to its inherent slowness relative to the deterministic methods, it cannot be used at present for all routine calculations. However, it can provide reference values which are transparent to physicists and engineers.

Monte Carlo codes are more flexible than the currently available deterministic code schemes for treating reactor geometries and cross section data. They can be used to treat any reactor type (provided that the cross section preparation scheme is sufficiently accurate). However the validity of the cross section data must be checked. Not all of the available Monte Carlo codes have data libraries which are suitable for fast reactor applications, the reason being that they are not able to treat self-shielding effects in the unresolved energy region. This can be done, for

example, by applying the subgroup approach for group cross section data (MMKFK [132], or by using probability tables for continuous energy data. Most of recent Monte Carlo codes can treat probability tables (for example, MCNP4C or later, VIM, MVP, TRIPOLI, etc).

The probability table method, implemented in VIM, may be seen as a particular case of the subgroup approach suitable for a "continuous" cross section representation. The main steps to calculate probability tables for VIM are the following:

- For each spin series of resonances, the resonance spacing and width distributions are sampled to obtain a ladder of resonances;
- Pointwise cross sections are reconstructed from the resonance parameters with Doppler broadening to the desired temperature;
- The average values of the partial cross sections between energy points on the grid are then binned by total cross section value, with weight equal to the energy interval;
- The above steps are repeated until some test parameter is exceeded and the average cross section in each bin is then calculated;
- The comprehensive probability distributions thus formed are condensed into a library of tables with a small number of bands.

The VIM code was probably the first Monte Carlo code especially tailored to treat continuous energy neutron data in a manner suitable for general fast reactor problems. Mention can also be made of the MOCA Monte Carlo code, which has been used for fast reactor control rod calculations and is included in the ERANOS scheme. Hybrid schemes of coupling Monte Carlo and deterministic methods were also used. In this approach, the Monte Carlo method is applied only for treating sub-regions having complex geometry. Outside these complex domains, simpler and quicker deterministic methods are used. A detailed review of these combined methods is presented in [133].

As with deterministic methods, significant improvements have been made in Monte Carlo codes with the rapid advance of computing power. Parallel computation capabilities have been implemented in most production codes. Parallel processing has extended the applicability of Monte Carlo simulation to much wider range of problems. Library production approximations to accommodate limited computer memory have been reduced. The number of cross section points has been increased significantly, and the interpolation error thinning criteria have been tightened. To reduce the computational time by achieving acceptable statistics with fewer histories, efficient global variance reduction techniques have also been developed. For example, the variational variance reduction methods [134] have been developed for eigenvalue calculations. These approaches rely on global estimates of both forward and adjoint functions. The adjoint function is determined from a multigroup Monte Carlo simulation and is used to derive variance reduction parameters for the continuous Monte Carlo simulation of the forward problem. Some of these include hybrid approaches to determine efficiently the biasing parameters by using approximate deterministic calculations or defining accurate functionals for desired responses by using deterministic adjoint and Monte Carlo forward information.

There has recently been more reliance on Monte Carlo tools for depletion calculations. The method is particularly useful for analysis of specified designs but not sufficiently efficient for use in parametric and trade studies required for developing an optimized design. A lot of coupled Monte Carlo and depletion code systems have been developed for the analysis of advanced systems. The popular coupling is the linkage of MCNP with the ORIGEN2

depletion code [135] such as MONTEBURNS [136], MOCUP [137], MCODE [138], MCWO [139], and ALEPH [140]. The coupled systems based on the other codes have been also developed such as KENO/ORIGEN-S [141], MCNPX/CINDER90 [142], SWAT (MVP/ORIGEN2) [143], MVP-BURN [144], RACER [145], VMONT [146], etc. The Monte Carlo technique is attractive because of the ability to represent accurately nuclear data details and to treat complex geometries. Propagation of the Monte Carlo statistical uncertainty during depletion calculations has not been addressed in these tools and future work to quantify (and hopefully control) this problem is required. Without this, results from such methods would be questioned due to un-quantified uncertainty.

6.2.2.2. Computer codes

The most widely used tool in the USA for fast reactor neutronics calculations is the DIF3D/REBUS-3 system developed at Argonne National Laboratory. The DIF3D code system is a multi-group steady-state neutron diffusion and transport theory solver. It provides three flux solution options: finite-difference diffusion theory [99], nodal diffusion theory [118], and variational nodal transport theory [122] methods. Eigenvalue, adjoint, fixed source and criticality (concentration) search problems are permitted. Flux and power density maps by mesh cell or node and region balance integrals are provided. Although primarily designed for fast reactor problems, DIF3D treats up-scattering. The DIF3D finite difference option solves one-, two- and three-dimensional orthogonal and triangular geometry diffusion theory problems. The nodal option solves the multi-group neutron diffusion equations in two- and three-dimensional hexagonal and Cartesian geometries using the nodal expansion method. Equivalence Theory parameters (discontinuity factors) are permitted with hexagonal nodal models. The variational nodal transport theory option (VARIANT) solves the multi-group steady-state neutron transport equation in two- and three-dimensional Cartesian and hexagonal geometries. The nodal equations of the VARIANT option are derived by reformulating the even-parity transport equation as a variational principle and incorporating the odd-parity flux at the interface as a Lagrange multiplier. Anisotropic scattering up to P_5 is treated, and the even- and odd-parity fluxes are expanded in orthogonal trial functions of space (up to 50^{th} and 9^{th} order polynomials for even- and odd-parity fluxes, respectively) and angle (spherical harmonics up to P_{15} or simplified spherical harmonics up to order 99). The DIF3D-nodal and VARIANT options have the capability of performing pin flux and power reconstruction calculations.

The DIF3D-nodal and VARIANT options were extended to solve the multi-group time-dependent neutron diffusion and transport equations, respectively. These spatial kinetics capabilities are called DIF3D-K [147] and VARIANT-K [148], respectively. Two formulations were implemented for time discretization, the direct “theta” method and the space-time factorization method. The theta method is a variable time integration scheme which permits the resulting difference equations to range from fully explicit to fully implicit. For a given value of the variable parameter “theta”, the time-dependent problem reduces to a sequence of "fixed source" problems in which the fixed source term is composed of quantities computed from the solution of the previous time point. The factorization method allows the use of the improved quasi-static, adiabatic, or conventional point kinetics option for treatment of the time dependence. In the improved quasi-static option, the same algorithm (with theta = 1) used for the theta scheme is employed with large time-step sizes to determine the flux shapes. In the adiabatic option a series of time-independent eigenvalue problems are employed to obtain the flux shapes. In the conventional point kinetics scheme, the initial steady-state shape is used for the duration of the transient problem. In all these factorization

options, the flux amplitude is obtained from the solution of the point kinetics equations employing time-dependent kinetics parameters evaluated by the code. The DIF3D-K and VARIANT-K spatial kinetics capabilities were coupled with the SAS4A and SASSYS-1 system dynamics and safety analysis code system [149] for coupled neutronics/thermal-hydraulics transient analyses [150].

REBUS-3 [107] is a system of codes designed for the analysis of fast reactor fuel cycles. Two basic types of problems are solved: (1) the equilibrium conditions of a reactor operating under a periodically repeating fuel management scheme and (2) the explicit cycle-by-cycle, or non-equilibrium, operation of a reactor under a specified periodic or non-periodic fuel management programme. It allows flexible user-defined burnup chains, with no limit on the number of nuclides. The isotopes to be considered in the burnup equations, as well as their transmutation reactions, are specified by the user. Various neutronics flux solvers are available: all the options of DIF3D, TWODANT, and MCNP. The total reactor burn cycle time is divided into one or more subintervals, the number of which is specified by the user. An explicit nuclide depletion computation is performed in each region of the reactor over each of these subintervals using the average reaction rates over the subinterval. These average reaction rates are based on fluxes computed at both the beginning and end of the subinterval. The nuclide transmutation equations are solved by the matrix-exponential technique. REBUS-3 provides a general external cycle modelling capability: a flexible reprocessing scheme with user-specified allocation of discharged fuels to multiple reprocessing plants and isotope-dependent recovery factors, a flexible re-fabrication scheme with multiple reprocessing plant outputs and external feeds and a user-specified multi-level priority scheme for distributing available atoms to different fuel types, and modelling of time delays between various processes and radioactive decays. Four types of search procedures may be carried out in order to satisfy user-supplied constraints:

- Adjustment of the reactor burn cycle time to achieve a specified discharge burnup;
- Adjustment of the fresh fuel enrichment to achieve a specified multiplication constant at a specified point during the burn cycle;
- Adjustment of the control poison density to maintain a specified value of the multiplication constant throughout the reactor burn cycle;
- Adjustment of the reactor burn cycle time to achieve a specified value of the multiplication constant at the end of the burn step.

A companion code RCT [151] recovers detailed pin burnup characteristics from REBUS-3 fuel cycle calculations in hexagonal-Z geometry using the DIF3D-nodal option. It reconstructs intra-assembly distributions of multi-group fluxes, power densities, burnup, and nuclide number densities.

VIM [132] solves the steady-state neutron or photon transport problem in any detailed three-dimensional geometry using either continuous energy-dependent ENDF nuclear data or multigroup cross sections. Neutron transport is carried out in a criticality mode, or in a fixed source mode (optionally incorporating subcritical multiplication). Photon transport is simulated in the fixed source mode. The geometry options are infinite medium, combinatorial geometry, and hexagonal or rectangular lattices of combinatorial geometry unit cells, and rectangular lattices of cells of assembled plates. Boundary conditions include vacuum, specular and white reflection, and periodic boundaries for reactor cell calculations. VIM uses standard Monte Carlo methods for particle tracking with several optional variance reduction techniques. These include splitting/Russian roulette and non-terminating absorption with non-analog weight cutoff energy. The multiplication factor is determined by the optimum linear

combination of two of the three eigenvalue estimates - analog, collision, and track length. Resonance and smooth cross sections are specified point-wise with linear-linear interpolation, frequently with many thousands of energy points. Unresolved resonances are described by the probability table method, which allows the statistical nature of the evaluated resonance cross sections to be incorporated naturally into the representation of self-shielding effects. Neutron interactions are elastic, inelastic and thermal scattering; (n,2n); fission; and capture, which includes (n,t), (n,p), (n,α), etc. Photon interaction data for pair production, coherent and incoherent scattering, and photoelectric events are taken from the MCPLIB of the MCNP code. Trajectories and scattering are continuous in direction, and anisotropic elastic and discrete level inelastic neutron scattering are described with probability tables derived from ENDF/B data. VIM has an automatic restart capability to permit user-directed statistical convergence. In eigenvalue calculations, the beginning source sites are from a random guess or can be provided via ASCII input or from a previous calculation. The starting neutrons for each subsequent generation are randomly selected from the potential fission sites in the previous generation. Track-length or collision estimates of reaction rates are automatically tallied by energy group and edit region to facilitate comparison to other calculations. Group-wise edits include isotopic and macroscopic reaction rates and cross sections, group-to-group scattering cross sections, net currents, and scalar fluxes. Particle pseudo-collisions are used to estimate microscopic group-to group (n,2n), inelastic, and P_N elastic scattering rates. A serial correlation of eigenvalue estimates is computed to detect underestimated errors.

In the Russian Federation, most codes for neutronics calculations of fast reactors solve a transport equation in diffusion approximation. Now such codes are really used as TRIGEX [152], JARFR [42], GEFEST [153], and FACT-BR [154]. Their brief description is presented further in the report.

TRIGEX is developed for three-dimensional calculation of fast reactors in hexagonal geometry. Recently it allows calculating reactors with a square lattice also. An improved coarse mesh discretization of a transport equation in diffusion approximation is used for construction of the numerical scheme. The number of energy groups is limited to 26 now. The solution of a homogeneous problem and problem with an external source, and also joint problem is possible. Last problem allows carrying out calculation of functionals of the perturbation theory. Essential feature of the code is presence of the module for calculation of FFCP cell. The code carries out calculation of cylindrical or plane cell with use of a method of the first flight collision probability (FFCP). Resonance self-screening of cross-sections is taken into account in sub-group approximation. TRIGEX is widely used in research and design studies on SFR such as BN-600, BN-800, CEFR, innovative designs. The presence of the FFCP module allows using this code also for the analysis of experiments carried out on both operating reactors (BN-350, BOR-60, BN-600) and critical facilities (BFS) taking into account heterogeneous structure of last ones.

JARFR is widely used in design developments on SFR and also for analysis of innovative designs of fast reactors. It also provides calculation of neutronic reactor characteristics in multigroup diffusion approximation. The solution is defined by a method of source iteration and by a successive over relaxation (SOR) method in each energy group. The effective techniques of increased accuracy are realized. One of them is based on updating nonlinear Askew coarse mesh method, another is based on an approach specified for nodal methods when an additional set of unknown data is included into numerical scheme - unilateral surface neutron currents (IIS scheme). The code complex provides solution of homogeneous forward and joint problems, and also problem with an external source. The calculation algorithms of the first order classical perturbation theory and generalized perturbation theory for calculation

of sensitivity coefficients of fraction-linear functionals are realized. The code is intensively developing. Now the code version JAR-IQS is developed for solution of spatial neutron kinetics which will provide dynamic calculation for innovative reactors.

The code complex GEFEST is created for operational neutronic calculations of SFR in multigroup (from 1 up to 26 groups) diffusion approximation in three-dimensional hexagonal geometry. Now it is used in BNPP with BN-600 reactor. The code complex allows calculating neutron fields and energy release distributions in 20 000 nodes of reactor model taking into account a real position and movement of control rods. It is supposed that the basic calculations are carried out in two-group approximation.

The code HEX3D is used as a neutronics calculation program in the code complex, which provides finite-differences method of multigroup diffusion equation solution in three-dimensional hexagonal geometry with a calculation point at the centre of a cell. A step along height is variable. The fuel archive is an important component of the code complex, which contains passport data of fuel subassemblies (FSA), their characteristics reflecting a burnup mode during stay of FSA in reactor. There are realized algorithms of the perturbation theory for calculation of reactivity effects in the code complex. There is an opportunity to solve the kinetic equations in quasi-steady approximation. The necessary parameters of the equation for amplitude function (lifetime of prompt neutrons and fractions of delayed neutrons) also are determined in the code complex.

FACT-BR is based on the methodical approaches similar with those in above described codes. A multigroup (up to 26 groups) diffusion approximation is used for calculation of three-dimensional distribution of neutron flux density. The diffusion equation is solved either by finite-differences method or by nodal method. A method of incomplete factorization is used for solution of finite-differences equations of large dimensions. One-dimensional approximation dependences for each FSA are used for calculation of core thermal hydraulic parameters (fuel temperatures and densities lead coolant). A specially developed algorithm is used for calculation of three-dimensional power distribution up to each fuel pin. The development of a block of spatial neutron kinetic calculation is carried out to provide joint dynamic calculation together with thermal hydraulic dynamic code based on a porous body model. This code is the basic tool in design studies of BREST reactor with heavy liquid metal coolant.

The codes based on Monte-Carlo method are developed for a quite long time. Alongside with the Russian codes, foreign programs such as KENO and MCNP began to be used in calculations. Now there is developed a code complex MMKKENO [53] on the basis of the MMK-FK and KENO codes, which is applied at planning and analysis of experiments on critical assemblies, reference precise calculations of BN-600, BN-800 reactors.

The MMKKENO code is the essentially modified version of the US KENO-V$_a$ code [155] with the new geometrical standard modules included in it. This standard is closed to the standard of the Russian MMKFK code [156]. The code has higher calculation efficiency (by times and sometimes by order) in comparison with KENO VI code [157] which gives similar geometrical opportunities. Recently essentially new functional possibilities in comparison with KENO-Va are realized in MMKKENO code. There are created:

- Options for calculation of effective fraction of delayed neutrons β_{eff};
- Some options for calculation of k_{eff} perturbation due to change of materials in separate parts of reactor, which are based on a method of correlated weights or on a method of correlated trajectories;

– Some options for calculation of k_{eff} sensitivity coefficients to group macro-constants of materials, which are used for calculation of k_{eff} sensitivity coefficients to group micro-constants.

The Monte-Carlo MCNP code widely distributed in the world is used for problems requiring not group (detailed) performance of cross-sections of interaction of neutrons with substance, for tasks of calculation of shielding of complex geometry, and also for comparative calculations. The group constants ABBN-93 are connected to this code with the help of FORMCNP code [158] developed at the Institute of Physics and Power Engineering (IPPE) located in Obninsk, Russian Federation.

Perhaps one of the most important features of the described software is the maintenance of uniform binding to constant system of fast reactor calculations on the basis of library ABBN-93, and also close cooperation of the designers of the above described software. As result, it is possible to assert that now there is a stable system of software and constant maintenance of fast reactor calculations. Its scheme is presented in Fig. 6.2.

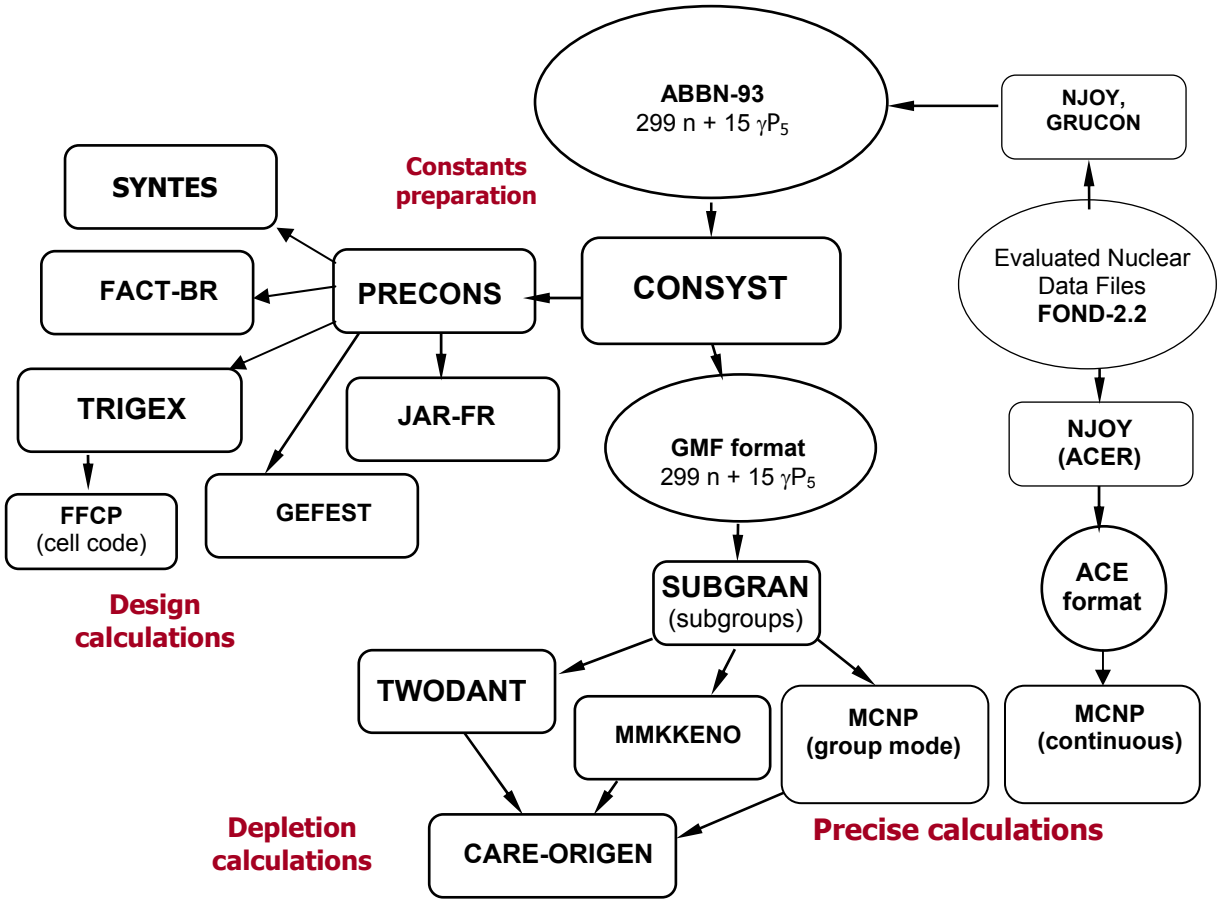

FIG. 6.2. Scheme of constant system and software for fast reactor neutronics calculation in the Russian Federation.

The task of association or creation of a uniform code instead of several similar ones is not yet urgent, since a system of the users has been also formed, each of them has chosen software with service functions optimally met his tasks.

In Germany, deterministic neutron flux calculations are performed at FZK mainly with the DANTSYS [111] and VARIANT [159] codes. The family of D3D/D3E [104] finite difference diffusion codes (developed at FZK in the past) is now used less often due to the fact that neutron transport codes are running rather quickly and avoid the diffusion approximation. The development of other FZK neutron transport codes was discontinued in early 1990s together with the fast reactor development; by that time these codes did not reach the level of maturity that would recommend their routine application.

The DANTSYS neutron transport S_n finite-difference code includes 1D (ONEDANT), 2D (TWODANT) and 3D (THREEDANT) models. These 2D and 3D models are currently incorporated in SIMMER-III [160] and SIMMER-IV [161]. DANTSYS can also be used as a stand-alone code linked either to KAPROS or to the C^4P data library. Routine reactor analyses are often performed at FZK with TWODANT in RZ geometry. Due to the application of the diffusion synthetic acceleration scheme, DSA [162], the code performance was improved dramatically compared to S_n neutron transport codes applied before. A significant effort was paid at FZK during the last decade [71] in order to improve the reliability of TWODANT and to optimize incorporated acceleration techniques, in particular for models with relatively coarse spatial meshes (as often applied in transient analyses due to computer resource limitations). A similar, but smaller effort was devoted to THREEDANT, that is applied at FZK more rarely, for 3D analyses in XYZ and R-Theta-Z geometry.

VARIANT, a nodal 3D hexagonal-Z/XYZ transport (2D and diffusion models are also available) code, is included in ERANOS and can also be used as a stand-alone code linked either to KAPROS or to the C^4P data library. The hexagonal-Z geometry capability is used for fast reactor applications. When appeared first, VARIANT offered an unprecedented performance with respect to hexagonal-Z full core transport calculations. It should be mentioned that the nodal transport calculations in hexagonal-Z fast reactor cores were pioneered by HEXNOD. However, the original HEXNOD neutron transport model was not able take into account suitably well neutron transport effects (as compared to diffusion theory based results) for some important cases (in particular for designs, in which the upper fertile blanket was replaced by a sodium "plenum" above core in order to reduce the coolant void effect).

The VARIANT solution scheme, based on the Variational Nodal Method [160], was shown to be sufficiently accurate for many fast reactor models analyzed. However, it may potentially encounter some problems if it is applied in a straightforward manner for analyses of e.g. distorted configurations, which contain very low density regions, due to its particular feature of using second-order form of the transport equation.

One may also mention using of BISTRO [109, 163], a module of ERANOS (BISTRO is similar to TWODANT in many respects), and CITATION [164], a finite-difference diffusion code linked to KAPROS. The BISTRO code has both S_n transport and diffusion options. The diffusion option is also used in the transport module for convergence acceleration. An efficient solution from BISTRO code is obtained by using the successive line over-relaxation method, the alternating direction implicit method or the strongly implicit method.

A module that extends the VARIANT application for kinetics and perturbation calculations, KIN3D [165], is used and extended at FZK since many years, the extended VARIANT version being often referenced as VARIANT-K. This kinetics capability (that includes spatial kinetics options) can be applied on the "stand-alone" basis for modelling transients provided that the transient conditions are known in advance (as may happen e.g. in a zero-power reactor experiment

or in a computational benchmark exercise aimed to validate a "coupled" - with thermal-hydraulics — dynamics model) or offers a basis for coupling with a thermal-hydraulics code. A particular feature of the KIN3D perturbation capability is the option to compute spatial distributions of reactivity coefficients for a finer axial mesh than applied in neutron flux calculations [166], thus facilitating coupling with Lagrangian thermal-hydraulics codes, like SAS4A.

Burnup and related studies are performed at FZK since long time by using KORIGEN [167], an extended in Karlsruhe version of ORIGEN [168]. The code is employed together with proprietary nuclear data libraries, which contain, in particular, 1-group cross-sections for different reactor types. For some applications, the 1-group cross-sections used by KORIGEN should be given for different burnup steps (in order to take into account variations of neutron spectra due to variations of the isotopic composition). Thus, additional burnup models can be applied to produce these data for KORIGEN, such as the KARBUS procedure of KAPROS [73] or the TRAIN code [169] linked to C^4P and auxiliary JEFF 3.1 libraries. The modelling options of KARBUS and TRAIN may not offer all options of KORIGEN, but they are coupled with data libraries, cell and neutron transport codes described before, thus providing an option to generate data for KORIGEN and to perform burnup simulations on a stand-alone basis if the set of the options that they offer is sufficient for a particular case.

In India, the computer code CHANDY [170] has been developed to compute fission products and actinide activities. Recently fuel isotopic composition change has been studied [171] using ORIGEN2 code. It was found that due the mixing of high quality Pu from radial blanket fuel with core fuel, it is possible to maintain nearly same Pu composition with several reprocessing cycles. The concept of ^{239}Pu equivalence can be applied to compensate for any variation. The ORIGEN2 code is being used for nuclide evolution studies also. Its database has been updated using recent data, viz. ENDF/B-VI for cross-sections and FP yields, and JENDL for the decay data. With this updated database, ORIGEN2 calculations have been done for Prototype Fast Breeder Reactor [172], and also a few variants of FBTR. For the fast breeder reactor model developed under the IAEA CRP on "Studies of Advanced Reactor Technology Options for Effective Incineration of Radio-active Waste", calculations were done using the updated database. The effect of spread in cross-sections over different evaluations, viz. ENDF/B-VI, JENDL-3.3, and JEFF-3.0 [173], on the prediction of safety-related parameters of this model, was found to be within ±10%.

In the Republic of Korea, fuel cycle calculations are carried out with the neutron flux and burnup calculation module consisting of DIF3D [99] and REBUS-3 [107] codes. The 25 group cross sections are used for all depletion analysis in the K-CORE System. Flux solution calculations solved the coarse-meshed nodal diffusion equation for hexagonal-Z reactor representation. The REBUS-3 burnup calculations use the complex U-Pu chain model having descriptions for all the U-Pu-MA isotopes to analyze the core composition change during a fuel cycle. The one type of burnup calculations: equilibrium cycle calculation is performed for burnup analysis. For an equilibrium core, the fuel cycle computations for the operating interval under a fixed fuel management scheme are solved; this equilibrium cycle calculation approach approximates reactor characteristics after many cycles of operation subject to a fixed, repetitive fuel management strategy. The equilibrium cycle analyses provide good estimates of integral parameters, mass flows, and global characteristics of a reactor after achieving an equilibrium state, while the non-equilibrium cycle analyses calculate reactor behavior when not in equilibrium, e.g., during the first several cycles from startup and provide a detailed local performance characteristics. All the fuel cycle calculations are performed with all the control rods withdrawn.

In order to improve the accuracy of the conventional diffusion nodal method such as the one in DIF3D code, the SOLTRAN [174] code was developed to employ an interface current nodal formulation for the solution of the multi-group SP_2 equations in a hexagonal geometry. The nodal SP_2 equations have been incorporated as an option in the framework of the conventional nodal diffusion equations. By introducing the SP_2 factor α and the SP_2 flux (ζ), the nodal SP_2 equations can be easily incorporated into the conventional diffusion nodal equations. The relationship between the surface-averaged flux and the partial currents at the intra-node interfaces in the SP_2 approximations gives rise to additional term, i.e., the surface-averaged source term, in the response matrix equations. This costs the total computing time of the SP_2 nodal to increase by about 50%.

Numerical comparisons were performed in LMR benchmark problems and it was found that the accuracies of the SP_2 nodal method were improved over the diffusion theory solution. Especially, the SP_2 nodal solutions reduced the error of the multiplication factor up to 50% and there are conspicuous improvements for estimating the region-averaged fluxes in the non-dense or blanket regions with higher neutron energies, where the transport effects are dominant.

6.2.3. Energy production, radioactivity and irradiation damage

Important products of nuclear interactions are energy release, radiation emissions, reaction products (some of which are radioactive) and irradiation damage of materials. The major sources of energy are fission reactions, but the contributions from other reactions are also significant. As a result of neutron interaction with material in a reactor, energy appears from fission reactions predominantly and from parasitic capture reactions. Most of the fission energy appears as kinetic energy of the fission fragments and is deposited close to the point of fission (within about 10 μm). Some recoverable energy after the fission reaction appears as β-and γ-rays when the fission fragments or compound nucleus decay, and some energy appears as prompt γ-rays and kinetic energy of fission neutrons. Not all of the fission energy is emitted promptly; a significant proportion is emitted as energy resulting from the radioactive decay of fission products. This is called fission product decay heat. This component of heating is important in connection with emergency core cooling, in heat removal from a shutdown reactor, and in the design of fuel transfer and transport casks.

A parasitic capture reaction usually leads to the production of γ-rays, and the γ-ray energy depends on the binding energy of the neutron to the compound nucleus. The γ-ray energy of both fission and parasitic capture reactions is deposited over a wide region of the reactor. The heat generation in structural materials is primarily by γ-ray energy deposition, with a partial contribution from neutron scattering. In a reactor static calculation, the recoverable energy generated from fission and parasitic capture reactions is used to normalize the flux level in the eigenvalue calculations. Knowledge of the energy transferred to materials by neutron scattering and γ-ray interactions is required in the design of cooling for control elements, reflector regions, breeder regions and experimental rigs in reactors. Shielding must be provided for biological protection from neutrons and γ-rays and also to protect components from irradiation damage. Materials damage mechanisms include atomic displacements resulting from nuclear recoils, primarily in scattering reactions and in γ-emission, and helium production in (n,α) reactions. Shielding is also required when handling radioactive materials.

The radioactive decay of transuranics and fission products makes a contribution to the decay heat following reactor shutdown and in fuel transport. Spontaneous fission and (α,n) reactions

provide a source in a shutdown reactor which can be used when monitoring the reactivity of the core. If the source is known and the flux is measured, then the reactivity can be derived and the approach to critical monitored. Radioactive decay must also be accommodated in the design of transport casks and in reprocessing plant studies. The long-term heat, radiotoxicity, and dose are dominated by the ^{241}Pu-to-^{241}Am-to-^{237}Np decay chain. The α-decay of ^{242}Cm and ^{244}Cm, and associated neutron emissions from (α,n) reactions, are important in fuel which has undergone a long irradiation. In addition, the high spontaneous fission of ^{252}Cf is also important if multiple recycled LWR spent fuel is introduced into a fast reactor.

Neutron irradiation in the reactor core gives rise to loss of ductility and fracture resistance due to the atom displacement within the material. Traditionally, reactor fluence calculations have been used to measure neutron irradiation damage based on the observation in EBR-II that the displacement per atom (dpa) is proportional to the fast fluence [175]. However, in recent years, displacement per atom cross sections are directly used to evaluate material damage because this approach provides a simpler correlation with ductility that is generally material dependent.

6.2.3.1. Energy release and damage data

The accuracy of the total energy released in fission is better than ±0.5% and the accuracy of the gamma component is better than ±10%. Although the accuracies assessed for the total delayed gamma and beta components are high (~ 1%), the time dependence of the decay heat is known typically only to about ±5%. In addition to the total gamma energies, the gamma spectra are required. This is because the energies of individual gamma rays determine the migration distances and also the probabilities for (γ,n) and (γ,f) reactions. Gamma spectra are stored in nuclear data libraries and converted into group form for reactor calculations. Coupled neutron-gamma cross-section sets are produced and used in coupled neutron-gamma flux and energy deposition calculations.

6.2.3.1.1. Fission product decay heat

Heat generated by fission product decay is calculated by summing the contributions from individual fission products. Summation codes, such as ORIGEN-2 [135] and many similar codes are used for these calculations. The data libraries they require contain fission product yields and decay data (the half-lives, beta and gamma total energy yields, and gamma energy spectra). Fission product capture reactions can have a significant effect on decay heat in some reactors, and the above codes are capable of treating these effects in a simple way, using few-group cross sections and fluxes. These reactions tend to increase the total decay heat by a few percent. For applications where the effects of fission product capture can be neglected or treated by means of a small correction factor, the decay heat can be represented by a sum of exponentials. About twenty exponentials are required to give a fitted accuracy of 1% over the time range of interest in reactor operations (this being more accurate than the actual accuracy of predictions).

The accuracy of fission product decay heat data has been assessed in two ways. The sensitivity of the summation calculations to changes in yield and decay data have been calculated and combined with estimates of the uncertainties in the calculations [176, 177]. The uncertainties estimated for *M(t)*, the decay heat following a long irradiation, are about ±3% for ^{235}U and ^{239}Pu. The uncertainties in *m(t)*, the decay heat following a single fission, are larger, particularly at short times following the fission. They are in the range ±5% to

±10% for times less than 100 seconds. There are larger uncertainties for these short decay times because of the uncertainties in the beta and gamma energy yields of short-lived fission products. Nuclear theory is used to provide some of these data, an example being the Gross Theory of Beta Decay [178] and the work of Klapdor and Metzinger [179]. The accuracies of the data are also assessed by comparing with micro-calorimetric measurements of total heat as a function of time and also with measurements of the separate total beta and total gamma heating components by means of β and γ ray detection [180-182]. The agreement between these measurements and the calculations is not as good as the summation calculation sensitivity studies suggest. The summation calculations tend to be about 5% to 10% lower than the total heat measurements at short cooling times, but there are also significant discrepancies between the different total heat measurements. Work is in progress in several countries to try to resolve these discrepancies, in particular the decay data measurements on short-lived fission products being made at Studsvik. The differences between fission product decay heat for fission in thermal and fast reactors are calculated to be small (<2%). The differences in fission product yields between thermal and fast reactor spectra are small but not well known. However, this source of uncertainty is not considered to be important, and it is not unusual to use thermal neutron fission yields in fast reactor decay heat calculations. At times of the order of 10^7 seconds (116 days), comparable to the time required to transport fast reactor fuel for reprocessing, just a few fission products contribute to the total decay heat, in particular the following:

$^{106}Rh + {}^{106}Ru$	30%
$^{95}Zr + {}^{95}Nb$	30%
$^{144}Ce + {}^{144}Pr$	24%
^{103}Ru	5%
^{89}Sr	1%
Remainder	6%

6.2.3.1.2. Actinide decay heat

The actinide decay heat at short times following the shutdown of a power reactor arises predominantly from the decay of ^{239}U (half-life 1410 seconds) and ^{239}Np (half-life 2×10^5 seconds). This component varies with fuel burnup because of the variation of the number of ^{238}U captures per fission. Alpha decay of ^{242}Cm (half-life 1.41×10^7 seconds) makes a significant contribution to the decay heat at longer decay times. This arises from neutron capture in ^{241}Am produced by the decay of ^{241}Pu (half-life 14.6 years). The fraction of ^{241}Am in the fuel depends on the length of time for which it was stored between the abstraction of plutonium from irradiated fuel and the loading of the plutonium into the reactor, and also the reactor residence time.

6.2.3.1.3. Structural material decay heat

Heat is generated in the steels of the fuel pin cladding and the subassembly wrapper of a fast reactor fuel subassembly by the decay of radioactive products. This component of the decay heat does not exceed 10% of the total decay heat at any time. Integral measurements have been made of the activity induced in structural materials, and these enable this component to be predicted to an accuracy of about ±10%.

6.2.3.1.4. Energy yields and energy deposition

Point energy yield is distinguished from distributed energy yield. The former is the kinetic energy of fission product nuclei produced in fission, nuclear recoil following neutron scattering, and the energies of alpha and beta emissions, and the latter is the energy of neutrons and gamma rays which distribute their energies over a wide range. The gamma energy yield arises from inelastic scattering, (n,γ) reactions, other capture reactions (in association with other emissions such as alpha particles) and from fission. The main sources of energy are fission and capture in the fuel isotopes. The energy produced by capture in the fissile isotopes is about 1% of the energy produced in fission. The energy produced by capture in the principal fertile isotope (^{238}U) is about 2% of the total energy. Thus, capture reactions contribute only about 6 MeV in a total of about 200 MeV per fission. A high accuracy is therefore not required for this capture component when calculating the total heat generation.

The gamma energy is of more importance in calculations of energy deposition in structural materials, for example, for calculating the temperatures of samples in an experimental rig in a reactor. Such a rig might contain samples of structural materials which are undergoing irradiation endurance testing. Irradiation effects are dependent on material temperatures. The main source of heating in many of these cases is the prompt and delayed gamma rays from fission (the two components being of about equal importance). To calculate this heating, the gamma spectrum must be known because this determines both the gamma migration distance and the energy deposition. Only about 3% of the energy is deposited outside the fuel, and about half of this energy is deposited in the fuel cladding.

6.2.3.1.5. Measurements of spatial distributions of gamma energy deposition

These are made in experimental critical assemblies using thermo-luminescent dosimeters. These are also sensitive to beta particles and to the neutron flux. The assumption that beta particle energy is deposited at the point of production cannot be made in the interpretation of these measurements. The migration of beta particles is usually calculated using a Monte-Carlo tracking method. The interaction cross sections of gamma rays with matter are more accurately known than the gamma energy sources and spectra. Consequently, these measurements provide a check on the gamma source data and the methods used for calculating the gamma flux from the source. Gamma interactions are strongly anisotropic, and Monte-Carlo tracking calculations are made when accurate predictions are required. More approximate methods, including equivalent diffusion theory methods, which involve the derivation of effective gamma diffusion coefficients, are used in simplified design methods.

6.2.3.1.6. Radioactivity of irradiated fuel

Kuesters [183] has reviewed the status and requirements for nuclear data relating to the radioactivity of irradiated fuel. He focuses attention on routes for the production of ^{238}Pu, ^{242}Cm and ^{244}Cm because of their strong activity and the neutron sources from spontaneous fission and (γ,n) reactions. In the fast reactors studied by Kuesters, α-decay of ^{242}Cm and the route ^{238}U (n,2n) ^{237}Np (n,γ) ^{238}Pu are the primary sources of ^{238}Pu. For the production of ^{242}Cm, the capture cross sections of ^{241}Am leading to the ground and isomeric states of ^{242}Am are required, and the ^{242}Pu (n,γ) and ^{243}Am (n,γ) cross sections are required for the calculation of the production of ^{244}Cm. The (n,2n) cross sections of both ^{238}U and ^{239}Pu are required for fast reactor irradiated fuel inventory calculations. Measurements of the compositions of irradiated fuel elements provide a check on the nuclear data and can also be analyzed to

provide spectrum-averaged data suitable for fuel inventory calculations. Irradiations of samples of isotopes provide the most accurate data, the PROFIL irradiations in the Phénix reactor being an example of this [184]. Spent fuel analysis is also of high importance in nuclear safeguards investigations. A method called the isotopic correlation technique, which correlates measured isotopic ratios with fuel burnup and plutonium content, is being evaluated as a potential way of monitoring plutonium production.

One requirement is to predict the neutron source in a shutdown reactor so that flux measurements can be used to monitor reactivity changes. Another requirement is for the design of shielding for spent fuel transport and reprocessing. The main neutron sources are ^{242}Cm decay at shorter times and ^{244}Cm decay at longer times. For predictions at shorter times, accurate data are needed for ^{241}Am (n,γ) ^{242g}Am (β decay) ^{242}Cm and the spontaneous fission branching ratio. Since the fission cross section of ^{242}Cm cannot be measured (because of the high background activity), improved nuclear theory methods are required. To improve the accuracy of predictions at longer times, more accurate values of the ^{242}Pu (n,γ) and ^{243}Am (n,γ) ^{244} Cm cross sections are needed.

6.2.3.1.7. Activation of structural and coolant materials

The buildup of strong gamma emitters within the coolant circuit and on reactor components causes maintenance problems. One source of gamma activity in the coolant arises from the decay of ^{58}Co and ^{60}Co. These are reaction products which result from trace quantities of cobalt and nickel which are dissolved into the coolant from components in the primary coolant circuit, activated in the core, and then plated out in various parts of the circuit, such as the pumps and heat exchangers. Integral measurements of reactions which lead to such strongly radioactive products can be readily made in low-power facilities, as well as in experiments made in power reactors (or samples taken from the reactors). Integral measurements made in zero-power critical facilities have accuracy of typically ±5%, and they can be used to predict the reaction rates in power reactors to a satisfactory accuracy of ±10%. However, measurements should also be made in power reactors to check on the importance of competing reactions and the transmutation of the radioactive products themselves. Two-stage reactions, and reactions less easily measured in zero power facilities (such as (n,n'p) which only occurs at high neutron energies), can also be found in this way.

The activity induced in the sodium coolant of a fast reactor is also of importance. The reactions ^{23}Na (n,γ) ^{24}Na (half-life 15 hr) and ^{23}Na (n,2n) ^{22}Na (half-life 2.6 years) are important, as is the activity induced in trace contaminants in the coolant, such as ^{41}K (n,p) ^{41}Ar (half-life 1.8 hr).

6.2.3.1.8. Irradiation damage effects

Atomic displacement damage in structural materials is a function of the nuclear recoil energy, E_r, the temperature, and the presence in the material of nucleation sites for void formation, such as helium (resulting from (n,α) reactions). The recoil energy must exceed threshold energy, E_j, for the atom to be displaced. For recoil energies higher than E_j the number of displacements is approximately equal to E_r/E_j but is less than this number by a factor which increases with increasing recoil energy. This is because there is a greater probability of a recoiling nucleus being displaced into an existing vacancy rather than an interstitial position. There are different models for calculating the number of displacements, one such model being the NRT Model [185]. This has been adopted for international reference use. Having chosen a

model, the displacement cross section can be calculated. It is equal to the sum of the cross sections for each reaction multiplied by the number of displacements for the corresponding recoil energy.

The number of atomic displacements depends on the element, I, and also on the particular alloy. However, this dependence on the alloy is usually neglected, and a displacement cross section for iron is calculated which is used for iron in all different types of steel. The variation of E_j with alloy is not so great as to be significant compared with other sources of variability in the effects of atomic displacements (e.g. temperature, manufacturing method). The (n,γ) reaction contributes to the atomic displacement cross section because of the nuclear recoil which occurs when the γ rays are emitted. Other reactions also contribute, in particular, inelastic scattering, (n,p) and (n,α) reactions. Atomic displacement cross sections have been calculated for a number of structural material elements by Doran and Graves [186], and the data are available in a fine-energy-group form (the SAND II 640-group structure).

Helium embrittlement is another structural material damage mechanism. Helium is produced in (n,α) reactions. Trace quantities of boron and nitrogen in structural materials can make a significant contribution to helium production. Consideration must also be given to (n,α) reactions in isotopes which are formed as a consequence of irradiation; for example: ^{58}Ni (n,γ) ^{59}Ni (n,α).

Integral measurements of (n,α) reactions in structural materials have been made by irradiating samples in power reactors and measuring the helium produced. Uncertainties in the amounts of trace quantities of elements such as boron and nitrogen can introduce large uncertainties into the results. Uncertainties in the shapes of reactor neutron spectra at high energies can also result in uncertainties in the derived data. It is usual to derive equivalent ^{235}U fission spectrum averaged values from these measurements by applying a calculated factor. These are the results quoted, for example, by Gryntakis [187]. For Fe, the values differ by ±30% from the mean value and this uncertainty is larger than the required accuracy of about ±15%.

6.2.3.1.9. Dosimetry

Irradiation exposure is monitored by means of foils or detectors. These are removed following the irradiation, and the induced activity is measured. This induced activity depends on the cross section for the reaction, the time history of the flux, the rate of decay of the activity, and the rate of burnup of the primary isotope and of the activation product. The activity must be sufficiently strong to be accurately measurable, sufficiently long-lived to measure the dose over the time period of interest, and the absorption cross sections of the isotope and the activation product must be sufficiently small for burnup to be negligible or to be a correction which can be accurately made. Dosimetry reactions suitable for different applications have been reviewed, and the chosen dosimetry reactions have been compiled in an IAEA recommended International Dosimetry File, IRDF [188].

Standardization is important because the measured information on irradiated damage effects is often correlated with dosimetry reaction dose measurements. The derived damage cross sections are less accurate than the correlated data because of uncertainties in the dosimetry cross sections used to deduce the flux and flux spectrum of the irradiation. By standardizing the dosimetry cross sections and measuring doses using the same dosimetry reactions, the materials damage can be predicted more accurately. Integral measurements of the dosimetry reactions in standard neutron spectra (or benchmark fields) are used to evaluate the

differential cross sections and, when appropriate, to adjust them, (and also to adjust the characteristics of the reference benchmark fields). These benchmark fields include the ^{252}Cf spontaneous fission neutron spectrum, the thermal-neutron-induced ^{235}U fission neutron spectrum, and a number of well-characterized spectra.

The BR-1 Research Reactor [189] at Mol, Belgium provides one such reference benchmark field facility.

The types of dosimetry reaction can be divided into fission and non-fission, threshold and non-threshold. The choice of the set of reactions to be used for a particular application depends on the intensity of the flux, the duration of the irradiation, the type of reactor spectrum (thermal reactor, fast reactor, core, shielding, vessel), and the neutron energy range of importance in the effect being monitored.

6.2.3.2. Computer codes

A typical code system used in the USA to generate a consistent set of coupled neutron and gamma heating rates involves the NJOY, SDX, and DIF3D codes. The NJOY code is used to produce gamma production and gamma interaction matrices on an intermediate neutron and gamma group basis (typically 230 groups for neutron and 94 groups for gamma). Neutron and gamma KERMA (Kinetic Energy Release in MAterials) factors and other response factors are also produced. Each element of the gamma production matrix represents the probability that a neutron in a given group will produce a photon in a given gamma group. Thus, the macroscopic gamma production matrix when multiplied by the neutron flux yields the gamma source. The TRANSXS [98] processing code is used to convert a MATXS dataset generated by NJOY into an AMPX master file format. For the later use of properly self-shielded neutron interaction group constants from MC^2-2/SDX, the gamma production matrices are transformed back into yield matrices.

The SDX code is used to spatially collapse both the neutron and gamma group structures. The intermediate group data for KERMAs, gamma yield and production matrices, and gamma interaction group constants are used along with user specified spatial region descriptions. A delayed neutron library based on a semi-empirical evaluation of delayed neutron data is also used to account for delayed neutron contributions, which are neglected in NJOY.

The neutron interaction group constants are collapsed using the standard MC^2-2/SDX path. The neutron KERMA factors are collapsed for each spatial region using the SDX calculated spectra. The gamma yield matrices are combined with the self-shielded neutron group constants to form self-shielded gamma production matrices. These matrices are collapsed using the regional neutron spectra.

The gamma collapsing spectra are calculated by considering each region as an infinite medium problem. These infinite medium regional gamma spectra are used to collapse the gamma KERMA factors and gamma interaction group constants.

Neutron and gamma transport calculations are performed using the diffusion or transport solution options of the DIF3D system or the TWODANT code. Following the neutron flux calculation, the gamma source distribution is determined by multiplying the neutron flux and the gamma production matrices. Using this gamma source distribution, the gamma flux calculation is performed as a fixed source problem. The neutron heating distribution is determined by multiplying the neutron flux by the neutron KERMA factors, and the gamma

heating distribution is determined by multiplying the gamma flux by the gamma KERMA factors. The total heating rate is appropriately normalized to the reactor power.

The ORIGEN-2 code and its modified version ORIGEN-RA are generally used for estimating detailed irradiated fuel characteristics by nuclide, including the concentration, mass, activity, total and gamma decay heats, dose hazard limits in air and water, gamma spectra, and neutron source.

The ORIGEN-RA was developed at ANL primarily for EBR-II spent fuel characterization. Various updates were made to nuclear data libraries, and the code was modified to allow the replacement of libraries with problem-specific cross section data, fission product yields, and energy releases per fission and capture. This code is used to perform detailed nuclide transmutation calculations based on the flux history determined from REBUS-3 whole-core depletion calculations and RCT pin burnup calculations.

6.2.4. Static neutronics

6.2.4.1. Power distributions

The predominant source of power in a reactor is the fission reaction. Most of the energy of fission (which is about 200 MeV in total) is the kinetic energy of recoil of the fission fragments, which appears as heat within the fuel. Some of the energy is in the form of kinetic energy of the emitted neutrons, the mean energy of each prompt fission neutron being about 2 MeV, making a total of about 6 MeV for ^{239}Pu. This is deposited as nuclear recoil energy in scattering interactions and in reactions over a wide volume of the reactor. There is also the emission of γ-rays in fission, both prompt emission and the delayed emission in the β-decay of fission product nuclei, about 15 MeV in total. The gamma ray energy is also deposited over a wide region. The heat generation in structural materials is primarily by γ-energy deposition, with neutron scattering also making a contribution. For the prediction of energy distributions the most important requirement is the accurate prediction of fission rate distributions. These are usually well predicted in uniform cores; the problems arise when there are control rods either partly or fully inserted into the core. There can also be discrepancies in the interface regions between different zones, such as core-blanket interfaces, particularly when diffusion theory is used. As an illustration of the types of measurement which have been made and the results obtained, the measurements made in the ZEBRA core BZB and in ZPPR are summarized.

The ^{239}Pu fission rate distribution was measured for eight different control rod configurations using the multi-chamber scanning system in ZEBRA Assembly BZB [190]. The control rod positions were: the center of the core, an inner ring of six, and an outer ring of twelve near the inner core-outer core boundary. Each control rod array studied had a combined reactivity worth of about 4% dk. All the arrays were symmetrical other than Array 5, which had one rod fully inserted in the outer ring, the remaining outer ring rods being 1/4 inserted. The other arrays included two with symmetrical patterns of rods fully inserted, Array 3 with the inner ring of six inserted, and Array 8 with nine of the outer ring of twelve inserted. In the other arrays, there were different degrees of insertion in the inner and outer rings and in the central position. There were changes in both the axial and radial fission rate distributions of up to about 30%. The fission rate distributions were analyzed using XYZ geometry diffusion theory. For the values averaged over radial and axial regions, it was found that, relative to Array 1, the mean

deviations for each region were less than ±0.5% and the variations about the mean were less than ±1%.

An extensive series of reaction rate distribution measurements has been made in the ZPPR Assemblies. They include ^{239}Pu, ^{235}U and ^{238}U fission, together with ^{238}U capture. Detailed analyses have been made for the 600 litre assemblies 10D (rods withdrawn) and 10D/2 (rods inserted) [191]. These cores have an approximate diameter of 2.8 m. The analyses were made using XYZ geometry diffusion theory with S4 transport theory corrections. As was also found in the ZPPR core analyses, the calculation results of ^{239} Pu fission rates in the outer core relative to the core centre with the latest library and analytical methods are quite satisfactory within 1% discrepancy between experiments and calculations. The overall effects of the control rods on reaction rate distributions were well predicted. However, the incorrect prediction of the reactivity worth of sodium-filled control rod channels by diffusion theory has a significant effect on the power distributions in these large cores. Exploratory calculations made using axial buckling adjustment factors to account for axial transport effects in the sodium-filled channels gave reaction rate corrections of up to 2% in ZPPR-10D. Diffusion theory calculations also gave discrepant results within breeder regions close to the core-breeder boundary. It can be concluded from these analyses that a refined treatment of control rods and control rod follower regions is required for the calculation of reactor core reaction rate distributions.

It is known that radial power distribution in reactor has significant non-uniformity. For a homogeneous core, the radial distribution of neutron flux is described by function close to Bessel function (some discrepancy is due to perturbed influence of radial blanket). Radial coefficient of non-uniformity of power distribution in this case reaches ~ 1.7. Therefore various ways of flattening radial power distribution are used. The most widespread way is related to changing fuel enrichment. Usually two or three subzones with different fuel enrichment are used in fast reactor cores. For example, there are three zones with different fuel enrichment in the BN-600 and BN-800 reactors - low enrichment zone (LEZ), medium enrichment zone (MEZ) and high enrichment zone (HEZ). The chosen algorithm of definition of feeding fuel enrichments should provide the minimal non-uniformity of power distribution during core lifetime. Thus, in essence, the task of definition of feeding fuel enrichments is related to tasks of optimization. There are also other ways of flattening power distribution: flattening by using fuel pins of different diameter with the same fuel enrichment, flattening by insertion of inner fertile zones into the core, flattening by using subzones of different height etc.

In Japan, previous analytical results by JENDL-2 indicated that calculation-to-experiment ratio (C/E) values of reaction rate distribution systematically changed with radial positions in the core. This persistent “C/E space-dependency” of JENDL-2 was found to be largely alleviated by using the new JENDL-3.2 library. The sensitivity analysis showed the great improvement of space dependency by JENDL-3.2 came from the combination and cancellation of many nuclides and reactions contributions [192].

In India, COHINT was developed to treat both cluster and plate type heterogeneities found in fast neutron power and experimental reactors. It uses first flight collision probability method for cylindrical clusters and interface current method for 2D plates. For the design of PFBR reactor in India, COHINT generated absorber rod cross-sections are fed to 3D hexagonal-Z diffusion theory code FARCOB [193] for computing absorber rod worth and power distribution. For obtaining the peak pin power an interpolation scheme using fluxes

from 12 adjacent triangular meshes is used. FARCOB [194] can also compute assembly wise evolution of fuel compositions and burnup. As mesh wise fuel compositions are stored, it is possible to handle changes in core configuration and core expansion.

6.2.4.2. Control rod worth

In the critical balance method, criticality (or reactor power) is maintained by making one of the following changes when a rod or group of rods is inserted:

(1) Moving calibrated or reference control rods. This method is usually only used to measure reactivity worth of single rods or small movements of a group of rods. The reference rods can be calibrated in terms of the delayed neutron fraction or the calculated effect of a compensating fissile material addition to the core;
(2) Increasing the radius of the core by adding extra fuel elements at the core edge. The reactivity worth is then related to the calculated effect of edge element addition. Consistency is checked by interchanging the added edge elements and comparing measurement and calculation for the different arrangements;
(3) Changing the fissile material content of a region of the core. The reactivity scale is then the calculated effect of the fissile material addition. This is an appropriate reactivity scale because one of the functions of the regulating rods is to compensate for the loss of fissile material in fuel burnup; and
(4) Comparing the reactivity worth of different arrays which are calculated to have about the same reactivity worth, with the worth of each array having been determined by using one of the reactivity changes (1), (2) or (3) discussed above.

The different reactivity scales can be interrelated in separate experiments (for example by measuring edge element worth in terms of calibrated rods or distributed fissile material). It is necessary to recalibrate rods when the size of the core is changed or experimental rods are added.

The principal method used to measure subcriticality is the source multiplication technique. The ratio of the total flux to the source is approximately inversely proportional to the subcritical reactivity. Flux calculations must be made to obtain the flux at the counter positions because of the changes in the flux shape caused by insertion of the rods and the effect of the position of the source on the flux distribution. Normalization of the reactivity scale involves a reference subcritical condition, such as that produced by inserting a calibrated control rod.

Measurements of subcriticality relative to the effective delayed neutron fraction can be made by calibrating a reference fine control rod by means of asymptotic period measurements following rod withdrawal, or by inverse kinetics analysis of the reactor power response following rod drop or rod withdrawal (fitting the response using the delayed neutron kinetics equations).There are uncertainties in total delayed neutron yields and in the time dependence of delayed neutron emission, the accuracy of this reactivity scale being estimated to be around 3% [195].

There are a number of techniques for measuring subcritical reactivity relative to a calibrated reference control rod, in addition to source multiplication. These include rod drop, rod jerk, source jerk, pulsed source and reactor power noise. Account must be taken of spatial flux transients (either by calculating them or measuring them with arrays of counters) and of the spatial distribution of natural neutron sources due to spontaneous fission and (α,n) reactions

and any fixed sources introduced to increase the subcritical flux level. The different methods have been reviewed and inter-compared, for example, at the 1976 Specialists Meeting [196].

Extensive programmes of measurements have been carried out in all the fast critical facilities and also in Superphénix during the start-up experimental programme. An illustration of the accuracy of current methods and data is given by the results of the Superphénix experimental analyses. These were made by four different groups, France/Italy, Germany (KfK and Interatom) and the UK using different methods and data). The calculations were made for four experimental configurations, and the deviation in C/E values was less than few percent. Interatom used a Monte-Carlo code, MOCA, and obtained particularly good agreement.

Most effective absorbers in fast neutron spectrum are materials containing boron-10 isotope [197, 198]. Therefore, the most widespread material for use in control and protection system rods is boron carbide. Europium oxide was used in some reactor designs (BN-600), whose efficiency is comparable with boron carbide of natural enrichment. In some Russian fast reactors (BN-350) fuel compensators were used for compensation of fuel burnup which in contrast with absorbing materials practically do not reduce breeding ratio. The total efficiency of and protection system of the fast reactor should be at the level of 8-10% $\Delta k/k$. The total amount of regulating rods (absorbing rods) depends on core size and sizes (diameter) of absorbing rods. The fast reactors do not permit to place a plenty of and protection system rods due to rather small sizes of their cores. Therefore, as a rule, it is necessary to use high-enriched boron carbide. It is necessary to note that advanced fast reactors designed in the Russian Federation are assumed to be providing high breeding ratio in the core (~ 1) by using core configurations with a high volumetric fuel fraction or by using denser fuels, for example, nitride fuel. It will permit to exclude from and protection system control rods compensating fuel burnup and thus to increase reactor safety in incidents with unprotected rod withdrawal.

6.2.5. Reactivity coefficients

Knowledge of temperature and power coefficients of reactivity is required to determine the control rod reactivity required to raise a reactor to power and to study the response of the reactor to malfunctions. The tempterature reactivity coefficient is characterized by uniform reactor heating by 1°C. The power reactivity coefficient is characterized by change of power by 1 MW and is connected with non-uniform reactor heating. A characteristic temperature reactivity coefficient for fast reactor of medium power (such as BN-600) is about -3×10^{-5} $\Delta k/k/°C$, and a characteristic power reactivity coefficient for the same type of fast reactor is about -0.4×10-5 $\Delta k/k/MW$.

The coefficients are of two types: those due to thermal expansion effects and those arising from Doppler broadening of resonances. A uniform expansion of a reactor core results in an increase in the leakage fraction and a reduction in reactivity. However, different materials have different coefficients of expansion, and so account must be taken of the relative changes in material densities, for example, the changes in the atomic fractions of coolant and structural materials relative to the atomic fraction of fuel. The expansion of the fuel can be affected by the expansion of the fuel cladding, if the fuel is bonded to the cladding. Axial core expansion and expansion of control rod structures can result in movements of control rod absorber sections relative to the core, with the consequence of an increased control rod insertion. The temperature gradients across subassemblies result in bowing of the assemblies. The way they bow depends on the points in contact between them. In some arrangements, an increase in temperature results in an increased inward bow and hence an increase in reactivity, a condition

to be avoided. The subassembly lower support structure is at the temperature of the coolant inlet flow, whereas the temperatures vary axially through the core depending on the power and the flow rate. Bowing can result from radial variations of temperature. Bowing of subassemblies also results from irradiation-induced swelling, the flux on one side of a subassembly being higher than on the other. However, this is a slowly varying effect. It can result in changes to the way subassemblies are in contact and hence to the way they bow in a temperature transient, however.

Coolant voiding is another effect which must be investigated. A subassembly might become voided as a consequence of a blockage and the vaporization of the coolant above the blockage. In a severe accident, the temperature could rise to a point at which the coolant throughout the reactor is vaporized. Sodium voiding studies have been made in many critical facilities for different axial sections of single subassemblies or groups of subassemblies at different radial positions, and also for whole cores. Accident configurations which could result from the partial meltdown of a region of a core have also been simulated in critical facilities. The calculation of the effects of voids in the core presented a problem in the past but now, with 3D transport theory codes being available, it is less of a problem.

The reactivity effects arising under sodium cooled fast reactors operation are quite well investigated at start-up and operation of such sodium cooled fast power reactors as BN-350, BN-600, Phénix, Superphénix, and also such experimental fast reactors as BOR-60, Rapsodie, and EBR-II. In addition, extensive researches have been carried out concerning development of advanced fast reactor designs: BN-800, BN-1600, EFR, etc.

6.2.5.1. Perturbation theory methods

Perturbation theory methods are used to calculate reactivity coefficients, such as Doppler effects and the effects of coolant density changes. They are also used to calculate the sensitivities of parameters to cross-section changes for use, for example, in cross-section adjustment studies. Perturbation theory requires the solution of an adjoint equation, a transposition of the normal transport theory equation, the transposition being in energy and direction. A distinction is made between reactivity perturbation theory and generalized perturbation theory. In reactivity perturbation theory, it is the change in reactivity resulting from changes in the macroscopic cross sections (or geometry) which is calculated.

The method distinguishes two systems: the unperturbed system, having cross sections Σ_u, and the perturbed system, having cross sections Σ_p. The flux is calculated for one of these systems (ϕ_u) and the adjoint flux (ϕ_p^*), for the other. The adjoint flux, or neutron importance, $\phi_p^*(x',E')$ is the probability of a neutron (at position x' and of energy E') contributing to the production of a fission neutron in the asymptotic fission distribution.In first-order perturbation theory, ϕ_p^* is replaced by the adjoint flux calculated for the unperturbed system, ϕ_u^*. This results in an ambiguity for the leakage term in the diffusion theory term because there is the option of replacing either the flux gradient or the current by the unperturbed value. This choice must be considered when calculating coolant density reactivity coefficients. For whole reactor effects, the flux distribution shape remains approximately unperturbed, and the approximation of grad ϕ_p by grad ϕ_u is acceptable. For small regions, the current is approximately unperturbed, and it is better to replace J_p by J_u.

Generalized perturbation theory permits changes in properties other than reactivity to be calculated. To calculate these, an appropriate adjoint equation must be solved which uses a

source corresponding to the property for which the sensitivities are to be calculated. For example, to calculate the sensitivities for a central fission rate ratio, the adjoint source is the fission ratio itself. Generalized perturbation theory can also be used to calculate the sensitivities of reactivity changes to changes in cross sections. For a review of these methods, reference can be made to [199].

The most widely used perturbation theory tools in the USA for fast reactor calculations are the VARI3D and DPT [200] codes. VARI3D is a generalized perturbation theory code that allows calculation of the effects on reactivity and reaction rate ratios of alterations in microscopic cross sections and/or material number densities. VARI3D is most frequently used to compute the reactivity coefficient distributions and kinetics parameters employed in reactor dynamics and safety analyses. VARI3D utilizes the DIF3D code for the flux and adjoint solutions required to compute these quantities. First-order and exact perturbation theory options are available, and several options are allowed for treatment of leakage term. It is currently limited to the finite difference diffusion theory option of DIF3D.

The DPT code is a depletion perturbation theory code, which solves the adjoint equations corresponding to the coupled neutron and nuclide field equations for non-equilibrium and equilibrium fuel cycle analysis of REBUS-3 and computes the sensitivity coefficients of various response functionals with respect to cross sections and initial nuclide densities. The responses include the local nuclide densities at the end of cycle (EOC), the effective multiplication factor at EOC, the local power densities at EOC, the core breeding ratio, and the burnup reactivity swing. The flux and adjoint solutions are obtained in R-Z geometry by the finite difference diffusion theory option of the DIF3D code.

In the Republic of Korea, various reactivity feedback effects and neutron kinetics parameters are calculated utilizing the DIF3D and PERT-K [201] codes. The perturbation code, PERT-K, for the hexagonal geometric core was developed at KAERI, based on Nodal Expansion Method. By coupling to the DIF3D code, PERT-K calculates reactivity changes caused by the perturbation of composition or/and neutron cross sections. The accuracy of the PERT-K code was assessed by calculating the sodium void worth, and sample reactivity worth measured at BFS-73-1 critical facility. Global feedback coefficients are determined by the results from direct flux computations for the unperturbed and perturbed systems. These coefficients include Doppler effect, uniform radial expansion and sodium voiding. These coefficients are calculated by using the 80 group cross sections. The BETA-K [202] and PERT-K codes are used for the perturbation computations to generate neutron kinetics parameters as well as spatial reactivity coefficients that are required for transient analysis. Normally Doppler calculations are performed for various fuel zones to separate the Doppler coefficients for the fuel zones. The direct flux solution approach based on hexagonal-Z geometry with 80 group cross sections is used to compute the sodium void worth by voiding the sodium in the core regions of interest using the sodium-voided cross sections. On the other hand, the spatial sodium density reactivity coefficients are obtained from the PERT-K calculations based on the first-order perturbation theory. The sodium void worth represents the estimated reactivity effect of voiding of sets of fuel assemblies in an active fuel region plus in the coolant channels of upper gas plenum. The control rod worth calculations are carried out with 80 group cross sections in the diffusion theory calculations with three-dimensional hexagonal-Z geometry.

6.2.5.2. Doppler effects

The Doppler-effect provides a fast-acting negative reactivity feedback compared to other reactivity feedback effects. The Doppler-effect has essential importance in a ceramic fuel because of a high fuel temperature (average fuel temperature is ~ 1200°C). In large cores, the Doppler-effect comprises ~ 70% of total power reactivity effect.

The effect arises predominantly from the increase in neutron capture in ^{238}U resonances. Smaller contributions arise from the resonances in plutonium isotopes and also from the narrow p-wave resonances in the structural material elements (e.g. the 1.15 keV resonance in ^{56}Fe). Thus, the increase of neutron capture by ^{238}U due to increase of temperature plays the determining role in large fast reactors and determines negative value of effect. The Doppler-effect for ^{239}Pu and ^{241}Pu brings in positive reactivity, but the total contribution from plutonium could be close to zero with a negative contribution from ^{240}Pu.

The main fraction of fissions in fast reactor occurs in the range of 1 MeV-1 keV, while the most resonances in heavy nuclides occur below ~ 10 keV. In this connection the accuracy of calculation of Doppler-effect essentially depends on accuracy of calculation of neutron spectrum at low energy that weakly influences accuracy of calculation of other reactor characteristics (critical mass, breeding ratio etc.). The decrease of Doppler-effect value in range of 2–4 keV is explained by presence of large scattering resonance in sodium.

One of the Doppler-effect features is its nonlinear dependence on temperature [197]. For weak resonances which have the cross-section of resonance interaction comparable with cross-section of potential scattering, it is possible to write down after some transformations:

$$d\sigma_o/dT \sim T^{-3/2},$$

where σ_o denotes a resonance cross-section. For strong resonances in which the probability of absorption of neutrons is very great, it is possible to write down:

$$d\sigma_o/dT \sim T^{-1/2}$$

In a fast reactor, both weak and strong resonances play a role in Doppler-effect, therefore temperature dependence of Doppler constant lays between these two functions. Practically, this dependence is well approximated by function 1/T that was confirmed experimentally. Experimental research on the Doppler-effect were carried out in reactor SEFOR, which was designed and constructed especially for these purposes [203].

To the present time in the different countries including the Russian Federation, the numerous analytical-theoretical researches are carried out on evaluation of Doppler-effect in fast reactors with various types of fuel, with various core compositions and configurations. For example, the results of calculations of Doppler-effect for a sodium cooled fast reactor with power of 1300 MWe are given [204]. The calculations have been carried out for three variants of core with axial heterogeneity and for one variant with a homogeneous core. The axial heterogeneity in considered variants was created by insertion into the core of a layer of fertile material with thickness of 15 cm. This heterogeneity provides flattening axial power distribution. Variants are as follows:

(1) A heterogeneous core with nitride fuel (fuel fraction - 51%);
(2) A heterogeneous core with nitride fuel (fuel fraction - 45%);
(3) A heterogeneous core with oxide fuel (fuel fraction - 47%);
(4) A homogeneous core with oxide fuel (fuel fraction - 47% as well).

Main reactivity parameters of such cores are presented in Table 6.4.

TABLE 6.4. MAIN SAFETY NEUTRONIC PARAMETERS

Safety parameter	Nitride fuel		Oxide fuel (E_f=0.45)	
	E_f=0.51	E_f=0.45	Heterogeneous	Homogeneous
TRC, (Δk/k)/°C	-1.2E-05	-1.22E-05	-1.6E-05	-1.35E-05
PRC, (Δk/k)/MWt	-1.5E-06	-1.7E-06	-2.6E-06	-2.8E-06
TRE, %Δk/k (from 200°C to 390°C)	-0.22	-0.23	-0.30	-0.26
PRE, %Δk/k (from 0 to 3200 MW)	-0.484	-0.559	-0.824	-0.889
β_{eff}	3.662E-03	3.659E-03	3.512E-03	3.510E-03
Prompt neutron lifetime, s	2.745E-07	3.151E-07	4.135E-07	3.7E-07

TRC = temperature reactivity coefficient
PRC = power reactivity coefficient
TRE = temperature reactivity effect
PRE = power reactivity effect

A spectral Doppler-effect distribution in a 26 group division of the ABBN constant library is presented in Fig. 6.3.

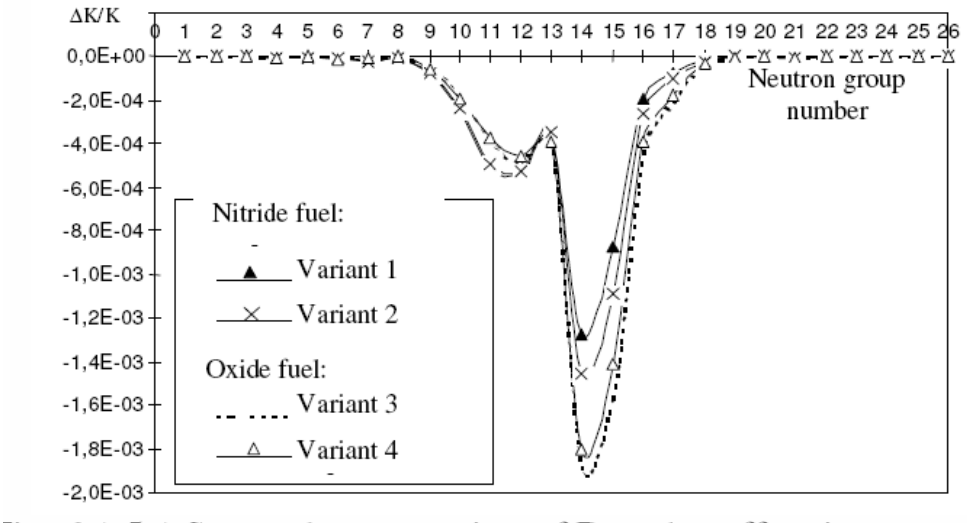

FIG. 6.3. Spectral presentation of the doppler-effect in a reactor heated from 900 K to 2100 K.

Different neutronic processes contribute to the Doppler-effect, the balance of these values for the Doppler constant is given for different temperature ranges in Table 6.5. The role of the Doppler-effect that reacts to fuel temperature increase with very small delay is very important for ensuring reactor safety. However, in accidents caused by stop of the primary pumps combined with failure of shutdown system (ULOF) a large value of Doppler-effect makes

obstacle for power decrease. At the reduced values of Doppler-effect, for example, due to increase of fuel enrichment, this accident proceeds much more softly.

TABLE 6.5. BALANCE OF DOPPLER-CONSTANT T(∂k/∂T) MAIN COMPONENTS IN DIFFERENT TEMPERATURE RANGES

Fuel	Nitride fuel (heterogeneous)	Oxide fuel (heterogeneous)	Oxide fuel (homogeneous)
Temperature range: 600–900 K			
Radial leak	5.32E-5	4.48E-5	4.36E-5
Axial leak	9.92E-5	7.78E-5	0.00011
Absorption	-0.00742	-0.00917	-0.00856
Moderation+(n,2n)	-0.00014	-0.00014	-0.00013
Fission	0.002364	0.003243	0.003044
Total	-0.00505	-0.00594	-0.00549
Temperature range: 900–2100 K			
Radial leak	3.14E-5	2.63E-5	2.43E-5
Axial leak	3.36E-5	2.12E-5	4.75E-5
Absorption	-0.00673	-0.00871	-0.00801
Moderation +(n,2n)	-0.00014	-0.00013	-0.00013
Fission	0.001357	0.00211	0.001837
Total	-0.00545	-0.00668	-0.00623

The problem of the Doppler-effect essentially becomes aggravated in fast reactors without uranium-238 which are supposed to be used for effective burning minor actinides. In such reactors, the sources of the Doppler-effect are plutonium-240 and steel components. It is possible to introduce resonance absorbers into fuel, among which most effective is iron. At the IPPE, the modelling of a fast reactor with ROX-fuel (fuel without uranium-238) on critical BFS-91-1 and BFS-91-2 assemblies has been carried out. The measurements of the Doppler-effect with plutonium samples have been carried out on these assemblies [205].

The BFS-91-1 and BFS-91-2 assemblies represented three-zoned systems consisting of the central area simulating investigated reactor, driver zone and lateral reflector. Axial and lateral reflectors contained depleted uranium dioxide. The critical assembly BFS-91-2 (with softened spectrum) differed by the following conditions: in a cell of the central zone two sodium pellets were replaced with one pellet of SiO_2, and polyethylene displacers were inserted into inter-tube gaps of the central insertion and driver.

Tables 6.6 and 6.7 represent results of measurements on BFS-91-1 and BFS-91-2 assemblies and appropriate calculations of Doppler-effect for two samples of depleted UO_2 and PuO_2 with the high and medium contents of plutonium-240. The calculations have been made by using the TWODANT code in two-dimensional R-Z geometry, with 299 groups and in the P_1S_8-approximation, with using ABBN-93 constant library and CONSYST code for preparation of constants [206].

TABLE 6.6. COMPARISON OF EXPERIMENTAL AND CALCULATION DATA FOR BFS-91-1 ASSEMBLY - REACTIVITY DIFFERENCE FOR HOT AND COLD SAMPLES (CENT)

Sample	Experiment	Calculation
UO_2 (depleted)	- 0.101 ± 0.006	- 0.100
PuO_2 (Pu-240: -89.22%)	- 0. 032 ± 0.003	- 0.030

TABLE 6.7. COMPARISON OF EXPERIMENTAL AND CALCULATION DATA FOR BFS-91-2 ASSEMBLY - REACTIVITY DIFFERENCE FOR HOT AND COLD SAMPLES (CENT)

Sample	Experiment	Calculation
UO_2 (depleted)	-0.353± 0.006	-0.279
PuO_2 (Pu-240: 16.76 %, Pu-241: 2.26%)	-0.080± 0.003	-0.062

A number of approximations are made in the usual calculation methods:

- The large variation in temperature across a fuel pin is usually replaced by the average temperature across the pin;
- The heterogeneity of the fuel pin and subassembly structure is often treated as homogeneous; and
- The Doppler effects in different axial and radial regions of a reactor are treated as dependent only on the local average fuel temperature. Uncertainties in predictions of Doppler effects can be separated into two components: the uncertainty in prediction of fuel temperatures and the uncertainty in the change of Doppler reactivity with temperature. The uncertainty in the fuel temperature, arising from uncertainties in the clad-fuel gap conductivity and the fuel conductivity, must therefore be considered. Separation of the uranium and plutonium in granular fuel could also have an effect, as could the radial migration of plutonium within the fuel caused by the high temperature gradient (although studies show this latter effect to be negligibly small). Although the uncertainty in prediction of Doppler effects could be assessed in terms of uncertainties in knowledge of resonance structure and the fraction of the reactions occurring in the resonance region, it is more usual to base the assessment on a comparison of calculations of Doppler reactivity feedback with measured values. However, because it is necessary to extrapolate up to much higher temperatures than those for which measurements have been made, some consideration must be given to the accuracy of the basic data and calculation methods.

In Japan, a methodology to make a sensitivity analysis for the Doppler reactivity was developed [207]. In this method, the temperature gradients of self-shielding factors, f, are treated as a kind of pseudo-cross-sections. Since the covariance of temperature gradients of self-shielding factors can be obtained from the covariance of resonance parameters numerically [208], the Doppler reactivity can be treated as other general core parameters like k_{eff}, control rod worth, etc. in the procedure of accuracy evaluation or cross-section adjustment.

The approximation is sometimes made that the Doppler coefficient has a 1/T dependence on temperature. The actual variation with temperature depends on the shape of the neutron spectrum through the resonance region and on the balance between the contributions from fertile and fissile isotopes. At low temperatures, chemical binding effects can become

important. These are usually taken into account by using an equivalent temperature (instead of the actual temperature) in the gas model Maxwellian velocity distribution. The equivalent temperature is usually expressed in terms of a Debye temperature which characterizes the lattice vibration motion of the uranium and plutonium isotopes in the solid. This can be different from the Debye temperature for the solid as a whole. Values of the Debye temperature for UO_2 used in the analysis of experiments range from about 250 K to 650 K, and this difference affects the conclusions drawn from Doppler coefficient measurements made over a range from ambient temperature to a temperature a few hundred degrees higher. The accuracy of Doppler effect predictions has been assessed by analyzing the SEFOR Doppler experiments [209].

In addition, an analysis can be made of structural material Doppler effect measurements made in the Japanese critical facility FCA [210]. Small sample reactivity worth measurements as a function of sample temperature have now been made for ^{238}U to about 2000 K. Measurements of neutron spectra and the use of spectral index measurements made with detectors sensitive to resonances in the Doppler effect energy range are also valuable. As well as the uncertainties in Doppler effect predictions, account must be taken of the variation of the effect throughout the fuel cycle, first as the reactor is brought to the equilibrium cycle condition and then from fuel loading to discharge, as control rod absorption is replaced by fission product absorption and the reduction in fissile material worth. The build-up of fissile material in breeder regions and the consequent increase in temperature has an effect. Changes in the isotopic composition of the fuel, both of the feed fuel (when different sources are used) and the variation with burnup, must also be allowed for.

In U^{238} the Doppler effect arises mainly from the s-wave resonances. Uncertainties in the subdivision of the capture cross section into s-wave and p-wave resonances (or between large and small resonances) are carried over almost directly into uncertainties in the Doppler effect. Less than 10% of the ^{238}U Doppler effect comes from energies above 10 keV, resolved resonance parameter data now being available up to this energy. It makes very little difference to the Doppler effect calculated for a power reactor whether the Debye temperature is 250 K or 650 K. At temperatures above the Debye temperature, q_D, the equivalent temperature T* is close to the actual temperature, being less than about 5% different. However, for the analysis of experiments in the range 300 K to 1000 K, this difference is significant. Analyses of cross-section shapes are more consistent with the lower value, but some analyses of reactor Doppler effect experiments are more consistent with the higher value.

The temperature distribution radially across a fuel pin is approximately linear in terms of the volume of annular regions. It departs from a linear variation because of the dependence of thermal conductivity on temperature and when there is a central hole in the pin. For a fast reactor spectrum, the effective temperature is estimated to be close to the average [211].

In a transient, the temperature of the fuel depends on the specific heat, which is temperature dependent. Fuel melting at the centre of the pin can change the temperature distribution, and these effects must be taken into account in calculations of Doppler reactivity feedback. For the ceramic fuel with gas gap between the fuel and cladding, gas gap conductivity is another source of uncertainty in the calculation of effective fuel temperature. The temperature change across the fuel-clad gas gap is about 25% of the difference between the mean fuel temperature and the inner clad surface temperature, so that a 10% uncertainty in gas gap conductivity results in a 1.3% uncertainty in mean fuel temperature.

A study of the effect of heterogeneity is described in [212], which presents a general review. The effect can be separated into two components: the fuel pin heterogeneity effect and the subassembly wrapper effect. Compared with the homogenized model, both effects are found to increase the Doppler constant by 2.5%, giving a total increase of 5%.

6.2.5.2.1. Experimental validation

The following types of measurements have been used to evaluate the accuracy of Doppler effect calculations:

- Measurements taken in the Southwest Experimental Fast Oxide Reactor (SEFOR), which was built and operated specifically to measure Doppler effects (or fast-acting fuel reactivity feedback effects with expansion effects minimized);
- Measurements of the dependence of reactivity on temperature in operating power reactors, such as Phénix and Superphénix (from the non-linearity of the temperature coefficient, for example);
- Measurements taken in the ZEBRA-5 Doppler Loop experiments, in which a test zone was heated, with experiments being performed with and without sodium present;
- Measurements of the temperature dependence of the reactivity worth of small samples oscillated at the centre of critical assemblies;
- Measurements of the differences in reaction rates in samples irradiated at different temperatures; and
- Temperature-dependent thick sample transmission and self-indication measurements, which are usually analyzed together with differential nuclear data to provide average resonance parameter data. The uncertainties in extrapolating from these comparisons to the conditions in an operating power reactor must also be taken into account.

6.2.5.2.2. SEFOR Doppler effect measurements

Two versions of the SEFOR core were built, SEFOR-1 and SEFOR-2. Both were sodium cooled and used 20 % enriched PuO_2/UO_2 fuel, but SEFOR-1 contained a number of beryllium oxide rods to soften the spectrum, whereas in SEFOR-2, these were replaced by stainless steel rods. The fuel pins were of large diameter so that a high mean fuel temperature could be achieved at low power. The experiments were of two types: static and transient. The first analyses were made by General Electric and by Karlsruhe. An improved analysis was later made by HEDL, and this included a correction for chemical binding effects (assuming a high Debye temperature). The correction is small, however, about 1.5% in the case of the SEFOR measurements. The choice of delayed neutron data affects the results. The agreement between measurement and calculation is within the uncertainties (1σ) for all of the analyses, including a recent one using JEF-2.2 data. Extrapolating these results to the spectra and fuel compositions of a conventional power fast reactor results in an increase in the uncertainties to ±15%. The additional uncertainties associated with burnup effects, for the target burnup considered (10% maximum), do not increase this uncertainty estimate, but for extrapolations to low and high temperatures, the uncertainties are increased to ±18%.

Recently, JAEA and CEA re-evaluated the SEFOR experiments from their original report. The re-evaluated Doppler constant is 3–5% larger than the original GE evaluation. The increase is mainly due to the update on the fuel thermal conductivity correlation. The new values look more reasonable than the recommended HEDL evaluation in that now the C/E values do not depend on the core type. In addition, the experimental uncertainty is significantly

reduced from 12% to 6%, and this is of the utmost importance according to current accuracy requirements [213].

6.2.5.2.3. Small sample Doppler experiments and the steel Doppler effect

Small sample Doppler measurements have been made in several critical facilities, including the ANL ZPR and ZPPR facilities, SNEAK and FCA. Measurements made for ^{238}U samples in ZPPR have been analyzed using ENDF/B-IV data, giving C/E values in the range 0.85 to 0.90. Measurements made in SNEAK and analyzed using KFKINR data give C/E values of about 0.89. These two data sets give similar values for the Doppler constants in the SEFOR cores. Measurements of the Doppler effect of iron samples have been made in FCA Assemblies V-2 (a mock-up of Joyo) and VI-2 (a mock-up of Monju). The samples were heated from room temperature to 823 K and 1073 K. In Japan, the C/E range of 0.95–1.05 for the Doppler reactivity has been obtained through the experimental analysis of ZPPR, FCA, BFS and SEFOR with the most detailed analytical methods and the JENDL-3.2 library [195].

6.2.5.2.4. Measurements on operating power reactors

Measurements have been made on operating power reactors of the reactivity response to changes in temperature, power and flow. There are problems in deriving the Doppler effect, which is only one component of the reactivity change. However, for some purposes it is unnecessary to separate out the Doppler component. The reactivity change on going from the normal shutdown temperature to full power operation can be measured directly (in terms of the compensating control rod movements), and the response to transient reactivity, power changes, or inlet coolant temperature changes can be measured. A separation of the components is required to enable deductions to be made about the response in transients for which measurements cannot be made, or to extrapolate to different fuel types and reactor designs.

However, this separation into Doppler effect and expansion effects need not necessarily be made. Separation into a fuel power coefficient (together with its temperature dependence) and other coefficients could be sufficient, and possibly even more useful because of uncertainties in temperature response and fuel plus cladding expansion effects and their interactions. It would be valuable if a reassessment could be made of the parameters which are required for different applications, together with the component breakdown required to extrapolate to different designs of fuel and reactor core.

Doppler effect measurements have been made in Phénix [214] and Superphénix [215]. The measurements were of the isothermal temperature changes at very low power. The Doppler effect is identified with the non-linear component of the temperature coefficient, assuming a dependence of the form b/T for the Doppler effect. The uncertainties in the analysis of the measurements arise from uncertainties in control rod reactivity worth and rod worth profile and from the statistical analysis of the data. It is concluded that the maximum uncertainty is ±15% and the probable error ±10%. A more recent analysis is presented in Ref. [216].

6.2.5.3. Sodium voiding and sodium density coefficients

The reactivity effects of voiding the sodium coolant from regions of a reactor core and the effects of sodium density changes resulting from changes in temperature can be considered in terms of two components: the central term (moderation plus capture) and the leakage term (capture being a small effect). A reduction in sodium density results in an increase in leakage,

a negative reactivity effect. The reduction in moderation which results from the density reduction has an effect which depends on the energy dependence of the neutron importance. In a conventional plutonium/uranium fuelled fast reactor, the reduction results in an increase in reactivity.

The effect is a balance between high energy and low energy effects. The reduction in the inelastic scattering contributed by sodium results in an increase in ^{238}U fission (at MeV energies) — a positive reactivity effect. At intermediate energies (above about 10 keV), the effect is also positive because of the increase in ^{239}Pu alpha (capture-to-fission ratio) and the ratio of ^{238}U capture to ^{239}Pu fission as one goes towards lower energies. However, below about 10 keV, ^{239}Pu alpha is approximately constant, and the fission cross section increases more rapidly than the resonance-shielded ^{238}U capture cross section. The effect of the reduction in moderation is negative at these lower energies. The net moderation effect depends on the plutonium enrichment of the fuel but is normally positive. For ^{235}U fuelled systems the net effect is normally negative, however. The balance of the moderation (or central) and leakage terms depends on the region of the core voided (or having the density reduced). In central regions the effect is predominantly due to the moderation term, and even for the core as a whole, for a reactor of the size of Superphénix, the net effect is positive.

Sodium reactivity effect is negative for very small cores with high neutron leakage outside. For sodium cooled fast reactors of medium and large power sodium reactivity effect is positive and can reach appreciable value. The largest positive void effect can be of the order of 10 $, when a large central region of the core is voided. Because of this, many studies have been made of heterogeneous core designs with a reduced voiding reactivity effect. For design options for reduction of sodium void worth, reference can be made to [217].

In the Russian Federation, nuclear safety rules very rigidly regulate sodium void reactivity effect (SVRE) value: “reactivity coefficient for specific volume of the coolant should be negative at normal operation, at abnormal events and design accidents.” There are various ways to decrease the SVRE to zero or, even, a negative value. During development of the BN-800 reactor design, a new concept of ensuring zero SVRE value was proposed. It is based on introduction of screens filled with sodium and transparent for neutrons. The basic idea is that decrease of sodium density or its disappearance from such screens will result in increase of neutron leakage outside from the core and accordingly to decrease of sodium reactivity effect. This concept was implemented in the BN-800 reactor design by means of creation of sodium cavity above core - in the field of the greatest sodium temperature [218, 219].

The disappearance of sodium from this cavity will result in occurrence of appreciable negative reactivity due to increase of neutron leakage. The essential point in creation of such cavity is the minimization of amount of steel in it. In BN-800 reactor the volumetric fraction of steel (FSA wrappers) in sodium cavity is equal to ~ 7%. The parameters of this screen can be chosen so that negative reactivity in sodium cavity will compensate positive reactivity in the core. Thus, the summary reactivity effect due to sodium disappearance from FSA in core will have zero or small negative value. It is necessary to note good compatibility of the proposed configuration with traditional core configurations of sodium cooled fast reactors.

The introduction of this idea into design of the BN-800 reactor has required execution of quite deep analytical-theoretical and experimental researches. The international benchmark model was organized on the basis of a variant of the BN-800 reactor with an axial blanket layer and sodium cavity, which was developed at the preliminary stage of development of the new core

design [219, 220]. Experts of the Russian Federation, the USA, the UK, Japan, India and Germany have taken part in these benchmark studies. The studies, as a whole, have confirmed an opportunity of achievement of zero or small negative SVRE value for the examined core configuration with sodium cavity, though there were also appreciable distinctions between results obtained by researchers of the different teams.

Experimental research on the SVRE has been carried out in a series of critical BFS assemblies. With this purpose in 1991–1995 at the critical BFS-2 facility there have been carried out experiments on four critical assemblies simulating the BN-800 reactor core with sodium cavity [221]:

- BFS-54-2 – assembly with uranium loading in the core;
- BFS-54-3 – assembly with uranium loading in the core and with central insertion of medium background plutonium;
- BFS-56 – assembly with mixed uranium-plutonium fuel on the base of low background plutonium;
- BFS-58 – full-scale model of the BN-800 core with mixed loading (uranium-plutonium fuel in low enrichment zone, fuel on the base of enriched uranium in medium and high enrichment zones).

The first three assemblies were modelling and intended for research of the sodium void reactivity effect only. The efficiency of using a sodium cavity for decrease of this effect was checked at these assemblies. The critical BFS-58 assembly was already a full-scale model of BN-800 reactor core design and, in addition to research one the SVRE, other physical reactor characteristics (power distribution, efficiency of control and protection system rods etc.) have been also investigated for this assembly.

The process of sodium removal was provided by reinstallation of fuel rods when sodium blocks were replaced with empty wrappers of sodium blocks. The replacement was carried out from centre of the critical assembly by portions of 12 fuel rods. Thus, the measurement of a reactivity difference between two sequential states was carried out by special digital device for reactivity measurements. Further additional loading (or unloading) of fuel rod on core periphery was carried out to ensure criticality of assembly with lifted control and protection system rods. Hence, number of the fuel rod and radius of critical assembly continuously change during measurements. The experimental researches executed at the critical assemblies of the BFS facility have shown that introduction of sodium cavity is sufficiently effective means for SVRE decrease in fast reactor cores.

The transfer of calculation results of studies of SVRE at critical assemblies with use of various isotope compositions of plutonium shows that irrespective of plutonium composition calculating value of SVRE exceeds experimental value. The performed analysis allows correctly enough evaluating integral value of SVRE in real core of the BN-800 reactor. The maximum value of sodium void reactivity effect is equal to:

- For variant of the core with axial layer: - 0.03 %Δk/k;
- For design variant of the core: + 0.07 %Δk/k.

Many experimental programmes have been carried out in critical assemblies to validate the methods and data used to calculate sodium voiding effects. The usual method of analysis is to derive bias factors and the associated uncertainties to be applied to the central term and the leakage term. Typical accuracies obtained are ±5% for each term [212].

In Japan, the C/E range of 0.90–1.05 for the sodium void reactivity has been obtained through the experimental analysis of ZPPR, FCA and BFS with the most detailed analytical methods and the JENDL-3.2 library [195]. The method of calculation is complicated by the need to treat heterogeneity effects and, in particular, the streaming in voided regions. In the experiments performed in plate geometry, the voiding is achieved by replacing the sodium-filled plates by empty cans. The streaming effects in these are significant. Experiments have also been performed in pin geometry assemblies (or mini-calandria), but even in this case, the streaming effect must be treated.

6.2.5.4. Radial and axial core expansion

The thermal expansion of reactor arises in the radial direction due to thermal expansion of the bottom collector (pressure head chamber) where FSA are fixed by bottom tails, and in the axial direction owing to thermal expansion of fuel pins. Some role in core deformation in radial direction is played by FSA bending due to different temperatures on opposite walls of FSA wrapper caused by radial non-uniformity of the power distribution.

In Tables 6.8 and 6.9, as examples, there are presented calculated values of temperature and power reactivity coefficients and reactivity effects, and also components of TRC and PRC for the 1300 MWe fast reactor described earlier [205].

TABLE 6.8. TEMPERATURE AND POWER REACTIVITY COEFFICIENTS AND REACTIVITY EFFECTS

Fuel	Nitride (heterogeneous)	Oxide (heterogeneous)	Oxide (homogeneous)
TRC, (Δk/k)/°C	-1.22E-05	-1.6E-05	-1.35E-05
PRC, (Δk/k)/MWt	-1.7E-06	-2.6E-06	-2.8E-06
TRE, %Δk/k (from 200 to 390°C)	-0.23	-0.30	-0.26
PRE, %Δk/k (from 0 to 3200 MW)	-0.559	-0.824	-0.889
β_{eff}	3.659E-03	3.512E-03	3.510E-03
Prompt neutron lifetime, s	3.151E-07	4.135E-07	3.87E-07

TABLE 6.9. TEMPERATURE AND POWER REACTIVITY COMPONENTS

Item	Nitride (heterogeneous)	Oxide (heterogeneous)
TRC components, (Δk/k)/°C		
Doppler	-8.73E-6	-1.03E-5
Axial expansion	-4.8E-7	-5.2E-7
Radial expansion	-7E-6	-7E-6
Density	3.83E-6	2.32E-6
PRC components, (Δk/k)/MW		
Doppler	-1.03E-6	-1.82E-6
Axial expansion	-8.7E-8	-1.8E-7
Radial expansion	-1.31E-7	-1.32E-7
Sodium density	7.62E-8	4.78E-8

6.2.6. Shielding

For shielding studies, the Iron Benchmark experiment was performed in the ASPIS facility on the NESTOR reactor at Winfrith [222] (a water-cooled, graphite-moderated MTR reactor operating at power levels up to 30 kW). The reactor provided a source of neutrons in a central

channel and also in the graphite reflector surrounding the reactor tank. Adjacent to the reflector were the four experimental caves, in one of which was the ASPIS shielding facility. A fission plate, containing 93% enriched uranium in the form of a uranium-aluminum alloy, provided the source of fission neutrons. This source could be modified by a suitable choice of moderating materials. The thermal neutrons from the graphite reflector caused fissions in the fission plate. The shielding configuration being studied was placed adjacent to the fission plate source configuration, and the reaction rate distributions through the shielding configuration were measured. The usual reaction rates chosen for this purpose were $^{32}S(n,p)^{32}P$; $^{115}In\ (n,n')^{115m}\ In$; $^{103}Rh\ (n,n')^{103m}Rh$- and $^{197}Au\ (n,\gamma)^{198}Au$ (with and without a cadmium cover). The resulting activation was then measured.

The experiments were analyzed using the MCBEND Monte Carlo code with its 8220 energy group library. Analyses have also been made using MCNP. The MCBEND code has associated with it the DUCKPOND module, which can be used to calculate the sensitivities of the measured quantities to cross-section changes. These methods of calculation are reference methods. For more routine evaluations, multigroup methods are used. Coupled neutron-gamma group data sets are used in S_n computer codes to calculate the properties of interest. A widely used set has the neutron cross-section data in the VITAMIN-J group structure [223].

In line with the international practice, to obtain the bias factors for shield design relevant to the PFBR [87], mockup experiments have been carried out in the shielding corner cavity of the APSARA reactor [228]. The neutron flux was enhanced to 1.03×10^{10} n/cm^2/s by displacing most of the water between the core edge and the stainless steel liner of the APSARA pool on the shielding corner-side with an air-filled aluminium box. Converter assemblies made of depleted uranium were used so that the emergent neutron spectrum represents the PFBR blanket leakage neutron spectrum. The following neutron experiments were conducted in phases with various shield models simulating PFBR radial and axial shields [224]:

- Steel-sodium models, steel-borated graphite-sodium models and steel-boron carbide-sodium models for simulating similar shields in the radial direction;
- Steel-graphite-boron carbide-sodium models to study the effect of replacing boron carbide by graphite in the radial shields;
- Steel-sodium models simulating upper axial shields to obtain bias factors for the flux at the detector location;
- Radiation streaming through the gas plenum model simulating the lower axial gas plenum to obtain bias factors for estimation of dpa at grid plate;
- Scaled down models of the top shield and transfer arm to validate the radiation streaming calculations.

While Monte Carlo computations are able to predict the measured results reasonably accurately, the deterministic transport method used in the PFBR design with 100 neutron + 21 gamma group cross-section library were prone to more errors.

In the case of transport through steel-sodium shields, calculations predict fluxes within a factor of 2. For shield models with borated graphite and boron carbide, the calculations generally under-predict the neutron fluxes by factors in the range of 3 to 5. The measurements for the plenum model show that the fast neutron fluence (above 0.1 MeV) and hence dpa are under-predicted by a factor of 1.5 to 3.5. Radiation streaming through the top shield models is

predicted within a factor of 2 and hence a bias factor of 2 in gamma shielding calculations is used. However, the fast neutron flux streaming is underestimated by a factor of 2. Similarly, in all the configurations of transfer arm model, fast neutron flux is under predicted by a factor of 2.

For the shielding applications, the 121 (100 n, 21 γ) group coupled cross-section set, called DLC-37 of US origin had been in use. In view of a few major drawbacks in this set, a new 121 group set, viz. IGC-S2, in the same format as the DLC-37, was created [229] from ENDF/B-VI with anisotropy considered up to P5. In the long run, in order to reduce the uncertainties to less than a factor of two, a new 175 neutron + 42 gamma group cross-section library has been derived from ENDF/B-VI. Use of this library with self shielded cross-sections and larger number of thermal groups led to better predictions [226]. This 175 group library is used for in-vessel shield design and local shield of the intermediate heat exchanger.

6.2.7. Validation of methods and data

The measurements available for validation studies comprise simple integral measurements, which can be used to adjust, or select, nuclear data, and mock-up type experiments, more appropriate for assessing the accuracy of methods, and possibly also for deriving bias factors. There also exists a large experimental database for validation of the overall depletion methodologies, derived from destructive measurements of EBR-II experimental test assemblies and processing irradiated EBR-II fuel assemblies in the Fuel Conditioning Facility (FCF) [227].

The main sources of fast reactor core integral data have been: the Argonne National Laboratory facilities ZPR-3, -6 and -9, and ZPPR, in the USA; ZEBRA (Winfrith) and VERA (Aldermaston) in the UK; MASURCA (Cadarache) in France; SNEAK (Karlsruhe) in Germany; FCA (Tokai) in Japan; and BFS-1 and -2 (Obninsk) in the Russian Federation. Of these, only MASURCA, FCA and the BFS facilities are currently in use for fast reactor studies. In addition to these, studies on small fast reactor core zones have been made in coupled fast-thermal systems, such as MINERVE (Cadarache) in France, PROTEUS at the PSI Institute in Switzerland, SEG/RRR (Dresden) in Germany and STEK (Petten) in the Netherlands. The latter two have been used for small sample reactivity worth measurements on fission product isotopes. The small Los Alamos criticals, such as Godiva and Jezebel, also provide a valuable check on higher energy data for fast reactors. A good range of integral data is to be found in the CSEWG Benchmark Book (ENDF-202), but this is far from complete. In addition to the measurements made in critical facilities, irradiations of samples in power reactors provide valuable data on spectrum-averaged cross sections.

The simple integral data are of the following types:

(i) Values of k_{eff} measured on simple geometry cores;
(ii) Critical buckling in the central regions of cores;
(iii) Central reaction rate ratios (fission rates and ratios of ^{238}U capture to ^{235}U or ^{239}Pu fission);
(iv) Central reactivity worth measurements for small samples;
(v) k_∞ values for zones having k_∞ close to unity, and
(vi) Neutron spectra measured using different techniques

These are all used in nuclear data adjustment studies.

The more complex mock-up assemblies represent two-zone cores with control rods or "rod-follower regions" in the core. Fission rate distributions are measured for different configurations of rods. Particularly large cores have been studied in ZPPR, corresponding to commercial sized fast reactors. Studies have also been made of different configurations of sodium voiding and possible fuel meltdown accident configurations.

Shielding studies have been made on a number of facilities such as the ORNL Tower Shielding Facility in the USA, NESTOR in the UK and HARMONIE in France (none of which are currently in use for shielding studies). The measurements are of two types: transmission through blocks of single materials (such as iron) and simple material combinations (iron and sodium), or mock-up configurations. Simple geometry measurements are used for the adjustment of nuclear data. Measurements are made not only of neutron transmission but also gamma ray transmission. Measurements have also been made of gamma energy deposition in core regions.

Inter-comparison exercises have been carried out, in particular of reaction rate ratio measurement techniques, a recent example being the IRMA inter-comparisons carried out in MASURCA [228].

The overall scope of the measurement programmes can be seen by referring to conference proceedings, such as the 1990 PHYSOR conference. One example is a summary of the comprehensive programme of measurements carried out at the start-up of Superphénix [229]. Also, the measurements carried out on the large critical assemblies ZPPR-18/19 at ANL are summarized in [230]. These include measurements of the reactivity worth of different configurations of control rods and the associated fission rate distributions. Measurements carried out in the JANUS programme of shielding benchmark experiments are described in [222]. This is a step-by-step sequence of measurements on stainless steel, sodium and boron carbide (including different combinations). Reaction rate distribution measurements have also been made through the core and shields of Superphénix and are discussed in [231]. The conference proceedings also cover gamma energy deposition measurements made in MASURCA, described in [232].

An International Handbook of Evaluated Criticality Safety Benchmark Experiments has recently been published under the International Criticality Safety Evaluation Project (ICSBEP), which is an official activity of the OECD/NEA Working Party on Nuclear Criticality Safety [55]. Currently, the handbook contains 442 evaluations representing 3955 critical, near-critical or subcritical configurations, 21 criticality alarm placement/shielding configurations with multiple dose points for each, and 20 configurations that have been categorized as fundamental physics measurements that are relevant to criticality safety applications. Among the 3955 critical, near-critical or subcritical configurations, 510 are fast systems.

An effort is ongoing to document the criticality experiments performed on Argonne National Laboratory’s plate-type fast critical assemblies as benchmarks in ICSBEP [233]. More than a hundred sets of critical assemblies were constructed between 1955 and 1990 at ANL Zero Power Reactor (ZPR) fast critical assembly facilities. In support of the national effort to develop fast reactors, three classes of ZPR assemblies were constructed: engineering mockups, engineering benchmarks, and physics benchmarks. Criticality was always measured, and typically, many other quantities of interest for fast reactor design were also measured, including reaction rate ratios, spatial reaction rates, control rod worth, sodium void

reactivity, Doppler worth, and flux rations. To date, twenty-six ICSBEP benchmarks based on ZPR critical assemblies have been prepared.In Japan, a new unified cross-section set for fast reactors, ADJ2000 [207], was successfully developed, the features of which are:
(1) JENDL-3.2 base;
(2) Adjustment of self-shielding factors;
(3) Application of the latest cross-section covariance;
(4) Experiments of various independent cores;
(5) aadoption of burnup- and temperature-related characteristics; and
(6) Full use of statistical chi-square values.

The ADJ2000 can predict wide-variety cores with high accuracy, from large to small size cores, and from critical experiments to power reactor, for various core parameters. The ADJ2000 was opened to public from JNC, and it is currently widely utilized in fast breeder reactor core analysis and design study.

(a) Integral data testing of ENDF/B-VII.0

As an effort to validate the ENDF/B-VII.0 library released in December 2006, integral testing was performed for more than 700 benchmark configurations in the ICSBEP handbook using primarily the NJOY and MCNP codes [2, 3]. This test included 98 fast critical benchmarks; 1 compound and 97 metal fuel forms. Compared to the ENDF/B-VI.8 library, significant improvement in the calculated k_{eff} was observed with the ENDF/B-VII.0 cross section data set. The average deviation of C/E values of k_{eff} from unity was: 0.18% for 16 intermediately-enriched uranium systems; 0.15% for 66 highly-enriched uranium systems; 0.19% for 4 mixed fissile systems; 0.23% for 7 plutonium systems; and -0.36% for 4 ^{233}U systems. Of nine bare or ^{238}U reflected LANL fast assemblies, seven C/E values for k_{eff} were within the estimated 1σ experimental uncertainty.

For additional highly-enriched uranium benchmarks, either base or with various reflector materials, the C/E values were within the experimental uncertainty in eight out of fourteen cases. Of the six cases that fall outside the estimated 1σ experimental uncertainty, the uncertainty was either very (to the point of being unrealistically) small or not given. For plutonium systems with various reflector materials, the C/E for k_{eff} was within the estimated 1σ experimental uncertainty in eight of ten cases. Calculated k_{eff} values with the VIM code for a suite of 26 Argonne ZPR and ZPPR benchmark also showed improvements, but significant deviations from unity still remained. In particular, the k_{eff} of the ZPR-6 assembly 10, which has an intermediate (soft) spectrum, was over-predicted by over 3.5% with ENDF/B-VII.0 and ENDF/B-VI, while it was very well predicted (C/E ≈ 1.001) with the ENDF/B-V data. The ZPR and ZPPR results suggested a need to review of the tungsten evaluation and the data in the resonance regions for ^{239}Pu, chromium, and manganese.

Delayed neutron data was also tested against measurements of the effective delayed neutron fraction β_{eff} in critical configurations. This test included five fast spectrum cores in MASURCA (R2 and ZONA2) and FCA (XIX-1, XIX-2 and XIX-3), whose β_{eff} were measured by several international groups [234]. The core R2 had ~ 30% enriched uranium as fuel, whereas ZONA2 had both plutonium and depleted uranium. Both cores were surrounded by a 50-50% UO_2-Na mixture blanket and steel shielding. The XIX-1, XIX-2, and XIX-3 cores respectively had highly enriched uranium, plutonium and natural uranium, and plutonium as fuel. The cores were surrounded by two blanket regions, one with depleted uranium oxide and sodium, the other with only depleted uranium metal. The ENDF/B-VII.0

data yielded improved results compared to the ENDF/B-VI.8 data. The C/E value for β_{eff} obtained with the MCNP code and the ENDF/B-VII.0 data deviated from unity by 1.2%, -2.7%, -1.3%, 1.0%, and -1.9% for R2, ZONA2, XIX-1, XIX-2, and XIX-3, respectively.

Reaction rates and spectral indices were also tested against the measurements in the LANL fast critical assemblies: Godiva, Jezebel, Jezebel-23, Flattop-25, Flattop-Pu, Flattop-23, Big-10, and Topsy. The calculated spectral indices with the ENDF/B-VII.0 data agreed with measurements very well, often within the (small) experimental uncertainties. A notable exception is for Godiva, where ^{238}U f/^{235f} U spectral index was calculated 4% low (over three standard deviations).

(b) Effective multiplication of a core at startup

At the initial startup of a reactor, none of the fuel has been irradiated, and the reactor fuel loading programme must be planned to move progressively to the equilibrium cycle in which a fraction, 1/N, of the core is replaced at each reloading. At the end of a stage of an equilibrium cycle, 1/N of the core will be at the maximum average end-of-cycle burnup, *b*, and the average burnup of the core as a whole at the end of an equilibrium cycle is ((N+1)/2N)·*b*. At the beginning of a new step in the cycle, when fresh fuel has been loaded into 1/N of the core, the average burnup is ((N-1)/2N)·*b.* The control rod requirements are designed to compensate for the change in reactivity with burnup, *b/N,* in each cycle, together with the safety requirements and the control required taking the reactor from the normal shutdown condition to operating power level. The safety requirements include a provision for the failure of some rods to enter the core at shutdown. The method usually adopted to progress from the initial startup condition to the equilibrium condition is to insert steel diluent assemblies in place of some of the core assemblies, to compensate for the reactivity change associated with burnup, ((N-1)/2N)·*b*. This initial core is therefore more complicated to analyze than the equilibrium core because of the added complexity of these diluent assemblies.

The equilibrium core must be analyzed to predict the fuel enrichment required to provide a critical state at the end of an equilibrium cycle and at normal operating power (and temperatures). Determining the required fuel enrichment requires accurately predicting the variation of reactivity with burnup and with power.

Measurements have been made on operating power reactors, such as Phénix, Superphénix and PFR, of the variation of reactivity with burnup and with power level. Measurements have also been made of the reactivity of the core loadings at initial startup. In the Superphénix startup configuration measurements, good consistency has been found with the results of analyses of measurements made on critical facilities, to within the expected accuracy of predictions of ±0.5% (or 500 pcm). These measurements also provide an accurate reference point for future predictions [235]. Measurements have also been made of the effect of replacing fuel subassemblies with steel diluent subassemblies. Agreement with calculation is good except for substitution experiments in the outer regions of the core [236].

In Japan, the prototype fast reactor Monju achieved initial criticality with 168 fuel subassemblies in April of 1994, and the first start-up core with 198 fuel subassemblies was assembled in May of 1994. Monju experimental data analysis was performed by using the detailed deterministic calculation scheme for fast reactor cores developed in Japan, the features of which are:

- Cell-heterogeneity treatment by collision probability;
- 3-D hexagonal modelling with transport theory, and
- Ultra-fine energy-group correction.

The C/E (calculation/experiment) values of Monju initial core criticality and the first start-up core criticality based on JENDL-3.2 was 0.9952 and 0.9964, respectively [237].

(c) Reactivity with burnup

There are two main effects on reactivity due to burnup. One is the reduction of the proportion of fissile isotopes in the fuel and the second is the buildup of fission products which capture neutrons. There is also the effect of the breeding of fissile material in blanket regions. Measurements have been made of the spectrum-averaged fission and capture cross sections of actinide isotopes (e.g. the PROFIL irradiations in Phénix) and also of the reactivity worth of samples having differing plutonium isotopic compositions (and also core zones having plutonium of different isotopic compositions, the PLUTO programme). Capture cross sections for ^{240}Pu, ^{241}Pu, and ^{242}Pu are overestimated by 13%, 24%, and 17%, respectively, in the calculations based on the JEF-2.2 library, whereas fission cross sections are better predicted (±3%). The measurements used to validate the fission product nuclear data include small sample reactivity worth measurements made in STEK and activation measurements made in CFRMF, ERMINE (the ZONA 1 and ZONA 3 programmes) and Phénix [238]. The measurements have been made for 40 fission products which contribute about 80% of the total reactivity effect. Measurements made on Phénix fuel pins have been used to develop a model for the time-dependent release of gaseous and volatile fission products. This reduces the fission product reactivity effect typically by about 5%, and the accuracy of the calculation of this reduction is estimated to be ±20% (1σ).

A general conclusion from the nuclear data in the JEF-2.2 library was that the inelastic scattering cross sections for many even-mass nuclides were about a factor of two low because of the neglect of direct interaction effects in the nuclear models used to calculate these cross sections. The contribution of inelastic scattering is of the order of 15% of the total fission product reactivity effect. The most important even-mass nuclei are ^{98}Mo and ^{100}Mo; ^{102}Ru, ^{104}Ru, and ^{106}Ru; ^{106}Pd and ^{108}Pd; ^{132}Xe and ^{134}Xe; ^{146}Nd and ^{148}Nd; and ^{152}Sm. Improved theoretical models have now been developed and validated by direct measurements of the differential cross sections of Pd isotopes. As a consequence of the analyses of the integral measurements, it has been concluded that the contribution of fission products to the variation of reactivity with burnup can be predicted to within ±5% (1σ) for a conventional fast reactor.

(d) Characterization of spent fuel

An extensive set of analytical laboratory measurements for EBR-II spent fuel samples were made at the Fuel Conditioning Facility (FCF) over the duration of the Spent Fuel Demonstration Programme [227]. A diverse set of measurements was performed on these chopped segment samples, including: sample mass; U mass / sample mass; Pu mass / sample mass; Zr mass / sample mass; Na mass / sample mass; burnup (via determination of La and Tc content); U isotopic fractions (^{234}U/U, ^{235}U/U, ^{236}U/U, ^{238}U/U); Pu isotopic fractions (^{239}Pu/Pu, ^{240}Pu/Pu); gamma spectroscopy (^{134}Cs, ^{137}Cs, ^{144}Ce, ^{106}Ru/^{106}Rh, ^{54}Mn, ^{60}Co, ^{95}Nb, ^{125}Sb, ^{154}Eu, ^{155}Eu, and ^{95}Zr). The U and Pu masses and the U and Pu isotopic fractions were experimentally determined by isotopic dilution mass spectroscopic (IDMS) analyses. The measurement of La content is accurately determined by inductively coupled plasma atomic

emission spectrometry (ICP-AES) measurements [239, 240]. This technique eliminates the separation of the fission product (or burnup indicator) by either ion exchange or solvent extraction and subsequent measurement by IDMS methods. The ICP-AES measurements have a number of advantages, including:

(i) Much shorter time and not so labour intensive;
(ii) Reduced waste generation; and
(iii) No mixed waste generation.

The ANL calculation methods were used to predict the radionuclide inventories of the irradiated EBR-II driver and radial blanket assemblies [241]. The Zr-alloy driver fuel was inserted into EBR-II rather late in its operational history (in February 1985), a large fraction of radial blanket assemblies resided in the EBR-II grid since its initial operation in August 1964. Experimental assemblies tended to be similar to driver assemblies in design, but may contain more than one type of fuel element or may have been reconstituted using some fresh fuel elements combined with some previously irradiated fuel elements. Most EBR-II assemblies were moved to more than one location in the reactor grid over their irradiation lifetime.

For the depletion analysis of the EBR-II driver-type assemblies, a multigroup library with 9 broad energy groups was generated using ETOE-2/SDX/ MC^2-2 with ENDF/B-V data. This library contains region- and unit-cell-dependent cross sections for all of the nuclides included in the Version V data files. These 9 group cross sections were used to perform core-follow calculations with the REBUS-3/RCT codes for each of the EBR-11 runs which contained the Zr-alloy fuel. The REBUS-3 model utilized hexagonal-Z geometry and included each reactor grid location (homogenized). Block depletion was performed using the nodal diffusion theory option of DIF3D. Each of these EBR-II runs were then analyzed using the RCT code which interpolated the three dimensional group fluxes and currents within the node of the assemblies and performed pin (fuel element) depletion. The REBUS-3 and RCT codes each used the same limited depletion chain that included only 19 “active” (or burnable) isotopes, ranging from ^{234}U through ^{246}Cm and lumped fission products. This extensive set of depletion calculations produced a complete set of three-dimensional 9 group fluxes for each pin in each fueled assembly.

For the depletion analysis of radial blankets, the lengthy sequence of actual EBR-II configurations was simulated with a much smaller sequence of seven “generic configurations” that capture the major core loading and geometry changes over the operating history of EBR-II. A set of 28 group fluxes were obtained for each of these configurations using full core 3-dimentsional (hexagonal-Z) models with the VARIANT nodal transport theory option of DIF3D. The 28 group cross sections were collapsed from an ENDF/B-V based ETOE-2/ MC^2-2/SDX generated 231 group library with a one-dimensional EBR-II model employed for spatial collapse. A flux reconstruction module was used to recover the detailed intra-assembly flux distribution from the nodal VARIANT results.

This module yields the multigroup flux as a function of time for each generic model at any blanket pin position. These fluxes were then used to derive one-group cross sections and one-group fluxes averaged over each run of the reactor appropriate for selected axial regions of each fuel element. The ORIGEN-RA analyses employed highly detailed nuclide transmutation chains, and provided the fuel element nuclide densities and radiation emission characteristics in detail.

A series of ORIGEN-RA calculations was then performed corresponding to each axial zone of each of the fuel element. The one-group fluxes input to these calculations trace the irradiation history of the fuel element. Furthermore, the default one-group cross sections in the ORIGEN-RA libraries were replaced at run-time with the appropriate flux-weighted one-group cross sections for all available nuclides.

A summary of the validation results based upon the complete Spent Fuel Demonstration Programme at the FCF has been presented in [227]. The mean calculated-to-measured (C/M) ratio for the U content for all samples taken near the axial centre of the fuel elements was 1.003; the standard deviation in these C/M values was ~ 2.2%. The mean C/M for the ^{235}U/U fraction was 0.997±0.001. This small bias in the ^{235}U enrichment indicated the calculations over-predicted the burnup. The larger spread or deviation in the C/M values for the U content of the sample reflects the larger variation of the U in the samples (than the variation of the ^{235}U in the U). This greater difficulty in measuring absolute values (such as U content) than relative values (such as ^{235}U/U) was observed in all of this validation data and was a by-product of the difficulty of obtaining and preparing samples from the irradiated fuel elements. The agreement between measurement and calculation of the other U isotopic fractions was also good. The mean C/M (±1σ) values for ^{238}U/U, ^{234}U/U, and ^{236}U/U were 1.005±0.001, 0.979±0.006, and 1.011±0.016, respectively. The mean C/M ratio for the Pu content was 1.063. This bias was observed over the duration of the Spent Fuel Demonstration Programme with a rather small deviation (1σ of ±0.043) and with no discernable correlation with core location, burnup, etc.

The agreement between calculation and measurement of the isotopic fractions of Pu was similar to the agreement observed for the U isotopic fractions, in the sense that there is excellent agreement (1.0000±0.0004) for the principal fissile nuclide fraction (^{239}Pu/Pu) and much poorer agreement for the remaining minor Pu nuclide fractions. The mean C/M (±1σ) values for ^{238}Pu/Pu, ^{240}Pu/Pu, and ^{241}Pu/Pu were 1.200±0.050, 0.944±0.024, and 1.097±0.131, respectively. There was a significant bias in the predicted La content - much like the bias in the predicted Pu content. The mean of these C/M values for La is 1.069±0.059. Again this bias was observed over the duration of the Spent Fuel Demonstration and again with no discernable correlation with core location, burnup, etc.

The over-predictions of both Pu and La (i.e., burnup) are likely the result of an incorrect normalization of the reactor power in the depletion calculations. The under-prediction in the ^{235}U/U fraction is also consistent with the over-prediction of the burnup (or depletion of ^{235}U). The magnitude of these biases is consistent with the uncertainty (~ 5%) in the power normalization of EBR-II.

The strong correlation between the Pu buildup and La content or burnup indicates a simple renormalization of the reactor power in the depletion calculations (by the inverse of the average bias on these quantities, i.e., reduction of the power by a factor of 1/1.065) would largely eliminate these biases. Such “renormalized” calculations were performed and shown, in fact, to bring the calculated values of ^{235}U, Pu, and La into excellent agreement with the measured data. Although most of these validation results displayed very good agreement between calculation and measurement, there remained a few notable unresolved discrepancies. There was a 20% bias for the calculated values of the ^{238}Pu/Pu weight fraction. The magnitude and consistency of this bias implied an error in the modelling of the production and/or destruction of ^{238}Pu. There was a consistent bias observed between the C/M

values for La content and Tc content. There was a bias of ~ 7% in the predicted La content of these samples.

However, there was essentially no bias (0.008±0.040) in the predicted Tc content of these samples. This consistency of the calculated and measured values of "burnup" via the Tc content of the samples was inconsistent with all the remaining validation data. In this case the size of the errors in both the calculations and measurements made it difficult to determine the source(s) of the error.

(e) Incineration of fission products

Feasibility studies on the incineration of actinide isotopes and fission products are being made in several countries. In the case of fission products, attention has been focused on the incineration of ^{99}Tc and ^{129}I. Following neutron capture, both nuclides decay rapidly to the stable isotopes ^{100}Ru and ^{130}Xe, respectively. One method being considered is the use of special moderating assemblies located in the breeder regions of fast reactors. (This technique has been used successfully in Phénix for the production of ^{60}Co from ^{59}Co). An irradiation test has been carried out in the Fast Flux Test Facility.The percentage of transmutations in a 10.5 equivalent full power days irradiation were about 0.7% for ^{99}Tc and 0.4% for ^{129}I. The agreement between the measured and calculated values is about 15%. One can foresee transmutation rates of about 10% per year being achieved in this way.

(f) High Pu carbide fuel and FBTR experience

In India, the FBTR used high Pu carbide fuel for the first time in 1985 [242]. The fuel was 70% PuC–30% UC. Progressively from the initial targets of linear heat rating at 250 W/cm and peak burnup of 25 GWd/t, the targets presently achieved are 400 W/cm heat rating and 155 GWd/t peak burnup [243]. The Doppler coefficient of the fuel is practically zero, but reactor safety is ensured by the prompt negative core expansion coefficients. Absorber rod worth, power and temperature coefficients of reactivity have been measured several times in FBTR. As absorber rod worth is measured using the inverse kinetics method, delayed neutron fractions arising from predominantly Pu fissions are important input parameters.

In ENDF/B-VI, the delayed neutron fractions of a delayed neutron group from a individual fissile isotope has been derived from neutron emission probabilities of delayed neutron emitter and yields of respective precursors. It was of interest to compare how this basic approach compared with the integral yields evaluated and incorporated in ENDB/B-V from the works of Keepin and Tuttle [244].

Between ENDF/B-V and VI, the total delayed neutron fraction of any fissile isotope is same even though the group values are different. This was because, after obtaining the individual group worth by summation method, totals were normalized to the old measured integral yields. Due to the high Pu content in FBTR, the differences in worth computed by the two sets of delayed neutron fractions were large enough for finding consistency with computed worth. From an analysis of FBTR absorber rod worth it was concluded that the summation method incorporated by Brady and England in ENDF/B-VI was deficient [245].

6.3. Thermal hydraulics

In a nuclear reactor, the proper thermal-hydraulic design for the detailed flow and temperature distributions in the reactor core is essential to ensure safe and reliable operation of the reactor

system. The evaluated thermal-hydraulic conditions should guarantee integrity of fuel rod, clad and structures during the normal and the transient operational states. Therefore, the reactor designers try to perform the thermal hydraulic design of core as accurately as achievable because the increased accuracy results in enhanced safety margin and also benefits in economics.

6.3.1. Subchannel analysis

For the thermal hydraulic design of a nuclear reactor core, subchannel analysis codes are frequently used. For this reason, it is required to improve the existing subchannel analysis codes by developing more accurate models. The accuracy in the thermal hydraulic design becomes more important in the design of a liquid metal cooled reactor (LMR) because the fuel pins are configured very compactly and the heat flux from the fuel rods is usually higher than that of a pressurized water reactor.

In a subchannel analysis approach, the temperature, pressure and velocity in a subchannel are averaged, and a representative thermal hydraulic condition specifies the state of a subchannel. Flow and temperature distributions in the core are obtained by modeling and solving the conservations of mass, momentum and energy in a subchannel. Therefore, it is essential to model the inter-subchannel heat transfer between the adjacent subchannels as accurately as possible to enhance the predictability of a subchannel analysis code. These techniques not only predict the mixing behaviour of coolant within the subassembly, also predict the inter-subassembly heat transfer effects. Inter subassembly heat transfer effects are very important in the design of coolant flow distribution through various subassembly especially in the periphery of the core.

6.3.1.1. Analysis methods

In a subchannel analysis, the minimum control volume is a ‘subchannel’ and it is assumed that the thermal-hydraulic state of a subchannel is constant. In other words, one subchannel is represented by one temperature, velocity, and pressure. This means that a fine structure of the velocity and the temperature in a subchannel is ignored and the averaged mass flow rates and temperatures are the main parameters in a subchannel analysis. In a subchannel analysis code, which is a practical method used for the thermal-hydraulic design of a nuclear reactor, the axial momentum and energy equations for an arbitrary subchannel ‘i’ are described as follows, respectively:

$$\frac{\partial m_i}{\partial t}+\frac{\partial}{\partial x}\left(\frac{m_i^2}{\rho A_i}\right)+\sum_j w_{ij}u^*+\sum_j f_T(w'_{ij}u'_i-w'_{ji}u'_j)=-A\frac{\partial p}{\partial x}-A\rho g-\frac{1}{2}\left(\frac{f}{D_h}+\frac{K}{\Delta x}\right)\left\langle \rho u^2\right\rangle_A A \quad , \quad (1)$$

$$A_i\frac{\partial}{\partial t}(\rho_i h_i)+\frac{\partial}{\partial x}(m_i h_i)+\sum_j w_{ij}h^*+\sum_j (w'_{ij}h_i-w'_{ji}h_j) = Q_{ij}+Q_{ext} \quad . \quad (2)$$

The notation of m_i means the axial mass flow rate and w_{ij} is the lateral flow rate between subchannels i and j. Further, Q_{ij} and Q_{ext} denote the heat transfer due to conduction between two adjacent subchannels and the external heat input per unit length of a flow channel, respectively. In the above equations, the last terms in the left hand sides represent the contribution by a turbulent mixing between subchannel ‘i’ and its surrounding subchannels.

6.3.1.2. Computer codes and experimental verification

In India, the steady state temperature distribution in a subassembly is determined using the multi-assembly code SUPERENERGY [246]. In this code, intra-assembly thermal hydraulic behaviour due to the presence of wire wrap around the pins is described in terms of two-correlated parameters, eddy diffusivity (ε^*) and swirl ratio (C). These parameters, coupled with numerical form of energy equations and along with a flow split model, provide a complete representation of the temperature under forced convection regime. The code takes into account the inter subassembly heat transfer as well. This code is well validated against many international benchmarks.

In the Russian Federation, experimental research on the substantiation of thermal hydraulics of fast reactor core with a square lattice of fuel pins cooled by liquid metal have been executed in the SSC RF-IPPE. Sodium-potassium eutectic alloy (22%Na+78%K) was used as coolant. The velocity fields and heat transfer coefficients have been investigated.

Experimental studies of velocity fields with reference to regular cells of smooth pins with pitch to diameter ratio, s/d = 1.25 and 1.34 were executed in Russia. The value s/d = 1.25 is provided in the regular model bundle consisting of 25 identical pins (diameter of pins is d_1=14 mm), and also in the irregular model bundle consisting of two sub-zones of pins (diameters d_1 = 14 mm and d_2 = 12 mm). In the second case, the instrumented pin (d_1 = 14 mm) with the sensor is located on the border of the sub-zones. It is surrounded with regular square cells with s/d=1.25 on one side, and on the other side with approximately regular square cells with $s/\overline{d}$ =1.34 (the pitch-to-diameter ratio is calculated using an average diameter of pin simulators $\overline{d}$ = (d_1+d_2)/2). Rotation of the instrumented pin with the sensor allows measurement of velocity fields over the perimeter. Measurements are carried out by using the electromagnetic technique [247]. The accuracy of measurements is 1-1.5%.

A permanent magnet is located inside the tube. It is surrounded with a ring of steel “armco” inside the tube and with a copper ring on the tube surface. Two mutually perpendicular pairs of electrodes are located near the end of the magnet. One pair of electrodes measures longitudinal velocity component, another pair measures cross velocity component. Value of the sensor signal is proportional to average velocity w_i in the subchannel which is formed by radial rays directed from sensor electrodes up to crossing with a line of maximum velocity. The angle between these radial rays is equal to 11°.

Figure 6.4 demonstrates distribution of coolant velocity over perimeter of the instrumented pin in the regular model bundle (s/d = 1.25) for two Reynolds numbers: Re = 84560 and 49570. Velocity amplitude $(w_\varphi^{\max} - w_\varphi^{\min})/\overline{w'}$ is 14-15% on average and it poorly depends on the Reynolds number, though it is slightly less for Re = 84560 than for Re = 49570. Here $\overline{w'}$ is the mean coolant velocity in the channel enclosing the instrumented pin.

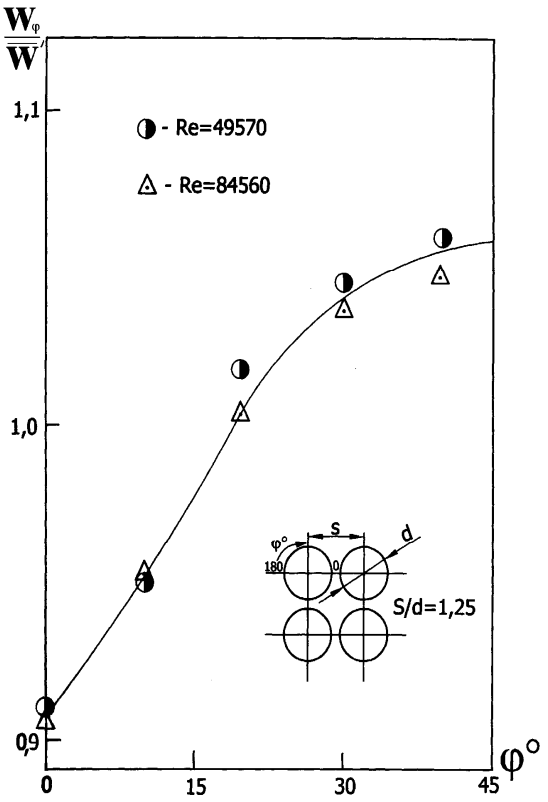

FIG. 6.4. Distribution of relative coolant velocity in a typical square cell (0-45°) for various Re numbers in the regular model bundle with s/d=1.25.

Figure 6.5 demonstrates the velocity field over the perimeter of the instrumented pin in the irregular model bundle (the sub-zone with s/d = 1.25 is in the perimeter section 270°–0°–90° and the sub-zone with s/d = 1.34 is in the perimeter section 90°–270°).

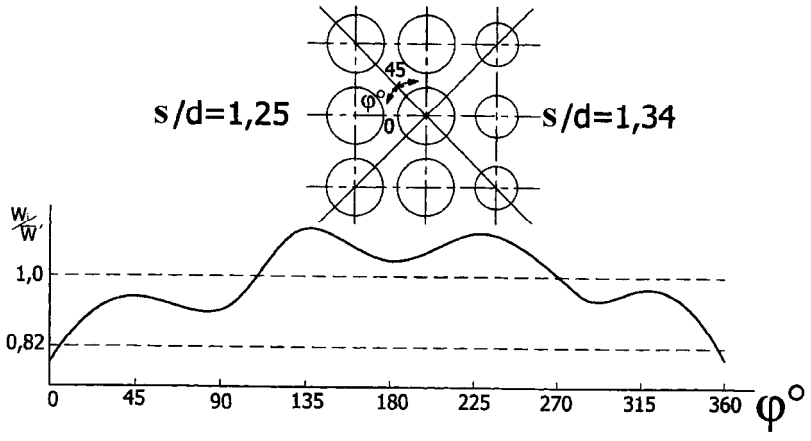

FIG. 6.5. Velocity field in the irregular (geometrically) square cells of smooth pins.

It is seen that for s/d=1.34 the maximum velocity non-uniformity $(w_\varphi^{max} - w_\varphi^{min})/\overline{w'}$ is ~ 10%, and for s/d=1.25 it is 15%. Distribution of velocity non-uniformity in the regular bundle and irregular bundle for cells with s/d=1.25 is in close agreement. This shows the absence of appreciable influence of velocity fields in the two sub-zones to each other. Data obtained in tests show that velocity non-uniformity in square cells is approximately two times larger than in triangular cells with the same relative pitch. Similar thermal hydraulic models with various relative pitches of pins (s/d=1.46; 1.34; 1.28 and 1.25) as that which are used for the study of flow hydraulics have been used for study of heat transfer in square lattice of pins cooled with liquid metal in the Russian Federation. The model assemblies consist of 25 smooth pins located in square lattice inside a rectangular wrapper (cross-section of the modelling assembly with s/d=1.25 is presented in Fig. 6.6.

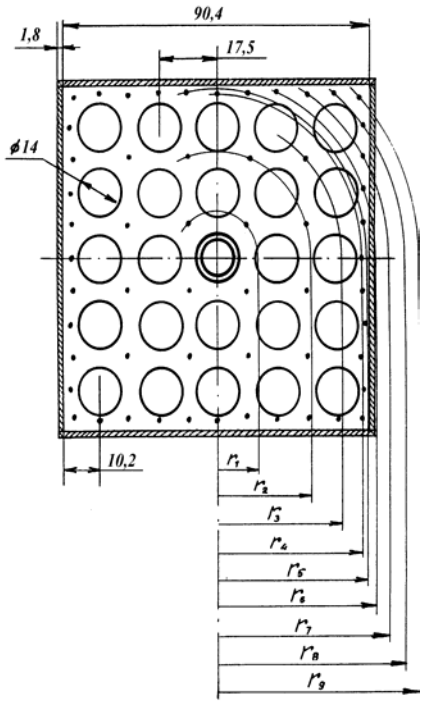

FIG. 6.6. Cross section of assembly (s/d=1.25) with location of thermocouples r_1–r_9 – radii of thermocouple locations.

The gap between outside pins and wrapper wall was chosen to provide equal coolant heating in central and peripheral cells. As a result, geometry of model cross-section in its central part provides a good approximation of conditions appropriate to “infinite” (regular) square fuel pin lattice of fast reactor core

The central pin is instrumented and it can be rotated. Twelve microthermocouples were attached on its surface with regular intervals along the pin length from the beginning of the heated zone and with equal azimuth step ($\Delta\varphi=30°$) along its perimeter. Rotation of the instrumented pin in an interval of corners $0\leq\varphi\leq360°$ allows measurement of temperature distributions on its surface. Other (not measuring) pins are made motionless. The uniform heat

flux is provided along the height and perimeter of pins. Coolant temperature is measured in all cells in the model bundle outlet and also in the inlet and outlet collectors of the model. The experimental data in the stabilized heat exchange area have been calculated in dimensionless form and they are represented as generalized relationships for the large interval of changing basic parameters.

The generalized relation obtained for Nusselt number (Fig. 6.7) shows dependence of heat transfer on Peclet number and pitch to diameter and gives limiting transition to the appropriate values for laminar coolant flow:

$$Nu = 7.55\ s/d - 14(s/d)^{-5} + 0.007\ Pe^{(0.64+0.246\ s/d)} \qquad (3)$$

For $1.2 \le s/d \le 1.5$ and $10 \le Pe \le 2500$

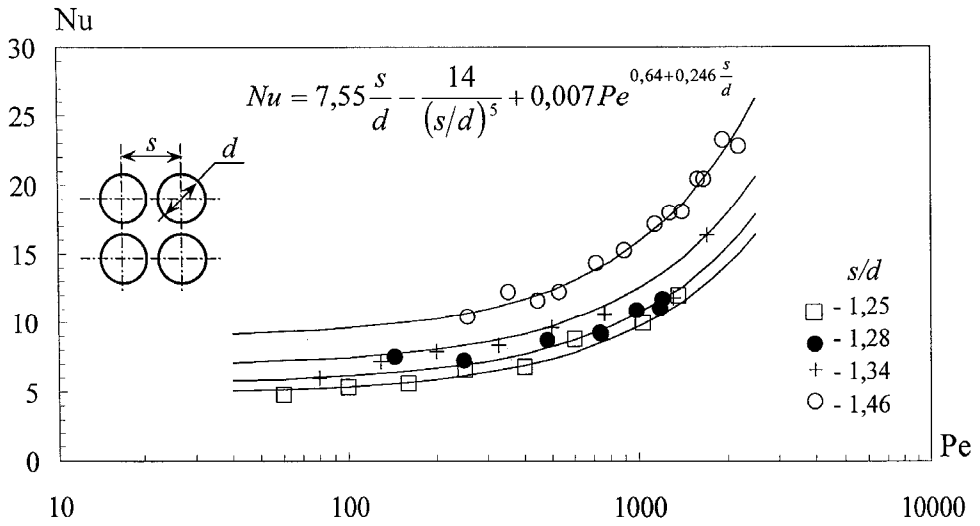

FIG. 6.7. Nu vs. Pe for square bundle with smooth pins for different s/d.

The hydraulic diameter of the central (regular) cells has been used as characteristic dimension in Nusselt and Peclet numbers. The Peclet number is calculated based on velocity of coolant in the central cells. The markers in Fig. 6.7 indicate experimental points and the solid line represents that calculated using Equation (3).

The heat transfer coefficients (Nu) for square lattices of pins are lower than those for triangular lattice of pins for the same equivalent thermal conductivity of pins. Periodic non-uniformity of temperature over pin perimeters corresponds to the cosine function. The generalized formula for the maximum periodic non-uniformity of temperature over pin perimeter (Fig. 6.8) shows dependence on Peclet number and pitch-to-diameter ratio, and gives limiting transition to the appropriate values for laminar coolant flow:

$$\Delta T = (t_w^{\max} - t_w^{\min})\lambda_f \Big/ \bar{q}R = \frac{\Delta T_л}{1 + 5 \cdot 10^{-4} \cdot Pe^{1{,}223\frac{s}{d} - 0{,}42}} \qquad (4)$$

For, $1.2 \le s/d \le 1.35$; $10 \le Pe \le 2500$; $\varepsilon \cong 1.4$

where (λ_f is thermal conductivity of coolant, $\bar{q}$ is average heat flux for surface over the pin perimeter, R is external radius of the pin cladding, ($T_л$ is limiting value of temperature non-

uniformity for laminar coolant flow for different s/d (for pins with equivalent thermal conductivity $\varepsilon \cong 1.4$) determined by the following correlation:

$$\Delta T_{л} = 1.5\ (s/d)^2 - 4.53\ (s/d) + 3.45\ , \quad 1.0 \le s/d \le 1.4. \qquad (5)$$

$\Delta T_{л}$ – value for corresponding s/d for laminar coolant flow

Temperature non-uniformities for square lattice of pins are higher than that for triangular lattices of pins for the same equivalent thermal conductivity of pins.

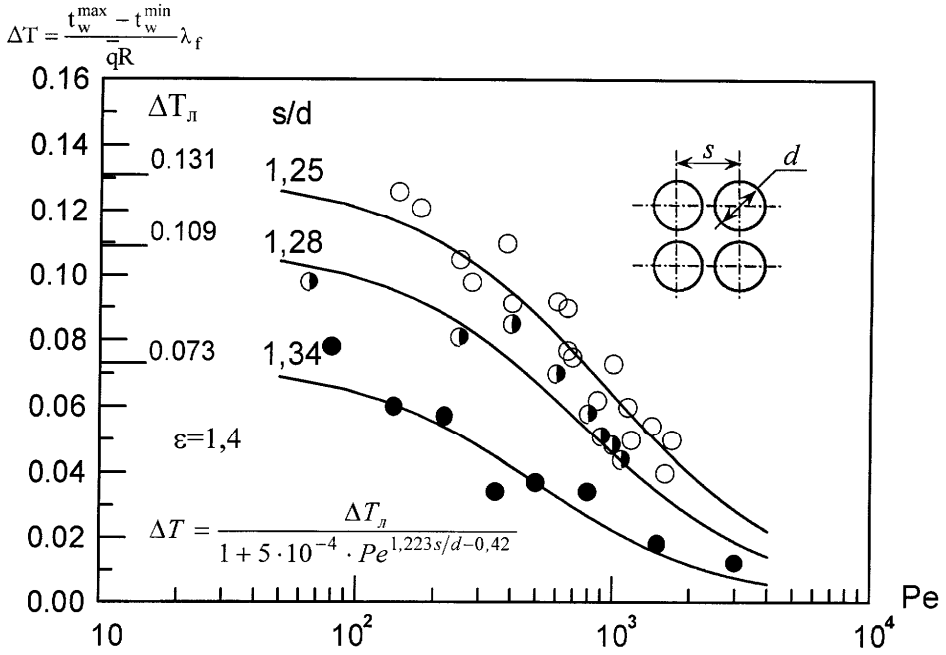

FIG. 6.8. Dependence of maximum temperature non-uniformity of pins Vs Pe for bundles of smooth pins with various s/d.

In Japan, a subchannel analysis code ASFRE was developed at Japan Atomic Energy Agency (JAEA) to calculate single-phase thermal-hydraulic phenomena in a wire-wrapped fuel pin bundle, taking into account of the fuel pin heat conduction and heat transfer to the fluid [248]. A triangular coordinate system is adopted to model the fuel pin bundle in accordance with a triangular pin array configuration, which is typical of LMFR fuel assemblies. The finite difference equations of mass, momentum and energy conservations are derived using the standard control volume integration method based on a specific subchannel control volume. Semi-implicit solution algorithm developed by Liles and Reed is used for time integration. As the pressure equation matrix solver, Incomplete LU decomposition Bi-conjugate Gradient method (ILUBCG) is adopted, which is both vectorized and parallelized in order to make it applicable to large problems such as real reactor full bundle geometry. Momentum or energy exchange at the fluid-fluid interface and fluid-solid interface at subchannel boundaries are modeled in terms of rather simple correlations such as friction factor, wire-forcing function, heat transfer coefficient and turbulence mixing coefficient. Emphasis is placed on the momentum exchange between fluid and wire-wrapped fuel pin wall. ASFRE adopts the distributed resistance model, which can deal with mixed convection as well as forced convection flow with more general treatment of wire spacer. Three dimensional fuel-pin heat conduction model and local blockage model are also available.

ASFRE has been validated through analyses of both water and sodium experiments. Table 6.10 shows examples of experimental data that were used for code validation. Predictability of axial pressure drop and circumferential pressure distribution along wrapper tube was checked against these water experiments carried out at JAEA. With respect to the coolant temperature distribution in a fuel subassembly, sodium tests with relatively small fuel assembly such as 37 pin bundle were utilized: PLANDTL for high flow rate conditions and CCTL-CFR for low flow rate conditions.

TABLE 6.10. LIST OF EXPERIMENTAL STUDIES CARRIED OUT BY JAEA FOR CODE VALIDATION

Purpose	Facility
Water experiments	
Axial pressure drop	JOYO Fuel assembly mock-up test (127 fuel pins)
	MONJU Fuel assembly mock-up test (169 fuel pins)
	Large fuel assembly mock-up test (271 fuel pins)
Circumferential pressure distribution along wrapper tube wall	MONJU Fuel assembly mock-up test (169 fuel pins)
Sodium out-of pile experiments	
Coolant temperature distributions	PLANDTL Test: Normal operation condition (37 fuel pins)
	CCTL-CFR Test: Natural circulation condition (61 fuel pins)

Maximum difference of 10% between the predicted and measured pressure drops is observed in the lowest Re number condition. At Re > 600, the prediction shows good agreement with the experimental data (within 3%). Circumferential pressure distribution along the wrapper tube wall was calculated and compared with the measured data. Figure 6.9a,b shows the horizontal cross-section of MONJU fuel assembly mock-up along with pressure measurement position.

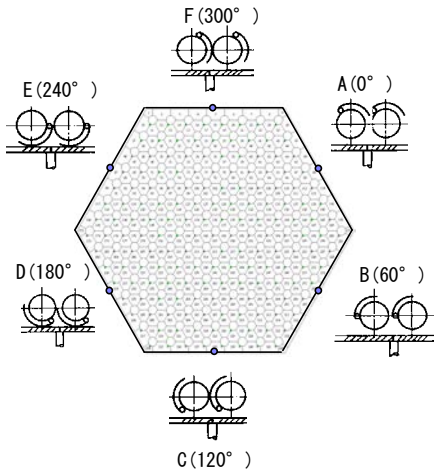

Pressure Measurement Tap Position and Its Relationship with Wire-Spacer Position

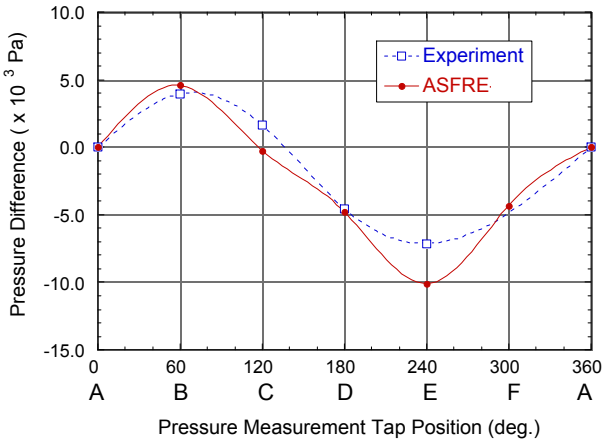

a) *b)*

FIG. 6.9a,b. Comparison of predicted and measured circumferential pressure distribution.

The relationship between pressure tap and wire-spacer position is also indicated (The wire is wrapped counter clockwise). At position B, the wire-spacer comes into the downstream of the pressure tap and blocks the main axial flow. Therefore, the highest pressure appears here. On the contrary, at the position E the lowest pressure appears because the pressure tap exists just behind the wire-spacer against main axial flow. The right hand side of this figure shows the comparison of the measured pressure distribution with the prediction, in which the pressure measured at position A is used as the reference. ASFRE can reproduce the tendency of the pressure distribution even though the pressure deviation due to the wire-spacer is relatively much smaller than axial pressure drop.

Figure 6.10 shows an example of the calculation results of the sodium experiment PLANDTL under the forced convection conditions.

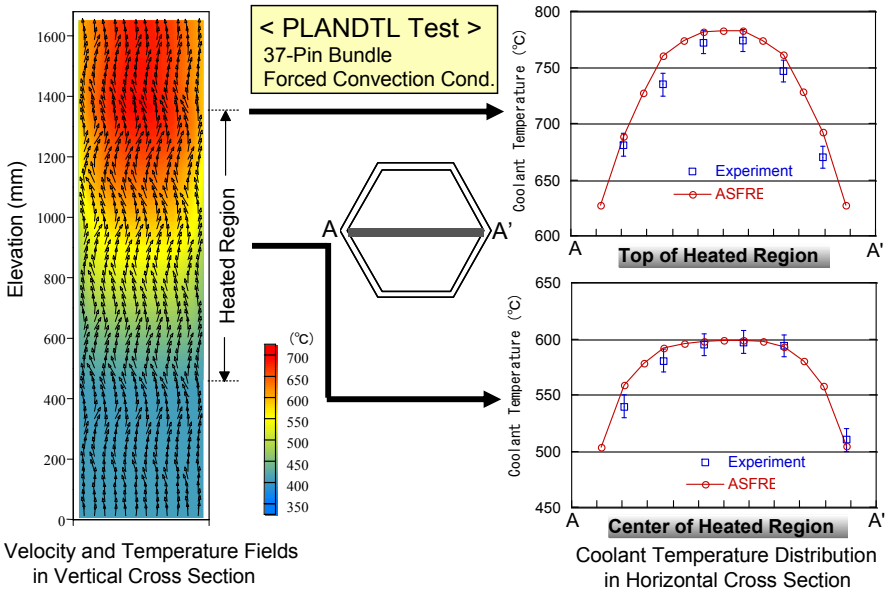

FIG. 6.10. Comparison of predicted and measured coolant temperature distributions.

The left hand side sketch displays the calculated velocity and temperature fields in the vertical cross section of the 37-pin bundle. Twisted flow field is clearly observed in this figure due to the presence of the wire-spacer. Right hand side shows the comparison of coolant temperature distribution in the horizontal cross section at the top of heated region and at the centre of heated region. The temperature distribution is not completely axi-symmetric owing to the effect of the wire-spacer. Considering measurement error and heat loss from test section, agreement between experiment and calculation is good. In the condition of low flow rate, the prediction with ASFRE also showed good agreement with experimental data.

In the Republic of Korea, a detailed subchannel thermal hydraulic analysis code for LMFBRs, MATRA-LMR [249], has been developed based on the COBRA-IV-I [250] and MATRA [251] codes. MATRA-LMR is intended for LMR applications. Thus, some improvements are implemented from the mother code MATRA, which is a code developed to analyse a wide variety of single and two phase flow problems for PWRs. Sodium property relations, correlations of sodium heat transfer coefficients and pressure drop correlations for wire wrap bundle viz. Novendstern [252], Chiu-Rohsenow-Todreas [253] and Cheng-Todreas [254] are included in the code. In order to validate MATRA-LMR code, the THORS tests performed at ORNL have been analysed. The selected THORS test is for the FFM-2A test section [255],

which simulates the normal flow path. In this test, the spacers are wire-wrapped around the fuel rods of 5.842 mm diameter arranged in triangular pitch within a hexagonal duct. The diameter of the wire wrap around the internal rods is 1.4224 mm and its diameter around the peripheral rods near the hexagonal duct is 0.7112 mm. Figure 6.11 shows the comparisons for the pressure drop models used in the MATRA-LMR code with the ORNL FFM-2A test. The accuracy of the pressure drop data is the most important parameter for predicting the temperature distribution in the fuel bundle. It is found that the CRT model is able to predict the pressure drop accurately, though it predicts a slightly higher temperature than the experimental results.

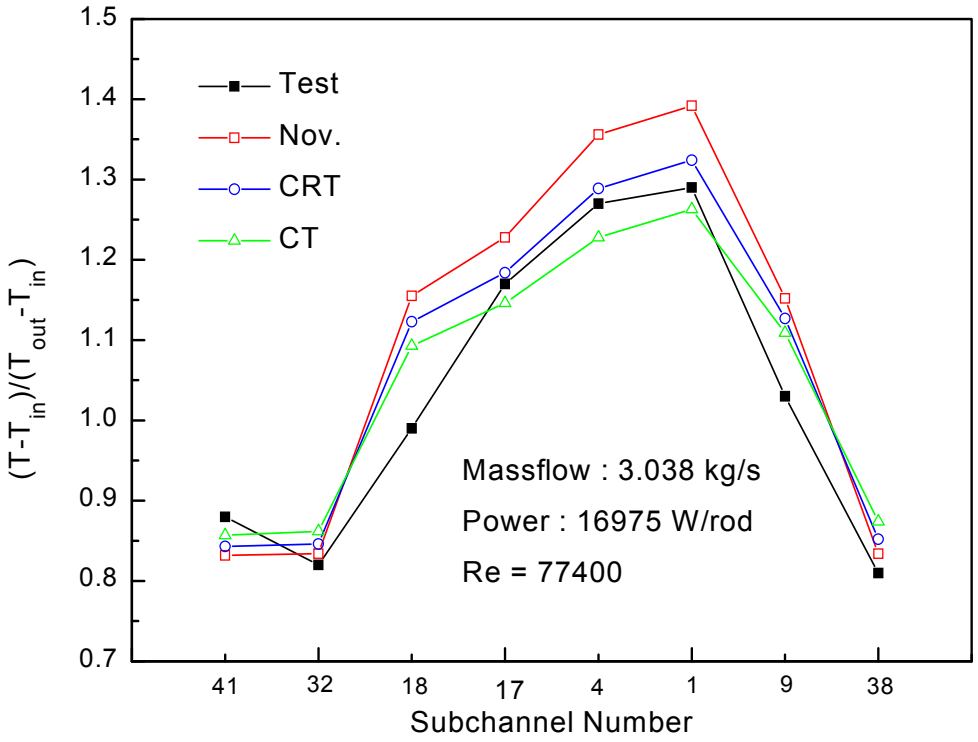

FIG. 6.11. Normalized temperatures at the end of the heated length predicted by MATRA-LMR code.

In France, for subchannel analysis, the CEA has developed the CADET [256] model included in the ELOGE global core modelling. For a fuel or breeder subassembly, the power is dissipated in a pin buddle. The pin bundle itself consists of fuel or breeder pellets, a clad and a helical wire wrap spacer in a hexcan. In the past, many hydraulic and thermal hydraulic studies were undertaken with two objectives: first to achieve optimum performance for each subassembly and the whole core, second to respect the safety criteria on the clad (and the hexcan) to avoid mechanical failure. The physical modelling comes from studies performed in the framework of Rapsodie, Phenix and Superphenix programs. It is based on theoretical and experimental experience. The estimation of maximum clad temperature requires a correct knowledge of the global and local thermal hydraulics of the pin bundle. One of the main effects to take into account is the mixing of the coolant due to the wire wrap spacer which imposes local thermal hydraulic couplings. The distinction between two next sub-channels is made by the fictitious border which is common and where the thermal hydraulic couplings occur. This approach is using physical models coming from theoretical, analytical and experimental data. Figure 6.12 shows a CADET computation of a particular blanket subassembly with a heterogeneous thermal field.

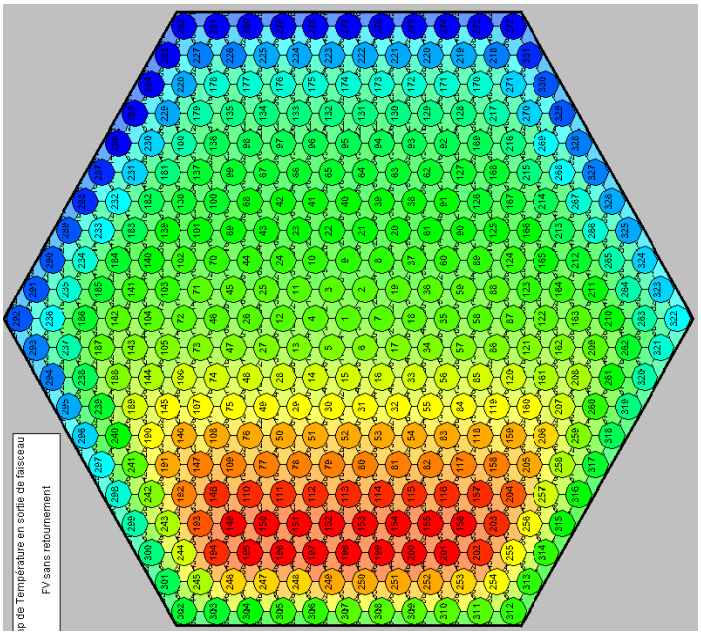

FIG. 6.12. CADET computation for blanket subassembly.

6.3.1.3. Detailed analysis of subassembly

Traditionally, subassembly analysis has relied upon subchannel analysis methods which utilize experimentally derived correlations to describe viscous forces and heat exchange within the sub-assembly and between subassemblies. While these correlations provide accurate predictions within the parametric range spanned by the experimental data from which they are derived, this approach confines the design of new systems to the state space in which all of the correlations used by the model are valid. To extend the state space available to new designs, the detailed thermal hydraulic characteristics must be determined by either new experiments or by detailed CFD simulation. Furthermore, CFD simulations of an assembly or group of assemblies can be coupled directly to neutronics or structural mechanics simulations for detailed evaluations of three dimensional effects, such as rod bowing or channel blockage, when needed. Computational simulation is particularly attractive for liquid sodium cooled systems because sodium experiments are challenging to design and operate. Sodium is liquid only above 98°C and all experiments must be heated experiments. Sodium reacts chemically with both air and water so care must be exercised to design a system which operates safely. Most importantly however, the opacity of liquid sodium renders modern optical measurement methods inapplicable and very detailed distributions of coolant velocity or temperature within a reactor sub-assembly are very time-consuming and costly to obtain. When a large number of parameters are involved or the range of interest for a single parameter is particularly large, numerical simulation is cheaper and faster.

The increasing power of computer systems allows more detailed analysis using CFD codes with refined meshes. The detailed geometry can be modelled and the explicit description of the wire wrap spacer is possible. Such a CFD approach can be a reference and serve as a validation tool for the sub-channel studies. In France, CEA has developed the CFD code named TRIO_U for all kind of thermal hydraulic studies in nuclear reactors, fuel cycle process and non nuclear applications. TRIO_U code is used for thermal hydraulic computations in Fast Reactor subassembly, global core, plenum and heat exchangers. For detailed subassembly analysis, TRIO_U code allows a refined modelling of the pins and wire

wrap spacer. Figure 6.13 shows TRIO_U calculation results of a 61 pins sub-assembly. Such a computation requires about 10^6 elements for one pitch of the helical wire. The computation performed in the year 2008 is using massively parallel 1000 number of processors. The verification of TRIO_U subassembly calculations is based on available global data as pressure drop correlations. A few data are available on velocity fields and flow visualisation in water or air experiments. A few sodium data are also available on temperature profiles. Further experimental velocity fields (in water or air) and temperature fields in sodium are needed to complete the verification of CFD calculations.

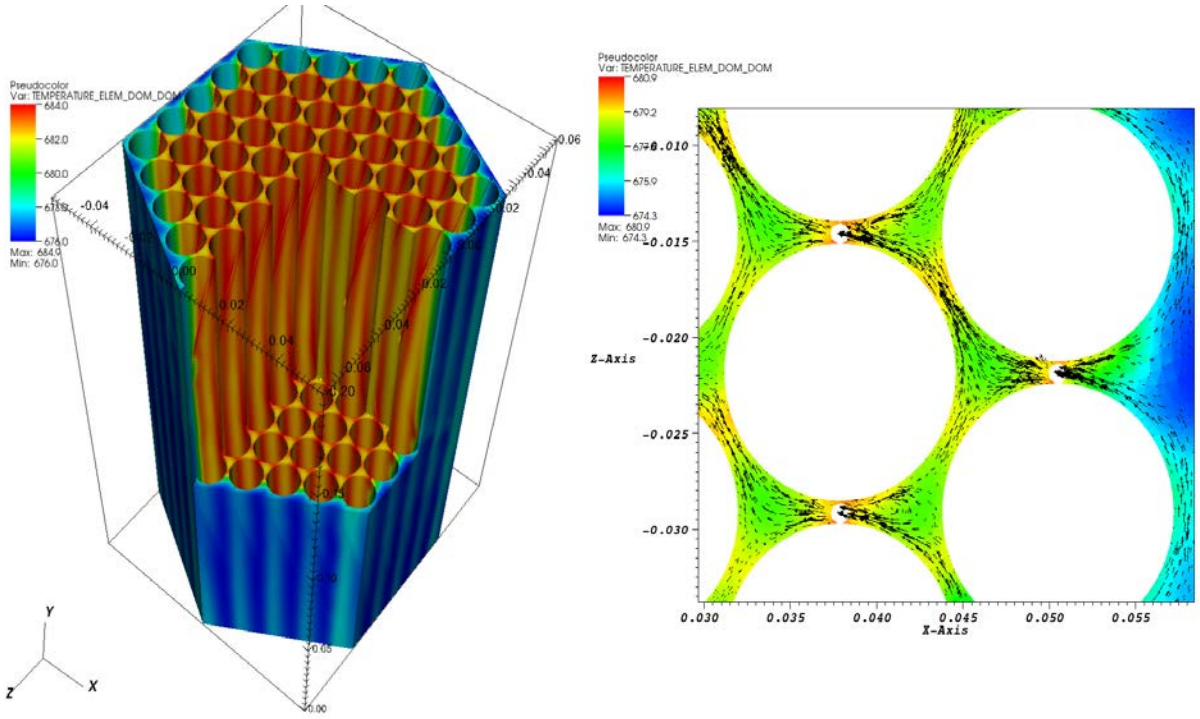

FIG. 6.13. TRIO_U computation of temperature (left) and velocity (right) distribution in a subassembly.

For multi-dimensional thermal-hydraulic analysis of fuel sub-assemblies in the United States, two computer codes are used – the in-house spectral-element method code Nek5000 [257, 258] and the commercial CFD codes Star-CD [259] and Star-CCM+ [260]. The code is based on the spectral element method (SEM), which is a high-order weighted residual technique that combines the rapid convergence of spectral methods with the geometric flexibility of the finite element method (FEM). The SEM employs E elements of order N, resulting in $n \sim EN^3$ grid points for three-dimensional problems, with $N = 4 - 15$ being typical. Nek5000 employs second or third order semi-implicit time stepping, in which the nonlinear term is treated explicitly and the linear viscous and pressure coupling is solved by using state of the art parallel multigrid algorithms. The formulations of the in-house and commercial codes are validated against data sets available for standard problems in the literature such as driven cavities, flow in ducts, backward facing steps, etc. A single span segment of a 7-pin wire-wrapped fuel rod sub-assembly is illustrated in Fig. 6.14.

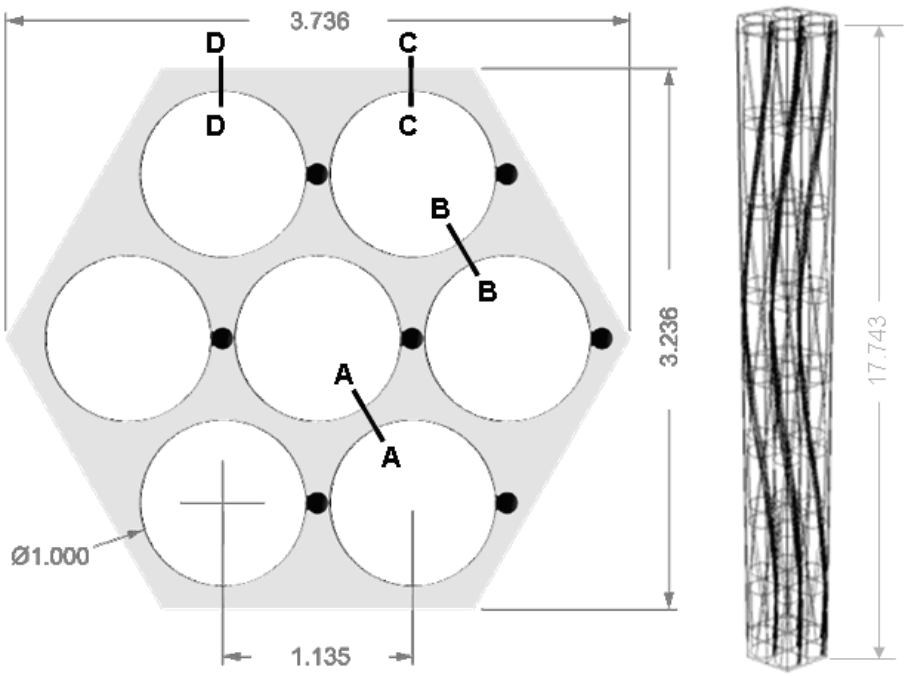

FIG. 6.14. Seven- pin wire wrapped fuel subassembly which is non-dimensionalized based on the fuel pin diameter.

Simulations have been completed using both Reynolds Averaged Navier-Stokes turbulence models available as part of the commercial CFD code Star-CD and the Large Eddy Simulation capabilities of the in-house code Nek5000. Predicted three dimensional flow distributions for a single wire wrap span of the 7 pin wire-wrapped fuel rod sub-assembly from Star-CD simulations are shown in Fig. 6.15. As a preliminary benchmark, cross channel flow rates predicted by each of the codes are shown in Fig. 6.16. The channels along the can do not exhibit cross flow in both directions (all velocities are positive) as a consequence of the bulk rotation of the fluid within the sub-assembly. This occurs because all of the wire wraps are wrapped in the same direction with the same axial span. The CFD-predicted cross-flow velocities have been used to develop improved cross channel flow functions for use in a fast running lower order model of the bundle for evaluation of heat transfer. Based on these preliminary it is expected that the less computationally expensive and faster running RANS models can be used to evaluate these parameters for wire-wrapped bundles. The sensitivity of the RANS model predictions to mesh density, mesh structure (Fig. 6.17) and turbulence model selection have been considered. Mesh converged solutions can be obtained for all mesh types. Solution variability as a consequence of turbulence model selection can be significant. Guidance and validation standards are needed to assure consistent results from code to code and user to user.

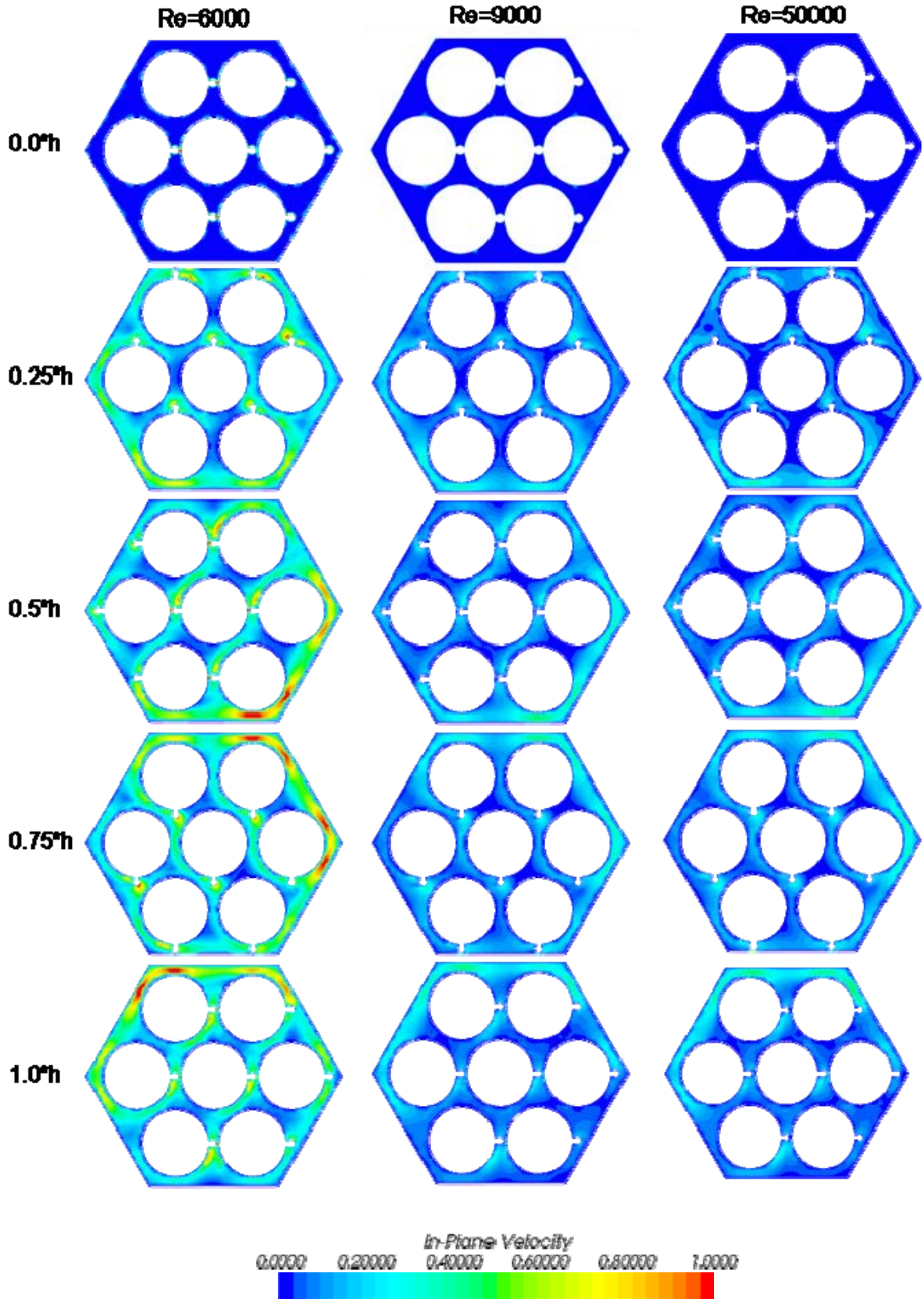

*FIG. 6.15. Predicted in-plane cross-flow velocity distributions in a 7-pin non-dimensionalized fuel assembly for three different Reynolds numbers: 6000, 9000, 50000. (Results are shown for a single axial span of the wire wrap of height h with constant velocity distribution at 0*h)*

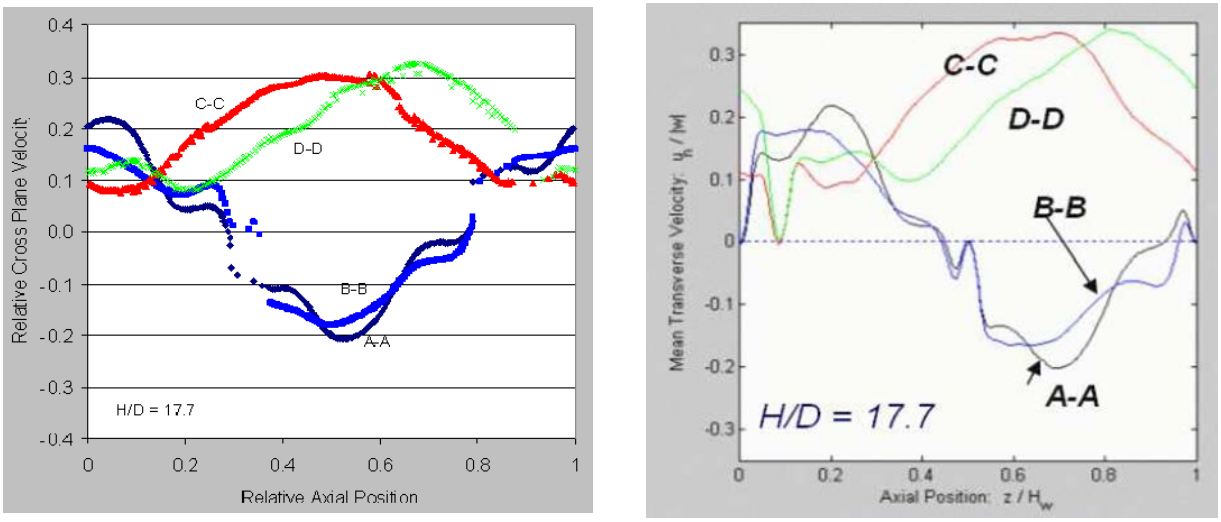

FIG. 6.16. Comparison of predicted cross channel velocities from (a) RANS and (b) LES simulations of a 7-pin fast reactor wire-wrapped fuel subassembly at the four locations shown in FIG. 6.14.

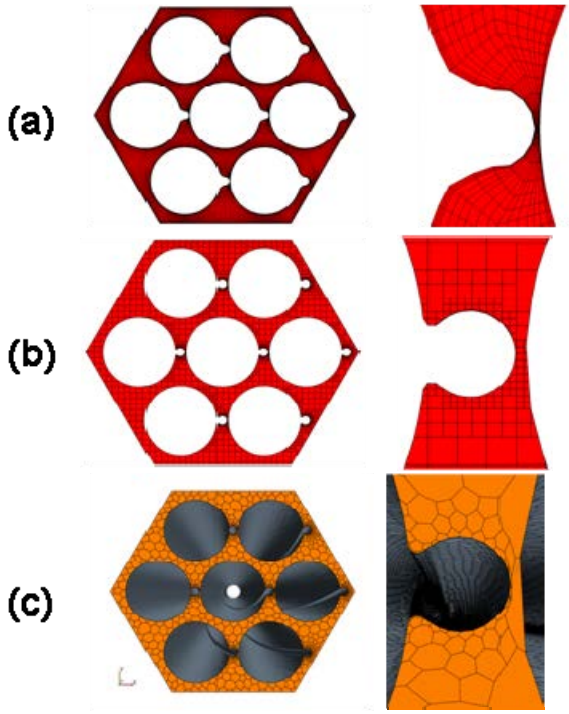

FIG. 6.17. Three mesh structures considered in sensitivity evaluation: (a) structured hexahedral, (b) unstructured trimmed cell, (c) unstructured polyhedral.

As an initial demonstration of the application of the RANS-based models to larger assemblies, a 19-pin sub-assembly has been considered. Results for a single wire wrap span of the of the 19-pin wire-wrapped fuel rod sub-assembly from Star-CD simulations are shown in Fig. 6.18. For assemblies larger than 7 pins the flow field develops a much more organized cross flow pattern in the space between rows of pins rather than primarily rotating around each individual pin as in the 7 pin case. The outer row of channels adjacent to the can wall continue to exhibit the bulk rotation seen in the 7 pin case.

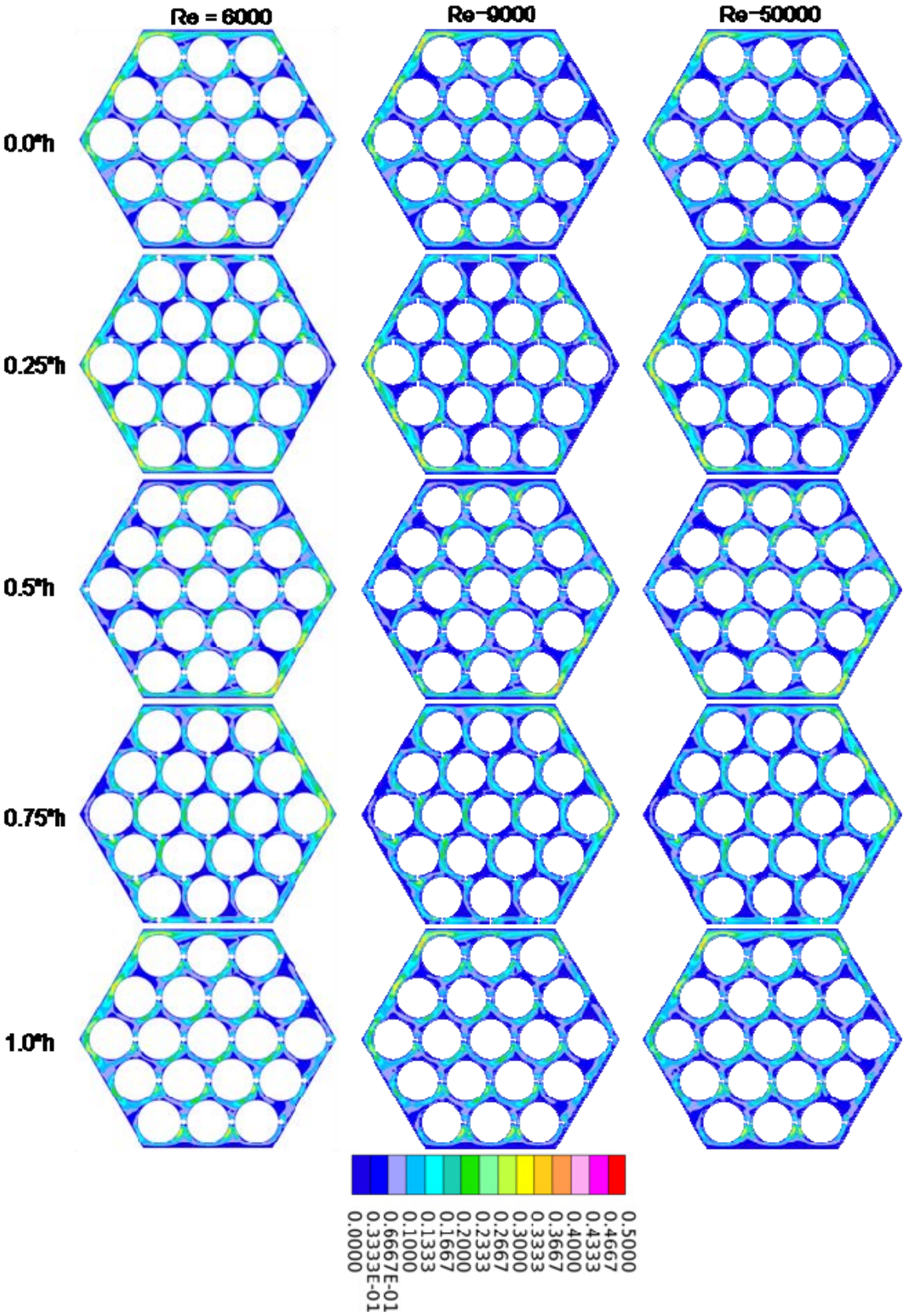

FIG. 6.18. Predicted in-plane velocity distributions in a 19-pin fast reactor wire-wrapped fuel sub-assembly for three different Reynolds numbers: 6000, 9000, 50000
(Results are shown for a single central axial span of the wire wrap of height h. Model includes multiple axial spans to limit boundary condition effects).

All simulations carried out in ANL discussed above were completed using 3.2 GHz Intel Em64t processors. Serial runs and all pre/post processing were completed using 64 bit operations on a workstation with 8 GB of RAM. Parallel computations were completed using a 100 node Beowulf cluster with 1 GB of RAM per node and a 1 GB Ethernet interconnect. Although there was some variability from case to case, for the 7-pin single span cases, total cpu time invested was approximately divided as follows:

- Serial generation of the surface mesh: 2 hours
- Serial generation of the volumetric mesh: 1 hour
- Parallel simulation using 8 CPUs: 1.5 hours
- Post processing to generate plots: 0.5 hours
- Post processing to extracted interpolated data: 4-8 hours

Investigations of the computational costs of simulating larger assemblies, such as the standard 217 pin or 274 pin arrangements typically used in fast reactor cores, is underway in ANL. While the commercial code solvers are not as easily scaled to very large machines as the algorithms used by Nek5000, the parallel simulation using the commercial code Star-CD is expected to scale well for one to a few full sized sub-assemblies since the 7 and 19 pin simulations are clearly CPU rather than memory limited. However, the need to complete some mesh generation steps, most notably the generation of an acceptable surface mesh, as a serial process requires significant effort on the part of the user to describe the problem in pieces which will fit within machine memory and be completed in a reasonable time. More efficient methods for extraction of detailed distribution data from very large data sets are also needed. In the CFD adventure for a complex fuel subassembly, generation of a structured mesh with adequate refinement around the clad and spacer wire surfaces is a challenging task, requiring concentrated efforts. The structured CFD mesh generated for a 217 pin PFBR fuel subassembly in India is depicted in Fig. 6.19.

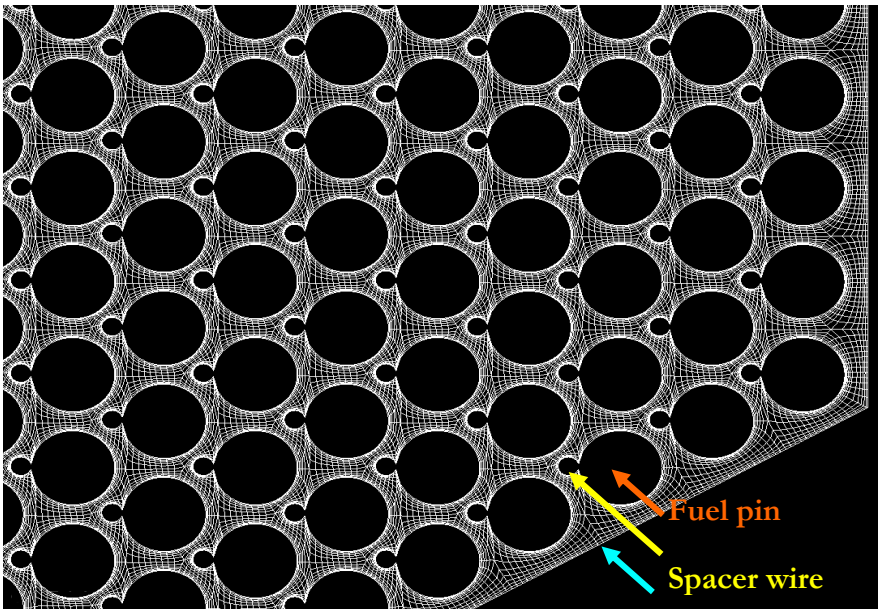

FIG. 6.19. Part of the structured finite volume mesh for 217 pin fuel subassembly.

The mesh requirement for a complete simulation of entire pin bundle is highly demanding in terms of memory and computational time. To circumvent this difficulty, the rotational

periodicity in the velocity and pressure distributions has been judiciously utilized. In this novel approach, detailed velocity and pressure distributions are estimated only for 1/6th length of the spacer wire pitch. Then the flow and pressure fields for the entire length of the fuel pins are established from the simulation results corresponding to 1/6th pitch. This flow field is utilized in the energy equation to determine the temperature distribution of sodium in the entire pin assembly, taking into consideration the axial and radial variation of the heat generation rate.

The predicted axial velocity and temperature distributions at the exit of the active zone are depicted in Figs 6.20 and 6.21.

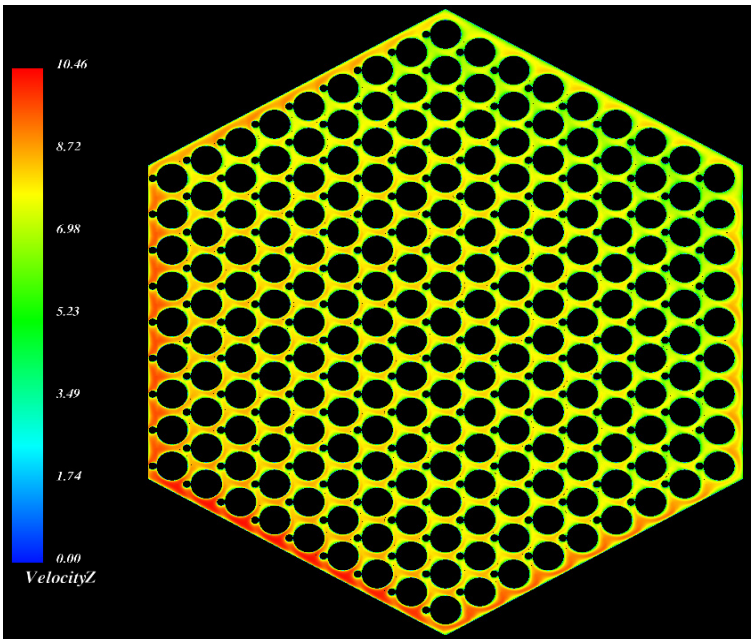

FIG. 6.20. Axial velocity distribution in the cross section of the central fuel subassembly of PFBR (m/s).

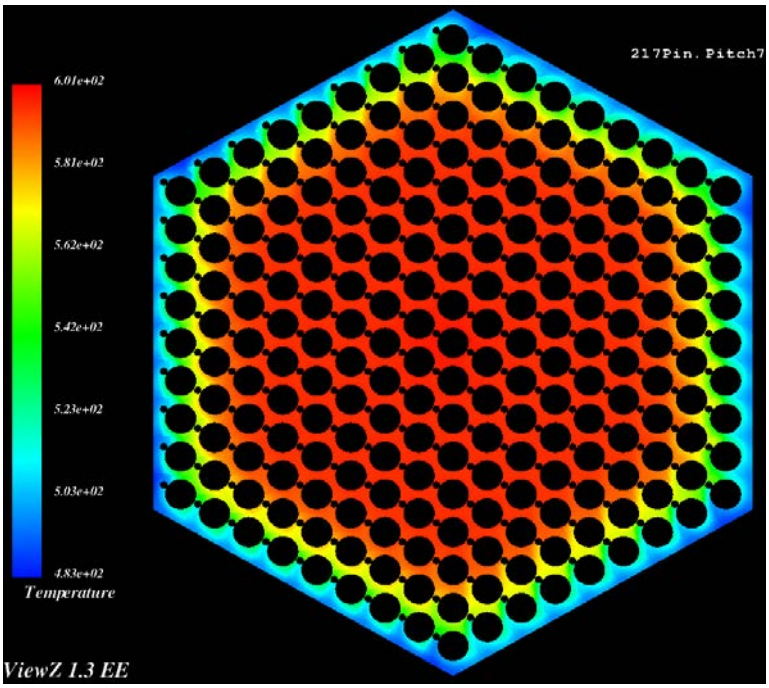

FIG. 6.21. Sodium temperature distribution at the top of active zone in central fuel subassembly (°C).

The velocity is highly non-uniform in the wall subchannels, varying from 10.5 m/s to 8 m/s. The velocity is maximum in the sub-channels housing the spacer wire, despite a larger hydraulic resistance. Since the spacer wire revolves around the pin, the location of the wall sub-channels with maximum velocity also revolves around the inner periphery of the hexcan.

It is evident from the temperature contours that the mixing induced by the spacer wires is insufficient. At the top of the active zone, there is a temperature difference of over 100 K between the central and wall sub-channels, with wall subchannels being colder due to flow by-pass. This temperature difference reduces in the top axial blanket region to 60 K. The value of non-dimensional peak clad temperature (ξ), defined as:

$$\xi = (T_{Peak\text{-}Clad} - T_{Na\text{-}Bulk})/(T_{Avg\text{-}Clad} - T_{Na\text{-}Bulk})$$

where :

$T_{Peak\text{-}Clad}$ is the peak clad temperature at any axial location,
$T_{Na\text{-}Bulk}$ is the bulk sodium temperature at that level and
$T_{Avg\text{-}Clad}$ is the average clad temperature,

is found to vary from 2 to 5, providing valuable information for use in the safety analysis.

In the Netherlands at NRG, a numerical engineering modeling approach using CFD with RANS turbulence modelling was validated using a stepwise approach [260a].

As the first step, CFD simulations were conducted for the heat transport in straight tubes. Results were compared to empirical correlations.

In the second step, CFD simulation results were compared to single heated rod experiments performed at KIT in Karlsruhe (Germany). The third step was to compare the hydraulics in a rod bundle to experimental results obtained in simulation fluids like e.g. water or air. Such fluids allow relatively easy, less costly and often more accurate measurements than liquid

metals. The last step is to compare thermal-hydraulic simulation results to experimental results obtained in a liquid metal rod bundle geometry. To this purpose, the four rod sodium TEGENA experiments of [260b] in Karlsruhe were used. This stepwise development and validation campaign has lead to clear recommendations and conclusions for a RANS-based CFD approach summarised in [260a].

The validated approach was subsequently used for simulation of a single subchannel of the fuel assembly of the European Lead-cooled System (ELSY) [260c]. These simulations have lead to recommendations for empirical correlations to be used for bare rod bundles which are also reported in [260a]. As the reference ELSY core design exists of square open fuel assemblies, new correlations are required to describe the heat transport in the gap between two fuel assemblies as shown in Fig. 6.21a.

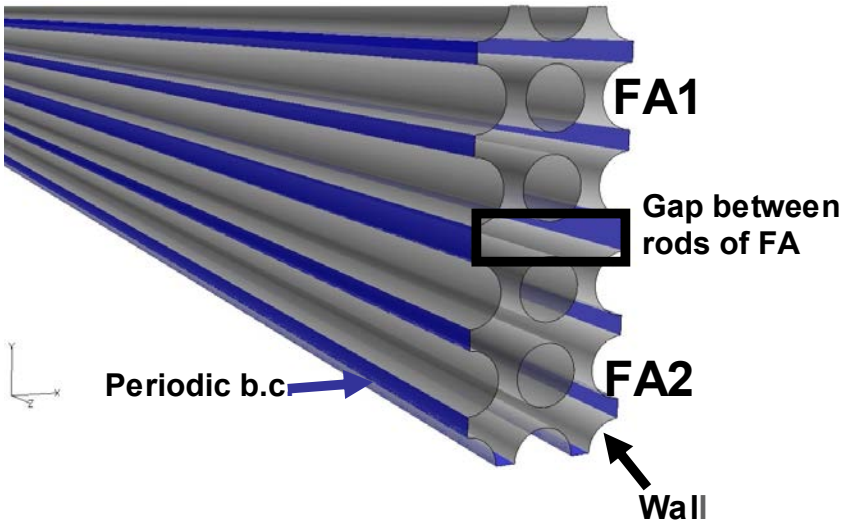

FIG. 6.21a. Open fuel assemblies (FA1 and FA2) and the analysed gap region.

To this purpose, the developed RANS approach was applied to a multiple subchannel domain which includes the gap between two fuel assemblies. The effects of variations of gap size were analysed, which showed that the maximum peripheral temperature difference along a rod is significant when the gap size between two fuel assemblies differs from the pitch of the rods within a fuel assembly. Such a temperature variation along a rod surface may lead to bending and ultimately in failure of the fuel rod. An optimum was found when the gap size between two fuel assemblies is chosen equal to the rod pitch within a fuel assembly. Furthermore, the heat transport between two fuel assemblies has been analysed for fuel assemblies with different power levels. For such a situation, a conservative heat transport correlation (see equation 6) has been derived which can be used in system codes. The comparison with RANS simulations for a 5.5 mm gap is presented in Fig. 6.21b [260d].

$$Nu_{gap} \sim 10.2 - 4.7\,|1\text{-}Power\ Ratio\,| \qquad (6)$$

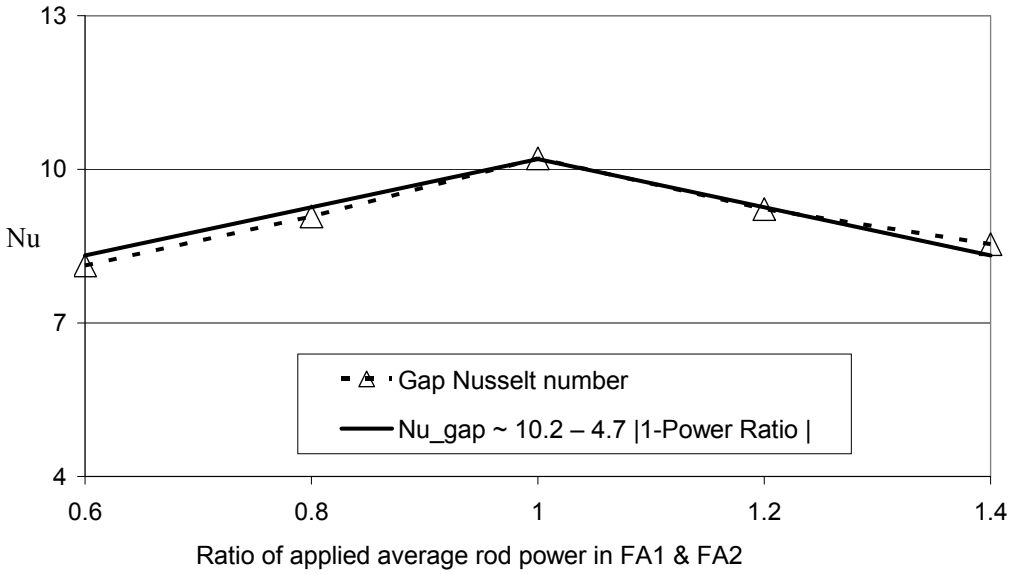

FIG. 6.21b. Analysed gap Nusselt number based on power level for the ELSY fuel assembly with gap size = 5.5 mm.

In order to bridge the gap between traditional fuel assembly simulation approaches using system codes, subchannel codes or porous medium approaches and the detailed CFD approaches to analyze single sub-channels, a Low Resolution Geometry Resolving (LRGR) CFD approach is applied by NRG in the Netherlands [260e]. First, a grid resolution study was performed in order to analyse the accuracy of the employed LRGR grids. Rod surface temperatures differed less than 15% to the results obtained with the detailed validated approach from [260a]. The LRGR CFD approach allows capturing 'medium scale' flow features such as recirculation zones, which cannot be captured by the system code, subchannel code and porous media approaches, and can serve e.g. to fine-tune the porous parameters which are important input for a porous medium approach.. However, it should be noted that the prediction of detailed flow features such as secondary flows is not feasible. Figure 6.21c shows computational domain and grid of the hexagonal closed ELSY fuel assembly employing the LRGR CFD approach.

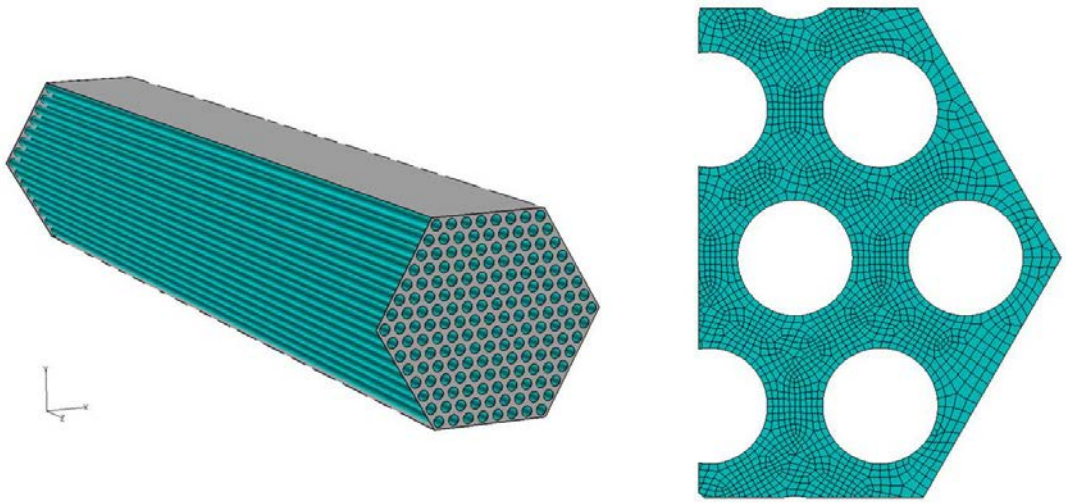

FIG. 6.21c. Computational domain and grid of the hexagonal closed ELSY fuel assembly employing the LRGR CFD approach.

6.3.2. Whole core thermal hydraulic analysis

The primary objectives of thermal hydraulic design of the core are to ensure that adequate flow of coolant is passed through each subassembly and to determine the temperature and coolant velocity distributions in the core, which are inputs for checking the structural integrity of core components, viz. subassembly bowing analysis, clad damage etc. Analyses are performed to obtain the behaviour of the core under static and event conditions.

Towards the commercialization of liquid metal cooled fast reactors, much effort should be devoted to enhance the economic performance as well as the plant system safety. As one of effective methods for this, the adoption of high performance fuel and natural circulation decay heat removal can be considered. In the former, the evaluation of the in-core structure deformation coupled with thermal hydraulic phenomena under the condition of high linear power and high burn-up is necessary. And in the latter, the decay heat removal capability should be estimated including the effect of inter-wrapper flow and core-plenum thermal-hydraulic interaction. Thus, the detailed temperature distribution in the core region is required for the core structure integrity evaluation or the safety assessment under various operating conditions.

6.3.2.1. Analysis methods

6.3.2.1.1. Static analysis

The flow distribution in the core in Indian reactors is designed based the following design criteria.

- Mixed mean coolant temperature at the core outlet is 150 K.
- Power and residence time of subassembly are restricted such that the temperature difference between the two neighbouring subassemblies does not exceed 100 K during its life time from thermal striping consideration.
- No cavitation even at 110% of rated flow through the subassembly.
- Clad mid-wall hotspot temperature of the subassembly is restricted such that that the cumulative structural damage is limited below predefined levels.
- Sodium (hotspot) cannot exceed the boiling point.

As the power distribution in the reactor is not uniform, flow through each subassemly has to be allocated such that temperatures at the outlet of the subassembly are nearly uniform. However, it is cumbersome to allocate flow for each subassembly individually and hence subassembly having similar powers are grouped together and are assigned the same flow.

In PFBR, about 90% of the total power is generated in the fuel, 8% in the blanket, 0.4% in the control and 0.15% in the shielding regions. The power in the blanket region increases with the burnup due to accumulation of fissile material while the fuel power decreases. This results in change of radial power profile from beginning of life to end of life. Given the total power and the temperature rise in the reactor, the total flow through the core gets fixed and this flow is to be distributed through various regions such that the design criteria are met under operating conditions of individual subassembly.

While allocating the flow through each subassembly it is necessary to take into account the mixing in the subassembly as this factor improves the subassembly average temperature for a given hot spot temperature. Also, for blanket subassembly, where coolant flow rate is less compared to fuel subassembly, inter subassembly heat transfer plays an important role.

Hence, unless these factors are considered while allocating the flow for a given hot spot temperature, flow through the subassembly will be over predicted. Hence, a judicious estimate of these factors is necessary.

6.3.2.1.2. Dynamic analysis

PFBR fuel pins are designed for a peak burnup of 100 000 MWd/t after accounting for few transient events during the residence time in the reactor. This corresponds to about 2 years of residence time inside the reactor. For the target burnup, fuel pin integrity is to be ensured for category 1, 2 and 3 design basis events and design allows certain failures under category 4 events. Analysis has been carried out to check the integrity of fuel pins under various design basis events. The design of fuel pins is based on the cumulative damage fraction (CDF) approach.

The entire life of the fuel pin is taken as 1 in which a CDF of 0.25 each is apportioned for the first three design basis event categories and balance 0.25 is allocated for any damage to the subassembly during spent fuel storage and transit outside the reactor vessel. The maximum channel temperature around a pin is chosen and the clad mid-wall temperature under hotspot conditions are estimated for all the pins. At the end of each equilibrium cycle, BOEC and EOEC, burnup undergone by each pin is estimated along with the fission gas pressure and the hoop stress. From the knowledge of residence time of the pin, clad mid-wall hotspot temperature and the hoop stress and for the given ramp rate on temperature, the CDF is estimated. In addition to the CDF apportionment, temperature limits which are called 'Design Safety Limits' (DSL) are established for fuel, clad and coolant for all the DBE categories. For the clad, allowable transient time duration is also defined commensurate with the apportioned CDF limit. In order to ascertain the margin to the DSL, the clad temperatures are compared with the allowable temperature limit which can be considered as an index for the clad failure. The fuel pin clad temperature at the end of a transient event is estimated as:

$$\begin{array}{l}\text{Fuel pin clad}\\ \text{temperature at}\\ \text{end of transient}\\ \text{event}\end{array} = \begin{array}{c}\text{Fuel pin clad temperature}\\ \text{under normal operation}\\ \text{under hotspot condition}\end{array} + \begin{array}{c}\text{(temperature ramp rate)} \times\\ \text{(time duration of transient)} \times\\ \text{(hotspot factor for channel}\\ \text{temperature rise)}\end{array}$$

6.3.2.2. Computer codes and experimental verification

6.3.2.2.1. Static analysis

For designing the mass flow rate through various subassembly based on the design criteria, a computer code FLONE [261] has been developed in India. Analysis has been carried out for a 30^{o} symmetry sector of the core and flow optimization is carried out. A factor for taking into account the mixing characteristics within a subassembly and inter subassembly heat transfer due to the presence of adjacent subassembly is obtained for each subassembly using SUPERENERGY code and suitably incorporated in FLONE. Based on the flow optimization and rationalization, subassembly with forced cooling are divided into 15 flow zones. Accordingly, fuel region is divided into 7 zones, blanket into 3 zones, the control, reflector and shielding having 1 zone each and storage into 2 zones (1 for spent fuel subassembly and 1 for failed fuel subassembly).

The necessary flow through subassembly is realized by providing flow control device like an orifice at the foot of each subassembly. The pressure drop through each subassembly is estimated for designing the orifice and fixing the primary sodium pump head. Pressure drop through pin bundle is estimated using Cheng's correlation [262] as it covers a wide range of Reynolds number, pin pitch-to-diameter ratio and wire wrap pitch-to-diameter ratio.

The pressure drop values for fuel subassembly predicted by SAPD compares well with the experimental results and are shown in Fig. 6.22.

The pressure drop for the maximum rated subassembly is ~ 57 m of sodium column. After determining the flow rate through each subassembly, steady-state temperature distribution in a subassembly is determined using multi-assembly code SUPERENERGY.

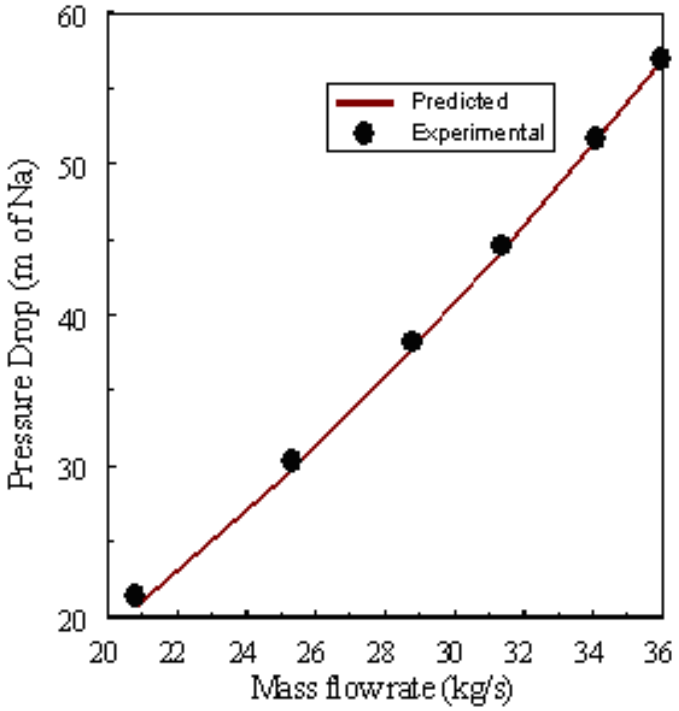

FIG. 6.22. Comparison of predicted pressure drop of PFBR fuel subassembly with experimental results.

6.3.2.2.2. Transient analysis

Analysis has been carried out to check the integrity of fuel pins under various design basis events. For the Indian analysis, SUPERENERGY coupled with the transient plant dynamics code DYANA-P is used. General methodologies adopted in the formulation of the DYANA-P code have been validated through the commissioning tests carried out in the Fast Breeder Test Reactor (FBTR) in Kalpakkam [263].

Towards demonstrating the safety margin to the DSL, a study was carried out in which the clad temperatures at hot spot conditions were calculated for all the fuel pins in 1/6th of the core. Number of pins in different temperature ranges was estimated for enveloping events of category 3 and 4 DBE.

The enveloping events considered for category 3 is primary pump seizure and for the category 4, it was primary pipe rupture. As an example, number of fuel pins with different stress ranges and different clad temperatures at BOEC & EOEC for the primary pump seizure (cat. 3) event are given in Fig. 6.23. Also, the temperature limit corresponding to these events is also indicated. These figures are meant to show that the clad temperatures are within the DSL indicative of the safety margins

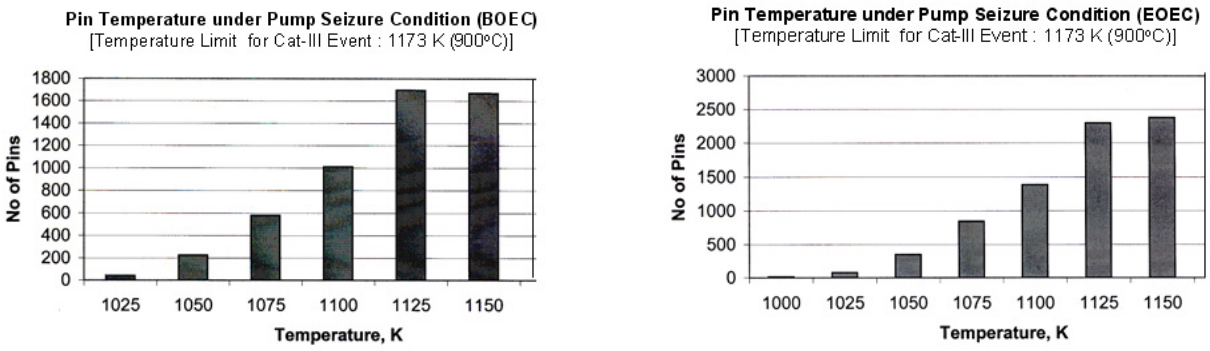

FIG. 6.23. Pin temperature under pump seizure condition (BOEC and EOEC).

A whole core thermal-hydraulic analysis program ACT was developed to satisfy such needs in Japan Atomic Energy Agency (JAEA) [264]. ACT consists of three kinds of analysis modules, i.e. a core analysis module (intra-subassembly, inter-wrapper gaps), an upper plenum module and a heat transport loop module. The upper plenum and heat transport modules give the proper boundary conditions to the core analysis module especially for the natural circulation decay heat removal simulation.

These modules were made based on three kinds of thermal hydraulic codes that have been developed and validated at JAEA: subchannel analysis code for each fuel subassembly and the inter-wrapper gaps (core analysis module), three dimensional thermal hydraulic analysis code for the upper plenum and one dimensional plant dynamics analysis code for the heat transport system.

These three modules are coupled with each other by a coupling algorithm, in which the conservation of mass, momentum and energy are considered, and calculate simultaneously on a parallel computer using Message Passing Interface (MPI). ACT was applied to analyzing a sodium experiment performed at JAEA [265] for the code validation, which simulated the natural circulation decay heat removal under the operation of reactor auxiliary cooling system.

Figure 6.24 shows the schematic of the sodium test loop.

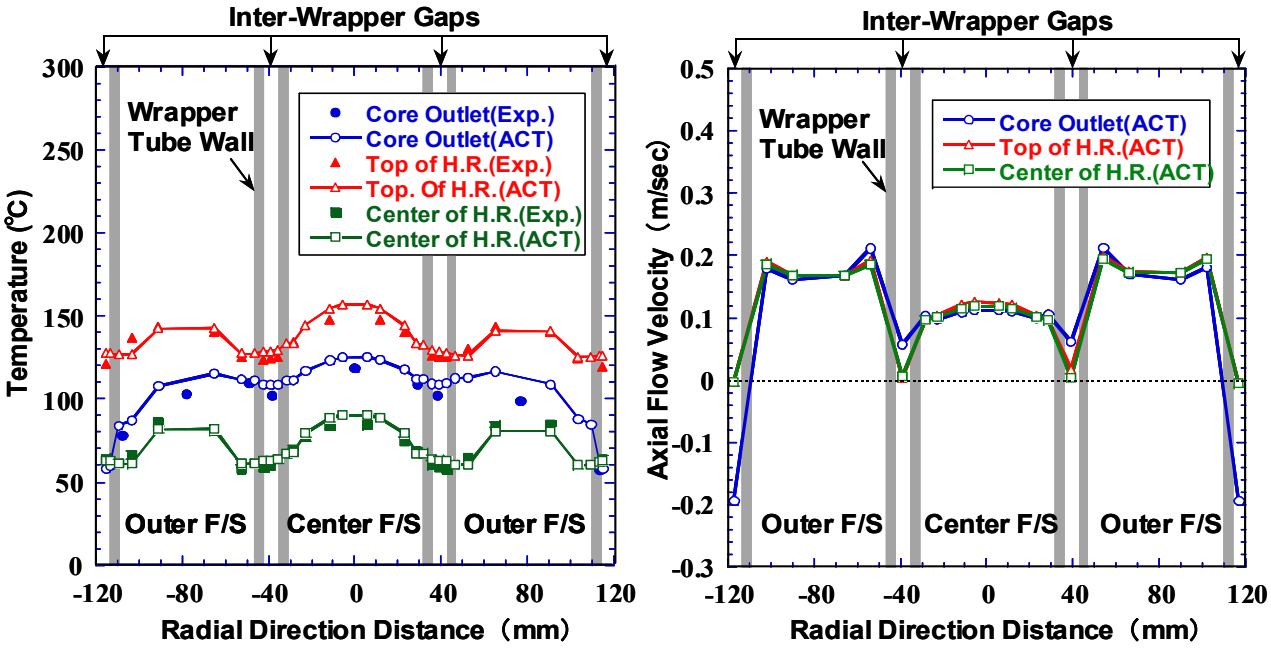

FIG. 6.24. Coolant temperature and velocity distributions predicted by ACT code.

The test loop consists of the test section, upper plenum including immersed cooler of direct reactor auxiliary cooling system (DRACS), IHX, pump and lower plenum. Primary reactor auxiliary cooling system (PRACS) is also implemented at the upper part of the IHX.

The test section simulating a small part of the core consists of seven fuel subassemblies and inter-wrapper gaps. The central fuel subassembly has 37 electrically heated with spacer-wire.

Outer 6 fuel subassemblies have the same specification, that is, 7 electrically heated pins with spacer-wire. In the experiment, the influence of not only the inter-wrapper flow but also the reverse flow in fuel subassemblies on the temperature field were observed. As an example of the calculation results, the predicted coolant temperature and velocity distributions on the axial cross section of the test section under DRACS and PRACS operating condition are shown in Fig. 6.25 with the measured data.

Predicted coolant temperatures are in good agreement with the measured data at the top of the core, at the top and the centre of the heated region and inter-wrapper gap region. Through these calculations, it was confirmed that ACT has the capability to simulate such complicated thermal hydraulic phenomena.

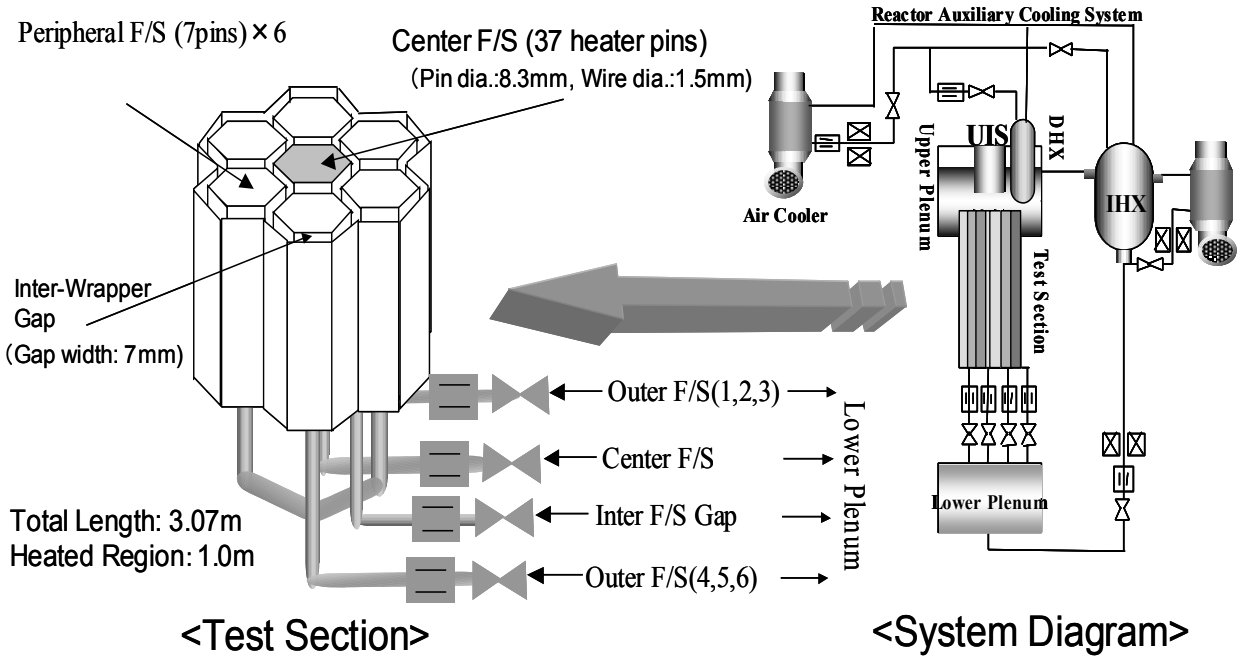

FIG. 6.25. Sodium test loop of natural circulation decay heat removal.

A two level modelling approach is adopted in France for whole core analysis. The level is decided according to the purpose of the calculation and according to the accuracy required [266]. The first level is the system analysis to describe the global behaviour of the whole plant during transient situations. The core is modelled with a few 1D parallel channels. The second level is the global core modelling with a sub-channel description of each subassembly based on correlations, a 3D modelling of the inter-wrapper space and a 3D modelling of the connection with the plenum. The present tool used at CEA is included in the ELOGE global core modelling, with CADET sub-channel modelling of subassembly described in Section 6.2.1.2 and TRIO_U 3D modelling of the inter-wrapper space and plenum.

The CADET sub-channel modelling of subassembly could be replaced in the future by TRIO_U to have a unique tool for the core thermal hydraulic modelling. Another possibility is to couple a global core modelling with a refined CFD description of one subassembly. This coupling process allows for example a detailed description of the hottest subassembly in tight connection with the global core behaviour.

Figure 6.26 shows a TRIO_U core calculation with 469 sub-assemblies using a sub-channel modelling of subassembly, coupled with the 3D inter-wrapper space and connected to the 3D lower and upper plenum. The verification of whole core calculations requires experimental data taking into account the thermal hydraulic interactions between the sub-assemblies, the inter-wrapper flow and the lower and upper plenum. A few water tests were performed in the past to study the inter-wrapper flow in connection with the plenum pressure effect. A few sodium tests are available on the thermal interaction between subassemblies and inter-wrapper flow. Further experimental programs in sodium are needed to complete the verification of core calculations.

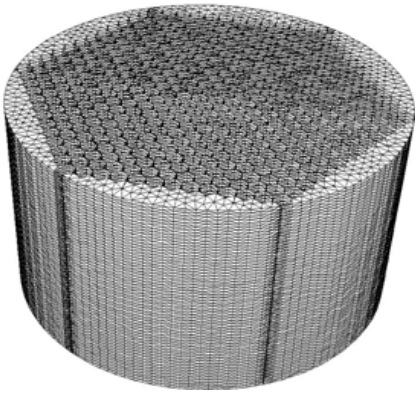

Mesh

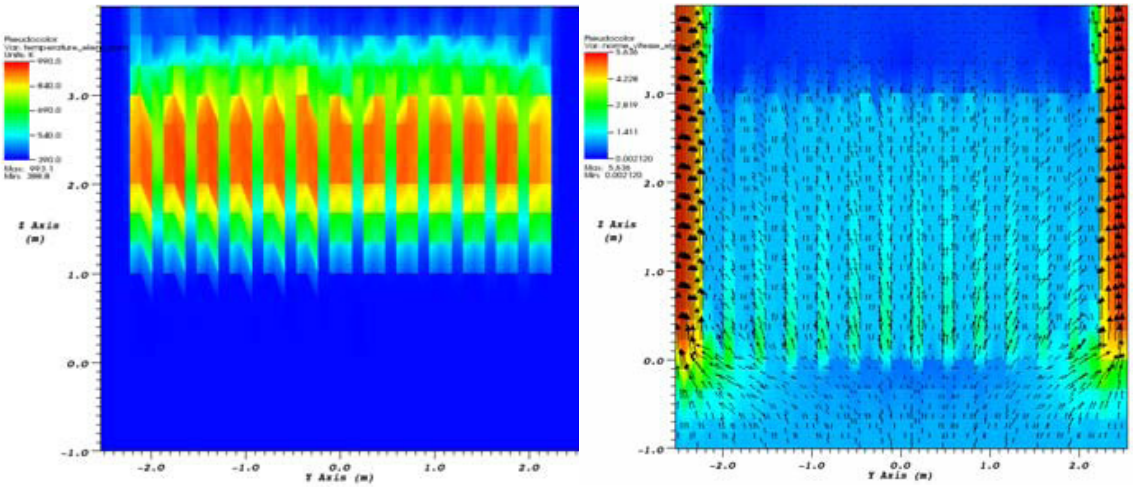

Temperature distribution *Flow distribution*

FIG. 6.26. TRIO_U core computation of whole core thermal hydraulics.

6.3.2.3. Sodium boiling

Thermal-hydraulic phenomena linked to sodium boiling has been investigated for about 35 years (mainly between 1960 to 1995) in laboratories involved in LMFBR safety all over the world. Most of the work was dedicated to safety problems so that results are closely related to special applications and specific conditions. Considerable progress in this field has led to good general knowledge of single and two-phase forced convective flows and natural convective flows. The scientists involved in the development set up a working group (Liquid Metal Boiling Working Group or LMBWG) to give emphasis to fundamental, but also to applied aspects. One can find a synthesis of the work of this group edited by H.M. Kottowski who was for a long time the coordinator of the LMBWG [267].

Basic boiling mechanisms have been investigated, such as nucleation and superheat [268]. A major challenge was associated to initial superheat, since superheat could lead to the initiation of a major accident. The major finding in this field was that superheat is associated with very clean sodium before boiling starts and that there was sufficient theoretical and experimental evidence that, in a reactor environment, superheat is reduced by various factors.

Extensive investigations of the characteristics of sodium boiling and two-phase flow have been performed. Two-phase pressure drops have been measured in single channel and bundle configurations and the frictional pressure drop prediction with the Lockhart-Martinelli [269] correlation proved to work sufficiently well. Despite the difficulty to perform the

measurements, many critical heat flux (CHF) data have been collected. However, no analytical predictions were considered reliable at the end of the program. As a guide it was proposed to consider that dryout conditions usually occur at high vapour qualities (i.e. >40%).

Sodium boiling induced by local flow perturbations (local blockages) in a subassembly has extensively been studied in many laboratories [270]. Transient sodium boiling has been investigated for application to unprotected loss of flow (ULOF) accidents and unprotected transient over-power (UTOP) accidents. In ULOF, the kinetics of the transient decrease of the flow is linked to the pump inertia. Theoretical and experimental investigations have shown that the onset of boiling can result in a flow instability called "flow excursion". This flow excursion is induced by a significant increase of the two-phase frictional pressure drop over the boiling length in the fissile region and upper fertile cover. The characteristic time duration of the flow excursion is controlled by the thermal inertia of the core structure and the power level. During the flow excursion, the two-phase mixture penetrates into the fissile length, which may lead to a power excursion. Under ULOF conditions, critical heat flux is practically obtained when the flow rate reaches zero. When the hydraulic diameter in the upper fertile cover is large enough, and provided that the subassembly outlet tube is also long enough, the flow instability may be avoided and a stable natural convection boiling may install. Under such conditions, boiling only affects the outlet of the subassembly and does not significantly penetrate into the fissile zone [271]. Subassembly voiding under instantaneous inlet flow blockage has mainly been studied in the frame of the SCARABEE programme. The voiding kinetics of the fissile zone under UTOP has been thoroughly analysed in several experiments and in particular in the CABRI programme. These programmes have shown that the voiding kinetics is controlled by the thermal inertia of the fissile zone.

The modelling of sodium boiling was initially based on the so-called "bubble model approach". This model was initially connected with the superheat question. In the absence of superheat, sodium boiling revealed to present characteristics that are similar to water boiling flows at low pressure. Therefore, the theoretical approach that has been developed for the description of boiling water flow [272] has been adapted to sodium boiling. Thus, the "bubble model" has latter on been replaced by the homogeneous model approach that proved to be more pertinent to describe sodium boiling in a bundle under various accidental conditions. The homogeneous boiling model has been used in all subassembly (bundle) boiling calculation tools. The "bubble model approach" still subsists in the SAS code.Many codes have been developed:

- General codes: CAFCA, COMMIX, HEV-2D, INCA, ROBOT, SIMMER, THERMIT,
- Single channel bubble: BLOW, SAS;
- Single channel homogeneous: ESSO, FLINA/FLINT/NATREX/MANDRIN, NASLIP, SEMPLICE;
- Bundle geometry: BACCHUS, MULTICANA, SEETHE, VELASCO, ASFRE, SABENA, SABRE, THEBES, UZU;
- System codes: EAC, SSC.

Also instrumentation and detection techniques have been developed (~50 publications in the frame of the LMBWG), as for instance:

- Sodium-steel thermocouples have been tested for sodium boiling detection;
- Acoustic sensors have been developed and tested for sodium boiling detection.

Boiling noise is related to bubble implosion and is, consequently, very similar to cavitation noise. Thus, acoustic noise proved to be difficult to use, mainly because the existence of strong background noise related to existing cavitation noise in the reactor.

Many technological developments have been performed in support of the sodium boiling experiments, among which the development of reliable heaters. As sodium has high electrical conductivity, direct heating is not possible (such as in water) and the electrical heating had to be indirect, which imposed to use a high temperature resistant electrical insulation of the heating wires (but with elevated thermal conductivity). These heaters were designed to deliver high heat fluxes (~ 1.5 MW/m²) at elevated temperatures (~ 1500°C) and were thoroughly instrumented with thermocouples for the detection of CHF.

IPPE carried out several experimental studies on heat exchange and coolant flow stability during liquid-metal boiling in parallel channels under natural convection conditions. An experimental facility for studying the liquid-metal boiling in parallel assemblies was set up in the sodium-potassium loop of the AR-1 installation [277, 278]. The facility consists of two natural circulation loops which have a common downcomer with a cooler to remove the heat released in the model assemblies. Each loop contains electrically heated pin-bundle simulators (model assemblies). The gas volumes located above the assemblies are also connected to each other. Each model assembly (loop) can operate independently through its own circulation circuit.

The geometry of the pin-assembly simulated were typical assemblies of the BN-600 and BN-800 fast reactors. The diameter of the heated fuel pin simulators was 8 mm, the pitch to pin diameter ratio s/d = 1.19, and the length of the heat-release section was 830 mm. The heat generating elements were located in the bundle that contained 12 unheated elements to simulate the geometry of an infinite lattice. In the upstream of the heating section, there was 130 mm long section for the hydrodynamic stabilization of the flow. An unheated section of 800 mm length was put above the heated zone. The coolant outlet from the assembly to the upper plenum was an assembly head of smaller dimension. Other elevations of the loop viz. arrangement of cooler relative to the heated section, the height of the preinstalled section and the distance between the pin bundle and the assembly head were similar to that of BN-600 geometry.

Initially experiments on studying heat transfer and coolant circulation stability under boiling of NaK eutectic alloy in the model assembly were performed separately for the left and right loops. Then, the experiments were performed with parallel operation of these loops under natural circulation condition. The experiments were conducted with a stepwise increase in power supply to the pin simulators. The increment in the heat flux at the pin surface was not more than 10–20 kW/m^2. After each step of the power increase, a certain time period was provided to allow the parameters being measured to stabilize. The pressure in the gas volume was approximately 0.4 bar which corresponded to a level of pressure in the upper part of the heat release section of the assembly of 0.49-0.52 bar. The measurement system enabled to monitor the following parameters: electric power supplied to the pin simulators and auxiliary electric heaters of the installation, coolant flowrate, static pressure and pressure oscillations in the boiling zone, pressure drop at the pin assembly models over the heating section, pin simulator surface temperature in three cross sections along the heating section height, coolant temperature in three cross sections along the heating section height and at different points of the circulation circuit, the flowrate of the cooling water. The main results of the experimental studies are as follows [273, 274]:

- Boiling starts in the assembly at a heat flux of ~95 kW/m^2, which is accompanied by bubble flow of coolant and is characterized by stable oscillations of the thermal hydraulic parameters (pressure, flow rate and temperature of coolant, surface temperature of heating element). These oscillations have small amplitude, their period is from 1 s to 5 s.
- At a heat flux of approximately 130 kW/m^2, the bubble flow regime changes over to the developed slug flow with strong oscillations of the coolant flow rate and other parameters with a period varying from 150 s to 200 s and weak oscillations of small amplitude and period (3–5 s) being superimposed on them.
- Oscillations of all thermal hydraulic parameters in separate loops have the same temporal characteristics.
- Onset of the oscillations during coolant boiling in one of the parallel assemblies initiates antiphase oscillations in the second assembly; further, these oscillations of the thermal hydraulic parameters in different loops proceed in the antiphase mode.
- Hydrodynamic interaction between the loops provides a significant growth of the coolant flow rate amplitude ("resonance" of flow rate oscillations) and possible "lock" of the flow rate or flow reversal in the loops. It may also result in increase of the coolant and pin cladding temperature (the effect of inter-channel instability) and in the incipience of the heat transfer crisis (Fig. 6.27).
- The difference in the heat fluxes on the surface of heat-generating pins in parallel assemblies provides the enhancement of the "resonance" of the oscillating process.
- Heat transfer coefficients under liquid-metal boiling in a single assembly or in assemblies arranged in parallel agree with each other as well as with such data for liquid metal boiling in tubes and exceed the values of the heat transfer coefficients for liquid metal under pool boiling. The solid line in the plot in Fig. 6.28 is the calculation by the following empirical formula [275]:

$$\alpha = Aq^m p^n \qquad (6)$$

where:

p = pressure,

q = heat flux,

m = 0.7,

n = 0.1-0.15,

d A = 4.5-7.5.

The other points on the plot are experimental data from studies on potassium and sodium-potassium eutectic (IPPE data) [273, 274] on a 7-pin bundle of length l = 840 mm.

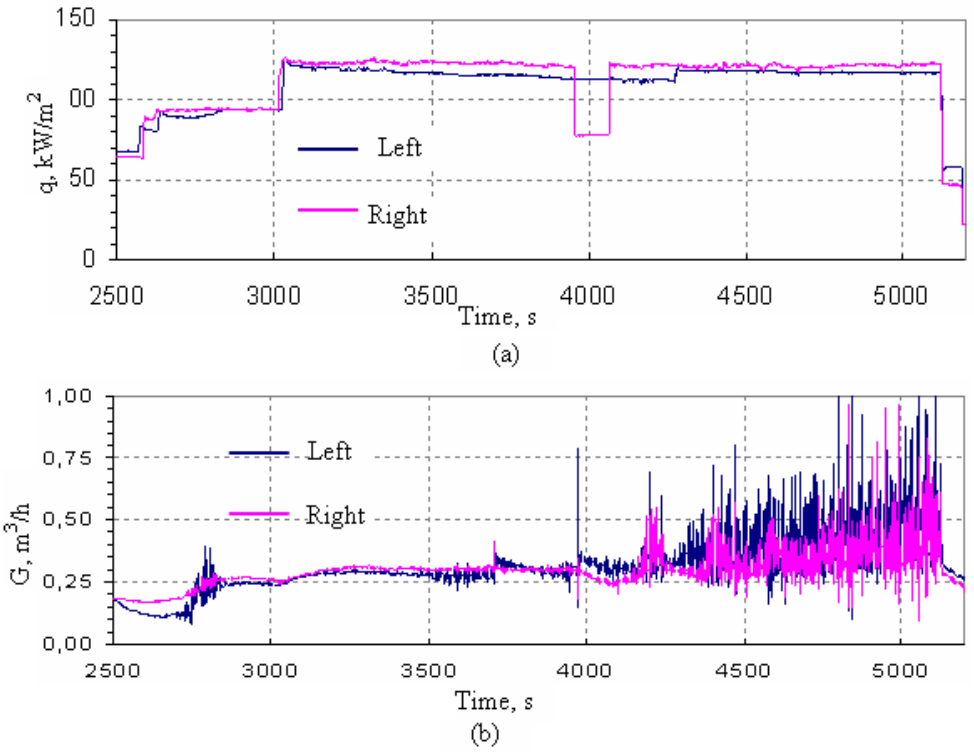

FIG. 6.27. Changes in flow parameters under parallel operation of assemblies with similar heating conditions: (a) heat flux from pins in the left and right bundles (b) coolant flow rate at the inlet to the left and right bundles.

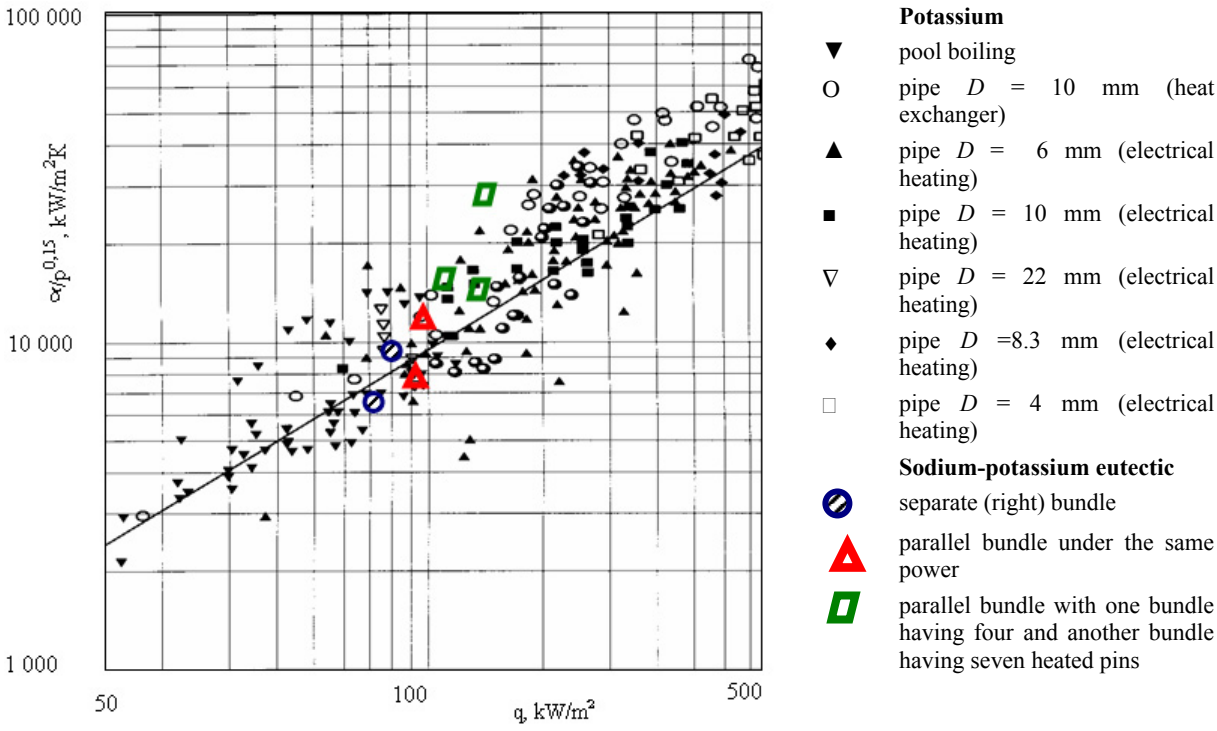

FIG. 6.28. Comparison of heat transfer data under liquid metal boiling.

6.3.3. Thermal fluid system: Thermal hydraulic analysis

Thermal hydraulic characteristics of an LMFBR pose considerable challenges to the analyst. In the primary sodium system, forced, natural and combined convections co-exist at all operating power levels. For thin structures of LMFBR (~ 15-30 mm thickness), the Biot number is of the order of unity, since the sodium heat transfer coefficient is large, indicating the conductive and convective resistances are of similar order. This suggests that a multidimensional conjugate convection-conduction heat transfer analysis is required for the estimation of structural temperatures. When the Richardson number in the pools is of the order of unity, a stratification interface, where a large temperature change occurs over a short height, is developed.

The stratification interface is unstable with respect to position and it leads to low frequency (~ 0.01-2 Hz) temperature oscillations of large amplitude. Since the heat transfer coefficient of sodium is very large, the fluid temperature fluctuations are transmitted to the adjoining structures with minimum attenuation. Similarly, the mixing interface of sodium jets (of different temperature) issuing out of various subassemblies is unstable and it leads to temperature oscillations in the structures, known as thermal striping.

The operating temperature of primary sodium in an LMFBR is large (~ 550°C) and the temperature requirement of various sub-systems bounding the primary system falls in the range of 65°C (reactor vault) to 120°C (roof slab), that natural convection and radiation heat transfer through the gaseous media take place simultaneously. The natural convective flow is generally turbulent. Moreover, the structural temperature distributions are often required for the estimation of thermal stresses in them. Hence, this calls for a conjugate multi-dimensional heat transfer analysis considering simultaneous interaction between surface radiation, natural convection and conduction in the structures. In a large size LMFBR, the free surface of the pool is not static and it fluctuates when the sodium pumps are in operation. The fluctuating sodium free level leads to high cycle thermal fatigue in structures which are partly immersed in sodium and partly in cover gas (such as IHX, inner vessel, control plug). If the free level sodium velocity is sufficiently large, the sodium can entrain droplets of cover gas. The size of gas droplets that get entrained in sodium varies proportional to the square of the sodium velocity. Entrainment of gas in sodium and its subsequent passage through the core leads to reactivity perturbations. Hence it is essential to have a free surface with low velocities.

6.3.3.1. Analysis methods

The above mentioned thermal hydraulic problems of LMFBR can be analyzed either by experimental simulation or by numerical simulation. Large scale experiments in sodium are costly and time consuming. Normal fluids like air and water cannot simulate sodium heat transfer due to large difference in the values of the Prandtl numbers. But hydraulic conditions of sodium can be nearly simulated by water models. Even for gases such as argon and nitrogen, the numerical simulation is cheaper and faster especially when the number of parameters involved is large. But numerical models and the codes developed need to be necessarily validated through experiments. For a successful design, a judicious combination of experimental and numerical approaches is a must. The method adopted at IGCAR is to perform many large scale water experiments and limited sodium experiments to validate computer codes and then use these validated computer codes for numerical prediction of sodium flow and temperature distributions in the reactor.

6.3.3.2.Static and transient thermal hydraulic analysis computer codes and experimental verification

For system transient analysis in India, plant dynamics code DYANA-P is used. General methodologies adopted in the formulation of the DYANA-P code have been validated through the commissioning tests carried out in the Fast Breeder Test Reactor (FBTR) in Kalpakkam 263]. For multidimensional fluid flow and heat transfer analyses, two computer codes THYC-2D and THYC-3D have been developed in house in India. They respectively solve 2- and 3- dimensional transient Navier-Stokes and energy equations in Cartesian and cylindrical coordinate systems using the control volume based discretisation method. The pressure-velocity coupling is resolved either by the SIMPLE algorithm or one of its variants such as SIMPLER, SIMPLEC, SIMPLEST etc. The convective and diffusive fluxes are combined by Upwind, Hybrid or Power-law schemes. The discretisation equations are solved by Tri-Diagonal Matrix Algorithm and its extended forms for penta and septa diagonal matrices, employing multi-directional sweeps. The Boussinesq approximation is used to take care of buoyancy effects. Turbulence is modelled using the standard k-ε model or by the constant turbulent viscosity model. Porous body formulation is used to model submerged small scale structures. These codes have been validated against numerical / experimental results published in open literature and experiments carried out in house. In addition to these codes, the general purpose commercial thermal hydraulic codes PHOENICS and STAR-CD are also being used. The predictions of the codes have been validated against experiments carried out in-house.

The velocity distribution at the entry to IHX inlet windows, predicted by the code and the same extrapolated to the reactor based on 1/4 scale water model tests, carried out at IGCAR are compared in Fig. 6.29.

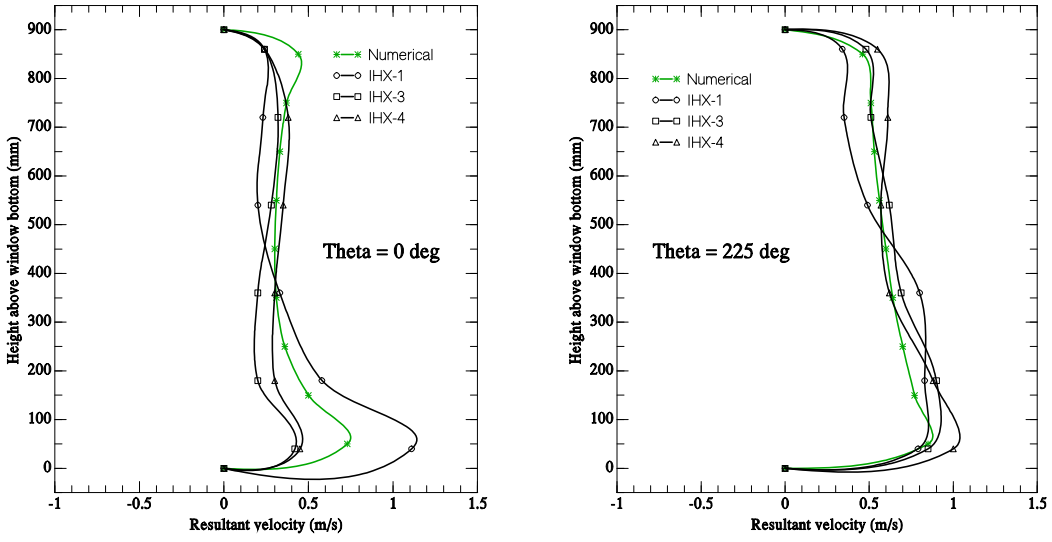

FIG. 6.29. Comparison of velocity distribution at IHX inlet window of PFBR.

In these figures, “Theta” refers to various circumferential locations around the IHX. IHX-1, 2, 3 and 4 refer to 4 IHXs in the reactor. Due to symmetry, the numerical result is the same for all the IHX. The comparison is quite satisfactory. Mixing characteristics of multiple jets entering into the main vessel cooling annulus of PFBR has been studied in a 1/5 scale water model. The flow pattern inside the annulus visualized by dye injection and flow distribution predicted by CFD code are compared in Fig. 6.30. The CFD model is able to predict major and minor recirculations accurately.

FIG. 6.30. Comparison of mixing characteristics of multiple jets in main vessel cooling system.

For system analysis of Fast Reactors, CEA is using CATHARE code. CATHARE code has been originally developed by CEA, EDF, AREVA and IRSN for Pressurized Water Reactors. It has been adapted by CEA to other reactors such as Boiling Water Reactors, VVER, Super Critical Water Reactors, Gas Cooled Reactors and Sodium cooled Fast Reactors.

CATHARE code describes the global behaviour of the whole plant during transient incidental or accidental situations (except severe accident scenario). The core is modelled with several 1D parallel channels. The plenum can be modelled with one or several volumes. The heat exchangers and steam generators are modelled with 1D parallel channels. Specific models are implemented for mechanical and electromagnetic pumps.

Figure 6.31 shows a CATHARE calculation of the primary circuit of a Small Fast Reactor concept during an Unprotected Transient Over Power (control rod withdrawal).

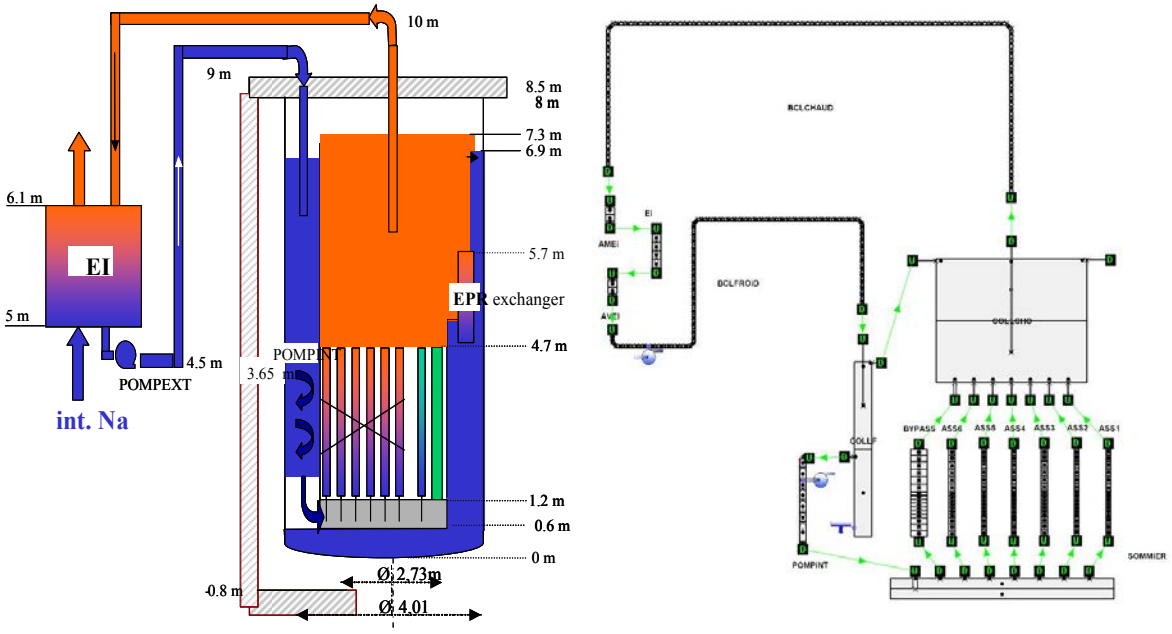

Reactor system *Nodalisation*

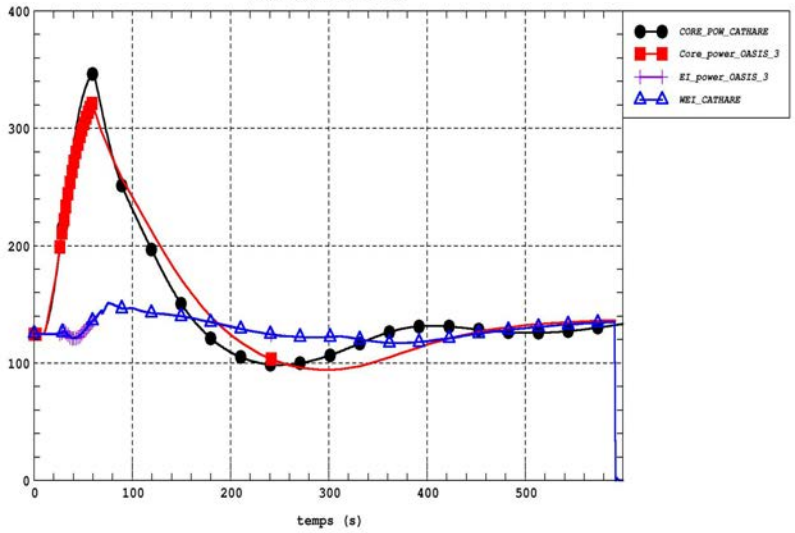

FIG. 6.31. CATHARE SMFR computation.

The core outlet temperature takes into account various reactivity effects implemented in CATHARE. The verification of CATHARE system calculations is based on existing reactor data during transient situations. The tests performed in Phénix, Superphénix and Monju are used in priority. New tests on future reactors will be used as soon as they are available.

6.3.3.3. Pool thermal hydraulics

Pool thermal hydraulics includes various situations in steady-state or transient conditions, in forced convection or mixed convection or natural convection. Flow configurations such as mixing jets, recirculation, thermal stratification are important areas to be addressed. For pool thermal hydraulics studies, CEA is using TRIO_U code. Several turbulence models are implemented in TRIO_U such as k-ε, Large Eddy Simulation and Direct Simulation [277]. Turbulent Prandtl number takes into account the liquid metal specificity. In the past, the pool

thermal hydraulic calculations were verified by comparison with experimental data from reduced scale models of the reactor using water. Moreover, some sodium experiments as CORMORAN were performed to assess a generic validation on typical phenomena as thermal stratification and heat transfer correlation for various flow regimes. New experimental data will be required to verify the CFD calculations of new concepts of reactors, mainly water reduced scale experiments.

Figure 6.32 shows the comparison of a TRIO_U calculation and the CORMORAN cavity experiment performed at CEA with a thermal stratification configuration.

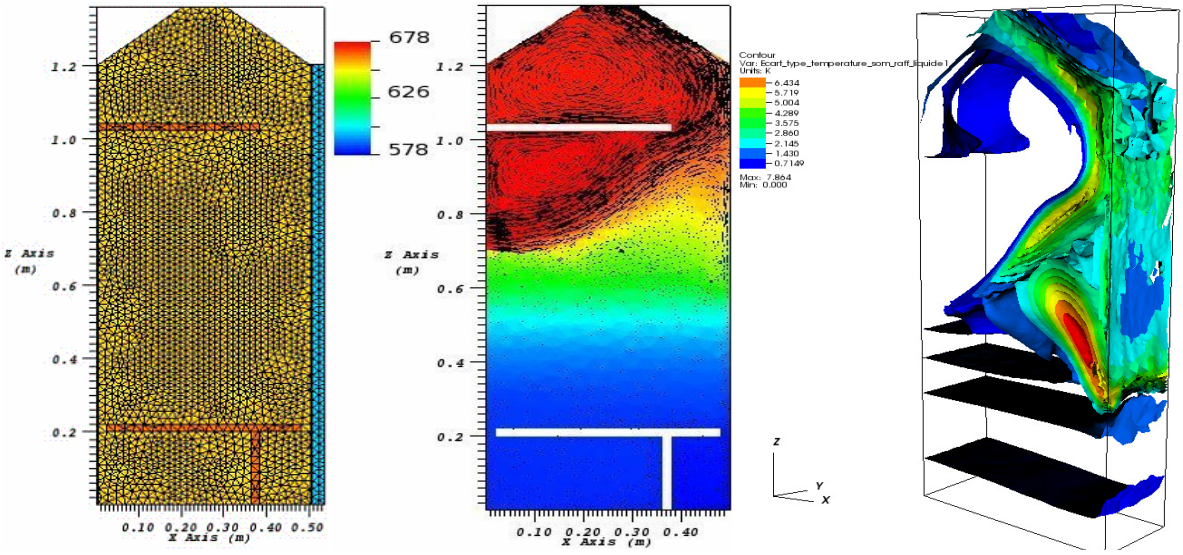

FIG. 6.32. Mean temperature distribution and peak-to-peak sodium temperature fluctuation.

Figure 6.33 shows a TRIO_U calculation of the cold plenum of an advanced pool Sodium Fast Reactor with three Decay Heat Removal systems in the cold plenum. CFD calculations are needed for validating such design options.

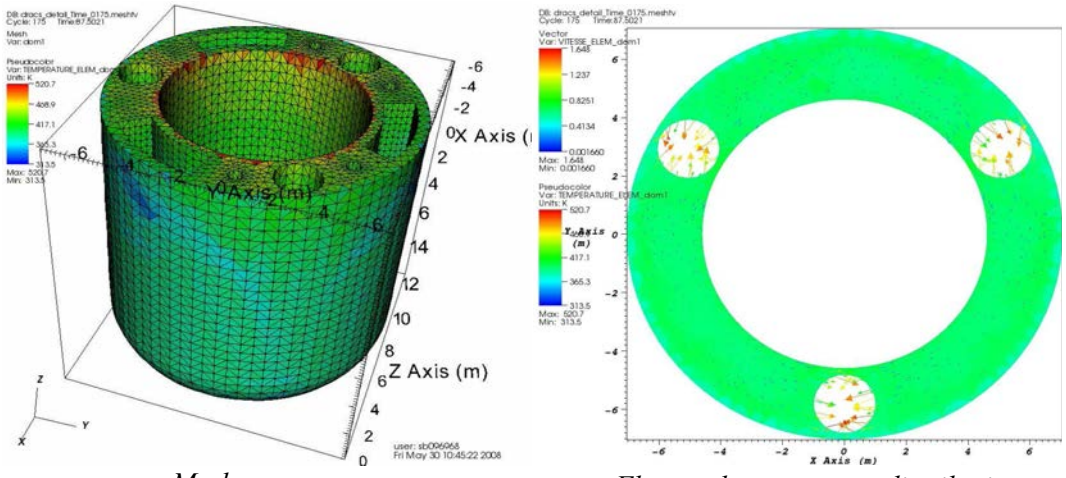

Mesh *Flow and temperature distribution*

FIG. 6.33. TRIO_U calculation of the cold plenum of a pool type fast reactor concept.

Three-dimensional flow and temperature distributions of primary sodium in the hot pool under various power levels have been predicted for PFBR. It was found to be stratified at full power. To break the stratification, the radial velocity of sodium entering the pool has been increased by providing a skirt below the control plug. The flow and temperature distributions after this modification are depicted in Fig. 6.34a and Fig. 6.34b.

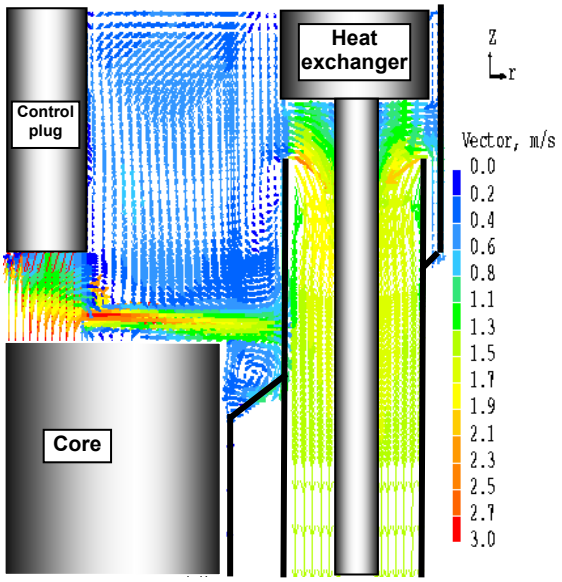

FIG. 6.34a. Flow field in hot pool .

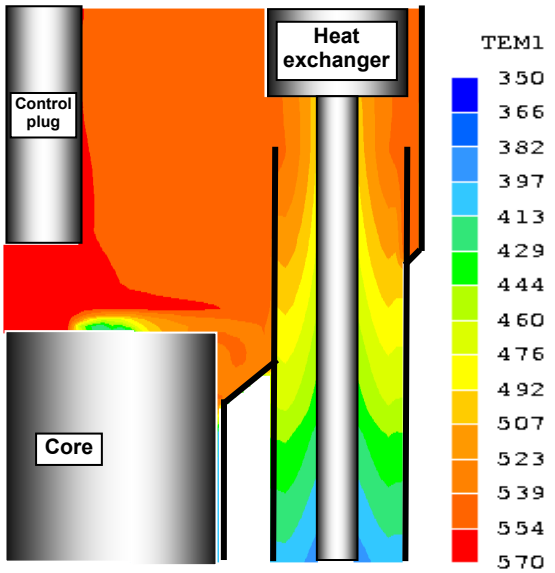

FIG. 6.34b. Temperature field in hot pool.

Based on a detailed parametric study, the porosity of the skirt, its effectiveness at low power and its influence on core monitoring thermocouple locations, intermediate heat exchanger (IHX) primary inlet velocity distributions (from flow induced vibration considerations), mixing in the hot pool and free surface velocity have been assessed. Based on steady and transient studies, the thermal loads on the submerged structures viz. inner vessel and control plug etc have also been predicted. Large sodium velocities at the free surface are of concern from gas entrainment considerations.

To minimize the free surface velocity, baffles are to be provided at suitable locations in the hot pool that breaks the vertical sodium jets leading to a calmer free surface. The size and location of these devices are optimized based on CFD investigations.

Delayed neutron detectors (DND) are provided in the hot pool of PFBR for detection of fuel clad failure. In order to have a low background field, the detectors are located as far away from the core as possible. But, farther the distance between the core and detectors, the longer would be time taken by the delay neutron precursors, to reach the detector. It is highlighted that the precursors decay during their travel from core to detector. The paths taken by sodium streams, which transport the precursors from fuel subassembly to detector, are different for different subassemblies. Also, the number of detectors has to be as minimum as possible.

To optimize the number of detectors and finalize their locations, considering the constraints from reactor assembly, 3-D transient thermal hydraulic analysis of hot pool has been carried out and the evolution of fission product concentration in hot pool sodium after the failure of a fuel subassembly has been predicted. It has to be ensured that clad failure in any subassembly

is detected by DND within the stipulated time, considering dilution in the concentration of fission products in hot pool both by mixing as well due to their radioactive decay.

Based on this study, the number and position of detectors in hot pool for effective detection of cladding failure in any of the subassembly been arrived at. It is found that 8 DND, located one on either side of the IHX, can detect 10 cm^2 failures in any fuel subassembly within 70 s [278]. The shortest path traversed by a precursor from the failed fuel subassembly in a radial plane where IHX is located and the longest path traversed by a precursor from a failed fuel subassembly away from IHX are depicted in Figs 6.35a and 6.35b respectively. In these figures PSP, CP and IV refer to primary sodium pump, control plug and inner vessel respectively.

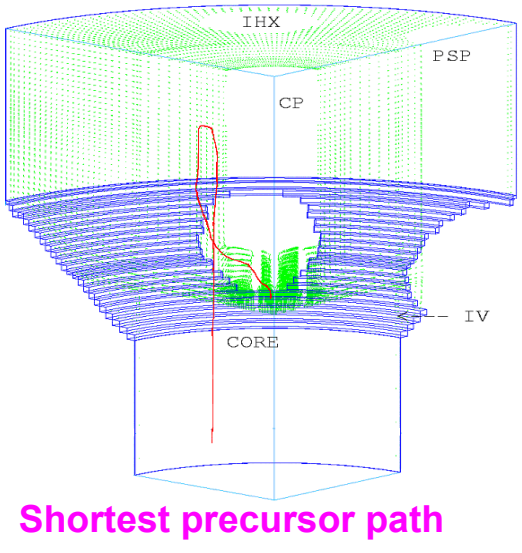

FIG. 6.35a. Shortest path traversed by a precursor.

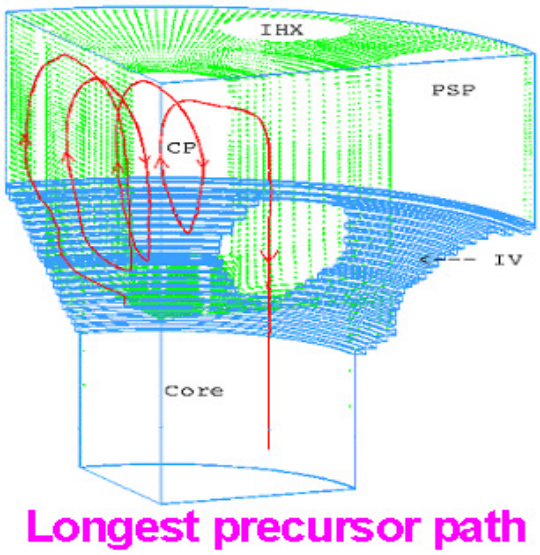

FIG. 6.35b. Longest path traversed by a precursor.

The outlet temperatures of all fuel subassembly are continuously monitored by thermocouples (TC) mounted in the core cover plate. The accuracy of the prediction of subassembly outlet temperatures depends on the location of the TC, temperature profile within the subassembly and dilution by the neighboring subassembly. Hence, a thermal hydraulic study has been carried out for PFBR to study the effects of the location of the TC with respect to the subassembly position by considering subassembly movement due to irradiation bowing.

In this study using CFD code PHOENICS, the stream line paths and temperature distribution of sodium around core monitoring thermocouple tips have been determined.

The results are shown in Fig. 6.36.

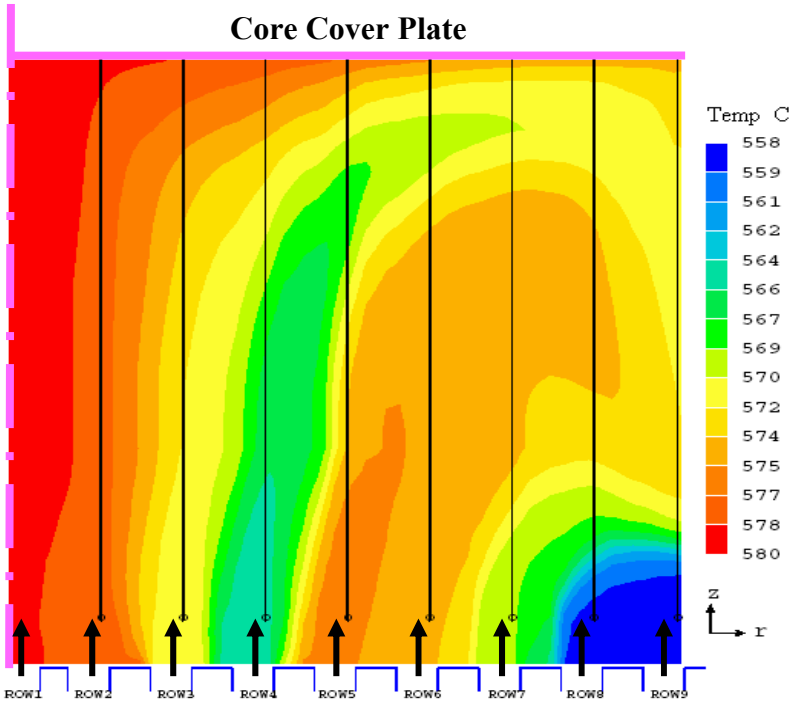

FIG. 6.36. Temperature distribution below CCP at full power conditions.

It has been found that the TC tips are required to be shifted by 20 mm radially for proper temperature monitoring. With this radial shift it has been established that the thermocouple tips (located at 95 mm above subassembly top) are immersed in their respective fuel subassembly sodium streams for full and part load conditions of the reactor. The temperature attenuation of sodium streams is negligible at the location of thermocouple tips.

The non-uniform temperature distribution at the subassembly top can cause fluctuations in the temperature reading recorded by the TC in the central region of core. This has been investigated further [279]. The fluctuations are caused due to the phenomenon of jet instability. In order to analyse this, 2 D direct numerical simulation of a representative region of hot pool near core center has been carried out. Temperature fluctuation in sodium near the TC mounted above the central subassembly is shown in Fig. 6.37.

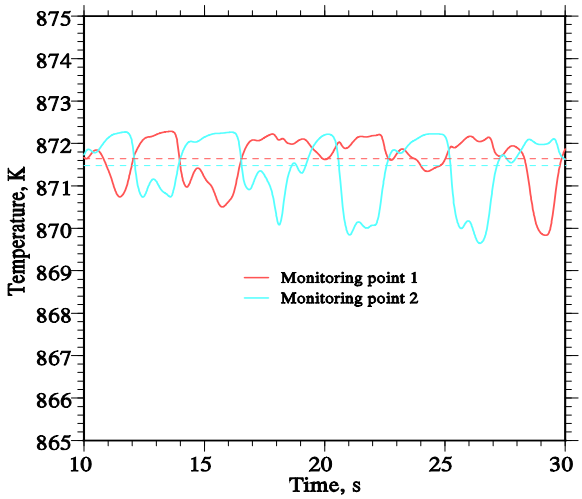

FIG. 6.37. Temperature fluctuation at TC above central fuel subassembly.

The dominant frequency of fluctuation of sodium temperature at the TC location has been estimated to be 0.25 Hz, which would be sensed comfortably by the central subassembly temperature monitoring bare TC (0.3 s time constant). The maximum fluctuation in the temperature reading recorded by this TC has been found to be ±2 K. The SCRAM threshold on the parameters based on this TC measurement is fixed at +10 K. Thus, this fluctuation together with the effect of subassembly bowing is below the scram threshold and hence there is no concern.

Sodium flow and temperature distributions in hot pool of PFBR, in the region between subassembly top and core cover plate, have been investigated using the general purpose CFD code PHOENICS at full power condition for various values of flow reduction in a particular subassembly compared to others. The analysis has been carried for the blocked subassembly located at each and every row in core. The stream line paths and temperature distribution of sodium around core monitoring thermocouple tips of the blocked subassembly have been given special attention. Based on the analysis, it has been established that the thermocouple tips are immersed in their respective fuel subassembly sodium streams for all the cases of flow reduction studied. It is also established that plugging in any subassembly can be detected for 6% flow reduction itself. This value of 6% reduction is much less than the permissible value of ~ 30%. In the Republic of Korea, pool hydraulics studies have been carried out using COMMIX-1AR/P code. Figure 6.38 shows the steady state temperature distribution of an elevation view in the r-z plane passing through the center of IHX.

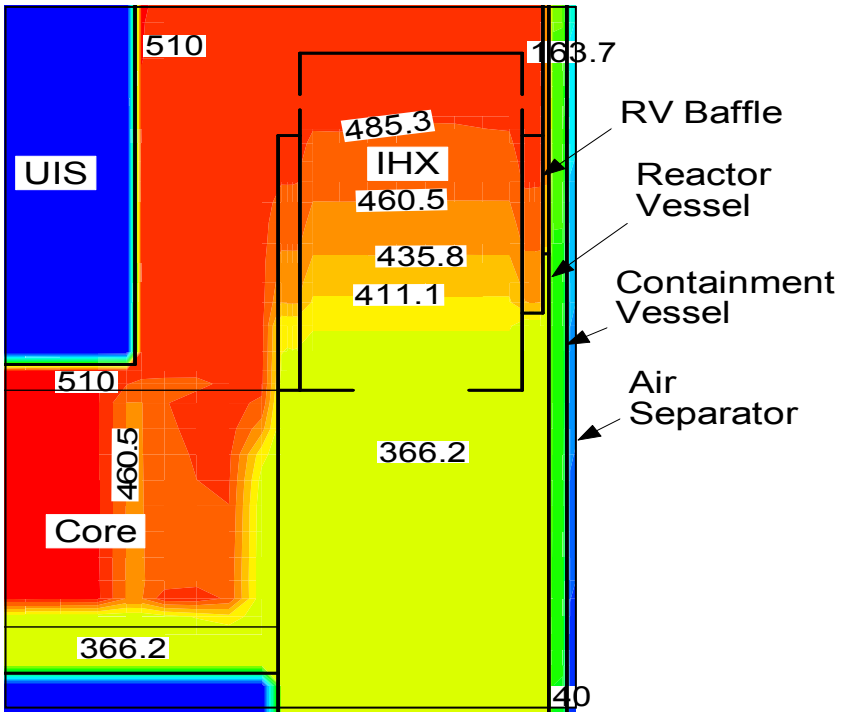

FIG. 6.38. Temperature and velocity distributions in the reactor pool at a plane passing through IHX center.

This figure also shows the velocity distribution in the same plane. The isothermal lines are showing the increase in temperature through the fuel assembly region. The temperature in the cold pool, fixed shielding, and core inlet plenum is uniform at 390°C, and that in the hot pool is at 545°C. The flow field shows the circulation pattern with a small velocity in the vicinity of the support barrel at the level of the core exit.

The results of the steady state analysis show that the sodium is well mixed and nearly isothermal in the hot and cold pools and there are no unexpected conditions that are of concern to the designer. The transient calculation is performed for the case of the loss of heat sink using the same code and the steady state results are used as the initial conditions. The transients of the core inlet and outlet temperatures and the percentage of mass flow rate are shown in Fig. 6.39.

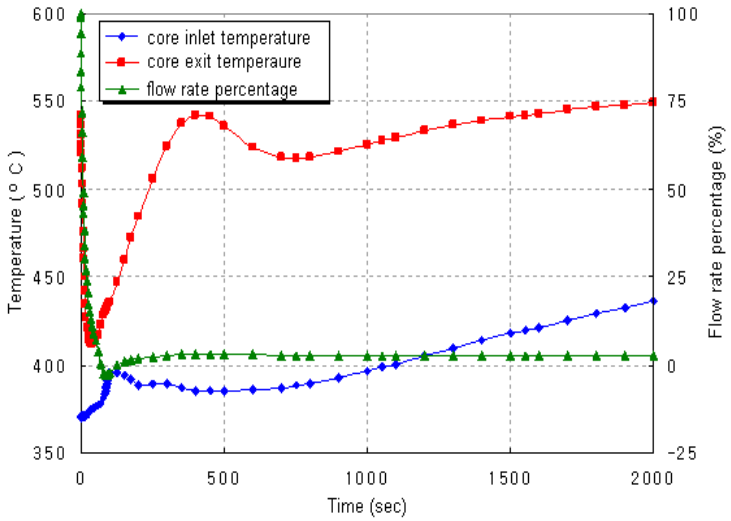

FIG. 6.39. Transients of core inlet and outlet temperatures and percentage of mass flow rate.

As the pump starts coasting down, the flow rate at the core inlet starts decreasing. Flow reversal happens at 70 s and then the flow rate increases slowly and is nearly saturated at 250 s. As the heat generated in the core drops suddenly due to reactor SCRAM, the core exit temperature decreases rapidly to 410°C within 40 s.

The predicted flow and temperature distribution in the sodium pools at various instants during the transient are depicted in Fig. 6.40.

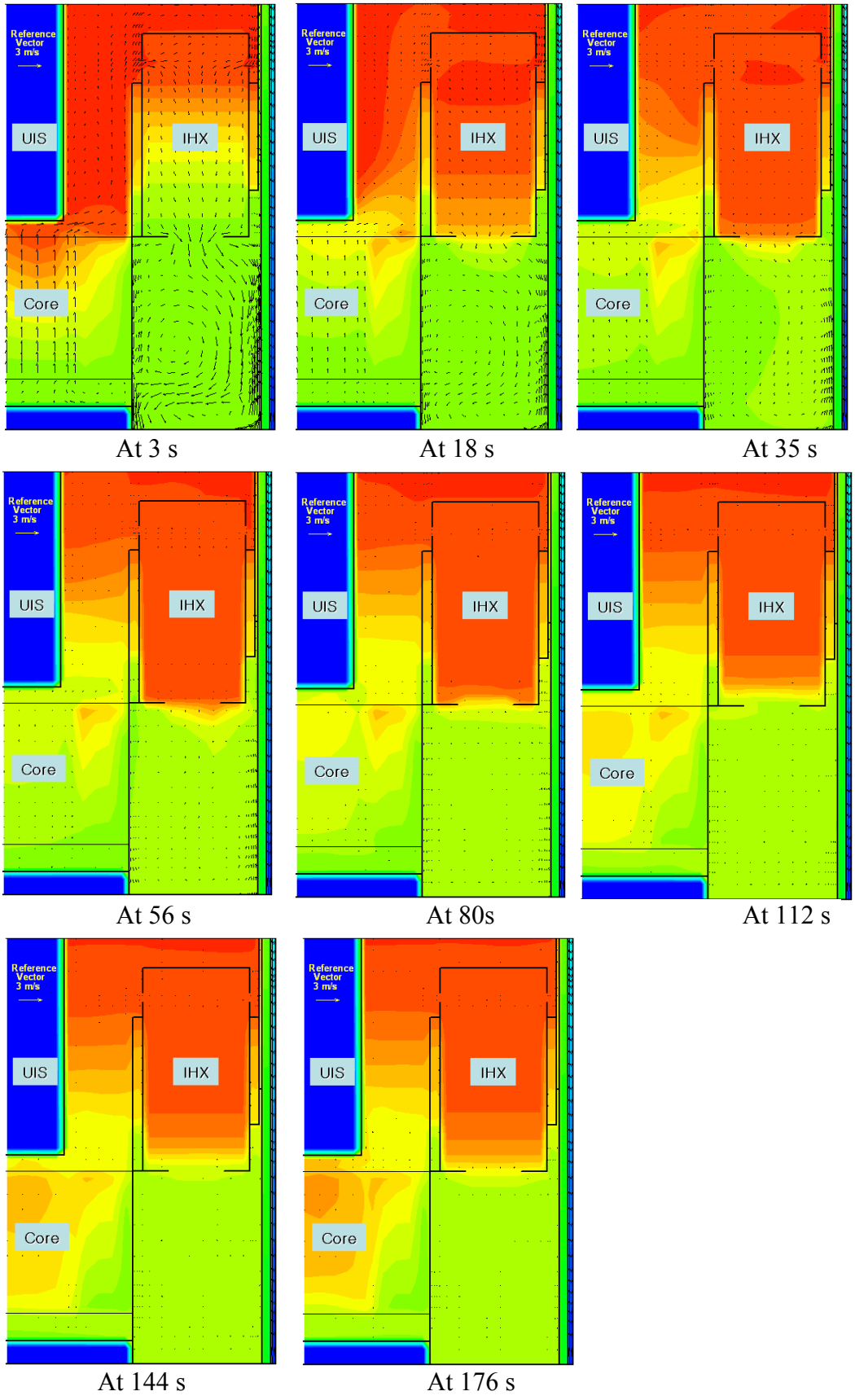

FIG. 6.40. Transient distributions of flow and temperature in the reactor pool.

Within the framework of the European THINS (Thermal Hydraulics for Innovative Nuclear Systems) project, a reliable database for qualification of CFD approaches for the simulation of flow phenomena in a large pool like e.g. convection patterns, thermal stratification and fluid-structure thermal exchange, will be established on the basis of experiments with suitable instrumentation. A new experimental installation called E-Scape (European Scaled Pool Experiment) depicted in Fig. 6.40a will be built up at SCK·CEN in Belgium based on a scale model of a representative liquid-metal pool-type vessel and its components with an envisaged scaling factor of about 1:5 or 1:8 using lead-bismuth. The experiments will aim at characterizing the convection patterns in different forced flow conditions as well as at monitoring the free surface level fluctuations.

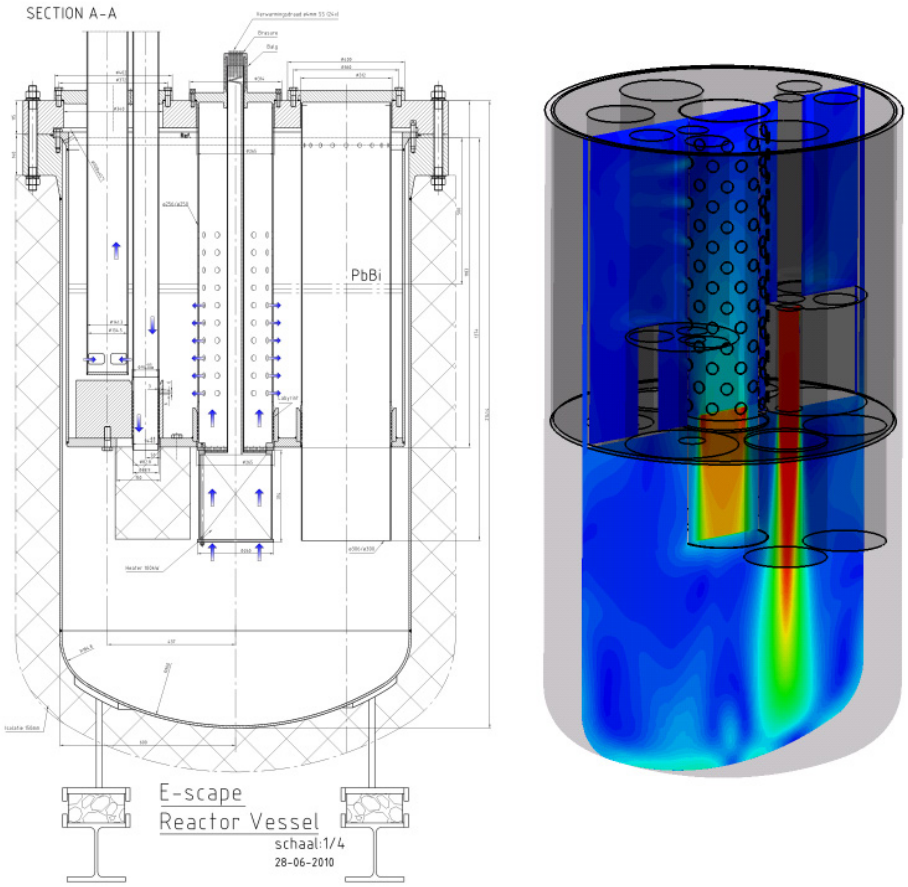

FIG. 6.40a. E-Scape drawing (SCK·CEN) and scaling simulation (NRG).

For each phenomenon investigated, similarity laws and modelling criteria have to be established. Proper simulation requires similarity of geometry, velocity and temperature fields and of the boundary conditions. In view of this, the governing dimensionless numbers that characterise the behaviour of the liquid metal in the reactor pool for a particular phenomenon (e.g. Reynolds, Froude, Weber, Euler, Richardson's and/or Peclet number) will be maintained whereas a compromise will be accepted in the distortion of others.

CFD simulations were used by SCK·CEN and NRG [279a] to validate this approach, to determine the scaling factors and transposition of the experimental results to the real scale situation for the different phenomena as was done in a preliminary. It was found that various scaling approaches can be used which more or less give similar results.

An appropriate instrumentation will be installed with the support of the German HZDR from Rossendorf consisting of pressure transducers, thermocouples, surface characterisation and velocity probes, including UDV for local velocity measurements.

6.3.3.4. Modelling of decay heat removal in primary sodium system

Decay heat removal is an important issue for fast reactors. The sodium cooled fast reactors have the advantage of possible passive decay heat removal by natural circulation. Nevertheless, the onset and the efficiency of natural circulation in the primary circuit and in the decay heat removal circuits have to be demonstrated. Success of decay heat removal depends on the deployment of final heat sink and healthiness of the heat transport path from the heat source to the heat sink.

The passive decay heat removal path of PFBR includes two sodium pools between the heat source and the decay heat exchangers (DHX) and a sodium loop between DHX and air heat exchangers (AHX). A part of the cold sodium entering the hot pool from DHX flows to the bottom of the subassembly along the core periphery and then flows radially inwards and upwards through the inter-wrapper space between subassembly. This flow is termed as inter-wrapper flow. A part of the total decay heat is transferred to hot pool by the sodium passing through the subassembly, while the rest of the decay heat is transferred to the hot pool by the inter-wrapper flow.

Flow distribution in the hot and cold pools is multi-dimensional in nature. Sodium flow in the intermediate circuit and air flow in the AHX are by natural circulation and is prone to stability and flow reversal problems. The natural circulation of air in the AHX stack is likely to get influenced by the atmospheric wind conditions and the presence of nearby structures. Because of these complexities, the heat removal capability needs to be established through an integrated multidimensional computational analysis or by experiments.

Towards assessing the temperature evolution in critical structures of hot and cold pool and clad of the fuel and storage subassemblies, a multi-zone model, depicted in Fig. 6.41 has been used for PFBR. The predicted temperature evolution in hot and cold pools is depicted in Fig. 6.42.

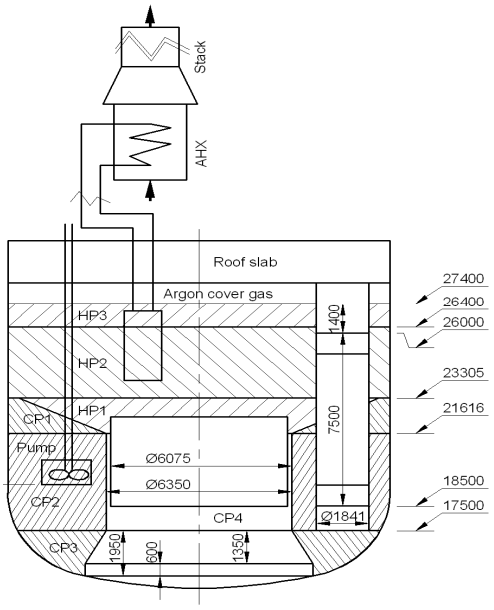

FIG. 6.41. Multi-zone model of hot and cold pools.

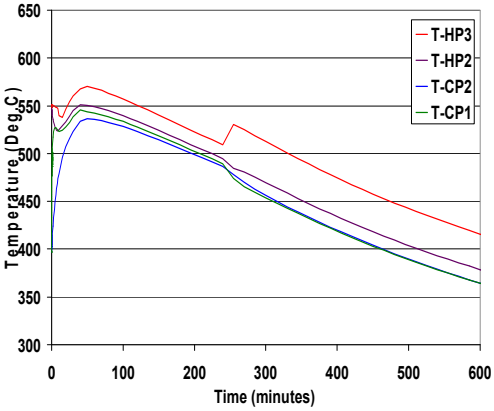

FIG. 6.42. Evolution of hot and cold pool temperatures during decay heat removal.

The cold sodium from DHX removes significant amount of the decay heat while it flows through the inter wrapper space (Fig. 6.43a). The heat removal capability of this flow has been established based on a combined "system level – multidimensional" thermal hydraulics model. Based on this study, it is found that the temperature limits of the core are satisfactorily met under natural convection condition. The predicted instantaneous temperature distribution in the pool, 490 s after the power failure event, is depicted in Fig. 6.43b.

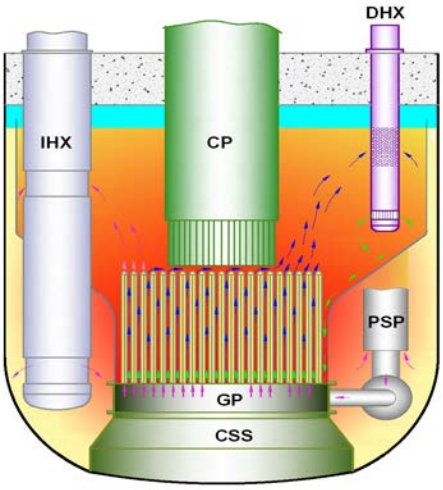

FIG. 6.43a. Inter-wrapper flow.

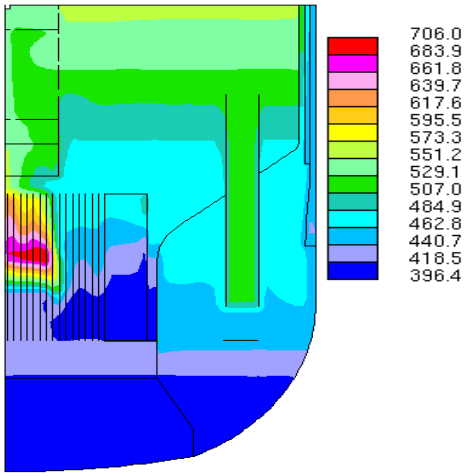

FIG. 6.43b. Transient temperature (°C) in pools at time = 490 s.

CEA is using CATHARE system code with possible coupling with TRIO_U code to take into account 3D effects [280]. In the past, the calculations of the onset and the efficiency of natural circulation in the primary circuit and in the decay heat removal circuits were verified by comparison with experimental data.

Reduced scale water models were used to verify the calculations of the primary circuit with immersed coolers. Sodium facilities were used to assess the calculations on natural circulation in the decay heat removal circuits. New experimental data will be required to verify the CFD calculations of new concepts of reactors, mainly water reduced scale models of the primary circuit. Figure 6.44 shows the CATHARE modelling of the primary and secondary circuits of a sodium cooled fast reactor for decay heat removal analysis.

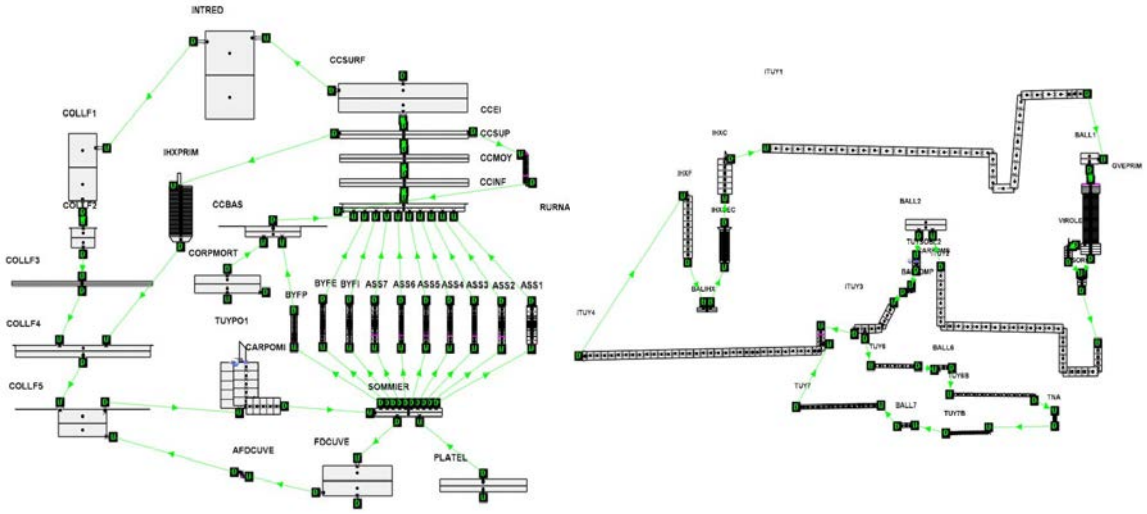

FIG. 6.44. CATHARE modelling of primary and secondary circuits for DHR analysis.

Natural circulation is used in the primary circuits of SFRs, as a rule, to remove decay heat. The major investigations on decay heat removal systems carried out are: (i) an investigation on water models of reactor facilities, (ii) modifying and validation of computational codes by using the experimental data (iii) calculation of thermal hydraulic performance of decay heat removal by natural convection in the reactor conditions by using validated code.

The following are the main stages related to emergency reactor shutdown viz. (a) operation at nominal power, (b) reactor power decrease due to reactor SCRAM and (c) natural convection development. A system of differential equations which describes the above mentioned processes gives the following set of similarity criteria [285]:

$$Ri = g\beta\Delta T_0 L / U_0^{\,2}, \quad Eu = \Delta P_0 / \rho U_0^{\,2}, \quad Ho = \tau_0 U_0 / L, \quad Pe = U_0 L / a, \quad \mathrm{Re} = U_0 L / \nu,$$
$$N = Q / \rho c U_0 L^2 \Delta T_0 .$$

It is difficult to achieve equality of the all listed similarity criteria in both model and prototype, therefore an approximate simulation is applied, i.e. simulation of some of the most important similarity criteria alone. H. Takeda and T. Koga proposed to use a method of representation of experimental time dependency of coolant temperature at the core outlet in dimensionless form: $\Delta T^*=\Delta T/\Delta T_0=f(\tau^*)$, where $\tau^*=\tau/\tau_0$ [281].

Results of studies implemented for cases with sudden power increase of model heaters revealed auto modeling for $\Delta T^*=f(\tau^*)$ dependency at Q > 1 kW. This fact has been confirmed by results of experimental studies carried out on a flat water model in SSC RF IPPE.

These tests derived dependencies of temperature difference Δt as a function of time for various values of power, which demonstrate a process of natural convection development in a

heated part of the model [286]. The similar dependencies were obtained in operating reactor facilities (BR-10, BOR-60, BN-600) [286].

Analysis has showed that experimental data obtained for coolants with different values of Prandtl number (water, sodium-potassium alloy, sodium) and presented in dimensionless form $\Delta t / \Delta t_m = f(\tau / \tau_m)$ are well generalized by relation:

$$\Delta t / \Delta t_m = 1 - \exp(-2\,\tau/\tau_m)^3 \qquad (7)$$

in wide range of power and Prandtl number (0<Pr<10).

Figure 6.45 shows a comparison of the experimental data to the data presented in [281] with the proposed equation.

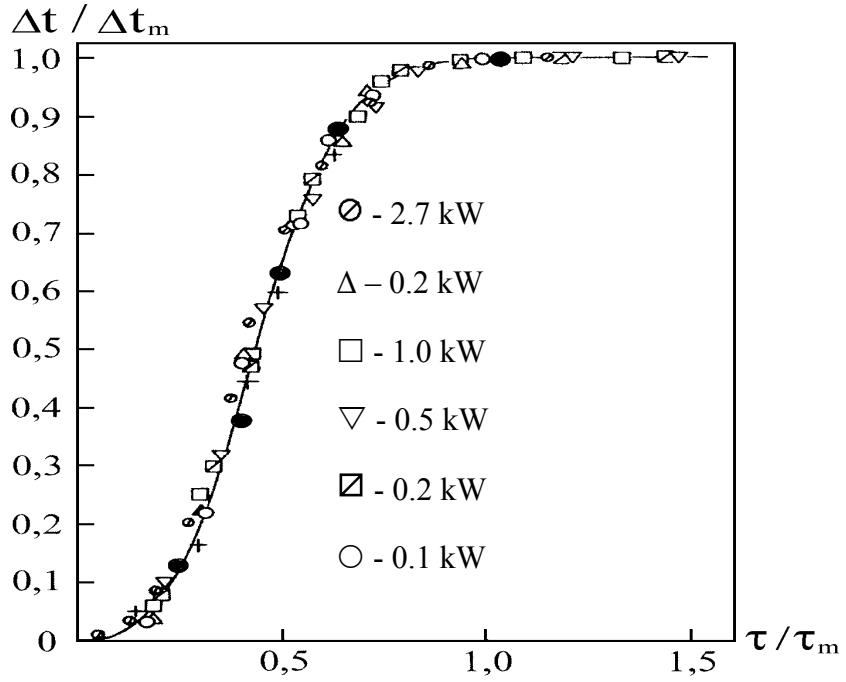

FIG. 6.45. $\Delta t/\Delta t_m$ *Vs* (τ/τ_m) *at different power levels.*

It is clear that this relation well generalizes these data in all range of change of the power in tests (0.1-2.7 kW). It should be noted that each of relations $\Delta t=f(\tau)$, irrespective of power, is characterized by availability of a singular point, in which the temperature difference Δt reaches a maximal value Δt_m. The time $\tau=\tau_m$ corresponds to this value Δt_m. From all variety of parameters describing dynamical characteristics of process, the parameters Δtm and τ_m are interesting for us.

At first, as the coordinates of special characteristic point describing dynamical process, Δt_m and τ_m are reciprocal dependent parameters, this gives the basis for generalization of the experimental data for non-stationary natural convection.

Secondly, each of these parameters can be used as a reference scale at development of similarity criteria which include characteristic temperature difference and characteristic time.

The characteristic scales of a temperature difference Δt_m and time τ_m depend on a level of power reproducing a decay heat.

The specific data presented in works which were reviewed in [281] allow establishing the relation

$$\Delta t_m = f(N),\ \tau_m = f(N).$$

Thus, the generalized dependence of dimensionless temperature on dimensionless time reflects dynamics of development of temperature changes under conditions of natural convection at sudden change of power of heaters.

6.3.3.5. Thermal striping

There are many places where hot and cold fluids meet and temperature fluctuation occurs in a nuclear power plant. One such location is fuel breeder interface. Due to the difference in the heat generation rates among the fuel, breeder and storage subassemblies, the temperatures of sodium jets leaving these subassemblies are not the same. Thermal striping is a phenomenon, which leads to random temperature fluctuations at the interface between non-isothermal streams, arising out of jet instability. Due to the large heat transfer coefficient associated with liquid sodium, these temperature fluctuations are transmitted to the adjoining structures with minimal attenuation, which eventually lead to high cycle fatigue and crack initiation in the structures. Sodium cooled fast reactors had some incidents due to the thermal striping [282].

Detailed thermal hydraulic investigation has been carried out to quantify the amplitude and frequency of temperature fluctuations in the structures of primary sodium system of PFBR. The investigation consists of CFD simulations at two levels [283].

In the first level, locations prone to thermal striping were identified, by performing a global conjugate 3-D simulation of hot and cold pools, employing the standard k-ε turbulence model.

In the second level, transient transport equations were solved by Direct Numerical Simulation (DNS) method, to predict detailed flow and temperature fluctuations. The computed peak-to-peak values of sodium temperature fluctuations (Fig. 6.46) and the corresponding values on the structural surfaces are found to be less than the acceptable temperature limits, evaluated by detailed structural mechanics studies.

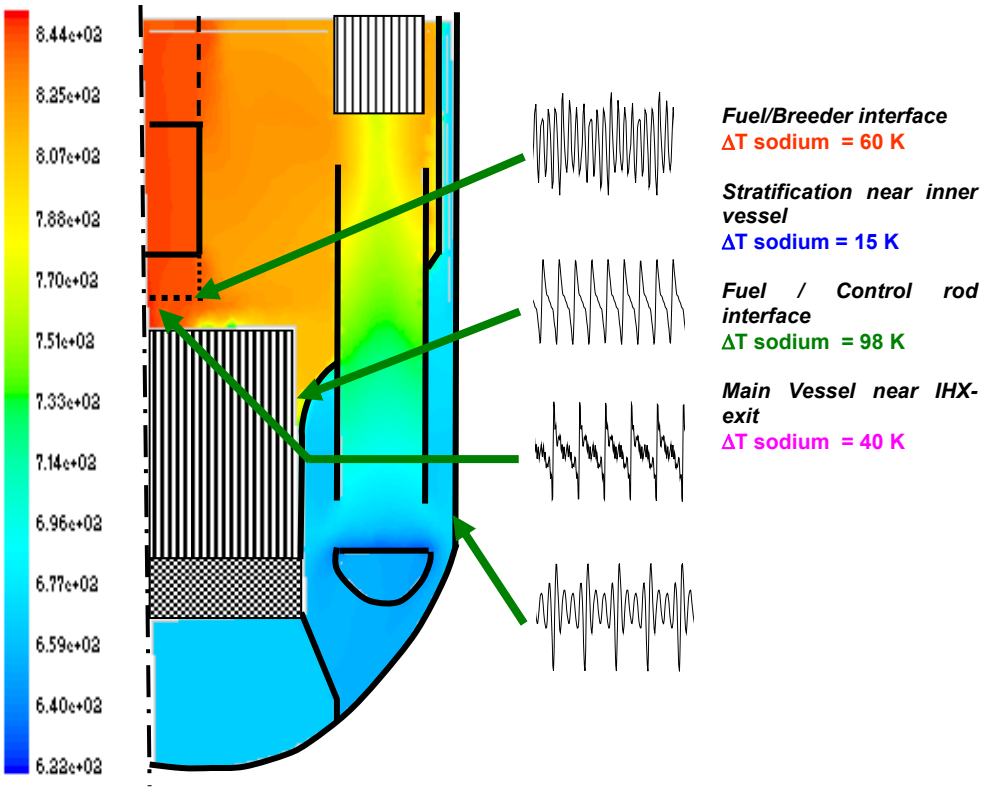

FIG. 6.46. Mean temperature distribution and peak-to-peak sodium temperature fluctuation.

Water and sodium experiments [284, 285] were carried out in Japan to evolve thermal hydraulic aspects of thermal striping. A configuration of triple parallel jets along a wall was selected as the test geometry.

Detailed temperature and velocity fields were measured by a movable thermocouple tree and particle image velocimetry (only in the water experiment). The test sections in the water and sodium experiments were nearly identical in geometry and dimensions.

Figure 6.47 shows the schematic of the test section of the sodium experiment.

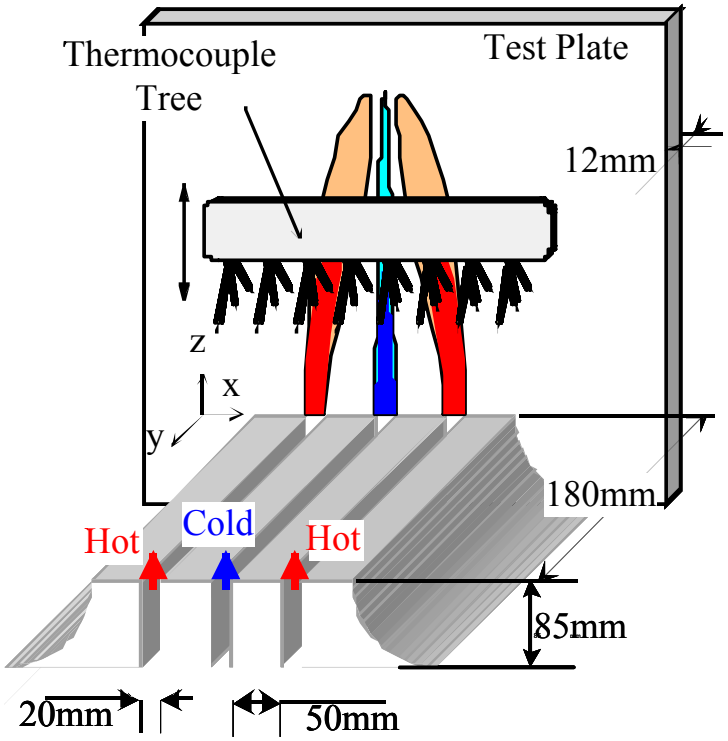

FIG. 6.47. Schematic of parallel triple jet test section in sodium.

The cold jet in the center mixes with two hot jets which flow in parallel to the center jet. This flow geometry is a simplified model of an outlet of control rod channel surrounded by core fuel subassemblies. In the triple jet experiment, a vertical wall stands in parallel to the three jets. There is one more vertical wall at the opposite side and the triple jet flows are sandwiched by these two plates. The distances of two walls are 180 mm and 170 mm, in the sodium and the water tests respectively. Each of the jets is discharged vertically from a rectangular nozzle.

The representative length, D, is set as the nozzle width, 20 mm, and the pitch of the three nozzles is 70 mm. Each nozzle has three porous plates in upstream region and a quadrant reducer. It is believed that the discharged velocity profile at the nozzle outlet is flat.

As for the coordinate system: the x-axis is the horizontal direction, the y-axis is the normal direction of the wall surface and the z-axis is the vertical direction along the wall surface. The origin is the centre of the cold jet horizontally, the height of the nozzle exit vertically and the surface of the structural wall in normal direction of the wall. The walls are made of stainless steel (type-316) in the sodium test and acrylic resin in the water test.

Each array has 25 thermocouples. In the water experiment, the movable tree has one array of 30 thermocouples and it can move in vertical (z) and depth (y) directions. The thermocouples in the tree and test plate are non-contact CA-type and the diameters of the thermocouple are 0.3 mm or 0.5 mm in the sodium test and 0.25 mm in the water test. The temperature distributions in fluid were measured by moving the thermocouple tree in z and/or y directions.

The time interval of the temperature measurement was 0.01 s and the number of the recorded temperature readings was 20000 (time length = 200 s) at each position. Velocity measurement using Particle Image Velocimetry (PIV) was applied to the water experiment.

Table 6.11 shows the experimental conditions of the water and sodium tests.

Flow visualization was done in the water experiment.

TABLE 6.11. TEST CONDITION OF TRIPLE PARALLEL JET EXPERIMENT

		Water	Sodium
Flow velocity m/s	Hot jet	0.5	0.5
	Cold jet	0.5	0.5
Temperature °C	Hot jet	39	350
	Cold jet	29	310

Figure 6.48 depicts a $1/15^{th}$ of a second time sequence of the triple jet under homogeneous temperature condition. The images have been taken with laser-sheet (argon laser) illumination from the side and Uranine dye added to the water. It was observed that the side-to-side swaying in unison of the three jets.

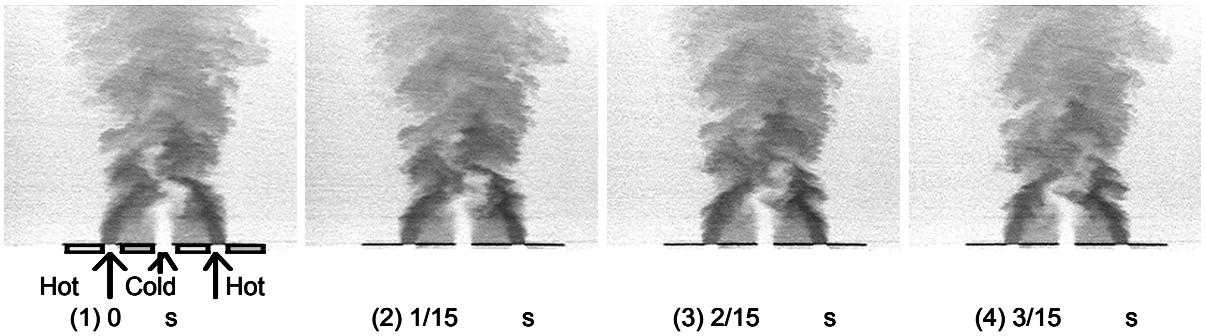

FIG. 6.48. Visualization of triple parallel jet flows.

Temperature distributions were measured in the sodium and water experiments.

Figure 6.49 shows the comparisons of transverse temperature distributions at y/D=4.5 and 0.025 from the wall between water and sodium experiments. Overall temperature distributions in the sodium test are similar to those in the water test. In the downstream region (z/D=10), the temperature distribution near the wall is steeper than at mid plane. One of reasons will be a flow along the wall due to the Coanda effect.

Temperature fluctuation intensity is shown in Fig. 6.50.

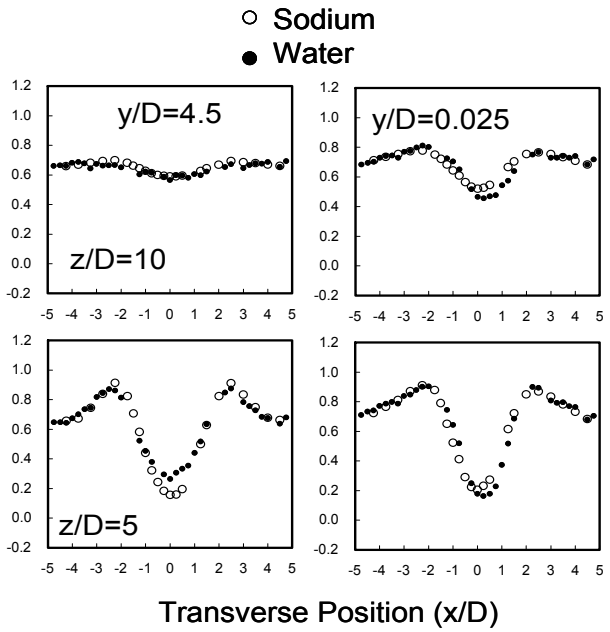

FIG. 6.49. Transverse temperature distribution in sodium and water.

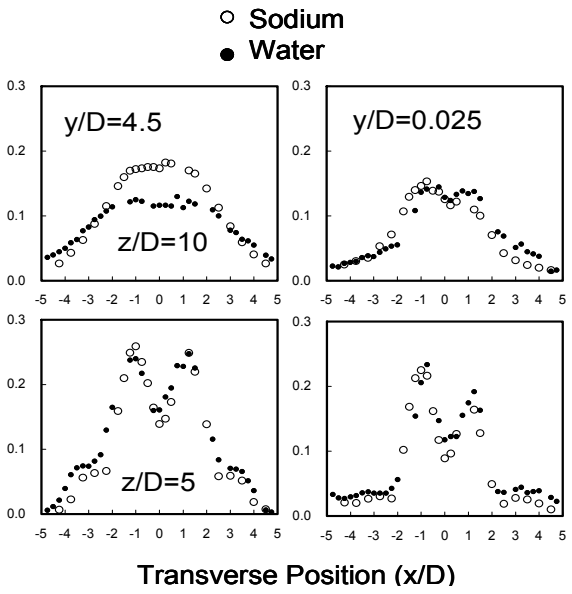

FIG. 6.50. Transverse distribution of intensity of temperature fluctuation.

The highest intensity at the high mixing region (z/D=5) decreases closer to the wall. The profiles in the sodium experiment are quite similar to those in the water except at the downstream mid plane, z/D=10 and y/D=4.5. In the downstream region mid plane, the fluctuation intensity in the water decays earlier.

Theoretical analyses [286] were carried out by using an in-house numerical code based on a finite difference method and a second order numerical scheme for the convection terms. Temperature profile and fluctuation characteristics were well predicted.

In KAERI (Korea Atomic Energy Research Institute), Nam and Kim [287] provided detailed experimental data for the thermal striping, mainly to test the turbulence models and LES (Large Eddy Simulation). The test sections are planar double-jet and planar triple-jet, and the working fluid is air. Several experiments are performed by varying the inlet temperatures and velocities. In the present study these experimental data will be used for testing the turbulence models for the simulation of the thermal striping.

For the numerical works, Ushijima et al. [288] carried out numerical calculations for a coaxial-jet with different temperatures using the high-Reynolds-number differential stress and flux model. The time average of the velocity and temperature generally agreed with the measured data, however, some discrepancies were found in the turbulence quantities, such as the turbulent heat fluxes.

Nishimura et al. [289] performed a numerical calculation for the triple-jet experiment conducted by Tokuiro and Kimura [290] using the low-Reynolds-number differential stress and flux model (LRSFM) together with the k-ε model. They showed that the LRSFM could simulate appropriately the experimental results most importantly with respect to the oscillatory motion and consequently the mean profiles of the flow pattern, while the k-ε model consistently under predicted the extent of mixing, such that a transverse mean temperature difference exists far downstream of the jets.

Kimura et al. [291] performed the same computations for the triple-jet flow, but added the computed results using the DNS. They showed that coherent oscillation observed in the experiment could be properly simulated by LRSFM and DNS, and that the k-ε model and LRSFM over-predict amplitude of temperature fluctuation. They also showed that the power spectrum density profiles of temperature fluctuations predicted by DNS were in good agreement with the experimental data and the prominent frequency component of jet oscillation could be predicted by LRSFM.

Another study has been carried out to test three turbulence models such as the shear stress transport (SST) model by Menter [292], the two-layer model by Chen and Patel [293] and the elliptic relaxation (V2-f) model by Durbin [294]. The practical implementation of the LRSFM such as the model developed by Nishimura et al. in a general purpose code is still difficult due to the existence of many wall related parameters. Thus, the primary emphasis of the present study is placed on the test of the two-layer model, SST model and V2-f models for the thermal striping since (1) the three models have been very successful in many kinds of flow situations, (2) the three models are very easy to implement in the general purpose codes.

The capability of predicting the oscillatory behavior of the ensemble averaged temperature is examined, and the accuracy of the prediction of the mean and root-mean-square of temperature by the three models is investigated through a comparison with the experimental data as shown in Figs 6.51 to 6.53.

It is seen that only the elliptic relaxation model is capable of predicting the oscillatory behavior of the ensemble averaged temperature. But the amplitude of the temperature fluctuation predicted by this model is smaller than the experimental values. It is also shown that the elliptic relaxation model predicts best the mean and RMS values of the temperature. However, this model predicts a slower mixing at a location far downstream of the jet.

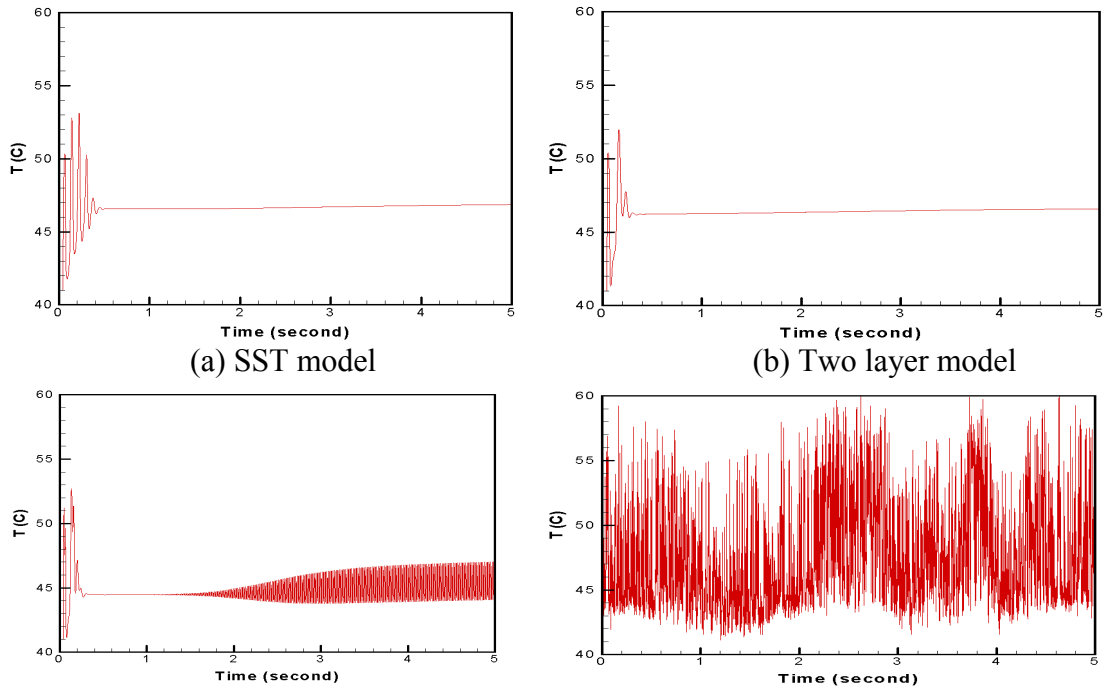

FIG. 6.51. Temperature evolution during first five seconds.

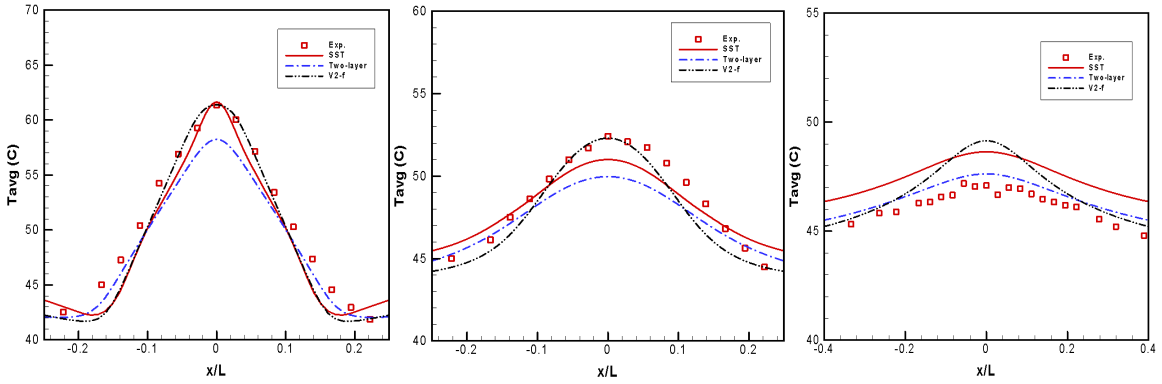

(a) y=98mm, (b) y=273mm, (c) y=523mm

FIG. 6.52. The time averaged temperature distributions at various vertical locations.

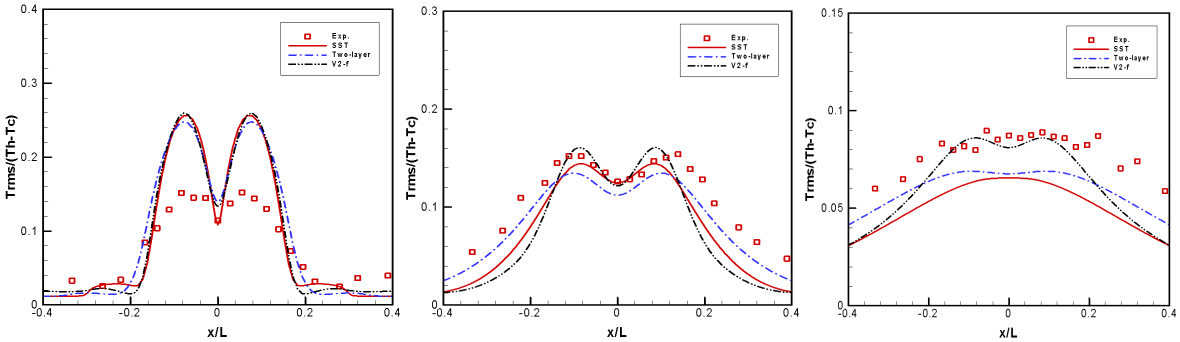

(a) y=98mm, (b) y=273mm, (c) y=523mm

FIG. 6.53. The root-mean-square of temperature distributions at various vertical locations.

Thermal striping in fast reactors has been studied for a long time in France as some problems occurred in Phénix reactor. CEA is using the TRIO_U code to estimate the temperature fluctuations in mixing regions or in stratified regions. The Large Eddy Simulation model implemented in TRIO_U is well adapted to determine the amplitude and the frequency of the fluctuations. Of course, experimental data are needed for the verification of such calculations. In the past, air, water and sodium tests were performed on core outlet mixing regions, mixing tees and other mixing regions. This data base can be used but new data may be required for specific configurations.

Figure 6.54 shows the comparison of a TRIO_U calculation and the WATLON water mixing tee experiment at JAEA [295, 296]. Figure 6.55 shows the comparison of a TRIO_U calculation and the sodium PLAJEST mixing experiment performed at JAEA [297].

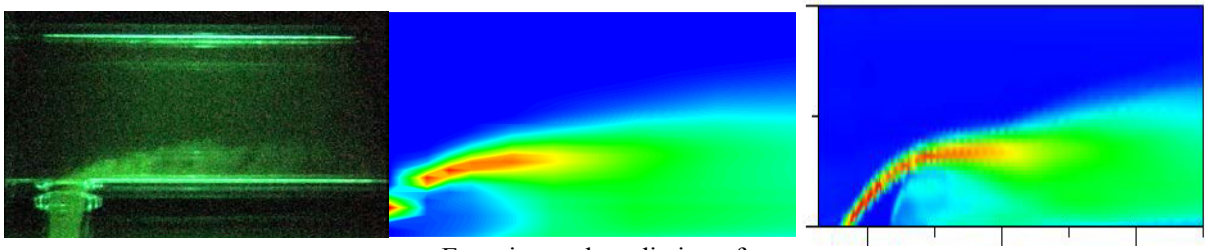

Experimental visualization

Experimental prediction of temperature fluctuation

TRIO_U prediction of temperature fluctuation

FIG. 6.54. TRIO_U calculation of WATLON experiment at JAEA.

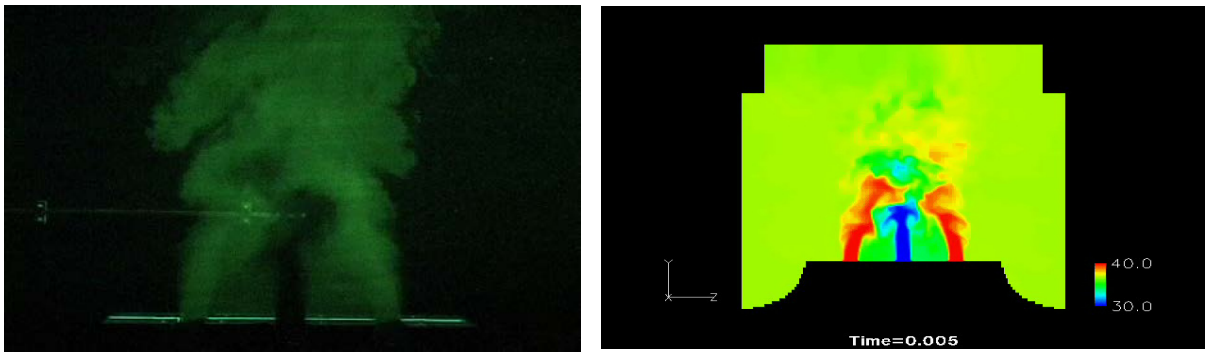

Experimental visualization

TRIO_U prediction of temperature field

FIG. 6.55. TRIO_U calculation of PLAJEST experiment at JAEA.

6.3.3.6. Cover gas thermal hydraulics

An inert cover gas is maintained between sodium free level and top shield. The top shield is filled with concrete for the purpose of shielding and the temperature of the concrete cannot exceed 120°C. Hence, the top shield is cooled. The primary sodium temperature in the hot pool is ~ 550°C during normal operating condition. As a result of these temperature conditions, natural convection of argon takes place, which transports sodium vapour from free level and deposits in the colder regions of the top shield. Solidification of sodium vapour in the colder regions causes difficulties in free movement of the components. The roof slab has many narrow enclosures opened at the bottom due to component penetrations.

The annular gap widths of the enclosures have to be minimum to resist natural convection so that the heat load to the roof slab cooling system is low. Narrow gap widths are also preferred to have compact layout. From the points of view of easier insertion/removal of components, a finite gap width has to be provided.

Typical gap width is of the order of 15-30 mm whereas the enclosure height is about 1.8 m. Because of the large aspect ratio of the enclosure (~ 100), the resulting natural convection is asymmetric (Fig. 6.56).

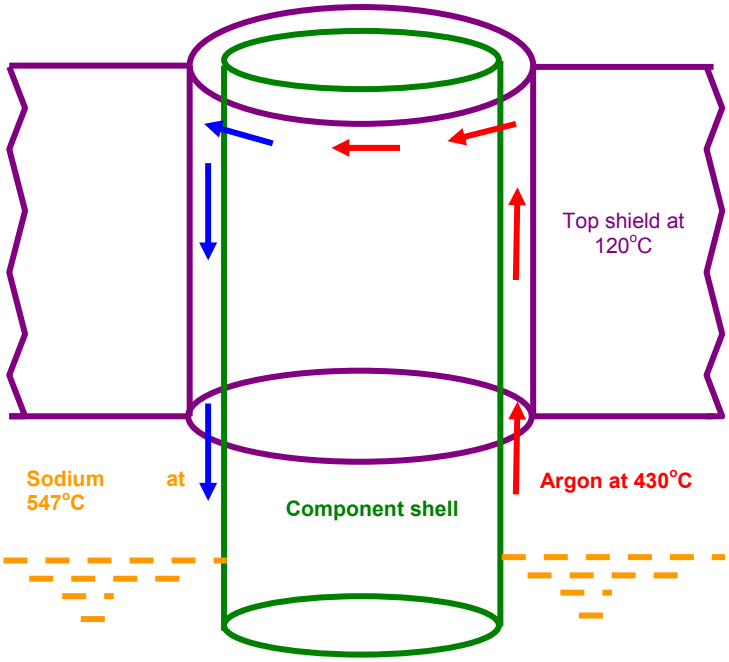

FIG. 6.56. Asymmetric convection of cover gas.

This leads to circumferential non-uniformity in the temperature of the enclosure walls which, leads to uneven vertical expansion and stress. Apart from natural convective heat exchange between the fluid and the walls, the walls interact via. surface radiation.

Also the walls are thick enough to conduct heat in the vertical and circumferential directions. Analysis of these phenomena is essential to estimate the temperature distribution in the walls and to estimate the cooling load and to decide upon the cooling arrangement.

Flow and temperature distributions of argon in rotating plug penetration, evaluated from a coupled convection-conduction-radiation simulation for PFBR, are shown in Fig. 6.57.

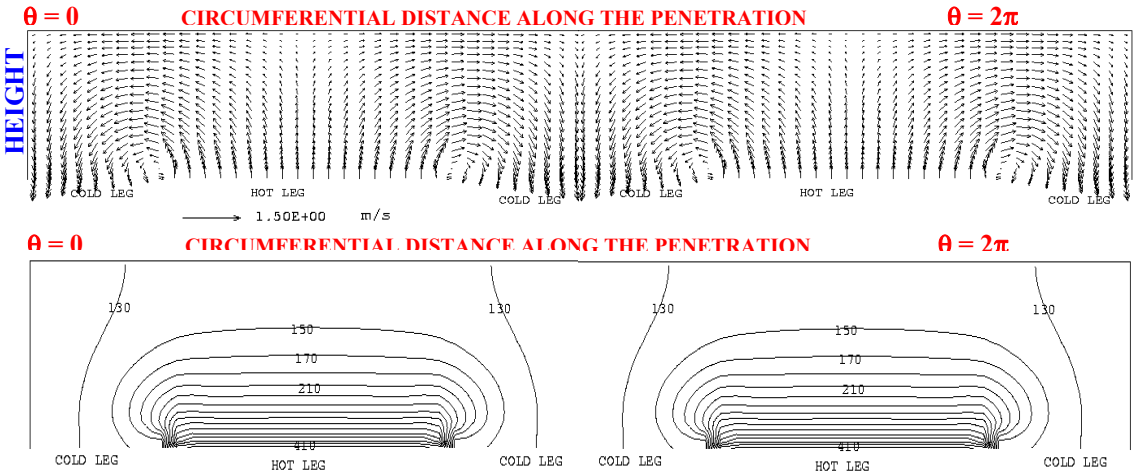

FIG. 6.57. Velocity (top) and temperature (bottom) distribution in component penetration.

The primary circuit of KALIMER-600 is closed at the top by a reactor head. This structure supports various components and the rotating plugs. The space between the free surface of sodium and the reactor head is filled with helium gas. Also, the insulation plates are installed in the space to reduce the heat transfer from the pool surface to the reactor head. Penetrations are provided in the reactor head for various components. Seals are provided to prevent the leakage from these penetrations. In order to maintain the integrity of sealing material and to prevent severe stress in the reactor head, the reactor head should be cooled during the reactor operation. Therefore, the heat transfer between free surface and reactor head must be known to design the cooling circuit and to determine thermal stresses. 3-dimentional the steady-state heat and flow analysis has been performed by CFD method in the cover gas region including solid structures.

The analysis domain is shown in Fig. 6.58 with the applied boundary conditions.

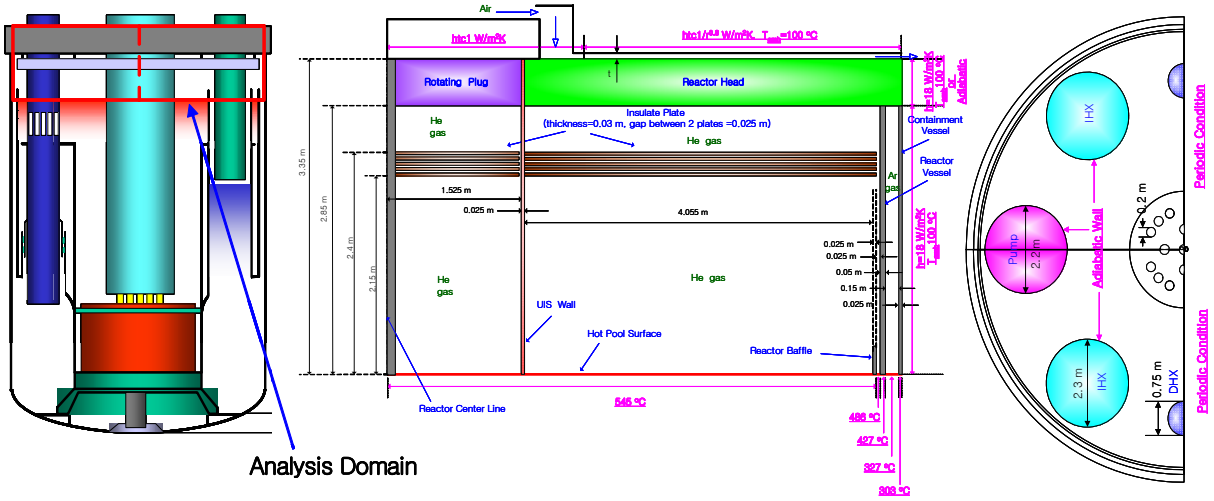

FIG. 6.58. Analysis domain and applied boundary conditions.

The effect of sodium aerosols present in the cover gas on the heat transfer was neglected in the analysis. Natural convection of helium along with conjugate heat transfer considering radiation was solved using CFX-10.0. Discrete Transfer Model was applied for the radiative heat transfer, and Shear Stress Transport Model was used for modelling turbulence. These models were selected based on the results from a benchmark test for the natural convection with radiation heat transfer in square enclosure.

Typical radial temperature distributions predicted are shown in Fig. 6.59.

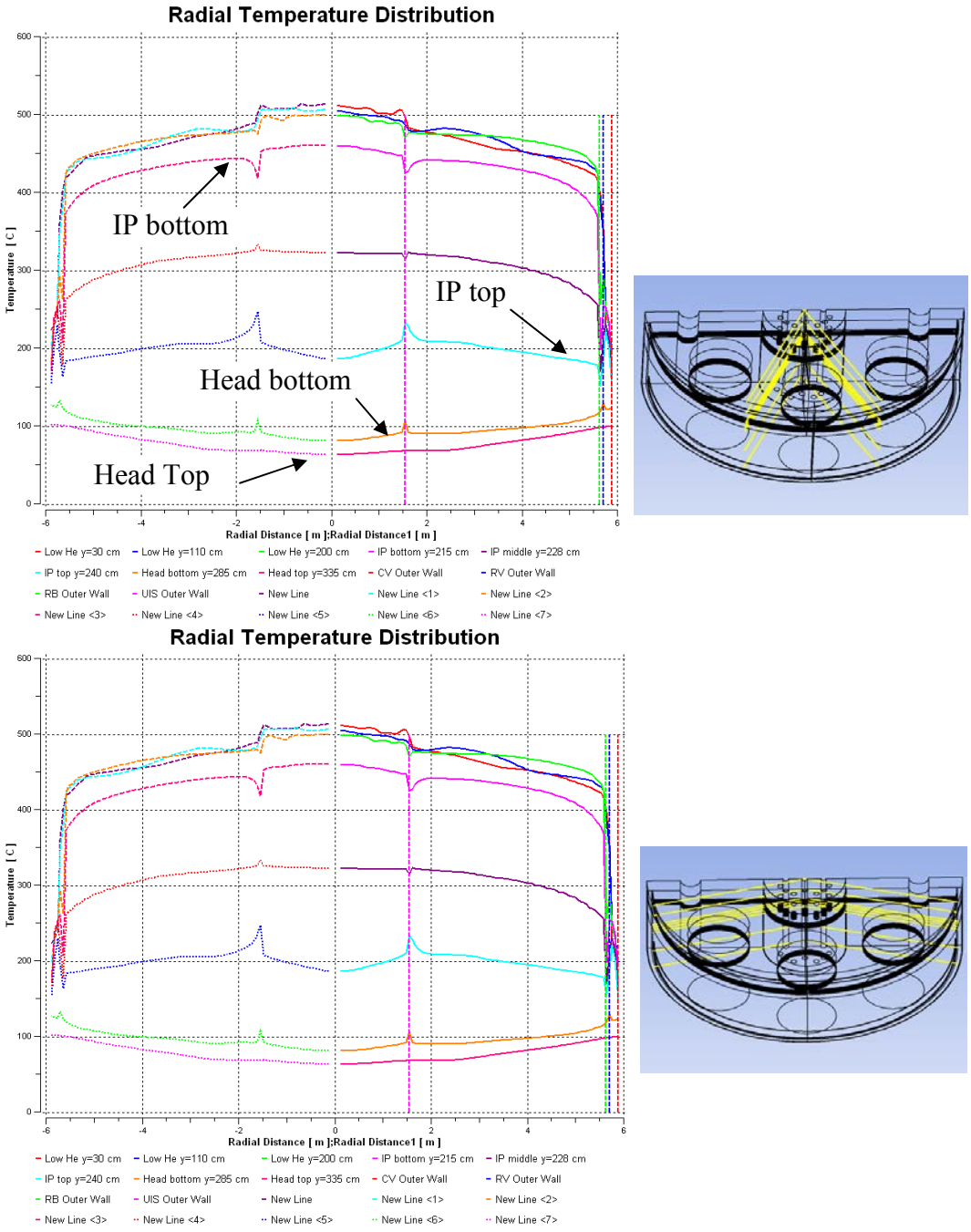

FIG. 6.59. Radial temperature distributions.

Temperature gradually decreases from the reactor centre line to reactor vessel wall, and then abruptly decreases outside the reactor vessel wall due to the cooling of containment vessel. On the other hand, the temperature drops axially across the insulation plates by about 200°C. Figure 6.60 shows axial velocity distribution in the space between the insulation plate and the reactor vessel. The helium gas with ascends from the lower part of the insulation plate to the upper part near the pump. Then the gas is cooled down in the upper part, and descends to the lower part near DHX. Thus high temperature region in the reactor head is formed around the reactor vessel near pump. The ratio of radiative to convective heat transfer was estimated to be 5.27–5.66 at free surface and 1.28-1.47 at the upper most surface of insulation plate. This

indicates that the radiative heat transfer is the main heat transfer mode from the free surface to the insulation plate, and the insulation plates sufficiently block the heat transfer to reactor head.

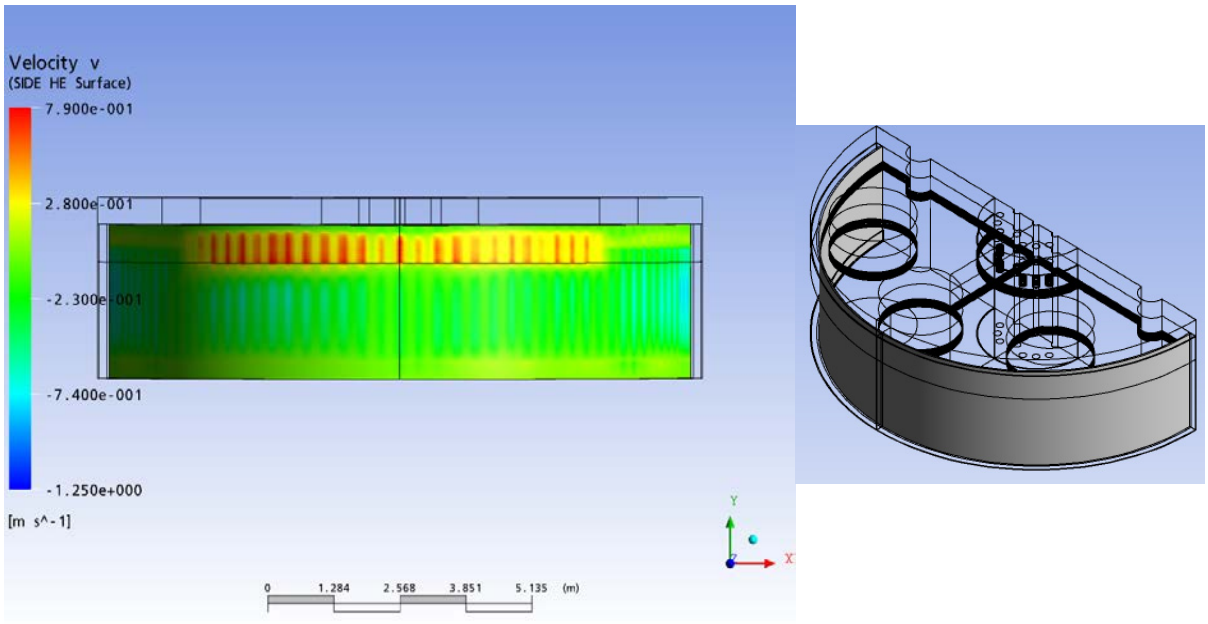

FIG. 6.60. Axial velocity distribution between the insulation plate and the reactor vessel.

6.3.3.7. Gas entrainment at the free surface

The free surfaces of sodium pools are not static and are associated with significant vertical and horizontal velocities. These velocities lead to free level fluctuations and formation of vortices, which are potential sources for gas entrainment in the sodium pools. Mechanisms of gas entrainment, transportation of gas to the grid plate through the IHX, agglomeration of gas inside the grid plate and its final passage through the core need to be understood well. This is an important safety problem as passage of argon gas through core leads to positive reactivity. The risk of gas entrainment is increased when the diameter of the vessel is reduced and the free surface velocity is higher. The research of increasing compactness requires detailed study of gas entrainment at the free surface. Special devices may be required to reduce gas entrainment and then efficiency of such devices must be confirmed.

In PFBR, core flow enters the hot pool as a horizontal jet in between the control plug skirt and subassembly top. It induces a large anti-clockwise circulation zone, which occupies almost the entire hot pool (Fig. 6.61a). The maximum horizontal velocity with which the jet enters the hot pool is ~ 3 m/s and as a result of this, the maximum horizontal velocity on the free surface is ~ 1.0 m/s. The reason for this high free surface velocity is the presence of skirt. By keeping the free surface velocity low, sodium free level can be made quiescent and possibility of gas entrainment can be avoided. To achieve this, the free surface velocity has to be less than 0.5 m/s. Reduction of free surface velocity is possible by altering the hot pool flow pattern such that the influence of core jet is minimized near the free surface. Detailed 3-D thermal hydraulic studies are carried out to see the efficacy of using baffles in reducing free level velocity. It is seen that by having a horizontal baffle of 0.5 m width attached to the upper shell of inner vessel and lowering the top shield inner shell up to IHX inlet, the free surface velocity could be reduced to 0.40 m/s (Fig. 6.61b).

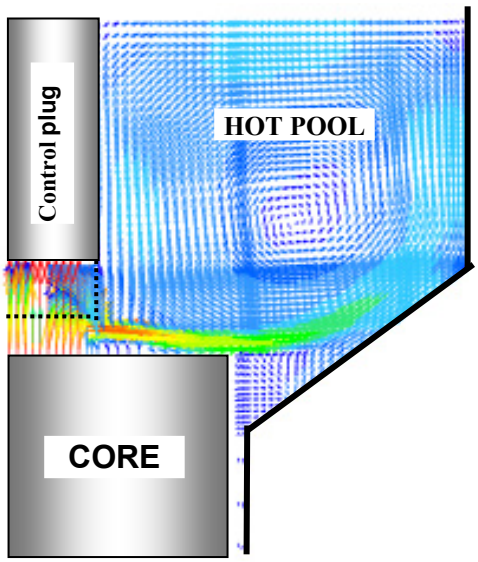

FIG. 6.61a. Velocity in hot pool (Free surface velocity = 1 m/s).

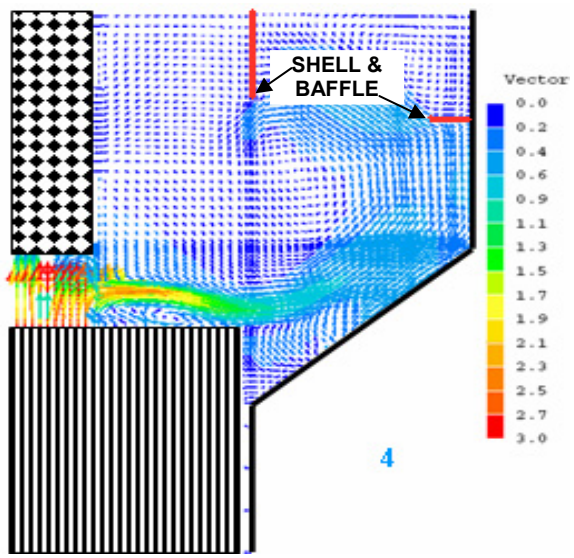

FIG. 6.61b. Velocity in hot pool (Free surface velocity = 0.4 m/s).

The Japanese Sodium-cooled Fast Reactor is designed to have the compact reactor vessel, which leads to the high coolant velocity in the vessel. In order to prevent gas entrainment from the liquid surface, there is a dipped plate near the free surface. The dipped plate is sufficiently effective to stabilize the coolant velocity near the free surface and prevent gas entrainment induced by the free surface disturbance or the waterfall. However, narrow gaps existing between the dipped plate and component structures in the upper plenum can promote strong downward flow depending on the gap position. Such kind of downward flow tends to induce gas entrainment from a dimple vortex at the liquid surface. Gas entrainment phenomenon from a surface vortex dimple strongly depends on the local flow conditions, such as velocity, local circulation, vorticity, turbulence intensity and surface waves. These flow conditions are difficult to predict without experiment. Therefore, the gas entrainment prevention in the design has been achieved by many scaled experiments [298].

One of the alternate procedures for flow optimization is the use of a CFD method. Sakai et al. [299] performed numerical analyses for existing gas entrainment data to investigate the prediction capability for the gas core depth of the surface vortex dimple. The gas core depth is able to be predicted by using the compensational vortex model with the CFD results. To evaluate the gas entrainment occurrence criterion, non-dimensional numbers by using local vortex parameters of CFD results were proposed [300]. In this method, the gas entrainment was classified based on the driving force to induce gas entrainment and the criterion was determined for each classified mode of gas entrainment. The vortex induced gas entrainment was classified into two types. One is a gas core extension directly to the outlet piping level, which results in large amount of gas entrainment. The other is continuous bubble detachments from the tip of the vortex dimple. Gas volume entrained by the bubble detachment is less than that by the gas core extension phenomenon. The bubble detachment, however, occurs continuously. Both phenomena have to be avoided.

6.3.3.7.1. Criterion for gas core extension type gas entrainment

The gas core extension type gas entrainment was evaluated by the gas core length. To predict the gas core length, the Burgers model was utilized as follows.

$$L_{gc} = \frac{\ln 2 \cdot \alpha \Gamma_{\infty}^2}{4 g \nu (2\pi)^2} \qquad (8)$$

where Γ (=$2\pi r u_\theta$) is the circulation and α is the vertical velocity gradient. Both of them are determined appropriately from CFD results. The onset condition of the gas core extension type gas entrainment can be evaluated by the ratio of L_{gc} and liquid level (height) from the outlet position (L_{gc}/h). Then, the non-dimensional equation is derived from the Eq.(8) as

$$\frac{L_{gc}}{h} = \frac{\ln 2}{16\pi^2}\left(\frac{\alpha \nu}{g h}\right)\left(\frac{\Gamma_{\infty}}{\nu}\right)^2 = K \cdot \alpha^* \cdot \Gamma^{*2} \qquad (9)$$

Here, K is 4.389×10^{-3}, α*is a non-dimensional velocity gradient which shows a ratio of viscous force and gravity force and Γ* is a non-dimensional circulation. Figure 6.62 shows the results of the gas core depth prediction by the CFD non-dimensional number in Eq. (9). The gas core depth ratios measured in experiments are plotted in the vertical axis. The Burgers model line in Fig. 6.62 means the theoretical prediction by Eq. (9). The error bar of the lateral values means the range of transient fluctuation in CFD results. The measured data are scattered in the three times range of the Burgers model prediction. Therefore, if we consider the three-times allowance to the theoretical model, the criterion can be determined as follows.

$$\alpha^*_{CFD} \cdot \Gamma^{*\,2}_{CFD} < 76 \qquad (10)$$

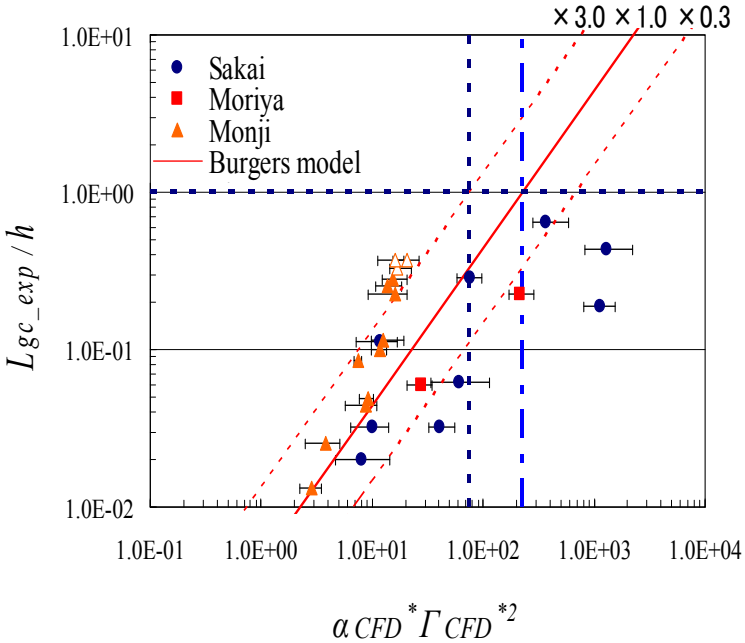

FIG. 6.62. Prediction of gas core length.

6.3.3.7.2. Criterion for bubble detachment type gas entrainment

The bubble detachment phenomenon from the tip of the gas core seems to be induced by the steep vertical velocity gradient near the liquid surface. Figure 6.63 shows the map for the bubble detachment phenomenon. The open plots mean the bubble detached case in

experiments. It was clearly divided in detached and non-detached regions by the non-dimensional velocity gradient. Therefore, we determine the second criterion for the gas entrainment prevention by the bubble detachment phenomenon empirically as follows.

$$\alpha^{*}_{CFD} < 10^{-7} \tag{11}$$

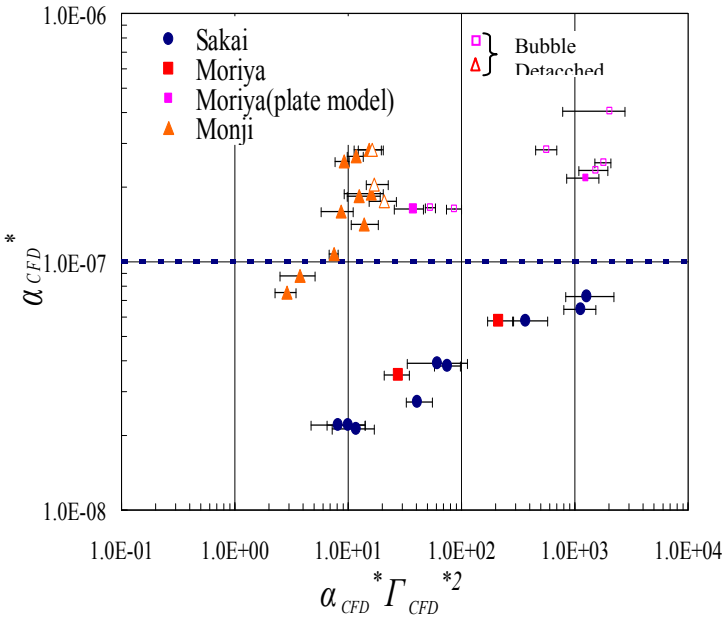

FIG. 6.63. Bubble detachment criterion.

Experimental studies have been carried out in the Repulic of Korea to establish critical conditions for the inception of gas entrainment at the free surface. There exist some previous experimental works to investigate the condition for inception of gas entrainment. Baum and Cook [301] performed a small scale experiment using four different working fluids including sodium in which the flow enters tangentially into the vessel and exits through a pipe at the center of the base of the vessel. They found that the critical condition (height) of the gas entrainment is nearly independent of the surface tension of fluid, but is proportional to the magnitude of inlet velocity. A correlation for the height of free surface for the onset of the gas entrainment has been developed in terms of Froude and Webber numbers.

Takahashi et al. [302] explained the gas entrainment by the following three mechanisms:

(1) Vortex-induced entrainment;
(2) Conically depressed surface with an entrainment of relatively large bubbles; and
(3) Falling flow along the suction pipe with an entrainment of the fine bubbles.

The characteristics of the above three mechanisms are investigated experimentally and an analytical model for the air entrainment rate of the vortex-induced entrainment was proposed. The proposed model agrees well with the experimental data in the presence of forced circulation. Takahashi et al. [303] investigated the onset of the vortex induced air entrainment for the suction flow into a vertical drawing pipe in a cylindrical test vessel. They found that the onset conditions can be represented by the two types of empirical criteria and showed that their empirical criteria represented all the experimental data well.

Madarame and Chiba [304] showed that the gas entrainment inception is determined by the flow patterns, such as the vortex formation, breaking of the surface wave, waterfall formation, and by the product of the Froude and Weber numbers based on the local velocity at the bubble formation point.

Govindaraj et al. [305] performed a small scale experiment and observed that the gas entrainment phenomena varied depending on the inlet and outlet nozzle positions of the surge tank. They also showed that the minimum liquid level required to avoid the gas entrainment was correlated by the Froude number.

Eguchi et al. [306] studied the effects of the scale and flow properties on the gas entrainment phenomena. Three models with different scales but of a similar geometry were used to examine the effects of the scale and viscosity. They showed that the critical Froude number, above which a gas entrainment appears, drastically decreases as the scale increases and proposed a prediction method that takes into account the Froude and Reynolds number effects.

Eguchi et al. [307] performed a similar study for the effects of the scale and flow properties on the onset of a gas entrainment for the free surface flow in an IHX vessel of the Japanese demonstration FBR. They showed that the critical Froude number decreases in proportion to the -0.5th power of the scale.

Currently in the Republic of Korea, an experimental study is performed to understand further the effects of the size of a tank, the inlet nozzle diameter, the level between the free surface and inlet nozzle and the flow rate on the onset of a gas entrainment in a water facility. The experimental data shown in Fig. 6.64 are obtained for the analysis of the critical conditions for gas entrainment by breaking of the surface wave, and an experimental correlation that describes the critical condition for the gas entrainment is proposed.

The effect of the various kinds of dimensionless variables on the formation of the bubbles is analyzed, and one equation that can describe the formation of the gas entrainment is found and is given below;

$$(W_e^*)^{-1/8}\ (\frac{D}{H}) \le\ 0.6209\ + 0.113\ \ln\left(F_r^*\ \frac{D}{H}\right) \qquad (12)$$

where

$$W_e^* = \frac{\rho g D}{\sigma / D}\ ,\ F_r^* = \frac{d_n}{H}\frac{V}{\sqrt{gH}}$$

and D is the diameter of the test section, d_n is the diameter of the inlet nozzle H is the average water level, V is the average velocity at the nozzle. For the fluid properties, ρ is the density of the water and σ is the surface tension coefficient. An experimental study has been carried out to find the critical conditions for air entrainment by a breaking of a surface wave at the free surface. Following conclusions are made from the study.

- An experimental correlation that describes air entrainment condition is developed in terms of modified Froude and Weber numbers.

- Two kinds of air entrainment are observed. The first one is the air entrainment due to the destruction of surface wave from the centre, and the other one is due to the crashing of water wave on the vessel wall. These two cases occur irregularly and the entrained air bubble distributes uniformly in water.
- In the smallest test section (ID=380 mm), bubbles appeared at the highest Reynolds number, and the critical Reynolds number decreased with decrease of the diameter of test section. The smallest critical Reynolds number is observed when the diameter of the test section is 680 mm except that the critical level is 0.89 m. The critical Reynolds number slowly increased with an increase of the diameter of the test section.

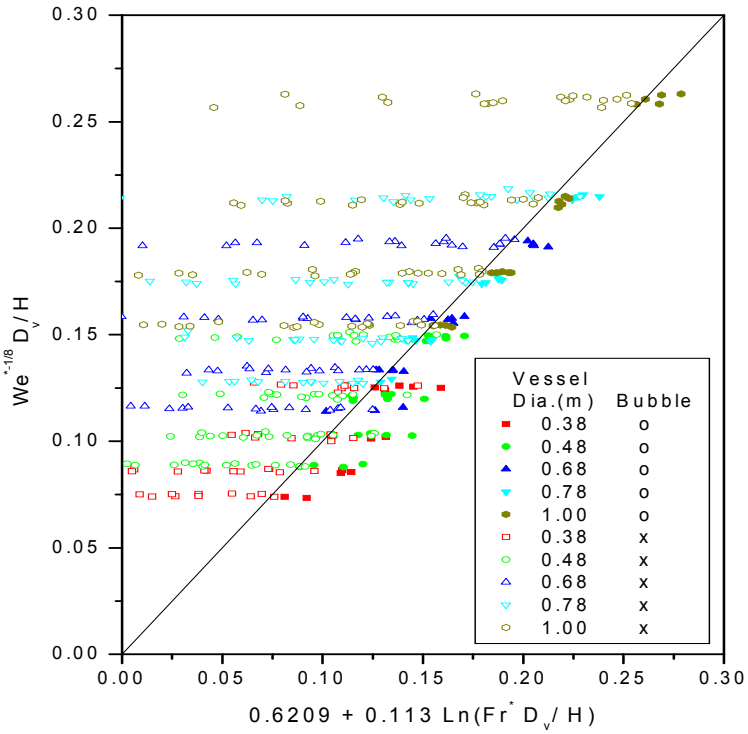

FIG. 6.64. The critical gas entrainment condition by the surface wave at the free surface.

In France, CEA is using TRIO_U code to predict the free surface deformation, the occurrence of vortex and the possible gas entrainment. The Front Tracking method implemented in TRIO_U code is well adapted to predict these phenomena. Of course, experimental data are needed for verification of such calculations. In the past, water tests on reduced scale models were performed at CEA for the EFR project. These tests were used to design special devices to reduce the risk of gas entrainment. At that time, CFD computation of gas entrainment was not possible. Now, experimental data are available for the verification of the calculations.

Figure 6.65 shows an experimental vortex in a JAEA experiment and TRIO_U calculation of a single stable vortex. This figure also shows free surface deformation and vortex occurrence for two converging flows.

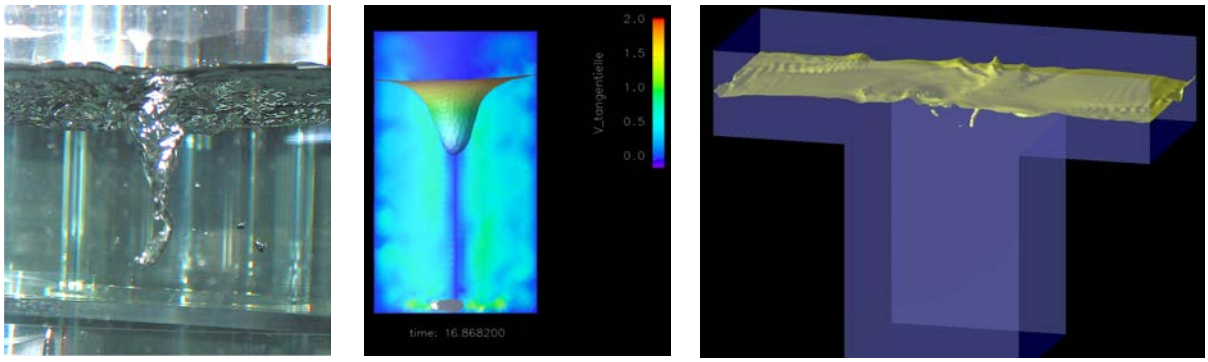

Vortex in a JAEA experiment

Single stable vortex predicted by TRIO_U

TRIO_U prediction of vortex occurrence for converging flows

FIG. 6.65. Vortex visualization (JAEA) and TRIO_U calculations of vortex at free surface.

Seismic qualification of (heavy) liquid metal cooled reactors is an issue because of the high density and possible sloshing effects of the coolant. Within the framework of the European ELSY project, complementary to finite element analyses (FEA), a CFD modelling approach was developed by NRG in the Netherlands to assess sloshing effects in the ELSY reactor vessel.

The approach is based on a standard Volume of Fluid (VOF) CFD approach combined with coupled solid body motion of the reactor vessel. The approach has been validated [307a] against the analytical solution for sloshing in a two dimensional tank. This showed the feasibility of this approach for the current purposes. In order to validate the numerical model for the determination of the sloshing forces, a three dimensional dam break experiment performed at the Maritime Research Institute Netherlands (MARIN) was simulated. Numerical simulations showed a good agreement with the force evolutions found in the experiments. Figure 6.65a shows The ELSY vessel design and the geometrical representation in the simulations.

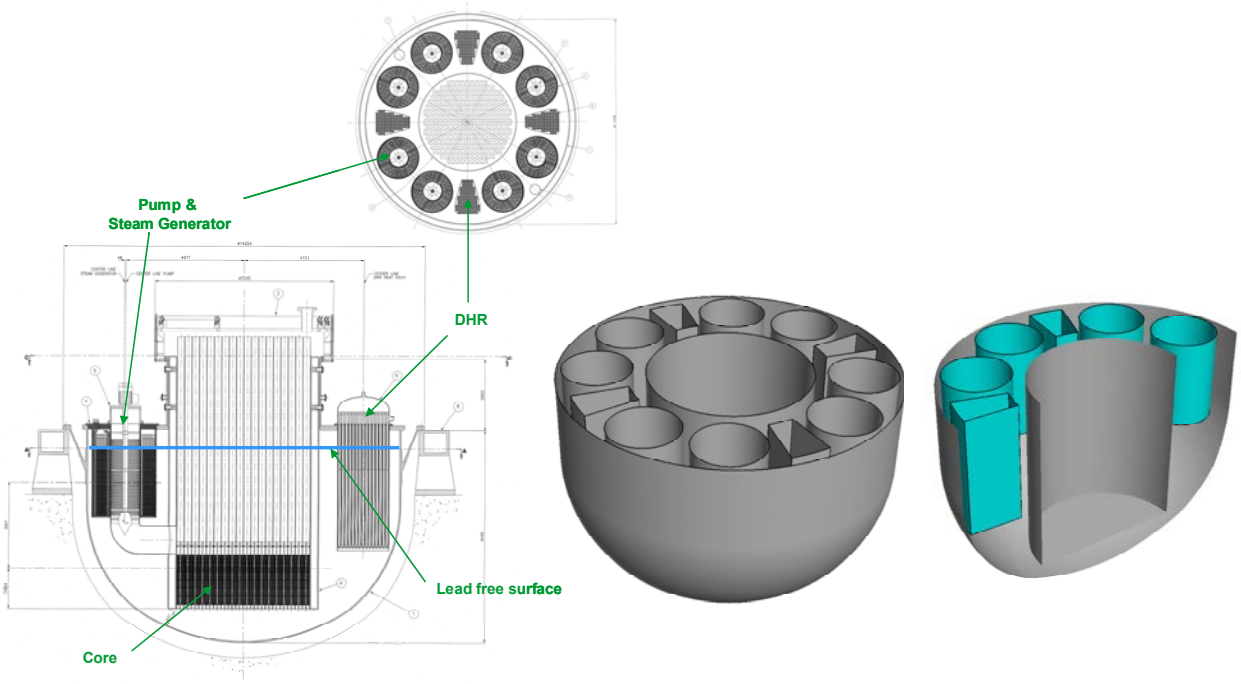

FIG. 6.65a. The ELSY vessel design and the geometrical representation in the simulations.

Seismic induced lead sloshing in the ELSY reactor vessel was then analysed providing sloshing induced loads to structural engineers. Figure 6.65a shows the ELSY vessel design. This figure also shows the computational model, which includes 8 pump/steam generator units and 4 decay heat removal systems. Figure 6.65b shows two snapshots of the simulated seismic induced lead sloshing in the ELSY vessel.

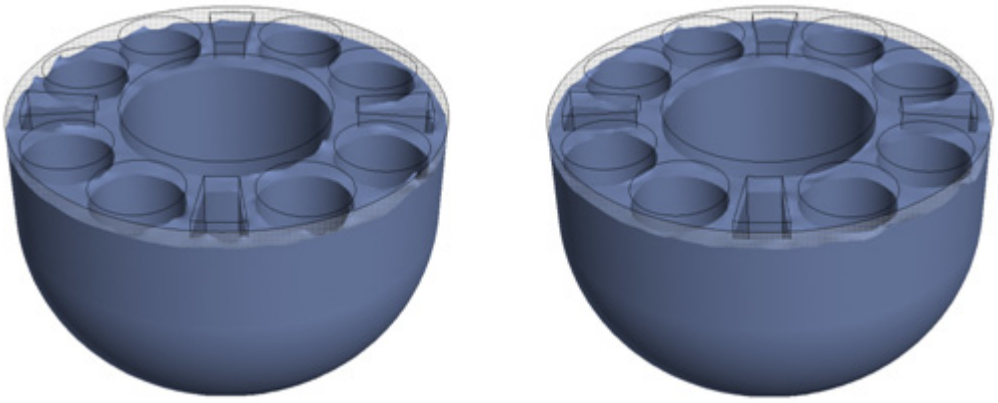

FIG. 6.65b. Snapshots of seismic induced lead sloshing in the ELSY vessel.

6.3.4. Coolant channel blockage

Evaluation of the coolant thermal-hydraulic behaviour in a fuel assembly with local deterioration of the cooling capability is necessary for the safety assessment of liquid metal fast reactors. The local deterioration of cooling might lead to cladding failure or fuel melting due to the tight package of fuel pins and the high power density in the assembly. The possible initiators of the local cooling disturbance can be categorized into three groups:

(1) Local blockages formed at an inlet, outlet or in the assembly or flow distribution error (insufficient flow type);
(2) Local over-rated power caused by some positive reactivity insertion, e.g. implementation of fuel pellets with excessive enrichment (power-density increase type); and
(3) Random pin failure

The local blockage event is often represented as the initiator of the local fault not only from the viewpoint of occurrence probability and its effect on fuel defect, but also from the fact that the event also appears in each sequence of the other two events. If a local fault reaches a critical size at a given coolant flow rate, it may cause local sodium boiling, dry-out and melting of fuel pin and cladding. The consequences could be either a non-energetic dispersion of the fault or accumulation of larger amount of molten material with the possibility of a fast coolant vaporisation, pressure generation and fast damage propagation to the whole fuel subassembly. The effect of the local faults on the reactor safety depends on several factors: size and thermo-physical properties of blockages, its location in the subassembly, fuel pin power and coolant velocity in the subassembly.

In PFBR, Total Instantaneous Blockage (TIB) is classified as a BDBE. Local blockages may be initiated due to the fuel loading error, failure of spacers, pin thermal deformation, pin swelling, bundle deformation, foreign materials left during construction, loose parts from structures, chemical products during operation and fragments from failed fuel. Protection

against subassembly plugging is provided at two levels, in design and safety action. The scenario with respect to protection against subassembly plugging is illustrated in Fig. 6.66.

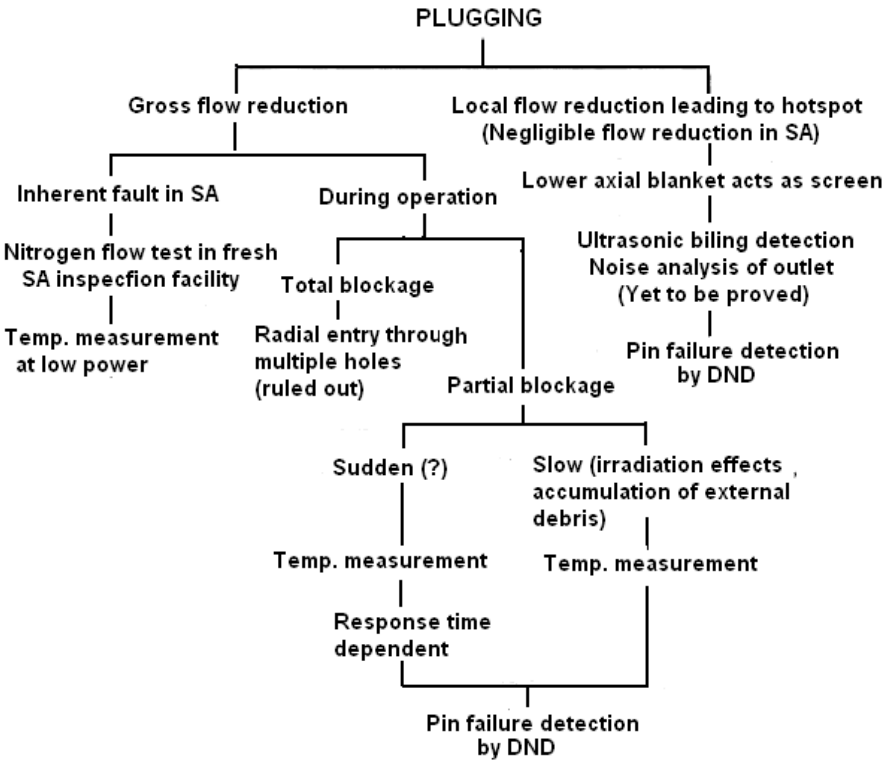

FIG. 6.66. Scenario with respect to protection against SA plugging.

6.3.4.1. Analysis methods

In the assessment of the local blockage event, it is important to investigate the blockage formation, influence of the formed blockage on temperature field, probability of fault propagation, and means of fault detection. With regard to the consequence of the formed blockage, various experimental studies were conducted in the past to clarify thermal-hydraulic behavior in a partially blocked subassembly assuming impermeable and planar blockage. On the other hand, some experiments were performed in France, Germany and Japan to find out the mode of the blockage buildup. They revealed that the most possible blockage formation in a wire-wrapped pin bundle would be a relatively thick porous one consisting of trapped particles whose diameter range is roughly between the wire-spacer diameter and the maximum gap width in the flow area [308]. In comparison with the impermeable and planar form, porous blockages have many parameters which should be considered in the assessment of the porous blockage event. Therefore, computational approach is useful for quantitative evaluation of the influence of porous blockages on thermal hydraulics in a fuel assembly.

For PFBR, the length of bottom plenum together with the bottom axial blanket is about 1 m. Hence, most of the debris is expected to be deposited in this length. Since, there is no heat generation, the blockage formation in this portion will have little effect. The following steps are adopted for the analysis of local blockage in PFBR.

- Determine the temperature profile behind the blockages as a function of flow, power, leakage flow through the blockage and inlet temperature;
- Establish the margin between the onset of boiling and onset of dry-out behind the blockages and characterize the types of boiling events;
- Collect the data for validating codes;
- Pin point the limitation of the detection of blockages in relation to the measuring devices,
- Demonstrate whether the blocked subassembly can be cooled during power operation and by natural convection.

In the design of an LMR, the consequence of formation in a fuel assembly is deliberately analyzed with a subchannel analysis code. Since the blockage disturbs the normal flow field it is important to simulate the flow and temperature field correctly in the analysis. When a blockage in the flow path occurs, the axial flow rate decreases drastically up to a certain distance downstream from the blockage and a re-circulating wake is formed. This re-circulating wake is characterized by a reverse flow and a large lateral cross flow. This is accompanied by an increase of the local temperatures of the coolant and the fuel rod surface. Therefore, the analysis code for the flow blockage requires a proper numerical scheme and thermal-hydraulic model to deal with the re-circulating flow.

6.3.4.2. Computer codes and experimental verification

A porous blockage model was developed and implemented into a subchannel analysis code ASFRE which is an in-house code of JAEA [314]. The concept of the porous blockage model is shown in Fig. 6.67.

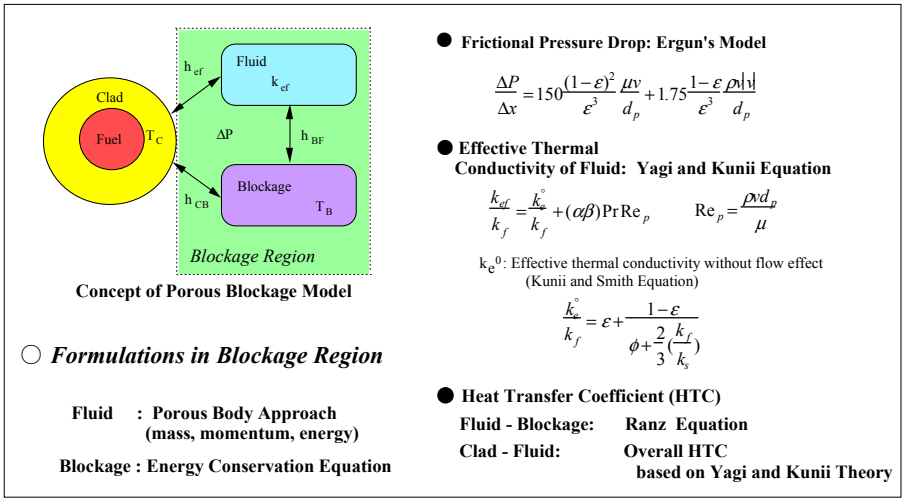

FIG. 6.67. Concept of porous blockage model.

Porous blockage region is modeled by porous body approach and energy equations of all the subchannel components, i.e. coolant, fuel pin, duct and blockage material, are solved interactively. Frictional pressure drop in the blockage region is calculated with the correlation based on the Ergun's model and the overall heat transfer coefficient derived by Yagi and Kunii is employed for evaluating heat exchange between the fuel pin and coolant in the blockage region. With regard to the heat transfer coefficient between the blockage and coolant, the Ranz equation is applied. The effective thermal conductivity based on the Yagi and Kunii equation is adopted to the thermal conduction of particles with flowing fluid in the blockage region. ASFRE with the porous blockage model was applied to calculate

temperature distribution in a fuel assembly with existence of central porous blockage for code validation. The Scarlet-2 experiment, which was performed by Electricité de France (EDF) was utilized. Figure 6.68 shows the horizontal cross section of the Scarlet-2 test section. The assembly was composed of 19 heater pins that simulated fuel pins of French FBR, Superphénix. The porous blockage made by sintered titanium particles was fixed on the six central subchannels between 587 mm and 647 mm downstream from the beginning of the heated region. Figure 6.69 shows the comparison between the calculated and experimental results of the axial temperature profile of sodium through the blockage region.

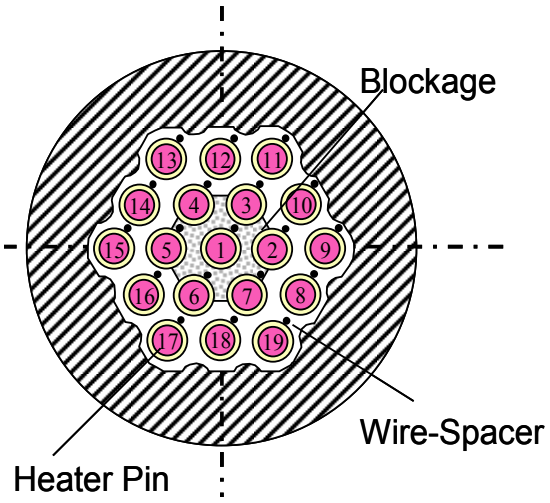

FIG. 6.68. Cross section of Scarlet-2 test section.

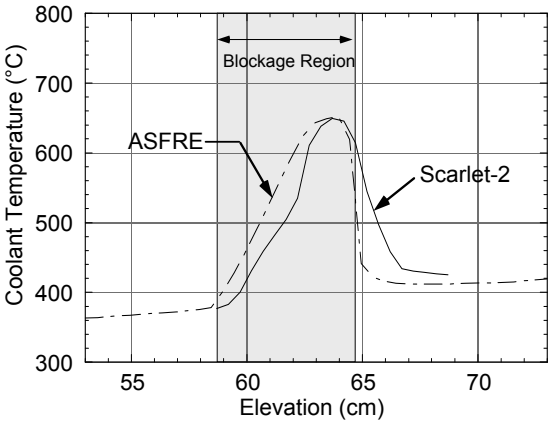

FIG. 6.69. Comparison of axial coolant temperature distributions.

As for the experimental data, the peak temperature position is shifted from the centre of the blockage region to the downstream side due to the effect of the flow passing through the permeable blockage. Although ASFRE underestimates the shift of the temperature peak position, the predicted peak temperature agrees with the measured one.

In PFBR, 211 positions in the core are continuously monitored for temperatures by thermocouples hanging from the bottom of control plug. Any change from the expected reading would indicate the change from the nominal scenario. Also, delayed neutron detectors are provided to detect the delayed neutrons emanating from the breached clad. These safety provisions help in the detection and prompt safety action. Engineering analyses have also been carried out to find out the permissible flow reduction during local blockage events to limit the consequences within the design safety limits of various category of events. Experimental programs have been undertaken to establish the mechanism of blockage formation. The main objectives of these studies are:

- General characterization of the flow blockages in subassembly with helical spacer wire as a function of location, and properties of material of blockage;
- To study the size distribution of particles that induce blockage;
- To study the effect of the ratio of wire-wrap pitch to the wire diameter on the blockages;
- To study propagation/progression of blockages as a function of time; and
- To define Maximum Credible Damage for PFBR subassembly.

It is also necessary to ensure that the total blockage in a fresh subassembly, which is loaded in the refuelling campaign preceding start up, does not lead to melt down below the detection threshold. This requires data on the heat transfer from the blocked subassembly to its

neighbouring subassembly. Hence, an experimental programme with a totally blocked subassembly has been undertaken with the following objectives:

- Assessment of steady state heat transfer from a blocked subassembly to the neighbouring subassembly taking into account natural convection inside the blocked subassembly;
- Establishment of the reactor power level beyond which the subassembly temperature monitoring is necessary;
- Evolution of transient temperature in the blocked subassembly in all details and the transient temperature distribution in the adjacent subassembly;
- Validation of computer codes

Special engineering care has been taken in the design of subassemblies of PFBR to minimize the probability of total blockage. In the foot of the subassembly, holes in the coolant entry sleeves are provided in the radial direction at two elevations to avoid total blockage. Similarly, at the top of the subassembly in the handling head, a blockage adaptor is provided. This prevents blockage due to any falling object from the top. The provision of blockage adaptor ensures about 53% flow even when the top is blocked. The arrangements are shown in Fig. 6.70.

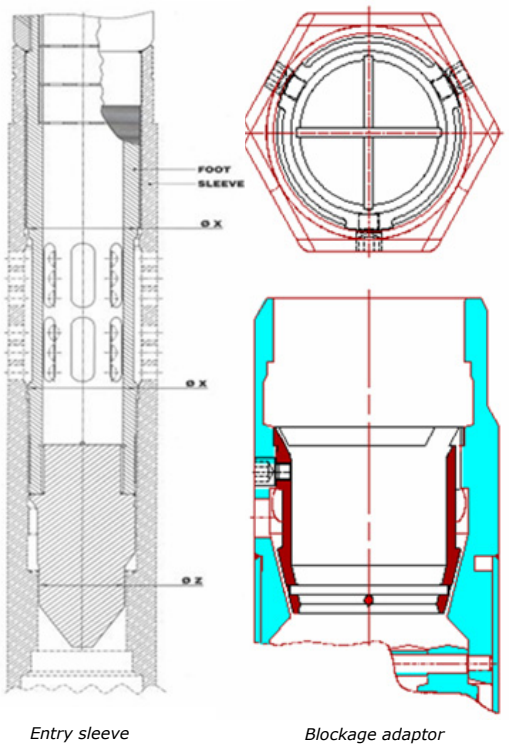

FIG. 6.70. Engineering features in SA to avoid blockage.

For the analysis of blockage accident, the Korea Atomic Energy Research Institute (KAERI) has developed the MATRA-LMR-FB code [309]. The MATRA-LMR-FB code uses the distributed resistance model (DRM) [310] to describe the sweeping flow formed by the wire-wrap around the fuel rods and to model the re-circulation flow after a blockage. The hybrid difference scheme is also adopted for the description of the convective terms in the re-circulating wake region of a low velocity. Some state-of-the-art turbulent mixing models

are implemented in the code as an effort to describe correctly the mixing phenomena after a blockage. For the modelling of a porous type blockage, a suitable pressure drop model is implemented.

The effects of each model in MATRA-LMR-FB code have been evaluated and the capability of the code has been estimated for ORNL THORS [311] experiments. The effects of the distributed resistance model and the hybrid difference scheme are depicted in Fig. 6.71.

The experimental data of ORNL THORS shows clearly that the outlet temperature downstream from the blockage increases when there exists a blockage in the flow path.

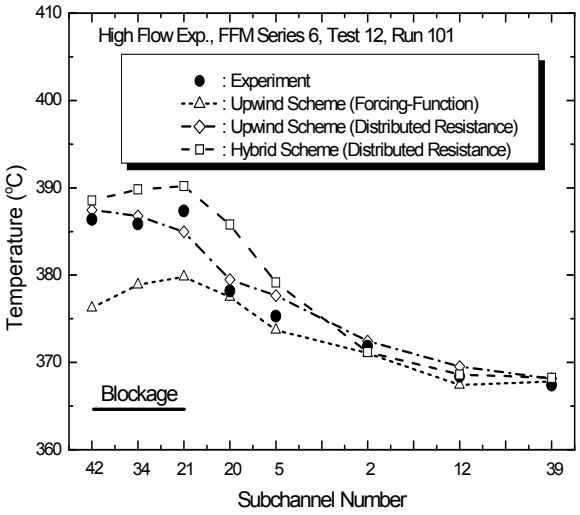

FIG. 6.71. Comparison of the distributed resistance model and hybrid scheme against

As can be seen in Fig. 6.72, the general trend of the outlet temperature profile is predicted reasonably with the wire forcing function but the magnitude of the peak temperatures are underestimated due to the lateral flow rates being not estimated correctly. With the distributed resistance model combined with the hybrid difference scheme, it is clearly shown in the figure that the degree of temperature increase due to the blockage agrees well with the data within 5°C. This improvement is mainly due to the treatment of energy equation with hybrid difference scheme. The overall temperature difference between the blocked region and the unblocked region, which amounts to about 20°C, is calculated well with these models even though the temperatures estimate at the blockage boundary region are slightly over-predicted.

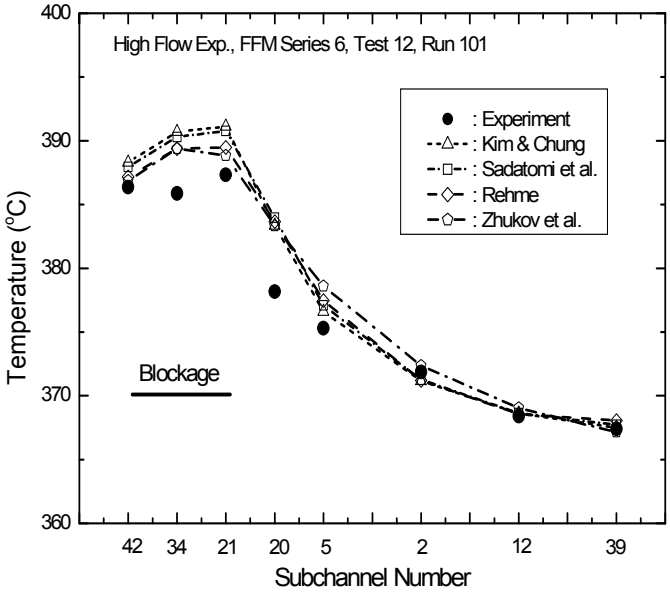

FIG. 6.72. Comparison of the turbulent mixing models against ORNL Test.

It is usual in a subchannel approach to perform the analysis with a constant value of the turbulent mixing coefficient. However, the application of a constant mixing coefficient does not reflect the changes of the local mixing depending on the flow regime. Therefore, the state-of-the-art turbulent mixing models are implemented in the MATRA-LMR-FB code and their influences on the analysis of a flow blockage are evaluated. The predicted outlet temperatures with different turbulent mixing models are compared for THORS test 12, run 101. The Re number at the centre subchannels are about 58 000 in this case. The models of Rehme [312] and Zhukov et al. [313] predict the data more accurately than the other models. The models by Kim and Chung [314] and by Sadatomi et al. [315] underestimate the mixing downstream from the blockage, thus, result in higher outlet temperatures. Kim and Chung's model includes some experimental coefficients whose appropriateness should be investigated further. On the other hand, Sadatomi et al.'s model is analyzed to underestimate the turbulent mixing due to the flow pulsation for the triangular arrayed bundle. By the phenomenological turbulent mixing models in the flow blockage analysis, the enhancement in the predictions is seen clearly at the edge of the blockage and also at the boundary of the blocked and the unblocked subchannels.

Using the already described LRHR CFD approach, NRG has analysed blockage effects in the ELSY open square and closed hexagonal fuel assembly design options. These analyses have shown that a partial blockage of a closed hexagonal fuel assembly design at the inlet of up to 16% cross section, leads to an average temperature increase at the assembly outlet of only ~2°C. Thus, detection of blockages at the outlet header of each single fuel assembly will strongly depend on the mixing in the outlet header. The maximum cladding temperature observed is ~673°C, so failure of fuel cladding will not occur.

Consequences of a large area inlet blockage of an open square fuel assembly structure were also analyzed with the LRGR CFD approach. Figure 6.72a shows the selected computational domain which includes an area of four fuel assemblies. This figure also reveals the employed grid for the analyses.

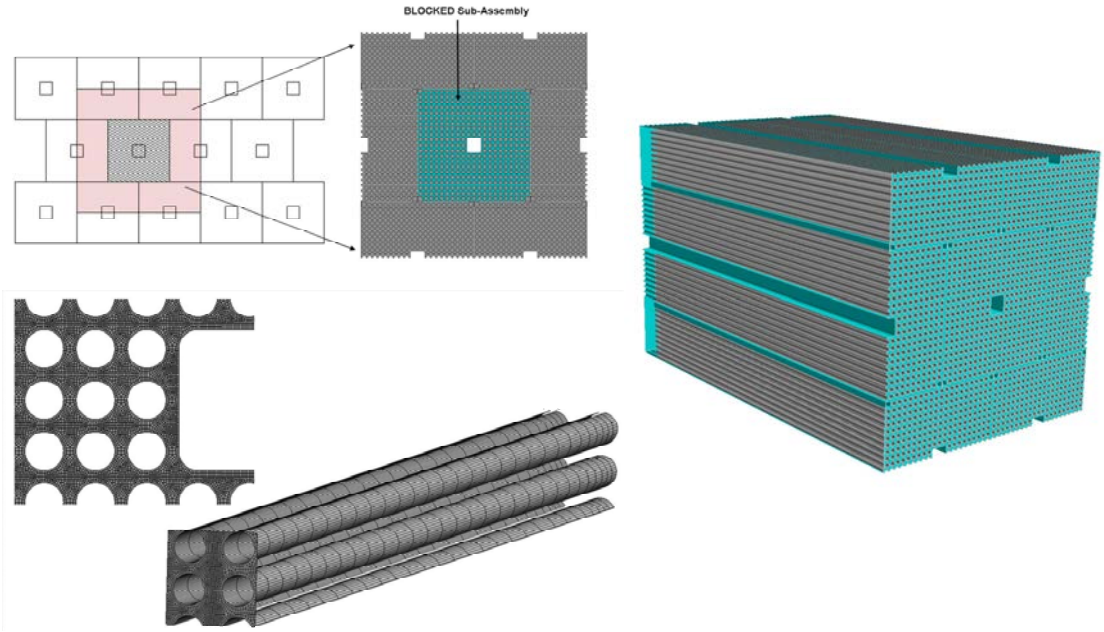

FIG. 6.72a. Computational domain and grid of the square open ELSY fuel assembly employing the LRGR CFD approach.

In Ref. [260f] has been shown that under the assumed conditions failure of fuel cladding will occur. If there is a possibility to measure temperatures at the outlet of individual subassemblies with high precision, then an early detection of a total inlet blockage for the open square fuel assembly design might be possible. However, most probably fuel pin failure has already occurred when coolant outlet temperatures increase by a detectable amount. A time dependent simulation of consequences of an inlet blockage increasing with time would become necessary to evaluate detection capabilities of massive inlet blockages by a single average coolant outlet temperature measurement at each subassembly without entering into massive fuel pin failures.

6.4. Fuel

Fuels considered for use in fast reactors include oxide, metal, carbide and nitride concepts, which incorporate depleted, natural and recycled uranium as well as (multiply) recycled plutonium. Detailed information on the description and irradiation performance of fast reactor fuels has been provided in former fast reactor status reports [316, 317]. The status and trends of oxide, metal, carbide and nitride fuels technology for sodium-cooled fast reactors (SFRs) have recently been documented in a report by the IAEA's Technical Working Group on Nuclear Fuel Cycle Option and Spent Fuel Management (TWG-NFCO). It represents the first in a series of technical reports that cover the status and trends of (i) nuclear fuels technology for SFRs, (ii) the back end of the fast reactor fuel cycle, and (iii) structural materials for fast reactor fuel assemblies. Further information on the manufacturing processes, out-of-pile properties and irradiation behaviour of mixed uranium plutonium oxide, metallic U-Zr and U-Pu-Zr, monocarbide and mononitride fuels, including minor actinide bearing variants of these fuels, is available there.

The idea to use fast reactors that enhance utilization of transuranics created the need to develop fuel containing minor actinides. In order to qualify such fuels, a large number of

experiments have been performed, especially in Phénix, but also elsewhere. Many of these experiments are awaiting post-irradiation examination. In the following, the most important experiments are listed or described.

6.4.1. European irradiation experiments

The following is a list of some of the most important European irradiations experiments, relevant to the development of minor actinide bearing fast reactor fuel [318, 319].

6.4.1.1. SUPERFACT

The SUPERFACT 1 experiment was launched as a collaborative effort by the Institute for Transuranium Elements (ITU) and the Commissariat à l'Énergie Atomique (CEA) to demonstrate the feasibility of the transmutation of ^{241}Am and ^{237}Np. The fuel design and production was performed by the ITU while the design basis studies, assembly of the irradiation device and irradiation in the Phénix reactor were carried out by the CEA (1986-1988); both partners participated in the post-irradiation examinations and analyses (1989-1992). The experiment served as a first successful demonstration of the technical feasibility of the homogeneous transmutation of minor actinides in a fast reactor, and moreover showed that, with the optimization of the pin dimensions, a reactor fuelled with minor actinide bearing fuel with up to 2.5% minor actinides by mass would perform as well as one fuelled with fuel without minor actinides.

6.4.1.2. TRABANT 1

The TRABANT 1 experiment to test the incineration of ^{237}Np in the presence of Pu was performed as part of the CAPRA programme and involved collaboration among the CEA, the ITU and the Forschungszentrum Karlsruhe (FZK). The TRABANT 1 fuel (mixed oxide containing 40% Pu and 5% Np by mass) was irradiated from June 1996 to May 1997 in the High Flux Reactor (HFR) to a burnup of 9.3 at%. The experiment has shown that fuel containing Np behaves as adequately as standard fast reactor fuel, as well as it has confirmed the conclusions reached by the SUPERFACT 1 experiment with regard to the Np content and achievable burnup which can be achieved for homogeneous transmutation in a fast reactor.

6.4.1.3. METAPHIX

The METAPHIX irradiation experiment was performed in fulfilment of a contract between the ITU and the Central Research Institute of Electric Power Industry (CRIEPI) of Japan. It involved the production at the ITU and irradiation in Phénix of UPuZr metal fuel and variants thereof containing small quantities of minor actinides (MA) and lanthanides (rare earths, RE):

- Areference U-Pu-Zr alloy;
- An alloy containing, by mass, 5% MA (3% Np, 1.6% Am and 0.4% Cm), with the composition 66U-19Pu-10Zr-5MA;
- An alloy containing, by mass, 2% MA (1.2% Np, 0.6% Am and 0.2% Cm) and 2% RE, with the composition 67U-19Pu-10Zr-2MA-2RE;
- An alloy containing, by mass, 5% MA (3% Np, 1.6% Am and 0.4% Cm) and 5% RE, with the composition 61U-19Pu-10Zr-5MA-5RE.

Each fuel was tested after it reached burnups of approximately 2.4at% (METAPHIX 1), 7at% (METAPHIX 2) and the maximum target burnup of 11at% (METAPHIX 3). The

transmutation rates expected with METAPHIX 3 are 40% for Np and 50% for Am. The experiment was approved by the safety authority in 2003 and was completed in May 2008.

6.4.1.4. ECRIX B and ECRIX H

The ECRIX experiments (Experiments on targets under slowed neutrons for incineration in Phénix), which commenced in 1998 and have since been completed, had as a goal to test the feasibility of the incineration of americium in heterogeneous mode in the context of monorecycling in a fast reactor. They consisted of the ECRIX B and ECRIX H irradiations which involved identical targets (microdispersed americium oxide in a magnesium oxide matrix; the americium content was 0.7 g/cm^3) but differed by the assemblies in which each was irradiated: ECRIX B in a DMC1 assembly ($^{11}B_4C$ moderator), and ECRIX H in a DMC2 assembly (CaH_x moderator). The targeted transmutation rates were 80% for ECRIX B and 90% for ECRIX H.

6.4.1.5. CAMIX-COCHIX

The CAMIX-COCHIX experiments were proposed in 2001 to optimize the compounds and americium target concepts investigated in the ECRIX experiments. CAMIX 1 (Compounds of americium in Phénix) pertained to the optimization of the actinide compound and used a solid solution of the cubic structure $(Am_{0.06},Zr_{0.78},Y_{0.16})O_{2-x}$ as the compound. CAMIX 2 used the same concept of microdispersion in a magnesium oxide matrix as was tested in ECRIX, instead with the compound $(Am_{0.2},Zr_{0.66},Y_{0.14})O_{2-x}$. The fissile particles ranged in size between 40 and 60 mm, corresponding to an anticipated damaged matrix volume fraction of 60-100%. COCHIX (Optimized design in relation to microstructures in Phénix) sought to test the macrodispersion concept under representative conditions and used the same type of actinide compound and matrix as in CAMIX 2 but the fissile particles were between 100 and 125 mm in size, corresponding to an anticipated damaged matrix volume fraction of 25-30%.

6.4.1.6. FUTURIX FTA

FUTURIX FTA irradiation experiment involved the irradiation in the Phénix reactor of 8 pins of TRU fuel concepts submitted by Europe, Japan and the USA under similar conditions:

- Two pins of uranium-free oxide CERCER fuel: $(Pu,Am)O_2$+MgO with differing TRU compositions (the Pu/Am ratios were about 50/50 and 20/80);
- Two pins of uranium-free oxide CERMET fuel: $(Pu,Am,Zr)O_2$+Mo and $(Pu,Am)O_2$+Mo;
- Ttwo pins of sodium-bonded nitride fuel, one non-fertile: (Pu,Am,Zr)N and one fertile: (U,Pu,Am,Np)N;
- Two pins of sodium-bonded metal fuel, one non-fertile: Pu-Am-Zr and one fertile: U-Pu-Am-Np-Zr.

All pins were irradiated up to a burnup of 11–16% h.a., corresponding to an Am transmutation rate of about 25%.

6.4.1.7. HELIOS

The goal of the HELIOS irradiation in the HFR is to study the in-pile behaviour of fuel of an optimized microstructure and composition. These experiments are designed to examine the CERMET and CERCER concepts designed to limit the fission product damage to the supporting matrix. The following aspects are studied:

- Matrices of MgO and Mo;
- New complex americium compounds, namely the solid solution $(Am,Zr,Y)O_2$ and the pyrochlore $Am_2Zr_2O_7$;
- CERCER fuel with a high rate of open porosity;
- The temperature dependence of fuel swelling.

6.4.1.8. BODEX

The goal of the BODEX experiment is to investigate the helium build-up and release mechanisms through irradiation tests in the HFR on boron-doped inert matrices (which is intended to simulate the ^{241}Am production via ^{242}Cm). Boron is introduced as either a boride (ZrB_2) or a borate ($Mg_3B_2O_6$). The behaviour (swelling, porosity creation, release rate) of helium gas will be studied in the inert matrix materials MgO, Mo and $(Zr,Y)O_2$.

6.4.1.9. CONFIRM

One (Pu,Zr)N fuel pin irradiated in the HFR as part of the CONFIRM programme is to have its post-irradiation examination performed at the Paul Scherrer Institute (PSI). The main aspects to be examined are fuel swelling, pin corrosion and fuel redistribution in order to qualify the fuel modelling codes developed in the European Commission's Fifth Framework Programme. The results of the post-irradiation examination will also be compared with those of the (Pu,Zr)N fuels irradiated in the BOR-60 reactor as part of the CEA-MINATOM bilateral collaboration.

6.5. Irradiation performance of absorber elements

The absorber material absorbs neutrons in the reactor and it may perform the power regulation, reactor control and reactor safety function of the reactor. It also acts as shielding material to limit the dose on certain components. This section provides a summary of the materials considered for use as an absorber material in fast reactors, their properties with implication to their advantages and disadvantages, as well as a review of the data collected on the irradiation performance of the reference fast reactor absorber material, boron carbide (B_4C).

6.5.1. Properties

The principal materials used as absorbers in fast reactors are boron, europium and tantalum. They are generally used in the form of oxide or carbide. Presently, B_4C, EuB_6 and Eu_2O_3, are treated as potential absorber materials. For the selection of one of these candidates as the reference material for a particular project, one has to consider the following aspects: reactivity worth, physical properties, irradiation behaviour, compatibility with Na and steel, fabrication technology, and irradiation experience. The properties of the candidate materials are compared in Table 6.12.

TABLE 6.12. COMPARISON OF PHYSICAL PROPERTIES OF ABSORBER MATERIALS [320]

Material	B_4C	EuB_6	Eu_2O_3
Thermal conductivity, $W \cdot cm^{-1} \cdot K^{-1}$	0.27	0.28	0.03
Melting point, °C	2450	2580	2050
Linear thermal expansion coefficient, $m \cdot m^{-1} \cdot °C^{-1}$	5.7×10^{-6}	7.4×10^{-6}	10.3×10^{-6}

6.5.2. Advantages, disadvantages and development status

The most important aspect in the development of the control and safety system is the choice of absorber material. In the early FBRs, enriched boron carbide was chosen for control and safety rods. Later on, however, at various laboratories studies were carried out on other absorbing materials. The main reason for these studies was a lack of confidence in boron carbide irradiation resistance prevailing at that time. One of the alternative absorber chosen and validated was CrB_2 (alloyed with Ta) which showed good radiation stability. However, because of lower reactivity worth as compared to boron carbide and more complex manufacturing technology, it was withdrawn and replaced with boron carbide.

The potential alternative to boron carbide is europium oxide (Eu_2O_3). In natural $_{63}Eu$, 47.8% Eu^{151} and 52.2% Eu^{152} are present. The averaged fast neutron cross section of Eu is twice that of B_4C. Eu_2O_3 is substantially superior to boron carbide by its main characteristics such as its high stability of reactivity worth during operation of the reactor, absence of gas release [due to (n, γ) reaction] and swelling. Daughter nuclei of Eu are also good neutron absorbers and hence the life of an absorber rod can be extended. However, because of the self-shielding effect, the effective worth of Eu_2O_3 is only equivalent to that of natural B_4C. Its thermal conductivity is also low. This material was used in burnup compensation rods of the BN-600 reactor which was successfully operated till 1988. Only disadvantage is its high residual activity which substantially complicates the spent rods handling.

Reactivity worth of EuB_6 is about 10% more than Eu_2O_3; i.e., equivalent to that of 25% B^{10} enriched B_4C. Its conductivity is better than that of Eu_2O_3. However, its gas release problem is much worse than for B_4C. Hence venting out is essential. Being a rare earth element, the supply of europium is quite limited. Both Eu_2O_3 and EuB_6 are expensive.

Tantalum is considered as another alternative to boron carbide. In natural $_{73}Ta$, 99.9% Ta^{181} with trace amount of Ta^{180} is present. The absorption cross section is about one third of that of B^{10}. The advantages of the tantalum are that there is no gas release, the daughter product Ta^{182} is also a good absorber, high thermal conductivity and it is not expensive. However, it is soluble in sodium and it has decay heat removal problem due to the 115 days half-life β^- decay of Ta^{182} [321].

Summing up the advantages and disadvantages of the different absorber materials, B_4C emerged as a most preferable absorber material for the control and shutdown systems.

6.5.3. Irradiation performance of B_4C pin

Boron carbide in the form of sintered pellet is extensively used as an absorber material in the control rod and as shielding material in fast reactors, because of its superior properties such as great neutron absorption capacity, high melting temperature, light weight and chemical stability at elevated temperatures. In natural boron, B^{10} which is the primary absorbing material is 19% and the remaining is B^{11} To increase the absorption cross section, the B^{10} concentration can be increased by enrichment. The (n,α) reaction of boron is given below:

$$_5B^{10} + n \rightarrow {}_3Li^7 + {}_2He^4$$

$$_5B^{10} + n \rightarrow 2\ {}_2He^4 + {}_1T^3$$

The properties of boron carbide relevant to the absorber pin design are the following:

- Irradiation-induced swelling (micro- and macro-swelling);
- Helium release;
- Compatibility of B_4C with Na and stainless steel cladding;

- Thermal conductivity;
- Thermal expansion;
- Mechanical properties (elasticity modulus, Poisson's ratio, tensile strength);
- Melting point.

These properties are influenced more or less by parameters such as burnup, temperature, specific density, B^{10} enrichment, stoichiometry and grain size. However, there are some limitations in using B_4C as an absorber material due to generation of helium by the absorption of a neutron. Significant experience has been accumulated on the irradiation behaviour of B_4C from irradiation experiments carried out in Rapsodie, Phénix, BN-600 and Joyo.

6.5.3.1. Helium release

In the process of absorbing neutrons, helium is produced by an (n,α) reaction in the pellets. The helium thus generated can either be retained or can be released depending on the burnup, temperature, etc. It is very important to know the helium release as it pressurizes the cladding and also changes the heat transfer characteristics. Helium retained in the matrix reduces the thermal conductivity of B_4C and affects its thermal performance. The helium retained also accelerates the pellet swelling which may result in the absorber-clad mechanical interaction. The helium release as function of burnup is shown in Fig. 6.73. Up to 100×10^{20} captures/cm^3, the release rate is very much less than the generation rate. The helium release rate slowly increases with burnup and at 150×10^{20} captures/cm^3 and over 1000°C, the release rate is almost the same as that of the generation rate [322]. It is understood that for the same burnup, the helium release increases linearly with irradiation temperature as shown in Fig. 6.74. At a higher burnup, the influence of the effect of burnup is more significant than the irradiation temperature.

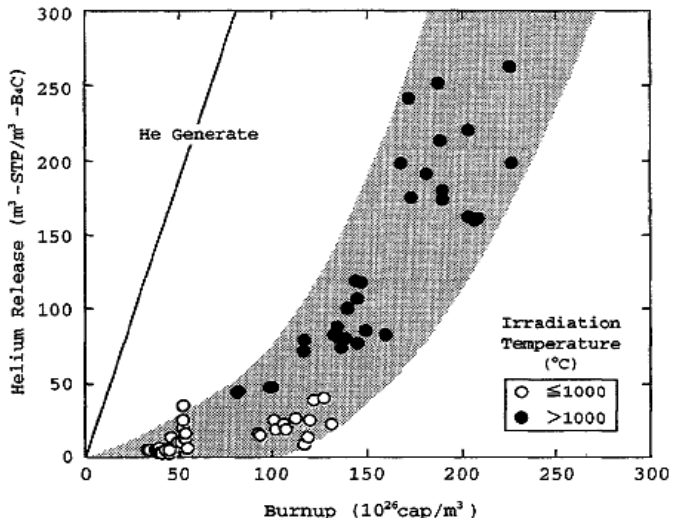

FIG. 6.73. Burnup dependence of helium release [322].

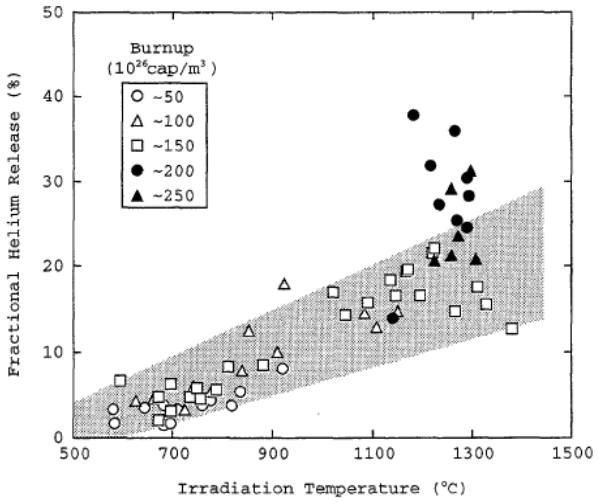

FIG. 6.74. Irradiation temperature dependence of fractional helium release [322].

Russian studies indicate that the release rate first increases with burnup 15×10^{26} captures/m^3 and then decreases as shown in Fig. 6.75 [323]. This is in contrast to the irradiation data reported in Figs 6.73 and 6.74 by Japan, which shows a release rate of 40% maximum.

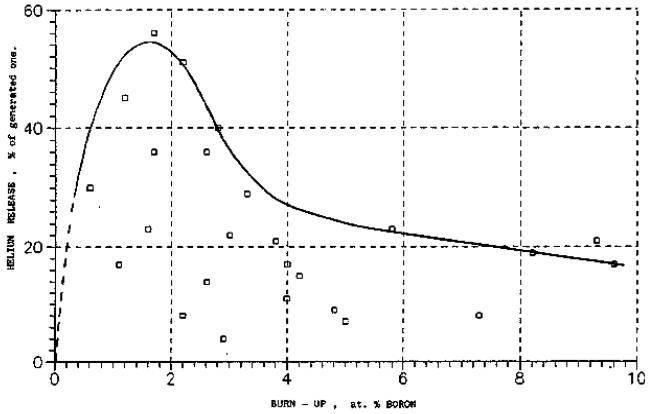

FIG. 6.75. Helium release from B_4C (20 at% B^{10}), irradiation temperature 500–800ºC [323].

6.5.3.2. Helium retention

The helium retention in the pellets is shown in Fig. 6.76.

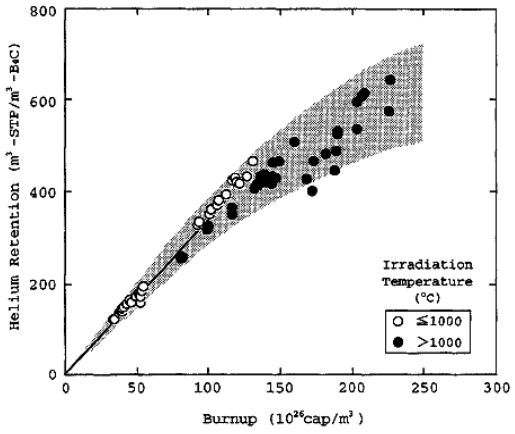

FIG. 6.76. Burnup dependence of helium retention [322].

Helium retention linearly increases with burnup up to 100×10^{26} captures/m^3 and beyond that it saturates. The helium retained in the pellets causes pellet swelling. Figure 6.77 shows the measurements of helium retention in B_4C reported by France and the UK.

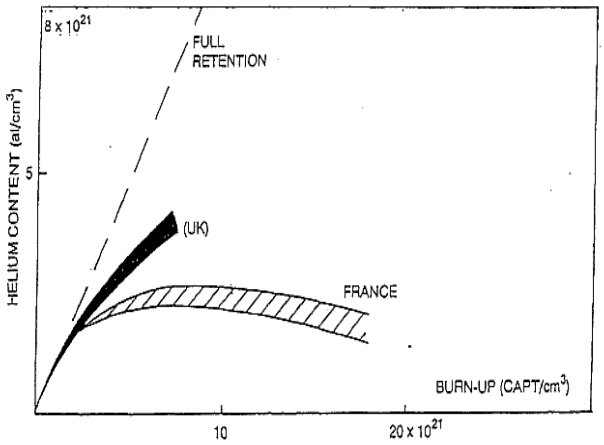

FIG. 6.77. Measurements of helium retention in B_4C [324].

6.5.3.3. Pellet swelling

Due to retention of the helium, the volume of the pellet increases. Diametral swelling of boron carbide pellets with burnup is shown in Fig. 6.78. Swelling increases linearly and saturates with burnup. The decrease in the swelling rate at higher burnup is due to increase in the helium release rate. Figure 6.79 shows the swelling data of the materials with various densities in the temperature independent range. Swelling is found to be linear dependent on burnup, i.e. on helium concentration up to a burnup of 1.5×10^{22} captures/cm^3 [324]. Russian studies reported that with an increase in temperature, the swelling decreases first and then it increases. Also, a decrease in enrichment increases the swelling [323].

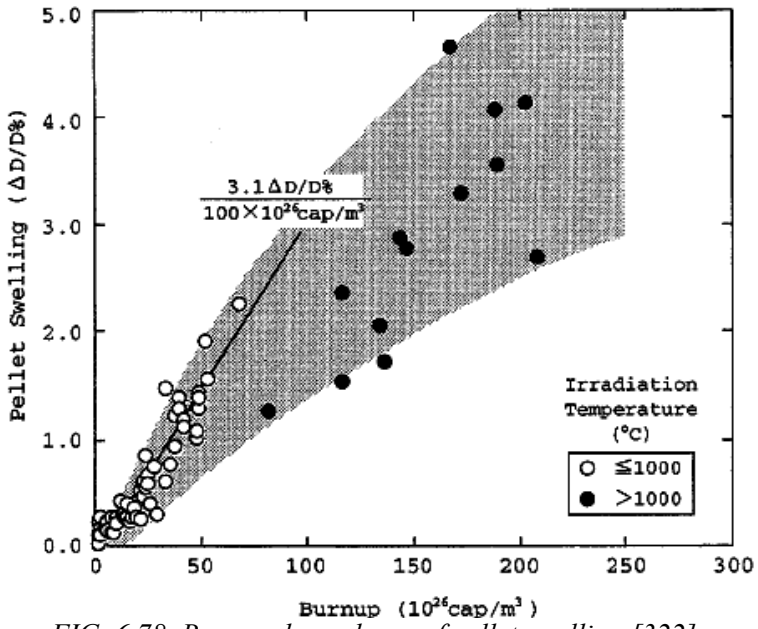

FIG. 6.78. Burnup dependence of pellet swelling [322].

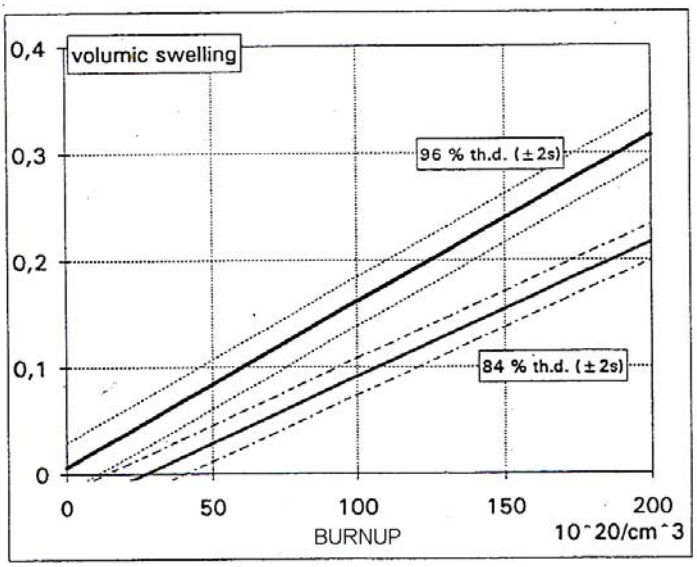

FIG. 6.79. Evolution of B_4C swelling of various densities vs. burnup [324].

6.5.3.4. Thermal conductivity

The thermal conductivity dependence on temperature is shown in Fig. 6.80. The thermal conductivity decreases with the temperature due to the decrease in the phonon conductivity. It also shows the decrease in the thermal conductivity due to burnup. A drastic reduction in thermal conductivity (more than a factor of five relative to unirradiated material) is observed as shown in Fig. 6.81. At higher burnup the thermal conductivity is almost constant and independent of temperature. Figure 6.82 shows the measurements performed in different laboratories on irradiated B_4C at low burnup (up to 40×10^{20} captures/cm^3) and low temperature (500°C).

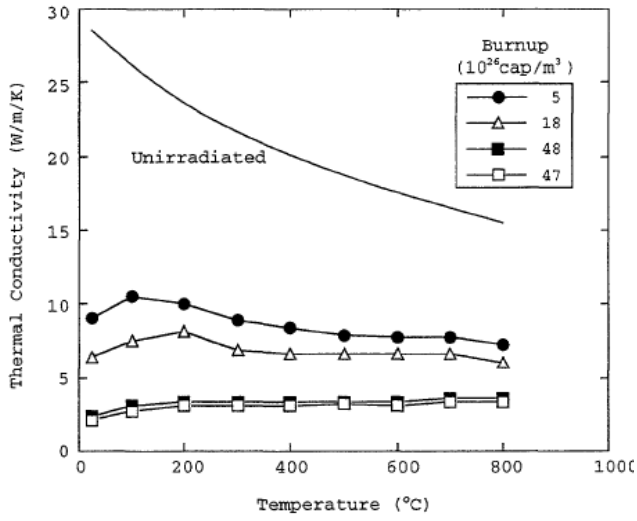

FIG. 6.80. Temperature dependence of thermal conductivity [322].

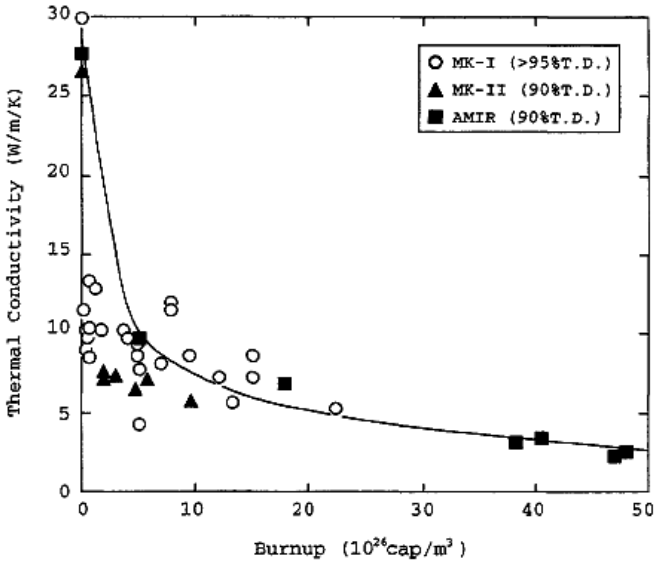

FIG. 6.81. Burnup dependence of thermal conductivity [322].

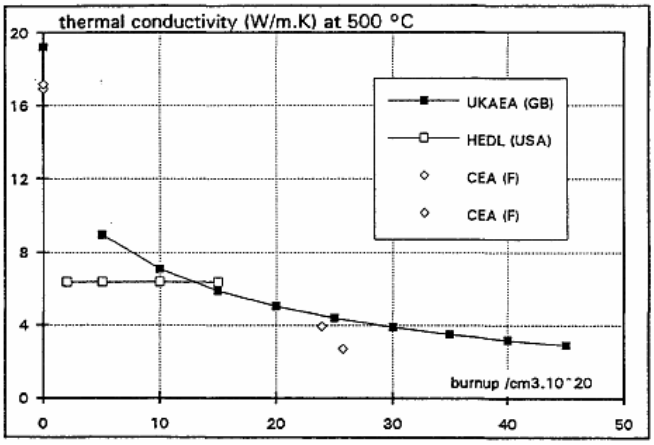

FIG. 6.82. Thermal conductivity of irradiated B_4C versus burnup [324].

6.6. Sodium coolant

After many detailed investigations on coolant options (e.g. heavy liquid metals, gas, water), sodium has turned out to be a favourite coolant for fast reactors. Nearly all fast reactor projects use sodium as the coolant. The main advantages are as follows: good heat transfer properties, low density allowing low pressure systems, fairly high boiling point and others.

Significant experience in the operation of sodium-cooled fast reactors has been acquired to date. There are disadvantages of sodium,which require special engineering measures to control the consequences of sodium-water or sodium-air interactions, as well as measures to overcome inspectability issues due to its opacity.

The comprehensive description of thermal-physical properties of sodium is given in other reports [325, 326].

In this chapter, the necessary safety measures are described in some detail. In addition, the experience gained in Russian sodium-cooled fast reactors is depicted.

6.6.1. Review of sodium coolant technology development status with respect to safety

6.6.1.1. Sodium-water reactions in steam generators

All highly-rated heat exchangers have a risk of failure, and the possibility of leaks has to be taken into account in the design. If the primary sodium of a sodium-cooled reactor were used to generate steam directly, a leak in the steam generator would allow the possibility of radioactive ^{24}Na being released to the environment. Until now the likelihood of such an event has been assessed as being unacceptably high, so all sodium-cooled power reactors have had intermediate circuits of non-radioactive sodium which accept heat from the primary coolant via intermediate heat exchangers (IHXs) and deliver it to produce steam in steam generating units (SGUs). The IHXs are part of the primary containment barrier.

The secondary sodium circuits operate at low pressure so that the IHXs are normally subject only to thermal stresses. A leak in a SGU results in high-pressure steam or water being injected into the secondary circuit where it reacts chemically to form corrosive materials.

The primary safety consideration in relation to SGU leaks is to ensure that neither the pressurisation of the secondary circuit nor the corrosive reaction products will jeopardise the integrity of the IHXs.

The secondary consideration is to limit the damage caused by a leak, preferably so that it can be repaired, failing that so that at most only the affected tube bundle has to be replaced while the rest of the secondary circuit can be re-qualified for continued use.

Unless protective action is taken, a leak in a SGU tube will both grow (i.e. the hole will enlarge so that the leak rate increases) and also escalate (i.e. leaks in other tubes will be caused, again increasing the overall leak rate). Safety against leaks is therefore ensured by appropriate means of detecting leaks quickly so as to prevent or minimise escalation, and a protective system to isolate and make safe the affected SGU.

Foerster et al. [327] review the current understanding of SGU leak behaviour and the design provisions necessary to protect against the consequences of leaks.

6.6.1.2. Leak behaviour

6.6.1.2.1. Sodium-water reactions

When sodium and water interact various chemical reactions compete; for example:

$2Na + 2H_2O \rightarrow 2NaOH + H_2$ (35 kcal/mole)
$2Na + H_2O \rightarrow Na_2O + H_2$ (31 kcal/mole)
$2Na + H_2 \rightarrow 2NaH$

The first of these reactions dominates under the conditions in a SGU, so that the main reaction products are sodium hydroxide and hydrogen, but depending on the initial conditions and quantities of the reactants and on the final pressure, some sodium oxide or hydride may be present. If the mixing ratio of sodium and water is not stoichiometric (i.e. equal numbers of moles), there will also be excess water or sodium, either of which may be present as liquid or vapour.

If the reaction is stoichiometric and adiabatic the temperature of the reaction products is a maximum which depends on pressure, rising from about 1250°C at 1 bar to 1450°C at 5 bars.

6.6.1.2.2. Classification of leaks

The behaviour of a leak and the opportunities for detection depend on its size. It is convenient to define four classes as follows:

- Microleak: < 0.1 g/s. This is a leak which is too small to be detected. It might be due for example to an inter-granular crack in an imperfect weld. Reaction products are formed so slowly that they do not damage other tubes.
- Small leak: 0.1-10 or 50 g/s. This is a leak which produces a reacting jet capable of impinging on adjacent tubes and damaging them. It might be due to a fatigue crack 1 cm or more long in a tube. The upper leak rate of the small leak depends on the SGU design and is considered 10 g/s for a Japanese type SGU.
- Intermediate leak: 0.01 or 0.05-2 kg/s. This is a leak which engulfs many other tubes in reaction products and produces significant excess pressures in the secondary circuit. Depending on the SGU design, it might be caused by a complete failure of a single tube so that steam flows unimpeded from both the broken ends (this is sometimes known as a "Double-Ended Guillotine Failure", DEGF). However, if water rather than steam flows from a DEGF, flow rates of 10 kg/s may be possible.
- Large leak: >2 kg/s. This is a leak which pressurises the whole secondary circuit and expels the majority of the sodium from the affected SGU. It might be caused by failure of several tubes.

6.6.1.2.3. Leak growth

Aqueous sodium hydroxide attacks steels notably by inter-granular corrosion. The corrosion rate is higher in ferritic than austenitic steels and higher still in Incolloy. The flow rate through a microleak is so small that the corrosion products are not swept away but remain in place. In some cases this has been observed to seal the leak so that the flow of water or reaction products to the sodium is stopped. However, the leak may still be active in the sense that water and sodium continue to diffuse through the corrosion-product plug, interact to form sodium hydroxide and then attack the metal, so that the plug of corrosion products grows. Eventually it is no longer able to support the pressure in the tube and blows out, leaving a hole up to 1 mm in diameter. The result may be a "small leak", with a flow rate of 10 g/s or more, appearing instantaneously with no detectable warning. The incubation period, from formation of microleak to the sudden appearance of a small leak, may last several days or weeks [328].

A small leak grows by a combination of corrosion and erosion. Although a high velocity jet of steam or water blows out of the leak, there is back-diffusion of sodium round the jet into the hole, where it reacts with water and corrodes the metal. Grains are loosened by inter-granular corrosion and swept away by the jet. Small leaks grow at an accelerating rate. A leak of 1 g/s may grow over a period of minutes, while a leak of 50 g/s grows significantly in a few seconds depending on the SGU design.

6.6.1.2.4. Leak escalation

The jet issuing from a small leak forms a turbulent under-sodium "flame" [329] (Fig. 6.83).

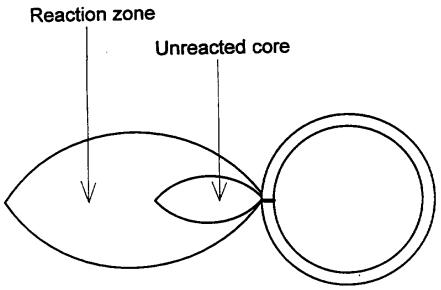

FIG. 6.83. Sodium-water reaction "flame".

The centre of the flame is a core of un-reacted steam at a temperature of 300-500°C. This is surrounded by a reaction zone in which the sodium concentration is low on the inside, high on the outside. In the centre of this reaction zone, where the molar concentrations of sodium are equal, temperatures of 1200-1400°C (depending on pressure) are reached. Outside there is a sodium-rich zone where the temperature is around the sodium boiling point of 900-1000°C (again depending on pressure).When the flame from a small leak impinges on another tube it causes wastage by corrosion and erosion.

Currie et al. [330] give typical data on wastage rates in austenitic steels. A leak of order 1 g/s impinging directly on to an adjacent tube causes wastage at a rate of about 0.01 mm/s, so secondary tube failure in a period of a few minutes can be expected.

When the leak rate rises into the intermediate range the reaction flame becomes large and affects many other tubes. The flame interacts with the flowing sodium and the result is a chaotic turbulent interaction region characterized by widely fluctuating temperatures.

The flame from a large leak can cause significant overheating. At temperatures above 1000°C, a steam tube subject to the normal operating internal pressure has a limited life. The higher is the temperature the shorter the life. For example an austenitic tube at 130 bars might fail in 2 minutes at 1100°C, but fail instantaneously at 1300°C. At lower temperatures the failure is characterised by extensive plastic deformation and ductile flow leading to thinning of the tube wall and a knife-edged trans-granular fracture. At high temperature there is little deformation or thinning of the wall because inter-granular fracture occurs before significant plastic flow can take place.

On the other hand, Wada et al. [331] develop an evaluation method for tube structural integrity considering the creep strength with time-dependence based on the high temperature strength tests of the 2.25Cr-1Mo tube material. Moreover, Hamada et al. [332] examine the heat-transfer characteristics of the flame and propose a simple model of effective heat-transfer coefficient by applying a two-phase flow model that consists of sodium and hydrogen to the flame from a leak.

Suda et al. [333] proceed with new approach to clarify sodium-water reaction phenomena by a numerical simulation. The simulation method of multi-phase reacting flow (SERAPHIM code) is developed to investigate the mechanism of the flame from a leak. SERAPHIM is composed of a compressible multi-fluid and one-pressure model for multi-phase calculation, and surface and gas-phase reaction models. A numerical simulation was carried out regarding experimental results of sodium water reaction test rig (SWAT-1R), which was test equipment

with forty-three heat transfer tubes under small water leakage condition, located at the Japan Atomic Energy Agency (JAEA).

The temperature reached by a tube depends not only on the temperature of the sodium-water flame outside it, but also on the temperature and flowrate of the water or steam inside it. For as long as the steam flows it acts to keep the tube cool, below the temperature at which it will fail rapidly. The cooling effect is more marked if the tube contains water. Concerning a large leak in a PFR superheater in 1987, for example, it is indicated that the tube would fail in a few seconds after the trip due to the lowering of cooling effect inside the tube because the depressurization in the slow dump system would not start immediately after SG isolation [334].

Once the leak has escalated to become a large leak, with the equivalent of DEGF ruptures of 5 tubes or so, the steam flow rate is so large that the majority of the sodium is swept out of the SGU. In the main the sodium-water reaction is quenched by excess steam, temperatures fall and further tube failures are suppressed. Small sodium volumes may, however, remain trapped (for example in crevices in the tube support grids) giving rise to local hot spots.

Because of the complexity of these processes, it is in general not possible to predict the evolution of a SGU leak event in a deterministic way. There is inevitably a substantial random component in the development due mainly to the highly turbulent nature of the flows. It may be possible, nevertheless, to place upper bounds on the rate and extent of leak escalation. Typically it may be possible to show that failure of more than a few - a few tens of tubes (in a SGU containing say 140 - 1000 tubes) is very unlikely and that these failures cannot be simultaneous but will be spread over a period of a few seconds.

This understanding of leak behaviour was confirmed by observations of the consequences of a large leak in a PFR superheater in 1987 [334, 335]. It was initiated by failure of a single tube, and although a total of 40 tubes failed over the next 8 seconds, the pressures in the secondary circuit were mild, and no significant damage was done, apart from to the superheater tube bundle itself.

6.6.1.2.5. Pressures in the secondary circuit

The above conclusion is very important because it sets a limit on the pressures experienced by the secondary circuit components and in particular the IHXs. It implies that whatever pressure changes occur they take place relatively slowly so that the effects of sodium compressibility are negligible. Thus the IHXs and the rest of the secondary circuit are subject to considerably less than the SGU steam-side pressure, typically 120-180 bars, because of the mitigating effect of the protective system (see below).

If the leak escalates much more rapidly, in a period of ms for example, compressibility effects may become important. Pressure waves may give rise to large impulsive forces, analogous to "water hammer" in water pipes, which could damage the IHXs.

Escalation as rapid as this cannot be caused by the corrosion-erosion or overheating mechanisms described above. An external mechanical cause either from a seismic event, impact of a foreign body, or sudden catastrophic failure of a tubeplate, would be needed. To predict the consequences of such an event in which the sodium side of a SGU is suddenly raised to the steam-side pressure, the flow and pressure in the secondary circuit and the protective systems have to be calculated taking account of the compressibility of the sodium.

6.6.1.3. Leak detection

A comprehensive survey of leak detection in steam generators is given by Hans and Dumm [336].

6.6.1.3.1. Hydrogen formation

A sodium-water reaction always generates hydrogen, which can be detected easily. This affords the most sensitive method of detecting a leak, in the sense that the hydrogen generated by very small quantities of water or steam in the sodium can be observed. A change of hydrogen concentration as small as 0.1 wpm in the secondary sodium, which may correspond to the leakage of a few hundred grams of water into a secondary circuit containing of order 100 tonnes of sodium, can be detected.

The major disadvantage of hydrogen detection is that it is not prompt. There is inevitably a transport delay of at least a few - a few tens of seconds while the sodium containing the hydrogen is convected to the detection device. This is often made longer because the detectors are situated in an auxiliary loop which takes a representative sample of the main sodium flow. On the other hand hydrogen detection is an integral technique in that it measures the total quantity of steam or water entering the sodium over a period. It is therefore able to detect very small leaks. A leak of 1 mg/s of water, for example, is nearly 100 g per day, which gives a measurable change in hydrogen concentration over a few days.

Leaks are not the only source of hydrogen in the secondary sodium. If the steam generator tubes are made of ferritic steel they are continually undergoing oxidation on the water side, where a steadily-growing film of magnetite (Fe_3O_4) builds up. Some of the hydrogen generated by this reaction diffuses through the tube walls into the sodium. In normal operation the oxidation takes place steadily and the change in hydrogen concentration in the sodium can be predicted. A leak is then shown by a higher-than-normal rate of increase of hydrogen concentration.

The steady generation of hydrogen by formation of magnetite can be accelerated if the magnetite layer becomes cracked or spalled, by a rapid temperature change due to a plant trip for example. This can expose un-oxidised metal to the water, which begins to oxidise rapidly, generating hydrogen at an increased rate. This may give the appearance of a leak for a time.

6.6.1.3.2. Detection of hydrogen and oxygen

The simplest way to detect hydrogen in sodium is by means of a plugging meter [337] (Fig. 6.84). This is a device in which a sample sodium flow is cooled and passed through an orifice. The cooling is increased until the pressure drop across the orifice increases, indicating that it has been "plugged" by precipitated impurities. The temperature of plugging is then an indication of the impurity concentration.

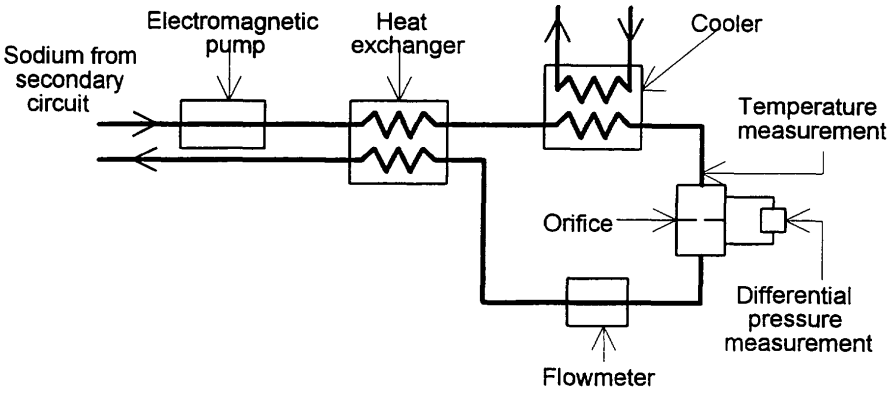

FIG. 6.84. Plugging meter for measuring impurity levels in sodium.

A plugging meter is sensitive to both oxide and hydride impurities. However, in the secondary sodium (unlike the primary) there is usually little oxide and its plugging temperature can usually be interpreted in terms of hydrogen concentration alone. Ambiguity can be removed, however, by measuring the "unplugging" temperature (the temperature to which a plugged orifice has to be heated to clear it). Hydride dissociates more readily than oxide dissolves, so the unplugging temperature is related more strongly to the oxide concentration and this can be used to correct the evaluation of the hydrogen concentration.

Diffusion affords a more selective means of detecting hydrogen alone. Hydrogen diffuses very readily through nickel at high temperature. A typical detection system takes a sample of the sodium flow, heats it, and passes it over a nickel membrane, through which the hydrogen diffuses into a carrier gas. The hydrogen concentration in the carrier gas can be measured either by a katharometer, which measures the thermal conductivity of the gas mixture (which is sensitive to small quantities of hydrogen) (Fig. 6.85), or by other means such as a mass spectrometer [336].

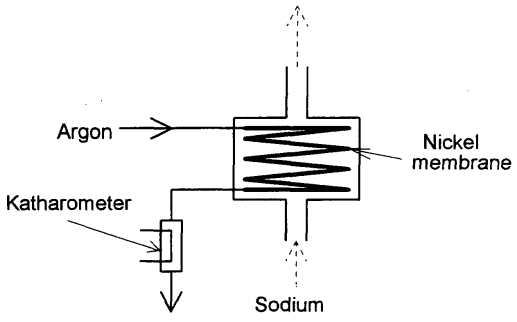

FIG. 6.85. Diffusion monitor to measure hydrogen concentration in sodium.

Oxygen and hydrogen concentration can also be measured by electro-chemical methods [338-340]. An electro-chemical cell can be used in either an absolute mode, in which the electric potential of the contaminated sodium relative to a reference electrode is measured directly, or alternatively in a differential mode. In the latter case the relative potential of sample sodium streams from inlet and outlet of a SGU is measured directly. This enables the change in hydrogen or oxygen concentration as the sodium flows through the SGU and therefore the leak rate, to be measured directly. Figure 6.86 shows a typical design for an electrochemical oxygen meter.

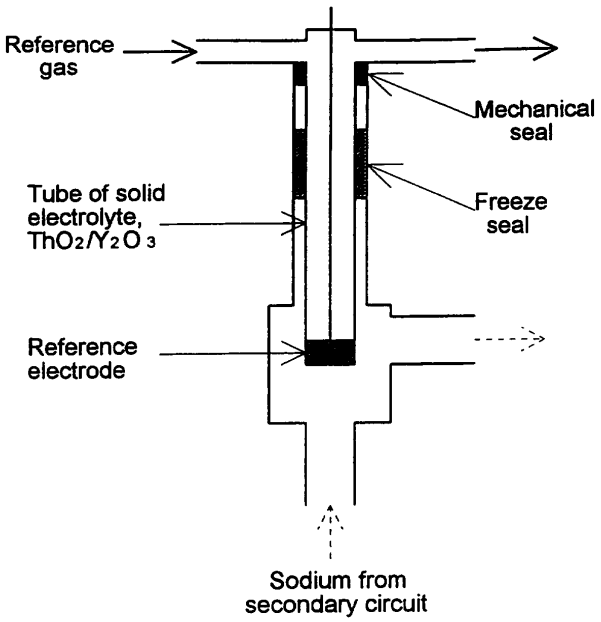

FIG. 6.86. Electrochemical meter for measuring oxygen concentration in sodium.

6.6.1.3.3. Acoustic methods

The use of acoustic techniques for detecting steam generator leaks is given below. The great advantage is that they give a much more rapid response than hydrogen detection because they are not subject to the transport delay. It is possible to detect a 1 g/s leak within 1 s by acoustic means, depending on a SGU design. Use of the two techniques together therefore gives a very wide coverage, with hydrogen detection giving warning of microleaks which may be growing over periods of hours or more, while acoustic detection of small leaks enabling protective action to be taken before significant escalation of the damage has time to take place.

6.6.1.3.4. Flow and pressure measurement

A leak detection system using hydrogen and acoustic methods, as outlined above, is still limited in that a response time of less than 1 s is not possible, so protection against sudden large leaks, caused by earthquakes for example, is imperfect. An alternative diverse means of protecting the IHX integrity may therefore be necessary. This function can be fulfilled by measuring the pressure in the secondary sodium circuit. Conventional pressure transducers located in expansion tanks can detect intermediate or large leaks in less than 1 s.

Alternatively, sodium flowmeters can be used. The signals from flowmeters at the inlet to and the outlet from a SGU can be compared to give a rapid indication of changes in the fluid volume, and hence the presence of intermediate leaks. Conventional electromagnetic flowmeters can give a response time of the order of 1 ms.

Figure 6.87 shows a complete leak detection system for a SGU, incorporating various devices to respond to leaks of all sizes.

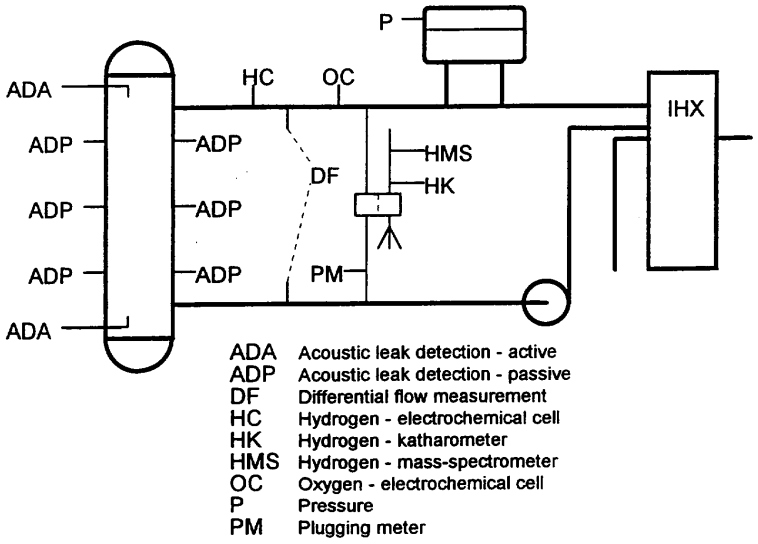

FIG. 6.87. Steam generator leak detection system.

6.6.1.3.5. Leak location

If a leak is detected it has to be repaired. In the event of a small leak there is usually no difficulty in locating it, when the plant has been shut down, by pressurising individual tubes.

A microleak can be much more difficult to locate because it is likely to become blocked by reaction and corrosion products, either while the plant is running or during and after the shutdown process. It is hardly possible to visually examine all the tubes in a SGU (which might number 1000 or more, each 20 m long).

Fortunately it has been found that, in spite of the pressure difference, sodium tends to diffuse back through a microleak to the steam side, and shows in the form of hydroxide impregnating the oxide layer. This can be detected chemically by swabbing individual tubes. A moist absorbent plug, or "mole", is driven through each tube in turn by compressed air and examined for the presence of hydroxide. The presence of the microleak can be confirmed visually, and the affected tube can then be plugged.

6.6.1.4. Plant protection

The most important consideration is to prevent damage to the IHXs, which are part of the primary containment boundary. This can be done by providing bursting discs set to burst at a pressure below that which will overstress the IHXs, and with sufficient capacity to discharge the sodium, steam and reaction products from a large leak. The bursting discs should be of robust and reliable design and be entirely passive, in that venting should be independent of any signal from the leak detection system. They should vent into a system which will receive the reaction products, including hydrogen, safely. There should be traps and filters to ensure that the release of sodium and other reaction products to the atmosphere is within acceptable limits.

6.6.1.4.1. Plant isolation

In the event of a major leak, the affected SGU has to be isolated quickly in order to prevent the spread of corrosive reaction products.

The sodium can be dumped to a dump tank by opening fast-acting valves in a drain line. The drain line has to be permanently trace-heated to a temperature which will prevent solidification not only of pure sodium but of sodium which is highly contaminated with reaction products, depending on the SGU design. The plugging temperature may be 300°C or more, and to ensure an unimpeded dump the drain line has to be kept above this temperature all the time.

In some systems the secondary sodium circuits are fitted with isolation valves, so that the affected SGU can be emptied of sodium while the rest of the circuit remains full. This may make the cleanup of the rest of the circuit easier, if sodium can be circulated in it. The disadvantages are that the isolation valves may pass, they may be difficult to maintain, and it may be hard to design them to withstand the pressure transients associated with a large leak. In addition if the secondary circuits have a role in the rejection of decay heat under emergency conditions the presence of isolation valves, which might be closed inadvertently, may decrease their availability significantly.

The steam side of the affected SGU has to be depressurised to stop the flow of steam or water into the sodium. Fast-acting isolation valves disconnect it from the rest of the steam system, and relief valves open to vent the steam to the atmosphere.

The placing of the relief valves in the steam circuit is critical. It is desirable to avoid stagnation of the water or steam in the SGU tubes before the pressure has fallen. If the flow stops, the tubes will no longer be cooled and they will be more likely to fail due to overheating by the sodium-water reaction flame. If the SGU is vented from one end only the pressure is relieved by the water or steam flowing through the tubes, the cooling does not stop until the pressure is low and the damage to tubes will be less extensive.

Particular care has to be given to the venting of sodium-heated reheaters, if these are fitted. When the SGU is isolated the entire steam plant is shut down and, among other things, the turbine stop valve closes. This exposes the whole of the turbine and the steam side of the reheaters to the condenser, so the pressure falls rapidly and may go below atmospheric. If there is a leak in the reheater this would allow sodium to pass into the steam pipework and even possibly the turbine, where it could do extensive damage.

In general it is important that during the isolation and dump sequence the steam side pressure does not fall below the sodium side pressure in any SGU, to avoid back-flow of sodium through any leaks which may be present.

After steam and sodium have been removed the SGU and secondary circuit must be filled with inert gas. Air must be excluded to avoid any moisture in it forming sodium hydroxide, which at low temperature may be aqueous and therefore particularly corrosive.

At higher temperatures sodium containing high oxygen concentrations is corrosive [341]. This is a particular problem with the secondary sodium left in the IHXs. In most cases this cannot be removed or circulated if the rest of the secondary sodium is dumped. It is therefore necessary to protect it from oxidation, especially if the reactor is to continue in operation. It is desirable to have a means of determining the impurity levels in the IHX secondary sodium.

Figure 6.88 shows the various components of the protective system for a SGU and secondary sodium circuit.

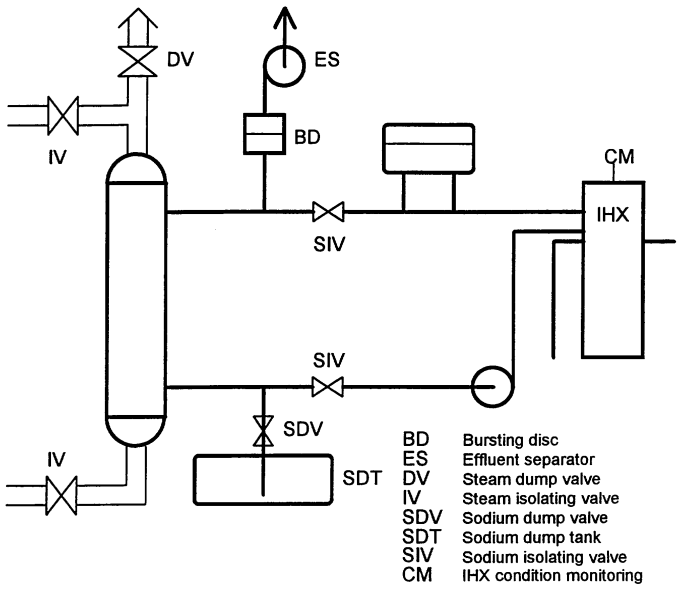

FIG. 6.88. Steam generator protective system.

6.6.1.4.2. Acoustic leak detection

The word "acoustic" is used to refer to sound in the audible range or a little above it, with frequencies up to around 100 kHz and wavelengths of a few centimetres or more in sodium.

Acoustic methods have a very important role in the detection of steam generator leaks. A leak of water or steam into sodium reacts chemically to form a mixture which is corrosive and hot. These reaction products may attack adjacent tubes, causing them to fail, and resulting in very rapid escalation of the accident. This can be prevented if the leak is detected quickly and the steam generator is isolated and depressurised. In the case of very small leaks, of the order of 1 mg/s or less, escalation is slow and detection by chemical means - usually of the hydrogen liberated - is quick enough. Larger leaks, of the order of 1 kg/s, can be detected readily by means of the pressure in the sodium system, but are so large that extensive damage to the steam generator is inevitable. A leak initially of the order of 1 g/s or so however might grow rapidly enough to damage other tubes within 10 s, too quickly for hydrogen detection systems to respond. Valuable protection is afforded therefore by a leak detection system capable of detecting such a leak within 1 s, so that action can be taken in time to protect the steam generator from extensive damage. This can be done by acoustic means. There are two distinct approaches: passive and active.

Passive detection relies on the fact that the effect of the leak is quite similar to boiling, in that it gives rise to rapidly-expanding bubbles. As a result the noise generated is similar to that generated by boiling and can be detected by similar, though not identical, means. Greene [342] describes different approaches to leak detection by passive means.

The IAEA Co-ordinated Research Programme on "Acoustic Signal Processing for the Detection of Sodium Boiling or Sodium/Water Reaction in LMFRs" covered acoustic leak detection as well as acoustic boiling noise detection. It made use of experimental recordings of leak noise from test rigs in the Russian Federation and elsewhere, and of background noise from operating steam generators, and showed that a 1 g/s leak can be detected within 1 s with high reliability and a false indication rate of the order of one in 25 years. A passive acoustic

leak detection system can make use of the same detectors as a plant monitoring system to detect vibration, will be described below. Active acoustic leak detection makes use of the changes to the acoustic properties of the steam generator caused by the gas liberated. The cloud of bubbles formed increases the acoustic attenuation of the sodium. This can be detected by means of acoustic pulses transmitted along the length of the steam generator between the tubes.

High frequency pulses of around 10 kHz are transmitted from one transducer, along the tube bundle to a receiving transducer, with a pulse repetition rate of around 1 Hz. If there is a significant fall in amplitude of the received pulses it is concluded that a leak is present. An advantage of this system is that it is fail-safe and self checking. Both passive and active acoustic leak detection methods are described in the report of an IAEA Specialists' Meeting.

6.6.1.5. Sodium fires

According to experience from existing fast reactors and Na test facilities, leakage from Na-containing systems and components cannot be excluded.

6.6.1.5.1. Definition of events and associated risk

In the event of a leak, sodium will escape. Many sequences have to be considered. The Na may be forced out or merely exposed. Typically a leak may start in the first mode and develop to the latter if the environment is such that chemical reactions cause plugging of the breach by reaction products. Corrosion by these products may subsequently enlarge the leak area thus reopening the leak after a time interval. The Na escaping from the leak may impose loads on other structures by the jet force. If oxygen is available, sodium will react leading to a fire, which may increase the thermal loadings and raise the gas pressure with aerosol generation.

The burning rate varies. The highest rate will be achieved when a sodium jet bounces against other structures and is dissipated into small droplets, thus increasing the Na surface in contact with air (spray fire). A low rate can be assumed when sodium only runs down the structures and collects in a catch pan (pool fire). Usually a combination of both extreme cases (spray fire and pool fire) has to be assumed. This situation is termed a combined fire.

The relation between leak rate and leak size depends on the system geometry, the location of the leak, and system characteristics such as the cover gas volume and pressure. Risks associated with a Na leak depend on the type of leak considered. In the case of the primary circuit heat removal from the core must be ensured, so loss of Na must be limited to allow decay heat removal via the DRC system.

Primary Na being radioactive, leaks must be contained and possible releases controlled. Secondary leaks are of less importance, but they must be collected and guided out of the building without affecting any installation inside. Large and long-lasting sodium concrete reactions having potentially severe consequences must be excluded. In the beyond design basis range, potential risks associated with severe Na leaks and fires include:

- Loss of the system function in which the leak occurs;
- Radiation release;
- Loads resulting from jet force;
- Corrosion;
- Sodium fire and associated phenomena;

- Sodium-concrete reactions;
- Sodium-water reactions if water circuits are involved.

6.6.1.5.2. Prevention, detection and mitigation

Sodium fires can be largely prevented by surrounding the sodium pipes and components with an inert gas, a Na-tight leak jacket, and steel-lined confinement cells. Outlets equipped with valves allow the build-up of pressure in the case of spray fire to be limited. Such design measures were used for FFTF and Superphénix.

In Superphénix, the four large areas (1000 m^3) of the secondary loops were modified by the installation of partitions creating 100 m^3 zones to limit the build-up of pressure in the outbreak of a fire, the venting of the boundary via outlets equipped with valves set to open at 10 mbar to evacuate the hot gases outside the reactor building, and the cladding of the concrete walls with stainless steel sheeting to contain the secondary sodium in the event of a leak and to avoid Na-concrete reactions.

In the Japanese prototype fast reactor Monju, a sodium fire mitigation system was introduced in the secondary loops and their function was experimentally confirmed to be valid [343].

The system consisted of thermal insulation cover of sodium pipe to prevent the sodium jet from impinging on concrete wall, steel-lining to prevent direct contact of sodium with concrete floor, and fire suppression plate to smother and extinguish the burning sodium after collecting the leaked sodium to a limited space in the secondary loop.

After experiencing sodium leakage from a secondary circuit in December 1995, comprehensive design review activities concluded to make additional improvement to the countermeasures as follows [344]:

- Installation of new sodium leakage detectors (TV monitors, smoke sensors) to enable the operators to be alerted of incidents quickly;
- Remodelled drain system to shorten the sodium draining time;
- Installation of a nitrogen gas injection system to extinguish sodium fires;
- Division of the secondary circuit area into several smaller zones to limit the aerosol spreading.

Other design measures against pool-type sodium fires are so called catch pan systems (Fig. 6.89). These collect leaking hot Na in such a way that it can run through holes into a leak recovery tank where it is isolated from the oxygen component of the air.

Various sodium fire-extinguishing powders have been developed and especially good experience has been obtained with graphite powders to quickly and effectively extinguish Na fires. Leak detection plays an important role. Wire detection has been developed in many countries. Superphénix was equipped with "sandwich detectors" to cover welds on the piping exceeding 200 mm in diameter, on which insulating material may react with Na and prevent it from getting into contact with the classical wire detection system. Other detection systems such as flame spectrometers and smoke detectors are commonly used. The objectives pursued are the following:

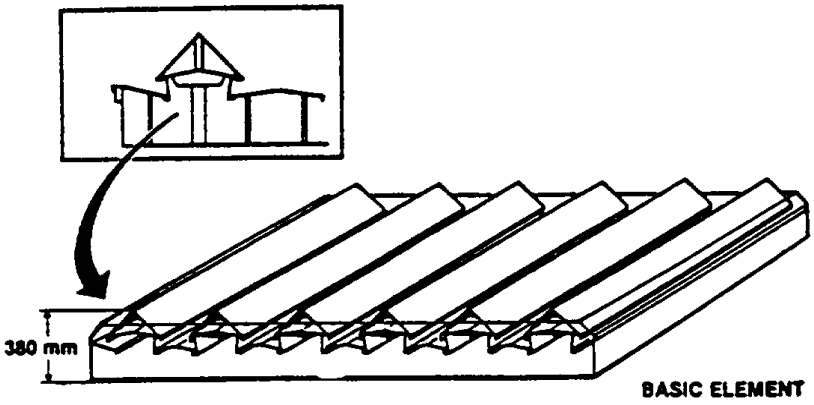

FIG. 6.89. Superphénix smothering catch pan system.

- In all cases to prevent large leaks, corrosion, and fires by early detection;
- To exclude large leaks from the design by extensive application of the Leak Before Break (LBB) criterion;
- To minimize large pressurized gas volumes which could act as driving forces for combined sodium fires in the event of leaks;
- To limit the duration of fires (15 minutes may be considered as an order of magnitude of an acceptable fire duration) to avoid serious damage to heavy structures by heating above acceptable limits;
- To preclude pressurization by relief openings; and
- To limit the drop height of any spray fire by arranging catch pans every 5 meters vertically (again this figure has to be considered as an order of magnitude).

Combined sodium fires develop according to the well known exothermic reactions:

$$4\,Na + O_2 \rightarrow 2Na_2O \text{ (sodium oxide)}$$
$$2\,Na + O_2 \rightarrow Na_2O_2 \text{ (sodium peroxide)}$$

The first reaction is the predominant mode. The evolution of a fire is very sensitive to the conditions of contact between oxygen and Na. That is why the extreme cases are pool and spray fires, the real case of a combined fire being a combination of the two.

6.6.1.5.3. Pool fires

A sodium pool fire will not normally ignite below about 250°C (if the pool is at rest). Since the fire occurs only at the pool surface it is appropriate to characterize the reaction rate on an area basis. A standard rate for a pool fire is 25 $kg \cdot m^{-2} \cdot h^{-1}$.

The evolution of the fire depends on many parameters linked to the volume of the cell and the heat transfer conditions. In reality the phenomena are more complex due to the fact that the pool is not really at rest and contact between Na and air is modified. The various phenomena have to be modelled in codes (see below).

6.6.1.5.4. Sodium spray fires

The ignition temperature for Na spray fires is lower than for pool fires and can be as low as 120°C depending on the Na droplet size. The sodium oxide aerosol production rates are much

higher than for a pool fire (a factor of 5 or even more). Again the various phenomena involved have to be modelled in the codes.

6.6.1.5.5. Models and codes

A common experimental programme concerning sodium combined fires was developed in France and in Germany [345]. It mainly focused on prediction of the thermodynamic consequences due to upward vertical jets with a Reynolds number of about 10^6 and a nozzle diameter of 10 to 26 mm. Due to the lack of direct measurements of the spray parameters during the fire and the difficulty of predicting those parameters accurately in the case of a real fire, a simplified approach has been developed: in the NABRAND code [346], an appropriate data set of droplet parameters was derived from realistic sodium fires, and in the FEUMIX code [347], a global interfacial area between oxygen (air) and sodium droplets was found correlated with the jet Reynolds number. For both NABRAND and FEUMIX, the comparison between calculation and experiment indicates that a simplified approach is valid for modelling the complex phenomena resulting from Na combined fires in the case of jet break up or impact.

In Japan, both experiments and computer code development for pool fire, spray fire and their combined fire have been performed [343]. The experimental study mainly aimed at a large-scale sodium leak, since it had been chosen as a design basis accident of the prototype FBR in Japan. The measured and evaluated value in the experiments were therefore pressure rise of atmosphere in a closed vessel and temperature increase in the structural material existing around the fire. After the sodium leak accident in Monju, a lot of works and sodium leak and fire tests were conducted to investigate the cause, the consequence, and the burning behaviour. These activities led to the understanding that small-scale sodium leak was also important, and to subsequent development of new numerical sodium fire analysis methodology.

To analyze the sodium fire phenomena and the related thermodynamic consequence, conventional sodium fire computer codes such as SOFIRE-II [348], SPRAY [349] and ASSCOPS [350] have been used. Other codes, such as SPM [362] with a sophisticated combustion model and SOLFAS [351] with multi-dimensional gas thermal hydraulics were developed. The ABC-INTG [352] code is a program to analyze the behaviour of aerosols which are generated as reaction products of sodium fire.

Integrated analysis code CONTAIN-LMR [353, 354] has also been developed to predict the physical, chemical, and radiological consequences of a postulated severe accident in FBRs. The CONTAIN-LMR code was developed around 1990 under an international collaboration among SNL/USA, PNC/Japan, KfK and GRS/Germany, AEA/UK, and CEA/France. The program includes sodium fire model based on SOFIRE-II and NACOM [355], sodium aerosol behaviour model based on MAEROS [356], sodium-concrete reaction model SLAM [357], and other models necessary for severe accident analysis. Most of sodium-related models have been validated with existing experimental data [354].

In the several years after the Monju sodium leakage accident, the primary focus was the small-scale sodium leak because it might result in locally higher temperature of structural material when compared to the large-scale sodium leak. It was implied from several experiments and analyses [358] that sodium combustion and subsequent thermodynamics were complicated, the coupled phenomena of chemical reaction with heat transfer. Thus numerical methodology for sodium combustion has been developed in order to investigate

these wide and complicated phenomena [359]. The methodology includes a fast-running zone model computer program SPHINCS [358], a field model program AQUA-SF [360] for multi-dimensional thermal hydraulics, method of particle for sodium spillage phenomena MPS-3D in discontinuous geometry [361], the COMET program with pseudo-DNS of single liquid droplet combustion and 3D thermal hydraulics [362], and a chemical reaction analysis program BISHOP based on chemical equilibrium theory [363]. In these computer codes, SPHINCS and AQUA-SF are available for the safety evaluation of FBRs with utilizing other detailed-level simulation codes as supporting methods.

6.6.1.5.6. Release of sodium fire aerosols to the environment

Experimental and analytical programmes were conducted in France and in the UK. At Cadarache, realistic release tests were carried out in Esmeralda Facility [364]. At Dounreay, tests were conducted in the SOFA programme. All these experimental and analytical studies into the behaviour of sodium fire aerosols released into the environment demonstrate that there are problems arising from the characteristics of the source and the behaviour of the aerosols within the plume. These problems are being solved and the programmes have given a lot of useful information allowing the evolution of parameters of interest to be predicted under a large range of weather conditions. However, the effect of the building is important and has to be studied carefully.

6.6.1.5.7. Filters

Special filters have been developed to separate sodium oxide and fission product aerosols from air. The design criteria for these filters reflect the physical and chemical properties of sodium oxide and sodium hydroxide as well as the temperatures of these aerosols. Special Sanahed filters have been developed which attain a separation efficiency of 99.7 to 99.9%. They can be combined with wet scrubbers which can remove 70% of the sodium aerosols in a first step.

6.6.1.5.8. Sodium-concrete reaction

Sodium-concrete reactions have been studied thoroughly [347]. Workers in the USA have suggested a generalized sodium-concrete reaction model shown schematically in Fig. 6.90.

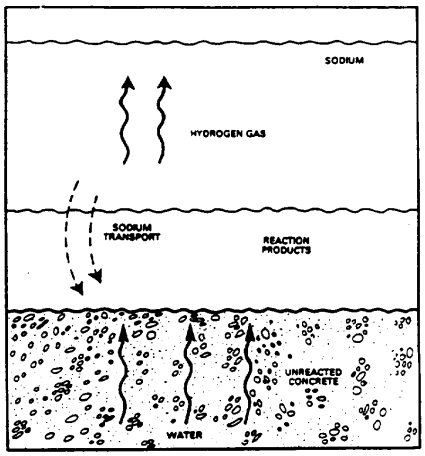

FIG. 6.90. Diagram of the sodium-concrete reaction model.

In essence hot sodium, placed on top of ambient temperature concrete, heats the concrete, driving water to the hot surface where it reacts with Na to form hydrogen and NaOH according to the exothermic reaction:

$$2Na + 2H_2O \rightarrow 2NaOH + H_2$$

Chemical energy from the reaction adds to heat from the Na to heat the concrete further and continue to drive off more water. When the concrete surface has been heated to about 500°C, sodium and NaOH both react with concrete solids to produce more chemical energy. The extent of water release is determined by heat transfer in the concrete rather than sodium penetration of the concrete.

The resulting NaOH phase at the concrete interface will generally form a barrier layer of reaction products, limiting the penetration into the concrete to a few centimetres of hard, rock-like consistency. In some cases, mechanical effects may cause disruption of the protective layer, resulting in rapid penetration of the dehydrated concrete by liquid sodium. The penetration rate is strongly dependant on Na temperature and varies from less than 0.5 mm/h at 200°C to 20 cm/h above 550°C.

The reaction products associated with deep rapid penetration of Na in dehydrated concrete are characterized by a loose, friable, cinder-like consistency. Sodium penetration of concrete is of indirect concern due to possible effects on the structural integrity of the concrete. Moreover, the release of sodium aerosols and fission products during the reaction is also important from a viewpoint of accidental source term evaluation, as is experimentally investigated [365].

6.6.1.5.9. Models and codes

A sodium-concrete ablation model SCAM has been developed by Sandia [366].

More recently the RESSORT and SORBET Codes [367] have been developed and tested. Modelling covers chemical decomposition, thermodynamic equilibrium, and mass transfer of water, air, H_2 and CO_2. Heat transfer remains very important and may be strongly influenced by bubbling at the interface. Further developments are necessary.

6.6.1.5.10. Choice of concrete for minimizing interactions

The behaviour of concrete presented above varies considerably according to its composition. Various types of concrete have been investigated (Portland cement, granite concrete similar composition to basalt, hydrous alumina cement, etc.). Some differences appear above 500°C.

The most promising way to minimize interaction is to use refractory concrete which can be obtained by a combination of the following: aggregate of Al_2O_3, MgO, high alumina cement, and firing of the concrete. The use of refractory concrete may be limited to a protective layer on conventional concrete.

The CEA have tested Corindon, Secar concrete (EdF) and PHLOX 188 (Lafarge Cement Co). The main conclusions were that the behaviour in contact with hot sodium at 350°C is satisfactory. It is difficult to apply refractory concrete to industrial buildings, and in consequence a new aluminous concrete was successfully tested and qualified: the INTRACAST AS 701 (produced by the Lafarge Refractaire Monolithique Co). The EFR anchored safety vessel option was tested with this concrete. The results were very satisfactory,

but the cost is high so that the use of such concrete should be strictly limited to zones where the possible consequences of Na-concrete interaction would be unacceptable.

6.6.1.5.11. Liner systems

Long-lasting and large Na-concrete reactions are not acceptable, so liners are used extensively. Rapid heating to very high temperatures with large compressive stresses in the liners raises many problems which require careful design. In addition a considerable amount of heat can be transferred to the concrete, resulting in release of water vapor and other gases, with the potential to produce pressures behind the liner if the concrete is not adequately insulated and vented.

6.6.2. Review of sodium coolant technology development status and experience with respect to operational performance and availability in the Russian Federation

6.6.2.1. Introduction

The purpose of this section is to:

- Present the achieved performance of the main sodium equipment operation in SFR;
- Evaluate the statistical data on service of sodium systems and failures in them from the point of view of influence on value of load factor of SFR.

It should be noted that experience gained in power plants is most representative from the standpoint of evaluation of effect of sodium systems and components on the NPP performance, and therefore analysis described below is mainly based on data obtained in the BN-600 reactor [368, 369].

6.6.2.2. Influence of sodium technology on operational performance of SFR

By now the essential experience in the world has been accumulated for SFRs (~ 250 reactor-years from experimental SFRs and ~140 reactor-years from NPPs with SFRs). This experience has confirmed the practical feasibility of SFR technology at the industrial level. From this point of view, the operational performance of the industrial fast reactor BN-600 is most valuable and impressive. It demonstrates a stable work over more than 30 years as one of the best Russian NPPs and improving its parameters from year to year. It is possible to make some conclusions on the basis of operating experience of the BN-600 NPP and also other SFRs.

The achievement and even exceeding design values on operation time and lifetime of the large-sized sodium equipment is one of the important results obtained during SFR operation.

Table 6.13 shows the data on the achieved parameters during operation of the different facilities with sodium cooled fast reactors in the Russian Federation.

TABLE 6.13. THE ACHIEVED PARAMETERS ON OPERATION TIME AND LIFETIME OF THE SFR EQUIPMENT WITHOUT OVERHAUL, HOURS

	BR-5/10 (1958)	BOR-60 (1969)	BN-350 (1973)	BN-600 (1980)
Non-replaceable equipment				
Reactor vessel	150 000	200 000	170 000	130 000
Primary piping	300 000	200 000	170 000	130 000
Sodium pumps	170 000 (electromagnetic)	130 000 (mechanical)	100 000 (mechanical)	100 000 (mechanical)
Intermediate heat exchangers	300 000	200 000	170 000	130 000
Steam generators	-	Test models of different SG types	150 000	105 000 (evaporators)

The presented data testify to good compatibility of sodium coolant with structural materials used and its low corrosion activity in the mastered range of SFR parameters. The technology of replacement and repair of sodium components, including main equipment (pumps and steam generators), is also mastered.

Taking the BN-600 reactor as an example, it can be demonstrated that, with the appropriate sodium technology, competent personnel and stable power operation, the total outage time of the plant is not dominated by the sodium systems, but rather by repair and maintenance of the tertiary circuit, for example the turbine-generator system.

Accumulated statistical data on the unscheduled shutdowns and power decrease modes of the BN-600 power unit caused by failures of sodium components and systems show their low fraction in the total number of unscheduled shutdowns and power decrease modes of the power unit and, hence, insignificant influence on the power unit performance. It should be noted that such failures mainly occurred in the early stage of the BN-600 operation, i.e. in the period of assimilating of sodium technology features by the personnel. For example, the last sodium leak outside took place in the BN-600 reactor in 1994, and the last SG leak was in 1991. Analysis of SG leak events performed in 1996 has shown that the decrease in the availability of the BN-600 plant caused by the 12 water-to-sodium leaks was as low as 0.3%.

Although this section does perform a full scale study of economical characteristics of the SFR as a whole, nevertheless, it should be noted that the use of a three-circuit reactor heat removal system in SFR design results in certain increase of cost of the NPP. However, according to the estimates, this cost increase does not exceed 10-15% of the total NPP construction cost.

Analysis of the effect of sodium leaks from the circuit on the BN-600 reactor performance shows that a significant fraction of the leaks occurred with the reactor out of operation, on the stage of reactor start-up or during scheduled preventative repairs, or in the auxiliary sodium systems, and therefore these did neither result in the long reactor outages nor made any significant effect on its economical characteristics. The share of additional expenses caused by introduction of special components and systems into the NPP structure for confining sodium leaks is not considerable in the total capital and operating cost of the NPP.In the last 10 years, there was only one event of unscheduled load factor decrease in the BN-600 power unit due to failure related to sodium systems. In 2002, it was made replacement of MCP-2 in one loop of the secondary circuit caused by revealed defect in it.

6.6.2.3. Conclusion

The analysis of the effect of sodium technology on operational performance of SFR made mainly on the basis of statistical data on the BN-600 power unit operation testifies to a high degree of mastering sodium technology and its minimum effect on the power unit performance.

6.6.3. Review of data on sodium leaks in Russian sodium-cooled fast reactors

6.6.3.1. Introduction

The purpose of this section is to review sodium leaks which occurred in sodium systems and equipment of Russian experimental and industrial SFRs and estimate the character and extent of their influence on safety of these SFRs. Both sodium leaks outside and within the SG are considered in this review [370, 371]. Review of leaks outside is implemented for BR-5/10, BOR-60, BN-350 and BN-600 reactors. Review of leaks in the SG is done on the basis of the BN-600 operation.

6.6.3.2. Influence of sodium leaks on SFR safety

In spite of a rather long period of operation of the Russian SFRs, there has not been one severe accident, thus showing a high degree of self-protection of these reactors against severe accidents. All failures and abnormal operating conditions that occurred in the sodium systems did not result in any severe consequences and were successfully overcome by existing safety systems.

Analysis of experience gained in these cases is important for the real estimate of how such events related to sodium coolant features could influence SFR safety, as well as impact personnel, inhabitants and the environment.

6.6.3.2.1. Sodium circuit leaks

There have been 61 incidents of sodium leaks from the circuits during operation of SFR in the USSR and Russia (BR-5/10, BOR-60, BN-350 and BN-600):

BR-5/10 (~44 years of operation)	19 events
BOR-60 (~40 years of operation)	0 events
BN-350 (~26.5 years of operation)	15 events
BN-600 (~30 years of operation)	27 events

The majority of leaks occurred in the early stage of mastering sodium technology and these were caused by the lack of experience in operation, designing and manufacturing of sodium equipment and systems. The more frequent reasons of leaks were at this stage: erroneous actions of the personnel (improper procedure of sodium unfreezing, mechanical formation of holes due to wrong actions of personnel), design deficiencies in electrical heating system, defects of sodium valves, flange joints, sodium level indicator sensors, manufacture defects, insufficient self-compensation of pipeline thermal expansion etc. It is very important that in the process of operation of any SFR, no increase of sodium leak frequency with time has been observed, but, on the contrary, there is a pronounced trend of its decrease resulting in the long time periods without any sodium leaks. Further on, as the experience was gained and sodium technology was developed, sodium leak frequency decreased significantly. For instance, in

the BR-10 reactor, no sodium leaks have occurred since 1986, the last sodium leak in the BN-600 reactor was detected in 1994 and in BOR-60 reactor almost no sodium leaks from the circuits have occurred during the whole period of its operation.

According to their initiation causes the leaks have been distributed as shown in Table 6.14.

TABLE 6.14. INITIATING CAUSES OF SODIUM LEAKS IN BR-5/10, BN-350 AND BN-600

Cause	BR-5/10	BN-350	BN-600
Pipe burn-through by electric heaters	2	-	-
Failures of pump-vessels level indicator sensors	6	-	-
Sodium valve failures	7	-	2
Improper procedure of sodium unfreezing	2	6	4
Manufacture defect	1	-	3
Crack formation on a pipe	1	-	6
Flange joint defects	-	2	5
Intercircuit leaks in steam generators	-	2	-
Mechanical formation of holes as a result of direct actions by personnel	-	4	2
Steam generator sodium valve seals	-	-	5
Uncertain reason (may be, corrosion)	-	1	-
TOTAL	19	15	27

Experience gained on sodium leaks from the circuit outside shows that:

- Sodium leaks do not influence reactor safety due to appropriate systems and technical decisions;
- The analysis of leaks occurred and the character of their origin and further development shows that the small leaks with slow rate of their development (frequently without sodium burning) are most typical at low pressure characteristic for SFR sodium circuits. Finally, it allows ensuring their timely detection and localization excluding by this any appreciable radioactivity release outside;
- The frequency of sodium leaks is minimal once sodium technology has been mastered and thus does not render a practical influence on the operational performance of a SFR.

Besides, the approach of placing all sodium systems of the primary circuit inside a reactor vessel provided in the advanced SFR designs reduces the probability of radioactive sodium release does not exceed the value valid for the residual risk.

However, there were no severe consequences of failures that occurred in the sodium systems of the Russian SFRs. As it was mentioned above, one of the features of a SFR is low pressure in the sodium circuits. As a rule, this results in the low rate of defect expansion in the sodium systems and, hence, the slow increase of the sodium leaks. This makes it possible to detect the leak on its early stage, i.e. when the leak is still small. As mentioned in the section devoted to description of the BN-600 operational experience, all 27 sodium leaks that occurred during its operation were detected in due time by control systems or operators.

There was only one case of leak and fire of radioactive sodium from the primary circuit, for which the design measures against the consequences of sodium fire were used: in this case, radioactivity release (10.7 Ci) was well below the permissible limit. The effect of this low radioactivity release on the boundary of the NPP controlled area is equivalent to 0.001 of natural background radiation. This incident was classified by the level 1 of INES scale. There was no need to use drainage-based fire fighting systems.

Thus, experience of operation of SFR and sodium systems gained in Russia shows that safety is reliably assured in the case of sodium leak outside by implementing certain technical decisions and equipment, as well as appropriate system of quality control on the stages of designing and manufacturing of sodium components and systems.

6.6.3.2.2. Steam generator leaks

In order to eliminate the possible effect of accidents caused by SG leaks and the resulting sodium-water interaction on reactor safety, three-circuit heat removal systems are used for SFRs.

The presence of an intermediate, non-radioactive sodium circuit isolating the SG from the radioactive primary circuit and spatial separation of the primary circuit and SG premises makes it possible to eliminate possible effect of the SG on either reactor core or integrity of the primary circuit as a whole.

Thus, the construction and layout decisions provided in SFR designs exclude a danger of development of failure caused by SG leak to radiation accident or nuclear accident with core disrupture. The incidents caused by SG leaks influence only equipment and systems of the secondary circuit. From the point of view of this influence, SG leaks are subdivided into two categories: “large” and “small” leaks. In the first case, the leak is accompanied by change of integral parameters of the secondary circuit; in the second case, change of integral parameters of the secondary circuit is not observed.

The special systems of emergency protection are provided for SG protection against leaks which should prevent an emergency at a stage of the “small” leak and exclude its development into the “large” leak.

During the whole period of BN-600 SG operation, 12 leaks of steam and water into sodium have occurred; half of these leaks took place in the first year of operation as a consequence of hidden manufacturing defects. Inter-circuit leaks took place mainly in the superheaters (6 events) and reheaters (5 events), while only one leak occurred in the evaporator. In all cases, these leaks have not resulted in SG failure, indicating the fact that the systems of emergency SG protection have demonstrated reliable operation and performance of their functions.

6.6.3.2.3. Conclusion

Review of sodium leaks shows that they do not make a significant influence on safety of the SFR. There was only one incident for all period of operation of Russian SFRs which was estimated by a level 1 in accordance with INES scale. The gained experience confirms an opportunity of the practical decision of SFR safety problems caused by sodium leaks outside and in SG.

6.7. Structural material

6.7.1. Structural material for fuel pin cladding

6.7.1.1. Austenitic steels

Extensive R&D work has been devoted to austenitic steels by all the countries developing fast reactors. The status of development in the main national groups can be summarized as follows.

Europe [372]

The national programmes in France and Germany led to the selection of titanium-stabilized (0.4-0.5%) cold worked (15-20%) steels as reference candidates, namely the French 15-15 Ti alloy (10 Cr Ni Mo Ti B) and the German DIN 1.4970 alloy (10 Cr Ni Mo Ti). For these cladding materials, more than 10 000 pins with oxide fuel and peak cladding temperature up to 650°C have reached dose values of 100 dpa (NRT) and about 1000 pins have exceeded 125 dpa with a maximum value of 148 dpa for an experimental sub-assembly (217 pins). No actual endurance failure occurred with the reference fuel design. These large numbers of irradiated pins have emphasized the beneficial effects of an adjustment of cold work level and the addition of some minor elements (Ti, C, Si, P), on the swelling and irradiation creep behaviour where the increase of incubation dose before swelling occurs is the most important factor.

The mechanical properties of these materials have also been accurately investigated through tensile tests performed both in the longitudinal and transverse directions using specimens machined from defuelled Phénix fuel elements. The results showed that the mechanical behaviour depends not only on the test and irradiation conditions but also on the swelling resistance. The effect of irradiation varies with temperature: hardening at low temperatures and softening at high temperatures was observed, associated with dislocation re-arrangements, but no recrystallization occurred. It appears that, at least up to about 120 dpa, these alloys have sufficiently high temperature strength and adequate ductility in the temperature range of fuel pin cladding.

The post-irradiation results have also confirmed the excellent resistance of these materials to external sodium corrosion (maximum depth of 30 mm measured on a Phénix pin irradiated to 13,6 at% over 826 EFPD (equivalent full power days). Development work has been carried out, within the framework of the European Collaboration, leading to the specification of a reference cladding material, the so-called AIM1 (Austenitic Improved Material number one), designed to meet the European Fast Reactor (EFR) project target (170 dpa).

In parallel, an R&D programme has been performed to develop advanced austenitic cladding materials (10.15 Cr/15.15 Ni type - Ti Nb stabilization - high P content...). Ti stabilized material containing 12 Cr and 25 Ni has been irradiated in Phénix with promising results: its swelling resistance is clearly higher than the best alloy 15.15 Ti, even Si modified.

United States of America

Valuable experience has been gained on the 20% CW titanium stabilized stainless steel designated "D9", irradiated in the Fast Flux Test Facility (FFTF) with oxide fuel at peak cladding temperatures up to 675°C. On the basis of more than 2000 highly irradiated pins, a

target exposure of 100 dpa was demonstrated and exceeded up to a maximum value of about 140 dpa. Alloy D9 reached 37% volume increase at a peak fluence of 24×10^{22} n/cm^2. D9 exhibits a longer fluence incubation period at higher temperatures than 316 SS. The D9 alloy has not, however, fulfilled the early promise of optimistic swelling correlations. This extensive experience demonstrated that the performance of the D9 alloy at large exposure was quite good, but it was also observed that when swelling is large (e.g. greater than 10% diametral), this type of cladding material is prone to brittle failure, particularly at handling temperatures (when examined in hot cells), attributed to localized channel fracture. Therefore, a functional limit of about 110 dpa was used for designs with 5.84 mm diameter cladding for the FFTF.

Austenitic stainless steels, like grade 316, will have densification when held at a constant temperature. This mainly occurs because of the formation of carbides as well as the annealing out of the dislocations from cold working. The effect increases for materials with a larger cold working. The densification competes with radiation-induced void swelling, which in turn causes a volume expansion with the increase in radiation dose.

The swelling in austenitic stainless steels is a strong function of its composition. The effect of the bulk nickel concentration on swelling is shown in Fig. 6.91.

The addition of cold working to 316 stainless steel will also decrease the swelling, which is evident in Figs 6.92 and 6.93 [373].

In Fig. 6.93 it is noted the diminishing effect of higher cold working. A cold working of 20% was used in the US fast reactor cladding and duct programmes for swelling resistance. The general trend for swelling in cold worked 316 stainless steel in depicted in Fig. 6.94 [374].

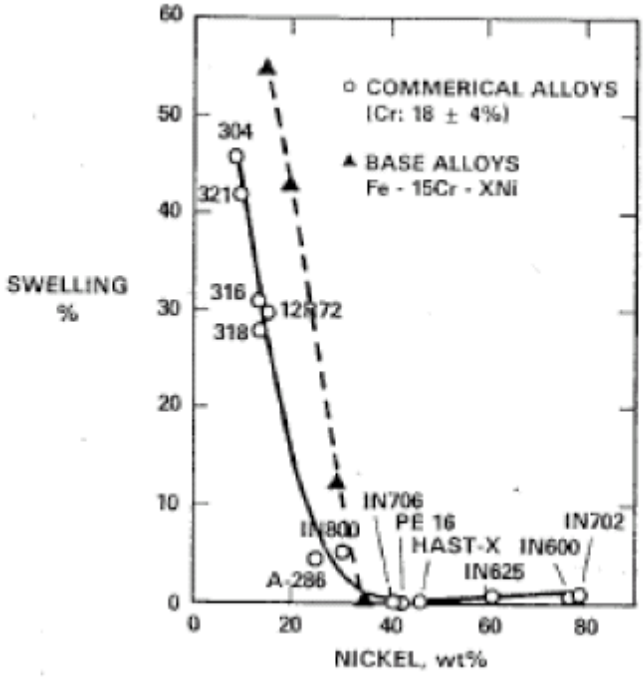

FIG. 6.91. Void swelling for austenitic stainless steels when irradiated at 625°C [373].

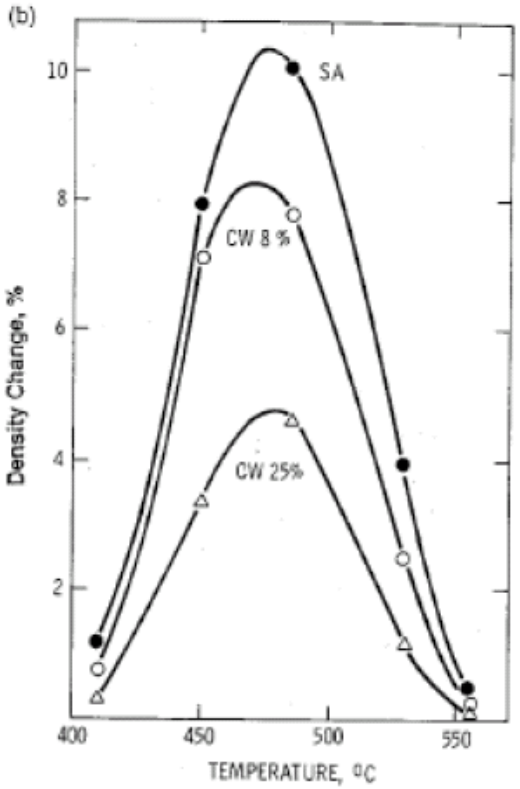

FIG. 6.92. Effect of cold working on void swelling for austenitic stainless steels as a function of cold work [373].

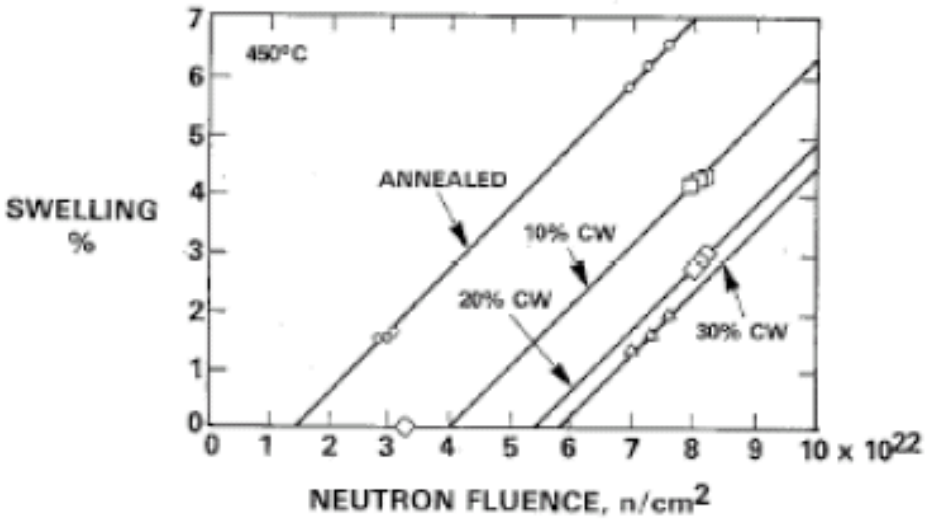

FIG. 6.93. Effect of cold work on void swelling in 304 stainless steels [373].

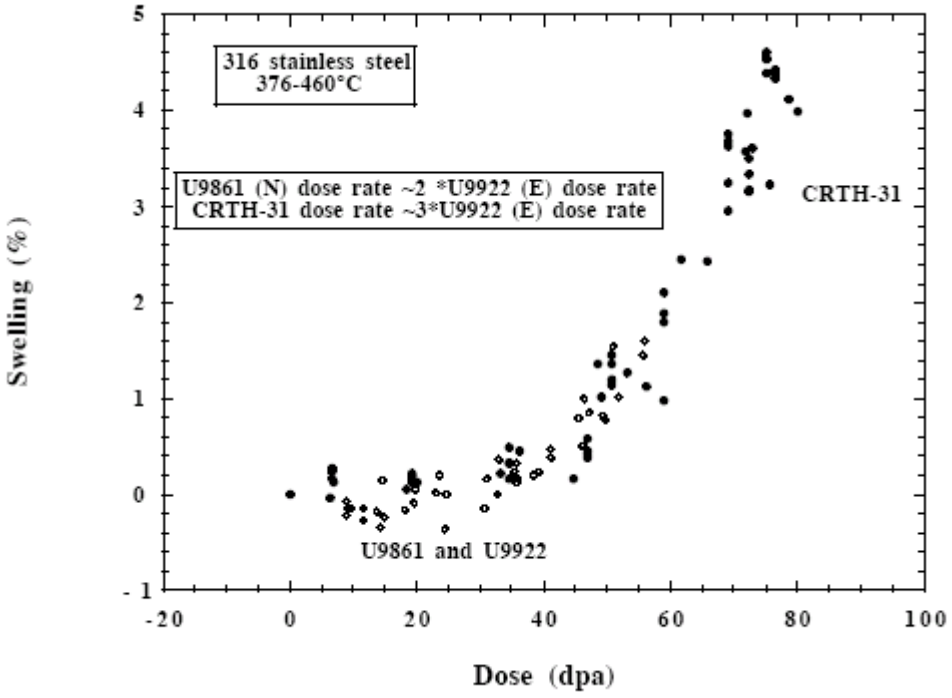

FIG. 6.94. Void swelling of three different 316 stainless steel ducts irradiated in EBR-II with 12% cold working [374].

Japan [397]

Standard type 316 austenitic stainless steel has been modified for fuel pin cladding material by optimizing alloying elements, cold-work conditions, and grain size, and then examined by out-of-pile and in-pile tests in Joyo and foreign fast reactors (Rapsodie, Phénix, DFR, EBR-II, FFTF). The optimized one has been defined as PNC316 [375], and applied to Monju fuel. Material specimens of PNC316 have been irradiated up to 185 dpa at elevated temperatures ranging from 415°C to 670°C. Also, out-of-pile testing demonstrated that creep rupture strength of PNC316 at 650°C for 10000 hr is more than 200 MPa. Pressurized tube specimens were irradiated in FFTF up to 100 dpa and have been irradiated in Joyo up to 10 dpa in order to investigate in-pile creep rupture property. In addition, more than 27 000 driver fuel pins have been irradiated in Joyo over 50 dpa, and a subassembly was irradiated in FFTF up to 120 dpa.

Russian Federation

Conventional austenitic stainless steels have been optimized by addition of B, Ti and Mg. Extensive experience, involving more than 100 000 fuel pins, has been gained on the 20% CW TchS-68 steel irradiated in BN-600 with oxide and MOX fuels at peak temperatures up to 700°C. More than 2500 fuel pins reached doses more than 80 dpa, with a maximum dose of 94 dpa. This steel has been used successfully as the standard cladding material since the beginning of 1991. Post-irradiation profilometry has shown quite high volume increase of the TchS-68 steel: up to 12% at doses 85-90 dpa. Destructive post-irradiation examinations (PIE) resulted in brittle failures of this type steel at handling temperatures. Development work has been carried out for the further improvement of austenitic steel in order to increase its strength and ductility and to decrease its swelling by optimising the additive composition and

improving the metallurgical and technological processes. Samples made of improved austenitic steels have been irradiated in BN-600 up to 108 dpa.

India

Alloy D9 stainless steel (SS) has been chosen as the fuel clad and fuel subassembly wrapper material for India's Prototype Fast Breeder Reactor (PFBR) in view of its higher void swelling resistance as compared to 316 SS. In PFBR, the fuel clad tubes experience temperatures in the range of 673-973 K under steady state operating conditions. For a target burnup of 100 000 MWd/t, the maximum neutron dose is 85 dpa. Major loads on the fuel clad are the internal pressure due to accumulated fission gases released from fuel matrix (~ 5 MPa) and moderate fuel-clad interaction. The hexagonal sheath of the core subassembly operates at relatively lower temperatures than the fuel clad. The typical operating temperature range is 673-873 K. Alloy D9 SS has been developed by adjusting the composition of 316 SS, from considerations of lower void swelling and irradiation creep. It contains controlled additions of silicon and titanium, higher level of nickel and lower level of chromium as compared to 316 SS. Small addition of boron (10-20 ppm) is made to improve creep ductility. Grain size is specified between ASTM No. 7 and 9 for clad and 5 and 9 for wrapper tubes. Chemical composition of Alloy D9 SS, specified for PFBR is given in Table 6.15.

TABLE 6.15. CHEMICAL COMPOSITION OF ALLOY D9 CLAD AND WRAPPER TUBE (VALUES IN MASS PERCENT, UNLESS OTHERWISE SPECIFIED)

Element	C	Ni	Cr	Mo	Ti	Si	Mn	S	P	B	N	Fe
PFBR Spec	0.035-0.05	14.5-15.5	13.5-14.5	2.0-2.5	5-7.5×C	0.5-0.75	1.65-2.35	0.01 max	0.02 max	10-20 ppm	0.005	Balance
Clad tube	0.053	15.9	15.0	2.3	0.35	0.57	1.55	0.004	0.01	-	0.042	Balance
Wrapper tube	0.045	15.24	13.88	2.12	0.23	0.64	2.12	<0.005	<0.005	12 ppm	0.002	Balance

Since the clad and wrapper tubes will be used in 20% cold worked condition, the high temperature stability of the cold worked microstructure was studied to arrive at the optimum level of cold work. The main fabrication variables which influence the stability of the cold worked alloy D9 SS are the solution annealing treatment, percentage cold work and Ti/C ratio. The stability of cold worked microstructure was found to be enhanced in the temperature range 873–1023 K due to precipitation of secondary titanium carbide (TiC), which has been found to have a strong influence on the retardation of recovery and recrystallization processes. To increase the amount of secondary TiC precipitates and reduce the amount of coarse primary Ti(C,N) precipitates, the solution annealing temperature should be increased. Stability of the cold worked microstructure was observed to increase as the solution annealing temperature was increased in the range of 1343–1473 K. However, the grain size increased above the specified upper limit of about 60 μm, at the highest solution annealing temperatures.

Creep rupture properties of alloy D9 SS clad tubes were evaluated at 923 and 973 K at various stress levels. The tubes have been procured in (20±4)% cold worked condition. Chemical composition of the material corresponds to Ti/C = 6. The results are compared with the creep properties of 20% cold worked 316 SS cladding tubes. A power law relation ($\dot{\varepsilon}_s = A\sigma^n$,

where $\dot{\varepsilon}_s$ is the steady state creep rate, σ is the applied stress, n is the stress exponent, and A is an empirical constant) was obeyed between applied stress and steady state creep rate by both the materials. At 973 K, a two-slope behaviour was observed. The creep laws at 923 and 973 K for D9 SS clad tubes are given below:

$\dot{\varepsilon}_s = 2x10^{-13}\sigma^2$ at 973 K; stress 125 to 200 MPa

$\dot{\varepsilon}_s = 2x10^{-38}\sigma^{13}$ at 973 K; stress 200 to 250 MPa

$\dot{\varepsilon}_s = 1x10^{-37}\sigma^{12}$ at 923 K; stress 200 to 250 MPa

The variation of rupture life with applied stress for these materials is shown in Fig. 6.95.

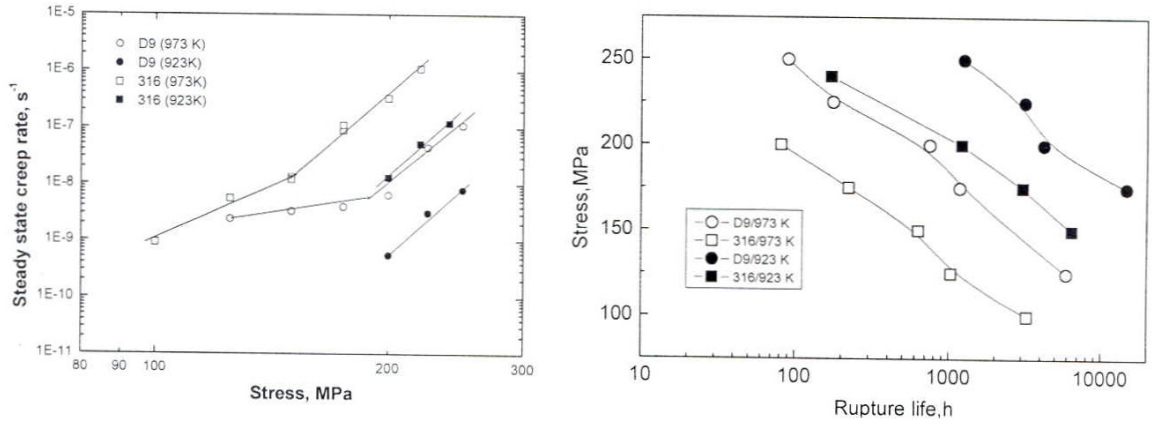

FIG. 6.95. Variation of steady state creep rate and rupture life with stress.

Creep strength of alloy D9 SS was higher than that of 316 SS by a factor of six at 973 K and by a factor of four at 923 K.

6.7.1.2. High nickel alloys

Europe

A high nickel alloy, designated STA Nimonic PE 16, was developed in the United Kingdom [372] as reference cladding material for PFR fuel and candidate for EFR fuel. This alloy was selected because of its high temperature strength and subsequent irradiations in both DFR and PFR showed an inherent resistance to void swelling. Much experience has been gained with PFR oxide fuel pins (5.84 mm and 6.6 mm OD). Of a total 96 200 pins irradiated, approximately 3500 pins have exceeded a dose level of 100 dpa and 265 pins have reached a maximum exposure of 155 dpa; of the failure events which have occurred only a very limited number have been associated with the high burnup designs. The maximum diametral strain measured so far in any STA PE 16 clad pin in UK has been about 1% and there have been no indications of any rapid rise in swelling rate at high dose, so that diametral strains of around 2-3% are predicted at 200 dpa. The PFR pin irradiation programme which

involved 30 different casts and over 100 different batches has shown no significant variation from the expected swelling behaviour of the pins examined to date, implying little sensitivity to composition variation within the specification given to the tube manufacturers. Post irradiation mechanical properties tests show considerable strength is retained at high doses with values similar to these measured at around 40 dpa. Ductility appears to be decreasing with increasing irradiation temperature and at temperatures above 500°C falls below 1%. It would appear that this is related more to the structure developed during high temperature irradiation than to test temperature.

Japan

In Joyo, a high nickel alloy with 15% Cr and 35% in mass has been applied to reflector elements in order to improve core performance, and several types of solution or precipitation hardened high nickel alloys have been irradiation-tested by use of the core material irradiation rig [375].

6.7.1.3. Ferritic/martensitic alloys

Ferritic/martensitic alloys are being developed as cladding materials, both in their standard form (a) and as oxide dispersion strengthened steels (ODS) (b).

(a) Traditional ferritic/martensitic alloys

France

In France, EM 12 (9.6Cr-0.12Ni-l.91Mo-0.92Mn-0.37Si-0.41Nb-0.28V-0.086C-0.019P) has been tested in the Phénix reactor where two subassemblies reached a maximum exposure of 120-130 dpa at a moderate peak cladding temperature (600–630°C max).

Russian Federation

In the Russian Federation, the EP 450 alloy (13%Cr-2Mo-Nb-P-B-V), also used as duct material, has been successfully irradiated in one BOR-60 demountable subassembly beyond 180 dpa at a peak cladding temperature of 680°C at the beginning of life. Subassemblies of standard design based on vibropac, polydispersive MOX fuel with metal uranium powder getter additions and EP-450 cladding, were tested in BOR-60 up to 26 at.% burnup (140 dpa). PIE revealed no corrosion damage of the internal surface of the cladding.

United States of America

A large amount of experience has been accumulated on the so-called HT-9 alloy considered as reference material for metallic driver fuel of EBR-II and FFTF. The highest exposure doses were reached with FFTF oxide fuels at limited peak cladding temperature (600°C), with a record level of about 200 dpa, without cladding failure. Furthermore, some of the lead tests were performed at cladding temperatures in the range of 640°C-660°C. Post irradiation results confirmed the inherent characteristics of this type of material to be very good resistance to void swelling, very small diameter changes (0.5% at 120-130 dpa) except, in some pins, a peak cladding deformation (up to 1.7% at 120-130 dpa) towards the top of the fuel column, associated with cesium build-up and reduced creep strength at high temperatures in this upper part of the pins; limited high temperature strength which implies stringent design limits and raises some concern with regard to pin failure behaviour, especially in the context of current commercial reactor conditions (peak cladding temperature of about 650°C).

Information on radiation properties for ferritic and martensitic steels of HT-9 material has been reported by T. Allen, et al. [376]. The main candidate material for cladding and duct material is HT-9 which was developed as part of the US Liquid Metal Fast Breeder Reactor (LMFBR) development program. Current advanced reactor studies in the United States are considering HT-9 for both the cladding and duct material [377] for the Advanced Burner Test Reactor (ABTR). The ABTR primary system is configured in a pool-type reactor arrangement, which is similar to the EBR-II reactor, with the reactor core immersed in a pool of sodium coolant within the reactor vessel.

The nominal composition of the HT-9 material by Sandvik is Fe-12.0%Cr-1%Mo-0.6Mn-0.6Ni-0.3%V-0.5%W-0.38Si-0.2%C [378]. When the material was first introduced into the fast reactor cladding and duct program, the heat treatment of HT-9 after fabrication had a short time, of approximately five minutes, normalizing anneal at 1038°C with a rapid argon cool-down. The annealing was followed by a tempering treatment at 760°C for 30 minutes followed by a rapid argon cool-down [379].

An improved thermo-mechanical treatment was later developed to improve the stress-rupture lifetime. The thermo-mechanical treatment annealed at 1100°C followed by tempering at 675°C (annealing and normalizing times were similar to the original treatment) and was chosen as the thermo-mechanical treatment for the FFTF Core Demonstration Experiment (CDE). Ductile-to-brittle transition temperature (DBTT) generally increases with increasing grain size by increasing the austenitizing temperature. Based on a given grain size, tempering at the higher temperature lowers the strength, which should improve fracture properties. Thus the improved heat treatment provides gains in creep-rupture strength via an increase in the DBTT.

Swelling and creep can cause bow and distortion of subassembly ducts leading to unacceptably high loads which will not allow retrieval from the core. HT-9 material was chosen for fast reactor duct and cladding application because of its low swelling and low thermal expansion.

Recent data on HT-9 swelling indicates the possibly of significant variation in swelling based on irradiation conditions and/or material heat. The irradiation conditions may also affect swelling and has been showed that for Fe-Cr model alloys irradiated in two different reactors (EBR-II and FFTF), the transient period of swelling was much shorter in EBR-II (Fig. 6.96). So the transient period of swelling may be shorter than expected and should be monitored for new types of operating regimes.

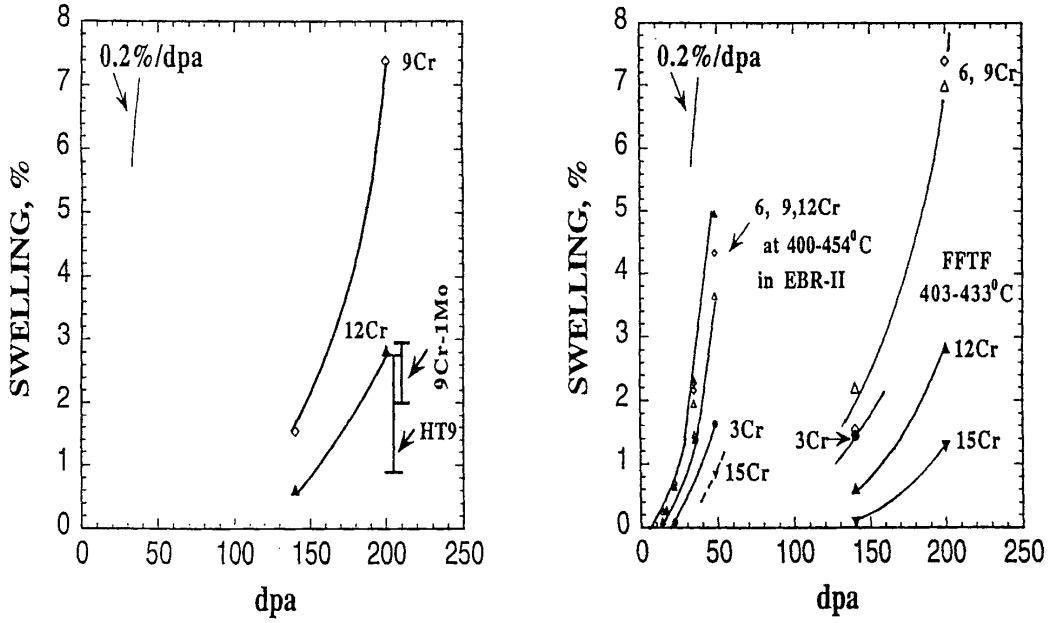

FIG. 6.96. Comparison of the swelling observed in HT-9 and modified 9Cr-1Mo steels irradiated in FFTF and the swelling of Fe-Cr binary type alloys in EBR-II and FFTF at 400-454°C.

The variability of swelling can also occur with different material lots. Swelling was measured in stress-free tubes fabricated from different heats of HT-9 irradiated in the FFTF at temperatures ranging from 384-427°C and to doses as high as 165 dpa. The swelling rate was essentially absent until about 100 dpa, at which point constant swelling rates of 0.00216%/dpa and 0.00975%/dpa were established for two separate heats. The maximum swelling observed was 0.9% at 165 dpa.

It has been suggested that the following items are not understood with respect to swelling in bcc alloys:

- At high temperatures of around 600°C, swelling may occur at high doses especially under lower dose rate conditions. Such conditions were not previously explored because swelling was not expected at these temperatures.
- Swelling in bcc types of steels may be more susceptible when subjected to high levels of helium and hydrogen.
- Well-controlled materials irradiation tests will most likely yield conservatively low amounts of swelling when compared to those conditions of a more typical temperature history based on normal reactor operation.

When HT-9 material is employed, swelling is not a primary concern, but the understanding of the swelling variability due to material variability and irradiation spectrum variability should be considered in the reactor design phase.

Republic of Korea

The fuel cladding material in reference fast reactor design, KALIMER was selected as HT9 for its low swelling characteristics upon irradiation. However, it was estimated that HT9 cladding material was not conservative enough to satisfy the discharge burnup goal, because of the high coolant outlet temperature and low creep resistance characteristics [380]. Therefore the researches on these materials have been focused on increasing the creep rupture

strength. Formation of a more stable and fine precipitation is the key issue to improve the creep rupture strength of ferritic/martensitic steels. Nitrides are more stable and less soluble than the corresponding carbide because the enthalpy of formation of nitrides is higher than that of carbides. So an addition of nitrogen contributes to an increase of the creep rupture strength. Nitrogen of up to 0.10 wt% is added to form stable nano nitride particles in ferritic/martensitic steels. And the effect of a nitrogen addition and tempering temperature on the formation of nano particles in high Cr ferritic/martensitic steels has been studied. At about 500°C, a tempering produced fine needles of M_2X which was predominantly Cr_2N in ferritic/martensitic steels. Generally Cr_2N particles are less stable than $M_{23}C_6$ particles at a higher tempering temperature in ferritic/martensitic steels, and they are gradually replaced by Cr rich $M_{23}C_6$ particles. But the Cr_2N particles remained as a stable phase at a higher tempering temperature by increasing the nitrogen content. The shape of these particle was a fine needle type which was very similar to V(C,N) particles. These precipitates were not dissolved or largely coarsened during a creep deformation at 600°C. So it seems that they acted as an effective obstacle against a dislocation glide during a creep deformation, thus contributed to an increase of the creep rupture strength in ferritic/martensitic steels. Another approach is the replacement of Mo by W in high nitrogen ferritic/martensitic steel. The creep rupture strength of the alloy was about 150 MPa for 10^5 hours at 600°C. Application of ferritic/martensitic alloys to alternative fast reactor concepts:

Other fast reactor studies for the Generation IV programme include the options of the gas-cooled fast reactor (GFR) and the lead-cooled fast reactor (LFR). Current preliminary designs for GFR option use SiC composites for the fuel pin cladding and hex can wrapper (duct).

Recent studies in the LFR [381] programme are considering using ferritic/martensitic steels and modified ferritic/martensitic steels for additional corrosion resistance. Currently the fuel cladding for LFR is proposed to use existing ferritic/martensitic steels such as T91 or HT9. These steels have been shown to be corrosion resistance to lead-bismuth eutectic with active oxygen control at temperatures below approximately 550°C [382]. The active maintenance and control of the dissolved oxygen potential in lead-bismuth eutectic (LBE) and Pb coolants is an established technique for providing corrosion protection for steel. By maintaining the dissolved oxygen concentration within a proper range such that protective oxide layers of Fe_3O_4 (below approximately 570°C) form on the cladding and steel structures, but solid PbO does not precipitate in the coolant. Operating peak cladding at temperatures of up to 650°C will require the development and testing of new materials for service in Pb. A promising approach for the cladding makeup may be the weldment of a surface layer of Si-enhanced steel upon ferritic/martensitic steel to form a layered billet, which is then co-extruded [383]. This Si-enhanced steel layer will provide an improved corrosion resistance but has inherently poor irradiation stability. The ferritic/martensitic substrate of T91 or HT-9 will provide the structural strength and irradiation stability.

(b) Oxide dispersion strengthened ferritic/martensitic alloys

Some efforts have been made, particularly in Europe and in Japan to improve the high temperature strength of the ferritic alloys by optimizing their composition (out-of-pile development of a high Mo material in Japan) and, significantly, by adding TiO_2 or YO_2 to develop a dispersion-strengthened type, designated "ODS" steels. A first generation of these ODS alloys (DT and DY MOL ODS), manufactured by mechanical alloying, was tested in reactor, up to a maximum dose of about 90 dpa and exhibited post irradiation embrittlement which led to numerous and severe cladding failures in PIE hot cells. Microstructure and

tensile properties of these commercial alloys have been investigated as a function of their processing route [384]. Macro and microstructural evolution of the MA 957 type material has been determined as a function of time. Experimental observations have shown that, for the MOL ODS alloys, the main damage mechanism consists of microcracking of X phase precipitates on grain boundaries. Recrystallization phenomena have been seen in MA 956 and MA 957 alloys. Tensile properties of these materials are illustrated in Fig. 6.97.

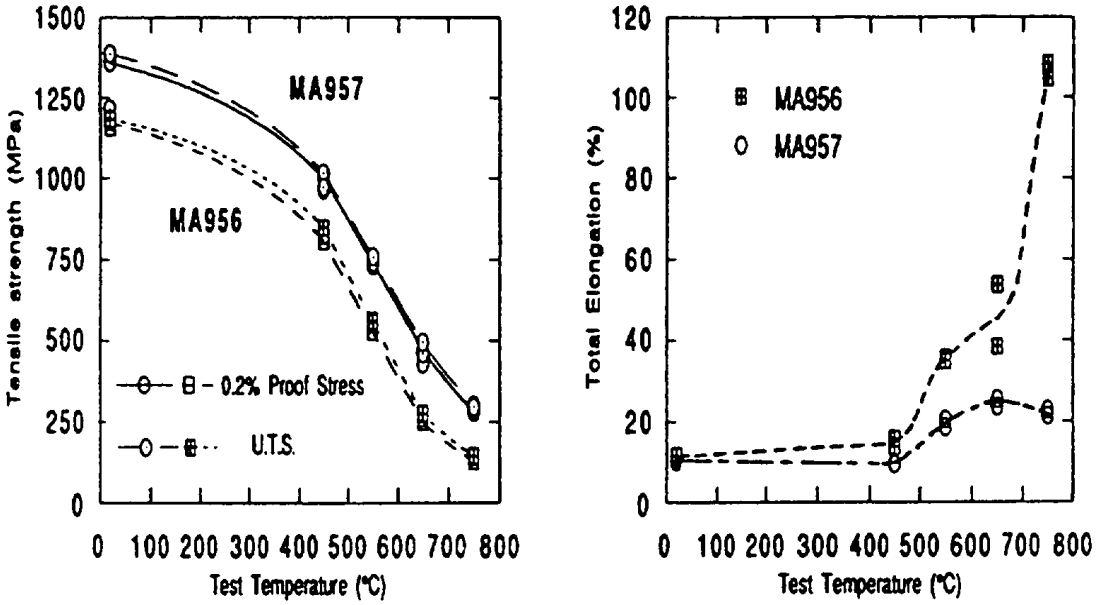

FIG. 6.97. Comparison of tensile properties of 25% cold-drawn specimens of MA 956 and MA 957 alloys.

Japan [397, 423-434]

The ferritic-martensitic alloy designated as PNC-FMS (0.12C-11Cr-0.5Mo-2W-0.4Ni-02V-0.05Nb-0.05N) has been irradiation-tested in Joyo. Even though PNC-FMS exhibits superior high temperature strength compared with conventional high chromium ferritic steels, it is much less than austenitic stainless steels such as PNC316. So, its utilization is limited up to around 650°C, since it will lose precipitation hardening mechanism over 650°C due to rapid coarsening of carbides and nitrides.

In order to overcome such disadvantage in precipitation hardening, oxide dispersion strengthened (ODS) ferritic steels have been developed since 1987 in JAEA [385-389, 390-394]. Oxide dispersion strengthening is the only mechanism which will enable to attain maximum cladding temperature over 650°C. ODS ferritic steel is recognized as the best prospective candidate cladding material for the sodium-cooled fast reactor. Two types of ODS steel claddings have been developed; 9Cr-ODS steel focusing mainly on radiation resistance with a basic chemical composition of Fe-0.13C-9Cr-2W-0.2Ti -0.35Y_2O_3 as well as 12Cr-ODS steel on corrosion resistance with a basic chemical composition of Fe-0.03C-12Cr-2W-0.3Ti-0.23Y_2O_3.

The ODS steels strengthened by the Y_2O_3 particles tend to be too hard to manufacture cladding by the cold-rolling. Also, the manufactured ODS steel claddings will have inferior creep

strength and ductility loss in the cladding hoop direction if their grains extensively grows toward a rolling direction. These technical problems have been successfully solved through a grain structure control by means of α to γ phase transformation for 9Cr-ODS steel and recrystallization technique for 12Cr-ODS steel with appropriate intermediate heat treatments [385, 386]. In order to evaluate the tensile strength in the hoop direction of the manufactured ODS steel claddings, the ring tensile tests were carried out. The tensile properties of the manufactured ODS steel claddings are represented in Fig. 6.98 and that of the conventional ferritic-martensitic steel (PNC-FMS) claddings is also plotted. All manufactured ODS steel claddings show the improved tensile strength over the entire temperature region. The uniform elongation of PNC-FMS tends to decrease with increasing temperature, whereas in ODS steel claddings the uniform elongation is adequately maintained and increases over 500°C. The improved uniform elongation in ODS steel claddings could arise from the retardation of recovery and continuing work-hardening due to pining the dislocation by Y_2O_3 particles. The creep rupture test for the manufactured ODS steel claddings was carried out under internal pressure conditions.

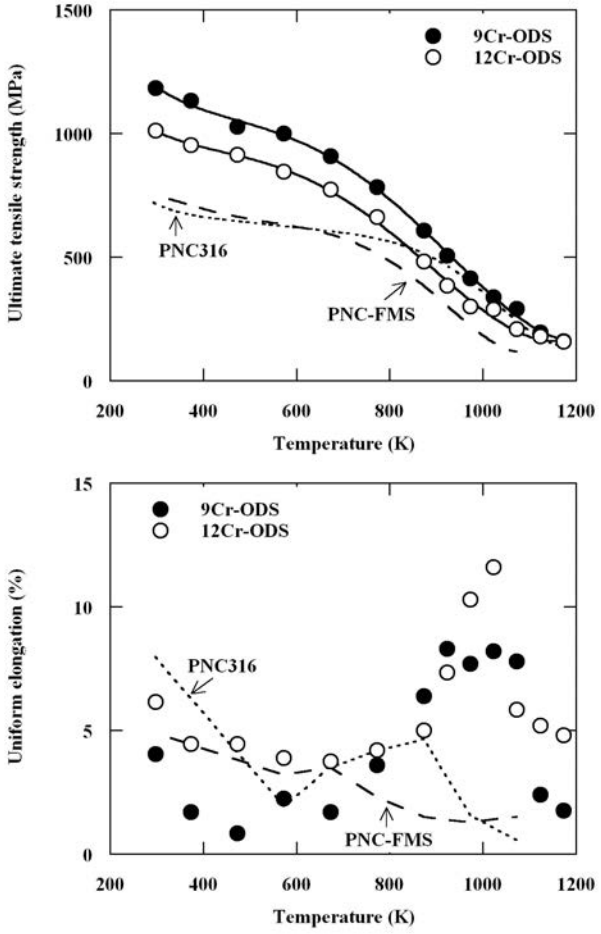

FIG. 6.98. Tensile properties of manufactured ODS steel claddings as a function of temperature: ultimate tensile strength (top) and uniform elongation (bottom).

Figure 6.99 shows the comparison of PNC-FMS and PNC316 [375, 395]. These curves were predicted on the basis of the Larson-Miller parameter method. The strength anisotropy perfectly disappears in the hoop and longitudinal directions, and the internal creep rupture strength level approaches the target of 120 MPa for 10 000 hr at 700°C that is required from the advanced fast reactor fuel design. This strength level is far beyond that of PNC-FMS, and

superior to even PNC316. In order to confirm and demonstrate the ODS fuel pins integrity to high burnup conditions, the irradiation tests in BOR-60 have been conducted under the collaborative works between JAEA and Research Institute of Atomic Reactors (RIAR) in the Russian Federation [386]. The first irradiation test had been already completed to the burnup of 50 GWd/t and neutron dose of 21 dpa. In addition, the ODS fuel pins irradiation tests in Joyo are also scheduled. These irradiation tests data will be applied to the licensing of ODS driver fuels in the Monju up-grade core.

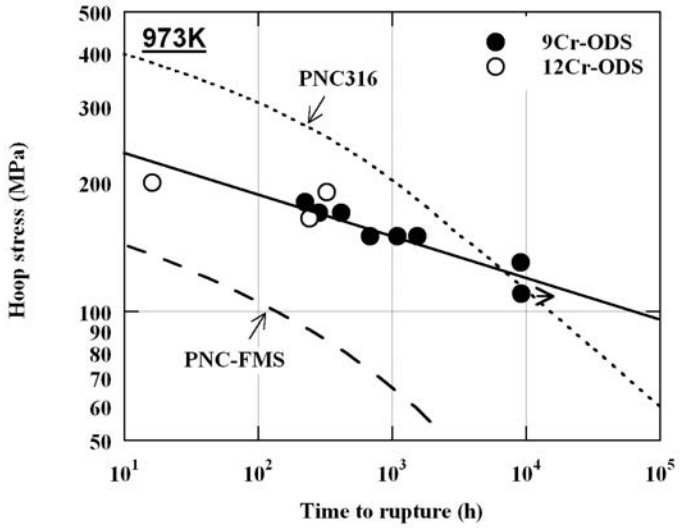

FIG. 6.99. Creep rupture properties of manufactured ODS steel claddings, comparing with those of PNC-FMS and PNC316.

Russian Federation

For a number of years there has been work on the technology and investigation of the properties of ODS alloys in the Russian Federation. A considerable amount of work has been carried out on development and investigation of a model ODS alloy based on steel 13Cr-2Mo. The effect of alloying this steel with V, Ti, Al, W, Nb has been studied. Oxides of Y, Ti, Ca were used as hardening particles.

The transition of ODS steel with ferritic structure to a two-phase ferritic-martensitic structure is of great interst. Samples of newly-developed ODS alloys with a ferritic content of 40-60% have been made and irradiated in the BR-10 reactor at temperature 650°C to study their high-temperature strength.

6.7.1.4. Conclusions on cladding material development

World-wide research and development work on various cladding materials has reached a very high level of understanding of the basic phenomena involved as well as of the operational requirements to be met by a well-designed fuel element. Austenitic alloys (15.15 Ti, 1.4970, PNC 316, D9, PNC 1520) have proved their ability to reach exposure rates as high as 150 dpa and their advanced versions (AIM1, CEA 12.25,...) are very promising candidates for the current target doses (170 dpa) of the commercial fast breeder reactors. Ferritic/martensitic alloys (HT 9, EM 12, PNC-FMS, EP-450) are also able to fulfill these objectives, if a limitation on peak cladding temperature is acceptable. For more ambitious targets (over 200 dpa), a large amount of R&D is still required for qualification of the most promising candidates, namely the ODS steels.

6.7.2. Wrapper-tube (duct) materials

The first generation of ducts were manufactured in austenitic steels which have since been progressively improved until they now satisfactorily reach neutron exposures as high as 140 dpa for the D9 alloy in FFTF [390] and approximately 125 dpa for the 15.15 Ti alloy in Phénix. In most of the countries developing fast reactors, attention is now currently focused on ferritic-martensitic steels.

In Europe, two candidates are under consideration, a plain 9Cr1Mo martensitic steel (EM 10) and a 10.12 Cr Mo V Nb (FV 448/1.4914). The highest doses achieved at present are 155 dpa for a FV 448 wrapper in PFR, and 115 dpa for 1.4914 and 146 dpa for EM 10 wrappers in Phénix. In the United States, the HT 9 alloy has been successfully irradiated in FFTF to the record dose level of around 200 dpa. In Japan [395-397], duct material of the ferritic-martensitic alloy designated as PNC-FMS [395] has been irradiation-tested in Joyo to beyond 90 dpa. PNC-FMS is identified as the candidate duct material for sodium cooled fast breeder reactor (SFR) cores in the Feasibility Study on Commercialized Fast Reactor Cycle Systems in Japan. Efforts have been made to establish material strength standards including heavy neutron irradiation data over 200 dpa (Fe), and to develop a dissimilar weld technique between PNC-FMS duct and SUS316 entrance nozzle or handling head [396, 397]. The dissimilar weld technique has been successfully developed without delta-ferrite formation. Material irradiation test of the dissimilar weld joint as well as standard part is under way using the core material irradiation rig in Joyo. In the Russian Federation, the most extensively studied alloy was a 13% Cr-Mo-Nb-P-B stabilized alloy (EP-450) irradiated in BOR-60 up to 140 dpa and in BN 600 up to 94 dpa.

Europe

The principal results obtained for the majority of ferritic-martensitic duct materials studied in Europe have been reviewed, [398]. It was noted that dimensional stability is very good, which correlates with a low swelling rate, especially for the fully martensitic alloys (less than 0.5% at all temperatures, Fig. 6.100) with a maximum at the lowest temperatures (below 400°C).

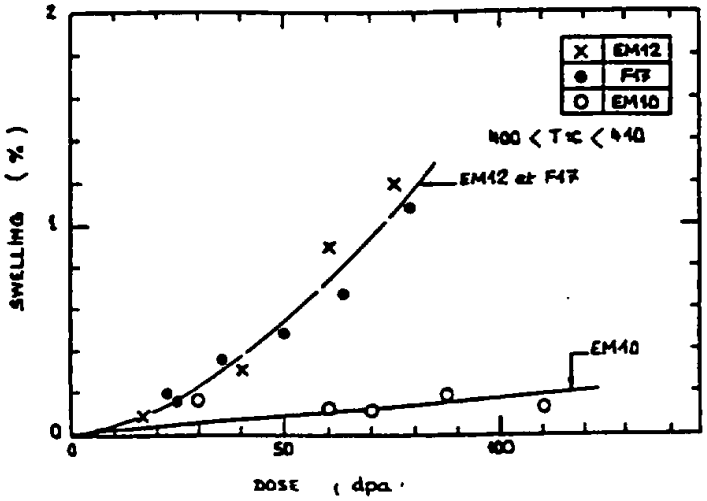

FIG. 6.100. Dose dependence of the swelling of EM 10, EM 12 and Fl 7 steels.

Tensile, charpy and fracture toughness tests were performed either on samples irradiated in experimental rigs, or machined from wrapper tubes. The results indicate that irradiation hardening can only be observed at temperatures below 500°C, that this effect saturates at low doses and that the properties of the alloys investigated are quite similar. The post-irradiation UTS and uniform elongations of EM 10 and 1.4914 have been plotted in Fig. 6.101 as functions of the irradiation temperature, which is equal to the test temperature; one can see that despite the wide range of doses investigated there is a single plot for both materials, and that the uniform elongation always remains above 1%.

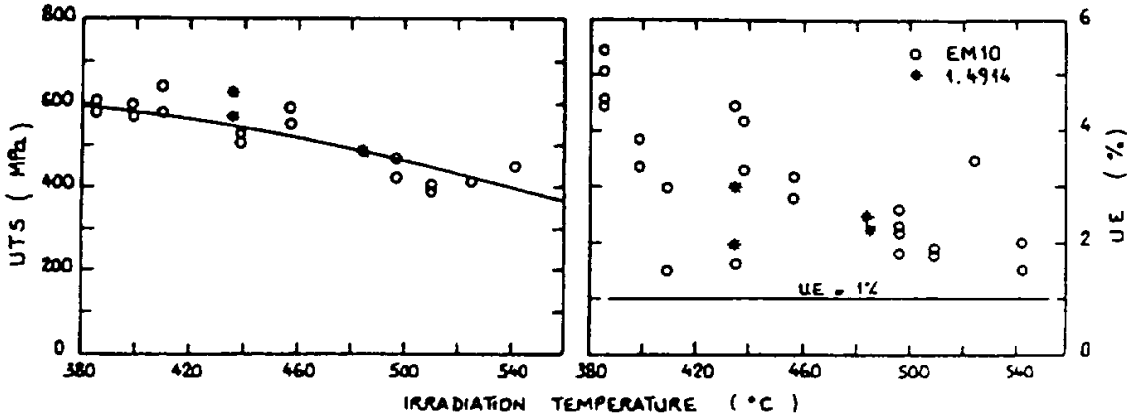

FIG. 6.101. Tensile properties of EM 10 and 1.4914 irradiated between 33 and 100 dpa.

Figure 6.102 gives, as a function of the irradiation temperature, the post-irradiation DBTT of various ferritic-martensitic alloys. The measured values, which do not depend significantly on dose, differ only slightly from one ferritic martensitic alloy to another. The DBTT shifts are relatively small and clearly compatible with the use of these materials for wrapper applications. Furthermore, test results at low dose rate on martensitic FV 448 indicate that the post-irradiation fracture toughness above DBTT remains high.

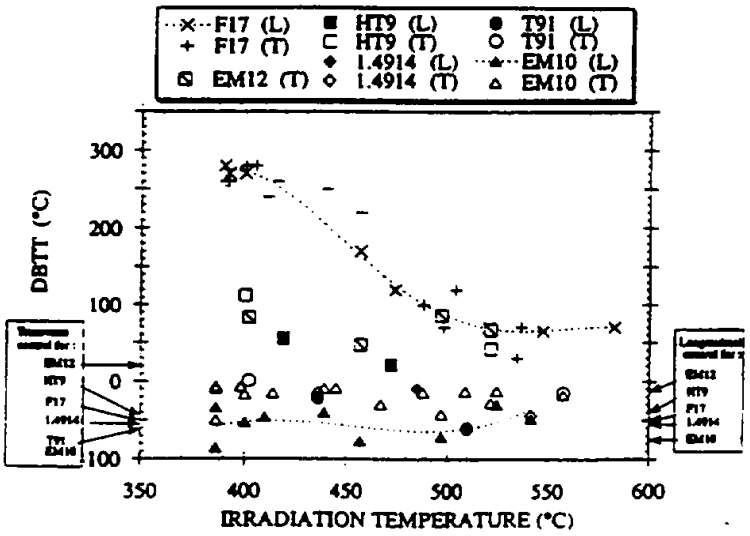

FIG. 6.102. Comparison of the DBTT observed after irradiation for various ferritic-martensitic steels.

Russian Federation

A large amount of experience has been accumulated in Russia on the irradiation behaviour of wrappers made of EP-450 steel: more than 400 subassemblies with EP-450 wrappers have been irradiated in BN-600 to a maximum dose of 94 dpa. Valuable experience on EP-450 wrapper irradiation was gained also in the BN-350, the peculiarity of this reactor being low inlet sodium temperature (280°C). These irradiations showed the high dimensional stability of EP-450 steel. Profilometry of a large number of wrappers in a water pool produced the following information:

- There is very smooth temperature dependence of EP-450 swelling with a maximum at 385-400°C;
- The dose dependence of EP-450 swelling is quite low: 0.004%/dpa;
- The mean value of the irradiation creep modulus is equal to 0.25×10^{-6} $(MPa\cdot dpa)^{-1}$ in the temperature range of T < 480°C;
- There is a trend for the irradiation creep modulus to increase at temperatures 350-360°C.

Destructive PIE of samples machined from BN-350 and BN-600 wrapper tubes demonstrated the following:

- The maximum changes in tensile and impact (Charpy) toughness occur at the bottom of the core in the zone with the minimum irradiation temperatures: the minimum value of ductility (0.5% at T=280°C) and the maximum value of DBTT (+175°C) were observed on samples machined from the bottom section of a wrapper with maximum dose 85 dpa.
- An irradiation hardening effect was observed at temperatures below 500°C. The dependence for a temperature of 350°C was as follows: in the dose range 20-25 dpa hardening increases; then an effect of saturation was observed; and for doses higher than 40 dpa there was a smooth decrease of the hardening.

In conclusion, on the basis of present knowledge, the more promising martensitic duct alloys can be considered as able to meet the dose requirements (170 dpa) for commercial fast breeder reactors and even to reach more ambitious targets (over 200 dpa).

India

Alloy D9 stainless steel (SS) has been chosen as the fuel clad and fuel subassembly wrapper material for India's Prototype Fast Breeder Reactor (PFBR) in view of its higher void swelling resistance as compared to 316 SS. Characteristics of alloy D9 wrapper tube are described along with D9 clad tube in Section 6.6.1.1. Tensile properties of alloy D9 SS wrapper tubes were evaluated at room temperature, after thermal ageing the tubes at various temperatures in the range of 823–1123 K for various ageing times from 10 to 10 000 hours. The wrapper tubes were manufactured in (20±4)% cold worked condition.

Figure 6.103 shows the effect of thermal ageing on room temperature tensile properties of the tubes. Significant changes in tensile properties were observed in the aged condition.

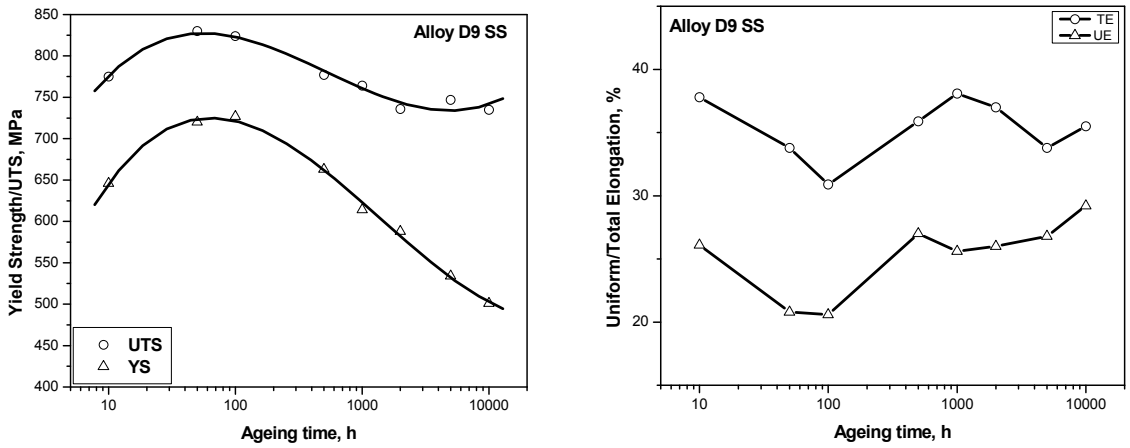

FIG. 6.103. Effect of thermal ageing at 923 K on room temperature tensile properties of wrapper tubes of PFBR.

6.7.3. Structural materials for shielding

Many materials have been used for shielding and/or as a reflector. For example, stainless steels, refractory materials (e.g., Inconel), graphite, boron carbide and depleted uranium have all been invoked. Traditionally these materials have been used to protect the core barrel from neutron irradiation damage as well as minimising activation. The proposal to use moderator materials is quite new, and therefore some aspects are discussed in this report.

Metal hydrides have been eligible for shielding materials (neutron moderators) because of their high hydrogen number density and resultant large neutron slowing down power. Zirconium hydride had been used as neutron moderators and reflectors in KNK reactor core, and irradiation-tested in EBR-II and BOR-60 reactors [399, 400]. Yttrium hydride has been preferred at higher temperature applications than zirconium hydride, and, in practice, had been applied to a cobalt-60 production subassembly in the FFTF [401]. It is noteworthy that zirconium hydride has been used as inert matrix for TRIGA fuel since 1960s [402].

6.7.3.1. Zirconium and yttrium hydrides [447-454]

For sodium cooled fast breeder reactor (SFR) core environments, zirconium and yttrium hydrides are candidate materials for in-pile applications, in case that metal hydrides are screened from a view of cost of raw metal, melting point, hydrogen number density, parasitic neutron absorption, activated products, dissociation properties, and phase stability (disproportionate reaction). In design studies of medium and large scale SFR cores in the Feasibility Study on Commercialized Fast Reactor Cycle Systems in Japan, zirconium hydride is applied to in-reactor radial shielding subassemblies in order to effectively reduce displacement damages [403]. Since cubic crystal structures are inherently resistant for anisotropic growth induced by radiation damage, Inoue and Ukai have determined the standard H/Zr and H/Y atomic ratios to be 1.65±0.02 and 1.80±0.03, respectively, in order to be dominated by a face centered cubic crystal structure phase (delta phase) at the service temperatures [404]. In addition, both hydrides specimens have been fabricated in laboratory scale and provided to measure physical and chemical properties. For example, thermal conductivity of zirconium hydride up to 923 K has been recently measured and, as shown in Fig. 6.104, thermal conductivity of zirconium hydride is comparable with an austenitic stainless steel [404]. It is noteworthy that Yamanaka et al. have conducted fundamental

studies on zirconium hydride to investigate the effect of hydride formation on mechanical properties of zirconium alloy claddings for light and heavy water reactors [405-410]. Zirconium and yttrium hydrides were immersion-tested at 823 K for 3000 hours in stagnant and high purity liquid sodium whose impurity oxygen content was 1.1 ppm by mass [404]. Weight measurements, optical microscopy, and electron probe microanalysis after the immersion revealed that both zirconium and yttrium hydrides are highly compatible with the liquid sodium.

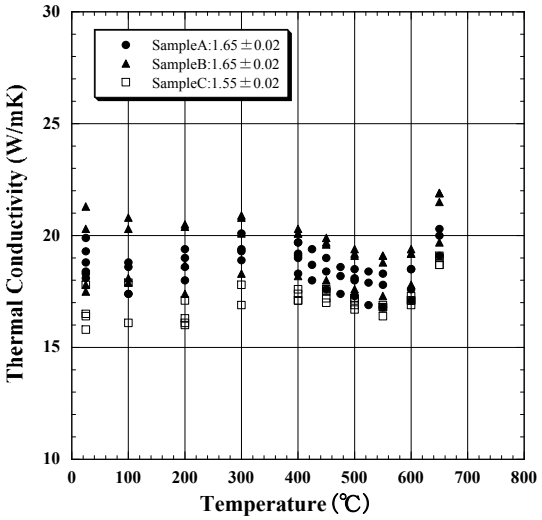

FIG. 6.104. Thermal conductivity of zirconium hydride disk specimens (H/Zr=1.65 or 1.55).

6.7.3.2. H ydrogen permeation barrier on cladding inner surfaces.

In a shielding subassembly loaded in the SFR core, zirconium hydride in pellets or blocks are clad with steel tubes, bonded with sodium or inert gas, and sealed by plugs. To prevent from dimensional instability due to void swelling at higher doses than 90 dpa (Fe), a cladding tube material should be ferritic and/or martensitic steel. Dissociated hydrogen from the hydride pellets chemically diffuses through cladding wall by a gradient of hydrogen gas partial pressures, and escapes into primary coolant. Excessive hydrogen loss will degrade shielding performance, induce phase instability of the hydride, and overload cold traps of coolant purification systems. The hydrogen loss practically limits a lifetime of the subassemblies. Therefore, development of hydrogen permeation barrier is necessary to reduce hydrogen loss in service. Inoue and Ukai have screened various coating processes and materials to be laminated out of commercially available techniques for the barrier. Since highly reductive liquid sodium coolant washes cladding outer surfaces, the barrier should be coated or laminated only to cladding inner surfaces. Also, the barrier coating process needs to be coherent with specific heat treatment condition of each cladding steel; for example, PNC-FMS, which is one of the candidate ferritic-martensitic alloys for fuel pin cladding, is normalized at 1373 K for 10 minutes followed by tempering at 1053 K for one hour. Thin layers of some inorganic compounds such as carbides, nitrides, and oxides are highly effective to be the barrier. In addition, much smaller hydrogen solubility metals including aluminum, copper, molybdenum, and tungsten than stainless steels also act as the barrier when laminated. In order to maximize the volume fractions of metal hydrides in the subassembly, thinner surface coating is desired. In conclusion, calorizing process has been selected as the most promising candidates. It is well known that calorizing process has been also paid attention for fusion reactor blankets for tritium production operated at elevated temperatures [411].

Hydrogen permeation rates with or without calorizing for PNC-FMS tube specimens are compared in Fig. 6.105. Oxidations under relatively low oxygen potential conditions practically produce the barrier function for calorized PNC-FMS surfaces.

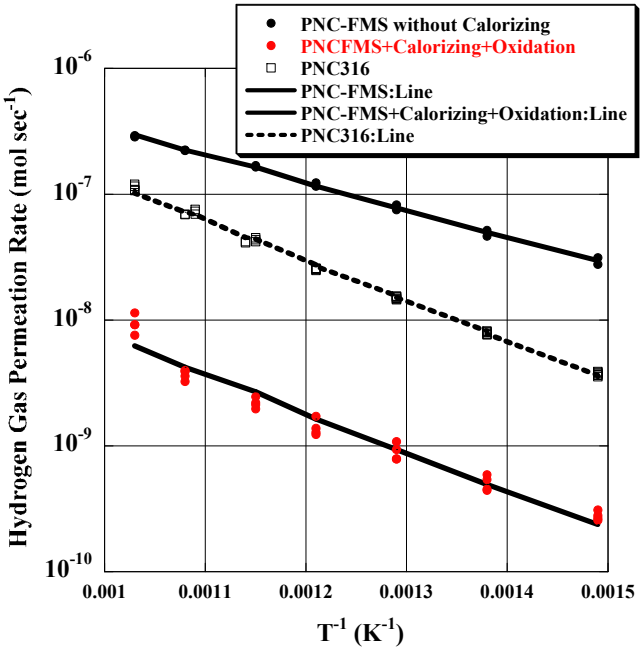

FIG. 6.105. Hydrogen permeation barrier by calorizing on PNC-FMS tube inner surface (PNC316: austenitic stainless steel).

6.8. Instrumentation and control system

This section describes the typical instrumentation in a fast reactor plant. In addition, some specific instrumentation systems are explained. The general and common knowledge of these fields is omitted for brevity.

6.8.1. Plant control system (PCS)

In a nuclear power plant the instrumentation and control (I&C) systems are generally grouped into three types:

(a) Plant monitoring and display systems that monitor plant variables and provide data to other I&C systems and to plant operators for use in controlling the operation of the plant. Typical examples include systems that monitor and display the status of the fire protection system, fluid flow temperatures and pressures. These systems also normally provide data visual and audible alarms at various control stations, particularly the main control room that notify operators of trends or particular values requiring actions by the operator to avert an actual problem of emergency.

(b) Plant control systems that are used to control all the normal operations of the plant. They are used in startup, power operations, shutdowns and plant control of normal operations of the plant. Typical examples include moderating fluids (liquid metal cooled) and steam control systems turbine generators controls and the myriad systems used to control the many circuit breakers, pumps and valves throughout the plant.

(c) Plant protection and mitigation systems. These systems are an additional separate layer of systems that monitor the plant variables. If they detect that the above described plant

monitoring and plant control systems have not kept the plant within a predefined set of conditions they take action automatically to rapidly shut down the plant.

Nuclear plants operate in the analogue mode with no centralized control system; instead they use the local pneumatic control and analogue field devices (transmitters and control valves). This approach has become problematic, because equipment was becoming obsolete and qualified safety-related spare parts were very hard to procure. Another factor that will have an effect is that large numbers of staff that know how to maintain analogue systems are retiring.

With these two issues in mind the nuclear industry has to transform to digital systems which means that they will have to transition into today's state-of-the-art instrumentation with a first step that may be the implementation of a centralized control system to provide better visibility to process operators. These digital devices can communicate by sending real-time information back to the centralized control system, providing vital information of the state of the process and the devices themselves. This two-way communication can effectively deliver a condition-based on-line, in service predictive maintenance programme that greatly enhances process yield, while reducing the cost of maintaining the infrastructure with time.

6.8.2. Leak detection

In a sodium-cooled fast reactor, diverse types of leak detectors and leak detection systems are employed, depending upon the sodium and ambient conditions. Below, several different sodium leak detectors are identified, along with their applications, and examples of steam generator leak detection systems are provided on the basis of PFBR.

6.8.2.1. Sodium leak detectors

6.8.2.1.1. Wire type leak detector

This detector is used where the leaked sodium does not get collected at a particular place and where the areas to be covered are larger. There are many factors influencing the detection time and the smallest leak that can be detected.

6.8.2.1.2. Spark plug type leak detector

This detector is used where the leaked sodium is accumulated at a place such as leak collection trays. Response time of the spark plug leak detector is better than the wire type leak detector since spark plug type detector is placed close to the expected leak point and the quantity of sodium leak it can detect depends on the volume where it is installed.

6.8.2.1.3. Mutual inductance type detector

This detector consists of a primary winding excited with high frequency constant current source and a secondary wiring. The design of the detector is such that it is noninvasive and it can be located external to the leak-collecting pocket provided in the system. Presence of sodium in the pocket changes the output of secondary, which is used as the leak signal. Mutual inductance type leak detectors are used to detect leaks in double envelope tubes, as the leaked sodium remains in liquid form (due to high temperature and inert interior), permitting it to spread and reach the collection pocket since the pipe is inclined.

6.8.2.1.4. Sodium aerosol detector

A sodium aerosol detector is highly sensitive to sodium aerosols and the minimum detectable concentration is around 1 nano-gram per cubic centimetre of the carrier gas. Because of this high sensitivity, it is used as an area monitor. Sampling tubes are provided to collect the aerosols from the areas of interest and directed to the detector.

6.8.2.1.5. Smoke detectors

Optical type smoke detectors are used for detecting smoke arising out of sodium fire. This detector is used as an area monitor. Overall response time depends on the time required for the smoke to reach the detector, which responds instantaneously.

6.8.2.1.6. Video smoke detection

Video camera is used at remote and inaccessible areas to confirm sodium leak before initiating the draining of sodium from the system. This helps to mitigate the damages to the system due to sodium leak.

6.8.2.2. Steam generator tube leak detection (India)

Early and reliable detection of water leaks is essential to prevent the propagation of sodium-water reactions and increase the operating safety of a sodium-cooled fast reactor. Figure 6.106 shows the leak detection system for the PFBR. A steam generator (SG) tube leak is broadly classified as a small leak, a medium leak or a large leak depending on the leak rate.

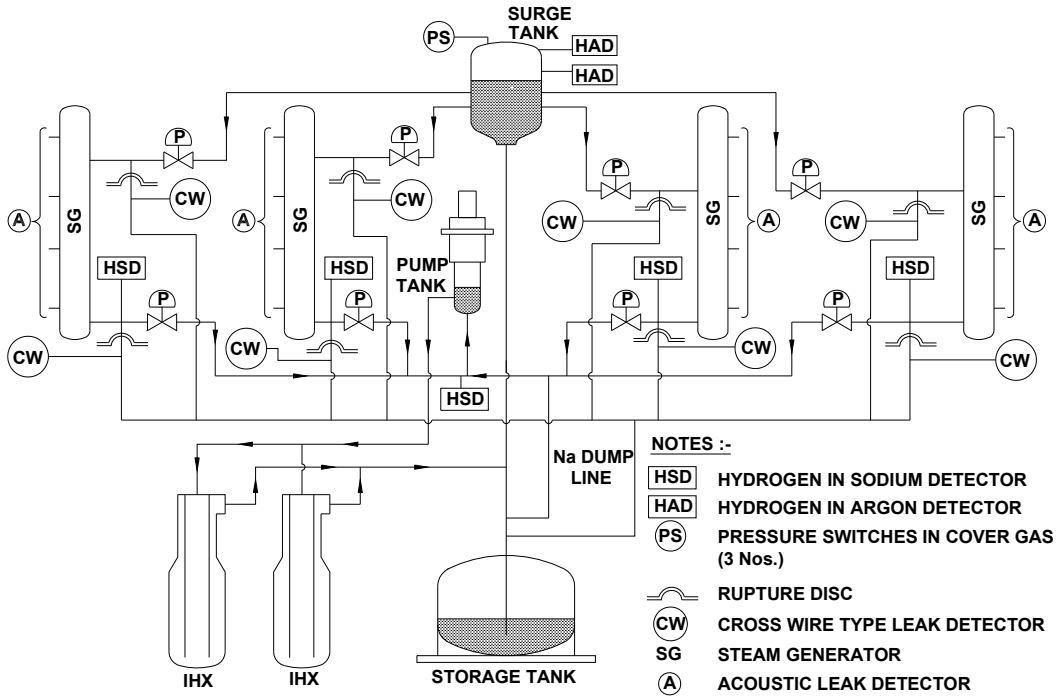

FIG. 6.106. SG Leak detection system in the PFBR.

The leak detectors provided for detecting each category of leak are listed in Table 6.16 and elaborated upon in the discussion that follows.

TABLE 6.16. LEAK DETECTORS USED IN THE PFBR

Leak classification	Detector(s)	Detector location
Small (< 10 g/s)	Hydrogen in argon detectors Electrochemical hydrogen meter Hydrogen in sodium detectors – sputter ion pump based	Cover gas space of surge tank Outlet of SG units Common line to pump tank
Medium (10 g/s–2 kg/s)	Pressure switches	Cover gas space of surge tank
Large (> 2 kg/s)	Cross wire type detectors	Downstream of rupture disc assembly at SG inlet and outlet

6.8.2.2.1. Hydrogen in argon detector (HAD) circuit

HADs are for detecting small leaks when the sodium temperature in the loop is below 623 K. They are effective only during the startup and shutdown of the reactor when sodium temperature is lower. In the PFBR, the HAD system (comprising two detectors) is provided at the surge tank cover gas of the secondary circuit. This is required to detect water leak during startup and shutdown of the reactor as the hydrogen-in-sodium detectors are not effective when the sodium temperature is below 623 K.

The HAD system consists of a nickel tube maintained at 773 K inserted into the cover gas. The hydrogen is diffused into the nickel tube and monitored using a thermal conductivity detector (TCD). The TCD signal is processed to compute the increase in hydrogen concentration with respect to background for initiating safety actions.

6.8.2.2.2. Hydrogen in sodium detector (HSD) with electrochemical hydrogen meter (ECHM)

Electrochemical hydrogen meters (ECHMs) using $CaBr_2$–40 mol% CaHBr solid electrolyte and a mixture of CaO-Mg-MgO-CaH_2 as the reference electrode were developed for use in sodium systems of fast reactors for detecting steam leaks in sodium circuits. This is based on the principle of concentration cell and is used to measure the hydrogen pressure:

The performance of the ECHM in FBTR as well as in large sodium circuits such as the Steam Generator Test Facility and the Sodium Water Reaction Test Facility proved that this type of detector can reliably detect a change of 10 ppb of hydrogen in sodium at a background level of 50 ppb, shows an instantaneous response and is adequate to detect steam leaks at micro levels at the time of their inception.

The hydrogen level is compared with the background hydrogen concentration and three levels of alarm are defined. The rate of increase in concentration is also computed and three additional levels of alarm are defined to identify fast escalating leaks.

6.8.2.2.3. Hydrogen in sodium detector circuit (HSDC) with sputter ion pump (SIP)

The HSDC is for detecting a water/steam leak in the SG when the sodium temperature is above 623 K. One detector is provided in the common return line to the pump tank from the SG for confirmation of the leak.

This detector consists of a nickel tube assembly. The shell side of the assembly is connected to vacuum pumps through a pneumatically operated isolation valve. Sodium from the common outlet line is passed through the economiser, electric heater, tube side of the nickel detector assembly, and returned to storage tank through the economiser. The sodium temperature is controlled at (723±1) K. Hydrogen in the sodium diffuses through the nickel tubes to the shell side of the nickel detector assembly. The vacuum circuit and signal processing are similar to the HAD. The sputter ion pump current is processed and converted into an equivalent hydrogen concentration in sodium. The hydrogen level is compared with the background hydrogen concentration and three levels of alarm are defined. The rate of increase in concentration is also was computed and three additional levels of alarm are defined to identify fast escalating leaks.

6.8.3. Acoustic/ultrasonic instrumentation

6.8.3.1. Acoustic technique for drop time measurement of diverse safety rod (India)

In the PFBR, there are three diverse safety rods (DSR), in addition to the normal control rods to shut down the reactor. During a reactor SCRAM, the electromagnet holding the DSR is de-energized and the DSR falls under the force of gravity into the reactor core and at the end of the free fall, it is decelerated by a sodium dashpot and it is brought to rest. Development of a system for measuring the free fall time and total travel time of the DSR is in progress.

The free fall time is the time elapsed between the instant at which the electromagnet de-energizes and the instant at which dashpot action initiates. At the end of free fall, the DSR hits the top end of the dashpot and generates a shock signal. Similarly, at the end of braking (deceleration in dashpot), another shock pulse is generated. By measuring the time delays between the step transition of the electromagnet signal and the above shock signals, the free fall and braking times can be estimated. The feasibility of using high frequency accelerometers for measuring the shock pulse produced was studied during the performance testing of the DSR drive mechanism (DSRDM) in sodium at 550°C (reactor condition). An accelerometer sensor mounted on the wave-guide and in the DSRDM showed very good response to the shock pulse generated. Experiments were carried out for different drop heights of DSR in sodium and the free fall and braking times were measured.

For the drop height of 1075 mm in sodium at 550°C, the measured total drop time/travelling time of DSR is 751 ms, which is less than the allowable time of 1 s. Both accelerometer signals from the DSRDM and wave-guide are observed to be similar in nature. From the experimental results, it is concluded that acoustic measurement technique can be used to determine the drop time of the DSR in PFBR. Experimental setup for the DSR drop-time measurement is shown in Fig. 6.107.

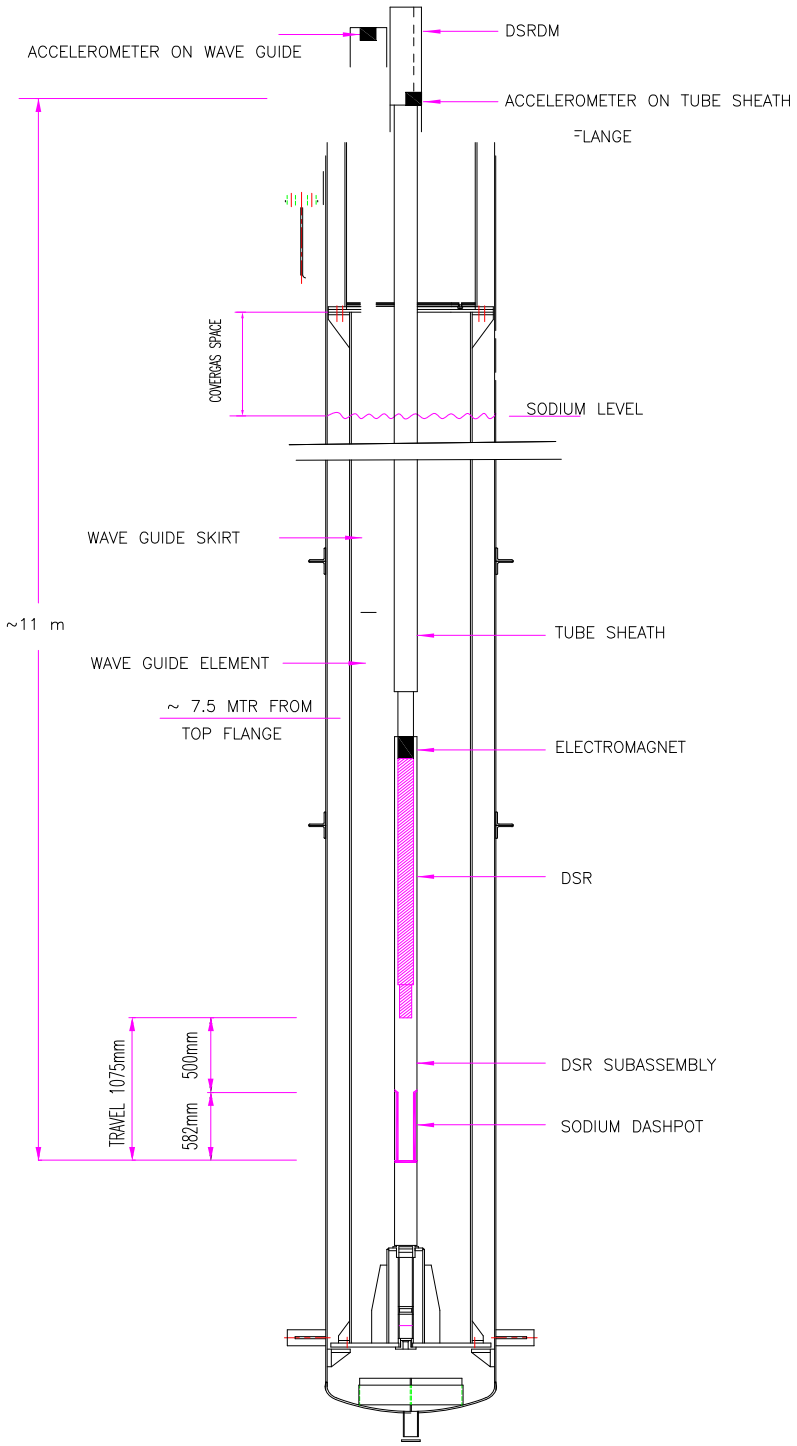

FIG. 6.107. Experimental setup for the DSR drop-time measurement.

6.8.3.2.Ultrasonic technique for sodium boiling detection (USA)

The monitoring of nuclear reactors has, up to now, been carried out by measurement and observation of the mean value of the relevant state parameters such as power, coolant temperature and coolant flow. Variations in the mean signals of these values indicate some kind of malfunction and in turn activate the control safety system. It is therefore possible in principle by analysis and monitoring of the fluctuations in suitable parameters to detect small disturbances in the reactor before more serious accidents occur or larger areas of the core are affected. During the height of the LMFR programme at various institutions, various sodium boiling experiments were performed. It will be needed to re-establish such programs that will require development or continuation of high temperature ultrasonic transducers like the ones that were placed in EBR II. Boiling and cavitation was detected at that time.

6.8.3.3.Acoustic technique for other parameters (USA)

Acoustic/ultrasonic sensors have shown great promise for measuring process parameters such as flow, level temperature and use for under sodium viewing, boiling detection, leak detection and location and on-line in situ non-destructive (NDE) characterization of materials. To address the needs of acoustic/instrumentation, it is essential to develop new transducers that can withstand the adverse environments of liquid metal reactors (LMRs). This means materials development and qualifications for radiation environments. In the late 1970s work on lithium niobate transducers at Argonne National Laboratory produced devices for both detection and under sodium viewing as well as transducers to be used for flow and temperature measurements.

Measurement of flow (single phase or multiphase) has received considerable attention in the past at universities and national laboratories. Instrument manufacturers have concentrated on conventional single-phase instrumentation. The commercially available sensors can be categorized as:

(i) Intrusive i.e. penetrates the flow stream (head-type, drag-type, sequential wedge and a variety of impedance probes); and
(ii) Non-intrusive i.e. does not penetrate the flow stream (acoustic, optic, electromagnetic and nuclear).

The future of measuring flow for LMRs will be in the traditional permanent magnet flowmeters and the development of a number of acoustic techniques such as upstream/downstream transit time flowmeter for single phase flow; development of active acoustic cross correlation for steam/water flows and the acoustic Doppler for void monitoring. These technologies are available commercially but have to improve on sensitivity and calibration ease as well as qualification for use in nuclear power plants.

In the case of temperature measurements, the acoustic/ultrasonic technology of time domain reflectometry can be used for temperature profile measurement in the core. This technique requires an intrusive device, but it is easy to implement and requires no calibration.

Pressure measurement by using acoustic techniques can be used but requires an interface and new membrane development to implement it.This technology can be implemented in conjunction with the development of level measurement probe based on acoustic/ultrasonic principles. The probe can be intrusive like the acoustic temperature probe or nonintrusive by attaching the transducer on the containment vessel.

6.8.4. In-service inspection (ISI) and repair

The objective of in-service inspection (ISI) of a nuclear power plant is to confirm the functional integrity of components necessary for safety, to protect plant investment and to achieve high plant performance and availability. Inspection techniques required for a commercialized sodium-cooled fast reactor (SFR) will be prepared by combining innovative techniques and conventional techniques that have been developed for existing SFRs. This area should be on-line inspection technologies by using non-destructive evaluation methods (NDE). In the past the nuclear industry has used NDE technologies such as acoustics/ultrasonic or eddy current. Eddy current was implemented for leaks in steam generators, while acoustic/ultrasonic technologies were implemented for cracks in steel alloys.

For new LMR reactors it will be important to implement NDE technologies on-line in situ that can continuously monitor the structural integrity of components. Ongoing research in this area has been largely associated with life-extension and management of light water reactors. A wide range of NDE technologies including electromagnetic and acoustic methods have been evaluated in the past for in-service inspection of components (e.g. tubing, piping and pressure vessel). R&D work was carried out with the aim of developing resources needed for a volume inspection of the internal sodium structures.

Regarding non-destructive tests on structures, no device currently exists that is able to generate ultrasounds in high-temperature sodium. Two non-destructive test methods were considered.

The first method was based on electromagnetism using electro-magnetic acoustic transducer (EMAT) probes. These probes generate ultrasounds in sodium by means of eddy current signals.

The second method uses piezoelectric composite probes. Probes that are acoustically and chemically compatible with sodium must be developed to evaluate their technological feasibility. A method using phased array probes has also been considered, with the aim of developing a technique capable of exploring the entire volume of sodium when traditional probes prove to be are inadequate. The small space available for probe movement is compensated by an angular scanning.

6.8.4.1. In-service inspection technology in France

6.8.4.1.1. Using ultrasounds to inspect sodium environments

It is useful to be able to inspect sodium environments for the three reasons:

(1) To guide and position an inspection apparatus carrier within the reactor;
(2) To establish and locate any missing reactor elements; and
(3) To perform remote-control measurements.

Sodium is an opaque liquid; therefore, to be able to “see” through liquid sodium to conduct dimensional inspections from a distance, it is necessary to use a type of wave capable of propagating with little attenuation, such as ultrasounds, at frequencies of several megahertz. It is therefore possible to obtain an attenuation coefficient of about 0.1 dB/m with ultrasounds.

The next step involves applying techniques similar to those found in the active sonar used by submarines or medical ultrasounds – non destructive tests using ultrasounds.

6.8.4.1.2. Principle of an active sonar

In its simplest form, an active sonar is composed of one unique sensor, still called a probe, which emits an ultrasonic wave, receives this wave after it has been reflected by the surrounding structures and then delivers an electrical signal. The probe uses “directivity”, which means that it only transmits and receives within a limited beam range, schematically speaking in the shape of a cone. By rotating the cone to cover all or part of the zone, information concerning the presence, absence and distance of objects in the scanned areas can be collected continuously. The distance (L) between the probe and the located object is calculated using the time of flight information (t) according to the equation; $L = (c \cdot t)/2$, where c represents the celerity of ultrasounds in the sodium. The cone is rotated by either rotating the probe or by dividing the probe into small electronically piloted elements.

6.8.4.1.3. Accessing back-scattered information

The reflection of a metallic structure is in fact composed of three components that all together form the received signal [412]. These components are, in decreasing order of amplitude:

- Specular echoes, occurring with a delay in time in relation to the transmitted ray that, in the beginning, depends on the distance between the probe and the closest part of the structure. Even if the beam is rotated, the echo takes the same time to be received, which gives the impression that a structure in the shape of a spherical dome is cantered on the probe – regardless of the reflecting structure – and whose aperture only depends on the probe’s directivity.
- Diffraction echoes, from structure edges help locate the edge of structures.
- Back-scattered echoes, generated by each point of the structure, provided that the local roughness is significant enough for the wavelength.

Optical waves are used to locate and visualize objects in three dimensions. Ultrasonic visualization also uses backscattered acoustic energy.

To separately access backscattered acoustic signals, it is necessary to direct the beam in a direction where it is stronger than the specular and diffracted acoustic signals. The beam must therefore be narrow enough so that only a slight misalignment in relation to the specular direction is enough to eliminate specular echoes. Sodium visualization systems, known as "VISUS" [413], already exist in the Phénix and Superphénix reactors. These systems are used to detect and locate possible obstacles preventing the rotating plugs from functioning during handling operations. However, these systems are not directional enough and do not enable the separation of acoustic components from the signal. Therefore, in reality, these systems only deal with specular echoes. The sodium rapid imaging programme, IMARSOD (IMAgerie Rapide en SODium), was carried out to explore such problems.

6.8.4.1.4. IMARSOD system characteristics

The IMARSOD system is composed of two perpendicular antennas, one transmitting and the other receiving (Fig. 6.108) [414, 415]. These antennas are designed so that their focal zones approximately represent a horizontal and vertical line, respectively. The focal point that is detected by the system is located at the intersection of the two lines. To move the focal point in a

3-D space, the antennas are divided into elements each equipped with an electronic device enabling electronic focusing by exploiting the time delay laws intervening between elements. An example of a system measuring technique that designed for Superphénix is provided in the Fig. 6.108.

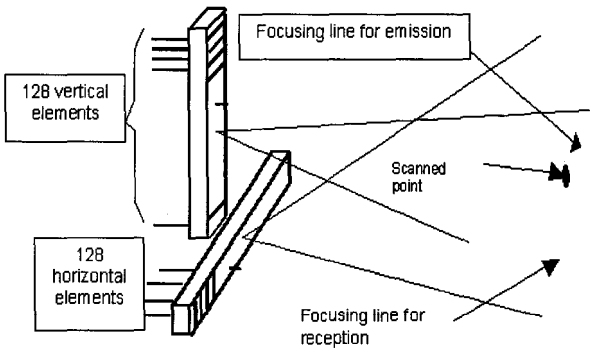

Antenna size (horizontal et vertical)	L = 500 mm
Number of elements per antenna	N = 128
Aperture of image	30°
(equivalent to a range of 1020 mm to 2 m in distance)	
Frequency	1,6 MHz (λ = 1.5 mm)
Axial resolution	4 mm
Spatial resolution	0.33°
(equivalent to a range of 11 mm to 2 m in distance)	
Image acquisition time (anolog solution)	
- sectorial (= one segment)	dt = 65 ms
- total (= 64 sectorial images)	64 dt = 4 s

FIG. 6.108. Orthogonal ultrasonic imaging.

6.8.4.1.5. Validating the "active sonar" principle through tests in water

Approximate calculations of the ratio between the backscattered echo and the specular echo for a system dimensioned as illustrated above, with estimated reactor surface roughness of approximately 10 μm indicated the fact that separating the echoes is possible but rather complicated. Tests were necessary to confirm these calculations and establish whether the acoustic dispersion "originated" from the electronic noise.

An experimental system was installed in the ultrasound container, by "synthetising" the receiver antenna using a single-element moved to the successive positions of the antenna elements. Transmission was carried out using a big single-element antenna, which generated a focalization line at a normal distance of 2 m. The "B-scan" image provided by the system when using a flat plate with a width of 700 mm placed 2 m from the antennas revealed that all points of the plate were visible, with glare due to the specular echo coming from the point found closest to the antennas, with excess intensity from the edge of the plate due to edge diffraction echoes.

6.8.4.2. In-service inspection technology in Japan [416]

6.8.4.2.1. Design approach for implementation of ISI

It is essential for the commercialization of the SFR that plant systems are designed for maintenance. As a part of design study for maintenance of the JSFR, an ISI program was studied that took into consideration characteristics of the JSFR design such as the double

walled coolant boundary structures and the double wall straight tube SG. The JSFR has two characteristics related to ISI. The first is that all sodium coolant boundary structures have a double-wall system. Continuous monitoring of the sodium coolant boundary structures is adopted for inspection. The second characteristic is the SG with double-wall-tubes. Volumetric testing is adopted to make sure that one of the tubes can maintain the boundary function in case the other tube fails. A rational ISI concept was developed taking these features into account. Future studies will focus on giving shape to the ISI concept for application to the JSFR.

6.8.4.2.2. Development of inspection technologies

In order to realize the design approach for implementation of the ISI, feasibility studies of inspection techniques were performed, such as the under sodium area monitor system, under sodium vehicle and volumetric inspection technique for the double-wall-tube of a SG. The under-sodium viewing system consisted of multi ultrasonic scanning transducers, which was used for imaging under-sodium structures. The under-sodium viewing system was mounted on the under-sodium vehicle and was delivered to core internals.

The prototype of under-sodium viewing system and vehicle were fabricated and performance tests were carried out under water. The laboratory experiments of volumetric testing for the double-wall-tubes of the SG, such as ultrasonic testing and remote-field eddy current testing, were performed and technical feasibility was assessed. Application of these techniques to sodium awaits further studies.

6.8.4.3. In-service inspection technology in the United States of America

Under the NRC's control, scientists all over the world have collaborated to assess the reliability of conventional and emerging NDE technologies and have carried out research on advanced ISI technologies. They have established a mock-up test facility at Argonne National Laboratory (national users' facility) in order to test and validate inspection technologies. To accomplish that, expertise in the area of analytical and numerical modelling of thermal acoustic and electromagnetic interaction with complex media as well as advanced signal processing, imaging and data analysis was utilized.

In addition to ISI related technologies, various other NDE areas are expected to play a major role toward advancement of inspection technologies for advanced nuclear reactors such as sodium cooled fast reactors. Inherent to their design, in addition to high temperature metal alloys, there will be a more widespread use of ceramic components in advanced reactors. This means that more emphasis would be placed on reliable NDE techniques that are capable of examining ceramic, composites and higher degree of sensitivity. These advanced methods include phased array ultrasonics, X-ray computed tomography, thermal wave imaging, optical coherence tomography (OCT), confocal microscopy, microwave/millimetre-wave (MW/MMW) sensing, eddy current (EC) testing and optical laser backscatter.

For optically translucent engineering materials such as many structural ceramics (e.g. Si_3N_4, SiC, Al_2O_3), OCT has been used for the detection of near-surface defects. Advanced X-ray CT techniques have been developed for high-resolution volumetric imaging of engineering materials using high power microfocus sources. High temperature materials such as monolithic ceramics have small critical flaw sizes. Phased array ultrasonics, which utilizes the interference of multiple excitation sources to increase signal to noise ratio, has been used extensively for inspection of ceramic components. Pulsed thermal imaging techniques have

also been developed to probe internal material property, structure, and to detect surface and subsurface defect/damage. Polarized laser scatter and confocal microscopy technologies have been developed for subsurface detection of cracks, voids, spalling and inclusions in ceramic components. The technique has been used to determine defect size, shape, severity and distribution that are critical to the strength of critical components. Cross-polarized confocal microscopy has been used for 3D imaging of subsurface microstructure for translucent materials. Pulsed thermal imaging systems have been used to determine thermal property distribution in three directions, detect delamination, defect size, depth, severity, etc.

A specialized technique was developed for imaging of multilayer material structures including their thickness, conductivity and health monitoring in general. Electromagnetic testing methods have also been used extensively. Specialized EC methods have been developed for inspection of conductor and semiconductor materials. In addition to probe design, engineers have developed software-based tools for efficient and reliable analysis of EC inspection data in an automated manner. Both active and passive MW/MMW sensing techniques have been developed for NDE of composite materials including ceramic components. Reliable pre- and in-service inspection, condition monitoring and assessment of fabrication processes for advanced reactors are expected to utilize a wide range of NDE technologies.

6.8.5. Primary sodium flow measurement by eddy current flowmeter (India)

Sodium flow through the core is an important parameter for monitoring core cooling. The ratio of the neutronic power to the flow through core (P/Q) is the parameter which is used to initiate SCRAM. It is used to protect the reactor.

In the Indian design, an eddy current flowmeter is installed in a thimble located in a bypass line from pump discharge volute to suction chamber. Two thimbles are provided in each pump with two flowmeters in each of them. A small part of the sodium is flowing through this thimble and joins at the pump suction. This flow through the thimble is proportional to the square root of the pump head developed from which pump discharge flow is derived. Out of the four flowmeters, three are normally used and the fourth one serves as an in situ spare.

The location of the eddy current flowmeter in the primary sodium pump is shown in Fig. 6.109.

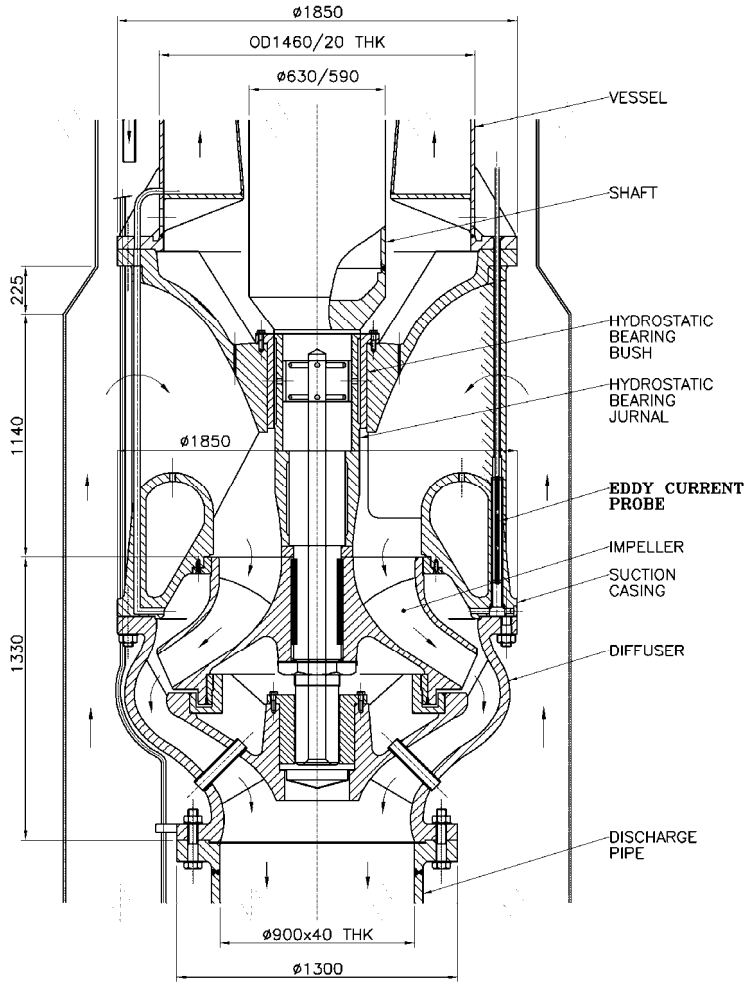

FIG. 6.109. Primary sodium pump with eddy current flowmeter.

The signal from each flowmeter is processed by dedicated independent hardware units. The signal from one flowmeter of each pump is wired to one panel and the total primary flow is obtained by adding the signals from the flowmeters provided in each pump. The flow through core (Q) is then calculated by subtracting the leakage flow from the total primary flow. The power to flow ratio is computed based on individual pump discharge flow. If either P/Q1 or P/Q2 rises above 1.1, the SCRAM signal is generated. The primary sodium flow measurement channel schematic is shown in Fig. 6.110.

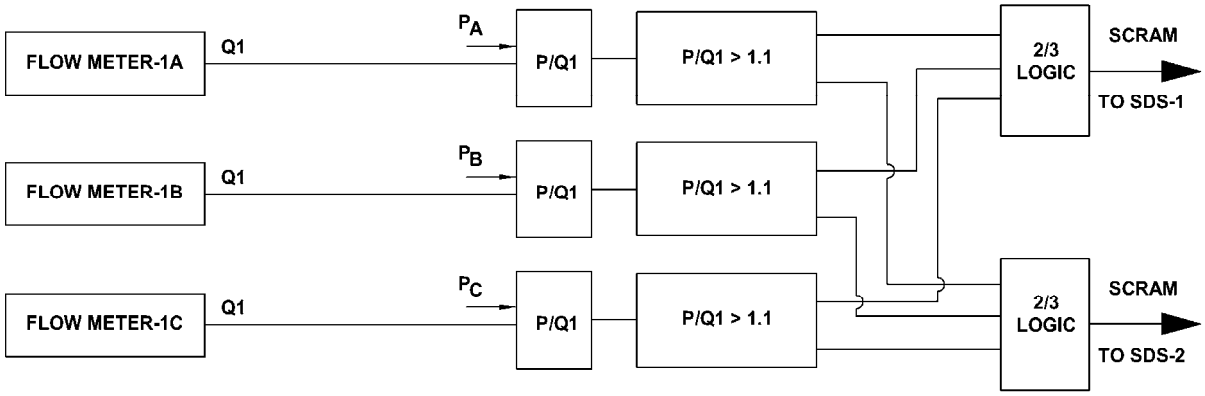

FIG. 6.110. Primary sodium flow measurement.

When the pump discharge flow is more than 105% of the nominal value, a high flow alarm is generated in control room and when the pump discharge flow is less than 95% of the nominal value, a low flow alarm is generated in the control room.

6.8.6. Inspection technique of fuel pin and subassembly (India)

6.8.6.1. Inspection of irradiated fuel pins

6.8.6.1.1. Neutron radiography of irradiated fuel pins

Neutron radiography of irradiated fuel pins is carried out as a part of post irradiation examination. The transfer method using a dysprosium converter screen and a neutron flux on the order of 10^6–10^7 n/cm^2/s is used. The exposure time varies depending on neutron flux, film speed and sensitivity requirements. Different radiographic parameters are employed to reveal the hardware portions and for assessing the integrity of the pellets. Real time neutron radiography using a gadolinium oxysulphide screen is also carried out.

The quality of the neutron beam from a source is studied using suitable beam purity indicators and sensitivity studies are made as per ASTM E545 standards. A typical neutron radiograph showing pellet to pellet gaps in an irradiated fuel pin is given in Fig. 6.111.

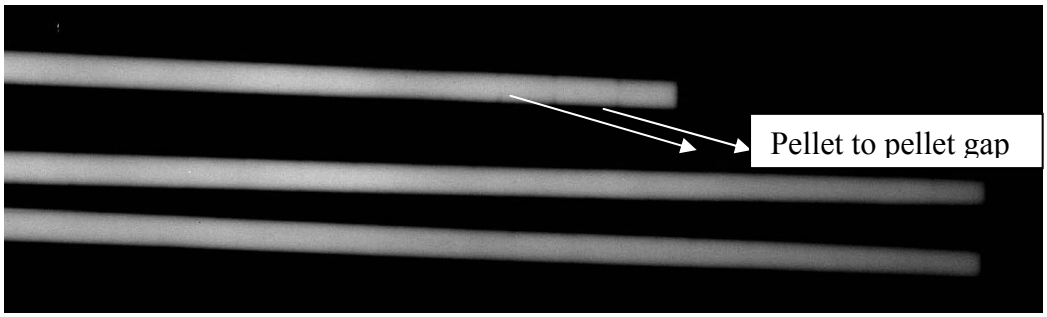

FIG. 6.111. Typical neutron radiograph showing pellet to pellet gaps in an irradiated fuel pin.

6.8.6.1.2. Gamma scanning of irradiated fuel pins

Gamma scanning is used to obtain information such as burnup distribution in fuel pins, fission product redistribution, increase in fissile column length due to swelling and location of fuel-cladding failure. The detectors employed for high resolution gamma spectrometry of fuel pins include semiconductor detectors such as high purity germanium detectors which have an energy resolution better than 2 keV for a gamma energy of 1.33 MeV. A typical gamma spectrum obtained during gamma scanning of the irradiated fuel pins is shown in Fig. 6.112.

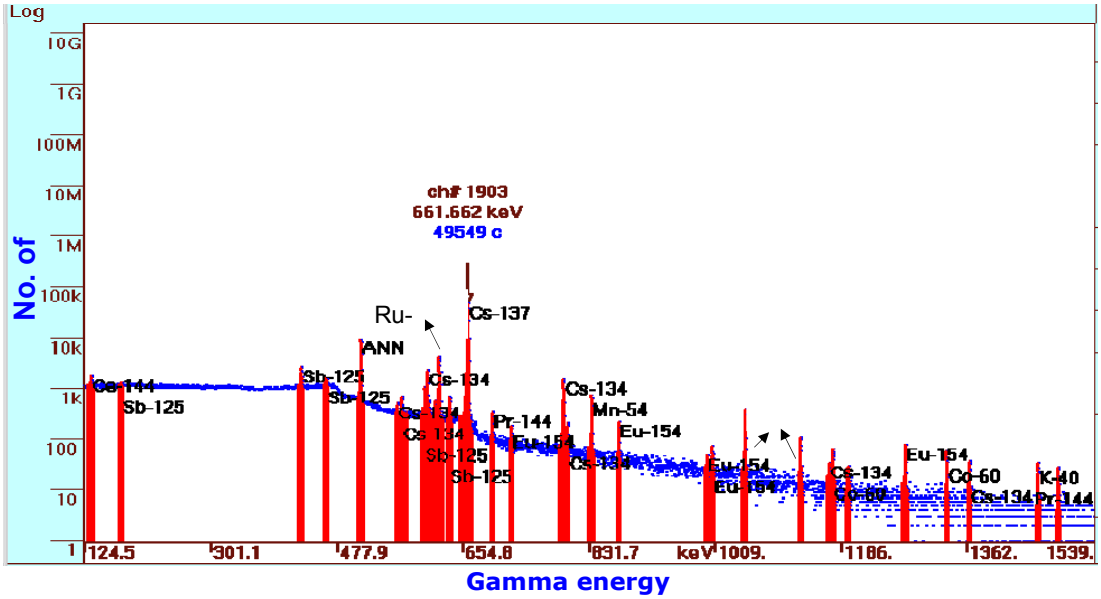

FIG. 6.112. Typical gamma spectrum obtained during gamma scanning of the irradiated fuel pins.

6.8.6.2. Ultrasonic testing of fuel pins

X-radiography, which is usually used in the fuel inspection, has a limited ability to detect tight discontinuities with shorter circumferential extents and at angles to the X-ray beam. For small backlash discontinuities, tight lack of fusion/penetration anomalies and to achieve almost 100% coverage, the ultrasonic technique is preferred.

Furthermore, the detection of tight laminar type defects oriented radially to the surface is expected to be detected better by the ultrasonic technique [417]. The ultrasonic technique used for inspection of fuel pins is the immersion type, which employs a highly damped point focussed probe, positioned precisely to generate a 45º shear wave into the tube that is intercepted by any discontinuity in the weld joint. The discontinuity is displayed as an A-scan signal in pulse-echo mode. A good correlation has been established between radiography, metallography and ultrasonic techniques.

An advanced ultrasonic phased array technique is considered for inspection of end plug welds. Typically a 17 MHz, 128 element linear phased array immersion probe is used. The phased array probe is maintained at a 19 degree angle inclined to the axis of the tube, which provides maximum reflection from the defect. When the ultrasonic beam falls on the surface of the weld, it goes into the tube material and further penetrates into end plug region.

An intensity plot with the angular position of the tube on the x- axis, the elements position on the y-axis and the amplitude at a given depth (which corresponds to reflected wave from weld) as a colour scale was used to image defects in the welds.

Typical images obtained from non defective and defective end plug welds are shown in Fig. 6.113, where white represents the minimum amplitude (0%) and red represents the maximum amplitude (100%). From these images, it is possible to estimate the angular location and angular length of the defect.

Moreover, the colour will give an idea of how severe is the defect.

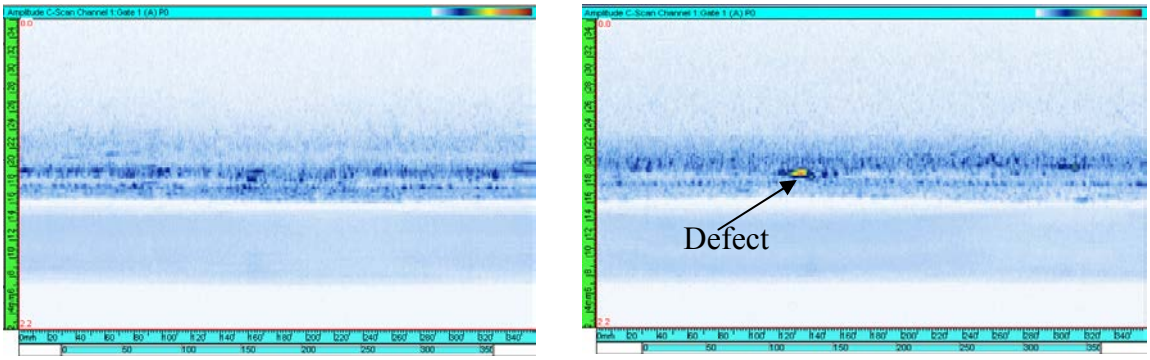

FIG. 6.113. Images of weld regions of the end plug welds obtained by ultrasonic phased array technique.

6.8.6.3. Eddy current testing of sodium bonded metallic fuel pins [418]

One unique requirement for metallic fuel pins consisting of sodium bonded metallic fuel slugs is their examination for the detection of voids in the sodium column, in addition to any localised defects in the cladding tube wall. Eddy current testing is employed for this purpose. Systematic experimental studies have been carried out on fuel cladding tubes with simulated aluminium inserts (electrical conductivity equivalent to that of sodium) having a series of artificial defects such as flat bottom holes of different diameters and electric discharge machined notches of different sizes, using rotating pancake eddy current test probes. By proper optimization of probe dimensions and test frequency, voids in sodium larger than 1 mm^3 and defects in the fuel cladding wall can be detected with good repeatability.

6.8.6.4. Ultrasonic inspection of seal welds of FBR subassembly hexcan

The complex geometry and weld thickness (about 3 mm) demand the adoption of a new methodology to test the hexcan weld. The developed ultrasonic methodology involves testing the weld from the thinner plate side using Rayleigh waves at a frequency of 1 MHz, which would penetrate complete thickness (3 mm, approximately one wavelength) of the weld. This methodology is quite fast and can be used for detection of both axial and circumferential defects. A hexcan weld having natural defects and simulated equivalent weld specimens with artificial defects are used as calibration standards, to establish the sensitivity of the developed methodology.

The ultrasonic signals received from natural defects and their radiographs taken after suitably machining out excess thickness portions, are shown in Fig. 6.114 a,b,c.

(a) (b) (c)

FIG. 6.114. (a) Radiograph showing incomplete penetration, (b) corresponding ultrasonic A-scan signal and (c) A-scan signal corresponding to a defect free location.

6.8.7. Fiber optics technology for nuclear power plants

The process of incorporating emerging fiber optic technology into sensor systems for nuclear power plants should be evaluated:

- Examine use of light energy as a source of primary sensor power;
- Measure parameter magnitude, convert to a light signal and transmit to local area network (LAN) or data highway; and
- Demonstrate performance of the required function in an operating nuclear plant environment.

The use of fiber optic transmission systems is an available technology that is being used in communications and computer industries. The use of fiber optics eliminates the need for wire conductors, thereby eliminating conduction and radiation of electromagnetic energy responsible for electromagnetic interference. However, sufficient work has not been done for use of fiber optics in the nuclear industry. The strategy for the nuclear industry should be to review developments of fiber optic systems and components and select design concepts for nuclear applications. Develop fiber optics by:

- Establishing requirements;
- Evaluating current state-of-the-art and establishing areas requiring modifications and development;
- Designing, developing and fabricating associated optical electronics;
- Conducting laboratory testing and development to demonstrate operability when exposed to a nuclear power plant environment; and
- Conducting an extended duration test programme in an operating plant.

Development of fiber optics and wireless transmission systems will reduce electromagnetic interference and vessel penetrations for cables.

REFERENCES TO CHAPTER 6

[1] ROSE, P.F., DUNFORD, C.L., ENDF-102 Data Formats and Procedures for the Evaluated Nuclear Data File ENDF-6, BNL-NCS-44945 (1990).

[2] CHADWICK, M.B., ENDF/B-VII.0: Next Generation Evaluated Nuclear Data Library for Nuclear Science and Technology, Nuclear Data Sheet, Vol. 107, No. 12, p. 2931 (2006).

[3] VAN DER MARCK, S.C., Benchmarking ENDF/B-VII.0, Nuclear Data Sheet, Vol. 107, No. 12, p. 3061 (2006).

[4] OECD/NEA, Index to the JEF-1 Nuclear Data Library, JEF Report 1, OECD/NEA Data Bank (1985).

[5] JEF-2.2 Radioactive Decay Data, JEF Report 13, OECD/NEA Data Bank (1994).

[6] The JEF-2.2 Nuclear Data Library, JEF Report 17, OECD/NEA Data Bank (2000).

[7] OECD/NEA, KONING, A., The JEFF-3.1 Nuclear Data Library, JEF Report 21, OECD/NEA Data Bank (2006).

[8] IGARASI, S., NAKAGAWA, T., KIKUCHI, Y., ASAMI, T., NARITA,. T, Japanese Evaluated Nuclear Data Library, Version-1 - JENDL-1 -, JAERI 1261 (March 1979).

[9] NAKAGAWA, T., Summary of JENDL-2 General Purpose File, JAERI-M 84-103 (June 1984).

[10] SHIBATA, K., NAKAGAWA, T., ASAMI, T., FUKAHORI, T., NARITA, T., CHIBA, S., MIZUMOTO, M., HASEGAWA, A., KIKUCHI, Y., NAKAJIMA, Y., IGARASI, S., Japanese Evaluated Nuclear Data Library, Version-3 - JENDL-3 -, JAERI 1319 (June 1990).

[11] NAKAGAWA, T., SHIBATA, K., CHIBA, S., FUKAHORI, T., NAKAJIMA, Y., KIKUCHI, Y., KAWANO, T., KANDA, Y., OHSAWA, T., MATSUNOBU, H., KAWAI, M., ZUKERAN, A., WATANABE, T., IGARASI, S., KOSAKO, K., ASAMI, T., Japanese Evaluated Nuclear Data Library Version 3 Revision-2: JENDL-3.2, Journal of Nuclear Science and Technology, Vol. 32, No. 12, pp. 1259-1271 (December 1995).

[12] SHIBATA, K., KAWANO, T., NAKAGAWA, T., IWAMOTO, O., KATAKURA, J., FUKAHORI, T., CHIBA, S., HASEGAWA, A., MURATA, T., MATSUNOBU, H., OHSAWA, T., NAKAJIMA, Y., YOSHIDA, T., ZUKERAN, A., KAWAI, M., BABA, M., ISHIKAWA, M., ASAMI, T., WATANABE, T., WATANABE, Y., IGASHIRA, M., YAMAMURO, N., KITAZAWA, H., YAMANO, N., TAKANO, H., Japanese Evaluated Nuclear Data Library Version 3 Revision-3: JENDL-3.3, Journal of Nuclear Science and Technology, Vol. 39, No. 11, pp. 1125-1136 (November 2002).

[13] IWAMOTO, O., NAKAGAWA, T., OTUKA, N., CHIBA, S., OKUMURA, K., CHIBA, G., OHSAWA, T., FURUTAKA, K., JENDL Actinoid File 2008, Journal of Nuclear Science and Technology, Vol. 46, No. 5, pp. 510-528 (May 2009).

[14] SHIBATA, K., et al., JENDL-4.0: A New Library for Innovative Nuclear Energy Systems, to be published.

[15] YOUXIANG, Z., CENDL-3: Chinese Evaluated Nuclear Data Library, Version 3, Journal of Nuclear Science and Technology, Supplement 2, 33 (2002).

[16] SCHMIDT, J.J., Neutron Cross-sections for Fast Reactor materials, Kernforschungszentrum Karlsruhe, Part.1 Evaluations, KFK 120.

[17] OBLOZINSKY, P., Status of Work on the ENDF/B-VII Library, paper presented in Workshop on Nuclear Data Needs for Generation IV Systems, Brookhaven National Laboratory, USA, 24-25 April 2003.

[18] OBLOZINSKY, P. AND HERMAN, M., Recent Progress in the Development of the ENDF/B-VII Library, Nuclear Data Needs for Generation IV Nuclear Energy Systems, paper presented in International Workshop, Antwerpen, Belgium, 5-7 April 2005.

[19] ALIBERTI, G., PALMIOTTI, G., SALVATORES, M., KIM, T. K., TAIWO, T. A., ANITESCU, M., KODELI, I., SARTORI, E., BOSQ, J.C., TOMMASI, J., Nuclear Data Sensitivity, Uncertainty, and Target Accuracy Assessment for Future Nuclear Systems, Annals of Nuclear Energy, Vol. 33, p. 700 (2006).

[20] KAWANO, T., MATSUNOBU, H., MURATA, T., ZUKERAN, A., NAKAJIMA, Y., KAWAI, M., IWAMOTO, O., SHIBATA, K., NAKAGAWA, T., OHSAWA, T., BABA, M., YOSHIDA, T., Simultaneous Evaluation of Fission Cross Sections of Uranium and Plutonium Isotopes for JENDL-3.3, Journal of Nuclear Science and Technology, Vol. 37, No. 4, pp. 327-334 (April 2000).

[21] KAWANO, T., SHIBATA, K., Uncertainty Analyses in the Resolved Resonance Region of 235U, 238U, and 239Pu with the Reich-Moore R-Matrix Theory for JENDL-3.2, Journal of Nuclear Science and Technology, Vol. 39, No. 8, pp. 807-815 (August 2002).

[22] SHIBATA, K., Uncertainty Analyses of Neutron Cross Sections for 235U in the Resonance Region, Journal of Nuclear Science and Technology, Vol. 42, No. 1, pp. 130-133 (January 2005).

[23] SHIBATA, K., NAKAGAWA, T., Uncertainty Analyses of Neutron Cross Sections for Nitrogen-15, Lead-206, 207, 208, Bismuth-209, Plutonium-238, Americium-242m, and Curium-244 in JENDL-3.3, Journal of Nuclear Science and Technology, Vol. 44, No. 1, pp. 1-9 (January 2007).

[24] NAKAGAWA, T., Estimation of Covariance Matrices for Nuclear Data of Np-237, Am-241 and Am-243, Journal of Nuclear Science and Technology, Vol. 42, No. 11, p. 984-993 (November 2005).

[25] SEGEV, M., A Theory of Resonance-Group Self-Shielding, Nuclear Science and Engineering, Vol. 56, No. 72 (1975).

[26] GRIMSTONE, M.J., TULLET, J.D., RIMPAULT, G., Accurate Treatment of Fast Reactor Fuel Assembly Heterogeneity with the ECCO Cell Code, Proc. PHYSOR'90, Marseille, France, 23-27 April 1990 (5 Vols), NEA-1828.

[27] TOPPEL, B.J., HENRYSON II, H., STENBERG, C.G., ETOE-2/MC^2-2/SDX Multigroup Cross Section Processing, Proc. RSIC Seminar-Workshop on Multigroup Cross Sections, Conf-780334-5, Oak Ridge, Teneessee, USA, 14-16 March 1978.

[28] MACFARLANE, R.E., MUIR, D. W, The NJOY Nuclear Data Processing System, Los Alamos National Laboratory, LA-12740-M, 1994. Oak Ridge National Laboratory, RSICC PSR-480 NJOY-99.0. http://t2.lanl.gov/codes/njoy99/.

[29] MACFARLANE, R.E., NJOY 99/2001: New Capabilities in Data Processing, paper presented in Workshop on Reactor Physics and Analysis Capabilities for Generation IV Nuclear Energy Systems, Argonne National Laboratory, Argonne, Illinois, USA 18-19 February 2003.

[30] WEISBIN, C.R., MINX: A Multigroup Interpretation of Nuclear X-Sections from ENDF/B, LA-6486-MS (ENDF-237) (September 1976).

[31] RIBON, P., MAILLARD, J. M., Probability Tables and Gauss Quadrature: Application to Neutron Cross Sections in the Unresolved Energy Range, paper presented in ANS Topical Meeting on Advances in Reactor Physics and Safety, Saratoga Springs, NY, USA (September 1986).

[32] SINITSA, V.V., RINEISKIJ, A.A., GRUKON - A Package of Applied Computer Programs. System Input and Operating Procedures of Functional Modules, INDC(CCP)-334, Vienna (1993).
[33] TRUBEY, D.K., HENDRICKSON, H.R., A Review of Multigroup Nuclear Cross Section Processing, paper presented in RSIC Seminar-Workshop on Multigroup Cross Sections, Conf-780334-5, Oak Ridge, Tenessee, USA, 14-16 March 1978.
[34] HENRYSON II, H., TOPPEL, B.J., STERNBERG, C.G., ETOE-2/MC^2-2/SDX, Multigroup Neutron Cross Section Processing System, paper presented in Seminar on Nuclear Data Processing Codes, Ispra, Italy, 1973.
[35] DUNN, M., Status of ORNL Cross-section Processing & Library Generation Capabilities, paper presented in GEN-IV Nuclear Data Working Group Meeting, Antwerpen, Belgium (April 2005).
[36] HENRYSON II, H., TOPPEL, B.J., STENBERG, C.G., MC^2-2: A Code to Calculate Fast Neutron Spectra and Multigroup Cross Sections, ANL-8144, Argonne National Laboratory (1976).
[37] HWANG, R.N., A Rigorous Pole Representation of Multilevel Cross Sections and Its Practical Applications, Nucl. Sci. Eng., 96, 192 (1987).
[38] HWANG, R.N., Efficient Methods for the Treatment of Resonance Integrals, Nucl. Sci. Eng., 52, 157 (1973).
[39] STACEY JR., W.M., Continuous Slowing Down Theory Applied to Fast-Reactor Assemblies, Nucl. Sci. Eng., 41, 381 (1970).
[40] ALCOUFFE, R.E., BRINKLEY, F.W., MARR, D.R., O'DELL, R.D., User's Guide for TWODANT: A Code Package for Two-Dimensional, Diffusion-Accelerated, Neutral-Particle Transport, LA-10049-M, Los Alamos National Laboratory (1990).
[41] SERYOGIN, A.S., KISLITSYNA, T.S., Abstract of TRIGEX-CONSYST-ABBN-90, Preprint IPPE-2655, Obninsk, Russian Federation (1997) (in Russian).
[42] YAROSLAVTSEVA, L.N., Code package JAR for analysis of nuclear reactor neutronics, Issues of Nucl. Sci. & Tech., Series: Phys. & Tech. of Nucl. Reactors, Iss. 8 (37) pp. 41-43 (1983) (in Russian).
[43] SELEZNEV, E.F., Annotation of code complex SYNTES, Issues of Nucl. Sci. & Tech., Series: Phys. & Tech. of Nucl. Reactors (1984) (in Russian).
[44] INTERNATIONAL ATOMIC ENERGY AGENCY, MANTUROV G.N., BNAB-93 Data Library Part I, Nuclear Data for the Calculations of Neutron and Photon Radiation Function, INDC (CCP-409), Vienna, Austria.
[45] ABAGYAN, L.P., Group Constants for Reactor and Shielding Calculations, Energoizdat, Moscow, Russian Federation (1981).
[46] KOSCHEEV, V.N., et al., The FOND-2.2 Evaluated Neutron Data Library, Report IAEA-NDS-199 (2002).
[47] MANTUROV, G.N., NIKOLAEV, M.N., TSIBOULYA, A.M., Code for Constants Preparation CONSYST, Preprint IPPE-2828, Obninsk, Russian Federation (2000).
[48] BARANOV, O.V., The PRECON code: User Guide, Preprint IPPE-1847, Obninsk, Russian Federation (1987) (in Russian).
[49] BAZAZYANZ, N.O., The ARAMACO-F system for neutronic data processing for Reactor and Shield Calculations, Moscow, IAM (1976).
[50] BEZBORODOV, A.A., et al., Evaluation of Heterogeneous Effects by Method of the First Flight Collision Probability in Fast Neutron Critical Assemblies, Issues of Nucl. Sci. & Tech., Series: Phys. & Tech. of Nucl. Reactors, Issue 2, p. 8 (1986) (in Russian).

[51] NIKOLAEV, M.N., et al., Subgroup method for accounting cross-section resonance structure in neutronic calculations, Atomic Energy, Vol. 29, No. 1, p. 11 (1970) (in Russian).
[52] KOCHETKOV, L.A., ZCYKUNOV, A.G., "Scientific Research Program on Actinide Transmutation by Use of Fast Reactors", Use of Fast Reactors for Actinide Transmutation, IAEA-TECDOC-693, IAEA, Vienna (1993).
[53] BLYSKAVKA, A.A., MANTUROV, G.N., NIKOLAEV, M.N., TSIBULYA, A.M., A Code CONSYST-MMKKENO for calculations of nuclear reactors by the Monte-Carlo method in multi-group approximation with scattering order in Pn approximation, Preprint IPPE-2887, Obninsk, Russian Federation (2001) (in Russian).
[54] ICSBEP: International Handbook of Evaluated Criticality Safety Benchmark Experiments, OECD/NEA, NEA/NSC/DOC (95)03 (September 2006 Edition).
[55] OECD/NEA, IRPhEP: International Handbook of Evaluated Reactor Physics Experiments, OECD/NEA, NEA/NSC/DOC(2006) (March 2006 Edition).
[56] SINBAD: International Database for Integral Shielding Experiments, OECD/NEA and RSICC (April 2004).
[57] MANTUROV, G.N., Codes and Archives INDECS System, Issues of Nucl. Sci. & Tech., Series: Nuclear Constants, Issue 5(89), Moscow, p. 20 (1984) (in Russian).
[58] MANTUROV, G.N., MATVEEV, V.I., NIKOLAEV, M.N., et al., Requirements on the Accuracies of Calculation of Neutron Physics Reactor Characteristics in Fast Breeder Reactors and Ways to Meet Them, Atomic Energy, Vol. 67, No. 3, pp. 181-186 (1989) (in Russian).
[59] CHAUDAT, J.P., Data Adjustment for Fast Reactor Design, Trans. Am. Nucl. Soc., Vol. 27, No. 877 (1977).
[60] ROWLANDS, J.L., Production and Performance of the Adjusted Cross-Section Set FLG5, paper presented in Int. Symp. Fast Reactor Physics, Tokyo, Japan (1973).
[61] DEAN, C.J., EATON, C.R., PEERANI, P., RIBON, P., RIMPAULT, G., Production of Fine Group Data for the ECCO Code, Proc. PHYSOR'90, Marseille, France, 23-27 April 1990 (5 Vols), NEA-1828.
[62] RIMPAULT, G., PLISSON, D., TOMMASI, J., JACQMIN R., The ERANOS Code and Data System for Fast Reactor Neutronic Analysis, Proc. PHYSOR 2002, Seoul, Korea, Republic of, 7-10 October 2002, ANS, ISBN: 0-89448-672-1.
[63] JAPAN ATOMIC ENERGY RESEARCH INSTITUTE, JAERI Fast Reactor Group Constants System, JAERI-1995-70 (1995).
[64] ONO, S., WACHI, E., TAKEDA, I., SEKITA, T., CASUP: Cell Calculation Code for Fast Reactor Analysis, Technology Reports of Osaka University, Vol. 33 (1983).
[65] TAKEDA, T., KITADA, T., AND IKEDA, H., High-Precision Transport Calculation Methods for Fast Reactor Cores, paper presented in Joint Int. Conf. on Mathematical Methods and Supercomputing in Nuclear Applications, Karlsruhe, Germany, April 1993.
[66] HAZAMA, T., et al., Development of a Fine and Ultra-Fine Group Cell CalculationCode SLAROM-UF for Fast Reactor Analyses, Journal of Nuclear Science and Technology, Vol. 43, No. 8, pp. 908-918 (August 2006)
[67] KIEFHABER, E., The KFKINR-Set of Group Constants; Nuclear Data Basis and First Results of its Application to the Recalculation of Fast Zero Power Reactors, Kernforschungszentrum Karlsruhe, KFK 1572 (1972).
[68] FRÖHNER, F.H., Evaluation of the Unresolved Resonance Range of U238, Nucl. Sci. Eng, 103, 119 (1989).

[69] KIEFHABER, E., Updating of an 11-groups nuclear cross section set for transmutation applications, Forschungszentrum Karlsruhe, FZKA-6480, p. 582 (2000).
[70] KONDO SA., MORITA K., TOBITA Y., SHIRAKAWA N., SIMMER-III: An Advanced Computer Program for LMFBR Severe Accident Analysis, Proc. Int. Conf. on Design and Safety of Advanced Nuclear Power Plants (ANP'92), Tokyo, Japan, 25-29 October 1992, paper No. 40-5.
[71] KIEFHABER, E., Forschungszentrum Karlsruhe, private communication (2005).
[72] MASCHEK, W., RINEISKI A., SUZUKI T., WANG, S., MORI, M., WIEGNER, E., WILHELM, D., KRETZSCHMAR, F., TOBITA, Y., YAMANO, Y., FUJITA, S., COSTE, P., PIGNY, S., HENRIQUES, A., CADIOU, T., MORITA, K., BANDINI, G., SIMMER-III and SIMMER-IV Safety Code Development for Reactors with Transmutation Capability, paper presented in Int. Conf. on Mathematics and Computations M&C 2005, Avignon, France, 12-15 September 2005.
[73] BROEDERS, C.H.M, Entwicklungsarbeiten für die neutronernphysikalische Auslegung von Fortschrittlichen Druckwasserreaktoren (FDWR) mit kompakten Dreiecksgittern in hexagonalen Brennelementen, Kernforschungszentrum Karlsruhe, KFK 5072 (1992).
[74] BACHMANN, H., BUCKEL, G., HOEBEL, W., KLEINHEINS, S., The modular System KAPROS for Effi-cient Management of Complex Reactor Calculations, paper presented in Int. Conf. on Computational Methods in Nuclear Energy, CONF-750413, Charleston, USA, l5-l7 April l975.
[75] DAGAN, R., BROEDERS, C.H.M., STRUWE, D., Modifications of the Code SAS4A for Simulation of ADS Designs, Forschungszentrum Karlsruhe, FZKA 6334.
[76] CAHALAN, J.E., Advanced LMR Safety Analysis Capabilities in the SASSYS-1 and SAS4A Computer Codes, paper presented in Int. Topical Meeting on Advanced Reactors Safety, Pittsburgh, Pensylvania, USA, 17-21 April 1994.
[77] DORIATH, J.Y., MCCALLIEN C.W., KIEFHABER E., WEHMAN U., RIEUNIER J.M., ERANOS 1: The advanced European system of codes for Reactor Physics Calculations, paper presented in Int. Conf. on Mathematical Methods and Supercomputing in Nuclear Applications (M&C+SNA'93), Karlsruhe, Germany, 19-23 April 1993.
[78] RIMPAULT, G., Algorithmic features of the ECCO cell code for treating heterogeneous fast reactor subassemblies, paper presented in Int. Topical Meeting on Reactor Physics and Computations, Portland, USA, 30 April-4 May 1995.
[79] SMITH, P., RIMPAULT, CABRILLAT, J.C., MARTINI, M., JACQMIN, J., OHKI, S., The CIRANO Experimental Programme for CAPRA Core Physics Studies, paper presented in CAPRA International Seminar, CEA Cadarache, France, June 1997.
[80] RIMPAULT, G., et al, Experimental Validation of Nuclear Data and Methods for Steel Reflected Plutonium Burning Fast Reactor, Proc. PHYSOR 2006, Vancouver, Canada, 10-14 September 2006, ANS, ISBN: 0-89448-697-7, CD-ROM.
[81] RIMPAULT, G., et al, ERANIS Neutronics Calculations of B4C-moderated Subassembly and Experimental Validation in MASURCA, Proc. PHYSOR 2000, Pittsburgh, Pennsylvania, 7-11 May 2000, ANS, ISBN: 0-89448-655-1, CD-ROM.
[82] O'DELL, R.D., Standard Interface Files and Procedures for Reactor Physics Codes, Version IV, Los Alamos National Laboratory, LA-6941-MS (1977).
[83] BRIESMEISTER, J.F.(Editor), MCNP4C—a general Monte Carlo n-particle transport code, version 4c, Los Alamos National Laboratory, LA-13709-M (2000)

[84] RINEISKI, A., SINITSA V., MASCHEK W., C4P, a Multigroup Nuclear CCCC Data Processing System for Reactor Safety and Scenario Studies, Proc. Jahrestagung Kerntechnik, Nürnberg, Germany, 10-12 May 2005.
[85] RINEISKI, A., SINITSA V., Extended Probability Tables for Approximating Neutron Multigroup Cross-Sections, paper presented in Int. Conf. on Mathematics and Computations M&C 2003, Gatlinburg, Tennessee, USA, 6-11 April 2003.
[86] BHOJE, S.B., Design and Construction of Fast Breeder Test Reactor, paper presented in International Symposium on Fast Breeder Reactors, Lyon, France, 1985.
[87] CHETAL, S.C., The Design of Prototype Fast Breeder Reactor, Nucl. Engg. And Design, Vol. 236, p. 852 (2006).
[88] DEVAN, K., GOPALAKRISHNAN, V., MOHANAKRISHNAN, P., SRIDHARAN, M.S., Preparation of Multigroup Lumped Fission Product Cross-sections from ENDF/B-VI for FBRs, Annals of Nuclear Energy, Vol. 25, p. 161 (1998).
[89] MAHALAKSHMI, B. MOHANAKRISHNAN, P., Analysis of Radially Heterogeneous ZPPR-13A Benchmark for Investigating the Spatial Dependence of the C/E of Control Rod Worths, Nucl. Sci. and Eng., Vol. 115, p. 341 (1993).
[90] MANTUROV, G.N., NIKOLAEV, M.N., TSIBOULYA, A.M., The ABBN-93 Group Data Library. Part 1: Nuclear Data for Calculation of Neutron and Photon Radiation Fields, INDC(CCP)-409/L, IAEA, p. 65 (1997).
[91] GOPALAKRISHNAN, V. GANESAN, S., Self-shielding and Energy Dependence of Dilution Cross-sections in the Resolved Resonance Region, Annals of Nuclear Energy, Vol. 25. No. 11, p. 839 (1998).
[92] GOPALAKRISHNAN, V., Temperature Dependence of Unshielded Cross-sections in Multigroup Cross-section Sets, Annals of Nuclear Energy, Vol. 27, p. 1029 (2000).
[93] KESHAVAMURTHY, R.S., HARISH, R., Use of Pade Approximation in the Analytical Evaluation of J(θ, β) and its Temperature Derivative, Nucl. Sci. and Eng., Vol. 115. p. 81 (1993).
[94] DEVAN, K. KESHAVAMURTHY, R.S., Rational Approximations to Reich-Moore Collision Matrix of Non-Fissile Nuclides, Annals of Nuclear Energy, Vol. 26, p. 1253 (1999).
[95] DEVAN, K., AND KESHAVAMURTHY, R.S., Extension of Rational Approximations to p-wave Collision Amplitudes in Reich-Moore Formalism, Annals of Nuclear Energy, Vol. 28, p. 1013 (2001).
[96] KIM, Y.I., Nuclear and Thermal-Hydraulic Design and Analysis of KALIMER Breakeven Equilibrium Cycle, LMR/CD112-ER-01 Rev. 0, KAERI (2000).
[97] KIM, J.D., KAFAX-E66, Calculation Note No. NDL-23/01, Nuclear Data Evaluation Lab. Internal Report, KAERI (2001).
[98] MACFARLANE, R.E., TRANSX 2: A Code for Interfacing MATXS Cross-Section Libraries to Nuclear Transport Codes, Los Alamos National Laboratory, 16 December 1993.
[99] DERSTINE, K.L., DIF3D: A Code to Solve One-, Two-, and Three-Dimensional Diffusion Theory Problems, ANL-82-64, Argonne National Laboratory (1982).
[100] SEREGIN, A.S., Documentation of the TRIGEX program for small-group neutron physics calculations of a reactor in three-dimensional hexagonal geometry, Problems of Atomic Science and Technology, Series Physics and Technology of Nuclear Reactors, No. 4 (33), 59 (1983).
[101] LUCAS, A., User's Manual for DEGEN, Los Alamos National Laboratory (1988).

[102] FOWLER, T.B., VONDY, D.R., CUNNINGHAM, G.W., Nuclear Reactor Core Analysis Code: CITATION, ORNL/TM-2496, Oak Ridge National Laboratory (1969).
[103] HARDIE, R.W., LITTLE JR., W.W., 3DB-A three-dimensional diffusion theory burn-up code, BNWL-1264, Pacific Northwest Lab (1970).
[104] STEHLE, B., D3D und D3E - Zweige eines FORTRAN-Programms zur Loesung der stationaeren dreidimensionalen Multigruppenneutronendiffusionsgleichungen in Rechteck-, Zylinder- und Dreieckgeometrie, Kernforschungszentrum Karlsruhe, KFK-4764 (1991).
[105] LAWRENCE, R.D., The DIF3D Nodal Neutronics Option for Two- and Three-Dimensional Diffusion Theory Calculations in Hexagonal Geometry, ANL-83-1, Argonne National Laboratory (1983).
[106] WAGNER, M.R., Three-dimensional Nodal Diffusion and Transport Theory Methods for Hexagonal-Z Geometry, paper presented in Int. Reactor Physics Conference, Jackson Hole, Wyoming, USA, 18-22 September 1988.
[107] TOPPEL, B.J., A User's Guide for the REBUS-3 Fuel Cycle Analysis Capability, ANL-83-2, Argonne National Laboratory (1983).
[108] FLETCHER, J.K., A User's Guide to the MARC and PN Computer Codes, TRG Report 2911(R), The Reactor Group, United Kingdom Atomic Energy Authority (September 1976).
[109] PALMIOTTI, G., Optimized Two-dimensional S_n-transport (BISTRO), Proc. Int. Topical Meeting on Advances in Reactor Physics. Mathematics and Computation, Paris, France, 27-30 April 1987.
[110] BANDO, M., Three-dimensional Transport Calculation Method for Eigenvalue Problems Using Diffusion Synthetic Acceleration, Nucl. Sci. Tech., 22 (1985).
[111] ALCOUFFE, R.E., BAKER, R.S., BRINKLEY, F.W., MARR, D.R., O'DELL, R.D., WALTERS, W.F., DANTSYS: A Diffusion Accelerated Neutral Particle Transport Code System, LA-12969-M (June 1995).
[112] WAREING, T.A., MCGHEE, J.M., MOREL, J.E., ATTILA: A Three-Dimensional, Unstructured Tedrahedral Mesh Discrete Ordinates Transport Code, Trans. Am. Nucl. Soc., 75, 146 (1996).
[113] YAMAMOTO, T., Three-Dimensional Transport Correction in Fast Reactor Core Analysis, Journal of Nuclear Science and Technology, Vol. 23, No. 10, pp. 849-858 (October 1986).
[114] ALCOUFFE, R.E., BAKER, R.S., DAHL, J.A., TURNER, S.A., PARTISN Abstract, Proc. PHYSOR 2000, Pittsburgh, Pennsylvania, USA, 7-11 May 2000, ANS, ISBN: 0-89448-655-1, CD-ROM.
[115] HAGHIGHAT, A., SJODEN, G.E., PENTRAN™ (Parallel Environment Neutral-article TRANsport) Code System, Proc. PHYSOR 2000, Pittsburgh, Pennsylvania, USA, 7-11 May 2000, ANS, ISBN: 0-89448-655-1, CD-ROM.
[116] SIMPSON, D.B., DOORS 3: Discrete Ordinates Oak Ridge System, Proc. PHYSOR 2000, Pittsburgh, Pennsylvania, USA, 7-11 May 2000, ANS, ISBN: 0-89448-655-1, CD-ROM.
[117] SOOSLOV, I.R., Method of Characteristics in Fast Reactor Control Rod Calculations, paper presented in IAEA Specialists Meeting, Winfrith, UK, 6-8 December 1988.
[118] LAWRENCE, R.D., DORNING, J.J., A Nodal Green's Function Method for Multi-dimensional Neutron Calculations, Nucl. Sci. Eng., 76 (1980).

[119] SUGINO, K., An Improvement of the Transverse Leakage Treatment fro the Nodal SN Transport Calculation Method in Hexagonal-Z Geometry, Journal of Nuclear Science and Technology, Vol. 33, No. 8, pp. 620-627 (Aug. 1996).
[120] LEWIS, E.E., MILLER, W.F., Computational Methods of Neutron Transport Theory, Wiley, New York, USA (1984).
[121] DILBERT, I., LEWIS, E.E., Variational Nodal Methods for Neutron Transport, Nucl. Sci. Eng., 91, 132 (1985).
[122] PALMIOTTI, G., CARRICO, C.B., LEWIS, E.E., VARIANT: Variational Anisotropic Nodal Transport for Multidimensional Cartesian and Hexagonal Geometry Calculation, ANL-95/40, Argonne National Laboratory (1995).
[123] GRABEJNOI, V.A., USANOV, V.I., A Collision Probability Method Applied to Neutron Shielding Calculations, Preprint-2270, Institute for Physics and Power Engineering, Obninsk, Russian Federation (1992).
[124] DORIATH, J.Y., Reactor Analysis Using a Variational Nodal Method Implemented in the ERANOS System, paper presented in Topical Meeting on Advances in Reactor Physics: Reactor Physics Faces the 21st Century, Knoxville, Tennessee, USA (1994).
[125] MAJOROV, L.V., GOMIN, E.A., Collision Probability Calculations in a System With Complex Geometry Structure, Problems of Atomic Science and Technology, Series Physics and Technology of Nuclear Reactors, Issue 8 (1981).
[126] BROWN, F.B., ED., MCNP – A General Monte Carlo N-Particle Transport Code - version 5, LA-UR-03-1987, Los Alamos National Laboratory (2003).
[127] STRAKER, E.A., The MORSE Code - A Multigroup Neutron and Gamma-ray Monte Carlo Transport Code, ORNL-4585, Oak Ridge National Laboratory (1970).
[128] PETRIE, L.M., CROSS, N.F., KENO IV: An Improved Monte Carlo Criticality Program, ORNL-4938, Oak Ridge National Laboratory (November 1975).
[129] NAGAYA, Y., OKUMURA, K., MORI, T., NAKAGAWA, M., MVP/GMVP II: General Purpose Monte Carlo Codes for Neutron and Photon Transport Calculations on Continuous Energy and Multigroup Methods, JAERI 1348 (2005).
[130] BOTH, J.P., et al., User manual for version 4.3 of the TRIPOLI-4 Monte Carlo method particle transport computer code, CEA-R-6044 (2003).
[131] BLOMQUIST, R.N., VIM Continuous Energy Monte Carlo Transport Code, paper presented in Int. Conf. on Mathematics, Computations, Reactor Physics and Environmental Analysis, Portland, Oregon, USA, 30 April-4 May 1995.
[132] KAZAKOVA, L.B., Developing the Functional Possibilities of the MMKFK Programs for Modeling Neutron Gamma-Quanta Transport, paper presented in VII All-Union Conference Monte Carlo Methods in Mathematics and Mathematical Physics Calculations, Novosibirsk, Russian Federation (1985).
[133] KOROBEJNIKOV, V.V., USANOV, V.I., Combined Methods in Transport Irradiation Problems, Energoatomizdat, Moscow, Russian Federation (1994).
[134] DENSMORE, J.D., LARSEN, E.W., Variational Variance Reduction for Monte Carlo Eigenvalue and Eigenfunction Problems, Nucl. Sci. Eng., 146, 121 (2004).
[135] CROFF, A.G., ORIGEN2 - A Revised and Updated Version of the Oak Ridge Isotope Generation and Depletion Code, ORNL-5624, Oak Ridge National Laboratory (1980).
[136] POSTON, D.I., TRELLUE, H.R., User's Manual Version 2.0, for Monteburns, Version 1.0, Los Alamos National Laboratory, LA-UR-99-4999 (1999).
[137] BABCOCK, R.S., WESSOL, D.E., WEMPLE, C.A., MASON, S.C., The MOCUP Interface: A Coupled Monte Carlo/Depletion System, Proc. Topical Meeting on

Advances in Reactor Physics, Knoxville, Tennessee, USA, 11-15 April 1994 (3 Vols and 1 supplement), Item ID: 700215.
[138] XU, Z., An Improved MCNP-ORIGEN Depletion Program (MCODE) and Its Verification for High-Burnup Applications, Proc. PHYSOR 2002, Seoul, Korea, 7-10 October 2002, ANS, ISBN: 0-89448-672-1, CD-ROM.
[139] CHANG, G.S, MCWO - Linking MCNP and ORIGEN2 for Fuel Burnup Analysis, Proc. Monte Carlo 2005 Topical Meeting, Chattanooga, Tennessee, 17-21 April 2005, ANS, ISBN: 0-89448-695-0, CD-ROM.
[140] HAECK, W., VERBOOMEN, B. AIT ABDERRAHIM, H., ALEPH: An efficient Approach to Monte Carlo Burnup, Proc. Monte Carlo 2005 Topical Meeting, Chattanooga, Tennessee, USA, 17-21 April 2005, ANS, ISBN: 0-89448-695-0, CD-ROM.
[141] BOWMAN, S.M., DEHART, M.D., PETRIE, L.M., Integrated KENO Monte Carlo Transport for 3-D Depletion with SCALE, Proc. Monte Carlo 2005 Topical Meeting, Chattanooga, Tennessee, USA, 17-21 April 2005, ANS, ISBN: 0-89448-695-0, CD-ROM.
[142] PELOWITZ, D.B., (Editor), MCNPX User's Manual, Version 2.5.0, LA-CP-05-0369 (2005).
[143] MOCHIZUKI, H., SUYAMA, K., OKUNO, H., SWAT2: The Improved SWAT Code System by Incorporating the Continuous Energy Monte Carlo Code MVP, paper presented in 7th Int. Conf. on Nuclear Criticality Safety (ICNC2003), Tokai-mura, Japan, 20-24 October 2003.
[144] OKUMURA, K., MORI, T., NAKAGAWA M., KANEKO, K., Validation of a continuous-energy Monte Carlo burn-up MVP-BURN and its application to analysis of post irradiation experiment, J. Nucl. Sci. Technol., Vol. 37, No. 128 (2000).
[145] KELLY, D.J., Depletion of a BWR lattice using the RACER continuous energy Monte Carlo code, Proc. Int. Natl. Conf. on Mathematics and Computations, Reactor Physics, and Environmental Analyses, Portland, Vol. 2, p. 1011 (1995).
[146] MORIMOTO, Y., MARUYAMA, H., ISHII, K. AOYAMA, M., Neutronic analysis code for fuel assembly using a vectorized Monte Carlo method, Nucl. Sci. Eng., 103, p. 351 (1989).
[147] TAIWO, T.A., DIF3D-K: A nodal kinetics code for solving the time-dependent diffusion equation in hexagonal-Z geometry, ANL/NPR-92/17, Argonne National Laboratory (1992).
[148] TAIWO, T., RAGLAND, R., PALMIOTTI, G., FINCK, P.J., Development of a Three-Dimensional Transport Kinetics Capability for LWR-MOX Analyses, Trans. Am. Nucl. Soc., Vol. 79, No. 298 (November 1999).
[149] CAHALAN, J.E., Advanced LMR Safety Analysis Capabilities in the SASSYS-1 and SAS4A Computer Codes, Proc. Int. Topical Meeting on Advanced Reactors Safety, American Nuclear Society, Pittsburgh, Pennsylvania, USA, 17-21 April 1994, Vol. 2, pp. 1038-1045 (1994).
[150] CAHALAN, J.E., Development of a Coupled Dynamics Code with Transport Theory Capability and Application to Accelerator-Driven Systems Transients, Proc. PHYSOR 2000, Pittsburgh, Pennsylvania, USA, 7-11 May 2000, ANS, ISBN: 0-89448-655-1, CD-ROM.
[151] YANG, W.S., FINCK, P.J., KHALIL, H., Reconstruction of Pin Power and Burnup Characteristics from Nodal Calculations in Hexagonal Geometry, Nucl. Sci. Eng., Vol. 111, No. 21 (1992).
[152] SERYOGIN, A.S., A summary of TRIGEX code for small-grouped calculation of reactor in three-dimensional hexagonal geometry, Issues of Nucl. Sci. & Tech.,

Series: Phys. & Tech. of Nucl. Reactors, Issue 4, No. 33, pp. 59-60 (1983) (in Russian).
[153] ALPEROVICH, M.N., GRIGORIEVA, N.M., SYSOEVA, O.V., SELEZNEV, E.F., YABLOKOV, S.L., A summary of GEFEST code, Issues of Nucl. Sci. & Tech., Series: Phys. & Tech. of Nucl. Reactors, Issue 4, pp. 36-43 (1994) (in Russian).
[154] BARINOV, S.V., RADKEVICH, A.V., Use of system of preparation of multigroup neutron data CONSYST/ABBN in a code complex FACT-BR for three-dimensional neutronics calculation of BREST-OD-300 reactor, paper presented in All-Russian seminar "Neutronics-99", Obninsk, Russian Federation, 2000 (in Russian).
[155] PETRIE, L.M., LANDERS, N.F., KENO 5A - An Improved Monte Carlo Criticality Program with Supergrouping, NUREG /CR-0200. Rev. 2 (ORNL/NUREG/CSD-2/R2) (December 1984).
[156] POLEVOI, V.B., TARASOVA, O.B., A code complex MMKFK-2 for calculation of transport processes of neutrons and gamma-quantums in reactor physics, paper presented in All-Russian seminar "Neutronics-98", Obninsk, Russian Federation, 1999 (in Russian).
[157] HOLLENBACH, D.F., PETRIE, L.M., LANDERS, N.F., KENO VI: A General Quadratic Version of the KENO Program, NUREG /CR-0200. Rev. 5 (ORNL/NUREG/CSD-2/V2/R5) (1995).
[158] BLYSKAVKA, A.A., POLYAKOV, A.YU., TSIBULYA A.M., FORMCNP – a code of formation of group constant library for MCNP, Preprint IPPE-2924, Obninsk, Russian Federation (2001) (in Russian).
[159] LEWIS, E. E., CARRICO C.B., PALMIOTTI G., Variational Nodal Formulation for the Spherical Harmonics Equations, Nucl. Sci. Eng., Vol. 122, No. 194.
[160] BUCKEL, G., HESSELSCHWERDT, E., KIEFHABER, E., KLEINHEINS, S., MASCHEK, W., A New SIMMER-III Version with Improved Neutronics Solution Algorithms, Forschungszentrum Karlsruhe, FZKA 6290 (1999).
[161] FUJITA, S., AND KIEFHABER, E., O-arai Research and Development Center of JAEA and Forschungszentrum Karlsruhe, private communication (2005).
[162] ALCOUFFE, R.E., Diffusion synthetic acceleration methods for the diamond-differenced discrete ordinates equations, Nucl. Sci. Eng. Vol. 64, No. 344.
[163] PALMIOTTI, G., RIEUNIER, J.M., GHO, C., SALVATORES, M., Optimized Two-Dimensional Sn Transport (BISTRO), Nucl. Sci. Eng. Vol. 104, No. 26.
[164] FOWLER, T.B., et. al, Nuclear Reactor Core Analysis Code: CITATION, ORNL-TM2496, Rev. 2 (1971).
[165] RINEISKI, A., KIN3D: Module de cinétique spatiale et de perturbations pour TGV2, Cadarache, SPRC/LEPh 97-203 (1977).
[166] RINEISKI, A., Intra-Nodal Reactivity Calculations Based on the Variational Nodal Method, Proc. Int. Conference on Mathematics and Computations M&C 2001, Salt Lake City, USA, 9-13 September 2001.
[167] WIESE, H.W., Status und Weiterentwicklung des Inventarcodes KORIGEN, der Szenariocodes KORREC und SOLEQ sowie des Nachwärmecodes CALOR, Forschungszetrum Karlsruhe, FZKA 6741 (2002).
[168] BELL, M.J., ORIGEN – The ORNL Isotope Generation and Depletion Code, Oak Ridge National Laboratory, ORNL-4628 (CCC-217).
[169] RINEISKI, A., Decay Heat Production in a TRU Burner, paper presented in Symposium Innovative Nuclear Energy Systems (INES-2), Yokohama, Japan, 26-30 November 2006.

[170] SRIDHARAN, M.S., MURTHY, K.P.N., An Assessment of Fission Product Data for Decay Power Calculation in Fast Reactors, paper presented in Specialists Meeting on Data for Decay Heat Predictions, Studsvik, Sweden (1987).
[171] PANDIKUMR, G., Multiple Recycling of Fuel in PFBR, paper presented in DAE-BRNS Theme Meeting in Advances in Reactor Physics: Design, Analysis and Operation of Nuclear Reactors, BARC, India (2007).
[172] PANDIKUMAR, G., GOPALAKRISHNAN, V., MOHANAKRISHNAN, P., Prediction of Inventories, Activities and Decay Heats in PFBR, National Symposium on Radiation Physics (NSRP-16), Chennai, India, 18-20 January 2006.
[173] DEVAN, K., A Fast Breeder Reactor Model for Incineration of Long-lived Minor Actinides, paper presented in IAEA Research Coordinated Meeting on the Coordinated Research Project on Studies of Innovative Reactor Technology Options for Effective Incineration of Radioactive Waste, Chennai, India, 15-19 January 2007.
[174] KIM, T.K., KIM, Y.J., KIM, Y.I., Interfaces Current Nodal Formulation of Simplified P2 Equations in Multi-Dimensional Hexagonal Geometry, Proc. PHYSOR 2000, Pittsburgh, Pennsylvania, USA, 7-11 May 2000, ANS, ISBN: 0-89448-655-1, CD-ROM.
[175] GILBERT, E.R., BATES, J.F., Dependence of Irradiation Creep on Temperature and Atom Displacement in 20% Cold Worked Type 316 Stainless Steel, J. of. Nucl. Materials, Vol. 65, No. 204 (1977).
[176] KATAKURA, J., IIJIMA, S., Analysis of Uncertainties in Summation Calculations of Decay Heat Using JNDC FP, Nuclear Data Library, Jour. Nucl. Sci. Tech., 29 (1992).
[177] REBAH, R. Sensitivity and Uncertainty Analysis for Fission Product Decay Heat Calculations, Proc. Int. Conf. on Radiation Shielding, Arlington, Virginia, USA, ANS, p. 63 (1994).
[178] TACHIBANA, T., YAMADA, M., YOSHIDA, Y., Improvement of the Gross Theory of beta-Decay. II --One-Particle Strength Function--, Prog. Theor. Phys., 84, p. 641 (1990).
[179] KLAPDOR, H.V., METZINGER, J., Predictions of the Decay Heat of Nuclear Reactors by Microscopic Beta Decay Calculations, paper presented in Int. Conf. Nuclear Data for Science and Technology, Mito, Japan (1988).
[180] TOBIAS, A., Decay Heat, Prog. Nucl. Energy, 5 (1980).
[181] TASAKA, K., Recommendation on Decay Heat Power in Nuclear Reactors, Jour. Nucl. Sci. Technol., 28, p. 1134 (1991).
[182] AMERICAN NUCLEAR SOCIETY, ANSI/ANS-5.1-2005: Decay Heat Power in Light Water Reactors (2005).
[183] KUESTERS, H., Nuclear Data Needs for the Analysis of Generations and Burn-up of Actinide Isotopes in Nuclear Reactors, KfK-2917, Kernforschungszentrum Karlsruhe (1980).
[184] D'ANGELO, A., Calculation and Experiment Comparison for Sample and Fuel Pin Irradiation Experiments in PHENDC, Proc. Topical Meeting Reactor Physics and Safety, Saratoga Springs, USA (1986).
[185] NORGETT, M.J., ROBINSON, M.T., TORRENS, I.M., Proposed Standard for Calculating Displacement Dose Rates, Proc. Specialists' Meeting on Radiation Damage Units for Ferritic and Austenitic Stainless Steels, Seattle, Washington, USA 31 October – 1 November 1972, paper CONF-721037-1.
[186] DORAN, D.G. GRAVES, N.J., Displacement Cross Sections and PKA Spectra; Tables and Applications, Hanford Engineering Development Laboratory Report HEDL-TME 76-70 (UC-79) (1976).

[187] GRYNTAKIS, E.M., A Compilation of the Fission Spectrum Average Neutron Cross-Sections for (n,α) Reactions, Jour. Radioanalytical Chem., Vol. 52, No. 1, p. 219 (1979).
[188] SZONDI, E. J., The Cross-Section Library IRDF-90/NMF-G and Its User-Friendly Processing for Practical Applications, paper presented in Int. Conf. on Nuclear Data for Science and Technology, Gatlinburg, USA (1994).
[189] FERNANDEZ, A.F., et al, Gamma dosimetry using Red 4034 Harwell in mixed fission neutrons and gamma environments, IEEE Trans. on Nuclear Science (2005).
[190] ROWLANDS, J.L., Development and Validation of Control Rod Calculation Methods, paper presented in Int. Symp. Fast Reactor Physics, Aix-en-Provence, France (1979).
[191] CARPENTER, S.G., et al, Experimental Studies of 6000 Liter LMFBR Cores at ZPPR, paper presented in Int. Conf. Advances in Reactor Physics and Shielding, Sun Valley, USA (1980).
[192] ISHIKAWA, M., Consistency Evaluation of JUPITER Experiment and Analysis for Large FBR Cores, Proc. Int. Conf. Reactor Physics (PHYSOR 96), Mito, Japan, pp. E36-E45 (September 1996).
[193] MOHANAKRISHNAN, P., COHINT, A Computer Code to Treat Control Rod Heterogeneity and its Application to Fast Reactor Core Analysis, IGC-130 (1992).
[194] MOHANAKRISHNAN, P., Development and Validation of Fast Reactor Core Burnup Code FARCOB, Accepted for Publication in Annals of Nuclear Energy (2007).
[195] ISHIKAWA, M., Recent Application of Nuclear Data to Fast Reactor Core Analysis and Design in Japan, Proc. Int. Conf. on Nuclear Data for Science and Technology (ND2004), Santa Fe, USA (Sep. 2004).
[196] NEACRP, Proc. of Specialists' Meeting on Control Rod Measurement Techniques: Reactivity Worth and Power Distributions, NEACRP-U-75, Cadarache, France (1976).
[197] ORLOV, VV, MATVEEV, VI, ZHUKOV, A.V., et al, Basic principles of control rods selection for fast reactors and the temperature and power effects in fast reactors, “Kernenergie” 12. Jahrgang Heft (4/1969).
[198] MATVEEV, V.T. et al., “Review of Technical Approaches and Solutions for LMFR Control Rods Development”, Absorber Materials, Control Rods and Designs of Shutdown Systems for Advanced Liquid Metal Fast Reactors, IAEA-TECDOC-884, IAEA, Vienna (1996).
[199] GANDINI, A., Time-Dependent Generalized Perturbation Theory for Burnup Analysis, Comitato Nazionale per l'Energia Nucleare, Casaccia, Rome, Italy RT/FI(75) 4 (1975).
[200] YANG, W.S., DOWNAR, T.J., Depletion Perturbation Theory for the Constrained Equilibrium Cycle, Nucl. Sci. Eng., 102, p. 365 (1989).
[201] KIM, T.K., Development of A Perturbation Code for Hexagonal Core, paper presented in ’98 KNS Autumn Meeting, Korea Nuclear Society (1998).
[202] KIM, T.K., et al, Measurement of k_{eff} in the Fast Critical Assembly BFS and Validation of k_{eff} Computation Code, BETA-K, Journal of the Korean Nuclear Society, Vol. 31, No. 4, pp. 401-7 (1999).
[203] MEYER, R.A., et al Design and Analysis of SEFOR Core 1. GEAP- 13598 (June 1970).
[204] POPLAVSKY, VM, MATVEEV, VI, ROGOV, VY, et al., Physical and engineering problems of enhancing safety and efficiency of actinides burning in an advanced fast reactor. The book, printed in IPPE, Obninsk, Russian Federation (2001)

[205] ISTC Project 1321, Final Report, Volume IV, Measuring of the Doppler effect of ^{239}Pu and ^{240}Pu at the BFS critical facility, Obninsk, Russian Federaton (2003).
[206] MANTUROV, GN, NIKOLAEV, MN, TSIBOULYA, AM, System of Group Constants ABBN-93. Part 1: Nuclear constants for the calculation of neutron and photon radiation transport, Journal 'News of Atomic Science and Technique', Serial: Nuclear constants. Issue 1, Moscow, Russian Federation, p. 59 (1996).
[207] ISHIKAWA, M., Development of a Unified Cross-section Set ADJ2000 based on Adjustment Technique for Fast Reactor Analysis, Journal of Nuclear Science and Technology, Supplement 2, pp. 1073-1076 (August 2002).
[208] OTUKA, N., ZUKERAN, A., TAKANO, H., CHIBA, G., ISHIKAWA, M., Covariance Analyses of Self-Shielding Factor and Its Temperature Gradient for Uranium-238 Neutron Capture Reaction, Journal of Nuclear Science and Technology, Vol. 45, No. 3, p. 849 (March 2008).
[209] CALDAROLA, L., SEFOR Experimental Results and Applications to LMFBR's, Proc. Int. Conf. on Engineering of Fast Reactors, Vol. 3, p. 1312, Karlsruhe, Germany (1972).
[210] ISHIGURO, Y., Measurements and Analysis of the Doppler Effect of Structural Materials, Proc. Int. Symp. Physics of Fast Reactors, Vol. 2, p. 964, Tokyo (1973).
[211] DE KRUIJF, W.J., JANSSEN, A.J., The Effective Fuel Temperature to be Used for Calculating Resonance Absorption in a $^{238}UO_2$ Lump with a Non-uniform Temperature Profile, Nucl. Sci. and Eng., Vol. 123, No. 121 (1996).
[212] BUTLAND, T., An Assessment of Methods for Calculating Doppler Effects in Plutonium Fuelled Sodium-Cooled Fast Reactors, Proc. Int. Symp. on Fast Reactor Physics, Vol. 1, p. 257, Aix-en-Provence, France (1979).
[213] HAZAMA, T., TOMMASI, J., Re-Evaluation of SEFOR Doppler Experiments and Analyses with JNC and ERANOS systems, Proc. PHYSOR 2004, Chichago, Illinois, USA, 25-29 April 2004, ANS, ISBN: 0-89448683-7, CD-ROM.
[214] GAUTHIER, J.C., et al., Comparaison calcul-experience pour la mesure de l'effet Doppler sur PHENIX, Proc. Int. Symp. Fast Breeder Reactors, Lyon, France (1985).
[215] VANIER, M., SUPER-PHENIX Reactivity and Feedback Coefficients, Nucl. Sci and Eng., 106 (1990).
[216] RIMPAULT, G., SEFOR and SUPER-PHENIX Start-up Doppler Experiments Analysis with the European Code Scheme JEF2/ECCO/ERANOS, paper presented in Int. Conf. Mathematical Methods and Super-computing in Nuclear Computations, Arlington, Virginia, USA (1994).
[217] KHALIL, H.S., HILL, R.N., Evaluation of Liquid-Metal Reactor Design Options for Reduction of Sodium Void Worth, Nucl. Sci. Eng., 109, 221 (1991).
[218] MATVEEV, V.I., CHEBESKOV, A.N., CHERNY, V.A., et al., Studies, Development and Justification of Core with Zero Sodium-Void Reactivity Effect of the BN-800 Reactor, paper presented in Int. Topical Meeting on Sodium Cooled Fast Reactor Safety, Obninsk, Russia, 3-4 October 1994.
[219] IAEA/CEC, Summary Report of the Consultancy on Benchmark Evaluations of Sodium Void Reactivity Effect in Fast Reactor Core, Vienna, Austria, 23-25 November 1992.
[220] KRIVITSKY, IY, MATVEEV, VI, Calculation of the test model of the reactor core of BN-800 with zero SVRE (Sodium Void Reactivity Effect) using the BNAB-93 (ABBN-93) constants. Preprint IPPE 2541, Obninsk, Russian Federation (1996).
[221] KRIVITSKY, IY, MATVEEV, VI, BELOV, S.P., SHAPAR, AV, Study of SVRE at BFS critical facility simulating the reactor core of the BN-800 with sodium cavity. Preprint IPPE - 2538, Obninsk, Russian Federation (1996).

[222] CALAMAND, D., CURL, I.J., A Review of Progress with the JANUS Program of Fast Reactor Shielding Experiments, paper presented in Int. Conf. on the Physics of Reactors: Operation, Design, and Computation, Marseilles, France, 1990.
[223] SARTORI, E., Standard Energy Group Structures Of Cross Section Libraries For Reactor Shielding, Reactor Cell and Fusion Neutronics Applications: VITAMIN-J, ECCO-33, ECCO-2000 and XMAS, OECD/NEA, JEF/DOC-315, Revision 3 (1990).
[224] INDIRA, R., Fast Reactor Bulk Shielding Experiments for Validation of Shielding Computational Techniques, Proc. Conf. Nuclear Mathematical and Computational Science, Gatlinburg, Tennessee, USA, ANS (2003)
[225] DEVAN, K., Generation and Validation of a New 121 Group Coupled (n,γ) Cross-section Set for Fast Reactor Applications, Annals of Nuclear Energy, Vol. 23, p. 791 (1996).
[226] DEVAN, K., Effects of Cross-section Sets and Quadrature Orders on Neutron Fluxes and on Secondary 24 Na Acivation Rate of a Pool Type 500 MWe FBR, Annals of Nuclear Energy, Vol. 30, p. 1181 (2003).
[227] MCKNIGHT, R.D., KRSUL, J.R., Validation Results Based on the Spent Fuel Demonstration Program at FCF, Proc. ANS Fourth Topical Meeting on DOE Spent Nuclear Fuel and Fissile Material Management, San Diego, CA, USA, 4-8 June 2000.
[228] SCHLTYSS, W., IRMA: Interlaboratory Comparison of Fission and Capture Rate Measurement Techniques at MASURCA, Proc. ANS Int. Symp. Reactor Physics, Jackson Hole, USA (1988).
[229] CABRILLAT, J-C, Common Lessons Drawn from Different Laboratories Analyses of SUPER-PHENIX Startup Experiments, Proc. Int. Conf. Physics of Reactors: Operation, Design, and Computation, Vol. 1, p. VII-10, Marseilles, France (1990).
[230] BRUMBACH, S.B., Experiments and Analysis for Large Conventional Fast Reactors in ZPPR-18/19, paper presented in Int. Conf. Physics of Reactors: Operation, Design, and Computation, Marseilles, France (1990).
[231] ROBINSON, P.J., Comparison of Calculation and Measurements of Reaction Rates in the Outer Regions of SUPER-PHENIX, paper presented in Int. Conf. Physics of Reactors: Operation, Design, and Computation, Marseilles, France (1990).
[232] DE WOUTERS, R., Measurements and Analyses of Gamma-ray Energy Deposition in a Critical Assembly Containing a Central Simulated Diluent, paper presented in Int. Conf. Physics of Reactors: Operation, Design, and Computation, Marseilles, France (1990).
[233] SCHAEFER, R.W., LELL, R.M., MCKNIGHT, R.D., Criticality Safety Benchmark Experiments Derived from Argonne National Laboratory Zero Power Reactor Assemblies, Nucl. Sci. Eng., 145, 84 (2003).
[234] OKAJIMA, T., Summary on International Benchmark Experiments for Effective Delayed Neutron Fraction, Progress in Nuclear Energy, 41, 285 (2002).
[235] NEWTON, T., The Evaluation of SUPER-PHENIX Core Reactivity Levels, paper presented in Int. Conf. on the Physics of Reactors: Operation, Design, and Computation, Marseilles, France, 1990.
[236] BERGEONNEAU, P., Analysis and Interpretation of the Neutronic Experimental Results at the SUPER-PHENIX Restart-up in 1989, paper presented in Int. Conf. on the Physics of Reactors: Operation, Design, and Computation, Marseilles, France, 1990.
[237] SUGINO, K., MONJU Experimental Data Analysis and its Feasibility Evaluation to Build up the Standard Data Base for Large FBR Nuclear Core Design, Proc.

PHYSOR 2006, Vancouver, Canada, 10-14 September 2006, ANS, ISBN: 0-89448-697-7, CD-ROM.
[238] ROWLANDS, J.L., SALVATORES, M., Fission Product Data Needs for Reactor Applications, paper presented in Specialists Meeting on Fission Product Nuclear Data, Tokai, Japan (1992).
[239] GIGLIO, J.J., CUMMINGS, D.G., MICHLIK, M.M., GOODALL, P.S., JOHNSOU, S.G., Determination of Burnup in Spent Nuclear Fuel by Application of Fiber Optic High-Resolution Inductively Coupled Plasma Atomic Emission Spectroscopy (FO-HR-ICP-AES), Nuclear Instruments & Methods in Physics Research A, 396, pp. 251-256 (1997).
[240] CUMMINGS, D., CARNEY, K., KRSUL, J., CRANE, P., MCKNIGHT, R., Measurement of Lanthanum and Technetium in Uranium Fuels by Inductively Coupled Plasma Atomic Emission Spectroscopy, Proc. Global'99, Jackson Hole, Wyoming, USA, 29 August-3 September, ANS, ISBN: 0-89448-641-1, CD-ROM.
[241] MCKNIGHT, R.D., ANL Calculational Methodologies for Determining Spent Nuclear Fuel Source Term, Proc. ANS Fourth Topical Meeting on DOE Spent Nuclear Fuel and Fissile Material Management, San Diego, California, USA, 4-8 June 2000.
[242] GANGULY, C., Development and Fabrication of 70% PuC- 30%UC Fuel for Fast Breeder Test Reactor in India, Nucl. Tech., Vol. 72 (1986).
[243] SRINIVASAN, G., Nucl. Eng. and Design, Vol. 236, p. 852 (2006).
[244] COX, S.A., Delayed Neutron Data- Review and Evaluation, ANL/NDM-5 (1974).
[245] MOHANAKRISHNAN, P., Estimation of Measured Control Rod Worths in Fast Breeder Reactor - Effect of Different Delayed Neutron Parameters, Nucl. Sci. and Eng., Vol. 122, p. 359 (1996).
[246] CHENG, S., AND TODREAS, N.E., Hydraulic models and correlations for bare and wire wrapped hexagonal rod bundles- bundle friction factors, sub channel friction factors and mixing parameters, Nuc. Eng. Des., pp. 227- 251 (1992).
[247] ZHUKOV, A.V., SOROKIN, A.P., MATJUKHIN, N.M., Inter-channel exchange in the fuel assemblies of fast reactors, M., Energoatomizdat (1989).
[248] OHSHIMA, H., NARITA, H., NINOKATA, H.,. Thermal-hydraulic analysis of fast reactor fuel subassembly with porous blockages, Proc. of Forth Int. Seminar on Subchannel Analysis (ISSCA-4), Tokyo Institute of Technology, Tokyo, Japan, pp. 323-333 (1997).
[249] KIM, W.S., KIM, Y.G., KIM, Y.J., A subchannel analysis code MATRA-LMR for wire wrapped LMR subassembly, Ann. Nucl. Energy, Vol. 29, pp. 303-321 (2002).
[250] STEWART, C.W., WHEELER, C.L., CENA, R.J., MCMONAGLE, C.A., CUTA, J.M., TRENT, D.S., COBRA-IV: The model and the method, BNWL-2214, Pacific Northwest Laboratories (1977).
[251] YOO, Y.J., HWANG, D.H., SOHN, D.S., Development of a Subchannel Analysis Code MATRA applicable to PWRs and ALWRs, J. Korean Nucl. Soc., Vol. 31, p. 314 (1999).
[252] Novendstern, E.H., Turbulent Flow Pressure Drop Model for Fuel Rod Assemblies utilizing a Helical Wire-Wrap Spacer System, Nucl. Eng. Des., Vol. 22, p. 19 (1972).
[253] CHIU, C., ROHSENOW, W.M., TODREAS, N.E., Flow-Split Model for LMFBR Wire-wrapped Assemblies, COO-2245-56TR, Rev. 1, MIT (1978).
[254] CHENG, S.K., TODREAS, N.E., Hydrodynamic Models and Correlations for Bare and Wire-Wrapped Hexagonal Rod Bundles – Bundle Friction Factors, Subchannel Friction Factors and Mixing Parameters, Nucl. Eng. Des., Vol. 92, pp. 227-251 (1986).

[255] FONTANA, M.H., et al., Temperature distribution in the duct wall and at the exit of a 19-rod simulated LMRBR fuel assembly (FFM Bundle 2A), Nucl. Technol., Vol. 24, pp. 176-200 (1974).
[256] VALETIN, B., "The thermal hydraulics of a pin bundle with an helical wire wrap spacer, modeling and qualification for a new sub-assembly concept", LMFR Core Thermal Hydraulics: Status and Prospects, IAEA-TECDOC-1157, IAEA, Vienna (2000).
[257] FISCHER, P.F., Parallel multi-level solvers for spectral element methods, Houston Journal of Mathematics, pp. 595–604 (1996).
[258] FISCHER, P.F., LOTTES, J.W., SIEGEL, A., PALMIOTTI, G., Large eddy simulation of wire wrapped fuel pins, paper presented in Joint Int. Topical Meeting on Math. and Comp. And Supercomputing in Nuclear Applications, Monterey, California, USA (2007).
[259] Star-CD v4.02, distributed by CD-adapco Group, Inc., Melville, NY, USA.
[260] Star-CCM+ v2.02 distributed by CD-adapco Group, Inc., Melville, NY, USA.
[260a] CHANDRA, L., ROELOFS, F., HOUKEMA, M., JONKER, B., A., Stepwise Development and Validation of a RANS based CFD Modelling Approach for the Hydraulic and Thermal-hydraulic Analyses of Liquid Metal Flow in a Fuel Assembly, Nuclear Engineering & Design, Vol. 239, pp. 1988-2003 (2009).
[260b] MÖLLER, R., TEGENA: Detaillierte experimentelle Untersuchungen der Temperatur- und Geschwindigkeitsverteilungen in Stabbündel-Geometrien mit turbulenter Natriumströmung, KfK 4491, Karlsruhe, Germany (1989).
[260c] ALEMBERTI, A., CARLSSON, J., MALAMBU, E., ORDEN, A., CINOTTI, L., STRUWE, D., AGOSTINI, P., MONTI, S., European Lead Fast Reactor: ELSY, paper presented in FISA 2009, Prague, Czech Republic, 2009.
[260d] CHANDRA, L., ROELOFS, F., Inter Fuel Assembly Thermal-Hydraulics for the ELSY Square Open Reactor Core Design, Nuclear Engineering & Design (in Press) (2010).
[260e] ROELOFS, F., GOPALA, V.R., CHANDRA, L., Fuel Assembly Simulations using LRGR CFD, Submitted to NURETH-14, 25-30 September 2011, Toronto, Canada.
[260f] GOPALA, V.R., CHANDRA. L., Determination of the Effect of Blockages in ELSY Fuel Assemblies using Low Resolution Geometry Resolving CFD, NRG-21962/09.99234 Vol. 1, Petten, Netherlands (2010).
[261] ROYCHOWDHURY ET AL., "Thermal Hydraulic Design of PFBR core", LMFR Core Thermal Hydraulics: Status and Prospects, IAEA-TECDOC-1157, IAEA, Vienna (2000).
[262] CHENG, S., TODREAS, N.E., Prediction of coolant temperature field in a breeder reactor including inter assembly heat transfer, COO- 2245- 20 TR, Rev. 1.
[263] VAIDYANATHAN, G., et al., Dynamic Tests Related to Undercooling Events in FBTR, paper presented in Int. Topical Meeting on Sodium Cooled Fast Reactor Safety, Obninsk, Russian Federation, Vol. 1, pp. 156-165 (1994).
[264] OHSHIMA, H, OHTAKA, M., Development of Computer Program for Whole Core Thermal Hydraulic Analysis of Fast Reactors, Proc. of 10th Int. Conf. on Nuclear Engineering (ICONE-10), Arlington, USA (2002).
[265] KAMIDE, H., et al., An Experimental Study of Inter-subassembly Heat Transfer during Natural Circulation Decay Heat Removal in Fast Breeder Reactors, Nucl. Eng. & Des., Vol. 183, pp. 97-106 (1998).
[266] DUCROS, F., CIONI, O., PERDU, F., VANDROUX, S., BARTHEL, V., QUÉMÉRÉ, P., FAUCHET, G., JAMET, D., BIEDER, U., GEFFRAYE, G., CHANDESRIS, M., TENCHINE, D., A proposal for a global multi-scale / multi

resolution thermalhydraulic approach for Gen IV concepts, paper presented in International Workshop on Thermal-Hydraulics of Innovative Reactor and Transmutation System (THIRS), Karlsruhe, Germany (2008).
[267] KOTTOWSKI, H.M., Liquid Metal thermal-hydraulics, Inforum Verlag ISBN: 3 926956-22-4 (1994).
[268] DWYER, O.E., On incipient boiling wall superheats in Liquid Metals, Heat and Mass transfer 12, 1403-19 (1969).
[269] LOCKHART, R.W., MARTINELLI, R.C., Proposed correlation of data for isothermal two-phase two-component flow in pipes, Chem. Eng. Progress (1949).
[270] HUBER, F., PEPPLER, W., Summary and Implications of Out-of Pile Investigations of Local Cooling Disturbances in LMFBR Subassembly Geometry under Single-Phase and Two-Phase Conditions, KfK 3927 (May 1985).
[271] RAMEAU, B., SEILER, J.M., LEE, K.W., Low heat flux sodium boiling experimental results. Application to natural convection boiling in reactor conditions, ASME, 84-WA/HT-5 (1984).
[272] DELHAYE, J.M., GIOT, M., RIETHMULLER, M.L., Thermohydraulics of two-phase systems for Industrial Design and Nuclear Engineering, Van Karman Institute book, Hemisphere, Mc Graw Hill (1980).
[273] IVANOV, E.F., SOROKIN, A.P., IVANOV, V.V., BOGOSLOVSKAYA, G.P., VOLKOV, A.D., Experimental Studying of Heat Transfer and Stability of Liquid-Metal Coolant Boiling in a Natural-Circulation Circuit, Obninsk: Preprint FEI-3023 (2005) (in Russian).
[274] EFANOV, A.D., SOROKIN, A.P., IVANOV, EU.F., BOGOSLOVSKAYA, G.P., IVANOV, V.V., VOLKOV, A.D., ZUEVA, I.R., RYMKEVICH, K.S., Liquid-metal boiling heat transfer in a system of channels under natural circulation conditions, Eleventh International Topical Meeting on Nuclear Reactor Thermal Hydraulics (NURETH-11), Avignon, France, 2-6 October 2005.
[275] ZEIGARNIK, YU.A., LITVINOV, V.D., Alkali Metal Boiling in Channels, Moscow: Nauka (1983) (in Russian).
[276] BORISHANSKII, V.M., KUTATELADZE, S.S., NOVIKOV, I.I., FEDYNSKII, O.S., Liquid Metal Coolants, Moscow: Atomizdat (1976) (in Russian).
[277] BENARAFA, Y., CIONI, O., DUCROS, F., SAGAUT, P., RANS/LES coupling for unsteady turbulent flow simulation at high Reynolds number in coarse meshes, Computer Methods in Applied Mechanics and Engineering, Vol. 195, pp. 2939-2960 (2006).
[278] NATESAN, K., et al., Thermal hydraulic study on random failure of fuel by delayed neutron detection system, Journal of Nuclear Engineering and Design, Vol. 237, pp. 2219-2231 (2007).
[279] CLEMENT RAVI CHANDAR, S., et al., Thermal Hydraulic Investigation of PFBR core, paper presented in 11th International Meeting of the Working group on advanced nuclear reactors thermohydraulics, Obninsk, Russia (July 2004).
[279a] VAN TICHELEN, K., KEIJERS, S., VANDERHAEGEN, M., JAYARAJU S., ROELOFS, F., Scaling Analysis for the European Heavy Liquid Metal Scaled Pool Facility E-Scape, Submitted to NURETH-14, 25-30 September 2011, Toronto, Canada.
[280] PERDU, F., VANDROUX, S., System/CFD coupling for reactor transient analysis. An application to the Gas Fast Reactor with CATHARE/TRIO_U, Proc. PHYSOR 2008, Interlaken, Switzerland, 14-19 September 2008, Paul Scherrer Institute (2008).
[281] MATJUKHIN, N.M., SOROKIN, A.P., Approaches for modelling of fast reactor thermohydraulics with liquid metal cooling in regime of accident cool down reactor,

In the collection of the reports “Thermophysics-2005”: Thermohydraulic aspects of safety NNP with fast reactors, Obninsk, Russian Federation, p. 25 (2005).
[282] GELINEAU, O., et al., High Cycle Thermal Fatigue: experience and state of art in French LMFRs, SMiRT16, Paper #1311 (2001).
[283] VELUSAMY, K., et al., Investigations of Thermal Striping in Primary Circuit of Prototype Fast Breeder Reactor, Proc. ICONE 13, Beijing, China, 16-20 May 2005, JSME (2005).
[284] KIMURA, N., NISHIMURA, M., KAMIDE, H., Study on Convective Mixing for Thermal Striping Phenomena (Experimental Analyses on Mixing Process in Parallel Triple-Jet and Comparisons between Numerical Methods), JSME International Journal, Series B, Vol. 45, No. 3, pp. 592-599 (2002).
[285] KIMURA, N., MIYAKOSHI, H., KAMIDE, H., Experimental study on thermal striping phenomena for a fast reactor -Transfer characteristics of temperature fluctuation from fluid to structure, Proc. 6th ASME-JSME Thermal Engineering Joint Conference, TED-AJ03-159 (2003).
[286] KIMURA, N., IGARASHI, M., KAMIDE, H., Investigation of convective mixing of triple jet - Evaluation of turbulent quantities using particle image velocimetry and direct numerical simulation, Proc. 8th Int. Symposium on flow modeling and turbulence measurements, Tokyo, Japan, pp. 651-658 (2001).
[287] NAM, H.Y., KIM, J.M., Thermal Striping Experimental Data, Internal Report, KAERI, LMR/IOC-ST-002-04-Rev. 0/04 (2004).
[288] USHIJIMA, S., TANAKA, N., MORIYA, S., Turbulence Measurements and Calculation of Non-Isothermal Coaxial Jets, Nuclear Engineering and Design, 122, pp. 85-94 (1990).
[289] NISHIMURA, M., TOKUHIRO, A., KIMURA, N., KAMIDE, H., Numerical Study on Mixing of Oscillating Quasi-planar Jets with Low Reynolds Number Turbulent Stress and Heat Flux Equation Models, Nuclear Engineering and Design, 202, pp. 77-95 (2000).
[290] TOKUHIRO, A., KIMURA, N., An Experimental Investigation on Thermal Striping Mixing Phenomena of a Vertical Non-Buoyant Jet with Two Adjacent Buoyant Jets as Measured by Ultrasound Doppler Velocimetry, Nuclear Engineering and Design, 188, pp. 49-73 (1999).
[291] KIMURA, N., NISHIMURA, M., KAMIDE, H., Study on Convective Mixing for Thermal Striping Phenomena (Experimental Analyses on Mixing Process in Parallel Triple-Jet and Comparisons between Numerical methods), JSME International Journal Series B, Vol. 45, No. 3, pp. 592-599 (2002).
[292] MENTER, F.R., Two Equation Eddy-Viscosity Turbulence Models for Engineering Applications, AIAA J., 32, pp.1598-1604 (1994).
[293] CHEN, H.C., PATEL, V.C., Near-wall Turbulence Models for Complex Flows Including Separation, AIAA J., 26, pp. 641-648 (1988).
[294] DURBIN, P.A., Separated Flow Computations with the k-ε-$\bar{v}^2$ Model, AIAA J., 33, pp. 659-664 (1995).
[295] COSTE, P., QUÉMÉRÉ, P., ROUBIN, P., EMONOT, PH., TANAKA, M., KAMIDE, H., Large Eddy Simulation of a Mixing-T Experiment, Proc. ICAPP’06, Reno, Nevada, 4-8 June 2006, ANS, ISBN: 0-89448-698-5, CD-ROM.
[296] COSTE, P., QUÉMÉRÉ, P., ROUBIN, P., EMONOT, P., TANAKA, M., KAMIDE, H., Large eddy simulation of highly-fluctuational temperature and velocity fields observed in a mixing-T experiment, Nuclear Technology, Vol. 164, pp. 76-88 (2008).

[297] KIMURA, N., KAMIDE, H., EMONOT, P., NAGASAWA, K., Study on thermal striping phenomena in triple-parallel jet. Investigation on non-stationary heat transfer characteristics based on numerical simulation, Proc. NURETH-12, Pittsburgh, Pennsylvania, USA, 30 September-4 October 2007, ANS, ISBN: 0-89448-058-8, CD-ROM.

[298] EGUCHI, Y., YAMAMOTO, K., FUNADA, T., TANAKA, N., MORIYA, S., TANIMOTO, K., OGURA, K., SUZUKI K., MAEKAWA, I., Gas Entrainment in the IHX of Top-Entry Loop-Type LMFBR, Nuclear Eng. and Design, Vol. 146, pp. 373-381 (1994).

[299] SAKAI, T., EGUCHI, Y., IWASAKI, T., OHSHIMA, H., YAMAGUCHI, A., Numerical Analysis of Gas Core depth Prediction in a Steady Free Surface Vortex, paper presented in NTHAS4: Sapporo, Japan, 28 November - 1 December 2004.

[300] SAKAI, T., EGUCHI, Y., MONJI, H., IWASAKI, T., ITO, K., OHSHIMA, H., Proposal of Design Criteria for Gas Entrainment From Vortex Dimples Based on a Computational Fluid Dynamics Method, paper presented in NTHAS5, Jeju, Korea, Republic of, 27-29 November 2006.

[301] BAUM, M.R., COOK, M.E., Gas Entrainment at the Free Surface of a Liquid: Entrainment Inception at a Vortex with an Unstable Gas Core, Nuclear Eng. Des., 32, pp. 239-245 (1975).

[302] TAKAHASHI, M., INOUE, A., ARITOMI, M., Gas Entrainment at Free Surface of Liquid, (I): Gas Entrain Mechanism and Rate, J. of Nuc. Sci. & Tech., Vol. 25, No. 2, pp. 131-142 (1988).

[303] TAKAHASHI, M., INOUE, A., ARITOMI, M., Gas Entrainment at Free Surface of Liquid, (II): Onset Conditions of Votex-Induced Entrainment, J. of Nuc. Sci. & Tech., Vol. 25, No. 3, pp. 245-253 (1988).

[304] MADARAME, H., CHIBA, T., Gas Entrainment Inception at the Border of a Flow-Swollen Liquid Surface, Nucl. Eng. & Des., 120, pp. 193-201 (1990).

[305] GOVINDARAJ, et al., Gas Entrainment in Surge Tank of Liquid Metal Gast Breeder Reactors, J. of Nucl. Sci. & Tech., Vol. 30, No. 7, pp. 712-716 (1993).

[306] EGUCHI, et al., Gas Entrainment in the IHX Vessel of Top-entry Loop-type LMFBR, Nucl. Eng. & Des., 146, pp. 373-381 (1994).

[307] KOYAMA, K., et al., Study on local blockage in FBR fuel assembly, Proc. of Fast Reactors and Related Fuel Cycles, Kyoto, Japan (1991).

[307a] GOPALA, V.R., ROELOFS, F., Numerical Simulation of Liquid Lead Sloshing in the ELSY Reactor Vessel, paper presented in 5th Int. Workshop on Materials for HLM-cooled reactors and related technologies (HeLiMeRT), Mol, Belgium, 2009.

[308] OHSHIMA, H., NARITA, H., NINOKATA, H., Thermal-hydraulic analysis of fast reactor fuel subassembly with porous blockages, Proc. 4th Int. Seminar on Subchannel Analysis (ISSCA-4), Tokyo Institute of Technology, Tokyo, Japan, pp. 323-333 (1997).

[309] JEONG, H.-Y., HA, K.-S., CHANG, W.-P., KWON, Y.-M., LEE, Y.-B., Modeling of Flow Blockage in a Liquid Metal-Cooled Reactor Subassembly with a Subchannel Analysis Code, Nucl. Technol., Vol. 149, pp. 71-87 (2005).

[310] NINOKATA, H., EFTHIMIADIS, A., TODREAS, N.E., Distributed Resistance Modeling of wire-wrapped Rod Bundles, Nucl. Eng. Des., Vol. 104, pp. 93-102 (1987).

[311] DOMANUS, H.M., SHA, W.T., Numerical Results for a Hexagonal Fuel Assembly with a Planar Blockage using the COMMIX-1A Computer Code, NUREG/CR-0483, U.S. Nuclear Regulatory Commission (1978).

[312] REHME, K., The Structure of Turbulence in Rod Bundles and the Implications on Natural Mixing between the Subchannels, Int. J. Heat Mass Transfer, Vol. 35, p. 567 (1992).
[313] ZHUKOV, A.V., KIRILOV, P.L., SOROKIN, A.P., MATJUKHIN, N.M., Transverse Turbulent Momentum and Energy Exchange in the Channels of Complicated Form, Proc. Heat Transfer, Brighton, UK, Vol. 4, p. 327 (1994).
[315] KIM, S., CHUNG, B.-J., A Scale Analysis of the Mixing rate for various Prandtl number flow fields in Rod Bundles, Nucl. Eng. Des., Vol. 205, p. 281 (2001).
[321] SADATOMI, M., KAWAHARA, A., SATO, Y., Prediction of the Single-phase Turbulent Mixing rate between two parallel Subchannels using a Subchannel Geometry Factor, Nucl. Eng. Des., Vol. 162, p. 245 (1996).
[316] INTERNATIONAL ATOMIC ENRGY AGENCY, Status of Liquid Metal Cooled Fast Breeder Reactors, Technical Reports Series No: 246, IAEA, Vienna (1985).
[317] INTERNATIONAL ATOMIC ENERGY ABENCY, Status of Liquid Metal Cooled Fast Reactor Technology, IAEA-TECDOC-1083, IAEA, Vienna (1999).
[318] EUROPEAN COMMISSION, Sixth Framework Programme, Partitioning and Transmutation European Roadmap for Sustainable Nuclear Energy (PATEROS), State-of-the-art of the transmutation fuels and fuel fabrication facilities (August 2008).
[319] EUROPEAN COMMISSION, Sixth Framework Programme, Partitioning and Transmutation European Roadmap for Sustainable Nuclear Energy (PATEROS), Needed fuel fabrication facilities up to the industrial deployment of partitioning and transmutation (April 2008).
[320] BIRNEY, K.R., et. al., United States Experience with LMFBR Control Material Selection, paper presented in Specialists' meeting on absorber materials and control rods for fast breeder reactors, Obninsk, Russian Federation, 7-10 June 1983.
[321] WALTER, A.E., REYNOLDS, A.B., Fast Breeder Reactors, Pergamon press (1981).
[322] KAITO, T., et al., “Irradiation Behaviour of Boron Carbide Neutron Absorber”, Absorber Materials, Control Rods and Designs of Shutdown Systems for Advanced Liquid Metal Fast Reactors, IAEA-TECDOC-884, IAEA, Vienna (1995).
[323] TARASIKOV, V.P., et al., “The Experience of Post Irradiation Investigations of the BN-600 Control Rods”, Absorber Materials, Control Rods and Designs of Shutdown Systems for Advanced Liquid Metal Fast Reactors, IAEA-TECDOC-884, IAEA, Vienna (1995).
[324] KRYGER, B., GOSSET, D., ESCLEINE, J.M., “Irradiation Performances of The SUPERPHENIX Type Absorber Element”, Absorber Materials, Control Rods and Designs of Shutdown Systems for Advanced Liquid Metal Fast Reactors, IAEA-TECDOC-884, IAEA, Vienna (1995).
[325] INTERNATIONAL ATOMIC ENERGY AGENCY, Thermophysical Properties of Materials for Nuclear Engineering: A Tutorial and Collection of Data, IAEA-THPH (February 2009).
[326] INTERNATIONAL ATOMIC ENERGY AGENCY, Comparative Assessment of Thermophysical and Thermohydraulic Characteristics of Lead, Lead-Bismuth and Sodium Coolants for Fast Reactors, IAEA-TECDOC-1289, IAEA, Vienna (2002).
[327] FOERSTER, K., et al., LMFBR Steam Generators-realistic Investigations on Leakage Accidents, paper presented in 4th Int. Conf. Liquid Metal Engineering and Technology, Avignon, France, October 1988.
[328] DESMAS, T., LEMOINE, P. A., Study of Small Leaks of Water in Sodium-heated Steam Generators: Self-evolution and Wastage, Proc. 3rd Int. Conf. on Liquid Metal

Engineering and Technology in Energy Production, Oxford, UK, British Nuclear Energy Society, Vol. 1, p. 1. (April 1984).
[329] GREENE, D.A., Sodium-water Reaction Phenomena Associated with Small Leaks Ion LMFBR Steam Generators, Proc. 3rd Int. Conf. Liquid Metal Engineering and Technology in Energy Production, Oxford, UK, British Nuclear Energy Society, Vol. 1, p. 13 (April 1984).
[330] CURRIE, R., et al., Sodium-water Reactions: Production of Data for the European Steam Generator Accident Common Code System: Small Leak Wastage and Steam-sodium Surface Corrosion Investigations, Ibid. 1, p. 308.
[331] HAMADA, H., TANABE, H., WADA, Y. et al., Study of Overheating Tube Rupture for FBR Steam Generators, Proc. ICONE 8, Baltimore, Maryland, 2-6 April 2000, ASME, ISBN: 0791819922 (2000), CD-ROM, paper ICONE-8240.
[332] HAMADA, H., KURIHARA, A., NISHIMURA, M., Study of Thermal Influence on Tubes due to Sodium-Water Reactions in LMFBR Steam Generator, Proc. ICONE 12, Arlington, Virginia, 25-29 April 2004, ASME (3 Vols) (2004) Print Book, paper ICONE12-49064.
[333] SUDA, K., WATANABE, A., OHSHIMA, H., Numerical Simulation of Sodium-Water Reaction Phenomena under Small Leakage Condition in a Steam Generator, Proc. ICONE 14, Miami, Florida, 17-20 July 2006 (5 Vols), ASME, paper ICONE12-49064.
[334] JUDD, A.M., CURRIE, R., LINEKAR, G.A.B., HENDERSON, J.D.C., The Under-sodium Leak in the PFR Superheater 2, Nuclear Energy,Vol. 31, No. 3, p. 221 (1992).
[335] ROBERTSON, C, WALFORD, J.D., The Leak in Superheater 2 - PFR February 1987, Proc. 4th Int. Conf. on Liquid Metal Engineering and Technology, Avignon, France, Vol. 3, p. 712 (October 1988).
[336] HANS, R., DUMM, K., Leak Detection of Steam or Water in Steam Generators of Liquid-metal Fast Breeder Reactors, Atomic Energy Review, 15, 4, p. 611 (1977).
[337] BOUCHACOURT, M., et al., EdF Experience on Analysis of Non-metallic Impurities in Sodium, Proc. 3rd Int. Conf. on Liquid Metal Engineering and Technology in Energy Production, Oxford, UK, British Nuclear Energy Society ,Vol. 1, (April 1984) p. 45.
[338] SMITH, C.A., SIMM, P.A., Calibration and Performance of Galvanic Cell Hydrogen and Oxygen Meters in Sodium, Proc. 3rd Int. Conf Liquid Metal Engineering and Technology in Energy Production, Oxford, UK, British Nuclear Energy Society, Vol. 3, (April 1984) p. 103.
[339] ASHER, R.C., et al., Recent Developments in the Design, Performance, and Application of Harwell Oxygen Sensors and Harwell Carbon Meters, Proc. 4th Int. Conf. on Liquid Metal Engineering and Technology, Avignon, France, Vol. 3, p. 602 (October 1988).
[340] GNANASEKARAN, T., et al., Experience with on-line Meters for Measuring Hydrogen in Sodium Coolant, paper presented in 4th Int. Conf. on Liquid Metal Engineering and Technology, Avignon, France, October 1988, 3, 604.
[341] THORLEY, A.W., BLUNDELL, A., BARDSELY, J.A., LLOYD, R., Mass Transfer Behaviour of Stainless Steels in Flowing Sodium Environments at Different Oxygen Levels, Ibid, 3, 532.
[342] GREENE, D.A., et al., Acoustic Leak detection Development in the USA, paper presented in 3rd Int. Conf. Liquid Metal Engineering and Technology in Energy Production, Oxford, UK, April 1984.

[343] HIMENO, Y., et al., Engineering Scale Test on Sodium Leak and Fire Accident and its Consequences in Auxiliary Building of Fast Breeder Reactors, paper presented in 4th Int. Conf. Liquid Metal Engineering and Technology, Avignon, France (1988).
[344] MIYAKAWA, A., et al., "Sodium Leakage Experience at the Prototype FBR Monju", Unusual Occurrences during LMFR Operations, IAEA-TECDOC-1180, IAEA, Vienna (2000).
[345] CHAPPENEL, J., et al., Combined Sodium Fires - Experiments and Code Development, Ibid, Vol. 1.
[346] MALET, J.C., European Experimental and Analytical Studies Concerning Sodium Combined Fires, paper presented in International Fast Reactor Safety Meeting, Snow-bird, USA (1990).
[347] DUFRESNE, J., et al., Sodium Concrete Interaction, paper presented in LMFBR Topical Meeting, Lyon, France (1982).
[348] SHIRE, P.R., SPRAY Code User's Report, HEDL-TME 76-94 (1977).
[349] BEIRIGER, P., et al., SOFIRE II User Report, AI-AEC-13055 (1973).
[350] MIYAKE, O., et al., Sodium Pool Combustion Codes for Evaluation of Fast Breeder Reactor Safety, J. Nucl. Sci. Technol., 28, pp. 107-121 (1991).
[351] SEINO, H., et al., Computer Code Development for Sodium Fire and Source Term Evaluation of FBR, Proc. Int. Topical Meeting Sodium Cooled Fast Reactor Safety (FRS'94), Vol. 2, Obninsk, Russian Federation (1994) pp. 176-189,
[352] MIYAHARA, S., et al., Development and Validation of ABC-INTG Code, Proc. CSNI Specialist Mtg. Nucl. Aerosols in Reactor Safety, Karlsruhe, Germany, pp. 416-427 (1984).
[353] MURATA, K.K., et al., CONTAIN LMR/1B-Mod.1, A Computer Code for Containment Analysis of Accidents in Liquid-Metal-Cooled Nuclear Reactors, SAND91-1490 (1993).
[354] MIYAKE, O., et al., Development of CONTAIN Code for FBR Severe Accident Analysis, paper presented in Int. Conf. Design and Safety of Advanced Nuclear Power Plants (ANP'92), Tokyo, Japan, 1992.
[355] TSAI, S.S., The NACOM Code for Analysis of Postulated Sodium Spray Fires in LMFBRs, NUREG/CR-1405 (1980).
[356] GELBARD, F., MAEROS Users Manual, NUREG/CR-1391 (1982).
[357] SUO-ANTTILA, A.J., SLAM – A Sodium-Limestone Concrete Ablation Model, NUREG/CR-3379 (1983).
[358] YAMAGUCHI, A., et al., Validation Study of Computer Code SPHINCS for Sodium Fire Safety Evaluation of Fast Reactors Nuclear Engineering and Design, 219, pp. 19-34 (2003).
[359] YAMAGUCHI, A., et al., Numerical Methodology to Evaluate Fast Reactor Sodium Combustion, Nuclear Technology, Vol. 136, pp. 315-329 (2001).
[360] TAKATA, T., et al., Numerical Investigation of Multi-Dimensional Characteristics in Sodium Combustion, Nuclear Engineering and Design, 220, pp. 37-50 (2003).
[361] IIDA, M., Three Dimensional Particle Method Code for Sodium Leakage Analysis in Liquid Metal Reactor, Proc. 7th Int. Conf. Nucl. Engineering (ICONE), Tokyo, Japan (1999).
[362] OKANO, Y., et al., Direct Numerical Simulation of Liquid Sodium Droplet Combustion in Forced Convection Air Flow, Proc. 7th Int. Conf. Nucl. Engineering (ICONE), Tokyo, Japan (1999).
[363] OKANO, Y., et al., Direct Numerical Simulation of a Combustion Experiment of a Free-Falling Liquid Sodium Droplet, Proc. ICONE 8, Baltimore, Maryland, 2-6 April 2000, ASME, ISBN: 0791819922 (2000), CD-ROM.

[364] MUHLESTEIN, L.D, Application of Na Concrete Reaction data to Breeder, Reactor Safety Analysis, Nuclear Safety, Vol. 25 (April 1984).
[365] MIYAHARA, S., Sodium Aerosol Release Rate and Non-Volatile Fission Product Retention Factor during a Sodium-Concrete Reaction, Nuclear Technology, Vol. 97, pp. 212-226 (1992).
[366] Puo-Antilla,-a Sodium Concrete Ablation Model, NUREG/CR-2099, SAND 81-0415, (October 1981).
[367] MALET, J.C., et al., Sodium Concrete Interaction Experimental Studies and Modeling, paper presented in Fourth International Conference (LIMET) 1988, Avignon, France.
[368] OSHKANOV, N.N., POTAPOV, O.A., GOVOROV, P.P., The evaluation of an operational performance of the power unit with the BN-600 fast reactor of Beloyarsk NPP for 25 years of operation, Nuclear Energetics, No. 1 pp. 3-9 (2005).
[369] OSHKANOV, N., et al., The Main Results of Beloyarsk NPP Unit 3 Operation, paper presented in IAEA Technical Meeting on the Coordinated Research Project on Analyses of and Lessons Learned from the Operational Experience with Fast Reactor Equipment and Systems, Obninsk, Russian Federation, 14-16 February 2005.
[370] ASHURKO, Y.M., et al., "Fast Reactor Operating Experience Gained in Russia: Analysis of Anomalies and Abnormal Operation Cases", Unusual Occurrences During LMFR Operation, IAEA-TECDOC-1180, IAEA, Vienna (2000).
[371] POPLAVSKY, V.M., et al., "Review of Fast Reactor Operational Experience Gained in the Russian Federation", Operational and Decommissioning Experience with Fast Reactors, IAEA-TECDOC-1405, IAEA,Vienna (2004).
[372] BROWN, C, LANGUILLE, A., MUEHLING, G., Journal of Nuclear Materials, Vol. 204, p. 33 (1993).
[373] GARNER, F.A., Irradiation Performance of Cladding and Structural Steels in Liquid Metal Reactors, Materials Science and Technology A Comprehensive Treatment, Vol. 10A, Chapter 6 (VCH Publishers) pp. 419-543 (1994).
[374] ALLEN, T.R., COLE, J.I., TSAI, H., UKAI, S., MIZUTA, S., YOSHITAKE, T., The Effect of Low Dose Rate Irradiation on the Swelling of 12% Cold-Worked 316 Stainless Steel, Proc. 9th Int. Symp. Environmental Degradation of Materials in Nuclear Power Systems-Water Reactors, Newport Beach, CA, (Editors: S. Bruemmer, P. Ford, G. Was), TMS, Warrendale, Pensylvania, USA, p. 1035 (August 1999).
[375] TATEISHI, Y., YUHARA, S., SHIBAHARA, I., ITO, M., NOMURA, S., SATO, Y., YOSHIDA, E., SHIKAKURA, S., Development of modified SUS316 stainless steel as core material for fast breeder reactors, Journal of the Atomic Energy Society of Japan, Vol. 30, No. 11, p. 1005-1019 (1988).
[376] ALLEN, T., KLUEH, R.L., UKAI, S., Fuels and Materials for Transmutation, OECD NEA report 5419 (2005).
[377] CHANG, Y.I., FINCK, P.J., GRANDY, C., Advanced Burner Test Reactor Preconceptual Design Report, ANL-ABR-1, ANL-AFCI-173 (September 2006).
[378] KLUEH, R.L., HARRIES, D.R., High-Chromium Ferritic and Martensitic Steels for Nuclear Applications, ASTM, West Conshocken, PA (2001).
[379] LAURITZEN, T., BELL, W.L., KNOZE, G.M., VAIDYANATHAN, S., GEFR-00575 (September 1981).
[380] LEE, B.O., et al., Design Limits Analysis of the Claddings for KALIMER, Proceedings of KNS 2006 Autumn Conference (2005).
[381] SIENICKI, J.J., WADE, D.C., MOISSEYTSEV, A., Role of Small Lead-Cooled Fast Reactors for International Deployment in Worldwide Sustainable Nuclear

Energy Supply, Proc. ICAPP '07, Nice, France, 13-18 May 2007, ISBN: 9781604238716, Curan Associates, Inc. (February 2008) paper 7228.
[382] LI, N., Lead-Alloy Coolant Technology and Materials – Technology Readiness Level Evaluation, paper presented in 2nd COE-INES Int. Symp. Innovative Nuclear Energy Systems, INES-2, Yokohama, Japan, 26-30 November 2006.
[383] LIM, J.Y., BALLINGER, R.G., Alloy Development for Lead-Cooled Reactor Service, paper presented in MIT-Tokyo Tech Symposium on Innovative Nuclear Energy Systems, Massachusetts Institute of Technology, Cambridge, Massachusetts, USA, 2-4 November 2005.
[384] ALAMO, A., REGIE, H., BECHADE, J.L., Novel Powder Processing - Advances in Powder Metallurgy and Particulate Materials, Vol. 7 (1992).
[385] UKAI, S., MIZUTA, S., FUJIWARA, M., OKUDA, T., KOBAYASHI, T., Development of 9Cr-ODS martensitic steel claddings for fuel pin by means of ferrite to austenite phase transformation", J. Nucl. Sci. Technol., Vol. 39 (7), p. 778 (2002).
[386] UKAI, S., KAITO, T., SEKI, M., MAYORSHIN, A.A., SHISHALOV, O.V., Oxide dispersion strengthened (ODS) fuel pins fabrication for BOR-60 irradiation test, J. Nucl. Sci. Technol., Vol. 42, No. 1, p. 109 (2005).
[387] SEKI, M., HIRAKO, K., KONO, S., KONO, S., KAITO, T., Pressurized resistance welding technology development in 9Cr-ODS martensitic steels, J.Nucl. Mater., Vol.329-333, p. 1534 (2004).
[388] UKAI, S., KAITO, T., OHTSUKA, S., NARITA, T., FUJIWARA, M., KOBAYASHI, T., Production and properties of nano-scale oxide dispersion strengthened (ODS) 9Cr martensitic steel cladding, ISIJ Int., Vol. 43, No. 12, p. 2038 (2003).
[389] UKAI, S., MIZUTA, S., FUJIWARA, M., OKUDA, T., KOBAYASHI, T., Consolidation process study of 9Cr-ODS martensitic steel tubes, J.Nucl.Mater., Vol. 307-311, p. 758 (2002).
[390] OHTSUKA, S., UKAI, S., FUJIWARA, M., KAITO, T., NARITA, T., Improvement of 9Cr-ODS martensitic steel properties by controlling excess oxygen and titanium contents, J. Nucl. Mater., Vol. 329-333, p. 372 (2004).
[391] YOSHITAKE, T., ABE, Y., AKASAKA, N., OHTSUKA, S., UKAI, S., KIMURA, A., Ring-tensile properties of irradiated oxide dispersion strengthened ferritic/martensitic steel claddings, J. Nucl. Mater., Vol. 329-333, p. 342 (2004).
[392] AKASAKA, N., YAMASHITA, S., YOSHITAKE, T., UKAI, S., KIMURA, A., Microstrucutural change of neutron irradiated ODS ferritic and martensitic steels, J. Nucl. Mater., Vol. 329-333, p. 1053 (2004).
[393] YAMASHITA, S., AKASAKA, N., OHNUKI, S., Nano-oxide particle stability of 9-12Cr grain morphology modified ODS steels under neutron irradiation, J. Nucl. Mater., Vol. 329-333, p. 377 (2004).
[394] BOTTCHER, J., UKAI, S., INOUE, M., ODS steel clad MOX fuel-pin fabrication and irradiation performance in EBR-II, Nucl.Technol., Vol. 138, p. 238 (2002).
[395] SHIKAKURA, S., NOMURA, S., UKAI, S., SESHIMO, I., KANO, Y., KUWAJIMA, Y., ITO, T., SAWARAGI, K., FUJITA, T., Development of high-strength ferritic/martensitic steel for FBR core materials, Journal of the Atomic Energy Society of Japan, Vol. 33, No. 12, pp. 1157-1170 (1991).
[396] NARITA, T., UKAI, S., KAITO, T., OHTSUKA, S., FUJIWARA, M., Development of manufacturing process of PNC-FMS wrapper tube with SUS316 short joint, J. Nucl. Sci. Technol, Vol. 42 (9), p. 825 (2005).

[397] UEHIRA, A., UKAI, S., MIZUNO, T., ASAGA, T., YOSHIDA, E., Tensile properties of 11Cr-0.5Mo-2W,V,Nb stainless steel in LMFBR environment, J. Nucl. Sci. Technol, Vol. 37 (9), p. 780 (2000).
[398] SERAN, J.L., private communication.
[399] HARDE, R., STOHR, K.W., A sodium-cooled power reactor experiment employing zirconium-hydride moderator, Proc. Third Geneva Conference (United Nations), Geneva, Session 1.5 P/537, Vol. 6, pp. 353-362 (1965).
[400] PONOMARENKO, V.B., et al., "Experience in development, operating and material investigation of the BOR-60 reactor control and safety rods", Absorber Materials, Control Rods and Designs of Shutdown Systems for Advanced Liquid Metal Fast Reactors, IAEA-TECDOC-884, IAEA, Vienna (1996).
[401] WOOTAN, D.W., RAWLINS, J.A., CARTER, L.L., BRAGER, H.R., SCHENTER, R.E., Analysis and results of a hydrogen-moderated isotope production asembly in the Fast Flux Test Facility, Nuclear Science and Engineering, Vol. 103, pp. 150-156 (1989).
[402] SIMNAD, M.T., The U-ZrHx alloy: its properties and use in TRIGA fuel, Journal of Nuclear Engineering and Design, Vol. 64, pp. 403-422 (1981).
[403] MIZUNO, T., OGAWA, T., NAGANUMA, M., AIDA, T., Advanced oxide fuel core design study for SFR in the Feasibility Study in Japan, Proc. GLOBAL 2005, Tsukuba, Japan, 9-13 October 2005, Editor: Hajimu Yamana, Atomic Energy Society of Japan, ISBN: 4-89047-133-2 (2005) CD-ROM, Paper No. 434.
[404] INOUE, M., UKAI, S., Research and development of neutron moderators with metal hydrides for sodium cooled fast breeder reactors, Proc. GLOBAL 2005, Tsukuba, Japan, 9-13 October 2005, Editor: Hajimu Yamana, Atomic Energy Society of Japan, ISBN: 4-89047-133-2 (2005) CD-ROM, Paper No. 591.
[405] YAMANAKA, S., YOSHIOKA, K., UNO, M., KATSURA, M., ANADA, H., MATUDA, T., KOBAYASHI, S., Thermal and mechanical properties of zirconium hydride, Journal of Alloys and Compounds, Vol. 293-295, p. 23-29 (1999).
[406] YAMANAKA, S., YAMADA, K., KUROSAKI, K., UNO, M., TAKEDA, K., ANADA, H., KOBAYASHI, S., Thermal properties of zirconium hydride, Journal of Nuclear Materials, Vol. 294, pp. 94-98 (2001).
[407] YAMANAKA, S., YOSHIOKA, K., UNO, M., KATSURA, M., ANADA, H., MATUDA, T., KOBAYASHI, S., Isotope effects on the physicochemical properties of zirconium hydride, Journal of Alloys and Compounds, Vol. 293-295, pp. 904-914 (1999).
[408] YAMANAKA, S., YAMADA, K., KUROSAKI, K., UNO, M., TAKEDA, K., ANADA, H., MATSUDA, T., KOBAYASHI, S., Characteristics of zirconium hydride and deuteride, Journal of Alloys and Compounds, Vol. 330-332, pp. 99-104 (2002).
[409] YAMANAKA, S., YAMADA, K., KUROSAKI, K., UNO, M., TAKEDA, K., ANADA, H., MATSUDA, T., KOBAYASHI, S., Analysis of the electronic structure of zirconium hydride, Journal of Alloys and Compounds, Vol. 330-332, pp. 313-317 (2002).
[410] YAMANAKA, S., YAMADA, K., KUROSAKI, K., UNO, M., TAKEDA, K., ANADA, H., NAGASE, F., UETSUKA, H., Analysis of the fracture behavior of a hydrided cladding tube at elevated temperatures by fracture mechanics, Journal of Alloys and Compounds, Vol. 330-332, p. 400-403 (2002).
[411] SMITH, D.L., KONYS, J., MUROGA, T., EVITKHIN, V., Development of coating for fusion power applications, Journal of Nuclear Materials, Vol. 307-311, pp. 1314-1322 (2002).

[412] THURSTON, R.N., PIERCE, A.D., Ultrasonic Measurement Methods, collection PHYSICAL ACOUSTICS, Volume XIX, Academic Press (1990).
[413] BERTON, J.-L., LOYER, G., Continuous monitoring of the position of two subassembly heads of Phénix at 350 MWth power and 550°C temperature, paper presented in SMORN VII Conference, Avignon, France (1995).
[414] IMBERT, C., Ultrasonic imaging of immersed metallic structures, using a numerical dynamic focalisation imaging. Simulation and tests, paper presented in 4th French Acoustic Congress, Marseille, France (1997).
[415] IMBERT, C., Realization of ultrasonic images of immersed metallic structures using a digital beamforming system. Experimental study, Proc. ICONE 5, Nice, France, 25-29 May 1997, ASME/SFEN/JSME, ISBN: 0791812383 (1997) CD-ROM.
[416] ANDO, M., et al., Study on in-service inspection program and inspection technologies for commercialized sodium-cooled fast reactor, Proc. ICONE 14, Miami, Florida, 17-20 July 2006 (5 Vols), ASME, (2006), paper ICONE14-89558.
[417] MUKHERJEE, D., et al., Development of an Ultrasonic Testing Technique for the NDT of Breeder Reactor End Cap Welds, Materials Evaluation, pp. 1097-1101 (November 2006).
[418] SASI, B., et al., Development of Eddy Current Techniques for NDE of Fuel Cladding Tubes, Proc. Mtg. Recent Advances in PIE (RAP-2008), 22-24 May 2008, Kalpakkam, India, paper C4.

CHAPTER 7
REACTOR PLANT ENGINEERING TECHNOLOGY DEVELOPMENT

7.1. Introduction

A large number of sodium-cooled fast reactor designs have been successfully realized in the past, thereby proving that the technology, by and large, is available. Improvements are still possible with respect to economics, lifetime or safety. In this chapter, engineering advances made in Member States in the areas of plant design and main components are discussed in detail. The chapter concludes with a qualitative discussion on the innovative design trends under consideration in the Member States for use future sodium-cooled fast reactor designs so that they may attain improved economics and safety.

In the following, specific designs or projects, which are presently under consideration, are being used to point to the basic choices in the design, as well as to the remaining problems.

7.1.1. India

Selection of main options for a large fast breeder reactor (FBR) power plant is an important phase of the project as it gives a definite shape to the plant. Satisfactory plant operation depends on the correct selection of robust concepts. The concepts, which affect not only PFBR but also the future FBR programme, are selected based on the energy situation in the country, economic competitiveness of the plant, design trends in other countries, operating experience of other fast reactors including FBTR, PHWR experience in India, industrial infrastructure, design and construction codes, available materials, O&M requirements, electric power grid, site characteristics, R&D requirements, safety and engineering judgement.

7.1.1.1. Pool-type concept

The loop and pool concepts have been discussed qualitatively in several forums. Both types are in use. The pool concept was selected for the PFBR due to following reasons:

- Simple shape of reactor vessel without any nozzles, low neutron fluence and its easy in-service inspection results in high reliability;
- Large thermal inertia of the pool attenuates thermal shocks; results in slow temperature rise during decay heat removal and load throw conditions, and gives longer time for operator action;
- Capability to withstand higher work potential under core disruptive accident;
- Radioactive components and fluids are contained within the reactor vessel;
- Compact primary sodium circuit layout. Based on experience with loop (BN-350) and large pool (BN-600) reactors, Russians prefer the pool-type concept for plants with generation capacity more than 300-400 MWe;
- Leakage in primary sodium circuit will not lead to a loss of coolant accident (LOCA) and hence there exists high reliability of core cooling.

The pool-type concept, however, calls for a few challenging aspects to be resolved successfully:

- Complex pool hydraulics: Specially developed computer codes and several scaled down water models have solved these problems successfully. Operation of EBR-II, Phénix, PFR, BN-600 and Superphénix has demonstrated the agreement with the predicted thermal hydraulic behaviour;

- Complex seismic design of thin vessels with large mass of sodium requires robust analysis techniques with experimental validation;
- There is more interdependence for overall optimisation in component designs (including, for example, the primary sodium pump, the intermediate heat exchanger, the inner vessel, and the reactor vessel roof);
- Large vessels require onsite construction and assembly;
- Difficulty in maintenance on the top of pile: Close layout of many components on reactor assembly resulting in space constraint can prolong maintenance works.

7.1.1.2. Reactor power

The following considerations led to the selection of a 500 MWe capacity:

- Specific capital cost is lower for 500 MWe than for lower power, say 250 MWe (~ 30%).
- Medium power is desirable for constructing additional similar follow on plants before a large commercial scale plant is built.
- Coal fired power plants and PHWRs of 500 MWe capacities have been designed; the coal fired plants are in operation and the PHWRs are under construction. The conventional power equipment of this size, particularly the turbine generator (TG) set, is readily available.
- Design and development efforts for 250 MWe and 500 MWe plants are comparable.
- Constructability of 500 MWe size components was assessed based on the experience of 220 and 500 MWe PHWRs and the FBTR. The Indian industries are equipped with necessary infrastructure.
- Pool-type reactors of this power range have been successfully operated in other countries (e.g. BN-600).

7.1.1.3. Core

7.1.1.3.1. Fuel

PuC-UC was chosen as fuel for FBTR due to the unavailability of enriched uranium for mixed oxide option. For PFBR, enriched uranium is not required. Though carbide gives high breeding ratio, it raises safety problems in fabrication because of its pyrophorocity. Fabrication cost is also high. Fuel burnup is lower compared to oxide because of its high swelling rate. Reprocessing on prototypic scale has not yet been done anywhere and this cost is also expected to be more. Being a large power plant, a proven fuel cycle is essential. High breeding is not the objective for PFBR. As the design of entire plant revolves around the fuel, a firm decision is essential.

Most of the large sized FBRs use MOX fuel. This choice was natural since the technology of mixed oxide fuels is very similar to that of UO_2, which is used in thermal reactors. MOX fuel has shown excellent performance in all FBR where it has been used, with respect to high burnup (up to 200 000 MWd/t on full size subassemblies) and has proven reprocessing technology. A large experimental data base with respect to satisfactory behaviour under off-normal operating conditions is available. Extensive experience is also available in India from thermal reactors. Therefore, MOX is chosen as fuel for PFBR.

7.1.1.3.2. Core layout

A conventional homogeneous type of layout is selected for the core and blankets configuration, in spite of advantages of higher breeding ratio and reduced sodium void coefficient, is not considered due to increase in higher fissile inventory, larger core size, reduction in Doppler coefficient, requirement of increased thermal striping protection arrangements for the above core internal structures and possible difficulty in achieving optimum neutronic coupling between core zones without extensive experimental studies (Fig. 7.1).

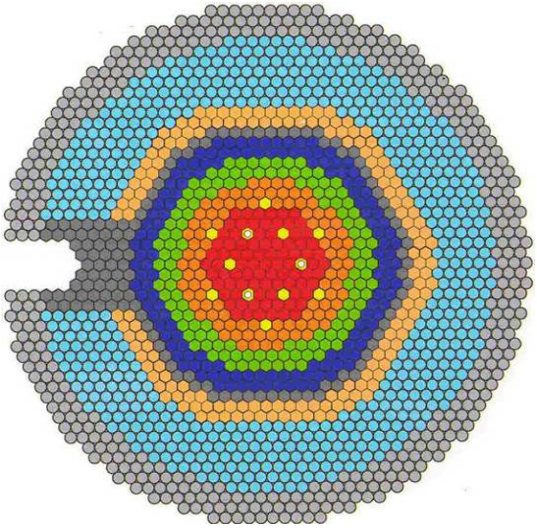

SYMBOL	TYPE OF SUBASSEMBLY	No.
	FUEL (INNER)	85
	FUEL (OUTER)	96
	CONTROL AND SAFETY ROD	9
	DIVERSE SAFETY ROD	3
	BLANKET	120
	STEEL REFLECTOR	138
	B_4C SHIELDING (INNER)	125
	STORAGE LOCATION	156
	STEEL SHIELDING	609
	B_4C SHIELDING (OUTER)	417
	TOTAL SUBASSEMBLIES	1758

FIG. 7.1. PFBR core layout.

7.1.1.3.3. Core height

Core height has effect on both physics and engineering design parameters. These have been studied in detail. The advantages of small core heights are: increased fuel volume fraction for the same coolant pressure drop, reduced subassembly length, easier fuel fabrication and reduced sodium void coefficient. The disadvantages include: increased fissile inventory, larger number of pins and larger core radius. Based on the parametric study to limit the penalty on fissile inventory, an active core height of 1 m with height/diameter ratio of ~ 0.5 has been selected.

7.1.1.3.4. Pin and subassembly sizes

The choice of pin diameter significantly affects the fissile inventory, fuel cycle cost and doubling time. Parametric studies made for doubling time and fuel cycle cost considerations for oxide fuel indicate that the optimum pin diameter is 8 to 9 mm depending on the out-of-pile time. In order to reduce the Pu inventory, a small pin diameter of 6.6 mm has been selected. The Pu inventory for a 6.6 mm pin is lower by ~ 15% in comparison to optimum pin diameter range.

Considering factors such as subassembly worth, decay heat of spent fuel, handling loads, number of positions on grid plate, core monitoring positions, core average burnup, handling time, fabrication cost etc, 217 fuel pins per subassembly has been selected. The active core consists of 181 fuel subassemblies of which 85 are in the inner enrichment zone and 96 are in the outer enrichment zone, as shown in Fig. 7.1.

7.1.1.4. Shutdown systems

For reactor shutdown, the PFBR is provided with two independent, fast acting and diverse shutdown systems, namely SDS-1 and SDS-2, to detect any abnormalities in reactor core and to initiate safety action. Each system consists of sensors, signal-processing systems, logic systems, drive mechanisms and neutron absorber rods. The absorber rod of the first system is called the Control and Safety Rod (CSR) and that of the second system is the Diverse Safety Rod (DSR). Enriched B_4C pellets are used as neutron absorbing material in both CSR and DSR. The respective drive mechanisms are Control and Safety Rod Drive Mechanism (CSRDM) and Diverse Safety Rod Drive Mechanism (DSRDM). The overall scheme of the shutdown systems is shown in Fig. 7.2.

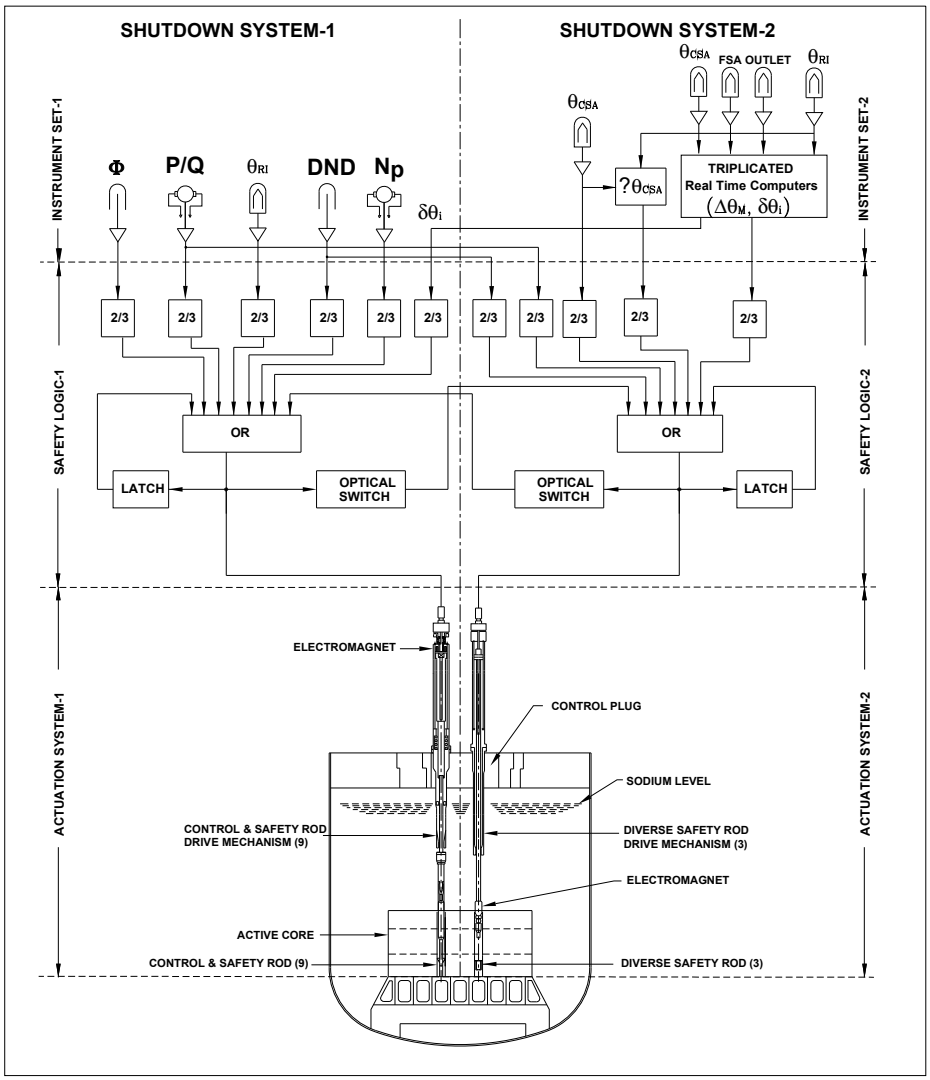

FIG. 7.2. PFBR shutdown systems.

There are nine CSRs and three DSRs in two radial banks of reactor core. The CSRDM and DSRDM are housed in the control plug and are in-line with the respective CSR and DSR in the core. Figure 2 shows the CSR and DSR with their drive mechanisms in the reactor assembly. Core subassemblies are arranged in a hexagonal array and the nine CSR and three DSR subassemblies are kept in two pitch circles as shown in Fig. 7.1.

7.1.1.4.1. Safety criteria

Safety of the reactor as a whole depends on the reliable performance of both the shutdown systems. This demands very detailed design and analysis, prototype manufacturing and testing under simulated reactor-operating conditions to check and ensure the intended functions in the reactor. The safety criteria pertaining to the shutdown systems are as follows:

- Provision of at least two reliable, independent, automatic, fast acting shutdown systems, operating to the greatest extent possible on diverse principles. At least one of the systems needs to meet all functional requirements even in case of postulated core deformation. The reliability of each system is such that its non-availability is less than 10^{-3} per reactor year and the overall non-availability of the two systems is less than 10^{-6} per reactor year.
- Provision of sufficient redundancy in the design so that failure of a single most effective absorber rod of a shutdown system does not result in impairment of that system to an extent that it will not meet the minimum specified requirements.
- One of the shutdown systems could be used for reactivity control, provided that its functional capability to shut down the reactor is not jeopardised.
- The reactivity worth, speed of action and delay in actuation of each shutdown system is such that during all operational states and postulated accident conditions of the reactor, including the most reactive state of the core, the following criteria are met:
  (a) The reactor is rendered sufficiently sub-critical and maintained sub-critical under cold condition, taking into account uncertainties in the neutronic calculations or measurements,
  (b) The specified fuel design limits are not exceeded,
  (c) The reactor coolant system design limits are not exceeded.
- The total reactivity worth of the shutdown systems is such that in the shutdown state, with all absorber rods in the core, the reactor is sub-critical with k_{eff} not more than 0.95, such that the reactor remains sub-critical under postulated fuel handling errors (e.g., replacement of the most reactive absorber rod by most reactive fuel subassembly, removal of absorber rods).
- Maximum reactivity worth of an absorber rod, together with its maximum possible withdrawal speed, is limited such that the fuel, coolant and cladding design limits are not exceeded.
- The availability of safety support systems necessary for actuation of a shutdown system is commensurate with the availability requirements of the shutdown system.
- All equipment is designed such that its probable failure modes will not result in an unsafe condition.
- Maintenance and availability testing which may be required during reactor operation can be carried out without a reduction in the effectiveness of each shutdown system below the minimum allowable requirements.
- Each shutdown system can be actuated manually from the main and emergency control rooms.
- It is not readily possible for an operator to prevent a safe automatic action from taking place.
- Design of the control logic of the absorber rods and their drive mechanisms to prevent unintended movement in the directions that add reactivity.

7.1.1.5. Main heat transport system

The main heat transport system comprises primary sodium, secondary sodium and steam-water circuits. Sea water is the ultimate heat sink. A secondary sodium circuit is interposed between the primary and steam-water circuits from the consideration of safety. It avoids entry of

moderating and corrosive material into the core during a sodium-water reaction in the steam generator (SG). Further this avoids radioactive contamination of SG and steam-water system.

It is worth noting that the investment cost is the major contributor (~ 75%) of the unit energy cost in comparison with 15% and 10% for O&M and fuel cycle costs, respectively. Out of 75% investment cost, ~ 25% is contributed by sodium heat transport systems. This indicates that the major efforts should be directed towards reducing the capital cost and construction schedule, which, in turn, calls for a less number of systems and components.

A study on 2 / 3 / 4 primary and secondary sodium loops was made. Due to adoption of design improvements, the increase in size of components, when the number of loops is decreased, is not large and the increased component dimensions are within the Indian industrial capability. The reduction in number of components helps to reduce the capital cost, construction time and the outage time due to generic design failure or inspection and repair of components. Hence the capacity factor is expected to be marginally higher for the case with lower number of components and/or loops, except for the SG, where more units offer a higher capacity factor as failure is linked to number of tube to tubesheet welds. Reduction in number of loops also reduces instrumentation and control, electrical systems and the space required for layout of components. Hence, a two loop concept has been selected which results in two primary sodium pumps, four IHXs and two secondary sodium pumps. Each primary pump is flanked by two IHXs as in other large pool reactors to optimise the main vessel size and economics. Figure 7.3 shows the flow sheet of main heat transport system.

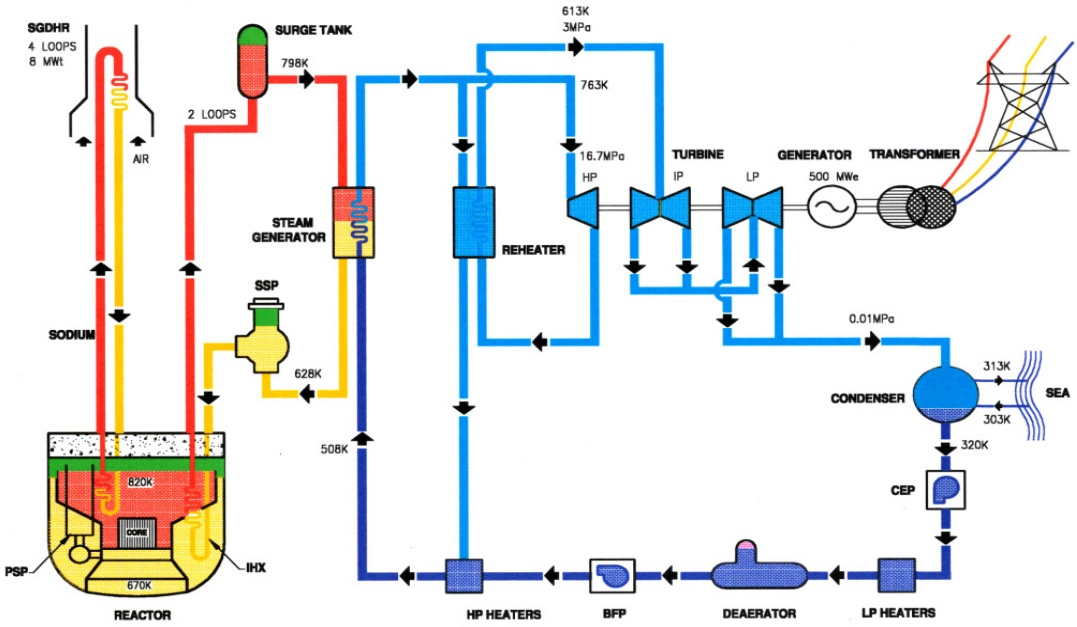

FIG. 7.3. Diagram of PFBR main heat transport system.

Liquid sodium is circulated through the core using two sodium pumps. The sodium enters core at 397°C and leaves at 547°C.

The hot primary sodium is radioactive and is not used directly to produce steam; instead, it transfers the heat to secondary sodium through four intermediate heat exchangers. The non-radioactive secondary sodium is circulated through two independent secondary loops, each having a sodium pump, two intermediate heat exchangers and four steam generators. The choice of four steam generators per loop is based on overall optimization studies carried out considering capital cost, outage cost and operation cost with three steam generators in the affected loop in case of a leak in one steam generator. The primary and secondary pumps are vertical, single stage and single suction centrifugal type, with variable speed AC drives are provided with flywheels to meet the flow coast down requirements of 8 s and 4 s, respectively. An AC pony motor of 30 kW rating is additionally provided for each of the primary pumps. The steam generator is a once through integrated type design using straight tubes and an expansion bend in each tube. The decay heat is removed using the operation grade decay heat removal system of maximum 20 MWt capacity in the steam water system under normal conditions. In case of off-site power failure or non-availability of steam-water system, the decay heat is removed by a passive safety grade decay heat removal circuit consisting of four independent loops. Each safety grade decay heat removal loop is rated for 8 MWt and consists of a decay heat exchanger immersed in the hot pool, one sodium-air heat exchanger, associated sodium piping, tanks and air dampers. Diversity is provided for decay heat exchanger, air heat exchanger and dampers. The circulation of sodium and air is by natural convection.

The once through concept is selected for the SG because of reduced water inventory which minimises the consequences of large sodium water reaction and improves economics. Considering the advantages of simplification in design, manufacture, reduction in capital costs, construction schedule, operation and availability of proven turbine, steam reheat cycle has been chosen. Most of the FBR designs use steam reheat concept to reduce the complexity. Saturation steam cycle does not permit the exploitation of higher steam temperatures possible in FBR. Hence, super heated steam cycle is adopted.

For the SG, a modular type concept (i.e. greater number of units per secondary loop), is selected because of inherent advantages in design and construction of smaller units. In the modular concept, the tubesheet size is also relatively small. The choice of four SG modules per loop has been arrived at based on optimisation of capital cost and outage cost in case of a tube leak, with due consideration to construction schedule, while permitting (n-1) module operation.

From economic considerations, the integrated design, combining evaporator and superheater, is preferred over the split up units. Since steam pressure is high, the instability problem can be easily resolved.

Finally, the combination of 2 primary sodium pumps / 4 IHX / 2 secondary loop / 4 SG per loop is selected from both economic and availability considerations as compared to other combinations.

7.1.1.6. DHR system

Even after the reactor is shutdown, there is heat generation in the core due to radioactive decay of fission products. This heat, called decay heat, needs to be removed to prevent unacceptable temperature rise. When offsite power is available, the decay heat is removed through normal heat transfer path of primary sodium, secondary sodium and steam-water circuits. Under loss of offsite power or non-availability of either the secondary sodium circuit

or the steam water circuit, the decay heat is removed through independent safety grade decay heat removal system (SGDHRS).

Various options are available for the SGDHRS. Main options are Radiant Vessel Auxiliary Cooling System (RVACS), wherein the heat is transferred from fuel to main vessel through natural convection and then, from main vessel by conduction, convection and radiation (e.g. Phénix, Superphénix and PRISM), Independent Na-air HX riding on the secondary sodium circuit with the primary and secondary sodium pumps having emergency power supply (e.g. Superphénix and Monju),

Direct Reactor Auxiliary Cooling System (DRACS) wherein the decay heat is removed by sodium to sodium heat exchangers immersed in the hot pool which in turn transfers the heat to sodium air heat exchanger (e.g. Superphénix, EFR, DFBR, BN-600M). RVACS does not provide adequate heat transfer capabilities for the large pool type plants (>350 MWt). The function of DHR system attached with secondary sodium depends upon the availability of the later and also requires safety grade design for the secondary sodium system. Hence for PFBR, DRACS option is selected.

Four independent loops of 8 MWt capacity each have been selected in order to provide adequate redundancy. Even with one of these loops not being available on demand, it is possible to keep the temperatures within the acceptable values for upset conditions. Each of these loops comprises one sodium-sodium heat exchanger dipped in reactor hot pool, one sodium-air heat exchanger, associated piping and tanks. Except for the dampers on the air side, this system is entirely passive. In order to enhance the availability, dampers are motorised with the provision for manual operation. NaK, which has low melting point, is not considered as coolant in the loops of the SGDHRS because of its higher chemical affinity for air, inferior thermal properties, higher cost compared to sodium and possibility of NaK leaking into primary sodium. Sodium is used as the intermediate coolant. There is no risk of sodium freezing in the SGDHRS as dampers are closed whenever the sodium temperature falls below 433 K.

7.1.1.7. Main structural materials

20% CW D9 material is selected for the cladding and the hexcan because of its improved resistance against swelling due to neutron irradiation, high strength at operating temperature and good corrosion resistance against Na and fuel. Ferritic steel will be considered for the hexcan of future cores. AISI 316M has been used in the FBTR for sodium components, except for the SG. There has been no problem with this material. It is decided to adopt the same grade with some improvements. SS 316 LN minimises risk of sensitization during welding and avoids risk of intergranular stress corrosion cracking (IGSCC), while maintaining high temperature strength. The embrittlement due to thermal ageing is also within acceptable limits and operating experience of other FBR has indicated satisfactory performance of this material. Hence it is selected for out of core sodium components. Use of SS 304 LN for the cold leg is chosen, except for parts where there is risk of mix up (e.g. sodium piping). Modified 9Cr-1Mo steel has been selected for SG because of its high mechanical strength, freedom from the risk of stress corrosion cracking (problem with stainless steels) and also decarburization (problem with 2.25Cr-1Mo). Based on economic considerations, A516 Gr 65 / A 48 P2 (French AFNOR Std) type carbon steel is selected for top shield of the reactor because of low operating temperature, good impact strength and compatibility with sodium vapour.

7.1.1.8. Operating temperatures

High reactor outlet temperature is always preferred for achieving high thermodynamic efficiency. However, this is limited by fuel clad and component structural integrity considerations. In order to satisfy the allowable clad hotspot temperature of 973 K, the reactor outlet temperature can be as high as 833 K with $\Delta T = 150$ K across the core. As regards structural integrity of high temperature components, with the recent advancements in high temperature design codes and structural analyses methodology, the reactor outlet temperature is limited to 825 K. Detailed inelastic and viscoplastic analyses have been performed for control plug, inner vessel and IHX using ORNL and Chaboche viscoplastic models. While the permissible reactor outlet temperature is about 770 K in order to satisfy the design rules of RCC-MR through 'elastic' route, the viscoplastic analysis indicates that the acceptable temperature can be 825 K. Modified 9Cr-1Mo can permit up to 775 K steam temperature. The turbines used in conventional thermal power plants allow steam temperature of 811 K. The reactor inlet temperature and hot and cold temperatures of the sodium in the secondary sodium circuit are arrived at from overall cost optimisation studies.

- Primary Na core inlet/outlet 670/820 K
- Primary Na inlet/outlet to IHX 817/667 K
- Secondary Na inlet/outlet to IHX 628/798 K

7.1.1.9. Reactor assembly

The primary sodium circuit is housed in a single vessel called the main vessel (MV). This is closed at the top by the top shield, which includes the roof slab, the large and small rotatable plugs (LRP and SRP, respectively) and the control plug (CP). The roof slab supports the major components like the main vessel, the rotatable plugs, the two primary sodium pumps, the four intermediate heat exchangers, the four decay heat exchangers, the eight delayed neutron detectors, etc. The CP houses the nine control and safety rod drive mechanisms (CSRDMs) and the three diverse shutdown rod drive mechanisms (DSRDMs), the core thermocouples and the three failed fuel localisation modules (FFLM). The main vessel is surrounded by the safety vessel (SV) to ensure that the sodium level inside the reactor even in the case of unlikely leak in main vessel will be sufficient send the sodium in to the IHX and DHX for the decay heat to get removed. To achieve this, a nominal gap of 300 mm is chosen between main vessel and safety vessel. It is ensured that the robotic ultrasonic inspection device developed for the inspection of the main and safety vessels has free access for the smooth operations.

The interspace between the main and safety vessels is inerted with nitrogen. The SV is supported directly on the reactor vault independent of the support for main vessel. On the outer surface of the SV, metallic insulation is provided to limit the heat transfer to the vault. The core subassemblies are supported on grid plate and their combined load is transferred to the main vessel through core support structure (CSS). The main vessel contains about 1150 t of primary sodium. The sodium pool is divided into two parts viz. hot pool and cold pool by the inner vessel. Argon is used as the cover gas above the sodium pool. The cover gas height is chosen as 0.8 m giving due considerations to thermomechanical behaviour apart from other functional requirements. A core catcher is provided below the core support structure and prevents the core debris from coming in contact with the main vessel during the extremely unlikely event of CDA. Inner vessel is incorporated to separate the hot and cold pools of sodium. The assembly of main vessel and its internal and top shield along with safety vessel is

called reactor assembly (Fig. 7.4). The reactor vault which supports the reactor assembly consists of two walls: the inner wall supports the safety vessel and top shield carrying other components is supported on the outer wall.

The top shield is a box structure made from special carbon steel plates and is filled with heavy density concrete ($\rho = 3500$ kg/m^3) and provides thermal and biological shielding in the top axial direction. The principal material of construction is SS 316 LN for the vessels and boiler quality carbon steel for top shield. The biological shielding in the radial and bottom axial direction outside the main vessel is provided by the reactor vault concrete.

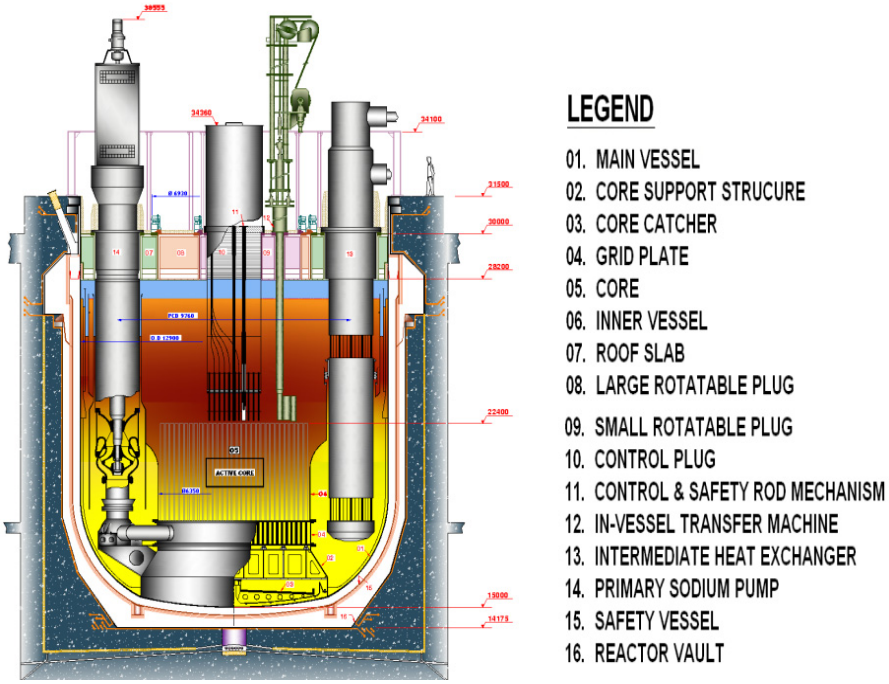

FIG. 7.4. PFBR reactor assembly.

7.1.1.10. Component handling

Fuel handling is done after 185 effective full power days with the reactor in shutdown condition at a sodium temperature of 200°C. Two rotatable plugs and a transfer arm are provided for in-vessel handling of core subassemblies. For ex-vessel handling, an inclined fuel transfer machine and cell transfer machines are used. The preheated fresh subassemblies are transferred to the core using cell transfer machine and inclined fuel transfer machine. The spent fuel subassemblies are stored inside the main vessel for one campaign and then shifted to a demineralized water-filled spent subassembly storage bay pool located in fuel building. Sodium sticking to subassemblies is washed in a spent subassembly washing facility. Leak-tight shielded flasks are provided for special handling of components like primary sodium pumps, intermediate heat exchangers, decay heat exchangers, absorber rod drive mechanisms and transfer arm. The components are decontaminated in a separate facility provided within reactor containment building before they are taken for maintenance. After decontamination, the above components are shifted to a separate building for maintenance purposes.

7.1.1.11. Plant layout

The plant layout is evolved on the basis of a single unit. The reactor assembly, primary sodium purification, primary argon cover gas system including its tanks and cover gas purification and decontamination facility are housed in a rectangular reactor containment building. Each of the two steam generator buildings houses four steam generators and associated components and piping. The reactor containment building, steam generator building and fuel building are connected and laid on a common base raft (Fig. 7.5).

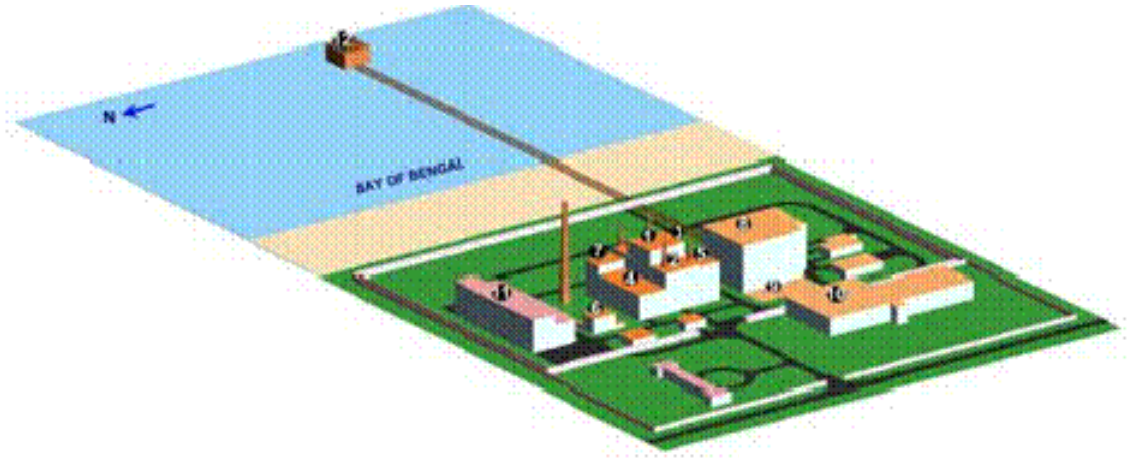

FIG. 7.5. PFBR plant layout.

1. REACTOR CONTAINMENT BUILDING
2. STEAM GENERATOR BUILDING
3. CONTROL BUILDING
4. FUEL BUILDING
5. ELECTRONICAL BUILDING
6. SERVICE BUILDING
7. RAD WASTE BUILDING
8. TURBINE BUILDING
9. SWITCH YARD
10. TRANSFORMET YARD
11. SITE ASSEMBLY SHOP
12. SEA WATER PUMP HOSE

This minimises the differential movement in piping and facilitates satisfactory working of inclined fuel transfer machine. In addition, the control building, two electrical buildings and the radwaste building are also laid on the common raft and connected to form a nuclear island, to reduce the magnitude of structural response under seismic loads and length of cables. The elevation of the raft is +12 m for reactor containment building and steam generator buildings and +14 m for the other buildings of nuclear island from functional, economic and seismic considerations (Finished floor elevation is +30 m). A service building is provided to cater to the needs of plant services. The turbine building layout is selected such that the turbine missile trajectory is outside the safety related buildings. The finished floor levels of all safety related structures are above the design basis flood level estimated for 1000 year return period. The finished floor levels of non-safety related structures is based on design basis flood level of 100 years and these structures are located 1.5 m lower than the safety related structures due to cost considerations. The diesel generators are housed in two separate safety related buildings. A 100 m tall stack is located close to the radwaste building.

7.1.2. France

In France, an important program was launched by the three partners CEA, AREVA and EDF in order to develop an innovative SFR concept [1]. The goals for innovation were identified by the partners and they are relative to safety, economic competitiveness, investment guaranty and sustainability.

This program aims at analysing the potential of different innovative technologies and design options for the primary system. First design (Fig. 7.6) studies were performed for:

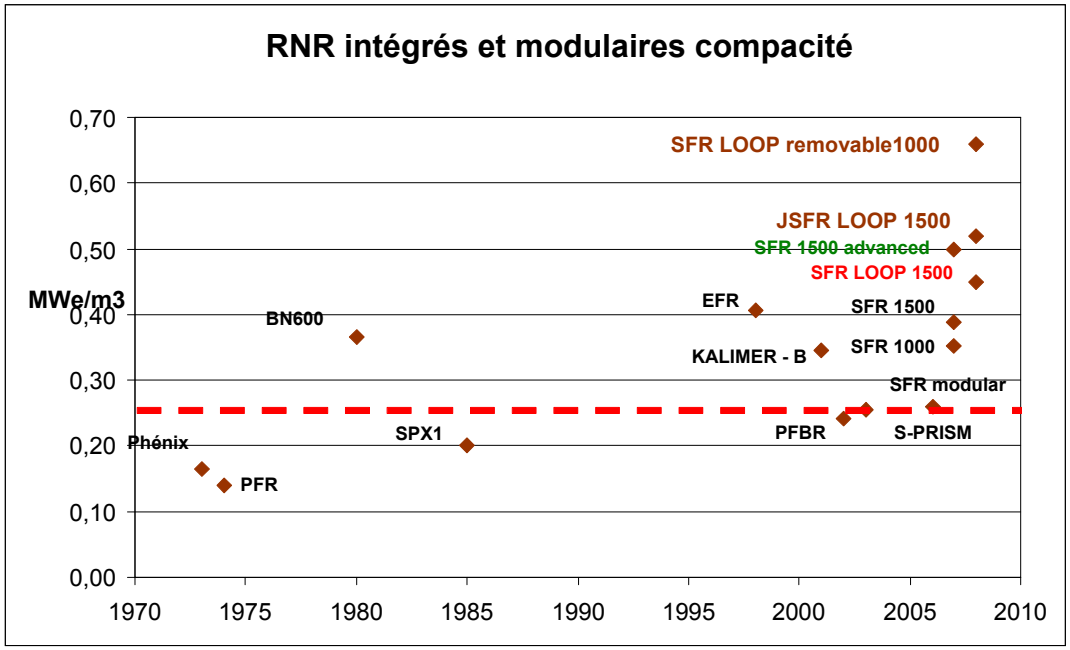

FIG. 7.6. Reactor block power density of existing and projected FBRs.

- The components and structures of the primary system (primary vessels, heat exchangers, primary pumps, reactor internals, core support structure, fuel handling, core catcher,…),
- The integration of these components in a pool, loop, hybrid, innovative reactors including in particular the integration of the primary pump and the intermediate heat exchanger in a dedicated vessel,...
- Different design options for the energy conversion systems and the safety related systems.

The different architectures of the system are examined for large power reactor (1500 MWe) medium size reactor (1000 MWe) and modular reactor (500 MWe). The gain obtained with reactor coupling / mutualisation (twin reactors) is also assessed. These different design and integration options are studied aiming at evaluating and comparing the different concepts regarding specific criteria (safety, economics, sustainability and in service inspection). An indicator about economics is the power density of the reactor block.

The retained option for the secondary heat transfer system has an important influence on the concept selection. For example, choice of alternative fluid or suppression of the intermediate

fluid may lead to loop or hybrid concepts to avoid water reaction or high pressurized gas in the reactor vessel. Furthermore, the primary system basic options (pool, loop, hybrid, innovative) give strong guidelines for the components (intermediate heat exchangers, primary pumps,...) and for the internal structures (reactor vessel, core support, sodium plenum arrangement).

Taking into account these conditions, the reflection is conducted first considering the classical option for the intermediate fluid (sodium) in the secondary circuit. Then, at this first stage the innovative solutions are proposed for the pool and for loop type reactors and comparison is achieved within the same hypothesis; that means equivalent:

- Power (electric and thermal);
- Temperature cycle;
- Core design.

7.1.2.1. Pool reactor 1500 MWe

The 1500 MWe primary system is based on six secondary loops (of 'Regain' type), three mechanical primary pumps and six DHR loops (six time 50% diversified for the half). The design (Fig. 7.7) is derived from the European Fast Reactor studies [2, 3].

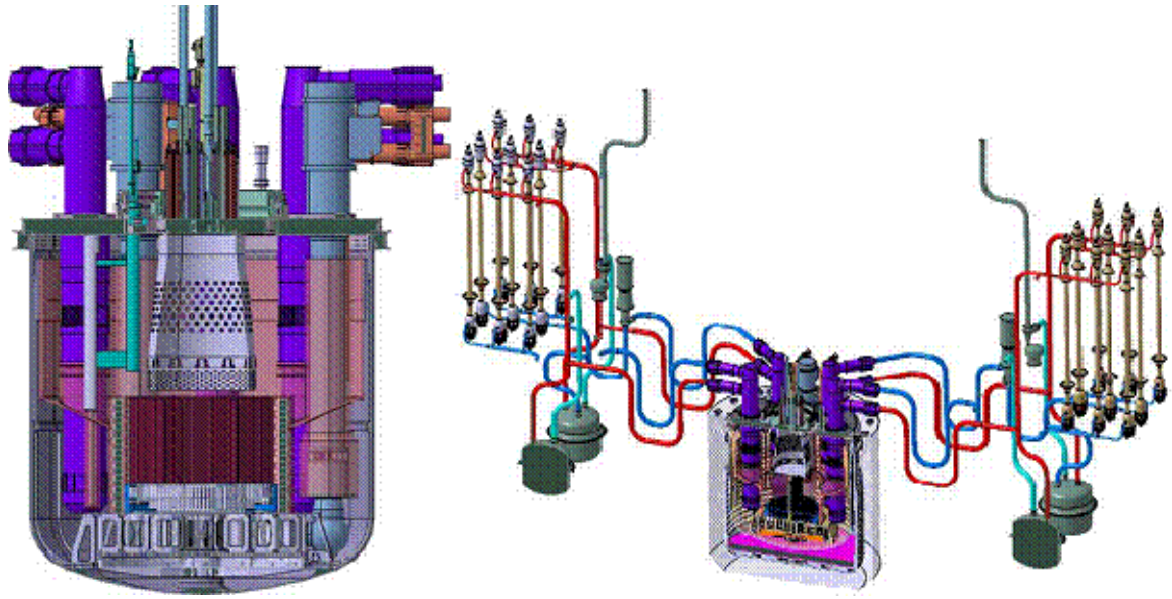

FIG. 7.7. SFR pool 1500 MWe - 3D views.

The primary system integrates six new options:

- Ferritic intermediate heat exchangers;
- Alveolus roof slab and improved anchorage to the vault;
- High pressure piping connected directly to core support strongback, the periphery of which is used as inlet core plenum;
- Strongback resting on the vessel bottom;
- Conical inner vessel;
- In-sodium fuel handling route;
- Internal and/or external debris tray able to cool and avoid the re-criticality of melted corium.

This integration design gives optimized sizes such as:

- Reactor vessel diameter: 16 000 mm
- Reactor vessel height: 18 000 mm
- Slab roof height: 900 mm
- LRP/SRP diameter: 8300/6200 mm

The power density of the reactor block is about 0.4 MWe/m^3. This concept suppresses the welded connection between the strongback and the main vessel. In-Service Inspection of the core support line is possible from outside (inter-vessel gap) using US-NDT and remote guided machine.

The same cooling system which cools the guard vessel participates in the decay heat removal function. However the efficiency is not sufficient but gives more grace time and reduces the mission duration of direct reactor cooling systems.

An external debris tray is proposed to be investigated to mitigate core melting and decay heat removal through specific cooling circuit acting in passive conditions.

7.1.2.2.Pool reactor 1000 MWe

A medium power version (SFR 1000 MWe) has been derived from the large power one. This integrated design is achieved considering four IHXs, three primary pumps and four secondary loops. The smaller vessel allows considering the innovative option of the integrated diagrid strongback which gives many advantages for the conception (e.g.: the diagrid is stiffer and the connection between diagrid and primary pumps is completely removed). The DHR system by the safety vessel is far from extracting enough power but the time saved for the DRC and the maximum temperature reached in case of accident are significantly improved. Main dimensions for this design are:

- Reactor vessel diameter: 14.2 m
- Reactor vessel height: 18.0 m
- Height of reactor vessel roof: 0.9 m
- LRP/SRP diameter: 7.1 / 5.2 m

The power density of the reactor block of the SFR pool 1000 MWe is not very far from that of the 1500 MWe; it is about 0.35 MWe/m^3.

7.1.2.3. Modular pool reactor

Modular pool reactor has been also designed aiming at extracting the decay heat through the vault thanks to a cooled guard vessel. For this purpose the power is limited to 375 MWe and the size of the reactor vessel is maintained relatively large. The general drawing is close to the 1000 MWe and the power density of the reactor block for the modular pool reactor is about 0.25 MWe/m^3.

7.1.2.4. Advanced pool reactor 1500 MWe

Advanced pool reactor has been proposed to investigate the reactor vessel diameter reduction possibilities toward ultimate ‘pool compactness’. Therefore this design exercise includes very innovative options such as cylindrical inner vessel linked to oval IHX through mechanical junctions of labyrinth type and pantograph fuel handling system associated to core cover plug

with fence or as gas fuel route without internal fuel storage. Primary pumps are also innovative (high net positive suction head (NPSH) type with axial feeding). These innovative options lead to a higher power density of the reactor block (0.5 MWe/m^3); however, at the same time, they present some technical risks and require further studies. The reactor vessel, 19 m in height, could be as small as 14.2 m in diameter. In order to accommodate fuel handling, the diameter has been increased to 14.8 m.

7.1.2.5. Loop reactor 1500 MWe

Study of the loop concept started with the analysis of the JSFR design [4] both from Safety and conceptual points of view. Preliminary assessment has been issued with three primary loops for safety reasons and with specific tanks for the primary pumps and IHX. The integrated IHX/primary pump has not been retained for maintainability reasons.

The compact design of reactor vessel leads to fuel handling system based on core cover plug with fence and pantograph machine as the advanced pool 1500 MWe.

The thick alveolus roof slab is proposed also for the loop concept and in the same way the core support on flange on cylindrical part of the reactor vessel is also retained. A cooling system (immersed weir system) is foreseen to avoid the hot reactor vessel (550°C) and creep/fatigue and progressive deformation loading during start-up and load variations.

The reactor block arrangement is given on Fig. 7.8.

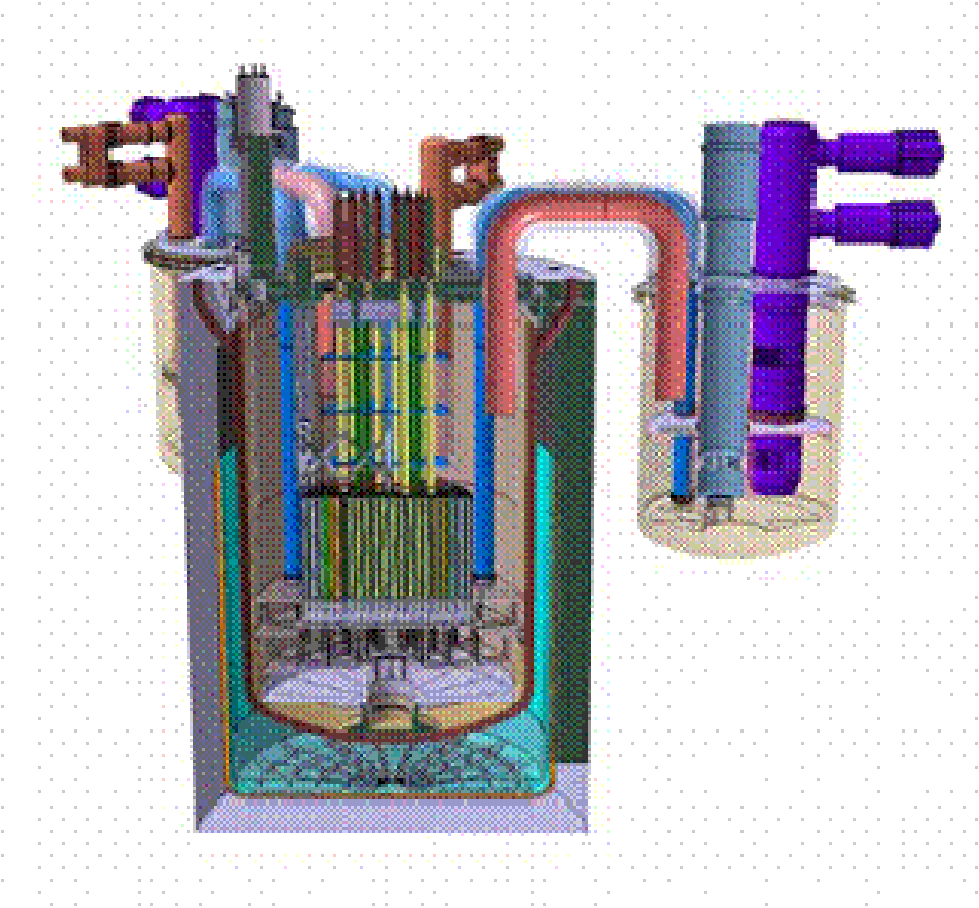

FIG. 7.8. SFR Loop reactor 1500 MWe – 3-D view.

7.1.2.6. Loop reactor with removable internals 1000 MWe

An analysis was performed to compare the pools and loops design from the view point of maintenance, inspection and repair. The conclusion is that both 'classical' concepts are quite equivalent with drawbacks on both sides. For the pool: large inventory of sodium, all the primary components in the same area. For the loop: primary piping difficult to inspect, reduced and narrow access possibilities. In consequence, an exercise has been launched aiming at defining the conditions for reactor vessel with fully removable internals. The starting hypotheses are the following:

- The reactor vessel diameter is limited to reduce the size of components to be handled (i.e. limited to 7 m);
- The number of primary loops is 3 for safety requirement in case of primary pump failure;
- The high pressure plenum is created by the reactor vessel and the inner vessel;
- The core is resting on reactor vessel flanges, and the core support line can be inspected from the outside;
- Direct nozzles are used for the primary loops;
- The primary loops are concentric in such a way the hot flow is inside and cold flow outside and so the nozzles are cooled;
- Simple device allows disconnection the hot piping and inner vessel.

The size limitation on the primary components leads to the retention of the loop option, which allows high power integration in a reduced reactor vessel.

The component vessel integrates two oval-shaped IHX and one primary pump at the centre. Direct Reactor Cooling heat exchangers (100%) are installed in the reactor vessel and one in each component vessel (100%). The guard vessels are cooled and the capability for decay heat removal through the vault including the components vessel is 100%. The installed capacity for the primary system is therefore 500%. The main characteristics of the SFR loop removable reactor are summarized in the Table 7.1.

TABLE 7.1. SFR LOOP CHARACTERISTICS

	Reactor vessel	Component vessels
Vessel		
Diameter, m	6.9	5.4
Height, m	17.5	11.5
Primary sodium mass, t	455	160
Steel mass, t	1300	680

The power density of the reactor block is high: 0.65 MWe/m^3.

Mechanical behaviour of nozzles under thermal expansion during start-up and seismic events show that for 80 mm thickness the stress level is acceptable.

The first assessment for the possibility internal component replacement has been done. A very large cask will be necessary for diagrid removal owing to its high radioactivity which requires about 0.4 m of steel shielding.

Gas based energy conversion cycles

SFRs have traditionally employed a Rankine steam cycle for power conversion. For instance, the Superphénix plant was based on a Rankine steam cycle for power conversion allowing a 40% net efficiency with 545°C for the core outlet temperature. Although the Rankine cycle is a well developed technology, the design and licensing safety evaluation must deal with the sodium-water reaction and the secondary sodium fire issues. Potential sodium-water reactions which result in formation of combustible hydrogen gas and exothermic energy release can be eliminated by adopting a gas based energy conversion cycle.

Moreover, the interest for other thermodynamic cycles to extract power can be argued by cost reduction (efficiency improvement with the same core temperature, energy conversion system (ECS) design simplification, operability and maintenance and the potential of suppression or simplification of the intermediate loop).

7.1.2.6.1. Classical gas indirect energy conversion system

The model consists of a closed-loop primary circuit with sodium as liquid metal coolant (Fig. 7.9). The intermediate circuit uses also sodium as coolant. The Brayton cycle consists of a closed-loop circuit with gas as coolant and two open-loop coolant circuit for the pre-cooler and the inter-cooler (water). The gas average pressure ranges between 30 and 250 bar.

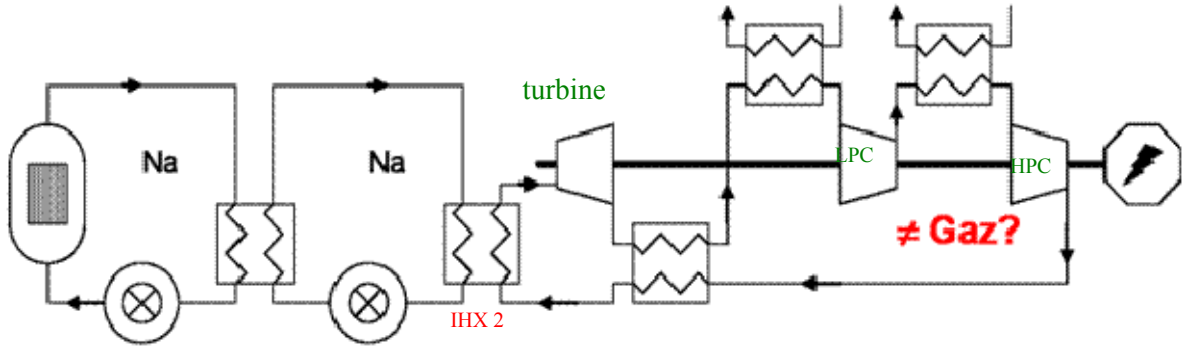

FIG. 7.9. Classical gas indirect energy conversion system.

Many sensitivity tests were performed on various parameters (gases, cycle arrangement, gas pressure, recuperator effectiveness, turbine and compressor efficiencies, core outlet temperature, IHX pinch point, cycle cold point) in order to analyse previous assumptions and conceptual choices. The overall cycle efficiency is currently used to compare cycles. Later on, a compromise between high values of overall cycle efficiency and economical/technological issues will have to be found. According to calculations, sub-critical CO_2 as coolant is the most efficient gas (Table 7.2).

TABLE 7.2. GASES (CORE OUTLET TEMPERATURE: 550°C, TIT: 520°C, 50 BAR, CYCLE COLD POINT: 21°C, WITH INTERMEDIATE LOOP)

Gas	$T_{in,core}$ (°C)	Π_T	net η (%)
He	390	1.7	35.5
He-N_2 (He mass percen 20%)	392	1.9	36.1
N_2	393	2.1	36.6
Air	394	2.1	36.3
Ar	381	1.,7	34.7
sub critical CO_2	403	2.8	37.4

But nitrogen at high pressure is also considered as a promising candidate; following coolants are, in order, air and He-N_2 mixture. Concerning sub critical CO_2, a test has been performed at 65 bar (pressure lower than critical pressure: 73.77 bar) with the turbine inlet temperature (TIT) at 530°C and without an intermediate loop: the net plant efficiency is 38.5%; in this case, the analysis must be pursued with a chemical evaluation to achieve compromise between thermodynamic properties and chemical specificities.

7.1.2.6.2. Cycle arrangement

Sodium properties make it necessary to use an intermediate loop in the reactor system between the core cooling and the power conversion.

An intermediate circuit leads to eliminate potential introduction of Na-gas reaction products into the primary system, and the potential for gas transport to the core (Fig. 7.10).

The elimination of the intermediate loop leads to a gain of 1% in plant efficiency and to the removal of one pump. The elimination of the intermediate loop is promising for future SFR; nevertheless, consequences of the gas circuit depressurisation as well as IHX tube failure have to be evaluated.

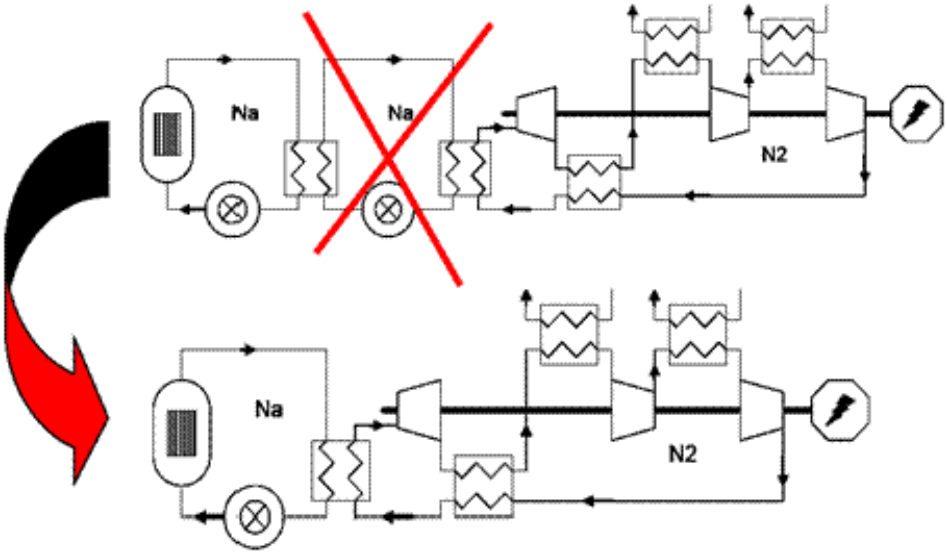

FIG. 7.10. Cycles with and without intermediate loop.

7.1.2.7. Reactors twinning

The study of the possibility of sharing systems has been performed aiming at cost reduction. If expensive systems and components, such as the control room, external storage and component handling devices could be shared, this would lead to a significant cost reduction. However, the studies performed point to the fact that it is very difficult to share safety related systems. An example is shown on Fig. 7.11.

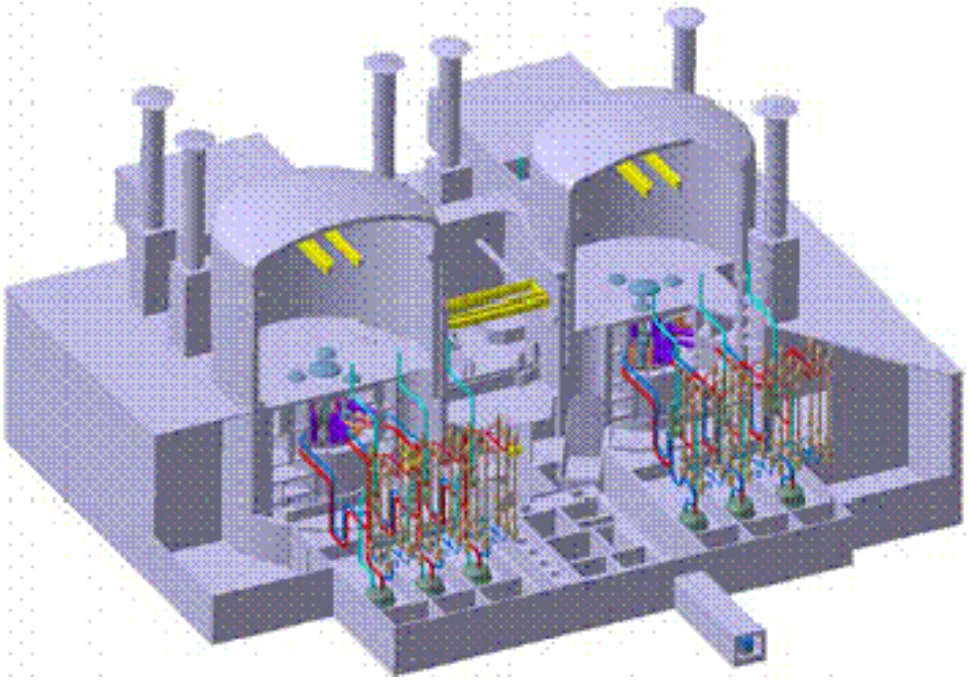

FIG. 7.11. SFR Reactor pool 1500 MWe twin.

7.2. Main components

Main components of sodium-cooled fast reactors must take into account the advantages and disadvantages of the coolant. The low system pressure certainly is an advantage, whereas e.g. the risk of sodium fires and the lack of optical transparency require special designs. In the following, the characteristics of main components such as the reactor vessel, main and safety vessel, sodium pumps, intermediate heat exchangers, steam generators, fuel handling and transfer systems, decay heat removal systems and seismic isolation, are discussed using SFRs which have operated in the past, those currently in operation and conceptual designs as examples.

7.2.1. Reactor vessel, main and safety vessel

7.2.1.1. Design features (including material selection and characteristics)

7.2.1.1.1. KALIMER-600

Reactor vessel

The reactor vessel is the boundary of the primary heat transport system and performs support and container functions during all temperature, pressure, and load variations which occur during the operating lifetime. The reactor vessel, which is made of Type 316 stainless steel, has overall dimensions of 18.0 m height, 11.41 m outer diameter, and 0.05 m thickness in the conceptual design and is composed with a 15.45 m long side cylinder with integral torispherical bottom

head. The reactor vessel is attached to the reactor head and supports the reactor internal structures, the reactor core, primary sodium, and includes IHXs, primary pumps and IVTM.

Safety vessel

The safety vessel, which is made of 2.25Cr-1Mo, has overall dimensions of 18.25 m height, 11.76 m outer diameter, and 0.025 m thickness in the conceptual design. The safety vessel is slightly greater than reactor vessel and encloses the reactor vessel. The gap, which is 15 cm, between the safety vessel and the reactor vessel contains argon gas and the instrument to detect sodium leakage from the reactor vessel will be installed in this gap region. It provides guard vessel for the primary sodium and cover gas if the reactor vessel leaks.

7.2.1.1.2. PFBR

Inner vessel

The inner vessel (Fig. 7.12) serves as a leak resistant barrier between the hot and cold pools of primary sodium and permits passage of the two primary sodium pumps, the four intermediate heat exchangers, the sodium purification line and the cold pool level detectors to the cold pool through suitable penetrations. It provides a plenum of hot primary sodium around the intermediate heat exchangers. The design of the component ensures that the path for decay heat removal from the core is not impaired under safe shutdown earthquake (SSE) conditions. Further, small leakage (design leakage < 2% of IHX flow at the mechanical seal) in the inner vessel does not affect the reactor operation or the component experiences severe thermal loadings and its geometry is optimized with respect to buckling resistance under normal and transient/incident conditions. Further, creep-fatigue interaction damage, risks of buckling, ratcheting and high cycle fatigue due to sodium free level fluctuations is also assessed over the reactor lifetime.

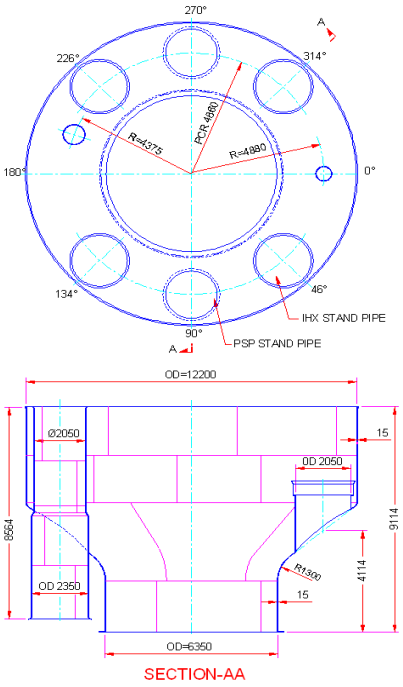

FIG. 7.12. PFBR inner vessel.

The dimensions of the safety vessel are decided by the allowable drop in sodium level in the main vessel (in the unlikely event of leak in main vessel) and the space required for in-service inspection of outer surface of main vessel (Fig. 7.13).

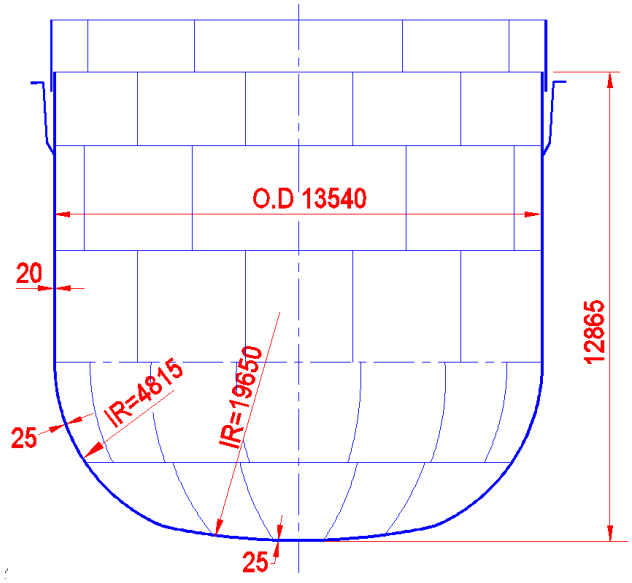

FIG. 7.13. PFBR safety vessel.

A nominal gap of 300 mm is selected for the inter-space between the main vessel and safety vessel and safety vessel is sized accordingly. The outer surface of the safety vessel is lined with insulation panels. The thickness of the insulation is fixed to limit the heat flux to reactor vault concrete and keep its temperatures within acceptable limits (in combination with a biological shield cooling system) during normal reactor operation and incident conditions. The temperature of the concrete is maintained below the permissible design limit of 339 K (66°C) under normal operation, 20% power operation, isothermal operation and 363 K (90°C) under safety grade decay heat removal (SGDHR) condition. At the top, the safety vessel is welded to the embedment in the reactor vault through a cylindrical support shell. The reactor vault is lined with carbon steel plates to keep the nitrogen atmosphere around the safety vessel.

Detailed experimental verification is done towards confirming the overall heat transfer characteristics of the insulation panel. Further, extensive qualification tests are performed on the insulation panels to assure their integrity under seismic conditions.

7.2.1.2. Design code

KALIMER-600

The reactor vessel is Class 1 component and the reactor vessel is designed to conform to the French code RCC-MR: Edition 2002. The safety vessel is Safety Class 2 component but the design of the safety vessel conforms to the Class 1 criteria. Establishment of the limiting values for design stress intensity includes allowances for any known or predictable degradation of mechanical properties that may occur as a result of irradiation, stress at service temperatures and changes in material properties over the design life. The reactor and safety vessels are designed as Seismic Category I structure.

7.2.1.3. Instrumentation and ISI&R

In France, the materials and techniques studied through R&D are the following:

- The instrumentation which allows a permanent surveillance of the structures and components (vessel, internal structures, steam generators,...),
- The materials aims at carrying out a regular inspection which should be as systematic as possible on these structures and components,
- Those which could be used for diagnosing anomalies,
- Finally, the tools which could be used to repair in situ the primary circuit components which cannot be moved.

In-service monitoring requirements

In-service monitoring of fast reactors is used to permanently control the good working order of the reactor. In-service monitoring involves two complementary activities:

(1) In-service monitoring
In-service monitoring enabling operators to follow the reactor state uninterrupted. For instance, the vibration behaviour monitoring process in which steel bars are plunged into liquid sodium and vibrations are recorded, which is used to analyze the evolution of sodium flows and neighbouring structures. This method enabled the researchers to quickly detect the presence of gas in the Superphénix primary sodium circuit in 1994.

(2) In-service inspection
In-service inspection composed of a series of main reactor structure examinations concerning the reactor block, secondary sodium circuits and the steam generators for the most part. Conducted during shutdowns, the inspection includes a series of global controls (telemetric measurements) and local inspections (non-destructive examinations of welds).

Repairs to structures are included in the same category as inspection, thus the acronym ISI&R. In-service inspection – a fundamental aspect of fast reactor technology [5] due to the presence of sodium which is hot (180°C during shutdowns), opaque and difficult to drain – began in France with the examination of main vessel welds in the Superphénix plant (using the MIR device, which is mentioned further on).

In-service inspection was extended to other structures located in the reactor block (Fig. 7.14) as well as other plant components, such as the steam generators.

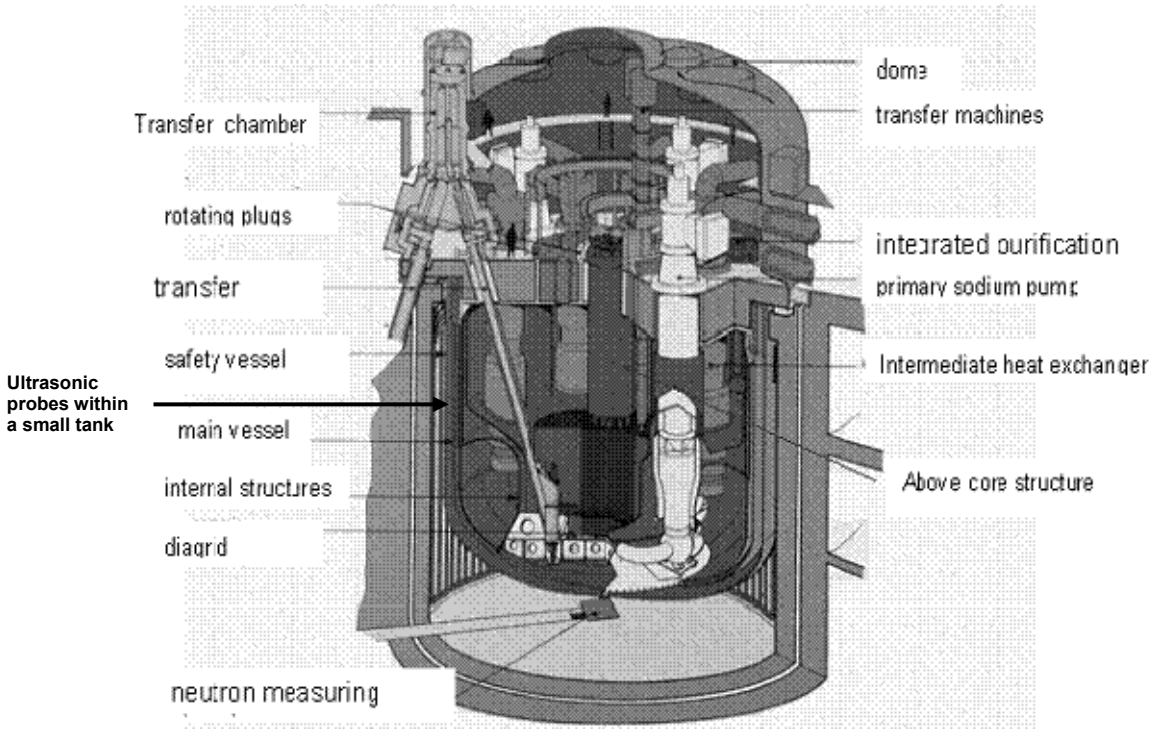

FIG. 7.14. Structures to be periodically inspected in the Superphénix reactor block.

The measures applied in Superphénix were updated to meet new inspection needs that compiled a list of possible failures for each component (cracking, rupture, progressive deformation, etc.). Two thresholds were defined for specific deformations: the alarm threshold or "recordable conditions" taking into account non-critical failures and the maximum threshold or "maximum acceptable conditions" related to level A of the RCC-MR regulations (design and construction regulations for fast nuclear reactor mechanical material).

The potential damage calculated for each structure is associated with the severity of the failure risk regarding its safety function. It is therefore possible to ascertain the vital components of the reactor for which R&D must illustrate the feasibility of applying the recordable and maximum acceptable thresholds. Therefore, each structure of the Superphénix reactor block has been classified as requiring low, medium or high monitoring.

The Phénix plant – based on an older concept – was not equipped with an inspection machine for the main reactor vessel such as the MIR device in Superphénix (Fig. 7.15).

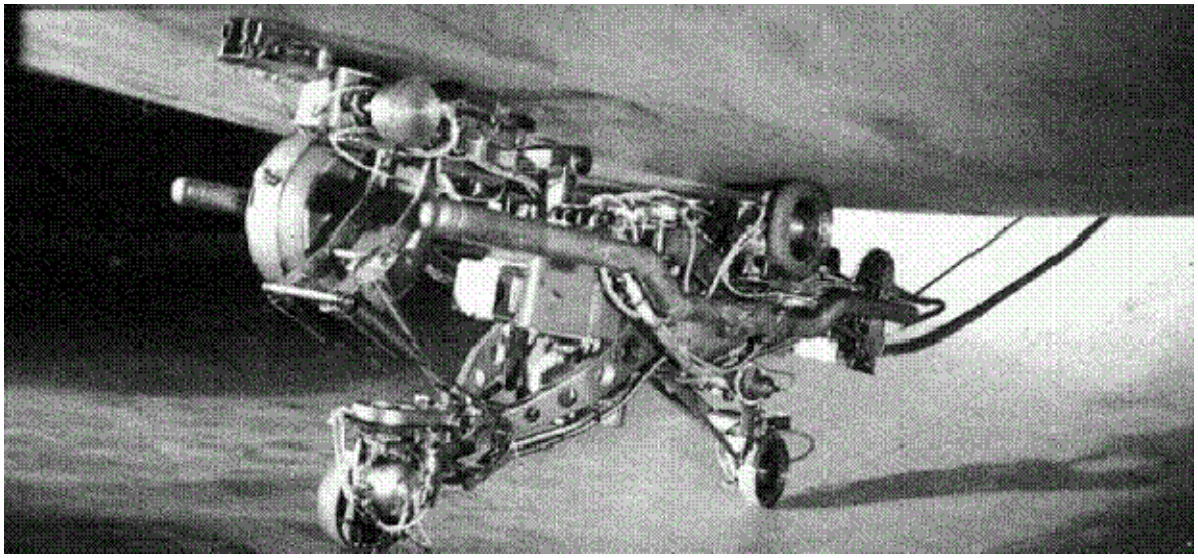

FIG. 7.15. MIR device designed to inspect welding in the Superphénix main vessel.

However, during safety re-evaluation studies [6] carried out from 1994 to 2003, the good condition of the structures containing core reactivity was confirmed by means of:

- Ultrasonic examination of conical shell supporting the reactor core (Fig. 7.16);
- Visual inspection of the above core structure, holding the control rods;
- Ultrasonic examination of the main reactor vessel hangers.

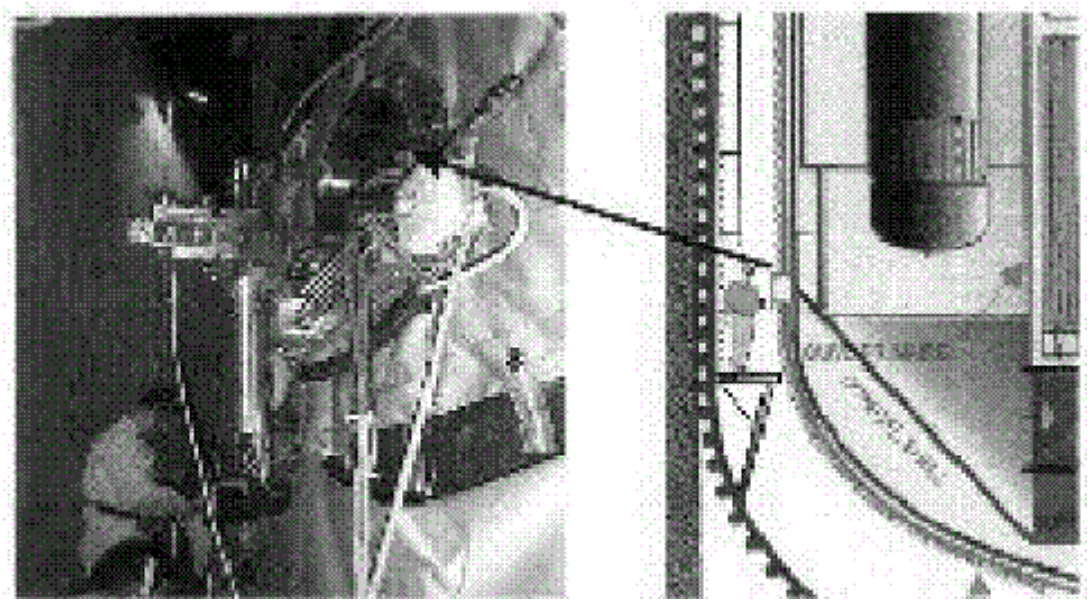

FIG. 7.16. Ultrasonic control of the conical shell in Phénix.

Non-destructive tests of sodium circuits, the fuel storage tank and the steam generators [7] were also performed in Phénix, with faulty components being repaired or replaced (cited as a reminder):

- Repairs to the secondary sodium circuits;
- Changeover of the primary coolant pumps;
- Cepairs to steam generator units [8];

- Replacing of the intermediate heat exchangers;
- Changeover of the control rod mechanisms.

Poles were also installed in the main reactor vessel to reinforce thermal (using thermocouples to measure sodium temperatures) and mechanical (using accelerometers and sight optical systems to measure structural displacement) monitoring.

Superphénix plant

New ultrasonic probe technologies were developed to improve the reliability of inspections. These probes are made from composite material and focusing is guaranteed by the piezoelectric pellet. These probes have greater detection and measuring capacities due to their enhanced sensitivity and damping [9].

A computer-aided tool designed to analyse results was developed [10] as the characterisation and measuring of defects in certain configurations was hindered by profile variations and echoes from geometrical surfaces (ex.: misaligned welds, triple point welding). Modelling is therefore extremely useful when analysing results [11, 12]. The simulation software programme currently being developed must be able to

- Predict geometry-based echoes caused by weld profiles;
- Evaluate the influence of the local geometry upon the defect ultrasonic response;
- Take into account the anisotropic and heterogeneous structure of welds on ultrasonic signals.

Specific studies were dedicated to the development of new inspection techniques using the MIR device. One of these studies dealt with the inspection, from the inter-vessel, of an

internal shell in the Superphénix vessel (Fig. 7.17). This inspection was conducted to detect defects located at great distances from the triple point weld.

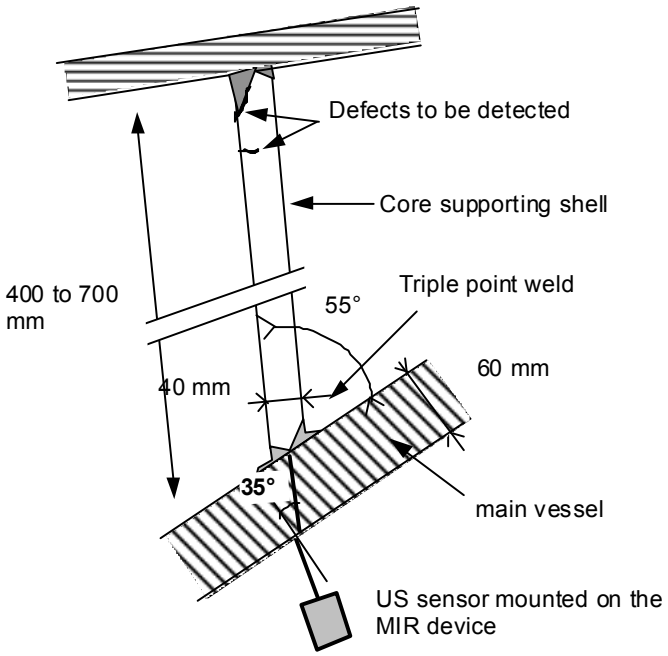

FIG. 7.17. Ultrasonic control of the Superphénix core supporting shell.

A method combining eddy current techniques and ultrasounds was considered to inspect the first few millimetres of the meridian welds of the triple point weld [13, 14] (Fig. 20). The use of phased array probes to inspect vessel welds prompted a long-term probe improvement program. It is possible to modify beam focusing parameters in relation to the geometry and thickness to be inspected when using phased array probes. The ability to optimize and adapt the probe to different inspection configurations improves defect characterization and measuring, while reducing geometry disturbances. A probe was designed and developed to inspect vessel edge-to-edge welds (Fig. 7.18). By adapting the time delay laws of each element, it is possible to obtain different configurations (angle of incidence of 45° or 70°, variable focusing depth) and rectify beam perturbations due to misaligned welds [15].

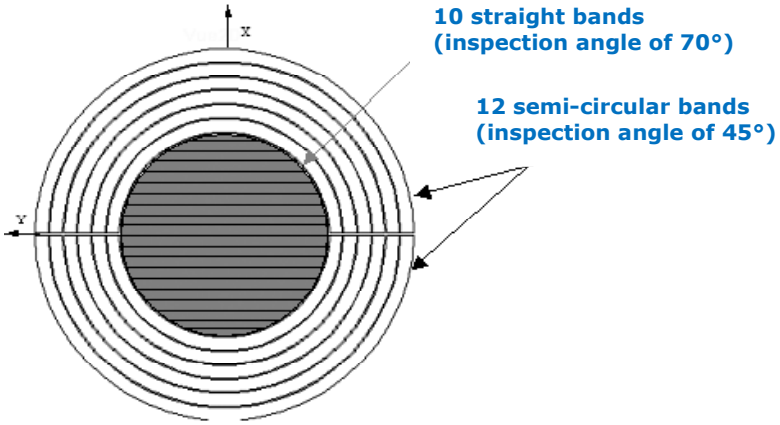

FIG. 7.18. Phased array probe used to inspect edge-to-edge welds in the main reactor vessel.

7.2.1.4. Safety issues

PFBR

The main vessel contains the bulk of primary sodium and serves as the boundary for primary sodium and argon cover gas (Fig. 7.19).

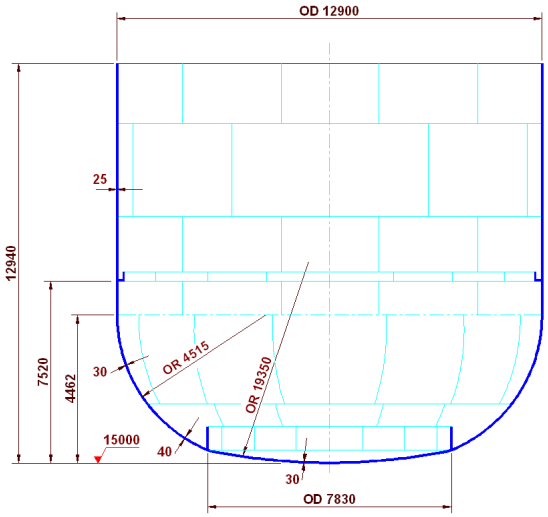

FIG. 7.19. Main vessel.

It supports the core support structure (CSS) along with the loads coming on it and also absorbs the energy released under "core disruptive accident" condition without breach of integrity. The core loads along with that of grid plate, inner vessel and core support structure are transferred to the dished end torus - sphere junction through CSS. The vessel is suspended from roof slab. No nozzle openings (penetrations) are provided on the main vessel to minimize the probability of sodium leaks.

Under SSE conditions, the vessel movement is limited such that safe shut down of the reactor is possible and the total reactivity addition in the core does not exceed 0.5 $ with integrity of the vessel maintained. In the unlikely event of leak from main vessel, a safe sodium level is maintained inside the vessel to ensure continued core cooling by the safety vessel, which is provided around main vessel.

The top support for the vessel ensures free thermal expansion in both radial and axial directions in regions away from the support location resulting in minimum thermal stress levels. The adequacy of thickness is also checked under CDA to limit the maximum plastic strain to less than about 4.65% in radial and 2.17% (averaged value) in axial directions and also to avoid buckling under external pressure with the axial temperature gradient in the vessel under SGDHR conditions. However, the condition of occurrence of external pressure on the vessel > 5 kPa does not arise due to the provision of a hydraulic relief pot, which relieves the pressure when it exceeds 5 kPa in the inter vessel space.

The main vessel is cooled by cold sodium to enhance the structural integrity by lowering the vessel temperature so as to minimise the formation of undesirable carbides and sigma phases in the austenitic stainless steel material and to maintain its temperature and temperature gradients (axial and circumferential) within acceptable limits (from creep and creep-fatigue aspects) during all operating conditions so that the dimensional limits for the main vessel are met over the design life. The main vessel cooling system consists of a system of two cylindrical shells called the 'thermal baffles' supported on the inside of the main vessel and a number of pipes equispaced all along the circumference to lead the coolant flow, from inside of core support structure, in to the annulus formed by the main vessel and the thermal baffles.

The leakage flow from the feet of the core subassemblies in the grid plate is used as coolant in the cooling system. The concentric annular spaces between the baffles are source of high external pressure loadings on the baffle shells, under seismic conditions, due to the mismatch between the frequency of out-of-phase movement/vibrations of the shells and the circumferential convective flow of the coolant within the annular gap. These complex loadings are analysed to demonstrate the adequate buckling resistance of the baffles, under external static pressure combined with the dynamic pressure created during seismic loadings.

Further, the stability of weir shell against fluid-elastic instability and creep-fatigue damage and ratcheting due to free level oscillations under steady operations, and free level variations under power variations and DHR operations are also taken into consideration for assuring the structural integrity of the free standing baffle shell structures. The safety vessel forms secondary containment for radioactive primary sodium and tertiary containment for fission product release from fuel and designed to contain the sodium that may leak from main vessel in the unlikely event and to ensure a safe sodium level in the main vessel. The main vessel is made of austenitic stainless steel SS 316 LN. The component design meets RCC-MR (edition 2002) requirements.

7.2.2. Sodium pumps

7.2.2.1. Functions and requirements

The purpose of a primary sodium pump is to circulate the sodium coolant from the cold pool (or leg) through the core, the IHX, and back into the cold pool. The purpose of a secondary sodium pump is to circulate the sodium coolant through the IHX and steam generator. Each pump must also provide low flow capability for decay heat removal and other low power standby conditions. Each pump must exhibit hydraulic and mechanical stability with no significant cavitation, and must be designed for service under the normal, standby, refueling, upset, emergency, and faulted conditions specified in the design documents. Pumps must be designed so that removal of the internals can be accomplished without cutting of primary or secondary sodium piping.

To minimize operational costs, the design objective of primary and secondary sodium pumps should be that minimal (if any) scheduled maintenance is required, and that the pumps should ideally last the full life of the plant

Nevertheless as removable components the minimum required lifetime is focused towards 10 to 15 years. Modification and repairs are feasible on pumps if they are drained and clean from residual sodium and sometimes decontaminated (in the case of primary pumps). Usually, the prevention of a large loss of availability factor of the reactor due to pumps maintenance or repair, spare components are available on the reactor site.

The sodium-wetted materials are selected from materials, such as 304 stainless or equivalent. Hard facing alloys are used in wear areas.

7.2.2.2. Primary and secondary sodium pump state of the art

7.2.2.2.1. Mechanical pumps

Based on the material presented below, the state-of-the-art of large mechanical pumps for application in primary and secondary sodium systems of the next generation fast reactors is a vertical, free surface, single suction, centrifugal pump with a lower radial hydrostatic bearing operating in sodium that is fed from the delivery side of the impeller. The pump shaft rotates in two bearings, the lower being a radial hydrostatic bearing and the upper usually a radial-axial roller bearing or a liquid or grease lubricated sliding bearing. The impeller is usually disposed below the hydrostatic bearing. There is an axial or radial guiding duct. A gas shaft seal is placed below the upper bearing, and a flexible coupling connects the shaft of the pump and its variable speed electric drive.

The design of sodium pumps must meet a complex set of specific requirements. First of all, the specified technical and economic characteristics have to be provided, the most important of which are delivery rate, dynamic head and efficiency. Meeting these requirements depends on the quality of the pump's hydraulic flow path including the impeller, guide duct or scroll, and the ducts for supplying sodium to the impeller and removing it. The pump design should provide for reliable performance, particularly for longevity and failure-free operation. The most important items of vane pumps responsible for meeting these requirements are the impeller (for cavitation-free operation) and the bearings. The bearings, in particular, must meet the following requirements:

- Minimal wear of working surfaces during the specified lifetime, taking into account of startups and shutdowns;
- Pump operation at any rotational frequency in the limits of the working range, to allow for reversing, and to consume minimum amounts of cooling, lubricating, or (for hydrostatic bearings) suspending liquids.

The chemical activity of sodium makes the requirement for sealing the pump inner cavities against ambient air very stringent. A mechanical face seal performs this function. The seal should eliminate the ingress of oil and oil vapors and cooling water into the sodium plenum. For safety reasons a gas blanket of inert gas (usually argon) under a pressure somewhat higher than atmospheric should be provided in the pump above the sodium surface.

Structural materials for a sodium pump should be chemically resistant to sodium, to decontaminating alkali-acid solutions and to steam-water or water spray washing media. The materials of the flow path should be also resistant to erosion by sodium at high velocity. As a rule these are stainless steels with various kinds of thermal or chemical-thermal treatment, with hard facing in places where enhanced hardness is required.

A vane pump can become a source of vibration because of unbalanced rotating masses, hydraulic forces, or misalignment of the pump and drive shafts. Therefore special design measures must be taken to ensure acceptable vibration levels. The pump drive has an important role. It should provide the capability to control the pump rotation frequency smoothly or stepwise over a wide range of rotation speeds from 10 to 100% of nominal value.

The design of a sodium pump is largely determined by its location within the reactor design. For example in the BN-600 reactor, where the primary coolant pumps are installed as integral parts of the primary circuit components in the reactor vessel, this dependence is manifest in the following way:

- The pump dimensions such as diameter, depth of submersion of the impeller and distance between the bearings are predetermined. For this reason the shaft dimensions, which were determined by mechanical design considerations, turned out to be such that the pump contribution to the total torque of the pump-coupling-electric motor assembly amounts to 30%. In contrast for the BN-600 secondary unrestricted conditions of the loop arrangement of the circuit this value is equal to 8%;
- The limited cover-gas pressure of the integral layout made the problem of cavitation free operation more complex, and enforced the use of a double-suction impeller which complicated the flow path considerably and made the pump heavier;
- The rigidity of the pump support (a shell 6.5 m in height on the reactor support belt) is less than that of a traditional ferroconcrete foundation, requiring additional restraint of the pump body in the region of the upper bearing;
- The location of the pump in the immediate vicinity of the reactor core causes non-uniform heating of the pump body along its height and radius, especially when cooling dependent on the pump delivery head becomes less effective. The resulting deformation of the pump body must be accounted for.

Placing the reactor coolant pump downstream of the heat exchanger (in the cold leg) is preferable for the following reasons:

(1) The pump circulates sodium at temperatures not higher than 400°C, which simplifies the choice of structural materials;

(2) Relatively low heat fluxes along the shaft and pump body do not influence the operation of the upper bearing and shaft seals in practice;
(3) The pump is better protected against thermal shocks and transients.

The majority of sodium pumps in current fast nuclear reactors are submersible with lower radial hydrostatic bearings operating in sodium that are fed from the delivery side of the impeller. With the introduction of hydrostatic bearings the structural scheme of sodium pumps coalesced more or less as follows: the pump shaft rotates in two bearings, the lower being a radial hydrostatic bearing and the upper usually a radial-axial roller bearing or a liquid or grease lubricated sliding bearing; the impeller is usually disposed below the hydrostatic bearing; there is an axial or radial guiding duct; a gas shaft seal is usually placed below the upper bearing; and a flexible coupling connects the shafts of the pump and its electric drive. For repairing the shaft seal without depressurizing the sodium circuit, a repair seal is sometimes provided below the main seal. In primary coolant pumps, a biological shield is needed and (if necessary) there is a check valve in the form of a shutter, float valve or obturator upstream or downstream of the guiding duct.

A scheme of thermal baffles was found to be necessary in FFTF, which had to be installed with the pump in the vertical position. The baffles were necessary to prevent shaft bending due to uneven heating caused by convection cells in the argon cover gas. These baffles consisted of three assemblies, installed in order from top to bottom. Each assembly was a segmented arrangement; the upper and lower assemblies consisted of four segments, the centre of six. The assemblies were installed sequentially from top to bottom, each segment of each unit being tack-welded in place first, until the complete assembly was fitted to the shield plug/support cylinder. The complete assembly was then welded and inspected before work was begun on the next assembly. After all three assemblies were installed, each baffle leaf was checked and adjusted as necessary.

Submersible pumps may be subdivided into deep- and shallow-submerged pumps. The axial dimension of a submersible pump is such that given any sodium level fluctuations (determined by the hydraulic resistance of the suction duct and thermal expansion of the circuit), a column of sodium sufficient to ensure cavitation-free operation remains above the impeller. This requires that the suction comes directly from the reactor tank (or expansion tank or pump tank) with no sealing devices between the tank and the pump assembly. For large capacity pumps, meeting these requirements might require very cumbersome fabrication.

For example the largest submersible sodium pumps for the Superphénix reactor weighed 120 tonnes, were 23 m in length, and 2.5 m in diameter. If, because of the reactor layout, it is impossible to ensure that the level in the pump tank follows the hydraulic resistance of the suction path, an artificial resistance has to be provided between the pump internals and the tank to retard or prevent the drop of sodium level. In emergency transients this helps to ensure the minimum allowable suction head at the impeller inlet and to prevent the entrainment of cover gas.

In the BN-600 primary pumps, which fall into the category of shallow-submerged pumps, the resistance is provided by an annular slot 1 mm wide between the pump internals and the reactor support, and four throttling orifices of 50 mm diameter. If the removable internals of a shallow-submerged pump are sealed completely from the tank, the risk of suction head loss is eliminated. The level rises due to leakage of sodium from the delivery side of the impeller

through the hydrostatic bearing, so a provision to return the leakage to the circuit is needed. This function is usually fulfilled by an overflow tube, which is connected to the suction portion of the flow path. Shallow-submerged pumps have better mass and size characteristics.

A pump with a small diameter will have less weight and cost less and will require less space. For the same reasons the length of the pump must be minimized. The need to reduce the dimensions of the pump leads to the demand to reduce the dimensions of the impeller. This can be achieved by increasing the speed of the pump. For a given suction pressure, the maximum speed is restricted by the cavitation phenomenon in the impeller. Until now, sodium pump designs have included excessive safety margins and restricted operating ranges. Thus the pump dimension depends on how accurately the designer can deduce the incipient cavitation limits of the impeller.

7.2.2.2.2. Primary pumps in the KALIMER concept

In the case of the Korean SFR design (KALIMER concept), two PHTS pumps circulate primary sodium through the reactor core. The pump is a centrifugal type mechanical pump installed in the annular area between reactor barrel and baffle. Each pump takes the primary coolant at the intake of the pump side and discharges the coolant to the core inlet plenum. The pumps are installed through penetrations in the fixed portion of the closure into an annular area above the core assembly shared with the intermediate heat exchangers. The primary sodium which is cooled by flowing through the IHX passes around the fixed core radial shield region in the lower plenum of the reactor vessel and then is drawn to the pumps via the inlet nozzles of the pumps and discharged to the inlet plenum through the discharge pipe. The design data for the pump are provided in Table 7.3.

TABLE 7.3. KALIMER PRIMARY PUMP DESIGN PARAMETERS

Item	Value
Pump type	Centrifugal type mechanical pump
Number of pumps/reactor	2
Flow rate (kg/sec)/pump	3866
Developed head, MPa	0.38
Sodium inlet temperature, °C	389.8
Electric Power (MWe)/pump	3.08
Efficiency, %	80
Length, m	15.35
Maximum diameter, m	2.15
Rotation speed, rpm	45-450
Available NPSH, m	11.02

The flow rate and head can be controlled by varying the rotating speed of the pump impeller. In order to change the rotating speed, two approaches are used. The first one is to change the frequency of the supplied power to the pumps. The other one is to reduce the rotating speed through the fluidic converter. For the case of refueling operations of very low flow rate, a pony motor is used to protect main motor of the pump.

The power to the primary pump is normally supplied from the normal power distribution system through a dedicated input transformer and solid state, variable frequency power-

conditioning unit. All PHTS pumps are equipped with flywheel for flow coastdown. Upon loss of the normal power supply, the stored kinetic energy in the flywheel of the pump is utilized to rotate the impeller for flow coastdown of the primary pump. The moment of inertia required for coastdown of flow rate about 50% during 5.5 seconds is around 7114 $kg \cdot m^2$.

7.2.2.2.3. Primary and secondary pumps in the PFBR concept

For the Indian design, the primary sodium pump is a mechanical, centrifugal, vertical type with a single stage top suction impeller having a free sodium level and running at a nominal speed of 590 rpm. The removable pump assembly is located inside a standpipe in inner vessel penetrating into the cold pool. The top flange of the pump is supported on the roof slab (cold) and the pump discharge nozzle plugs into the discharge pipe receptacle (hot) called the pump-pipe connection (PPC). A metallic seal ring is provided at the PPC to minimize radial clearance and to minimize vibration. The fixed intake skirt permits suction of cold sodium from the bottom of the cold pool. The single stage impeller about 1.48 m in diameter, delivers sodium into an axial diffuser and discharge casing from where it is led downward into the discharge nozzle. A long (around 11 m) shaft guided by a radial hydrostatic bearing at the bottom drives the impeller. The sodium flow to the hydrostatic bearing is supplied from the pump discharge through a strainer.

A Kingsbury tilted pad thrust bearing and a hydrodynamic bearing support the shaft at the top. The pump shaft in turn is coupled to the drive motor shaft by means of a flexible gear type spacer coupling. The drive motor is an AC induction motor driven by an AC variable speed drive capable of running the motor at any desired speed between 15 and 100% of the nominal pump speed. The rating of the motor is 3 600 kW. A flywheel with a flow halving time of 12 seconds is mounted on motor shaft. An eddy current flow meter is provided at pump discharge for flow measurement. The pump shaft is of composite construction with a hollow middle portion welded on either side to solid ends. A shaft based on critical speed alone is uniformly hollow

However, in order to reduce the diameter of the bearings, mechanical seals and also to provide shielding against radiation, shaft is made solid at the top. The shaft is made solid at the bottom from hydraulic considerations. The diameter at the various sections of the shaft is fixed based on torque and critical speed considerations.

The shaft sealing is achieved by means of a triple mechanical seal with oil as the buffer fluid. Two independent oil circuits are provided: one for the bottom mechanical seals and another for the top bearings and mechanical seal assembly. There are two oil catch pots in series, each with an oil deflector to direct any leaking oil to the respective catch pots. The entire hold up can be contained in the top catch pot itself.

One of the important areas in the mechanical design of the pumps concerns with the problem of accommodating the differential (both lateral and axial) thermal expansion between pump support 120°C and the discharge pipe 547°C max. This is achieved by providing a compliant upper support that permits the entire removable pump assembly except the shield plug to tilt up to a maximum of 0.4 degree from vertical. A spherical bearing assembly allows this pump inclination when any change in operating temperature of sodium (from 397°C) moves the pump bottom at PPC level laterally.

A pony motor is provided for each primary sodium pump and is used to maintain sodium circulation in the primary system, when the reactor is scrammed during off-site power failure.

The pony motor is used to run the pump at 15% of rated speed. Dedicated batteries are provided for pony motor to run the pump during a station black out for a maximum duration of 4 hours.

The PFBR has two primary sodium pumps (PSPs, Fig. 7.20) in the primary circuit for circulating the coolant sodium through the core and intermediate heat exchanger (IHX), thereby transferring the nuclear heat from reactor core to the secondary circuit. The sodium coolant circulated by the PSP extracts heat from the core and transfers it to the secondary sodium system via the IHX.

The secondary sodium system consists of two loops, with two IHX, one secondary sodium pump (SSP) (Fig. 7.21) and four SG per loop. The heat extracted by the secondary sodium coolant in the IHX is transferred to the steam water circuit through the SG.

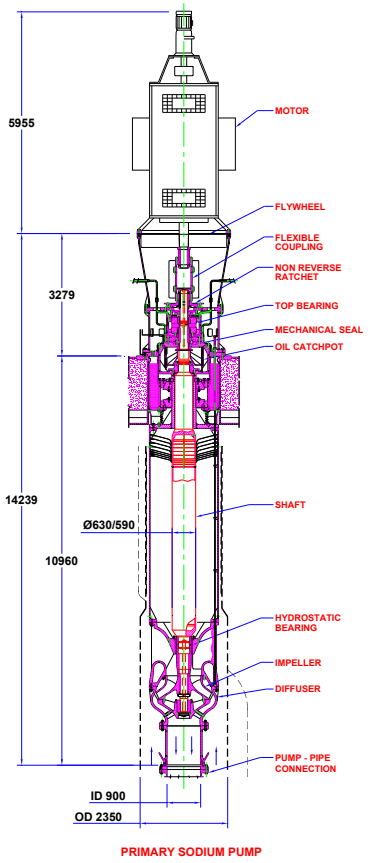

FIG. 7.20. PFBR primary sodium pump.

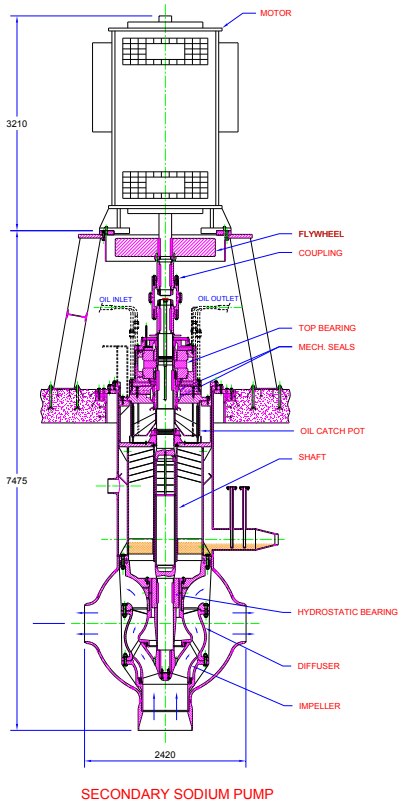

FIG. 7.21. PFBR secondary sodium pump.

The PFBR secondary pump design is a mechanical centrifugal, single stage, bottom suction, vertical shaft type and is housed in a fixed shell called pump tank having free sodium level. The space above the sodium is filled with an inert cover gas viz. argon. The pump cover gas is connected to the surge tank and storage tank cover gas. The pump is removable from the top. The pump is located in the cold leg of the circuit at lower elevation with respect to the SG.

Other design features of the pump like composite construction of shaft, radial hydrostatic bearing at the bottom, tilted pad thrusts bearing at the top and triple mechanical seals are similar to the case of the PSP. Since the SSP is in the loop, there is no need of differential thermal expansion as in the case of PSP and hence no tilting of the assembly. A flywheel with

a flow halving time of 4 seconds is mounted on motor shaft. The ratings of the pumps are shown in Table 7.4.

TABLE 7.4. PFBR PUMP RATINGS

Parameter	PSP	SSP
Flow rate, m^3/s	4.13	3.34
Head, m	75	65
Speed, rpm	590	900
NPSHA, m	16.02	30.12
NPSHR $_{3\%}$, m	10.6	16.9
NPSHR erosion, m	12	20
Motor rating, kW	3600	2700

7.2.2.2.4. Electromagnetic pumps

Based on the material presented below, the state-of-the-art of large electromagnetic (EM) pumps for application in primary and secondary sodium systems of the next generation fast reactors is the double stator, fully submerged, self cooled, annular linear induction pump.

Mechanical centrifugal-type pumps have been the choice for high flow capacity service in large prototype liquid metal fast breeder reactor power plant heat transport systems. The fact that their efficiency is approximately 50% greater than that of the EM pump has been viewed as an important positive consideration for larger plants designed to demonstrate commercial performance potential. However, it is evident that problems encountered in the exposure of mechanical pumps to the high temperatures and thermal transients of primary sodium heat transport systems become more severe as plant and pump sizes increase. In a 1979 EPRI study [16] evaluating the use of EM pumps in the primary and intermediate heat transport systems in large pool-type LMFBRs, it was shown that the impact of the lower efficiency of EM pumps on plant economic performance is moderate and judged acceptable in view of the potential benefits. The use of double-stator, self-cooled (fully submerged) electromagnetic pumps in both primary and intermediate heat transport systems in the EPRI reference plant was found to reduce the overall plant efficiency by only 0.4%, while it would further and considerably reduce the complexity of the pump. The double-stator design significantly increases the pumping efficiency by increasing the magnetic flux in the fluid gap of ALIPs, and is easily feasible for the large pumps required for primary and secondary system application.

EM pumps are less efficient than mechanical pumps; nevertheless, they are employed in much greater numbers in sodium cooled reactors, and they have a long history of extensive and successful use in these applications. The large majority of EM pumps are smaller than the main heat transport pumps and are applied in auxiliary, safety, and service systems. However, EBR-I, EBR-II, both SIR plants, and the SEFOR plant did use EM pumps in the main heat transport systems. EBR-I employed direct current electromagnetic pumps, and the original EBR-II concept incorporated direct current electromagnetic primary sodium pumps [17]. Tests were conducted to verify that operation submerged in sodium was feasible [18]. Their major drawback was the requirement for very high current at extremely low voltage. During this period (the early 1960s), an advance was made in mechanical pumps with the development of the hydrodynamic bearing, which was being used to pump fluids with poor

lubricating qualities. This type of bearing proved to be successful with sodium, and mechanical pumps were selected for use in the EBR-II primary sodium system.

More important than their efficiency is their impact on lifetime plant economics and power cost. Reliability issues of primary and secondary mechanical sodium pumps remain fundamentally a technological concern, while EM pumps have demonstrated high reliability and low maintenance; for example, the largest EM pump operated in the USA (the 24.6 m^3/min pump in the secondary circuit in EBR-II) ran successfully for thirty-five years with only one documented repair. Furthermore, the 1979 EPRI study found that EM pumps of the capacity needed for primary and secondary heat transport systems are smaller and lighter than equivalent mechanical pumps. Thus their first cost is potentially lower, further increasing their cost effectiveness over mechanical pumps. It was also concluded that these features can be utilized to minimize the size and complexity of the primary heat transport system.

EM pumps have many advantages over mechanical pumps: no rotating members, seals, or bearings, they are immune to failures in those parts; they require no free surfaces, bubblers, or overflow lines, and consequently have greater locational flexibility; and they generally require lower NPSH than mechanical pumps. Furthermore, an EM pump is mechanically passive and has unique operating and control characteristics; therefore, additional potential benefits in the areas of system operability, pump reliability, and pump maintenance requirements are foreseen. However, concern over the lower efficiency characteristics of EM pumps and uncertainty concerning mechanical design features have precluded their selection as the main system pumps in large reactor plant designs in the USA.

An EPRI-sponsored 1 000 MW(e) pool-concept LMFBR plant design study [19] revealed additional areas of concern related to mechanical primary pump installation support and sealing requirements unique to the pool configuration. Furthermore, the pump drive motors are large contributors to congestion of above-deck equipment that may aggravate major equipment maintenance problems in the head access area of a pool-type plant.

A 1984 study by Novatome and CEA researchers found that the use of EM pumps in an LMFBR intermediate sodium circuit would only marginally affect the plant efficiency. The drop in efficiency due to the electric power consumption of the EM pumps should be offset by the lower investment cost and the greater reliability of this type of pump. In view of the other advantages, such as locational flexibility, the study concluded that it appears reasonable to consider them for the IHTS.

Novatome/CEA preliminary studies on using an EM pump for the primary sodium pumping function in a pool-type LMFBR led to the definition of an IHX-EMP module in which a submerged pump, with no external cooling system, was coupled with the intermediate heat exchanger. After analyzing the various possible configurations and based on the preliminary dimensioning studies, the most promising approach appeared to be an EM pump in the cold sodium stream beneath the IHX partially withdrawn upward into the slab penetration and supplied with primary sodium by means of an argon hood. The study pointed out that the development of an IHX-EMP module first requires industrial implementation of coils for reliable high-temperature operation, which would not be expected for another decade (after 1984).

From the late 1980s to the mid 1990s, the ALMR program advanced the modular liquid metal reactor concept. In this proposed pool-concept plant, the EM pump was submerged in the primary system sodium that it pumps. The pump was self-cooled, i.e., heat generated in the pump stator would be conducted to the pumped fluid and would not require an externally

mounted auxiliary gas cooling system. Since these pumps were designed to operate without an active cooling system, relying instead on the pumped and surrounding sodium to remove internally generated heat, the electrical windings of these self-cooled annular linear induction pumps would reach temperatures near 538°C. Conventional high voltage coil winding insulation is limited to about 200°C. An insulation system for an EM pump was required that could operate continuously at 538°C for 40 years at 1000 volts AC, and be commercially available. These insulation systems are very sensitive to total insulation thickness, voltage gradient, and mechanical effects causing cracking. A program to develop and test this insulation system was carried out at Argonne National Laboratory between 1985 and 1992.

To bring this pump concept to reality, the Large Electromagnetic Pump (LEMP) program for application to the main circulation pumps was initiated in 1997. It was a multi-year program to design, build and test a fully submerged, self-cooled, 160 m^3/min annular linear induction pump for liquid sodium.

The Japan Atomic Power Company (JAPC), a consortium of Japanese utilities, funded the program as part of an overall program to develop an advanced, liquid metal cooled, nuclear reactor [20, 24].

But first, to prove the effectiveness of countermeasures against elevated temperature, a 1 m^3/min Na-immersed high temperature electromagnetic pump was tested, confirming the feasibility of a high temperature electromagnetic pump [21, 22]. Based on the 1 m^3/min pump result, a test of a 44 m^3/min Na-immersed high temperature electromagnetic pump, in which a full scale double stator design was adopted for the first time, was carried out [23]; about 10 000 hours of operation was acquired. Also the prospect of a manufacturing technology to scale up the electromagnetic pump capacity was confirmed. However, problems arose in that the pump efficiency was only about 20% at the rated conditions, which was lower than expected. Therefore the design of an improved heat-resistant structure was developed for the severe heat transient of a commercial scale reactor. The 44 m^3/min pump project was collaboration between JAPC and DOE.

Based on these results, in 1998–2000, the large capacity Na-immersed high temperature pump was designed and manufactured. Final assembly and testing of the pump in 2000–2001 was conducted at the Boeing Santa Susanna Test Facility, formerly known as the Energy Technology and Engineering Center (ETEC), located in the mountains north of Los Angeles, California.

The 160 m^3/min pump used high temperature electrical insulation and was designed to operate immersed in liquid sodium and be self-cooled by the sodium. Hence winding temperatures exceeding 450ºC were expected. Almost all the internal electrical losses are transferred to the surrounding sodium, which can be recovered as electricity by turbine generators. The test pump, the largest of its type known to have been built and tested, was a "proof-of-principle" design rather than being prototypic of a particular pump application. The double-stator design and output characteristics of the test pump were, however, very representative of pumps that have been proposed by the program participants for use in primary or secondary cooling loops of advanced sodium-cooled fast reactors in the United States and Japan, respectively.

The primary participants in the LEMP program, in addition to JAPC, were Toshiba, General Electric (GE), Kawasaki Heavy Industries (KHI) and Boeing. Toshiba and GE shared design and fabrication responsibilities for the test pump components and preparation of the test specifications (with JAPC and Boeing input). KHI provided program management and

assisted with data acquisition and reduction. A variable frequency, variable voltage, power converter was supplied by ALSTOM under contract to GE.

The following results were obtained from the testing [20]:

- Pump efficiency that exceeded 40% at the rating 160 m^3/min, 0.28 MPa was confirmed. This implies that this efficiency could be achieved for the station load equivalent to that of the mechanical pump, considering the energy recovery in the plant.
- Stable flow characteristics and the good controllability of the flow with the constant V/f ratio operation were shown in the area on the right-hand side of Q–H characteristics peak.
- Stator temperature fully satisfied the designed maximum working temperature of 600°C of the coil insulation. The stator support mechanism showed the behaviour expected for the design. Based on these results, the design and manufacturing technology of a large capacity electromagnetic pump were verified and also sufficient heat resistance for application to a plant was confirmed.
- As a result of the post-test inspection after the Na test for over 2550 hours, it was confirmed that there was no problem that exerted an influence on the function and performance of the pump. Based on this result, the applicability of a large capacity, double-stator, fully immersed, self-cooled electromagnetic pump to a plant was fully confirmed.

7.2.3. Intermediate heat exchanger

The Korean KALIMER concept and Indian PFBR are used to point to the important features of intermediate heat exchangers (IHXs).

7.2.3.1. KALIMER design features

The KALIMER reactor adopts four cylindrically shaped IHXs in the primary heat transfer system (PHTS) along with two primary pumps. The IHX is sized such that the PHTS can transfer the core heat to the IHTS for all operation modes when all the primary coolant pumps are in operation. The IHX is a counter current flow shell and tube type unit with a vertical orientation in the reactor vessel.

The design arrangement provides for downflow of the hot (primary) sodium and upflow of the cold (intermediate) sodium to enhance natural circulation for reactor decay heat removal. The IHXs are located above the reactor core assembly in the annular region between the reactor support barrel and the reactor baffle.

Each IHX is rated at 380.9 MWt for a total rating of 1523.4 MWt. The IHX is designed to operate in the vertical position within the primary sodium pool. It is supported by, and hung from the reactor closure head.

Primary sodium from the hot pool enters the shell side of IHX through the inlet nozzle that is located at an elevation just below the upper tube-sheet and flows downward. The primary sodium flows around and through the tube support plates into a plenum below the lower channel head where the primary sodium exits into the cold pool. Normal sodium level difference between the hot and cold pools is set at about 5 m in considering the prevention of the cover gas entrainment and the heat loss through the PDRC.

The upper tube-sheet is fixed and supported from the riser cylinder, intermediate sodium upper channel, and outer shell. The lower tube-sheet is floating and supported by the tubes to relax the thermal load between the IHX tube bundle and shell structure.

The safety objectives of the IHX are to isolate the radioactive primary sodium from the intermediate sodium and to provide a mechanical barrier to the transport of radioactive sodium out of the containment boundary. The mechanical integrity of the IHX tubes at a sodium-water reaction event is protected by the Steam Water Reaction Protection and Relief System (SWRPRS).

As shown in Fig. 7.22, the IHX consists of an upper and lower tube-sheet separated by straight tubes with a central downcomer for incoming intermediate sodium. The IHX cross section is a circular shape and the number of the IHXs was selected to minimize the radial space between the support barrel and reactor baffle.

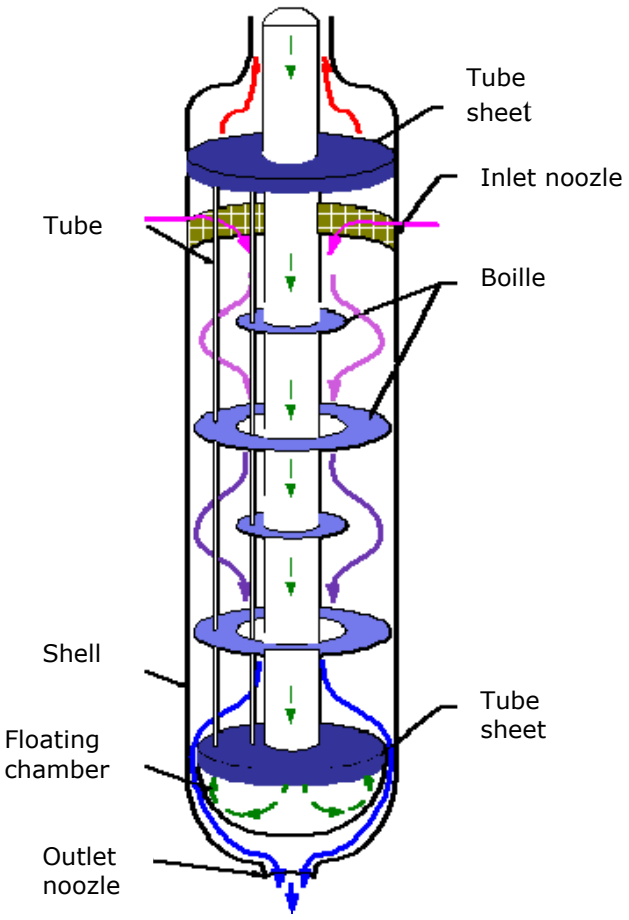

FIG. 7.22. KALIMER IHX schematic.

Table 7.5 shows the performance specification for an earlier design where the core exit temperature was 545.0°C.

TABLE 7.5. DESIGN SPECIFICATIONS FOR EARLY MODEL KALIMER IHX

Parameter	Value
Tube	
Number of tubes	4188
O.D., mm	15.9
I.D., mm	13.5
Thickness, mm	1.2
Length, m	6.0
Material	9Cr-1Mo
Bundle	
Pitch arrangement	Triangular
Pitch/tube O.D.	1.73
Flow hole diameter, mm	12.6
Number of holes	8376
Shell	
I.D., m	2.03
Length, m	7.81
Shape	TEMA type S

As is shown in Table 7.6, the tube bundle for each IHX contains 4188 straight tubes of 15.9 mm OD×1.2 mm wall thickness.

TABLE 7.6. PERFORMANCE SPECIFICATIONS FOR EARLY MODEL KALIMER IHX

Parameter	Value
Overall	
Number of IHXs	4
Thermal duty/IHX, MWt	380.9
LMTD, °C	32.54
UA total, MW/°C	11.98
DT, hot side, °C	13.11
DT, cold side, °C	65.23
Primary sodium (shell) side	
Flow rate, kg/s	1932.8
Inlet temperature, °C	544.8
Outlet temperature, °C	385.9
Pressure drop, kPa	25.73
Intermediate sodium (tube) side	
Flow rate/IHX, kg/s	1450.2
Inlet temperature, °C	320.7
Outlet temperature, °C	531.6
Pressure drop, kPa	40.59

The tubes are arranged on 27.5 mm triangular pitches. The tubes will be end-welded to the tube-sheet and then explosively expanded into the tube-sheet holes. The tube side, which is the high-pressure intermediate sodium side, of the IHX is designed for 2.5 MPa for normal operation. This design pressure is sufficient to withstand the pressure resulting from sodium-water reactions caused by low probability multiple tube failures of the steam generator or failures of the sodium-water reaction protection system. The shell side and the tube itself of the IHX are classified as a safety grade since the IHX tube provides the pressure boundary separation of equipment.

The support and the seals for the IHX are located at the separation plate and in the reactor closure head. The vertical support of the IHX occurs at the reactor closure head via pipes for IHTS sodium. The lateral support is provided at the baffle plate and the separation plate which acts as the vertical support for the reactor baffle.

Three design codes, CONFIG, ASTEEPL, 2DHX, are used for the design of the IHX. The CONFIG codes generate the number of tubes and the tube arrangement for a given geometry condition. The ASTEEPL code calculates the pressure drop in the primary (shell) and secondary (tube) sides of the IHX using the stream analysis method. The 2DHX code calculates the heat transfer in the axial and radial directions for both tube and shell sides of the IHX.

7.2.3.2. PFBR IHX design

The PFBR has two secondary sodium loops and a total of four intermediate heat exchangers (IHX), two for each secondary sodium loop. The IHX (Fig. 7.23) is a vertical counter-current flow, shell and tube heat exchanger with primary sodium flowing downwards on the shell side and secondary sodium flowing upwards on the tube side.

Each IHX is rated for 314.7 MW(t) and consists of a tube bundle having 3600 straight tubes of 19 mm OD and 0.8 mm thickness. Each tube is around 8050 mm in length and is made of austenitic stainless steel, rolled and welded to the tube sheets at both the ends. The tubes are arranged in circular pitch around an inner shell of size 579 mm OD and 16 mm thickness. This inner shell is welded to the tube sheets at both the ends.

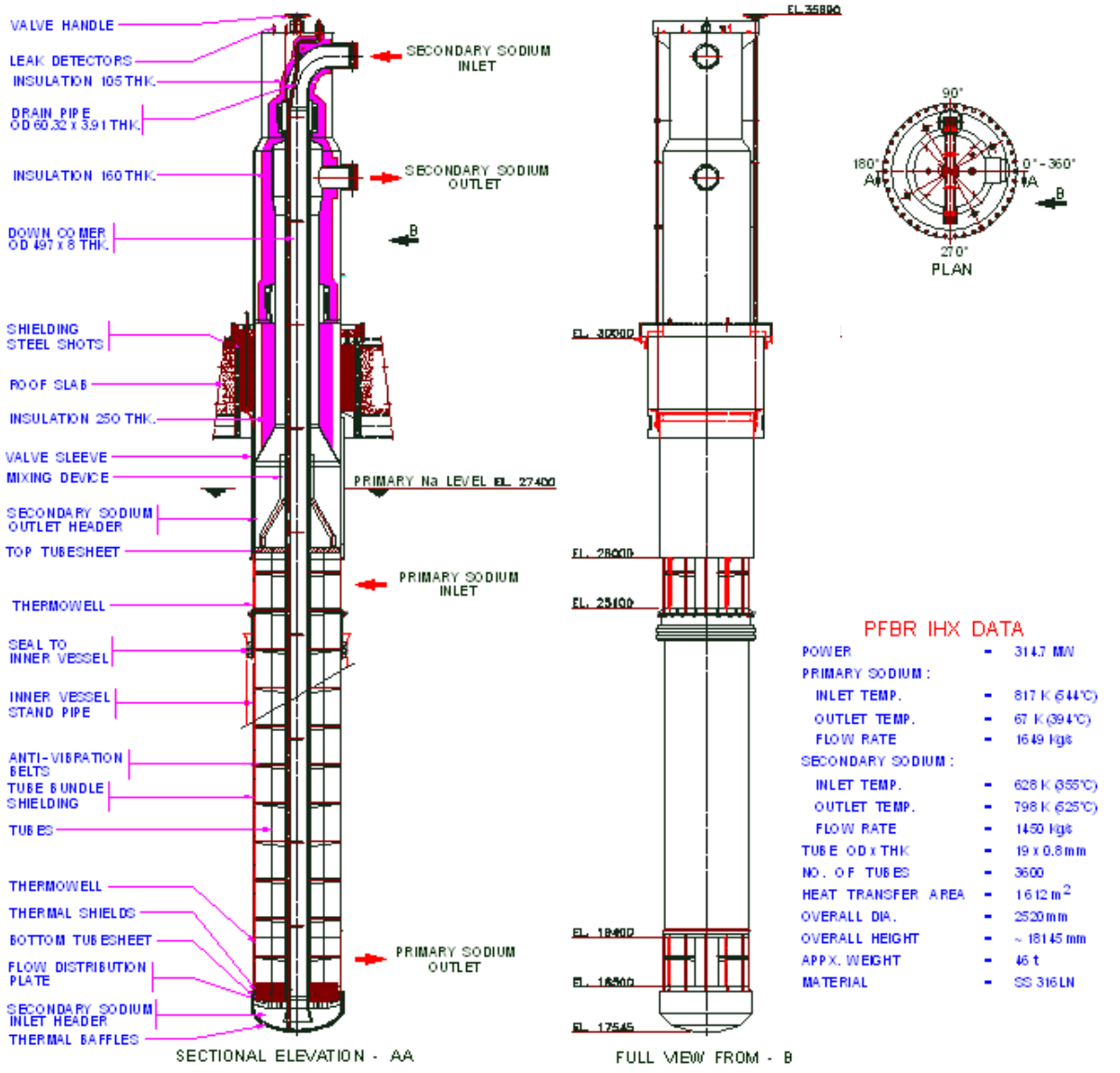

FIG. 7.23. PFBR IHX design.

The secondary sodium inlet pipe of size 497 mm OD×8 mm thickness passes inside this inner shell and is welded only to the bottom tubesheet. The annulus between these two is kept under argon atmosphere. There is a vertical outer shell around the tube bundle and inlet and outlet windows for primary sodium flow provided in this shell. Secondary sodium enters the IHX at the top, flows down to the bottom dished end (secondary inlet header), flows upwards through the tubes of the tube bundle, and is discharged at the outlet to the secondary outlet header.

The salient features consist of flow distribution plate at the bottom tubesheet and flow mixing device at the outlet of the secondary sodium to ensure uniform sodium temperature of the secondary sodium emerging from the separate tubes and further mixing to ensure minimum thermal stress due to temperature variation. Tubes are held at regular intervals by anti-vibration belts to minimize flow induced vibrations. There is provision to drain complete secondary sodium from the IHX by providing a pipe for the same up to the lowest elevation possible in the secondary side of the IHX.

At the roof slab penetrations, steel shots are filled to form biological shielding. The steel shots can be removed from the IHX. Thermal insulation is filled between secondary sodium inlet-outlet pipe/shell and the support/casing shells. A manually operated sleeve valve is provided to close the primary side inlet window to permit operation of the reactor with one secondary loop if required. At the penetration of the IHX in the inner vessel, a mechanical seal is provided to avoid bypass of primary sodium from hot pool to cold pool

7.2.4. Steam generator (SG) including leaks and safety issues

7.2.4.1. Functions and requirements

The function of the steam generator is the transfer of thermal energy between the intermediate sodium circuit and the steam turbine system. The steam generators must be designed for performance, reliability, protection in case of sodium-water reaction, inspection accessibility, and economical competitiveness.Reliability is important from the viewpoint of plant operational performance. Steam generator failures lead to plant shutdowns since they serve as the conduit to the final heat sink of the reactor during power operations. Tube-failure detection and pressure relief systems are required since a steam generator tube-failure can lead to sodium-water reactions and additional tube failures. Inspection of heat exchanger tubes and tube-to-tube sheet welds during normal plant shutdown is highly desirable as a means of reducing or eliminating unplanned plant shutdowns due to steam generator failures.

7.2.4.2. Historical experience

Several different designs for liquid-metal heated steam generators have been developed over the years. A summary of those developed in the US is provided in Table 7.7, while international developments are summarized in Table 7.8. These steam generators can generally be categorized by the tube type and flow mode, as detailed in Table 7.9.

TABLE 7.7. USA STEAM GENERATOR DEVELOPMENT

NAME	CAPACITY (MW)	TYPE	TUBE	OPERATION	FABRICATOR
EBR-I	1	EV+SH+RH	TUBE TO TUBE	1951	BECHTEL
APDA-U-TUBE	1	ONCE THROUGH	U TUBE	<1957	GRISCOM-RUSSELL
APDA-BAYONET	0.5	ONCE THROUGH	BAYONET	1958	GRISCOM-RUSSELL
LAMPRE PROTOTYPE	2	EV+SH	STRAIGHT	1960	LANL
SRE(SG #2)	30	ONCE THROUGH	U TUBE	1957	B&W
SRE (SG #1)	18	EV(NC)+SH(NC)	PANCAKE DOUBLE	1957	UNKNOWN
EBR-II	15.6	2EV+SH(NC)	STRAIGHT DOUBLE	1961	ANL
HNPF	84	EV+SH	BAYONET DOUBLE	1962	GRISCOM-RUSSELL
HNPF PROTOTYPE	3	EV+SH	BAYONET DOUBLE	<1960	GRISCOM-RUSSELL
FERMI	143	ONCE THROUGH	SERPENTINE	1962	GRISCOM-RUSSELL
CRBR	325	2EV+SH	HOCKEY STICK	-	-
CRBR FULL SCALE	70	EV	HOCKEY STICK	1982	WH,AI
CRBR FTTM	2	EV+SH	HOCKEY STICK	1977	AI
ANL SINGLE TUBE	1	SINGLE TUBE	STRAIGHT	1976	ANL
GE SINGLE TUBE	1	SINGLE TUBE	STRAIGHT	1976	GE
AI-MSG-30MW	30	ONCE THROUGH	HOCKEY STICK	1970	AI
ALCO/BLH SG	30	ONCE THROUGH	STRAIGHT+SINE	1966	ALCO/BLH
TST-1,2	1	ONCE THROUGH	STRAIGHT	<1970	WH
HTM-1	1	ONCE THROUGH	SERPENTINE	1970	WH
DWTSG-FTM		ONCE THROUGH	STRAIGHT DOUBLE	1980	WH
B&W HELICAL	70	ONCE THROUGH	HELICAL COIL	1987	B&W
DWTSG	70	ONCE THROUGH	STRAIGHT DOUBLE	1991	WH

TABLE 7.8. INTERNATIONAL STEAM GENERATOR DEVELOPMENT

COUNTRY	NAME	CAPACITY	TYPE	TUBE	OPERATION	FABRICATOR
UK	DFR		EV+SH	TUBE TO TUBE	1957	UNKNOWN
	PFR	210	EV+SH+RH	U TUBE	1974	B&W
FRANCE	PHENIX	16	EV+SH+RH	HAIRPIN	1973	STEIN
	PHENIX PROTOTYPE	16X3	3EV+3SH+3RH	HAIRPIN	1970	STEIN
	PHENIX PROTOTYPE	15	EV+SH+RH	HAIRPIN	1967	STEIN
	PHENIX PROTOTYPE	5	ONCE THROUGH	HAIRPIN DOUBLE	1964	STEIN
	SPX	750	ONCE THROUGH	HELICAL COIL	1985	NOVATOM
	GVE-1 (HELICAL COIL)	45	ONCE THROUGH	HELICAL COIL	1973	BABCOCK ATLANTIQUE
	STRAIGHT-TUBE	45	EV+SH	STRAIGHT	1973	STEIN
	PGV-1	45	EV+SH	STRAIGHT	1979	NIRA
	HELICAL COIL	6	ONCE THROUGH	HELICAL COIL	UNKNOWN	BABCOCK ATLANTIQUE
	CEA STRAIGHT TUBE	0.45	SINGLE TUBE	STRAIGHT	UNKNOWN	UNKNOWN
	SDP-1	1	SINGLE TUBE	HELICAL COIL	1970'S	NIRA
	SDP-2	1	SINGLE TUBE	STRAIGHT	1970'S	NIRA
GERMANY	KNK-II	29	ONCE THROUGH	HAIRPIN (TUBE IN)	1977	DURR-WERKE
	KNK-PROTOTYPE	5	ONCE THROUGH	HAIRPIN (TUBE IN)	1960'S	DURR-WERKE
	KNK-PROTOTYPE	5	ONCE THROUGH	HELICAL COIL	1960'S	VKW
	INTERATOM-BAYONET	2.27	EV+SH	BAYONET TRIPLE	1971	INTERATOM
	SNR-300 (STRAIGHT)	85.5	EV+SH	STRAIGHT	-	NERATOM
	SNR-300 (HELICAL)	85.6	EV+SH	HELICAL COIL	-	NERATOM
	HENGELO STRAIGHT	50	EV+SH+RH	STRAIGHT	1971	NERATOM
	HENGELO HELICAL	50	EV+SH	HELICAL COIL	1974	NERATOM
	SINGLE HELICAL TUBE		SINGLE TUBE	HELICAL COIL	<1978	NERATOM
	10-TUBE (FOR SNR-2)	5	EV+SH	STRAIGHT	<1984	UNKNOWN
JAPAN	MONJU	238	EV+SH	HELICAL COIL	1995	MHI, HITACHI
	MONJU PROTOTYPE #2	50	EV+SH	HELICAL COIL	1975	MHI
	MONJU PROTOTYPE #1	50	EV+SH	HELICAL COIL	1974	HITACHI
	ITR (INSTABILITY TEST RIG)	1	ONCE THROUGH	HELICAL COIL	1976	TOSHIBA
	PNC-1 MW#1, #2	1	ONCE THROUGH	HELICAL COIL	1971	HITACHI,MHI
	DWTSG-1MW	1	ONCE THROUGH	STRAIGHT DOUBLE	1991	HITACHI
	DWTSG-FTTM	1.7	ONCE THROUGH	STRAIGHT DOUBLE	1991	TOSHIBA/IHI

TABLE 7.9. STEAM GENERATOR CATEGORIES

Type	Circulation mode	Tube Categorization	Subcategory	Stages	Experience
tube-in-tube	forced	straight	triple wall	EV+SH+EC	EBR-I
		hairpin		once through	KNK, KNK prototype
tube-to-tube	forced	hairpin		EV+SH	DFR
shell-and-tube	natural	straight	double-wall	EV+SH	EBR-II
		pancake coil	double-wall	EV+SH	SRE #1 SG
		bayonet	double-wall	EV+SH	HNPF prototype, HNPF
	forced (horizontal)	straight		EV+SH	LAMPRE prototype
		U-tube		once through	APDA U-tube, SRE #2 SG
		bayonet	double-wall	once through	KNK prototype
	forced (vertical)	straight	single-wall	EV+SH	SPX prototype 45MW, PGV-1, SNR-300
				EV+SH+RH	SNR-300 prototype
			double-wall	once through	DWTSG-FTM, DWTSG-70 MW (US) DWTSG-1MW, DWTSG-FTTM (Japan)
			Hockey stick	EV+SH	CRBR, CRBR mockup, CRBR FTTM, AI-MSG
			sine wave	once through	ALCO/NLH SG
		U-tube		EV+SH	PFR
		hairpin		EV+SH+RH	Phenix, Phenix prototype
		bayonet	single-wall	once through	APDA bayonet, BN-350
		helical coil		once through	B&W helical 70 MW, SPX, SPX prototype
				EV+SH	SNR-300, SNR-300 prototype, Monju, Monju prototype
		serpentine		once through	Fermi, HTM-1

Early designs selected tube-in-tube (EBR-I, KNK) or tube-to-tube (DFR) layouts. For the tube-in-tube types, each steam tube was located within an outer tube that contained the liquid metal. In the DFR tube-to-tube type steam generators, both the sodium and steam tubes were installed within copper blocks; heat transfer between the tubes occurred by conduction through the copper. The advantage of this type of heat exchanger is that it is robust, thereby minimizing the chances of sodium-water reactions. The units are also easy to repair. The primary disadvantage is high construction cost due to the complex structure and large size that is mandated by the low thermal efficiency that can be achieved with this design. In terms of the traditional shell and tube heat exchanger approach, there were two early variants: i) horizontal tube configuration, and ii) natural circulation units. The horizontal steam generators experienced thermal stratification (steady temperature gradient) on the shell side containing the sodium, and also flow instabilities that developed during low power operations. EBR-II and Hallam Nuclear Power Plant (HNPF) adopted natural circulation systems since this approach was desirable from the viewpoints of system design simplicity and economic competitiveness. However, natural circulation steam generator systems generally operate at relatively low steam pressure that requires large heat transfer surface area per unit thermal power [1–5].Most recent liquid metal heated steam generators are forced circulation vertical shell-and-tube designs are shown in Fig. 7.24.

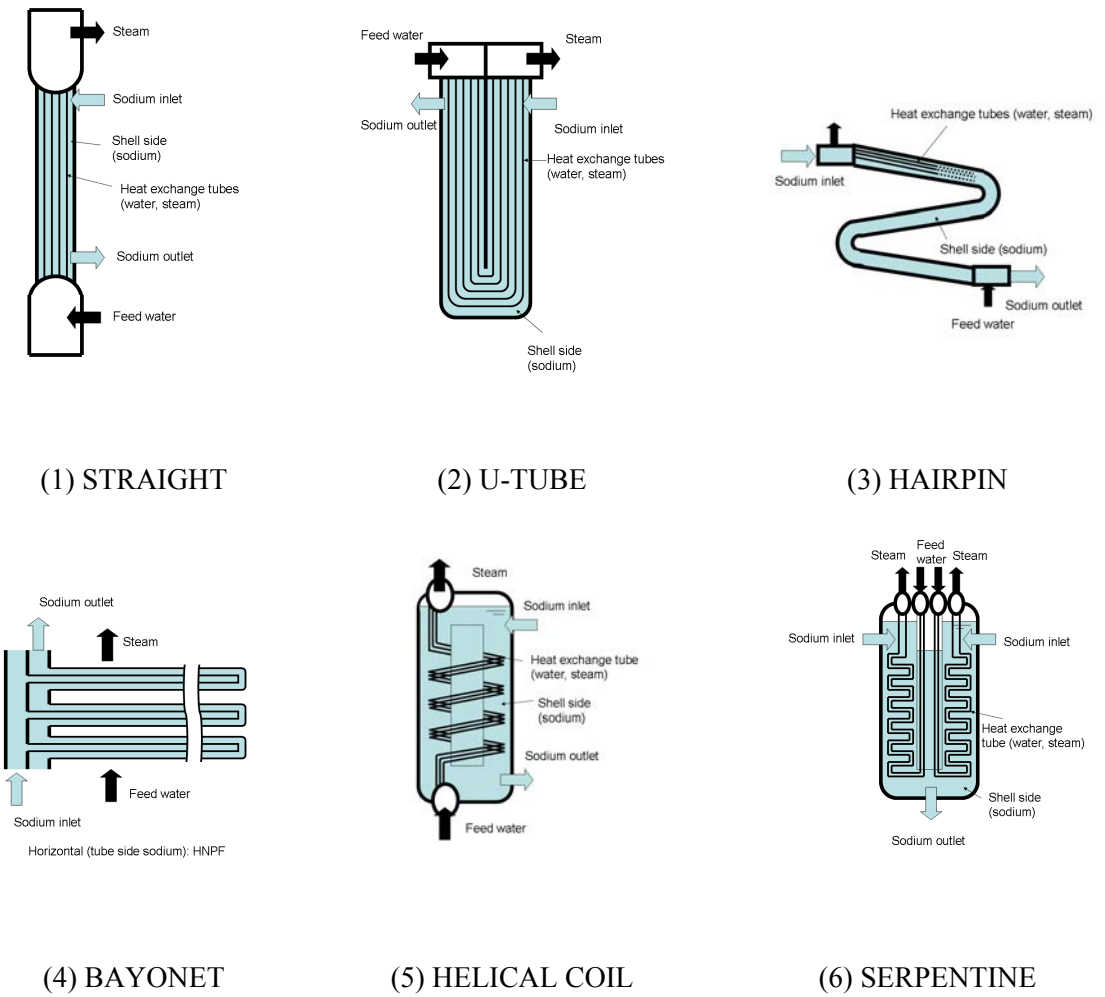

FIG. 7.24. Steam generator concepts.

There are a variety of tube types; i.e. straight, U-tube, hairpin, bayonet, helical coil and serpentine. In these designs, the liquid metal generally exists on the shell side since water/steam corrosion problems develop at crevices on the shell side, as has been observed in almost all PWR steam generators. Differences between PWR and liquid metal steam generators are discussed later in this review. From the viewpoint of tubing material, some early steam generators adopted austenitic stainless steel, because ferritic steels had not accumulated enough experience under sodium at that time. Early experiences indicated that austenitic stainless steel suffered from high thermal stress and chloride stress corrosion cracking. On this basis, ferritic steels were substituted for austenitic stainless steels in subsequent steam generator designs. Major national R&D programs have been carried out in order to develop reliable steam generators for liquid metal fast reactor applications. Thus, these developmental efforts are summarized on a national basis.

7.2.4.2.1. United States of America

Timelines showing the history of steam generator development in the USA for liquid metal reactors are provided in Tables 7.10 and 7.11. Chronologically, these developments can be divided into four major phases:

(1) Early development for the Submarine Intermediate Reactor (SIR) and experimental reactors;

(2) Development for early prototype reactors (Fermi and HNPF);

(3) Development for the Clinch River Breeder Reactor (CRBR); and

(4) Developments after CRBR.

TABLE 7.10. EARLY CHRONOLOGICAL DEVELOPMENT AND TESTING OF STEAM GENERATORS IN THE U.S.

Reactor	SG	49	50	51	52	53	54	55	56	57	58	59	60	61	62	63	64	65	66	67	68	69	70
EBR-I 1.2 MWt/0.2 MWe U-Zr, loop (NaK)	EBR-I tube to tube ANL	construction		critical (ANL)													shutdown						
								meltdown caused by fuel bowing															
Fermi 200 MWt/61 MWe U-Mo, loop	APDA U-tube, horizontal B&W								operation (APDA) 18months										1972 final shutdown 1974 APDA phase out				
										no difficulty other than slight stratification									1975 Fermi decommissioned 1975 PRDC dissolved				
	APDA-bayonet-0.5MW bayonet, vertical Alco										operation (APDA) 5months												
											performance < predicted												
	Fermi serpentine 67MW G-R				design (APDA)				construction (UEC)										repair				
															critical (PRDC)				core melt (local blockage)				
															SG tube failure (SCC, vibration)								
SRE 30 MWt/8.5 MWe, U graphite moderator, loop	SRE #1:pancake, #2:U-tube B&W							construction (AI)															
										power generation (AI)							shutdown						
											partial meltdown by loss of flow accident												
HNPF 256 MWt U-Mo graphite-moderator loop	Hallam prototype bayonet																		1967 NAA merged with Rockwell (AI was one of divisions of NAA)				
	HNPF bayonet, double wall, horizontal G-R										construction (AI)												
															operation				canceled				
																graphite moderator can leak							
LAMPRE 2 MWt molten-plutonium	LAMPRE straight, horizontal LANL												operation (LANL) 9500h										
														cracks found at sodium mixing after decommission									
EBR-II 62.5 MWt/20 MWe U-Pu-Zr	EBR-II straight, double wall ANL										construction (ANL)						repair						
														operation		critical							
																primary pump bind							

TABLE 7.11. LATER CHRONOLOGICAL DEVELOPMENT AND TESTING OF STEAM GENERATORS IN THE USA

Reactor	SG	63	64	65	66	67	68	69	70	71	72	73	74	75	76	77	78	79	80	81	82	83	84	85	86	87	88	89	90	91	92	93	94
CRBR 975MWt 350MWe MOX, loop	Alco/BLH 30MW sine wave	construction				SCTI upgrade																											
					operation (ETEC) terminated																													
					operation (AI) sodium-water reaction																													
	AI-MSG 30MW hockey stick (AI)					design and construction (AI)																											
									operation (ETEC)																									
												4000h steaming																					
	TST-1&2 straight (WH)							TST-1,2 (WH)																									
	HTM-1 1MW serpentine (WH)							construction (WH)																									
									operation (WH)																									
	GE single tube straight (GE)													construction (GE)																			
															operation (GE)																		
	ANL single tube straight (ANL)													construction (ANL)																			
															operation (ANL)																		
	FTTM hockey stick (AI)													design and construction (AI)																			
															operation (GE) 1900h																		
																	bypass flow caused by tube bowing																
	full scale EV hockey stick (AI,WH)																		design and construction (AI,WH)														
																					operation	at 60 % (ETEC)											
																							AI merged with Rocketdyne										
	CRBR 207 MW hockey stick DWTSG-FTM straight double (WH)																				construction												
																							canceled										
																		operation (WH)															
ALMR	helical-70MW helical (B&W)																									operation (ETEC) 4200h steaming							
	DWTSG straight double (WH)																													operation			
																														(ETEC)			
	-																						1996 Rockwell sold Rocketdyne to Boeing										
																							1998 DOE contract for ETEC expired										
																							2005 Boeing sold Rocketdyne to Pratt & Whitney										

Early development for SIR and experimental reactors

A major feature of steam generators for SIR and experimental reactors is that economical considerations are of secondary importance relative to the requirement of high reliability. As a result, the steam generator designs for these systems often deviate from those of prototype fast reactors intended for commercial power generation. For example, Experimental Breeder Reactor I (EBR-I) adopted a tube-in-tube type and Experimental Breeder Reactor II (EBR-II) adopted a natural circulation double-walled shell-and-tube type.

EBR-II was developed by Argonne National Laboratory and started construction in 1958 in Idaho. First criticality was achieved in 1961 and service with sodium started in 1963. This plant was a 62.5 MW(t) thermal (20 MW(e)) sodium cooled pool type reactor. The design incorporated one main cooling loop with eight 5.7 MW(t) evaporators and two 7.4 MW superheaters with double wall straight tubes fabricated of 2-1/4Cr steel. Two types of bonding techniques were utilized during the assembly of the double tubes: metallurgical (four evaporators and one superheater) and mechanical (four evaporators and one superheater). A water leak was found in the air space between the water and sodium tubesheets of one of the evaporators. This leak was caused by a defect at the tube-to-tubesheet weld. After repair, the steam generators were operated successfully. From 1974 to 1980, the superheater with mechanical bonded tubes experienced gradual degradation in performance caused by decreased contact pressure between the inner and outer tubes [25]. This superheater was replaced with one of the evaporators in 1981, leaving seven evaporators and two superheaters for subsequent operations. The EBR-II steam generators experienced no other difficulty and accumulated over 100,000 hours of operation under steaming conditions [26]. Although the EBR-II natural convection steam generator design was not typical of that used in commercial reactors, the long term operational experience showed excellent material compatibility of the 2-1/4Cr steel tubes [20-27].

Development for early prototype reactors (Fermi and HNPF)

In the USA, there were two prototype liquid metal cooled reactors constructed and operated in the 1960's. One was the Enrico Fermi Atomic Power Plant (Fermi) and the other was the Hallam Nuclear Power Plant (HNPF). The Fermi reactor was designed and developed by Atomic Power Development Associates (APDA) for Power Reactor Development Company (PRDC). APDA was incorporated for Fermi reactor development in 1952. The major members were the Detroit Edison Company (DEC), the Dow Chemical Company and Babcock & Wilcox Company (B&W). APDA tested two prototype steam generators for the Fermi reactor in their 1 MW NaK facility. One unit was a U-tube type proposed by B&W and the other was a bayonet type proposed by Alco Products. The main purpose of these tests was to develop an economical once through steam generator with single-wall tubes. The APDA U-tube steam generator was constructed from 304 stainless steel, and extreme care was taken to maintain water quality to prevent chloride stress corrosion cracking. The APDA U-tube design performed well except for slight thermal stratification. The APDA bayonet design also exhibited acceptable performance, although the actual thermal output was somewhat less than predicted.

A serpentine steam generator design fabricated from 2-1/4Cr steel was selected for Fermi, and three 67 MW units were fabricated by the Griscom-Russell Company (G-R). Before service with sodium, a water pressure test with the #2 unit revealed many tube leaks at the bends caused by stress corrosion cracking (SCC). The SCC was attributed to residual cleaning solution and all of the tubes were subsequently replaced. After sodium charge, flow induced

vibration caused a failure of several tubes and a sodium-water reaction occurred in 1962. A large number of leaks were found during helium leak tests in 1965, and 160 tube joints in Unit #1 and 270 joints in Unit #2 were repaired. After the reactor was returned to service in 1965, leaks were found in the tube to tubesheet welds. Another problem in the Fermi steam generators was instability caused by boiling in the downcomer tubes. This problem was solved by inserting smaller tubes with higher pressure drop within these downcomers.

In 1966, the Fermi reactor experienced a core melt accident due to a local blockage. During the subsequent four-year shutdown in which an investigation was conducted and repairs were made, all 3600 tube-to-tubesheet welds at the water headers were rewelded. After Fermi returned to operation, the steam generator failure rate was much lower, with only minor cracks in the tube sheet ligaments and small leaks at the manifold seal welds that developed. The reactor core reached its licensed burnup limit of 0.4 at. % in 1971. Although a new oxide core project was proposed, Fermi was eventually closed down in 1972 because of a lack of adequate financial support. APDA was phased out in 1974 and PRDC was dissolved after the reactor was decommissioned in 1975. DEC elected to switch to LWR technology, and General Electric (GE) constructed the Fermi 2 BWR which started operation in 1985 [13-18].

North American Aviation (NAA) established the Atomics International (AI) division and started construction of the Sodium Reactor Experiment (SRE) in 1955 at Santa Susana Field Laboratory (SSFL). SRE used unalloyed metal uranium fuel, graphite moderator, and sodium coolant and began operation in 1957. SRE tested two steam generator prototypes. Both units used doubled-walled tubes with mercury in the annular gap to increase the gap conductance. The first was a natural circulation pancake coil tube design with sodium flow on the tube side. The unit was composed of two evaporators and one superheater. This design experienced problems with the accumulation of rust and preservatives during construction and initial operation. In addition, there were unexpected problems with sodium recirculation and reverse flow patterns that developed in the bottom tubes due to natural circulation under low power operating conditions. The second SRE design was a horizontal U-tube type similar to the APDA U-tube design. In this design, sodium flow was on the shell side. This steam generator also experienced flow instabilities at low power, along with difficulties with thermal stratification that led to the development of 100°C temperature differences between the top and bottom tubes. The thermal stratification issue was solved by placing orifices in the tubes to increase pressure drop. After this change, the unit operated satisfactorily for 16,000 hours under steaming conditions. SRE experienced a partial core melt during a loss of flow accident in 1959 and was finally shutdown in 1964 [28–33].

The HNPF was a sodium-cooled, graphite moderated, prototype reactor developed and constructed by AI in Nebraska. The HNPF steam generator adopted the same design as prototypes developed in the SIR program and was a natural circulation, horizontal bayonet tube type with sodium flow inside the tubes. The double-walled tubes were fabricated from 304 stainless steel; interstitial helium was placed between the tubes to increase the gap conductance. HNPF started operation in 1962. Early difficulties were encountered with water carryover at high steaming rates. This problem was solved by modifying the water level control in the units. The steam generators operated satisfactorily after this modification. The reactor experienced leaks in the graphite moderator cans in 1963 and the reactor was shut down in 1966. The HNPF steam generators did not accumulate enough operating experience to adequately access their long-term reliability. North American Aviation eventually merged with Rockwell Standard in 1967 and became Rockwell International in 1973 [34–38].

Development for CRBR

The USAEC constructed the Liquid Metal Engineering Center (LMEC, subsequently the Energy Technology Engineering Center, or ETEC) at SSFL in 1966. ETEC featured a Sodium Components Test Installation (SCTI) that could test components in sodium at temperatures up to 700°C, and with power inputs as high as 35 MWt initially (SCTI was subsequently upgraded for testing at up to 70 MWt). Alco Products designed a 30 MW prototype steam generator for the USAEC. However, Alco Products eventually withdrew from the project, and Baldwin-Lima-Hamilton Corporation (BLH) completed the fabrication. The Alco/BLH steam generator was a 30 MWt once-through unit with a straight tube design that incorporated a sine wave bend in the tubes just below the top tube sheet to accommodate thermal expansion. The outer tubes were made of 316 stainless steel while the inner tubes were made from Inconel. This steam generator was tested at SCTI in 1966, accumulating 1 400 hours of operation until operations were interrupted for facility upgrades. The test was resumed in 1969, and an additional 900 hours of operating time was accumulated before a sodium-water reaction occurred. After repairs, the unit accumulated an additional 1 100 hours of operating time before experiencing a second sodium-water reaction in 1970. Tube failures and massive cracking at the feed water tubesheet (made of 316 stainless steel) were found, and testing was terminated. The main reason for the tubesheet cracking was thought to be a mismatch between the tubesheet material and tubes. Evidence pointed strongly towards stress corrosion cracking of the 316 stainless [39-40].

Westinghouse proposed a serpentine steam generator design and conducted material and weld tests using two Thermal Shock Models (TST-1, TST-2) that had 12 and 18 straight tubes, respectively. Westinghouse also conducted a steady state operation test using a 1 MW Heat Transfer Model (HTM-1) with nine serpentine tubes in their General Purpose Loop (GPL-1) at Waltz Mill, Pennsylvania [41].

AI developed a Modular Steam Generator (AI-MSG) that had 158 single-wall hockey stick tubes fabricated of 2-1/4Cr-1Mo steel that was rated for 30 MWt. This unit was tested at the SCTI from 1970 to 1973, accumulating 4000 hours of operation without any significant evidence of flaws. The hockey stick tube design and 2-1/4Cr-1Mo material were selected for the CRBR steam generators in 1974 [42–44].

Once the reference tube design and tubing material for the CRBR steam generators were chosen, fundamental experiments were conducted. Two single-tube test models were constructed at GE and Argonne National Laboratory (ANL) to study heat transfer and corrosion behavior of the CRBR steam generator tubes [45–47].

A Few Tube Test Model (FTTM) for the CRBR hockey stick steam generator was constructed for a 10,000 hour endurance test by AI. This steam generator consisted of an evaporator and a superheater, each with seven tubes (three active and four inactive). This module was tested in the 2 MW Steam Generator Test Rig (SGTR) at GE in San Jose, California from 1977 to 1978 until the test was terminated after 1915 hours of operation under power. Evidence of sodium bypass flow on the shell side was found in both the evaporator and superheater. This problem was caused by separation between the inner shroud and shell flange with accompanying bolt failures. Post-test disassembly and examination indicated that tube bowing had occurred in the superheater, along with gouging between tube supports and tubes in both the evaporator and superheater [10, 48].

AI and Westinghouse subsequently constructed a full-scale mockup of the CRBR evaporator and tested it at SCTI from 1982 to 1983. The capacity of the SCTI was increased from 35 MW to 70 MW for this operation. Since the full-scale evaporator was designed for 117 MW full power operation, the model was operated at 60% power in this experiment. The steady state performance of the test article was in good agreement with the prediction, and no significant difficulties were encountered during operation [49–55].

The CRBR project was canceled in 1984 and the steam generator development work was phased out. AI merged with Rocketdyne (another division of Rockwell International) and became Rocketdyne Propulsion and Power in 1984.

Development after CRBR

After CRBR, there were two prototype steam generator tests conducted at ETEC as part of the Advanced Liquid Metal Reactor (ALMR) programme to further support liquid metal reactor development. B&W constructed a 70 MW(t) helical coil steam generator with 2-1/4Cr steel tubes and tested it at ETEC from 1987 to 1989. This unit operated successfully with a steaming time of 4200 hours and was selected as the reference steam generator design for ALMR [75].

The DOE and Japan Atomic Power Company (JAPC) took part in a cooperative development programme for double-walled tube steam generators. In this programme, Westinghouse constructed a 70 MW(t) Double-Wall-Tube Steam Generator (DWTSG) with 2-1/4Cr steel tubes and tested it at ETEC from 1991 to 1993, accumulating more than 7700 hours of successful operation [63-69].

After these two prototype tests, developmental testing of steam generators at ETEC for fast reactor applications was terminated. Rockwell sold Rocketdyne, including the SSFL, to Boeing in 1996. The DOE contract for ETEC expired in 1998. Boeing sold Rocketdyne to Pratt & Whitney in 2005 and Pratt & Whitney was renamed Pratt & Whitney Rocketdyne.

7.2.4.2.2. France

A timeline showing the historical development of steam generators in France is provided in Table 7.12.

TABLE 7.12. CHRONOLOGICAL DEVELOPMENT AND TESTING OF STEAM GENERATORS IN FRANCE

Reactor	SG	62	63	64	65	66	67	68	69	70	71	72	73	74	75	76	77	78	79	80	81	82	83	84	85	86	87	88	89
Phenix 568MWt 250MWe MOX, pool	Stein 5 MW hairpin double (Stein)	construction (Stein et Roubaix)		operation (CEA)																									
	prototype 15 MW hairpin (Stein)					construction (Stein et Roubaix)																							
							operation (CEA) 8000h steaming																							
	Phenix prototype 15 MW hairpin (Stein)								construction (Stein Industrie)																				
										operation (EDF) 13000h (power 6200h)																			
								Stein Industrie was established																					
	Phenix hairpin (15MW)							construction (SG: Stein Industrie)								IHX repair						RH repair		IHX repair					
													operation																
																sodium fire (IHX break)						RH leaks		IHX leak				standby	
SPX 2990MWt 1200MWe MOX, pool	SDP-1 helical (Nera)												construction (Nera)																
														operation (CNEN)															
	SDP-2 straight (Nera)																	construction (Nera)											
																			operation (CNEN)										
	GVE-1 45MW helical coil (Babcock Atlantique)											construction (Babcock Atlantique)																	
													operation (EDF)						18460h (5610h power)										
													Babcock Atlantiques merged with Fives Lille-Cail to be Fives-Cail Babcock																	
	Stein-straight 45MW straight (Stein)												construction (Stein Industrie)																
														operation (EDF)															
															4088h (1507h power)														
	PGV-1 45MW straight (Nira)																construction (Breda T. and Nira)												
																		operation (EDF) tube bundle rotation											
																		4796h (1690h power)											
	SPX helical coil (750MWx4)															construction													
																									critical				
																				1998 terminated							EVST leak		

Chronologically, these developments can be divided into two major phases: (1) initial development for Phénix, and (2) subsequent development for Superphénix.

Development for Phénix

The first sodium fast reactor to be constructed in France was the experimental reactor Rapsodie at Cadarache. Construction was initiated in 1962, and first criticality was reached in 1967. Rapsodie had no steam generator.

A separate steam generator development program for Phénix was started in 1957 by Commissariat à l'Energie Atomique (CEA). In 1963, Stein et Roubaix constructed a once-through tube-in-tube steam generator with a thermal capacity of 5 MW and tested it at a CEA facility at Grand Quevilly. This unit had hairpin double-wall steam tubes and was fabricated from 321 stainless steel. NaK was used between the inner and outer tubes to increase the gap conductance [5, 70].

After the 5 MW test, the steam generator design for Phénix was selected to be a shell and tube type with a separate evaporator, superheater, and reheater. The tube design was a single-wall hairpin fabricated from 2-1/4Cr steel for the evaporators and 321 stainless for the superheaters and reheaters. In 1967, Stein et Roubaix constructed a prototype module with a total thermal capacity of approximately 14 MW. This unit was tested at Grand Quevilly from 1967 to 1969, accumulating 8 000 hours of operation under steaming conditions [70-72].

Electricite de France (EdF) constructed a sodium component test facility (CGVS) with a thermal power rating of 50 MW at Les Renardieres. Stein Industries constructed three modules of the prototype Phénix steam generator at the Les Renardieres facility with total thermal power rating of 47 MW. These modules were tested from 1970 to 1972, accumulating 6200 hours of operation [73–76].

Phénix construction was started in 1968 and first criticality was reached in 1973. Phénix is a pool type sodium cooled reactor with 568 MW thermal power rating and three secondary loops with 12 steam generator modules per loop. The steam generators were fabricated by Stein Industrie from 1969 to 1972 and were erected on the Marcoule site between 1971 and 1972 [73, 77, 78]. Detailed on-site test results for these steam generators have been reported in the literature [73]. The Phénix reheaters experienced two leaks in 1982 and two more in 1983. These tube failures were thought to be caused by a combination of some low quality welds and the startup operating procedure in which a steam/water mixture was inadvertently passed through the reheater tubes [79, 80].

Development for Superphénix

Development of the steam generators for Superphénix was carried out collaboratively between France and Italy. Two steam generators with 45 MW power were tested at the CGVS from 1973 to 1975 to select a steam generator design.

Babcock Atlantique constructed a 45 MW once-through helical coil steam generator (GVE-1) with tubes made of Incoloy 800 and accumulated 1001 hours of operation under steaming conditions during testing in 1973. Stein Industrie constructed a straight tube steam generator composed of a 33 MW evaporator with 7CD9.10 tubes and a 12 MW superheater with 316 stainless steel tubes. This unit was tested in 1974 and accumulated 1507 hours of operation.

As a result of the competition, the once-through helical coil steam generator was selected for Superphénix. The prototype unit GVE-1 was returned for more testing and accumulated a total of 5610 hours of operation under steaming conditions. [75, 76, 78–82]

The Italian company Nira also constructed a straight tube steam generator composed of a 33 MW evaporator with 2.25Cr tubes and a 10 MW superheater with 316 stainless steel tubes (PGV-1). This unit was tested at the CGVS and accumulated 1690 hours of operation from 1979 to 1980. A post-test examination was carried out on the evaporator and it was observed that a rotation of the tube bundle had occurred that caused a 1.7 mm tube deformation. This tube bundle rotation was caused by shrinkage of the shell seal welds [86–89].

Superphénix construction began in 1976 and the reactor first achieved criticality in 1985. Superphénix was a pool type sodium cooled reactor with a thermal output of 2990 MWt. The reactor employed four secondary sodium loops, each with a once-through helical coil steam generator rated at 750 MW thermal. The detailed design and fabrication of the Superphénix steam generators was carried out by Novatom from 1977 to 1982. Superphénix experienced an ex-vessel storage tank (EVST) leak in 1987 and air contamination of the primary side sodium in 1990. Operations were finally terminated in 1998 [90-94].

7.2.4.2.3. Germany

A timeline showing the history of steam generator development in Germany is provided in Table 7.13. Chronologically, these developments can be divided into two phases:

(1) Initial development for KNK;

(2) Subsequent development for SNR-300.

TABLE 7.13. CHRONOLOGICAL DEVELOPMENT AND TESTING OF STEAM GENERATORS IN GERMANY

Reactor	SG	64	65	66	67	68	69	70	71	72	73	74	75	76	77	78	79	80	81	82	83	84	85
KNK-II 58MWt 20MWe MOX, loop	Interatom 5 MW hairpin, tube in tube (Durr-Werke)	Durr-Werke	operation																				
	Interatom 5 MW helical (VKW)																						
	Interatom 5 MW bayonet (Interatom)								operation (Interatom)														
	KNK-II 29 MW hairpin, tube in tube			construction (Interatom)					critical (KNK)			modification (Interatom)			critical (KNK-II)								
									SG leak							power generation						1991 final shutdown	
SNR-300 762MWt 327MWe MOX, loop	test module 1 MW																						
	Hengelo 50 MW straight					design and construction (Neratom)			operation (TNO) 3003h			bending of flow skirt, wear at the tube support, rotation of tube supports											
									leak at RH and RH removed														
	Hengelo 50 MW helical							design and construction (Neratom)				operation (TNO) 3268h as EV, 6700h as once through											
	SNR-300 85 MW straight (loops 1-2) helical coil (loop 3)									construction													
																						sodium fire	
																						1991 canceled	

Development for KNK

Interatom (a Siemens subsidiary) constructed a 5 MW sodium component test facility for KNK plant development and tested two prototype steam generators at the facility. One was a helical coil tube type proposed by VKW and the other was a hairpin tube-in-tube type by Durr-Werke. The double wall hairpin tube-in-tube type was selected for the KNK steam generator because it was easy to fabricate and repair in case a sodium-water reaction occurred. These considerations took precedence over economics for this experimental reactor design.

KNK was constructed by Interatom for Karlsruhe Nuclear Research Center (KfK) from 1966 to 1971. KNK was a loop type reactor with a thermal power of 58 MW. This plant achieved first criticality in 1972 with a thermal spectrum core. KNK was then modified to utilize a fast spectrum core from 1974 to 1977 and first achieved criticality in that configuration in 1977. As noted, the steam generators were hairpin tube-in-tube type and each of the two loops had one steam generator with a thermal rating of 29 MW. One of the steam generators experienced a sodium water reaction during the course of low power commissioning. The leak was located at the end of a weld of a tube spacer fin. Since the steam generator was a tube-in-tube type, detection and repair of the damaged tube was not difficult. The damaged tube was removed and a standby tube was attached in six weeks. KNK-II was operated without any more difficulties related to the steam generators and the reactor was finally shut down in 1991 [5, 95–99].

Development for SNR-300

SNR-300 development was started in 1968 with a collaborative agreement among Germany, Belgium and the Netherlands. International Natrium Brutreaktor Baugesellshaft (INB) was established for the construction of SNR-300. A Dutch company of INB members, Neratom, was responsible for the steam generator development.

The original steam generator design for SNR-300 was a straight tube type, and Neratom constructed a prototype 50 MW steam generator composed of a 26 MW thermal power evaporator, a 17 MW superheater, and a 7 MW reheater. This steam generator was tested in the Sodium Component Test Facility (SCTF) at Hengelo, Netherlands from 1971 to 1972. Soon after start-up, there was a sodium-water reaction in the reheater. The reheater was removed and the test was resumed with the evaporator and superheater, accumulating 3003 hours of operation under steaming conditions. The heat transfer performance of the evaporator was 20% less than predicted due to sodium bypass flow between the tubes and shroud. A radial temperature difference of 40°C was measured in the tube bundle. Post-test examination of the evaporator revealed that the flow shroud had bent, creating an opening with a maximum clearance of 3 mm at the flange. The tube support had also rotated. These defects were thought to have been caused by a stress relief procedure that was carried out during fabrication. In particular, the unit was annealed at ~ 740°C after assembly, and this procedure caused permanent deformation of the flow shroud, as well as overstressing of the bolts. The tube support rotation was thought to be caused by a non-symmetrical sodium temperature distribution. In 1970, Neratom began design of a helical coil tube steam generator due to the fact that the SNR-300 designers had decided to have two different types of steam generators in the plant. Neratom constructed a prototype helical coil evaporator rated for 53 MW and tested it at the Hengelo SCTF in 1974, accumulating 3268 hours of operating time. Post-test examinations revealed no defects in this module and it was reassembled to serve in a once-through operational mode in the Hengelo SCTF [100–106].

SNR-300 construction was started in 1971 by INB. SNR-300 was a 327 MW electric (762 MWt) loop-type reactor with three primary loops. Each loop was outfitted with three intermediate heat exchangers (IHXs). Each of the nine IHXs fed intermediate sodium to one steam generator; in total, there were six straight tube and three helical coil tube-type units. Both designs consisted of 55 MW evaporators and 30 MW superheaters. Fabrication of the straight tube and helical coil steam generators was completed by Neratoom in 1983 and 1984, respectively, and subsequently installed in the plant. SNR-300 experienced a sodium fire in a secondary sodium circuit in 1984 before fuel loading, and was cancelled in 1991 [115–121].

7.2.4.2.4. United Kingdom

The UK designed, built, and operated two liquid-metal cooled fast reactors. The first was the Dounreay Fast Reactor (DFR), while the second was the Prototype Fast Reactor (PFR). DFR construction was started at Dounreay in 1954 and achieved criticality in 1959. DFR was a 60 MWt (15 MW electric) sodium-potassium eutectic cooled loop type reactor. The design incorporated 24 primary and 12 secondary circuits with one evaporator and one superheater in each secondary circuit. The steam generators were tube-to-tube type in which both the steam tubes and secondary coolant tubes were placed within copper blocks. There were no major problems with these steam generators, but this design was not adopted for PFR due to the low thermodynamic conversion efficiency of nominally 25% that would have adversely impacted the plant economics [126].

PFR construction was started at Dounreay in 1968 and first achieved criticality in 1974. This plant was a 600 MWt thermal (200 MW electric) sodium cooled pool type reactor. The design incorporated three main coolant loops, each with a 210 MWt steam generator consisting of a 130 MW evaporator, a 55 MW superheater, and a 25 MW reheater. These U-tube type units were fabricated by Babcock and Wilcox. In the evaporator, 2-1/4Cr steel was used for the tubing material, while in the superheater and reheater, 316 stainless steel was used [127–131].

In the early stages of operation, PFR availability and output were limited because of steam generator leaks. During the period from 1974 to 1984, PFR experienced a total of 36 tube-to-tubesheet leaks; 33 of these leaks were in the evaporators, two in the superheaters, and one in a reheater. Two superheater leaks occurred in 1974 and one reheater leak occurred in 1976. Evidence of rapid caustic stress corrosion cracking, caused by sodium side impurities introduced during leak events, were observed at tubesheets fabricated of 316 stainless steel in the failed units. The # 3 reheater was eventually removed because of severe cracking at the tubesheet, and PFR continued to operate without it. Because of this unexpected rapid failure mechanism, the tube bundles in all superheaters and reheaters were replaced with new bundles fabricated of 9Cr steel over the period from 1984 to 1987.

The tube-to-tube sheet leaks in the evaporators increased in 1980-81. Two weld cracking mechanisms were observed: (i) pure water stress corrosion cracking, and (ii) caustic stress corrosion cracking. The principal reason behind the pure water cracking was the hardness of the welds and the residual stresses caused by the absence of post-weld heat treatment. Caustic cracking on the sodium side was caused by impurities in the secondary sodium that were introduced during previous leak events. This problem was fixed with sleeves welded over the defective tube-to-tube sheet welds inside the tubes. The sleeve installation in the three evaporators was completed in 1984 [131–138].

After the initial leaks in 1974 and 1976, there were no further leaks in the superheaters or reheaters until 1986. During this phase, PFR continued to operate without the #3 reheater that was removed in 1976. Full three loop operation resumed in 1984 when the #3 reheater was upgraded with a new tube bundle fabricated of 9Cr steel. Although new tube bundles fabricated with 9Cr steel were prepared for the other five units by 1985, PFR experienced two additional sodium-water reaction accidents in the superheaters before these new bundles could be installed. In 1986, a leak occurred in the #3 superheater and the damaged tube bundle, fabricated from 316 stainless steel, was replaced with a new bundle fabricated of 9Cr steel. During this time, the plant continued to operate with the two remaining loops. In 1987, a leak occurred in the #2 superheater that resulted in a large sodium-water reaction. The burst disks on the Sodium Water Reaction Pressure Relief System (SWRPRS) ruptured and the reactor tripped automatically. This particular leak was initiated by a tube that failed due to fretting caused by flow-induced vibration. Thirty nine additional tubes were damaged in this event as a result of the sodium-water reaction. Inspection after disassembly revealed that the main mechanism driving the tube failure propagation was loss of physical strength caused by overheating from the sodium-water reaction. On this basis, the steam generator safety case underwent extensive additional review. Based on findings from this investigation, the steam generator protection system was refined with improved hydrogen detection systems, reliable water isolation valves, and burst disks with diverse designs [139, 140].

In 1987, 1988 and 1990, additional leaks from the steam generator vessels occurred and subsequent inspection revealed large non-penetrating cracks on the vessel walls in the superheaters. These cracks were repaired with patches attached to the defective areas. In 1991, PFR experienced contamination of the primary sodium by oil. In this accident, up to 35 L of oil from the primary pump upper bearing entered the primary circuit. PFR was stopped for 18 months for repair and restarted operations in 1992. The reactor was permanently shut down in 1994 [140-143].

7.2.4.2.5. Japan

Japan has developed two sodium-cooled reactors: the experimental fast reactor Joyo, and the prototype fast breeder reactor Monju. Joyo construction was started in 1970 and criticality was first achieved in 1977. Joyo is a 50 MWt (Mark-I core) loop type reactor located at Oarai, Japan. Joyo has no power conversion system.

Two 50 MWt prototype steam generators were constructed for Monju. Both units were of the helical coil type and each was composed of an evaporator with 2-1/4Cr steel tubes, and a superheater with austenic stainless steel tubes (type 304 for #1 and type 312 for #2). The first prototype was fabricated by Hitachi and tested from 1974 to 1975 for the Power Reactor and Nuclear Fuel Development Corporation (PNC), accumulating 3400 hours of operation under steaming conditions for the evaporator and 1100 hours for the superheater. The second prototype was fabricated by Mitsubishi Heavy Industries (Mitsubishi) for PNC and tested from 1975 to 1987, accumulating 16,104 hours of operating time for the evaporator and 5025 hours steaming for the superheater. There were no major problems with these two steam generators [144–152].

A timeline showing the historical development of steam generators in Japan is provided in Table 7.14.

TABLE 7.14. CHRONOLOGICAL DEVELOPMENT AND TESTING OF STEAM GENERATORS IN JAPAN

Reactor	SG	70	71	72	73	74	75	76	77	78	79	80	81	82	83	84	85	86	87	88	89	90	91	92	93	94	95	96	97	98
Joyo 140MWt MOX,loop	Joyo no SG	construction							operation																					
																						2006 operating								
Monju 714MWt 280MWe MOX,loop	PNC-1MW #1 helical coil (Hitachi)	construction (Hitachi)																												
			operation (PNC)																											
	PNC-1MW #2 helical coil (MHI)			construction (MHI)																										
					operation (PNC	4800h steaming																								
					sodium leak x2																									
	ITR-1MW helical coil (Toshiba)						construction (Toshiba)																							
								operation																						
	prototype 50MW #1 helical coil (Hitachi)		construction (Hitachi)																											
						operation (PNC)																								
							4200h (EV:3400h SH:1100 steaming)																							
	prototype 50MW #2 helical coil (MHI)				construction (MHI)																									
							operation (PNC)		EV:16104, SH:5025 steaming																					
	Monju 238 MW helical coil																construction													
																	SH: Hitach		1994 critical							operation	stanby			
																	EV: Mitsubishi		1995 sodium leak (stanby)								sodium leak			
DWTSG	DWTSG-FTTM-1.7MW straight double Toshiba/IHI																						operation (ETEC)							
	DWTSG-1MW straight double Hitachi																						operation (PNC)							

Monju construction was started in 1985 and the first criticality was achieved in 1994. Monju is a loop type plant with a thermal power rating of 714 MW and an electrical output of 280 MW. There are three main loops, and each loop has a 238 MWt steam generator consisting of a 191 MW evaporator (fabricated by Mitsubishi with 2-1/4Cr steel tubes) and a 47 MW superheater (fabricated by Hitachi with 312 stainless steel tubes). Monju experienced a sodium leak in the secondary piping system in 1995, resulting in an outage of over fourteen years [153].

The Japan Atomic Power Company (JAPC) and DOE carried out a cooperative R&D program on a double walled steam generator design. In this program, Westinghouse constructed a 70 MW Double-Wall-Tube Steam Generator (DWTSG-70MW) with 2-1/4Cr steel tubes. This unit was tested at ETEC from 1991 to 1993. In the same project, Toshiba and Ishikawajima-Harima Heavy Industries (IHI) constructed a 1.7 MW Few Tube Test Model (DWTSG-FTTM) with modified 9Cr steel tubes and tested it along with the DWTSG-70MW test at ETEC. At the same time, Hitachi constructed a 1 MW thermal power model (DWTSG-1MW) for PNC and JAPC and tested it at the PNC facility at Oarai, Japan [55, 153–155].

7.2.4.2.6. Russian Federation

Russia has developed three sodium-cooled reactors with steam generators: BOR-60, BN-350 and BN-600. In BOR-60, which first achieved criticality in 1968, several prototype steam generators were tested. However, detailed operating experience and specifications for the steam generators were not found in open literature publications describing the work carried out at this reactor. [156, 157] The BN-350 reactor, which first achieved criticality in 1972, was a 750 MW thermal power plant with six secondary loops including one reserve loop. Each loop had two bayonet type evaporators and two U-tube superheaters. Numerous tube failures were reported for these steam generators. [143, 158] BN-600, which first achieved criticality in 1980, is a 1470 MW thermal power reactor with three main coolant loops. Each loop has eight sets of straight tube evaporators, superheaters, and reheaters. In this design, a failed module is isolated in case of a tube failure incident and reactor operation continues at power. The BN-600 steam generators accumulated 100 000 hours of operation while experiencing a total of 12 tube failures, including three large sodium-water reactions [143, 158].

7.2.4.2.7. India

The PFBR SG (Fig. 7.25) is a vertical, counter-current shell and tube type heat exchanger with sodium on shell side, flowing from top to bottom, and water/steam on tube side. The flow to the tube bundle entry is made uniform by the flow distribution device (annular perforated plates) located in the annular region before sodium entry to the tube bundle. The tubes are placed in triangular pitch. The ligament (minimum gap between two tubes) of 15mm is provided to balance between resistance to adjacent tube wastage due to small leak sodium-water reaction and cost. Each SG is rated for 158 MW(t). Each tube is OD 17.2×2.3 mm thickness and there are 547 tubes per steam generator. Orifices are provided in each tube at feed water inlet from flow stability considerations. The pressure drop in each orifice is around 10 bars.

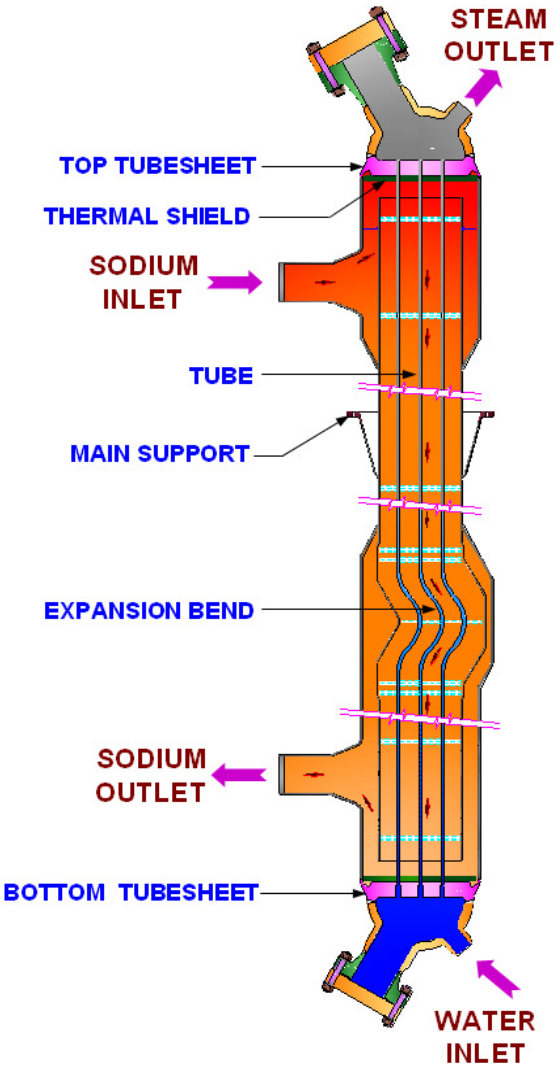

FIG. 7.25. PFBR steam generator.

Each tube is provided with expansion bend in sodium flow path. Its location is in lower portion of single water phase water zone for steady state operation of 20 to 100% power operation. In both the inlet and outlet plenum the outer shell is far away from last row of tubes. The tubes are supported at various locations including at the middle of tube expansion bend. Tube to tube sheet joining is by internal bore welding with raised spigot type joint.

Long seamless tubes of each 23 m is provided to get less number of tube to tube sheet weld, hence improved reliability of SG. Top and bottom tube sheets are protected by thermal shields. Sodium inlet and outlet shell nozzle junctions are in the form of pullouts. A manhole is provided on water-steam dished heads to allow access to tubes for ISI and plugging, if required. SG is supported by conical skirt arrangement attached to the centre of the unit.

7.2.4.2.8. Republic of Korea

A helical coil steam generator (HCSG) was chosen as the reference steam generator design for the KALIMER-600 which is being developed at KAERI due to the following advantages offered by the HCSG design in terms of meeting the requirements for reliability, availability and safety imposed by the adverse effects of potential sodium-water reactions that may occur in sodium-cooled fast reactors:

- Relatively small number of tubes with longer length, larger diameter, and thicker wall;
- Smaller number of welds of tube-to-tubesheet and sodium to water pressure boundary;
- Easier accommodation of tube-to-tube and tube-to-shell thermal expansion differentials;
- Compact heat transfer surface arrangement;
- More efficient heat transfer performance by extended nucleate boiling region.

The KALIMER steam generator is a vertically oriented helical coil type heat exchanger with sodium-to-water counter-cross flow. For the tube side, water flows and is converted to steam. For higher plant efficiency, a once-through superheated steam cycle has been considered in the KALIMER steam generating system [179].

The KALIMER-600 SG system consists of two independent steam generation loops for the reactor and each loop is arranged so that operating conditions or casualty events in one loop will not affect the operation of the other.

The SG system can, when all the related equipment functions normally, cool the intermediate heat transfer system (IHTS) sodium to the temperature levels required for reactor cooling during transient and steady state conditions, and is capable of cooling the IHTS down to refueling temperature of about 200°C.

The SG system is designed such that, with the design features of IHTS, any failure of the sodium-steam/water boundary in the steam generator and resulting sodium-water reactions will not result in a breach to the IHX. The system consists of the following subsystems and a component:

- Steam generator;
- Main steam and feedwater system;
- SG auxiliary feedwater system;
- Water and steam leak detection system;
- Water and steam dump system.

The steam generator is a helical coil, vertically oriented, shell-and-tube type heat exchanger with fixed tube-sheet. Flow is counter-current, with sodium on the shell side and water/steam on the tube side. Sodium flow enters the SG through the upper inlet nozzles and then flows down through the tube bundle. Feedwater enters the steam generator through the feedwater nozzles at the bottom of steam generator. The desired feedwater distribution among the tubes is achieved by the flow restrictor at the tube-sheet.

Also, the flow restrictor prevents the possibility of flow instability in steam generator tube side where two-phase steam water flow exists during normal operating condition. Water entering the tubes from the inlet tube-sheet flows through the helical coil tube bundle, and exits at the outlet tube-sheet as superheated steam for normal power operation. The steam generator is designed to withstand the normal, upset, emergency and faulted operating

conditions. The system parameters of the KALIMER-600 steam generator are summarized in Table 7.15.

TABLE 7.15. KALIMER-600 STEAM GENERATION SYSTEM PARAMETER SUMMARY

	Item	Value
Intermediate heat transport system	Sodium hot leg temperature	526°C
	Sodium cold leg temperature	320°C
	Sodium flow rate	5800.7 kg/s (total)
Steam generator system	Steam generator power	1528.9 MWt (total)
	Steam cycle	Superheat cycle
	Design life	60 years
	Steam temperature	503.1°C
	Steam pressure	16.5 MPa
	Steam flow rate	663.25 kg/s (total)
	Feedwater temperature	230°C
SG tube bundle	Bundle height	8.5 m
	No. of tubes	715
	Tube I.D.	16 mm
	Tube thickness	3.5 mm
	Tube length	71.8 m
	Tube material	9Cr-1Mo
	Pressure drop	1.12 MPa

There are two steam generators (1 SG/loop) and each is designed to transfer 764.45 MWt and generates 331.63 kg/s of superheated steam at 16.5 MPa and 503.1°C at the rated full load condition. The gas region above the free sodium surface is filled with inert cover gas, Ar, designed to accommodate the following:

- Sodium expansion or contraction by a rapid change in the sodium temperature;
- Pressure pulse associated with a large sodium water reaction;
- Space for the installation of the leak detection instrument.

The size of the lower and upper plenum regions is determined under the consideration of tube bundle arrangement and the size of the feedwater inlet and steam outlet nozzles.

The SG is designed for the thermal/hydraulic requirements at full load conditions and the structure of the SG is designed to accommodate the worst possible loading from the duty cycle and operational stresses. The main material for tubing, internal structures and shell of steam generator is modified 9 Cr-1Mo steel, which has a reasonable resistance to erosion and stress corrosion cracking.

Main steam and feedwater system

The steam and feedwater system configuration for the Steam Generator System is shown in Fig. 7.26.

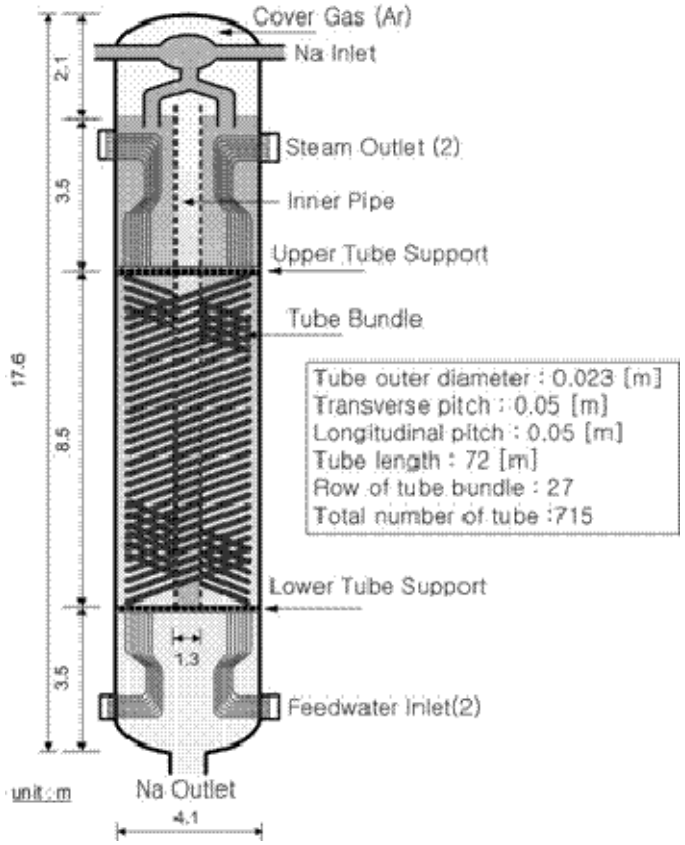

FIG. 7.26. KALIMER-600 steam generator.

The number of feedwater pumps is two and each pump has a 100% capacity for one SG. The main feedwater is pumped at pressure of 19.5 MPa and flow-rate of 331.63 kg/s. The feedwater is heated at 230°C by the feedwater heater by using high pressure steam extracted from turbine. The feedwater from HP heater is separated into two parts for two steam generators. It flows through remotely actuated stop and control valves. The stop valve is for stopping flow of feedwater to any steam generator side in case of failure. The feedwater passes through a flow-meter, a check valve, two water isolation valves, a nozzle, and a tube-sheet, and enters the steam generator tubes. A flow-meter measures the feedwater flow-rate and its signal is transmitted to and recorded at the control room. A check valve makes the feedwater flow only to the forward direction. Two water isolation valves are installed in series and used to isolate the feedwater flow to the steam generator. The water in the main feedwater pipe can be drained through several drain lines. Feedwater is transported through sample lines to a monitoring station for measurement of specific feedwater quality.

The feedwater which enters the two tube-sheet headers is distributed to 715 tubes. The water flows upward in the helical coiled tube and heated to superheated steam by the IHTS sodium flowing in a counter-current way in the shell side. The superheated steam exits the steam generator and flows to the upper two steam tube-sheets of which size are the same as those of

the lower tube-sheets. The steam from two steam tube-sheet headers flows in two lines and then merges into a single line. The steam line contains safety and power operated pressure relief valves for preventing overpressure. The steam line also has a flow-meter, a check valve, and two remotely operated isolation valves. The steam from two steam generators is combined at the steam common header.

Water and steam leak detection system

There are several water/steam leak detection systems in the KALIMER-600 steam generator in order to detect the leak as soon as possible. Each leak detection system monitors and alerts the leak of water or steam into the sodium. The detection of the possible leak of the steam/water from the tube to the sodium in the SG shell is made using hydrogen concentration measurement, acoustic detection, and/or measurement of the pressure at the rupture disk piping. The steam generator leak detection system monitors and alarms water or steam leak in a steam generator and identifies the faulted steam generator. The small scale leak detection subsystem utilizes the measurement of hydrogen concentration in the liquid sodium stream as the method of leak detection. Leakage of water/steam into the sodium stream increases the hydrogen and oxygen concentration in the sodium. The measurement of hydrogen in sodium is accomplished by allowing hydrogen to diffuse through a thin nickel membrane, one side of which has a high vacuum held by an ion pump. These detector modules are installed on the main sodium piping at the steam generator outlet and cover gas space. The purpose of this detection is early detection in the event of a water/steam to sodium leak. In order to have adequate coverage, redundant detectors are provided to accommodate detector malfunctions during operation. A minimum of two operational hydrogen meters is installed to ensure leak detection coverage at any time.

Intermediate leak generally continues for about 30 seconds and the leak can be identified within 3 seconds by the acoustic detection system, and steam generator protective actions are initiated. The acoustic system provides leak detection reliability in intermediate leak region and diversity in the overlapping region of small leak.

Large leak generally continues for several seconds and causes to burst the rupture disk. This leak can be detected by detecting the pressure of sodium or sodium water reaction product in the pipe region between the two rupture disks serially installed at the bottom of the steam generator.

Critical components of leak detection, most susceptible to failure, are outside of the sodium boundary. Replacement of vacuum system components and electronic parts, and replacement of critical components will be accomplishable during planned shutdowns.

Water and steam dump system

The water dump system is to provide rapid blow-down of the water/steam side of the steam generator. This system is provided for each loop to accept and store the water from the steam generator when rapid depressurization of the steam generator is required. In the event of sodium water reaction, the leak detection system alerts its occurrence to operator. The steam generator relief/safety valves are opened at high steam overpressure. The water dump system isolates steam generator from the water and steam system by closing the isolation valves. The isolation valves are located in the feedwater line and steam line in series on each steam generator. These valves are closed automatically in conjunction with the blow-down in the event of a large sodium/water reaction. The water and steam mixture is dumped into the dump tank by two quick opening dump valves in parallel, which are located on inlet line to the

steam generator. In the dump tank, the flashed steam is vented to the atmosphere. Since nitrogen gas pressurizes the tube side through steam line, the water/steam dump to the dump tank is accelerated. This water/steam dump with the safety valve opening can reduce the steam generator pressure to about 2 MPa in less than one minute, and the system effectively minimizes the amount of water leakage.

To facilitate the sodium drain from the SG, there is an inner pipe at the centre of the steam generator and it serves as a bypass channel to equalize pressure differentials between the inlet and outlet sodium nozzle regions. The bypass flow channel and the low pressure drop in the tube bundle ensure the prevention of steam movement into the IHX through the SG cover gas space and IHTS hot leg pipe by the differential pressure between the inlet and outlet sodium nozzle regions in the event the steam isolation valves fail to close. Thus, passive protection of IHX tubes from a worst-case steam generator tube leak is assisted.

Design code

A computer code, named HSGSA (Helical coil Steam Generator Sizing Analyzer), was developed for the thermal sizing analysis of the KALIMER steam generator [180]. HSGSA can analyze the thermal sizing and performance of a steam generator and simulate the operating conditions of recirculation and once-through modes applicable to the following parameter ranges:

- Steam generator type: once-through superheated helical coil steam generator;
- Operating pressure: 5 Mpa ~ 20 Mpa;
- Operation Mode: recirculation (saturated cycle) and once-through modes (superheated steam).

The heat transfer phenomenon between the shell-side sodium and tube-side water/steam, which is two-phase flow, through the tube wall is modeled one-dimensionally. The governing equations of continuity, momentum and energy are discretized in a computational node. A mass conservation equation, one-dimensional energy balance equation, and pressure loss equation are used for the tube and shell sides. The governing equations are of a steady state and the energy balance equation consists of a convection term and a source term for the heat transfer between the tube and shell side flows. The sodium flow rate per control volume is assumed to be the total sodium flow rate divided by the total number of tubes. The total pressure drop for each control volume consists of accelerational, frictional, and gravitational pressure drops. Tube arrangement is determined by longitudinal pitch, transverse pitch, and tube pitch angle. Major assumptions used in the calculation are as follows:

- Constant heat load for each control volume;
- Properties at the i-th control volume correspond to the average values of the i-1-th and i-th nodes;
- The same convergence criterion, 10^{-5}, is applied to relative variations of temperature and pressure for each control volume with respect to the previous iteration values, respectively.

The input parameters are the SG heat transfer rate, flow rate, exit and inlet temperatures of the shell and tube sides, and steam exit pressure. The systems of linear algebraic equations are solved iteratively with Gauss-Seidel method. The tube side flow patterns for a helical coil tube are similar to that of a vertical straight tube in single-phase flow. In the case of two-phase flow, the centrifugal force and the body force due to gravity influence the flow pattern. For the steam generator operating conditions, the gravity effect becomes negligible

except for a low load operation. In the coiled tube, the centrifugal force produces a radial velocity component which results in a secondary flow pattern superimposed on the main flow along the tube axis. The secondary flow pattern makes the helical coil tube very efficient in distributing the liquid on the tube surface, even at high quality. The heat transfer and pressure drop correlations that account for the effects of the coiled tube geometry are presented in Table 16. In the analysis model, the water/steam flow is classified into preheat region, saturated region, film boiling region and superheated region. Table 7.16 shows applied heat transfer and pressure drop correlations.

TABLE 7.16. APPLIED HEAT TRANSFER AND PRESSURE DROP CORRELATIONS

	Region	Correlation
Heat transfer correlation	Preheat water	Seban-McLaughlin Mori-Nakayama
	Nucleate boiling in water	Chen (Modified for hc) with Modified Forster-Zuber equation Owhadi
	Film boiling of water/steam	Bishop et al.
	Critical quality of water/steam	Duchatelle et al.
	Sodium	Kalish-Dwyer Lubarsky-Kaufman
Pressure drop correlation	Preheat or superheat water/steam	Mori-Nakayama Duchatelle
	Two-phase water/steam	Homogeneous Equilibrium Model Modified Martinelli-Nelson or Jones Model Thom Void Fraction - Thom Friction Factor
	Sodium	Gunter-Shaw

Instrumentation

Sodium ionization detectors and sparkplug sensors will be located in the cooling annulus. Steam generator tube leakage will be monitored using the hydrogen detectors and the acoustic leak detectors. Steam generator tubes will be done by volumetric inspection such as remote field ECT or ultrasonic test to detect the flaws and measure the tube wall thickness. Volumetric inspection of steam generator requires draining the sodium in SG to reduce to the ambient temperature and inserting an ECT probe inside the tubes. During these test, some surface and volumetric test of the selected weld of SG shell will be also performed. The major maintenance operations of SG system involve valve operator servicing, recirculation pump seal replacement, tube plugging and cleaning. The maintenance activities are performed during normal refuelling outages.

Sodium-water reaction phenomenon

The sodium-water reaction (SWR) is an important issue for the design of the steam generator and related systems of the LMR. Since the system dynamic responses during the SWR event show obviously different characteristics between the initial stage of an acoustic wave propagation and the long-term period of a bulk motion, its analysis should also be performed for the two major events in general. One is the peak pressure pulse generation, called the spike pressure, during the very initial stage of the chemical reaction, and the other is the bulk

motion including the mass and energy transfer during several seconds or minutes after the leak initiation. In the long-term period of the SWR event, the acoustic wave propagation effects of a sharp and short-lived pressure pulse are subsided and thus the system dynamic response depends only on the characteristics of the bulk motion with the quasi-steady pressurization of the system due to a continuous chemical reaction [181].

Although various numerical approaches to simulate the long-term system transient behavior of the SWR event have been performed in many preceding works [182, 183], complex physical models and numerical schemes have been applied to its simulation, because it has been treated as an extended work of the initial wave propagation stage. The physical model for a long-term mass and energy transfer during the SWR event, named the LMET model, was developed to simplify the quasi-steady SWR phenomena, and the computer code SELPSTA (Sodium water reaction Event Later Phase System Transient Analyzer) was formulated by using the LMET model.

When a large quantity of steam or water suddenly leaks into the shell-side sodium due to defects or ruptures of the SG heat transfer tubes, the sodium water reaction will occur and large amounts of hydrogen gas and exothermic heat will also be generated in the system. Though various chemical reactions occur competitively during the reaction period, it is very difficult to consider all of these possible reactions. Therefore, to analyze the system transients during the reaction, it is necessary to simplify the complex reaction phenomena. The representative reaction between the sodium and water/steam can be expressed by the following general form [186, 187], where A, B, C and D are the reaction constant and Q is an exothermic reaction energy produced by the reaction. Also the term α is a molar conversion ratio of unit mole of water/steam to hydrogen gas.

$$A \cdot Na + H_2O \rightarrow B \cdot Na_2O + C \cdot NaOH + D \cdot NaH + \alpha H_2 + Q \qquad (1)$$

As shown in the relation, the sodium reacts with the unit mole of the water/steam and then various reaction products, such as NaOH, NaH, Na_2O and hydrogen gas, are produced with an exothermic reaction heat. Among these main reaction products, it is well known that a gaseous product like hydrogen gas plays an important role in a system pressure transient [186, 187]. Since the molar conversion ratio (α) of steam to hydrogen gas is also one of the most important factors in the analysis of the SWR event, it should be quantitatively defined to verify the system transients caused by the hydrogen gas and exothermic heat generation. From previous researches conducted in various organizations such as PNC in Japan, GE in USA, and EDF in France, etc., the value of α has been reported experimentally as about 0.5-0.7, and the absolute temperature of the hydrogen gas produced by the reaction has a value between 1000 K and 1660 K in a large-leak SWR analysis [184-186]. In the present study, to consider a large safety margin for a system design, the molar conversion ratio was set up as 0.7 and the absolute temperature of the hydrogen gas is assumed as a constant value of 1300 K. Accordingly, the hydrogen quantity produced by the SWR can be considered as a function of the existent quantity of the water/steam in the shell-side sodium and the steam to hydrogen conversion ratio.

Analysis code

For investigating the system pressure and temperature responses during the SWR event, actual mock-up sodium experiments are desirable. However, since sodium experiments are costly in general, numerical quantifications of the SWR are available to give an account of the

phenomena. For this reason, the analysis of the thermal-hydraulic SWR phenomena in KALIMER has been performed by numerical simulations using the SPIKE [187] and the SELPSTA code. The SPIKE code is developed only for the prediction of the system transient behaviour of the very initial stage of the pressure pulse generation, called as the spike pressure, incurring acoustic wave propagations in the system. It is based on the numerical scheme of MOC (Method of Characteristics) [7, 9] for solving wave equations. Since the scheme, however, is only used to solve an acoustic wave propagation phenomena, it does not have a proper method to consider the mass and energy transfer phenomena in a quasi-steady pressure transient. Figure 7.27, for example, shows the pressure variations of the rupture disk line mounted on the lower part of the SG unit as results of the SPIKE calculation [187, 188].

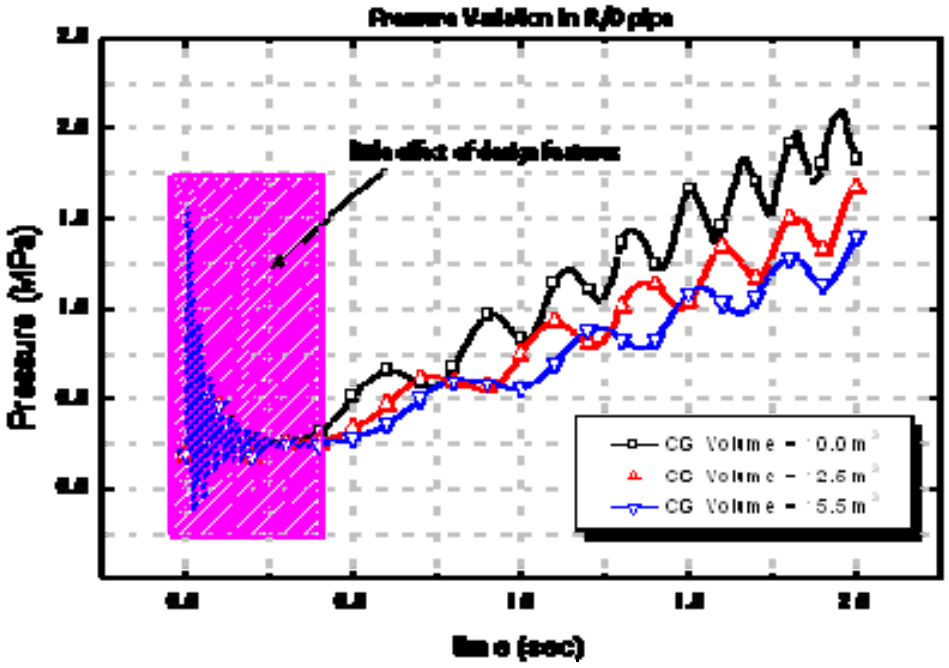

FIG. 7.27. Pressure variation in R/D line (SPIKE calculation).

As shown in Fig. 7.27, in the very initial stage of an acoustic wave transfer regime, it can be seen that the pressure variations are independent of a specific design parameter like the cover gas volume because of the characteristics of the acoustic wave propagation. To the contrary, it can be seen that the pressure variations in the mass and energy transfer during several seconds show a different trend with respect to the design parameter changes. For the quasi-steady system transients just after the subsidence of the wave propagation phenomena, the use of the SPIKE code may incur an improper or unreasonable prediction because the code has drawbacks in the mass and energy transfer calculations. In other words, the SPIKE code was developed under the assumptions that the pressure wave is generated only by the single hydrogen bubble formed by the reaction and that the initial spike pressure behaviour strongly depends on the single bubble growth [187, 189]. As the reaction progresses, the bubble size rapidly increases and is finally bigger than the diameter of the SG unit. This is the reason why the SPIKE code predicts physically unreasonable calculation results in the longer term period of the SWR event [189]. That is, the system design features in the mass and energy transfer phase cannot be properly reflected in the SPIKE calculation, and thus the applicable range of the SPIKE code should be limited just for the very initial wave propagation stage up to 100 msec ~ 1 sec [189]. Accordingly, for the long-term period of the SWR event, it is suitable

to use another analysis method rather than the SPIKE code. This is the motivation to develop the numerical simulation method to effectively reflect the quasi-steady system design features. The detail physical models and algorithm for the numerical quantification are provided in the following sections.

The analysis of the later phase of the SWR event is mainly treated as a none acoustic wave propagation during several milliseconds but a quasi-steady system transient including the rupture disk breakage and pressure relief system behavior during several seconds or minutes. Since the IHTS is a closed loop before the rupture disk break, the system transients in the quasi-steady state of the SWR event can be regarded as the pressure and temperature transients of the cover gas space because it accommodates the entire system thermal-hydraulic responses as mentioned previously. For this reason, to simplify the quasi-steady SWR phenomena, the physical model for a long-term mass and energy transfer (LMET) was developed by using the assumptions that (1) the reaction occurs instantaneously if a water/steam leaks into the sodium phase, (2) non-reacted quantity of water/steam in the sodium phase is negligible, (3) the generation quantity of the hydrogen gas totally depends on the steam to hydrogen conversion ratio, (4) all of the hydrogen gas and exothermic energy due to the reaction itself flow into the cover gas space, and (5) the hydrogen dissolution ratio into the sodium phase is negligible. In particular, Hiromichi [190] experimentally evaluated the hydrogen dissolution ratio during the SWR event and reported that the quantity of the hydrogen gas that dissolves into the sodium before reaching the sodium free surface in the shell-side SG is 5% - 15% as a function of the steam leak rate. This fact means that more than 85% of the generating hydrogen gas flows into the cover gas region without any dissolution. From this finding, the physical assumptions implemented in the LMET model are feasible and practicable for a long-term SWR analysis in view of a conservative manner. Based on the physical model and assumptions, the system pressure variation can be regarded as the cover gas pressure transient and the energy balance between the cover gas and the shell-side sodium.

The energy balance presented here does not contain terms representing the phase change of the reaction products, such as Na_2O and NaOH, for a simplification of the phenomena. The code has capabilities to calculate the system pressure and temperature, the SDT pressure, the sodium discharge flow rate, the sodium free surface level in the shell-side SG, the termination time of the reaction, etc.

SWR long-term transient analysis

To analyze the quasi-steady system transient during the SWR event, the systems and components including the faulted SG, IHTS, rupture disk mounted on the lower part of the SG unit, and the SDT are reasonably modeled using the design data of KALIMER [191] as listed in Table 7.17.

TABLE 7.17. MAJOR INPUT DESIGN PARAMETERS FOR THE SELPSTA CODE

Parameter	Unit	Value
System pressure at normal operation	MPa	0.1
Initial cover gas volume	m^3	9.23
Initial sodium temperature in SG (average value)	^oC	400
Cover gas pressure (at 1 sec)	MPa	0.78
Water/Steam leak rate (design basis leak in KALIMER)	kg/sec	21.57
Hydrogen gas temperature (constant)	K	1300
SDT free volume	m^3	150
Initial SDT gas temperature	^oC	200
R/D bursting pressure	MPa	1.5

The yielding rate of the hydrogen gas corresponding to the steam leak rate with the steam to hydrogen molar conversion ratio of 0.7 is shown in Fig. 7.28.

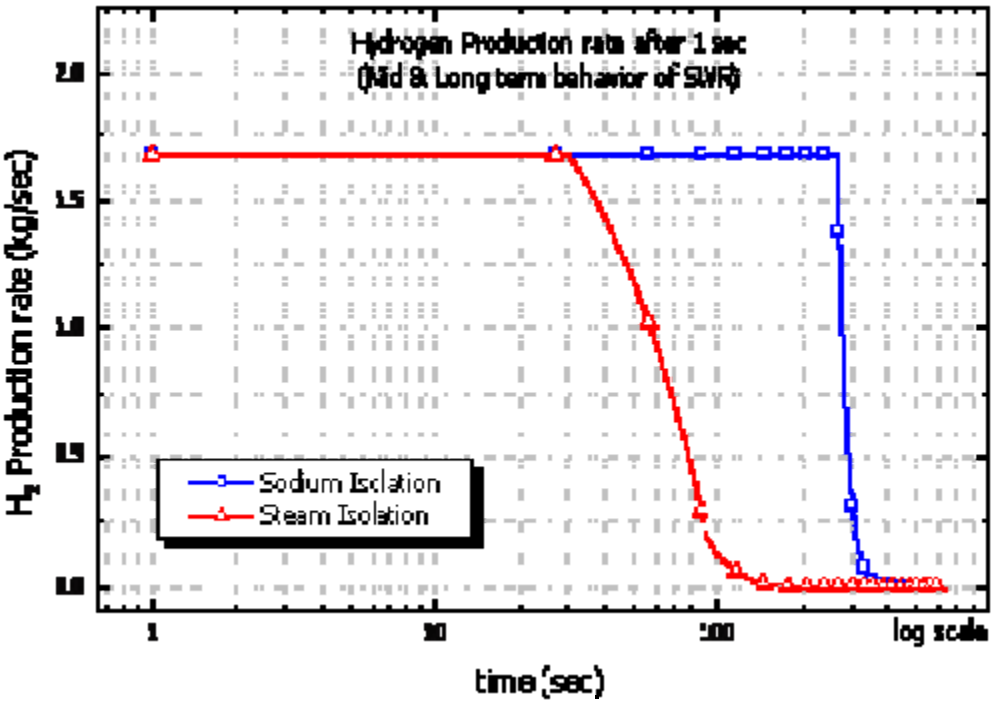

FIG. 7.28. Variation of H_2 generation rate.

As shown in the figure, the yielding rate of the hydrogen gas is initially maintained at a constant value of the design basis leak, and it can be seen that the terminating time of the hydrogen gas generation is different between the tube-side steam isolation and the shell-side sodium clearing. This is because the steam isolation time is faster than the sodium clearing time, quantitatively about 3 minutes [187, 191], since the feed water isolation system will be activated as soon as the sodium-water reaction is detected. On the other hand, since the shell-side sodium clearing is strongly dependent on the design features, such as the pressure difference between the system and the SDT, geometric effects in the shell-side SG, etc., it can be said that the sodium-side isolation is more conservative than the steam isolation from the aspect of the system design. Based on these features, for a more conservative approach, it is

assumed that the reaction is terminated only by the shell-side sodium clearing related to the level decrease of the shell-side sodium.

The temperature and pressure transients of the system including the cover gas and SDT are shown in Fig. 7.29.

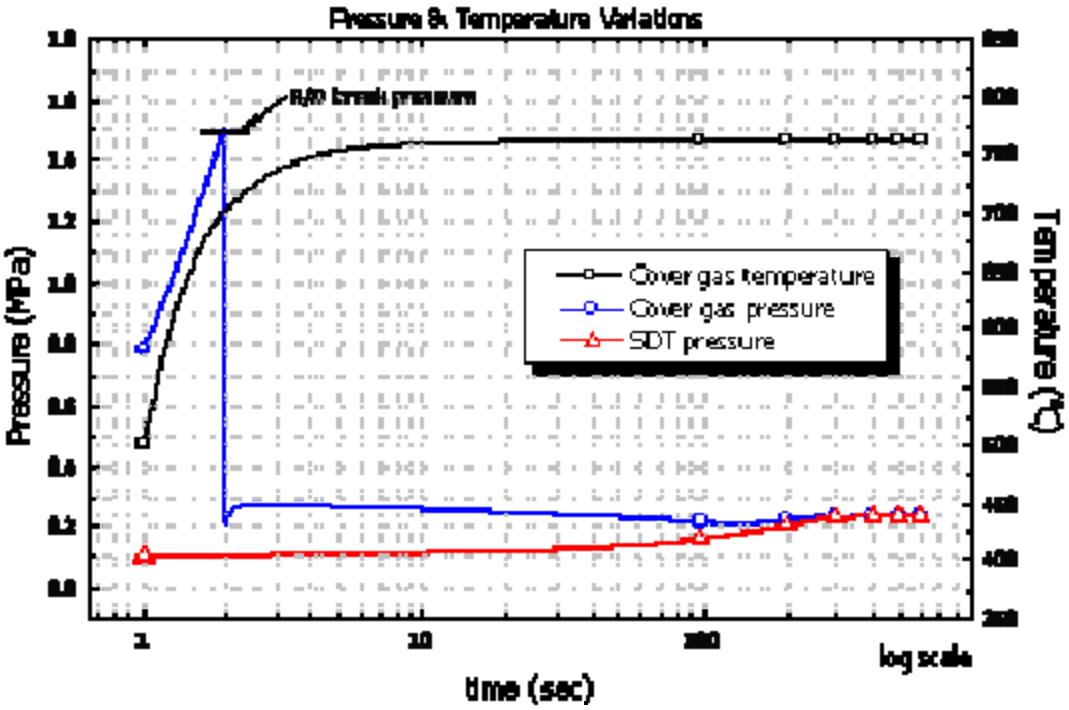

FIG. 7.29. Temperature and pressure transients of the system.

The system pressure rapidly increases until the rupture disk break, and it promptly decreases to the normal system pressure range with some pressure oscillations. The rupture disk break time is about 2 sec after a leak initiation. A relatively small pressure rise is shown just after the rupture disk break time because the continuous steam leak rate is still maintained during this time period. The SDT pressure remains at the initial SDT pressure of 0.1 MPa before the rupture disk break, and it begins to rise corresponding to the system pressure decrease caused by the sodium discharge after the rupture disk break. This is because the free volume of an inert gas in the SDT is sufficiently large enough to accommodate the entire sodium volume of the IHTS loop including the SG. Accordingly, the pressure variation is relatively small when compared to the system depressurization. At the end of the reaction period about 4 minutes after a leak initiation, the SDT pressure is nearly equal to the system pressure since the shell-side sodium is almost cleared and the pressure difference between the system and the SDT becomes very small.

The cover gas temperature also rapidly increases up to the rupture disk bursting time because the cover gas volume is fixed before the rupture disk break. In other words, since the rigid boundary condition is applied to the cover gas region and the exothermic reaction energy flows into the fixed volume with the mass inflow of the hydrogen gas, the compressible cover gas experiences a drastic pressure and temperature transient. However, after the rupture disk break, the cover gas volume is expanded and the moving boundary condition is applied to the region, so the temperature increment very slowly appears or almost diminishes due to the net effects between the energy term added by the hydrogen gas generation and the volume

expansion term in an adiabatic system. The cover gas volume begins to increase just after the rupture disk break time because the sodium discharge also begins at that time. On the contrary, the sodium level begins to decrease due to the sodium discharge, and it shows a little bit of a different trend from the cover gas volume increase.

This is because the sodium level is determined by the relation between the discharged volume and the effective flow area reflecting the complicated geometric effects of the shell-side sodium flow path. Using the level change of the shell-side sodium, the terminating time of the reaction due to the shell-side sodium clearing can be calculated and it is about 4 minutes after the rupture disk break. However, since a quicker termination of the SWR is desirable to secure the safety, the termination of the reaction can usually be accomplished by a tube-side water/steam isolation, and a quantitative shortening time by using the steam isolation at about 23% [187]. It should be noted that the termination of the SWR event in the present study was assumed only by the shell-side sodium clearing, but, in the SELPSTA code, the tube-side isolation model can be optionally selected according to the purpose of the analysis. It is concluded that the SELPSTA code has the capabilities to simulate the long-term system transient of the SWR phenomena with respect to the various design conditions associated with the pressure relief system and operational strategy against the SWR event. The numerical quantification method implemented in the SELPSTA code is also practicable to the system design purpose.

Safety issues

The possibility of a water-steam leak into the sodium in a steam generator of LMR is the major safety issue. The chemical and physical aspects of the exothermic reaction of sodium-water could be followed by a pressure pulse and an over-pressurization of the secondary system. To mitigate a continuous sequential SWR and to protect the system from an over-pressurization of the sodium in the SG, the sodium and the reaction product should be released expeditiously through an adequate pressure relief system (PRS). From a view of licensing for the construction, the SWR PRS is essential. The set pressure, the position and the number of pressure relief devices as a design basis are significant parameters in designing a PRS and IHTS, since these parameters are dominant during abnormal transient operating conditions. Improperly designed pressure relief devices diminish the reactor's operational availability. The determination of the proper parameters is essential to satisfy the safety requirements and the elimination of an excessive conservatism and thus can lead to a satisfactory design. The system's integrity should be confirmed by simulations and an adequate complement of system parameter by feedback is also necessary.

By means of the methodology for the PRS conceptual design, the number, the locations and the type of PRS of KALIMER were determined. The two sets of decision trees were adopted for the determination of appropriate design of PRS [188]. The design concept of a reverse dome-type rupture disk in the bottom of each SG of the secondary loop in the present KALIMER design was validated and the suitability of the PRS design was evaluated with calculations. For the correspondence of the design requirements, an allowable set pressure range which secures the system's structural integrity in the IHX tube and SG pipe was estimated as 0.31 ~ 2.30 MPa with an uncertainty margin of 20% and the validity of the present set pressure of the rupture disc of 1.23 MPa was shown by the calculations and comparisons with reference liquid metal reactors [189]. The transient system behaviour, especially the system pressure is simulated with the computer code SPIKE, and the pertinence of the PRS design of KALIMER was shown.

7.2.4.3. Future trends in SGs

7.2.4.3.1. Steam generator type

As this literature survey indicates, there were many types of steam generators developed for liquid metal reactor applications before the 1970s. In the early stages, the tube-to-tube (DFR), tube-in-tube (EBR-I, KNK) and natural circulation (EBR-II, HNPF) designs were developed based on the requirements of high reliability and ease of repair. Some of these steam generators were operated successfully, but it was apparent that significant cost reduction and improved economic efficiency would be required if they were to find widespread use in commercial plant applications.

Subsequently, efforts were focused on achieving cost reductions for steam generators to support commercial electric generation applications. In the development of Fermi and PFR, the designers tried to apply single-wall tube steam generator designs for large thermal power applications. Fermi was equipped with 67 MW once-through serpentine tube steam generators, while the PFR employed a U-tube design that included a 130 MW evaporator, a 55 MW superheater and a 25 MW reheater. Both of these plants experienced numerous steam generator failures during operation that limited plant availability since shutdowns were required to repair the steam generators.

In France, the steam generator for Phénix was developed using prototype modules. Phénix achieved first criticality in 1973 and did not experience major steam generator problems until two reheater failures occurred in 1982. Even though the Phénix steam generators performed well, helical coil type units were adopted for Superphénix in order to reduce capital costs [87].

The straight (including single-wall-tube straight, hockey stick and double-wall-tube straight) and helical coil tube type steam generators have undergone extensive design and development work since 1960 with a focus on high economical performance. There were many prototype tests for both kinds of steam generators and three reactor plants were equipped with them. SNR-300 had both straight and helical coil tube steam generators, but this plant was terminated before operation. Superphénix had helical coil steam generators. The plant experienced problems with the EVST and the primary sodium circuit and was permanently shutdown before extensive steam generator operating experience could be gathered. Monju also has a helical coil type steam generator.

A design comparison between straight and helical coil steam generators suggested that the single wall straight tube type has an advantage in compactness and the ability to perform inspections [109,111]. However, prototype tests showed that the straight tube design is more likely to encounter technical problems; e.g. shroud deformation and tube bowing in CRBR-FTTM, tube bundle rotation in PGV-1, and shroud deformation and tube support rotation in the Hengelo straight tube evaporator. On the other hand, there have not been major difficulties reported in the operation of helical coil modules.

In the ALMR study [75], a design competition between a single-wall helical coil and double-wall straight tube steam generator types was conducted. The straight double-wall unit was estimated to cost approximately twice that of the helical coil counterpart. The major purpose of the double-wall design was to increase reliability by reducing the likelihood of tube boundary failure between the sodium and water sides of the unit. However, failure probability analyses showed that the failure frequency of the double wall tube design was only slightly less than the helical coil design (i.e. 0.65 and 0.81 failures per plant life time, respectively, in

a nine reactor-unit plant with a 60-year plant life). Therefore, the single-wall helical coil type was selected as the reference steam generator design for the ALMR.

In recent conceptual design studies, the European Fast Reactor (EFR) and Japan Sodium-cooled Fast Reactor (JSFR) have adopted single-wall straight tube and double-wall straight tube steam generator designs, respectively. Both designs employ advanced materials for the tubing; i.e., EFR utilized T91 steel, while JSFR utilized 12Cr steel. Fundamental studies examining operational stability, sodium leak protection, and inspection techniques were conducted to support these designs. However, the designs are not yet fixed and no prototype steam generator testing has been conducted [76–78].

7.2.4.3.2. Tube material

The most established material for evaporator and once-through steam generator tubes is 2-1/4Cr steel. There have been a large amount of fundamental experiments in the areas of fabrication, welding, corrosion resistance, and thermal transients. The tubes of: (i) the Fermi, EBR-II, and SNR-300 steam generators, (ii) the Phénix, PFR, and Monju evaporators (including the prototype modules), and (iii) the B&W 70 MW helical coil steam generator and the Westinghouse 70 MW DWTSG were all fabricated with 2-1/4Cr steel (including niobium stabilized 2-1/4Cr steel). These fundamental and prototype tests have all demonstrated the feasibility of 2-1/4Cr steel as a tubing material [146, 87-89, 168-174].

Superphénix adopted a once-through steam generator with Incoloy-800 tube material. Cracks were found at the tube welds of the prototypes. However, fundamental experiments and numerical calculations after crack detection showed that Incoloy-800 is still acceptable for plant operations [172]. Nickel based alloys (Inconel-600 and Incoloy-800) were also studied in the United States as candidate materials [173, 174]. However, the CRBR, 70 MWDWTSG, and B&W 70 MW helical coil steam generators all used 2-1/4Cr steel based on superior resistance to stress corrosion cracking [168, 169].

High chromium steels such as 9Cr and 12Cr have been studied in the interest of using higher performance materials for steam generator tubes [165-170]. This research has shown that 9Cr and 12Cr steel tubes have high-temperature strength, high thermal conductivity, and good resistance against stress-corrosion cracking. Thus, steam generators manufactured with these steels can be designed to be more compact than those made with 2-1/4Cr steels. Although there have been many fundamental experiments on high-temperature strength and corrosion, there have only been two small-scale prototype steam generator tests with 9Cr steel; i.e., DWTSG-FTTM and DWTSG-1MW.

7.2.4.3.3. Comparison with PWR steam generators

PWR steam generators have experienced many more tube failures relative to liquid metal steam generators [26, 158]. In terms of unscheduled PWR plant outages, 25% are reported to be caused by problems related to the steam generators. In the United States, there are essentially two types of PWR steam generators: i) recirculating U-tube, and ii) once-through straight tube. In both types, the tubes are fabricated of Inconel-600 with primary system water on the tube side, and secondary water on the shell side. PWR steam generator problems can generally be categorized as follows:

- Wastage - Early PWRs utilized phosphate for pH control on the secondary side. Phosphate concentrated as sludge on the tube surface and caused corrosion. This problem

was solved by utilizing an all-volatile treatment (AVT) for pH control, as opposed to the use of phosphate.

- Denting - Magnetite builds up at clearances between the tubes and tube supports, causing pressure to increase to the point where the tubes dent.
- Pitting - Pitting is caused by local corrosive attack from chlorides, oxygen and copper contaminants in the secondary system water.
- Inter-granular attack (IGA) - IGA occurs at the tube-to-tubesheet interface and tube support clearances. This mechanism is caused by caustic impurities that concentrate in these crevices causing clearance problems.
- Inter-granular stress corrosion cracking (IGSCC) - IGSCC is usually observed near locations where IGA occurs. IGSCC is caused by a combination of a caustic environment and elevated mechanical stress, while IGA does not require stress to proceed.
- Fretting - Fretting is caused by flow induced vibration that results in rubbing between the tubes and tube supports.
- High-cycle fatigue - High-cycle fatigue is also caused by flow induced vibration. This type of failure was observed at the North Anna Unit 1 plant.
- Pure water stress corrosion cracking (PWSCC) - PWSCC is observed in high stress tube regions: tubesheet expansion transition, sharp U-bend and dented tube regions. Locations where PWSCC occur suggest that this mechanism is caused by high residual tensile stress.

As this list indicates, most PWR steam generator problems are caused by water chemistry issues on the shell side with the exception of fretting, high-cycle fatigue and PWSCC. Since sodium - heated steam generators use sodium on the shell side, they do not suffer from most PWR steam generator problems. However, flow induced vibration (fretting and high-cycle fatigue) and PWSCC failures on the tube side were also observed in early sodium - heated steam generators, but these failures were addressed in the early developmental phase. Furthermore, the helical coil steam generator has not experienced fretting, high-cycle fatigue, or PWSCC because the tube support and tube-to-tubesheet welds are different from those used in straight and U-tube steam generator designs.

7.2.5. Fuel handling and transfer system

The reactor refuelling system provides the means of transporting, storing and handling reactor core subassemblies, including fuel, blanket, control, and shielding elements. The system consists of the facilities and equipments needed to accomplish the scheduled refuelling operations.

The tasks that a fuel handling system (FHS) has to fulfil are the following (including the loading and unloading of Fuel Assembly (FA) are:

- Arrival of new assembly;
- New fuel storage;
- Preparation of loading (with potential conditioning);
- Loading (using the same handling route as the unloading);
- Internal transfer (including the internal storage);
- Unloading (can include an External Vessel Storage Tank: EVST);

– Out of vessel transfer;
– Evacuation (can or cannot include a cleaning operation);
– Storage for fuel cooling (in sodium, gas or water).

Based on this very general principle, several technological options can be chosen and have been applied on reactors. The aim of the next part is to present the various major options that can be selected and then illustrated by the choice made on the French SFRs.

7.2.5.1. Potential options for the fuel handling route design

Before defining the several routes chosen in the past and that could be investigated for the future, a review of the different options has been carried out using the Fast Reactor Database [237] and recent technological development in SFR design. This list is not exhaustive but is considering the main options. The major innovations in the FHS routes are described in Fig. 7.30.

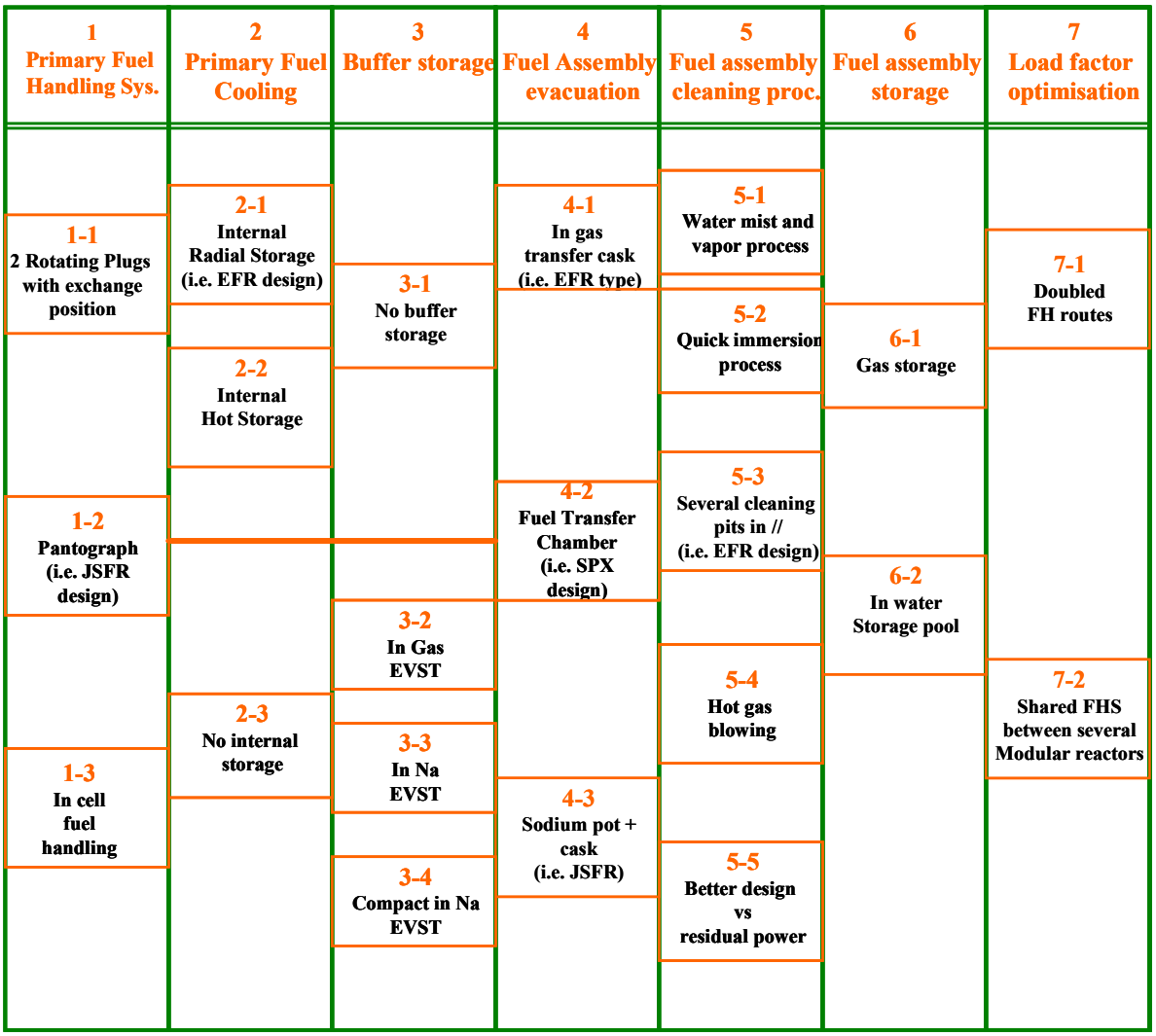

FIG. 7.30. List of different technical options for the FHS route.

Column 1: Primary fuel handling systems

In the primary FHS, the French reference design is a system with two rotating plugs associated with an exchange position (option 1-1). This design is particularly suitable with the pool type reactor where the FHS is not in the critical sizing for the primary vessel diameter. In the case of a loop type reactor, the FHS is directly involved in the critical value for the primary vessel diameter optimisation. In that case, a slotted Upper Internal Structure (UIS) with pantograph type FHS (option 1-2), as it is foreseen on the JAEA Sodium-cooled Fast Reactor design [4], or an in-cell FHS (option 1-3) can be envisaged.

Column 2: Primary fuel assembly cooling

Three solutions are considered for the primary fuel cooling. The most known consists to realize an internal radial storage as on EFR reactor vessel [2, 3]. In that case, the reactor vessel can accept a large number of fuel assemblies (i.e. 244 locations at EFR), by designing two rows of assemblies after the neutronic shielding. This solution impacts the reactor vessel minimum diameter. The second solution is characterized by a cooling zone on the upper part of the core structure, around the Upper Inner Structure. In the third solution, there is no internal storage.

Column 3: Buffer storage

The buffer storage vessel (also named External-Vessel Storage Tank) is an essential component designed to allow assemblies thermal power decay before their cleaning and unloading. Nevertheless, in different situations some SFR have been designed without any buffer storage. The main reason to suppress this component can be argued by its high investment cost: for instance the Superphénix EVST had roughly the size of the Phénix primary vessel. In that case, the core management must be adapted to this option. This is what was designed for instance on the EFR reactor concept, or on the Superphénix solution adapted strategy after the replacement in 1987 of the sodium EVST by an in argon fuel transfer chamber with no buffer storage.

If an EVST is taken into account, two solutions can be adopted. The most known is the use of an in sodium EVST as it is done for Phénix reactor, for Superphénix reactor before 1987, and for several SFRs in operation or under project all over the world. The major improvement in an in Na EVST is to design a storage concept providing the optimized storage compactness with equivalent functions of cooling the fuel assembly for the same residual power, and avoiding any criticality risk.

Thus, the Phénix EVST compactness is calculated to be 2.63 FA/m², Superphénix EVST compactness was 5.88 FA/m², the target is to reach over 10 FA/m² with a modification of the handling principle.

The second way is to use an in gas EVST. This solution was for instance used during the Rapsodie operation even if it was not integrated in the first design. Indeed, in 1972 in argon EVST has been constructed for Rapsodie to be able to disconnect the primary and the secondary fuel handling. This cooling buffer tank was constituted of 30 locations for FA in pots. The residual power was limited to only 0.4 kW per assembly.

Column 4: Fuel assembly evacuation

Three solutions are identified for the FA evacuation from the primary vessel: in gas through a transfer cask, in sodium pot through a fuel transfer chamber and in sodium pot + cask (mixed solution). Each solution is technologically feasible and has been already used on operating SFRs. The major differences between these options are principally the transfer time and the maximal residual power accepted by the solution. These two parameters can directly influence the core management and the availability factor.

Column 5: Fuel assembly cleaning process

The cleaning process aims at removing the residual amount of sodium retained on the FA after its extraction before a safe storage in water or in gas (Figs 7.31 and 7.32).

FIG. 7.31. Superphénix fuel assembly before cleaning.

FIG. 7.32. Superphénix fuel assembly after cleaning.

During this process, the purpose is to realize in a short time:

(i) The safe removal of the residual sodium (estimated to a range of 300 to 700 grams of residual sodium per assembly on Superphénix assemblies);
(ii) The continuous cooling of the assembly to prevent from any pin failure.

The process used a series of water atomization phase mixed with carbon dioxide gas (option 5.1). Two challenges are considered for this process: a quicker process (option 5.2) and a process allowing the possibility to clean FA with higher residual power (option 5.5). Today the limitation is set on Superphénix to 7.5 kW. The aim is to raise it up to 10 kW and ideally 15 kW. These new operating conditions would have a large influence of the defuelling rate and could ease the whole core management. To accelerate the cleaning rate another solution could be to double (or multiply) the cleaning facilities (option 5.3). Another way investigated is to reduce the residual amount of sodium with hot argon blowing prior to its fast cleaning (option 5.4). At least another solution should be to improve the SA design to allow a better draining and avoid sodium retentions.

Column 6: Fuel assembly storage

Two solutions are available: in water storage or in gas storage. These two technical options are just mentioned but are not subject to be investigated in this study.

Column 7: Load factor optimisation

The load factor optimisation can be envisaged in several ways: by doubling the sensitive components identified on the fuel handling route (i.e. the cleaning pit is considered to be on the critical path). Another innovative solution is to share the whole FHS between several modular reactors. Several ideas are presented in Fig. 7.33.

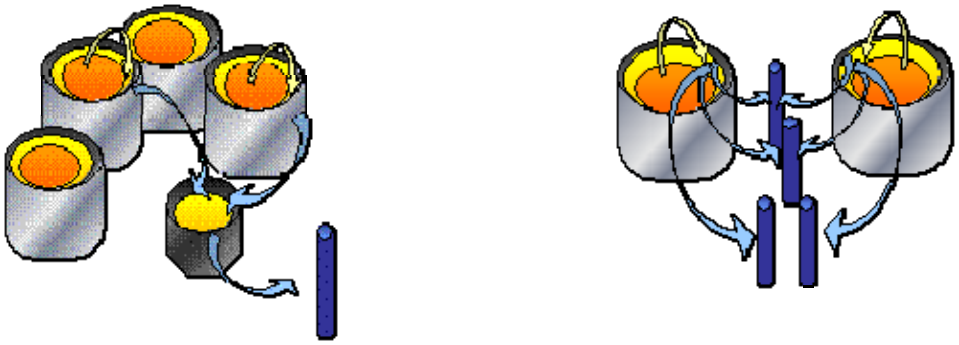

FIG. 7.33. Two different ways for load factor optimization.

The basic idea is to have a unique FH route used for several reactors. It would give gains in investment cost and also in the FHS load factor. To identify the best options a computer tool is under development, where the optimized parameters will be the availability factor and the investment cost.

7.2.5.2. Review of national SFR FHS options

7.2.5.2.1. Review of some French fuel handling system design options

The past and current operation of French sodium fast reactors (Rapsodie, Phénix and Superphénix) is providing a substantial experimental feedback of the several options chosen on FHS. The scaling up from Rapsodie (40 MWth) to Superphénix (1 200 MWe), passing through Phénix (250 MWe), is also an illustration of some solutions available for small size reactors that cannot be applicable to larger scale. Therefore, this part presents the several options chosen on the French reactor and provides much experimental feedback. A detailed review of the three French reactors can be found in the Refs [9, 10].

The Rapsodie fuel handling system and experimental feedback

The Rapsodie reactor operated from January 1967 until October 1983. The basic principle of Rapsodie fuelling/defuelling route was based on an in gas transfer with a multi-purpose cask. With time and experience, this unique cask has been changed to multiple casks adapted to specific situations but easier to handle and with less technological integrated systems. Two rotating plugs were able to access every assemblies. An internal storage was designed and every FA could be transferred at a peripheral position for internal cooling when its residual power had reached 25 kW. For unloading of the reactor vessel, the admissible residual power

was first 2 kW with an argon blowing cooling system. After several troubles and mainly due to sodium aerosol production, the argon blowing had been suppressed and the acceptable residual power had been decreased down to 0.4 kW. In 1972, an argon EVST was built to decouple the primary and secondary fuel handling. This buffer storage solved numerous situations and allowed the reactor to have an acceptable load factor.

The Phénix fuel handling system and experimental feedback

Phénix is a 250 MWe demonstration reactor that operated from March 1974 to May 2009, with extensive modification works in the 1990s for lifetime extension [6–8]. The Fuel Handling System is based on an internal storage (that can store one half of the core) plus and in sodium EVST (that can store one core). The access of every assembly is done by one single rotating plug and a Fixed Arm Charge Machine (FACM). The assembly can be transferred to the peripheral area for internal cooling at a residual power of 40 kW. The transfer to the EVST could be done at 6 kW Residual Power. The cooling time in the EVST is set to a minimum of one month. A significant amount of knowledge in fuelling/defuelling operations has been acquired, and no major difficulty was noticed in the 35 years of operation.

The Superphénix fuel handling system and experimental feedback

Superphénix is a 1200 MWe power reactor that reached criticality in September 1985 and was prematurely stopped in February 1998. The fuel handling route was first very similar to the one designed for the Phénix reactor with a scaling up of the several components. In principle it was composed of two rotating plugs associated with a transfer machine that put the assembly in the adequate position for the load/unload station that connects the primary vessel to the in Na EVST. In this configuration the rules to transfer an assembly were at a maximum residual power of 28 kW to go to the EVST. There was no internal storage.

The cleaning process could be done at 7.5 kW residual power. The core management was defined at Frequency 2. In 1987, a sodium leak occurred on the primary tank of the EVST [13], and after several investigations [14], it has been decided to replace it by an in argon Fuel Transfer Chamber (FTC) with no buffer storage for the assemblies. As a consequence it has been obliged to change the core management and to adapt the fuel handling route. The core management was defined at Frequency 1 (the whole core changed in one time) and an internal cooling zone has been prepared after core rearrangement for internal decay heat (from 35 kW down to 7.5 kW).

As an experimental feedback, it can be said that the major trouble of this system was the EVST leak. A technological solution has been found to replace it, involving a new component (FTC) associated to a new core management. The overall system has not been tested in time due to the premature shutdown of the Superphénix reactor. No refuelling was done on this reactor and the first significant use of the FH route was for the final unloading.

The Superphénix 2 project fuel handling system

The Superphénix 2 project uses the Superphénix options as regards handling equipment layout in the secondary confinement – favourable from a safety standpoint – and maintenance of the fuel transfer machine in the reactor block to limit the duration of shutdowns for removal of failed sub-assemblies from core. The small-number of sub-assemblies being handled (i.e. 97 fissile subassemblies per cycle) makes it possible to simplify the equipment on the basis on one-by-one sub-assembly handling.

The fuel transfer machine services all the diagrid and lateral neutron shield support holders, together with the in-reactor fuel handling station. Its rigid arm design allows centring of the core – vessel – large rotating plug assembly. The sub-assemblies, transferred in upright position, are gripped at the top by the machine which provides vertical motion, then translated by motions of the rotating plugs. The sub-assembly is transferred into the hot pool directly from the initial holder to the final holder. An ultrasonic viewing device (VISUS) incorporated in the above core structure provides assurance that there are no obstacles above the sub-assembly heads before any handling operation. The charge-discharge system provides transfer of new and irradiated sub-assemblies between the in-reactor fuel handling station and the secondary charge-discharge facility outside the reactor block. The system is designed to accept an irradiated sub-assembly hang-up of unlimited duration in the worst-case position on the transfer path. The rotating transfer lock is removable after isolation of the reactor block and of the secondary charge-discharge facility.

Local running of the handling systems simplifies the control/instrumentation hardware and facilitates servicing. The irradiated fuel assembly chain allows three types of disposal:

(1) Wet route disposal after washing of the subassemblies and decay storage in a cooling pond, allows subsequent shipment under gas atmosphere to reprocessing plant. It is used for sound fissile sub-assemblies (with a decay heat of about 2.3 kW) and fertile sub-assemblies (removed after a decay period of about 6 months). This route takes the sub assembly to the cooling pond rack then, after decay, the sub-assembly takes a reverse path to the gas-blanketed shipping cask for final disposal;
(2) Dry route disposal, after washing and storage in a gas atmosphere, is used for absorber subassemblies. These are then routed to the dry storage pit in shipping casks;
(3) Sodium route disposal is for fuel subassemblies which cannot stay in the internal storage.

Removal of the sub-assemblies from the reactor building takes about 16 weeks, at a rate of one cask per week.

The new fuel sub-assemblies chain comprises:

- A receiving hall for the containers coming from the fuel fabrication plant;
- An upender elevator for transferring the sub-assembly from the hall to the control station;
- A transfer tube for routing the sub assembly from the control station to the handling corridor;
- A control station.

Sub assembly control-conducted both before storage and before transfer into the reactor block is carried out in a sealed cell. For this operation, the operator has viewing windows and a remote monitoring system.

Concerning the global fuel handling systems, major simplifications have been made since Superphénix:

(1) Integration of the cooling pond in the reactor building, yielding a gain on investment and an increase of operating throughputs (paths to be covered are much shorter).
(2) The elimination of the storage drum and its replacement by the secondary charge-discharge facility, which is a simple input-output station.

The EFR project fuel handling system

The European Fast Reactor (EFR) is a 1500 MWe SFR project reactor. This project officially started in 1988 (even if some previous studies for a large commercial SFR were done before, known as Superphénix 2). This project stopped in 1998 with a detailed design of the reactor [2]. The fuel handling route is described by: two rotating plugs with a Fixed Arm Charger Machine and a Direct Lift Charge Machine (Fig. 7.34), no EVST, an internal cooling area and two cleaning pits operating in parallel to enhance the defuelling rate.

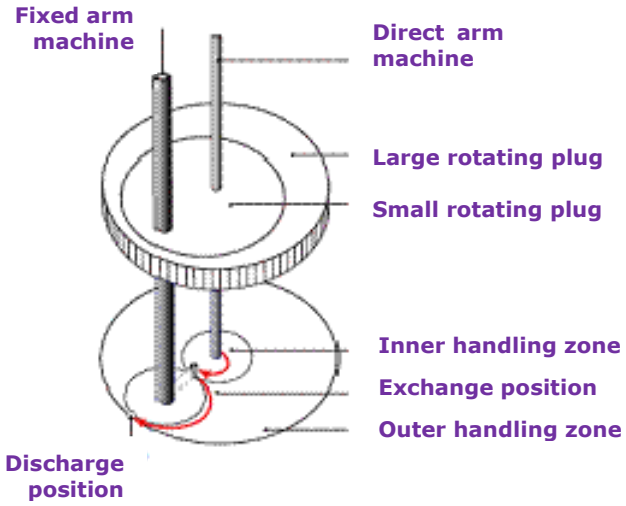

FIG. 7.34. EFR primary FH.

The EFR core management was at Frequency 5 (meaning 20% of the assemblies are changed every 425 days). As the project was not finalized by an industrial realization, the experimental feedback of this solution cannot be reported.

Conclusion of the experimental feedback on the French fuelling/defuelling systems

The Rapsodie and Phénix reactors have provided enough operating time to allow to have a significant experimental feedback. It has been shown that the in gas transfer for Rapsodie was efficient but has proven some limitations due to its low acceptance regarding to residual power. The Phénix system providing a redundancy in cooling solutions (internal plus EVST) and operating integrally under sodium is an industrial example of a simple, reliable and efficient solution for SFR FHS. Its optimisation regarding to cost investment and primary vessel diameter has not been the first concern during this design. In this subject area, the following part is presenting an extensive study of the Fuel Handling System optimisation regarding its compactness.

7.2.5.2.2. Review of Korean SFR FHS2

The KALIMER-600 Reactor Refueling System (RRS) provides the means of transporting, storing and handling reactor core assemblies, including fuel, control, and shield.

The system consists of the facilities and equipment needed to accomplish the normal scheduled refueling operations and all other functions incident to the handling of core assemblies.

The system consists primarily of the in-vessel transfer machine (IVTM), the two rotating plugs, and the fuel transfer port which are located entirely within the reactor area. The IVTM has two lifting devices, one is a direct core-assembly lift machine (DLM) and the other is a rotatable fixed-arm type lifting machine (FALM).

The DLM is installed at the center of the UIS in the small rotating plug and covers the inner driver fuel zone of the core.

The FALM is also located on the small rotating plug, outside of the UIS. There are two rotating plug drives, small and large sizes. These have an electromechanical system in which the electrical power to the motor of the plug drive is controlled to rotate and position the reactor rotating plugs and IVTM during refueling. In the drive, the output torque of the motor is transmitted through a reduction gear set to impart rotational motion to the reactor rotating plug. By controlling the electrical power to the motor, clockwise (CW) motion, counter-clockwise (CCW) motion, accurate angular positioning of the plug is achieved. Fifteen days have been allotted for an average reactor refueling. This begins with reduction of reactor power from 100% to the power level from which the reactor is shut down. The sodium in the reactor vessel is cooled down to a refueling temperature 200°C, the control rod drive-lines are disconnected from the absorber assemblies and raised, permitting rotation of the rotating plug in the reactor head, and the above the rotating plug, IVTM drive mechanism is installed. Concurrently, the reactor cover gas is purged and purified to reduce radioactivity levels in the gas to a very low level.

7.2.5.2.3. Review of Indian SFR FHS

Core subassembly handling includes handling of both fresh and spent subassemblies (SA). The types of subassemblies handled are fuel, blanket, absorber and reflector subassemblies. Fresh SA handling involves receipt, inspection, storage and loading of SA into main vessel. The spent SA handling involves in-vessel transfer, storage within the main vessel at in-vessel storage locations, discharge from main vessel, washing, storage outside main vessel and shipping of spent SA in shielded cask.

The in-vessel handling scheme uses a combination of two rotatable plugs (large and small) and an offset arm type fuel handling machine called the transfer arm (TA). Positioning of the TA to the required core location is carried out by the combined rotation of both rotatable plugs and transfer arm. The large rotatable plug is located concentric to the core and the small rotatable plug is nested within the large rotatable plug and is eccentric by 667.5 mm from the centre of large rotatable plug. The TA is located in small rotatable plug at a radial distance of 1275 mm from the centre of the small rotatable plug.

Fuel handling is carried out after about 185 effective full power days (EFPD), which is equivalent to 8 calendar months. This is roughly one third of average residence time (2 y) of fuel for a target burnup of 100 MWd/kg. 62 fuel SA, 33 blanket SA and 4 absorber SA are replaced during every fuel handling campaign. It is estimated to take ~ 20 d to complete one fuel handling campaign. The sodium temperature in main vessel during fuel handling is reduced to 473 K (200°C) and the argon cover gas pressure is lowered to 0.3-0.5 kPa (3-5 mbar) to reduce radioactive argon leak into reactor containment building. Before commencement of the fuel handling campaign, the cover gas in the main vessel is flushed with fresh argon if radioactivity of cover gas is more than the specified limit. This reduces the leakage of radioactivity from the main vessel to the reactor containment building.

During handling, the maximum clad nominal temperature is limited to 923 K (650°C) and a limit of 5 kW is fixed for the decay heat of spent fuel SA at the time of its discharge from main vessel. This level is expected to be reached after 100 d of in-vessel storage.

Internal storage locations for 156 SA beyond the blanket is provided. The number of fuel SA to be discharged in the scheme of batch refueling is determined by the maximum burn-up of fuel, the decay period in the in-vessel storage, the limit on decay heat during handling and the number of in-vessel storage positions provided. A reduced sodium flow is provided in the in-vessel storage positions.

Shielding for the core is provided in the form of steel and B_4C shielding subassemblies. The outer steel and B_4C shielding SA (beyond storage locations) are designed for a life of 40 years and are not handled normally. Handling of these SA will be required only during decommissioning. These SA will be handled by a pantograph type machine, which will be introduced through an opening in large rotatable plug. The pantograph machine is under design and will be used when the need arises. The inner B_4C shielding/reflector subassemblies are designed for a life of 10/20 years and hence require handling during the life of the reactor.

At a time only, one SA is handled in the core and at any other working position. The subassemblies remain vertical during handling and storage. Only after a SA discharged from the core has been replaced by a fresh SA, the next SA is discharged from the core. Absorber rod SA is replaced first during a fuel handling campaign followed by blanket and fuel subassemblies.

During in-vessel handling operations, the SA is kept submerged (except top 170 mm which is in argon cover gas) in sodium to ensure adequate cooling (decay heat of spent fuel SA is 28kW, 2d after reactor shutdown). When absorber subassembly (ASA) is being removed, an alarm is provided in the control room to alert the operator. To prevent inadvertent removal of ASA, its level is kept 40 mm below other SA.

The entire core is divided into 14 flow zones. The flow decreases from inner to outer zones and is achieved by changing the hydraulic resistance of SA. The foot profile of SA is such that a fuel SA cannot go into ASA location. The foot profile is such that SA of outer zone cannot be fully inserted into inner zones where lower enriched fuel SA is loaded. Failed fuel subassemblies if any, are transferred to internal storage locations to reduce the decay heat before they are discharged and canned inside the fuel transfer cell located in fuel building.

During fuel handling, the signals from neutron detectors are processed by pulse channels and the signals are taken through trailing cables. A minimum count rate is ensured, which is used as reference to detect any inadvertent handling of absorber SA or increase in count rate due to any reason. If the count rate exceeds the preset value, further handling operations are suspended.

Fresh SA handling scheme

Fresh fuel SA produces, on contact, radiation dose of 4 mSv/h (400 mrem/h) due to neutrons and 6 mSv/h (600 mrem/h) due to gammas. Fresh blanket SA produces negligible neutrons and a dose of 7.75 mSv/h (775 mrem/h) due to gammas on contact. The shielding for the core SA handling is designed based on the highest source of radiation from the SA being handled. The scheme of handling fresh SA is shown in Fig. 7.35.

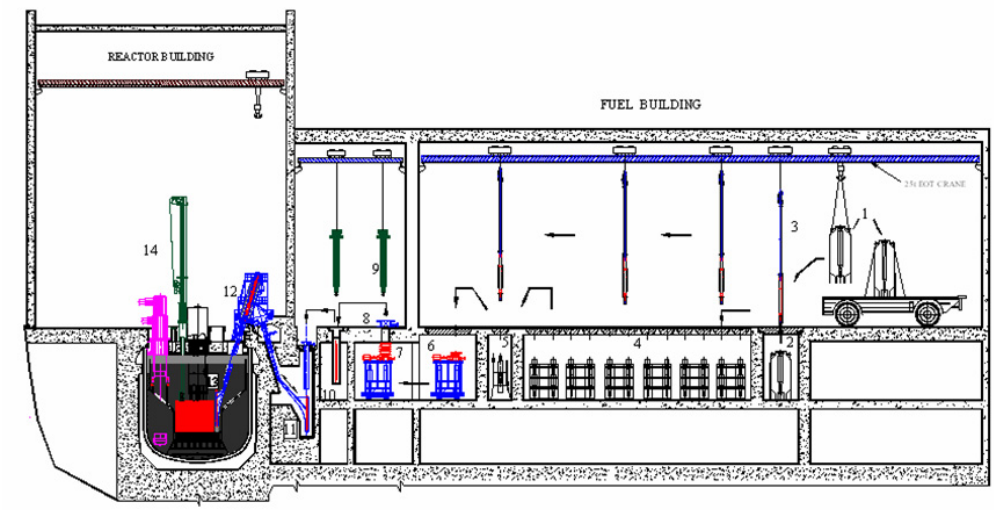

1. FRESH SA SHIPPING CASK
2. FRESH SA RECEIVING FACILITY
3. FRESH SA TRANSFER GRIPPER
4. FRESH SA STORAGE BAY
5. FRESH SA INSPECTION FACILITY
6. NITROGEN FILLING FACILITY
7. FRESH SA TRANSFER CHAMBER
8. FRESH SA ENTRY PORT
9. CELL TRANSFER MACHINE (FSA)
10. FRESH SA PREHEATING FACILITY
11. EXVESSEL TRANSFER POSITION
12. IFTM
13. INVESSEL TRANSFER POSITION
14. TRANSFER ARM

FIG. 7.35. Fresh subassembly handling scheme in PFBR.

The fresh SA are transported from the fuel fabrication plant to PFBR in Fresh fuel transport cask (FFTC). The cask is brought on a trailer into fuel building through the truck entry area. The cask is unloaded using the 100 t crane provided in the spent SA storage area on to the carriage for fresh fuel transport cask (CFTC). The carriage moves the cask from the spent SA area to the fresh SA area. The cask is then handled to the fresh SA receiving facility (FSRF) using the 25 t crane.

The fresh subassemblies are transferred one at a time to the fresh SA inspection facility (FSIF) using the fresh SA transfer gripper (FSTG). At the inspection facility, the subassemblies are checked visually for any apparent damage, checked for length to distinguish between fuel and absorber SA, checked for serial number and core zone for identification and proper loading. The accepted SA is then stored in fresh SA storage bay (FSSB) in separate stainless steel containers. The rejected subassemblies are stored similarly in the same storage bay at segregated earmarked locations.

During fuel handling campaign, the subassembly is once again transferred to the inspection facility and checked for enrichment level to identify the enrichment zone to which the subassembly belongs in case of fuel SA and checked for coolant flow to verify absence of blockage, after which it is placed in the fresh SA transfer chamber (FSTC). The chamber has provision to store 11 subassemblies and one failed fuel container. The chamber is evacuated after loading of subassemblies and filled with nitrogen in the nitrogen filling facility (NFF). The chamber is then handled and loaded on to the transfer chamber carriage (TCC). The carriage is moved to align the fresh SA transfer chamber with the fresh SA entry port (FSEP). The entry port connects the transfer chamber with the fuel transfer cell (FTC) through a gate valve. Within the fuel transfer cell, two cell transfer machines (CTM-FS and CTM-SS) are provided, one for fresh SA and the other for spent SA. The fresh SA cell transfer machine lifts the SA from the transfer chamber and transfers it to the Fresh SA preheating facility (FSPF)

where the SA is preheated to 473 K. The preheated SA is then transferred by CTM-SS to the ex-vessel transfer position (EVTP) located within FTC.

The EVTP is connected to the reactor containment building (RCB) by an inclined chute opening provided in the common wall between fuel building and RCB. The inclined fuel transfer machine (IFTM) located in RCB transfers the fuel SA from EVTP to the in-vessel transfer position (IVTP) located on the periphery of the reactor core. From the IVTP, the SA is transferred to the required core location using a combination of rotations of the Large and small rotatable plugs (LRP and SRP) and transfer arm (TA).

Spent SA handling scheme

The handling of spent SA from the core to EVTP is similar to that of a fresh SA indicated earlier except that the operations are carried out in reverse order. Using transfer arm and the large and small rotatable plugs, a spent SA is transferred first from an in-vessel storage location to IVTP and a SA from the fuel location is transferred to the in-vessel storage location. From IVTP, the IFTM transfers the SA to EVTP located within FTC. Thus, EVTP is a common port used for both fresh and spent SA handling beyond which, the spent SA handling route is separate from fresh fuel. From EVTP, the cell transfer machine (CTM-SS) transfers the spent SA to the spent SA washing facility (SSWF) located within FTC. The SA after washing is transferred to Under water trolley (UWT) through the Spent SA exit port (SSEP). The under water trolley moves on inclined rails and shifts the SA to a water filled bay.

The Spent SA storage bay transfer machine (SSTM) transfers the spent SA from the UWT to the storage racks located in the water filled spent SA storage bay (SSSB).Selected SA are transferred to the spent SA inspection facility (SSIF), checked for dimensions and then transferred to storage racks using SSTM. In case of failed SA, after sodium washing, the SA are loaded in separate leaktight water filled containers and stored separately in the storage bay. The absorber SA are not washed but stored in nitrogen filled leaktight containers at Absorber subassembly storage facility (ASSF) located within the fuel transfer cell.

The scheme of handling spent SA is shown in Fig. 7.36.

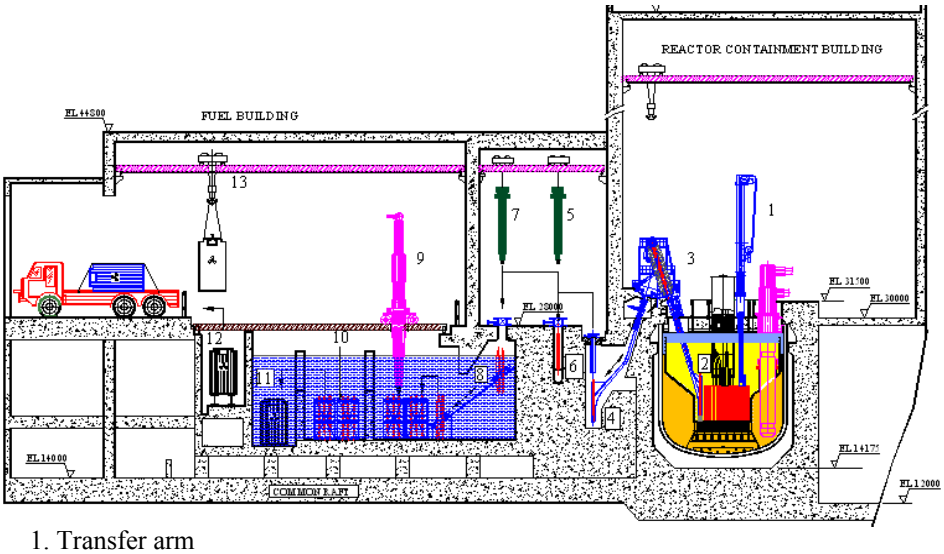

1. Transfer arm
2. In vessel transfer position
3. Inclined fuel transfer machine
4. Ex vessel transfer position
5. CTM (fresh SA)
6. Spent SA washing facility
7. CTM (spent SA)
8. Under water trolley
9. Spent SA transfer machine
10. Spent SA storage bay
11. Cask loading bay
12. Cask washing bay
13. Shipping cask

FIG. 7.36. Spent subassembly handling scheme in PFBR.

After cooling in the storage bay for 100 days in order to reduce the decay heat of the SA to 2.5 kW suitable for reprocessing, the subassemblies are transferred to a shielded shipping cask located in the cask loading bay. The cask is then shifted to the cask washing bay where it is washed and then loaded using the 100t crane on to a trailer. The trailer is used to shift the cask to the reprocessing plant. The absorber SA from ASSF are handled similar to that of a spent SA. In the case of failed SA stored in SSSB, the SA along with its container is again brought back to UWT using SSTM and the SA is transferred to a leaktight nitrogen filled container kept in Canned SA storage (CSAS) located within FTC. The water filled and the nitrogen filled containers are transferred to the reprocessing plant similar to a normal SA.

Cooling of SA, in fuel transfer cell, in case they are stuck, is effected by forced nitrogen flow through the gripper of CTM (SS). For spent SA storage bay, air is exhausted through ventilation ducts located close to the top of the pool in order to maintain the humidity in the accessible areas around the bay. A description of the important machines/facilities associated with core subassembly handling namely transfer arm, inclined fuel transfer machine and spent SA storage bay is given in the following sections.

Transfer arm

Transfer arm (TA) is permanently located on the small rotatable plug. Figure 7.37 shows the details of transfer arm.

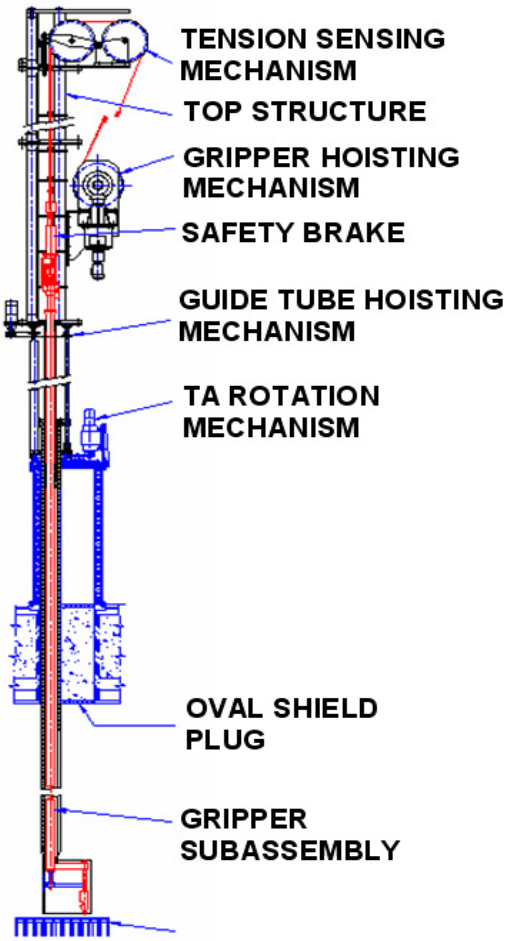

FIG. 7.37. PFBR Transfer arm.

The machine consists of gripper assembly, guide tube, gripper hoisting arrangement, safety brake, guide tube hoisting arrangement, tension sensing mechanism, gripper finger drive and oval shield plug. The gripper assembly consists of gripper head with three fingers, fixed to the gripper outer tube inside which moves the gripper inner tube. The gripper inner tube is connected to a linear actuator at one end and to an actuator rod at the other end, which by its translational movement opens or closes the gripper fingers. The gripper head is mounted offset with respect to the gripper tube. The gripper tube is hoisted vertically up and down using a wire rope. The gripper tube moves within the guide tube which protects the gripper from flow induced vibration. During reactor operation, both the gripper and guide tube are kept raised by 4.5 m to avoid activation. The machine has been designed for the following conditions:

- Weight of heaviest SA to be handled: 3500 kN;
- Weight of fuel SA: 2400 kN;
- Deviation in elevation of SA top in core: +20, -5 mm;
- Mismatch capability of transfer arm: ± 35 mm;
- Max insertion capability of TA: 10 kN;
- Maximum withdrawal capability of TA: 25 kN.

As it is not possible to reorient hexagonal sheath of SA by rotating the machine around its own axis, auto-orientation feature is provided on the head and foot of each SA. The lower part of gripper is mounted on roller bearings and rotates along with SA automatically when SA is lowered into the core.

To differentiate control rod from other SA, the top level of control SA is kept lower by 40 mm as compared to other SA. In addition, the weight of gripper along with the SA held by it is monitored to distinguish between various SAs. A tension sensing device is also provided which cuts off the power supply to the hoist drive motor if there is excessive load / low tension in the wire rope. A safety brake is provided on the gripper, which limits the free fall of gripper under gravity to less than 200 mm in case of failure of wire rope. All the operations of transfer arm are carried out remotely from the handling control room.

Inclined fuel transfer machine (IFTM)

The IFTM is supported on the reactor vault within the reactor containment building and is used to transfer a spent SA from inside the main vessel to outside the reactor (Fig. 7.38).

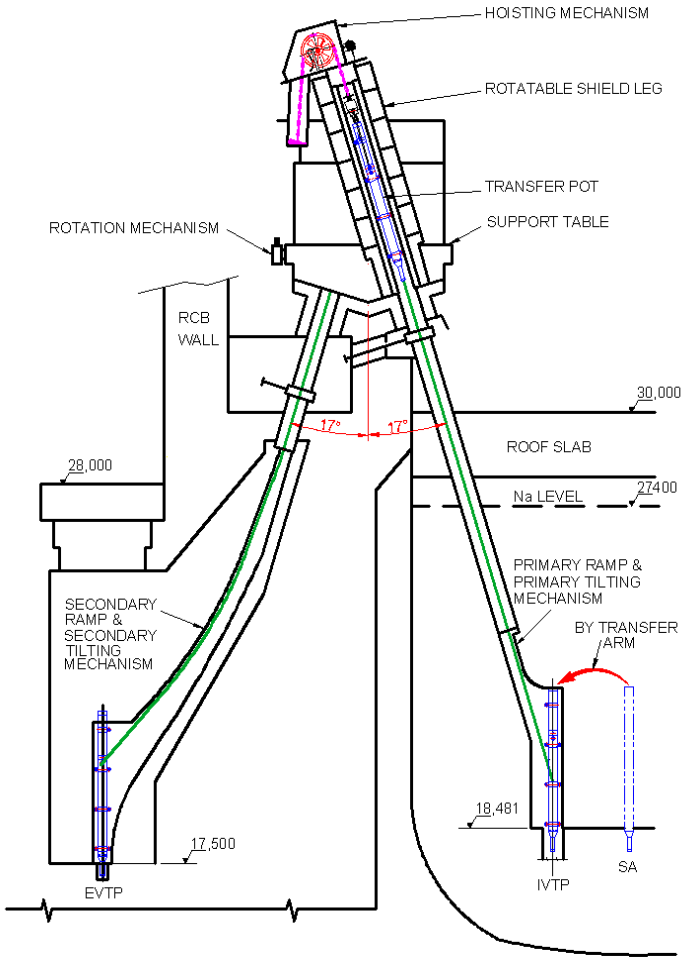

FIG. 7.38. PFBR Inclined fuel transfer machine.

The machine is 4.5 m in diameter, 24 m approx in height and weighs ~ 175 t. It consists of primary ramp, primary tilting mechanism, secondary ramp, secondary tilting mechanism and

rotatabe shield leg. The SA is loaded by the transfer arm into a sodium filled transfer pot, which moves on rollers. The pot is hauled up using a double chain arrangement into the rotatable shield leg. Rotation of the shield leg by 180^{o} aligns the transfer pot from the primary side to the secondary side. The pot is then lowered to the ex-vessel transfer port located in fuel building from where the SA to transferred by CTM to the washing facility. The spent SA is then exchanged with a fresh SA by CTM, which is then transferred to the core.

Spent SA storage bay (SSSB)

After sodium cleaning, the spent SA are stored in a dimenaralised water filled pool called the spent SA storage bay (SSSB). This is mainly required to reduce the decay heat of the SA to about 2.5 kW suitable for reprocessing. The bay has four compartments, two for storing fuel, one for cask loading and another for cask washing. The subassemblies are stored vertical in open storage racks. The spent SA storage bay transfer machine (SSTM) is used for transfer operations within the bay and for loading the SA into the shipping cask. The bay is provided with a cooling and purification system to maintain the temperature and chemistry of the water. It is also lined with stainless steel with leakage collection arrangement provided below the liner welds to monitor leakage of the liner. Adequate storage capacity is provided in the bay to permit full core unloading, if required.

Special handling scheme for PFBR

Special handling involves handling large sized radioactive components in a leaktight manner, cleaning and decontamination of the components before maintenance. All special handling operations are carried out inside the reactor containment building. To reduce the radioactivity of the components, two decay pits are provided for storage of the components if required. Two decontamination facilities are provided for sodium cleaning and decontamination and a wet CO_2 bubbling process is used. Special large sized flasks are used for handling of the components in a leaktight and shielded manner. A special handling frame with a tilting arrangement is also provided for tilting of components from vertical to horizontal before the components are sent out to maintenance building. Figure 7.39 shows the layout of equipment associated with special handling inside the reactor containment building.

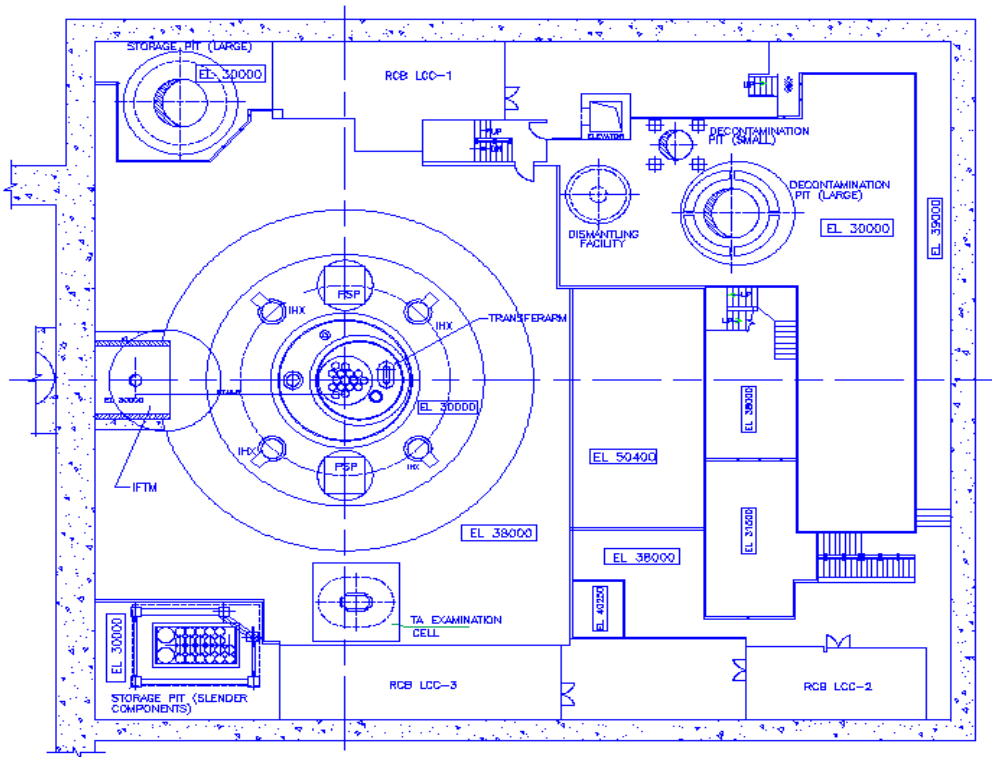

FIG. 7.39. Layout of special handling equipment in RCB.

Special engineering rigs have been established for full scale testing of the transfer arm and the IFTM. The transfer arm has been manufactured and is currently undergoing testing in air at Large component test rig (LCTR) (Fig. 7.40).

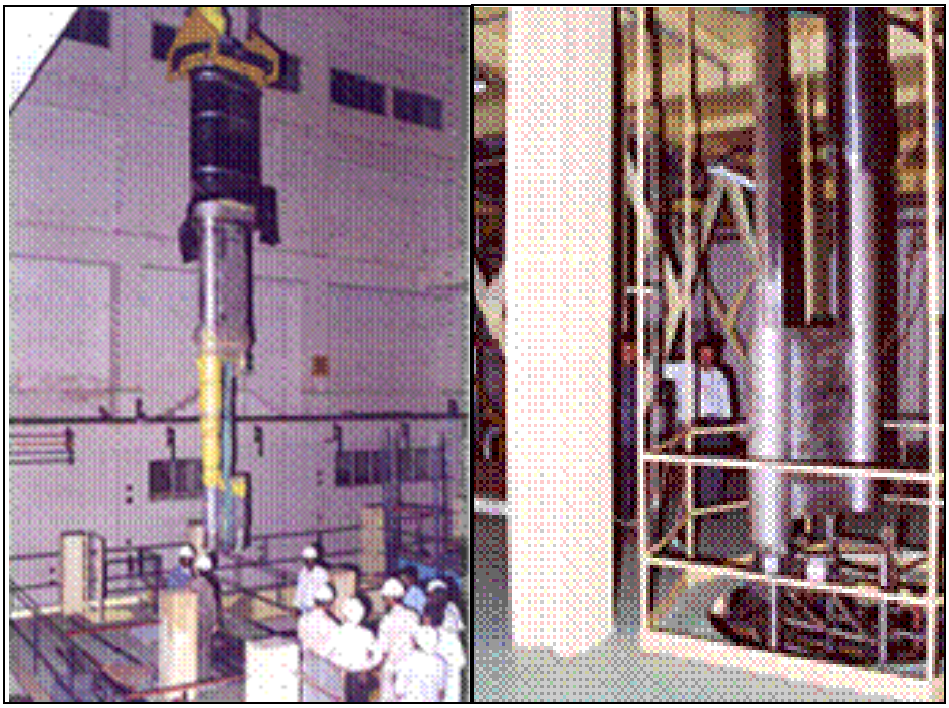

FIG. 7.40. Testing of PFBR transfer arm.

The machine carries out in-vessel handling operation of extracting a SA from a mockup core and grid plate, transferring the SA to a transfer pot and transferring it back to the core in a cyclic manner. Both air and sodium tests will be carried out. The IFTM is currently under manufacture and will also be cyclically tested in both air and sodium before it is used in the reactor.

About 10% of the total cycle life is planned during testing. In addition, separate tests are underway/planned to validate the subassembly washing process, sodium dripping time for transfer pot of IFTM and siphoning time for transfer pot of IFTM. The IFTM uses a set of three inflatable seals testing of which a separate test rig has been established.

7.2.6. Decay heat removal system

In the shutdown situation, as well as in the situation of the loss of the main heat transfer systems, the decay heat must be removed by additional decay heat removal systems. These systems can either make use of the still existing capabilities of the main heat transfer system or they will make use of additional subsystems specially designed for this purpose

In any case, it is preferable if the decay heat can be removed by passive means only (i.e. natural convection). Examples of decay heat removal are given below. The Korean KALIMER-600 design and the Indian PFBR designs are used for this purpose.

7.2.6.1. Passive heat removal system of the KALIMER-600

The residual heat removal (RHR) in the KALIMER-600 is safely accomplished by using a condenser cooling with a steam generator (SG) feed water system, intermediate reactor auxiliary cooling system (IRACS), and the passive decay heat removal circuit (PDRC) system. The normal heat transport path comprised of the PHTS, IHTS, and the main condenser cooling of the SGS is used for the normal power operation mode and a scheduled plant cool down process from the power operation to the refuelling mode. When the normal heat transport path is not available, an adequate emergency core decay heat removal methods should be provided to accomplish the safe cooling of the core and the sodium coolant boundary without exceeding the temperature limit.

Certain criteria have been established for an emergency decay heat removal (DHR) system design. That is, it has been decided that two independent diverse systems utilizing two different operating principals are needed to meet the licensing and design criteria. The potential candidates for these two systems in the KALIMER-600 are the non safety-grade IRACS and the safety-grade PDRC system. The IRACS is operated by using off-site power supplied active devices, and the PDRC system is passively operated by using natural circulations of the sodium and the air without any active components or operator action.

The IRACS is comprised of independent two loops connecting each IHTS loop, and it consists of the tube-side IHX, forced-type sodium-air heat exchanger (FAHX), sodium pipings connecting the IHX with the FAHX via a part of the IHTS loop, a motor-driven air blower and isolation dampers installed at the upper part of the air stack, a single electro-magnetic pump of each IHTS loop, and two isolation valves located at the IRACS cold leg and the IHTS side SG sodium exit pipe. The PDRC system is comprised of two independent loops, and each loop is equipped with a single sodium-sodium decay heat exchanger (DHX), single sodium-air heat exchanger (AHX), and the intermediate sodium loop connecting the DHX with the AHX.

Though both DHR systems have sufficient capacity for a scheduled or an emergency plant cooling process, the non-safety grade IRACS cannot be used if off-site power is not available. This is the reason why the PDRC system should be guaranteed as an ultimate shutdown DHR system in the KALIMER-600. To this end, the safety-grade PDRC system provides enough DHR capability during any abnormal condition, and it relies exclusively on natural convection heat transfer, i.e. a natural circulation on the sodium side and a natural draft on the air side.

The main function of the PDRC system is to remove the core decay heat generated just after a reactor trip such that the system is safely cooled down under upset conditions without damaging the mechanical integrity of the structures and components in the sodium coolant boundary. Since the PDRC system employs a completely passive concept without the provision of dampers being located in an air path of the sodium-air heat exchanger and isolation valves mounted on the hot and cold legs of the PDRC intermediate sodium loops, it has great advantages that an operational reliance of the DHR system can be considerably enhanced.

The DHX is a shell-and-tube type counter-current flow heat exchanger, and it consists of the cold sodium downcomer situated along the centre of the unit, and the plurality of the heat transfer tubes surrounding its outer circumference are concentrically arranged and are uniformly spaced apart from each other in a radial direction. The upper end of the cold sodium downcomer is connected to the cold leg of the PDRC loop, and the heated sodium collector located at the upper part of the heat transmitting unit is connected to the hot leg of the intermediate sodium loop. The DHX is located inside DHX support barrel which is situated in the hot sodium pool region, and each DHX support barrel has a lower end communicating with the cold sodium pool.

Hence, during normal plant operation, the sodium free surface inside the barrel is maintained at the same level as the cold pool free surface owing to the primary pumping head. The upper end of each barrel is positioned higher than the hot pool free surface to prevent undesirable inflow of the hot pool sodium during normal plant operation. Consequently, the DHX is positioned higher than the cold pool free surface, and thus the DHX heat transfer tubes do not directly come into contact with any pool sodium. This feature makes the heat loss through the PDRC system during normal plant operation pretty small even without air damper.

The AHX located above the reactor building is a counter cross flow shell and tube type heat exchanger, and it has the function of dumping the system heat load into the environment. The helical coil type AHX design was employed to properly accommodate heat transfer between the hot sodium and the cold air with fast thermal transients. The heat is transmitted from the hot pool into the intermediate sodium loop via the DHX, and a direct heat exchange occurs between the tube-side hot sodium and the shell-side atmospheric air through the AHX sodium tube surface. Cold atmospheric air enters the air inlet at the lower part of the unit and it flows upward across the heat transfer tube bundle located in the shell-side AHX. The inflow air is heated up in the bundle region and the heated air is collected at the top of the unit and then is discharged through the air outlet at the top of the air stack. The air stack of each AHX unit should be high enough to secure a required developing head, and it has rain protecting structures to limit inflows of rain water or harmful obstacles.

In a normal steady-state condition, DHX heat transfer tubes are not directly in contact with the pool sodium as depicted in Fig. 7.41.

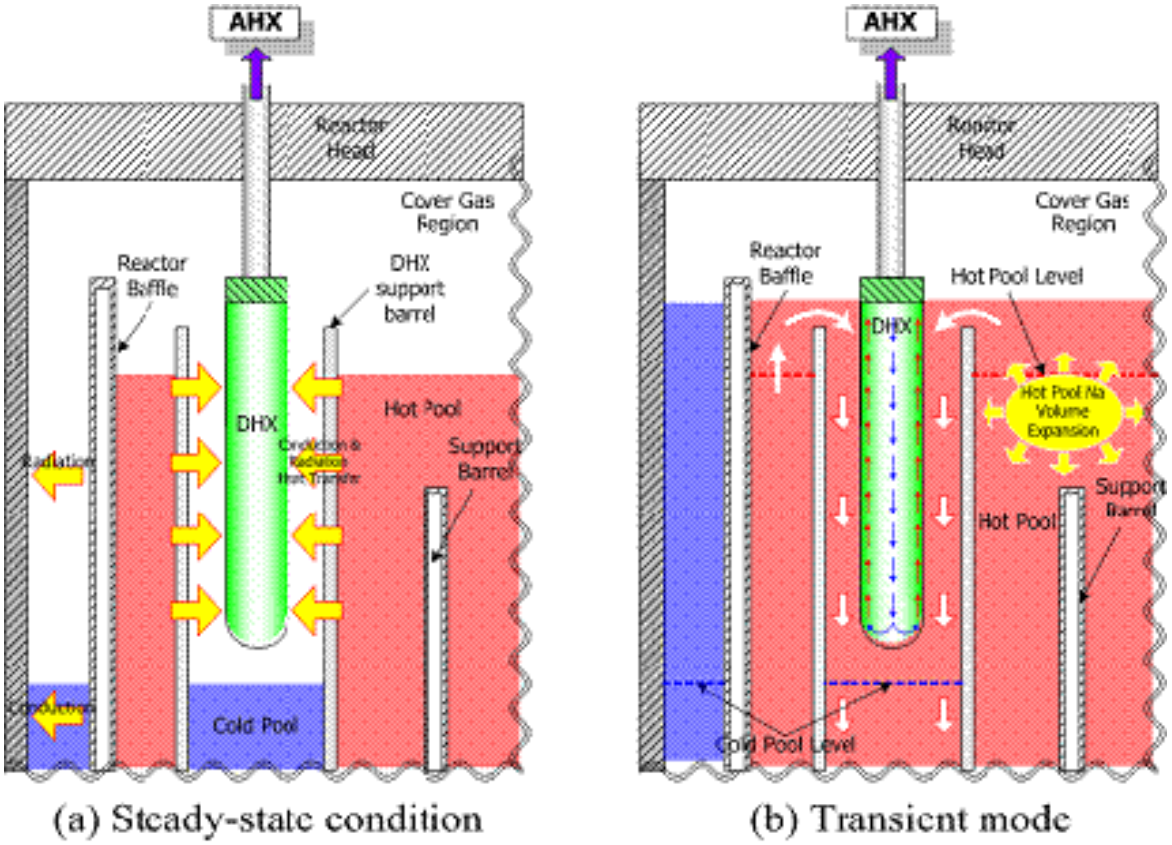

FIG. 7.41. DHR process of the PDRC system.

Consequently, the heat transfer in the shell-side DHX is achieved only by thermal radiation heat transfer. The DHX tube-side loop sodium, which has been cooled in the AHX unit, enters into the upper centre part of the DHX, and moves downward along the cold sodium downcomer. After turning 180 degrees inside the lower chamber connected with the bottom end of the cold sodium downcomer, the sodium moves upward along the heat transfer tubes. In this process, the DHX absorbs only the heat necessary for preventing loop sodium solidification by using thermal radiation process between the inner circumferential surface of the DHX shroud and the heat transfer tube surfaces. The heated sodium continuously moves upward by means of the density difference and is collected in the heated sodium collector located at the top end of the heat transfer tube bundle. The collected sodium is introduced into the AHX heat transfer tubes via the hot leg of the intermediate sodium loop, and then it is cooled down at the AHX sodium tube region by heat transfer between the tube-side loop sodium and the shell-side atmospheric air. Thereafter, the cold sodium returns into the DHX via the cold leg of the intermediate sodium loop, and the process is repeated during the whole period of the normal plant operation.

Under transient conditions such as a total loss of heat sink accident, the level difference between hot and cold pool disappears because the primary pump trip following the reactor shutdown. In this case, since the normal heat transport path is not available, the hot pool sodium is expanded due to a continuous decay heat generation. Consequently, hot sodium overflows into the shell-side DHX and then the cooled sodium flows into the cold pool region. As the naturally circulating sodium flow rate in the shell-side DHX increases, the heat transfer rate through the DHX is rapidly increased owing to the rapid increase of convection heat transfer. The system is self-regulating since the heat removal capacity of the PDRC

system is directly proportional to the pool sodium temperature variation. To this end, a transient decay heat removal accomplished by using the PDRC system is activated based on the total passive concept. Consequently, the core decay heat is continuously discharged into the environment without either an operator's action or any active component actuation.

7.2.6.2. Decay heat removal system of the PFBR

Safety criteria followed for plant design requires the non-availability of decay heat removal (DHR) function be less than 10^{-7} per reactor-year. To achieve this, two diverse and independent DHR systems are provided i.e., normal heat removal path consisting of secondary sodium loops, Steam Generators and Steam Water System (SWS) known as the Operation Grade Decay Heat Removal (OGDHR) system and SGDHR system. The availability of the OGDHR system depends on the number active components, so its reliability is low. The SGDHR (Fig. 7.42) system is a passive system, hence it is highly reliable.

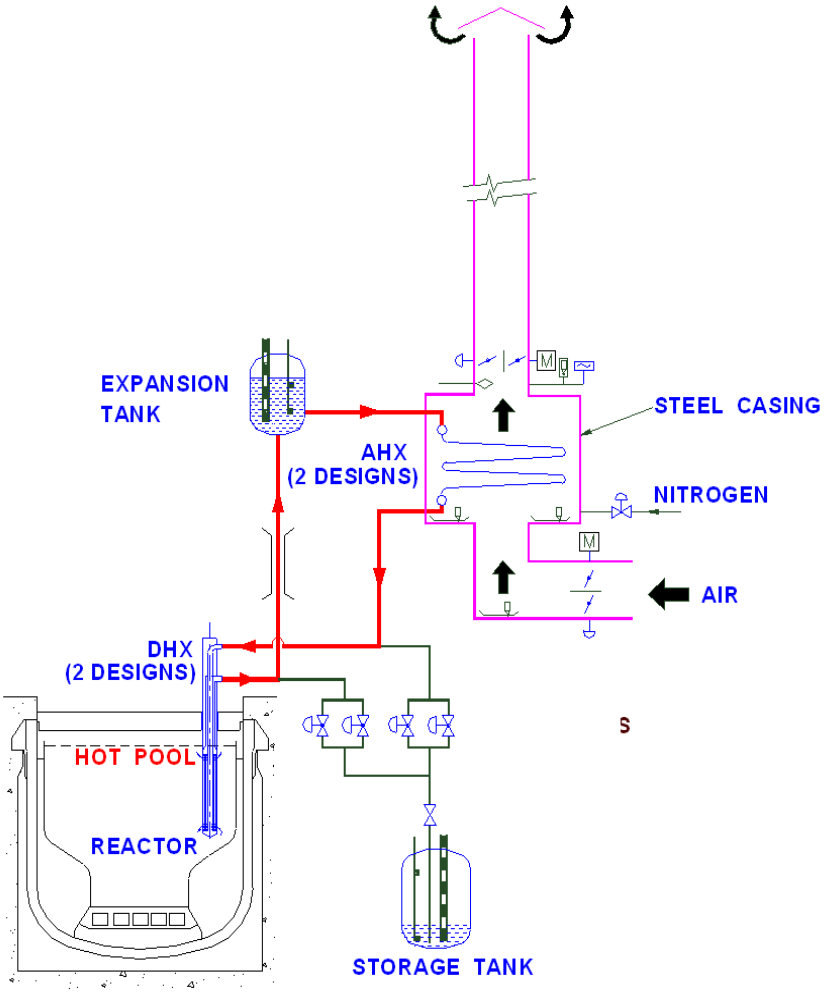

FIG. 7.42. PFBR SGDHR system.

The SGDHR system is used following any Design Basis Event (DBE), which incapacitates the Steam Water System (SWS) of both the secondary sodium loops by enabling heat removal directly from the hot pool. The bounding set of events that cause demand on SGDHR system is off-site power failure, loss of SWS and Station Blackout (SBO).

The SGDHR system consists of four independent loops, each having 8 MW heat removal capacity (at a hot pool temperature of 820 K). It is a passive system except for the air dampers on the airside. It is admissible to raise the reactor power to full power only when all the four circuits are available. In other words, if one SGDHR circuit becomes unavailable during normal operation of the reactor on power, reactor is shutdown through the controlled shutdown mode. Each circuit consists of a sodium to sodium heat exchanger (DHX) dipped in hot pool, a sodium to air heat exchanger (AHX) placed outside the Reactor Containment Building (RCB), an expansion tank, a storage tank and associated sodium piping and valves. The DHX and associated piping are housed in RCB and all other components and piping are placed outside RCB and are placed in the steam generator building. The AHX and expansion tank are placed on the roof of steam generator building. The stack top is provided with hood to avoid entry of rainwater, birds etc.

The DHX transfers heat from radioactive primary sodium to intermediate sodium. The primary sodium flows on the shell side of the heat exchanger (HX), whereas the intermediate sodium flows inside the tubes. This HX is supported on roof slab and its tube bundle is immersed in hot pool sodium. This HX is removable from top when reactor is shut down. The tubes are rolled and welded to the tube sheets. The shell at the primary sodium inlet is perforated with holes for sufficient length to permit primary sodium entry for the case of lower sodium level following leak in the main vessel, which is a category 4 event.

The AHX dissipates heat from intermediate sodium to atmospheric air. This mode of DHR is passive. The only active element in the system is the 2 air dampers (one at the inlet and one at the outlet) in the air circuit which have to be opened on demand. The air dampers at the inlet and outlet are (two-louvre type) divided in to two halves and one half is motor operated and the other half is pneumatically operated for ensuring diversity. The air dampers are opened on auto mode when the SGDHR system is required for DHR. The dampers can be opened by manual command (remove manual) from the control room. If manual operation from control room also fails, dampers can be opened manually by sending operators to the damper site. Provision is also there to open the dampers manually at damper site.

Diversity in the design of the DHX and AHX is adopted in SGDHR system to obtain the required reliability values. For diversity in the DHX, different tube size and tube arrangement is used in Type A and Type B (Fig. 7.43).

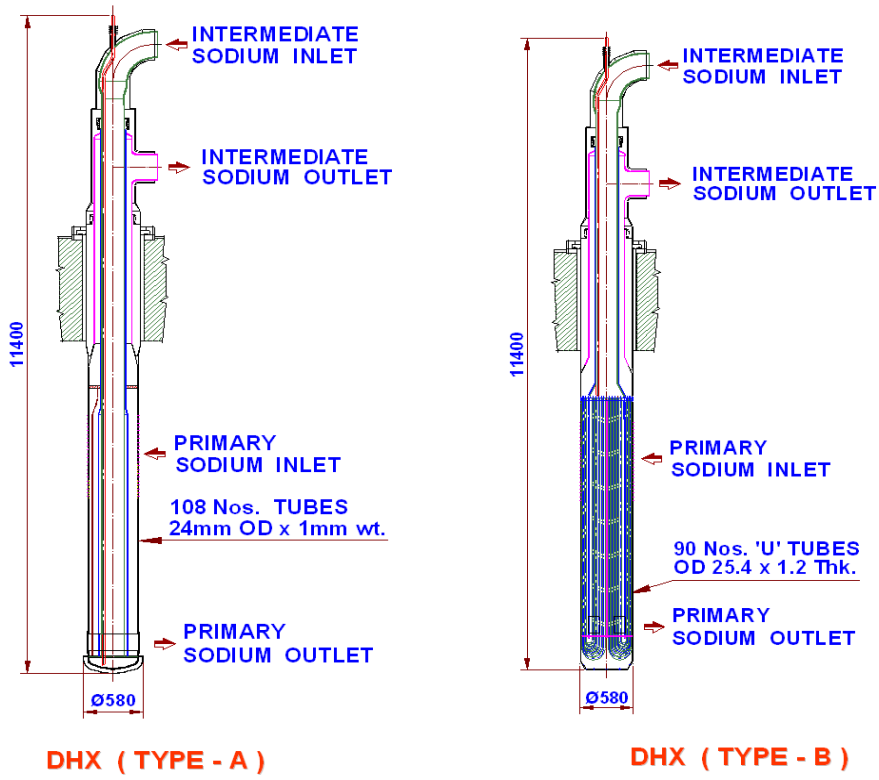

FIG. 7.43. Diversity in PFBR DHX designs.

The DHX (Type-A) is a vertical counter-flow shell and tube HX consisting of straight tubes with expansion bends in the argon space. The DHX (Type-B) is a vertical, U- tube shell and tube HX with expansion bends in the argon space and the tube sheet is of split type.

For diversity in the AHX, different fin type, fin height, number of fins per unit length and tube bundle arrangement are adopted. In Type A, a serpentine type horizontal tube bundle is used. In Type B, a straight vertical tube bundle is used.

Two SGDHR loops have one design of DHX (Type-A) and AHX (Type-A) and the other two SGDHR loops have different design concept for DHX (Type-B) and AHX (Type-B). There are two SGB in the plant, one on either side of the RCB. SGB1 contains 2 SGDHR loops, one of Type-A and other of Type-B and SGB2 contains 2 SGDHR loops, one of Type-A and other of Type-B. The intermediate sodium flow by natural circulation is obtained by placing the thermal centre of the AHX ~ 41 m above the thermal centre of the DHX (Fig. 7.44).

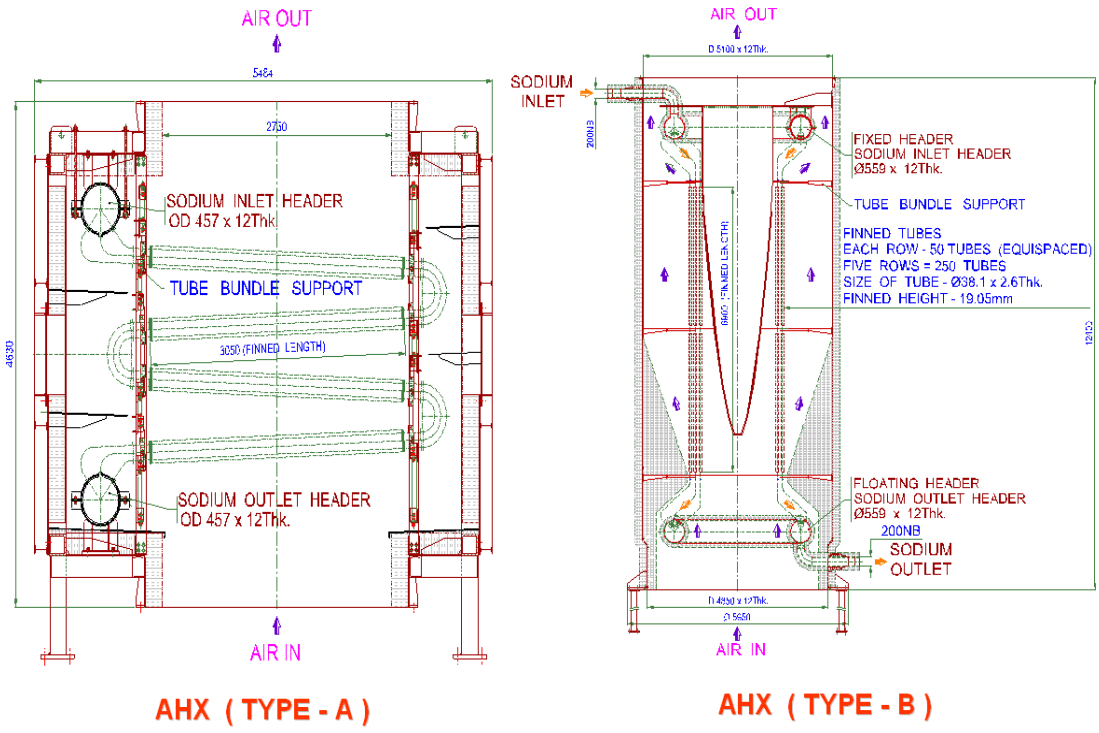

FIG. 7.44. Diversity in PFBR AHX designs.

The drive force for the flow of air over the finned tubes of the AHX is obtained by providing a stack of height 30 m. During normal plant operation, to minimize the heat loss, pneumatic and electrical motor operated air dampers provided at the inlet and outlet of the AHX are kept slightly open, permitting certain amount of natural circulation in the SGDHR to enable smooth change over to DHR mode when required. The heat removed during this poised state is about 0.33 MW per loop. The Primary Sodium Pump (PSP) main motor is provided with a Class 3 emergency diesel power supply. These pumps are also provided with pony motors powered through dedicated battery backed power supply for 4 hrs as a defence in depth. These provisions are for ensuring coolant circulation through the core during off-site power failure and SBO.

To minimize sodium side corrosion, the sodium purity is maintained by an off-line purification system (SGDHR purification circuit – common to two circuits). Sodium purity is checked by periodical sampling of sodium from the loop and also by plugging indicator provided in the loop. When leak detectors provided for pipes and components detect a sodium leak, the leak is confirmed by other means and then sodium from the loop is drained to the storage tank by opening the drain valves. In case of sodium leak in the AHX, two out of three logic from the leak detectors gives signal to close the air dampers automatically (if in open position) and nitrogen is supplied to the AHX cabin and sodium is drained to the storage tank. To prevent the risk of sodium freezing in AHX, dampers are closed automatically in case the sodium outlet temperature of AHX falls below 160°C. In case a damper fails to close and if the temperature continues to fall down, the sodium is drained from the loop on manual command, if the temperature falls below 150°C.

7.2.7. Seismic isolation

Mitigation of earthquake loads by the seismic isolation technology is expected to enhance both safety and economy of a nuclear power plant, through enabling rationalized and simplified design of structures, systems and components. In this subsection, work on seismic isolation in Japan, the Republic of Korea and the United States is discussed.

7.2.7.1. Seismic isolation in Japan

A comprehensive research program on the design methods of laminated rubber bearings [194] was carried out, and a design guide, "Technical Guidelines on Seismic Base Isolation System for Structural Safety and Design of Nuclear Power Plants, JEAG4614-2000", was issued by Japan Electric Association in 2001. Since fast reactor components are subjected to significant thermal loads at elevated temperatures and relatively vulnerable to seismic loads, mitigation of seismic loads is especially beneficial.

A design study of base-isolated demonstration FBR plants was conducted from 1989 to 1999 in Japan [195]. Figure 7.45 shows the configuration of seismic isolation devices. The seismic isolation devices are natural rubber sheets laminated in turn with thin steel plates, with steel rods for damping. The period of laminated rubber bearing is assumed to be 2 seconds. Rated load per one device is 500 to 1000 tons.

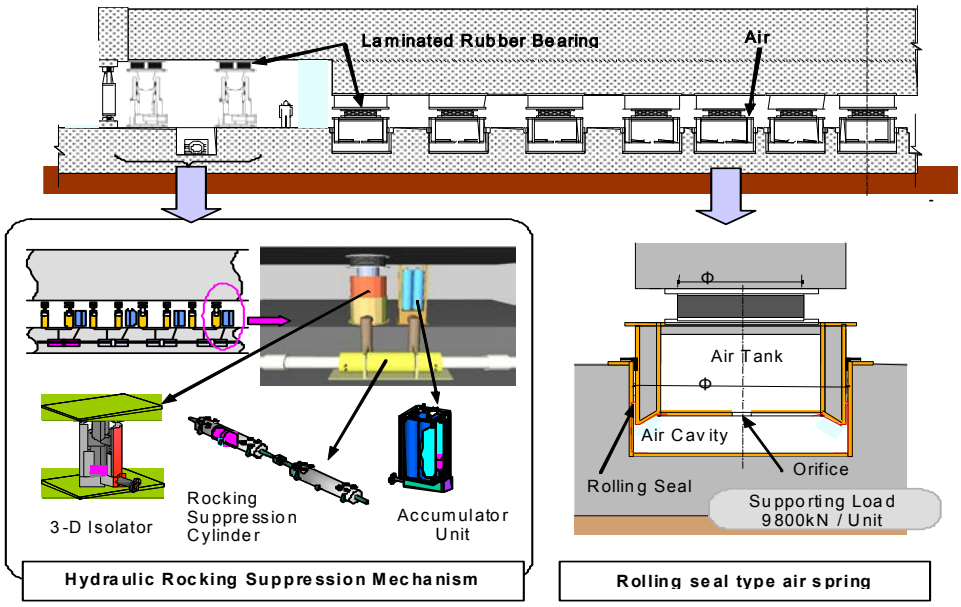

FIG. 7.45. Schematics of 3D base isolation system.

A true earthquake-load-free design may be realized by the three-dimensional seismic isolation, which is especially of benefit to the nuclear power plants located in high seismic zones such as Japan. A R&D project on three-dimensional seismic isolation for future FBR plants was carried out form 1999 to 2004 [196]. Within this program, a three-dimensional base isolation system with combined use of pneumatic springs and hydraulic devices has been developed. A vertical isolation system with coned dish springs has also been developed for major reactor components assuming a horizontally base isolated structure. For both systems,

detailed designs were made on the isolation devices, and seismic table tests of the systems with reduced scale models were carried out to confirm their basic technical feasibilities.

7.2.7.2. Seismic isolation in the Republic of Korea

Since the rubber in laminated rubber bearing (LRB) is the main element for shear deflection, the understanding of its mechanical response behaviour can provide insight into the behaviour of LRB. The effective ways of understanding the behaviour of LRB are to perform extensive tests on small specimens of the rubber and the reduced scale LRB.

To investigate the seismic isolation capability and produce the test data for verification of the seismic analysis methodology, shaking table tests are carried out with the test model designed to simulate a KALIMER reactor building and structures.

Various input ground motions such as the 1940 El-Centro NS, the artificial time history, which is numerically developed so that its response spectrum characteristics match those of the specified US NRC Reg.1.60, and the 1985 Mexico earthquake are used to investigate the effects of input motions. The seismic response analyses for a seismically isolated KALIMER reactor building and structures are performed to show the seismic isolation performance and the seismic margins.

The contents of the R&D program include the characteristic tests for the rubber specimen used in the LRB, the high damping LRB (HLRB), the lead inserted LRB, and the 3D-LRB, and the development of the numerical methodology to simulate the LRB behaviour, the seismically isolated KALIMER building, and the KALIMER reactor structures including reactor internals as shown in Tables 7.18 and 7.19 [179].

TABLE 7.18. SPECIFICATION AND DESIGN TARGETS FOR THE KALIMER-600 LRBS

	Prototype LRB	1/4 Scale HLRB	1/8 Scale HLRB
Design vertical load, t	320	18.4	5.0
Effective OD, cm / ID, cm	120 / 4	30 / 1.9	15 / 1.9
Rubber thickness, mm × no. layers	278 (9.6×29)	69.6 (2.4×29)	34.8 (1.2×29)
Steel thickness, mm × no. layers	3.2×28	2.3×28	1.8×28
Vertical stiffness, kN/m	51.6×10^5	12.9×10^5	6.4×10^5
Horizontal stiffness, kN/m	3080	770	385
Horizontal isolated frequency = 0.5 Hz Vertical natural frequency of isolated system = 21 Hz Damping coefficient = 12 % above Maximum shear strain = 300 % above Primary shape factor ($D/(4\cdot t_R)$) = 31.25 Secondary shape factor ($D/(n\cdot t_R)$) = 4.31			

TABLE 7.19.TEST RESULTS OF EQUIVALENT DAMPING (ζ_{eq}) AND STIFFNESS (K_{eq}) FOR KALIMER-600 REDUCED HLRB

Shear strain, %		50	100	150	200	300
		%				
1/8 Scale (0.01 Hz)	ζ_{eq} (%) K_{eq} (kN/m)	- -	10.64 395.6	- -	8.91 407.3	8.68 514.5
1/8 Scale (0.5 Hz)	ζ_{eq} (%) K_{eq} (kN/m)	18.0 495.	18.0 385.	16.5 380.	- -	- -
1/4 Scale (0.01 Hz)	ζ_{eq} (%) K_{eq} (kN/m)	11.30 1061.	11.94 775.4	11.18 736.4	- -	- -
1/4 Scale (0.5 Hz)	ζ_{eq} (%) K_{eq} (kN/m)	17.0 950.	16.0 800.	- -	- -	- -

The various tests for rubber specimens, LRBs, and isolated structural model, and the numerical simulations for the evaluation of LRBs and seismically isolated KALIMER structures have been done in this program to verify the performance and the effectiveness of the seismic base isolation.

The KALIMER-600 reactor building is represented in Fig. 7.46. The seismic isolation consists of lower base mat, pedestals, high damping rubber bearings, and upper basemat. The concrete upper basemat on which whole reactor building is seated is about 36 m wide and about 49 m long and 9 m deep. The gap between upper and lower basemat is about 2 m where 164 isolators will be installed and maintained. Figure 7.47 shows schematic arrangement of isolators on the lower basemat.

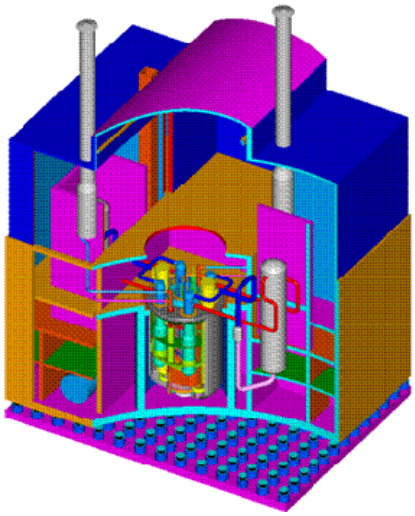

FIG. 7.46. KALIMER 600.

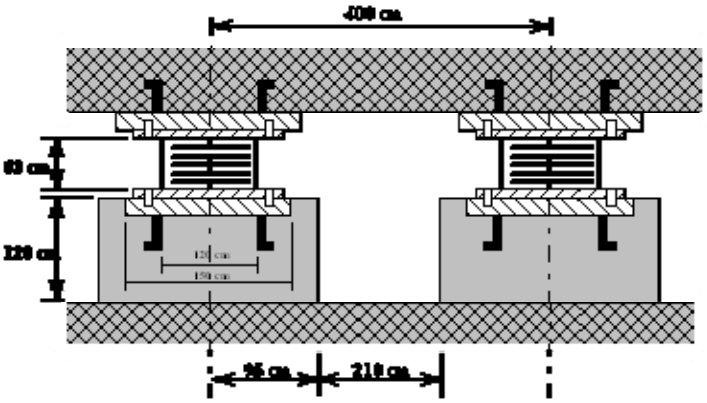

FIG. 7.47. Seismic isolator concept.

The seismic gap between isolated reactor building and non-isolated wall is about 1.2 m, which will allow no contact even when subjected to beyond design basis earthquake with peak ground acceleration 1.0·g.

High damping isolation bearings made of natural rubber have been selected to isolate the reactor building. The rubber compounds of the bearing contain a high amount of filler materials such as carbon black and the filler material achieves a non-linear behavior which increases the natural rubber‘s stiffness properties, tear and abrasion resistance, and damping. The design target and specification for the seismic isolators are listed in Table 7.18.

The rubber shear modulus varies as a nonlinear function of the shear strain. At low strains (50%) for 1/8 scale the equivalent stiffness is as high as 495 kg_f/cm, at higher strains (100%) the stiffness drops to 385 kg_f/cm and remains fairly constant beyond this strain level. This lower stiffness is necessary to achieve effective isolation. Test has also shown that for strains larger than 300%, the material hardens and the effective modulus begins to increase. This provides additional safety in the case of earthquakes exceeding the SSE value. The high rubber stiffness at low strains means that wind loads are adequately resisted by the isolated system without the use of mechanical fuses designed to break during a strong earthquake.

Another important feature of these bearings is the provision of sufficient damping to make additional external damping devices unnecessary. Tests have shown that 12% damping can be easily achieved for the entire shear strain range up to 100% as listed in Table 7.19. Another advantage with damping through the use of rubber is that it shows a complete recovery of its shear strain behaviour after cycling. In contrast, external damping devices rely on permanent plastic formations; thus, they have to be replaced after a seismic event. Furthermore, rubber-only systems provide the greatest protection to equipment housed in isolated buildings.

To minimize amplifications in vertical response due to the vertical flexibility of the isolators, a high vertical to horizontal stiffness ratio is provided. Tests have shown that bearings with stiffness ratios larger than 1000 can be designed. With stiffness ratios of this magnitude the vertical frequency is about forty-two times the horizontal frequency.

Another benefit of the isolators is that they are self centering so that there is no permanent displacement of the isolated structure. Reduced scale bearings tests indicate that they could sustain many maximum credible earthquakes and an unlimited number of smaller events without permanent internal changes. Thus, the system remains effective in foreshocks, the main event, and aftershocks without the need of adjusting the system.

7.2.7.3. Seismic isolation in the United States of America

This section reviews the development of seismic base isolation for nuclear applications in the USA, especially for liquid metal fast reactors. Base isolation technology is now considered to be a mature technology for building and bridge applications in the USA. There is no difference between the isolators that are applied to buildings and those applied to nuclear structures, except that for nuclear applications, more thorough analyses and tests will be required. Also, quality control for material, fabrication and field installation are more stringent. Currently, there are no base isolated nuclear structures in the USA. One of the obvious reasons is that no new nuclear plants have been ordered in the USA since 1978.

In the USA, consideration of base isolation in nuclear power plants started in 1979 when the Electric Power Research Institute (EPRI) founded a study to review the possibility of using

seismic isolation for nuclear structures [16]. In that study, several isolation devices were identified as feasible for use in nuclear structures, and the study recommended that detailed analyses be performed and validated by shaking table and field tests. In around 1980, Argonne National Laboratory proposed to Department of Energy (DOE) to initiate a study to explore seismic isolation for the US LMR plant designs and the proposal was accepted [17]. Argonne began the studies of this technology, particularly with regard to applications in nuclear reactor facilities. In the mid 1980s, seismic base isolation was chosen for the General Electric (GE) PRISM design and the Rockwell SAFR design [18]. The GE PRISM design was chosen by DOE for further development. A program funded by the Department of Energy and conducted by Argonne National Laboratory was carried out over 1988-92 to perform research on seismic base isolation to support the PRISM design and the DOE's New Production Reactors (NPR). However, seismic isolation was not selected for the NPR reference design, and the PRISM project was cancelled in 1994. Before the PRISM project was cancelled, GE had submitted the Preliminary Safety Information Documents (PSID) to the NRC for review. The review comments provided by the NRC indicate that NRC agreed, in principle, with the concept of seismic base isolation for nuclear application [19].

In 1992, the DOE Office of Risk Analysis and Technology and the DOE Office of Nuclear Safety Policy and Standards sponsored two meetings which focused on seismic base isolation. Both meetings were organized by Lawrence Livermore National Laboratory. The first meeting was the Workshop on Seismic Base Isolation for the Department of Energy Facilities and it was held in Marina Del Rey, California on May 13 to 15, 1992. Its goals were to introduce the concepts of base isolation and to illustrate that seismic isolation is a viable technology that can be applied to DOE facilities for natural phenomena hazards mitigation [201].

The second meeting was the Department of Energy Short Course on Seismic Base Isolation. It was held in Berkeley, California on August 10 to 14, 1992, and it emphasized the engineering details of seismic isolation. These two meetings, while producing three volumes of reports for technology transfer [202], did not result in DOE's acceptance of seismic isolation. As mentioned in Ref. [203], DOE does not endorse seismic isolation for their performance category 3 or 4 facilities (note that reactors are performance 4 facilities).

With the cancellation of the NPR and PRISM programs, the R&D activities for the development of seismic base isolation for nuclear applications in the US went into a state of hibernation. In 2006, the Global Nuclear Energy Partnership (GNEP) was announced. One of the GNEP's goals is to recycle the spent fuel generated from the light water reactors. The Advanced Burner Reactor (ABR) was selected for this purpose. An advanced burner reactor is an Advanced Liquid Metal Reactor (ALMR). So, with the inception of the Global Nuclear Energy Partnership (GNEP), the research activity on liquid metal fast reactor seems to be rejuvenated. To standardize the ABR design for cost reduction and to make the ABR design suitable for high activity seismic areas, the seismic base isolation was again proposed for the ABR. Currently, a gap analysis on seismic base isolation is being conducted at Argonne National Laboratory. The purpose of the gap analysis is to assess the readiness of base isolation technology for the ABR. From this study, two types of base isolation systems were identified to be potential candidates for use in the ABR design. They are the High-Damping Rubber Bearing (HDRB) and the Friction Pendulum System (FPS)/Multiple Friction Pendulum System (MFPS). The descriptions of these two systems are given below.

7.2.7.3.1. High-Damping Rubber Bearings

The High-Damping Rubber Bearing (HDRB), shown in Fig. 7.48, consists of thin layers of rubber sandwiched between steel plates. The manufacturing methods for vulcanization and bonding are used for making bearings. The damping in HDRB is increased by adding extra fine carbon black, oils or resins, and other proprietary fillers. The damping is increased to levels between 10 and 20% at 100% shear strains. This type of isolation system has been used in the first US isolated building, the Foothills Communities Law and Justice Center in Southern California [199] and has been proposed for the PRISM reactor [200]. This is the most popular type of bearing in the USA.

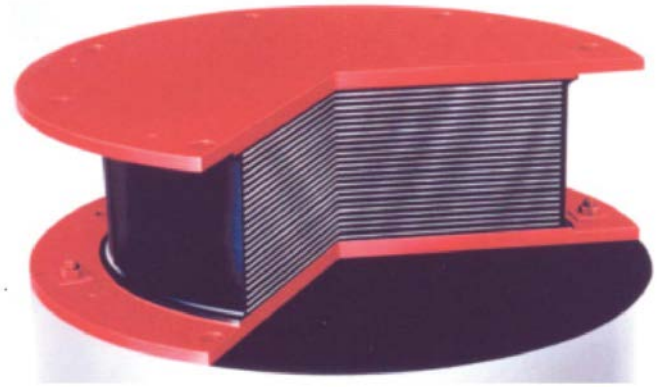

FIG. 7.48. High-Damping rubber bearing.

7.2.7.3.2. Friction Pendulum System

The Friction Pendulum System (FPS) isolator, shown in Fig. 7.49, is designed to remedy one of the drawbacks of flat-sliding bearings, namely lack of the restoring force.

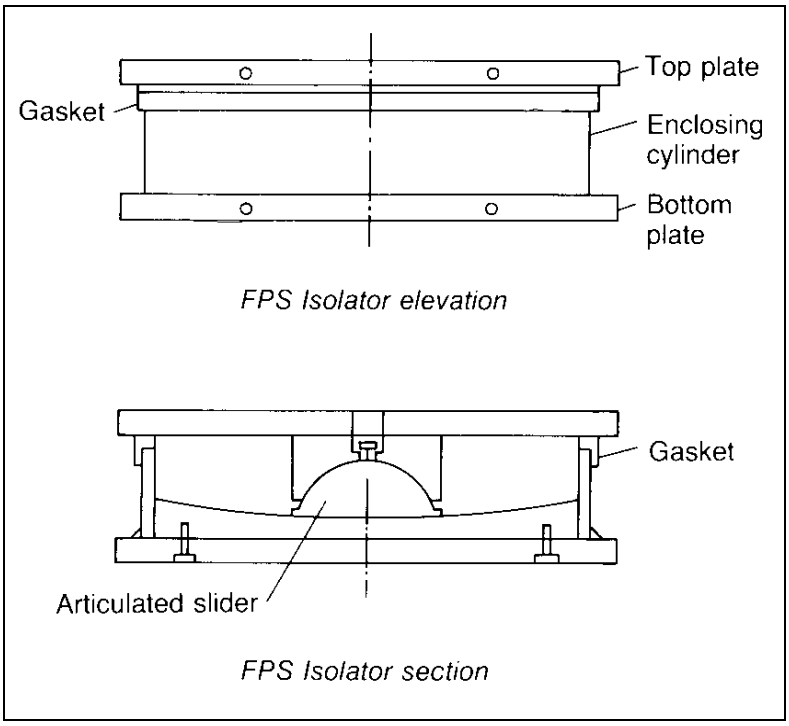

FIG. 7.49. Friction pendulum system [10].

It was invented by V.A. Zayas in 1987 [207, 208]. The device mimics the kinematics of a pendulum which utilizes the weight of the superstructure as the restoring force. It consists of a polished stainless steel concave surface coated with high density chrome, an articulated slider, and a cover plate. The slider is coated with a low friction self-lubricating composite material such as Teflon. During an earthquake, the slider slides along the concave surface, causing the superstructure to move along like a pendulum. The restoring force is therefore proportional to the weight of the structure; the period of oscillation is a function of the radius of the concave surface and is independent of the mass of the superstructure. The energy is dissipated by friction. A recent study [209] indicated that under the same design parameters, the displacement of a FPS is much smaller than that of a rubber bearing system. This trend is not surprising because a FPS system dissipates more energy (by friction) than a LRB system at comparable displacement/deformation of the isolator, thus reducing displacement [210]. A study by Mokha et al. also indicated that the FPS has low sensitivity to the frequency content of the time history of an excitation (e.g., earthquake ground motion), and has a high degree of stability under dynamic loadings [211].

7.2.7.3.3. Multiple Friction Pendulum System

Multiple Friction Pendulum System (MFPS), shown in Fig. 7.50, is also called a Double Concave Friction Pendulum [212].

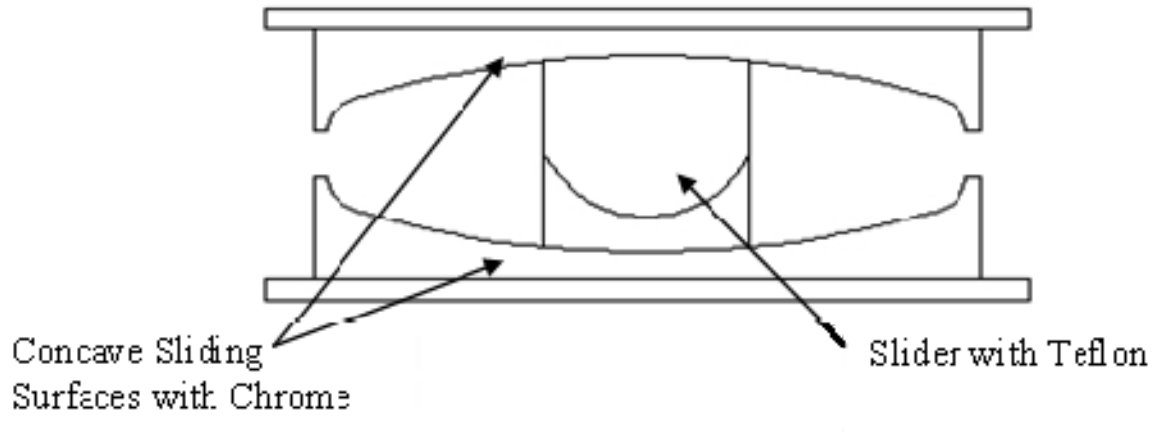

FIG. 7.50. Multiple friction pendulum system.

It is an improved version of FPS. Instead of one sliding surface in FPS, it consists of two facing concave sliding surfaces. As a result, the MFPS can accommodate a larger relative displacement at the isolator level (Fig. 7.51).

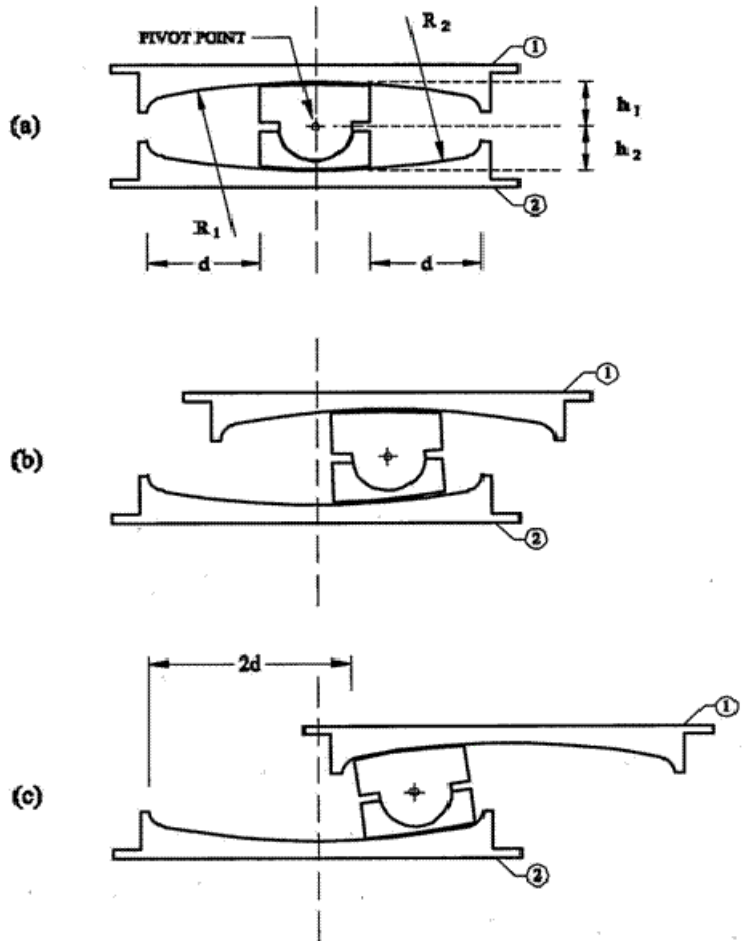

FIG. 7.51. Displacements of MPFS [16].

Moreover, by using two concave sliding surfaces having the same radii of curvature, the size of the MFPS isolator is 40% less than that of a FPS bearing having the identical vibration period. MFPS was invented by Tsai et al. [213] in 2002. Shaking table tests were performed to study the effectiveness of MFPS in reducing the seismic response of structures [214, 215]. The behaviour of MFPS during earthquake excitations was also studied by Fenz and Constantinou [216]. Since the properties of MFPS are almost identical to those of FPS, in the following discussion, FPS/MFPS will be used to designate either one of the devices.

The coating material used between two sliding surface usually is polytetrafluoroethylene (PTFE), more commonly known by its trademarked name Teflon. PTFE was discovered by Roy Plunkett of DuPont in 1938 [217]. It is inert to most chemicals and is the best material known to man for corrosion resistance. It was used in the Manhattan Project to coat valves and seals in pipes holding highly reactive uranium. The coefficient of friction of PTFE is 0.1 or less, which is the lowest of any known solid material.

According to DuPont its melting point is 327°C. PTFE is quite durable; the PTFE coating of a sliding bearing will wear out after travel of 10 km to 20 km according to Kelly [218]. For buildings, the sliding occurs only during an earthquake and the total travel is about several meters rather than kilometers; therefore, wearing out of the coating is not a concern. FPS/MFPS reduces the seismic excitations experienced by the superstructure by lengthening the system period and by friction mechanism; therefore, FPS/MFPS possesses characteristics of both

elastomeric and sliding type base isolators in reducing the seismic response. FPS/MFPS has the following advantages over HDRB:

(1) Design is simpler;
(2) Period is independent of the structural weight;
(3) Torsional effect is minimum;
(4) The energy dissipation due to friction is effective for a wide range of frequency input;
(5) No buckling concerns;
(6) Durable (made of stainless steel and inert to chemicals and radiations);
(7) Wider working temperature range;
(8) Better fire resistance and safe;
(9) Quality control is easier.

Despite these advantages, FPS is not as popular as HDRB in the USA. It was not even considered in the studies sponsored by the IAEA as a candidate for the base isolation system in nuclear power plants [218]. One of the reasons for this is attributed to timing. HDRB was developed by the Malaysian Rubber Producers' Research Association of the United Kingdom in 1982, and it was soon selected to be the isolation device for the ALMR reactors in the R&D program conducted at the Argonne National Laboratory.

In 1985, it was used in the first isolated building in the United States, and in 1986, it was proposed for the base isolation system in the PRISM and SAFR reactor designs [219]. By the time FPS was invented in University of California at Berkeley in 1987 [207], HDRB had already become the most popular base isolation device in the USA. The other reason is the modelling issue for the friction mechanism of the FPS.

During the early developmental years of FPS, the friction was modelled as Coulomb friction; whereas, the experimental study conducted by Tyler [220] has shown that the friction characteristic of the Teflon-steel interface depends on the pressure and velocity of the slider; therefore, Coulomb's law of friction is not applicable for the Teflon-steel interface. The reason cited for FPS being inferior to HDRB for nuclear applications was the lack of a proper model for the friction mechanism, so the maximum sliding distance could be calculated accurately [221].

However, in recent applications of base isolation, this trend seems to have reversed. In several base isolation projects, FPS was chosen for the base isolation system instead of HDRB. This is due to recent advancements in the FPS technology in recent years. Just to name a few, mathematical models for the nonlinear behaviour of the friction force at the Teflon-steel interface were developed [221–228], and a 3-D analytical model for FPS that considers the large deformation and the axial force variation has also have been developed [229–231].

Additionally, the long term material property of the FPS was addressed in a paper by Mokha et al. [232], and the dwell of load (self-welding) has been found to have no effect on the friction properties [233]. All these developments in FPS serve as the foundation for designing and analyzing the FPS for future nuclear applications. Therefore, FPS deserves further consideration as the isolation devices for the future ALMR design.

7.3. Future trends in the design of SFRs in order to improve economics and safety

7.3.1. Innovative design features to achieve improved economics

The basic approach for cost reduction involve design optimization, improved performance indices, innovative concepts and design leading to reduced consumption of materials and simplified manufacture and operation and use of advanced technologies for faster construction with modular concepts. Various Member States have been devising their strategies by adopting all the above the extent possible satisfying their national priorities and needs.

Capital cost for NPPs with FRs generally accounts for 70-80% of the total nuclear electricity generation cost, compared to 40-55% for LWR plants. The reason for the higher cost of equipment for fast reactors, as is shown in this report, is their wider range and higher per installed kilowatt metal content. A reduction of the nuclear grade metal content of the plant, and thus bringing down the use of expensive safety grade steels is one of the most important tasks facing the design and planning of fast reactors.

Because of the difference in electrical output between comparing designs, a straight forward comparison of components weight and buildings material (concrete) volume was not fully indicative of the cost reduction potential. More suitable indicators for an economic comparison and evaluation of different plants and design solutions have been taken as the 'specific amount' calculated in tonnes and/or in cubic metres per unit of electrical output (t/MWe, m^3/MWe).

A way forward to commercial utilization of fast reactors has been established. This approach is generally consistent with other studies, and indicates that the goal of competitive fast rectors may be within reach. The economic competitiveness of sodium cooled fast reactors (SFRs), are dependent on capital investment cost and uranium price. It has been shown in former studies that the economic advantages of SFRs are clearly improved if and when the prices of natural uranium are increased.

However, the most important "bearing in the cost of generated energy is the SFR capital cost" [251]. Therefore, the objective should be to achieve a SFR design the cost of which has to be equal or less that the one of the advanced light water reactor (LWR) designs.

Apart from the reduction of consumption of steel and concrete which is the basic factor which has a high impact on capital cost, the optimum plant parameters possibly with higher steam temperatures and pressure, longer plant design life, high burnup, optimum plant layout with reference to economy and safety, adopting the concepts involving less number of systems and components with possibly thinner vessel walls are the other key features which could bring down the capital cost. Adopting such innovative concepts call for in-depth R&D. Among these factors achieving high burnup would be the most challenging activity.

Development of advanced materials for the structural materials for the clad and wrappers for achieving high burnup, numerical simulation of fuel and structural materials under high irradiated condition, generation of material data for out of core components for long life (>60 years), development of constitutive material models for the numerical simulation of time dependent and time independent failure mechanisms in the metal are the important research to be pursued for realizing the targeted economic gain for the future reactors. It is acknowledged that seismic design is an important component of the engineering cost of the sodium cooled

reactors. Hence, reduction of seismic loads through adopting state of art base isolation system is an important factor to be critically investigated with respect to feasibility and economy.

Improved design features such as high thermal efficiency, high capacity factor, high burnup and multiple units on a single site offer potential for a competitive cost. The above features directly have the major and direct influence on the cost. It is possible to achieve the improved design features in light of the vast experience in nuclear reactor design operating experience supported by focused R&D programme. Some of the advanced features towards improved economy being implemented by various member states are briefly mentioned below.

7.3.1.1. France

The French approach involves (i) simplification of systems (ii) enhanced in-service inspection and repair (ISI&R) capabilities (iii) enhanced operations and maintenance (O&M) capabilities and (iv) twinning and modularity.

(i) In the category of simplification of systems, the following were pursued:

   (a) Simplification of Na circuits and auxiliary systems;
   (b) R&D on ferritic-martensitic steels for the IHX, the secondary piping and the SG;
   (c) Feasibility of alternative thermal fluids inside the heat removal system (e.g. Pb-Bi, molten salts, hydroxides) and gas cycle with or without an intermediate circuit with reduction in the number of auxiliary systems needed and even might allow the suppression of the secondary circuit. These alternative fluids discussed above are of interest in order to avoid the sodium-water reaction, and thereby reduce investment risks and improve availability.

(ii) In the category under enhanced ISI&R options, the following were addressed:

   (a) Need for improved in-service inspection techniques for continuous monitoring and periodic inspection;
   (b) Need for "industrial" through sodium viewing and volumetric inspection capabilities;
   (c) Improvements needed (accuracy, range, volumetric non-destructive testing capabilities, robots);
   (d) Focus on structures simplification, component removal capability, accessibility, core discharge and primary circuit draining provisions, repair capabilities.

ISI&R has to be significantly improved to minimize investment protection risks.

(iii) The following enhanced O&M options were addressed:

   (a) Systems need to be simplified to facilitate maintenance operations, reduce O&M costs and limit risks associated to the human factor;
   (b) Reduction in the number and length of piping;
   (c) Reduction in the number of auxiliary systems;
   (d) Refuelling and component handling to be optimized to improve availability factor
   (e) Reactor design to be optimized to minimize personnel exposure;
   (f) Appropriate selection of materials to facilitate maintenance (e.g. cobalt-free alternatives to stellites for surface hardening in sodium);
   (g) Balance between prevention of Na issues (e.g. Na fires) and ease of access for maintenance operations.

O&M and ISI&R options must be consistent with 90% availability target.

7.3.1.2. India

In the Indian approach, a simplified grid plate design is coupled with an optimized fuel handling system in order to achieve cost reduction. In addition, reactor internals will be adopted using simple design and optimized structural performance. Advanced core structural materials will be employed for higher burnup and reactor vessel diameter reduction is achieved by employing advanced shielding materials and optimization of the top shield component design and the rotating plug design. The SG will have longer lengths of tubes leading to enhanced safety which in turn give economic advantages. Twin reactor design will be the choice for future FBR deployments.

7.3.1.3. Japan

Cost-saving approaches employed by Japan are: a compact reactor vessel, a compact fuel handling machine, Zr-H shielding, simplified reactor internal structures, heat transport system with shortened piping. A new fuel handling system without large double rotating plugs enables the compact reactor vessel. The commodities of the reactor structure are decreased by about 40%.

The compact reactor vessel is achieved by simplifying the reactor internal structure by the following:

(i) No wall cooling system - By adopting single-forging ring where the liquid level is moving, together with advanced elevated temperature structural design standard;
(ii) Simple skirt-type core support structure; to be fabricated with single-forging ring and possible to be inspected. These will be supported by extensive experimental and analytical studies are carried out to manage the coolant flow and temperature transients in the upper plenum.

The heat transport system of the JSFR employs innovative design with shortened piping, made possible by the use of high chromium ferritic steel and inverse L-shape simple pipe works, and an integrated pump-IHX. These measures lead to drastic reduction of plant materials and a double boundary concept is proposed as the countermeasure against sodium leaks.

7.3.1.4 Russian Federation

The Russian studies on the BN-800 directed towards improvement of technical and economical characteristics of the power are:

(i) Increasing the thermal efficiency, leading to an increased electrical power (880 MWe instead of the previous 800 MWe) achieved by means of optimization of the third circuit;
(ii) Improvement of turbine parameters and elimination of steam extraction for heating purpose; and
(iii) Extending the lifetime from 30 years up to 40 years.

Research and development is being pursued in the conceptual development of small-size modular-transportable two-circuit NPP and gas turbine (concept of the BN GT nuclear co-generation power plant).

The advanced BN-1800 design includes: traditional three-circuit design of power unit, pool type arrangement of the primary circuit including cold traps located in the reactor vessel that makes it possible to eliminate in fact a danger of radioactive sodium release outside the reactor vessel and its fire, once-through vessel-type SG of integrated type, steam reheating and the exception of intermediate storage drums of fresh and spent fuel assembly (FSA) and optimization of in-reactor vessel storage (IVS) of spent fuel assembly storage, providing storage of spent fuel assemblies for more than 1.5 years allows the direct unloading of FSA from the IVS into the wash cells and the storage pool.

7.3.2. Innovative design features to achieve improved safety

In this section, challenges in the design of SFRs, innovations, breakthroughs and related R&D addressed by various countries are compiled based on the references [251].

7.3.2.1. SFR challenges

Unlike in the water-cooled reactor, the SFR core is not in its most reactive geometry. The core has a high power density, which can have a positive voiding effect. The physical-chemical characteristics of sodium cause sodium water reaction, chemical toxicity problems. There are difficulties for ISI of the structures under sodium due to opaqueness of sodium. Repairing circuits and components in post-accidental situation call for very challenging technologies. The SFR components, i.e. large size thin walled shell structures, are very sensitive to earthquake loadings. The requirement of high breeding ratio and enhanced safety with improved economy requires advanced materials and technologies which call for extensive experimental, modelling and simulation technologies. High Pu content in fuels has to be investigated critically with respect to criticality, release to environment, loss of fissile material in waste streams. High burnup targeted for the future reactors introduces higher levels of radioactivity during fuel handling and fuel reprocessing.

7.3.2.2. Hypothetical accidents

The design objective is to make every identified sequence which can lead to the whole core melting highly hypothetical. Although this is also an objective in the existing designs of SFRs, optimisation still seems to be possible, thereby all the situations which can lead to important mechanical energy releases will be practically eliminated. The confinement, however, will be designed to resist all the consequences of any hypothetical accident.

Towards achieving this, design adopts defence in depth philosophy which defines simple scenarios without any cliff edge effects, passive safety features in the core taking advantages of presence Na void at the upper portion of core, Doppler effects, core expansion behaviour, shutdown and decay heat removal systems without calling for active safety devices and preventive surveillance and in-service inspection (ISI) and repair provisions. Passive safety features are introduced carefully after confirmation. Sufficient grace time is provided until human actions are possible during the time period required for recovery of operation performance of the failed safety systems under beyond design basis accidents due to loss of off-site and on-site electric power supply of the power unit with simultaneous failure of all absorber rods and loss of heat removal from reactor to final heat sink.

7.3.2.3. Robust design features

The robust design starts with choosing high quality materials, adopting established design, construction and inspection standards, guidelines and methodologies. General guidelines for achieving robust core design are: reduced power density of the reactor core, minimised stresses and reduced core height. The reactor design should incorporate higher design margins for strength and seismic resistance, in-vessel primary circuit purification system, concrete reactor vault with sealed liner serves as a guard vessel, simplified fuel reloading technology with minimum number of operations, elimination of isolation valves in the secondary circuit loops and testing in simulated environment (sodium and temperature).

The design provisions, such as diversity in shutdown and decay heat removal systems are introduced to meet the safety limits with adequate margins for the design basis events, so as to prevent beyond design basis accidents. Further novel design features such as re-criticality free core, effective core catcher, and containment are introduced for the management of beyond design basis accidents.

Critical examination and consideration of the feedback experience, rationalization of the design approach by the deliberate adoption of the ALARA principle, reinforced treatment of the severe plant conditions; continuous improvement in the defence in depth implementation and achievement of design architecture are some of the features that demonstrate robustness.

7.3.2.4. Innovations towards enhanced safety

7.3.2.4.1. Core

Improvement of the core design to minimise the ratio of the sodium void coefficient to the Doppler coefficient, reduction of height/diameter ratio, moderate core size, annular core, use of metallic core, use of advanced cladding materials (15/15Ti, ODS, etc.) to gain higher margins for the cladding ruptures during transients, state of the art core monitoring instrumentations and improved core diagnostic systems (neutron and acoustic noises acquisition and analysis) are some of the innovations presently under consideration.

7.3.2.4.2. Sodium fire and sodium-water reactions

The main objective is to practically eliminate sodium fires and sodium-water reactions possibly degrading the safety functions in an unacceptable manner or to lead to unacceptable consequences to the environment. In order to achieve this, apart from the existing design features, reduction of welds in piping by reducing number of sodium loops, shortening of pipe length with high chromium content, use of double wall piping, double wall steam generator tubes, integrated pump-IHX and improved inspection and repair systems are being considered. The passive means for self-extinguishing the sodium fires when sodium leaks from the circuits include sodium discharge into a pan with hydrolock and sodium discharge into a tank blanketed by inert gas. Experimentation and validation of the passive systems are required.

7.3.2.4.3. Reliable and diverse shutdown systems

A few innovations are introduced in the shutdown systems. In case of power excursion, an automatic negative reactivity insertion occurs:

- By way of enhanced expansion of the core and shutdown systems;
- Use of Curie point electromagnets or magnet switches to de-energize the magnet holding the absorber rods;
- Hydraulically suspended rods which would lower automatically into the core in case of any loss of flow due pump seizure or primary pipe rupture;
- Gas expansion modules (GEM);
- Stroke limiting devices to arrest the uncontrolled withdrawal of absorber rods;
- Self-actuating devices to shutdown the reactor directly under class 4 power supply failure.

7.3.2.4.4. Decay heat removal systems

Use of pumps with high mass inertia to ensure heat removal while awaiting the establishment of a natural convection (electromagnetic pump), enhanced grace time for safety actions, passive decay heat removal features (e.g. shape memory alloys for enhanced and automatic opening of dampers with rise in temperature), implementation of redundant circuits and the minimization of risks of common mode failures are a few of the innovations being investigated by designers.

7.3.2.4.5. Core catcher

The core catcher is placed with the objective of maintaining integrity of the vessel in the case of a full or partial core meltdown. The robust design of core catcher involves definition of scenarios for the core melt down relocation, settling behaviour of debris within sodium, post-accident heat removal of corium (pool thermal hydraulics, DHR) and design analysis to demonstrate integrity of the main vessel.

7.3.2.5. Additional design features for future SFRs

Certain design features are under consideration for the future innovative reactors. In the core design, in order to eliminate the possibility of flow blockage and at the same time to achieve lower pressure drop, power flattening is achieved without orificing by the use of different core zones at identical Pu content with different pin sizes or adopting the design of sub-assemblies with perforated wrapper or without wrapper by use of advanced spacer concepts for pin bundle. Stable power shape with burnup, metal plate concept for gas cooled reactor core, fuel assembly design for enhancement of molten fuel discharge upon the unprotected core degradation (parallel path for molten fuel) and engineering for the stabilised sodium boiling in the upper part of the S/A without voiding the fissile part are some additional design features considered. In the natural decay heat removal circuit, multiple flow paths in the pool to facilitate increased natural circulation (e.g. thermal valve in the inner vessel) are proposed.

For the shutdown system, use of fusible shutdown devices (FSD) placed above the upper fissile zone which acts when a fusible threshold is reached. The core catcher would have features to achieve enhanced cooling of debris and to prevent re-criticality. These can be achieved by incorporating enlarged coolant plenum for molten fuel quenching and pelletising the debris, novel chimney for effective coolant circulations, multi-layer debris tray debris for debris retention within limited height for cooling and sub-critical state, well defined paths for debris, sacrificial layers, etc. Alternate coolants, comprehensive ISI and repair strategies are also the features being thought of for the future designs.

REFERENCES TO CHAPTER 7

[1] ANZIEU, P., SERPANTIE, J.P., VERWAERDE, D., DUFOUR, PH., MARTIN, PH., A Program on Innovative SFR in France, Proc. ICAPP'07, Nice, France, 13-18 May 2007 (5 Vols), Curran Associates, Inc. (February 2008).

[2] EBBINGHAUS, K., MITCHELLL, C., DEBRU, M., EFR Design Criteria, paper presented in Int. Conf. Fast Reactors and Related Fuel Cycles, Kyoto, Japan 28 October-1 November 1991.

[3] SERPANTIÉ, J.P., FENEMORE, P., HAMMERS, D., The EFR Primary System: Design and Improvements, paper presented in Int. Conf. Fast Reactors and Related Fuel Cycles, Kyoto, Japan, 28 October-1 November 1991.

[4] NIBE, N., SHIMAKAWA, Y., KASAI, S., ICHIMIYA, M., NOMURA, M., Feasibility Studies on Commercialized Fast Breeder Reactor System, paper presented in ICONE 7, Kyoto, Japan (1999).

[5] RODRIGUEZ, G., BAQUÉ, F., ASTÉGIANO, J.C., Experimental Feedback of the Support of Sodium Technology Applied on the Development, Operation, Final Shutdown and Decommissioning of Sodium Fast Reactors, Nuclear Technology (2004).

[6] GUIDEZ, J., MARITEAU, P., LE COZ, P., Lifetime Extension of the Phénix Plant, Nuclear Technology (2004).

[7] GIRAUD, M., et al., Ultrasonic Control of the Phénix Steam Generator Modules, Nuclear Technology (2004).

[8] GASTALDI, O., CAVAGNA, C., MARTIN, L., GRABON, V., Phénix Steam Generator Module Repair, Nuclear Technology (2004).

[9] CALMON, P., LHEMERY, A., CHAMPIGNY, F., Modelling of Echo Responses from Defects in Complex UT Configurations, paper presented in 14th Int. Conf. on NDE in the Nuclear and Pressure Vessel Industries, Stockholm, Sweden (1996).

[10] MAHAUT, S., CATTIAUX, G., ROY, O., BENOIST, PH., Improvement of Defect Characterization with Ultrasonic Adaptative Focusing Technique: The FAUST System, paper presented in 14th Int. Conf. on NDE in the Nuclear and Pressure Vessel Industries, Stockholm, Sweden (1996).

[11] SERRE, M., ROY, O., POIDEVIN, C., DE MATHAN, N., VILLARD, D., Ultrasonic Examination of Cast Stainless Steel, paper presented in 14th Int. Conf. on NDE in the Nuclear and Pressure Vessel Industries, Stockholm, Sweden (1996).

[12] CALMON, P., LHÉMERY, A., LECOEUR-TAÏBI, I., CHAMPIGNY, F., Modelling of Echo Responses from Defects in Complex UT Configuration, paper presented in 14th Int. Conf. on NDE in the Nuclear and Pressure Vessel Industries, Stockholm, Sweden (1996).

[13] BENOIST, B., MASIA, A., SIMARD, P., PIRIOU, M., Wavelet Transformation: Filtering of Eddy Current Signals, paper presented in 14th Int. Conf. on NDE in the Nuclear and Pressure Vessel Industries, Stockholm, Sweden (1996).

[14] LE BLANC, LE CHIEN, J.L., TALVARD, M., DELSARTE, G., PIRIOU, M., Subsurface Cracks Detection in Inconel using Pulsed Eddy Current Technique, paper presented in 14th Int. Conf. on NDE in the Nuclear and Pressure Vessel Industries, Stockholm, Sweden (1996).

[15] ROY, O., PINCEMAILLE, G., MORISSEAU, PH., ANCRENAZ, P., Examination of a Cladding Zone with an Adaptative System, paper presented in 14th Int. Conf. on NDE in the Nuclear and Pressure Vessel Industries, Stockholm, Sweden (1996).

[16] CAGE, J.F., Electromagnetic Pumps for Large Pool-Concept LMFBR, EPRI-NP-1265 (1979).

[17] BARNES, A.H., et al., The Engineering Design of EBR-II, A Prototype Fast Neutron Reactor Power Plant, Proc. Int. Conf. on Peaceful Uses of Atomic Energy, Vol. 3, Power Reactors, pp. 380–344(August 1955).

[18] KOCH, L.J., An Integrated Experimental Fast Reactor Nuclear Power Station, Experimental Breeder Reactor-II (EBR-II).

[19] Pool-Type LMFBR Plant 1000 MWe Phase A-Extension-2 Design. Part XIII: Balance of Plant-Evaluation of Pool-Related Areas Final report, EPRI-NP-1014, Vol. 11 (June 1979).
[20] OTA, H., et al., Development of 160 m^3/min Large Capacity Sodium-Immersed Self-Cooled Electromagnetic Pump, Journal of Nuclear Science and Technology, Vol. 41, No. 4, pp. 511–523 (April 2004).
[21] NAKAZAKI, M., TAGUCHI, J., KATSUKI, K., et al., Development of Sodium-Immersed Self-Cooled Electromagnetic Pump, paper presented in Int. Conf. on Fast Reactor and Related Fuel Cycle, Kyoto, Japan, 1991.
[22] NAKAZAKI, M., MATSUZAWA, H., AIZAWA, R., et al., Performance Evaluation of Sodium-Immersed Self-Cooled Electromagnetic Pump, Proc. ICONE5, Nice, France, 26-30 May 1997, ICONE-2330 (1996).
[23] KWANT, W., FANNING, A.W., DAYAL, Y., et al., In-Sodium Testing and Performance of a 43.5 m^3/min Electromagnetic Pump for LMR Application, Proc. ICONE 5, Nice, France, 25-29 May 1997, ASME/SFEN/JSME, ISBN: 0791812383 (1997) CD-ROM.
[24] FANNING, A., et al., Giant Electromagnetic Pump for Sodium Cooled Reactor Applications, Electric Machines and Drives Conference, 1-4 June 2003, (IEMDC'03), IEEE International, Vol. 1, pp. 477-482 (2003).
[25] NOVICK, M., MCGINNIS, F.D., WHITHAM, G.K., EBR-I and EBR-II Operation Experience, Proc. ANS National Topical Meeting on Fast Reactor Technology, Detroit, Michigan, USA, p. 25 (April 1965).
[26] ANDERSON, R.H., Heat Exchangers and Steam Generators, paper presented in 1957 Fast Reactor Information Meeting, Chicago, Illinois, USA, November 1957.
[27] YEVICK, J.G., Fast Reactor Technology: Plant Design, MIT Press, Cambridge, Massachutes, USA, (1966).
[28] MORABITO, J.J., Sodium Components in Nuclear Reactor Systems, Proc. of the Nuclear Power Conference, Vol. 26, p. 257 (1964).
[29] MARABITO, J.J., SAVAGE, H.W., Major Components and Test Facilities for Sodium Systems, Proc. of the ANS National Topical Meeting on Fast Reactor Technology, Detroit, Michigan, USA, p. 380 (April 1965).
[30] KOCH, L.J., United States Experience with Fast Power Reactors: EBR-II, Proc. of the American Power Conference, Vol. 33, p. 181 (1971).
[31] BROWN, W.H.G., Nondestructive and Dimensional Inspection of EBR-II Steam Generator Tubes, ANS Transactions, Vol. 35, p. 418 (1980).
[32] WHITHAM, G.K., LONGUA, K.J., Bore-Side Inspection of EBR-II Steam Generator Tubes, ANS Transactions, Vol. 27, p. 759 (1977).
[33] PERRY, W.H., LENZ, G.L., RICHARDSON, W.J., WOLZ, G.C., Seventeen Years of LMFBR Experience: Experimental Breeder Reactor II (EBR-II), Proc. The American Power Conference, Vol. 44, p. 801 (1982).
[34] TIPPETS, F.E., FORD, J.A., WRIGHT, E.A., BUSCHMAN, H.W., Progress of LMFBR Steam Generator Testing in the US, Proc. 2nd Int. Conf. Liquid Metal Technology in Energy Production, Richland, Washington, 20-24 April 1980, (Editor J. M. Kahlke), U.S. Department of Energy (1980).
[35] ONESTO, T., ZWEIG, H.R., GIBBS, D.C., CARLSON, R.D., RODWELL, E., KAKARALA, C.R., The Case for Endurance Testing of Sodium-Heated Steam Generators, Nuclear Technology, Vol. 103, p. 168 (1993).
[36] SHIELDS, J.A. JR., LONGUA, K.J., The Effects of Ten Years Experimental Breeder Reactor II Service on 2 ¼ Cr-1 Mo Steel, Nuclear Technology, Vol. 28, p. 471 (1976).
[37] PAULINE, E.A., Fermi-I New Age for Nuclear Power, ANS (1979).
[38] ALEXANDERSON, E.L., Contribution of the Fermi-I Project to Fast Breeder Reactor Technology, Proc. Int. Conf. Organized by British Nuclear Society – Fast Reactor Power Station, London, UK, p. 13 (March 1974).
[39] ALEXANDERSON, E.L., BRANYAN, C.E., FORD, J.A., NIMS, J.B., OLSON, W.R., Enrico Fermi Atomic Power Plant Operating Experience through 100°MW, Proc. of

National Topical Meeting-Fast Reactors, ANS-101, San Francisco, USA, p. 1-21 (April 1967).
[40] BRANYAN, C.E., OLSON, W.R., United States Experience with Fast Power Reactors: Fermi I, Proc. The American Power Conference, Illinois Institute of Technology, Vol. 33, p. 19 (1971).
[41] SLIPER, E.G., Enrico Fermi Steam Generator Experience, ANS Transactions, Vol. 11, p. 137 (1968).
[42] DUFFY, J.G., WAGNER, H.A., Operating Experience with Major Components of the Enrico Fermi Atomic Power Plant, paper presented in Symposium on Performance of Nuclear Power Reactor Components, Prague, Czechoslovakia, November 1969.
[43] STARR, C., DICKINSON, R.W., Sodium Graphite Reactors, Addison-Wesley Publishing Co. Inc. (1958).
[44] DURAND, R.E., Sodium Reactor Operating Experience, Chemical Engineering Progress, Vol. 57, No. 3, p. 54 (1961).
[45] STARR, C., DICKINSON, R.W., Sodium Graphite Reactors, Addison-Wesley Publishing Company Inc. (1965).
[46] WOODRUFF, R.W., DURAND, R.E., OWENS, J.E., SRE and HNPF Operating and Modification Experience, Proc. National Topical Meeting-Fast Reactors, ANS-101, San Francisco, USA (April 1967).
[47] GLASGOW, L.E., Sodium Reactor Experiment Operating Experience, ANS Transactions, Vol. 4, No. 2, p. 202 (1961).
[48] KELLER, L.E., DAVIDSON, R.H., Hallam Nuclear Power Facility Operating Experience, Nuclear Safety, Vol. 7, No. 2, p. 236 (1965).
[49] DICKINSON, R.W., BEELEY, R.J., MAHLMEISTER, J.E., Modern Steam Conditions for a 360-MWe Sodium-Graphite Reactor, Proc. American Power Conference, Vol. 24, p. 195 (1962).
[50] COCHRAN, J.D., Operating Experience at Hallam Nuclear Power Facility, Proc. American Power Conference, Vol. 25, p. 204 (1963).
[51] COCHRAN, J.D., OWENS, J.E., Initial Operation of the Sodium Graphite Reactor at the Hallam Nuclear Power Facility, Proc. American Power Conference, Vol. 26, p. 201 (1964).
[52] COCHRAN, J.D., MONSON, H.O., OWENS, J.E., Operating Experience with Large Sodium Cooled Reactor Plants, Proc. American Power Conference, Vol. 28, p. 241 (1966).
[53] GIMERA, R.J., Alco/BLH Steam Generator Operating Experience in the SCTI, paper presented in Symposium on the Progress in Sodium-Cooled Fast Reactor Engineering, Monaco, March 1970.
[54] JONES, D.R.H., Post-Test Examination of the LMEC Alco/BLH Steam Generator, ANS Transactions, Vol. 14, p. 787 (1971).
[55] HOBSON, R.G., EILBECK, E., LMFBR Steam-Generator Development and Testing, paper presented in Symposium on Progress in Sodium-Cooled Fast Reactor Engineering, Monaco, March 1970.
[56] MCDONALD, J.S., CASEY, D.F., MORGAN, W.T., Modular Steam Generator for the LMFBR Power Plants, Proc. The American Power Conference, Vol. 33, p. 284, Illinois Institute of Technology (1971).
[57] MCDONALD, J.S., HATY, R.B., DEBEAR, W.S., LMFBR Modular Steam Generator Test Results, Proc. American Power Conference, Vol. 35, p. 180 (1973).
[58] RANDALL, E., MCDONALD, J.S., FBR Modular Steam Generator Design, ANS Transactions, Vol. 12, p. 770 (1969).
[59] MCDONALD, J.S., FBR Modular Steam Generator Fabrication and Inspection, ANS Transactions, Vol. 13, p. 111 (1970).
[60] FRANCE, D.M., ROY, R., CARLSON, R.D., CHIANG, T., Dynamic Stability Experiments in Sodium-Heated Steam Generators, Proc. 3rd Int. Conf. on Liquid Metal Engineering and Technology, Oxford, UK, p. 195 (April 1984).
[61] FRANCE, D.M., CARLSON, R.D., CHIANG, T., ROY, R., Dynamic Stability Experiments in LMFBR Steam Generator Tubes, ANS Transactions, Vol. 45, p. 820 (1983).

[62] STEVENS, H.C., FRANCE, D.M., Development of a Thermal-hydraulic Test Facility for Full-Scale LMFBR Steam Generator Tubes, ANS Transactions, Vol. 22, p. 538 (1975).
[63] IMPELLEZERI J.R., CAMARET, T.L., Clinch River Breeder Reactor Plant Steam Generator Few Tube Test Model Post Test Examination, Proc. 2nd Int. Conf. Liquid Metal Technology in Energy Production, Richland, Washington, 20-24 April 1980 (Editor J. M. Kahlke), U.S. Department of Energy (1980).
[64] JACOBI, W.M., The Clinch River Breeder Reactor Project Nuclear Steam Supply System, Nuclear Engineering International, Vol. 19, No. 221, p. 846 (1974).
[65] LILLE, F., Design of the Clinch River Breeder Reactor Steam Generators, Proc. International Symposium on Design, Construction and Operating Experience of Demonstration Liquid Metal Fast Reactors, Bologna, Italy, p. 557 (April 1978).
[66] WHIPPLE, J.C., SPALARIS, N., Design of the Clinch River Breeder Reactor Plant Steam Generators, Nuclear Technology, Vol. 28, p. 305 (1976).
[67] MCCLUNG, R.W., SLAUGHTER, G.M., SPALARIS, C.N., LILLIE, A.F., Fabrication and Inspection Development for Clinch River Breeder Reactor Plant Steam Generators, Nuclear Technology, Vol. 28, p. 374 (1976).
[68] FOX, JR., C.H. PURCELL, W.J., WIESENECK, H.C., CRBR Steam Generator Testing Experience, Proc. 3rd Int. Conf. Liquid Metal Engineering and Technology, Oxford, UK, 9-13 April 1984, British Nuclear Energy Society (1984).
[69] LAY, D.M., PIPER, R.M., Modeling Considerations for the Analysis of LMFBR Steam Generator Tube Clamps, Journal of Engineering for Power, Vol. 105, p. 771 (1983).
[70] SPALARIS, C.N., RING, P.J., WRIGHT, E.A., Fabrication Technology Liquid-Metal Fast Breeder Reactor Steam Generators, Nuclear Technology, Vol. 55, p. 243 (1981).
[71] BERGLUND, R.C., TIPPETS, F.E., PRISM, the Plant Design Concept for the U.S. Advanced Liquid Metal Reactor Program, Proc. American Power Conference, Chicago, Illinois, p. 697 (1989).
[72] GOWER, G.C., PROBERT, P.B., Design of a 1000-MW Sodium-Heated Steam Generator for Superheat and Reheat, Proc. American Power Conference, Vol. 28, p. 109 (author: Illinois Institute of Technology, publisher: American Power Conference) (1966).
[73] STONE, C.C., FORD, J.A., TIPPETS, F.E., MCDONALD, J.S., GRANT, G., EPSTEIN, J.L., Experience with Liquid-Metal Fast Breeder Reactor Steam Generators – U.S. Design, Nuclear Technology, Vol. 55, p. 60 (1981).
[74] SMITH, D.C., GERHART, P.M., KAKARALA, C.R., Preliminary Multidimensional Thermal-hydraulic Analysis of a Helical Coil LMFBR Steam Generator, ANS Transactions, Vol. 44, p. 596 (1983).
[75] KWANT, W., BOARDMAN, C.E., DAYAL, Y., MAGEE, P.M., ALMR Plant Design and Performance, ANS Transactions, Vol. 66, p. 351 (1992).
[76] LAY, D.M., PIPER, R.M., Modelling Considerations for the Analysis of LMFBR Steam Generator Tube Clamps, Journal of Engineering for Power, Vol. 105, p. 771 (1983).
[77] GRANT, G., KAKARALA, C.R., HINTON, R.M., Material Selection for a Sodium-Heated Steam Generator, ANS Transactions, Vol. 27, p. 225 (1977).
[78] KUBOTA, J., MIURA, M., NAKAGAWA, H., SEMKO, J.W., GREEN, P.M., MORI, K., KUMAOKA, Y., YANO, K., SAKANO, K., A Cooperative Program of Development and Testing of the Double-Wall-Tube Steam Generator, Proc. Int. Conf. Fast Reactors and Related Fuel Cycles, Kyoto, Japan, 1991, Paper 2-6 (November 1991).
[79] HEBBAR, M.A., SESSIONS, C.E., LMFBR Steam Generator Materials Development at Westinghouse, Journal of Engineering for Power, Vol. 105, p. 779 (1983).
[80] CHO, S.M., SELTZER, A.H., Thermal Hydraulic Characteristics of a Double-Walled Tube Advanced Nuclear Steam Generator, Heat Transfer Engineering, Vol. 10, No. 3, p. 25 (1989).
[81] HEBBAR, M.A., SESSIONS, C.E., LMFBR Steam Generator Materials Development at Westinghouse, Journal of Engineering for Power, Vol. 105, p. 719 (1983).
[82] SESSIONS, C.E., UBER, C.F., Steam Generator Tubing Development for Commercial Fast Breeder Reactors, Nuclear Technology, Vol. 55, p. 280 (1981).

[83] SESSIONS, C.E., REYNOLDS JR., S.D., HEBBAR, M.A., LEWIS, J.F., KIEFER, J.H., Materials Development for a Fast Breeder Reactor Steam Generator Concept, Nuclear Technology, Vol. 55, p. 270 (1981).
[84] DUKE J.M., HEBBAR, M., REYNOLDS, S.D., LEWIS, J., Material Consideration for Large Sodium Heated Steam Generator, ANS Transactions, Vol. 27, p. 224 (1977).
[85] ROBIN, M.G., BEFRE, J., CACHERA, P., FOUCHE, L., LIONS, N., POUDEROUX, P., Developpement en France des Generateurs de Vapeur Chauffes par Sodium Liquide, paper presented in Symposium on Progress in Sodium-Cooled Fast Reactor Engineering, Monaco, March 1970 (in French).
[86] ROBIN, M.G., SAUR, J.M., SCHWAB, B., LIONS, N., BEAUFRERE, J., LECOCQ, P., PHÉNIX Steam Generator Development and Preliminary Operation, Proc. Int. Conf. Organized by British Nuclear Energy Society–Fast Reactor Power Station, London, UK, p. 205 (March 1974).
[87] DUCHATELLE, L., DE NUCHEZE, L., ROBIN, M.G., Theoretical and Experimental Study of Phenix Steam Generator Prototype Modules, Nuclear Technology, Vol. 24, p. 123 (1974).
[88] ROBIN, M.G., French Steam Generator Experience – Phénix and Beyond, Nuclear Technology, Vol. 28, p. 482 (1976).
[89] FONTAINE, J.P., LLORY, M., Ten Years of Steam Generator Tests on a 45 MW Sodium Test Loop, Proc. 3rd Int. Conf. Liquid Metal Engineering and Technology, Oxford, UK, 9-13 April 1984, British Nuclear Energy Society (1984).
[90] BEFRE, J.L., DELISLE, J.P., ROBIN, M.G., Circuits and Main Components, Nuclear Engineering International, Vol. 16, p. 567 (1971).
[91] ROBIN, M.G., SAUR, J.M., VIAL, B., BRACHET, A., Conception, Construction et Experience D'exploitation des Circuits de Sodium Secondaire de Reacteurs Rapides, Proc. Int. Symposium on Design, Construction and Operating Experience of Demonstration Liquid Metal Fast Reactors, Bologna, Italy, p. 527 (April 1978) (in French).
[92] ELIE, X., Operation Experience with the Phénix Prototype Reactor, Proc. Int. Conf. Fast Reactors and Related Fuel Cycles, Kyoto, Japan, Paper 5-1 (November 1991).
[93] SAUVAGE, J.F., GUIDEZ, J., CHAUCHEPRAT, P., MARTIN, L., Thirty Years of Operation of the Phenix Fast Breeder Reactor, Proc. ICAPP '05, Seoul, Korea, 15-19 May 2005, ISBN: 9781604236934, Curran Associates Inc. (April 2007) paper 5625.
[94] LECOEUVRE, J.M., HEMMERICH, P., Numerical Simulation in Unsteady-State Running of the 45 MW Scale Model Super-Phénix Steam Generator, Proc. 2nd Int. Conf. Boiler Dynamics & Control in Nuclear Power Stations, Bournemouth, UK, p. 87 (October 1979).
[95] CHELLI, L., PAPA, G., SALGO, C., Transient Calculations of a 45MWth Steam Generator Model for Sodium-cooled Fast Breeder Reactors, Proc. 2nd Int. Conf. Boiler Dynamics & Control in Nuclear Power Stations, Bournemouth, UK, p. 87 (October 1979).
[96] PERRIN, J., SIMEON, CH., Prediction of Dynamic Stability Limits of the 45 MW Scale Model of Super Phénix Steam Generator, Proc. 2nd Int. Conf. Boiler Dynamics & Control in Nuclear Power Stations, Bournemouth, UK, p. 87 (October 1979).
[97] VALETTE, M., A Heat Transfer Study for Vertical Straight-Tube Steam Generators Heated by Liquid Metal, Proc. 3rd Int. Conf. on Liquid Metal Engineering and Technology, Oxford, London, UK, 9-13 April 1984, British Nuclear Energy Society, p. 171 (1984).
[98] FABREGURE, J.P., LAURET, PH., MIREAU, J.P., SuperPhénix Steam Generators: Analysis of Thermal Hydraulic Behaviour under Steady State and Transient Condition, Proc. 3rd Int. Conf. Boiler Dynamics & Control in Nuclear Power Stations, Harrogate, UK, p. 267 (October 1985).
[99] BARBERIS, M., AVANZINI, P.G., CASALINI, P., SALGO, G., MANONI, A., 50-MW Prototype of the NIRA/CNEN Sodium Heated Steam Generator, Proc. 2nd Int. Conf. Liquid Metal Technology in Energy Production, Richland, Washington, 20-24 April 1980, Ed. J. M. Kahlke, U.S. Department of Energy (1980).
[100] AVANZINI, P.G., VALENTINI, P., BOTTIGLIONI, F., CASALINI, P., SALGO, C., CAVALLERI, P., CUMO, M., SCIBONA, G., DI SCIASCIO, N., PANZERI, D., RINALDI, F., VACCHIANO, S., Design, R&D and Manufacture of the Components of

Secondary Circuits for Fast Sodium Power Plant, Proc. Int. Symposium on Design, Construction and Operating Experience of Demonstration Liquid Metal Fast Reactors, Bologna, Italy, p. 605 (April 1978).
[101] CASALINI, P., SALGO, C., GEROSA, A., VALENTINI, P., DI LEO, S., AVAZINI, P.G., CAVALLERI, G., The Italian Programme of Sodium-Heated Steam Generators, Proc. Int. Conf. organized by British Nuclear Society – Fast Reactor Power Station, London, UK, Thomas Telford, Ltd., London, p. 137 (March 1974).
[102] SALGO, C., BET, M., VALENTINI, S., Tests on the 45 MW NIRA-ENEA LMFBR Prototype Steam Generator After Sodium Performance, Proc. 3rd Int. Conf. on Liquid Metal Engineering and Technology, Oxford, London, UK, 9-13 April 1984, British Nuclear Energy Society, p. 225 (1984).
[103] CRETTE, J.P., ZUBER, T., SuperPhénix 1 Steam Generator Fabrication, Nuclear Technology, Vol. 68, p. 171 (1985).
[104] ZUBER, T., The Creys-Malville Plant Steam Generator, Proc. 2nd Int. Conf. Liquid Metal Technology in Energy Production, Richland, Washington, 20-24 April 1980, (Editor J. M. Kahlke), U.S. Department of Energy (1980).
[105] SAUR, J.M., BALLOT, E., ROBIN, M.G., ZUBER, T., French Fast Breeder Reactor Main Components: The Steam Generators, ANS Transactions, Vol. 31, p. 615 (1979).
[106] FONTAINE, J.P., LLORY, M., MASSE, J., QUINET, J.L., Synthesis of Scale-Model Steam Generator Tests Proposed for the Super-Phénix Nuclear Power Plant, ANS Transactions, Vol. 20, p. 141 (1975).
[107] Construction of the World's First Full-Scale Fast Breeder Reactor, Nuclear Engineering International, Vol. 23, p. 43 (1978).
[108] STEIGER, W., SCHREIBMAIER, J., Some Experiences with Sodium Exposed Components in KNK, Proc. Int. Conf. Fast Reactors and Related Fuel Cycles, Kyoto, Japan, Paper 5-2, November 1991.
[109] MARTH, W., KNK Power Plant-Achievements and Future Programs, Proc. 1976 ASME-ANS International Conference–Advanced Nuclear Energy Systems, Pittsburg, Pennsylvania,USA, p. 89 (March 1976).
[110] LORENZ, H., HERBERG, G., KNK Steam Generator Damage, ANS Transactions, Vol. 20, p. 200 (1975).
[111] BUSCHER, E., HAUBOLD, W., JANSING, W., VINZENS, K., Testing of a Bayonet-Type Integrated Steam Generator System for Sodium-cooled Breeders, ANS Transactions, Vol. 20, p. 206 (1975).
[112] BRUDERMULLER, G., FINKE, G., GUTHMANN, E., HENDL, G., MARTH, W., Operating Experience with the KNK Reactor and Preparation for a Fast Mixed Oxide Core (KNK II), Proc. Int. Conf. Fast Reactor Power Station, London, UK, British Nuclear Energy Society, p. 111 (March 1974).
[113] DE CLERCQ, W.J.C., VAN WAVEREN, N.J., Steam-Generator and Intermediate Heat-Exchanger Development, paper presented in Symposium on Progress in Sodium-Cooled Fast Reactor Engineering, Monaco, March 1970.
[114] KNAAP, M.H., LUDWIG, P.W.P.H., SMIT, C.C., VAN WESTENBRUGGE, J.K., BROODMAN, J.J., VAN DER KROGT, C.A.J., Development, Design, Construction and Prototype Test Experience of Steam Generators for SNR 300, Proc. Int. Symposium on Design, Construction and Operating Experience of Demonstration Liquid Metal Fast Reactors, Bologna, Italy, p. 587 (April 1978).
[115] MANTE, J.H., BRAUN, A.R., JANSING, W.J., MAUSBECK, H., Operational Experience with Main Circuit Components for the SNR 300 Power Plant, Proc. Int. Conf. Fast Reactor Power Station, London, UK, British Nuclear Energy Society, p. 157 (March 1974).
[116] DE CLERCQ, W.J.C., VAN DER KROGT, C.A.J., RUYTERMAN, C., LUDWIG, P.W.P.H., POIESZ, M.J., BROODMAN, J.J., VAN DEN BOOMEN, M.A., The Development of Sodium-Heated Steam Generators in the Netherlands, Proc. Int. Conf. Fast Reactor Power Station, London, UK, British Nuclear Energy Society, p. 173 (March 1974).

[117] UNAL, H.C., VAN GASSELT, M.L.G., LUDWIG, P.W.P.H., Dynamic Instabilities in Tubes of a Large Capacity, Straight-Tube, Once-through Sodium Heated Steam Generator, International Journal of Heat and Mass Transfer, Vol. 20, p. 1389 (1977).
[118] BRASZ, J., VAN ESSEN, D., Experimental Determination of Density-wave Oscillations in Full-scale Sodium-heated Steam Generators, paper presented in 2nd Int. Conf.: Boiler Dynamics & Control in Nuclear Power Stations, Bournemouth, UK, p. 177 (October 1979).
[119] VAN WESTENBRUGGE, J.K., TROMP, T.J., DE MAEIJER, J.R.A., Result of the Test and Inspection Programme of the Prototype SNR-300 Steam Generators, Proc. Int. Conf. organized by BNES: Ferritic Steels for Fast Reactor Steam Generators, London, UK, p. 16 (June 1978).
[120] DREYER, S., The Heat Transfer System of SNR, Nuclear Engineering International, Vol. 21, p. 49 (1976).
[121] DE HASS VAN DORSSER, H., Main Heat Transfer Components for SNR-300, Nuclear Engineering International, Vol. 21, p. 49 (1976).
[122] DE HAAS VAN DOSSER, H., SNR Coolant System Components, Proc. 1976 ASME-ANS International Conference–Advanced Nuclear Energy Systems, Pittsburg, Pennsylvania, p. 181 (March 1976).
[123] BRANDSTETTER, E.A., GUTHMANN, A., STOHR, K.W., SNR Construction Experience, Proc. of the 1976 ASME-ANS International Conference–Advanced Nuclear Energy Systems, Pittsburg, Pennsylvania, p. 97 (March 1976).
[124] VANT' HOFT, J., DE JONG, J.J., VROOM, J.P., KUPERS, G.R., Fabrication of Interim Heat Exchangers, Steam Generators, and Sodium Pumps for SNR-300, Nuclear Technology, Vol.78, p. 262 (1987).
[125] MATTHEWS, R.R., HUTCHINSON, W.G., FENEMORE, A.S. Design and Construction of the Dounreay Fast Reactor Heat-Transfer Circuits, Steam-Generating Plant, and Reactor-Control System, Proc. Symposium on the Dounreay Fast Reactor, p. 27 (1960).
[126] HENRY, K.J., Technical Description of PFR, Nuclear Engineering International, Vol. 16, p. 632 (1971).
[127] SCOTT, R.W., PFR Components, Nuclear Engineering International, Vol. 16, p. 646 (1971).
[128] TAYLOR, D., MILLICAN, B.P., Erection and Testing of PFR Secondary Circuits and Steam Generator, Proc. Int. Conf. Fast Reactor Power Station, London, UK, British Nuclear Energy Society, p. 223 (March 1974).
[129] TAYLOR, D., Prototype Fast Reactor Heat-Transport System, paper presented in Int. Symposium Progress in Sodium-Cooled Fast Reactor Engineering, Monaco, March 1970.
[130] BOLT, P.R., CARRUTHERS, H.M., Some Comments on Sodium/Water Reaction Problems from the Viewpoint of a Power Station Purchaser and Operator, paper presented in Int. Symposium Progress in Sodium-Cooled Fast Reactor Engineering, Monaco, March 1970.
[131] TAYLOR, D., SMEDLEY, J., BROOMFILED, A.M., Operation of the PFR and Design of the CDFR Secondary Circuit, Proc. Int. Symposium Design, Construction and Operating Experience of Demonstration Liquid Metal Fast Reactors, Bologna, Italy, p. 509 (April 1978).
[132] HIND, J.R., TAYLOR, A.F., Sleeving Repair of Prototype Fast Reactor Evaporators, Proc. 3rd Int. Conf. on Liquid Metal Engineering and Technology, Oxford, London, UK, 9-13 April 1984, British Nuclear Energy Society (1984).
[133] EVANS, D., BROOMFIELD, A.M., SMEDLEY, J.A., BRAY, J.A., Operating Experience with the PFR Evaporators, Proc. of Int. Conf. organized by BNES: Ferritic Steels for Fast Reactor Steam Generators, London, UK, p. 509 (June 1978).
[134] KIRKLAND, G.R., DAVIES, E.R., LAMBERT, M.E., KENNETT, E.J., Metallurgical Examination of Tube-to-Tube-Plate Welds Removed from Dounreay Prototype Fast Reactor Evaporators, Nuclear Technology, Vol. 55, p. 289 (1981).
[135] BROOMFIELD, M., Operating Experience on the Prototype Fast Reactor, Nuclear Energy, Vol. 25, No. 2, p. 73 (1986).

[136] SMEDLEY, J.A., BROOMFIELD, A.M., ANDERSON, R., Dounreay Fast Reactor Boilers Get a New Lease of Life Part 1: The Problems Caused by Small Leaks and the Search for Solution, Nuclear Engineering International, Vol. 29, p. 26 (February 1984).
[137] HIND, J.R., MATHER, B., SIMMERS, A., Dounreay Fast Reactor Boilers Get a New Lease of Life Part 2: Design and Installation of Internal Sleeves, Nuclear Engineering International, Vol. 29, p. 40 (March 1984).
[138] TAYLOR, F., DICKINSON, F.S., THATCHER, G., Dounreay Fast Reactor Boilers Get a New Lease of Life Part 3: Development of the Sleeving Repair Techniques, Nuclear Engineering International, Vol. 29, p. 34 (April 1984).
[139] BRIERLEY, G., HAYDEN, O., Replacement Superheaters and Reheaters for the Prototype Fast Reactor, Proc. 3rd Int. Conf. on Liquid Metal Engineering and Technology, Oxford, London, UK, 9-13 April 1984, British Nuclear Energy Society (1984).
[140] JUDD, M., CURRIE, R., LINEKAR, G.A.B., HENDERSON, J.D.C., The Under-Sodium Leak in the PFR Superheater 2, February 1987, Nuclear Energy, Vol. 31, No. 3, p. 221 (1992).
[141] GREGORY, V., A Review of the Operation of the Prototype Fast Reactor, Nuclear Energy, Vol. 31, No. 3, p. 173 (1992).
[142] GREGORY, V., Operating Experience with the Prototype Fast Reactor at Dounreay, Proc. Int. Conf. on Fast Reactors and Related Fuel Cycles, Kyoto, Japan, paper 5-3 (November 1991).
[143] INTERNATINAL ATOMIC ENERGY AGENCY, Status of Liquid Metal Cooled Fast Reactor Technology, IAEA-TECDOC-1083, Vienna, Austria (1999).
[144] KAWAHARA, S., OGASAWARA, H., YAMANOUCHI, A., TACHI, Y., Design of the Sodium-Heated Steam Generator for the FBR Nuclear Power Station, paper presented in Int. Symposium on Progress in Sodium-Cooled Fast Reactor Engineering, Monaco, March 1970.
[145] NAGANUMA, T., NAKAI, Y., WATANABE, T., The Experimental Results of a Small-Scale Sodium-to-Sodium Heat Exchanger and Sodium-heated Steam Generator, Proc. Symposium on Progress in Sodium-Cooled Fast Reactor Engineering, Monaco, March 1970.
[146] NAKAI, Y., WATANABE, T., HOSHI, Y., HORI, M., SANO, A., Steam Generators for the MONJU Power Plant, Proc. Int. Conf. Fast Reactor Power Station, London, UK, British Nuclear Energy Society, p. 151 (March 1974).
[147] IMANAKA, N., NAKAI, Y., Design of the Monju Heat Transport System and the Related R&D Work, Including Steam Generator, paper presented in Int. Symposium Design, Construction and Operating Experience of Demonstration Liquid Metal Fast Reactors, Bologna, Italy, p. 573 (April 1978).
[148] NAKAI, S., ENDOU, H., IMAI, H., FUKUDA, T., Dynamic Characteristics of Steam Generator of LMFBR MONJU, Proc. 3rd Int. Conf.: Boiler Dynamics & Control in Nuclear Power Stations, Harrogate, UK (October 1985).
[149] KUBOTA, J., TSUCHIYAMA, T., IWASHITA, T., MONTA, K., Hydrodynamic Stability Tests and Analytical Model Development for Once-through Sodium Heated Steam Generator, Proc. 2nd Int. Conf. Boiler Dynamics & Control in Nuclear Power Stations, Bournemouth, UK, p. 105 (October 1979).
[150] TSUDA, H., KAWARA, M., SHIBATO, E., KANAMORI, A., Post-Performance Examination of the 50 MW Steam Generator for the Prototype Fast Breeder Reactor Monju, Proc. Int. Conf. Organized by BNES: Ferritic Steels for Fast Reactor Steam Generators, London, UK p. 22 (June 1978).
[151] SAKAI, T., YAMAGUCHI, A., METZ, P., Thermal-Hydraulic Analysis for a Sodium-Heated Steam Generator Using a Multi-Shell Method, Nuclear Engineering and Design, Vol. 2, No. 19, p. 35 (2003).
[152] NAKAI, Y., MOCHIZUKI, K., AOKI, T., YAMAKI, H., LMFBR Coolant System Components Development in Japan, Proc. ASME-ANS Int. Conf. Advanced Nuclear Energy Systems, Pittsburg, Pennsylvania, p. 193 (March 1976).
[153] SAKAI, S., NAKAMURA, S., SATO, M., KUROKAWA, M., WAKI, M., TSUDA, H., TAKEDA, S., Design and Construction of the Steam Generator and Water Steam Systems of

the Prototype Fast Breeder Reactor Monju, Proc. Int. Conf. on Fast Reactors and Related Fuel Cycles, Kyoto, Japan (November 1991) paper 8-5.
[154] KISOHARA, N., NAKAI, S., SATO, H., YATABE, T., Development of a Double-Wall-Tube Steam Generator–Evaluation of Thermal Hydraulic Tests on High Mass Flow Rate Condition, TN9400 2001-093 (2001) (in Japanese).
[155] KISOHARA, N., NAKAI, S., TANABE, H., KUBOTA, S., SAKAKIBARA, Y., INOUE, M., KASHIWAKURA, J., MOTOOKA, N., YANO, K., Feasibility Study on Double-Wall-Tube Type Primary Steam Generator, Proc. Int. Conf. Fast Reactors and Related Fuel Cycles, Kyoto, Japan (November 1991) paper 2-7.
[156] GRYAZAV, V.M., KRASNOYAROV, N.V., KEVROLEV, V.P., KONDRAT'EV, V.I., NECHAEV, B.N., SMIRNOV, A.M., Four Year's Operating Experience on the Experimental BOR 60 Nuclear Power Station, Proc. Int. Conf. Fast Reactor Power Station, London, UK, British Nuclear Energy Society, p. 21 (March 1974).
[157] MATAL, O., KUGLER, V., TOMES, V., LOCHMAN, K., SIMO, T., Chechoslovak Inverse Prototype 30 MW Steam Generator Heated by Liquid Sodium, Proc. 3rd Int. Conf. on Liquid Metal Engineering and Technology, Oxford, London, UK, 9-13 April 1984, British Nuclear Energy Society p. 211 (1984).
[158] BLAGOVOIN, S.M., BAKLUSHIN, R.P., FEDOROV, V.G., GRDLICHKO, E.M., GUBANOV, V.M., LOGVINOV, S.A., LUKASEVICH, B.I., NEKRASOV, A.V., STEKOL'NIKOV, V.V., YURCHENKO, D.S., Results of Experimental and Startup Adjustment Works on the Steam Generators of the BN 350 Installation, Proc. Int. Conf. Fast Reactor Power Station, London, UK, British Nuclear Energy Society, p. 21 (March 1974).
[159] BUKSHA, Y.K., BAGDASSAROV, Y.E., KIRYUSHIN, A.I, KUZAVKOV, N.G., KAMANIN, Y.L., OSHKANOV, N.N. VYLOMOV, V.V., Operation Experience of the BN-600 Fast Reactor, Nuclear Engineering and Design, Vol. 173, p. 67 (1997).
[160] BERGLUND, R.C., TIPPETS, F.E., PRISM, the Plant Design Concept for the U.S Advanced Liquid Metal Reactor Plant, Proc. of American Power Conference, Vol. 51, p. 697 (1989)
[161] DUMM, K., EBR-600MW Straight Tube Steam Generator-The Strategy Towards the Definition of a Design Basis Accident, Proc. Specialists' Meeting on Steam Generator Failure and Failure Propagation Experience, No. 1-4, Aix-en-Provence, France, September 1990.
[162] KONOMURA, M., ICHIMIYA, M., Design Challenges for Sodium Cooled Fast Reactors, Journal of Nuclear Materials, Vol. 371, p. 250 (2007).
[163] KISOHARA, N., MORIBE T., SAKAI, T., Flow and Temperature Distribution Evaluation on Sodium Heated Large-sized Straight Double-wall-tube Steam Generator, Proc. ICAPP'06, Reno, Nevada, 4-8 June 2006, ANS, ISBN: 0-89448-698-5 (CD-ROM).
[164] MATSUMOTO, K., OHTA, Y., KATAOKA, T., YUKITOSHI, T., MOROISHI, T., YOSHIKAWA, K., Carbon Transfer Behaviour of Materials for Liquid-metal Fast Breeder Reactor Steam Generator, Nuclear Technology, Vol. 28, p. 452 (1976).
[165] DEVAN, J.H., GRIESS, J.C., Clinch River Breeder Reactor Environmental Effects-Generator Water-side Corrosion, Nuclear Technology, Vol. 28, p. 398 (1976).
[166] NATESAN, K., CHOPRA, O.K., KASSNER, T.F., Compatibility of Fe-2 ¼ wt% Cr-1 wt% Mo Steel in a Sodium Environment, Nuclear Technology, Vol. 28, p. 441 (1976).
[167] YUKITOSHI, T., MOROISHI, T., KOIZUMI, I., ABEM, T., YOSHIKAWA, K., SHIDA, Y., Comparison of Various Chromium Molybdenum Low-alloy Steels for Liquid-metal Fast Breeder Reactor Steam Generators, Nuclear Technology, Vol. 28, p. 506 (1976).
[168] BRINKMAN, C.R., WILLIAMS, R.K., KLUEH, R.L., Mechanical and Physical Properties of 2¼ Cr-1 Mo Steel in Support of Clinch River Breeder Reactor Plant Steam Generator Design, Nuclear Technology, Vol. 28, p. 490 (1976).
[169] TAVASSOLI, TOURON, H., WEISZ, M., Effect of Decarburization on Structural and Mechanical Properties of Ferritic Steels, Nuclear Technology, Vol. 55, p. 302 (1981).

[170] KNAAP, M.H., NIEUWLAND, H.C.D., VRIJEN, J., VAN WESTENBRUGGE, J.K., HUSSLAGE, W., SCHEEPENS, C.P., SCHINKEL, J.W., SNR 300 Experience in Steam Generator Materials, Nuclear Technology, Vol. 55, p. 218 (1981).
[171] ROY, P., SPALARIS, C.N., Some Aspects of Materials Development for Sodium-Heated Steam Generators, Nuclear Technology, Vol. 55, p. 259 (1981).
[172] THEUS, G.J., Caustic Stress Corrosion Cracking of Inconel-600, Incoloy-800, and Type 304 Stainless Steel, Nuclear Technology, Vol. 28, p. 388 (1976).
[173] PATRIARCA, P., HARKNESS, S.D., DUKE, J.M., COOPER, L.R., U.S. Advanced Materials Development Program for Steam Generators, Nuclear Technology, Vol. 28, p. 516 (1976).
[174] ASADA, Y., DOZAKI, K., UETA, M., ICHIMIYA, M., MORI, K., TAGUCHI, K., KITAGAWA, M., NISHIDA, T., SAKON, T., SUKEKAWA, M., Exploratory Research on Creep and Fatigue Properties of 9Cr-steels for the Steam Generator of an FBR, Nuclear Engineering and Design, Vol. 139, p. 269 (1993).
[175] ITO, T., KATO, S., AOKI, M. YOSHIDA, E., KOBAYASHI, T., WADA, Y., Evaluation of Carburization and Decarburization Behavior of Fe-9Cr-Mo Ferritic Steels in Sodium Environment, Journal of Nuclear Science and Technology, Vol. 29(4), p. 367 (1992).
[176] VAN WESTENBRUGGE, J.K., VAN ESSEN, D., NERATOOM, B.V., Stability Tests in a 5 MW 10-Tube Sodium Heated Test Rig, Proc. 3rd Int. Conf. on Liquid Metal Engineering and Technology, Oxford, UK, p. 191 (April 1984).
[177] VRIJEN, J., WESTENBRUGGE, J.K., VAN DER WIEL, L., RADEMAKERS, P.L.F., SCHEEPENS, C.P., SCHINKEL, J.W., Material Selection and Optimization for Post-SNR-300 Steam Generator, Nuclear Technology, Vol. 55, p. 250 (1981).
[178] GREEN, S.J., Thermal, Hydraulic and Corrosion Aspects of PWR Steam Generator Problems, Heat Transfer Engineering, Vol. 9. No. 1, p.19 (1988).
[179] HAHN, D.H., KALIMER Design Concept Report, KAERI/TR-888/97 (1997).
[180] KIM, Y.S., et al., Proc. KNS Autumn Meeting, Taegu, Korea, Republic of, 24-25 October 1997, Proc. of the Korean Nuclear Society, p. 558 (1997).
[181] EOH, J.H., JEONG, J.Y., KIM, S.O., HAHN, D.H., PARK, N.C., Development and Experimental Verification of the Numerical Simulation Method for the Quasi-Steady SWR Phenomena in an LMR Steam Generator, Nuclear Technology, Vol. 152, pp. 286-301 (December 2005).
[182] SHIN, Y.W., VALENTIN, R.A., SWAAM-Code Development and Verification and Application to Steam Generator Designs, paper presented in IAEA Working Group on Fast Reactors, Aix-En-Provence, France, 26 September-3October 1990.
[183] MIYAKE, O., SHINDO, Y., HIROI, H., TANABE, H., SATO, M., Large Leak Sodium-Water Reaction Code SWACS and its Validation, paper presented in Int. Topical Meeting on LMFBR safety, Lyon, France, 19-23 July 1982.
[184] GREENE, D.A., Steam Generator Vessel Pressures Resulting from a Sodium/Water Reaction: A Computer Analysis with the SWEAR Code, Nucl. Technol. Vol. 14, No. 3, pp. 218-231 (1972).
[185] VAMBENEPE, G., Liquid Metal Fast Breeder Reactor Steam Generator Survey of the Consequences of Large Scale Sodium Water Reaction, paper presented in ENS/ANS Int. Topical Meeting on Nuclear Power Reactor Safety, Brussels, Belgium, 16-19 October 1978.
[186] HORI, M., Sodium/Water Reactions in Steam Generators of Liquid Metal Fast Breeder Reactors, Atomic Energy Review-Austria, Vol. 18, No. 3, pp. 707-778 (1980).
[187] PARK, J.H., CHOI, J.H., KIM, T.J., JEONG, K.C., Development of the SPIKE Code for Analysis of the Sodium Water Reaction, KAERI/TR-1123/98, Korea Atomic Energy Research Institute (KAERI), Daejon, Korea, Republic of (August 1998).
[188] EOH, J.H., KIM, E.K., KIM, S.O., Development of Tube Leak Model for Analysis Code of SWR in LMR, Proc. Korean Nuclear Society (KNS), 2002 Autumn Meeting, Yong-Pyeong, Korea, Republic of, 23-25 October 2001.
[189] KIM, Y.S., SIM, Y.S., KIM, E.K., EOH, J.H., Evaluation of the SWR's Early Pressure Variations in the KALIMER IHTS, J. Energy Engg., Vol. 11, No. 2, pp. 122-129 (2002).

[190] NEI, H., Dissolution ratio of Hydrogen Generated by Small-Leak Sodium-Water Reaction, J. Nuclear Science and Technology, Vol. 14, No. 9, pp. 652-660 (1977).
[191] HAHN, D.H., KALIMER Conceptual Design Report, KAERI/TR-2204/2002, Korea Atomic Energy Research Institute (KAERI), Daejon, Korea, Republic of, (May 2002).
[192] DIERS, Proc. Int. Symposium on Runaway Reactions and Pressure Relief Design, New York: The Design Institute for Emergency Relief Systems (DIERS), AIChE, (1995).
[193] KIM, S., EOH, J.H., KIM, S.O., Design and Validity Study of a Pressure Relief System for a Sodium-Water Reaction in KALIMER, paper presented in ICAPP '05, Seoul, Korea, Rep. of, 15-19 May 2005.
[194] ISHIDA, K., YABANA, S., SHIBATA, H., Distinctive Features of Proposed Technical Guidelines for the Design of Seismically Isolated Fast Breeder Plants, ASME, Vol. 319, pp. 309 (1995).
[195] INAGAKI, T., WATANABE, Y., UETA, M., et al, The Design of Seismic Isolated Demonstration FBR Plant, ASME, PVP-Vol. 341, pp. 129 (1996).
[196] TAKAHASHI, K., INOUE, K., MORISHITA, M., et al, Development of Three-Dimensional Seismic Isolation Technology for Next Generation Nuclear Power Plant Applications, ASME, PVP2005-71357, (2005).
[197] NP-1220-SR, A Review of Seismic Isolation for Nuclear Structures, Special Report, Electric Power Research Institute (1979).
[198] SEIDENSTICKER, R.W., R & D Activities at Argonne National Laboratory for the Application of Base Seismic Isolation in Nuclear Facilities, Proc. 7th Int. Seminar on Seismic Isolation of Nuclear and Non-Nuclear Structures, Nara, Japan 1991, pp. 167-182 (1991).
[199] TAJIRIAN, F.F., KELLY, J.M., AIKEN, I.D., Seismic Isolation for Advanced Nuclear Power Stations, Earthquake Spectra, Vol. 6, No. 2, pp. 371-401 (1990).
[200] NUREG-1368, Preapplication Safety Evaluation Report for the Power Reactor Innovative Small Module (PRISM) Liquid-Metal Reactor, Final Report, U.S. Nuclear Regulatory Commission (1994).
[201] SOMMER, S.C., Potential Role of Seismic Base Isolation in the DOE, paper presented in Fourth DOE Natural Phenomena Hazards Mitigation Conference, Atlanta, Georgia, USA, 19-22 October 1993.
[202] CONF-9205413, Technology Transfer Package on Seismic Base Isolation, Lawrence Livermore National Laboratory (3 Vols) (1995).
[203] DOE Standard, DOE-STD-1020-2002, Natural Phenomena Hazards Design and Evaluation Criteria for Department of Energy Facilities (January 2002).
[204] TARICS, G., WAY, D., KELLY, J.M., The Implementation of Base Isolation for the Foothill Communities Law and Justice Center County of San Bernardino, California, Report to the National Science Foundation and the County of San Bernardino, Reid and Tarics Associates (November 1984).
[205] TAJIRIAN, F.F., SCHRAG, M.R., Conceptual Design of Seismic Isolation for the PRISM Liquid Metal Reactor, paper presented in SMiRT-9 Conference, Lausanne, Switzerland, 1987.
[206] JANGID, R.S., DATTA, T.K., Seismic Behavior of Base-Isolated Buildings: a State-of-the-art Review, Structures and Buildings, Vol. 110, pp. 186-202 (1995).
[207] ZAYAS, V.A., LOW, S.S., MAHIN, S.A., The FPS Earthquake Resisting System: Experimental Report, Report no. UCB/EERC-87/01, Earthquake Engineering Center, University of California, Berkeley (June 1987).
[208] ZAYAS, V.A., et al, Feasibility and Performance Studies on Improving the Earthquake Resistance of New and Existing Buildings Using the Friction Pendulum System, Report no. UCB/EERC-89/09, Earthquake Engineering Center, University of California, Berkeley (September 1989).
[209] RYAN, K.L., CHOPRA, A.K., Estimating the Seismic Displacement of Friction Pendulum Isolators based on Non-Linear Response History Analysis, Earthquake Engineering and Structural Dynamics, Vol. 33, pp. 359-373 (2004).

[210] NAEIM, F., KELLY, J.M., Design of Seismic Isolated Structures: From Theory to Practice, John Wiley & Sons (1999).
[211] MOKHA CONSTANTINOU, M.C., REINHORN, A.M., ZAYAS, V.A., Experimental Study of Friction Pendulum Isolation System, Journal of Structural Engineering, Vol. 117, No. 4, pp. 1201-1217 (1991).
[212] CONSTANTINOU, M.C., Friction Pendulum Double Concave Bearing, Technical Report, State University of New York, Buffalo, NY (October 2004).
[213] TSAI, S., et al., An Improved FPS Isolator for Seismic Mitigation on Steel Structures, Proc. ASME Pressure Vessels and Piping Conference, Vancouver, Canada, pp. 237-244 (2002).
[214] TSAI, S., et al., Shaking Table Tests of a Full Scale Steel Structure Isolated with MFPS, Proc. ASME Pressure Vessels and Piping Conference, Ohio, USA, pp. 41-47 (2003).
[215] TSAI, S., et al., Component and Shaking Table Tests for Full-Scale Multiple Friction Pendulum System, Earthquake Engineering and Structural Dynamics, Vol. 35, pp. 1653-1675 (2006).
[216] FENZ, M., CONSTANTINOU, M.C., Behaviour of the Double Concave Friction Pendulum Bearings, Earthquake Engineering and Structural Dynamics, Vol. 35, pp. 1403-1424 (2006).
[217] KELLY, T.E., Base Isolation Structures – Design Guidelines, Holmes Consulting Group Ltd. (July 2001).
[218] KELLY, J.M., State-of-the-Art and State-of-the-Practice in Base Isolation, Proc. ATC-17-1 Seminar on Seismic Isolation, Passive Energy Dissipation, and Active Control, Applied Technology Council, San Francisco, CA, USA (March 1993).
[219] TYLER, R.G., Dynamic Test of PFTE Sliding Layers under Earthquake Conditions, Bulletin New Zealand National Society for Earthquake Engineering, 10, pp. 129-138 (1977).
[220] GLUEKIER, AOYAGI, S., Meeting Summary Discussion and Recommendations, paper presented in the IAEA Specialists' Meeting on Seismic Isolation Technology, GE Nuclear Energy, San Jose, California, USA 8-20 March 1992.
[221] MOKHA, A.M., CONSTANTINOU, M.C., REINHORN, A.M., Teflon Bearing in Base I solation. Part 1: Testing, Journal of Structural Engineering, ASCE, Vol. 116, No. 2, pp. 438-454 (1990).
[222] CONSTANTINOU, M.C., MOKHA, A.M., REINHORN, A.M., Teflon Bearing in Base Isolation. Part 2, Journal of Structural Engineering, ASCE, Vol. 116, No. 2, pp. 455-474 (1990).
[223] CONSTANTINOU, M.C., MOKHA, A.M., REINHORN, A.M., PTFE Bearings in Base Isolation: Modeling, Journal of Earthquake Engineering, Vol. 116, No. 2, pp. 455-472 (1990).
[224] MOKHA, M., CONSTANTINOU, M.C., REINHORN, A.M., Verification of Friction Model of PTFE Bearings under Triaxial Load, Journal of Structural Division, ASCE, Vol. 119, No. 1, pp. 240–261 (1993).
[225] TSAI, S., Seismic Behavior of Building with FPS Isolators, Proc. 2nd Congress on Computing in Civil Engineering, Atlanta, Georgia, USA, 5-8 June 1995, ASCE, ISBN-10: 0784400881; ISBN-13: 978-0784400883, pp. 1203-1211 (May 1995).
[226] TSAI, S., FEM with Local Effects for Flat Sliding System, Computer and Structures, International Journal, Vol. 61, No. 6, pp. 1003-1024 (1996).
[227] TSAI, S., Finite Element Formulations for Friction Pendulum Seismic Isolation Bearings, International Journal for Numerical Methods in Engineering, Vol. 40, No. 1, pp. 29-49 (1997).
[228] ALMAZAN, J.L., DE LA LLERA, J.C., INAUDI, J.A., Modelling Aspects of Structures Isolated with the Frictional Pendulum System, Earthquake Engineering and Structural Dynamics, 27, pp. 845-867 (1998).
[229] ALMAZAN, J.L., DE LA LLERA, J.C., Analytical Model for Structures with Frictional Pendulum Isolators, Earthquake Engineering and Structural Dynamics, 31, pp. 305-332 (2002).

[230] ALMAZAN, J.L., DE LA LLERA, J.C., Physical Model for Dynamic Analysis of Structures with FPS Isolators, Earthquake Engineering and Structural Dynamics, 32, pp. 1157-1184 (2003).
[231] MOKHA, A.M., NAVINCHANDRA, A., CONSTANTINOU, M.C., ZAYAS, V., Seismic Isolation Retrofit of Large Historic Building, Journal of Structural Engineering, ASCE, Vol. 122, No. 3, pp. 98-308 (1996).
[232] MOKHA, A.M., CONSTANTINOU, M.C., REINHORN, A.M., Further Results on the Frictional Properties of Teflon Bearings, Journal of Structural Engineering, Vol. 117, No. 2, pp. 622-626 (1991).
[233] PRELE, G., CAPITAINE, A., BISCARRAT, F., SANSEIGNE, E., SAEZ, M., RODRIGUEZ, G., MAJOT, C., CHASSIGNET, M., Some Experimental Feedback of the Fuel Handling System of French Sodium Fast Reactor regarding Specific Operations: Cleaning, Refuelling, Final Defuelling, paper presented in IAEA Technical Meeting on Fuel Handling Systems of Sodium Cooled Fast Reactors, 24–27 November 2007, Kalpakkam, India.
[234] ANZIEU, P., SERPANTIE, J.P., VERWAERDE, D., DUFOUR, PH, MARTIN, PH., A Program on Innovative SFR in France, Proc. ICAPP'07, Nice, France, 13-18 May 2007 (5 Vols), Curran Associates, Inc. (February 2008).
[235] MARTIN, P., ROUAULT, J., SERPANTIE, J.P., VERWAERDE, D., French Program towards a GEN IV Sodium Cooled Fast Reactor, ENC 2007, Brussels, Belgium, 16-20 September 2007.
[236] INTERNATIONAL ATOMIC ENERGY AGENCY, Fast Reactor Database 2006 Update, IAEA-TECDOC-1531, Vienna (2006).
[237] KONOMURA, M., ICHIMIYA, M., Design Challenges for Sodium Cooled Fast Reactors, J. Nucl. Mater, doi:10.1016/j.nucmat.2007.05.012 (2007).
[238] HISHIDA, M., MURAKAMI, T., KONOMURA, M., TODA, M., Progress on the Plant Design Concept of Sodium Cooled Fast Reactor, Proc. GLOBAL 2005, Tsukuba, Japan, 9-13 October 2005 (Editor: Hajimu Yamana), Atomic Energy Society of Japan, ISBN: 4-89047-133-2.
[239] EFR ASSOCIATES, European Fast reactor 98 – Outcome of design studies, Lyon, France (1998).
[240] HISHIDA, M., KONOMURA, M., UCHITA, M., IITSUKA, T., KAMISHIMA, Y., Construction of Sodium-Cooled Medium-Scale Modular Reactor in Consideration of In-service Inspection and Repair, Proc. of ICAPP 2005, Seoul, Korea Rep. of (2005) Paper 5112.
[241] RODRIGUEZ, G., BAQUE, F., ASTEGIANO, J.C., Evolution of Sodium Technology R&D Actions Supporting French Liquid-Metal Fast Breeder Reactors, Nuclear Technology, Vol. 150,·No 1, pp. 3-15 (April 2005).
[242] ASTÉGIANO, J.C., RODRIGUEZ, G., BAQUÉ, F., Status of Knowledge Preservation activities on Sodium cooled Fast Reactors in France, paper presented in IAEA Technical Meeting on Implementation of the Fast Reactor Data Retrieval and Knowledge Preservation Initiative, Obninsk, Russian Federation, 28 November-1 December 2006.
[243] GUIDEZ, J., MARTIN, L., Status of Phénix Operation and of Sodium Fast Reactors in the World, Proc. ICAPP'07, Nice, France, 13-18 May 2007 (5 Vols), Curran Associates, Inc. (February 2008).
[244] MARTIN, L., PEPE, D., DUPRAZ, R., Lifetime Extension of the Phenix Nuclear Power Plant, paper presented in IAEA Technical Meeting on Operational and Decommissioning Experience with Fast Reactors, Cadarache, France, 11-15 March 2002.
[245] RAHMANI, L., DECHELETTE, S., BANDINI, C., SPX significant events and whether it would have happened on EFR, Technical Committee Meeting on Unusual Occurrences during LMFR operation. Vienna (Austria) 9-13 Nov 1998, International Atomic Energy Agency, Vienna (Austria), IAEA-TECDOC-1180, pp. 63-102
[246] BERJON, R., DUPRAZ, R., La localisation de la fuite de sodium du barillet de SUPERPHENIX, LIMET 1988, Palais des Papes, Avignon, France, 17-21 October 1988.

[247] LEFEVRE, J.C., MITCHELL, C.H., HUBERT, G., European Fast Reactor Design, Nuclear Engineering and Design, Vol. 162, No. 2, pp. 133-143 (1996).
[248] INTERNATIONAL ATOMIC ENERGY AGENCY, Fast Reactor Database, IAEA-TECDOC-1531, IAEA, Vienna (2006).
[249] INTERNATIONAL ATOMIC ENERGY AGENCY, Status of Liquid Metal Cooled Fast Reactor Technology, IAEA-TECDOC-1083, IAEA, Vienna (1999).
[250] MOUROGOV, V.M., et al., Energy, Vol. 23, No 7/8, pp. 637-648 (1998).
[251] MARTIN, PH., Et al., French Program Towards an Innovative Sodium Cooled Fast Reactor, Nuclear Eng. and Technology, Vol. 39, No. 4 (August 2007).

CHAPTER 8
REACTOR SAFETY DESIGN AND ANALYSIS

8.1. Safety principles and goals

The fundamental objective for nuclear power plant safety is to protect both people and the environment against harm by radiological exposure [1]. The people to be protected include both the general public and those who work to operate and maintain the plant. Protection must be provided during normal operation of the plant, for anticipated events involving equipment failures and operator errors, and for unforeseen events.

The overall safety principle for nuclear power is to assure that the risk from operation of the fleet of plants must be small in comparison to the level of risk encountered in everyday activities and accepted by society. For the public and people who work in the plants, this risk is quantified by the health hazard associated with exposure to radiation. The goal for nuclear power plant safety is to provide the means to control risk by design.

The current generation of commercial light water reactors (LWRs) was constructed in accord with the above safety principle. Public acceptance of nuclear power has been based substantially on the safety performance of the commercial LWR fleet. For advanced liquid metal-cooled fast reactors, the challenge is to achieve an equivalent or superior level of risk reduction and public protection. World-wide experience with prototype liquid metal fast reactors has provided considerable experience to serve as basis for future safety requirements. However, the discussion is ongoing regarding the specific design features needed to achieve the desired level of safety.

For instance in France, the safety objectives retained for the EPR™ guarantee a very high level of protection; further and prescriptive reduction of the risk with regard to this level is not justified and could even be counterproductive. That is why these objectives would be kept for future SFRs. It is worth noting that the safety level for the EPR™ is reached through, among others:

(1) An extended design basis domain which, aside the classical “design basis”, includes the treatment of severe accidents considering both their prevention and the mitigation of their consequences, and
(2) The “*practical elimination*” of some situations which will be prevented and whose consequences will not be explicitly addressed by the design.

Some examples of potential practical eliminated situations are:

- Events that could lead to a prompt-critical state with kinetics that are incompatible with the reactivity control systems and the capabilities of the feedback reaction coefficients, as for instance an abrupt voiding of the core due to a large gas bubble, a significant reactivity insertion due to excessive core or fuel compaction, or a collapse of core support structures;
- Events that could lead to the loss of the decay heat removal means or their inefficiency, as for instance a long term loss of all decay heat removal circuits or an instantaneous whole loss of flow in the core.

The approach recommended for future sodium cooled fast reactors requires realization of a robust safety framework. Such a framework will rely primarily on the feedback of experience as well as on the selection of design options, and on the R&D programmes which must: (1)

enable the identification and the management of the uncertainties, and (2) contribute technology capable of rejecting possible threshold effects. Tools helping to demonstrate an exhaustive, gradual, tolerant, forgiving and balanced defence against all initiating events or hazards must be developed and applied.

The role of reactor safety design and analysis is to provide meaningful estimates of reactor and plant performance in normal operation and in accident sequences. Specifically, deterministic analyses employ data and models qualified by test results to predict radiological releases for postulated events. Probabilistic analyses are performed to estimate the likelihood of a particular event. The risk spectrum is established by the combination of the probability and the consequences for all events.

8.1.1. Safety fundamentals: Defence-in-depth

From the earliest days of nuclear power, protection of people and the environment from the effects of radiological exposure was based on a design philosophy described as "Defence-in-Depth" [2]. The concept of defence-in-depth provides multiple layers of protection, so that failure of any one safety provision does not lead to uncontrolled risk.

In reactor design, application of the defence-in-depth principle results in multiple barriers (cladding, primary coolant system, containment building) between radiological material and the public, and multiple systems for reactor control and cooling to preserve the integrity of those barriers. Worldwide, implementation of defence-in-depth has progressed with variations, but the general consensus for layers of application includes the following:

- Provide inherent and basic design characteristics; conservative design approach and sound construction and operation practices; focus on reliable operation and on accident prevention using features of the plant design, construction, operation and maintainability; reliability enhancement through redundancy and diversification, quality assurance, testability, inspectability, and simplified fail safe system designs; prevent deviations from normal operation and system failures.
- Detect deviations from normal operational states and failures; monitor performance for activation of control, localization, and protection systems; limit challenges to protective barriers by external challenges (e.g. earthquakes) and component failures which may occur during the plant design life; control unlikely design basis accidents by engineered safety features and emergency procedures.
- Limit core damage and preserve protective barriers; control unlikely design basis accidents by engineered safety features and emergency procedures.
- Prevent severe accident progression and mitigate severe accident consequences; ensure fission product and molten fuel retention within the reactor vessel.
- Mitigate the radiological consequences of significant releases of radioactive materials by off-site emergency response. The Generation-IV International Forum [3] proposes a more challenging objective in order to support public acceptance: the future nuclear energy systems will eliminate the need for offsite emergency response.

8.1.2. Safety assessment: Analysis for risk determination

Figure 8.1 describes the safety design approach applied for a new European sodium fast reactor (SFR) design in order to determine and analyze its relevant operating conditions. Although the event classification discussed here is not universally applied world-wide, this European SFR example serves to illustrate the generally accepted safety approach.

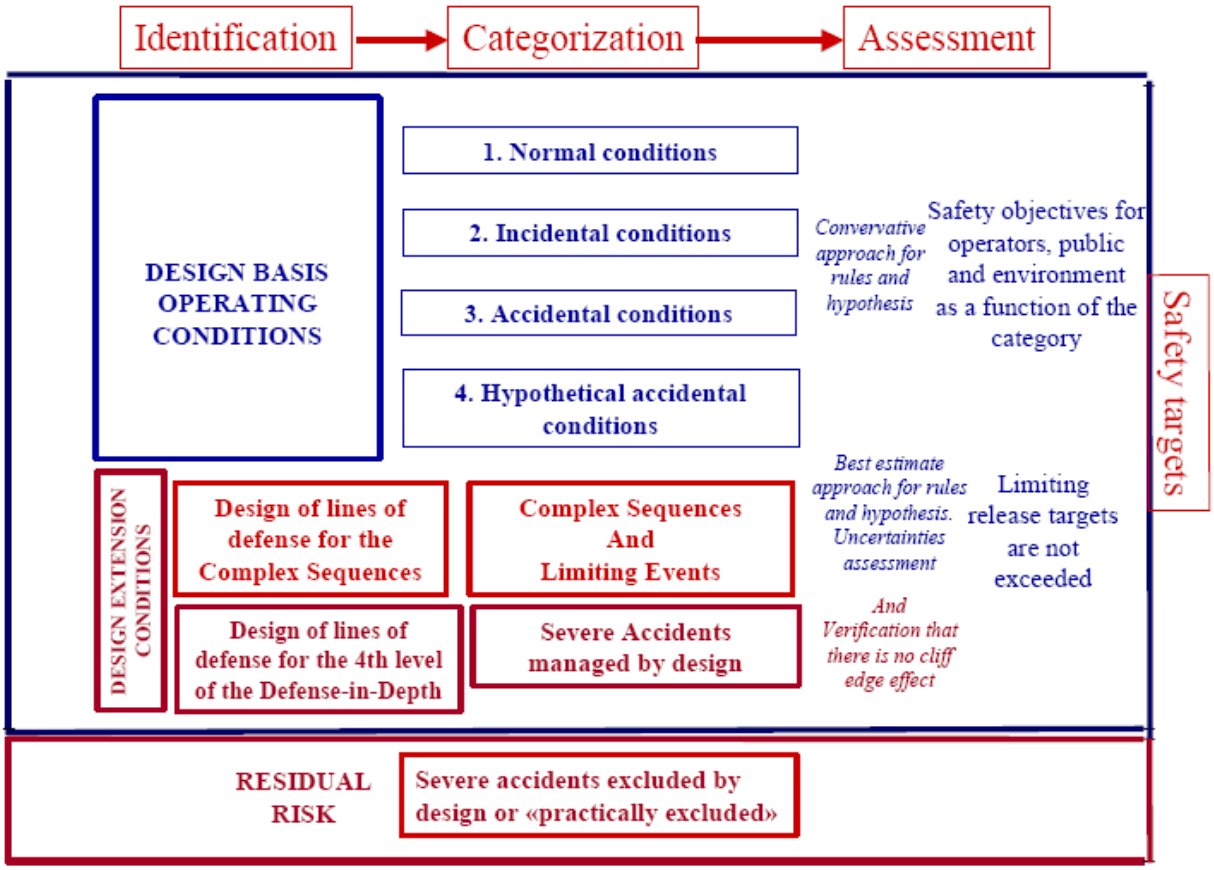

FIG. 8.1. General approach for the safety related design and assessment.

A Design Basis Condition is a plant condition resulting from the combination of a normal operating condition (category 1, see hereafter) and of an initiating event belonging to the Design Basis area, i.e. classified from category 2 to category 4 (according to its probability, see definition hereafter). Initiating events may arise due to component failure, operator errors, internal or external hazards. Their consequences affect the plant behaviour. The design basis conditions are grouped in four categories on the basis of the expected occurrence frequency of the corresponding initiating events. Definition of the categories, referring to the next European SFR, is as follows:

– Normal operating conditions

  Normal operating conditions are plant conditions planned and required. They include special conditions such as tests during commissioning and start-up, partial loading, shutdown states, handling states, partial unavailability for inspection, test, maintenance and repair. The decommissioning conditions are not included in the safety analysis of the operating plant; they will be specifically analyzed in good time. Nevertheless, considerations concerning the decommissioning have to be made. The goal of the safety analysis of normal operating conditions is to verify that their consequences on the staff and the public are As Low As Reasonably Achievable (ALARA) and in any case lower than the corresponding release criteria.

- Category 2 operating conditions

  Category 2 operating conditions are operating conditions not planned but expected to occur one or more times during the life of the plant (mean occurrence frequency estimated greater than 10^{-2} per year). Plant shall be able to return to power in short term after fault rectification. The goal of the safety analysis of category 2 operating conditions is to verify that their consequences on the staff and the public are ALARA and in any case lower than the corresponding release criteria.

- Category 3 operating conditions

  Category 3 operating conditions are operating conditions not expected to occur during the life of the plant (mean occurrence frequency between 10^{-4} per year and 10^{-2} per year) but after which plant restarting, by possible repair, is required for investment cost guarantee. The goal of the safety analysis of category 3 operating conditions is to verify that their consequences on the public are lower than the corresponding release targets.

- Category 4 operating conditions

  Category 4 operating conditions are operating conditions after which plant restart is not required because there is no expectation of occurrence during the plant life. The consequences of an operating condition must not exceed category 4 limits with a mean value of their frequency higher than 10^{-7} per year. The goal of the safety analysis of category 4 operating conditions is to verify that their consequences on the public are lower than the corresponding release targets.

Beyond the design basis, there exists a class of accidents of such low probability that they have been termed "hypothetical." These events involve multiple failures of safety grade systems, and usually are considered to have a frequency of less than 10^{-6} per reactor year of operation. Because of the potentially severe consequences of accidents in this class, they have received significant regulatory scrutiny in prior sodium-cooled fast reactor licensing reviews for the purpose of characterizing thermal and structural safety margins beyond the design basis.

Referring to the European SFR categorization, the Design Extension Conditions (DEC) are not defined on the basis of their occurrence frequency, but they are postulated to be bounding cases resulting from risks specific to the design or the process. Two kinds of design extension conditions are considered: the situations for which the consequences have to be demonstrated to be limited, and the severe accidents. The goal of the safety analysis of DEC is to verify that their consequences on the public are lower than the limiting release targets. In the safety approach developed in the European Utility Requirements (EUR), *complex sequences* are design extension conditions which are not covered by the safety analysis of category 2, 3 and 4 operating conditions, but the occurrence frequency of which is not demonstrated to be sufficiently low (i.e. well below the mean value of 10^{-7}/sequence/year/plant). In the European SFR safety approach, the complex sequences are complemented by limiting events defined for licensing purposes. They are bounding cases resulting from risks specific to the design or the process. The consequences of complex sequences and limiting events are investigated. This can lead to design enhancements in order to show that core damage is prevented, and then that the limiting release targets are not exceeded. *Severe accidents* are considered in order to verify that there is no "cliff edge" effect on the consequences even for very extreme hypothetical conditions. The goal of the analysis of severe accidents is to provide additional

verification of the containment measures for limiting the consequences of core damage accidents. The radiological consequences shall be lower than the limiting release targets.

Residual Risk (RR) situations are accident conditions for which the prevention regarding their occurrence is such that the analysis of their consequences is not required by the safety demonstration. On the other hand, the adequacy of the prevention of these accident conditions has to be demonstrated. Such a demonstration may be performed using probabilistic assessment. In this case, the goal is to show that accident conditions which the consequences may exceed the limiting release targets have a mean frequency well below to a threshold, as for example 10^{-7}/event/year/plant. One of the goals of the US reactor technology development program is to enhance prevention of severe accident progression to the point that severe accident conditions become part of the residual risk category.

Hazards must be considered in order to add provisions aiming to avoid that they provoke an accident and to protect the systems permitting to control the facility conditions. The hazards to consider in the design of a plant could result from internal causes or external ones and are qualified as internal hazards and external hazards. A typical list of internal hazards to be taken into account is: internal flooding, internal fire, electromagnetic perturbations (possibly externally caused, like lightning, but having an effect on control system of the plant), internal explosion, missile projection. The following external hazards are usually considered: earthquake, extreme weather conditions, aircraft crashes, industrial environment (explosion, fire…), external fire, external flooding. For SFRs, specific hazards from the use of sodium are studied due to fire or leakage or freezing of sodium.

In the safety architecture, additional provisions could be added in order to minimise the risk in a homogeneous manner and with a reasonable cost, under the frame of the ALARA approach.

Safety analyses are also carried out within the scope of a Probabilistic Safety Assessment (PSA) to determine a conditional reactor core damage probability (accident frequency) and an accident consequence measured in terms of release of radioactive materials from the plant. For sodium cooled fast reactor, design-specific risk sources may be considered in a PSA, as for example the risk of significant creep of the main vessel in SuperPhénix in the Level 1 PSA.

These analyses are performed for a selected list of the postulated design basis initiating events and for selected DEC sequences. Performance of a PSA has become a licensing requirement for future nuclear power reactors in most nations. The probabilistic safety assessment scope is depicted in Fig. 8.2.

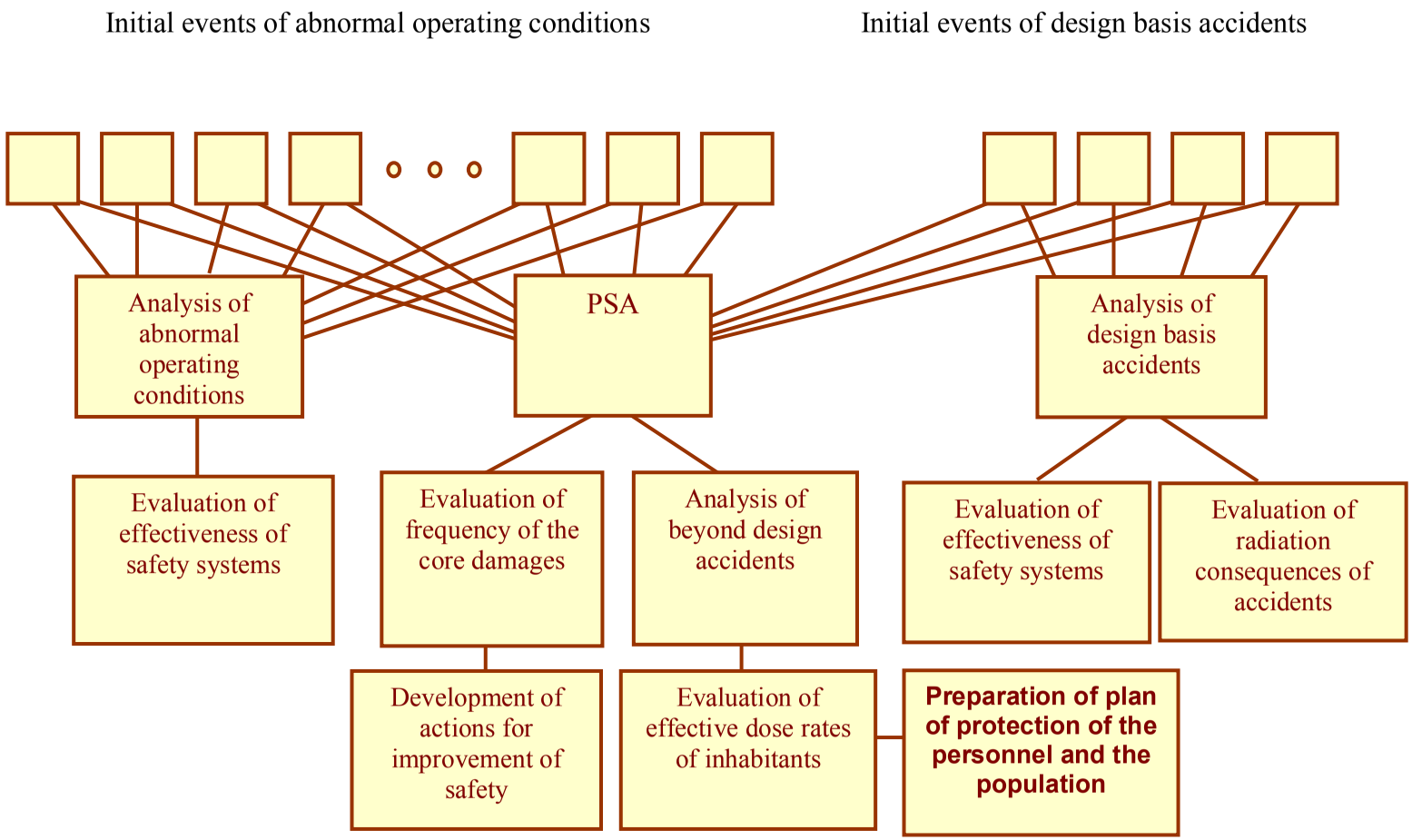

FIG. 8.2. Safety analysis scope.

8.2. Safety design goals

The safety goals in nuclear power reactor design and operation are to assure the health and safety of the public, to protect the plant operating staff from harm, and to prevent plant damage. Traditionally, these goals have been fulfilled by an approach that:

(1) Minimizes risk by maximizing safety margins;
(2) Reduces the likelihood of potentially harmful events; and
(3) Provides additional design features to mitigate the harmful consequences of low probability events. This approach is usually identified as "defence-in-depth."

8.2.1. Safety related systems, structures and components

The basic principle of "defence-in-depth" is to provide multiple levels of protection. The protective levels may be physical barriers, like the multiple barriers to release of radioactivity provided by the fuel cladding, the primary coolant system, and the reactor containment building. Alternatively, the multiple layers may be provided by active systems, like the reactor shutdown systems and the reactor cooling systems. The safety design approach implements the defence-in-depth strategy by adopting the traditional three lines of protection, and extension of the line of defence notion. A provision could be any inherent characteristics (for instance large inertia of Na), an implemented active or passive system, an operational or emergency procedure or organizational measures, selected for the design, the construction and the operation. For instance, the advanced design features have been selected to provide significant safety margin enhancements by inherent, passive safety responses to upset conditions and equipment failures.

Usually, several lines of protection are considered in the safety architecture of the plant. However, in all instances, the achievement of the defence in depth strategy depends on the independence of the protective measures, so that no single event can breech more than one protective level.

In support of the first line, the reactor is designed to operate with a high level of reliability, so that accident initiators are prevented from occurring. The first line is assured in part by selection of fuel, cladding, coolant, and structural materials that are stable and compatible, and provide large margins between normal operating conditions and limiting failure conditions. Next, the first line is assured by adopting an arrangement of components that allows continuous or periodic monitoring, inspection, and testing for performance changes or degradation. Finally, the reactor design provides for repair and replacement of components necessary to assure the efficiency of the first line of protection.

For the second line of protection, the reactor is designed to provide protection in the event of an equipment failure or an operating error. This level of protection is provided by engineered safety systems for reactor shutdown, reactor heat removal, and emergency power. All of these safety-grade systems have back-ups that function in the event of failure in the corresponding operating system, and are subjected to continuous monitoring and periodic testing and inspection.

The third and higher lines of protection provide additional assurance of the public health and safety in an extremely unlikely accidental event that is not expected to occur in the life of the plant, or which was not foreseen at the time the plant was designed and constructed. For example, the reactor guard vessel and the reactor containment building provide level 3 protection for cooling assurance and containment of radioactivity. The reactor guard vessel is designed to hold primary coolant in the extremely unlikely event of a leak in the primary

coolant system. The reactor guard vessel assures that the reactor core remains covered with sodium and cooled by the emergency heat removal system, even if the primary reactor vessel fails. In the extremely unlikely event that primary coolant leaks and oxidizes in the reactor building air atmosphere, or if cladding failures release gaseous fission products, the reactor containment building provides a low-leakage barrier to release of radioactivity.

8.2.2. Strategies for improving safety for reactor control and decay heat removal

8.2.2.1. Reactor Shutdown System (RSS)

The normal reactor shutdown system design consists of two independent active sub-systems with different design specifications and operational characteristics. Each of them is designed to prevent fuel failure in design basis events.

The European Fast Reactor (EFR) Project studied the development of additional protective provisions for mitigating the failure of the normal reactor shutdown system. Examples of such third shutdown systems are CREED (Control Rod Enhanced Expansion Device), GEM (Gas Expansion Module), SADE (electromagnetic system for uncoupling control rods) and some fusible shutdown systems.).

8.2.2.2.Decay Heat Removal (DHR)

The improvement strategy is based on the improvement of reliability of the systems related to the DHR function, by:

- Enhancing the natural convection capability;
- Minimizing common modes due to Na risks or for physical protection needs by some constructive dispositions (partitioning…), as the main systems are crossing the vessel head (see Fig. 8.3);
- Using probabilistic study for demonstrating the high level of reliability.

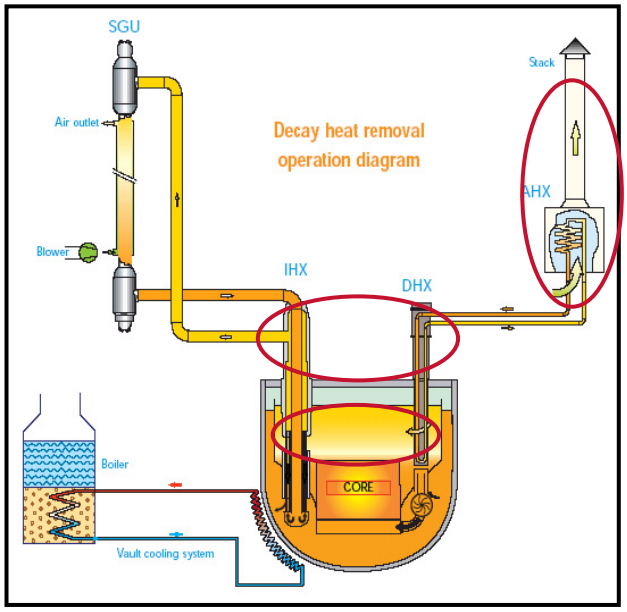

FIG. 8.3. Example of DHR architecture of a pool reactor from EFR.

On-going works for enhancing the reliability of the DHR function are based on the development of an efficient DHR system by the vessels. Such system could provide:

- A redundancy for small or medium reactor;
- For large reactor, at the beginning a complementary means for DHR and after a few hours a redundant DHR system.

8.2.3. Innovative safety systems

8.2.3.1. Reactor shutdown system

As an additional protective measure, an innovative self-actuated shutdown system (SASS) has been proposed by JAEA to prevent accident progression in design extension condition events [4]. The SASS features a latching device that employs a Curie point magnet to hold a withdrawn shutdown control rod (see Fig. 8.4).

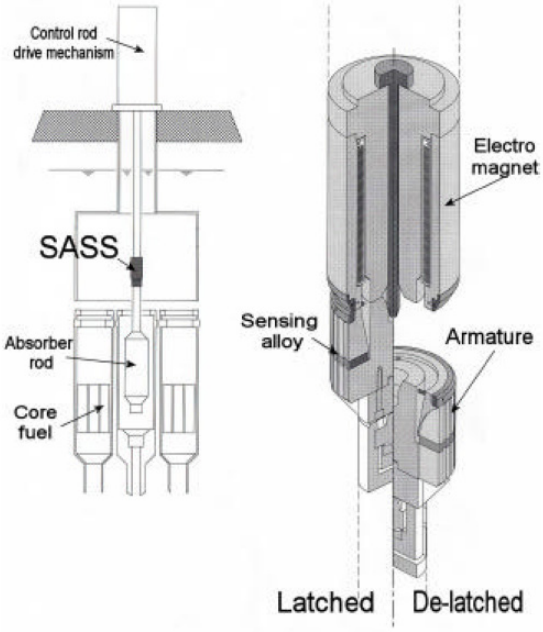

FIG. 8.4. JAEA Self actuated shutdown system (SASS).

In the event that both normal shutdown systems fail to operate in any transient resulting in high coolant temperatures, heating of the SASS latch to beyond the Curie point causes the shutdown control rod to fall into the reactor. The SASS is a backup passive shutdown feature that ensures prevention of accident progression in anticipated transients without scram (ATWS).

8.2.3.2. Elimination of energetic re-criticality event under Core Disruptive Accident (CDA) condition

In the consideration of core melt consequences in severe accidents, mitigation of core disruptive accident (CDA) energetics is an important objective. In order to achieve both social acceptance and a rational plant design, it is important to achieve in-vessel retention of a degraded core. This can be achieved by practically eliminating the severe mechanical energy release due to re-criticality events in the CDA scenarios, accompanied by stable post-accident heat removal. Together, these factors ensure debris retention without causing significant mechanical loadings to the reactor vessel.

The usual approach for designers is based on the analysis of several scenarios that could lead to CDA.

For each phase of the scenario (from in-pin behaviour to the core-catcher), the most influential parameters are identified from uncertainty and sensitivity studies. That result allows determining the most promising physical phenomena to enhance and to propose dedicated systems, in order to avoid criticality for the studied phase of the scenario. Classical ways are to:

- Promote the dispersion of the molten fuel, by using for instance FAIDUS described below for the subassembly scale, or the use of control rod guide tube at the scale of the core; and
- Insert absorber or diluents, as for example by including dedicated diluents layers in the core-catcher.

For this purpose, the positive sodium void worth may be limited to mitigate initiating phase energetics as sodium boiling tends to insert positive reactivity feedback.

Furthermore, JAEA has proposed special fuel assembly features (e.g. fuel assembly with inner duct structure named FAIDUS shown in Fig. 8.5) to enhance molten fuel discharge from the core [5].

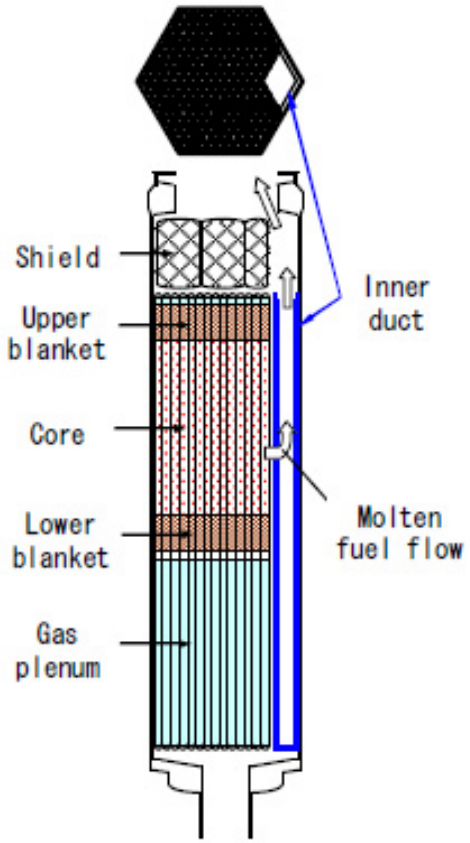

FIG. 8.5. JAEA FAIDUS type fuel subassembly.

Fuel removal prevents energetic re-criticality events by reducing core fuel mass below the criticality requirement. In order to achieve quenching of the molten fuel and stable cooling of the core debris, a multi-layered structure for core debris retention is installed at the bottom of

the reactor vessel. Quenching is attained by assuring sufficient sodium inventory in the lower plenum, and stable cooling is attained by providing sufficient surface area of the core debris on the multi-layered structure. Long-term coolability can be ensured by the natural circulation capability of decay heat removal system. These design features reduce loads on the containment and allow a compact containment design.

8.2.4. Containment design requirements and containment isolation concepts

Although the occurrence of hypothetical core meltdown accidents can practically be excluded, there are nevertheless requirements to the design of the containment.

Containment design requirements typically include the following:

- In order to keep the release of radioactivity to the environment within specified limits in normal and postulated accident conditions, the containment shall be provided.
- Calculation of the required strength of the containment structure including access openings, penetrations and isolation valves shall be based on the calculated internal pressure, vacuum and temperature conditions resulting from all the operational states and postulated accidents.
- At least two routes of egress shall be available for emergency evacuation.
- The containment wall shall provide sufficient shielding to permit post accident site occupancy requirements especially control room and backup control room habitability.
- Within the containment, the possibility of leaks shall be minimized in order to prevent any sodium reaction.
- The containment shall be maintained under negative pressure during all operational states of the reactor except during special operations (e.g. transportation of IHX from RCB in reactor shutdown state).

Containment isolation design concepts include the following:

- Detection of containment isolation signal shall be provided;
- Each line that penetrates the containment and is open to containment atmosphere or open to main vessel shall have two automatic isolation valves;
- For limiting the release of radioactivity to the atmosphere, the isolation devices shall close at a speed which takes proper account of the potential release hazard;
- Systems to control the release of fission products from containment to the environment following design basis events shall be provided;
- The containment leak rate shall be such as to keep the radioactivity release to environment within specified limits during all operational states of the reactor and postulated accident conditions, throughout the life of the plant;
- Provision shall exist for determination of leak rate of containment and associated equipment.

8.3. Design basis safety analysis

The normal safety design envelope considers design basis accidents (DBAs) that assume single failures. By definition, accidents within the design basis, usually taken to have a frequency of occurrence of once in a million reactor years or more, must be accommodated by the design and shown to present risks to the public that are within regulatory standards.

The objective of design basis analysis is to apply validated models to demonstrate that the reactor and plant design will perform in compliance with regulatory requirements.

8.3.1. Definition of design basis events

It is customary to define a number of Design Basis Events (DBEs) that can serve to verify that a proposed reactor and plant design will perform according to the design requirements. A DBE is defined as a combination of a plant state and a initiating event or operational process. Methods based on functional analysis and a Master Logic Diagram are used for identifying the initiating events, particularly for new design. When a new design is sufficiently mature, analyses of normal duty cycle events provide predictions of the performance of the proposed design, and a basis for assessment of the need for design revision. As the design evolves further, Design Basis Accidents (DBAs) are defined with the purpose of providing conditions and sequences that test the design against the safety design criteria.

A DBA may be defined as a DBE combined with a single aggravating failure, often the loss of external power sources or a failure of safety-grade component designed for limiting their consequences, under the assumption of the single failure criterion. Analyses of design basis accidents are performed with validated models, and include treatment of uncertainties. For these situations, uncertainties are usually taken into account by applying models that overestimate the behavior of the system, and so-called conservative input data that maximize load quantities and minimize resistance quantities.

Design basis events (DBEs) impose requirements on the design of components and systems that have safety-related functions, and define the range of conditions under which these functions are to be performed. For this, the consequences and the behavior of the safety functions provided by the defence-in-depth design are evaluated through extensive DBE analysis. Conservative assumptions are applied to the analysis of plant response during the postulated DBEs. Also, for each event category a single limiting event, whose postulated consequences envelope all of the other DBEs in that category, can be selected.

Specification of design basis events depends on the operational and safety requirements for a particular design, and the systems, structures, and components that collectively constitute the design. However, the set of design basis accidents provide an assessment of reactor shutdown, decay heat removal, and containment systems performance in normal operation, and in unlikely and extremely unlikely accident sequences.

8.3.2. Models and codes for design basis events

A survey of models and computer codes used for design basis analysis was conducted. It was found that modeling and code capabilities varied from nation to nation depending on favored design variations and regulatory requirements. However, a general set of codes and capabilities emerged as follows:

8.3.2.1. Systems analysis codes

The systems analysis codes are used for the analysis of reactor systems and component transient responses of multi-loop and multi-circuit fast reactors. In general, system analysis codes for sodium-cooled fast reactors include these models: point reactor dynamic model, core thermal hydraulic model, fuel/cladding behavior model, primary and secondary sodium loop thermal hydraulic models, tertiary water-steam thermal hydraulic model, pipelines thermal hydraulic model, reactor automatic regulation and control protection model, components models including pumps, heat exchangers, and steam generators.

Due to the hydraulic behavior of large plena, the distribution of flows within the volumes should be validated from experimental tests or verified with multidimensional (CFD) calculations.

8.3.2.2. Sodium fire analysis codes

Depending on sodium burning rate and other conditions, sodium fire type can be classified as pool fire, spray fire, or some combination.

8.3.2.2.1. Pool fire code

Pool type sodium fire is defined when the sodium flow itself is partially burning or not burning, the sodium flows to form a sodium pool and then burns on the surface of sodium pool, resulting in energy release.

8.3.2.2.2. Spray fire code

Spray fire analysis for calculating the consequences of sodium spray leakage caused by pressure in a pipeline or vessel.

8.3.2.3. Local fault analysis codes

Local fuel/cladding faults may occur due to flow irregularities within a subassembly or spurious control rod movement that cause cladding failures and fuel melting and lead to a significant radioactive release. The safety approach for local faults is to monitor and detect the fault, to provide protection for the reactor core, and to avoid the propagation to a core disruptive accident (CDA) situation. Consequently, computer codes for local faults analysis typically include detailed coolant thermal-hydraulics and fuel element heat transfer models.

8.3.2.4. Multidimensional thermal/hydraulic analysis codes

These codes are usually of a general purpose nature and may be used to analyze flows within a fuel subassembly or alternately in volumes within vessels, heat exchangers, and pumps. The calculated temperature and flow conditions yield information for design evaluation and prediction of instrumentation performance, as for example delayed neutron detection.

8.3.2.5. Mechanical/structural analysis codes

Analyses of stress loads and strains in weight-bearing structures, structures exposed to transient coolant temperatures, as well as fuel cladding are performed to evaluate life-cycle performance of structural materials.

In some countries, standards and code specifications have been developed for guiding structural designers; for example, well known standards are provided by ASME or RCC-MR in France.

8.3.3. Example design basis safety analyses

8.3.3.1. Design basis accidents in the JAEA Sodium Fast Reactor (JSFR)

Design basis safety analysis in the JAEA Sodium Fast Reactor (JSFR) is described in this section. Some preliminary safety evaluations were conducted to examine the feasibility of the

safety design concept. Here we show the results for the large-scale compact-type oxide core, the medium-scale high-conversion-type oxide core and the large scale compact-type metal core. The plant specifications of these three kinds of JSFR design concepts are listed in Table 8.1, which are samples of possible design options in order to cover various demands of the output capacity, fuel burn-up, breeding ratio, fuel inventory, etc.

TABLE 8.1. PARAMETERS FOR THE SAFETY EVALUATIONS

	Large oxide core (compact type)	Medium oxide core (high conversion type)	Large metal core (compact type)
Plant parameters			
Power output	1500 MWe / 3570 MWt	750 MWe / 1785 MWt	1500 MWe / 3750 MWt
Number of loops in PHTS	2	2	2
Primary coolant temperature	550°C / 395°C	550°C / 395°C	505°C / 350°C
Primary coolant mass flow rate	1.8×10^{4} kg/s	0.9×10^{4} kg/s	1.9×10^{4} kg/s
Steam generator	Double wall straight tube	Double wall straight tube	Single wall helical coil tube
DHRS	PRACS×2 + DRACS×1	PRACS×2 + DRACS×1	IRACS×2 + DRACS×1
Fuel pin conditions			
Fuel pin diameter	8.8 mm	10.4 mm	8.5 mm
Fissile length	800 mm	1000 mm	900 mm
Maximum linear power	420W/cm	420 W/cm	470 W/cm
Maximum cladding temperature	700°C	700°C	650°C
Maximum fuel temperature	~2200°C	~2200°C	930°C
Reactivity coefficients (at EOEC)	-	-	-
Doppler coefficient	-4.7×10^{-3}Tdk/dT	-5.3×10^{-3}Tdk/dT	-4.1×10^{-3}Tdk/dT
Coolant temperature coefficient	5.2×10^{-6} Δ k/kk'/°C	5.1×10^{-6} Δ k/kk'/°C	10.5×10^{-6} Δ k/kk'/°C

The medium scale reactor is designed to share one turbine generator by two reactors, while the large scale reactor has its own independent turbine generator.

The oxide fuel is recognized as the reference and there are mainly two options of the core design, i.e. smaller fuel inventory core (compact type) and higher internal conversion core (high conversion type). The compact type has smaller core diameter and is suitable for higher breeding ratio over 1.1 with radial blankets. On the other hand, the high conversion type can realize higher average burn up without radial blanket and its cycle length is longer more than 40% of the compact type. In the safety point of view, the high conversion type has larger diameter fuel pins with smaller specific power density of fuel, which would affect its transient behaviour.

The metal fuel is considered as advanced options for higher core performances by utilizing its higher concentration of the heavy metals. There are two kinds of options, i.e. smaller fuel inventory core (compact type) and higher outlet temperature core. The latter one can achieve the core outlet coolant temperature of 550°C, while the former has 505°C.

As typical DBEs, the primary pump stick accident, the control rod withdrawal and loss of offsite power were evaluated for the various types of designs. In the evaluation for DBEs, some typical conservative conditions, which include the single failure criterion, were applied.

8.3.3.1.1. Loss-of-flow type events

Since in JSFR the two-loop system without check valves is employed, the decrease of the core flow rate with a primary pump stick accident is larger than that of the conventional three- or four-loop design. The primary pump stick would become the severest accident in the DBEs. However, some design adjustments (e.g., a delay time of the primary pump trip in the intact loop and a halving time of the primary flow rate within the reasonable range) make it possible to restrict the maximum cladding temperature less than the tentative safety criterion. Each sub-system of RSS was designed so as to independently shut the core down within the limit of the cladding temperature. The main and the backup RSS are actuated by the signal indicating “low primary pump speed” and “low primary flow rate” respectively

Figure 8.6a shows a calculated result for the main RSS case for the large and medium scale reactors with oxide cores. The actuation signal was the “low primary pump speed” signal corresponding to 80% of normal speed. The maximum temperatures of fuel and cladding tube for both cases were less than their tentative criteria of 2650°C and 900°C. The major different conditions in these cases are not in the output power but in the heat capacity of the fuel pellets, i.e., the high conversion type has a larger diameter of fuel pin. The maximum fuel temperature and maximum linear power at the initial condition is almost identical for them. Therefore, the cladding temperature decrease just after the core shutdown is slightly slower in the high conversion type core. The fuel maximum temperature is not critical for oxide fuel in the loss-of-flow type events.

Figure 8.6b shows the result for the metal core case. The resultant maximum temperature of the cladding tube is rather lower than those of oxide core cases. This is due to the lower initial temperature of the cladding tube and due to the smaller cumulated heat in the fuel pellet. Due to the compatibility concern between the fuel and cladding, the maximum temperature of the cladding in normal operation was restrained lower by 50°C than that of oxide fuel. And higher thermal conductivity and smaller heat capacity of the metal fuel give significantly smaller

accumulated heat inside the fuel pellet, which causes temperature rise of the cladding tube in the loss-of-flow type events.

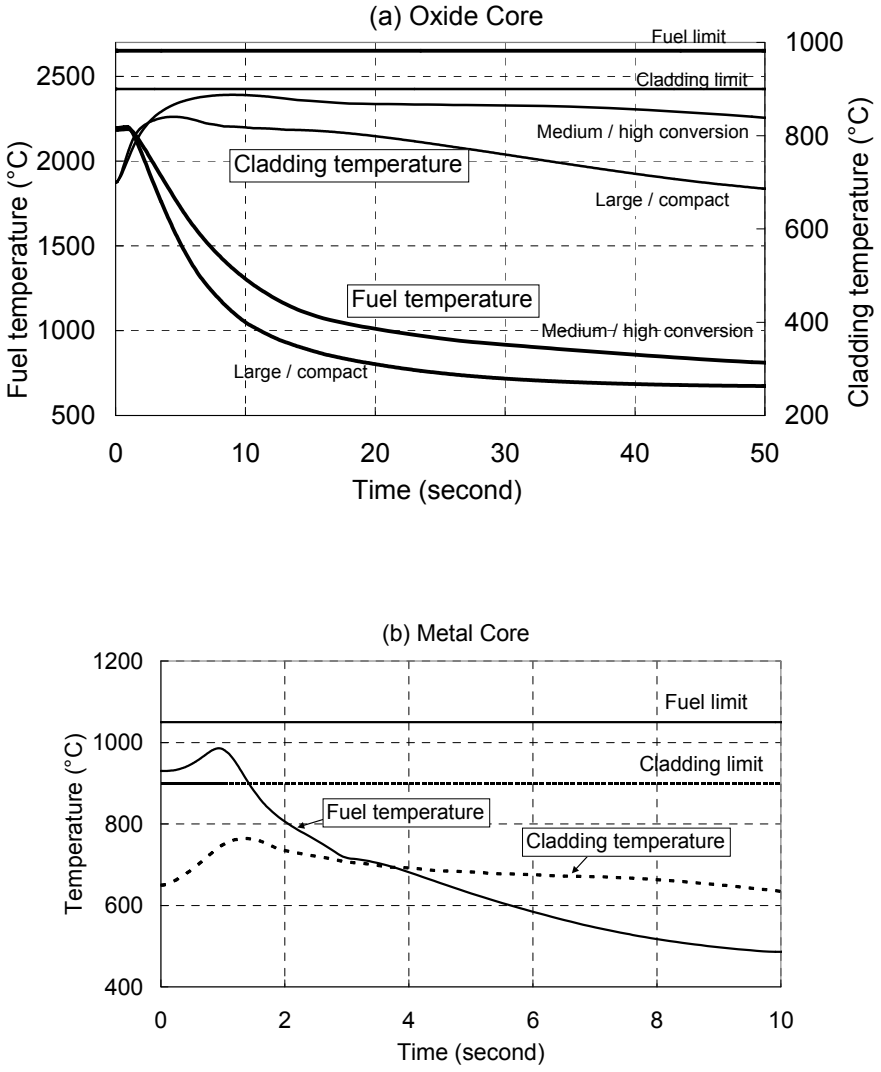

FIG. 8.6a,b. Calculated results of primary pump stick.

8.3.3.1.2. Transient-over-power type events

The control rod withdrawal events were also analyzed for the three cases, and the results met the criteria as presented in Fig. 8.7a,b.

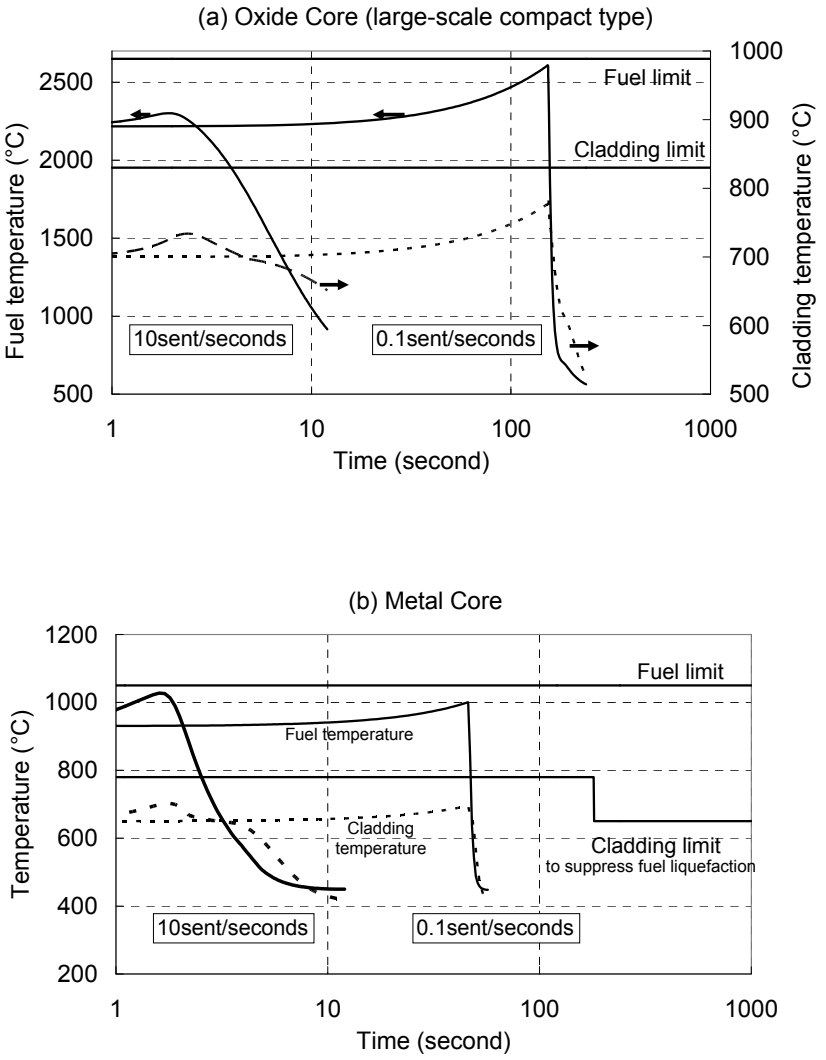

FIG. 8.7a,b. Calculated results of control rod withdrawal.

In these calculations, it was assumed to activate the primary RSS with the "high power range neutron flux" signal. In spite of the larger size of the core, the neutron monitor array equipped at outside of the core, which is used for the power range neutron flux, can detect entire range of the reactivity insertion rate from 0.1 cent/s to 10 cent/s, and shut the core down safely. For the two oxide core cases, the maximum fuel temperatures are quite similar in spite of the differences of the core size and core type. This is due to their similar maximum linear powers.

For the metal core case, the maximum fuel temperature is close to its melting temperature but still below it. In case of the abnormal transient, which is the case with the slower insertion rate around 1cent/second or less, it is necessary to be assured of immediate recovery to normal operation after termination of the transient. Therefore, it is required to suppress liquefaction of the fuel to a negligible level. Although the maximum cladding temperatures are slightly increased from their initial value and close to 700°C, the liquefaction are quite small because the duration, in which the cladding maximum temperature exceeds 650°C, is very limited. And below 650°C, the liquefaction does not occur.

Both of the primary and backup RSSs are effective with diverse actuation signals to prevent fuel pin failure. The outlet coolant temperature of the representative fuel assembly can be a good signal for the low reactivity insertion rate, while the relative deviation of the control rod positions can be a good signal for the high reactivity insertion rate. With help of these diverse detection means, fuel melting due to the control rod withdrawal events can be prevented safely.

8.3.3.1.3. Decay heat removal

For the fully passive feature like this DHRS, the evaluation for the abnormal transient is rather important from the viewpoint of the fuel integrity during the slower transient for the establishment of the stable coolant circulation. Typical results of loss of offsite power transient analysis for the three cases are shown in Fig. 8.8.

For the oxide core cases (compact type both for large-scale and medium-scale) after the first peak of fuel cladding tube maximum temperature just after reactor shutdown, second and third peaks appeared around 200 s and 1000 s, respectively, in the course of the transient. However, the cumulative damage fraction of the cladding tube was still within the acceptable range, and the temperature fluctuation was rather small.

The metal core case in Fig. 8.8 shows the analysis result of the reactor cooling system combined with two trains of IRACS (Intermediate Reactor Auxiliary Cooling System).

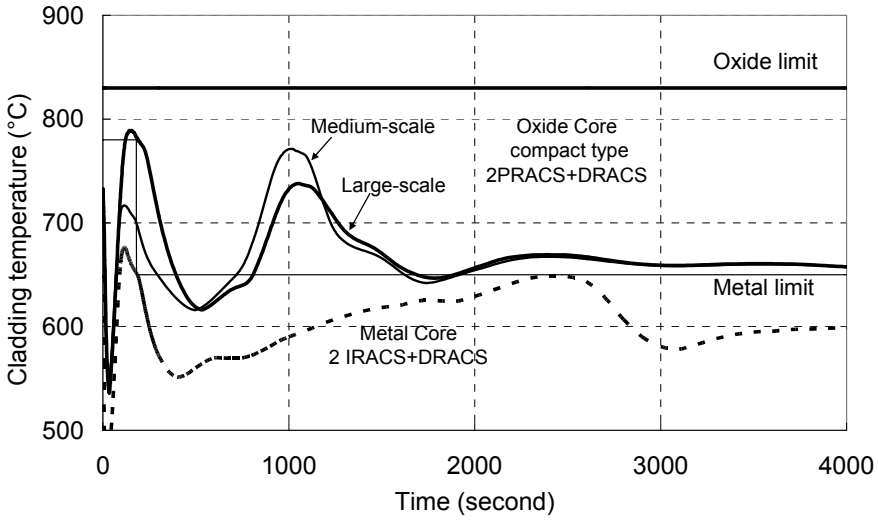

FIG. 8.8. Calculated results of loss of offsite power.

One train of DRACS shown in Fig. 8.9.

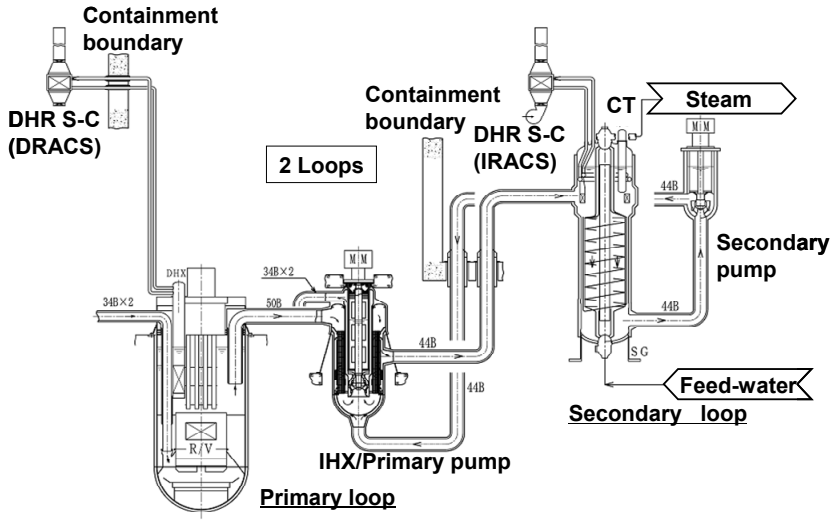

FIG. 8.9. Conceptual design of reactor and cooling system combined with IRACS.

In this case, single wall helical coil tube SGs, instead of double wall straight tube ones, were assumed, at the top of which the heat exchanger of IRACS was installed. The result satisfied the tentative criteria of the maximum cladding temperature and the cladding cumulative damage fraction. In this case, the liquefaction of the metal fuel is negligible. Because of its smaller accumulated heat, the maximum temperature both of fuel and of cladding tube can be lower than their criteria, which are lower than that of the oxide fuel case.

8.3.3.2. Pipe break and sodium fire analysis for China Experimental Fast Reactor (CEFR)

In the design of CEFR, pool fire was used as design basis. However, for sodium fire accident analysis, it was required by China safety authority that a sodium fire DBA should be analyzed in two modes: pool fire and spray fire.

For the analysis of primary sodium purified pipelines break in the corridor of the primary sodium purified system (Room 309), the initiator of the event is that the segment of pipeline with the size of 89×4.5 mm below the sodium surface breaks resulting in sodium leakage, assuming the break size of Dt/4. In the progress of the accident, the following monitoring and protecting measures work for early detection and mitigation:

- The parameters of room gas temperature, smoke and gas radioactivity and the signal of short circuit to the ground emitted by electrical heating system can monitor the leakage of sodium and form the command automatically: close the isolating valve, and transfer the normal ventilation condition to accidental ventilation condition;
- The alarming signal forms when the sodium surface lowers 150 mm, and the reactor scram will be triggered and then the isolating valve be closed automatically when the sodium surface lowers 250 mm;
- Monitoring of reactor cover gas pressure: the alarming signal forms when the argon pressure decreases to 0.040 MPa and the shutdown signal forms requiring action of the operator when decreases to 0.035 MPa.

In the analysis of the accident, SPOOL and FEUMIX codes were used for accident consequences of pool-type sodium fire and spray-type sodium fire and PAVAN code was used for diffusion of radioactive sodium aerosols to environment. The results are plotted in Figs 8.10-8.14.

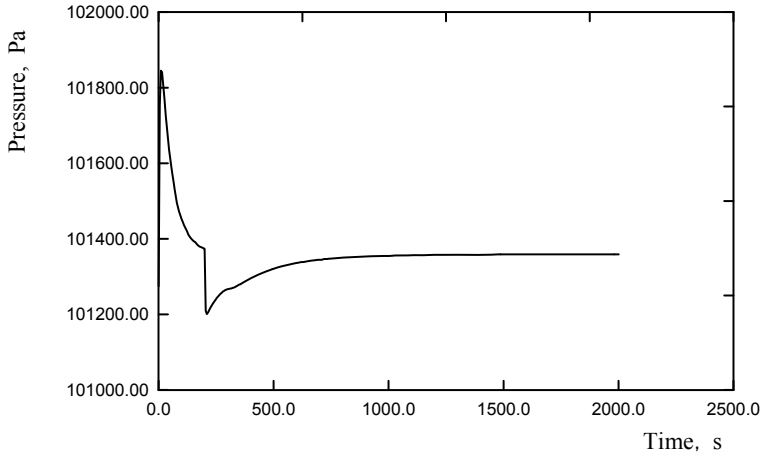

FIG. 8.10. Gas pressure (pool fire).

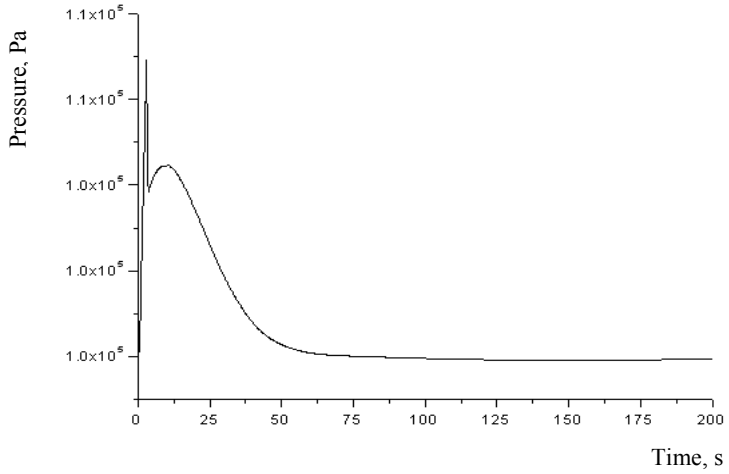

FIG. 8.11. Gas pressure (spray fire).

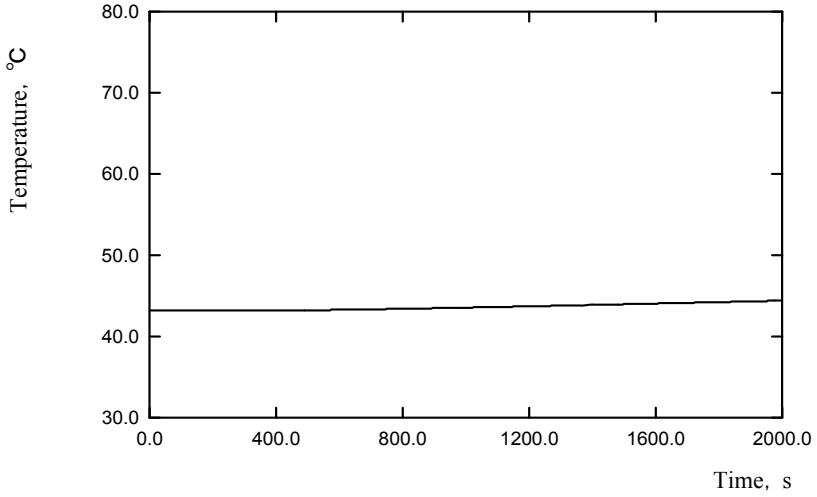

FIG. 8.12. Concrete temperature (pool fire).

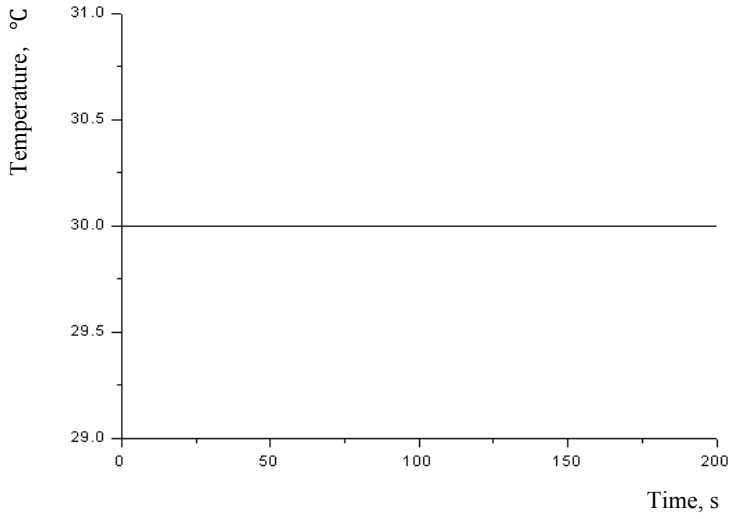

FIG. 8.13. Concrete temperature (spray fire)

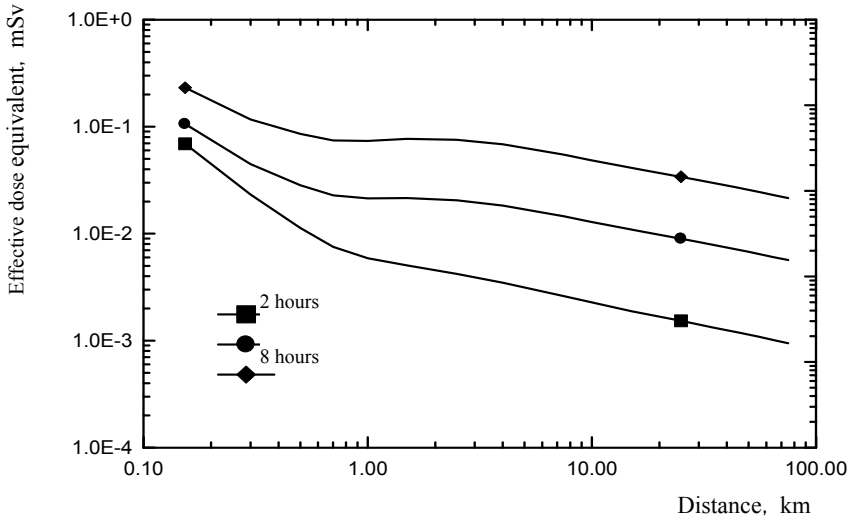

FIG. 8.14. Radioactive consequences to environment.

8.3.3.3. Example analysis from India: Off-site power failure analysis

Off-site power failure, one primary sodium pump seizure, one primary pipe rupture and transient over power are the events that have major impact on clad temperature and they only decide most of the SCRAM parameters and their threshold values.

Primary pipe rupture event is the most complicated design basis event that has been successfully analysed by the DYANA-P code. It brings out the consequences of sudden and double-ended guillotine rupture of one of the four primary pipes feeding the grid plate. Effects due to cavitation of the primary pump, intense heating up of the coolant in the core, and consequent reactivity feedback have all been brought out. SCRAM induced by the power to flow ratio and central subassembly sodium outlet temperature is shown to be adequate in assuring the clad and coolant temperatures below the design safety limit.

Consequences of one primary sodium pump trip, one secondary sodium pump trip and loss of steam – water system affect all the cold pool structures, especially primary pipe and main vessel. Hence, evolution of long-term IHX primary outlet and cold pool temperatures has been obtained and utilized in the estimation of fatigue damages. Decay heat removal through Safety Grade Decay Heat Removal System following loss of steam water system dictates creep damage in the hot and cold pool components.

For some of the major design basis events originating in the steam water system (other than boiler feed pump trip) like turbine trip, a power setback procedure where the reactor power is automatically reduced to 60%, has been incorporated. DYANA-P code has been used to arrive at the extent of Control and Safety Rod insertion required and other operating conditions during and after such an event.

All the enveloping design basis events are systematically anlysed and the evolution of process parameters are predicted. From these results, the SCRAM parameters, their threshold values and the response time of the instruments associated with the actuation of SCRAM have been optimized.

The SCRAM parameters and their threshold values determined through the plant dynamic studies are presented in Table 8.2.

TABLE 8.2. ESSENTIAL SCRAM PARAMETERS

Serial no. and SCRAM parameter		Description of the parameter	Threshold
1	τ	Reactor period for an 'e' fold increase	10 s
2	Lin P	Reactor power in linear channel	110 % nominal
3	ρ	Net reactivity	± 10 pcm
4	DND	Neutron flux at delayed neutron detectors	3 times the background value
5	P/Q	Power to flow ratio	1.10
6	θ_{CSAM}	Central subassembly sodium temperature	Nominal + 10 K
7	$\Delta\theta_M$	Core temperature rise	Nominal + 10 K
8	$\delta\theta_I$	Deviation from an expected value of a subassembly sodium temperature	10 K
9	θ_{RI}	Reactor inlet sodium temperature	Nominal + 10 K
10	$\Delta\theta_{CSAM}$	Central SA temperature rise	Nominal + 10 K
11	N_P	Primary pump speed	95% Nominal

Major design basis events and the SCRAM parameters that protect the system are presented in Table 8.3.

TABLE 8.3. MAJOR DESIGN BASIS EVENTS AND THE SCRAM PARAMETERS

Sl. no.	DBE		Event category	SCRAM parameters
1	One primary pump trip		2	P/Q, θ_{CSAM} , $\Delta\theta_{CSAM}$ and $\Delta\theta_M$
2	One primary pump seizure		3	P/Q, $\Delta\theta_{CSAM}$ and θ_{CSAM}
3	Off-site power failure		2	P/Q, θ_{CSAM} , $\Delta\theta_{CSAM}$ and $\Delta\theta_M$
4	Primary pipe rupture		4	P/Q, $\Delta\theta_{CSAM}$ and θ_{CSAM}
6	Transient over power during	≤ 5 % power	2	τ, Lin P, P/Q, ρ and $\Delta\theta_{CSAM}$
7		~ 15 % power	2	ρ, Lin P, P/Q and $\Delta\theta_{CSAM}$
8		≥ 15 % power	2	ρ, Lin P, P/Q, $\Delta\theta_{CSAM}$ and θ_{CSAM}
9	One secondary pump trip		2	θ_{RI} and θ_{CSAM}
10	Loss of steam – water system		2	θ_{RI} and θ_{CSAM}
11	IHX sleeve valve closure#		3	θ_{RI}
12	Feed water flow increase		2	P/Q and $\Delta\theta_M$
13	Secondary pump acceleration#		2	$\Delta\theta_M$ and P/Q
14	Primary pump acceleration		2	None

DSL are not challenged and hence manual SCRAM is sufficient.

Evolution of plant parameters during typical events are presented in Figs 8.15–8.18.

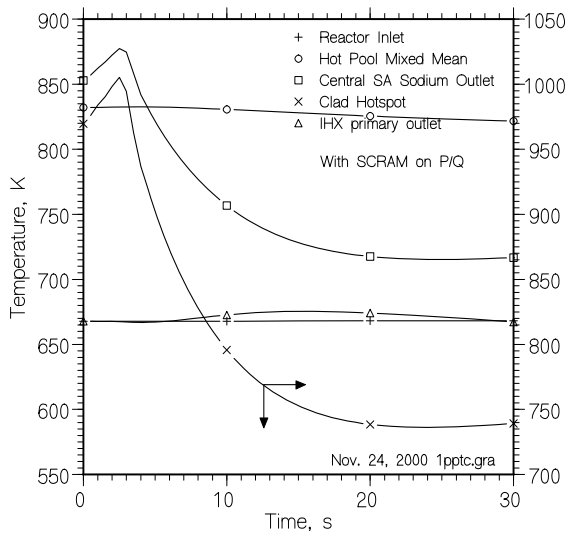

FIG. 8.15. One primary sodium pump trip: Evolution of core temperatures.

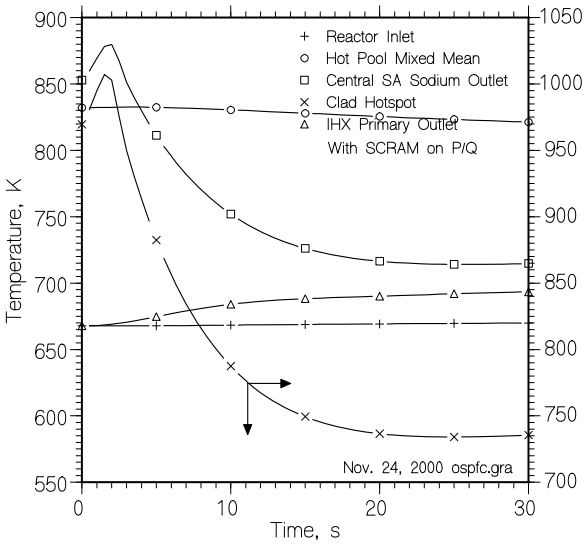

FIG. 8.16. Off-site power failure: Evolution of core temperatures.

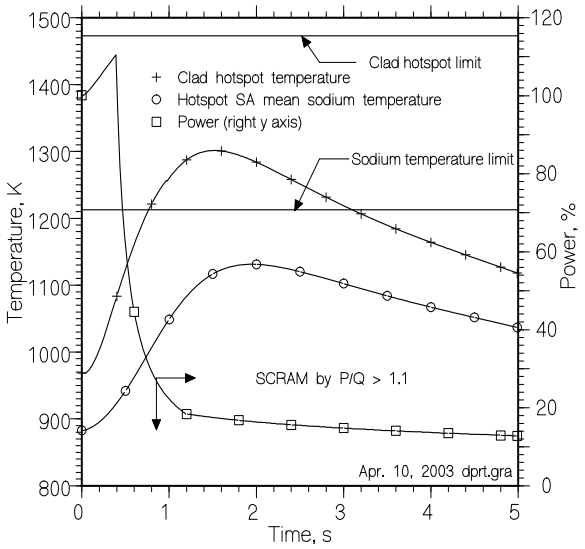

FIG. 8.17. Primary pipe rupture: Evolution of power and core temperatures.

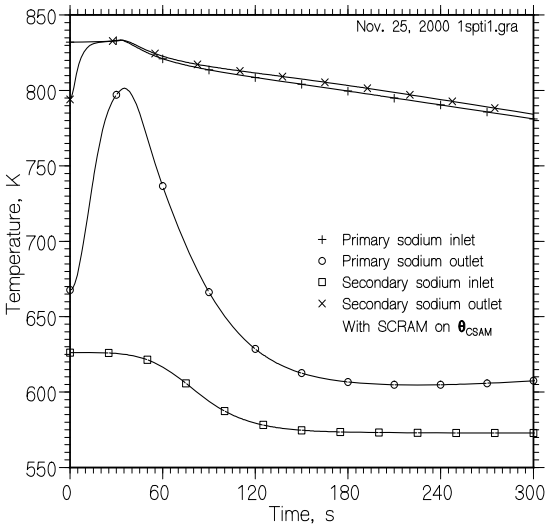

FIG. 8.18. One secondary sodium pump trip: Evolution of IHX temperatures.

8.3.3.4. Example analysis from India: design basis leak sodium-water reaction in a steam generator

Small leak sodium-water reaction propagates to large leak due to failure of safety actions envisaged by the steam generator leak detection system. Continued sodium-water reaction would cause overheating of many tubes, resulting in rupture of tubes. In order to limit over heating sodium need to be taken away from the reaction site. For this purpose two rupture discs have been provided: one at the top and one at the bottom of each steam generator. The leak rate at which both top and bottom rupture discs break has been taken as design basis leak. When both top and bottom rupture discs break, sodium moves out of the reaction zone in both directions. Because of fast movement of sodium out of the reaction zone, there is no time to overheat additional tubes. Therefore additional tube failures are suppressed. Studies have been carried out using the SWEPT computer code [6, 7] to find the design basis leak.

The design basis leak is calculated in terms of number of failed tubes to cause rupture of both top and bottom rupture discs in the leaking steam generator. From the studies it has been found that the design basis leak is instantaneous double ended guillotine failure of three tubes at the top of steam generator.

The design basis leak sodium-water reaction in the steam generator generates pressure waves which will travel throughout the secondary sodium system. The components of secondary sodium system like pump, intermediate heat exchanger, surge tank etc are designed to withstand these pressures (Fig. 8.19). For the secondary sodium pipe lines the effect of fluid-structure interaction has been taken into account [8].

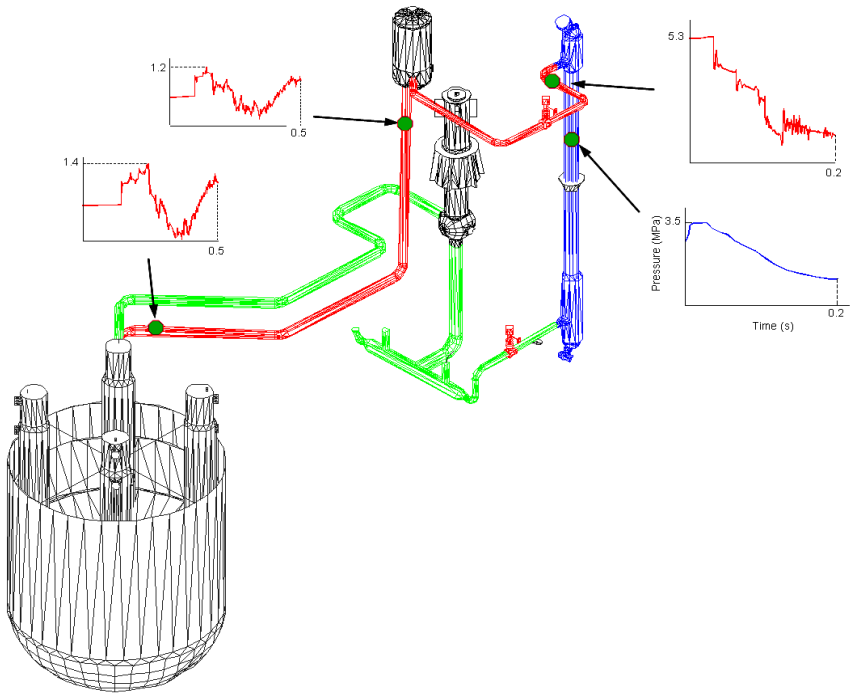

FIG. 8.19. Sodium-water reaction pressure transients at various locations.

8.4. Design extension condition safety analysis

Beyond the normal safety design envelope, there exists a class of beyond design basis accidents (BDBAs) that assume multiple failures. By definition, accidents beyond the design basis, usually taken to have a frequency of occurrence much less than once in a million reactor years, are considered to be "hypothetical", since none are anticipated to occur during the operation of the entire reactor fleet. However, because the consequences of these accidents can be quite serious and may exceed regulatory standards, estimates of their impact and exploration of the phenomena are sought in order to assist potential accident mitigation measures.

The objective of Design Extension Condition analysis is to apply best-estimate models to characterize thermal and structural safety margins beyond the design basis. The influence of uncertainty sources is studied for demonstrating the absence of any threshold effects; the methodology characterized as "Best Estimate Plus Uncertainty" is an example of the approach used.

Three DEC sequences, each involving failure of both safety-grade reactor scram systems, have received specific attention in past safety assessments. In the unprotected loss-of-flow (ULOF) sequence, it is assumed that all primary and secondary coolant pumps cease operation, and the reactor scram systems fail to activate. In the unprotected transient overpower (UTOP) sequence, it is assumed that one or more inserted control rods are withdrawn, and the reactor scram systems fail to operate. In the unprotected loss-of-heat-sink (ULOHS) accident, it is assumed that heat removal through the power conversion system is lost, and the reactor scram systems do not activate. Taken collectively, these three accident initiators encompass all the ways that an operating reactor can be perturbed, i.e. by a change in coolant flow, by a change in reactivity, or by a change in coolant inlet temperature.

Depending on the design features and performance characteristics, particularly the natural behavior of the core and the protection system performance, DEC sequences may or may not lead to core disruptive accident (CDA) conditions.

8.4.1. Models and codes for design extension conditions

A survey of world-wide capabilities for analysis of beyond design basis events shows that two categories of models and codes exist. In one category, there are model and codes that focus on performance of reactor and plant designs for prevention of severe accident progression. The capabilities in these models and codes tend to emphasize reactivity feedbacks and reactor heat removal mechanisms in modes that are outside the normal operating range, but sufficient to prevent coolant boiling, cladding failure and fuel melting for the assumed accident sequences. These models and codes seek to estimate the margins between anticipated performance and the thresholds for development of severe accident phenomena. In the other category, there are models and codes that focus on the consequences of severe accident progression. These codes model fuel melting and relocation, and seek to provide bounding estimates of severe accident conditions (temperatures and pressures) for assessment of containment margins and release of molten fuel and fission products.

8.4.2. Examples of design extension conditions analyses

8.4.2.1. ATWS in KALIMER-600 at KAERI

The calculations of ATWS have been mostly accomplished over a short time interval covering the initial system transients. The events considered herein are: Unprotected transient over-power (UTOP), unprotected loss of heat sink (ULOHS), unprotected loss of primary flow (ULOF). A long-term analysis, however, has also been performed for a loss of heat sink scenario, activating the passive decay heat removal system for ensuring the long term safety requirement. The initial plant conditions are assumed to be the full power operation with the equilibrium decay heat level. Actions of the reactor protection system and reactor controller subsystem are assumed not to work completely in the analyses for conservatism.

The analyses for DECs clearly show that the inherent safety characteristics of KALIMER-600 from a negative reactivity feedback are ensured. Therefore, it is concluded that the KALIMER-600 breakeven core design accommodates the design extended conditions (DECs) of ATWSs without further propagation to a more severe hypothetical condition [9].

8.4.2.2. Passive shutdown with SASS in JSFR

Transient calculations were conducted in order to confirm the feasibility of SASS under ATWS condition for the large scale reactor with oxide core. Although the maximum coolant temperature reached 1010°C in the case of unprotected loss of flow (ULOF), it is below the boiling temperature at the pressure condition of the core outlet, so that the coolant bulk boiling was prevented and core cooling could be maintained. An unprotected transient over power (UTOP) calculation with 3 cent/s resulted in less than 30% of areal melt fraction of fuel pellet at the peak power position. An unprotected loss of hear sink (ULOHS) calculation with simultaneous loss of the secondary heat transportation system resulted in the maximum coolant boundary temperature of 670°C. From these results, one can say that SASS can prevent core damage in a typical ATWS event which is regarded as DEC.

8.4.2.3. Mitigation against CDA in JSFR

As for CDA, ULOF is postulated. It is preliminarily shown for the oxide cores that super prompt criticality does not occur at the initiating phase and that the core reaches shutdown state due to fuel discharge at the beginning of the transition phase without severe re-criticality events. In order to get these preferable results, the oxide cores were designed to fulfill the following conditions.

- The sodium void worth is less than 6 $;
- The core height is less than or around 1 m;
- The fuel specific power density is higher than 40 kW/kg;
- Special molten fuel discharge duct is installed in each fuel assemblies: fuel assembly with inner duct structure (FAIDUS).

Although these features give some drawbacks in the performance of the core, these could give significant effect for suppressing the severe mechanical energy release due to re-criticality. And it is expected to significantly contribute to achieve the in-vessel retention without too much heavy protective design against the internal mechanical energy release. The behaviors of the initiating phase have been well understood by computer codes, which have been verified through TREAT and CABRI experiments, and thus, the validity of this design may be confirmed by comprehensive evaluation. To make sure FAIDUS concept, some additional R&D works are under way using the IGR in-pile test facility in the National Nuclear Center in Kazakhstan.

For the metal core case, we are conducting some theoretical and analytical prediction with available data about the molten metal fuel behaviors. Currently we assume the following conditions for the elimination of the severe re-criticality:

- The sodium void worth is less than 8 $;
- The core height is less than or around 1 m;
- Shorten the lower structure of fuel pin for enhancing the molten fuel discharge.

The larger sodium void worth can be allowed because its early fuel dispersion can compensate it. This is due to the lower melting point and lower fuel failure threshold of metal fuel comparing oxide fuel. Concerning the molten fuel discharge, it is easier to shorten the lower pin part, because liquid sodium bond and upper gas plenum are adopted in our concept. An investigation of this concept to see its feasibility is under way.

8.4.2.4. Example analysis from India: Transient Over Power Accident (TOPA)

The average and maximum reactivity addition rate due to withdrawal of one Control and Safety Rod (CSR) are 2 and 3.6 pcm/s respectively [10]. In this analysis, the reactivity addition rate due to withdrawal of a CSR is taken as 4 pcm/s. The CSR withdrawal is assumed to be continuous without any limit on the total reactivity added in the accident. If the incident is initiated at steady state operation at full power, then the maximum reactivity that can be added is 500 pcm and if the event were initiated at the time of the calibration of a CSR, then it would be about 900 pcm.

In a continuous withdrawal of a CSR, the negative reactivity feedbacks are overridden by the positive reactivity from CSR withdrawal and so the net reactivity is always positive, leading to continuous power and temperatures rise. In the absence of modelling of deterministic fuel

pin failure condition (i.e., calculation of strain and strain rates in the clad), a 50% fuel melting is normally taken as the fuel pin failure criteria and is considered as a reasonable and adequate criteria [11]. With this criterion, it has been found that fuel pin fails slightly above the mid plane of the core in central channel and at 178 s after the start of the transient. At this time, sodium is still in liquid state in all the channels. So, on fuel pin failure, the molten fuel would come out and would react thermally with the liquid sodium leading to its vaporisation. This is called fuel coolant interaction (FCI). This would cause a momentary flow reversal and a positive reactivity due to voiding from FCI. But as the vapour pressure recedes, the flow would be restored. In the process much of the fragmented fuel would be swept out of the core and may result in the subcriticality of the reactor. This could be enough to absorb the external reactivity. However, if the external reactivity still remains, it may wipe out the negative reactivity from fuel sweep out and again the power excursion would start. This would further lead to fuel pin failure in other channels and would lead to fuel sweep out again.

Based on experimental and analytical results from sophisticated codes developed elsewhere, it is found that TOPA would be terminated by such fuel sweep out and would lead to permanent subcriticality without energetic disassembly of the core [12]. There is also a possibility that the swept out fuel would freeze in the upper axial blanket and would fall into the core due to melting from decay heat and leading to positive reactivity transient. Such a scenario is called transition phase and is studied by modelling the fuel/clad movement and relocation in detail. The modelling and evaluation of this scenario does not exist in the code, PREDIS.

Therefore, conservatively, the accident propagation is allowed till the one-third part of fissile zone is molten and fuel starts slumping and giving large positive reactivity. This happens at about 212.87 s in the present case. When the peak node fuel temperature reaches boiling point, the calculation of the code, PREDIS are stopped and the input is fed to the VENUS-II code. The rate of reactivity addition rates due to fuel slumping is of the order of 23 $/s. Uncertainty analysis on sodium and Doppler coefficient (20%) indicates that reactivity addition rates at the end of pre-disassembly phases change only by 10%.

Disassembly phase analysis has been carried out for different reactivity addition rates and the results are quite sensitive to this parameter. For reactivity addition rates of 25 $/s, the mechanical energy release is only 2.43 MJ and it is 46.2 MJ for reactivity addition rates of 50 $/s. Reactivity addition rates in the transient may not exceed 25 $/s.

However, to be conservative, mechanical energy release of 100 MJ has been assumed in the accident. Such an energy release results from reactivity addition rate of 66.26 $/s.

8.4.2.5. Example analysis from India: Loss of Flow Accident (LOFA)

The transient is initiated due to loss of primary coolant flow resulting from power supply failure to the primary pumps. The flow reduces with a flow halving time constant of 8 s. The inlet coolant temperature is assumed constant during the transient. Flow reduction in LOFA immediately leads to coolant temperature rise that gives positive reactivity. The heating of the spacer pads results in negative reactivity. These negative reactivity components dominate over the positive reactivity components from clad and coolant heating and hence the net reactivity is negative. However, the power to flow ratio is high which leads to coolant voiding in the upper part of the highly rated channels. Subsequently, core voiding spreads radially outward and axially downward. Because of the positive reactivity introduced when the sodium voiding propagates into the central part of the core, the net reactivity begins to increase and becomes positive. It leads to power excursion and finally to clad dry out that

leads to rapid increase in clad and fuel temperatures which results in clad and fuel melting. At this stage, molten fuel will be swept out of the core by shearing force of the coolant and clad vapours for fresh fuel and in addition by fission gas pressure for irradiated fuel. This will lead to large negative reactivity addition and hence the reactor would stay in sub-critical condition. Beyond this again the transition phase analysis, evaluating in detail the fuel and clad movement and the consequent reactivity effects, is to be done. But the entry to transition phase is non-energetic. But transition phase modelling feature is not in the code, PREDIS. All these uncertainties are covered by taking a conservative slumping model as assumed in TOPA. Fuel slumping leads to rapid positive reactivity insertion and rapid power rise. At 71.156 s, the peak node fuel temperature reaches boiling point and hence the transient enters the disassembly phase. It is found that the reactivity addition rates due to fuel slumping and coolant voiding are 13 $/s and 25 $/s respectively, for which mechanical energy release is small. In this case also, the uncertainty analysis on the sodium and Doppler reactivity coefficient (20%) indicates that reactivity addition rates change only by 10%. Assuming reactivity addition rate as 40 $/s, it is found that mechanical energy release in this case is about 27 MJ and for 50 $/s, it is of the order of 58 MJ.

Based on these results and again to be conservative, mechanical energy release of the order of 100 MJ is considered to be released in LOFA.

8.4.2.6. Example analysis from India: Parametric study

In addition to the parametric study with respect to reactivity addition rates in disassembly phase, a set of parametric study has been carried out by certain parameters of pre-disassembly phase.

(1) Change in coolant flow and pressure drop across the core: Coolant flow velocity is increased by 0.9% in core 1, and decreased by 7.7% in core 2. Earlier, the pressure values were constant (0.12 MPa) at the top of axial blanket for all channels. In the new calculations, the pressure is considered constant at the top of sub-assemblies (0.14 MPa), but varies channelwise at the top of axial blanket. The reactivity addition rates at the end of pre-disassembly phase remains less than 25 $/s and 100 MJ of energy is released from reactivity addition rates greater than the reference case.
(2) A set of calculations have been done by ignoring axial reactivity feedbacks from the case 1 discussed above. Again the reactivity addition rates are less than 25 $/s and 100 MJ of energy is released with reactivity addition rates more than reference case.
(3) A set of calculations have been done by ignoring further the radial expansion reactivity feedback. The reactivity addition rates at the end of pre-disassembly phase are of the order of 17 $/s, and 100 MJ of energy is released with reactivity addition rates of the order of 68 $/s.
(4) A set of calculations have been done by taking higher pin linear heat rating, representing the highest value in the ring of subassemblies considered. It has been found [13] that the reactivity addition rates at the end of pre-disassembly phase are of the same order and hence consequences of energy release are not more severe than the reference case.
(5) A set of calculations have been done to study the effect of temperature distribution in the core at the end of pre-disassembly phase. Results were obtained as a function of reactivity addition rates for three cases:
    - Reference case: Temperature profile as obtained deterministically from PREDIS code;
    - Artificially, temperatures in Core 1 and Core 2 are made same and 3023 K (fuel melting point);

- Artificially, temperatures are made 3023 K in all the meshes where temperature obtained from PREDIS are 3023 or more.

It was found that the energy release is sensitive to the temperature profile. This is mainly because, when temperature profile has a gradient, the displacement feedback starts acting sooner than the case when the profile is flat.

Based on the above parametric study, it is seen that the reactivity addition rates at the end of pre-disassembly phase are of the order of 25 $/s or less. Energy release in disassembly phase changes with reactivity ramp rate and is less than 30 MJ even for 40 $/s.

Reactivity addition rates being of the order of 25 $/s or less in all the cases, one can conclude that energy release is small in the CDA and a design value of 100 MJ can be considered a reasonably conservative value.

It is reported by Fauske [14] that reactivity ramp rate from sodium voiding in a typical large homogeneous core is less than 15 $/s and re-criticality effects will be limited to ramp rates of 10 to 25 $/s. It is also shown experimentally that in the fuel dispersal, large amounts of molten fuel is removed from the core region through several potential paths, including the axial blankets, inter-subassembly gaps and the control subassenmblies which lead to permanent subcriticality and unrealistic assumptions are required to produce energetic excursions [15]. The reported energy release in all other LMFBRs is less than or equal to 150 MJ except SPX1. The design value of PFBR is conservative and is similar to international trend [16-42].

8.4.2.7. Example analysis from India: Investigation of mechanical consequences of a Core Disruptive Accident for the PFBR

Core disruptive accident (CDA) is a very low probability event (< 10^{-6}/r-y) considered as beyond design basis event in fast breeder reactor. The energy release in CDA of PFBR is found to be small. CDA results in release of mechanical work by pressure energy stored in core bubble. Based on the reactor physics analysis with pessimistic assumptions, a mechanical energy release of 100 MJ is considered for the design. Mechanical consequences of CDA are strains in main vessel and its internals, sodium slug impact at the top shield bottom, sodium release to reactor containment building and finally temperature and pressure rises in reactor containment building which define the design loadings for reactor containment building.

Assessment of these mechanical consequences calls for sophisticated modeling features for treatment of large distortions in the fluid domains, strong geometrical & material non-linearities in structures, fast transient fluid structure interaction, sodium slug impact on the top shield, shock wave propagation, interactions between the moving interfaces of various fluids and automatic rezoning of finite element mesh. Addressing all the complexities, the computer code FUSTIN has been developed based on Arbitrary Lagrangean Eulerian (ALE) formulation for fluids and convected co-ordinate formulation for structures. It has been extensively validated using international benchmark problems viz. MANON (France), COVA (UK), CONT (UK), MARA (France) and TRIG (India) series.

Analysis has been completed for PFBR in stages, first without any internals to assess the potential of the main vessel and with essential internals. Figure 8.20 shows the numerically predicted core bubble expansion at a few discrete intervals during CDA.

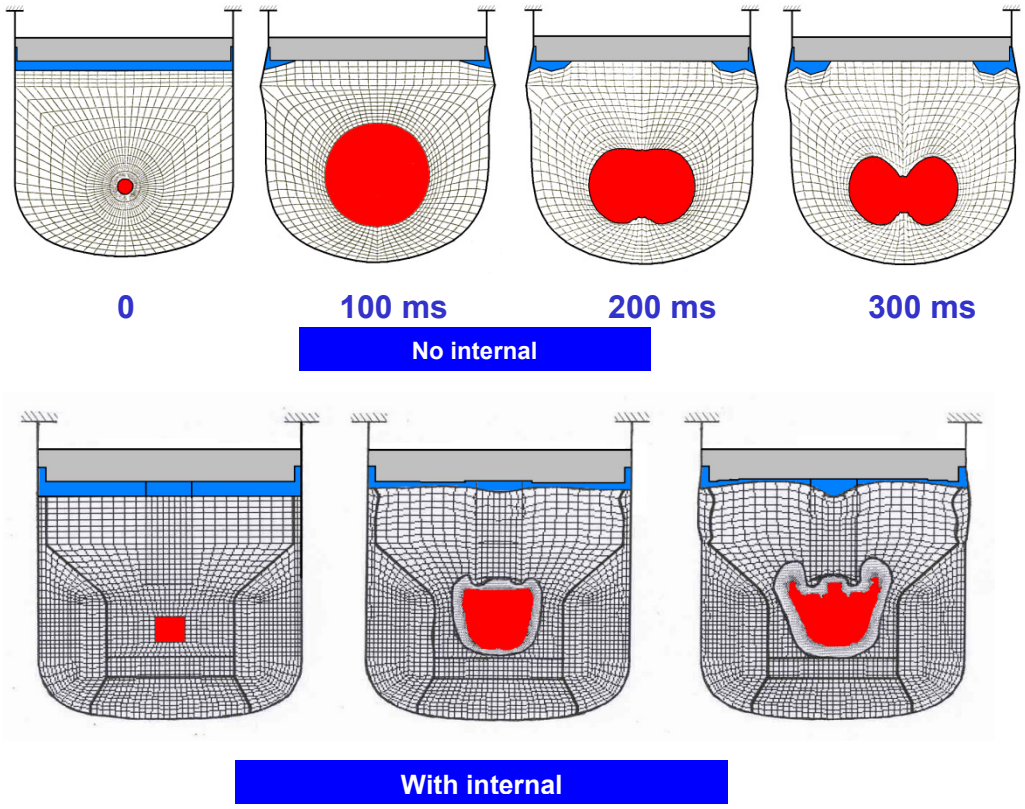

FIG. 8.20. Numerical simulation of mechanical consequences of CDA in PFBR.

Figures 8.21 and 8.22 show a few important results, viz. energy absorbed by the vessel and vessel strains with and without internals.

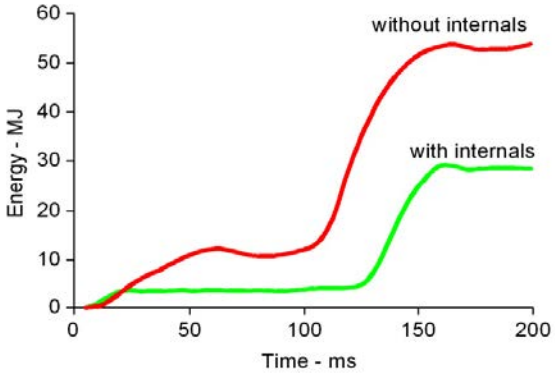

FIG. 8.21. Energy absorbed by main vessel.

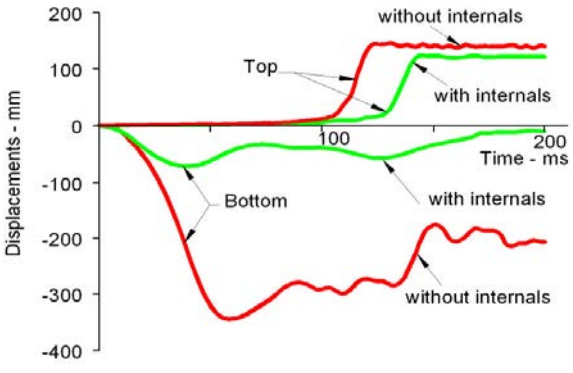

FIG. 8.22. Strains developed in main vessel.

8.5. Experimental studies on fast reactor safety

This section describes some experimental programmes in fast reactor safety that are ongoing. Specifically, contributions from India and Japan are provided.

8.5.1. Experimental studies on fast reactor safety in India

8.5.1.1. Experimental partial flow blockage studies in FBR fuel subassembly

Partial fuel subassembly blockage is one of the important safety issues in the fast reactors as it may lead to enhanced localized heating in the subassembly with a potential to cause fuel melt down. Steel chips or particles resulting from machining process in the construction stage or accumulation of non-fuel debris arising from corrosion and erosion or other reaction products of primary sodium with organic materials may be transported, trapped and settled in the fuel subassembly causing localized heating and flow reduction. Hence the phenomenon of transport and trapping of particulate debris in flowing water, in a 37-pin fast reactor test subassembly, has been experimentally investigated.

The schematic diagram of experimental loop and cross-section of the test subassembly are given in Figs 8.23 and 8.24, respectively.

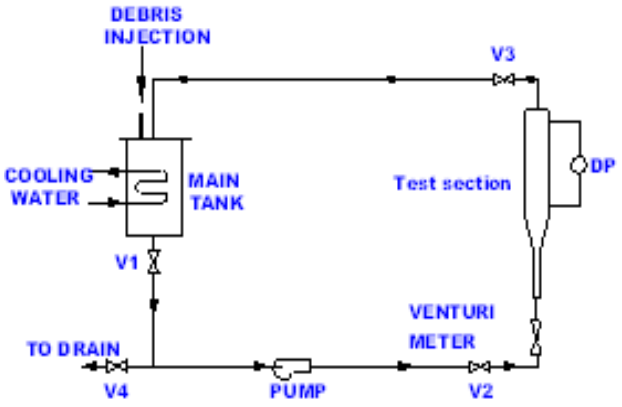

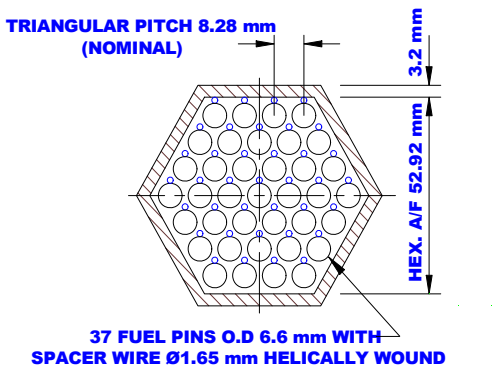

FIG. 8.23. Schematic layout of experimental loop.

FIG. 8.24. Cross-section of 37- pin subassembly.

Stainless steel piping of 50 mm nominal bore size is used in the loop. The geometrical features of the pin bundle are same as that for PFBR, except that the length of the test section is 800 mm (four helical pitches). A venturi meter with a range of 17 m^3/h to 30 m^3/h is used for flow measurement. Pressure drop across the test section is measured within a range of 0 to 1500 kPa. Water temperature is maintained at 50 ± 2 °C by an automated cooling water system during the experiments.

Experiments were carried out with stainless steel cylindrical debris (with diameter to height ratio of 1) of size 1.6 mm and 1.2 mm at different concentrations ranging from 3 to 20 ppm for varying flow values. The concentration is based on the volume of water in the loop, which is around 0.55 m^3. A debris concentration of 1 ppm occupies 0.06% of subassembly flow volume, in case all the debris are trapped within the test subassembly.

Figure 8.25 explains the maximum Sub-channel Passage Diameter (SPD) that is possible in the test section, which is 2.02 mm. Particles larger than this cannot enter the subassembly. The debris deposition pattern for a typical case, where the debris concentration in the loop was 5 ppm (or 0.3 vol.% of the test subassembly, when all the particles are trapped), is shown in Fig. 8.26.

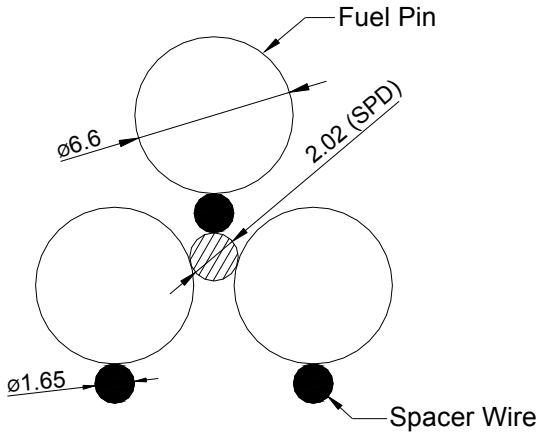

FIG. 8.25. Sub-channel passage diameter.

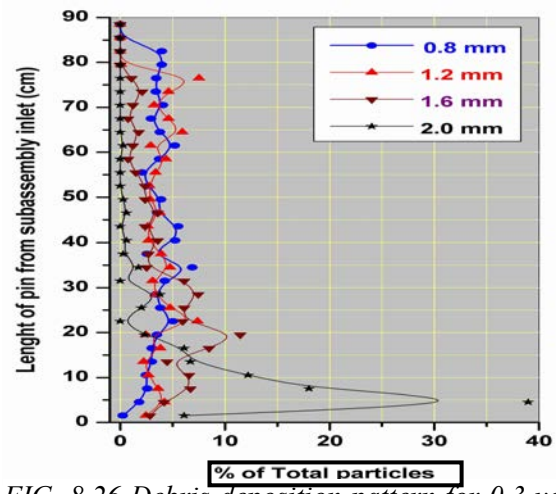

FIG. 8.26 Debris deposition pattern for 0.3 vol.

he 2 mm size debris is observed to penetrate up to one pitch length (i.e. 200 mm) of the subassembly. All the debris of 1.6 mm size were trapped within four pitches of test subassembly and around 80% of these debris settled in the first two pitches. Debris of size 1.2 mm showed almost uniform settlement throughout the length of the test subassembly and 90 to 95% of the debris was found to be trapped in the subassembly. The 0.8 mm size debris also settled uniformly but the percentage of debris settled in the subassembly was around 25% only.

The particle settlement pattern shows that the particles of sizes 1.6 mm and above will not penetrate to the active core region (which starts 5 pitches after inlet) in PFBR fuel subassembly. The particles of size less than 1.6 mm will penetrate and settle at the active core region causing local hot spots.

8.5.1.2. Analysis of enclosed sodium pool fire scenario in sodium fire experimental facility

If hot liquid sodium (temperature greater than ~ 200°C) leaks in air filled enclosures, it undergoes spontaneous combustion due to its high chemical reactivity with oxygen. Sodium combustion is characterized by very small flame with heat production rate approximately equal to about 7% of that is possible with a petrol fire and generating dense white smoke. This will lead to increase in the surrounding gas and structural temperature. The aerosols produced (mostly sodium hydroxide) in the sodium fire is a chemical hazard to the plant and operating personal thereby making it difficult to access the event spot for “fire fighting”. It is also essential to limit the impact due to the aerosols on public at the site boundary and the personnel within the plant boundary. In addition, the leaked and burning sodium damages the structural concrete. Thus in depth understanding of all the sodium fire associated phenomena is inevitable for the safe design and operation of a sodium cooled Fast Breeder Reactor (FBR). With this purpose in mind, a Sodium Fire Experimental Facility (SFEF) (Fig. 8.27) is being setup at the Safety Engineering Division (SED) of IGCAR. Major objectives of the facility are to obtain the evolutions of gas temperature, its pressure rise and wall / ceiling

temperatures due to different modes of large sodium fires (pool / spray / combined) under enclosed or ventilated conditions, to validate the mathematical models developed for the assessment of the consequences of such sodium fire events and to evaluate the performance of mobile or permanent sodium aerosol cleaning systems.

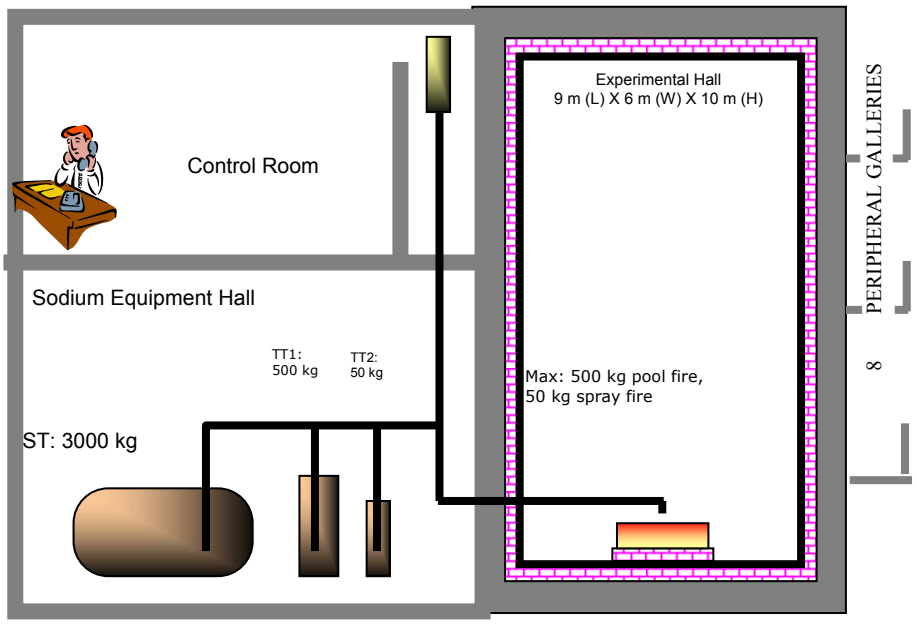

FIG. 8.27. Schematic of SFEF.

The facility consists of an experimental hall and sodium equipment hall in the ground floor and a control room in the first floor. Inside of the experimental hall is 9 m long, 6 m wide and 10 m in height (i.e. 540 m ^{3}volume). This is made up of 450 mm thick RCC floor, walls and ceiling with a design pressure of 50 kPa(g) and temperature of 65°C. All the four walls and ceiling are provided with 50 mm thick insulation and the floor with 150 mm insulation with calcium silicate boards. In order to prevent caustic attack on the concrete and to facilitate thorough washing after conducting an experiment, inside of the hall is completely lined with SS plates. Personnel and material access into the experimental hall is through an air-tight door of 1.8 m width and 2.1 m height in western wall. Several leak tight through wall penetrations are provided on all the four walls for sodium piping entry, inert gas supply, thermocouples, videography, air inlet and exhaust gas outlet and gas and aerosol sampling. Thermocouple trees are provided at various locations in the walls and also in ceiling to measure the concrete temperature at different depths.

Analysis has been carried out for typical enclosed sodium fire scenarios in SFEF, by using lumped model codes, SOFIRE II (pool fire analysis code) and NACOM (spray fire analysis code). Further pool fire analysis has also been carried out with 3-D CFD code to evaluate the maximum temperature of localized hot areas on ceiling and walls. The lumped parameter SOFIRE II code give the evolution of averaged gas and concrete surface temperature and gas pressure, whereas CFD codes give also the spatial variation in them (Figs 8.28 and 8.29). From these analyses it has been concluded that a maximum size pool fire of 500 kg at 550°C and 3 m^2 area and a maximum spray fire of 50 kg at 550°C and at 1 kg/s can be safely conducted within the structural limitations of the experimental hall.

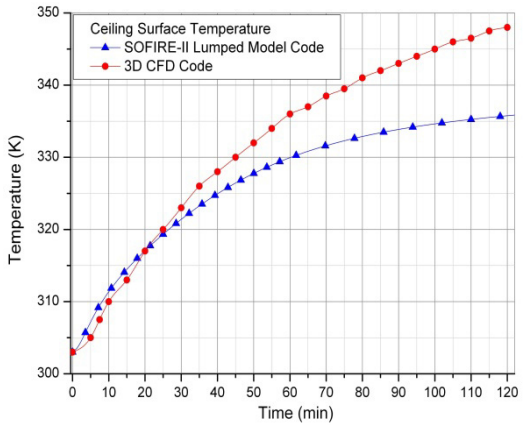

FIG. 8.28. Ceiling temperature in a typical confined pool fire.

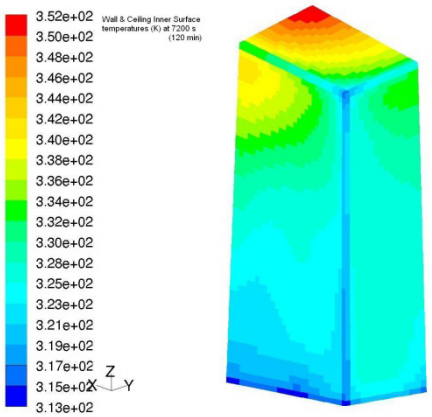

FIG. 8.29. Spatial variation of wall and ceiling surface temperature in a typical confined pool fire.

8.5.1.3. Evaluation of performance of sodium leak collection trays of PFBR

Liquid sodium is used as a coolant in Fast Breeder Reactor (FBR) systems. In the rare case of failure of a sodium bearing component, sodium can leak out and burn with consequences discussed above. In order to collect the leaked sodium and mitigate the consequences of sodium fire in the Steam Generator Buildings (SGB) of PFBR, Leak Collection Trays (LCT) are provided.

The leak collection tray mainly consists of two sloping plates (angle 200) forming a funnel like structure supported on the sodium hold-up vessel. These sloping plates with V-shape orientation rapidly guide the leaked sodium to a central drain-pipe, which ends at 20 mm above the bottom surface of the hold-up vessel. The drained sodium is accumulated in the hold-up vessel with limited exposure to air. A vent pipe of smaller diameter is provided on the slopping plates to facilitate the easy draining of the leaked sodium. The size of the bottom hold-up vessel of the tray chosen is 1200 mm×500 mm×500 mm and that of the top funnel like structure is 1200 mm×1000 mm. The capacity of the hold-up vessel is 300 L. Drain-pipe of 50 NB size and a vent pipe of size 25 NB are used. Figure 8.30 shows the details of LCT and Fig. 8.31 shows the sodium just being let into the tray in one of the tests.

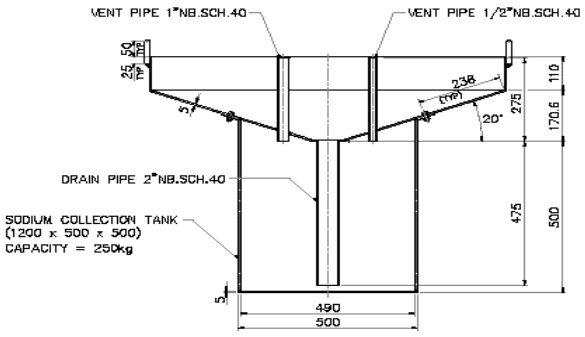

FIG. 8.30. Details of prototype of LCT.

FIG. 8.31. Performance testing of sodium leak collection tray.

Experimental studies on the evaluation of a PFBR leak collection tray have been carried out in the Safety Engineering Division. Three experimental runs were carried out by pouring sodium at 530-550°C into the tray in open-air conditions. Continuous records of temperatures at various important parts of the LCT were obtained. The chemical analysis of the samples indicated burning of sodium was only in the range of 4 to 25%, depending on the test conditions, as against about 70% that normally occurs in a large open pool exposed to air, which is considered as satisfactory.

Processes involved in the operation of the LCT are thermal hydraulics of the flow of hot sodium over the cold surface of the SCT, gravity draining into the SHV and combustion kinetics of sodium, with almost all the processes occurring simultaneously.

A simplified process model has also been derived based on the CFD results, which can be used for quick estimates. Reasonable validation of the simplified model could be achieved (Fig. 8.32) and it is being refined.

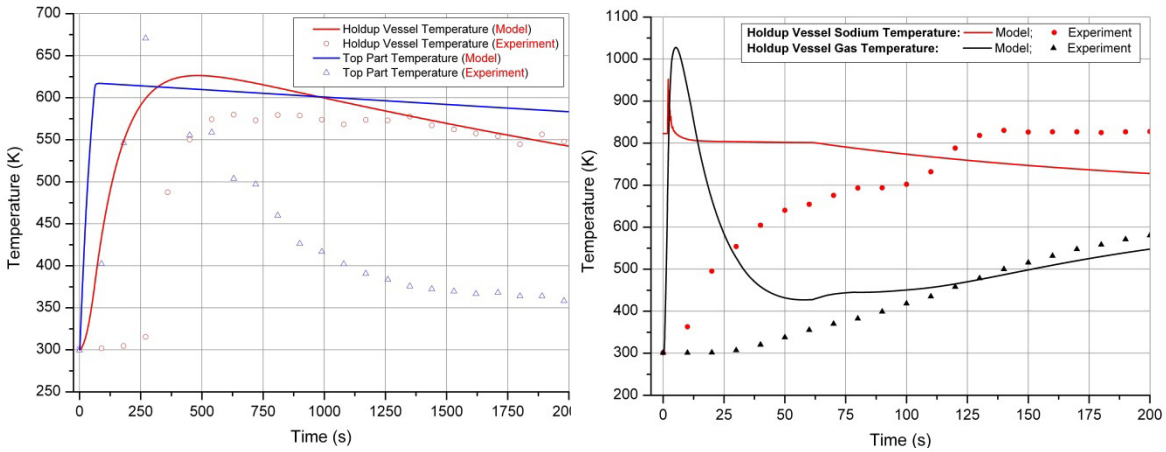

FIG. 8.32. Validation of the simplified model of LCT.

8.5.1.4. Heat transfer studies on model core catcher

In FBR, a core catcher is provided to collect, support, cool and maintain in sub-critical configuration, the core debris generated from fuel melting due to certain postulated beyond design basis event, as an in-vessel core debris retention device. This also acts as a barrier to prevent settling of debris on main vessel and keeps its maximum temperature within acceptable creep range. Experimental studies are carried out at Safety Engineering Division of Safety Group for validating the numerical model, which are being used for analysis of full-scale PFBR core catcher assembly. Experiments have been carried out in water with two versions of model core catchers to understand natural convective heat transfer and fluid flow in and around the core catcher assembly. First version is with a simple central cylindrical chimney and stagnant regions of coolant below the heat shield plate and core catcher support plate. Second version is with a chimney and necessary arrangement to avoid the stagnant regions of coolant present in the first version. Electrical heater coils laid on the heat shield plate is used as the heat source in the experiments. A schematic of the experimental setup is shown in Fig. 8.33.

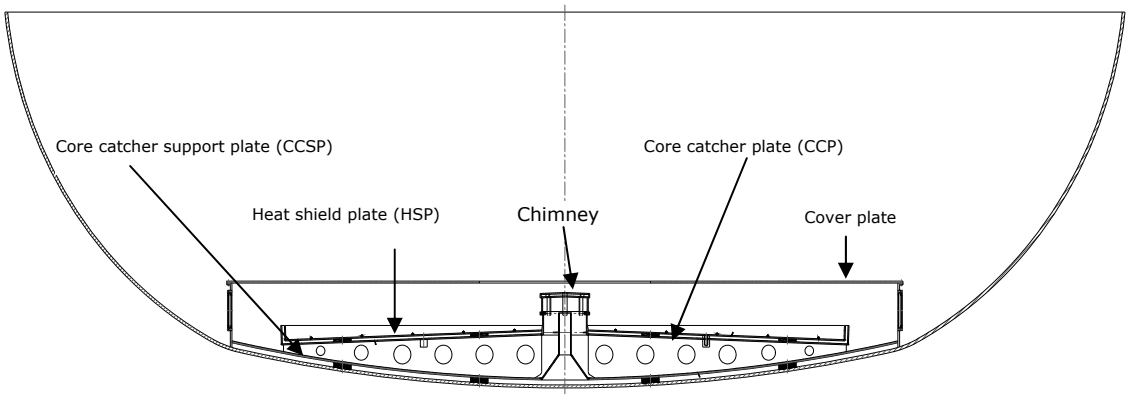

FIG. 8.33. Experimental setup of core catcher assembly.

Details of both the versions of core catcher models are shown in Fig. 8.34.

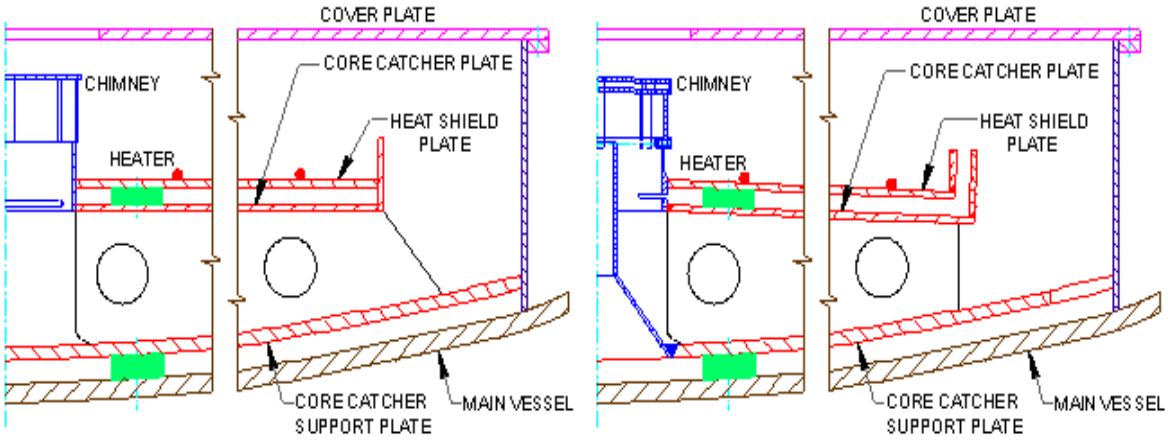

FIG. 8.34. Details of the two versions of model core catcher assemblies.

Experiments have been carried out in water for convenience of handling and transparency for flow visualisation. Steady state natural convective flow conditions are obtained for fixed Heat Shield Plate (HSP) temperatures for both the versions of the model. Several temperatures were measured in different locations of the facility and archived. In this report, attention is brought out on the salient features of the natural convection flow patterns and the water temperatures profile in the central axis.

The experimental temperature distribution over the HSP has been used as the boundary condition for the numerical analysis of the system through the FLUENT code. Figure 8.35 shows the comparison of the natural convection flow patterns in the two versions of the core catcher models.

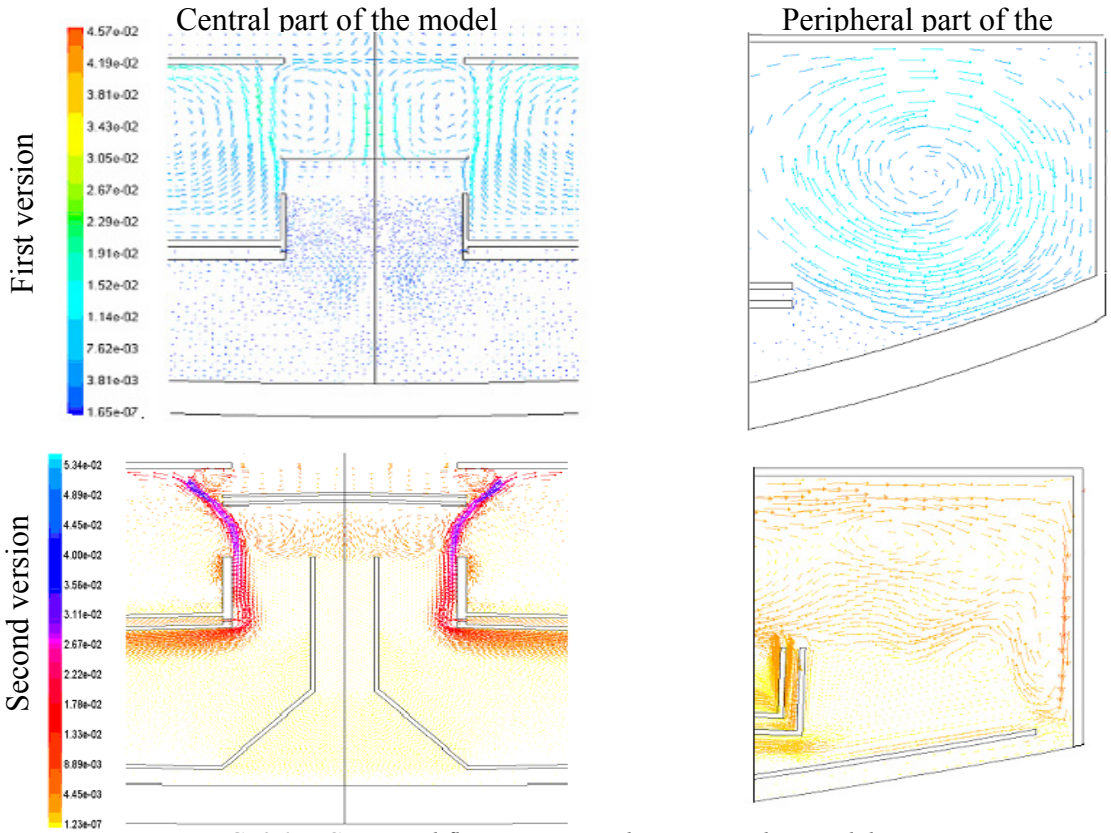

FIG. 8.35. Computed flow pattern in the core catcher models.

It is clearly seen from the flow patterns the modifications of the second version of the core catcher model leaves no stagnant region and cools the main vessel better. These numerical predictions on the flow pattern were in good conformity with the flow visualizations carried out in the experiments. Complex geometry and low velocities made it difficult to measure the actual velocities.

Axial fluid temperature profile obtained both experimentally and numerically along the depth of the cavity for both the versions of the core catcher models, for a HSP temperature of 328 K are shown in Fig. 8.36. Numerical result is generally in good agreement with experimental data in most of the region except in the confined zone where it is under predicted.

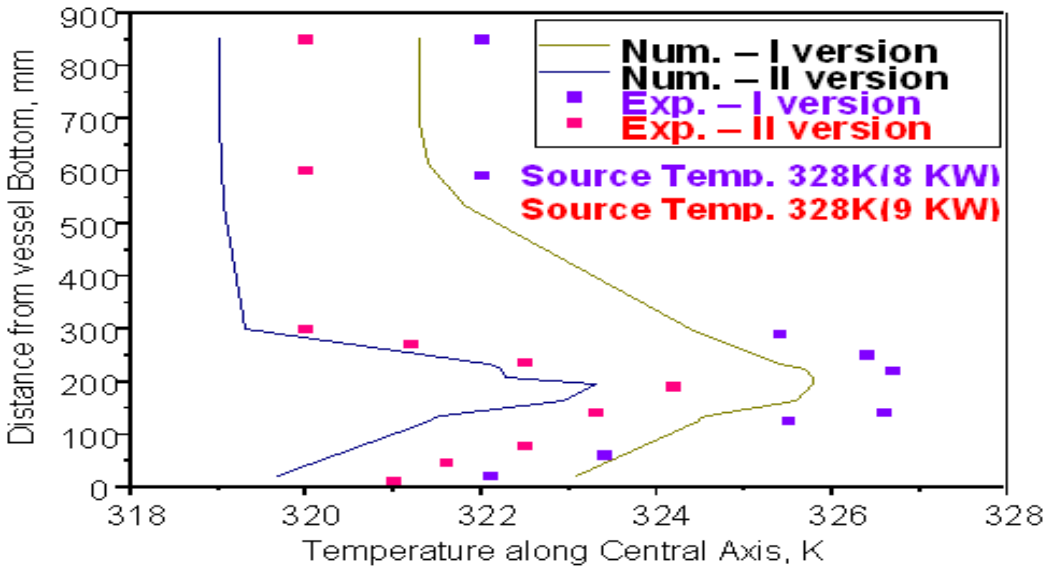

FIG. 8.36. Computed and experimental axial temperature profiles.

8.5.1.5. Atmospheric dispersal of sodium aerosols formed due to a large sodium fire in steam generator building of PFBR

In the event of a postulated sodium leak in SGB of PFBR, intense sodium fire would result and release dense sodium oxides as sodium aerosols. Sodium oxides are readily converted to sodium hydroxide in air due to the presence of moisture in it. Hence, sodium aerosols are invariably in the form of particulate sodium hydroxide. These aerosols may damage not only the equipment and instruments due to their corrosive nature but also pose health hazard to humans. Acceptable limit on the concentration of sodium aerosols in places of human habitat is 2 mg/m^3. Hence, it is essential to estimate the concentration of sodium aerosols within the plant and at site boundary for sodium leak events. The atmospheric dispersion of sodium aerosols at the site boundary is obtained by the Gaussian Plume Dispersion Model, which is applicable for evaluating the concentration for large open spaces. However, this model does not give accurate results for dispersion in spaces with buildings in between. For the latter case, a combination of Eularian Box Model for the velocity field and Monte-Carlo Particle Random Walk Model for the sodium aerosol dispersion has been used. Concentration of sodium aerosols at various distances from the point of release for PFBR have been computed, some recommendations on the ventilation of SGB made and the safety case of PFBR established.

Hot liquid sodium at temperatures greater than 250°C burns spontaneously when it comes in contact with atmospheric air at rates in the order of 20 kg/h/m^2 to 40 kg/h/m^2, depending on the leaked sodium temperature and availability of oxygen. Though the reaction products are in solid phase, due to the intense nature of the sodium fire, about 30% of the oxides are thrown out as fine dusty fume into the surrounding atmosphere. In the event of a sodium fire inside a ventilated building, it is known that about 80% of the aerosols get deposited within the building and rest escapes out through the ventilation. With these characteristics of sodium leak, it has been estimated that 552 g/s of sodium aerosol can come out of the SGB of PFBR, for prolonged periods, in case of a large sodium leak event. This conservative estimate is used as the source term for estimation of both the site boundary and plant premises impact.

The Gaussian Plume Dispersion Model is a simple, steady state, single point source dispersion model, which gives accurate results for plain, uninterrupted terrains from 100 m to 4000 m

from the point of source of release. The worst weather condition F (Stable) as defined by the Pasquill chart is considered for calculating the aerosol diffusion and a wind velocity of 1 m/sec is assumed. Sodium hydroxide reacts with the carbon-dioxide present in the air and gets converted to harmless sodium carbonate at a first order rate constant of 0.2 min-1. This is especially so in large open spaces, where there is no dearth of availability of carbon-dioxide. Particle deposition or absorption is neglected in this calculation. With these assumptions, airborne sodium aerosol concentration is given by:

$$C(x,y,z)=\frac{Q}{2\pi\sigma_Y\sigma_Z u}\left\{\exp\left(\frac{-(z-h)^2}{2\sigma_z{}^2}\right)+\exp\left(\frac{-(z+h)^2}{2\sigma_z{}^2}\right)\right\}\left\{\exp\left(\frac{-(y)^2}{2\sigma_y{}^2}\right)\right\}\{\exp(-x/u\tau)\}$$

where:

C = pollutant concentration at coordinates (x,y,z), g/m^3 or CU/m^3
(CU = Concentration units) averaged over time
x = the distance downwind from the source to the receptor (m)
y = the crosswind distance from the center of the plume to the receptor (m)
z = the height above ground level of the receptor (m)
Q = mass emission rate of pollutant (g/s or CU/s)
u = mean wind speed of the plume (m/s)
h = effective emission height (m) = 0 for a ground source
σ_y = standard deviation of plume concentration in the crosswind direction (m)
σ_z = standard deviation of plume concentration in the vertical direction (m)
τ = time constant for the first order reaction of sodium hydroxide conversion to sodium carbonate (s)

Ground level concentration profiles for the large open space extending to the site boundary is thus estimated for various elevations of source release and shown in Fig. 8.37.

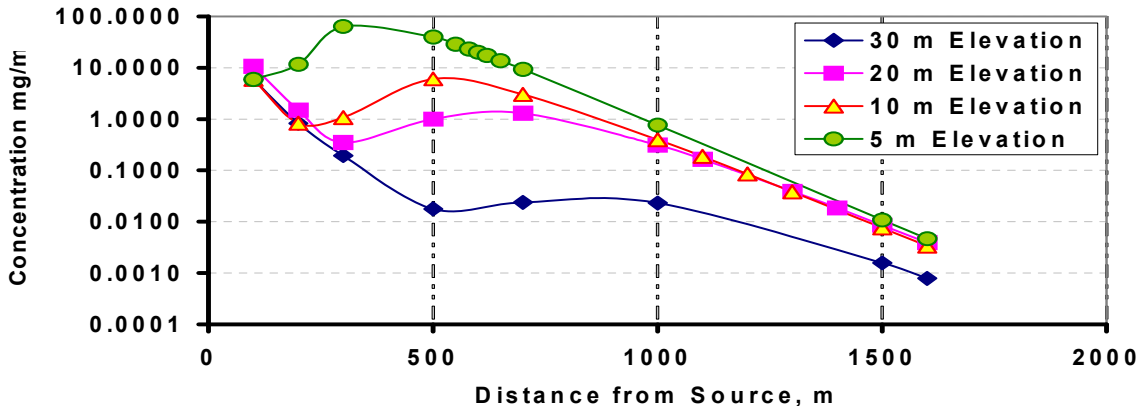

FIG. 8.37 Ground level sodium aerosol concentration profiles.

It can be seen that everywhere beyond the plant premises (500 m) and at the site boundary, airborne aerosol concentration is much less than 2 mg/m^3, if the aerosol release from the SGB is at or above 20 m elevation. For the estimation of impact within the plant premises, entire PFBR site (600 m×600 m) and major buildings are brought into a grid structure of 60 by 60 by 20 with a mesh size of 10 m ×10 m×5 m as shown in Fig. 8.38.

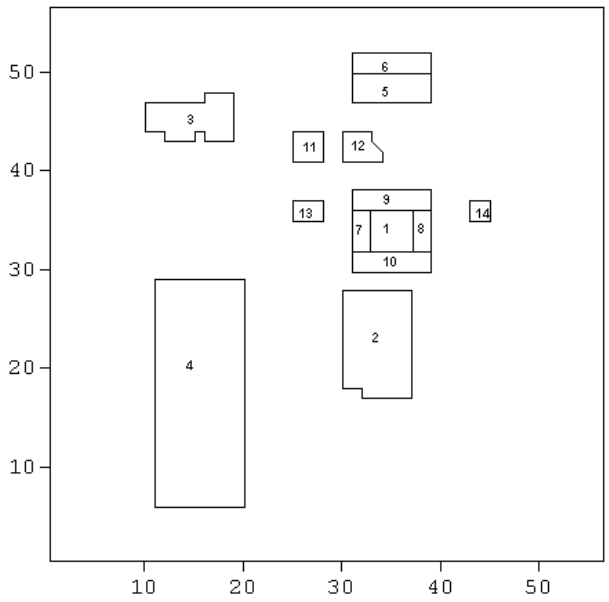

1. RCB
2. Turbine building
3. Administrative building
4. Switch yard
5. Workshop low bay
6. Workshop high bay
7. SGB2
8. SGB1
9. Fuel building
10. Electrical building
11. Service water pump house
12. Service building
13. Diesel generator building (DGB2)
14. Diesel generator building (DGB1)

FIG. 8.38. Grid Structure with important buildings in PFBR site.

A typical ground level concentration contours obtained through the combination of Eularian Box Model for the velocity field and Monte-Carlo Particle Random Walk Model for the sodium aerosol dispersion is shown in Fig. 8.39.

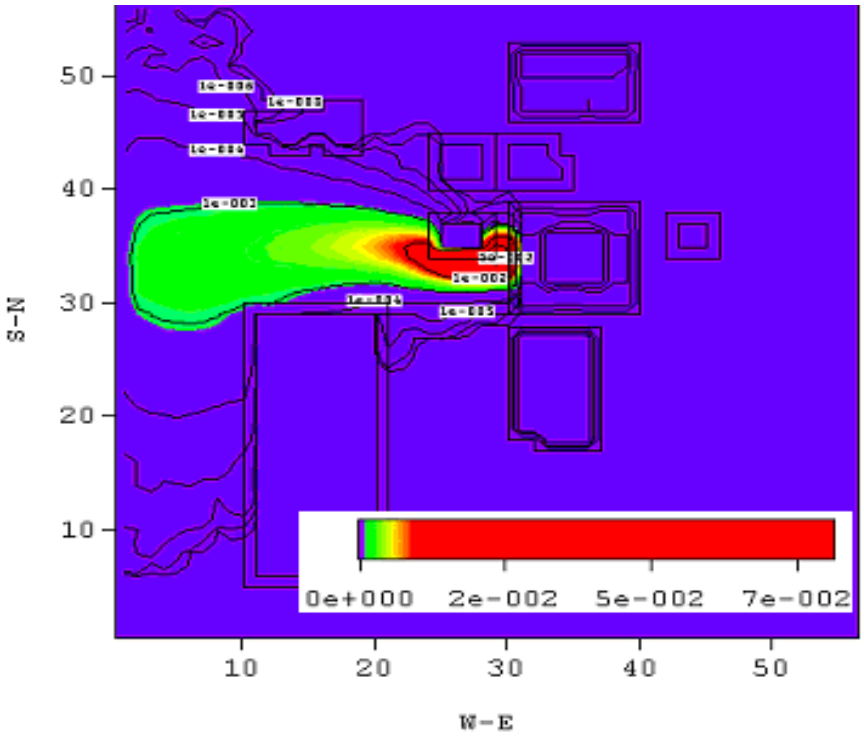

FIG. 8.39. Ground level concentration contours for aerosol release at 5 m

8.5.1.6. Experimental investigation of mechanical consequences of CDA

The tests were carried out in 3 stages (Fig. 8.40).

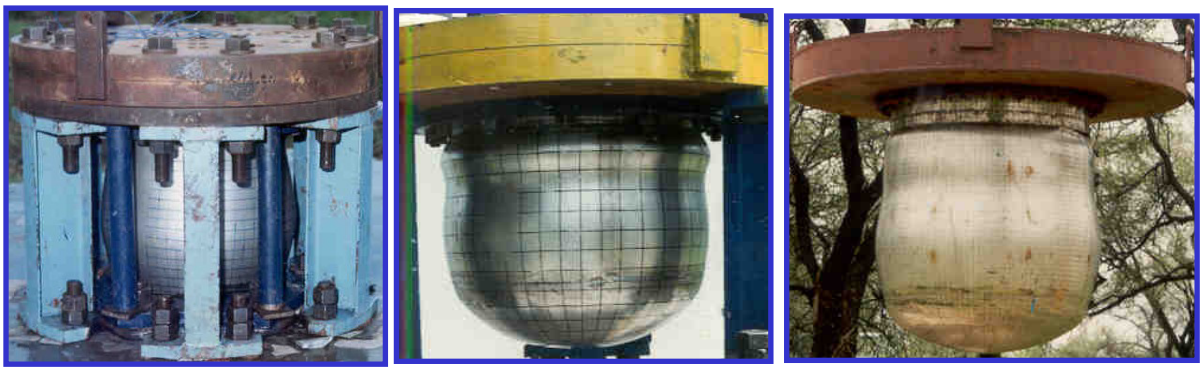

FIG. 8.40. TRIG series test vessels.

In the first stage under TRIG-I series, 17 tests were conducted in water filled cylindrical shells with rigid and fixed top and bottom plates of various dimensions to characterize the chemical charges (the energy conversion ratio, i.e. mechanical energy release per unit mass and the equation of state).

In the second stage under TRIG-II series, tests were conducted in the main vessel models without any internals. Under this series, 30 tests on $1/30^{th}$ scale models and 3 tests on $1/13^{th}$ scale models were conducted. Sufficient data have been generated for validating the FUSTIN code and also for establishing acceptable strain limits for the vessels under simulated CDA loading conditions.

In the third (last) stage, under TRIG-III, tests were conducted on $1/13^{th}$ scale mockups with the main purpose to demonstrate the structural integrity of intermediate heat exchanger (IHX) and decay heat exchanger (DHX) and also to estimate the sodium leak based on simulation principles. Totally 61 tests were completed during the period of 4 y.

TRIG-I and TRIG-II results were well predicted by FUSTIN. TRIG-III analysis is in progress. After characterizing the low density explosive specially developed for the test series based on TRIG-I rests, TRIG-II cases were analysed. Figure 8.41 shows transient pressure evolutions within main vessel model filled with water subjected to simulated low density chemical explosion (TRIG-II).

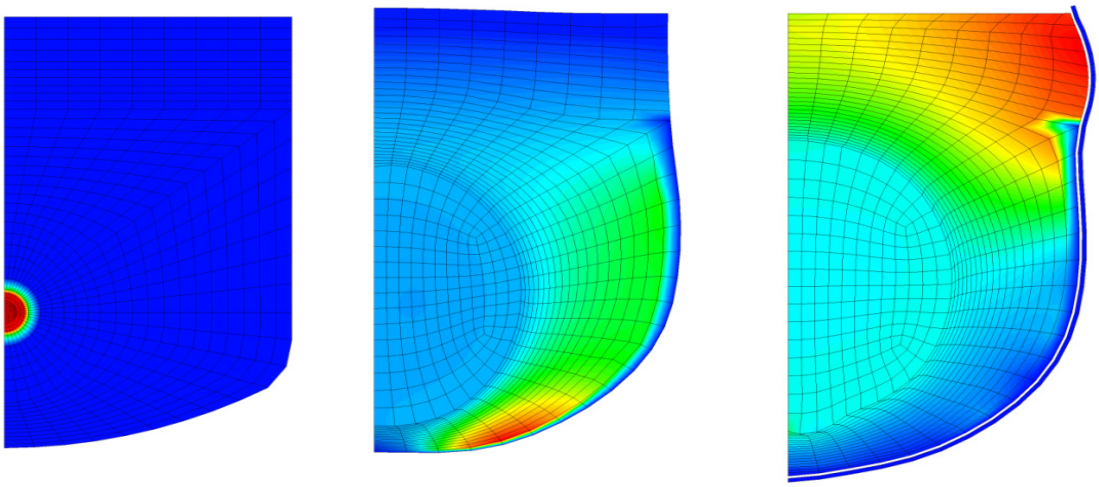

FIG. 8.41. Transient pressure distribution within the vessel predicted by FUSTIN.

The vessel deformations captured by high speed camera at a few discrete time steps are compared with the FUSTIN prediction in Fig. 8.42.

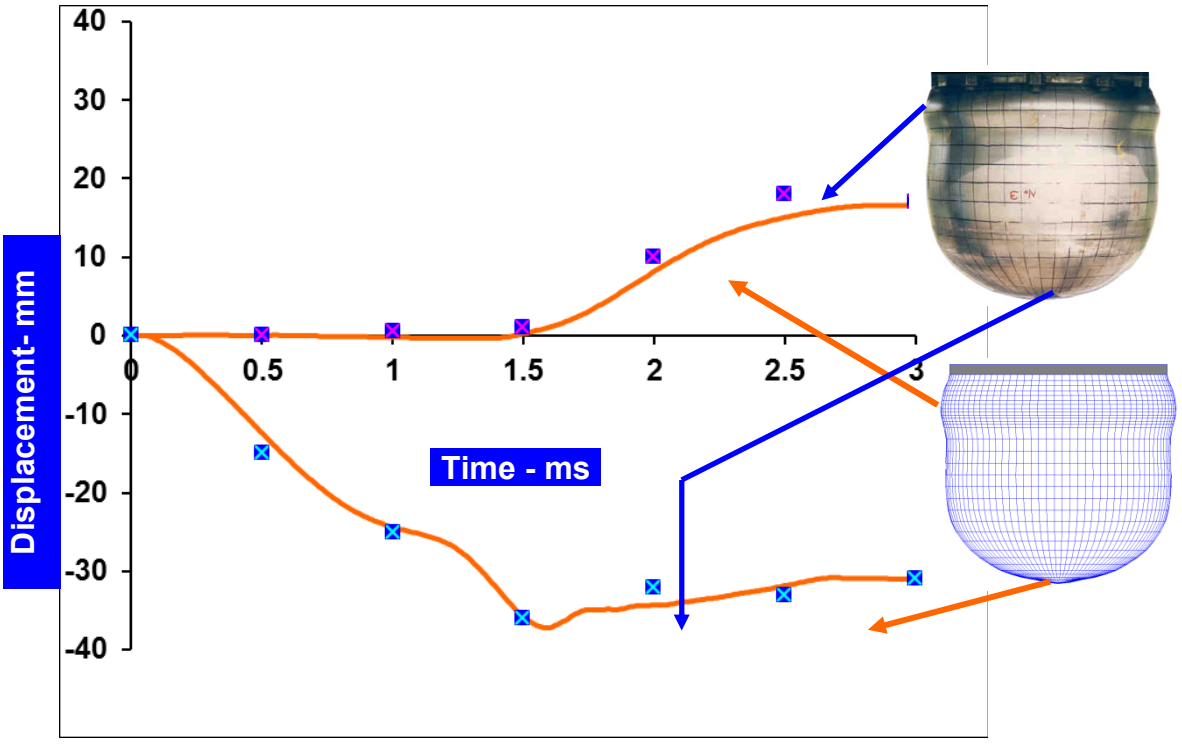

FIG. 8.42. Displacements by FUSTIN for TRIG-II vessel.

Further tests were conducted on 1/13th scaled reactor assembly mockup to assess the structural integrity of intermediate heat exchanger and decay heat exchangers as well as to estimate sodium leak through top shield penetrations (Fig. 8.43).

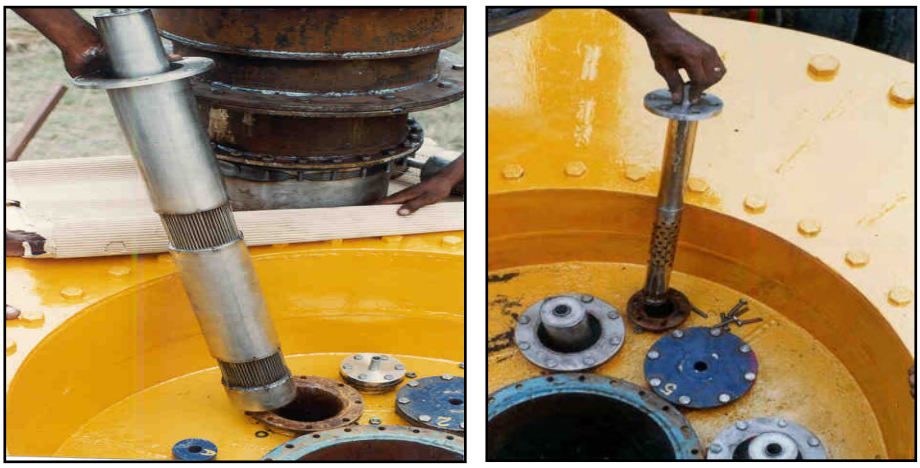

FIG. 8.43. IHX & DHX including tubes are integral for 200 MJ.

8.5.2. Experimental studies on fast reactor safety in Japan

8.5.2.1.CABRI-RAFT Project

Within the framework of the CABRI-RAFT project, seven in-pile experiments listed in Table 8.4 were performed under the collaboration between IRSN and JAEA (formerly IPSN and JNC) from 1997 to 2002.

TABLE 8.4. TEST MATRIX OF THE CABRI-RAFT PROJECT

Areas to be investigated	Test name	Power history	Test section	Objective	Facility
Control-rod withdrawal-type overpower transient (DBE study)	RB1	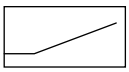	Single pin with a slit-type pre-defect on the cladding	Possibility of fuel ejection as a function of fuel melting and impact of fuel ejection	CABRI
	RB2	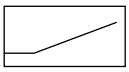			
Early transition phase of core disruptive accident (BDBE study)	LTX	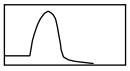	Single pin (without upper axial blanket)	Possible in-pin fuel motion before the pin failure and post-failure fuel motion in the coolant channel	
	TP2	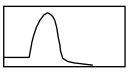	Three-pin cluster	Fuel relocation and blockage formation with presence of a prototypical coolant sub-channel focusing on initial material distribution for the transition phase	
	TP-A1	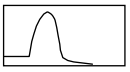			
	TP-A2	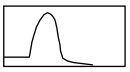	Capsule	Heat transfer within the molten fuel/steel mixture pool	
	TP3 (5 shots)	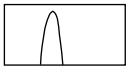	Capsule		SILENE

This project covers interests on (1) impact of fuel pin failure under an overpower condition corresponding to control-rod withdrawal-type incidents (DBE study), (2) reduction of the uncertainty of initial conditions of the transition phase of the ULOF accident (DEC study), and (3) basic study on heat-transfer characteristics of the fuel/steel mixture in the transition phase of the ULOF accident (DEC study).

8.5.2.1.1. RB1 and RB2 tests [43] (DBE study)

In the RB1 test, a pre-defected fuel pin with a slit-type defect shown in Fig. 8.44 was driven to fuel melting with a slow over-power transient.

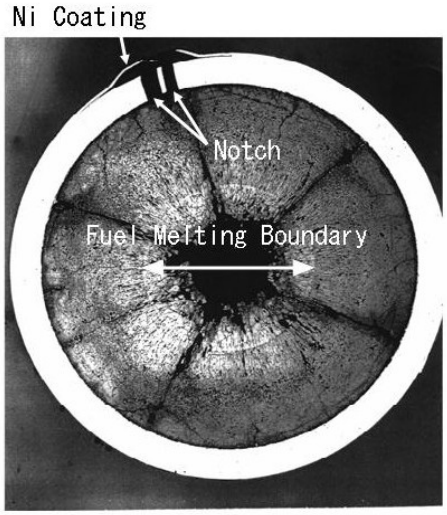

FIG. 8.44. Radial cut of the test pin after the RB1 test at around the pre-defect on the cladding.

Although maximum fractional melt radius of 0.57Ro (Ro is fuel outer radius) was observed in the radial cut and calculated molten fuel mass is approximately 10% of initial fissile fuel mass, molten fuel was maintained within the fuel pin suggesting that the outer solid fuel part has potential to prevent fuel ejection even in case of cladding failure. It should be noted that the low smear density fuel adopted in this test would have led to limited cavity pressure increase thereby contributing to the non-ejection result. It is also noted that there was a certain amount of DN-precursors released into the coolant flow even without fuel ejection. This information is encouraging from the viewpoint of anomaly detection by the DN observation.

Based on the RB1 test result, it was intended to get basic information on molten fuel ejection behavior in the RB2 test. Therefore, more pronounced fuel melting leading to fuel ejection was realized in this test. Calculated maximum fractional melt radius by computer codes for this test was 0.6-0.7Ro and corresponded to 15 to 20% of initial fissile fuel mass. With the fuel ejection into the coolant channel, sodium voiding took place. However, thermocouples placed in the coolant channel showed the temperature basically only up to the saturation level in the early phase of the transient suggesting that the coolant channel kept its wet characteristic. As for the later part of the transient, the single-pin test geometry with complete blockage formation, inevitably led to dryout. However, in the reactor condition, presence of sodium flow in the neighboring sub-channels would possibly prevent complete blockage formation in the later part of the transient. Therefore, although the RB2 test result is not directly applicable to demonstrate coolability of the ejected fuel, it provided basic information effective for consideration of the impact of the fuel ejection.

8.5.2.1.2. LTX, TP2 and TP-A1 tests (DEC study)

An early cladding failure in the LTX test prevented pre-failure in-pin fuel motion suggesting that this reactivity mitigation mechanism is quite dependent on the fuel and transient conditions.

TP2 and TP-A1 tests with the three-pin cluster condition, confirmed the effectiveness of the conventional single pin CABRI tests regarding fuel relocation and blockage formation showing that the fuel relocation/freezing is dominated by the local fuel enthalpy in both geometries. It was also suggested with a real time measurement of gas level inside the gas trap placed above the test fuel that the fuel blockage is tight enough to prevent significant gas escape from the disrupted fuel region. This result is suggesting that the disrupted core in the early part of the Transition Phase would be bottled up with certain pressurization.

8.5.2.1.3. TP-A2 and TP3 tests [44] (DEC study)

In the TP-A2 test, 1-mm size steel balls were placed within the fuel (pressed from fuel powder) and fuel melting was realized. Although energy injection was sufficient to generate certain steel vapor pressure if heat transfer was large enough, there was no sign of meaningful steel vapor formation in terms of molten fuel movement. However, microscope measurement on the post-test samples strongly suggested presence of local steel vapor formation. These experimental results suggested possible mechanism, which reduces fuel-to-steel heat transfer. A simulation study with a computer code showed a possible explanation of this mechanism with the steel-vapor blanketing effect, in which a thin layer of small steel-vapor bubbles prevents rapid heating of the steel ball. If this assumption is correct, fuel/steel mixture would not lead to a rapid steel vapor formation in case of rapid fuel heat generation, which often leads to dynamic core material relocation thereby causing reactivity insertion in the Transition Phase. Further study is necessary to apply this mechanism for the reactor evaluations.

In the TP3 test, single pressed fuel with a steel ball in it was contained in a tight capsule without expansion volume. The test consisted of five individual shots with different energy injections and steel ball sizes. In this test, high pressurization due to impurity gas release from the zirconia crucible realized a turbulent fuel-steel mixing condition leading to significant fuel-to-steel heat transfer. Through these tests, it was understood that fuel-to-steel heat transfer is quite dependent on the dynamic characteristics of the mixture.

8.5.2.2. EAGLE-1 programme [45, 46]

8.5.2.2.1. In-pile tests

In the EAGLE-1 programme, under cooperation between Japan (JAEA and JAPC) and Kazakhstan (NNC: National Nuclear Center of the Republic of Kazakhstan), experimental study on fuel relocation behavior under the Core Disruption Accident was conducted. This program put stress on demonstration of effectiveness of a design measure, which introduces a fuel discharge duct into each fuel sub-assembly, to eliminate the re-criticality issue on one hand. It is also intended to obtain basic information related to the core-material relocation behavior, which would be effective for evaluation of various design options on the other hand.

The test program was conducted utilizing IGR (Impulse Graphite Reactor) and out-of-pile facilities of NNC. As the in-pile part of this program, six experiments were performed along with establishment of the test techniques. In the final stage of the program, about 8 kg of UO_2-fuel was melted in IGR in three tests and molten-fuel-discharge behavior through the duct was

investigated. In one of these final stage tests, sodium was not used and served as basic information for the two main tests with sodium thereby providing clarification of sodium effects on the fuel discharge behavior.

Figure 8.45 shows the schematic of test channel of the final-stage tests with sodium. Energy release history in the test fuel was controlled so as to realize the molten fuel/steel mixture pool with enthalpy corresponding to a relatively high power part of the core during the ULOF accident.

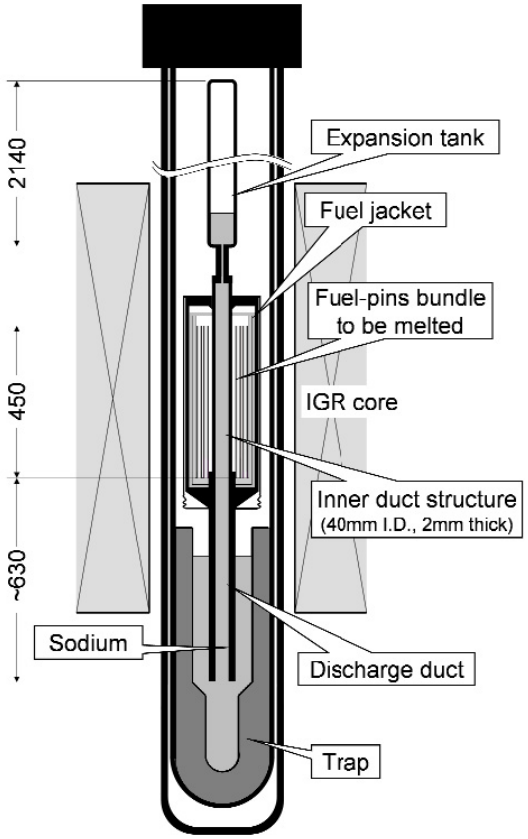

FIG. 8.45. Test section of the final-stage in-pile tests.

Early discharge of fuel from the core, which enhances capability to prevent re-criticality events, is one of the key elements in the present approach. Fuel discharge starts with failure of the thin duct-wall structure, which is initially filled with liquid sodium. Therefore, depending on the cooling capability of sodium inside the duct, the failure time can be delayed. The experimental results showed that heat transfer from the fuel/steel mixture to the duct is so high that duct-to-the-sodium heat transfer plays only a minor role. As a result, the presence of sodium inside the discharge duct delays the wall failure only shortly assuring an early fuel discharge scenario.

After the wall failure, the fuel discharge in the reactor condition is believed to be driven mainly by the gas pressure. Although significant pressure buildup is expected for the rector condition, it was intended to allow relatively low pressure condition in the final stage tests aiming at demonstration of discharge capability without significant pressurization. Based on this strategy, the pressure difference between the fuel/steel pool and the discharge duct was controlled at a low level (less than 0.12 MPa) in the first main final-stage test with sodium. As shown in Fig. 8.46, on ejection of fuel/steel mixture into the discharge duct, rapid sodium

vapor formation took place, which is dynamic enough to evacuate the liquid sodium from the discharge duct. As a result, the main part of the fuel/steel mixture discharged through the voided duct without significant freezing.

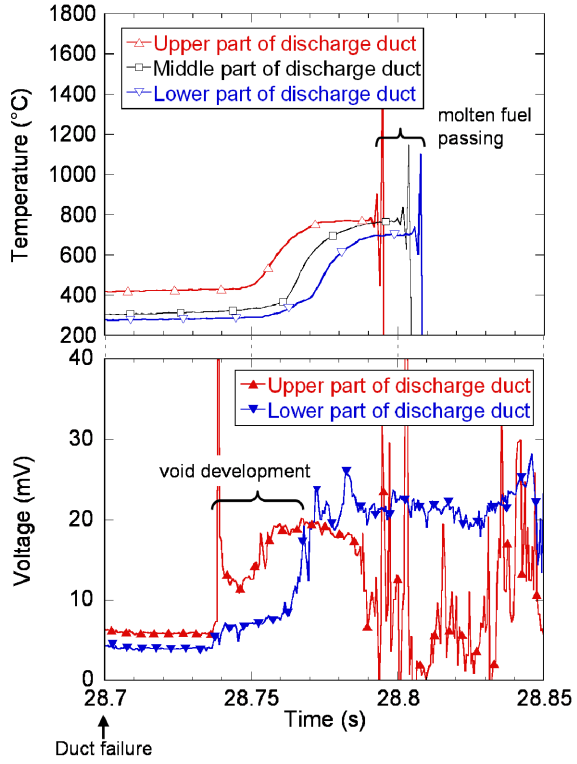

FIG. 8.46. Observed void development and temperature response in the duct in the first main final-stage in-pile test.

Above characteristics and some preliminary results from the post test examinations (PTE) strongly suggest the effectiveness of the design option enhancing the early fuel discharge characteristic to eliminate the recriticality issue. The ongoing PTE will supply more information leading to confirmation of the above preliminary conclusions.

8.5.2.2.2. Out-of-pile tests

The schematic of the test section is shown in Fig. 8.47. Alumina (Al_2O_3) was selected as a fuel simulant and was melted by the electro-magnetic induction heating in the furnace (EMF) which is located above the test section. The molten alumina generated in EMF was transported to the upper trap which simulated the molten core region. The lower trap vessel contained about 90 kg of sodium without cover gas, which is sufficient to simulate the lower plenum region during the early fuel discharge phase of the reactor condition. After establishment of the necessary test techniques through tens of preparatory tests, four main tests with sodium were performed.

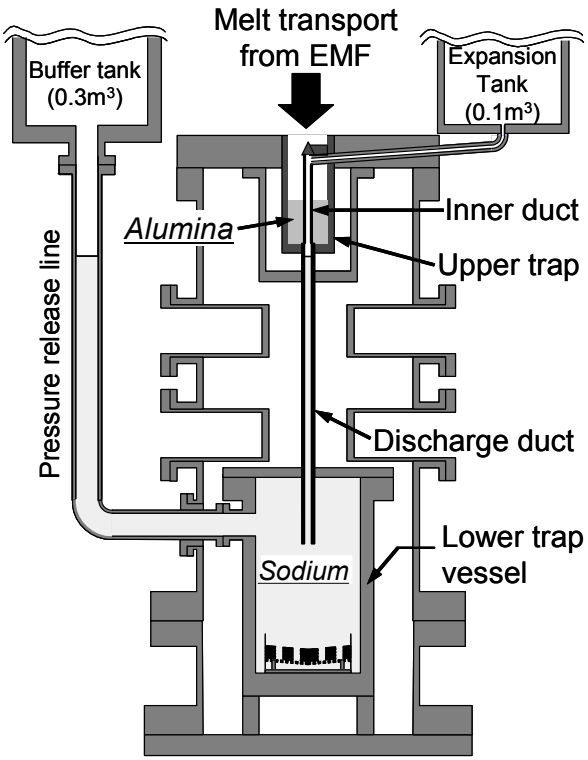

FIG. 8.47. Test section for the out-of-pile tests.

In the first main test, the short-term duct failure did not occur because the heat transfer from molten alumina to the duct was one order of magnitude lower than that observed in the in-pile tests. With this low heat transfer from the melt, duct wall was cooled by sodium without a short-term duct failure preventing observation of melt discharge behaviour. In the out-of-pile tests, fuel heating was absent after its transfer into the upper trap and no steel was included in the melt so that heat transfer within the melt would have been limited. These factors specific to the out-of-pile test condition are responsible for the limited heat transfer to the duct. Therefore, in order to realize a short-term duct failure and subsequent melt discharge, the sodium level in the discharge duct was set at the bottom of the upper trap in the later three tests. Although the absence of sodium at the axial level of duct failure would slightly delay the FCI in the duct, basic information on effects of sodium in the discharge duct and the lower trap on the melt-discharge behavior can be obtained.

Observed melt relocation behavior was common in these three tests. Right after the wall failure, the melt contacted with sodium in the discharge duct leading to rapid sodium vapor formation and downward void extension toward the lower trap vessel. With this void extension, an effective discharge path was formed prior to the main melt discharge phase. This rapid voiding behavior, which is effective to reduce the heat loss from the melt during the discharging phase, had been predicted in the fundamental experiments using simulant materials [47] and it was confirmed with these EAGLE-1 out-of-pile tests. Figure 8.48 shows a sample of pressure histories measured in the cover gas region of the upper trap and sodium pressure in the lower trap vessel. At the moment of melt penetration into the lower trap, FCI pressure build up was observed.

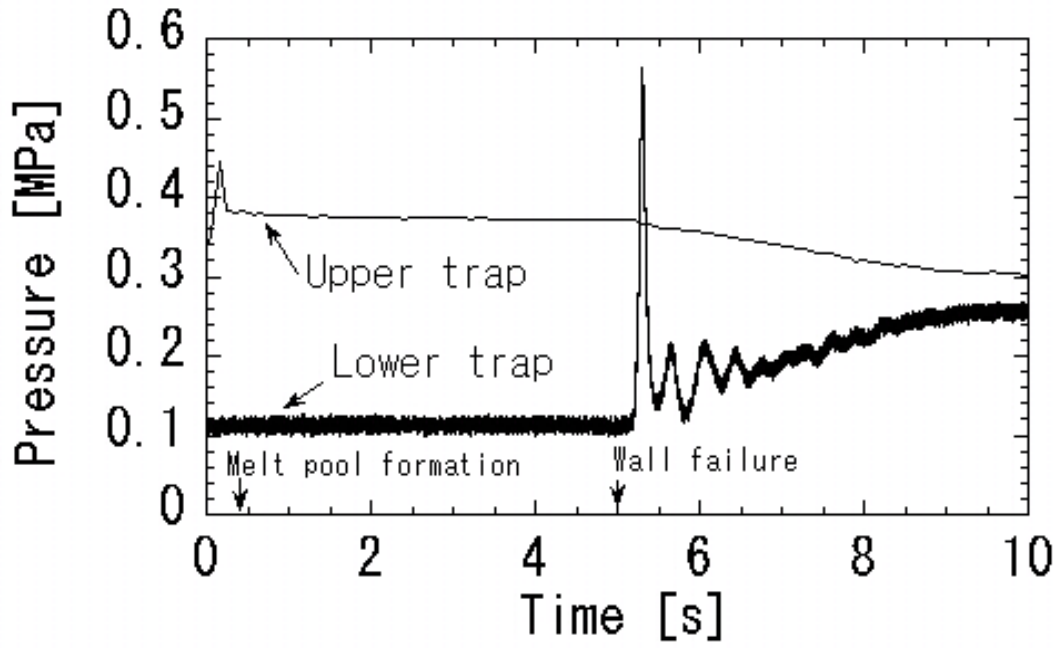

FIG. 8.48. Pressure histories measured in the out-of-pile test.

However, this FCI pressure level was not significant and decreased rapidly both by condensation of sodium vapor and the sodium flow toward the buffer tank. With this limited FCI pressure build up and its rapid decrease, melt discharge behavior was almost undisturbed. This FCI event, which is not at all energetic, effectively transferred the discharged melt into fine debris, which is the favorable geometry for cooling.

8.6. Future developments

8.6.1. Trends in safety design approach

As sodium-cooled fast reactor development has progressed from the demonstration phase to the commercialization phase, trends in fast reactor design approach have focused on improvements in economics, operation simplification, and the robustness of the safety architecture. Efforts to achieve cost reduction have emphasized design simplification for initial capital cost reduction, as well as extension of fuel and plant life for operating cost reduction.

In recent sodium-cooled fast reactor designs, designers have sought to make reactor and plant systems more compact to reduce the cost of commodities. At the same time, designers have sought to reduce the number of components and systems. From the safety perspective, these developments have brought new reliance on innovative safety design features to satisfy design basis safety requirements and to enhance prevention and consequence mitigation measures for beyond design basis accidents. Increased emphasis has been placed on inherent mechanisms for reactor power control and shutdown heat removal. Passive behavior of design features has received greater attention to permit reduction or elimination of active systems. The choice between passive or active provisions should be made on the basis of a cost-benefit approach and on the validation of the performance of the passive system when its performance is reduced (particularly for thermal-hydraulic passive system). Continued attention to severe accident prevention and mitigation has prompted the further development of traditional design features to

address beyond design basis accident phenomena. New design developments have been proposed to address severe accident phenomena, with the design objective to avoid a large, energetic, mechanical release that could damage the containment.

Regulatory authorities have responded to these changes in safety design approach with new requirements for safety analysis content and documentation. Of particular significance is a movement toward increased presence of risk-informed regulation in the determination of priorities for establishing a safety basis.

These new developments in safety design features and nuclear reactor regulation have determined the requirements for future safety analysis models and computer codes.

8.6.2. Developments for safety analysis models and codes

Trends in new safety analysis model and code developments have focused on higher fidelity deterministic methods and increased applications of probabilistic techniques.

With the rapidly increasing availability of large-scale, multi-processor computer systems, deterministic safety analysis methods are evolving toward higher fidelity models for both geometric detail and phenomenological scope. The success of commercial computational fluid dynamics (CFD) analysis methods in non-nuclear engineering and systems analysis has fostered their use in nuclear reactor coolant systems analyses. Building on the application of CFD methods, higher order simulation techniques for fluid dynamics analysis applications are currently being developed. These advanced techniques model physical transport phenomena at a level that promotes improved understanding and better utilization of experimental data. These techniques promise the possibility of eliminating many of the sources of uncertainty in current design basis calculations. Consequently, overall uncertainty margins will become smaller and allowable performance conditions may be enhanced accordingly.

The success of higher order analysis methods in fluid dynamics has prompted the extension of newly available software and hardware to solution of higher fidelity models in other phenomenological areas as well. New models for reactor physics and kinetics, heat transfer, structural mechanics, and fuel behavior are currently in development, as well as the coupling at different scales. These new models feature higher fidelity in both geometric and phenomenological depictions of reactor systems, components, and structures. Past models that were limited to single or few-pin geometric models of the reactor core are now being replaced by models that explicitly represent each fuel pin. Correlations for measured data are replaced with first-principles models whenever understanding of physical behavior permits. Application of advanced simulation to all areas of reactor design and safety analysis promises to make the design and safety analysis process more efficient, to reduce uncertainties and enhance reactor performance conditions, and to substantiate more completely the safety design basis.

As deterministic analysis methods become more detailed, establishment of a more secure safety basis has also benefited from increased use of probabilistic techniques in order to reach confident quantification of some risk measures or safety margins taking into account the various uncertainty sources. The use of probabilistic safety assessment has served to quantify more completely the comparative safety basis for a specific plant, and to integrate voluminous deterministic analysis results into a compact format that is more readily assimilated by regulatory reviews and the public. As risk-informed regulation becomes increasingly prominent, probabilistic safety assessment and the application of probabilistic analysis methods will become more significant in reactor safety and licensing analysis.

REFERENCES TO CHAPTER 8

[1] INTERNATIONAL ATOMIC ENERY AGENCY, Basic Safety Principles for Nuclear Power Plants, 75-INSAG-3 Rev. 1 INSAG-1, IAEA, Vienna (1999).

[2] INTERNATIONAL ATOMIC ENERY AGENCY, Defence in Depth in Nuclear Safety, INSAG-10, IAEA, Vienna (1996).

[3] US DEPARTMENT OF ENERGY, A Technology Roadmap for Generation IV Nuclear Energy Systems, U.S. DOE Nuclear Energy Research Advisory Committee and the Generation IV International Forum, U.S. Department of Energy (December 2002).

[4] MORIHATA, M., AONO, H., ARIYOSHI, M., IKARIMOTO, I., Development of Self Actuated Shutdown System for FBR in Japan, paper presented in 5th Int. Conf. Nuclear Engineering, Nice, France, 26-30 May 1997.

[6] NIWA, H., A Comprehensive Approach of Reactor Safety Research Aiming at Elimination of Re-criticality in CDA for Commercialization of LMFBR, Prog. Nucl. Energy, 32, 3/4, 621 (1998).

[6] SELVARAJ, P., SEETHARAMU, K.N., VAIDYANATHAN, G., Large leak sodium-water reaction analysis of an LMFBR steam generator using a variable temperature spherical bubble model, Nuclear Engineering and Design, Vol. 123, pp. 87-90 (1990).

[7] SELVARAJ, P., VAIDYANATHAN, G., CHEAL, S.C., Review of design basis accident for large leak sodium-water reaction for PFBR, paper presented in 4th Int. Conf. Nuclear Engineering, Louisiana, USA (March 1996).

[8] SREEJITH, B., JAYARAJ, K., GANESAN, N., PADMANABHAN, C., CHELLAPANDI, P., SELVARAJ, P., Finite Element analysis of fluid-structure interaction in pipeline systems, Nuclear Engineering and Design, Vol. 227, pp. 313-322 (2004).

[9] LEE, Y.B., et al., Safety Analysis for Key Design Features of KALIMER-600 Design Concept, KAERI/TR-3370/2007, Korea Atomic Energy Research and Institute (2007).

[10] FRIZONNET, T.M., RONGIER, C., Comparative Calculations for Unprotected Transient Over Power in BN-800 Type Reactor, Note Technique SEMAR 98/11, Cadarache, France (August 1998).

[11] WALTER, A.E., REYNOLD, A.B., Fast Breeder Reactors, Pergamon Press (1981).

[12] SRINIVASAN, G.S., SINGH, O.P., CDA Analysis with Conservative Radial Power Density Distribution, PFBR/01117/DN/1016 (2000).

[13] FAUSKE, H.K., Core Disruptive Accidents –Nuclear Reactor Safety Heat Transfer– OWEN (Editor C. Jones) McGraw-Hill International Book Company, pp. 481-494 (1981).

[14] GOVINDARAJAN, S., SINGH, O.P., VAIDYANATHAN, G., MURALIKRISHNA, G., KASINATHAN, N., Conceptual Design of Reactor Shutdown System, Task Force Report, PFBR/31000/TF/1014 (October 1999).

[15] INTERNATIONAL ATOMIC ENERGY AGENCY, Status of Liquid Metal Cooled Fast Breeder Reactors, IAEA Technical Report No. 246, IAEA, Vienna (1985).

[16] THEOFANOUS, T.G., BELL, C.R., An Assessment of CRBR Core Disruptive Accident Energetics, Proc. Int. Topical Meeting on Fast Reactor Safety, Vol. 1, Knoxville, Tennessee, 21- 25April 1985, p. 471 (1985).

[17] HARISH, R., SATHIYASHEELA, T., SRINIVASAN, G.S., SINGH, O.P., KALDIS: A Computer Code System for Core Disruptive Accident Analysis in Fast Reactors, Internal report, IGC–208 (March 1999).

[18] CARTER, J.C., et al., SAS1A - A Computer Code for the Analysis of Fast Reactor Power and Flow Transients, ANL-7607 (1970).
[19] JACKSON, J.F., NICHOLSON, R.B., VENUS-II: A LMFBR Disassembly Program, ANL-7951 (1972).
[20] SHARADA, B., SINGH, O.P., Validation of the Computer Code, POKIN against SEFOR Experiment and Analytical Results, ROD/01117/SNAS-32 (1990).
[21] NOBLE, L.D., et al., SEFOR Core 1 Test Results to 20 MWt, GEAP-13702 (1971).
[22] SRINIVASAN, G.S., SINGH, O.P., Validation of the Computer Code, PREDIS Against FBTR Experimental Reactivity Transients, RPD/SAS/FBTR/01100 /CR/011 (1999).
[23] SINGH, O.P., HARISH, R., Results of Transient Calculations Up to Onset of Boiling of a Comparative Calculation for Unprotected Loss of Flow Accident in BN-800 Type Reactor with near zero void reactivity coefficient, paper presented in Consultancy meeting Comparative calculations for severe accident in BN-800 reactor, Obninsk, Russian Federation, 2-16 June 1998.
[24] SATHIYASHEELA, T., HARISH, R., SINGH, O.P., A Comparative Study of ULOF for BN-800 Reactor with Non-Zero Sodium Void Coefficient, RPD/SAS-101 (1998).
[25] ROYAL, P., et al., Comparative Analysis of Hypothetical LOFA in LMFBR using Different Computer Programmes for a Common Benchmark Problem, EUR 63 18E (1979).
[26] DHARMADURAI, SINGH, O.P., Validation of PREDIS Code Against European LOFA Benchmark Problem, FRG/RPS-230 (1983).
[27] NIWA, H., Results of Boiling and Post Boiling Transient Analysis of ULOF in BN-800 Like Reactor, paper presented in Consultancy Meeting on the Comparative Calculations for Severe Accidents in BN-800 Like Reactor, Obninsk, Russian Federation, 2-6 June 1998.
[28] TOBITA, Y., MORITA, K., KAWADA, K., NIWA, H., NONAKA, N., Evaluation of CDA Energetics in the Prototype LMFBR with Latest Knowledge and Tools, paper presented in 7th Int. Conf. Nuclear Engineering (ICONE-7), Tokyo, Japan, 19-23 April 1999.
[29] BROADLEY, D., et al., Safety Design of EFR and Risk Minimisation, paper presented in FR'91, Int. Conf. on Fast Reactors and Related Fuel Cycles, Kyoto, Japan (1991).
[30] ENDO, H., et al., A Study of the Initiating Phase Scenario of Unprotected Loss of Flow in a 600 MWe MOX Homogeneous Core, paper presented in IAEA Technical Committee Meeting on Material Coolant Interactions and Material Movement and Relocation in LMFRs, O-arai, Ibaraki, Japan, 6-9 June 1994.
[31] WINTERTON, R.H.S., Cover Gas Bubbles in Recirculating Sodium Primary Coolant, Nucl. Eng. Design, Vol. 22, pp. 262-271 (1972).
[32] NIWA, H., Model Development for SAS4A and Investigation on the Initiating Phase Consequences in LMFRs Related with Material Motion, paper presented in IAEA Technical Committee Meeting on Material Coolant Interactions and Material Movement and Relocation in LMFRs, O-arai, Ibaraki, Japan, 6-9 June 1994.
[33] LEWIS, E.E., Nuclear Power Reactor Safety, John Wiley & Sons (1977).
[34] PROJECT MANAGEMENT CORPORATION, CRBR Plant Preliminary Safety Analysis Report, Vol. 14 & 15 (1975).
[35] BUKSHA, YU., KUZNETSOV, I., Current Status of Investigations on Molten Fuel – Coolant Interaction, Material movement and Relocation in LMFBRs in Russia, paper presented in IAEA Technical Committee Meeting on Material-Coolant Interactions

and Material Movement Relocation in Liquid Metal Fast Reactors, O-arai, Ibaraki, Japan, 6-9 June 1994.
[36] GOURIOU, A., et al., The Dynamic Behaviour of Super Phenix Reactor under Unprotected Transients, paper presented in L.M.F.B.R. Safety Topical Meeting, Lyon, France, 19-23 July 1982.
[37] BROADLEY, D., et al., Safety Design of EFR and Risk Minimisation, paper presented in Int. Conf. on Fast Reactor and Related Fuel Cycles, Kyoto, Japan (1991).
[38] BOUCHARD, J., LEVISOLEN, C., The History of Fast Reactor Safety in France, paper presented in Int. Fast Reactor Safety Meeting, Snowbird, Utah, USA, 1990.
[39] FUKANO, Y., CHARPENEL, J., The Adventitious Pin Failure Study under a Slow Power Ramp, Proc. ICONE 12, Arlington, Virginia, 25-29 April 2004, ASME (3 Vols) ISBN: 0791846873 / 0791846881 / ISBN: 079184689X (204) (2004).
[40] YAMANO, H., ONODA, Y., TOBITA, Y., SATO, I., Interpretation of the CABRI-RAFT TPA2 Test Investigating Fuel-to-Steel Heat Transfer Characteristics, paper presented in 6th Int. Conf. Nucl. Thermal Hydraulics, Operations and Safety (NUTHOS-6), Nara, Japan, 4-8 October 2004.
[41] KONISHI, K., et al., The result of a wall failure in-pile experiment under the EAGLE project, Nuclear Engineering and Design, Vol. 237, pp. 2165-2174 (2007).
[42] KONISHI, K., et al., The EAGLE Project to Eliminate the Recriticality Issue of Fast Reactors -Progress and Results of In-Pile Tests-, paper presented in 5th Korea-Japan Symposium on Nuclear Thermal Hydraulics and Safety (NTHAS5), Jeju, Korea Republic of, 26-29 November 2006.
[43] MATSUBA, K., et al., Experimental Study on Void Development Behavior in a Simulated Coolant Channel, paper presented in 6th Int. Topical Meeting on Nuclear Reactor Thermal Hydraulics, Operation and Safety (NUTHOS-6), Nara, Japan, 4-8 October 2004.

CHAPTER 9
NATIONAL STRATEGIES, INTERNATIONAL INITIATIVES, PUBLIC ACCEPTANCE AND FINAL REMARKS

9.1. National strategies

The research and development of fast reactors and the related nuclear fuel cycles (hereafter called R&D of FRs) is advanced in many countries of the world now. This section documents the current status of R&D of FRs and the national strategies from several of the major countries conducting fast reactor programmes, including France, India, Japan, the Republic of Korea, the Russian Federation and the United States of America.

As a common feature of the reports, we can see increasing needs and expectations for R&D of FRs in last few years, although there are many differences in the current status or the national strategies resulting from differences in the history, the experience and the related national interest in R&D of FRs. As a result, the R&D of FRs seems to be gaining greater importance in the nuclear policy or the energy policy in these countries.

The most important factor driving the needs and expectations for R&D of FRs in these countries is the potential for effective use of the world's uranium resources, recognizing that the demand for nuclear power is rapidly increasing worldwide. In addition, the possibility of burning transuranics in a fast reactor in a closed fuel cycle that leads to the reduction of the long-term radiotoxicity of the high level radioactive waste is also a very important component.

The most important issues to be addressed in the programmes of R&D of FRs to realize the above mentioned needs and expectations include ensuring compliance with the nuclear non-proliferation regime, achievement of economic competitiveness and ensuring safety.

The needs and expectations and issues to be addressed cited above are common targets in the programmes of R&D of FRs, and are also very important elements for promoting the sustainable and peaceful use of nuclear power of the world. It is desirable to promote cooperation and harmonization of programmes among countries performing R&D of FRs to achieve the common targets in both technical issues and political issues of the R&D of FRs, even if the programmes of R&D of FRs are advanced under each country's national strategy. This section will be useful and helpful, not only for the researchers and the engineers but also for policymakers and every stakeholder to understand the other countries' current status and strategies of R&D of FRs and to understand the backgrounds of the concrete R&D activities treated in this status report [1].

9.1.1. National strategy of France

Current fast reactor research and technology development (R&D) activities in France are determined by two recent Acts of the French Parliament: the Law 2005-781, enacted on 13 July 2005, and the Law 2006-739, enacted on 28 June 2006. Together, these laws stipulate the energy policy guidelines (Law 2005-781) and outline the policies for sustainable management of radioactive waste (Law 2006-739), requesting R&D on innovative nuclear reactors (i.e. those referred to in Law 2005-781) to ensure that, firstly, by 2012 an assessment of the industrial prospects of these reactor types can be made, and, secondly, a prototype reactor is commissioned by 31 December 2020 (with an industrial introduction of this technology in 2040 – 2050).

The responsibility to meet the stipulations of these laws falls under the auspices of the Commissariat à l'Énergie Atomique (CEA), which is currently implementing an ambitious R&D programme organized around two main topics: the sodium-cooled fast reactor (SFR) as the reference option and the gas-cooled fast reactor (GFR) as the longer-term option. The Advanced Sodium Technological Reactor for Industrial Demonstration (ASTRID) is the industrial prototype that is foreseen to be put into operation around 2020 in view of the former option, while ALLEGRO is an experimental reactor developed at the European level to demonstrate the feasibility of a GFR in view of the latter.

9.1.1.1. The SFR R&D programme

The R&D performed in France on SFRs is done in close collaboration between the CEA and its two industrial partners, AREVA and Électricité de France (EDF). The R&D programme comprises research in four domains of innovations:

- The development of an attractive and safe core, taking into account the specificities of the fast neutrons and sodium, and also able to transmute minor actinides;
- A better resistance to severe accidents and external hazards;
- The search for an optimized energy conversion system which reduces the sodium risks;
- The re-examination of the reactor and components design to improve the conditions of operation and the economic competitiveness.

Between 2007 and 2009, the R&D programme provided very useful results and valuable status reports were issued on the following topics:

- Reactor designs of both loop and pool configuration;
- Innovative design and technology options: advanced energy conversion systems, advanced pool/loop designs;
- Fuel handling;
- Impact of reactor power level on safety and costs;
- Core and fuel;
- Safety and severe accidents;
- Status of 9Cr potential for pipes and components;
- Status of oxide dispersion strengthened steel (ODS) as cladding tube material;
- ISI&R: sensors, inspectability, reparability, robotics.

With respect to safety, emphasis is placed on the relationship with the safety authority. Interactions started in 2008, including the organization of technical seminars. For the year 2010, the main topic of exchange will be the operational feedback of Phénix, Superphénix and other reactors. Current R&D includes passive safety devices as additional lines of defence in an enhanced core.

As far as the energy conversion system is concerned, the goal is to minimize the frequency and the consequences of sodium-water reactions. R&D is conducted in two directions: an alternative fluid to sodium in the secondary circuit, or to steam as working fluid (Brayton cycle), or design improvement to drastically improve the resistance to sodium-water reactions, like modular steam generators of double-wall tubes etc. Supercritical CO_2 is seen as a long-term promising option, with issues like sodium-CO_2 interaction to be investigated further.

In-Service Inspection and Repair (ISI&R) is of great importance and an extensive R&D programme in this area is being performed.

A large refurbishment and construction programme for testing facilities to support R&D activities and ASTRID development is presently underway. Sharing of facilities in other countries is also envisaged and harmonization of prototypes on an international level is considered as well.

9.1.1.2. The ASTRID programme [2]

The ASTRID prototype is seen as an industrial prototype prior to a first-of-a-kind reactor, meaning that the extrapolation of the technical options and of the safety demonstration is of great importance. The reactor will also provide some irradiation capabilities, especially in order to validate the properties of the new fuel (which exhibits large diameter pins and ODS clad) and the ability to fission minor actinides in an industrial way. The ASTRID programme defined by the CEA also includes a facility to manufacture the fuel for the reactor, of limited capacity from 5-10 tonnes of heavy metal per year. The refurbishment of existing testing facilities and the construction of new tools is part of the programme as well.

ASTRID, will be coupled to the grid with an electrical power of about 600 MW. It will integrate operational feedback of past and current reactors. It is seen as a Generation IV prototype reactor. The level of safety will be at least as good as current Generation III reactors, with strong improvements on core and sodium-related issues. After a learning period, the reactor will have a high load factor (e.g. more than 80%). The reactor will provide the capability for demonstration of transmutation of minor actinides at larger scale than previously done in Phénix. The investment costs of the prototype will be kept to the lowest possible, with technical options compatible with later deployment on a commercial facility.

The schedule of the ASTRID prototype is to be put into operation by the 2020's. First choices need to be made in 2010 in order to launch the pre-conceptual and the conceptual designs, and to start first discussions with the safety authority. Still, some options will be kept open until 2012. A second phase of conceptual design with the submission of the safety option file in 2014 will allow the basic and detailed designs to begin in 2015

9.1.1.3. The GFR R&D programme and ALLEGRO [3]

The French R&D programme on the GFR is conducted based on the principle that GFR is a potential fast neutron system for the long-term horizon. The main features of the GFR system yield potential advantages relative to the SFR; however, the same inherent features that lead to the advantages also present challenges which make it necessary to seek innovative solutions through detailed R&D.

The work performed thus far on the GFR has led to a first consistent design of the reactor and its fuel. Although the major design directions have been fixed, other aspects of the GFR design basis are constantly evolving. Great effort has been placed on the safety analysis which, to the extent carried out so far, indicates the acceptable performance of the current design in any accident situation. Considering the progress already made on the concept as a whole, the principal R&D priority is now the fuel technology (design, fabrication, behaviour at nominal conditions and high temperature, etc) and demonstration of the viability of the reactor and technology (i.e. the ALLEGRO reactor). The next step is to update the concept viability report by 2012.

In relation to ALLEGRO, the Gas Cooled Fast Reactor Specifically Targeted Project (GCFR STREP) of the EURATOM 6th Framework Programme included the pre-conceptual

Experimental and Technology Demonstration reactor (ETDR) – the predecessor to ALLEGRO – design and safety studies. In parallel to the pre-conceptual design process, the ALLEGRO R&D plan has been launched to qualify the appropriate calculation tools and gaseous coolant technology necessary, in addition to the VHTR mainstream development. The R&D plan has now been expanded at the European level through the 7th Framework Programme ADRIANA project. Central Europe countries (Czech Republic, Slovakia and Hungary) are currently candidate to host the ALLEGRO experimental reactor

9.1.2. National strategy of India

India is the largest democracy with the current population of about 1.05 billion and is on a road to rapid economic growth. An average gross domestic product (GDP) growth rate of about 8% per year has been achieved in 2006-07 and it is targeted to touch 10% per year for the next 10 years. Towards realizing this targeted growth, development activities are planned based on a well-conceived road map and a clear vision. Like elsewhere, the energy and electricity growth in India are also closely linked to growth in the economy. Indices of socio-economic development like literacy, longevity, GDP and human development are directly dependent upon the per capita energy consumption of a country. India aims to reach at least a per capita energy consumption equal to the present world average (2200 kWh/a) by 2030 from the current value of (660 kWh/a) as indicated in Fig. 9.1.

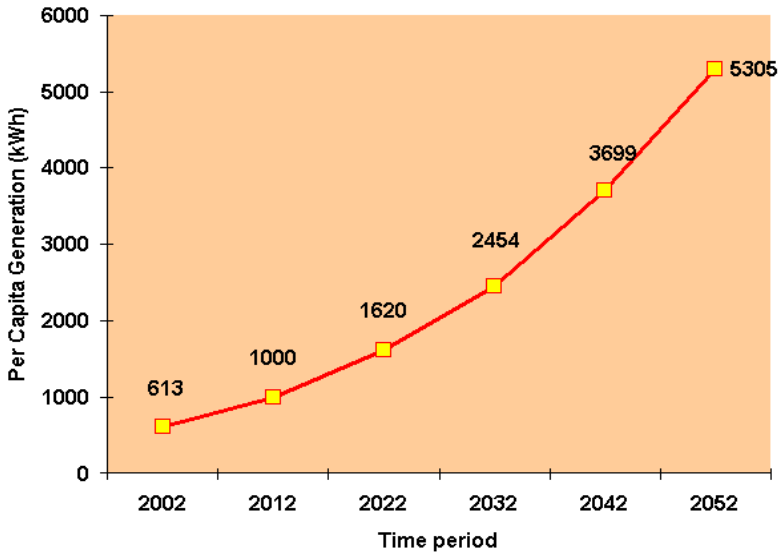

FIG. 9.1. Energy growth scenario in India.

The current installed capacity of ~ 138 GWe needs to be increased to about 600 GWe by 2030 assuming the population of about 1.4 billion.

Energy strategists in the country have realized the importance of a judicious mix of energy resources to meet this challenge. e of nuclear energy is an inevitable choice in this judicious energy mix from resources, sustainability and environment considerations. The nuclear share is expected to contribute about 63 GWe by 2030, which will be steadily increased to 275 GWe by 2052, against the total projected capacity of 1344 GWe. India ranks high in nuclear technology scale with strong R&D, high quality human resources, sound infrastructure,

unwavering government support and performance based public acceptance. In terms of providing clean, viable and sustainable energy and effective utilization of available nuclear resources, the development of fast breeder reactor (FBR) with a closed fuel cycle is theinevitable option for India. India has limited uranium and abundant thorium resources (Fig. 9.2).

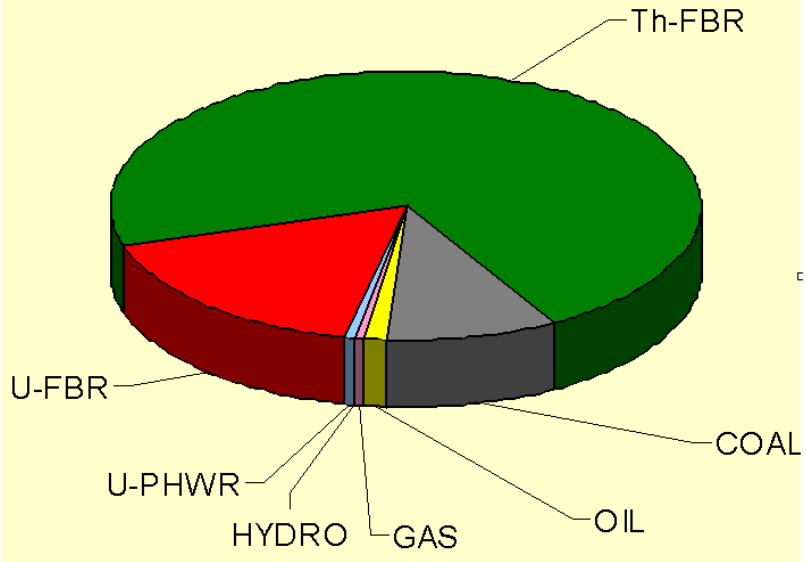

FIG. 9.2. Resource position in India.

The uranium resources reasonably assured plus inferred in India are 84 600 t. (<2% of world resource). However, the thorium resource in the country is 225 000 t (second largest reserve in the world), which has an energy potential 155 000 GWe-y. The uranium resource available in the country can feed 10 GWe capacity of pressurized heavy water reactors (PHWRs) for ~ 50 years with a thermal efficiency of 30%. Since FBRs can extract about 70 times more thermal energy from the same quantity of uranium and generate electricity with higher thermal efficiency (40%), the available uranium can also feed 275 GWe for about 200 years, when used in FBR after reprocessing. Thorium can feed 275 GWe capacity power plants for about 550 years.

Taking cognizance of India's nuclear resource profile, Dr. Homi Bhabha formulated a 'Three Stage Nuclear Power Programme' for achieving energy independence. The first stage of this programme ,which comprised setting up PHWRs, is now in the industrial domain. At present, 15 PHWRs and 2 Boiling Water Reactors (BWRs) are in operation and 3 PHWRs and 2 light water reactors (VVER type) are under construction. The second stage of India's nuclear power programme envisages setting up FBRs, backed up by reprocessing plants and plutonium based fuel fabrication plants. The third stage envisages exploiting the vast resources of thorium through the route of fast or thermal critical reactors and/or the accelerator driven sub-critical reactors (ADS). An Advanced Heavy Water Reactor (AHWR) designed to draw about two-thirds of its power from thorium fuel is under regulatory examination and will improve experience in all aspects of technologies related to the thorium fuel cycle. The third stage began with the commissioning of the 30 kWt thorium based ^{233}U fuelled research reactor, KAMINI at Kalpakkam. Enhancement of the PHWR programme through advanced uranium exploration, import of natural uranium for PHWRs, import of water reactors from outside under safeguards are the current plan of the department. Also planned, is the establishment of mega nuclear parks with co-located fuel cycle facilities.

The seed for fast reactor programme in India was sown through the establishment of a research centre (then called Reactor Research Centre) in 1971, dedicated to the research and development of fast reactor science and technology and the construction of the Fast Breeder Test Reactor (FBTR) at Kalpakkam. The FBTR is a sodium-cooled loop-type 40°MWt/13.2 MWe experimental fast reactor and was commissioned in 1985 with a unique plutonium rich carbide fuel as the driver fuel. Operating experience of the FBTR has thus far been positive and the reactor life is to be extended by 20 years to serve as an irradiation facility for the development of future fuels and in-core materials.

The experience gained in the construction, commissioning and operation of the FBTR, and comprehensive research and technology development programmes in collaboration with a large number of academic, research and industrial organizations have provided the necessary confidence to launch a Prototype Fast Breeder Reactor (PFBR) of 500 MWe capacity and fuelled by uranium-plutonium mixed oxide. The reactor construction was started in 2003 and the reactor is anticipated to be commissioned in 2010. The indigenous manufacture of the critical, large size components of the PFBR to close tolerances has given a high level of confidence to meet the requirements. The design of the reactor has incorporated the worldwide operating experience from the FBRs and has addressed all the safety issues reported in literature, besides introducing a number of innovative features.

Simultaneous with the construction of the reactor, the fuel cycle of the reactor has been addressed in a comprehensive manner and construction of a collocated fuel cycle facility has been initiated. As a follow-up to PFBR, it is planned to construct two twin units of 500 MWe reactors, with improved economy and safety during 2013-20. Various elements of reactor design are being carefully analysed with the aim of introducing innovative features towards further reduction in unit energy cost and enhancing safety in these reactors. Clear strategies have been identified to simplify the design without sacrificing safety, reduce construction time, enhance the burn-up and close the fuel cycle with minimum cooling and out-of-pile inventory. It is targeted to bring down the unit energy cost by ~ 25% and increase the mixed oxide fuel burnup to 20 at% using advanced structural materials for clad and wrapper.

All energy resources need to be exploited and achieving a judicious mix is both a challenge and opportunity. In terms of providing clean, viable and sustainable energy and effective utilization of available nuclear resources, the development of a fast breeder reactor with a closed fuel cycle is the inevitable option for India. The energy security is ensured through indigenous FBRs in the immediate horizon. A systematic road map has been conceived towards gradual introduction of FBRs to generate about 2.5 GWe by 2020. Metallic fuel is planned to be introduced through 1000 MWe units beyond 2020. FBRs will be an inevitable option, at least up to 2050.

9.1.3. National strategy of Japan

In the 20th century, developed countries benefited from science and technology which made rapid progress. Meanwhile problems such as waste of resources, environmental destruction, etc. became apparent. In the 21st century, a remarkable increase in energy demand is foreseen especially in developing countries, so energy and environment problems will get worse on a global scale. Therefore, the necessity of sustainable development is recognized in the world. Because there are few energy resources in Japan, development of technology which saves resources, emits little greenhouse gas and reduces an environmental burden is indispensable. Fast reactor cycle technology has been selected as one of technologies appropriate for such requirements in Japan, and has been developed to utilize its attractive potential of energy

supply, transuranic (TRU) burning, and so on. Fast reactor cycle technology needs to possess enough economic advantage while ensuring safety and taking account of nuclear non-proliferation issues to deploy commercial facilities in the context of electric utility deregulation. Moreover, it is important that fast reactor cycle technology has flexible performance to meet society needs in the future.

In Japan, the research and development (R&D) project on fast reactor cycle technology named "Feasibility Study on Commercialized Fast Reactor Cycle Systems (F/S)" was carried out from Japanese Fiscal Year (JFY) 1999 to 2005 by a Japanese joint project team of Japan Atomic Energy Agency (JAEA) and the Japan Atomic Power Company (JAPC). This project aimed at elucidating prominent fast reactor cycle systems that would respond to various needs of society in the future. The phase-I was implemented in the period from JFY1999 to 2000 and the phase-II from JFY2001 to 2005. Five development targets were established at the beginning stage, namely safety, economic competitiveness, reduction of environmental burden, efficient utilization of nuclear fuel resources, and enhancement of nuclear non-proliferation. Fast reactor concepts and fuel cycle concepts that adopted innovative technologies were investigated to satisfy the development targets. As the result of phase-II, the combination of the sodium-cooled fast reactor with oxide fuel, advanced aqueous reprocessing and simplified pelletizing fuel fabrication was selected as the most promising concept of the fast reactor cycle system, and a R&D plan for this concept until JFY2015 was proposed.

Recently, the significance of development of fast reactor cycle technology has been recognized once again in Japan. The Japan Atomic Energy Commission (AEC) issued the "Framework of Nuclear Energy Policy" in October 2005. The framework is the foundation of Japanese policy on research, development and utilization of nuclear energy. As for the target on development of fast reactor cycle technology, full-scale deployment in about 2050 is described. In March 2006, the Council for Science and Technology Policy (CSTP) of the Cabinet Office selected fast reactor cycle technology as one of key technologies of national importance in the third-term "Science and Technology Basic Plan". This means that fast reactor cycle technology was recognized as an essential technology to be invested intensively in a large-scale national project during the period of the basic plan. After this, the Ministry of Education, Culture, Sports, Science and Technology (MEXT) and the Ministry of Economy, Trade and Industry (METI) investigated action plans for development of nuclear technologies, respectively, to implement the "Framework of Nuclear Energy Policy" and published their reports in July and August 2006. These documents state a start-up of a demonstration fast reactor by 2025 and deployment of a commercial fast reactor cycle before 2050. Following the action plans, the council which consisted of METI, MEXT, electric utilities, manufacturers and JAEA was set up to discuss subjects aiming at smooth transition from a R&D stage to demonstration and deployment stages and to have good understanding together.

Following publication of the F/S phase-II result, MEXT reviewed the result by October 2006 and issued a report titled "Research and Development Policy on Fast Reactor Cycle Technology" in November 2006. As a result, the above-mentioned concept was confirmed as the main concept that should be developed toward its commercialization, and key development issues necessary for commercialization were defined. Moreover, AEC decided on the "Basic Policy on Research and Development of Fast Reactor Cycle Technologies over the Next Decade" in response to the review report on the result of F/S phase-II and the action plans of MEXT and METI in December 2006. Based on the conclusion of the F/S and the check and review by the government, a Fast Reactor Cycle Technology Development (FaCT) Project was launched as an advanced stage toward commercialization of fast reactor cycle technology.

Names of Documents on Japanese Policy

Framework of Nuclear Energy Policy (AEC)

Authorized by a Cabinet meeting on October 14, 2005

- The Japanese Government should promote the basic research to survey technological options that allow flexible responses in future to social conditions in the promotion of the nuclear fuel cycle activities. The Japanese Government should appropriately evaluate new knowledge and technical concepts developed at this stage and determine whether to designate them as activity targets for developing an innovative technological system.
- It is necessary to promote R&D toward commercialization of FR cycle technology from its potential of long-term energy security and reduction in radio-toxicity of radioactive waste.
- The operation of Monju should be resumed at the earliest possible time, and the priority should be placed on achieving the initial goals of demonstrating reliability as an operational power plant and establishment sodium handling technology within ten years or so. After that, Monju is expected to be utilized as a location for R&D activities toward commercialization of FR and its fuel cycle technology.
- The Japanese Government will evaluate the results of the F/S phase-II study and then present the subsequent R&D policy.
- Development of FR cycle aims at its commercial introduction at around 2050.

The third-term "Science and Technology Basic Plan" (CSTP)

Authorized by a Cabinet meeting on March 28, 2006

- FR cycle technology was selected as one of the key technologies of national importance.

Promotion Plan for Research and Development on Nuclear Energy (MEXT)

Committee Report issued on July 28, 2006

- Action plan to materialize the "Framework of Nuclear Energy Policy".
- A council was set up to investigate demonstration processes of fast reactor cycle technology by MEXT, METI, JAEA, the electric utilities and plant vendors.
- Development of a demonstration FR aims at its introduction by around 2025.
- Development of FR cycle aims at its commercial introduction before 2050.

Nuclear Energy National Plan (METI)

Committee Report issued on August 8, 2006

- Action plan to materialize the "Framework of Nuclear Energy Policy".
- A council was set up to investigate demonstration processes of fast reactor cycle technology by MEXT, METI, JAEA, the electric utilities and plant vendors.
- Development of a demonstration FR aims at its introduction by around 2025.
- Development of FR cycle aims at its commercial introduction before 2050.

Research and Development Policy on Fast Reactor Cycle Technology (MEXT)

MEXT Decision on November 2, 2006

- R&D policy based on the review of F/S phase-II results.
- Combined system of sodium-cooled, MOX-fuelled FR, advanced aqueous reprocessing and simplified pelletizing fuel fabrication was selected as the main concept for prioritization of future development.
- Innovative R&D subjects have been identified.
- R&Ds for FR cycle technology should be accelerated toward commercialization of the main concept.
- The conceptual designs of commercial and demonstration fast reactor cycle facilities will be presented by 2015 with development plan to realize them.
- All the innovative technologies are planned to be developed for reflecting their R&D results in the conceptual designs by 2015.
- A demonstration FR will start in operation in around 2025.
- A commercial FR will start in operation in around 2045.

Basic Policy on Research and Development of FBR Cycle Technologies over the Next Decade (AEC)

AEC Decision on December 26, 2006

- MEXT, METI and JAEA shall promote R&D regarding the main concept with electricity utilities, manufacturers and universities as a "Fast Reactor Cycle Technology Development Project", and present the conceptual designs of commercial and demonstration fast reactor cycle facilities with R&D programs to realize them in 2015.
- The JAEA shall resume operations of the prototype fast breeder reactor Monju in 2008 on the precondition of safety while promoting mutual understanding with local residents on the safety. The JAEA shall achieve its initial goals of demonstrating reliability as a power plant and establishing sodium handling technologies. Then, Monju shall be utilized for R&D activities toward commercialization of fast reactor technology.
- The Government and R&D organizations shall also promote the exploration and the proof of principle activities of innovative concepts for realizing alternative fast reactor cycle technologies as well as wide-ranging basic and fundamental R&D activities.
- MEXT, METI, JAEA, electricity utilities and manufacturers shall develop and continuously revise a roadmap to commercialization of fast reactor cycle technology in order to make it possible to promote effective and efficient R&D activities over a long time and facilitate smooth transition to the stage of demonstration. The roadmap shall specify requirements for demonstration facilities and activities in demonstration and commercialization stages including a plan for construction of demonstration facilities, as well as respective roles of all the parties concerned in each phase.

9.1.4. National strategy of the Republic of Korea

Nuclear power plants are playing very important roles in achieving energy self-reliance and in stabilizing the price of electricity in the Republic of Korea, because nuclear energy is less dependent on natural resources and more technology-intensive. Since the first commercial nuclear power plant Kori Unit 1 started its operation in 1978, there are now sixteen PWRs and four PHWRs in operation as of December 2008. In 2008, nuclear power plants claimed 24.4% of the total installed capacity, and generated as much as 35.6% of the total electricity demand.

According to “The Fourth Basic Plan for Long-term Electricity Supply and Demand” of December 2008, currently four OPR1000s (two at Kori and two at Wolsong) and two APR1400s at Kori are under construction, and an additional six APR1400s will be constructed by 2022 [4]. According to the “Basic Plan for National Energy” of August 2008, the nuclear share will be 41.0% of the total installed capacity and 59.0% of total electricity generation in 2030.

With the continuous operation of the nuclear power plants, the on-site spent fuel storage limit is expected to be reached from 2016. Therefore a decision making process for spent fuel management is under way.

In 2004, the Korea Atomic Energy Commission (KAEC) decided to construct a low and intermediate-level radioactive waste (LILW) repository separately from an interim spent fuel storage site, and to examine the spent fuel management plan under public consensus by considering national policy direction and the progress of technology development. In 2006, the government announced the Gyeongju site as the centralized LILW repository [5], construction started in 2007 and will be completed in 2010.

For the safe management of radioactive wastes including spent fuel, the National Assembly passed the Radioactive Waste Management (RWM) law on 26 February 2008. According to this law the Korea Radioactive-waste Management Corporation (KRMC) was established in January 2009, and RWM funds were managed under the administration of the KRMC.

It has been recognized that one of the most promising nuclear options for electricity generation is a fast reactor system which efficiently utilizes uranium resources and reduces radioactive wastes from nuclear power plants, thus contributes to a sustainable development. In response to this recognition, the widespread concern about the management of spent fuels caused the Republic of Korea to develop technologies for sodium-cooled fast reactors (SFRs) as one of the most promising future types of reactors in the country.

The PWR-SFR transition scenario study shows that SFRs can substantiate domestic waste management claims in the Republic of Korea [6]. A timely deployment of SFRs with recycle of transuranics (TRUs) from PWR spent fuels into SFRs can alleviate the potential limits to a domestic nuclear energy growth. This development is associated with the availability of uranium and the need to reduce nuclear waste disposal mainly constituted of PWR spent fuel. The SFR mix ratio in the nuclear fleet near the year 2100 is estimated to be approximately 35-40%. PWRs will remain as the main power reactor type until 2100, and SFRs will support the waste minimization and fuel utilization efforts.

The commencement of SFR technology development efforts in the Republic of Korea dates back to 1992 and basic research had been performed until 1996. The conceptual design of KALIMER-150 had been developed from 1997 to 2001. The conceptual design of KALIMER-600 [7] was developed from 2002 to 2006. KAERI is now developing a conceptual design of an advanced SFR under the third national mid- and long-term nuclear R&D program, a 5-year program launched in 2007.

The KALIMER-600 design serves as a starting point for developing an advanced design. This new design will adopt advanced design concepts and features with the potential to meet the Generation IV (Gen IV) technology goals of sustainability, safety and reliability, economics, proliferation resistance and physical protection. A conceptual design of the advanced SFR will be developed by 2011.

In order to provide a consistent direction to long-term R&D activities, the KAEC approved a long-term development plan for future nuclear reactor systems which include SFR, pyroprocess and VHTR on December 22, 2008. This long-term plan will be implemented through nuclear R&D programs of the National Research Foundation (NRF) with funds from the Ministry of Education Science and Technology (MEST), and a detailed implementation plan is now being developed.

The long-term SFR development plan approved by the KAEC will be carried out with the long-term vision of the construction of a SFR demonstration plant by 2028 in association with the pyroprocess technology development in three phases: (1) First Phase (2007 – 2011) - Development of an advanced SFR design concept, (2) Second Phase (2012 – 2017) - Standard design of a SFR demonstration plant, and (3) Third phase (2018 – 2028) - Construction of a SFR demonstration plant.

R&D efforts are being made for the conceptual design of the advanced SFR with emphasis on the development of the advanced SFR technologies necessary for the enhancement of safety and economic competitiveness. These R&D activities include the developments of a Passive Decay Heat Removal Circuit (PDRC) system, a supercritical carbon dioxide (S-CO_2) Brayton cycle system, an under-sodium viewing technique and a metal fuel. In addition, basic technologies are being developed, mainly focusing on validating computational tools and developing sodium technologies.

9.1.5. National strategy of the Russian Federation

9.1.5.1. Current status

At present there are two facilities with sodium cooled fast reactors in operation in the Russian Federation:

- Experimental reactor BOR-60 (SSC RF RIAR, Dimitrovgrad); its first criticality was in December 1968;
- Commercial power unit No. 3 of Beloyarsk NPP with reactor BN-600, put into operation in 1980 (BNPP, Zarechny).

Research reactor BR-10 (SSC RF-IPPE, Obninsk) is in the stage of preparation for its decommissioning after successful operation during ~44 years (1959-2002).

A large experience is gained as result of operation of these facilities and also the NPP with BN-350 reactor which belongs now to Kazakhstan and was shutdown in 1999. This experience has confirmed feasibility of sodium cooled fast reactors and has provided substantiation and implementation of this reactor technology in industrial scale.

The initial design lifetime of BOR-60 reactor facility was equal to 20 years, but its successful operation resulted in lifetime extensions, first to the end of 2009 and later to the end of 2014. Now the BOR-60 reactor is a main experimental base for implementation of reactor researches aimed at improvement of SFR technology.

The NPP with the BN-600 reactor that is now the largest power unit in the world with a FR has successfully operated during more than 30 years. It demonstrates high economical parameters including high load factor (average load factor during commercial operation of the BN-600 power unit from 1983 till 2007 is equal to 74.2%). The design lifetime of the BN-600

reactor plant expires in 2010; however, recently, lifetime extension works have been successfully completed and the reactor is now licensed to operate to the end of 2020.

The No. 4 power unit of the Beloyarsk NPP with sodium cooled fast reactor BN-800 (Zarechny) is under construction. Its initial operation is scheduled in 2012.

R&D is being carried out on prospective fast reactors with various coolants: sodium coolant (development of the conceptual design of large-size commercial fast reactor BN-1800, implementation of conceptual studies on a small-size modular-transportable two-circuit NPP with sodium cooled fast reactor and gas turbine - called the concept of the BN GT nuclear co-generation power plant); heavy liquid metal coolants (lead-bismuth - development of design of the SVBR-75/100 reactor facility, lead – implementation of R&D on justification of design of an NPP with a BREST-OD-300 reactor); gas coolant (conceptual researches on a two-circuit NPP with a helium cooled BGR-1000 reactor).

9.1.5.2. Tendencies and prospects of fast reactor development

NPPs with thermal reactors are the basis of nuclear power of the Russian Federation and such situation will be kept in the near future (up to 2040-2050). A significant increase in the share of nuclear power in total electricity production is expected (up to 25-30% of total electricity production to 2025-50 against 17% in 2006).

However, in the long-term future it is scheduled that fast reactors with closed nuclear fuel cycle (CNFC) and mixed uranium-plutonium fuel will be the basis of future nuclear power of Russia [8]. Implementation of a closed fuel cycle with reprocessing of spent nuclear fuel of both thermal and fast reactors will provide a solution to 1) the task of supplying fuel for nuclear power for the foreseeable time period and 2) the problem of radwaste including minor actinides.

The long-term technological policy provides for gradual insertion of nuclear power technology based on fast reactors with CNFC. Sodium cooled fast reactors are the single mastered fast reactor technology so SFR are considered to be the most likely and possible candidate for large-scale nuclear power in the future. At the first stage it is planned to fulfill the closed fuel cycle with use of BN-800 reactor. In this context the BN-800 reactor is considered as a pilot reactor that should play a key role in mastering basic elements and technologies of prospective CNFC of fast reactors and demonstration of practical implementation of the concept of the fast reactor in CNFC. It is supposed to reach this target by 2018-2020. At this stage the problem of recycling minor actinides should also be solved. It is necessary to note that in parallel with closing the fuel cycle on the basis of BN-800 reactor, development and mastering the technology of SFR decommissioning is also conducted. After resolution of these problems, it will be possible to say that complete complex mastering of the technology of nuclear power on the base of SFR in CNFC has been achieved.

The next stages are scheduled as follows:

- Construction of a demonstration large-size commercial SFR by 2018–2020, which should demonstrate competitiveness of sodium cooled fast reactors;
- Development on the basis of a demonstration facility and construction of a small series of large-size commercial SFRs by 2030;
- A large-scale introduction of serial SFRs in nuclear power by 2040–2050.

As probable alternative FR options, fast reactors with different types of coolant can be considered taking into account the necessity to implement the appropriate R&D and design studies.

On the whole, the scheduled scenario of FR development in Russia testifies to preservation of continuity and sequence in this area.

9.1.6. National strategy of the United States of America

9.1.6.1. Timeline of US fast reactor development

A fast reactor that would 'breed' plutonium and significantly extend the use of the earth's supply of uranium for electricity generation was described by Enrico Fermi in 1944. It remained a dream until after WW II. The peaceful uses of nuclear energy were then pursued with vigor in the USA, particularly at Argonne National Laboratory (ANL).

ANL work on fast reactors in the immediate post-war years culminated in the building and operation of the Experimental Breeder Reactor by 1951. It fired public imagination by generating electricity and confirmed the principle of breeding. Despite meltdown of its second core in 1955—which had no serious consequences but which demonstrated how fuel-pin bowing can cause reactivity insertion—work to understand fast neutron physics and the control of fast reactors continued with enthusiasm.

An industrial partnership in the mid 1950s gave birth to the design of a large-size fast reactor to be built near Monroe, Michigan, as the EFFBR. At about the same time work on a successor to EBR, the EBR-II, was begun by ANL. EFFBR would be an industrial prototype and EBR-II would demonstrate a closed fuel cycle for uranium; both reactors would use sodium instead of NaK and both would generate electricity. 'Wet' criticality was achieved at the two reactors in 1963.

The EBR-II operated safely and successfully throughout the 1960s and demonstrated fuel cycle closure by 1969; it then became a fuels and materials irradiation facility. But a fuel melting incident occurred at the EFFBR in 1966. Identifying and removing two damaged assemblies, finding and retrieving the object which had caused flow blockage, and preparing for reactor restart, took an agonizing 4 years. Although the EFFBR reached full power in 1970 and operated for a while without problems, it was permanently shut down in 1973 for financial reasons.

The mid 1960s saw reaffirmation of the need for fast reactors, and, as a consequence, the need for a new high-flux irradiation facility to test advanced fuels and commercial-size components. Thus the concept of the FFTF was born. It would use mixed-oxide fuel, the fuel of choice in France and the United Kingdom. After a lengthy design, construction and safety approval process, the FFTF achieved both wet criticality and full power in 1980. From 1982 onwards it was the facility for steady-state testing of LMR fuels and materials. The EBR-II complemented the FFTF in studying the off-normal behavior of fuels, while plant safety tests were performed at both reactors.

The FFTF and EBR-II operated almost flawlessly through the 1980s and into the 1990s, with only minor maintenance problems. US programmatic interest and support in fast reactors waned in 1992 and FFTF was instructed to shut down in 1993, and EBR-II in 1994, ending useful lives of 10 and 30 years, respectively.

Table 9.1 shows the major parameters of these four US LMRs.

TABLE 9.1. OPERATING US FAST REACTORS (1951–1994)

	EBR	EFFBR	EBR-II	FFTF
General information				
Wet criticality	1951	1963	1963	1980
Full power	1951	1970	1965	1980
Final shutdown	1963	1972	1994	1992
Thermal power, MW	1.2	200	62.5	400
Electrical power, MW	0.2	65	20	--
Core characteristics				
Height, m	0.22	0.77	0.36	0.91
Diameter, m	0.18	0.82	0.51	1.21
Volume, L	5.9	400	73	1040
Power density, kW/L	170	774	1002	730
Enrichment zones	1	1	1	2
Peak flux, $10^{15}/cm^2.s$	0.11	4.5	2.5	7.2
β effective	0.0068	0.007	0.01	0.0032
Doppler constant	NA	NA	0.0068	0.005
Core fuel				
Fuel type	U/Pu alloys	U-Mo	U-Fs/U-Zr	UO_2-PuO_2
Fuel form	Slug	Slug	Slug	Pellet
Fuel-clad bond	NaK, metallurgical	Metallurgical	Sodium	Helium
Clad type	SS, Zircalloy	Zircalloy	SS	SS
Clad thickness, mm	0.50	0.13	0.23/0.30	0.38
Pin diameter, mm	~10.0	4.01	4.4	5.8
Pins/assembly	None/31,60	120	91/61	217
#Assemblies	None/7	102	127/77	76
Radial blanket /reflector				
Fuel type	Nat. U	Nat. U-Mo	Dep. U	Inconel
Fuel form	Slug	Slug	Slug	Block
Rod diameter, mm	23.8	11.2		
Rods/assembly	138/--	25	6/19	
#Assemblies	--	537	162/366	199
Control rods				
Fuel type	U	B_4C	U + B_4C	B_4C
#Rods	12	10	10	9
Heat transfer				
Coolant	NaK/NaK	Na/Na	Na/Na	Na/Na
#Primary loops	1	3	1	3
Pump type	Electromagnetic	Centrifugal	Centrifugal	Centrifugal
Total flow, kg/s	36	1120	480	2200
Inlet temperature, °C	230	279	371	360
Outlet temperature, °C	322	418	473	503
#Secondary loops	1	3	1	3
Pump type	Electromagnetic	Electromagnetic	Centrifugal	Centrifugal
Total flow, kg/s		1120	302	2200
#Steam generators	1	8	3	None

9.1.6.2. The Advanced Fuel Cycle Initiative

The USA "will build the Advanced Fuel Cycle Initiative (AFCI) to work with other nations to develop and deploy advanced nuclear recycling and reactor technologies. This initiative will help provide reliable, emission-free energy with less of the waste burden of older technologies and without making available separated plutonium that could be used by rogue states or terrorists for nuclear weapons. These new technologies will make possible a dramatic expansion of safe, clean nuclear energy to help meet the growing global energy demand." AFCI seeks to bring about a significant, wide-scale use of nuclear energy, and to take actions now that will allow that vision to be achieved while decreasing the risk of nuclear weapons proliferation and effectively addressing the challenge of nuclear waste disposal. AFCI will advance the nonproliferation and national security interests of the United States by reinforcing its nonproliferation policies and reducing the spread of enrichment and reprocessing technologies, and eventually eliminating excess civilian plutonium stocks that have accumulated.

To enable the expansion of nuclear energy for peaceful purposes and make a major contribution to global development into the 21st century, the USA seeks to pursue and accelerate cooperation to:

- Expand nuclear power to help meet growing energy demand in an environmentally sustainable manner;
- Develop, demonstrate, and deploy advanced technologies for recycling spent nuclear fuel that do not separate plutonium, with the goal over time of ceasing separation of plutonium and eventually eliminating excess stocks of civilian plutonium and drawing down existing stocks of civilian spent fuel. Such advanced fuel cycle technologies would substantially reduce nuclear waste, simplify its disposition, and help to ensure the need for only one geologic repository in the United States through the end of this century;
- Develop, demonstrate, and deploy advanced reactors that consume transuranic elements from recycled spent fuel. Develop, demonstrate, and deploy advanced, proliferation resistant nuclear power reactors appropriate for the power grids of developing countries and regions;
- Establish supply arrangements among nations to provide reliable fuel services worldwide for generating nuclear energy, by providing nuclear fuel and taking back spent fuel for recycling, without spreading enrichment and reprocessing technologies;
- In cooperation with the IAEA, develop enhanced nuclear safeguards to effectively and efficiently monitor nuclear materials and facilities, to ensure commercial nuclear energy systems are used only for peaceful purposes.

The need for nuclear energy to play a major role in meeting base load electrical energy requirements is now recognized by most of the world's industrialized nations. Similarly, in the United States there is growing recognition of the need to start building new nuclear power plants as soon as possible and to rebuild our national nuclear infrastructure — needs supported by both the Energy Policy Act of 2005 and DOE's Nuclear Power 2010 program.

There are three facilities required to implement and thus affirm US commitment to AFCI:

(1) A nuclear fuel recycling center to separate the components of spent fuel required by AFCI;
(2) An advanced recycling reactor to burn the actinide based fuel to transform the actinides in a way that makes them easier to store as waste and produces electricity;
(3) An advanced fuel cycle research facility to serve as an R&D center of excellence for developing transmutation fuels and improving fuel cycle technology.

The pursuit of these three facilities constitutes a pathway with two complementary components. The first component, the nuclear fuel recycling center and the advanced recycling reactor, would be led by industry with technology support from laboratories, international partners, and universities. The second component, research and development led by the national laboratories, would include the advanced fuel cycle research facility funded by the Department and located at a government site. The two components would work closely together to move AFCI forward by integrating the national laboratories' capabilities with the needs of industry.

Sodium-cooled fast reactors suitable for adaptation as advanced recycling reactors already exist and there are proven separations processes. But there is a great deal of new technology that is needed to fully implement AFCI, and much of that technology can and must be developed at our national laboratories and universities in cooperation with similar international institutions.

However, to effectively bring AFCI into the commercial application we need to engage industry now. Through submittal of Expressions of Interest, industry has indicated not only its support for AFCI, but a potential willingness to invest very substantial sums of private money to build and operate AFCI fuel cycle facilities. At this early point, it should be recognized that potential industry participants have expressed interest, but certainly have made no commitments or fully explained what strings they might wish to attach to their participation. Nonetheless, an AFCI goal is to develop and implement fuel cycle facilities in a way that will not require a large amount of government construction and operating funding to sustain it. However, AFCI will also require a significant federal investment in supporting R&D and incentives to ensure that the long-term goals are sustainable. In sum, it is proposed to proceed in parallel to:

(1) Build and operate nuclear fuel recycling center and advanced recycling reactor facilities using the latest commercial technology available after final designs are validated; and
(2) Continue an aggressive R&D programme to complete development of advanced spent fuel separations techniques and transmutation fuel fabrication and recycle technologies and develop validated simulation and computation techniques to advance the development and approval of fuel cycle technology.

The parallel activities will have strong cross-connections with industry requested technical information provided by R&D according to the technology roadmap.

A nuclear fuel recycling center would be designed to incorporate the advanced separations and fuel fabrication modules, with construction scale paced by success in the R&D validating these modules and the prospect for use of separated product as fuel in fast reactors. The output of a nuclear fuel recycling center would be fuel including transuranics for fast spectrum reactors. It would not produce MOX for Light Water Reactors. Once the nuclear fuel recycling center is approved to accept spent fuel, shipments of fuel could begin from utilities, which would be a significant step in providing confidence in the country's ability to meet its nuclear waste management responsibilities.

A prototypical advanced recycling reactor would aim to reduce capital and operating costs in order to economically produce electricity while consuming plutonium and other transuranics. R&D would continue on technology for recycling used transmutation fuel for further burning an advanced recycling reactor, with one goal being to minimize the risk that such facilities would be abused to produce pure plutonium.

It is reasonable to expect that in the decade or more that design, approval and construction of these "base technology" facilities would take place, allowing the successful proof and incorporation of the vital actinide separations steps and development and qualification of a minor actinide bearing fast reactor fuel. Even if the advanced R&D effort was not fully successful or is delayed, proven advancements will still have been made over facilities in operation elsewhere in the world and could make a policy judgment at that time how best to proceed. The current focus is on making the integrated AFCI system work.

The advantage of the parallel approach is that the US could save nearly a decade in time and a substantial amount of money, while still engaging and reinvigorating the nuclear community with new facilities and continued long-term R&D. Development by the US of a credible program for construction of commercial fuel cycle facilities is a critical element of a strategy to convince any other nation considering beginning a nuclear energy programme that they can rely on the US for any of their fuel cycle needs. Making the USA a player in fuel cycle technology is vital to fulfilling the AFCI vision.

9.2. International initiatives

9.2.1. European Sustainable Nuclear Industrial Initiative (ESNII)

The European Sustainable Nuclear Industrial Initiative (ESNII) is exists as one of the European Industrial Initiatives (EIIs) supported established by the Sustainable Nuclear Energy Technology Platform (SNETP) in order to attain the goals set forth by Europe's in the frame of the European Union's Strategic Energy Technology (SET) Plan [10]. The EIIs are industry-led programmes which serve to enhance research and development and to accelerate the deployment of low carbon CO2-free energy the technologies on which they focus. In the case of the ESNII, the initiative addresses the need to demonstrate and accelerate the time-to-market of Generation IV fast neutron reactor technologies in tandem with the supporting research infrastructures, fuel cycle facilities and R&D necessities. The strategy and priorities of the ESNII are aligned with those of Sustainable Nuclear Energy Technology Platform (SNETP) in order to meet Europe's long-term energy needs in the areas of security of supply, safety, sustainability and economic competitiveness [19]. As outlined in the Strategic Research Agenda (SRA) of SNETP [11], it is proposed to develop two fast reactor technologies in parallel, namely:

- Te sodium-cooled fast reactor as the reference solution, with the construction of a prototype around 2020 in France;
- A alternative (lead- or gas-cooled) fast reactor, with the construction of an experimental reactor to demonstrate the technology in another European country willing to host the plant programme.

The initiative encompasses three principal areas:

(1) *Design, construction and operation of demonstration/prototype facilities* for each of the three (sodium-, lead- and gas-cooled) fast reactor technologies (respectively referred to as the ESNII-1, ESNII-2 and ESNII-3 components) in order to demonstrate that fast reactors:
   - Are able to exploit the full energy potential of uranium by extracting up to 100 times more energy than current technology from the same quantity of uranium;
   - Have the ability to transmute the minor actinides produced in the fuel during reactor operation by recycling them in fresh fuel, and in so doing significantly

reduce quantities, heat production and (by factors of up to 1000) hazardous lifetime of the ultimate waste for disposal;

- Attain safety levels at least equivalent to the highest levels attainable with Generation II and Generation III reactors;
- Eliminate proliferation risks by avoiding separation of weapons grade fissile material at any point during the fuel cycle;
- Can attain levelized electricity and heat production costs on par with other low carbon energy systems.

(2) *Refurbishment and/or design, construction and operation of support infrastructures* necessary to support the design and/or operation of prototype and demonstration fast reactors (known as the ESNII-4 component), in particular:

- Fuel fabrication facilities to develop and manufacture driver fuel and minor actinide bearing fuels for the prototype and demonstration fast reactors;
- Facilities for the development of materials and components, code validation and qualification, and design and validation of safety systems.

(3) *Comprehensive research and development programmes* to support all aspects of the design, construction and operation of the prototype and demonstration fast reactors, as well as the support infrastructure. Cross-cutting R&D will also benefit current reactors in terms of maintaining safety and radiation protection, increasing performance and competitiveness, ensuring lifetime management, and implementing solutions for waste management.

The ESNII components can be further elaborated upon as follows:

ESNII-1 the sodium-cooled fast reactor (SFR)

The objectives of ESNII-1 are to design, construct and operate an innovative demonstration sodium-cooled fast reactor that is coupled to the grid. The role of the reactor will be fulfilled by the ASTRID prototype. The programme includes the investigation of innovative paths leading to a significant progress on sodium-cooled fast reactors technology in the main areas in need of improvements, including: safety, economic competitiveness, ability to meet the operator's needs and capability to recycle and transmute all actinides extracted from spent nuclear fuel. These features will be demonstrated through the acquired operating experience of the reactor.

The work programme consists of:

- *ESNII-1.1 Innovation* through the investigation of innovative paths to allow significant progress in domains such as safety, economy, in-service inspection and actinides incineration through close collaboration among R&D organizations, industry, utilities and safety authorities. The programme, which uses the past R&D, engineering, construction, operating and licensing experience of former European sodium-cooled fast reactors as a basis, includes investigations and developments in the following main technical tracks:
  (i) Core and fuel: core design which reduces or exludes the risks of energetic accidents; non-swelling claddings to decrease the sodium content in the core and to increase the fuel burnup potential; strengthened lines of defence against core fusion risks; efficient use of depleted or reprocessed uranium and recycling of minor actinides.

(ii) Safety: reliable detection of sodium leaks and mitigation of the consequences of sodium fires; advanced sodium-water reaction detection and secondary loop designs; mitigation provisions and simulation methods for defence-in-depth situations.

(iii) Reactor and systems design: adapted reactor design and under-sodium telemetry or nondestructive examination techniques to enable efficient and practical in-service inspection campaigns; advanced steam generators to improve the global efficiency of the plant; efficient fuel and components handling systems to improve the overall availability; advanced instrumentation and control systems adapted to the challenges of sodium-cooled fast reactors.

— *ESNII-1.2 Prototype conception, licensing and construction*, the realization of which includes the tasks of: pre-conceptual design, conceptual design and safety options report, basic design and preliminary safety analysis report, detailed design and final safety analysis report, construction and commissioning and start-up. The R&D activities will be continued in parallel with the dual purpose of validation of the innovative concepts and recovery of industrial competencies. Particular emphasis is placed on:
  (i) Primary system components;
  (ii) Steam generators;
  (iii) Fuel handling and absorber mechanisms;
  (iv) Subassemblies;
  (v) Instrumentation and in-service inspection;
  (vi) Safety innovations;
  (vii) Cladding material.

— *ESNII-1.3 Prototype operation and experimental programme* which will include:
  (i) Demonstration of the consistency with industrial objectives;
  (ii) Irradiations programme focused on innovative cladding materials, innovative non-proliferating fuel fabrication processes, actinides recycling solutions and performances.

ESNII-2 the lead-cooled fast reactor (LFR)

The objectives of ESNII-2 are to design, construct and operate an innovative lead-cooled fast demonstrator reactor. This system should equal the sodium-cooled reference technology in terms of safety, economic competitiveness, uranium utilization and reduction of waste. It will be realized through first finalizing the design of, obtaining a license for the construction of, and putting into operation the European Technology Pilot Plant (ETPP), in this case the MYRRHA experimental device. Subsequently, the design will be finalized and a license for construction will be obtained for the demonstration reactor, which will be connected to the grid with an electrical power of about 100 MW. The results obtained through the operational feedback of the demonstration reactor will ultimately lead to the design and construction of a prototype lead-cooled fast reactor of about 600 MW_e, which will in turn contribute to the industrial deployment of a lead-cooled fast reactor by 2050. Aspects and objectives of the work programme include:

— *ESNII 2.1 Support R&D programme*, consisting of:
  (i) Materials qualification;
  (ii) Fuel development and qualification;
  (iii) Heavy liquid metal technology masterization;
  (iv) Components development;
  (v) Development of models and tools;

(vi) Conducting large scale integral tests;
(vii) Starting the zero power facility Guinevere in 2010.

— *ESNII 2.2 LFR ETPP conception, licensing and construction*, carried out in parallel with the support R&D programme. The MYRRHA project will fulfil the role of the LFR ETPP.

— *ESNII 2.3 LFR ETPP experimental programme*, to demonstrate fuel and heavy liquid metals technologies, and the endurance of materials, in service inspection and repair, components and systems.

— *ESNII 2.4 LFR demonstrator conception, licensing and construction*, consisting of the conceptual design, final design decisions, detailed engineering, specifications drafting and tendering, construction of components and civil engineering, on site assembly and commissioning. In parallel, the feedback from design and experience from the LFR ETPP will serve to optimize the final design of the LFR demonstrator called ALFRED.

— *ESNII 2.5 LFR demonstrator operation and feedback from experience*, to demonstrate the correct operability of all heat transport systems with connection to the grid. The demonstration reactor is a scaled down version of the (industrial) prototype, with similar characteristics. Specifically, the objectives of the LFR demonstrator are to:
(i) Achieve the safety standards required at the time of deployment and to enhance non-proliferation resistance;
(ii) Assess economical competitiveness of LFR technology, including high load factor;
(iii) Demonstrate better use of resources by closing the fuel cycle;
(iv) Validate materials selection.

ESNII-3 the gas-cooled fast reactor (GFR)

The objectives of ESNII-3 are to design, construct and operate an innovative gas-cooled fast demonstrator reactor. This fast neutron system should offer an alternative solution to the liquid metal-cooled fast reactors through the use of an inert and transparent coolant, with uranium utilization and reduction of waste comparable to the sodium-cooled reference technology. The programme involves the investigation of fuel, materials, components and the reactor design, ultimately leading to a safe and economic reactor technology. Additionally, improvements to the safety demonstration are studied, in particular by reducing the risk of severe accidents, and taking benefit from simpler in-service inspection and repair and coolant management. The innovative technologies will be implemented through the development, licensing and operation in a European country of a demonstration scale prototype, in this case the ALLEGRO reactor. The demonstration reactor will test high temperature heat delivery and utilization for industrial purposes, as well as demonstrate safety and waste minimization performance through operational feedback, ultimately leading to the design and construction of a GFR prototype which will be coupled to the grid. The work programme includes:

— *ESNII-3.1 Support R&D programme*, namely:
(i) Fuel development, specifically: fuel element and assemblies modelling and design; clad and fuel material studies; core material studies; development of clad and fuel fabrication processes; fuel element and assembly development and irradiation testing; analysis of behaviour during fault conditions.
(ii) Development and qualification of analysis tools comprising five principal areas: (1) core thermal-hydraulics; (2) core neutronics; (3) systems operation; (4) fuel performance; and (5) others (materials performance, structural assessment, codes and standards, etc.).

(iii) Helium technology and components development, including: the management of gas impurities; the development and qualification of heat insulation techniques; the construction and qualification of main specific components; the development of advanced instrumentation techniques in hot gas.

— *ESNII-3.2 ALLEGRO: A GFR demonstrator*

(i) ALLEGRO design studies, of which the main goal is to design the ALLEGRO reactor consistent with the GFR choices and to include specific devices and monitoring systems for experimental purposes; the work is divided into three areas:
- Review of the exploratory and pre-conceptual studies;
- Core studies;
- Mission and design consistency monitoring.

(ii) ALLEGRO safety studies, which is essentially the same as for GFR but is dedicated to the ALLEGRO specific case and has thus a tighter schedule. The work makes use of the ALLEGRO safety options report as input.

— *ESNII 3.3 Future GFR plant prospects*

(i) GFR design studies aimed at defining a consistent, high-performance gas-cooled fast reactor which:
- Has, at a minimum, a self-sustaining core in terms of the consumption and production of plutonium and should be capable of plutonium and minor actinide multi-recycling;
- Has an adequate power density to meet requirements in terms of plutonium inventory and breeding gain, economics and safety;
- Permits coupling between the reactor and process heat applications.

(ii) GFR safety studies necessary to establish a safety case for GFR and based upon the definition of a relevant safety approach; it consists of the following main tasks:
- Recommending and evaluating specific safety systems and requirements for fuel and material behaviour to manage accident conditions;
- Analyzing accident transients to establish both the natural, unprotected, behaviour of the system, and to demonstrate that adequate protection systems are available;
- Implementing a core melt exclusion strategy;
- Conducting a probabilistic risk assessment for the system.

ESNII-4 the support infrastructures

The objectives of ESNII-4 are to design, construct (or upgrade, if appropriate) and operate the necessary devices and facilities that are essential to the successful deployment of a demonstration fast neutron reactor, whether it is sodium-, lead- or gas-cooled, as defined in the framework of the ESNII. This includes: irradiation tools and devices to test materials and fuels; fuel fabrication workshops dedicated to uranium-plutonium driver fuels and minor actinide bearing fuels; and experimental facilities for component design, system development, code qualification and validation.

The R&D work programme comprises:

— *ESNII-4.1 Research and testing facilities*

(i) Update the existing set of European irradiation facilities; three reactors are currently under consideration: the Jules Horowitz Reactor under construction at

CEA-(Cadarache, (France), MYRRHA (Mol, Belgium) and PALLAS (Petten, Netherlands).

(ii) Development of new irradiation devices for experiments, which take into account cutting edge progresses in modelling, instrumentation and modern safety standards.

(iii) Establishment of experimental facilities for reactor physics which will enable components design, system development and code qualification and validation, which are mandatory to sustain the safety analysis.

(iv) Establishment of experimental facilities for civil, structural and safety case support work, as defined by each technology.

— *ESNII-4.2 Fuel manufacturing capacities*

(i) Establishment of an industrial-scale facility to produce the MOX driver fuel to be loaded in the core of the prototype and demonstration reactors.

(ii) Establishment of a pin-scale facility to produce experimental pins to be irradiated in experimental facilities during the early phases of the design of possible future fuels.

Figure 9.3 shows the timeframe associated with the ESNII-1, ESNII-2 and ESNII-3 components.

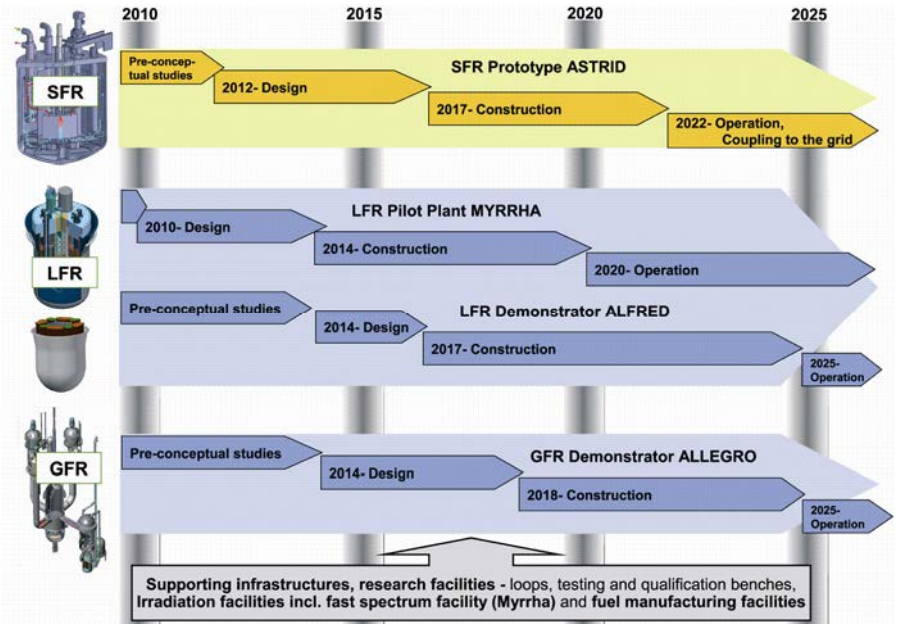

FIG. 9.3. ESNII roadmap (figure courtesy of SNETP).

9.2.2. Generation IV International Forum (GIF)

Created in 2000, GIF is a cooperative international endeavour organized to develop the research necessary to test the feasibility and performance capabilities of fourth generation (Generation IV) nuclear systems with the goal of making such systems deployable in large numbers by 2030, or earlier. The goals of fourth generation nuclear plants are to improve:

(1) Sustainability (including effective fuel utilization and minimization of waste);
(2) Economics (competitiveness with respect to other energy sources);
(3) Safety and reliability (e.g. no need for offsite emergency response);
(4) Proliferation resistance and physical protection.

There are six generic systems for further R&D:

(1) Gas-cooled Fast Reactor (GFR);
(2) Lead-cooled Fast Reactor (LFR);
(3) Molten Salt Reactor (MSR);
(4) Sodium-cooled Fast Reactor (SFR);
(5) Super-Critical Water Reactor (SCWR);
(6) Very High Temperature Reactor (VHTR).

9.2.2.1. GIF SFR design requirements

The broad design requirements for the SFR systems, shown in Table 9.2, are established in order to satisfy the development targets corresponding to the Generation IV goals.

TABLE 9.2. MAJOR BROAD DESIGN REQUIREMENTS FOR SFR SYSTEM

SFR Design requirements		Generation IV goals	
Actinide management TRU transmutation Radioactive release	Breeding ratio: 0.5-1.3* TRU transmutation under fast reactor multi-recycle and long-term storage of LWR spent fuel Equivalent to or less than present LWRs	Sustainability	(1) Resource utilization (1.0-1.3) (2) Waste minimization and management
PR&PP	Excludes pure plutonium state throughout system flow	Proliferation resistance and physical protection	Minimize diversion or undeclared production; reactors have passive features that resist sabotage
Safety	Operability, maintainability and repairability	Safety and reliability	(1) Operations will excel in safety and reliability (2) Very low likelihood and degree of reactor core damage (3) Eliminate the need for offsite emergency response
Electricity generation cost Operation cycle Construction duration	Cost-competitiveness with other means of electricity production and a variety of market conditions, including highly competitive deregulated or reformed markets ** 18 months, and more As a goal, large-scale: 42 months, medium-scale modular type: 36 months	Economics	(1) Life-cycle cost advantage over other energy sources (Low overnight construction cost, Low production cost) (2) Level of financial risk comparable to other energy project

* Conversion ratio of 0.5-1.0 might be taken to pursue Sustainability-2: waste minimization and management.

** Bus-bar cost will be evaluated using the methods specified by the Generation IV Economic Methodology Working Group; some expected targets for a First-of-a-kind (FOAK) plant are ~ 4¢/kWh and Construction cost: ~ 2 000 $/kWe. For a future Nth-of-a-kind plant, the cost target is to be competitive with advanced LWR system costs evaluated with a similar technique.

Three major options are considered: a large size (600 to 1 500 MWe) loop-type reactor with mixed uranium-plutonium oxide fuel, supported by a fuel cycle based upon advanced aqueous processing at a central location, serving a number of reactors as shown in Fig. 9.4a; an intermediate-to-large size (300 to 1 500 MWe) pool-type reactor as shown in Fig. 9.4b; and a

small size (50 to 150 MWe) modular-type reactor with uranium-plutonium-minor-actinide-zirconium metal alloy fuel, supported by a fuel cycle based on pyrometallurgical processing in facilities integrated with the reactor. The outlet temperature is 500-550°C for all three options.

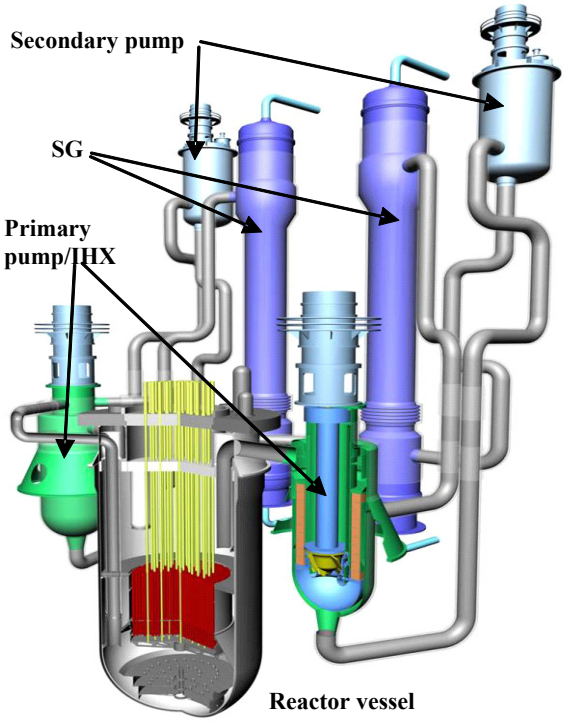

FIG. 9.4a. Loop-configuration SFR.

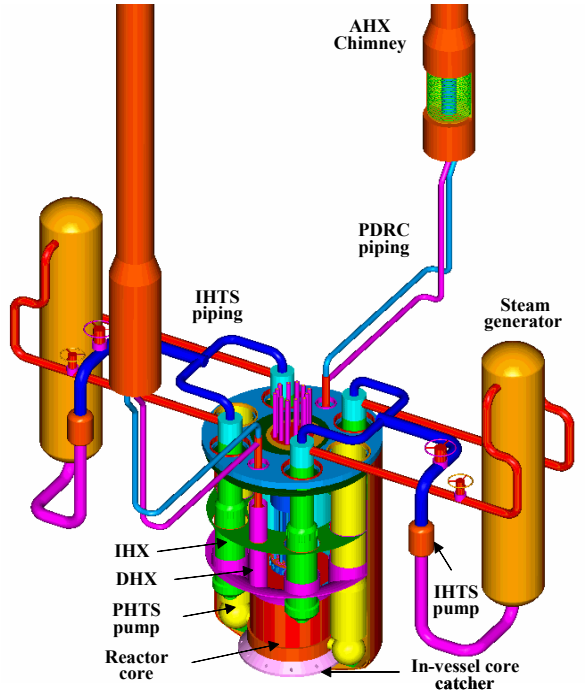

FIG. 9.4b. Pool-configuration SFR.

Table 9.3 gives an overview of the design parameters of Generation IV SFR.

TABLE 9.3. DESIGN PARAMETERS OF GENERATION IV SFR CONCEPTS

SFR Design parameters	Loop	Pool	Small modular
Power rating, MWe	1500	600	50
Thermal power, MWth	3570	1525	125
Plant efficiency, %	42	42	~ 38
Core outlet coolant temperature, °C	550	545	~ 510
Core inlet coolant temperature, °C	395	370	~ 355
Main steam temperature, °C	503	495	480
Main steam pressure, MPa	16.7	16.5	20
Cycle length, years	1.5-2.2	1.5	30
Fuel reload batch, batches	4	4	1
Core diameter, m	5.1	3.5	1.75
Core height, m	1.0	0.8	1.0
Fuel type	MOX (TRU bearing)	Metal (U-TRU-10%Zr Alloy)	Metal (U-TRU-10%Zr Alloy)
Cladding material	ODS	HT9M	HT9
Pu enrichment (Pu/HM), %	13.8	14.3	15.0
Burnup, GWd/t	150	79	~ 87
Breeding ratio	1.0-1.2	1.0	1.0

9.2.2.2. GIF SFR R&D

The SFR development approach builds on technologies already used for SFRs that have successfully been built and operated in France, Germany, Japan, the Russian Federation, the United Kingdom and the United States. As a benefit of these previous investments in technology, the majority of the R&D needs for the SFR are related to performance rather than viability of the system. Based on international SFR R&D plans, the research activities within GIF have been arranged into five projects.

9.2.2.2.1. System Integration and Assessment (SIA) Project

The main objectives of system integration and assessment are: to maintain and refine system options, reflecting continuous trade-off studies and technology development; to recognize R&D needs and assure that the work scopes of the PMBs are based on these needs; to apply the GIF assessment methodologies to various concepts; and to integrate and assess the R&D results from the other projects.

9.2.2.2.2. Safety and Operation (SO) project

In the field of safety, experiments and analytical model development are planned to address both passive safety and severe accident issues. Options of safety system architectures will be investigated also. The research on operation covers reactor operation and technology testing campaigns in existing SFRs (e.g. Monju and Phénix, including its end-of-life tests).

9.2.2.2.3. Advanced Fuel (AF) project

Fuel-related research aims at developing high burn-up MA bearing fuels as well as claddings and wrappers capable of withstanding high neutron doses and temperatures. It includes: research on remote fuel fabrication techniques for fuels that contain MA and possibly traces of fission products as well as performance under irradiation of fuels, claddings and wrappers. Candidates under consideration are: oxide, metal, nitride and carbide (since 2008) for fuels; and Ferritic/Martensitic & Oxide-Dispersion Strengthened (ODS) steels for core materials.

9.2.2.2.4. Component Design and Balance-Of-Plant (CDBOP) project

Research on component design and balance-of-plant covers experimental and analytical evaluation of advanced in-service inspection and repair technologies including leak-before-break assessment, and development of alternative energy conversion systems. The Brayton cycle, e.g., if shown to be viable, would reduce the cost of electricity generation significantly as compared with the Rankine steam cycle, owing to its compactness. In addition, the significance of the experience that has been gained from SFR operation and upgrading is recognized.

9.2.2.2.5. Global Actinide Cycle International Demonstration (GACID) project

The project of Global Actinide Cycle International Demonstration aims at demonstrating that the SFR can effectively manage all actinide elements — including uranium, plutonium, and minor actinides (MAs: neptunium, americium and curium) — by transmutation. The project includes fabrication and licensing of MA-bearing fuel, pin-scale irradiations, material property data preparation, irradiation behavior modeling and post-irradiation examination, as well as transportation of MA raw materials and MA-bearing fuels. Bundle-scale demonstration will be included. This technical demonstration will be pursued using existing fast reactors in a reasonable time frame.

9.2.3. International Project on Innovative Nuclear Reactors and Fuel Cycles (INPRO)

INPRO is a global forum for cooperation on innovative Nuclear Energy Systems and innovative deployment strategies. International studies and collaborative projects are mechanisms for meeting INPRO's objective of fostering innovation and sustainable nuclear energy development. To this end, INPRO has developed, with contributions from 300 international experts, an evaluation method — the INPRO methodology — that can be used to assess [in seven assessment areas, *viz*. economics, infrastructure (institutional arrangements), waste management, proliferation resistance, physical protection, environment (impact of stressors and resource depletion), and safety of reactors and nuclear fuel cycle facilities] whether or not a given nuclear energy system will contribute to meeting a country's energy needs in a sustainable manner, or if it requires follow-up actions including R&D studies to achieve sustainability [12].

The INPRO methodology was used to evaluate a number of Nuclear Energy Systems, including a joint assessment of a nuclear energy system based on a closed fuel cycle with fast reactors [13]. This activity resulted in the initiation of further collaborative projects that are relevant to fast reactors.

While INPRO considers all nuclear energy technologies (both reactor and fuel cycle systems), there are several Collaborative Projects relevant to fast reactor systems are being implemented under its framework

9.2.3.1. *Assessment of Nuclear Energy Systems Based on a Closed Nuclear Fuel Cycle with Fast Reactors (CNFC–FR)*

The objectives of this assessment were to assess an innovative nuclear energy system (INS) based on a closed nuclear fuel cycle with fast reactors (CNFC-FR) to meet the criteria of sustainability, determine milestones for the INS deployment, and to establish frameworks for, and areas of, collaborative R&D work.

The assessment was implemented in several steps. First, experts analysed the country/region/world data, discussed national and global scenarios for introducing the INS CNFC–FR, identified technologies suitable for the INS, and broadly defined a common INS CNFC–FR. In the second step, the study examined the characteristics of the INS CNFC–FR for compliance with INPRO criteria. It was agreed to use as a reference system a near term INS CNFC–FR based on proven technologies, such as sodium coolant, MOX pellet fuel and aqueous reprocessing technology. The main results and findings of the study concerning the multidimensional assessment of the reviewed INS are summarized as follows:

- Although the safety characteristics of near term INS CNFCFRs comply with INPRO requirements, further study is required to achieve a lower level of risk of severe accidents.
- In some countries, the introduction of fast reactors contributes to an efficient use of nuclear fuel resources by increasing the use of plutonium fuels and denaturated uranium fuel, to be generated in the fast reactor blankets, if needed.
- The INS CNFC–FR has the potential to meet all of today's requirements of waste management. By developing and introducing novel technologies for an optimal management of nuclear fissile products and minor actinides, the INS CNFC–FR would have the potential for a 'breakthrough' in meeting sustainability requirements related to waste management.
- Due to the intrinsic, i.e. technological features of the INS CNFC–FR, its proliferation resistance could be comparable to, or higher than, that of a once-through fuel cycle (OTFC).
- A CNFC–FR requires a regional or multilateral approach to front and back end fuel cycle services and the transition to a global nuclear architecture.
- The design of currently operating nuclear energy systems with CNFC–FRs will not meet economic requirements. The Joint Study showed that simplifying the design, increasing the fuel burnup and reducing costs by R&D, along with small series constructions, would make the costs of nuclear power plants with fast reactors comparable to those of thermal reactor and fossil fuelled power plants.

Based on this assessment and other INPRO activities, several studies and collaborative projects were initiated as described next.

9.2.3.2. *Global Architecture of Innovative Nuclear Systems based on Thermal and Fast Reactors including Closed Fuel Cycles (GAINS)*

The objectives of this collaborative project are to develop a standard framework — including a methodological platform, assumptions and boundary conditions — for assessing future nuclear energy systems taking into account sustainable development, and to validate the results through sample analyses. The scope of the project includes:

- Estimating, as a basis for modelling work, nuclear energy needs during the 21st century at the global and regional levels (non-geographical);

- Establishing, and analysing using existing modelling tools, a representative set of nuclear energy systems, taking into account the dynamic interactions between the different elements of the fuel cycle and evolution of the technologies;
- Evaluating analytical tools to address these two objectives in the near future, and ranking the potential needs of development.

The following elements illustrate the approach followed to implement this collaborative project:

- Two nuclear energy demand scenarios are considered (high and moderate) to the end of the 21st century considering both electric and non-electric demand.
- Nuclear technological development is defined in terms of a "heterogeneous" grouping of countries (i.e., different countries move differently in terms of technical development). While more complex, a heterogeneous model is more realistic than a 'homogeneous' model which assumes that the whole world moves technically as one homogeneous group. In the heterogeneous model, countries can be grouped either geographically or, preferably, and as done in GAINS, in 'non-geographical' groups (NG) of countries. The NG groups have similar fuel cycle approaches, especially for back end strategies. This makes modelling more complex, but also more detailed and realistic. A special procedure was developed in cooperation with IAEA experts on energy planning and economics to estimate global nuclear power demand profiles in non-geographical groups.
- The non-geographical groups are defined as follows:
  (b) NG1: Countries which are most involved in the development and deployment of the INS and, consequently, would be able to incorporate them as soon as commercially available.
  (c) NG2: Countries with significant experience in the use of nuclear energy and have most of the necessary infrastructure, but which are not ready to incorporate the most advanced nuclear energy systems.
  (d) NG3: Newcomer countries.
- Analysis of the technical possibilities — 'supply scenarios' — for meeting the nuclear energy needs defined in the two selected demand scenarios, including material flows for different fuel cycles and nuclear technologies, and the transition from the current fleet of nuclear reactors to future possible fleets. Considerations and assumptions used in the technical modelling include:
  - Reactor types and fuel cycle installations and their expected time for introduction.
  - A set of indicators on sustainability in the areas of economics, infrastructure, waste management, proliferation resistance, physical protection, environment and safety.
  - The main technical parameters characterizing all the reactor types and fuel cycle installations (e.g. initial load, reload, discharge, and full core discharge at retirement).
  - A preliminary set of the nuclear energy systems to be modelled and calculated.
- The simulations and analysis are performed using different fuel cycle modelling codes available to the participants.

This Collaborative Project is ongoing but the results to-date have demonstrated the importance of using the more realistic heterogeneous modelling approach to gain insight into the synergies between current and future technologies. In addition, this approach highlighted the importance of striking an appropriate balance between national efforts and multilateral cooperation.

9.2.3.3. *FINITE (Fuel Cycles for Innovative Nuclear Energy Systems based on Integrated Technologies)*

This Collaborative Project focuses on feasibility analyses of advanced and innovative nuclear fuel cycle options for the Closed Nuclear Fuel cycle option, and the assessment of the sustainability of the corresponding Nuclear Energy Systems. The INPRO Methodology will be the reference framework for the assessment. Special emphasis is provided to reprocessing technologies and fuel manufacturing for reactor types having the potential for deployment in the 21st century. The objectives of the CP include to:

- Develop a standard framework (methodological platform, assumptions and boundary conditions) for the assessment;
- Carry out assessment studies on the sustainability of selected options using the INPRO methodology;
- Provide an overview of feasible technical alternatives on closed nuclear fuel cycle technologies useful to decision makers, identifying key areas of innovation and improvement;
- Enhance the INPRO methodology for its application to these cases; and
- Identify potential R&D areas for international cooperation on closed nuclear fuel cycle.

Specific tasks in the development of the CP include to:

- Adopt nuclear energy demand scenarios for the 21st C in the countries considered;
- Describe the national strategies to be assessed, including deployment considerations (such as collocated, centralized and/or multinational facilities), and to identify nuclear materials flow;
- Model and to analyse such national strategies by using existing computational tools and agreed matrix of parameters;
- Assess the results by using the INPRO methodology, including recommendations for its enhancement; and
- Identify key innovations and recommendations for further international cooperation.

The conclusions from this CP will be considered as an essential element in the preparation of the INPRO Global Vision report on sustainable development of nuclear energy in the present century.

9.2.3.4. *COOL (Investigation of Technological Challenges related to the Removal of Heat by Liquid Metal and Molten Salt Coolants from Reactor Cores Operating at High Temperatures)*

Next generation reactors, to be used for hydrogen production and other applications, will need to incorporate innovative approaches to further enhance their reliability and safety for large scale deployment in different regions of the world. An important feature of these reactors will be the use of coolants at temperatures that are much higher than those in current generation reactors. This involves addressing a wide range of issues concerning the design and safety of these reactors.

The INPRO Collaborative Project on COOL investigates the technological challenges of cooling reactor cores that operate at temperatures of up to 1000°C in advanced FRs, high temperature reactors and accelerator driven systems by using liquid metals and molten salts as coolants.

9.2.3.5. DHR (Decay Heat Removal System for Liquid Metal Cooled Reactors)

Decay heat removal (DHR) after reactor shutdown of a fast reactor is one of the most important safety functions which must be accomplished with a very high degree of reliability. For a typical pool or loop type sodium cooled FR, one DHR system design is based on the heat transferred to the atmospheric air, as an ultimate heat sink from the reactor pool system via an intermediate loop having sodium as coolant.

This Collaborative Project investigates multidimensional thermohydraulic phenomena in the primary sodium circuit of an FR with a core under natural convection conditions, and specifically the performance of the safety grade DHR system when the secondary loop has lost its heat removal function. It addresses methodologies for analysing pool hydraulics and heat transfer in sodium–sodium and sodium–air heat exchangers, taking into consideration thermohydraulic effects of the elements of the core contributing to heat production and removal.

The data used in the analyses were provided by India and correspond to a 1250 MW(th), 500 MW(e), pool type fast breeder reactor which consists of a primary sodium circuit, two secondary sodium circuits and a steam water circuit. The primary sodium circuit includes the core, control plug, hot pool, cold pool, two primary sodium pumps, four intermediate heat exchangers (IHX), DHR system, etc.

The DHR system has four redundant and totally independent circuits capable of removing decay heat from the hot pool through natural convection in the primary and intermediate sodium sides as well as in the air side (stack). Each circuit consists of a sodium– sodium heat exchanger (DHX) and a sodium–air heat exchanger (AHX) connected by an intermediate sodium circuit. A tall air stack provides the driving force for the natural convection air flow through the AHX, when the dampers are opened.

9.2.3.6. PGAP (Performance Assessment of Passive Gaseous Provisions)

Innovative reactors are expected to increase the use of passive systems to enhance safety. The lack of operating experience and data covering relevant phenomena over a wide range of operating conditions may cause challenges to the designers of such systems. This is particularly true of a certain class of passive systems that involve a moving fluid under natural circulation. In these systems, the driving forces and uncertainties associated with important parameters that affect natural circulation raise questions regarding their performance and reliability. Several methodologies have been developed to assess the performance and reliability of such systems. These methodologies have different features and employ different definitions for reliability.

The objective of the INPRO Collaborative Project on PGAP is to contribute to an international consensus in two areas: (i) a unified definition of the reliability of a passive system that involves natural circulation and (ii) a unified methodology to assess this reliability. This new methodology will be based on existing methodologies developed in Europe, i.e. reliability methods for passive systems, and in India, i.e. assessment of passive systems reliability, and will use the results of a benchmark exercise that models decay heat removal transients for the Commissariat à l'Energie Atomique (CEA) gas cooled fast reactor design.

The above are examples of INPRO collaborative projects that are relevant to fast reactors. As these projects progress and as more assessments are carried out using the INPRO

methodology, it is anticipated that more projects will be initiated for different types of reactors and their associated fuel cycles and fuel cycle facilities.

9.3. Public acceptance of fast reactors

Along with ensuring operational safety, public acceptance is an indispensable factor for advancing nuclear energy. Securing public acceptance in this context means increasing the number of people who are interested in, familiar with, and understand nuclear energy and the related activities. This goal is to be achieved through information outreach, communication with the public and adequate consideration given to the opinions and concerns of the public. If successful, the outcome would then be increasing the public confidence in and support for nuclear energy and the related activities.

Since the beginning of the peaceful use of nuclear power, the people engaged in the related activities worldwide have made continuous efforts for ensuring long term nuclear safety. These accumulated efforts in the field of nuclear safety are mostly related to the technology of thermal reactors, on which the current utilization of nuclear energy is based. These efforts have resulted, in some cases, in a fair amount of public confidence in and support for the current nuclear power technology based on thermal reactors. However, the effective use of uranium resources and the need for volume and radio-toxicity reduction of the ultimate radioactive waste have triggered renewed interest in the fast reactor technology. In this context, one must be aware of the inherent difference that seems to exist in public perception and acceptance of the fast reactor research and technology development activities, as compared to the thermal reactor ones.

People are relatively familiar with thermal reactor technology because of decades-long experience and the public awareness of the role of these reactors in electricity generation. Public perception of research and technology development activities in the area of fast reactors seems to be more negative, perhaps due to difficulties in fully grasping, on the one hand side, the particular role of this technology with regard to sustainable energy production, and, on the other side, the questions linked to the safety of sodium technology and the risks associated with plutonium utilization from the view points of non-proliferation and toxicity.

The Japanese Fast Breeder Prototype Reactor Monju offers a good example for these difficulties. After the 1995 secondary sodium leakage accident at Monju, public confidence and support were seriously compromised by the inadequate handling of accident communication with the public. In spite of the sustained efforts over the last 14 years, which were devoted to recover the public confidence and support especially from population in the local area around the Monju reactor site, Monju was not allowed to restart and a 2008 opinion poll in Japan showed that only 5.8% of the public has manifested interest in Monju, a fast breeder reactor development, against 23.8% who have interest in nuclear power development in general. This example points out the difficulties encountered when trying to raise the public's awareness in and interest for specific fast reactor research and technology development topics.

This section compiles valuable status reports from Belgium, France, India, Japan, the Russian Federation, and the United States of America. These contributions share the country specific information about public acceptance issues in relation to fast reactor research and technology development activities. The reports do highlight the common recognition of the importance of public acceptance in order to continue fast reactor research and technology development activities, differences in the perception of the public and the experiences with activities

aiming at improving public acceptance. These differences might be due to the difference between the various national fast reactor development policies and program histories; the difference in the extent the public recognizes the needs for nuclear power, and by other factors.

On the other hand, the individual status reports show that practical activities, experiences and basic data such as current status of public acceptance focussing on the specific field such as research and technology development of fast reactors has been low in the past in each of the countries.

If we recognize the existence of difficulties, the lack of experience and basic data in the past, and the differences in member countries' current efforts related to the public acceptance for fast reactor related research and technology development activities as compared with those for thermal reactors, it then becomes meaningful to share each other's information, experience and activities as a first step towards finding a better way to successfully implement public acceptance activities.

It is expected that IAEA's Technical Working Group on Fast Reactors (TWG-FR) will continue and deepen this kind of activity with interested Member States to find better ways, in the future, of enhancing public acceptance in the field of fast reactor research and technology development.

9.3.1. Public acceptance of nuclear energy technology in Belgium

9.3.1.1. Introduction

Public acceptance of nuclear energy technology is now regarded as an essential element for any energy policy that envisages the use of nuclear power as a part of the energy mix. Nevertheless, there seems to be no clear idea, in the nuclear community or in the national governments of countries with nuclear programs, of how public acceptance should be achieved.

While the broader spectrum of engaged stakeholders of civil society are more or less aware of the variety of existing nuclear technology options (water or gas-cooled or fast reactors, open or closed fuel cycle) and of the consequent implications with regard to safety, waste and proliferation risk, it can be said that the awareness and knowledge about these technologies that the public at large has, is either limited or non-existent. With this in mind, the following reflections can be interpreted in the framework of public acceptance of nuclear power in general, or specifically in the context of Fast Reactor Technology (FRT).

Due to recent emphasis on the efficient use of resources and responsible waste management, recent nuclear policy developments have revealed a special attention to the role of FRT for the mid- to long-term future. Due to the special character of the FRT fuel cycle management and the possible consequences in the context of proliferation, it can be said that FRT policy brings along with it a special responsibility towards society. Therefore, it is as useful to start a reflection on the societal justification of future nuclear technology with the case of FRT as it is to dwell on the

aspects of public acceptance of nuclear power in general in the context of a report on fast reactors. This text[2] argues that until today, most communication efforts initiated through nuclear energy policies have mainly been strategic and not sufficiently 'deliberative'. Communication with civil society and the public at large is still seen as a next step after completion of the technology assessment exercise internally. The result is that the nuclear community tends to step outside seeking acceptance for a product, instead of engaging civil society in a justification process.

9.3.1.2. From strategic communication to joint justification

The use of nuclear technology brings along with it, a variety of well-known societal implications. In addition to the rational supportive arguments such as the stability and reliability of the fuel market for nuclear power, the low carbon dioxide burden of the nuclear fuel cycle and the competitive price of nuclear electricity in base load production, there remain the issues of reactor safety, the need to manage and dispose of radioactive waste in a responsible way and the proliferation risk. Despite the fact that nuclear technology has reached a certain operational maturity, and although significant technical improvements have been made relating to the above mentioned issues, the technology is still associated with risk and uncertainty and consequentially it's usage remains, what philosophers tend to call, a 'complex problem'. We should keep in mind here that, in this philosophical context, 'problem' is understood in the sense of 'question' or 'challenge' (similar to a mathematical problem) instead of as something to get rid of as soon as possible. In this way, we understand that, in the context of energy policy, not only nuclear, but also fossil fuels and renewables can be characterised as complex problems.

The aspects of a complex problem can be characterised in the following way:

- Uncertainty: aspects of inherent uncertainty with regard to the causality-risk relation;
- Multidimensionality: in space (local, global); in time (intra-generational, inter-generational);
- Interconnection: there is no single issue, but a related web of issues;
- Incompatibility: different points of view are possible, inspired by different scientific disciplines (economy, sociology etc.);
- Pluralism of values: lack of generally accepted standards and values.

Assessing nuclear technology as a 'complex problem' consequentially requires evaluation of both the (scientific) facts and the values at stake. In this sense, assessment of nuclear technology can be characterised as an *unstructured* problem, as (Table 9.4) obviously in civil society, there exists no consensus on the science, on the relevant values or on the way these values might be taken into account (and respected).

[2] This text is based on the presentation 'Nuclear technology assessment – on the complexity of justification', Gaston Meskens, Project on Integration of Social Sciences into Nuclear Research (PISA), SCK•CEN, presented at the European Nuclear Conference 2007 , Brussels, 19 September 2007.

TABLE 9.4. CHARACTERISTICS OF THE NUCLEAR ENERGY ASSESSMENT

Nature and governance of a 'Complex Problem'	Consensus on values	Consensus on scientific facts
'unstructured' *deliberation*	no	no
'moderately structured '*pacification*	yes	no
'moderately structured' *negotiation*	yes	no
'structured' *regulation*	yes	yes

It is clear that assessing nuclear technology in terms of its acceptability in society requires a joint deliberation exercise on the aspects of *justification*, rather than a strategic unidirectional communication of its benefits or problems alone.

9.3.1.3. Assessing nuclear technology – the difficulty of gathering in the deliberation arena in our politico-economic society

It is generally understood that the development and use of nuclear energy technology requires a stable economic and political climate, backed by well-funded research programmes and broad and robust societal support. Today, nuclear licensing and regulation remains on the national level, and international energy policies still insist on recognising the national sovereign right to develop and use nuclear technology for peaceful purposes.

Taking into account that global negotiations on sustainable development in general and on energy policy and climate change in particular, struggle with taking a joint position on nuclear issues due to diverging views of nation states, we can argue that the conditions and contexts wherein one has to start deliberation seem to be more complex than ever before.

Highlighted below, are three recent societal trends that have a specific influence on public perception and hinder, each in their characteristic way, a deliberative joint justification process.

9.3.1.3.1. Governance of radioactive waste, or the strategic involvement of civil society

In theory, national authorities that aim to maintain current or develop future nuclear technology should find themselves in the somewhat paradoxical situation of seeing the need for seeking public support 'locally' on the one hand while strengthening their position in the global economic system by 'tuning in' to international nuclear research and development programmes on the other hand

In practice however, political initiatives for an involvement of civil society remain restricted to the area of radioactive waste management. (In the last decade, international research programmes on governance of radioactive waste have successfully engaged civil society in research on themes such as long term governance, risk perception and organising public involvement through local communities. In parallel, more and more governments acknowledge their essential responsibility in involving local communities in the siting process for radioactive waste disposal. Although it is clear that a reflection on 'public acceptance of radioactive waste' has a logical connection to the question on the role of nuclear energy in national and international energy policies,) we can observe that, broadly speaking, civil society is still left out of these essential energy policy negotiations.

9.3.1.3.2. Climate change polarising public perception on nuclear

Climate change is nowadays regarded as one of the biggest threats to society. Since the third Conference of the Parties to the United Nations Framework Convention on Climate Change in 1997 in Kyoto, the debate on climate change has been brought into the public sphere. Also, since then, the nuclear community has positioned itself into this debate as a part of the solution to climate change. Their rationale is that the beneficial role of nuclear power as a virtual CO_2 free base load energy source makes it an optimum energy source. However, it has been observed that, in fact, this argument has caused a greater polarisation on the role of nuclear power, rather than a consensus on the value of this argument in a deliberative negotiation process.

9.3.1.3.4. A nuclear renaissance supported by societal acceptance?

Recent evolutions in national and international energy policies have resulted in, what the nuclear community tends to call, a nuclear renaissance. Analysis of recent history shows that this nuclear renaissance is inspired and supported by geo-political and market-economic strategies aimed at ensuring national security of energy supply for an affordable price, rather than on a better public acceptance of nuclear technology as such. The argumentation that nuclear power is part of the solution to climate change is used as additional evidence, despite the fact that, until today, this role of nuclear power has not been officially recognised on the international political negotiation level. In any case, the role of civil society, whether on national or international level, in steering the nuclear renaissance has been negligible.

The fact that countries position themselves internationally by either openly favouring or rejecting the nuclear option in their energy policies, and the fact that international policy organizations such as the EU and the UN insist on the state-sovereign right of choosing nuclear power gives the technology a definite political-strategic character, with the somewhat perverse effect that it strengthens the connotation with misuse in warfare and terrorism.

In conclusion, we state that acquiring societal acceptance of nuclear energy technology would require at first a societal dialogue on the energy policy level instead of a dialogue confined to radioactive waste management programmes or in the margin of the climate change debate.

9.3.1.4. On argumentation and perplexity in the deliberation arena

Any political deliberation on the use of nuclear energy technology obviously has to take into account the historical industrial development and use of the technology in various countries already, as well as the fact that any decision on introducing or phasing out nuclear technology has serious implications on future energy policies. One cannot just switch the nuclear option on or off, so to speak. This means that a political decision to introduce or phase out nuclear is mainly symbolic at first instance, and that it has to be backed by a robust follow-up policy sensitive to future economic and political dynamics.

Even in an ideal setting for deliberation on the complex problem of nuclear technology assessment, the complete spectrum of stakeholders (including nuclear experts and political decision makers) will face difficulties in generating a joint insight into the evidence that would (or would not) justify the use of nuclear technology. (We argue that these difficulties have nothing to do with emotional or irrational perceptions and expectations of the distinct stakeholders, but essentially with the inherent character of complexity of the issue as such, and that these difficulties provoke a double perplexity in the political arena).

A nuclear expert arguing on the benefits of using nuclear energy would rely on the well-known rational arguments with regard to the safety of the reactor, the insight into the future performance of a waste disposal site and the regulations that ensure the protection against low levels of radioactivity. Knowing that these arguments are based on the science of probabilistic safety assessment, performance assessment and radiobiology of stochastic effects, and thus on a probability, a prognosis and a hypothesis respectively, one can understand that it is impossible to deliver scientific proof of benefits and risks in a deliberation arena.

The expert may point at the substantive scientific and practical experience acquired already in the field of reactor operation, but cannot do the same in relation to waste disposal. In short, backed by insight in phenomenological scientific evidence, the nuclear expert enters the deliberation arena with what he/she believes but cannot prove.

On the other hand, due to the uncertainties with regard to the causality-risk relation and the complexity of distribution of benefits and burdens connected to the risky practice, the citizen or layperson will enter the arena with a concern that is not easily translatable into a rationale for acceptance (or rejection) of that perceived risk. Both parties face a certain perplexity when it comes to defending their case.

The consequence is that both parties realise that it is apparently impossible to reach full consensus on science and values in a deliberation exercise. In the interest of moving the process forward, in addition to scientific insight and mapping of values, a certain kind of trust in the future process is necessary in order to reach consensus *on a decision*.

9.3.1.5. Deliberation in a society steered by visual culture

A recent Eurobarometer survey showed that 80% of the EU25 citizens declare television as their main source of information on nuclear matters. Obviously, this has serious implications for public perception on nuclear power technology, especially taking into account that most communication on nuclear technology is still essentially strategic (both by advocates and opponents). One cannot overestimate the overwhelming influence of public media in steering public opinion: every idea on nuclear power (whether positive or negative) that lives among citizens is generated or influenced by the media.

While political philosophers up till now underestimated or even ignored the influence of images in generating perceptions among civil society, many philosophers engaged in studying visual culture state that, in our ‘digitalised’ and ‘mediatised’ society, visual images have replaced words as the dominant mode of expression. One can immediately understand the consequences for perceptions on nuclear technology, if only by realising that it is much easier to depict or show the dangers and harms of the technology than the benefits. Going back to our previous argument in favour of deliberation instead of strategic communication, this means that the way we visualise our argument has to be subject to careful critical reflection. The saying goes that 'a picture is worth a thousand words', but nobody can guarantee that it says the same thing.

9.3.1.6. Joint justification: a new way of generating knowledge, a new way of policy making

The argument in the previous paragraphs was meant to show that the only way robust public acceptance for nuclear can be generated is through a joint deliberative justification exercise, taking into account that the outcome of this exercise can well be a rejection of the nuclear option. As giving proof of scientific evidence and of public concerns is faced with specific

limitations, it was stated that that 'trust' is the essential 'additional' element that would ensure a certain robust consensus for a (jointly taken) decision. In summary, it can be said that it is essentially based on:

- Insight: recognizing inherent complexity and uncertainty and understanding the historical legacy;
- Transparency: explaining scientific facts, but also being open about unresolved issues and 'the real agenda';
- Accountability: responsibility of all involved stakeholders;
- Participation: as a right of all involved stakeholders - in both research and political decision making.

In practice, this generation of trust requires a new way of generating knowledge and a new way of policy making. In short, these new ways can best be described by sketching the responsibilities of the specific major stakeholders that are to be engaged in deliberation:

9.3.1.6.1. Research and business

- Better insight in complexity through joint integrated research;
- Overcoming ‘positioning’ and achieving simplicity in communication;
- Joint problem definition;
- Interdisciplinary research;
- Stakeholder involvement in research and development;
- Transparency and accountability towards society;
- Corporate social responsibility.

Or, in other words: if researchers and businesses in the nuclear community are serious about seeking societal acceptance for nuclear power, they should realise that public acceptance cannot be achieved by only responding to a concern by way of a (popularised) scientific argument or good communication. If it is not complemented with joint reflection, this unidirectional communication remains solely strategic.

In addition, corporate social responsibility is more than transparency, ecological and ethical awareness and good conduct. In the spirit of the previous arguments, it is clear that there is also the responsibility to actively participate in the societal debate on potential misuse of a technology. Especially with regard to FRT, this implies that the nuclear community can no longer afford to stay out of the proliferation debate. It should actively participate in the debate and stimulate the political world in initiating and steering this debate.

9.3.1.6.2. Politics

- Fostering interdisciplinary research and deliberative decision making;
- Responsibility for designing unambiguous rules for the market;
- Responsibility for steering deliberation;
- Promoting interdisciplinary research;
- Setting a good example by proper use of knowledge in policy making (no ‘science shopping’);
- Responsibility for involving stakeholders in deliberation on justification (deliberative democracy in practice).

When it comes to justifying nuclear energy and other complex risk-inherent technological applications, it is upon civil society to decide. This requires at first instance the political responsibility to organise true societal deliberative decision-making processes on (nuclear) energy policy, both in the case of introduction or re-launch of nuclear power, and in the face of an envisaged phase-out.

9.3.1.6.3. Civil society

- Awareness (awareness of its own responsibility);
- Recognizing the inherent complexities and uncertainties of our modern technological society;
- Awareness of the right to get involved;
- Awareness of the responsibility to get involved in research and deliberation.

(Both opponents and advocates of nuclear power who want to engage in a real debate on the role of nuclear power in energy policy should acknowledge that the public does not exist, which implies that it cannot be irrational or emotional and that you cannot claim to represent it.)

9.3.1.7. Status of public acceptance in Belgium

As stated earlier, the EC Eurobarometer studies are the chief source of information about the perception of nuclear power in Belgium and elsewhere in Europe. They conclude that the television plays an important role in influencing public opinion.

Multi-purpose Hybrid Research Reactor for High-tech Applications (MYRRHA), is a flexible fast spectrum research reactor, which will replace the ageing BR2 reactor, is currently under construction in Belgium. It is expected to be operational at full power in 2023. SCK-CEN hopes to put together a team of international collaborators to work with MYRRHA.

The Belgian Nuclear Center SCK-CEN has in the past, taken the initiative to address the public at large to allay concerns about nuclear power. However, most of the communication with the public is done through the Belgian Nuclear Forum. The forum also disseminates information that is related to non-electric applications of nuclear technology such as the production of radioisotopes for medical purposes.

Furthermore, SCK-CEN also has a PhD programme, which promotes education in the field of nuclear science and engineering. This program has generated a lot of interest in fast reactor related research from both within and outside Belgium.

Activities in the field of research and education as well as efforts made on by SCK-CEN and the Belgian Nuclear Forum have helped to promote nuclear power in the country and increase acceptance of it.

9.3.1.8. General conclusions

Historical analyses of the development of peaceful nuclear technology show that, until today, engagement of civil society with regard to public acceptance of nuclear technology has been more strategic than deliberative. Public information campaigns, hearings and internet forums remain to keep a character of unidirectional reassurance with regard to risks and benefits. Even referenda cannot be regarded as a deliberation activity, as they lack the joint problem definition exercise and the mapping of relevant norms and values.

As argued in the text, the FRT community could play a very important role in engaging civil society in deliberation on justification of nuclear technology, and this by starting and supporting real trans-disciplinary and inclusive reflection exercises as a part of the future R&D programmes; especially scientific and societal aspects of waste management and proliferation should be put at the centre of attention. Needless to say, the support and involvement of both.

9.3.2. Public acceptance of fast reactors in France: The French perspective

France has been involved for over forty years in the development of nuclear power. This energy policy has been maintained since the first oil crisis in the 1970s. France has no natural energy resources and the nuclear choice was first linked to energy security and energy independence.

The French context: a long experience in fast breeder reactors and fuel recycling

Nuclear power is well accepted in France, as it is perceived as necessary for economical reasons and, since the 2000s, for environmental ones (the necessity to reduce CO_2 emissions). The nuclear choice has been explained by decision makers as a long term commitment since the very beginnings of the nuclear programme. Consistently, France has early chosen to develop a closed fuel cycle, with the La Hague reprocessing plant.

Nevertheless, there have been ups and downs in public opinion on nuclear power in France. In this regard, there is no evidence that fast breeder reactors, as any other technological option, have influenced the public opinion in favour or against nuclear power. It seems that those against nuclear have argued that fast breeder reactors are more dangerous than other reactors because they are plutonium plants and therefore they increase the risks of proliferation, and because they are not economically competitive, but it is doubtful that these arguments have significantly influenced the general public opinion.

After Chernobyl, during the 1990s, one could observe an increasing distrust of nuclear power and more generally of scientific and technological progress, particularly in France but more generally in developed countries. In France, in 1998, an electoral agreement between the Socialist Party and the Green Party led to the political decision to shut down Superphénix, a 1200 MW sodium fast reactor. In the public perception, the breeder Superphénix remains a failure even if there are no sound or decisive technical arguments to support this viewpoint. The arguments evoked by the anti-nuclear population against Superphénix were on the one hand the risks linked to plutonium production and to sodium technology, and on the other hand the lack of economic competitiveness compared to thermal reactors.

Since the 2000s, public consciousness of new issues in energy policies (the greenhouse effect as a major concern, energy security in the context of geopolitical tensions and fossil fuel exhaustion…) has generated a "nuclear revival" worldwide, and public opinion in France has been influenced by this dynamic. On another hand, several 'public debates' on energy matters were organized by the Government and the National Committee of Public Debate (CNDP): the Energy Debate in 2003, aiming to give a broad information to the public on energy policy issues; and in 2005 and 2006, the EPR Debate and the Sustainable Waste Management Debate; before passing a law on Waste management on June 2006. Few people from the general public participated in these debates, except near the areas impacted by the construction of a new nuclear facility. But the general opinion and the media coverage have evolved in favour of nuclear energy, seen as cleaner than coal. The existence of solutions to manage the radioactive waste is slowly being recognized more and more. Safety concerns

remain important but people are more and more convinced by the fact that up to now, there has been no significant incident with external impact in western countries.

In this context of relatively good acceptance of nuclear power, what about the perception of fast reactors in the future?

- Firstly, it must be stressed that the difficulties will not come from the general public, that has no detailed knowledge nor opinion on fast reactors, but can hear contradictory arguments: those from anti-nuclear proponents against the risks linked to plutonium (proliferation, toxicity…) and to the sodium technology (safety); and, on the other hand, the arguments developed by the nuclear community on sustainability, better use of resources and minimization of ultimate waste. Furthermore, in France, the Safety Authority will not license a SFR design until it has been proven to be as safe as the best 3rd generation reactor (up to now in France, the EPR).

- As far as can be said, it seems that the argument of better use of natural resources, with a full recycling of plutonium and uranium, will be a decisive factor in favour of fast reactors. Contradictory to the USA, French public opinion has never been very concerned by the 'Carter doctrine' and plutonium elimination. The attempts of the anti-nuclear population to mobilize against reprocessing have never been successful. The concept of 'recycling' has positive ecological connotations. This is more and more the case since the consciousness of the scarcity of natural resources is increasing, as is the topic of sustainable development.

- The waste minimization argument may also be a factor in favour of fast breeder reactors, since the 2006 Act on "Sustainable Management of Radioactive Waste" includes the partitioning and transmutation as a milestone and an objective for the future French 'prototype' fast breeder reactor. The possibility to reduce the volume and the toxicity of ultimate waste, and perhaps to have no more ultimate waste than the fission products, with no more than two or three centuries of radiotoxicity, would certainly contribute to the acceptance of waste disposal methods or repositories. It would change the public perception of radioactive waste, since the lifetime of the waste would not be 'eternity', as it is currently perceived to be, but it would become an ordinary period of time on an historical time scale.

- Even if the general public is not very convinced by anti-nuclear arguments, it will be necessary to answer to their criticisms, particularly about the safety of fast breeder reactors. In this regard, it will be necessary to have strong answers to the questions about sodium fire, resistance to external aggression, and proliferation resistance.

To sum up these remarks, the concept of fast reactor may be a decisive building block to support the idea of nuclear power as a tool for sustainable development. However, it must be linked to the other main arguments – the role of nuclear power in a less CO_2-emitting energy mix and the sustainability of resources. The concerns about safety have to be addressed with regard to the current level of safety of 3rd generation reactors. Innovations regarding safety are therefore the most decisive breakthrough to be made by future R&D on 4th generation fast breeder reactors.

9.3.3. Public acceptance of nuclear power plants in India

Starting a nuclear power project in a new site attracts greater resistance from the public compared to any other industrial activity. Reasons are unfounded fear, lack of knowledge of safety features of the reactor and lack of understanding of the advantages that will accrue to the public during and after plant construction.

However, opposition to nuclear power plants (NPPs) in India is low compared to that in many other countries. Yet, the conscious population wants information before the project is launched. NPPs in India are spread across the length and breadth of the country. There is a large population living in the vicinity of the plants. Having knowledge of the safety record maintained by NPPs and recognising the benefit accrued to the society in the past, especially due to the corporate social responsibility discharged by the NPP management, the questioning is less when new projects are launched at an existing site. The issues raised are rather large when a new site is opened. Experience indicates that NPP management handles the issues with great sensitivity and is able to provide thorough satisfaction to the population surrounding the plant.

India drew a nuclear energy road map in the 1950s. The three-stage nuclear power programme of India was given wide publicity over the years and is quite well known among the conscious population. The people of the country have recognized well that long term energy needs can be met only by the fast breeder route. They also recognise that coal quality in India is inferior, oil reserves are scarce and hydro potential is limited. Although wind energy is expanding fast, its limitations are well recognised by the public at large. That energy scarcity is affecting industrial growth is well known to Indians. Major parts of the country have an electricity shortage and thus often experience power cuts. People are anxious for early narrowing of the gap between energy demand and supply. The global warming concerns have generated enormous support for NPPs. We have adequately advertised that NPPs do not emit carbon dioxide.

The scarcity of uranium and abundance of thorium in India is well known to the people. Years of public information effort by the Department of Atomic Energy of India has resulted in awareness among the people that there is no option but to go for fast breeder reactors in India to meet long term energy needs of the country. The indigenous nature of fast breeder technology, the indigenous components and possibility of 350 GWe by indigenous fuel has adequately enthused the Indian population to go ahead with nuclear reactors based on indigenous fast breeder technology.

The safety record of the Fast Breeder Test Reactor (FBTR) has also been well advertised and the public at large knows that the radiation releases, the contamination spread and radiation safety issues in fast breeder reactors are far less compared to those of thermal reactors.

Public hearings are arranged prior to the launch of an NPP at an existing or new site. The government machinery is activated to invite people's representatives. The government observers ensure that the entire concern and expectations of people at large surface during such public hearings and fair discussions are held. The government officials also ensure that the issues raised and commitments made are recorded and they pursue their implementation in a meticulous and timely manner.

The fast breeder reactor under construction at Kalpakkam (PFBR) is operating in a 'fishbowl.' Management in a fishbowl requires management effectively in an open environment. The

PFBR officials communicate project progress, the highs and the lows to the public in real time as the project progresses and new developments occur. The fast breeder management has recognized that NPPs have not to be made subtly but highly visible. To gain a broad base of support, the PFBR is being constructed in full public view and scrutiny (or in a 'fishbowl').

NPPs by their nature, involve heightened interest by the public in general and the inhabitants of neighbouring villages in particular, along with the peoples' elected representatives, government agencies, intelligentsia and students. The PFBR management team has demonstrated that the NPP activities are being managed honestly and effectively. The PFBR management is conscious that there should be no perception that the project is fertile ground for physical and financial irregularities and only investigations can uncover hidden data, or that there are surprises waiting to be uncovered. The PFBR management team has demonstrated that the project is being managed honestly and effectively and thus the management of PFBR has instilled great public confidence.

The management team of PFBR is working to improve public perception on a continual basis. As the projected and expected timeline is met, public confidence and trust has risen. It is recognised that when the projected schedules are met, the management credibility improves and the public perception of management capability of meeting commitments in all aspects, including safety of NPPs, improves. On the contrary, for projects that are affected by cost and time overrun, the management credibility comes into question and thus public perception of meeting stipulated safety standards too falls flat. Providing access despite the perceived risks, it is vital to invite government officials, students and professors, residents of neighbouring villages, press and media in large numbers throughout the project life cycle and during the operating phase of an NPP to maintain public trust in NPP management. More than 8000 students from different science disciplines, engineering college students, teachers, and people residing in the vicinity of PFBR have visited the construction site and carried the message that a high technology project of national importance is undertaken by the PFBR team, maintaining high standards of safety and quality.

The right of information to the public was provided by an act of Parliament of India in the year 2005. The act popularly known as RTI Act casts an obligation on public authorities to grant access to information and to publish certain categories of information. Information of a strategic nature is however excluded. The act lays down the machinery for the grant of access to information to public. Public authorities have designated Public Information Officers and Assistant Public Information Officers whose responsibility is to deal with the request for information in a timely manner and also to assist persons seeking information.

The operations of all public authorities including the actions and decisions of NPPs have thus become transparent to every Indian national. This has substantially boosted the confidence of the public. The press and media play vital role in creating public perception regarding a project. It is essential to ensure that the press and media are updated about the project regularly. The Prototype Fast Breeder Reactor project has kept the press and media updated about the project execution on continual basis. The nuclear power plants are constructed only by government agencies in India as yet. Government organizations once may have guarded information carefully but have undergone a dramatic change and now we see the value in nurturing a trusting relationship with the public.

Acceptance of people's expectations and need for keeping people closely informed of progress, issues, and upcoming events is essential for the NPP management team. This also minimizes the potential for blindsiding the public. In brief the public acceptance of the

forthcoming FBRs will depend on public information effort, visible progress, delivery on promises, involvement of large section of society and educating them about safety features, maintaining a relationship of trust and cooperation with the public, as well as updating the press and media on continual basis. The full array of delivery methods for information will have to be kept ready and released appropriately.

Those associated with the fast breeder programme in India recognize that the people who are influenced by the nuclear power plants are not only important but are an obligation to the utility. Even after public acceptance of the impact analysis of the project, completion of the public hearing and consultation process, and even after concluding the project, it is essential that the public is given confidence that nuclear power plant authorities are listening to their concerns and responding accordingly.

The philosophy the PFBR management team follows is that coordination and communication with the press and other interested parties alone is not enough. A constant focus on public perception is required and it must be ensured that the press periodically hears their message.

Keeping the public informed is important, but maintaining a dialogue that encourages openness and a free exchange of information and ideas with the general public is even more crucial for public acceptance of a new nuclear power project venture.

9.3.4. Public acceptance of fast reactors in Japan: JAEA's public relations activities

9.3.4.1. Introduction

Many scientists have pointed out that global warming has had a significant impact on animals and plants everywhere in the world, from the Arctic to the Antarctic. A major cause of this is said to be the increased emission of exhaust gases, such as carbon dioxide and nitrogen oxide, from expanding industrial activities and the improvement in people's living standards. Countries like China and India are expected to use more and more fossil fuels, driven by recent changes in their social environment and the expansion of industrial activities. This constitutes a large source of concern from the viewpoint of preventing global warming. At the G8 Hokkaido Toyako Summit held in Japan in 2008, world leaders affirmed that preventing global warming was an urgent issue to the world and that nuclear power was expected to play a significant role in solving environmental problems.

Nuclear energy is an essential energy source for life and also indispensable for long term energy security. Under this guideline, the Japan Atomic Energy Agency (JAEA) has programs as an independent administrative institution covering the entire range from basic research to supporting industrial activities. JAEA has been significantly contributing to creating and improving various innovative technologies related to nuclear energy. In the field of fast breeder reactor (FBR) cycle technology, designated as one of the "Key Technologies of National Importance" by the Government, JAEA has made great efforts to resume operation of the fast breeder reactor prototype 'Monju' and JAEA also promotes R&D of the FBR cycle for commercialization. Under such circumstances, public relations activities on nuclear power in Japan are positioned as important efforts to increase public acceptance. These activities should focus on communicating the attractive features of nuclear energy and expectations on its potential contribution to combating global warming, while easing people's anxiety and concern about radioactive contamination and exposure that may be caused by a potential accident at a nuclear power plant.

Japan is a country of few natural resources, with an energy self-sufficiency rate of only about 18% (if nuclear energy is assumed as a semi-domestic energy source). There are 55 nuclear power plants in Japan (see Fig. 9.5).

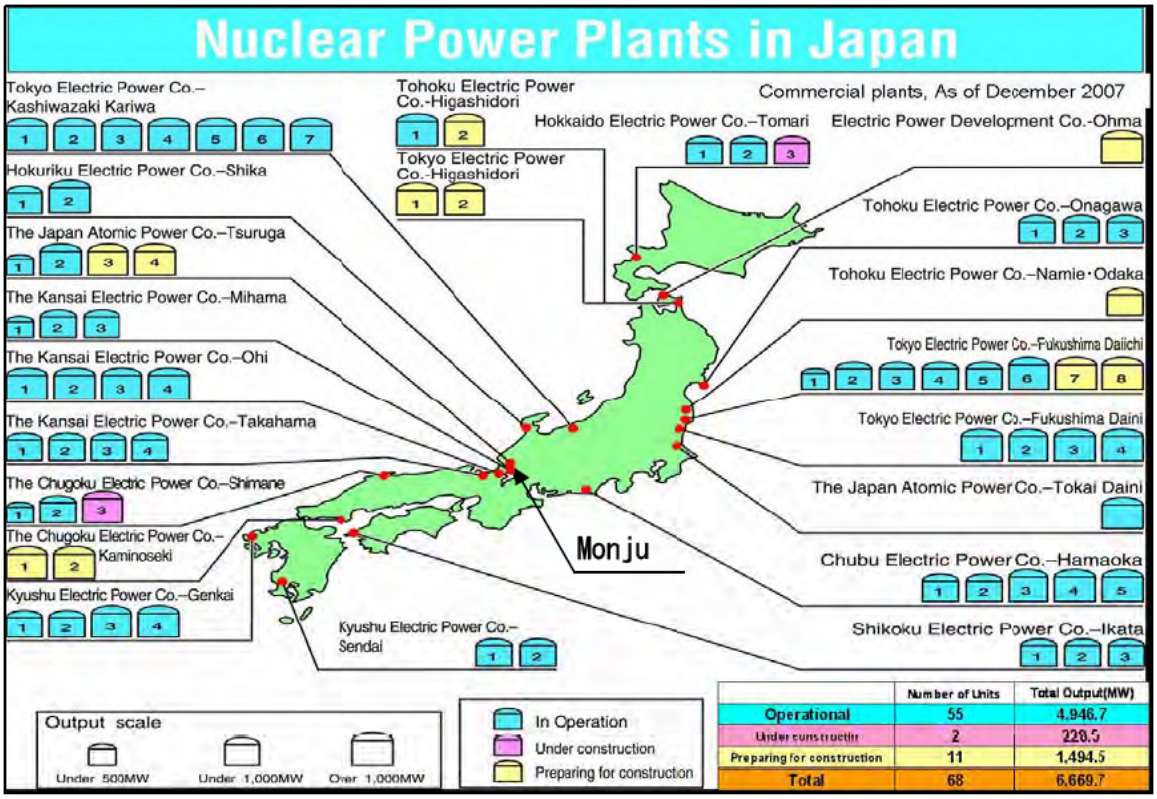

FIG. 9.5 Nuclear power plants in Japan.

Therefore, while it is important for Japan to develop renewable energy sources such as photovoltaic power generation and wind power generation, these sources have the weakness of low energy density. Japan should also bear in mind that the reserves of uranium, a fuel for nuclear power generation, are finite, as are the reserves of oil, natural gas and other fossil fuels.

Looking ahead the rest of the 21st century, Japan should diversify its energy sources by achieving the best mix of renewable energy (solar, wind), fossil fuels (e.g., oil), and nuclear power generation. This nuclear power generation should preferably centre on nuclear fuel cycles based on the next-generation reactors, for which uranium resources are recycled and plutonium is used as fuel.

We believe that face-to-face activities for mutual understanding are essential when many aspects are taken into account, including global environmental issues, energy affairs in Japan, and the need for efforts to foster public acceptance in metropolitan areas of Japan as well as in regions containing nuclear power plants, or supplier regions. How JAEA addresses public relations activities in these areas is described below in detail.

9.3.4.2. Public relations activities for Prototype Fast Breeder Reactor "Monju"

The prototype fast breeder reactor 'Monju' is located in Tsuruga-shi, Fukui Prefecture near the centre of the coast of the Sea of Japan (Fig. 9.6).

FIG. 9.6. Prototype fast breeder reactor Monju.

Fukui Prefecture has four distinct seasons with winter's north-westerly winds bringing heavy precipitation, making it a very moist place blessed with abundant water resources. The population of Fukui Prefecture is about 800 000 people.

Monju was out of service for over 14 years, since the sodium leak accident on 8 December 1995 until 6 May 2010. Activities to put Monju back into operation could not be started without acceptance of the Japanese people, especially local residents. From the viewpoint of working in harmony with society and local communities, it was also essential to create peace of mind and confidence in our operations by ensuring transparency of operations and by forging ahead with efforts to maintain and improve the public and local residents' confidence in this plant.

The JAEA holds explanatory meetings for different domestic groups and in different regions, including local communities and metropolitan areas, in order to widely communicate information on Monju-related issues. The JAEA has also been working to ensure transparent operations, for example, by publishing information on its efforts to assure the safety of Monju and on failures and problems that had occurred there. In the local region of Fukui Prefecture, JAEA staff members even visit residents to offer an explanation in person. The above interactive explanatory meetings, called Cycle Meetings, have been continuously held as part of JAEA's public hearing and public relations activities. These are opportunities for interaction and opinion exchange with local residents through which we can learn about their views.
To be more specific, these involve "visit and talk" activities, which have been continued since the accident. JAEA staff members have visited all of the 17 municipal governments in Fukui Prefecture, local council members, local community association heads and other organizations to explain developments in the JAEA. The JAEA also has been making efforts to increase local acceptance under the slogan of "Seeing is Believing." An example is the organization of tours to visit Monju-related facilities. In addition to these efforts, the JAEA takes advantage

of every opportunity to communicate information and increase public acceptance, such as explanatory meetings it holds at municipal councils in Fukui Prefecture.

The JAEA has been strengthening ties with local industries in order to build a better relationship of trust with them. For example, the JAEA is engaged in activities such as technology exchange with local companies, an R&D results application program (for disclosure and use of JAEA patents), a technological consultation program, and holding open seminars. Activities centring on local partnership constitute a pillar of the JAEA's business operations.

9.3.4.3. Outreach activities

The JAEA's outreach activities are aimed at supporting efforts to prevent youths from moving away from the sciences. At its International Nuclear Information and Training Center, the JAEA owns comprehensive FBR cycle training facilities, where training in sodium handling techniques and related maintenance techniques is provided, and the Monju Simulator, a system designed for Monju operation training. The JAEA also offers energy and environmental education through the "Science School" (science lab) programme of its science exhibition hall "Aquatom" in Tsuruga. Training and scientific experiments at these facilities, combined with onsite learning programs in Monju facilities, meet the diverse needs of domestic and international communities wishing to develop human resources.

With the aim of supporting and cooperating on environmental and energy education directed at the next generation, the JAEA provides educational programs for students in elementary, junior high and high schools and universities at its facilities and even sends staff to give lectures at such schools (see Fig. 9.7).

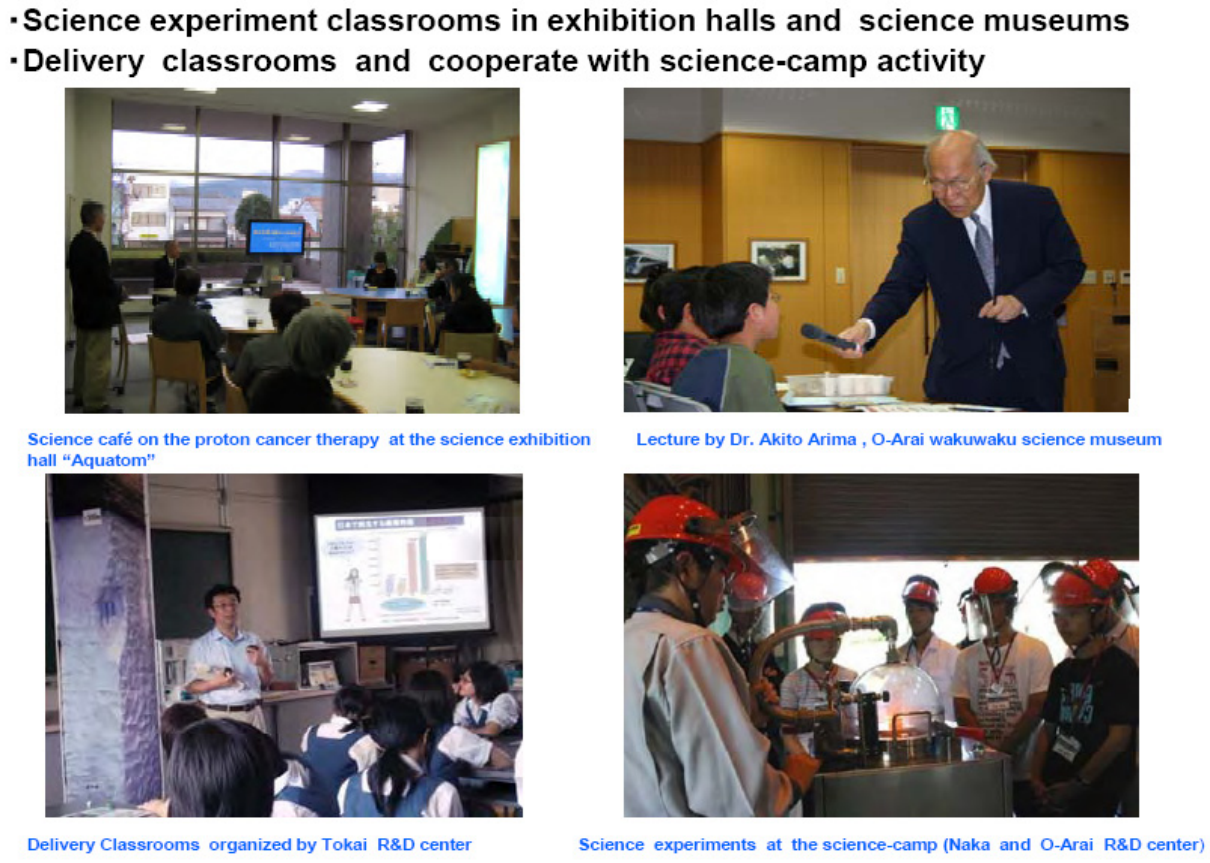

FIG. 9.7. Outreach activities by scientists and engineers.

On the other hand, the Fukui Prefectural Government is implementing a program to evolve the region into Japan's R&D center for energy and nuclear power. The JAEA has been actively cooperating with them in strengthening local R&D capabilities, developing and exchanging human resources, and creating and fostering industries.

9.3.4.4. Proactive provision of information

Considering the importance of communicating information to society, the JAEA has enhanced its capacity to provide information on its website. The information being posted includes the JAEA's current R&D activities and their results, day-to-day operations, and real-time environmental radiation monitoring data for areas in and around the nuclear facilities. The JAEA also gathers public opinions on its online information provision and actively responds to questions on the website. The JAEA provides information on its research activities and press releases for people in and outside Fukui Prefecture by sending e-mail magazines.

The JAEA contributes articles to newspapers, R&D journals and general-audience magazines. For example, the JAEA provides information for a comic writer whose work appears in Shukan Morning, a weekly comic magazine with a market-leading circulation in Japan, and posts advertisements jointly with power companies in Bungei Shunju, Japan's most popular monthly magazine. For communicating information to people in metropolitan areas, the JAEA posts an advertisement on a signboard at Otemachi Station of the Chiyoda Line, a Tokyo subway station where more than 5 million passengers get on and off trains in a month (Fig. 9.8).

FIG. 9.8. Signboard at Otemachi Station of the Chiyoda Line (Tokyo subway).

This is to publish R&D information, as well as recruitment information for new researchers and staff. In Osaka, the JAEA continues an exhibition on Monju at the Science Satellite exhibition hall next to the Ogimachi Kids Park, a facility designed for children and their parents. This way, the JAEA widely communicates its information to the public.

The JAEA attends open forums organized by groups opposing nuclear power and explains to them its R&D activities and the current state and future plans concerning Monju. In these

forums, the JAEA participates in panel discussions with members of opposing groups on the stage and sincerely answers questions from the audience.

9.3.4.5. Public hearing and public relations activities

Public hearing and public relations activities as part of the JAEA's efforts to increase public acceptance in the Fukui Prefecture are described below.

Since the sodium leak accident in December 1995, the JAEA has continuously engaged in "visit and talk" activities for 17 municipal governments in Fukui Prefecture, local council members, local community association heads and other organizations. JAEA reports its up-to-date information through these visits. The JAEA has made every effort to increase local acceptance; this includes inviting local residents to plant tours and holding explanatory meetings at municipal councils in Fukui Prefecture. Large-scale explanatory meetings at community centres (Fig. 9.9) that had been held right after the accident have been replaced by "Cycle Meetings" since October 2001 (Fig. 9.10).

FIG. 9.9. Explanatory meetings at local community centres at Tsuruga.

FIG. 9.10. "Cycle Meeting" at Atom Plaza, Tsuruga.

Under the slogan of “Anytime, Anywhere,” members of the JAEA have visited and participated in meetings organized by companies, organizations and schools in Fukui Prefecture to actively communicate with their members. As of the end of October 2008, 865 direct communication sessions were held with a total of 24 367 people. The “Cycle Meeting” is considered as an effective means of mutual communication because a friendlier atmosphere can be created when we are given a specific time period during the other party’s meeting. While maintaining these activities, the JAEA launched the “JAEA Briefing Session” in February 2008, with the upcoming restart of Monju in view. This is a meeting aimed at reporting progress at Monju and Fugen (an advanced heavy water thermal reactor) to Fukui Prefecture’s 17 municipalities.

Based on the concept of “Seeing is Believing,” the JAEA has been offering plant tours that include a look at the accident site, since September 1996, the year following the sodium leak accident. These tours were conducted even on national holidays. Although tour participants are not permitted to enter the protected areas because of international situations in the post-9/11 era, they can have a look at the sodium metal cutting and combustion processes at the sodium handling facility, see training with the operation simulator (or sometimes even touch the simulator), and observe how radiation monitoring is conducted, followed by an explanation of safety activities for Monju. As of the end of October 2008, a total of 106 052 people have participated in the plant tours.

As part of efforts to ensure operations open to the local society, the JAEA, in cooperation with the Ministry of Education, Culture, Sports, Science and Technology, has been hosting forums and explanatory meetings mainly in the cities of Tsuruga-shi and Fukui Prefecture in order to report business results and future plans. International forums are also held every two years with the aim of presenting information from Tsuruga to the world through lectures and discussions on different national energy policies and prospects in different countries and the international role of Monju. The JAEA also owns a large vehicle-mounted display, which is sent out to public events in Fukui Prefecture for cooperative and public relations purposes.

The local media of Fukui Prefecture, such as newspapers and TV and radio stations, are used in an integrated manner to communicate information, either periodically or occasionally. The JAEA publishes “Four Seasons in Tsuruga,” a public relations magazine aimed at local residents, “JAEA Newsletter,” “Genki (which means “Health” in Japanese),” a PR magazine designed for people all around Japan, and even an e-mail magazine, which has a nationwide readership of about 500. These publications are issued periodically to announce events and report JAEA’s activities and local topics. The same information is also made available on the JAEA website to give access to a wider audience. JAEA sets up a booth at events held in the local community and other parts of Fukui Prefecture to disseminate information, and actively participates in events and volunteer activities.

Public hearing activities include establishing the “Fukui Advisory Group” and the “Tsuruga Advisory Group,” in both of which representatives of different communities of Fukui Prefecture and Tsuruga-shi have been asked to serve as members. The JAEA periodically reports its operation status to these advisory groups and ask their views on JAEA activities. The same has been done with three JAEA supporter associations in Fukui, Tsuruga-shi and Mihama-chou, which have been formed under the local initiative. A survey program was launched in July 1996 with the aim of directly gathering public opinions. The JAEA called for participants from the local prefecture, and those who have registered have taken part in plant

tours, opinion exchange sessions, and questionnaires. To date, about 1 600 people have participated in this program and offered opinions.

In preparation for the restart of Monju, risk communication was conducted on the assumption that "humans make mistakes and machines fail." This included explanations of how to avoid mistakes and failures by citing examples of preventive measures. A brochure summarizing this risk communication has been distributed to local residents, municipal governments, municipal council members and the news media. This topic has attracted wide attention of the media. The brochure is a case study designed to be easy to understand for the public, and it describes some 120 potential accidents and problems that may occur during Monju operations and how to troubleshoot them. Problems that took place in other nuclear facilities in Japan and abroad have been analyzed in preparing this document.

Regarding media relations, the JAEA continues to put out weekly press releases, which started just after the accident, to report the status of Monju and Fugen, these include even the slightest problems with them. If any anomaly occurs, a press release is immediately issued. Explanatory meetings and plant tours are organized for the media as needed, as an opportunity to communicate up-to-date information on Monju. The media's requests for plant tours, seminars and interviews are accepted whenever possible, in an effort to foster understanding by giving them opportunities for onsite observation.

In the future, JAEA will ensure transparent operations by providing the public and local residents with information on failures and problems in Monju and on activities to assure its safety. JAEA will also continue public hearing and public relations activities and interactions with local residents to learn about their views.

9.3.4.6. Technology exchange and consultation programmes

To build stronger ties with local communities, the Tsuruga Head Office launched the R&D results application program in 1998. Moreover, in 2004 a group dedicated to the promotion of technology application in the local industries was established in the Policy Planning and Coordination Department at the Head Office. This has allowed the JAEA to conduct well-organized activities.

The technology exchanges with companies in many different sectors are aimed at allowing the JAEA and its partner companies to contribute to each other in advancing technologies, developing new products and creating new industries. Since 2004, 38 technology exchange sessions have been held.

For example, in a session focused on Echizen-yaki pottery, which has a history of about 800 years, representatives and researchers of the local ceramic industry and JAEA participants performed testing and study using anagama, or a tunnel kiln, that is actually used for firing pottery. This was an attempt to scientifically examine the firing process by means of analysis techniques achieved through the R&D of fast reactors and to thereby elucidate pottery craftsmanship, which has traditionally been dependent on intuition and experience.

In the 2008 fiscal year, the JAEA started a technology exchange program together with people engaged in the traditional industry "Echizen uchihamono," a 700 year old forged cutlery industry based in Echizen City. Its aim is to develop new products jointly with engineers of local forged cutlery companies by leveraging knowledge and know-how that the JAEA has gained through its laser technology development.

The JAEA offers technological consulting services through the consultation offices in the Tsuruga Head Office and the Community Collaboration Office in Fukui City. As of the end of October 2008, 163 technological consulting requests have been received from a wide range of fields. For example, some of them refer to methods of disposing of rubber crawlers, measures to counter plum tree resin, how to improve the properties of materials used to produce eye glasses, and how to improve the sesame tofu manufacturing method. The JAEA's technologies have been applied in many fields that apparently have nothing to do with nuclear power, such as heshiko (fish preserved in rice-bran paste), a local specialty of the Wakasa region, and Echizen washi (Japanese paper), a traditional handicraft product of Fukui Prefecture. Some of them have developed into projects under the R&D results application program. Figure 9.11 gives the photo of an Technical consulting with local companies at the Chamber of Commerce and Industry in Fukui.

FIG. 9.11. Technical consulting with local companies at the Chamber of Commerce and Industry in Fukui.

The Tsuruga Head Office advertises JAEA patents and technologies via the Internet and newsletters and by extensively hosting open seminars and other events. Technological Consulting System Terminals are available at the consultation offices in Tsuruga, Fukui and Takefu so that consultation requests can be accepted any time. The system has been in operation since FY 2006.

The JAEA conducts the R&D results application program, which is aimed at facilitating the use of the JAEA's patents and other R&D results to develop new products. In one of the projects under this program, JAEA patented technologies were used for a decision-making system that supports anti-snow and anti-ice measures by accurately assessing the road surface conditions in winter. This system is being advanced to create a new industry. The products developed through this joint research have been received well for their abilities to reduce costs and energy consumption (e.g. reducing the number of road service providers and eliminating the need to spread snow-melting agents), and have been adopted by expressway companies and civil engineering contractors in many prefectures since 2006.

A hydro-gel that the JAEA's Takasaki Advanced Radiation Research Institute successfully produced by applying radiation has helped the development of a new type of Echizen washi paper, Fukui's traditional handicraft product. The addition of the gel as a raw material has made the paper less likely to shrink from moisture absorption, while increasing its strength. After the commercialization of this new paper became feasible through the R&D results application program, the project was selected to receive support from the Ministry of Economy, Trade and Industry through its "Regional Resource Utilization R&D Program," with an eye toward mass production. The project is still underway to increase the use of this paper as material for interior decoration. To date, 23 projects have been implemented in Fukui Prefecture under our R&D results application program, prodding local companies to develop new products.

At the Tsuruga Head Office, there are more than ten business coordinators as well as external experts familiar with local companies. The JAEA promotes its established activities, with the aim of encouraging local companies to use its technologies and ensuring that it will be able to effectively create new businesses and provide support and cooperation for companies.

9.3.4.7. Efforts to develop and exchange human resources

At its comprehensive FBR cycle training facilities and the Monju Simulator located next to Monju, the JAEA provides training for staff of the JAEA and related companies, as well as for engineers in Fukui. It also offers summer workshops for college students studying nuclear energy in and outside Fukui, and internships and science camps for high school students.

Training sessions have been provided at the comprehensive FBR cycle training facilities since FY 2000. Currently, there are seven sodium handling courses, ranging from an introductory course, in which students learn about the properties of sodium, to one involving drills to fight sodium fires. The number of participants totalled about 1 700 by the end of FY 2007. The JAEA also offers seven maintenance courses, ranging from one to learn about Monju system equipment and devices specific to Monju, to one centred on the power supply panel and measuring and control equipment. About 700 individuals have taken these maintenance courses. Simulator-based training started in FY 1991. There are 13 courses, including those to qualify as an operator (introductory/intermediate/advanced-level), as an assistant shift supervisor, and as an operation supervisor. About 500 people have been qualified through these courses.

The Fukui Prefectural Government formulated in March 2005 the "Energy Research and Development Centralization Plan," which is aimed at fostering partnerships with nuclear-related institutions and developing the region. It stipulates that education on nuclear power and energy should be enhanced in elementary, junior high, and high schools. In line with this, the JAEA has started to provide active support for energy-related science education for schools and teachers. The JAEA supports lessons at elementary and junior high schools by working in cooperation with teachers to develop educational materials and lesson plans

For high schools (mainly Super Science High Schools, or SSHs), the JAEA assists lectures on world energy, global warming and contribution of nuclear power in these areas, and gives preliminary lessons as part of the Monju plant tour. In FY 2007, about 5 000 students and teachers participated in these programmes. This way, the JAEA, as a research institute, is committed to supporting local human resource development.

The JAEA and the Fukui Prefectural Institute for Educational Research jointly designed and offered a science class in which a fuel cell car was used. In March 2008, this program received the Committee Chairman Award of the Information Center for Energy and Environment Education in the 17th Energy Public Relations Activities Program organized by the Agency for Natural Resources and Energy. At Aquatom, a science exhibition hall centred on the sea and energy that is located in downtown Tsuruga, science workshops for young elementary school students have been provided. In addition to this, the exhibition hall launched "Aquatom Science School" in December 2007 as a means to support energy and environmental education.

In cooperation with local schools, this Science School gives older elementary school students, junior high school students, and high school students in Fukui Prefecture hands-on classes based on scientific experiments at either the exhibition hall or the school. The classes cover global environment and energy issues (Fig. 9.12), as part of integrated learning, and science topics such as substances and electricity.

FIG. 9.12. Energy and Environment Education at the Aquatom.

Using special funds to develop equipment to support science exhibition halls from the Japan Science and Technology Agency (JST), the JAEA built a hybrid cart driven by a combination of three power sources (hydrogen fuel cells, solar cells, and lead-acid batteries). The optimal mix of these power sources is created by a computer-controlled system. The cart is used to offer hands-on experience of clean energy that emits no carbon dioxide. During its first seven months after the opening, Aquatom Science School taught about 1 000 students in 27 sessions.

Through these education support activities, the JAEA has been explaining to students how principles and laws learned in science classes at school are utilized for everyday lives and industries as practical science and technologies. It is expected that more and more local students will become interested in science and mathematics and become able to scientifically and logically think about energy and environmental issues from the global point of view, as they understand that the global warming problem is no longer solvable by the Japanese people's day-to-day efforts alone

The JAEA hopes to help the local communities to produce human resources that will contribute to the world in new scientific and technological fields in the future, thereby fostering the development of local industries. As part of efforts to make Monju an international R&D centre, the JAEA promotes university student education in coordination with the international training programme of the Ministry of Education, Culture, Sports, Science and Technology (MEXT) and with the CEA of France (Fig. 9.13).

FIG. 9.13. Training in the Monju simulator room.

The JAEA also contributes to improving nuclear safety technologies in Asian countries. For example, the JAEA has been offering "Sodium Technology Training" (two months) under MEXT's nuclear researchers exchange programme since FY 2004. Eight trainees have been accepted so far from a Chinese institution operating a fast demonstration reactor. In addition, the JAEA has trained 16 engineers from eight Asian countries (China, Indonesia, Thailand, Vietnam, Sri Lanka, Bangladesh, the Philippines and Malaysia) through the "Training in Nuclear Reactor Safety" (three weeks), which has been conducted under the international nuclear safety promotion programme since FY 2006.

In cooperation with France's CEA, the JAEA has been offering an educational seminar called "Summer College for Nuclear Energy in Tsuruga" since FY 2006. This programme is part of Fukui Prefecture's "Energy Research & Development Centralization Plan," and the JAEA organizes it jointly with the University of Fukui and the Wakasa Wan Energy Research Center as a "Nuclear Energy Hands-on Trial Program" supported by the Ministry of Economy, Trade and Industry. This one-week training programme consists of a wide range of activities, including not only lectures but also things that students would not experience on campus (e.g. hands-on training, discussion in English, and plant tours). It has been very well-received by some 40 participants every year.

The JAEA hopes to use these facilities in combination with training programmes and scientific experiments so as to meet the needs of domestic and international communities wishing to develop human resources.

9.3.5. Public acceptance of nuclear power in the Russian Federation

9.3.5.1. Introduction

The negative attitude about nuclear power formed in society after the Chernobyl accident has pushed organizations and enterprises at all levels that are involved in development, designing, construction and operation of NPPs and development of nuclear power strategy to give more attention to formation of a positive attitude of society toward modern nuclear power and to plan the appropriate activities.

These activities are carried out through mass media of various levels and directions (general periodical publications at federal and regional levels, scientific periodical publications, Internet) and by means of contacts with authority bodies at federal and regional levels.

Formation of a positive attitude toward the fast reactor (FR) is a component of activities on creation of a positive attitude of the community toward nuclear power as a whole.

9.3.5.2. Activities in mass media

Activities in mass media are aimed at the following tasks:

- Informing and interacting with the public of certain regions or of the country as a whole;
- Exchange of information and its discussion within the scientific community.

The following means of interaction and informing various segments of the public can be selected in accordance with the issue to be addressed and the audience:

- Regional and local periodical editions (newspapers, magazines);
- Federal printed editions (newspapers, magazines, books);
- Branch periodical publications;
- Internet;
- Scientific periodical editions.

So, for example, when a point on acceptance of the decision about NPP construction on a certain site is discussed, the local public is informed and involved in discussion of the question using local and regional mass media. Thus, the coordinated decision of federal and local authorities on NPP construction is made necessarily taking into account opinion of the local population. At a stage of consideration of design materials of the NPP, public representatives who desire can participate in discussion of results of evaluation of the NPP's ecological influence on the environment.

As an example, it is possible to describe the process leading to acceptance of the decision about renewal of construction of the BN-800 power unit. In 2004-2005, when this decision was accepted, the following measures had been carried out:

- Two field sessions of the Committee of the State Duma on power, transport and communications in the State Scientific Center of the Russian Federation-IPPE;
- Parliamentary hearings in the State Duma;
- Numerous discussions at the All-Russian Public Movement 'Ecological Forum'.

Based on the results of the conducted discussions, the decision on renewal of construction of the BN-800 and its inclusion in the list of priority state tasks was approved.

The branch periodical editions are used for informing specialists of the branch about current activities of the branch enterprises and institutes, results of certain works and urgent questions of its development. An example is the weekly newspaper of the Russian nuclear workers, *Atom-press*, issued since 1991.

The Internet is a quite new form of information exchange that, nevertheless, has become wide spread. Each organization or enterprise has, as a rule, its own Internet site, and anyone wishing can learn about the activity of this organization/enterprise at the site. Examples of such sites include: www.minatom.ru, www.rosatom.ru, www.rosenergoatom.ru. The last of these sites provides on-line information on the current state of each Russian NPP. There are also specific sites for information exchange in the nuclear power area and discussion of urgent points of its development: www.nuclear.ru, www.atominfo.ru, www.proatom.ru etc. The obligatory and timely informing of the local population through local, federal editions and Internet about all significant events and incidents occurring at the nuclear power plants is provided.

The discussion of specific scientific and technical aspects of nuclear power, including those concerning prospects of its development, is carried out through special scientific periodical magazines, such as "Atomnaya Energiya", "Issues of Nuclear Science and Technology", "Nuclear Energetics", "Thermal Energetics" etc. Here it is necessary to note the significance of scientific periodical editions in discussion of a role and the place of FR technology in the future nuclear power installations, as well as in the creation of an objective professional look at these questions.

9.3.5.3. Activities in authority bodies

The authorities represent interests of the population, both in separate regions and in the country as a whole. Therefore urgent interaction with the authorities at all levels is an integral component of the work of all organizations and enterprises of Rosatom. The main tasks of this interaction are as follows:

- Informing authorities in a timely manner about the current state of NPPs and other subjects of the branch;
- Coordination with local and regional authorities of plans on siting and construction of new NPPs;
- Submission to authorities of objective information about tasks and needs of nuclear power, prospective ways of its development, etc.

Among certain results in this area, it is necessary to mention close interaction with the State Duma concerning discussion of prospects and tasks of nuclear power, and for near- and long-term prospects, including of the decision for construction of the power unit with BN-800 reactor on the site of the Beloyarsk NPP.

9.3.5.4. Conclusion

Now in the Russian Federation, much attention is paid to activities that help create a positive attitude in society toward nuclear power as a whole and toward fast reactors in particular. This activity is carried out both through mass media and by using close interaction with the population and the authorities at the federal and regional levels. This policy provides openness of nuclear power in the Russian Federation to a civil society.

9.3.6. Public acceptance of nuclear power and fast reactors in the United States of America

Although this report addresses fast reactors, it is not possible to provide any information on public acceptance of fast reactors distinct from public acceptance of nuclear power in general. There are no fast reactors operating in the USA and public opinion is based largely on experience and perceptions based on the current fleet of 104 nuclear power plants now operating in the USA.

Surveys conducted for the Nuclear Energy Institute (NEI) show that since the beginning of this decade, the proportion of the US public that favours nuclear energy as one of the ways to provide electricity has varied between about 60 and 70%. The most recent NEI survey showed 63% in favour and 31% opposed. A recent survey by the MIT Center for Advanced Nuclear Energy Systems (CANES) showed that slightly over 60% of Americans felt that use of nuclear energy for electricity generation should increase or stay the same in the next 25 years, while slightly fewer than 40% felt that its use should be reduced or eliminated. In a 2002 study in which the same question was asked, the results were about 53% in favour and 47% opposed. This comparison suggests a modest increase in favourable public opinion in the five-year interval.

Over the past few years, the issues of climate change (global warming), the role of 'greenhouse gas' emissions in climate change, and the role of nuclear power in reducing greenhouse gas emissions has received increasing attention in the media. Statements from high government officials and highly-respected scientists and environmentalists have been generally favourable to the increased use of nuclear power in the future as part of an energy mix aimed at reducing CO_2 emissions and air pollution in general. However, the CANES study showed only a remote connection between electricity generation and global warming in public opinion, and no significant correlation between concern over global warming and attitudes towards nuclear energy. The latest NEI survey showed that fewer than half of the public have heard or read about the benefits of nuclear energy in reducing air pollution and greenhouse gas emission. Among people who had heard about the clean-air benefits of nuclear energy, the proportion in favour rose to 73%, while only 49% of those who had not heard about the clean-air benefits were in favour. This result suggests that awareness of the benefits of nuclear energy as a clean energy source is important to improving public acceptance.

At this time, it is expected that the vast majority of the current nuclear power plants (NPPs) will apply for extension of their operating licenses from 40 to 60 years. According to the above-cited survey conducted for the Nuclear Energy Institute, 81% of the public agree that the US should renew licenses for plants that continue to meet federal safety standards. In the same survey, 72% agreed that the option to build more NPPs in the future should remain, and 71% agreed that electric companies should prepare now so that new NPPs could be built if needed in the next decade. A slightly smaller proportion, 66%, would accept a new reactor at the nearest existing plant site. A still smaller proportion, 56%, would definitely build more NPPs in the future. Thus, it seems that there is a substantial segment of the public that is favourable to the existing plants, and to keeping the nuclear option open. A smaller fraction, but still a majority, is favourable to making a definite commitment now.

While electricity generation and the use of nuclear power as the primary energy source remain in the private sector, the US Congress and the Administration have supported initiatives intended to facilitate new reactor construction and development of next generation nuclear power technologies. In addition, the Nuclear Regulatory Commission has taken measures to

improve the regulatory process, most notably by introducing the design certification, early site approval and combined operating license process.[3] These initiatives reflect recognition at the political level of the value of nuclear power in the national energy mix. In the recent past, many electricity generating companies have expressed interest in building new nuclear plants, either through participation in government supported programmes or through public statements of intent to file license applications. At this writing, a few reactor orders have been placed and a limited number of orders for long-lead time procurements, such as heavy steel forgings, have been entered.

The CANES study identified waste management as one of the critical obstacles (along with cost) to further development of the technology in the USA The study found that a large majority of the public (about 65%) would support expansion of nuclear power if there were a safe and effective way to deal with nuclear waste. Public support for use of the Yucca Mountain facility was weak; a plurality (39%) thought that it should not be used at all. Opinion about distributed storage in deep boreholes near existing nuclear facilities was about equally divided.

However, the CANES study found significant public support for current DOE proposals to introduce a large reprocessing facility in the USA and for a significant expansion of nuclear power if spent fuel were reprocessed. The survey question did not include specifics of the technologies involved, but the results suggest public support for the idea of reprocessing in principle. Along the same lines, an NEI survey in May 2006, found that 77% of the public would approve of US collaboration with other countries to develop technologies for recycling spent fuel and reducing radioactive waste. However, the question did not address the specific technologies involved.

To extrapolate the current public climate for nuclear power in the USA to public acceptance of the introduction of fast reactors requires some speculation. In the near term, public acceptance of fast reactor technology in the USA would seem to be closely connected with acceptance of the concept of spent fuel recycling. The above mentioned survey results suggest that the reprocessing and international collaboration in developing fuel cycle technologies have good public support in principle.

However, introduction of a fast reactor and reprocessing of spent fuel will also surely lead to renewed public discussion of the risks of proliferation of weapons-usable materials, the risks of transportation of spent fuel from reactor sites to a limited number of fuel cycle facilities and the safety of fast reactor technology. The first two of these issues remain in the public mind with respect to the current fleet of NPPs and the Yucca Mountain geological repository and will certainly be raised in any public debate of the merits of fuel reprocessing and recycling of actinides. It will be necessary to convince the public that the benefits to be derived from recycling the actinides are significant and outweigh proliferation and transportation risks.

The current fleet of NPPs is regarded as safe by a majority of the public. In an October 2006 NEI survey, 60-65% of the public rated today's plants as safe. The next generation of thermal

[3] This process is codified in Title 10, Code of Federal Regulations, Part 52 (10CFR52, for short).

reactors will be safer than the current generation. In the U.S. licensing process, it will be necessary to demonstrate that advanced fast reactors are as safe as next-generation thermal reactors. A clear demonstration of safety and an open and transparent regulatory process will be essential to retaining public acceptance of safety.

While public acceptance of fast reactors as a part of an integrated fuel cycle must pass some hurdles, it is starting from a position of a generally favourable public climate for nuclear power in general, and for the concept of recycling spent fuel in particular.

9.4. Final remarks

There is widespread agreement that fast reactor technology will eventually be needed to provide abundant energy free from pollution. The only possible alternative to breeder fission power, on a timescale of centuries, is fusion, and even the most favourable view of the prospects has to concede that there is a large chance that fusion will not be available in time to meet the energy needs, particularly of the rapidly developing nations of Asia and South America. The need for fast reactor technology, possibly even the need for breeding, may become necessary within 50 years or so.

It has been demonstrated in the preceding chapters that the technology of fast reactors is available and evolving and that acceptable safety standards can be reached. Fast reactors have intrinsic safety advantages which promise low radiation doses to the operating staff and the public. It is becoming increasingly clear that safety and economics are not incompatible: a reactor which is built and operated to high safety standards tends to be a reliable reactor which is economically viable.

REFERENCES TO CHAPTER 9

[1] INTERNATIONAL ATOMIC ENERGY AGENCY, Country Nuclear Power Profiles, Vienna, Austria (2009 Edition).

[2] INTERNATIONAL ATOMIC ENERGY AGENCY, Fast Reactors and Related Fuel Cycles: Challenges and Opportunities (FR09) (Proc. Int. Conf. Kyoto, 2009), IAEA, Vienna (2012).

[3] GARNIER, J., MALO, J., BERTRAND, F., ANZIEU, P., “Recent progress of gas fast reactor program”, Fast Reactors and Related Fuel Cycles: Challenges and Opportunities (FR09) (Proc. Int. Conf. Kyoto, 2009), Paper No. 01-10, IAEA, Vienna (2012) CD-ROM.

[4] The 4th Basic Plan of Long Term Electricity Supply and Demand (2008-2022 year), MKE announcement 2008-377, 29 December 2008.

[5] Atomic Energy White Paper, MEST (October 2008).

[6] KIM, Y.I., HONG, S.G., HAHN, D.H., "SFR Deployment Strategy for the Re-Use of Spent Fuel in Korea," Nuclear Engineering and Technology, Vol. 40, No. 6, pp. 517-526 (2008).

[7] HAHN, D., et al, KALIMER-600 Conceptual Design Report, KAERI/TR-3381/2007, Korea Atomic Energy Research Institute, Daejon, Korea, Republic of (2007).

[8] ATOMINFORM, Strategy of Nuclear Power Development in Russia in the First Half of XXI Century, Moscow (2001).

[9] ESNII Task Force and SNETP Secretariat, ESNII - The European Sustainable Nuclear Industrial Initiative - Concept Paper (May 2010).

[10] European Commission, Communication from the Commission of 22 November 2007 - A European strategic energy technology plan (SET Plan) - Towards a low carbon future [COM(2007) 723].
[11] SNETP Secretariat, Strategic Research Agenda (May 2009).
[12] INTERNATIONAL ATOMIC ENERGY AGENCY, Guidance for the Application of an Assessment Methodology for Innovative Nuclear Energy Systems, INPRO Manual – Overview of the Methodology, IAEA-TECDOC-1575, Rev. 1, IAEA, Vienna (2008).
[13] INTERNATIONAL ATOMIC ENERGY AGENCY, Assessment of Nuclear Energy Systems Based on a Closed Nuclear Fuel Cycle with Fast Reactors, IAEA-TECDOC-1639, IAEA, Vienna (2010).
[14] Perspective on Public Opinion, prepared for the Nuclear Energy Institute (May 2007).
[15] ANSOLABEHERE, ST., Public Attitudes Toward America's Energy Options: Insights for Nuclear Energy, MIT-NES-TR-008 (June 2007).

CONTRIBUTORS TO DRAFTING AND REVIEW

Abram, T.	The University of Manchester, United Kingdom
Alekseev, P.	Russian Research Center "Kurchatov Institute (RRC KI), Russian Federation
Andropenkov, S.	National Atomic Company "Kazatomprom", Kazakhstan
Anzieu P.	Commissariat à l'Energie Atomique et aux Energies Alternatives (CEA), France
Arai, M.	Japan Atomic Energy Agency (JAEA), Japan
Ashurko, Y.	Institute for Physics and Power Engineering (IPPE), Russian Federation
Bakanov, M.	Beloyarsk NPP (NNPP), Russian Federation
Baqué, F.	Commissariat à l'Energie Atomique et aux Energies Alternatives (CEA), France
Binachi, F.	National Agency for Energy, New Technologies and the Environment (ENEA), Italy
Cahalan, J.	Argonne National Laboratory (ANL), United States of America
Chang, Jinwook	Korea Atomic Energy Research Institute (KAERI), Republic of Korea
Charlent, O.	Commissariat à l'Energie Atomique et aux Energies Alternatives (CEA), France
Chellapandi, P.	Indira Gandhi Centre for Atomic Research (IGCAR), India
Denisov, V.	Gidropress Experimental Design Bureau (OKB Gidropress), Russian Federation
Devictor N.	Commissariat à l'Energie Atomique et aux Energies Alternatives (CEA), France
Dubuisson, Ph.	Commissariat à l'Energie Atomique et aux Energies Alternatives (CEA), France
Dufour, Ph.	Commissariat à l'Energie Atomique et aux Energies Alternatives (CEA), France
Efanov, A.	Institute for Physics and Power Engineering (IPPE), Russian Federation
Ershov, V.	St Petersurg-based AtomEnergoProekt (SPbAEP), Russian Federation
Fomichenko, P.	Russian Research Center Kurchatov Institute (RRC KI), Russian Federation
Fujita, E. †	Argonne National Laboratory (ANL), United States of America
Ganesan, V.	Indira Gandhi Centre for Atomic Research (IGCAR), India

† Deceased

Garnier, J.C.	Commissariat à l'Energie Atomique et aux Energies Alternatives (CEA), France
Guerin, Y.	Commissariat à l'Energie Atomique et aux Energies Alternatives (CEA), France
Heusener, G.	Germany, Consultant
Hill, R.	Argonne National Laboratory (ANL), United States of America
Ivanov, E.	Institute for Physics and Power Engineering (IPPE), Russian Federation
Jacqmin R.	Commissariat à l'Energie Atomique et aux Energies Alternatives (CEA), Cadarache, France
Kamaev, A.	Institute for Physics and Power Engineering (IPPE), Russian Federation
Karpenko, A.	Beloyarsk NPP (NNPP), Russian Federation
Karsonov, V.	Gidropress Experimental Design Bureau (OKB Gidropress), Russian Federation
Kim, Beong-Ho	Korea Atomic Energy Research Institute (KAERI), Republic of Korea
Kim, Seong-O	Korea Atomic Energy Research Institute (KAERI), Republic of Korea
Kim, Taek-K.	Argonne National Laboratory (ANL), United States of America
Kim, Yeong-il	Korea Atomic Energy Research Institute (KAERI), Republic of Korea
Korolkov, A.	Research Institute of Atomic Reactors (RIAR), Russian Federation
Kryuchkov, E.	Institute for Physics and Power Engineering (IPPE), Russian Federation
Kuzavkov, N.	Experimental Designing Bureau of Machine Building (OKBM), Russian Federation
Kuznetsov, I.	Institute for Physics and Power Engineering (IPPE), Russian Federation
Latgé, Ch.	Commissariat à l'Energie Atomique et aux Energies Alternatives (CEA), France
Lee, Chan Bock	Korea Atomic Energy Research Institute (KAERI), Republic of Korea
Lee, Jae-Han	Korea Atomic Energy Research Institute (KAERI), Republic of Korea
Lee, Yong-Bum	Korea Atomic Energy Research Institute (KAERI), Republic of Korea

Leonov, V.	Research and Development Institute of Power Engineering (RDIPE), Russian Federation
Lambert, J.	Argonne National Laboratory (ANL), United States of America
Manturov, G.	Institute for Physics and Power Engineering (IPPE), Russian Federation
Martin, L.	Commissariat à l'Energie Atomique et aux Energies Alternatives (CEA), France
Maschek, W.	Karlsruhe Institute of Technology (KIT), Germany
Matveev, V.	Institute for Physics and Power Engineering (IPPE), Russian Federation
Meskens, G.	Belgian Nuclear Research Center (SCK•CEN), Belgium
Monti, S.	International Atomic Energy Agency
Orlov, V.	Research and Development Institute of Power Engineering (RDIPE), Russian Federation
Oshkanov, N.	Beloyarsk NPP (NNPP), Russian Federation
Poplavsky, V.	Institute for Physics and Power Engineering (IPPE), Russian Federation
Portyanoi, A.	Institute for Physics and Power Engineering (IPPE), Russian Federation
Rineiski, A.	Karlsruhe Institute of Technology (KIT), Germany
Rodriguez G.	Commissariat à l'Energie Atomique et aux Energies Alternatives (CEA), France
Rouault, J.	Commissariat à l'Energie Atomique et aux Energies Alternatives (CEA), France
Seryogin, A.	Institute for Physics and Power Engineering (IPPE), Russian Federation
Sienicki, J.	Argonne National Laboratory (ANL), United States of America
Sofu, T.	Argonne National Laboratory (ANL), United States of America
Sorokin, A.	Institute for Physics and Power Engineering (IPPE), Russian Federation
Stanculescu, A.	International Atomic Energy Agency
Stepanov, V.	Gidropress Experimental Design Bureau (OKB Gidropress), Russian Federation

Suknev, K.	St. Petersburg-based AtomEnergoProekt (SPbAEP), Russian Federation
Tenchine D.	Commissariat à l'Energie Atomique et aux Energies Alternatives (CEA), France
Toshinsky, G.	Institute for Physics and Power Engineering (IPPE), Russian Federation
Tsibulya, A.	Institute for Physics and Power Engineering (IPPE), Russian Federation
Vasile, A.	Commissariat à l'Energie Atomique et aux Energies Alternatives (CEA), France
Vasilyev, B.	Experimental Designing Bureau of Machine Building (OKBM), Russian Federation
Vrai, B.	Electricité de France (EDF), France
Zabudko, L.	Institute for Physics and Power Engineering (IPPE), Russian Federation
Zhang, D.	China Institute for Atomic Energy (CIAE), China
Zhukov, A.	Institute for Physics and Power Engineering (IPPE), Russian Federation
Zrodnikov, A.	Institute for Physics and Power Engineering (IPPE), Russian Federation

IAEA
International Atomic Energy Agency

Where to order IAEA publications

In the following countries IAEA publications may be purchased from the sources listed below, or from major local booksellers. Payment may be made in local currency or with UNESCO coupons.

AUSTRALIA
DA Information Services, 648 Whitehorse Road, MITCHAM 3132
Telephone: +61 3 9210 7777 • Fax: +61 3 9210 7788
Email: service@dadirect.com.au • Web site: http://www.dadirect.com.au

BELGIUM
Jean de Lannoy, avenue du Roi 202, B-1190 Brussels
Telephone: +32 2 538 43 08 • Fax: +32 2 538 08 41
Email: jean.de.lannoy@infoboard.be • Web site: http://www.jean-de-lannoy.be

CANADA
Bernan Associates, 4501 Forbes Blvd, Suite 200, Lanham, MD 20706-4346, USA
Telephone: 1-800-865-3457 • Fax: 1-800-865-3450
Email: customercare@bernan.com • Web site: http://www.bernan.com

Renouf Publishing Company Ltd., 1-5369 Canotek Rd., Ottawa, Ontario, K1J 9J3
Telephone: +613 745 2665 • Fax: +613 745 7660
Email: order.dept@renoufbooks.com • Web site: http://www.renoufbooks.com

CHINA
IAEA Publications in Chinese: China Nuclear Energy Industry Corporation, Translation Section, P.O. Box 2103, Beijing

CZECH REPUBLIC
Suweco CZ, S.R.O., Klecakova 347, 180 21 Praha 9
Telephone: +420 26603 5364 • Fax: +420 28482 1646
Email: nakup@suweco.cz • Web site: http://www.suweco.cz

FINLAND
Akateeminen Kirjakauppa, PO BOX 128 (Keskuskatu 1), FIN-00101 Helsinki
Telephone: +358 9 121 41 • Fax: +358 9 121 4450
Email: akatilaus@akateeminen.com • Web site: http://www.akateeminen.com

FRANCE
Form-Edit, 5, rue Janssen, P.O. Box 25, F-75921 Paris Cedex 19
Telephone: +33 1 42 01 49 49 • Fax: +33 1 42 01 90 90
Email: formedit@formedit.fr • Web site: http://www. formedit.fr

Lavoisier SAS, 145 rue de Provigny, 94236 Cachan Cedex
Telephone: + 33 1 47 40 67 02 • Fax +33 1 47 40 67 02
Email: romuald.verrier@lavoisier.fr • Web site: http://www.lavoisier.fr

GERMANY
UNO-Verlag, Vertriebs- und Verlags GmbH, Am Hofgarten 10, D-53113 Bonn
Telephone: + 49 228 94 90 20 • Fax: +49 228 94 90 20 or +49 228 94 90 222
Email: bestellung@uno-verlag.de • Web site: http://www.uno-verlag.de

HUNGARY
Librotrade Ltd., Book Import, P.O. Box 126, H-1656 Budapest
Telephone: +36 1 257 7777 • Fax: +36 1 257 7472 • Email: books@librotrade.hu

INDIA
Allied Publishers Group, 1st Floor, Dubash House, 15, J. N. Heredia Marg, Ballard Estate, Mumbai 400 001,
Telephone: +91 22 22617926/27 • Fax: +91 22 22617928
Email: alliedpl@vsnl.com • Web site: http://www.alliedpublishers.com

Bookwell, 2/72, Nirankari Colony, Delhi 110009
Telephone: +91 11 23268786, +91 11 23257264 • Fax: +91 11 23281315
Email: bookwell@vsnl.net

ITALY
Libreria Scientifica Dott. Lucio di Biasio “AEIOU”, Via Coronelli 6, I-20146 Milan
Telephone: +39 02 48 95 45 52 or 48 95 45 62 • Fax: +39 02 48 95 45 48
Email: info@libreriaaeiou.eu • Website: www.libreriaaeiou.eu

JAPAN
Maruzen Company Ltd, 1-9-18, Kaigan, Minato-ku, Tokyo, 105-0022
Telephone: +81 3 6367 6079 • Fax: +81 3 6367 6207
Email: journal@maruzen.co.jp • Web site: http://www.maruzen.co.jp

REPUBLIC OF KOREA
KINS Inc., Information Business Dept. Samho Bldg. 2nd Floor, 275-1 Yang Jae-dong SeoCho-G, Seoul 137-130
Telephone: +02 589 1740 • Fax: +02 589 1746 • Web site: http://www.kins.re.kr

NETHERLANDS
De Lindeboom Internationale Publicaties B.V., M.A. de Ruyterstraat 20A, NL-7482 BZ Haaksbergen
Telephone: +31 (0) 53 5740004 • Fax: +31 (0) 53 5729296
Email: books@delindeboom.com • Web site: http://www.delindeboom.com

Martinus Nijhoff International, Koraalrood 50, P.O. Box 1853, 2700 CZ Zoetermeer
Telephone: +31 793 684 400 • Fax: +31 793 615 698
Email: info@nijhoff.nl • Web site: http://www.nijhoff.nl

Swets and Zeitlinger b.v., P.O. Box 830, 2160 SZ Lisse
Telephone: +31 252 435 111 • Fax: +31 252 415 888
Email: infoho@swets.nl • Web site: http://www.swets.nl

NEW ZEALAND
DA Information Services, 648 Whitehorse Road, MITCHAM 3132, Australia
Telephone: +61 3 9210 7777 • Fax: +61 3 9210 7788
Email: service@dadirect.com.au • Web site: http://www.dadirect.com.au

SLOVENIA
Cankarjeva Zalozba d.d., Kopitarjeva 2, SI-1512 Ljubljana
Telephone: +386 1 432 31 44 • Fax: +386 1 230 14 35
Email: import.books@cankarjeva-z.si • Web site: http://www.cankarjeva-z.si/uvoz

SPAIN
Díaz de Santos, S.A., c/ Juan Bravo, 3A, E-28006 Madrid
Telephone: +34 91 781 94 80 • Fax: +34 91 575 55 63
Email: compras@diazdesantos.es, carmela@diazdesantos.es, barcelona@diazdesantos.es, julio@diazdesantos.es
Web site: http://www.diazdesantos.es

UNITED KINGDOM
The Stationery Office Ltd, International Sales Agency, PO Box 29, Norwich, NR3 1 GN
Telephone (orders): +44 870 600 5552 • (enquiries): +44 207 873 8372 • Fax: +44 207 873 8203
Email (orders): book.orders@tso.co.uk • (enquiries): book.enquiries@tso.co.uk • Web site: http://www.tso.co.uk

On-line orders
DELTA Int. Book Wholesalers Ltd., 39 Alexandra Road, Addlestone, Surrey, KT15 2PQ
Email: info@profbooks.com • Web site: http://www.profbooks.com

Books on the Environment
Earthprint Ltd., P.O. Box 119, Stevenage SG1 4TP
Telephone: +44 1438748111 • Fax: +44 1438748844
Email: orders@earthprint.com • Web site: http://www.earthprint.com

UNITED NATIONS
Dept. I004, Room DC2-0853, First Avenue at 46th Street, New York, N.Y. 10017, USA
(UN) Telephone: +800 253-9646 or +212 963-8302 • Fax: +212 963-3489
Email: publications@un.org • Web site: http://www.un.org

UNITED STATES OF AMERICA
Bernan Associates, 4501 Forbes Blvd., Suite 200, Lanham, MD 20706-4346
Telephone: 1-800-865-3457 • Fax: 1-800-865-3450
Email: customercare@bernan.com · Web site: http://www.bernan.com

Renouf Publishing Company Ltd., 812 Proctor Ave., Ogdensburg, NY, 13669
Telephone: +888 551 7470 (toll-free) • Fax: +888 568 8546 (toll-free)
Email: order.dept@renoufbooks.com • Web site: http://www.renoufbooks.com

Orders and requests for information may also be addressed directly to:

Marketing and Sales Unit, International Atomic Energy Agency
Vienna International Centre, PO Box 100, 1400 Vienna, Austria
Telephone: +43 1 2600 22529 (or 22530) • Fax: +43 1 2600 29302
Email: sales.publications@iaea.org • Web site: http://www.iaea.org/books

12-12241

INTERNATIONAL ATOMIC ENERGY AGENCY
VIENNA
ISBN 978–92–0–130610–4
ISSN 1011–4289